



September 2, 2020

By e-mail only: OSMiningReportsPlans@aer.ca

Alberta Energy Regulator
2nd Floor, Provincial Building
9915 Franklin Avenue
Fort McMurray, Alberta
T9H 2K4

Attention: Charles MacDonald
Mining Authorizations, Manager Oil Sands West

**Subject: Syncrude Canada Ltd. Composite Tailings Capping Knowledge Synthesis
OSCA Approvals 8573Q (Clauses 27 and 28) and 10781L (Clause 22)**

Dear Sir,

Syncrude Canada Ltd. (Syncrude) has developed sand capping over composite tailings (CT) as one of the methods to construct landforms for reclamation and closure. In accordance with *Oil Sands Conservation Act (OSCA)* Approval No. 10781L (clause 22) and OSCA Approval No. 8573Q (clauses 27 and 28), Syncrude submitted its Aurora North and Mildred Lake CT deposit assessment/engineering analysis and research plans to the Alberta Energy Regulator (AER) on September 30, 2019 and February 27, 2020, respectively.

The following Composite Tailings Capping Knowledge Synthesis is submitted by Syncrude to the AER to fulfil the commitments made in the abovementioned plans. The learnings from Syncrude's greater than 20 years of research, development and operational experience have been compiled and synthesized to provide the current state of knowledge on sand capping CT from both the tailings treatment and tailings closure perspectives.

Syncrude trusts that the AER will find this information satisfactory. Please contact the undersigned if there are any questions regarding the attached.

Regards,

A handwritten signature in black ink that reads "R. Young".

Rochelle Young
Regulatory Advisor
Syncrude Canada Ltd.
825-409-7090
Young.Rochelle@syncrude.com

Ec. Shelvey.Isabelle@syncrude.com
Charles.MacDonald@aer.ca
Eric.Chiu@aer.ca
Tara.Wang@aer.ca



Composite Tailings Capping Knowledge Synthesis

Submitted to:

Alberta Energy Regulator

Submitted by:

Syncrude Canada Ltd.

August 31, 2020

Table of Contents

1	Regulatory Overview	3
2	Background	3
2.1	Composite Tailings	3
2.2	Capping of CT	5
2.2.1	Tailings Process and Deposit Considerations	5
2.2.2	CT Sand Capping	5
3	CT Capping Synthesis	5
3.1	Summary of Learnings	6
3.1.1	Physical: Syncrude’s Experience with Capping and Trafficking Composite Tailings.....	6
3.1.2	Chemical: Hummock Technology Learnings to Support Water Management on Reclaimed Landforms	6
3.1.3	Ecological	7
4	Next Steps	8
5	References Cited	9

Appendices

Appendix A: Syncrude’s Experience with Capping and Trafficking Composite Tailings

Appendix B: Hummock Technology Learnings to Support Water Management on Reclaimed Landforms

Appendix C: Sandhill Fen Watershed: Learnings from a Reclaimed Wetland on a CT Deposit

Appendix D: Development of Composite Tailings Technology at Syncrude Canada

1 Regulatory Overview

Syncrude Canada Ltd. (Syncrude) has prepared this submission to fulfil the commitments made in plans recently filed with the Alberta Energy Regulator (AER) to satisfy Clause 22 of *Oil Sands Conservation Act (OSCA)* Approval No. 10781L for Aurora North and Clauses 27 and 28 of *Oil Sands Conservation Act (OSCA)* Approval No. 8573Q for Mildred Lake. The plans previously submitted include:

- 1) Aurora North Composite Tailings Engineering Analysis and Capping Research Plan, Syncrude Canada Ltd. (OSCA Commercial Scheme Approval No. 10781M, Clauses 11 and 22) submitted on September 30, 2019; and
- 2) Mildred Lake Composite Tailings Deposit Assessment and Research Plan, Syncrude Canada Ltd. (OSCA Commercial Scheme Approval No. 8573Q, Clauses 27 and 28) submitted on February 27, 2020.

As proposed in the plan submissions (i.e. Sections 3 and 4 for the above plans), Syncrude has prepared an integrated research and monitoring plan. The two key elements of this integrated research and monitoring plan are:

- 1) Research and monitoring of the East-In-Pit (EIP) CT deposit; and
- 2) CT capping synthesis.

The objective of this document is to deliver on the CT Capping Synthesis.

2 Background

2.1 Composite Tailings

Bitumen extraction results in the production of fluid fine tailings (FFT). The geotechnical characteristics of FFT require long term storage in geotechnically secure tailings facilities. Composite tailings (CT) are produced by mixing a coarse tailings stream with a FFT stream and adding a coagulant to form a slurry that releases water when deposited and binds the FFT in a coarse tailings/FFT mixture. This allows for the fines to be stored in the soil matrix, which reduces the inventory of fluid-fine tails and enables a wider range of landforms for reclamation and closure (Matthews et al 2002). Research and Development of the CT process was started in the early 1990's and the CT process was piloted at Syncrude in 1997. Commercial CT production began in 2000.

Significant knowledge has been gained through the greater than 20 years of research, development and operational experience with capping of various deposits at Mildred Lake. Most notably, from the research and development programs at the CT Prototype and on the EIP Sandhill Fen Watershed (SFW). These learnings have been applied to operational scale capping and reclamation activities on CT deposits at SWIP Junior and EIP (Kingfisher Valley and southern EIP areas) (Figure 2-1).



Figure 2-1 Mildred Lake CT Capped Deposits

The learnings from these programs and the experience gained from the operational activities have been compiled and synthesized to provide the current state of knowledge on CT capping.

2.2 Capping of CT

Capping of soft sediments is a common activity worldwide, most notably in the dredging and mining industries. At its most basic level, a capping strategy includes decisions regarding: placement (hydraulic beaching, hydraulic cell construction, mechanical placement, or various combinations), capping materials (water, coke, uncapped, tailings sand, glacial materials, mine waste [lean oil sands, Kc and Kcw], and various mixtures), reclamation soil cover, and land use considerations (lake, upland forest, or wetlands).

2.2.1 Tailings Process and Deposit Considerations

A capping strategy is linked to the selected tailings technology. In order to support or facilitate effective capping, underlying tailings should be strong enough to support a cap, and should be dense enough that post-reclamation settlement meets its design basis. The density and strength of tailings are strongly correlated. The capping strategy employed will be a major determinant of the maximum elevation of the tailings, and is an iterative part of the process. These process considerations are critical to the success of any tailings management plan and landform design but are not within the scope of this synthesis.

2.2.2 CT Sand Capping

Syncrude has developed sand capping over CT as one of the methods to construct landforms for reclamation and closure. This process primarily involves hydraulic sand-capping using beaching to create a trafficability layer, then using cell construction of tailings sand to create a hummock topography. Some landform grading (mechanical) is required to achieve the designed topography. The final component of the cap is the reclamation soil cover which is typically comprised of one or two layers of soil (Pleistocene and Holocene materials salvaged from the mine advance).

This cap serves a number of objectives that can be considered in three interconnected categories: physical, chemical and ecological outcomes. Physical objectives are related to the design objectives of CT consolidation, release water flux management and the creation of a trafficable surface to support activities related to the chemical and ecological outcomes. To achieve chemical outcomes, the substrate cap, or soil cover design ensures that the resultant soil and water chemistry, and rates of its change and movement are appropriate to allow wetland and terrestrial plants to grow. Connected to the physics and chemistry objectives are the capping design components that support ecological outcomes, in essence, to provide enough water of appropriate quantity and quality to support both wetland and forest plants and animals to achieve equivalent land capability. The ecological outcome results from the physical and chemical state created through the capping design.

3 CT Capping Synthesis

This submission is structured into the three categories (physical, chemical and ecological components) of the CT cap. Appendix A is focused on the physical components of the CT cap. It is a summary of the operational experience with the construction of the sand cap to create a trafficable surface. Appendix B focuses on the chemical aspects of CT deposits. It provides a summary of the cap design

to produce a topography that provides water of appropriate quantity and quality to support a range of ecological outcomes. Appendix C addresses ecological considerations; it summarizes the research and monitoring program on SFW that validates the achievability of positive ecological outcomes on a CT deposit.

This synthesis presents the complete state of knowledge of CT capping that addresses capping from both a tailing treatment perspective as well as a closure perspective.

3.1 Summary of Learnings

The following is a brief summary of important key information from the physical, chemical and ecological components of Syncrude's historical work on capping and reclamation of CT deposits. This body of work demonstrates technical and operational understanding and confidence and serves to assert that CT is a commercially established tailings technology. It supports the approach that ongoing deposit performance monitoring is more appropriate going forward given the commercially proven status of the technology rather than a formal research and development plan. Monitoring performance in support of an Adaptive Management Approach is a necessary and important element of ongoing CT capping and reclamation. For specific technical details for each component, refer to the appropriate Appendix.

3.1.1 Physical: Syncrude's Experience with Capping and Trafficking Composite Tailings

Syncrude has systematically brought CT production and capping through the research, development, and commercialization phases for 20 years and is now in the commercial and continuous improvement phase. Processes and requirements for successful CT capping are mature and well-understood. Syncrude has implemented all stages of the CT technology at commercial scale (i.e. designing, planning, constructing, testing, and reclaiming CT) and to date has capped over 1100 ha (11 square kilometres) of CT successfully. The capped deposits are trafficable for reclamation material placement and proposed land uses. In 2020, about 50% of the sand-capped CT at Syncrude is fully reclaimed (which involves construction of hummock-and-swale topography, placement of reclamation material, and revegetation). Post-reclamation settlements are modest, occur within a few years, and can be managed through landform design.

3.1.2 Chemical: Hummock Technology Learnings to Support Water Management on Reclaimed Landforms

Hummock technology describes how Syncrude incorporates topographic relief on capped and reclaimed CT deposits. Over the last two decades, Syncrude has developed and advanced hummock technology through numerous applied research programs. Syncrude now has a thorough understanding of how to design and construct hummocks to meet targeted hydrologic functions on capped and reclaimed CT deposits. Where uncertainties remain, Syncrude is committed to the continuous improvement of hummock technology through its adaptive management framework.

Hummocks are essential components of the closure topography on CT deposits because they provide important hydrological, operational, and ecological functions. Results from research and monitoring

indicate that in terms of hydrologic function, hummocks are capable of achieving targeted water quantity, water quality, and landform drainage functions. Syncrude monitors and evaluates hummock performance relative to these hydrologic functions (see Section 4).

Hummocks have proven effective at providing separation between the water table and rooting zone. Hummocks prevent saturation and salinization of the rooting zone for upland vegetation when water table depths are maintained approximately 2 m below the land surface. The necessary separation between the water table and rooting zone is dependent on the specific material properties, soil cover, and vegetation on a hummock. Convex hummock shapes/slopes, with abrupt hummock-lowland interfaces, limit the areal extent of shallow water tables across hummocks compared to concave hummock shapes/slopes.

Constructed hummocks can be used to control the partitioning of precipitation to different water balance components. Given that overland flow is generally rare in the region, precipitation is primarily partitioned between recharge and evapotranspiration. The amount of water partitioned to these two water balance components represents a trade-off between vegetation productivity and water for downstream environments. Inter-annual climate cycles, soil cover characteristics (and corresponding vegetation assemblages), and hummock heights determine the magnitude of water partitioned to recharge versus plant water uptake.

Constructed hummocks can be used to passively manage and flush process-affected water. In typically horizontally-dominated groundwater flow systems, this can happen through freshwater percolating into the groundwater system forming freshwater lenses that displace saline-sodic water. In systems where the vertical component of groundwater is more pronounced, hummocks focus groundwater and solute discharge by facilitating the formation of local-scale groundwater flow systems. The discharge of deeper groundwater associated with the saline-sodic water entrained in the CT deposit appears to be a minor flux of water to the near-surface over the timescales considered.

Water table configurations beneath hummocks, and associated patterns of flow, are controlled by the ratio of recharge to hydraulic conductivity, hummock lengths, the thickness of the sand cap, and hummock heights. In relative terms, the water table more closely follows the closure topography when there is higher recharge, lower hydraulic conductivity, greater hummock lengths, shorter hummocks, and lower sand cap thickness.

Deposit-scale factors may override the influence of hummock morphological and hydrogeological properties, thereby controlling water table configurations and the pattern of groundwater flow/landform drainage. The propensity for hummock-scale factors to predominate over deposit-scale factors is largely dependent on the relative size and configuration of a hummock compared to the influential deposit-scale characteristics.

3.1.3 Ecological

SFW was designed, constructed, reclaimed, and revegetated as an instrumented watershed between late 2007 and 2012, and has had an active research and monitoring program since then. The goals of the project were to design and establish the initial conditions necessary to allow for development of a

fen wetland and its watershed over time, and to develop techniques for reclamation of CT deposits. A fen is a peat-accumulating wetland with a water table at or near the ground surface, and consisting of mineral-rich water primarily from groundwater.

Although the SFW is a newly reclaimed system, there is much that Syncrude has learned through the entire process, from concept, to design, to construction, to reclamation to research and monitoring.

Results from the research and monitoring indicate that successful ecological outcomes were achieved. The SFW project has demonstrated success with respect to establishing a range of natural fen vegetation in the wetland area.

An assessment of the ecological performance of the plants and invertebrates indicates that thresholds of salinity are much higher than previously thought, and the OSPW influenced chemistry is similar to natural wetlands in the region. There is evidence that hummock topography has created local-scale groundwater systems as expected, and although there are many drivers in the water balance, the watershed appears to be hydrologically sustainable. Structural and functional aspects of fen wetlands are achievable, even in short timeframes and on CT landforms. However, the wetland cannot be classified as a “fen” using conventional wetland classification. Achieving peatland targets as described in the Alberta Wetland Classification System, are not possible within the timeframes of closure (i.e. due to the requirement for 40cm of *accumulated* peat). Knowledge and understanding gained through the SFW will continue to inform the design, construction and reclamation of other CT deposits, including EIP. Continued performance monitoring of SFW will support understanding and prediction of other in-pit CT deposit reclamation. The work done on SFW is a key component of the adaptive management of EIP and other CT deposits.

4 Next Steps

At this time, Syncrude asserts that the adaptive management approach outlined in the “Aurora North Composite Tailings Engineering Analysis and Capping Research Plan” and the “Mildred Lake Composite Tailings Deposit Assessment and Research Plan” is the appropriate course of action going forward. This approach is also being successfully employed in the Base Mine Lake Monitoring and Research Program. Syncrude’s current plan with respect to sand capped CT deposits is focused on performance monitoring of the EIP CT deposit. The SFW and the Kingfisher Valley make up the northern portion of EIP. The southern half of Syncrude’s EIP is in the advanced stages of final sand placement, land forming and reclamation.

Learnings from this submission have been incorporated into the design of the EIP commercial scale sand capped CT deposit and the progressive reclamation that has taken place presents an opportunity for the first full scale integrated landscape performance evaluation of a commercial sand capped CT deposit in the mineable oil sands. Learnings from EIP will continue to inform the design and construction of future CT deposits planned at Syncrude.

5 References Cited

Matthews, J.G., Shaw, W.H., MacKinnon, M.D., Cuddy, R.G. 2002. Development of Composite Tailings Technology at Syncrude. *International Journal of Surface Mining, Reclamation and Environment*, 16, 24–39.

Appendix A

Syncrude's Experience with Capping and Trafficking Composite Tailings

McKenna Geotechnical were retained by Syncrude to carry out the studies presented in this publication and the material in this report reflects the judgment of McKenna Geotechnical in light of the information available at the time of document preparation. Permission for non-commercial use, publication or presentation of excerpts or figures is granted, provided appropriate attribution is cited. Commercial reproduction, in whole or in part, is not permitted without prior written consent from Syncrude. An original copy is on file with Syncrude and is the primary reference with precedence over any other reproduced copies of the document.

Reliance upon third party use of these materials is at the sole risk of the end user. Syncrude accepts no responsibility for damages, if any, suffered by any third party as a result of decisions made or actions based on this document. The use of these materials by a third party is done without any affiliation with or endorsement by Syncrude.

Additional information on the report may be obtained by contacting Syncrude.

The report may be cited as:

McKenna Geotechnical. 2020. Syncrude's Experience with Capping and Trafficking Composite Tailings. Prepared by McKenna Geotechnical for Syncrude Canada Ltd. 2020.



Syncrude's Experience with Capping and Trafficking Composite Tailings

AUGUST 28, 2020



McKENNA GEOTECHNICAL

About this document

This document was created by McKenna Geotechnical to describe Syncrude's experience capping and tracking composite tailings. This report contends that composite tailings (CT) capping is a routine and successful activity at the company, and part of routine planning and operations at Syncrude's Mildred Lake and Aurora North operations in Alberta's oil sands. The report will be combined with two others into a single document for submission to the Alberta Energy Regulator (AER) in August 2020. One of the other reports will cover closure topography (specifically hummock-and-swale technology) and learnings to support upland vegetation and water quantity/quality design objectives, while the other one will address the Sandhill Fen Watershed (learnings of a reclaimed wetland on a CT deposit). This report was written for a technical audience familiar with oil sands tailings and reclamation activities.

Authors

Syncrude contracted McKenna Geotechnical Inc to write and produce this document in close collaboration with Mr Dallas Heisler, PEng, a hydrogeological research engineer with Syncrude. The editorial team included:

- Gord McKenna, PhD PEng PGeol, McKenna Geotechnical Inc
- June Pollard, MSc PGeol, Engineering Geologist, 2222179 Alberta Ltd
- David Wylynko and James Hrynyshyn, Editorial and Design, West Hawk Associates
- Derrill Shuttleworth, Illustrator.

About McKenna Geotechnical Inc

McKenna Geotechnical is a Canadian engineering and consulting firm specializing in mining geotechnique, landform design, and mine reclamation. The firm develops mine closure plans, landform and watershed designs, and technical guidance documents. We provide expert consulting engineering and geotechnical review services for mines in Canada and abroad. We also offer courses for practitioners and students on landform designs and closure planning.

MCKENNA GEOTECHNICAL INC

5223 Laurel Drive.

Delta, BC, V4K 4S4 Canada

Phone: +1-604-838-6773

mckennageotechnical.com

info@mckennageotechnical.com

© 2020 McKenna Geotechnical Inc



McKENNA GEOTECHNICAL

Table of Contents

Executive Summary	4
1.0 Introduction	5
1.1 Scope of work	8
1.2 A concise history of CT and CT capping at Syncrude	8
2.0 CT and CT capping explained	15
2.1 Tailings definitions	15
2.2 Components and function of the CT cap	18
3.0 Technologies for CT cap design and construction	20
3.1 Landform design for a CT deposit	20
3.2 Design and deposition of CT	20
3.3 Types of CT capping and methods of selection	21
3.4 Design of the cap	26
3.5 Bearing capacity analysis	27
3.6 Deposition of trafficability cap	29
3.7 Trafficability testing	30
3.8 Prediction of post-reclamation settlement	33
3.9 Other technologies	35
3.10 Summary	35
4.0 CT capping case histories	36
4.1 NST Field Demonstration	38
4.2 CT Prototype	42
4.3 East In-Pit (EIP)	46
4.4 Southwest In-Pit (SWIP)	54
4.5 Aurora East Pit South (AEPS)	55
4.6 Other relevant studies	55
4.7 Summary	56
5.0 Assessment of technologies	57
5.1 Analysis of technology readiness levels	57
5.2 Residual challenges	58
6.0 Conclusions	61
7.0 Closing remarks	62
References	63
Appendix A: Case history summaries	A-1
Appendix B: Satellite imagery of case histories	B-1
Appendix C: Technology readiness levels	C-1

Executive Summary

In 2019, Alberta's provincial regulator asked Syncrude to submit a research and development plan regarding composite tailings (CT) capping and reclamation. This report contends that Syncrude already completed such a program over the past 20 years and is now in the monitoring and ongoing improvement phase.

The focus of this particular report is the research, development, and commercialization of CT capping to form a trafficable cap for construction of the closure topography layer, reclamation material placement by mining equipment, and future land uses.

Syncrude has compiled 19 case histories of CT capping, ranging from a pilot (NST Field Demonstration), to a prototype (CT Prototype), to a commercial scale project (East In-Pit, Southwest In-Pit, and the floating coke cap at Suncor Pond 5). Deposition of CT began at Syncrude Aurora East Pit South (AEPS), for which hydraulic sand capping is planned.

In affirming the contention, this report makes the following conclusions:

- Syncrude has systematically brought CT production and capping through the research, development, and commercialization phases for the past 20 years and is now in the commercial and continuous-improvement phase. The company has a mature understanding of the processes and operational requirements for successful CT capping.
- Syncrude is routinely designing, planning, constructing, testing, and reclaiming CT at a commercial scale and to date has successfully capped more than 1100 ha (11 square kilometres) of CT.
- The capped deposits are trafficable for reclamation material placement and proposed land uses. Approximately half of the sand-capped CT has been fully reclaimed (which involved construction of the closure topography layer, placement of reclamation material, and revegetation).
- Post-reclamation settlements tend to be modest, occur within a few years, and can be managed through landform design.
- A formal research and development plan for CT capping is not required. However, close monitoring and ongoing continuous improvement are recommended and are a necessary and important element of ongoing CT capping and reclamation.

1.0 INTRODUCTION

To manage growing inventories of fluid tailings, Syncrude Canada is using composite tailings (CT) technology to sequester oil sands fine tailings in tailings-sand pore spaces. The process entails mixing cycloned tailings sand slurry with fluid tailings and a flocculant, which allows production of a dense but soft and non-segregating deposit that can consolidate within a decade with manageable (< 2 to 4 m) post-reclamation settlement. CT can be capped and reclaimed with a growth medium to safely support productive boreal forest ecosystems. Figure 1-1 locates Syncrude and Suncor CT deposits.

Beginning in the early 1980s, Syncrude spent many years conducting laboratory research and field trials on various tailings technologies. This R&D work culminated in the 1997/98 CT Prototype, which is a large (1100 m long × 500 m wide × 10 m deep) deposit that was sand capped in 1998, with some portions reclaimed in 1999 and 2000. This natural laboratory was used to develop and refine capping and reclamation methods. Commercial-scale CT deposition began at Syncrude's Mildred Lake operation in 2000 and at Aurora North in 2014. Since 2005, successful commercial-scale capping of the new CT deposits has been nearly continuous and has become a routine practice at Syncrude.

The Alberta Energy Regulator has instructed Syncrude to provide details of a CT capping research program¹. In response, Syncrude contends that CT capping is already a commercial technology and part of routine planning and operations at Syncrude's Mildred Lake and Aurora North operations. To support the assertion that capping CT (and indeed building CT watersheds) is a common commercial activity, Syncrude is crafting three reports:

- Experience with capping and trafficking CT (this report)
- Hummock²: Technology Learnings to Support Water Management on Reclaimed Landforms
- Sandhill Fen Watershed: Learnings from a Reclaimed Wetland on a CT deposit

Syncrude will combine these documents into a single report, which will be submitted to the regulator in August 2020. While the primary audience for the report is the regulator, it will also be used to document Syncrude experience as a resource for staff.

This report's central assertion is that capping CT is a routine, successful, commercial-scale activity at Syncrude. The findings are based on Syncrude's 25 years of experience as evidenced by:

¹ This request came as part of the regulator's response to the Syncrude Aurora North Tailings Management Plan under the Oil Sands Conservation Act (OSCA) Approval no.10781L [Clause 22]: "Submit a capping research plan for composite tailings (CT) deposits at Aurora North."

² Hummocks are sometimes referred to as ridges (and hummock-and-swale topography as ridge-and-swale topography). The meanings are identical. More generally, this is the closure topography layer.

- the company designs and produces CT deposits suitable for capping hydraulically or mechanically.
- CT deposits are routinely capped, typically with hydraulically beached tailings sand. To date more than 1100 ha (11 square km)³ of CT has been successfully capped, of which approximately 50% has been fully reclaimed (construction of closure topography layer, placement of reclamation material, and revegetation).
- capped deposits are trafficable for reclamation material placement and proposed land uses.
- post-reclamation settlement to date has been modest, occurs within a few years, and can be managed through landform design.

This document provides a theoretical basis for CT capping for trafficability, and describes 19 supporting case histories that demonstrate Syncrude's experience producing, depositing, capping, and reclaiming deposits. Figures 1-2 through 1-7 show CT deposits and sand-capping operations at Syncrude and Suncor, which in this report are grouped geographically as follows:

- NST Field Demonstration
- CT Prototype
- East In-Pit (EIP)
- Southwest In-Pit (SWIP)
- Aurora East Pit South (AEPS)

Chapter 1 and Chapter 2 of this report provide an introduction, background, and definitions. Chapter 3 describes the technologies employed, and Chapter 4 consists of case histories (which are also summarized in Appendix A). Chapter 5 assesses technologies according to their readiness level and Chapter 6 provides formal conclusions and closing remarks.

³ Hectares are the common measure of land area for Canadian land reclamation. One hectare (ha) is 10,000 square metres. One hundred hectares is a square kilometre. It is perhaps easiest to visualize a hectare as square 100 m x 100 m. One hectare is 2.47 acres, an area of 1.23 CFL football fields. Syncrude's EIP is a large tailings facility with an area of about 1050 ha (10.5 km²).



Figure 1-1. Sand-capped CT locations at Syncrude and Suncor.

1.1 Scope of work

Table 1-1 is an overview of the scope for this report.

Table 1-1. Scope of work

Task	Description
Task 1. Compile data and available literature	Compile and read approximately 120 papers, reports, and presentations related to CT capping at Syncrude. Adapt and update case histories of CT capping from the 2017 capping workshop hosted by COSIA.
Task 2. Establish the framework	Build on the framework established by the R&D and prototype-scale capping at the CT prototype to develop and describe the key technologies used to cap CT.
Task 3. Conduct interviews	Interview key technical staff to fill in gaps and update the CT capping case histories.
Task 4. Compile the case histories	Compile case histories for capping performance at Syncrude's Mildred Lake Operation and Suncor Pond 5.
Task 5. Write, edit, illustrate, and prepare report.	Integrate research, writing, editing and illustrations to provide a draft and final report.

1.2 A concise history of CT and CT capping at Syncrude

This section provides a brief overview of the research, development, and commercialization of CT at Syncrude. Further details are provided in Chapter 3 and Chapter 4.

Research

CT is Syncrude's term for non-segregating tailings⁴. CT was developed in the laboratory by Dave Caughill, along with University of Alberta professors Norbert Morgenstern and Don Scott (Caughill et al. 1993). Their research was an extension of various coagulated-tailings research and development by Syncrude, the UofA, and others. Over recent decades, the oil sands industry has invested billions of dollars in research and development and commercialization of various tailings technologies (CTMC 2012). In the 1980s and 1990s, the focus was development of methods to sequester fines such as silt and clay particles less than 44 microns (COSIA 2012). A major focus was the capture of coagulated fines within a sand matrix. CT was the most successful of these efforts (see Pollock et al. 2000; CTMC 2012).

Composite tailings are oil sands tailings that are treated with a coagulant to form a non-segregating deposit. They may be comprised of whole extraction tailings (which average 20%

⁴ Suncor uses the term consolidated tailings (CT). Other oil sands operators use the term non-segregating tailings (NST). Internationally, mixtures of tailings are sometimes called "codisposal" – a term with a different meaning at Syncrude.

fines) or may be created by cycloning the whole tailings (WT) slurry (to remove excess water) and adding fluid fine tailings (FFT), which allows for greater control of density and fines content. Gypsum is the most commonly used coagulant, with a typical dose of 1600 g/m³ of tailings slurry.

The resulting CT slurry, typically composed of 65% solids and 20% fines, is discharged subaerially on a beach and deposited either subaerially, subaqueously, or sub-MFT, forming beaches 500 to 2000 m long. CT density reaches approximately 70% solids within minutes or hours after deposition, and fully consolidates to a loose sand deposit within a few months or years, nominally at 82% solids (2000 kg/m³ saturated density; 1630 kg/m³ dry density). The consolidation release water is recycled back to the extraction plant for re-use.

When discharged and deposited in low-energy environments, this mix of slurry exhibits little segregation, provided it has a sufficient density, high enough fines content, and a high enough coagulant dose. Where these conditions are not met, the slurry partially segregates, creating a low-fines (trafficable-sand) beach near the discharge and a high-fines fluid tailings zone at the distal end of the deposit. Often, tailings sand slurry is co-deposited with CT slurry (the streams intermingle during deposition) and forms an interfingered or layered deposit of tailings sand and CT.

Development

Syncrude's first CT trial (the 1995 NST Field Demonstration) was conducted in a U-shaped cell 600 m long and 30 m wide (see Figure 1-2 and Appendix B-1). In 2008, the CT was capped using mechanical placement to create 28 small test wetlands (fens) in anticipation of the Sandhill Fen Watershed.

The positive results of this large field pilot paved the way for the CT Prototype at the north end of MLSB (see Figure 1-3 and Appendix B-2) constructed in 1997 and 1998. About 40 ha of the 55-ha deposit, which was 1100 m long, 500 m wide and 10 m deep, was successfully sand-capped (mechanically and hydraulically) and a third of the capped area was reclaimed to boreal forest. In 2014, Syncrude successfully encapsulated the CT Prototype using 400-tonne trucks with 40 m of overburden as part of the W4 Dump construction. The CT Prototype was monitored for many years with respect to consolidation, water-table development, and reclamation.

In the late 1990s, Syncrude worked closely with Dr Richard Dawson, PEng, PGeol of Norwest Mine Services (now Stantec) to develop methods of capping and reclaiming CT, with most of the effort focused on the CT Prototype. Methods of capping, trafficability testing, and winter reclamation placement were advanced and commercialized at this deposit and have been successfully applied to many soft tailings deposits.

Commercialization

The positive results from the CT Prototype allowed Syncrude to move to commercial deposition and capping of CT at its Mildred Lake Operation, including the East In-Pit (EIP; Figure 1-4 and Appendix B-3) starting in 2000. CT deposition started at Southwest In-Pit in 2008 (Figure 1-5 and Appendix B-4). Each of these CT deposits has been hydraulically and mechanically sand-capped in whole or in part and reclamation material placement is continuing at EIP.

Starting in 2008, the northwest corner of EIP was developed into the Sandhill Fen Watershed, a 50 ha instrumented watershed for reclamation research. Building on that experience, most of the 1054-ha EIP has been hydraulically sand-capped and roughly half has been reclaimed to upland boreal forest and wetland. Reclamation efforts are expected to be completed in the next few years.

In 1998, CT was selected as the best tailings technology for Syncrude Aurora North. Active in-pit deposition began in the Aurora East Pit South (AEPS) area in 2014 (Figure 1-6; Appendix B-5).

In parallel, Suncor deposited CT in its Ponds 5 and 6 between 1995 and 2008 (Abusaid et al. 2011). Considerable segregation occurred, causing the formation of sandy beaches with large sandy fluid fine tailings ponds. The beaches are trafficable but the sandy FFT required a novel approach, in which a commercial-scale floating coke cover was constructed at Suncor Pond 5 (Figure 1-7 and Appendix B-3). This approach demonstrates that off-spec CT deposits can be capped mechanically, albeit at great effort, even if they are fluid.

Additional key references from the commercialization period include:

- BGC 2010a and 2010b – Review of tailings technologies and review of reclamation options for oil sands tailings substrates
- CTMC 2012 – Oil Sands Tailings Technology Deployment Roadmap.
- CEMA 2014 – Guidelines for Wetland Establishment on Reclaimed Oil Sands Leases (3rd Edition).
- Jakubick and McKenna 2001 – Stabilization of soft tailings practice and experience.
- McKenna et al. 2016 – Shear strength and density of oil sands fine tailings for reclamation to a boreal forest landscape.

Continuous improvement

Syncrude continues to produce CT at its Mildred Lake and Aurora North operations and capping continues at Mildred Lake. Such work is in an informal commercial continuous-improvement phase. While it is a routine activity, room for improvement in CT production and capping remains, mostly in terms of efficiency. In 2017, COSIA organized an internal workshop with representatives from each oil sands company and international experts in soft tailings and soft ground capping. The case histories in Chapter 4 and Table A-1 build on results from that workshop.



Figure 1-2. Syncrude 1995 NST Field Demonstration during deposition (NST U-shaped cell and reclamation cell).



Figure 1-3. Syncrude CT Prototype shortly after sand-capping.



Figure 1-4. Syncrude East In-Pit (EIP) CT deposit during deposition.



Figure 1-5. Syncrude Southwest In-Pit (SWIP) (from Google Earth 2019).



Figure 1-6. Syncrude Aurora East Pit South (AEPS) (from Google Earth, downloaded 2020-04-26).



Figure 1-7. Suncor Pond 5 CT during initial floating coke cap construction.

2.0 CT AND CT CAPPING EXPLAINED

2.1 Tailings definitions

Extraction tailings is a pipelined slurry resulting from the extraction of a bitumen from oil sands, comprised of water (typically 50% by mass), sands (40%) and fines (10%), with some residual bitumen. If deposited as **conventional tailings**, the unamended tailings are overboarded behind a dyke to form a sand **beach**, with a fines-rich water runoff. Initially this fines slurry is referred to as **thin fine tailings (TFT)**, but when it has dewatered to about 30% solids over a period of three years after deposition, it is referred to as **mature fine tailings (MFT)** and behaves as a viscous fluid with the consistency of chocolate milk. **Fluid fine tailings (FFT)** is liquid suspension of oil sands fines in water with a solids content greater than 2% but less than the solids content corresponding to the liquid limit.



Figure 2-1. Extraction tailings slurry being discharged from a 24-inch-diameter pipeline for deposition onto a tailings sand beach.

Composite tailings (CT) is a non-segregating mixture of chemically amended fine and coarse tailings which consolidates relatively quickly into solid landforms. CT is produced to consume legacy fines (MFT) and new fines and create a land surface reclaimable to predominantly upland vegetation. To this end, CT typically has a **sand-to-fines ratio (SFR)** between 5:1 (to permit useful levels of fines capture) to 3:1 (to allow rapid consolidation). A 4:1 SFR (20% fines) is the most common recipe. CT starts as a slurry and quickly consolidates to a semi-solid, loose, saturated, silty sand deposit. As noted above, **non-segregating tailings (NST)** and **consolidated tailings** are terms used by other oil sands operators to describe CT.



Figure 2-2. The initial few centimetre thick layer of freshly deposited CT in a test cell, about 70% solids content (NST Field Demonstration 1995).

The CT **amendment** is typically gypsum, but other amendments such as lime, CO₂, alum, and polymers are also used; each has its own operational and environmental issues. The purpose of the amendment is to coagulate and strengthen the fines matrix enough to support the sand grains during discharge and deposition, in order to retain the fines in the void spaces within the sand grains and keep the fines from being flushed out (segregated) of the CT by the consolidation release water.

For largely historical reasons, oil sands tailings have a unique nomenclature related to grain size. In many cases just two types are recognized: sand and fines. **Fines** are grains with diameters less than 44 microns (specifically those passing a #200 wet sieve). The rest of the material (i.e., anything > 44 microns) is defined as **sand**. Accordingly, the SFR is the mass of dry sand (> 44 microns) to the mass of dry fines (< 44 microns). The **fines content** is the dry weight of fines to the dry weight of solids. Fines content is $1/(1+SFR)$. A fines content of 20% is a 4:1 SFR. Many oil sands ore bodies average 20% fines. The **clay content** is the dry mass of clay particles (< 2 microns as determined by a hydrometer) to the total dry mass of solids. The clay content of MFT is typically 30% to 50%. Clay is defined by grain size in this case, rather than by mineralogy; many clay mineral particles (mainly kaolinite) are > 2 microns in diameter. It is clay content, rather than the fines content, that governs geotechnical behaviour, although at Syncrude the 44-micron fines content is a useful metric for predicting the slurry behaviour of CT and MFT.

The **solids content** is the dry weight of solids to the total mass of slurry; when the tailings are saturated, it is analogous to bulk density. The solids content of CT slurry in the pipeline is typically 60% to 70%⁵. Fully consolidated CT typically has a solids content of 80% to 82%. The **water content** is the mass of water as a proportion of the total mass of slurry. The **bitumen content** is the mass of bitumen as a proportion of the total mass of slurry. CT is typically <1% bitumen. The solids, water, and bitumen contents sum to 100%. The **geotechnical moisture content** is often confused with the water content but is defined differently; it is the mass of water to the mass of solids. Such a formulation means that geotechnical moisture content is proportional to the mass of water in a sample, which is a good indicator of geotechnical performance.

Discharge is the condition at the end of the CT pipe — it may be tremmied to become sub-CT discharge, or overboarded (over even spigotted) to be discharged subaerially. Subaqueous discharge can lead to increased segregation. **Deposition** is what happens to the slurry after it leaves the discharge area. It settles to form a beach that may be subaerial (in the air; visible from the air), sub-aqueous (flowing and depositing underwater), or sub-MFT.

Segregation is the process of separation of fines from the sand — it typically refers to the deposition of sand-rich tailings on the beach, where the fines are carried with the release water down to the pond. Conventional oil sands tailings are dominated by this depositional mechanism. **Zonation** refers to the tendency of CT deposits to exhibit a higher SFR near the discharge end of the deposit and a lower SFR near the distal end of the deposit as a result of partial segregation or variation in discharge fines or solids contents. Zonation typically has only minor impacts on performance. **Fines capture** is the ratio of the dry tonnes in the CT deposit to the dry tonnes of fines in the CT slurry, and the fines not captured create a thin fine tailings (TFT) that eventually densifies to mature fine tailings (MFT). **CT sand efficiency** is the ratio of the amount (dry mass) of tailings sand in a CT in a deposit to the total tailings sand in the deposit (including dyke, underdrain, segregated sand, sandy MFT, and the sand cap). Other efficiency definitions are also employed.

Consolidation is the loss of excess pore-water pressures through the transient flow of water out of the deposit. The expelled water is referred to as **CT release water**, which either rejoins the operational **recycle water system** or is eventually released to the natural environment. One of the results of consolidation is **post-reclamation settlement** of the deposit. Because the deposit is saturated, each millimetre of release water results in a millimetre of settlement of the reclaimed landscape. Deposit strengths increase until full consolidation is reached. Even at full consolidation and unless desaturated, CT remains untrafficable.

Capping is the placement of a trafficability layer on the CT, then placement of hummock-and-swale topography (also known as the **closure topography layer**) on the trafficability layer. **Reclamation** involves placement of a **reclamation material** growth layer (typically a peat-mineral

⁵ These values are based on testing of deposits at the CT Prototype and East In-Pit (EIP).

mix) on the cap, and **revegetation** by planting of native trees and shrubs in the uplands and allowing aquatic vegetation to invade the swale wetlands.

2.2 Components and function of the CT cap

The CT cap involves additional nomenclature at Syncrude. As shown in Figure 2-3, a **soft tailings cap** can comprise several components: a **stabilized tailings layer** (often dried/crusted or cemented), a **geogrid and/or geofabric layer**⁶ on top of the soft tailings, a **trafficability cap** of constant thickness, and often **hummock-and-swale topography** (or doming), all capped with a **growth medium**. **Wetland** and **upland vegetation** are typically seeded or planted.

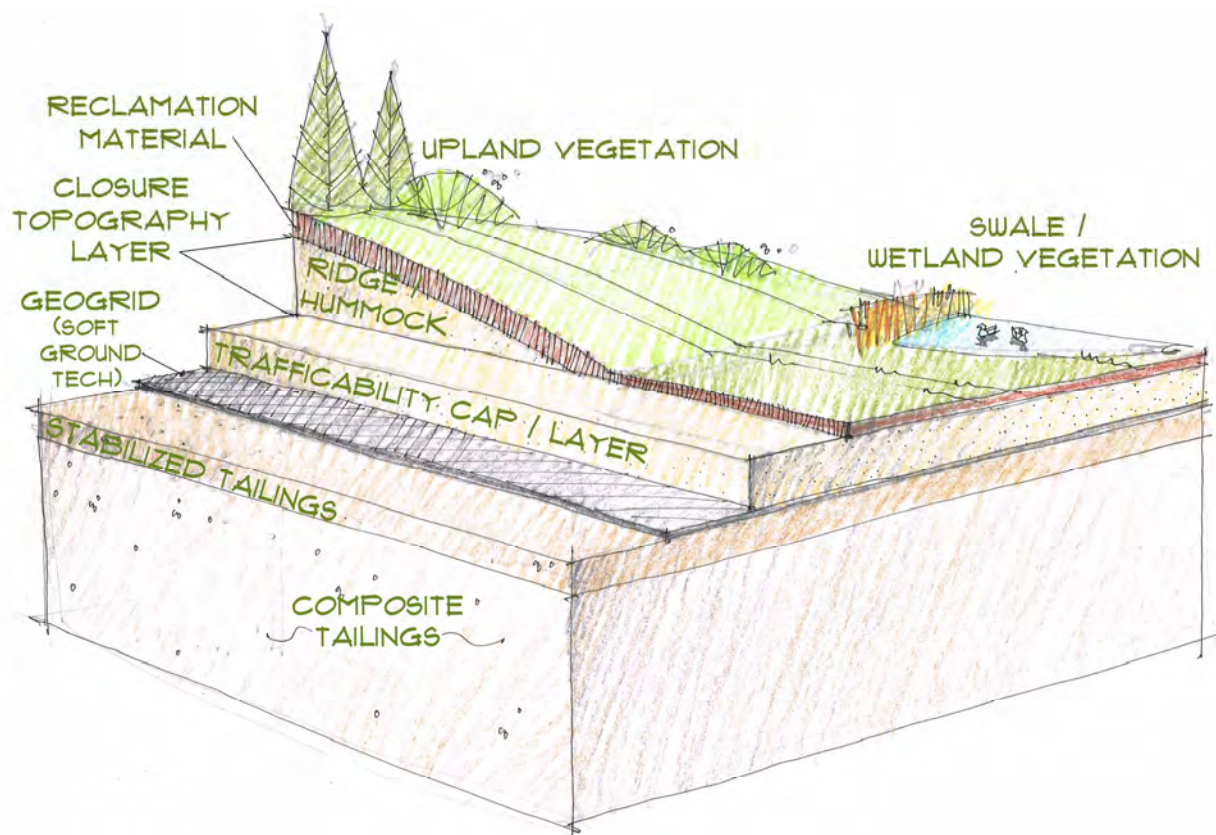


Figure 2-3. Components of a soft tailings cap/cover.

A **trafficability cap** is designed for the CT. This typically involves a pervious layer at least 2 m thick that allows for access by people and small equipment for construction of hummocks and placement of reclamation material. Trafficability caps are commonly 3 to 5 m thick.

Mechanical placement refers to capping by placement of sand or by motorized equipment, in some cases small equipment (for example 5-tonne trucks and D3-sized dozers) or more

⁶ Syncrude has not needed to employ soft tailings stabilization (beyond consolidation) or a geogrid / geofabric layer for its CT capping. These have been used in pilots and were employed at Suncor Pond 5 coke capping (see Section 4.6).

traditional mine-reclamation equipment (40-tonne trucks and D6 dozers). **Hydraulic placement** involves capping by discharging and depositing a slurry, typically through beaching from the perimeter of the CT deposit or raining-in from a barge floating on a water cap over the deposit. Syncrude uses both mechanical and hydraulic placement for CT capping. For mechanical placement, a **non-woven filter cloth** can be rolled out onto the tailings (sometimes in winter) to avoid allowing the tailings to boil up into the trafficability cap. In some cases, the filter cloth provides foot trafficability. **Geogrid** is a plastic reinforcing layer similar to plastic snow fencing, but much stronger. It is sometimes used to strengthen the interface, reduce the thickness of the trafficability cap for bearing capacity, minimize the risks of equipment becoming mired or punching into the soft tailings, and improve edge stability for fill placement. In some cases, strong geotextile panels are used instead of geogrid (as was done at Suncor Pond 5 coke capping (Abusaid et al. 2011)). As noted above, Syncrude has not needed these geomaterials for its commercial mechanical placement operations.

Hummock-and-swale topography and doming the deposit provide topographic relief needed to:

- Direct surface water away from the crest and toward the central swale, and prevent water from ponding in the geotechnical critical zone
- Favour runoff in the water balance
- Separate the root zone and the water table to promote upland vegetation and limit salinization of the reclamation material
- Provide topographic diversity for robustness, resilience, and ecological patch size
- Provide trafficability for larger mine equipment to deliver reclamation material
- Provide additional storage volumes for mine wastes
- Manage water quality downstream by enhancing the fresh-water component of the tailings plateau with hummock-and-swale topography.

As noted above, reclamation cap (coversoil and subsoil, typically a total of 0.1 to 0.5 m thick) is placed on the cap and revegetated. Release water, seepage water, and runoff are managed and directed toward the outlet for passive or active water treatment downstream. The resulting landform has considerable topographic diversity, where the upland areas are connected by a network of swales with creeks and wetlands.

3.0 TECHNOLOGIES FOR CT CAP DESIGN AND CONSTRUCTION

This chapter describes the framework that Syncrude employs to place a trafficability cap on CT. It involves various technologies that Syncrude has developed over the past 20 years with many hard-won learnings. Essentially this work is the result of the 20 years of research and development which has been commercialized. Chapter 4 (case histories) describes how Syncrude uses these technologies to plan, design, and cap CT. Chapter 5 assesses the technology readiness level (TRL) for each technology.

For capping CT, Syncrude combines an analytical and empirical framework, as typically done in dredging and other industries. The framework was largely developed in the late 1990s, and builds on work by the US Army Corps of Engineers for capping of dredge spoils and other soft ground environments.

3.1 Landform design for a CT deposit

The design of a CT landform is adapted from the life-of-mine closure landscape design and includes the outlet location and invert elevation, and sets the CT production, discharge, and deposition specifications, methods, volumes, and schedules. The landform design is based on a site investigation of the deposited tailings (a compilation of historical deposition data augmented by sampling and cone penetration testing from an amphibious rig). The trafficability cap is an integral part of the site-specific landform design as discussed below.

3.2 Design and deposition of CT

The success of capping depends on the production of a CT deposit that can be readily capped, and post-reclamation settlements that can be managed. To achieve this outcome, the following measures are required:

- Choosing a robust CT recipe that limits segregation and produces deposits that have small settlements over acceptably short timeframes. This typically means that the CT recipe has a fines content and density high enough to minimize segregation, but low enough to promote rapid consolidation/settlement.
- Closely monitoring the CT production to ensure it stays on-spec at discharge.
- Monitoring and adjusting CT discharge and deposition to ensure it remains non-segregating. Some segregation is inevitable, and any segregated material that cannot be capped can be removed by a dredge at the distal end of the deposit (typically this is fluid fine tailings and water). Some zonation is also inevitable so capping designs for the distal areas (which will be enriched with fines) are adjusted if needed.

CT behaves as a loose sand. There has been extensive cone penetration testing (CPT) and vane-strength test of existing CT deposits to understand CT behaviour and properties. CT tends to behave with an underdrained strength according to the vertical effective stress (Equation 3-1) based on triaxial data and back analyses of trial embankments on CT.

$$\frac{s_u}{\sigma_v'} = \frac{s_u}{\gamma' d} = 0.1 \quad (3-1)$$

where s_u is the peak undrained shear strength, σ_v' is the vertical effective stress, γ' is the buoyant unit weight of tailings, and d is the depth⁷. Bare, uncrusted CT at the surface has essentially zero shear strength, although the strength increases linearly with depth.

In many cases, there is a (usually desaturated) crust with 10 to 30 kPa⁸ of peak shear strength that is only 10 to 50 cm thick and provides little additional bearing capacity for equipment or embankments. However, in the particular case where there is underdrainage, the top few metres of the CT deposit are in suction and up to 100 kPa⁹ of peak undrained shear strength near the surface is observed (as was seen at the NST Field Demonstration Reclamation Cell (see Section 4.1)).

3.3 Types of CT capping and methods of selection

McKenna et al. (2016) provide a framework for capping oil sands tailings based on both soft tailings density and peak undrained shear strength (Figure 3-1) and capping methods based on empirical data from field trials on CT and other oil sands soft tailings (Figure 3-2). Six methods of capping are described (Figure 3-3):

- Water capping: almost any tailings can be capped with water, which “floats” on the denser tailings fluid or solid below.
- Coke capping: can be employed as a floating cover if the bulk unit weight of the coke is less than that of the underlying tailings, even if the tailings are fluid and are supported by geogrid / geofabric (Figure 3-4).
- Raining-in sand: a common technique of placing thin lifts (each just 5 to 10 cm thick). This approach is generally suitable for CT, but is typically more costly and operationally intensive than other methods.
- Sand beaching: the most common method in oil sands. The energy of deposition needs to be kept low to avoid excessive mixing or displacement (Figure 3-7).
- Soft ground techniques: mechanical placement is common in oil sands, but much more expensive than beaching. It controls and minimizes the use of sand (Figure 3-5).
- Standard earthworks construction: this method is suitable where the trafficability cap is strong enough to support equipment, namely 40-tonne trucks and CAT D6-

⁷ A saturated tailings sand cap has a buoyant unit weight of about $\gamma' = 7$ to 9 kN/m^3 and fully consolidated saturated CT has a buoyant unit weight of about 10 kN/m^3 .

⁸ Measured for example at the NST Field Demonstration U-Shaped Cell.

⁹ Measured for example at the (underdrained) NST Field Demonstration Reclamation Cell.

sized dozers which weigh between 13 and 22 tonnes. Larger equipment can be employed in some cases.

Syncrude routinely uses the last three of these technologies for capping CT. Suncor Pond 5 benefits from use of the first two. Designers select the best combinations of caps for each deposit and adjust designs as experience at that specific deposit is gained.

Early research at the NST Field Demonstration and the CT Prototype examined the use of enhanced CT surface strength (frost, or a crusted or vegetated surface) to support equipment operating on CT. Silva (1999) and Smith et al. (2018) provide some research results regarding the use of vegetation to stiffen the surface of soft tailings. Analysis and field testing quickly indicated that these enhancements could not be relied upon to support mining equipment, but can strengthen the interface.

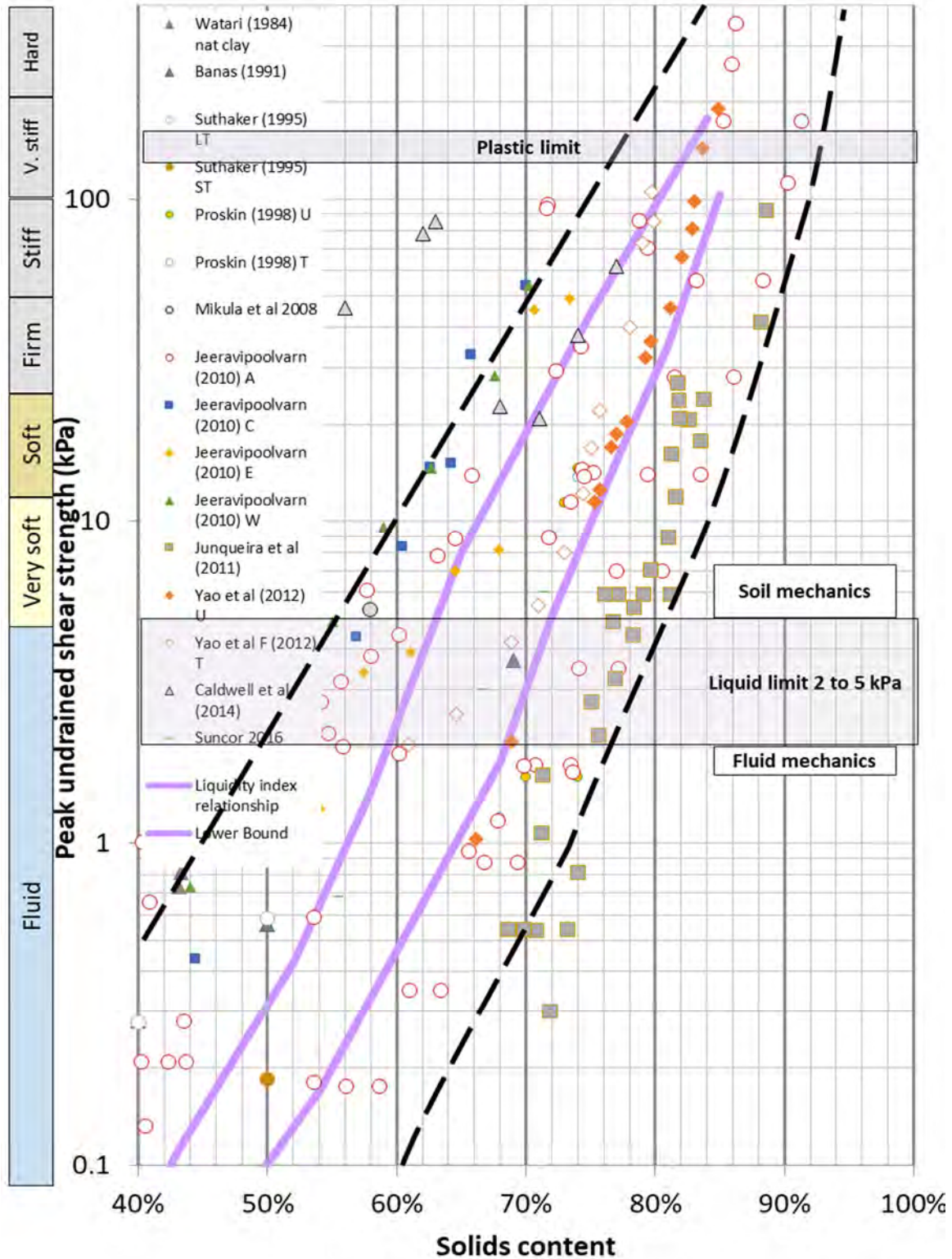


Figure 3-1. Oil sands soft tailings strength and density chart.

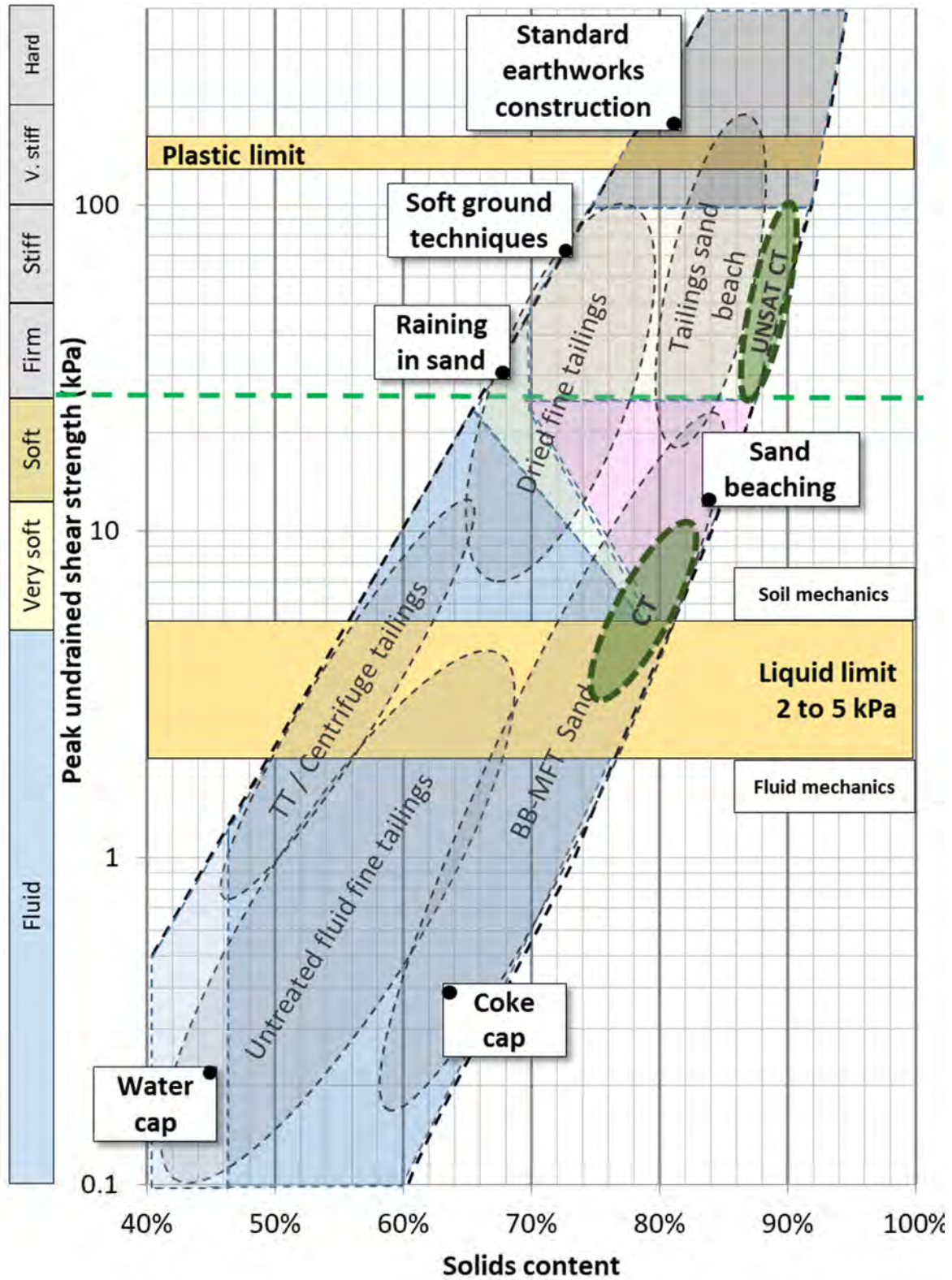


Figure 3-2. Oil sands soft tailings capping.

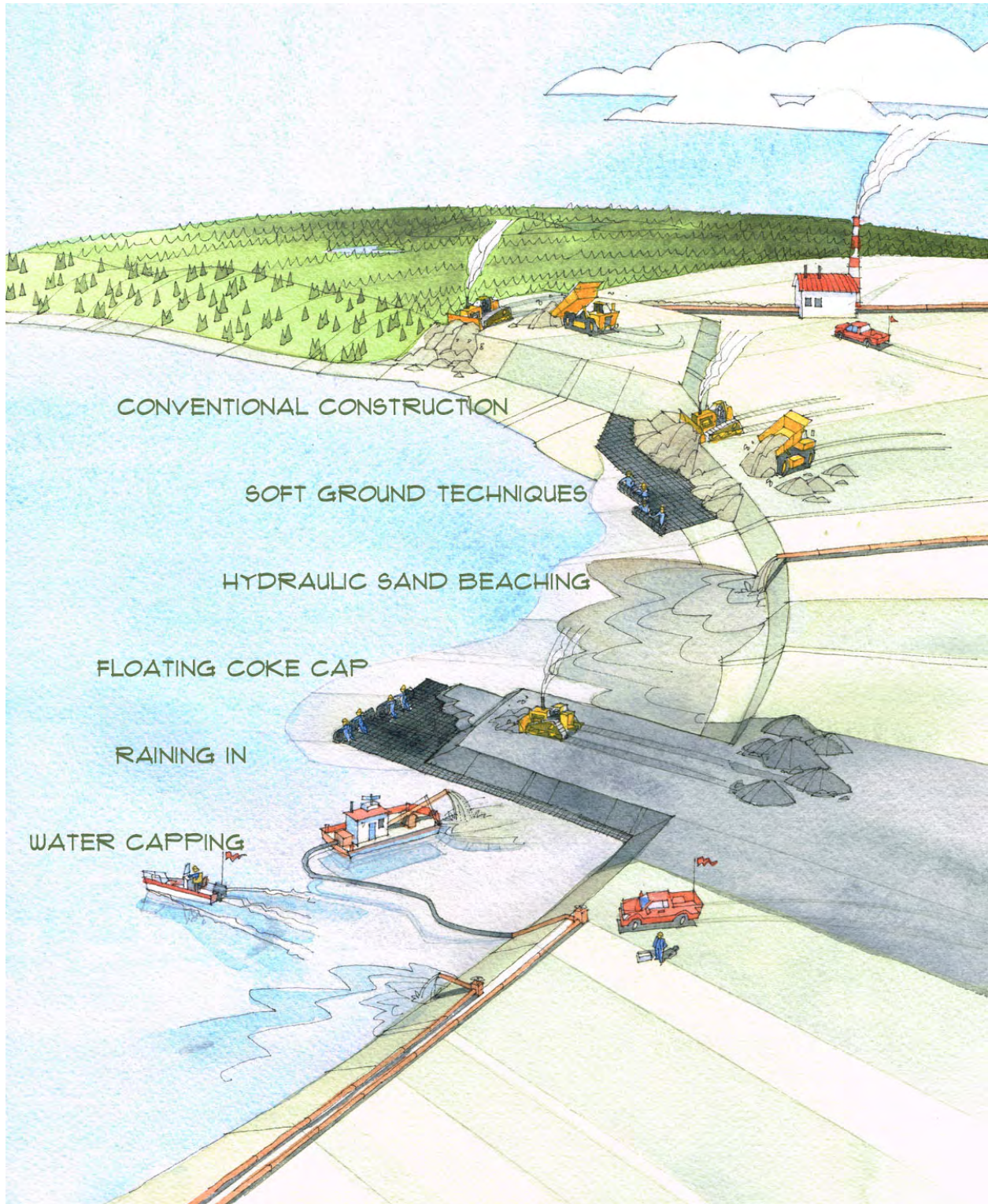


Figure 3-3. The six pack of tailings capping methods.



Figure 3-4. Mechanical placement of coke on off-spec CT at Suncor Pond 5 in 2010 (coke roads on strong geofabric).



Figure 3-5. Mechanical placement of tailings sand on CT at Syncrude CT Prototype in 2000.

3.4 Design of the cap

Syncrude geotechnical staff design the trafficability cap to meet trafficability requirements, support the closure topography layer, and to meet water quality and water quantity objectives for the reclaimed landscape (the groundwater regime in the closure landscape depends on the cap to act as a surface aquifer). A site investigation

is used to characterize the deposit and as input into the site-specific design of the trafficability cap. A semi-analytical design approach is used which includes equipment bearing capacity calculations (see next section), slope stability analysis for the hummocks, and integrated surface-water / groundwater modelling to support the reclamation design.

3.5 Bearing capacity analysis

The trafficability cap design is based primarily on meeting requirements to support specific reclamation equipment. Bearing capacity calculations are confirmed by trafficability testing (see Section 3.6).

Using soil mechanics, the ultimate bearing capacity (q_{ult}) (the bearing pressure that the soil will support at the onset of failure / instability) of a thick homogeneous anisotropic granular material, can be predicted by the Terzaghi (1943) bearing capacity equation:

$$q_{ult} = \frac{1}{2}\gamma BN_{\gamma} + cN_c + \gamma DN_q \quad (3-2)$$

Based on analysis and testing at the CT Prototype, it was determined that the main failure mode for trafficability was undrained punching (of wheeled or tracked equipment) into CT. This means that Equation 3-2 can be simplified to:

$$q_{ult} = s_u N_c = 5.14 s_u , \quad (3-3)$$

where s_u is the operational underdrained shear strength of CT, and N_c is a Terzaghi bearing capacity coefficient for cohesive materials and equal to $2 + \pi = 5.14 \approx 5$. The allowable bearing capacity q_{allow} typically uses a factor of safety FS of 2 to 3 as shown:

$$q_{allow} = \frac{q_{ult}}{FS} \quad (3-4)$$

The remolded (large-strain) undrained strength of CT is approximately 10% to 25% of the peak (which corresponds to a sensitivity of 4 to 10 as measured by the field vane). The designer takes into account that the CT may strain upon loading, and that the operational strength is some fraction of its peak undrained strength.

The bearing pressure of tracked equipment is estimated by dividing the operating weight of the equipment by the bearing area measured in the field. Small-dozer tracks have bearing pressures of 25 to 40 kPa. For trucks, the bearing pressure is the weight of the loaded truck divided by the combined contact area of the tires; this pressure is usually close to the tire air pressure, which is, for example, about 300 kPa for a 40-tonne truck.

Where CT is not capped and not underdrained, it is only trafficable by small, tracked, amphibious equipment (5 kPa bearing pressure), or specialized swamp buggies (often used for sampling and drilling). Hovercraft and airboats may also be used. Where the crust is sufficiently thick and strong, the CT may support human foot traffic. In all cases, Syncrude develops site-specific safe work plans.

Larger equipment requires either suitable frost thickness or a cap to spread the load. Ice bridge technology (e.g., USACE 2006) is employed to estimate the load capacity for equipment on frozen CT (the typical measured CT frost depth is 0.6 to 1.2 metres in late winter), restricting loading to modest-sized dozers and light vehicles (no haul trucks). Unlike the bearing capacity described above, which is a function of bearing pressure and fails in shear, ice-bridge technology considers the load (weight) of the equipment and assumes the frost cap to be a floating and brittle solid that can fail in bending. Extensive testing of frost depth is required before loading by equipment because the depth and strength of the frost varies spatially and temporally.

As a result, capping is generally required to traffic equipment on CT. Because layered bearing capacity theory cannot reliably predict or design soft tailings, a simpler load-spreading approach is used (Figure 3-6).

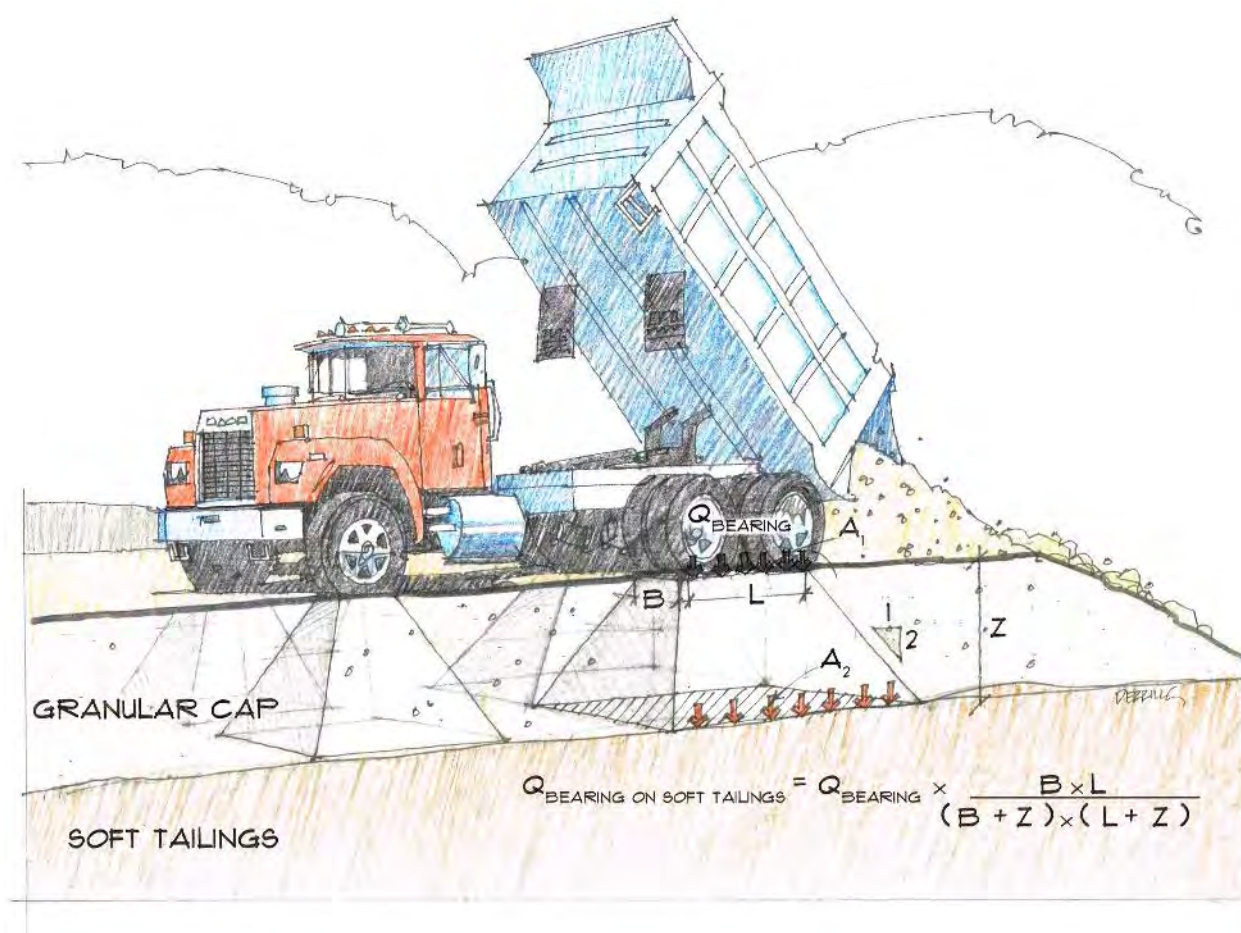


Figure 3-6. Accounting for spreading of bearing pressure through a granular cap on CT.

The thickness of the cap is not chosen by its frictional strength. Instead, it is assumed the cap spreads the wheel or track loads at 1V:2H onto the soft tailings below, according to the bearing width (B) and bearing length (L) and the cap thickness (Z). The peak undrained strength of the CT under the cap is estimated using Equation 3-1 (benefiting from the increased vertical effective stress under the cap), using Equation 3-3 for ultimate bearing capacity, and by employing

Equation 3-4 for a suitable factor of safety. Testing at the CT Prototype (see Section 4.2) indicated this approach was operationally effective and that a cap 2 to 3 m thick can support a 100-tonne loaded haul truck on fully consolidated CT (Figure 4-10).

3.6 Deposition of trafficability cap

At Syncrude, CT is generally capped using hydraulic sand beaching — discharge of tailings sand slurry around the perimeter of the deposit, beaching over the CT. Prior to deposition of the cap, CT is allowed to partially or fully consolidate, and tailings sand slurry is pumped to the deposit. A discharge spoon or header pipe is sometimes used to reduce the energy of discharge (Figure 3-7). Capping is enhanced by the fact that sand slurry during deposition is less dense than the CT. But experience has shown that effective capping involves understanding the concurrent depositional or geological mechanisms that create a complex deposit.

- Some of the CT is displaced by the sand cap, particularly near the discharge where discharge energies are high (Figures 3-7 and 3-8).
- Some depositional mixing of the CT and sand forms a mixing zone, a gradational interface of fines-enriched sand that can be centimetres to metres thick.
- There is also some interlayering or interfingering of the sand and CT, forming lenses and beds that can be centimetres or even a metre or more thick. Some of these beds are comprised of segregated CT.
- Sand slurry segregates during capping, forming a layer of fine tailings on the deposit which is typically displaced to a dredge. Some of these fines are incorporated back into the cap during deposition through entrainment or entrapment.
- Lensing (discrete lenses of CT or sand) can form through a variety of mechanisms (not just capping), resulting in a sometimes highly heterogeneous deposit.

These mechanisms are considered during the design of the capping and the impact on the properties of the sand cap. The main operational impact is the need to control discharge energies. Allowing the CT to more fully consolidate, and enhancing the strength of the top of the CT (with crusting, vegetation, or other stabilizing amendments), can help reduce this intermixing if needed though this has not been done at a commercial scale.



Figure 3-7. Tailings sand hydraulic beaching over CT using a spoon at the discharge – CT Prototype in 1998.

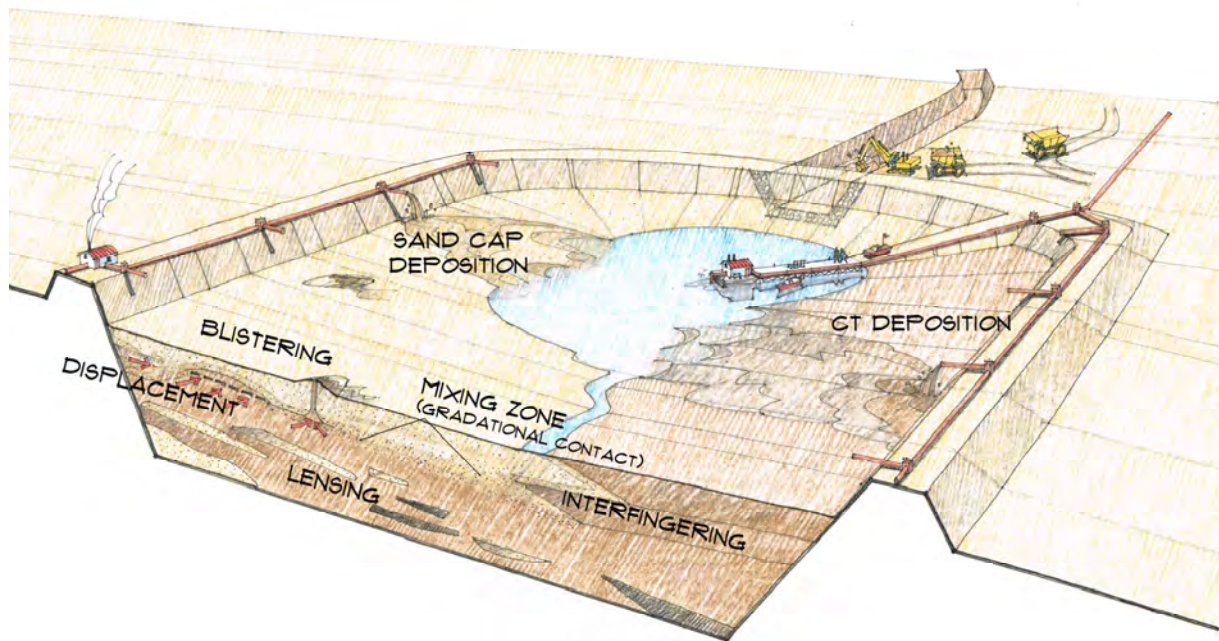


Figure 3-8. Complex depositional mechanism for CT and sand-capping (resulting in a complex deposit).

3.7 Trafficability testing

Syncrude backs up its semi-analytical design approach, described in Section 3.4, in two ways. First, Syncrude has developed summer and winter trafficability proof-roll testing of the capped CT

beaches, with larger and larger equipment advancing straight down the beach (Figure 3-9 and Figure 3-10). As the equipment progresses, it is closely monitored by the operator and a geotechnical engineer. The equipment reverses back up the beach when trafficability is reduced. The site where the equipment stopped is marked with a stake and a GPS survey position is measured. Subsequently, larger equipment is allowed no farther than that stake. A typical summer progression is an amphibious hunting vehicle, D3 dozer (8-tonne), D6 dozer (20-tonne). In summer, the heaviest equipment used is a D6/D7 dozer.

In winter, the frost depth at various locations is measured using the amphibious hunting vehicle, then operational techniques are employed to increase the frost depth. When frost depths exceed about 55 to 60 cm, the area is tested with a D9/D10 dozer. When frost depths exceed 90 to 100 cm, trafficability is tested with an empty then loaded 40-tonne truck, a loaded 100-tonne truck, then a loaded 140-tonne truck.

Equipment is parked on the dyke that can immediately extract any mired test equipment. A beach trafficability map and report are produced. A design for what equipment can work in which zone is then produced and followed in the field.

For areas that are too soft for the desired equipment, various stabilization or alternative capping measures are available, such as waiting for further consolidation, crusting, geogrid placement, hydraulic sand-capping, and enhanced frost penetration.

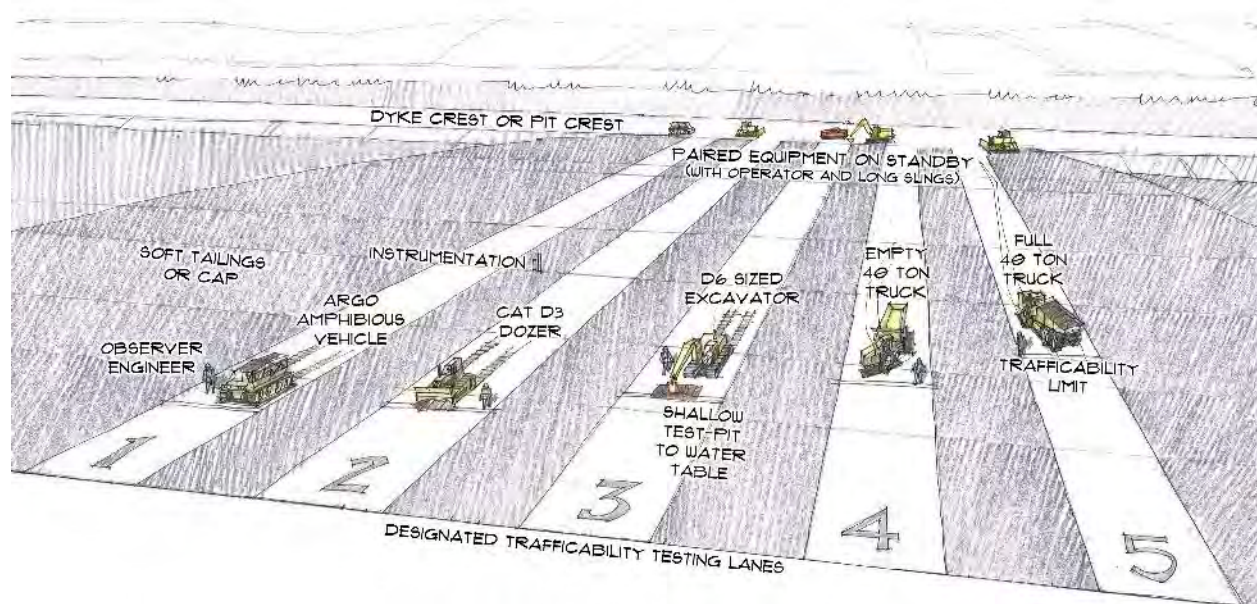


Figure 3-9. Example of trafficability proof-roll testing technology for sand-capped CT.



Figure 3-10. Trafficability testing with a Cat D3 dozer on the sand-capped CT Prototype in 1999.

This empirical testing approach has been successful, as indicated in the case histories (Chapter 4). Sometimes equipment becomes mired during proof-roll testing, but it can be quickly extricated using prepositioned equipment.

Second, trafficability risks are further reduced, and efficiency increased, by conducting reclamation material placement in the late winter, which takes further advantage of frost that penetrates the sand cap. This is the normal placement schedule for oil sands reclamation, as it also takes advantage of the frozen peat borrow areas. Syncrude has commercialized techniques for winter trafficability testing taking advantage of (measured) frost penetration: Argos, D6 dozers, 40-tonne, 100-tonne, and 140-tonne trucks. These techniques have been developed and used extensively at the Syncrude EIP area.

To further enhance operational trafficability, finger hummocks perpendicular to the dyke crest have been used to provide roads for haul trucks, as noted in Chapter 4 (capping by conventional earthworks). Haul trucks dump reclamation material near the crest of hummocks, and the material is then spread by dozers working on the hummocks and the intervening swales. Swale widths less than 100 m allow for simple and economical pushes by the dozers. This method is used at the EIP (Chapter 4).

3.8 Prediction of post-reclamation settlement

Post-reclamation settlement prediction is important for identifying areas that may have excessive settlement (predicted to affect drainage patterns and create ponding water) and is also used as part of the closure watershed water balance.

CT settlement is generally predicted using large-strain consolidation theory, and by employing commercially available one-dimensional analyses. Data from laboratory consolidation testing and field back-analysis (of settlement rates and dissipation of excess pore-water pressures) are used (see Pollock et al. 2000). Typically, several models for different areas of the deposit are run, then used to estimate post-reclamation consolidation magnitudes and timeframes. The model runs cover the lifecycle of the CT, from initial deposition in the base of the pit, through final filling, capping, and into the post-reclamation period until full consolidation is reached. In some cases, settlement is complete before the reclamation material is placed (for example at Sandhill Fen Watershed, full consolidation occurred during deposition – piezometers installed after deposition indicated no excess pore-water pressures and settlement monuments installed at the same time indicated less than 25 mm of settlement).

A settlement map is produced (Figure 3-11). Up to about 2 to 4 m of CT settlement can be managed through good design and construction. Because most CT, when capped, already has sand-to-sand contact, predicted post-reclamation settlements are generally small, typically less than a metre or two for on-spec CT.

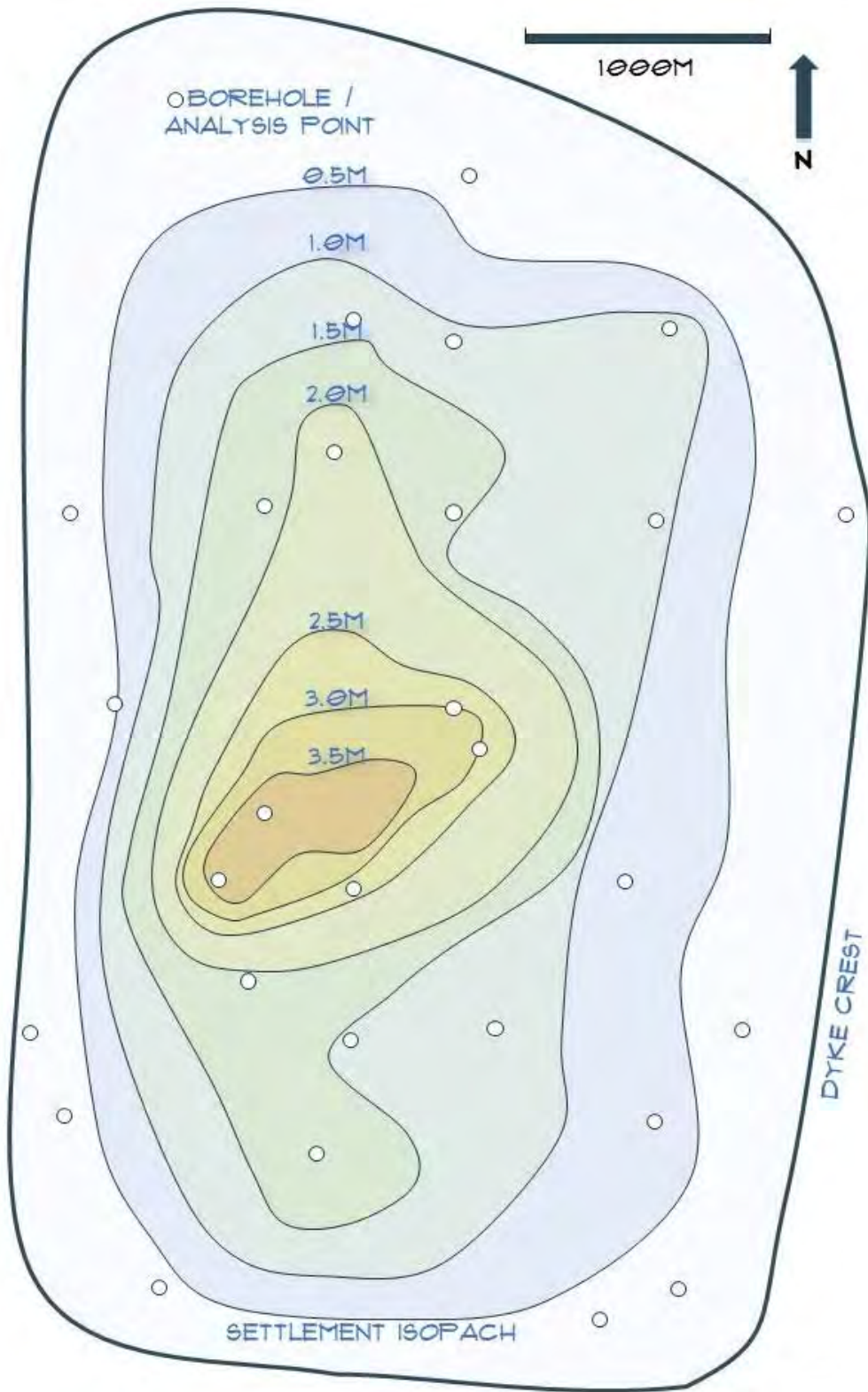


Figure 3-11. Example of settlement prediction map (hypothetical data).

3.9 Other technologies

The technologies for design of closure topography (the hummocks and swales), managing water quantity and quality, and reclamation of sand-capped CT deposits are described in the companion documents (by Syncrude and Advisian) to this report. These include:

- Design of the hummock-and-swale surface topography to manage the quality and quantity of seepage water in the reclaimed landscape
- Design and placement of reclamation material on the closure (final) topography sand / overburden surface
- Design and field activities related to revegetation of the CT deposits, including integration between upland and wetland areas
 - Monitoring techniques for landscape performance of the substrates, waters, and vegetation/ecosites.

3.10 Summary

The above framework provides the methods and processes that Syncrude uses to design, deposit, and test trafficability caps. Using this framework has allowed Syncrude to make capping CT a routine commercial activity at numerous sites. It is supplemented by an informal improvement process (Chapter 4).

4.0 CT CAPPING CASE HISTORIES

This chapter documents 19 supporting case histories that demonstrate Syncrude's experience, over the past 25 years, producing, depositing, capping, and reclaiming CT deposits using the technologies described in Chapter 3. The case histories are organized geographically:

- NST Field Demonstration
- CT Prototype
- East In-Pit (EIP)
- Southwest In-Pit (SWIP)
- Aurora East Pit South (AEPS)

Table A-1 (Appendix A) presents the histories. Figure 1-1 shows the first four of these locations and Figure 4-1 shows Aurora East Pit South (AEPS). Table 4-1 provides details on all 19 case histories.



Figure 4-1. Syncrude's Aurora East Pit South (AEPS)

Table 4-1. Case histories summary table

No.	Case history name	Year	Coordinates (UTM, NAD 83)	Area (ha)
Syncrude NST Field Demonstration				Total capped: 4 ha
01	Syncrude NST Field Demonstration U-Shaped Cell Loading Test	1999	460,279 E; 6,323,055 N	4 x 100 m ²
02	Syncrude NST Underdrained Reclamation Cell Test	1999	460,304 E; 6,323,172 N	1 ha
03	Syncrude NST Field Demonstration U-Shaped Cell (mechanical placement for cell and fen construction)	2008	460,224 E; 6,323,164 N	1.5 ha
Syncrude CT Prototype				Total capped: 50 ha
04	Syncrude CT Prototype (hydraulic sand cap)	1998	458,680 E; 6,329,060 N	25 ha
05	Syncrude CT Prototype (1 ha reclamation cap)	1999	459,111 E; 6,329,347N	1 ha
06	Syncrude CT Prototype (sand cap ditching prototype)	2000	458,933 E; 6,329,539 N	2 ha
07	Syncrude CT Prototype (mechanical sand cap)	2000	458,321 E; 6,328,861 N	~ 2 ha
08	Syncrude CT Prototype (winter placement of reclamation material on sand cap)	2001	458,812 E; 6,329,475 N	10 ha
09	Syncrude CT Prototype (W4 dump construction)	2014	458,653 E; 6,328,987 N	50 ha
Syncrude East In-Pit				Total capped: ~1000 ha
10	318 Closure Divide	2007 to 2009	464,697 E; 6,321,609 N	32.5 ha
11	Southeast Pond Junior (SEP Jr)	2008	464,014 E; 6,320,367 N	110 ha total
12	Sandhill Fen Watershed (hydraulic beach construction)	2008	464,039 E; 6,321,897 N	70 ha
13	Sandhill Fen Watershed (mechanical hummock construction)	2009 to 2011	464,020 E; 6,321,935 N	50 ha
14	Sandhill Fen Watershed (winter reclamation material placement)	2012	464,020 E; 6,321,935 N	50 ha
15	Kingfisher Watershed (hydraulic sand capping)	2012	464,685 E; 6,322,251 N	32 ha

No.	Case history name	Year	Coordinates (UTM, NAD 83)	Area (ha)
16	Kingfisher Watershed (mechanical sand capping)	2014 to 2016	465232 E; 6,321,717 N	54 ha
17	Syncrude EIP (hydraulic sand capping)	2008 to present	465,100 E; 6,320,980 N	500 ha
Syncrude Southwest In-Pit (SWIP)				Total capped: 32 ha
18	North Filter Berm CT (SWIP Jr)	2012 to 2014	459,712 E; 6,319,324 N	32 ha
Syncrude Aurora East Pit South (AEPS)				
19	Aurora East Pit South (AEPS)	2014 to present	No capped deposit (ongoing active CT deposition only)	0 ha
Approximate total capped CT at Syncrude to date				1186 ha

4.1 NST Field Demonstration

Following early lab scale demonstrations (Matthews 2002), CT demonstrations and research began with the Syncrude 1995 NST Field Demonstration in the southwest corner of the Mildred Lake Settling Basin (Figure 4-2 and Appendix B-1). The goal of the program was to demonstrate the production, deposition, and consolidation of on-spec CT and to gain operational knowledge and experience. Three deposits were successfully constructed: the **NST U-shaped cell** (600 m long, 30 m wide, lined flume), an underdrained reclamation cell 2 m thick (for reclamation trials), and a CT-under-MFT demonstration deposit. The key findings were that all three deposits were made with negligible segregation, and consolidation was rapid. The first two deposits were used for follow-on research and development as described next.

The first capping trial pilot was the Syncrude **NST Field Demonstration U-Shaped Cell Loading Test** (Case History 01; Figures 4-2, 4-3, and 4-4). The research goal was to develop techniques for placing and monitoring small embankments on CT and understand the resulting deformation mechanisms. Four 100 m² test embankments were constructed where the CT was approximately 2 m thick; two embankments were placed directly on CT, a third site had a filter cloth at the interface, and the last site had geogrid and fabric. The key learning from the project was that a soft ground technique can be used to cap consolidated CT with only a small mud wave out front of the embankment. Visual monitoring is necessary and sufficient for a safe and efficient operation. Crusting simplified placement of the geofabric and geogrid.



Figure 4-2. Loading of the trial embankment at the NST Field Demonstration U-Shaped Cell in 1999.



Figure 4-3. Embankment loading trial at the NST U-Shaped Cell in 1999.



Figure 4-4. Embankment loading trial at the NST U-Shaped Cell in 1999.

Syncrude returned to the Syncrude 1995 NST Field Demonstration in 1999 (Case history 02; Figure 4-5) to conduct the **Syncrude NST Underdrained Reclamation Cell Test**. The goal was to undertake an excavator trafficability test on an underdrained CT deposit. The work involved construction of a CT cell deposit 2 m thick over an unsaturated tailings sand foundation. Key learnings were that the deposit drained in a few months to become unsaturated to the full 2 m depth. This resulted in a hard, table-top-like surface that was difficult to penetrate with a hand spade or shovel, and which had a peak undrained strength of approximately 90 kPa (due to suction). The excavator left only slight cleat indents on the deposit. The deposit was subsequently capped with a few metres of fill to serve as a laydown area with no reports of any capping difficulties.

In 2008, Syncrude began building 28 pilot fen wetlands at the U-shaped cell (Case History 03; Figure 4-6). The goal was **mechanical placement for cell and fen construction** on the U-shaped cell deposit. The work involved construction of small embankments 1 to 2 m high to form cells on CT and the subsequent construction of HDPE-lined cells using various reclamation material treatments to form about two dozen pilot fen wetlands. Key learnings were that, after a decade, the deposit had a 60-cm deep crust that could support a medium-sized tracked excavator (CAT 322B 50T, similar to a D6 dozer). Though the highest part of the deposit could support a loaded 40-tonne truck, it became mired about 200 m down the beach.

Overall findings from the NST Field Demonstration

These successful pilot capping experiments showed that capping CT was feasible using soft-ground techniques, which is the most common approach for soft tailings worldwide (Jakubick and McKenna 2001) and allows for the development of monitoring techniques. The high cost of this capping approach indicated that hydraulic sand capping would likely be much more economical, and that this soft-ground technique is best reserved for small areas of particularly soft tailings.



Figure 4-5. Equipment loading trial at the NST U-Shaped Cell in 1999.



Figure 4-6. Trafficability testing on uncapped CT at the NST U-Shaped Cell in 2008.

4.2 CT Prototype

The **CT Prototype** (Figure 1-1; Appendix B-2) was constructed and filled with CT in the summers of 1997 and 1998 to scale up CT technologies, including discharge and deposition, consolidation and settlement monitoring, trafficability and hydraulic sand capping, and terrestrial and aquatic reclamation. Various CT-capping projects at the CT Prototype are described in the following paragraphs.

Hydraulic sand capping (beaching) of tailings sand over CT and trafficability of the cap were trialed in 1998 and 1999 at the CT Prototype (Case History 04; Appendix A-1). The goal of the study was to place a hydraulic sand cap on the CT Prototype and monitor its performance. The work consisted of hydraulic tailing sand beaching using a flip spoon on a 24-inch-diameter tailings line (Figure 4-7). Key learnings were that there was some zonation (the deposit's SFR averaged 3 near the discharge, trending linearly, to 5 near the distal toe), some displacement during capping of fresh non-segregated tailings (to depth of 0 to 6 m), and a mixing zone 2 m thick between the sand cap and underlying CT. The dense sand cap was prone to cyclic liquefaction under equipment loads (Wood 2003), sand volcanoes, and consolidation water upwelling. The water table was close to the beach surface in all areas, except those adjacent to the dyke crest. This prototype-scale trial was successful, but the amount of displaced CT indicated a need to allow more consolidation of CT before capping (only two days had been allowed).



Figure 4-7. Hydraulic sand-capping of the CT Prototype in 1998.

A **reclamation trial covering 1-ha (10,000 m²)** (Case History 05; Figure 4-8) was constructed in 1999 at the east end of the saturated sand cap. The goal was to test reclamation methods on the saturated sand beach. The work consisted of track-packing with various sizes of equipment (Caterpillar D3 and D6 dozers and 30-tonne rock trucks) to improve trafficability and reduce consolidation water upwelling, followed by placement of 20 cm of secondary material and 15 cm of peat mineral reclamation cap. Key learnings were that, despite these efforts and the use of only small dozers and small haul trucks for reclamation material placement, the beach had marginal trafficability for small equipment and that saturated tailings are often untrafficable to large mining equipment. Considerable upwelling of tailings pore water took place during placement and the reclamation material became waterlogged and salinized. Within a few years, salts had flushed, moisture contents decreased, and vegetation performed well (without intervention). This development-scale work was ultimately successful, but indicated the need for improved water-table control through the use of hummock-and-swale topography.



Figure 4-8. Mechanical compaction of 1-ha trial at the CT Prototype in 1999.

Trial ditching was conducted in 2000 and 2001 at the CT prototype (Case History 06; Figure 4-9). The goal was to evaluate field-scale use of water-table control methods for tailings sand caps on CT. The work was a randomized ditching trial with ditches 2 m deep down the beach, and shallow standpipe piezometers installed to monitor changes in the phreatic surface (water table)

due to drainage. Key learnings were that ditching below the water table is challenging and issues arose with the rising of ditch bottoms (from a depth of 2 to 3 m up to 1 m within hours), miring of equipment, spalling, and slumping of side slopes. Piezometric response to the ditching was minor and attempts to dewater the ditches were largely ineffective. Ditching for water-table control was discounted by Syncrude in favour of hummock construction. This development-scale work was ultimately unsuccessful.



Figure 4-9. Ditching trial at the sand capped CT Prototype in 2000.

Mechanical placement of sand using small trucks and small dozers to create hummocks was trialed in 2000 (Case History 07; Figure 3-5). The goal was to investigate the placement of hummocks as an alternative to ditching. The work involved loading the CT Prototype sand cap at the west end with a 2- to 3-m lift of tailings sand. Key learnings were that hummocks were a viable option for water-table control despite minor toe bulging, local dewatering, and some cracking at the crest, and that mechanical placement of hummocks is relatively straightforward if the tailings substrate is sufficiently dense, and strong enough, to support the slopes and equipment (see McKenna et al. 2016). This work was successful at the prototype scale.

Winter placement of reclamation material on sand cap was trialed in 2001 (Case History 08; Figure 4-10). The goal was to reclaim the area using standard mining equipment. The work involved summer trafficability testing, which indicated it would be safe to place reclamation

material on the sand-capped CT with loaded 100-tonne haul trucks. Reclamation material was successfully placed with these trucks in winter (Figure 4-10). Key learnings were that placement of reclamation material was feasible with standard mining equipment (100-tonne haul trucks and Cat D6 dozers) under non-frozen and frozen conditions with no deformations under winter conditions. This work is considered prototype-scale research.



Figure 4-10. Winter placement of reclamation material at sand capped CT Prototype in 2001.

The CT Prototype was buried by **W4 Dump construction** in 2014 and is no longer accessible (Case history 09; Figure 4-11). The goal was commercial-scale construction of the overburden dump using mining techniques and equipment and geotechnical stability of the constructed dump. The work involved improvement of the frozen surface and then winter placement, and advancing the overburden fill onto the frozen surface using initially smaller, and subsequently larger, mining equipment and lift thicknesses. Additional safety and contingency measures were put in place, initially using smaller equipment, offsets for trucks back-up, day-shift placement of lifts only, and leaving a “hole” in case excess CT needed to be removed and to act as a sump for pumping water from spring melt / surface runoff. Key learnings were that the first lift of overburden was successfully placed (using a horse-shoe pattern to control deformations), despite some isolated areas where the frozen cap heaved up with some cracking on the lift, which were remediated with a reduction in lift thickness. Tens of metres of overburden fill overlies the CT prototype with no evidence of deformation.



Figure 4-11. W4 Dump construction on CT Prototype in 2014.

Overall findings from the CT Prototype

The CT Prototype provided a sizeable outdoor laboratory for CT deposition, capping, and reclamation. It showed that mechanical capping of CT could be done efficiently with mining equipment, that CT could be capped with normal beaching operations (although waiting for consolidation would be required to reduce CT displacement volumes), and that ditching for water-table control was impractical. It also demonstrated that sand-capped CT can be trafficked with normal mining equipment for reclamation, taking advantage of winter frost conditions to limit deformations and to limit upwelling of consolidation water. The overburden capping indicates that CT deposits can be capped with tens of metres of overburden taking advantage of frost and closely monitoring dumping conditions. This work provided the confidence needed to advance to commercial-scale production and sand capping of CT at EIP.

4.3 East In-Pit (EIP)

EIP is a mined-out pit to the south of Highway 63 and Mildred Lake. EIP is typically divided into two areas: Northeast In-Pit (NEP) and Southeast In-Pit (SEP). The pit was mined from 1989 to 2000. Deposition of CT began in 2000 and capping of the CT began in 2007. The capping work at EIP described below provided Syncrude with numerous R&D opportunities and the ability to develop and refine a commercial capping operation in the southern end of EIP. The progression of work at EIP, from initial filling to near-final reclamation, is presented in a sequence of satellite images in Appendix B-3. Figure 4-12 presents two recent cross-sections of the EIP deposit.

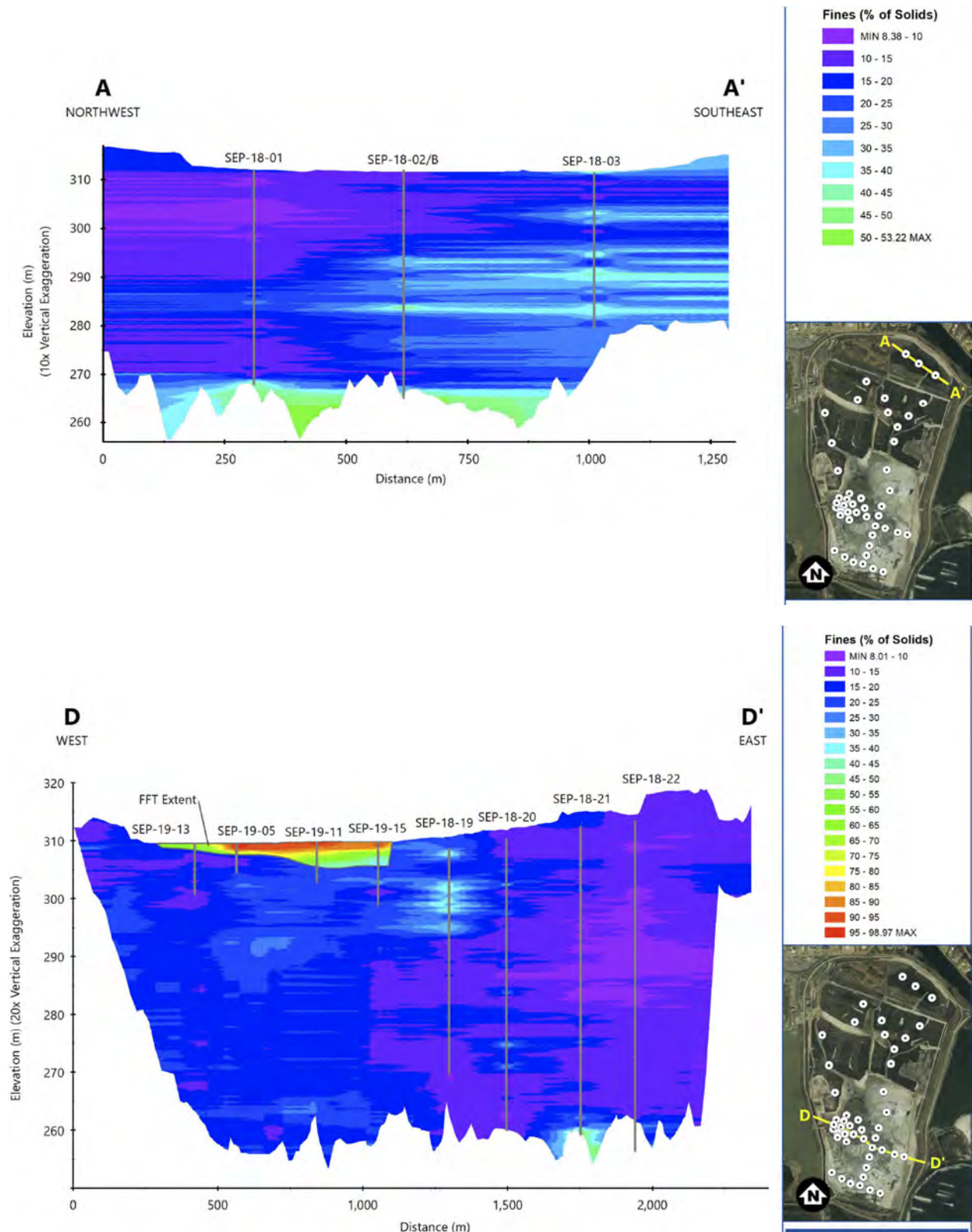


Figure 4-12. Two EIP cross-sections indicating fines contents (dark blue is the typical target for CT) (From Barr 2019).

The **318 Closure Divide** was one of the first capping structures constructed on CT at EIP, taking place from 2007 to 2009 (Case History 10; Figure 4-13). The closure divide is 2500 m long, 180 m wide, and 6 m high, and extends east-west across the northern half of EIP. The closure divide was constructed to create two separate watersheds in EIP for closure; a northern watershed that will ultimately drain surface water to Mildred Lake and a southern watershed which will drain surface water to Base Mine Lake (BML). The closure divide is also intended to provide gradient to the SEP outlet to BML. The closure divide was advanced onto the CT deposit using cell construction from both sides to meet in the middle; work on the western end began in late 2007 and the eastern end in November 2008. Key learnings were twofold: 1) the operational learnings from construction and 2) from geotechnical instabilities during construction of the west end of the closure divide in summer 2009 (cracks, sand boils in the surrounding CT, depressions in the closure divide). Construction continued following these instabilities using modification to side-slope design (setbacks), wait periods to allow for drainage, and modifications to placement plans to achieve final construction. These instabilities were investigated by Syncrude and slope-stability back-analysis was undertaken.



Figure 4-13. The 318 Closure Divide constructed on CT at EIP using hydraulic cell construction in 2007–2009.

The **Southeast Pond Junior (SEP Jr)** hummocks (Case history 11; Figure 4-14) were constructed in 2008. The hummocks were constructed as a closely investigated and monitored trial of hummock construction on CT that had been deposited at an operational scale (with a targeted SFR of 4:1) instead of a prototype. The construction was open-end cells with the initial lift beached onto CT. As the lift developed to approximately 2 m above the original CT surface, dozers were able to start pushing side dykes while still allowing the tailings to flow out of the open-ended cell. As this built up, the side dykes were advanced further. Eventually, the end dyke could be established with a spill box installed. The result was a 2.5 to 3 m thick hummock (as measured from the original CT surface), and a track-packed cell was constructed. A second lift was

constructed on top and the final result was a hummock 8 m high¹⁰ on CT. Key learnings were that the hummocks were successfully constructed on commercially deposited CT using beaching and open-cell construction. Several noteworthy operational learnings were produced. First, a combined beach and hummock-and-swale construction could be done simultaneously. Second, the side of the second lift initially did not have any offset from the first lift and some cracking developed along the edge. To resolve this, an offset of 5.2H:1V was implemented with no further cracking or instability noted. Third, sand losses from the open-ended cell formed a beach and, due to the fan that developed, resulted in poor drainage between the hummocks where the swale was intended to be. A design change to resolve this issue was proposed to create a hummock wider at the start and narrower at the end. Fourth, with regard to geotechnical stability, no visual evidence of sand boils appeared (unlike during construction of the 318 Closure Divide). A slight strength gain of the CT was noted from the sand capping in the following two years, with only 0.2 m of post-construction settlement.

Syncrude Sandhill Fen Watershed was constructed in the northwestern corner of EIP (see Wytrykush et al 2012). The goal of this instrumented watershed is to allow Syncrude to undertake research to gain additional experience and knowledge regarding wetland (and watershed) design and reclamation. The project took place in three phases, utilizing separate capping technologies: 1) **Hydraulic beach construction** (Case History 12), 2) **Mechanical hummock construction** (Case History 13), and 3) **Winter reclamation material placement for fen construction** (Case History 14). See Figure 4-15.

The **hydraulic beach construction** consisted of commercial deposition of tailings sand over CT from an open-pipe discharge in 2008. The resultant sand layer varied from 10 to 13 m thick (much of the volume of this cap was designed to provide closure topography). Key learnings were that the summer trafficability of the sand cap was found to be fair for mining equipment where saturated, but that poor trafficability was evident in the few locations that had standing water. Trafficability in winter was excellent since there was more than 1 m of frost. Underdrains that ploughed through the frost cap resulted in heaving/flow of the sand up through the trench and similar difficulties for the CT Prototype trenching.

Mechanical hummock construction, from 2009 to 2011, involved construction of seven rounded "island" hummocks, each 4 to 8 m high on the hydraulically placed sand cap. Construction involved mechanical placement of tailings sand utilizing 40-tonne trucks and small dozers, placed in lifts of 1 m. Key learnings were that the mechanical hummock construction was successful; no deformation of the hummocks was observed (apart from minor deformations of wet sand in one hummock) and there were no observations of deformation to the hydraulically placed sand cap from the loading of the mounded hummocks.

¹⁰ The ridges were originally designed to be twice as high as needed, then pushed down with dozers. Syncrude decided to keep with the as-built topography instead and allow wider swales.

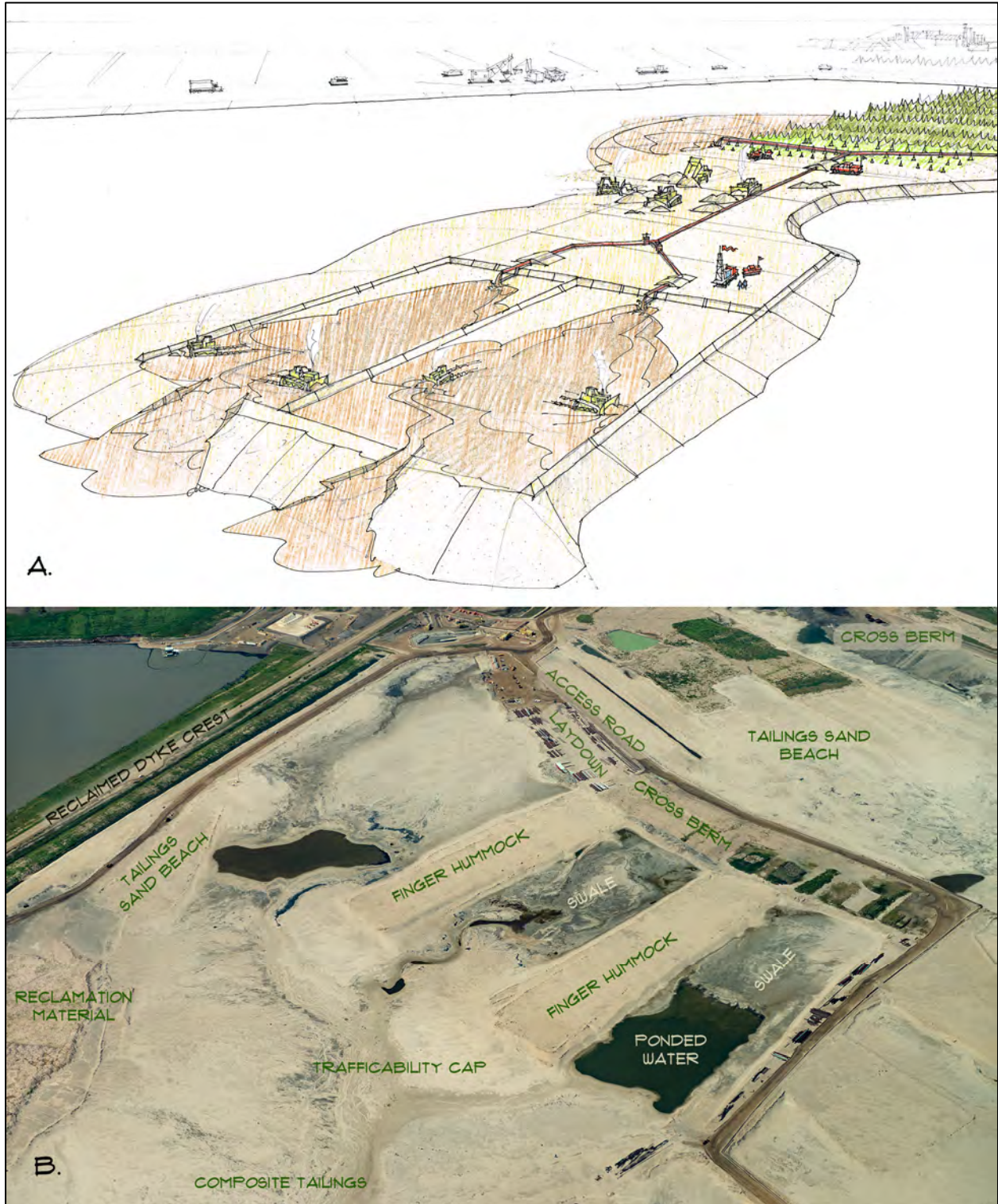


Figure 4-14. Sand-capping and hummock construction at Syncrude SEP-Jr in 2014.



Figure 4-15. Sandhill and Kingfisher (2015/2017).

Winter reclamation material placement for fen construction was undertaken in 2011 and 2012 and involved placement of 0.5 m of clay till and 0.5 m of peat mineral mix in the 15 ha fen between the mounded hummocks. Work was completed using 40-tonne trucks, a D6 dozer, and excavators (see Figure 4-16). Key learnings were that, in cases where there was more than 1 m of frost, the trafficability for winter reclamation placement was adequate for smaller equipment. The capping methodologies used could support the placement of reclamation material. The performance likely benefited from the thick sand cap. Subsequent performance of this research area has been documented by Synocrude in a companion document.

Kingfisher Watershed is in the northeastern corner of EIP. The watershed was hydraulically sand capped in 2010 (Case History 15) and mechanically sand capped in 2014 to 2016 (Case History 16) with the goal of creating closure topography. The underlying deposit in this area of EIP is layered CT and tailings sand with some areas of sandy MFT (4 to 10 kPa peak shear strength, 20% to 40% fines), which creates a challenging area to cap.

Hydraulic placement of tailing sand in Kingfisher Watershed took place in 2012 and was beached from the perimeter with a 24-inch-diameter line to create a dish-shaped watershed between 318 Closure Divide and the EIP boundary to the north. The beaching created a 0- to 10-m tailing sand cap. Key learnings were that while the sand capping of weak deposits is achievable, large volumes of sandy MFT were likely displaced during the beaching (a positive outcome but not entirely controllable).



Figure 4-16. Winter placement of coarse woody debris at Sandhill Fen Watershed by mining equipment.

Mechanical placement of a tailing sand cap in the Kingfisher Watershed was undertaken in 2014 to 2016. In summer, upland construction was completed; base preparation (dewatering, no track packing) was followed by tailing-sand placement using 40-tonne trucks (wiggie wagons) for the first lift, and then 100-tonne (CAT 777) haulers with D6 and D7 dozers. In winter, lowland construction involved base preparation of frost pounding¹¹ by dragging tires using a low-ground-pressure ATV; D7s were used once the frost depth was sufficient. Wiggie wagon trucks were used to bring sand in and D6/D7 dozers for placement. The area was reclaimed using commercial reclamation techniques. Key learnings were that the watershed was reclaimed successfully using hydraulic and then mechanical techniques. From the summer construction, some deformation from the displacement of segregated high-fines CT (edge and lift settlement) was evident and sand boils were seen mainly on the north and east side of the watershed. From winter construction, no deformations were observed. Once thawed, no significant deformations or sand boils were evident, just minor settlement from melting frozen sand lumps.

For the remainder of **Syncrude EIP, commercial hydraulic sand capping** (Case history 17) has been ongoing in NEP and SEP since 2008. The goal was commercial capping of the CT to create a trafficable surface to enable the subsequent creation of stable closure topography. The CT was

¹¹ Northern operators have often used “frost pounding” to “drive” frost into the ground, essentially deepening / thickening the frost cap in a certain area. The mechanics of such work is uncertain, but likely relates to keeping snow / loose frost from remaining on the surface, accelerating heat loss from the tailings to the atmosphere.

capped with hydraulic sand capping (beaching) to create a trafficability cap and using cell construction to create hummocks which have since been reclaimed (Figure 4-17). The remaining lowland areas (non-hummock) in the west of the deposit are planned to be capped in 2020. Key learnings were that the deposit characterization is important to understanding the final constructed closure landscape; creation of various watersheds in the northern end of EIP likely displaced some of the CT that was redeposited in the southern end. The majority of the deposit was hydraulically capped and can be trafficked by a D6 dozer; some CT may have been displaced during this capping. The resulting trafficability cap is considered to be an integral part of the closure topography design. Operational learnings (safe work practices, timings, schedules, methods) during construction continue to be incorporated into Syncrude operational practices.



Figure 4-17. Newly reclaimed sand hummock over CT at EIP.

Overall findings from the EIP

The EIP is the first commercial-scale CT deposit to be capped and reclaimed. The results to date have been judged extremely successful, with Syncrude applying learnings to its remaining CT deposits. Although originally designed to be homogenous, the heterogeneous CT deposit facilitated rapid consolidation (the sandier layers likely acting as interdrains), and drainage due to the sandy Boundary Dyke likely increased the ease of hydraulic sand capping. On the one hand, the 13-m-thick sand cap at Sandhill Fen Watershed provided excellent trafficability for reclamation, while the off-spec CT in Kingfisher and under the 318 Closure Divide proved more challenging (but ultimately successful). This deposit shows that CT capping and reclamation can be carried out effectively and efficiently. Future deposits can benefit from more analysis of the EIP, especially with respect to increasing the fines storage efficiency for in-pit deposits.

4.4 Southwest In-Pit (SWIP)

Hydraulic sand capping of CT has been ongoing at **North Filter Berm CT (SWIP Jr)**, **Southwest In-pit (SWIP)** (Case History 18; Figure 4-18; Appendix B-4) since 2012 at a commercial scale. The goal was to take the learnings from the successful creation of the 318 Closure Divide and create a sand trafficability cap on CT at SWIP for the SWIP North End Dam. In 2014, 22 m of sand cap was placed on CT with an SFR of 3.8:1 using cell-construction techniques working from east to west. Key learnings were that sand-capping CT continues to be affirmed operationally. Cell construction adjacent to the pond allowed greater sands capture, letting Syncrude conserve sand rather than having it interbed with the CT in SEP Major. This is an example of innovative improvement, and demonstrated Syncrude's capacity to react to local conditions. The Mildred Lake CT Plant continues to operate efficiently, meeting end-of-pipe CT specifications almost all of the time.



Figure 4-18. SWIP Jr beaching operation in 2019 (from Google Earth).

4.5 Aurora East Pit South (AEPS)

CT production at Syncrude's Aurora North operation started in 2014 with deposition to the AEPS site (Case history 19; Figure 4-1; Appendix B-5). Some difficulties with CT production (mainly related to gypsum handling and excessive component wear) continue to affect Syncrude's target CT production. These issues are being dealt with through sequential design upgrades. Hydraulic sand capping of the completed deposit is planned for 2029. Experience at EIP shows that the off-spec CT material can be entrapped or displaced, but there is some urgency to improve the CT plant reliability to manage this situation.

4.6 Other relevant studies

Suncor is a majority owner of Syncrude, and has two relevant case histories for capping of CT, both of which are detailed below. The progression of work at Pond 5 is presented in a sequence of satellite images in Appendix B-3.

In 2008, Suncor undertook a small-scale trial on Pond 5 CT deposit of a coke cap overlying non-segregating tailings. The trial was 25 m² and involved mechanical placement of coke from shore with a backhoe to a cap thickness of 1 m. The testing was limited to a backhoe on shore. The deposit was found to be trafficable by foot but not equipment. This early pilot work was a useful precursor to the commercial-scale floating coke cover operation that followed.

A large volume of off-spec CT deposit was created due to CT segregation during deposition at Pond 5. The capping goal was to place a floating coke cap on the off-spec CT (segregating sandy coagulated MFT) to create a trafficable surface (Abusaid et al. 2011). A series of coke roads over strong geosynthetics was constructed using small equipment for the first lift, followed by medium-sized mining equipment for subsequent lifts. The surrounding poulder areas were later backfilled with coke, and wick drains have been installed to speed consolidation of the deposit. Key learnings were that Suncor coke can be successfully used as a floating cover to cap low-density fluid tailings. Laying out and stitching of the geofabric on the frozen pond was straightforward. Placement of the first layer of coke required considerable trial and error but ultimately proved successful with subsequent lifts being placed with larger equipment. While expensive, it is a useful contingency technology for capping oil sands soft tailings. The coke cap was successfully tested with a loaded 100-tonne truck, although scrapers and 40-tonne haul trucks were preferred for operation (See Figure 4-19). The coke cap provided a good platform for wick drain installation using large excavators. The landform is designed to accommodate large settlements through use of a reclamation lake. Key learnings were that off-spec CT can be capped using a floating coke cover, though at great expense and – if the off-spec material is deep – results in high settlements.



Figure 4-19. Placement of floating coke cap on Suncor Pond 5 off-spec CT.

4.7 Summary

The database and experience of 19 CT-capping case histories, combined with the learnings from 30 other soft tailings case histories and from international experience, provide an excellent basis for future designs and operation for capping of CT at Syncrude. The case histories provide a real-world example of scaling from the research laboratory, through development pilots and prototypes, to implementation of full-scale commercial technology. The work allows Syncrude to design, plan, and cost its CT production and capping and integrate these efforts with the overall mine and tailings plans.

5.0 ASSESSMENT OF TECHNOLOGIES

This chapter presents an analysis of the technology readiness levels for CT production and CT capping, a list of residual challenges that Syncrude is addressing, and a list of geotechnical monitoring activities.

5.1 Analysis of technology readiness levels

Syncrude and other oil sands operators follow a formal method to assess new tailings technologies (McKenna et al. 2011), moving from the conceptual description, through to bench-scale tests, field pilots, field prototype, and on to commercial implementation. Table C-1 (Appendix C) provides a description of technology readiness levels (TRL) for the oil sands based on a scale by NASA (2017). Production of CT and sand capping has followed this general approach, as demonstrated by the case histories in Chapter 4. As a guide to the following paragraphs:

- TRL 1-4 Research involves paper studies and bench-scale laboratory work and finishing in lab-pilot scales tests.
- TRL 5-6 is the Development scale, running small then large-scale field pilots.
- TRL 7-8 is the Commercial scale, involving successful full-scale prototypes and continuous ongoing commercial operations.
- TRL 9 is the mature Commercial scale, where no additional major changes are expected beyond standard continuous improvement.

CT Production

As demonstrated by the case histories, Syncrude's research and development teams worked diligently on CT Capping starting in the 1990s to develop the technologies required for CT sand capping. Only a few small-scale capping experiments were run in the laboratory, as many of the mechanisms of interest exist solely at the commercial scale.

Taking promising technology from the University of Alberta laboratories (TRL 4), Syncrude's 1995 NST Field Demonstration (TRL 6) confirmed that CT could be produced on-spec, with 0.6% beach slope angles, and quickly consolidated. The CT Prototype (TRL 7) demonstrated that CT could be deposited on-spec in what would become known as a dedicated disposal area at full commercial rates. Results from these tests were used to design the CT Plant for deposition into Syncrude EIP and SWIP (TRL 8/9). Learnings from this plant and from the deposits were used to design the Syncrude Aurora North CT Plant (TRL 8/9) and its deposits. That Syncrude is still refining its CT production indicates there is still room to bring these commercial-scale activities to a mature stage over the next decade.

CT Capping

Capping technology development followed a similar path, building on years of experience with soft ground in the oil sands region and experience in capping of soft sediments by the dredging

industry. Pilot-scale trial embankments on the NST Field Demonstration (TRL 5) were conducted and a tailings sand cap was placed by hydraulic beaching on the CT Prototype (TRL 7). Both areas continued to act as outdoor laboratories for development of capping technologies, and learnings were applied to the EIP and SWIP CT deposits (TRL 8). The Sandhill Fen Watershed area of EIP was capped with hydraulically placed tailings sand and then with mechanically placed tailings sand hummocks (TRL 8) to act as a large, instrumented watershed for reclamation research; the technology development and results from this work are described in the companion documents. The Kingfisher area of EIP (TRL 8) was more difficult to cap and reclaim due to its higher fines content; but it was capped successfully without incident and is in its monitoring phase. Capping of almost the entire 1054-ha area of the EIP is a commercial-scale success, whose learnings have been replicated at SWIP Jr. While challenging, the sand capping of CT to form a trafficable cap is now commercial and routine at Syncrude.

5.2 Residual challenges

This document argues that CT sand-capping is a routine commercial-scale activity at Syncrude. That said, the technology has several operational challenges and requires strict controls, as noted in Table 5-1. Syncrude continues to further address these challenges to optimize CT efficiencies.

Table 5-1. CT production and capping operational challenges

Challenge	Potential impact	Control
CT process control producing too much off-spec material.	Reduced fines capture and increased fines rehandle and cost.	CT processing improvements, monitoring and testing, additional capacity for dredging of fluid fine tailings.
Excessive segregation of CT during discharge and deposition where the CT composition or discharge/depositions are out of spec.	Reduced fines capture, and excessive volumes of sandy fluid fine tailings accumulating at the distal toe of the deposit.	Syncrude uses enhanced CT process controls and closely monitors its CT production, annually measures the CT deposit performance, and adjusts its practices if there is persistent segregation.
Competing demands for tailings sand used for sand capping.	Increased costs for alternative materials or borrow sources for dyke construction or capping.	Syncrude uses the latest tools and processes for long-term tailings planning to optimize tailings sand usage. Contingencies if sand volumes fall short include using existing tailings facilities as borrow sources, or capping with petroleum coke (Pond 5).
A saturated tailings sand cap can be prone to cyclic liquefaction/cyclic mobility even if originally dense (Wood 2003).	Poor trafficability for dozers and trucks.	Careful operation of dozers on this material, avoiding too many passes at a single location, allowing induced excess pore-water pressures to dissipate where the beach does become soft, and by restricting reclamation material placement to such areas to winter when the frost cap largely precludes this mechanism.

Challenge	Potential impact	Control
The CT beach slope angle is often different than that of the tailings sand cap beach (the CT angle is often a little flatter, and neither is actually a constant slope).	Reduced volume of CT that can be deposited near the dyke, and increased volume of sand needed for capping.	Syn crude uses tailings deposition modelling software to guide design and operations, avoids overfilling deposits with CT, extends discharge points down the beach to effectively flatten tailings sand cap beach angles, and retains the option for mechanical placement where sand is in short supply.
When placing the sand hummocks on the trafficability cap, there is risk of triggering slumps along the toe of the hummock.	Operational delays and the need to redesign the hummock. Toe of slump may block drainage of the intervening swales. Such slumping is typically an operational rather than safety issue.	Syn crude manages this slumping through design and site investigation prior to placement, but mostly through visual monitoring of the hummock slopes during placement. Where slumping occurs, operations are halted. Technical and operations staff work together to adjust the field work to avoid excessive slumping.
Dry beaches are prone to wind erosion (dusting) during the few hours of high winds experienced each year.	Visibility concerns, deposition of sand onto adjacent reclaimed areas, decreased air quality.	Syn crude reclaims these beaches as quickly as practical and takes measures to avoid sand deposition onto newly reclaimed areas. Where practical, it attempts to keep the beaches wet through its tailings deposition activities.
Tailings or bitumen springs/blisters where lower density tailings flow up along cracks in the cap to deposit on surface.	Degrades reclamation material. Only seen during active operations and reclamation activities.	Visual monitoring and repair where needed. Additional controls being considered.
A soft area forms near the final outlet of CT deposits.	Costly to mechanically cap, and complicates construction of the outlet structure.	Minimizing the production and deposition of off-spec CT, and careful operation of the recycle dredges to minimize the volume and area of off-spec CT remaining at the end of final deposition. Allowance for use of soft-ground techniques and coke capping for the residual area.

Despite being a commercial or even mature technology, enhancements are always possible (see challenges in Table 5-1). Syn crude continually refines its operational procedures and technology on an informal basis to reduce costs, increase reliability, and enhance the landscape performance of these CT deposits.

Syn crude staff monitor the performance of the CT plants, deposits, operational capping, and reclamation performance of its CT deposits. Results from monitoring are used to adjust the day-

to-day operations and the designs of existing and future deposits. Geotechnical monitoring activities include:

- Process control to produce CT that is on-spec at the end of pipe.
- Routine sampling and in situ geotechnical testing of active CT deposits, and monitoring of dredging activities to ensure the deposit is on-spec and suitable for capping.
- Visual monitoring of deposition of trafficability caps and hummocks.
- Settlement monitoring and pore-water pressure modelling of capped CT deposits to refine models for prediction of water-release rates and post-reclamation settlement.

6.0 CONCLUSIONS

This report has demonstrated the following:

- Syncrude has systematically brought CT production and capping through the research, development, and commercialization phases for the past 20 years and is now in the commercial and continuous-improvement phase. It has a mature understanding of the processes and the required operation for successful CT capping.
- Syncrude is routinely designing, planning, constructing, testing, and reclaiming CT at commercial scale and to date has capped over 1100 ha (11 square kilometers) of CT successfully.
- The capped deposits are trafficable for reclamation material placement and proposed land uses. By 2020, about 50% of the sand-capped CT at Syncrude had been fully reclaimed (which involves construction of closure topography layer, placement of reclamation material, and revegetation).
- Post-reclamation settlements are modest, occur within a few years, and can be managed through landform design.
- A formal research and development plan for CT capping is not required. However, close monitoring and ongoing continuous improvement are recommended and are a necessary and important element of ongoing CT capping and reclamation.

7.0 CLOSING REMARKS

We trust the above satisfies your requirements at this time. Should you have any questions or comments, please do not hesitate to contact us.

McKENNA GEOTECHNICAL INC.

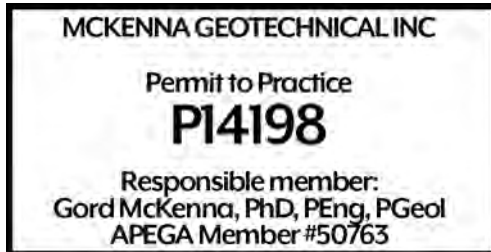
per:



Gord McKenna, PhD, PEng, PGeol
Geotechnical Engineer, Landform Designer

Reviewed by:

June Pollard, MSc, PGeol
Senior Engineering Geologist
2222179 Alberta Ltd.



Gord McKenna 2020-08-28

References

- Abusaid A, Pollock G, Fear C, McRoberts E, & Wells S. 2011. An Update to the Construction of the Suncor Oil Sands Tailings Pond 5 Cover. Tailings and Mine Waste Conference. Nov 6-9. Vancouver.
- BGC. 2010a. Oil Sands Tailings Technology Review. OSRIN Report No. TR-1. BGC Engineering Inc. Vancouver. 136 pp.
- BGC. 2010b. Review of Reclamation Options for Oil Sands Tailings Substrates. OSRIN Report No. TR-2. BGC Engineering Inc. Vancouver. 59 pp.
- Caughill DL, Morgenstern NR, & Scott JD. 1993. Geotechnics of non-segregating oil sands tailings. Canadian Geotechnical Journal. Volume 30. pp. 801–811.
- CEMA. 2014. Guidelines for Wetland Establishment on Reclaimed Oil Sands Leases (3rd Edition). Cumulative Environmental Management Association. Fort McMurray. 436 pp.
- COSIA. 2012. Technical Guide for Fluid Fine Tailings Management. Canada's Oil Sands Innovation Alliance. Calgary. August 30, 2012. 131 pp.
- CTMC. 2012. Oil Sands Tailings Technology Deployment Roadmap: Project Report – Volume 2, Component 1 Results. Consultants' report to Alberta Innovates – Energy and Environment Solutions. Consortium of Tailings Management Consultants. June 22, 2012. 112 pp.
- Jakubick AT and McKenna GT. 2001. Stabilization of soft tailings. practice and experience. Eighth International Conference on Radioactive Waste Management and Environmental Management (ICEM'01). Brugge Belgium. American Society of Mechanical Engineers.
- Matthews JG, Shaw W, MacKinnon MD, Cuddy RG. 2002. Development of composite tailings technology at Syncrude. International Journal of Surface Mining, Reclamation and Environment. 16:1 p24-39.
- McKenna G, Mooder B, Burton B, and Jamieson A. 2016. Shear strength and density of oil sands fine tailings for reclamation to a boreal forest landscape. IOSTC International Oil Sands Tailings Conference. Lake Louise. Dec 4 to 7. University of Alberta Geotechnical Group. Edmonton.
- McKenna G, O'Kane M, and Qualizza C. 2011. Tools for bringing mine reclamation research to commercial implementation. Tailings and Mine Waste 2011 Conference. Vancouver. Nov 6-9. 11 pp
- NASA. 2017. Technology readiness levels demystified. NASA Website: https://www.nasa.gov/topics/aeronautics/features/trl_508.html. Accessed 201-02-18.
- Pollock GW, McRoberts EC, Livingstone G, McKenna GT, Matthews JG, and Nelson JD. 2000. Consolidation behaviour and modelling of oil sands composite tailings in the Syncrude CT Prototype. International Conference on Tailings and Mine Waste 7:121-130.

- Silva MJ. 1999. Plant dewatering and strengthening of mine waste tailings. PhD Thesis in Geoenvironmental Engineering. Department of Civil and Environmental Engineering. University of Alberta. Edmonton. 293 pp.
- Smith W, Olauson E, Set J, Schoonmaker A, Nik R, Freeman G, and McKenna G. 2018. Evaluation of strength enhancement and dewatering technologies on a soft oil sands deposit. International Oil Sands Tailings Conference (IOSTC 2018). University of Alberta Geotechnical Centre. Edmonton.
- Terzaghi K. 1943. Theoretical Soil Mechanics, New York, Wiley.
- USACE. 2006. Engineering and Design: Ice Engineering. US Army Corps of Engineers. Third edition. EM 1110-2-1612. Sept 30, 2006. Washington. 475 pp.
- Wood RK. 2003. Response of Dense Beach Above Water Tailings to Cyclic Equipment Loading at Syncrude's Southwest Sand Storage Facility. MSc Thesis. Department of Civil and Environmental Engineering. University of Alberta. Edmonton. 223 pp.
- Wytrykush C, Vitt DH, McKenna G, and Vassov R. 2012. "Designing landscapes to support peatland development on soft tailings deposits: Syncrude Canada Ltd.'s Sandhill Fen Research Watershed initiative." Restoration and reclamation of boreal ecosystems: Attaining sustainable development. Cambridge University Press New York New York. pp. 161-178.

APPENDIX A: Case History Summaries

Case number and name	Location and timeframe	Tailings substrate description	Cap and capping details	Observations/notes/references	Illustrative site photo
01 Syncrude NST Field Demonstration U-Shaped Cell Loading Test	Syncrude Mildred Lake Operation – 1995 NST Field Demonstration, U-Shaped Cell Southwest West corner of MLSB 460,279m E 6,323,055 m N October 1999 Pilot scale Area = 4 x 100 m ² each	NST (composite tailings) 80% solids 20% fines Fully consolidated 40cm crust. Deposit approx. 2 m thick on plastic liner. NST crust vane strength 20 to 30 kPa. Non-crusted NST 5 to 10 kPa peak, 2 to 4 kPa remoulded.	Tailings sand, moist, mechanically placed, with and without geofabric and geogrid.	<ul style="list-style-type: none"> Highly instrumented. Bare NST supported a 2 m sand cap with a small mud wave. Nilex BX 1200 geogrid allowed a 3.5 m high pile with similar sized mud wave. Movements likely partially confined by the plastic liner 2 m below top of NST. Current Syncrude name for NST is Composite Tailings (CT). 	
02 Syncrude NST Underdrained NST Reclamation Cell Test	Syncrude Mildred Lake Operation – 1995 NST Field Demonstration, underdrained reclamation cell 460,304 m E 6,323,172 m N 1999 Area = 1 ha	Underdrained NST (composite tailings). Cell constructed tailings sand foundation drained the deposit within months. 90% solids 20% fines Unsaturated to full 2 m depth Vane strengths of 30 to 90 kPa.	Excavator trafficability test. Area later simply capped with a few metres of fill by operations staff to create a laydown area.	<ul style="list-style-type: none"> Hard, table-top like surface, hard to penetrate with a hand spade/shovel. Cleat marks of excavator barely visible. No reports of difficulties capping. Current Syncrude name for NST is Composite Tailings (CT). 	
03 Syncrude NST Field Demonstration U- Shaped Cell Mechanical placement for cell and fen construction	Syncrude Mildred Lake Operation – 1995 NST Field Demo, U-Shaped Cell. Trial fen construction. 460,224 m E 6,323,164 m N July 2008 Pilot scale Area = 1.5 ha	NST (composite tailings) 82% solids 20% fines Fully consolidated 40 to 60 cm crust Deposit 2 to 6 m thick. Aged 13 years.	Small 1 to 2 m high embankments constructed on NST to form cells. HDPE-lined cells constructed using various reclamation material treatments to form about two dozen pilot fen wetlands.	<ul style="list-style-type: none"> Able to support medium sized tracked excavator (CAT 322B 50T, similar to a D6 Dozer). Half of the deposit was able to support a loaded 40T truck, but became mired about 200 m down the NST beach. 20 cm cap formed a few weeks after deposition in 1995; 40 cm within a couple of years; 60 cm after a decade. Site had good surface drainage but a permanent pond in the lower half. Current Syncrude name for NST is Composite Tailings (CT). 	

Case number and name	Location and timeframe	Tailings substrate description	Cap and capping details	Observations/notes/references	Illustrative site photo
04 Syncrude CT Prototype Hydraulic Sand Cap	Syncrude Mildred Lake – outer perimeter of CT Prototype, Cell 16 North end of MLSB 459,063 m E 6,329,190 m N 1998 Prototype scale Area = 25 ha	NST (composite tailings) 77% to 82% solids 15 to 20% fines partially consolidated 10 m thick	Hydraulic tailings sand beaching using flip spoon on 24" tailings line. 0 to 6 m thick tailings sand cap covered about half of the deposit.	<ul style="list-style-type: none"> • Some displacement of fresh NST (to depth of 0 to 6 m). • MFT generation. • 2 m thick mixing zone between sand cap and underlying NST. • Dense tailings sand cap prone to local liquefaction under equipment loads, sand volcanoes, water upwelling. • Excess pore-water pressures in sand cap dissipate in about 12 hours after equipment removed. 	
05 Syncrude CT Prototype 1-Hectare Reclamation Cap	Syncrude Mildred Lake – East end CT Prototype 459,111 m E 6,329,347 m N Aug 1999 Pilot scale Area = 1 ha	Approx. 5 m sand cap over 7 m of NST Nominally 80% solids 20 to 25% fines Fully consolidated. Water table about 1 m down near top of end of beach, near surface at bottom.	Nominally 35 cm of peat mineral mix (peat and Pleistocene lacustrine clay) spread in one lift.	<ul style="list-style-type: none"> • Note: Saturated tailings sand is often untrafficable to large mining equipment and behaves as soft tailings. • Even after considerable track packing earlier in the season, equipment caused local liquefaction, sand volcanoes, expression of pore-water. • Marginal trafficability for small equipment (small dozers and small haul trucks). • Pore-water caused waterlogging and salinization of lower half of reclamation material deposit affected the new trees and shrubs. • Within a few years, salts had flushed, and moisture contents decreased, and vegetation performed well (no intervention). • Blowing sand was an issue at this exposed site. 	

Case number and name	Location and timeframe	Tailings substrate description	Cap and capping details	Observations/notes/references	Illustrative site photo
06 Syncrude CT Prototype Sand Cap Ditching Prototype	Syncrude Mildred Lake – Periphery of CT Prototype at north end Cell 16 MLSB. Summer 2000 458,933 m E 6,329,539 m N 2001 Area = 2 ha	4 to 6 m of beached tailings sand over 4 to 6 m of NST (CT) 80% solids 20% fines Fully consolidated Water table near surface (0 to 1 m).	Ditching through tailings sand cap. Six ditches at random spacing as part of dewatering trial for sand cap.	<ul style="list-style-type: none"> Unable to dig more than about 1 to 2 m through tailings sand cap – tailings sand cap (or CT below) liquefied and raised bottom of ditch within an hour or two of excavation. There may have also been NST upwelling from below sand cap leading to ditch infilling. Cracking of side slopes. Tried various strategies over the month, including progressive lowering of water table (pumping ditches), but to no avail. Project abandoned. 	
07 Syncrude CT Prototype Mechanical Sand Cap	Syncrude Mildred Lake – West end of CT Prototype at north end of MLSB. 458,321 m E 6,328,861 m N May 2000 Area = Approx. 2 ha	NST (composite tailings) 80 to 82% solids 15 to 20% fines Fully consolidated 20cm crust.	Rapid mechanical placement of a 2 to 3 m lift of unsaturated tailings sand fill. No geogrid.	<ul style="list-style-type: none"> Minor toe bulging, local dewatering, some cracking at crest. Borrow material was subexcavated from nearby channel. Keyano College heavy equipment operator students conducted work without incident. 	
08 Syncrude CT Prototype Winter Placement of Reclamation Material on Sand Cap	Syncrude Mildred Lake – Periphery of CT Prototype at north end Cell 16 MLSB. 458,812 m E 6,329,475 m N 2001 Area = 10 ha	4 m of tailings sand cap over 6 to 8 m of NST 82% solids 20% fines Fully consolidated. About 1 to 1.5 m of frost in sand cap.	Reclamation material placement.	<ul style="list-style-type: none"> Previously tested for summer trafficability with loaded 100T haul truck. No deformations under 100T haul trucks and Cat D6 dozers and none expected due to presence of frost cap. Area since capped with Kc (new W4 Dump). 	
09 Syncrude CT Prototype W4 Dump construction	Syncrude Mildred Lake – CT Prototype (north end of MLSB) 458,653 m E 6,328 987 m N Prototype scale Q1 2014 Area = 50 ha	NST (CT) 78 to 84% solids 14 to 20% fines $s_u = 5$ to 15 kPa NST approx. 10 m deep, some already sand capped.	3 m thick mechanically placed KC overburden cap. 1.5 m thick NST frost cap.	<ul style="list-style-type: none"> Some bow wave deformations. Some fracture and flow of tailings up through cap during placement of first lift. 	

Case number and name	Location and timeframe	Tailings substrate description	Cap and capping details	Observations/notes/references	Illustrative site photo
10 Syncrude East In-Pit 318 Closure Divide	Syncrude Mildred Lake – East InPit (EIP) 318 Closure Divide 464,697 m E 6,321,609 m N 2007 to 2009 Commercial scale Area = 32.5 ha	Layered NST (CT) and tailings sand 77 to 81% solids 20 to 40 fines $s_u = 4$ to 10 kPa Some areas of sandy MFT (“MFT snothole”)	Hydraulic sand capping. Open end cell construction to construct trafficable base. Push up cell construction side and back dykes and pour as closed cell.	<ul style="list-style-type: none"> Constructed with system of contained beaching then cell construction. No issues capping NST area, but soft NST/MFT area at centre triggered 370m long translational failure with sand boils and NST liquefaction. NST strength $c/p' = 0.05$ from back analysis, ($c_u = 6$ kPa), matches CPT data. 0.4 m of settlement. Piezometers indicate nearly fully consolidated (rapid consolidation). 	
11 Syncrude East In-Pit Southeast Pond Junior (SEP Jr)	Syncrude Mildred Lake – East In-Pit (SEP Jr) 464,014 m E 6,320,367 m N 2008 Prototype scale Area = 17 ha (hummocks), Area = 110 ha total (including beaches)	NST (composite tailings) Nominally 80% solids, 20% fines.	Hydraulically placed tailings sand cap (open ended cell construction). Integrated with hydraulically placed sand beach. 8 m high hummocks.	<ul style="list-style-type: none"> Closely investigated and monitored. Successful placement of hummocks on consolidated composite tailings using beaching and open cell construction. Open end cell construction to construct trafficable base. Push up cell construction side and back dykes and pour as closed cell. One rotational slope failure in beach, resolved by waiting and then stepping in with next lift for a flatter slope. NST strength 10 kPa by back analysis. $c/p' = 0.05$ from back analysis. Final result from CPT – 8 m of sand over 4 m of NST. Water table near base of hummock. 0.2 m settlement recorded. 	
12 Syncrude East In-Pit Sandhill Fen Watershed Hydraulic Beach Construction	Syncrude Mildred Lake – East InPit 464,039 m E 6,321,897 m N 2008 Commercial scale Area = 70 ha	NST (composite tailings) interlayered with tailings sand. NST nominally 80% solids, 20% fines.	Hydraulically beached tailings sand (open pipe discharge).	<ul style="list-style-type: none"> 10 to 13 m thick sand cap. Fair cap trafficability to small equipment where saturated. Poor trafficability where standing water. Good cap trafficability in winter (>1 m frost). Heaving / flow of sand up through trench cut through frost during ploughing in underdrains. 	

Case number and name	Location and timeframe	Tailings substrate description	Cap and capping details	Observations/notes/references	Illustrative site photo
13 Syncrude East In-Pit Sandhill Fen Watershed Mechanical hummock construction	Syncrude Mildred Lake – East In-pit (EIP) 464,020 m E 6,321,935 m N 2009-2011 Prototype scale Area = 50 ha	10 to 13 m thick saturated tailings sand beach cap over interbedded tailings sand and NST.	7 hummocks, each 4 to 8m high. Mechanically placed tailings sand – 40T trucks and small dozers, placed in 1 m lifts.	<ul style="list-style-type: none"> Placed mostly in winter. Only minor deformations of wet sand seen in one face of one hummock. 	 <p style="text-align: right; font-size: small;">Sandhill Fen – looking west</p>
14 Syncrude East In-Pit Sandhill Fen Watershed Winter reclamation material placement	Syncrude Mildred Lake – East In-Pit (EIP) 464020m E 6321935 m N 2012 Prototype scale Area = 50 ha	10 to 13 m thick saturated tailings sand beach cap over interbedded tailings sand and NST. Hummock and swale topography (closure topography layer) constructed in 2012.	Clay layer 0.5 m Peat mineral mix 0.5 m Mechanically placed with 40T trucks, a D6 dozer and excavators	<ul style="list-style-type: none"> Trafficability for winter reclamation placement was adequate for smaller equipment where there was greater than 1m of frost. The capping methodologies used could support the placement of reclamation material. No major deformations. The performance likely benefited from the very thick sand cap. 	

Case number and name	Location and timeframe	Tailings substrate description	Cap and capping details	Observations/notes/references	Illustrative site photo
15 Syncrude East In-Pit Kingfisher Watershed Hydraulic sand capping	Syncrude Mildred Lake – northeast corner of East In-Pit 464,685 m E 6,322,251 m N 2012 Prototype scale Area = 50 ha	Layered NST (CT) and tailings sand 77 to 81% solids 20 to 40% fines $s_u = 4$ to 10 kPa Some areas of sandy MFT (“MFT Snothole”)	Hydraulically placed tailings sand cap beached from perimeter. 24in dia line.	<ul style="list-style-type: none"> 0 to 10 m thick cap. Sandy MFT likely partially displaced. 	
16 Syncrude East In-Pit Kingfisher Watershed Mechanical sand capping	Syncrude Mildred Lake – NE corner of East Inpit 465,232 m E 6,321,717 m N 2014 to 2016 Prototype scale Area = 54 ha	Layered NST (CT) and tailings sand 65 to 80% solids 6 to 26% fines $s_u = 10$ to 20 kPa Some areas previously hydraulically sand capped.	3 m mechanically placed tailings sand cap.	<ul style="list-style-type: none"> Minor bow wave formation. Dewatering of underlying tailings apparent. 	
17 Syncrude East In-Pit Syncrude EIP Hydraulic sand capping	Syncrude Mildred Lake– East In-pit (EIP) 465,100 E; 6,320,980 N 2008 to present Commercial scale Area = 500 ha	NST (composite tailings) interlayered with tailings sand. NST nominally 80% solids, 20% fines.	Hydraulically placed sand cap and hummocks. Cap placed in a clockwise horseshoe from east to the south and then west.	<ul style="list-style-type: none"> Deposit characterisation important for capping. CT segregation/displacement occurred from earlier construction of other structures and watersheds on EIP. Commercial capping successful. 	

Case number and name	Location and timeframe	Tailings substrate description	Cap and capping details	Observations/notes/references	Illustrative site photo
18 Syncrude Southwest In-pit (SWIP) North Filter Berm CT (SWIP Jr)	Syncrude Mildred Lake – north end of South West In-Pit 459,712 m E 6,319,324 m N 2012 to 2014 Commercial scale Area = 32 ha	NST (CT) 75 to 80% solids 14 to 26% fines $s_u = 7$ to 10 kPa	13 m thick hydraulic beach tailings and cap.	<ul style="list-style-type: none"> Successful. 	
19 Syncrude Aurora North Syncrude Aurora East Pit South (AEPS) CT	Syncrude Aurora North 2014 to present	Ongoing active deposition	No capped deposit		

Notes

All locations UTM Zone 12 V and based on representative location on Google Earth.
Some observations / noted copied directly from COSIA capping workshop database and PowerPoint presentations.

Definitions

Fines defined as percentage dry mass passing 44-micron wet sieve. Solids content defined as mass of mineral solids to total mass of slurry. (In the table above, some solids contents may be the result of oven drying and may include bitumen in with the mass of mineral solids).
Soft tailings can include petroleum coke and saturated tailings sand beaches.
 S_u is peak undrained strength measured by either the vane or estimated from cone penetration tests (CPT) using an N_{KT} factor.
NST is non-segregating tailings aka CT, composite tailings, consolidated tailings – a mixture of sand and fines with a coagulant (typically gypsum).
TT is thickened tailings.
MFT is mature fine tailings, often also known as FFT fluid fine tailings.

Appendix B-5 Aurora East Pit South (AEPS)



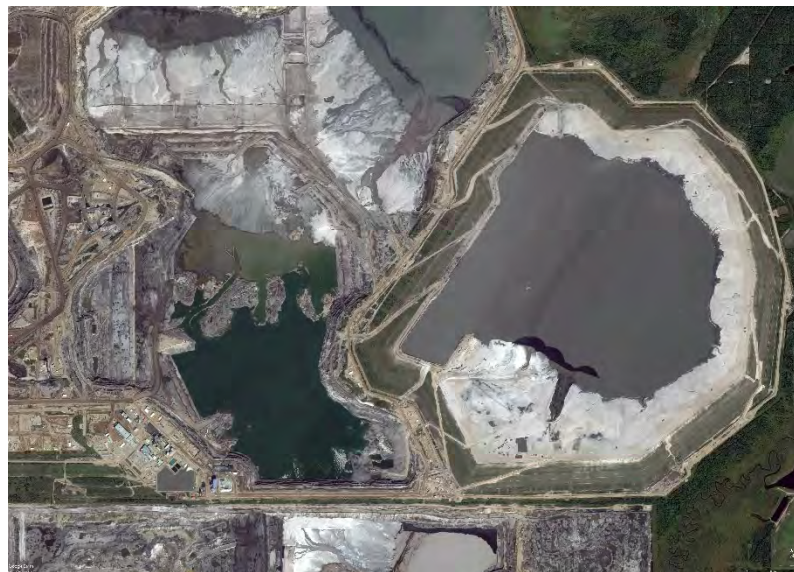
2004-06-21



2007-05-09



2010-09-22



2015-09-09



2017-07-05



2020-04-22

APPENDIX B: Satellite imagery of Case Histories

- Appendix B-1 NST Field Demonstration
- Appendix B-2 CT Prototype
- Appendix B-3 East In-Pit (EIP)
- Appendix B-4 Southwest In-Pit (SWIP)
- Appendix B-5 Aurora East Pit South (AEPS)

These are selected images from Google Earth downloaded in March 2020. They show the progression of various sites through time.

The image dates are copied from Google Earth, but the reader is cautioned they may not be exact. Note that Suncor Pond 5 is shown in the Appendix B-3 images.

Appendix B-1 NST Field Demonstration



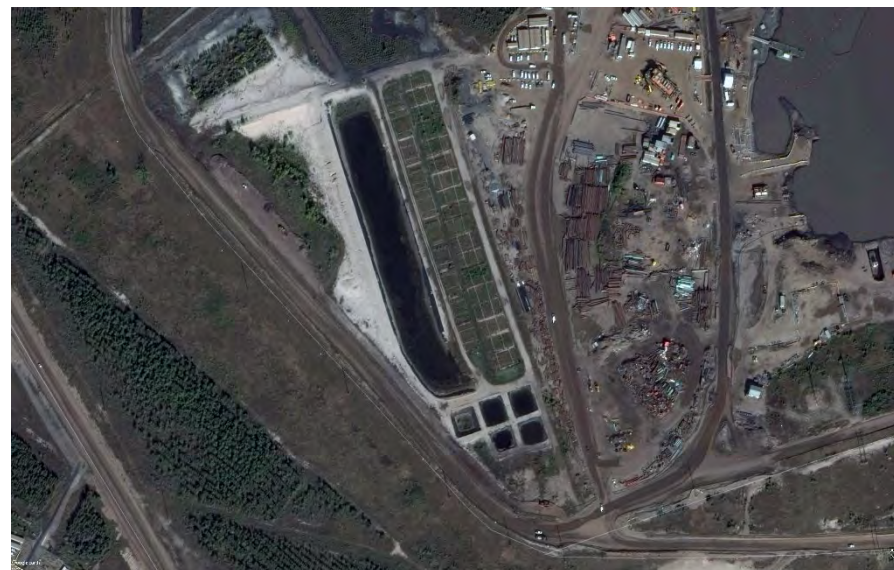
2006-06-24



2008-09-30



2010-07-21



2014-09-13



2016-09-11



2020-04-15

Appendix B-2 CT Prototype



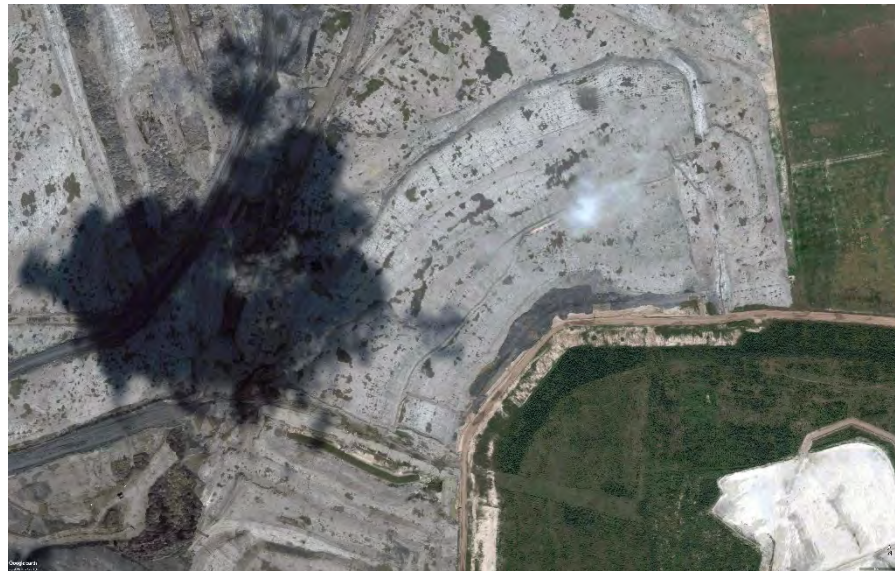
2006-06-24



2011-08-04



2014-08-11



2015-07-26



2016-09-11



2019-06-19

Appendix B-3 East In-Pit (EIP)



2006-06-24



2008-09-30



2011-08-04



2012-09-21



2018-10-24



2019-10-10

Appendix B-4 Southwest In-Pit (SWIP)



2006-06-24



2009-08-31



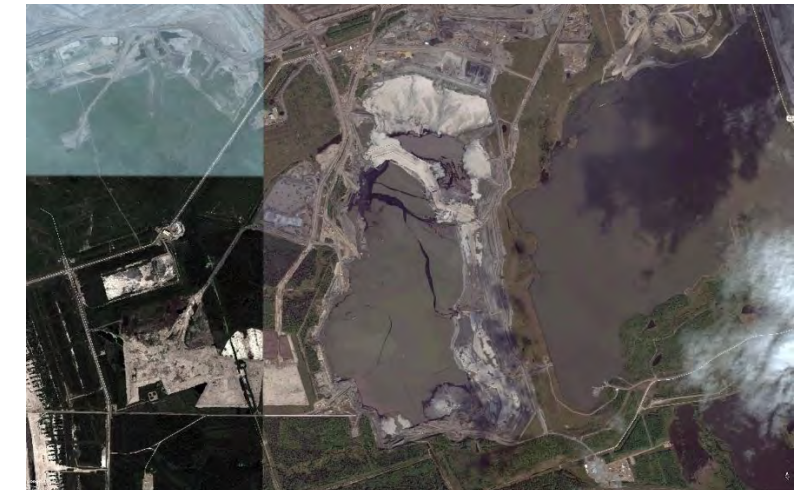
2012-09-05



2012-09-21



2013-08-19



2014-09-13



2016-09-11



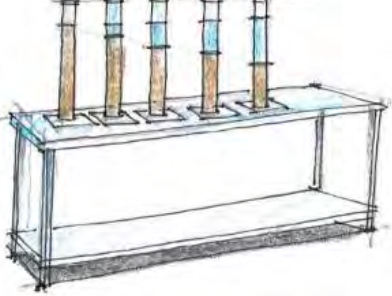
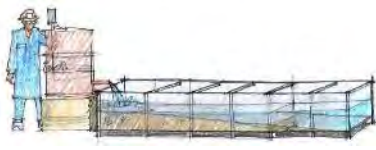
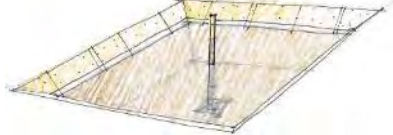
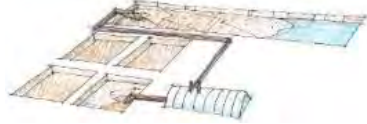
2018-08-07

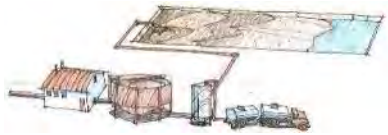


2020-04-15

APPENDIX C: Technology Readiness Levels

Table C-1. Description of technology readiness levels

Phase	NASA (2017) description	Oil sands adaptation, typical dimensions	Illustration
TRL 1	Basic principles observed and reported. Basic scientific research that can be turned into an application or a concept under a research and development program is considered. Examples might include paper studies of a technology's basic properties.	Concept or idea described in a paragraph.	
TRL 2	Technology concept or application formulated. An idea is proposed for the practical application of current research, but there are no experimental proofs or studies to support the idea. Examples are limited to analytic studies.	Paper study , literature review, technology assessment, perhaps index tests.	
TRL 3	Concept or application proven through analysis and experimentation. Active research and development begin, including analytical laboratory-based studies to validate the initial idea, providing an initial "proof of concept."	Lab bench scale. Progress report. $V = 0.01 \text{ m}^3$ (10L) $A = 1 \text{ m}^2$ $D = 0.2 \text{ m}$	
TRL 4	Basic prototype validated in laboratory environment. Examples of the proposed technology are built and put together for testing to offer an initial vote of confidence for continued development.	Lab pilot scale (batch or continuous). R&D report. $V = 5 \text{ m}^3$ $A = 10 \text{ m}^2$ $D = 3 \text{ m}$	
TRL 5	Basic prototype validated in relevant environment. More realistic versions of the proposed technology are tested in real-world or near real-world conditions, which includes initial integration at some level with other operational systems.	Small field pilot with highly controlled conditions over hours or a few days. R&D report. $V = 500 \text{ m}^3$ $A = 0.1 \text{ ha}$ $D = 3 \text{ m}$	
TRL 6	System or subsystem model or prototype demonstrated in a relevant environment. A near-final version of the technology in which additional design changes are likely is tested in real-life conditions.	Large field pilot with several variables run over weeks or months. R&D report. $V = 10^4 \text{ m}^3$ $A = 2 \text{ ha}$	

Phase	NASA (2017) description	Oil sands adaptation, typical dimensions	Illustration
TRL 7	System prototype demonstrated in a relevant environment. The final prototype of the technology that is as close to the operational version as possible at this stage is tested in real-world conditions	<p>D = 5 m</p> <p>Field prototype run at commercial scale and rates under favourable conditions.</p> <p>V = 10⁶ m³</p> <p>A = 50 ha</p> <p>D = 10 m</p>	
		TRL 8	Actual system completed and qualified for flight through test and demonstration. The technology is thoroughly tested, and no further major development of the technology is required. Its operation as intended is demonstrated without significant design problems.
TRL 9	Actual system proven through successful operation. The final operational version of the technology is thoroughly demonstrated through normal operations, with only minor problems needing to be fixed.		

Appendix B

Hummock Technology Learnings to Support Water Management on Reclaimed Landforms

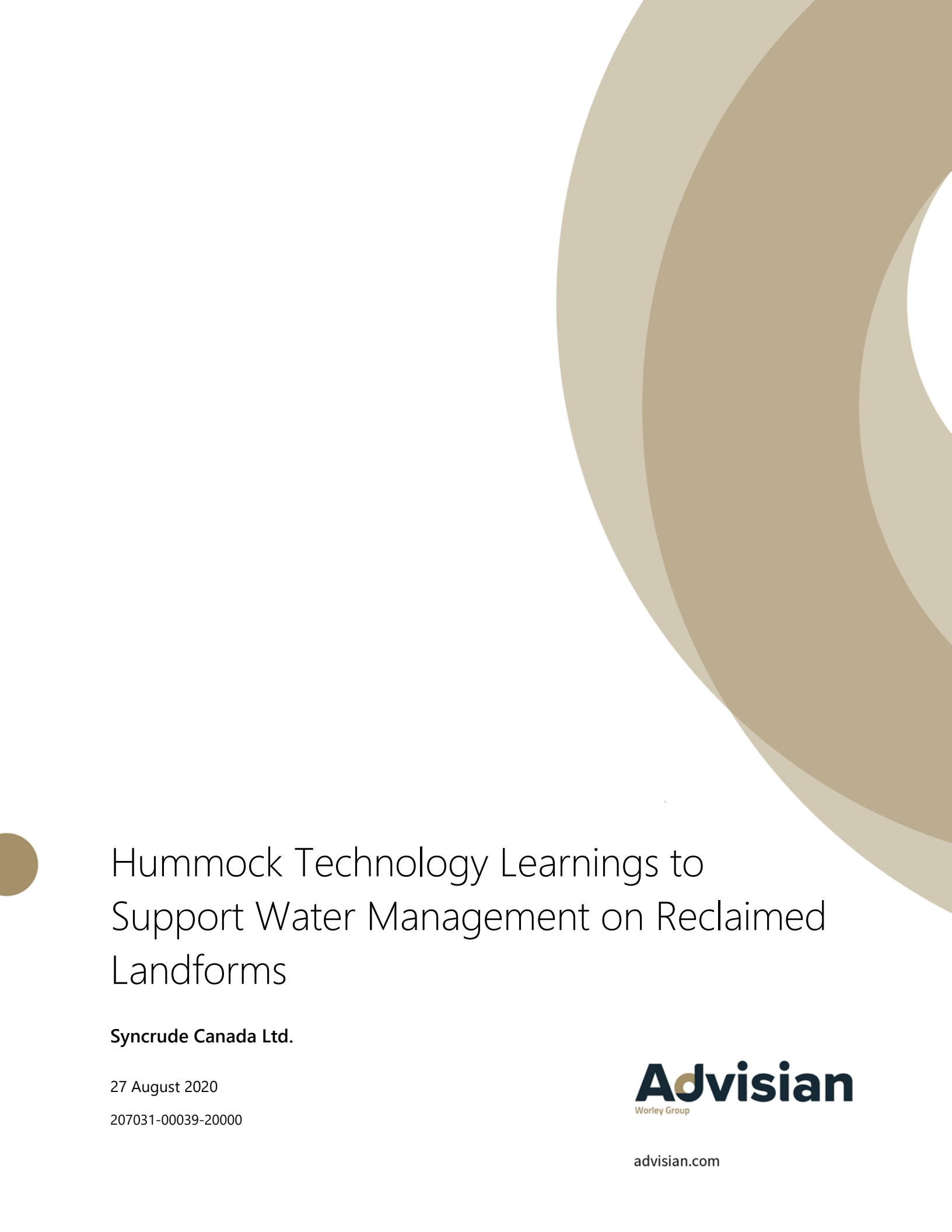
Worley Canada Services Ltd., operating as Advisian were retained by Syncrude to carry out the studies presented in this publication and the material in this report reflects the judgment of Advisian and BGC Engineering Inc. in light of the information available at the time of document preparation. Permission for non-commercial use, publication or presentation of excerpts or figures is granted, provided appropriate attribution is cited. Commercial reproduction, in whole or in part, is not permitted without prior written consent from Syncrude. An original copy is on file with Syncrude and is the primary reference with precedence over any other reproduced copies of the document.

Reliance upon third party use of these materials is at the sole risk of the end user. Syncrude accepts no responsibility for damages, if any, suffered by any third party as a result of decisions made or actions based on this document. The use of these materials by a third party is done without any affiliation with or endorsement by Syncrude.

Additional information on the report may be obtained by contacting Syncrude.

The report may be cited as:

Advisian. 2020. Hummock Technology Learnings to Support Water Management on Reclaimed Landforms. Prepared by Advisian and BGC Engineering Inc. for Syncrude Canada Ltd. 2020.



Hummock Technology Learnings to Support Water Management on Reclaimed Landforms

Syn crude Canada Ltd.

27 August 2020

207031-00039-20000

Advisian
Worley Group

[advisian.com](https://www.advisian.com)

Disclaimer

This report has been prepared on behalf of and for the exclusive use of Syncrude Canada Ltd., and is subject to and issued in accordance with the agreement between Syncrude Canada Ltd. and Advisian. Advisian accepts no liability or responsibility whatsoever for it in respect of any use of or reliance upon this report by any third party. Copying this report without the permission of Syncrude Canada Ltd. and Advisian is not permitted.

COVID-19

Worley Canada Services Ltd., operating as Advisian (Advisian), is committed to providing the services to you in a timely and professional manner. Advisian is also committed to ensuring the health and safety of all of its people and its clients.

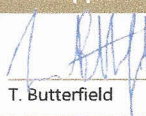
The COVID-19 pandemic has caused us to modify our business behaviour. This means that Advisian may only provide you with services in a manner which it deems safe. Advisian employees may provide some or all of the Services from their home and travel to business meetings or site may be affected. Advisian will take steps to mitigate any delays associated with the provision of services to you but accepts no liability or responsibility for the delayed or non-performance of any services caused by the modification of its behaviour to ensure the containment of COVID-19 or the health and safety of its people.

Company details

Worley Canada Services Ltd., operating as Advisian
Suite 300, 8615 - 51 Avenue NW
Edmonton, AB T6E 6A8
CANADA

Tel: 780-496-9055

PROJECT: 207031-00039-20000-WW-REP-0001: Hummock Technology Learnings to Support Water Management on Reclaimed Landforms

Rev	Description	Author	Review	Advisian approval	Revision date
0	Issued as Final	 M. Lukenbach / P. Twerdy	 T. Butterfield / C. Mendoza	 T. Butterfield	27-Aug-20

U:\EDM\GBS\217031-00039\20000-Technology_Synthesis\10.0_Technical_Specialist\10.4_Groundwater\Reporting\217031-00039-20000-WW-REP-0001-Rev0.docx

Table of Contents

Executive Summary	ix
1 Introduction	1
1.1 Scope of Work.....	1
1.2 Report Outline.....	2
2 Hummock Technology Background.....	3
2.1 Hummock Technology and Functions.....	3
2.2 Hummocks as Units of Reclaimed Landscapes.....	4
2.3 Hummock Technology within the Water Balance Framework.....	8
3 Hydrogeology of Hummocks.....	13
3.1 Water Table Configuration Analysis.....	14
3.2 Recharge-Discharge Dynamics.....	18
4 Case Studies of Constructed Hummock Performance: Observations and Controlling Factors.....	19
4.1 Syncrude Sandhill Fen Watershed.....	19
4.1.1 Performance Based on Water Table Configuration Metric.....	21
4.1.2 Overview and Key Learnings.....	24
4.2 Syncrude Southwest Sand Storage Facility.....	26
4.2.1 Performance Based on Water Table Configuration Metric.....	27
4.2.2 Overview and Key Learnings.....	29
4.3 Hydrogeology of Open-Pit Reclamation.....	30
4.3.1 Pit-Scale Simulations.....	30
4.3.2 Hummock-Scale Simulations.....	32
4.4 Summary.....	34
5 Modelling Water Table Positions in Hummocks	36
5.1 Analytical Modelling Framework	36
5.1.1 Steady-State Analytical Models	36

5.1.2	Transient Analytical Models	39
5.1.3	Model Calibrations.....	39
5.2	Parameter Ranges.....	39
5.2.1	Hummock Dimensions (<i>L, d, and s</i>)	41
5.2.2	Hydrogeologic Properties (<i>K, H, C</i>).....	41
5.2.3	Recharge (<i>R</i>).....	42
5.2.4	Correlations Between Factors	42
5.3	Sensitivity Analyses	43
5.3.1	Variation in <i>R/K</i>	43
5.3.2	Covariation in <i>R/K</i> and <i>L/d</i>	46
5.3.3	Covariation in <i>R/K</i> and <i>L/H</i>	48
5.4	Application of Analytical Models to Specific Design Scenarios.....	50
5.4.1	Long-Term Water Table Configurations.....	51
5.4.2	Short-Term Transient Influences on Water Table Configurations	54
5.5	Summary.....	57
6	Discussion of Uncertainties	58
6.1	Logistical Considerations	58
6.2	Factors Affecting Spatial Variability	58
6.3	Factors Affecting Temporal Variability and Trajectories.....	59
6.4	Modelling Limitations.....	59
7	Conclusions	61
8	References	63
9	Closure	67

Tables Within Text

Table 2-1	Defined Scales for Reconstructed Landscapes (Pollard and McKenna 2018).....	5
Table 3-1	Sensitivity of the water table-topography relationship for various hydraulic conductivity values for a constructed tailings sand hummock on a capped and reclaimed CT deposit.	15
Table 4-1	Summary of Case Study Findings.....	34
Table 5-1	Parameter ranges considered in modelling framework based on literature values and Syncrude's reclamation experience.....	40

Figures Within Text

Figure 2-1	Representative spatial scales (see also Table 2-1) in a hypothetical capped CT deposit (i.e. landform-scale/deposit-scale) containing hummocks (landform elements) with an outlet at the right side of the diagram. Scaled arrows indicate how a far greater volume of water migrates through the trafficability cap and closure topography layer than underlying CT/coarse tailings. Note that upwelling of tailings water due to consolidation is not considered in this work.	6
Figure 2-2	Fundamental hydrologic landscape unit (FHLU) of a scale-less upland-lowland unit. Adapted from Winter (2001). Note that the shape illustrated is arbitrary. Shading represents the lowland within the FHLU. Note that water can flow in either direction (i.e. from upland to lowland or lowland to upland), depending on the spatial scale of the FHLU and hydrologic properties.....	7
Figure 2-3	Nesting relationships between fundamental hydrological landscape units within a hypothetical landform (e.g. capped CT deposit). Adapted from Winter (2001). Shading represents the lowlands within the FHLUs.	7
Figure 2-4	Schematic defining water balance at any scale of the reclaimed landscape (from Devito et al. [2012]). ΔS indicates the amount of water storage, P is precipitation, ET is evapotranspiration, R is runoff (inflows or outflows), and GW is groundwater (inflows or outflows).....	8
Figure 2-5	Long-term, typical intra-annual trends in precipitation (P) and potential evapotranspiration (PET) for the Athabasca Oil Sands Region. Note that a seasonal water deficit is the norm and that units are millimetres (mm). From Devito et al. (2012).	9
Figure 2-6	a) Inter-annual trend in precipitation (P) and the associated magnitude of the water surplus (green) or deficit (red) for a given year indicated by the solid line and coloured shading. In top panel, the 30-year climate normals for precipitation and potential evapotranspiration (PET) are shown as dashed lines. In the lower panel, the same data is expressed as a cumulative departure from long-term mean (CDYrM) precipitation, showing how multi-year water deficits and surpluses occur over time as a function of inter-annual precipitation patterns. From Devito et al. (2012).	10

Figure 3-1 Conceptualized groundwater flow associated with constructed hummocks and potential water table configurations under contrasting hydrogeologic regimes for a) topography-controlled and b) recharge-controlled. Recharge-controlled describes how the shape of the water table is determined solely by the magnitude of recharge, all other factors being equal. Shading represents the lowlands. Adapted from Haitjema and Mitchell-Bruker (2005)..... 14

Figure 3-2 The different zones of hummock (crest, midslope, toe) identified for a) convex versus b) concave slopes with three potential water table configurations shown as dashed lines. Precipitation (P), evapotranspiration (ET), and recharge (R) are denoted with arrows, along with their conceptualized spatial variation on each slope. Note that evapotranspiration (ET) is conceptualized to increase in regions where upflux (U) occurs (i.e. negative net recharge)..... 17

Figure 4-1 Hummocks, hummock analogues, and other features in SFW and the associated soil, groundwater, and meteorological monitoring networks. Coloured shading denotes topography. Note that hummock numbering is not sequential due to deviations from planned construction due to limited material availability. Adapted from Lukenbach et al. (2019)..... 21

Figure 4-2 Depth to water table during moderate, lower, and higher water table periods in SFW; time series plots show transducer traces for two locations (indicated by stars on map), with shaded windows on the graphs indicating the time period for which the snapshot of the spatial water table configuration is shown. Percentages in colour bars indicate the percent area occupied by a given water table depth interval..... 23

Figure 4-3 Southwest Sand Storage Facility (SWSS) cross-sections showing instrumented transects through the dyke at Cell 32 (cross-section A) and Cell 46 (cross-section B) of the dyke. The water table is indicated by the solid black lines and inverted triangle, with the dashed line indicating where the water table's configuration is interpreted. Groundwater flow paths are indicated with black arrows. (Adapted from Price, 2005.) 28

Figure 4-4 a) Pit-scale simulations adapted from Schwartz and Crowe (1987), with water table configurations shown for different combinations of recharge, spoil hydraulic conductivity, and the hydraulic conductivity of the surrounding geologic medium. b) Same factors were varied as in a) but with a different lowland configuration..... 31

Figure 4-5 Hummock-scale simulations adapted from Schwartz and Crowe (1987), with water table configurations (black lines with inverted triangles) shown for different recharge (R) and hydraulic conductivity (K) combinations (solid versus dashed black lines) and as a function of different hummock lengths (L). Maximum hummock height (d) was constant for the shown set of simulations and the aquifer thickness (H) underlying the hummock was assumed to be 10 m, while the estimated maximum rise in the water table at the centre of each hummock (Δh) is related to d as a ratio ($\Delta h/d$). $\Delta h/d$ calculated assuming an aquifer shape factor (C) of 8. For further details on dimensionless ratios and variables, see Section 3.1 and Table 3-1..... 33

Figure 5-1 Schematic showing how the different analytical models and variables represent the hydrogeological processes and characteristics of hummocks. 37

Figure 5-2 a) Sensitivity of parameters ($\Delta h/d$, i) describing the water table (WT) configuration to the recharge over hydraulic conductivity ratio (i.e. R/K, log10 scale x-axis). The black (red) curve corresponds with the black (red), left (right) y-axis. $\Delta h/d= 1$ (i.e. WT at crest of hummock) and $\Delta h/d= 0.5$ (i.e. WT 2 m below crest of hummock) are denoted with a black and blue dashed line, respectively. Gray shading indicates unlikely R/K ratio ranges. Black points on panel a correspond to WT configurations (coloured lines) associated with specific R/K values (exact values shown in coloured text) in panel b. In b), the gray line denotes the hummock topographic profile, with two differing hummock toe slopes (s): concave slope (left, lower s), convex slope (right, higher s). WT gradient (i) $> s$ for concave slope, and $i < s$ for convex slope. Propensity of local-scale groundwater (GW) flow systems to develop indicated by vertical, black arrow. See Section 3 and 5.1 for further details and conceptual overview.45

Figure 5-3 Sensitivity analysis of $\Delta h/d$ and i to hummock dimensions (represented by different panels) and R/K values. Hummock length (L) increases from left to right across the diagram, while hummock height (d) decreases from top to bottom. The light gray, diagonal arrow indicates the decreasing trend of L/d across the panels. Select black and red points, corresponding to $\Delta h/d$ and i , respectively, indicate the position actual constructed hummocks (two from SFW, and the 318 Closure Divide in EIP). Layout as in Figure 5-2a (see above).....47

Figure 5-4 Sensitivity analysis of $\Delta h/d$ and i to aquifer thickness (H ; represented by different panels) and R/K values. Aquifer thickness (H) decreases from left to right across the diagram, while hummock height (d) decreases from top to bottom. The light gray, diagonal arrow indicates the decreasing trend of L/H across the panels. Layout as in Figure 5-2a (see above).....49

Figure 5-5 Map of EIP with modelled transects. Transects A, B, and C correspond to the Kingfisher Terrace Hummock, the Finger Hummock, and the East-side Terrace Hummock, respectively. The locations of Sandhill Fen Watershed (SFW), Kingfisher Watershed (KFW), and the 318 Closure Divide are also denoted..... 51

Figure 5-6 Modelled water tables for three constructed hummocks in EIP. Black lines represent the topographic profiles of the hummock transects shown in Figure 5-5. The coloured lines indicate potential water table configurations as a function of R/K values..... 53

Figure 5-7 Transient scenario tests for the Kingfisher Terrace Hummock. Initial steady-state water tables are indicated by solid lines, while the dashed lines represent different maximum water tables for different S_y values following the addition of 100 mm of precipitation over 2 days. 55

Figure 5-8 Transient scenario tests for the Kingfisher Terrace Hummock for a 100 mm precipitation event over 2 days, showing the rise (Day 0 to Day 2) and fall (50 days, 100 days, 300 days, and 500 days) of the water table (coloured lines). Initial steady-state water table is indicated at Day 0..... 56

Appendix

Appendix 1 Detailed Description of Analytical Models, Assumptions, and Calibration

Executive Summary

Hummock technology describes how Syncrude incorporates topographical relief on capped and reclaimed Composite Tailings (CT) deposits. Over the last two decades, Syncrude has developed and advanced hummock technology through numerous applied research programs. These efforts demonstrate that Syncrude has a thorough understanding of how to design and construct hummocks to meet targeted hydrologic functions on capped and reclaimed CT deposits, which is directly applicable to future reclamation at Aurora North Mine. Where uncertainties remain, Syncrude is committed to the continuous improvement of hummock technology through its adaptive management framework.

Hummocks are essential components of the closure topography layer on CT deposits because they provide important hydrological, operational, and ecological functions. This synthesis details the current state of hummock technology with respect to hydrologic functions. Parallel reports that are part of this regulatory submission provide further information on the physical and ecological functions. Hummock hydrologic functions can be considered those related to water quantity, water quality, or landform drainage, all of which are indicative of hummock performance. These hydrologic functions reflect how hummocks are central in addressing water management challenges associated with the sub-humid climate of the region and the saline-sodic composition of water in capped CT deposits.

Syncrude's progress in developing hummock technology is demonstrated by several case studies. Extensive research and monitoring of constructed hummocks at Sandhill Fen Watershed, the first reclaimed watershed on a capped CT deposit, exemplifies Syncrude's ability to construct hummocks that meet targeted performance. Syncrude also has incorporated learnings from hummock analogues elsewhere on its leases as well as from relevant literature sources to advance its understanding of hummock technology. Syncrude's operational experience and learnings can be readily applied when constructing hummocks on capped and reclaimed CT deposits on Syncrude leases in the future.

Syncrude's learnings are the basis for a comprehensive conceptual understanding of how hummocks influence water quantity and quality on capped and reclaimed CT deposits. The conceptual understanding is further supported by developed analytical models that investigate the relative influence of primary factors controlling hummock hydrologic functions. Analytical models also allow Syncrude to determine suitable hummock designs for a wide range of reclamation scenarios. Overall, completed and ongoing studies demonstrate that a separate CT capping and research plan for Aurora North Mine is not needed. Instead, Syncrude can apply learnings from past and ongoing work from the Mildred Lake Lease when capping and reclaiming CT deposits in the future.

1 Introduction

Syncrude Canada Ltd. (Syncrude) retained Worley Canada Services Ltd. (Worley), operating as Advisian, to complete the synthesis: "*Hummock technology learnings to water management on reclaimed landforms.*" (the "Synthesis"). Advisian has partnered with BGC Engineering Inc. (BGC), McMaster University, and the University of Alberta to complete this scope of work. The Synthesis is part of Syncrude's Oil Sands Conservation Act (OSCA) Approval No.10781L, Clause 22 for Aurora North Mine, specifically addressing a request by the Alberta Energy Regulator (AER) to provide a Composite Tailings (CT) Capping Research Plan. Given that CT deposits at Aurora North Mine will not be capped until 2030, Syncrude is leveraging existing knowledge from over 20 years of development, research, and operational experience on reclaimed CT deposits at Mildred Lake Mine to inform the design and construction of future reclaimed CT deposits at Aurora North Mine and Mildred Lake Mine. Syncrude contends that the capping of CT deposits is already a commercial technology and part of routine planning and operations. In support of this assertion, Syncrude has compiled three reports:

- Hummock technology learnings to support water management on reclaimed landforms (this report);
- Operational learnings for capping CT (soft) deposits for trafficability; and
- Sandhill Fen Watershed learnings of a reclaimed wetland on a CT deposit.

Hummock technology describes Syncrude's approach to incorporating topographical relief in reconstructed, capped, and reclaimed CT deposits. The objectives of the Synthesis were to:

- Compile and document the current understanding of hummock technology and hummock performance on capped and reclaimed CT deposits with respect to hydrologic functions; and
- Synthesize and advance the understanding of how hummocks constructed on CT deposits can be designed to achieve performance objectives related to water quantity and quality.

Numerous applied research programs have contributed to Syncrude's understanding of hummock technology. These efforts are detailed in the Synthesis and demonstrate that Syncrude has a thorough understanding of how to design and construct hummocks to meet targeted hydrologic functions on capped and reclaimed CT deposits, which is directly applicable to future reclaimed CT deposits at Aurora North Mine.

1.1 Scope of Work

The following is an overview of the scope of work adapted from the Advisian proposal dated November 22nd, 2019:

- Document performance of constructed hummocks to date primarily at Syncrude sites with respect to performance metrics (e.g. minimum 2 metre [m] water table separation);
- Summarize and document any additional analyses and modelling completed as part of this project;
- Provide a prioritized list of key controls and the influence of hummocks on water quantity and quality, based on existing literature, water balance analyses, and modelling completed herein;
- Provide presentations/updates to Syncrude during execution of the project; and
- Complete a regulatory report documenting the methods and results of this project.

In documenting hummock performance and assessing the underlying mechanisms controlling how hummocks influence water quality and quantity on capped and reclaimed CT deposits, the following methods were employed:

- Literature reviews (peer-reviewed literature and internal reports);
- Supplementary analyses (e.g. newly synthesized data; visualizations); and
- Modelling (both conceptual and analytical).

The findings and interpretations detailed in this scope of this work are limited to constructed hummocks on capped and reclaimed CT deposits. Constructed hummocks are likely to be components of other reclaimed landforms; however, they are not considered herein.

1.2 Report Outline

Section 1 (this section) and Section 2 provide background information and context about how hummock technology addresses the challenges associated with managing water on capped and reclaimed CT deposits. Section 3 details Synocrude's conceptual understanding (model) of how hummock technology supports hydrologic functions on capped and reclaimed CT deposits. Section 4 details case studies contributing to the understanding of hummock technology. Section 5 details the analytical models that have been developed based on learnings to date, which clarify the relative influence of key controls on water quantity/quality and can be applied to future hummock designs. Uncertainties and Synocrude's ongoing efforts to address them are outlined in Section 6, while Section 7 provides conclusions.

2 Hummock Technology Background

2.1 Hummock Technology and Functions

Hummock technology describes Syncrude's approach for incorporating topographical relief in reconstructed, capped, and reclaimed CT deposits to achieve similar landscape services as found in natural boreal forest environments. Hummocks were historically constructed as elevated areas serving as trafficable surfaces when capping soft CT deposits during reclamation, and to support the growth of upland vegetation, most commonly in the form of forestlands. However, it is now understood that, in addition to creating trafficable surfaces and supporting upland vegetation growth, hummocks also provide important hydrological, hydrogeological, and pedological services related to managing water and solute migration on reclaimed CT deposits. Proper management of water and solute migration is critical when reconstructing landscapes comprised of CT because these deposits – and the materials generally used to cap them – have elevated salinity concentrations associated with bitumen processing and the marine nature of the oil sands deposit (Johnson and Miyanishi 2008). Landscape reconstruction practices, including the application of hummock technology, should minimize the influence of solutes on reclaimed environments as well as provide adequate water supply and quality to down-gradient hydrological systems, which have long-term implications for mitigating hazards and achieving reclamation targets.

Currently, hummock functions have been categorized as those relating to: 1) water (i.e. quantity, control, and quality), 2) ecology (i.e. soils, vegetation, rooting zones, wildlife), or 3) operations (i.e. trafficability, material storage, and maintenance), with water and operations functions taking precedence for Syncrude, particularly during landscape reconstruction. This synthesis focuses on hydrologic functions, with parallel reports detailing the physical and ecological functions (McKenna Geotechnical 2020; Syncrude 2020).

Three primary hydrological functions of constructed hummocks have been identified:

1. Water quantity function – to manage water quantity by partitioning precipitation between evapotranspiration, soil storage, net recharge to the water table, and overland flow, or to manage consolidation water.
2. Water quality function – to influence water quality by flushing process-affected waters from tailings sand, to manage the water table location to allow upland, riparian, and wetland ecosystems to flourish, or to control salinity and toxicity to receiving systems.
3. Landform drainage – to direct water into a landform-scale drainage system to support downstream wetlands and end pit lakes, manage settlement, or to avoid ponding of waters near dyke crests, which would preclude dyke de-licensing.

Managing hydrologic functions following oil sands mining is challenging because the sub-humid climate of the region limits water availability (Devito et al., 2012), which also increases the complexity of capping and reclaiming saline-sodic CT deposits. Recent work has demonstrated that meeting hydrological functions in capped and reclaimed CT deposits generally requires the construction of hummocks to manage groundwater/surface water quantity and quality; however, there may be select locations on Syncrude's leases where hummocks may not be needed. Hummock technology is effective for meeting hydrological functions because it can control the movement of water through the landscape (i.e. landform drainage function in Life of Mine Closure Plan; Syncrude 2016). Furthermore, constructed hummocks are effective at controlling the position of the water table and increasing separation between the land surface

and the saturated zone, thereby facilitating solute flushing and minimizing the impact of tailings water on the rooting zone (i.e. water table control function in the Life of Mine Closure Plan; Syncrude 2016). Such hummock function is critical to ensuring that water quantity and quality are adequate for receiving water bodies (e.g. pit lakes) or eventual off-lease releases, thereby minimizing potential risks at closure.

Recent research, studies, and assessments have advanced the understanding of how to best construct hummocks to meet performance objectives and hydrologic functions. This body of work was initiated in the mid to late 2000s, and key questions included:

- What is the appropriate size (i.e. length, width, height), form (e.g. slope, shape) and configuration of constructed hummocks to meet hydrologic functions?
- How should hummock size and form account for a hummock's position within a larger CT deposit and under the influence of the sub-humid climate of the oil sands region?
- Given that hummock composition (e.g. lithology, permeability) is relatively fixed for a particular capped CT deposit, how can hummock size, shape, and configuration be optimized to meet hydrologic functions?
- What is the influence of the coversoil on hummock performance?

Much progress has been made in addressing these questions and this report documents the scientific basis that comprises the current understanding of these aspects of hummock technology.

During the last two decades, Syncrude has constructed and studied hummocks on its Mildred Lake Mine lease. To date, the most common material used to construct hummocks is tailings sand, although other construction materials may be employed. Tailings sand hummocks are generally constructed by hydraulic placement or cell construction, although mechanical construction is sometimes employed. Hummock geometry may also be augmented by mechanical or hydraulic excavation. Three classes of hummock, distinguished by their geometry, are generally constructed on Syncrude's leases: 1) finger hummocks, 2) mounded hummocks, and 3) terraced hummocks, with intermediate forms occurring between these end-members. The performance of each hummock type is considered and analysed in Section 5 of this report.

2.2 Hummocks as Units of Reclaimed Landscapes

Hummocks are practical for landscape reconstruction and reclamation because of their scalability; hummocks may be down-sized or up-sized depending on their role in the post-mining landscape or other considerations. Reconstructed hummocks are landform elements typically built at the macro-topographic scale (see Table 2-1 for scale definitions, and Figure 2-1). In practical terms, constructed hummocks are typically on the order of hundreds of metres long and wide, and two to ten metres high. Larger hummocks often originate as features that are part of mining operations (e.g. berms, dykes, dams) prior to becoming components of the reclamation environment. Comparatively, smaller hummocks may be constructed solely for meeting reclamation targets.

Less commonly, hummocks may be constructed as meso-topographic and micro-topographic features in the reclaimed landscape. Such hummocks may be constructed to increase habitat diversity and meet other ecological functions. However, it is generally not practical to target the design towards meso- and microtopographic features (i.e. length scales < 10 m) during reclamation. Rather, there is a generalized

acceptance that heterogeneity at the meso- or microtopographic scale, in the form of small-scale roughness or undulations, should either be targeted or not during reclamation, depending on the desired role of a specific landform or landform element.

Table 2-1 Defined Scales for Reconstructed Landscapes (Pollard and McKenna 2018)

Term	Representative Length Unit (km)	Description	Example	
Region	100 km	Area with similar hydrological, geological, and ecological characteristics	Athabasca Oil Sands Region	
Landscape	10 km	Oil sands lease-scale	Mildred Lake Mine	
Landform	1 km	A single feature of the reclaimed landscape; deposit-scale	Tailings drainage basin, CT deposit, overburden dump	
Landform Elements	Macro-topography	0.10 km	Localized feature within a landform; may be constructed with mining equipment	Hummocks, dykes, berms, lowlands, swales
	Meso-topography	0.01 km	Noticeable patterns superimposed on macro-topographic features	Hummock-lowland interfaces
	Micro-topography	0.001 km	Small-scale undulations; affects your footing	Pits, roughness of hummocks

Hummocks are part of the capping process on CT deposits. To facilitate the construction of landform elements (such as hummocks) during reclamation, it is necessary to create a trafficable surface (i.e. trafficability cap) by capping CT with tailings sand or another pervious material (McKenna Geotechnical 2020). The trafficability cap is generally 2 to 5 m thick (McKenna Geotechnical 2020). Hummocks are a component of the closure topography layer constructed on top of the trafficability cap (McKenna Geotechnical, 2020). Because CT generally has a sands-to-fine ratio between 5:1 and 3:1, the permeability of CT and/or the combination of CT with coarser tailings is generally understood to be lower than the overlying trafficability cap and closure topography layer (Thompson et al. 2011). As a result, the current understanding is that the trafficability cap and landform elements that are part of the closure topography layer (e.g. hummocks) predominantly influence water and solute movement on reclaimed CT deposits (Figure 2-1, Twerdy 2019).

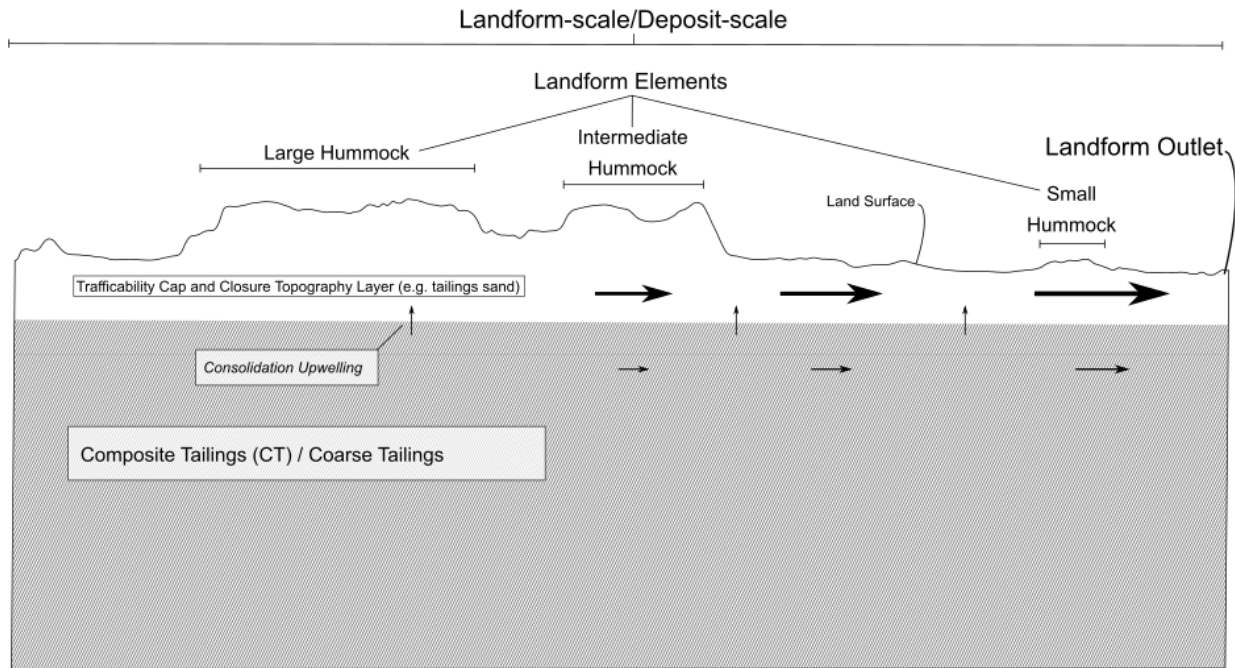


Figure 2-1 Representative spatial scales (see also Table 2-1) in a hypothetical capped CT deposit (i.e. landform-scale/deposit-scale) containing hummocks (landform elements) with an outlet at the right side of the diagram. Scaled arrows indicate how a far greater volume of water migrates through the trafficability cap and closure topography layer than underlying CT/coarse tailings. Note that upwelling of tailings water due to consolidation is not considered in this work.

Hummocks are constructed at a range of scales and their corresponding hydrological function/role varies as a function of their size and location relative to the other characteristics of the reconstructed landform. Hummocks are part of the mosaic of constructed features that comprise the closure topography layer on reclaimed CT deposits; therefore, their performance and function are inherently linked to the hydrology and hydrogeology of the overall landform that they are constructed upon (i.e. deposit-scale). Hummocks constructed on CT deposits are units nested within larger tailings drainage basins (Figure 2-1). As such, the deposit-scale characteristics, including permeability, slope, and prescribed outlet locations/elevations, relative to the size of a constructed hummock affect and constrain the possible functions of constructed hummocks.

A useful framework for conceptualizing how hummocks and landform elements influence water flow, landform drainage, water tables, and associated solute migration in reclaimed landscapes is that proposed by Winter (2001). In this framework, the fundamental hydrologic landscape unit (FHLU) is a scale-less upland transitioning to a lowland (see Figure 2-2), with the potential for upland-lowland transition areas to be nested within one another (Figure 2-3). At the scale of an entire oil sands mine lease, uplands could be elevated overburden dumps or out-of-pit tailings deposits, which transition into low-lying areas adjacent to in-pit lakes. Nested within these larger-scale FHLU deposits are hummocks, which comprise a FHLU with their adjacent lowland. Lowlands adjacent to hummocks are often referred to as swales, which act as shallow, trough-like channels designed to convey surface water during wet periods, as well as potentially

provide locations for groundwater discharge and wetland development. Hummocks and swales are complementary landform elements, comprising a FHLU, and their hydrological functions must be considered together. Conceptualizing constructed hummocks and the overall capped CT deposit as nested scales of flow and water movement is essential to describing their hydrologic behaviour and achieving targeted water functions. The integrated hydrological behaviour of many constructed hummocks influences the water quantity and quality associated with the overall landform and that arriving at down-gradient ecosystems and water bodies.

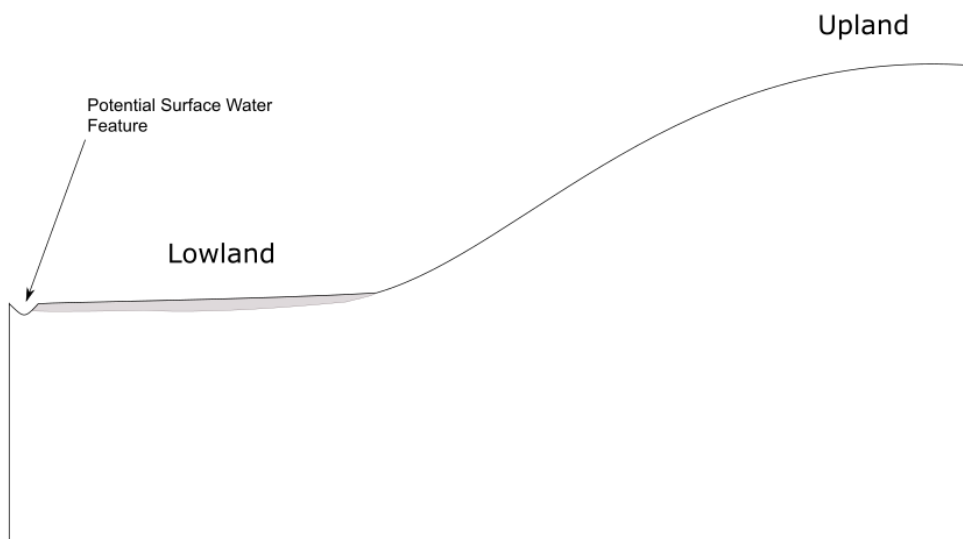


Figure 2-2 Fundamental hydrologic landscape unit (FHLU) of a scale-less upland-lowland unit. Adapted from Winter (2001). Note that the shape illustrated is arbitrary. Shading represents the lowland within the FHLU. Note that water can flow in either direction (i.e. from upland to lowland or lowland to upland), depending on the spatial scale of the FHLU and hydrologic properties.

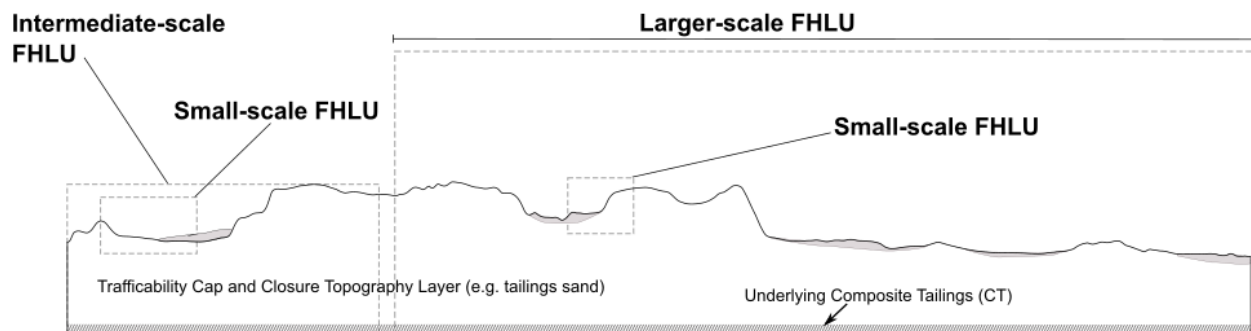


Figure 2-3 Nesting relationships between fundamental hydrological landscape units within a hypothetical landform (e.g. capped CT deposit). Adapted from Winter (2001). Shading represents the lowlands within the FHLUs.

2.3 Hummock Technology within the Water Balance Framework

The water balance describes the distribution of water across a given landscape, both spatially and temporally. It can be used as a quantifiable measure of the water source/sink function of different scales of FHLUs within the reclaimed landscape. The water balance defines fluxes into and out of a unit of the reclaimed landscape as well as the amount of water stored (i.e. storage) in that unit. Storage, whether in the form of groundwater, water stored in coversoils/substrates, or surface water in depressions, is defined as the residual remaining after accounting for inflows and outflows. The water balance equation for any scale of the reclaimed landscape can be defined using the form of Devito et al. (2012) as (see Figure 2-4):

$$\Delta S = P - ET + (R_{in} - R_{out}) + (GW_{in} - GW_{out})$$

2-1

where ΔS indicates the amount of water storage, P is precipitation, ET is evapotranspiration, R is runoff (inflows or outflows), and GW is groundwater (inflows or outflows).

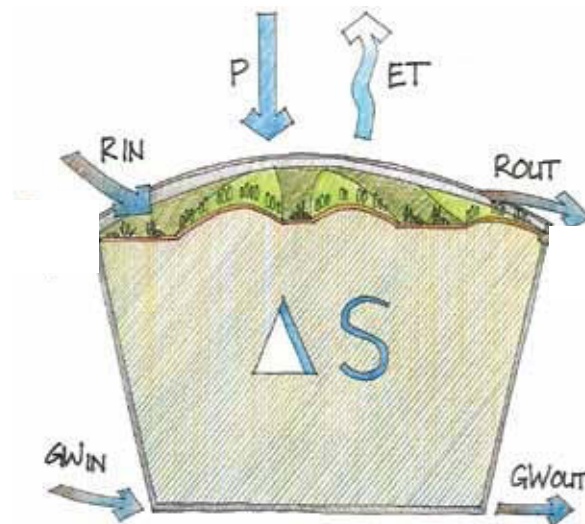


Figure 2-4 Schematic defining water balance at any scale of the reclaimed landscape (from Devito et al. [2012]). ΔS indicates the amount of water storage, P is precipitation, ET is evapotranspiration, R is runoff (inflows or outflows), and GW is groundwater (inflows or outflows).

The water balance equation demonstrates that a first-order control on all hydrological, hydrogeological, and ecological interactions occurring in reclaimed oil sands mining landscapes is the climate of the Athabasca Oil Sands Region (AOSR). The region's climate is sub-humid (i.e. long-term and average annual potential evapotranspiration is greater than precipitation) and water deficits are common (Figure 2-5; see Devito et al., 2012 for detailed overview). Most precipitation in a given year occurs during the growing season (Figure 2-5; i.e. synchronicity between precipitation and vegetative water demand), which facilitates root water uptake and ET at the expense of outflows via groundwater flow and runoff (Devito et al. 2012). Decadal-scale wet and dry climatic cycles are also characteristic of the AOSR climate and impart additional controls on water availability and flow (Figure 2-6), including lagged hydrological and ecological responses throughout the groundwater-soil-plant continuum (Devito et al. 2012).

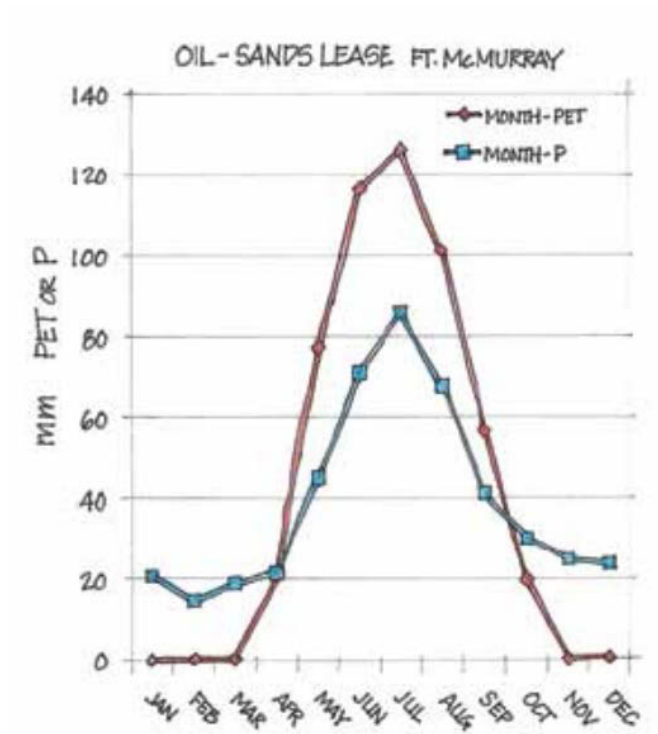


Figure 2-5 Long-term, typical intra-annual trends in precipitation (P) and potential evapotranspiration (PET) for the Athabasca Oil Sands Region. Note that a seasonal water deficit is the norm and that units are millimetres (mm). From Devito et al. (2012).

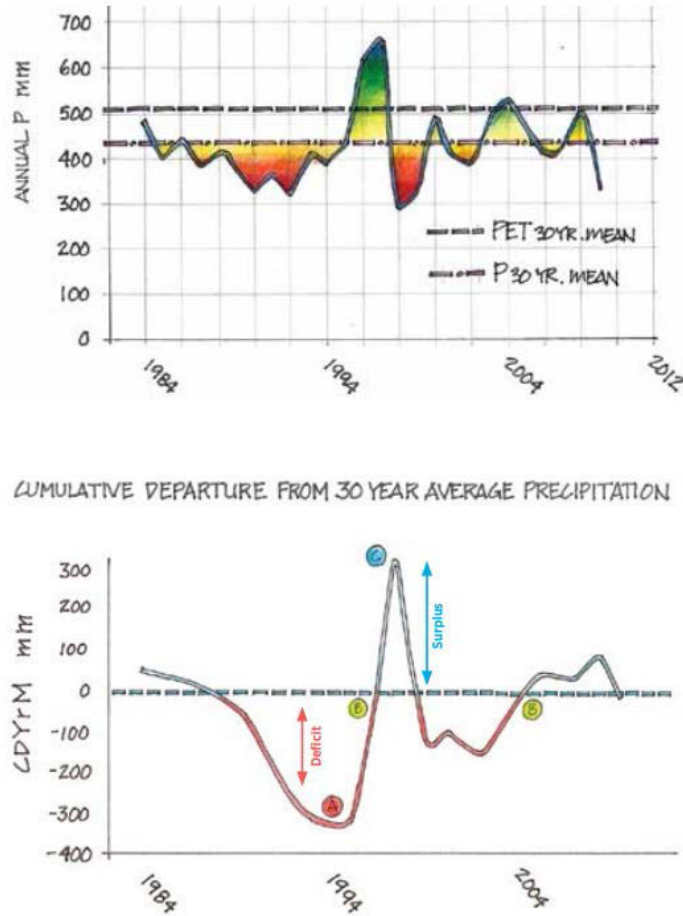


Figure 2-6 a) Inter-annual trend in precipitation (P) and the associated magnitude of the water surplus (green) or deficit (red) for a given year indicated by the solid line and coloured shading. In top panel, the 30-year climate normals for precipitation and potential evapotranspiration (PET) are shown as dashed lines. In the lower panel, the same data is expressed as a cumulative departure from long-term mean (CDYrM) precipitation, showing how multi-year water deficits and surpluses occur over time as a function of inter-annual precipitation patterns. From Devito et al. (2012).

Inflows to and outflows from units of the reclaimed landscape in the AOSR are represented by R and GW in the water balance equation and are components that describe fluxes associated with landform drainage. Given the water deficit imparted by the sub-humid climate, the high storage capacity of materials used to reconstruct landscapes, and the relatively permeable nature of materials used to cap CT deposits, landform drainage through the trafficability cap and closure topography layer (e.g. hummocks) generally occurs as groundwater flow (Twerdy 2019). Surface water runoff and overland flow in these landforms are typically limited, generally constrained to wet climatic periods (WorleyParsons Canada Services Ltd.

[WorleyParsons] 2013) and may occur immediately following the placement of reclamation materials (Ketcheson and Price 2016), and/or may be local-scale occurrences due to infrequent transient hydrologic events, including concrete frost or high intensity rainfall (Biagi and Care 2020). Overall, the current

understanding is that overland flow represents a small component of the overall water balance on capped CT deposits (Biagi and Carey 2020).

To adequately cap and reclaim CT deposits in sub-humid environments that store near-surface process-affected water, it may be necessary to minimize ET in the water balance to enhance the fresh-water component (i.e. meteoric water inputs not taken up by plants). At the deposit-scale, water not taken up by plants becomes recharge and reflects the amount of water available to down-gradient receiving water bodies, as well as the potential to freshen near-surface process-affected water. Moreover, the deposit-scale water balance is the summation of the water balances of individual landform elements, such as hummocks. This relationship is important because the deposit-scale water balance and the water balance of landform elements (e.g. hummock-scale) interact to alter water and solute movement patterns.

The water balance has applications for quantifying fluxes and flow rates at the deposit-scale. However, it only provides a high-level indication of flow patterns and flow paths within the capped CT deposit and is not necessarily indicative of how landform elements, such as hummocks, influence hydrological function. In addition to the water balance, geomorphological (e.g. geometry, slope, shape), hydrogeological (e.g. hydraulic conductivity), pedological (e.g. coversoils), and ecological (e.g. vegetation type) factors of the overall landform (i.e. capped CT deposit) and landform elements (e.g. hummocks) influence the migration pathways of water and solutes.

Given that water movement on capped and reclaimed CT deposits predominantly occurs via groundwater flow, the water table configuration reflects the summation of water balance components as well as the influence of geomorphological, hydrogeological, pedological, and ecological factors of landform elements and the overall reclaimed landscape. For this reason, the water table configuration is indicative of a hummock's water quantity, water quality, and landform drainage functions because:

1. it is an expression of how hummocks function as sources/sinks of water and, more specifically, how hummocks partition precipitation between root water uptake, soil storage, and recharge (i.e. water quantity function);
2. its position relative to the ground surface is indicative of the proximity of process affected water to the rooting zone of forestland vegetation and the capacity of a hummock to flush process affected waters from tailings sand (i.e. water quality); and
3. it is indicative of the hydrologic connectivity and flow paths that define the movement of water between recharge areas and outlets on a landform (i.e. landform drainage).

Therefore, the water table configuration is a useful and readily measurable quantity that Syncrude has used as a metric to indicate hummock performance when capping and reclaiming CT deposits (Syncrude 2016).

Since some factors controlling the hydrological behaviour and performance of reclaimed CT deposits are uncontrollable (e.g. climatic factors) or difficult to modify (e.g. availability and/or prior placement of reconstruction materials), reclamation managers should focus on managing the remaining factors that can be manipulated through design to meet performance objectives. One of the primary ways and scales at which it is possible to manage water and solute movement when capping CT deposits is the use of landform elements, including hummocks, as modifiers of flow and solute movement. More specifically, the geomorphology (hummock geometry and shape), pedology (thickness of coversoils and coversoil type),

and ecology (selective of vegetation/ecosites) of hummocks can be designed to optimize water balance components as well as the configuration of the water table. Consequently, hummocks can be constructed at specified scales and strategically placed to achieve desirable hydrological functions within a reconstructed landscape.

3 Hydrogeology of Hummocks

The water table is often assumed to be a subdued replica of topography in humid climates (Haitjema and Mitchell-Bruker 2005). However, the influence of topography at smaller spatial scales (i.e. the scale at which many hummocks are constructed) can diverge from this paradigm in regions with sub-humid climates (i.e. moisture deficit; see Section 2.3) that have low-relief (Haitjema and Mitchell-Bruker 2005; Hokanson et al. 2020). CT deposits and their capping methods result in low-relief closure topography that, when coupled with the sub-humid climate of the AOSR, can reduce the influence of closure topography on water table configurations. Whether the water table configuration in capped and reclaimed CT deposits mimics the topography will depend on the hydrogeologic properties and topographic relief characterizing a reclaimed CT landform (Haitjema and Mitchell-Bruker 2005).

The hydrogeology of capped CT deposits can be considered a generalized unconfined aquifer-aquitard system (Figure 2-1), where the closure topography layer, comprised of hummocks and lowlands/swales, combined with the trafficability cap constitute an unconfined aquifer overlying a much lower hydraulic conductivity CT material or CT material with coarser tailings. In unconfined aquifers, the degree to which topography influences the water table configuration, and associated groundwater flow patterns, is primarily related to the following hydrogeologic factors (Haitjema and Mitchell-Bruker 2005):

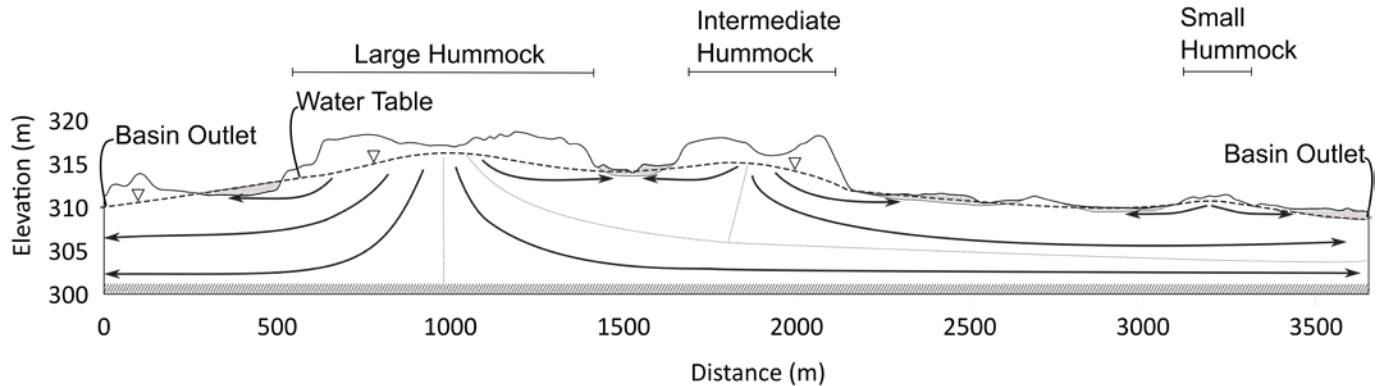
- The hydraulic conductivity of the unconfined aquifer;
- The amount and timing of recharge;
- The thickness of the unconfined aquifer;
- The distance between hydrological boundaries (i.e. surface water drainage features); and
- The topographic profile of the land surface itself.

While each of these factors plays a role in the expression of the water table, topography tends to have a greater influence on the water table configuration when recharge is high (i.e. water is in abundance), hydraulic conductivity is low, the distance between hydrological boundaries is large, and the aquifer thickness is less. Constructed hummocks can be manipulated to various degrees to control these factors, with some factors more readily altered than others. Given that the lithological composition and thickness of the trafficability cap are not readily altered on a CT deposit (i.e. logistical constraints posed by material availability), hummocks primarily influence the distance between surface water drainage features (e.g. swales, lowlands), the local elevation of the closure topography, and the spatial distribution of recharge. For example, the areal extent of a constructed hummock (i.e. length, width) can be altered to change the distance between hydrological boundaries that serve as drainage features. Similarly, coversoil prescriptions that control the amount of precipitation partitioned to recharge can be readily modified (e.g. thickness or texture).

Figure 3-1a and Figure 3-1b shows two end-member cases (i.e. water table closely related to topography vs. unrelated to topography) for how hummocks may or may not alter water table configurations and nearby associated groundwater flow patterns. Constructed hummocks with high recharge (i.e. water in abundance/excess moisture) and/or low hydraulic conductivity result in the water table closely following topography (Figure 3-1a). If the water table rises due to the presence of a hummock, defined as groundwater mounding, a nested flow system forms that alters the groundwater flow pattern. Comparatively, a hummock may not partition enough precipitation to recharge, be of sufficient areal

extent, and/or have hydraulic properties to alter the water flow pattern near it (Figure 3-1b). This may be because the characteristics of a particular capped CT deposit (i.e. deposit-scale), including its hydraulic conductivity, slope, and prescribed outlets, exert a far larger influence on flow patterns relative to the size of a constructed hummock.

a) High recharge and/or low hydraulic conductivity landform elements



b) Low recharge and/or high hydraulic conductivity landform elements

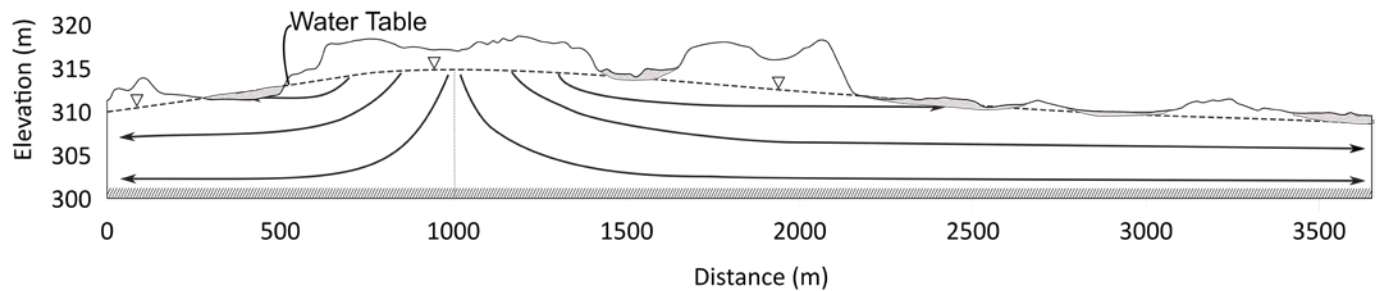


Figure 3-1 Conceptualized groundwater flow associated with constructed hummocks and potential water table configurations under contrasting hydrogeologic regimes for a) topography-controlled and b) recharge-controlled. Recharge-controlled describes how the shape of the water table is determined solely by the magnitude of recharge, all other factors being equal. Shading represents the lowlands. Adapted from Haitjema and Mitchell-Bruker (2005).

3.1 Water Table Configuration Analysis

Absolute values of recharge, hydraulic conductivity, and hummock dimensions (i.e. length, width, height) are important in many aspects of mine reclamation, but their relative values are what matter in determining the water table configuration. It follows that the relationship between the water table and the wide range of hummock morphological and hydrogeological characteristics can be related in terms of dimensionless ratios, where recharge (R), hydraulic conductivity (K), the distance between hydrological boundaries (L), aquifer thickness (H), and maximum hummock height (d) can be related to the expected rise in the water table (Δh) in the following form (Haitjema and Mitchell-Bruker 2005, note that this equation is also detailed in Section 5.1.1):

$$\frac{\Delta h}{d} = \frac{R}{K} \times \frac{L}{H} \times \frac{L}{d} \times \frac{1}{C}$$

3-7

when $\Delta h/d > 1$, water table closely follows topography

when $\Delta h/d \ll 1$, water table does not closely follow topography

The right side of the equation expresses the controlling variables as three key ratios (R/K , L/H , L/d) with an additional constant describing the shape of the aquifer (C). On the left side of the equation, when the rise in the water table (Δh) is greater than the maximum hummock height (d), the water table intersects the ground surface. Thus, a $\Delta h/d$ ratio ≥ 1 indicates that the water table closely follows topography. For $\Delta h/d$ modestly below 1, the water table may still be shallow and approximate the general topographic form of a hummock. Comparatively, for $\Delta h/d \ll 1$, the water table does not align with the topography of any but the largest landform features (e.g. perhaps streams or channels).

An illustrative example of the application of this dimensionless criterion for a tailings sand hummock is shown below in Table 3-1. The hydraulic conductivity of tailings sand can span a potentially large range from 10^{-7} m/s to 10^{-4} m/s, although the likely bulk hydraulic conductivity of landforms comprised of tailings sand generally appears to be between 10^{-6} m/s and 10^{-5} m/s (Goddard 2017; Price 2005; Thompson et al. 2011; Twerdy 2019). To evaluate the influence of this hydraulic conductivity range on the topographic control of the water table, ratios of $\Delta h/d$ are calculated and shown in Table 3-1, assuming realistic parameters of a hummock with a length of 300 m, height of 4 m, aquifer thickness of 10 m at the edges of the hummock, and relatively high recharge of 100 mm/yr.

Table 3-1 Sensitivity of the water table-topography relationship for various hydraulic conductivity values for a constructed tailings sand hummock on a capped and reclaimed CT deposit.

Hydraulic Conductivity (m/s)	R/K^a (dimensionless)	L/H^b (dimensionless)	L/d (dimensionless)	$\Delta h/d$ (dimensionless) ^a	Topography-Controlled Water Table?
10^{-4}	3.2×10^{-5}	29.9	75	0.01	No
5×10^{-5}	6.3×10^{-5}	29.9	75	0.02	No
10^{-5}	3.2×10^{-4}	29.5	75	0.09	No
5×10^{-6}	6.3×10^{-4}	29.0	75	0.17	No
10^{-6}	3.2×10^{-3}	26.0	75	0.77	Intermediate
5×10^{-7}	6.3×10^{-3}	23.5	75	1.39	Yes
10^{-7}	3.2×10^{-2}	15.6	75	4.63	Yes

^acalculated assuming a recharge value of 100 mm/yr = $3.2 \cdot 10^{-9}$ m/s, hummock height = 4 m, hummock length = 300 m, and shape factor = 8 (value of 8 or 16 typically applied aligning to planar or radial flow, respectively)

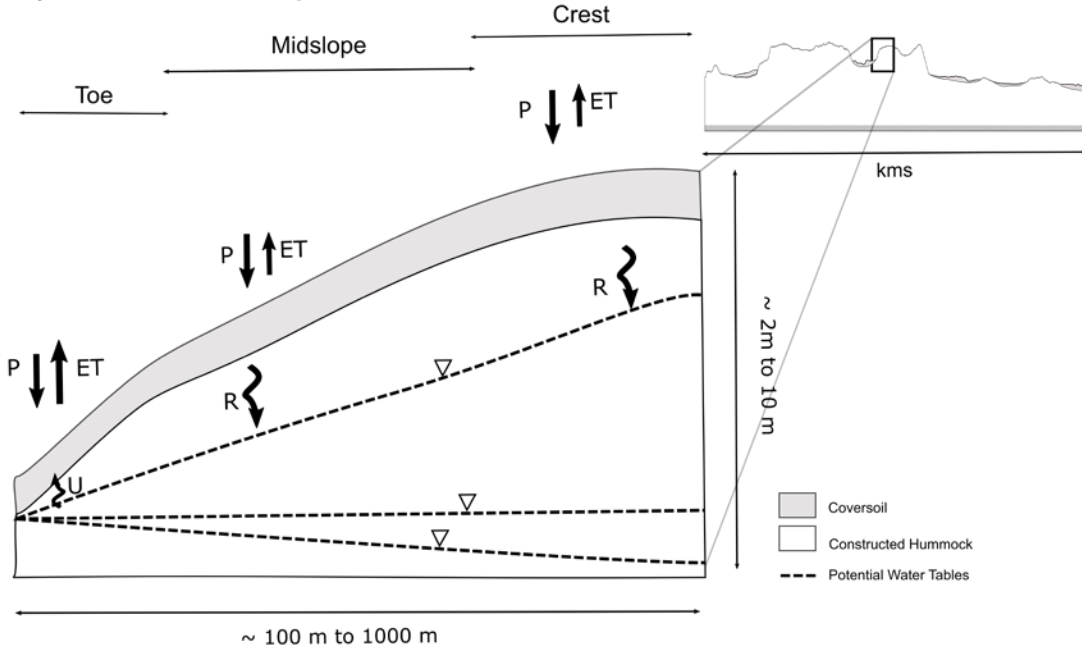
^b L/H varies because H increases as the height of the groundwater mound increases. H represents the average aquifer thickness of the groundwater mound beneath the hummock, calculated by taking the average of the water level at the centre and edge of the groundwater mound (see Section 5.1.1)

This simple example in Table 3-1 demonstrates that the observed range of hydraulic conductivities for materials used to construct the trafficability cap and closure topography layer (e.g. tailings sand) on CT deposits may or may not result in the water table being controlled by topography. Other variables could have been varied in the analysis (e.g. hummock height or size) to arrive at the same conclusion. In other words, the water table exhibits a range of possible interactions with topography, encompassing the situations where we expect the water table to closely and not closely follow topography.

While the above analysis represents a first order approximation of the water table configuration beneath a hummock, it does not explicitly recognize how the shape, form, and geometry of a hummock influences the water table depth. Additional shape factors are important for determining hummock-lowland interactions and whether a large or small proportion of a hummock provides adequate separation between the water table and rooting zone. Figure 3-2 shows the different zones on a hummock: 1) the crest, 2) the midslope, and 3) the toe, with the potential for a hummock to have a convex (panel a) or concave (panel b) slope. Hummock construction methods influence hummock shape, where hydraulic-placement typically results in more concave slopes and smaller crests compared to cell construction that leads to more convex slopes and larger crests.

Three potential water table configurations between the hummock and the adjacent lowland/swale are also shown on Figure 3-2. For the same water table configuration, concave slopes have a greater proportion of the water table near the ground surface, and the water table more easily intersects the land surface, compared to convex forms. Furthermore, these water table configurations represent different outcomes of $\Delta h/d$, where the flat water table configuration and the water table sloping from the toe to crest both have $\Delta h/d \ll 1$. Comparatively, the third water table configuration shows a groundwater mound developing beneath the hummocks, implying a $\Delta h/d$ close to or modestly below 1. Water table configurations with $\Delta h/d \ll 1$ represent cases where the hummock length/width is small, overriding deposit-scale factors govern the water table configuration, and/or hummocks function as sinks of water (i.e. negative net recharge potentially resulting in a water table depression; Hokanson et al. 2020). It should also be noted that hydrological and ecological processes can vary between different areas of the hummock (e.g. crest vs. toe) and as a function of the convex versus concave orientation of the hummock slope (Lukenbach et al. 2019). These may lead to additional complexity in water flow and water table configuration at small scales (Winter et al., 2003), which can have important geochemical and ecological consequences.

a) Convex Slope



b) Concave Slope

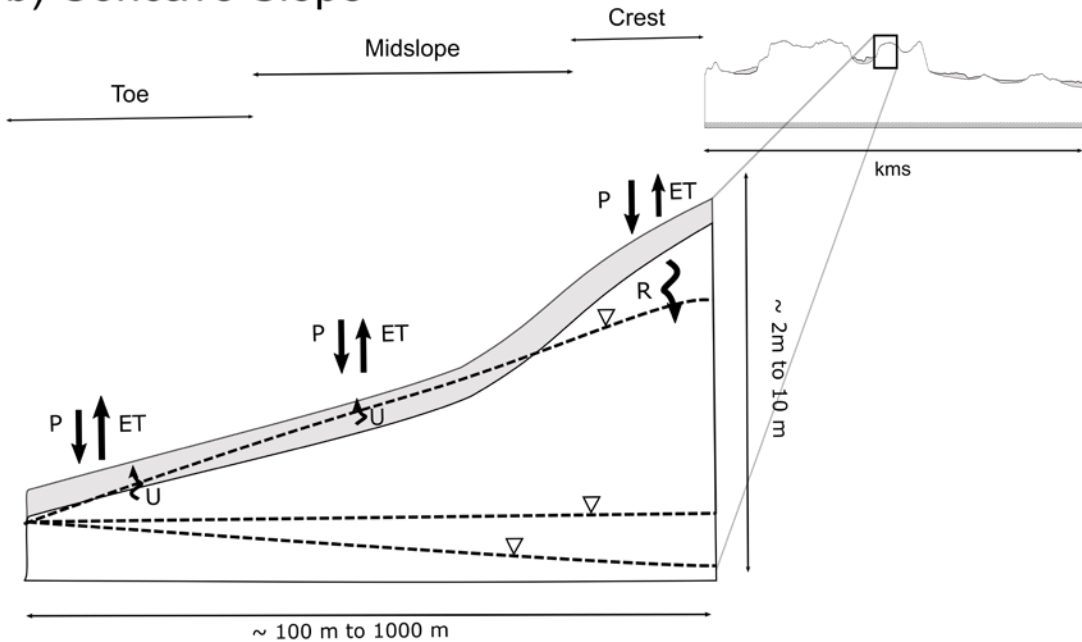


Figure 3-2 The different zones of hummock (crest, midslope, toe) identified for a) convex versus b) concave slopes with three potential water table configurations shown as dashed lines. Precipitation (P), evapotranspiration (ET), and recharge (R) are denoted with arrows, along with their conceptualized spatial variation on each slope. Note that evapotranspiration (ET) is conceptualized to increase in regions where upflux (U) occurs (i.e. negative net recharge).

3.2 Recharge-Discharge Dynamics

The water table configuration reflects the spatial and temporal distribution of recharge and discharge zones within reclaimed landforms. When the water table more closely approximates topography and groundwater mounds form beneath hummocks, local-flow systems tend to characterize the groundwater flow pattern (Figure 3-1a). Local-scale flow systems may exhibit temporal permanence across a range of climatic conditions, or they may be short-lived and transient in nature (Winter 2001). Comparatively, intermediate-scale flow patterns are predominant when the water table does not follow topography, and groundwater discharge may only occur near the outlets of a reclaimed landform. Additionally, in intermediate-scale flow systems, groundwater flow across hummock-lowland interfaces may be best described as “flow through”, where the horizontal component of flow dominates (Figure 3-1b).

The formation or absence of nested, local-scale flow systems is closely associated with solute migration patterns in reclaimed landforms (Twerdy 2019). Constructed hummocks aim to passively manage solute migration in capped and reclaimed CT deposits by: 1) affecting the tendency for local-scale flow systems to develop and 2) influencing the amount of precipitation partitioned to recharge. Where local-scale flow systems develop, solute discharge patterns are more likely to be an expression of hummock-scale dynamics (i.e. hummock to adjacent lowland). The smaller spatial scale of local-scale flow systems generally results in solute flushing occurring over shorter timescales than intermediate-scale flow systems.

Even if hummocks do not alter flow patterns, they may still be important sources of freshwater, where the timing and magnitude of recharge they facilitate determine the rate and magnitude of solute flushing. Under such circumstances, recharge through hummocks contributes to the amount of freshwater available at the landform-scale. Ultimately, the rate and magnitude of solute loading are related to the landform drainage patterns determined by the interaction between closure topography (i.e. constructed hummocks) and deposit-scale characteristics.

4 Case Studies of Constructed Hummock Performance: Observations and Controlling Factors

Section 4 provides case studies that demonstrate Syncrude's experience constructing hummocks and evaluating their performance. Additionally, this section discusses relevant hummock analogue studies from other mining operations that have helped inform Syncrude's understanding for how to design constructed hummocks that meet desired hydrologic functions. These case studies demonstrate that Syncrude has conducted, and continues to conduct, numerous investigations of constructed hummock performance; where uncertainties remain, Syncrude is actively undertaking work on the Mildred Lake Lease to advance their understanding of hummock and closure topography design. Learnings from these case studies can be readily applied to reclamation at Aurora North Mine and other Syncrude leases in the future.

Most of the synthesized findings presented here are based on data collected from study areas located at Syncrude's Mildred Lake Mine:

- Sandhill Fen Watershed (SFW); and
- South West Sands Storage Facility (SWSS).

Other reconstructed tailings areas on Syncrude's leases have infrequent field observations and/or did not contain constructed hummocks or hummock analogues. However, the geometry, type, and configuration of the hummocks at some locations, such as the hummocks constructed in the remainder of East in-Pit (EIP), are available for review. Hummocks currently under construction, in the design phase, and those presently lacking field data (e.g. elsewhere in EIP), can be evaluated using the tools developed in Section 5.

The other applicable case study detailed in Section 4 is a modelling exercise (Section 4.3), that evaluated the performance of hummocks across a range of hydrological conditions and/or design scenarios for analogous reclaimed mine sites.

4.1 Syncrude Sandhill Fen Watershed

Sandhill Fen Watershed (SFW) is the first reclaimed watershed constructed on a CT deposit and is one the most extensively studied reclamation projects in the AOSR, encompassing rich datasets from all aspects of the hydrological, hydrogeological and ecological systems. SFW is a 52 hectare (ha) watershed located on Syncrude's Mildred Lake Mine lease, constructed in 2012 on the northwest corner of the former mine pit, EIP. The tailings deposit in EIP consists of ~30 m of CT that was capped with 10 m of hydraulically placed tailings sand (BGC, 2008a, b), with tailings sand hummocks and lowlands mechanically constructed on top of the tailings sand trafficability cap to create the final closure topography layer (Figure 4-1). Constructed hummocks in SFW varied in size, height, morphometry, and coversoil prescriptions (Lukenbach et al. 2019; Twerdy 2019). Hummock analogues within SFW included a gently-sloping upland area, termed the south slope, as well as the 318 Closure Divide finger hummock (Figure 4-1). Hummocks and hummock analogues associated with SFW are a component of the larger, interdisciplinary work ongoing at SFW. Full details on the watershed's goals, research, construction, and design are provided by Wytrykush et al. (2012), Syncrude (2020), BGC (2008), BGC (2014a), and BGC (2014b).

Because it is an experimental research watershed, the SFW is more heavily instrumented and monitored compared to other reclaimed areas on Syncrude's leases. Groundwater monitoring activities have included manual and continuous measurements of water level, electrical conductivity, temperature, and water chemistry in approximately 200 piezometers and wells (Figure 4-1). Soil water monitoring was conducted at approximately 120 manual and nine continuous sampling locations (Figure 4-1). Atmospheric fluxes were monitored using three micrometeorological stations and three eddy covariance stations (Figure 4-1). Ecological and vegetation data were collected throughout the watershed starting in 2012. Full details on the groundwater instrumentation and monitoring are provided by Twerdy (2019) and Longval and Mendoza (2014); full details on the soil water monitoring network are provided by Lukenbach et al. (2019); full details of the micrometeorological data are provided by Nichols et al. (2016) and Carey and Humphreys (2019); full details of the vegetation sampling networks are provided by Merlin et al. (2018) for the forestlands/uplands and Vitt et al. (2016) for the lowlands.

Given that the entire watershed was constructed with tailings sand, which contained remnants of process-affected water, one of the major challenges when designing SFW was to minimize the impact of solutes (i.e. sodium salts) on vegetation. The intent of constructing hummocks in SFW was to develop several fresh, shallow, local-scale groundwater flow systems (i.e. groundwater mounding; see Section 3.1 for conceptual overview) to provide adequate water quantity and quality to the central lowlands in SFW and downstream environments, as well as provide a suitable substrate for upland vegetation growth. Local-scale groundwater flow systems associated with hummocks were a practical and elegant solution to mitigate the expression of process-affected water in the near-surface of the watershed because of their ability to limit the discharge of deeper groundwater associated with process-affected water. A detailed discussion and assessment of the observations and modelling from SFW are provided by Lukenbach et al. (2019), Twerdy (2019), and Syncrude (2020).

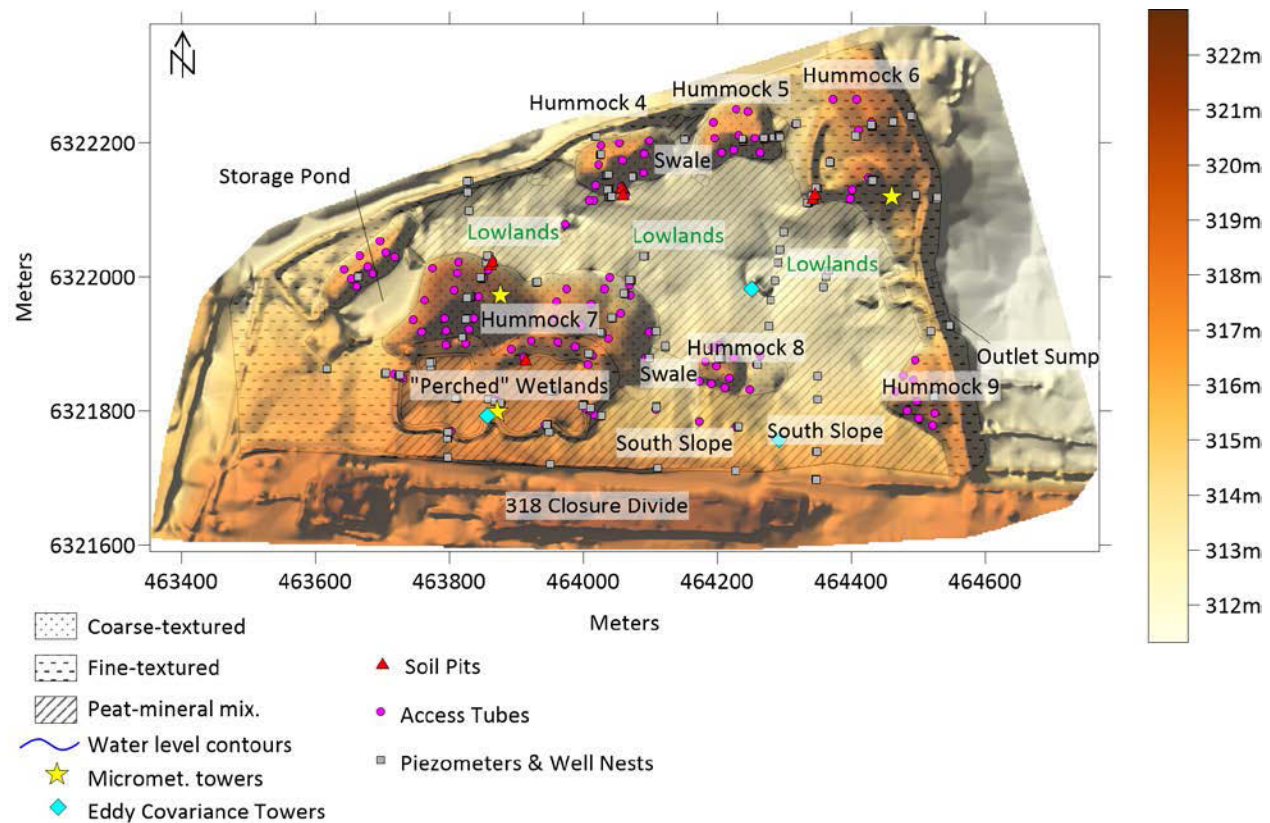


Figure 4-1 Hummocks, hummock analogues, and other features in SFW and the associated soil, groundwater, and meteorological monitoring networks. Coloured shading denotes topography. Note that hummock numbering is not sequential due to deviations from planned construction due to limited material availability. Adapted from Lukenbach et al. (2019).

4.1.1 Performance Based on Water Table Configuration Metric

Overall, groundwater preferentially flowed from the southern-most boundary of SFW towards the northeast; however, the water table below hummocks had a flatter, more linear configuration rather than exhibiting groundwater mounding as was anticipated (Twerdy 2019). Instead, the groundwater system was characterized by “flow-through” conditions, more influenced by intermediate-scale features (i.e. groundwater mound below 318 Closure Divide), where topographic features beyond the extent of SFW influenced the water table configuration more than constructed hummocks. It was also unexpected that some flow was diverted to the north, likely through a buried higher hydraulic conductivity gravel channel (Twerdy 2019).

While groundwater mounding below hummocks was not achieved, field observations of the water table configuration between 2013 to 2017 at SFW still provided an indication of how effectively hummocks and hummock analogues were able to isolate upland rooting zones from saturation and salinization. In general, hummocks of all heights and sizes increased the separation between the water table and the ground surface and exhibited limited temporal fluctuations during dry or wet periods in SFW (Figure 4-2). Moreover, separation between the water table and land surface was achieved even for small, localized

hummocks with limited spatial extent (e.g. Hummock 8; Figure 4-2). Additionally, the configuration of the hummocks was generally convex (recall Section 3.1 and Figure 3-2 for conceptual diagrams of hummock shape/form), which minimized the length of the hummock toe and, subsequently, the areal extent over which there were shallow water tables.

In contrast to the hummocks, the south slope was not constructed to an appreciable height. Instead, the shallow and gradual south slope essentially mimics the configuration of hummocks that are short and/or have concave slopes (recall Section 3.1 and Figure 3-2 for conceptual diagrams of hummock shape/form). As a result, the water table was in close proximity to the ground surface over large areas of this zone (Figure 4-2). Additionally, portions of the south slope adjacent to the lowlands frequently exhibited near-surface saturation, based on saturation mapping conducted by Twerdy (2019). Water tables were also more dynamic in this zone because there was limited soil water storage available above the water table (Figure 4-2). The temporal dynamics of the south slope were best demonstrated by two shallow piezometers where the water table responded rapidly to precipitation events and were consistently observed to be less than 2 metres below ground surface (mbgs), and often less than 1 m (Figure 4-2).

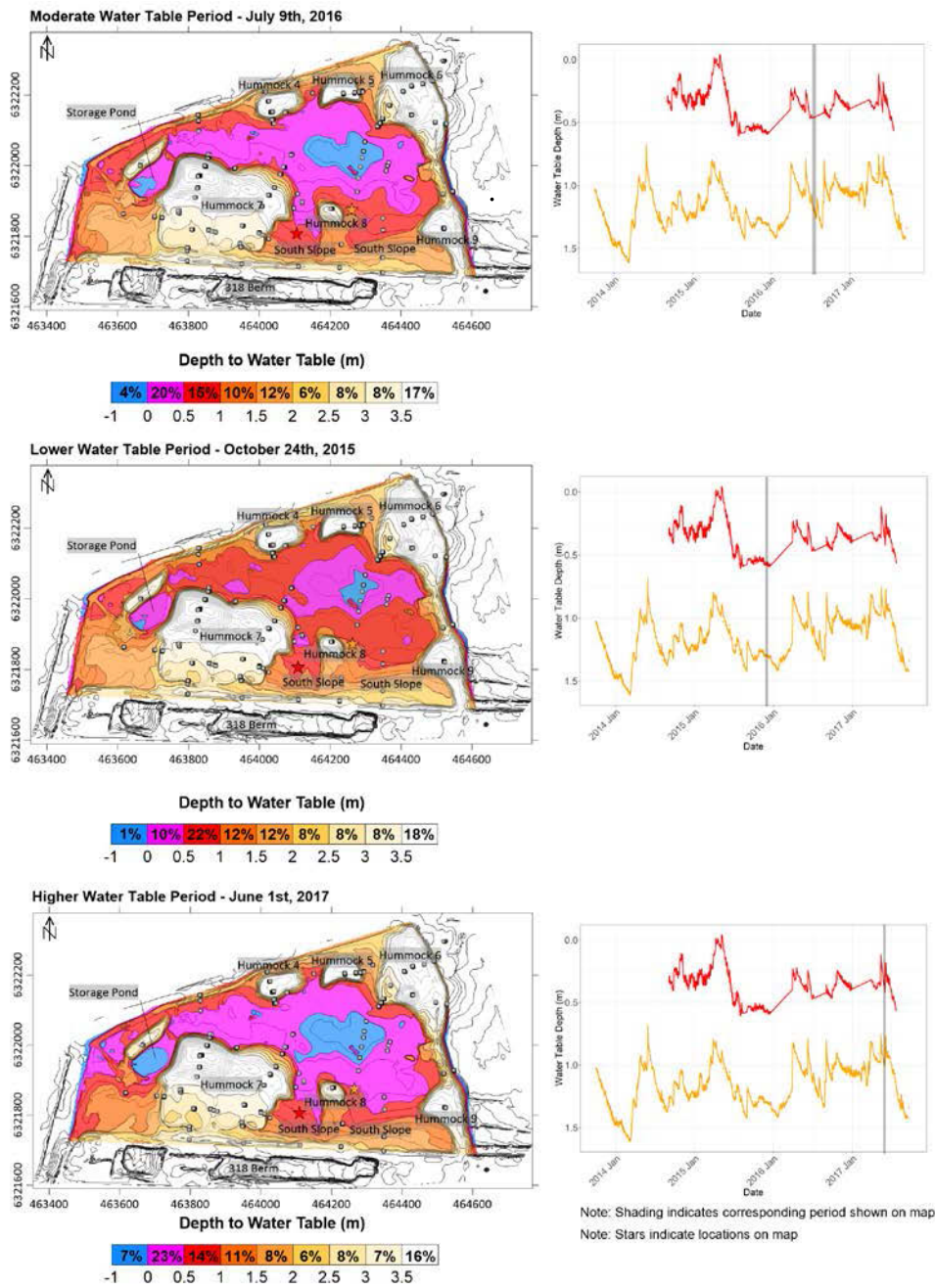


Figure 4-2 Depth to water table during moderate, lower, and higher water table periods in SFW; time series plots show transducer traces for two locations (indicated by stars on map), with shaded windows on the graphs indicating the time period for which the snapshot of the spatial water table configuration is shown. Percentages in colour bars indicate the percent area occupied by a given water table depth interval.

4.1.2 Overview and Key Learnings

Constructed hummocks in SFW were effective at increasing separation between the ground surface and water table, functioning to prevent saturation and salinization of the rooting zone (Section 4.1.1). Furthermore, hummocks greater than approximately 2 m in height were effective at partitioning precipitation to groundwater recharge, especially when prescribed coarse-textured coversoils (Lukenbach et al. 2019). Precipitation falling on hummocks was primarily partitioned to evapotranspiration and recharge, with overland flow representing a small component of the water balance (i.e. <10%; Biagi and Carey 2020; Carey and Humphreys 2019; Lukenbach et al. 2019). Local-scale groundwater flow systems did not develop beneath hummocks in SFW (Twerdy 2019), representing a departure between anticipated and actual function. The absence of local-flow cells forming beneath hummocks was a concern due to the potential discharge of solutes from deeper groundwater; however, recharge facilitated by hummocks led to freshwater lenses forming beneath several hummocks in SFW that limited the near-surface impact of solutes (Twerdy 2019). Thus, hummocks still functioned to freshen the groundwater system and passively managed process-affected water in SFW, comparable to the originally designed function.

Water transpired by plants directly reduced the amount of water available for freshwater recharge, highlighting the trade-off between vegetation productivity and recharge associated with the sub-humid climate (Lukenbach et al. 2019). Areas on constructed hummocks or hummock analogues with shallow water tables (i.e. < ~2 m below ground surface) not only had the potential to negatively impact the rooting zone, but also decreased recharge by allowing roots to readily draw water up from the saturated zone (Lukenbach et al. 2019). Threshold-like behaviour characterized the relationship between hummock height and recharge, where hummocks 2 m to 3 m in height were effective at consistently facilitating recharge, although the long-term water source/sink function of hummocks depended on the maximum rooting depth eventually reached (Lukenbach et al., 2019). The water source/sink function of hummocks was also largely controlled by the prescribed coversoil, where fine-textured coversoils limited recharge and partitioned water to evapotranspiration, thereby enhancing vegetation productivity (Lukenbach et al., 2019). A key learning was that the ability, or inability, of a coversoil to facilitate recharge can outweigh other hummock characteristics (lithology, geometry, height, width, convexity) in determining whether hummocks meet targeted water source/sink functions, with associated implications on the capacity of hummocks to freshen the groundwater system.

The absence of local-scale groundwater flow cells beneath hummocks can be explained in the context of the Haitjema and Mitchell-Bruker (2005) framework detailed in Section 3.1. Although constructed hummocks partitioned adequate amounts of precipitation to recharge, the hydraulic conductivity of the tailings sand used to construct the hummocks was approximately 10^{-5} m/s (Benyon 2014; Twerdy 2019). Assuming a rather high long-term recharge value of 100 mm/yr implies a R/K ratio of $\sim 3 \times 10^{-4}$. This R/K ratio indicates that even under elevated recharge conditions, the water table was recharge-controlled rather than topography-controlled, suggesting that larger-scale and/or intermediate-scale features were dominant in controlling the position of the water table in SFW (Haitjema and Mitchell-Bruker 2005). To develop groundwater mounds beneath hummocks with this relatively high hydraulic conductivity, more spatially expansive hummocks would be required (similar in size to the 318 Closure Divide), beyond what was logistically feasible given the area available for watershed construction.

The role of larger-scale features was exemplified by 318 Closure Divide, a finger hummock, which served as a groundwater/surface water divide within the overall reclaimed EIP landform and largely influenced water flow within SFW (Twerdy 2019). A key learning was that the spatial scale of targeted hydrologic functions should be carefully considered relative to the hydrogeologic properties of reconstruction materials. Importantly, groundwater flow patterns may evolve over time in SFW. The 318 Closure Divide hummock was not reclaimed until summer 2016; therefore, recharge on this feature was likely greater than it will be in the future. Over time, this will likely make the hydraulic gradient across SFW less steep, potentially allowing hummocks in SFW to develop transient, local-scale groundwater mounds (Lukenbach et al. 2017).

The discharge of deeper process-affected water, anticipated to develop in the absence of local-scale groundwater flow systems, was generally limited in spatial and temporal extent based on vertical hydraulic gradients measured at hummock-lowland interfaces (Twerdy 2019). When vertical hydraulic gradients did indicate flow towards the surface, the water flux associated with such occurrences was negligible due to their low magnitude, intermittent duration, and based on the low tailings sand hydraulic conductivity (Twerdy 2019). As such, areas with elevated solute concentrations were primarily related to shallow water tables at hummock-lowland interfaces and along the south slope. Potential mechanisms elevating solute concentrations included lateral seepage of water through process-affected tailings in the near-surface and/or enhanced root water uptake that limited solute flushing from the unsaturated zone (Twerdy 2019).

Given the targeted hummock hydrologic functions in SFW, optimally designed hummocks were those that were tall enough to consistently partition enough precipitation to recharge, featured convex slopes that minimized the spatial extent of shallow water tables at hummock-lowland interfaces, and had coarse-textured coversoils. Based on this, Hummock 7 was most effective at meeting targeted hydrologic functions, although Hummock 7 was likely taller than required. Particularly tall hummocks in SFW may take longer to flush solutes, given the larger volume of tailings used to construct them (thereby increasing storage potential), even if prescribed a coarse-textured coversoil.

Hummocks similar to the south slope in SFW, where a gradual slope and concave slope orientation resulted in shallow water tables across much of this feature's spatial extent, are likely to be undesirable. Due to shallow water tables at the south slope, recharge was limited, and solutes were poorly flushed beneath this zone. The south slope was interpreted to be analogous to short, broad hummocks constructed to inadequate heights that are ineffective at adequately separating the rooting zone from the water table. The south slope was a manifestation of material shortages during SFW construction, with the actual areal extent of constructed hummocks being approximately 15% to 20% less than designed. Nonetheless, findings from SFW contributed to the overall understanding of how material balances can be better managed during landform construction (e.g. shorter hummocks in some areas to allow elevation in other areas) and understanding of the limits of desirable hummock configurations.

The targeted hummock hydrologic functions in SFW may be different from those on other reclaimed landforms, and learnings from SFW contributed to this overall understanding. For example, in some reclaimed hummocks or landform elements, it may be best to limit recharge to lower water tables and increase geotechnical stability. In such cases, findings from SFW demonstrated that thick, fine-textured coversoils or those comprised of peat-mineral mixtures would be more suitable for such a targeted function.

4.2 Syncrude Southwest Sand Storage Facility

Southwest Sand Storage Facility (SWSS) is an aboveground tailings storage facility constructed to impound water and store tailings sand at Syncrude's Mildred Lake Mine lease prior to the advent of CT technology (Figure 4-3). The deposit is approximately 50 m high and 23 km² in size. It was constructed with a gently-sloping tailings sand perimeter dyke that extends downstream to a perimeter toe ditch. The tailings facility is subdivided into 21 operational areas, or cells, where tailings sand was deposited and mechanically reworked into a series of terraced slopes and/or benches (Price 2005), with variable geometries (i.e. orientation of slope or bench) and configurations (i.e. number of bench-slope pairs per cell) in different locations as part of the final closure topography. The tailings dyke was initially an undrained structure, constructed using the upstream method, but lateral drains were installed in 2010 to facilitate water management. Investigations between 2001 and 2010, prior to the installation of drains, are particularly informative for hummock technology and are the focus of interpretations herein.

The overall reclamation challenges, goals, materials, and outcomes of SWSS are analogous to those of hummocks. Many aspects of the dyke contribute to the understanding of hummock technology because the dyke is similar in composition (i.e. tailings sand) and form to large, terraced hummocks that will be incorporated into the closure topography layer when capping and reclaiming CT deposits. Moreover, the local-scale topography (i.e. terraced benches) constructed on some slopes of the SWSS dyke are representative of smaller-scale hummocks. The research outcomes from work completed on two intensively studied transects of the dyke on Cell 32 and Cell 46 are considered representative hummock analogues for post-mining closure landscapes on CT deposits; the dyke at both Cell 32 and 46 is representative of a large-scale hummock and the terraced benches on Cell 32 represent smaller scale hummocks (Figure 4-3).

The overall properties and form of the dyke and smaller-scale hummocks were designed to develop local-scale groundwater flow (Price 2005; Booterbaugh et al. 2015) to satisfy two goals: limit the proximity of the water table relative to the ground surface for geotechnical stability, and passively manage groundwater and vegetation by isolating the water table from the ground surface to prevent saturation and salinization of the rooting zone. Importantly, the hydrogeology of SWSS differs from capped and reclaimed CT deposits because the tailings sand that comprises the aquifer pinches out (Figure 4-3). Therefore, the wedge shape of the overall deposit, characterized by the gradual thinning of the tailings sand aquifer, and small cross-sectional area near the dyke's perimeter causes more water to daylight (seep) at the toe and may promote higher water tables and more pronounced local-scale groundwater flow systems throughout the structure.

To assess hydrogeological performance, including the water table configuration, groundwater flow and solute transport in an undrained dyke under variable construction scales (i.e. local/bench-scale, and intermediate/dyke-scale) and dyke geometries (i.e. number of terraces and their configuration), transects at Cell 32 and Cell 46 were instrumented as long-term research monitoring networks (Figure 4-3). The dyke configuration at Cell 32 and 46 prior to drain installation in 2010 is shown in Figure 4-3, where Cell 32 included two back-sloped benches (Benches A and B) and three forward-sloped benches (Benches C through E). Where the back-sloped benches intersected the dyke in Cell 32 are herein referred to as channels, given their role in collecting groundwater discharge and subsequently conveying water elsewhere prior to the installation of lateral drains in 2010. Comparatively, Cell 46 included only two forward-sloped bench-slope pairs (Figure 4-3). The dyke was constructed on glaciolacustrine sediment

(silts and clays), essentially a low hydraulic conductivity foundation upon which the dyke pinches out. Further construction, design, and hydrogeology have been discussed by Booterbaugh et al. (2015), Goddard (2017), and Price (2005).

The groundwater monitoring networks in Cell 32 and Cell 46 consisted of approximately 95 piezometers and wells at 22 locations along transects that run from the crest of the dyke to the perimeter toe ditch (Figure 4-3). Unsaturated zone monitoring included discrete and automated soil moisture stations to assess water movement and storage in the unsaturated zone. Meteorological stations monitored inter-annual and intra-annual meteorological patterns. Full details on groundwater instrumentation and monitoring data are provided by Booterbaugh et al. (2015), Goddard (2017), Price (2005); meteorological data by Dobchuck et al. (2013) and O’Kane Consultants Inc. (OKC 2007); soil water installations and monitoring by Chaikowsky (2003), Dobchuck et al. (2013), and OKC (2007). This work was part of interdisciplinary work evaluating ecosystem performance in soil and vegetation plots discussed by Burgers (2005) and Naeth et al. (2011).

4.2.1 Performance Based on Water Table Configuration Metric

Groundwater in Cell 32 flowed eastward from the dyke crest to the proximal perimeter toe ditch. In Cell 46, groundwater flowed westward, from dyke crest to toe ditch (Figure 4-3). In both transects, a groundwater divide existed below the dyke crest. The larger-scale water table configurations in both transects were subdued replicas of topography and a reflection of overall hydraulic gradient controlled by the hydrogeologic properties, height, and length of each cell’s tailings dyke slope. The water table depth was greatest near the crest of the tailings dyke, and least near the perimeter toe ditches and the toes of bench-slope pairs (Figure 4-3). On the bench-slope pairs, deeper water tables were present at the most elevated parts of the benches (e.g. Bench B in Figure 4-3), while water tables were slightly above ground at the toes of slopes (Price 2005).

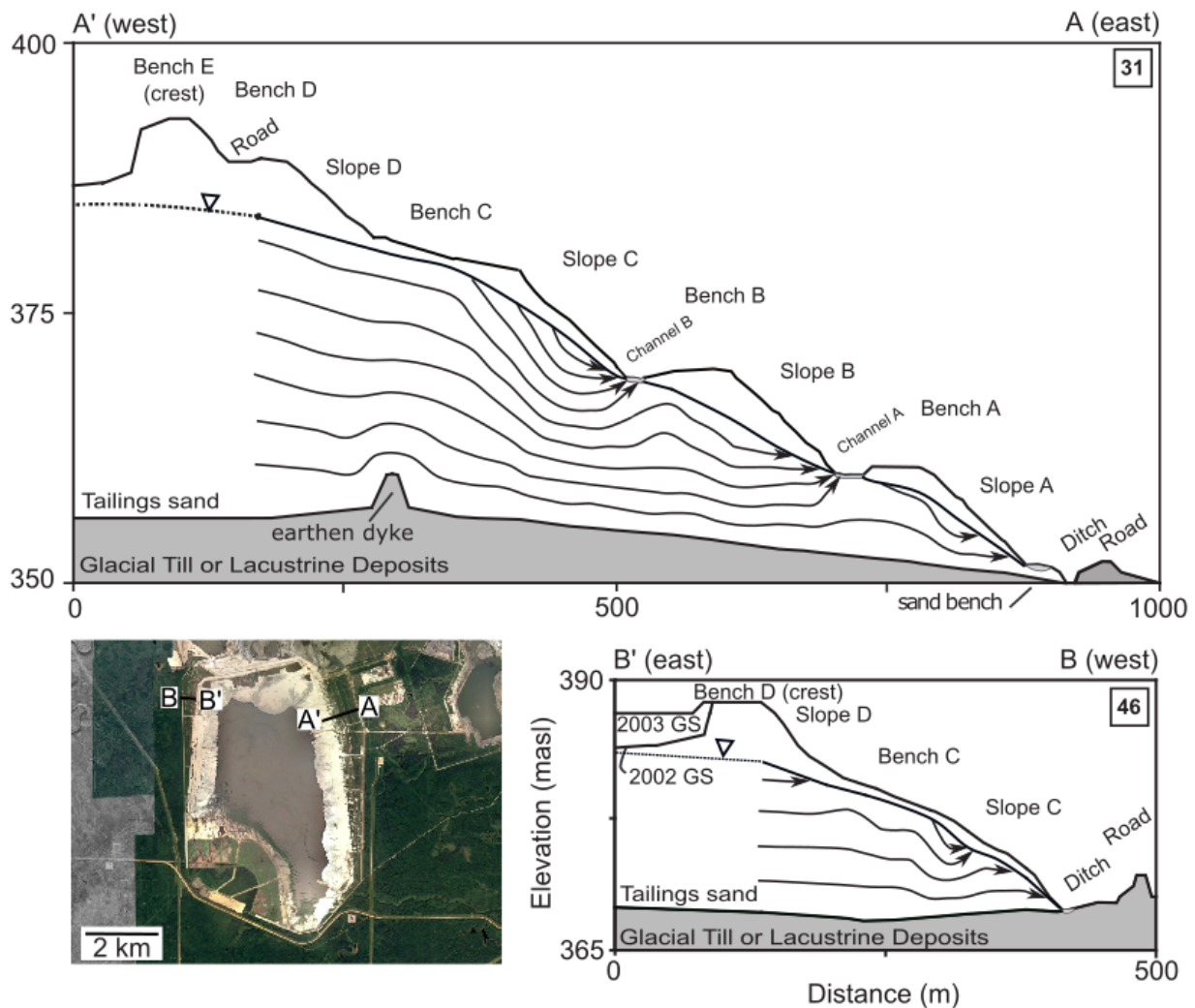


Figure 4-3 Southwest Sand Storage Facility (SWSS) cross-sections showing instrumented transects through the dyke at Cell 32 (cross-section A) and Cell 46 (cross-section B) of the dyke. The water table is indicated by the solid black lines and inverted triangle, with the dashed line indicating where the water table's configuration is interpreted. Groundwater flow paths are indicated with black arrows (Adapted from Price 2005).

Local-scale topography contrasts (i.e. presence/absence of small-scale hummocks) between Cell 32 and Cell 46 resulted in differences in local-scale water table configurations (Figure 4-3). Deeper water tables were associated with back-sloped benches in Cell 32, compared to the flat- to forward-sloped benches in Cell 46 (Figure 4-3). Furthermore, the materials used to construct Cell 46 had lower hydraulic conductivities than those used at Cell 32 (1×10^{-6} m/s vs. 3×10^{-6} m/s; Price, 2005), which made the water table shallower throughout Cell 46, even though Cell 32 was approximately twice as long (recall overview in Section 3.1). The result of different design characteristics meant that, for Cell 32, the water table was >10 m deep in some locations and was at the ground surface in other areas; ~25% of the transect had water table depths <1 m. In contrast, ~60% of the transect at Cell 46 had water table depths <1 m, with the water table >5 m

deep in some areas. Overall, the intermediate-scale topography remained the dominant control on the water table configuration at both Cell 32 and Cell 46; however, it was modulated by the local-scale topography to a greater or lesser degree (i.e. Cell 32 versus Cell 46, respectively) depending on the design (Price 2005).

4.2.2 Overview and Key Learnings

From a reclamation perspective, the intent of the topographic design and configuration of the SWSS tailings dyke and bench-slope pairs was to passively manage the water table's proximity to the ground surface, in turn increasing geotechnical stability and preventing saturation and salinization of the rooting zone. Since the tailings sand used to construct the dyke was a byproduct of bitumen processing, and the background geochemical signature of the groundwater was similar to process-affected water, the design of the dyke and bench-slope pairs sought to limit the expression of solutes at the surface and freshen the groundwater system. The combination of the gentle, subdued topographic relief of the dyke, and the variable geometry and configuration of the bench-slope pairs exhibited different degrees of effectiveness at modulating the water table configuration and developing local-scale groundwater flow cells.

The two transects (Cell 32 and 46) at SWSS provided the opportunity to evaluate hummock design at the scale of the entire dyke (i.e. larger-scale hummock) and in benches nested within the overall terraced structure (i.e. local-scale hummocks). Due to the more accentuated local-scale surface topography on the lower benches of Cell 32, the water table was more effectively separated from the rooting zone than at Cell 46, where the benches were characterized by less pronounced local-scale topographic relief (Figure 4-3). Furthermore, the presence of back-sloped benches at Cell 32 facilitated the formation of several groundwater discharge points, thereby lowering the overall water table in the dyke at Cell 32 compared to Cell 46, where all groundwater discharged at the dyke toe. It is worth noting that the back-sloped benches at Cell 32 (i.e. A and B) could be constructed to slightly lower heights, given the deep water tables observed at the crests of these locations.

The presence of back-sloped benches on Cell 32 also facilitated more pronounced nested local-scale flow systems superimposed on the intermediate-scale flow system (Price 2005; Goddard 2017), which resulted in more rapid solute flushing (Figure 4-3). Numerical modelling estimated that local-scale flow systems would flush solutes within decades, while the intermediate-scale flow system (i.e. dyke groundwater divide to perimeter ditch) would take centuries (Price 2005), largely constrained by recharge rates associated with the sub-humid climate. While the solute discharge at the toes of back-sloped benches associated with local-scale flow systems was generally detrimental to vegetation, these areas were small relative to the entire area of the dyke slope. Without the development of these local-scale flow systems, low-relief areas would freshen more slowly, and a greater proportion of the tailings dyke would likely have shallow, undiluted process-affected water.

A key learning was that when larger-scale hummocks are anticipated to have shallow water tables, perhaps due to low hydraulic conductivities (i.e. $< 5 \times 10^{-6}$ m/s) associated with construction materials, incorporating local-scale topographic relief on them may be effective at managing the water table and flushing solutes. Back-sloped benches resulted in focused groundwater discharge, forming localized areas of surface water ponding in corresponding channels. Therefore, the shape of the closure topography can be manipulated to focus groundwater discharge at specific locations. However, it is important to consider how designs that focus groundwater discharge, which are likely desirable under many reclamation

circumstances, affect geotechnical stability. One way to balance these end goals might be to rapidly reclaim hummocks with coversoils and vegetation to limit recharge and increase geotechnical stability. While drains were eventually installed in the SWSS dyke for geotechnical reasons, numerical simulations suggested that following full reclamation the undrained dyke would have had low recharge and water tables, with a groundwater divide shifted towards the tailings pond (Goddard 2017).

In some ways, the dyke and smaller local-scale hummock at SWSS departed from constructed hummocks on CT deposits. In particular, the dyke at SWSS was taller than hummocks likely to be constructed on most CT deposits. This design, combined with the relatively lower hydraulic conductivity of the tailings sand, likely contributed to the presence of steeper hydraulic gradients than will occur in most capped and reclaimed CT deposits (e.g. within EIP). Furthermore, the thinning of permeable aquifer materials from the dyke crest to the perimeter toe ditch may not be comparable to the design of capped in-pit CT deposits. The thinning nature of the aquifer likely made local-scale groundwater flow systems more pronounced and elevated the water table throughout the dyke. One important takeaway is that although the permeable trafficability cap and closure topography layer on CT deposits will generally have appreciable thickness throughout the deposit, resulting in recharge-discharge relationships that differ from those observed at the dyke at SWSS, it may be possible to focus groundwater discharge where desirable on reclaimed CT deposits by constructing a thinner trafficability cap/closure topography layer in some parts of the reclaimed landform.

4.3 Hydrogeology of Open-Pit Reclamation

Exploratory numerical modelling of reclaimed open-pit coal mine sites in Alberta by Schwartz and Crowe (1987) evaluated water table configurations at two spatial scales following reclamation: 1) the scale of an entire mine pit and 2) the scale of hummocks. Pit-scale simulations investigated the re-saturation of mine spoil as a function of different hydrogeologic factors, while hummock-scale simulations examined how a range of hummock morphological and hydrogeological properties influenced post-mining water table configurations. Overall, the objective of the work was to assist in reclamation planning to better understand the factors controlling the behaviour of the water table in reclaimed landforms.

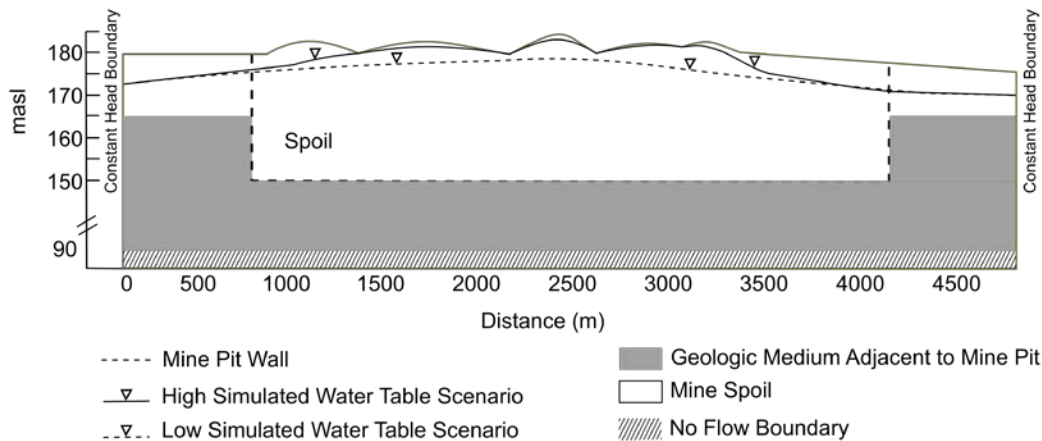
Both spatial scales investigated by the numerical modelling exercise are applicable to reclamation challenges on Syncrude's leases, and advance Syncrude's understanding of hummock design, construction, and performance. Given that many CT deposits will be constructed on former mine pits (e.g. EIP, Aurora East Pit), pit-scale simulations provide an understanding of the influence of deposit-scale factors (e.g. hydrogeology surrounding pit) on water table configurations. Similarly, hummock-scale simulations advance the understanding of how hummock morphological and hydrogeological properties interact at relevant spatial scales to influence water table configurations.

4.3.1 Pit-Scale Simulations

The model domain used in pit-scale numerical simulations is shown in Figure 4-4. Constant head boundary conditions (same elevation on either side) were prescribed on the left and right edges of the model domain, while a no flow boundary was specified at the base of the model domain. Recharge was applied along the top surface of the model domain. The relief of the prescribed in-pit closure topography was subtle, which is comparable to that found at reclaimed sites on Syncrude's leases. Recharge, the hydraulic conductivity of the spoil (i.e. material deposited in-pit after mining), the hydraulic conductivity of the

materials surrounding the pit, and the configuration of lowlands within the pit were varied to determine their influence on water table configurations.

a) Interaction Between Recharge, Spoil Hydraulic Conductivity, and Hydraulic Conductivity Surrounding Mine Pit



b) As in a), With Alternative Lowland Spacing Configuration

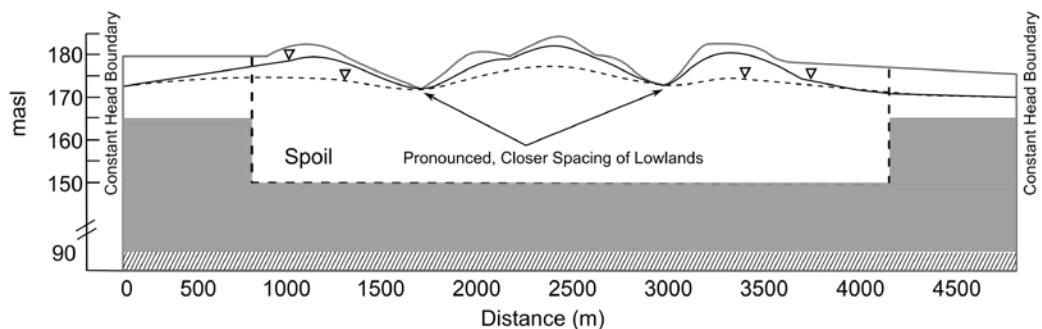


Figure 4-4 a) Pit-scale simulations adapted from Schwartz and Crowe (1987), with water table configurations shown for different combinations of recharge, spoil hydraulic conductivity, and the hydraulic conductivity of the surrounding geologic medium. b) Same factors were varied as in a) but with a different lowland configuration.

Two water table configurations that represent the range of modelled outcomes are shown in Figure 4-4a (solid and dashed black lines). The rest of the simulated water table configurations generally fell between these end-members, corresponding to alternative parameter combinations. The water table closely followed topography for scenarios with higher recharge and/or lower spoil hydraulic conductivity, corresponding to simulations that have R/K values $> \sim 6 \times 10^{-4}$. Comparatively, when R/K was $< 6 \times 10^{-4}$, the water table was lower throughout the pit (i.e. dashed line in Figure 4-4a). The fact that the water table still closely followed topography for rather low R/K values (see Section 3.1 for comparison) was because the closure topography was largely absent of well-defined lowlands or drainage features (i.e. L parameter in Section 3.1 and Table 3-1). The occurrence of near-surface water tables was appreciably mitigated by

the presence of lowlands (i.e. decreased distance between hydrological boundaries), as evidenced by alternative closure topography configurations with more pronounced lowlands that functioned to lower water tables (Figure 4-4b). Nevertheless, the influence of lowlands remained dependent on recharge and hydraulic conductivity throughout the rest of the reclaimed pit. These results can be interpreted in the context of Section 3.1, where constructing less expansive hummocks (i.e. decreasing the spacing between hydrological boundaries) can offset water table rises associated with lower hydraulic conductivity materials and/or coversoils that facilitate high recharge.

The simulations also showed that the influence of closure topography on the water table diminished near the edge of the pit (Figure 4-4), primarily due to the influence of the surrounding hydrogeology (i.e. deposit-scale factors). Pit-scale simulations examined a range of hydraulic conductivities characterizing the materials surrounding the pit. As the hydraulic conductivity of materials surrounding the pit increased, the in-pit water table configuration less closely followed topography. However, the influence of the surrounding hydrogeology was limited when in-pit materials had lower hydraulic conductivities less than $\sim 10^{-7}$ m/s. Thus, a key learning was that it is important to understand deposit-scale factors that influence the water table configuration, exemplified in this case study by the contrast between the hydrogeological properties of in-pit substrate materials relative to the surrounding geologic media. The interpreted influence of surrounding hydrogeology can also be expanded to infer the effect of prescribed outlets within a reclaimed landform, where the elevation and spatial positioning of outlets relative to the closure topography can have a large influence on the water table configuration. For example, in reclaimed landforms with relatively permeable substrates (i.e. hydraulic conductivities greater than $\sim 10^{-6}$ m/s), outlet elevations well below the average elevation of the closure topography function as drainage features that limit the rise of the water table throughout the deposit.

4.3.2 Hummock-Scale Simulations

Hummock-scale numerical simulations consisted of a model domain comprised of a cross-section of a symmetrical hummock (Figure 4-5), representative of a small-scale topographic feature from Figure 4-4. Hummock dimensions were varied in the simulations, with different combinations of hummock heights (5 m to 20 m) and the lengths (215 m to 1,075 m) investigated, corresponding to a range of slopes (2% to 20%). A no flow boundary was prescribed within 10 m of the base of the hummock, representing the initial aquifer thickness (i.e. prior to the application of recharge). Additionally, recharge, hydraulic conductivity, and the presence of drains were varied to determine their influence on the water table position.

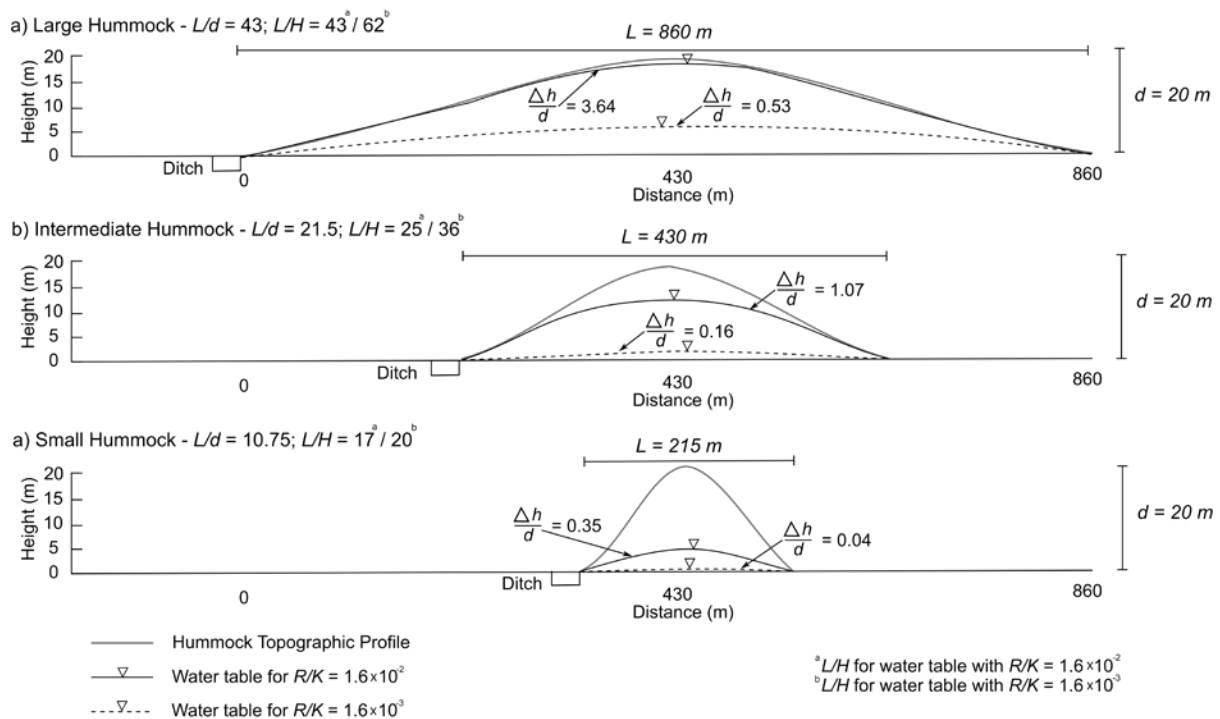


Figure 4-5 Hummock-scale simulations adapted from Schwartz and Crowe (1987), with water table configurations (black lines with inverted triangles) shown for different recharge (R) and hydraulic conductivity (K) combinations (solid versus dashed black lines) and as a function of different hummock lengths (L). Maximum hummock height (d) was constant for the shown set of simulations and the aquifer thickness (H) underlying the hummock was assumed to be 10 m, while the estimated maximum rise in the water table at the centre of each hummock (Δh) is related to d as a ratio ($\Delta h/d$). $\Delta h/d$ calculated assuming an aquifer shape factor (C) of 8. For further details on dimensionless ratios and variables, see Section 3.1 and Table 3-1.

Figure 4-5 shows a range of model outcomes for different parameter combinations. To readily relate these findings to the analysis detailed in Section 3.1, corresponding ratios between variables have been calculated. Longer, broader hummocks had shallower water tables due to the greater area over which recharge occurred and longer flow paths to discharge zones (i.e. less readily drained). Additionally, steeper slopes and taller hummocks limited the proportion of the hummock where water tables were shallow or intersected the ground surface. The water table closely followed topography for all combinations of recharge and hydraulic conductivity when the hummock was wide (i.e. 860 m and 1,075 m [not shown herein]). When hummocks were narrower (i.e. 215 m and 430 m), the water table was near the ground surface only for the high recharge (i.e. 50 mm/yr) and low hydraulic conductivity (i.e. 10^{-8} m/s) scenarios (i.e. R/K of 0.016 in Figure 4-5). Given the occurrence of near-surface water tables in several simulations, the effect of the position of surface drainage features, analogous to an adjacent lowland to a hummock, was investigated. Hummocks that had particularly low hydraulic conductivity ($< 10^{-7}$ m/s) or were particularly long (i.e. greater than 800 m) resulted in adjacent surface drainage features having a limited influence on hummock water tables because the drainage from the hummock was constrained by the hydraulic conductivity.

Interrelationships between factors identified by Schwartz and Crowe (1987) aligned with the simple water table configuration analysis detailed in Section 3.1. Notably, hummock-scale numerical simulations by Schwartz and Crowe (1987) focused on substrate materials that were less permeable than those used to cap CT deposits. For context, R/K ratios in Schwartz and Crowe (1987) ranged from 1.6×10^{-3} to 0.159, which was generally higher than reclaimed sites comprised of tailings sand on Synocrude's leases (i.e. Table 3-1). Nevertheless, findings demonstrated that the construction of long, broad hummocks (i.e. higher L/H and L/d ratios; Section 3.1) may be beneficial when the targeted hydrologic function is the formation of local-scale groundwater flow systems that redirect freshwater on capped and reclaimed CT deposits. However, there is a trade-off between constructing longer hummocks to develop local-scale flow systems and having a water table that is too shallow across a hummock. Design should consider the risk of the water table rising too close to the ground surface and affecting the rooting zone, which may be the case for broad hummocks paired with moderate hydraulic conductivity materials (e.g. $\sim 10^{-6}$ m/s) or a wide range of hummock sizes paired with low hydraulic conductivity materials. Taller hummocks could be constructed (i.e. increased slopes) to offset water table rises in longer hummocks, but this may be logistically infeasible. Overall, reclamation planners need to have a general sense of hydraulic conductivities and recharge for constructed hummocks to determine appropriate hummock heights and lengths and how they relate to lowland/swale positioning.

4.4 Summary

The case studies demonstrate Synocrude's applied experience constructing hummocks and monitoring and evaluating hummock performance (i.e. Sections 4.1 and 4.2). That understanding is supplemented by literature studies (i.e. Section 4.3). When related in terms of the conceptual framework outlined in Section 3, parallels between the findings from the case studies are evident. Table 4-1 summarizes the key findings from each case study.

Table 4-1 Summary of Case Study Findings.

Case Study	Key Findings
1. Sandhill Fen Watershed ¹	<ul style="list-style-type: none"> • Hummocks constructed to heights greater than approximately two metres are effective at providing separation between the water table and rooting zone; • Coversoil characteristics and corresponding vegetation assemblages control the partitioning of precipitation between recharge and evapotranspiration, where coarser (finer) and thinner (thicker) coversoils facilitate higher (lower) recharge (i.e. trade-off between upland vegetation productivity and water for downstream environments); • The magnitude of recharge facilitated by hummocks indicates the amount of water available to downstream environments; the integrated recharge flux across all hummocks and other landform elements determines downstream water availability at the landform scale. • Overland flow is a small flux on hummocks, constrained to extreme high intensity rainfall events and some snowmelt events (e.g. concrete frost); • Larger-scale (i.e. deposit-scale) factors primarily controlled the groundwater flow regime and water table configuration because relatively high hydraulic conductivity tailings sand was used to construct watershed, thereby limiting the formation of local-scale groundwater flow systems beneath constructed hummocks within SFW;

Case Study	Key Findings
1. Sandhill Fen Watershed ¹	<ul style="list-style-type: none"> • Discharge of deeper groundwater associated with process-affected water was limited, as evidenced by a lack of association between the deeper groundwater's geochemical signature and near-surface solute concentration patterns; • Hummocks facilitated solute flushing, resulting in the formation of freshwater lenses that displaced saline-sodic tailings water; • Shallow water tables and limited solute flushing was associated with short (i.e. < 2 m in height), gently-sloping features within the watershed (i.e. hummock toes, south slope); and • Successional trajectories of vegetation play a large role in determining how effectively hydrologic functions are met over the long-term.
2. Southwest Sand Storage Facility ¹	<ul style="list-style-type: none"> • Local-scale topographic relief (analogous to small-scale hummocks) was effective at mitigating the occurrence of shallow water tables and focusing groundwater discharge; • Focused groundwater discharge, while locally elevating solute concentrations, is effective at limiting the areal extent of elevated solute concentrations across entire hummocks/landform elements; • Thinning aquifer units (e.g. pinch-outs) reduce the depth of the water table and focus groundwater discharge, analogous to thin trafficability caps/closure topography layers on CT deposits; • Subtle variations in the hydraulic conductivity of hummock construction materials may appreciably alter the water table configuration, evidenced by an elevated water table in Cell 46 relative to Cell 32 (hydraulic conductivities of 1×10^{-6} m/s vs. 3×10^{-6} m/s at Cell 46 and Cell 32, respectively).
3. Schwartz and Crowe (1987) ²	<ul style="list-style-type: none"> • Deposit-scale factors impart a large influence on the water table configuration, where higher (lower) hydraulic conductivity geologic units adjacent to CT deposits, smaller (larger) distances between lowlands, and lower (higher) elevation outlet locations are associated with a decrease (increase) in water tables relative to closure topography. • Water table configurations beneath hummocks are governed by hummock morphological properties (i.e. hummock height, length) and hydrogeological properties (i.e. hydraulic conductivity, recharge), where the water table more closely follows topography when R/K ratios are higher, hummock lengths are greater, and hummocks are shorter. • There is a trade-off between constructing longer hummocks to develop local-scale groundwater flow systems and the occurrence of shallow water tables; and • A general sense of the hydraulic conductivities and recharge for constructed hummocks aids in determining appropriate hummock heights and lengths and how they relate to lowland/swale positioning.

¹Sites on Syncrude's Mildred Lake Lease

²Numerical modelling study

5 Modelling Water Table Positions in Hummocks

Section 5 details the analytical models that have been developed based on learnings to date and can be applied to future hummock designs. The developed models are founded on the conceptualizations outlined in Section 3 and informed by applying experiences outlined in the case studies of Section 4. These models also demonstrate Syncrude's in-depth understanding of hummock performance across a wide range of design scenarios and available substrate and reclamation materials. This allows Syncrude to holistically plan, adjust, and adapt hummock designs to target specific functions and performance outcomes. The analytical modelling framework is a tool that allows for different combinations of hummock morphological designs and coversoil prescriptions to be robustly and efficiently assessed when determining their suitability relative to available reconstruction materials and anticipated hydrogeological properties of a capped CT deposit. Syncrude intends to refine and improve the models by incorporating data from ongoing field investigations and monitoring on capped and reclaimed CT deposits, thereby aligning with its adaptive management framework.

Section 5.1 outlines the development and theoretical basis of the models, as well as their linkage to the hydrogeologic and hydrologic processes characteristic of constructed hummocks. Then, a thorough understanding of model parameter ranges are demonstrated in Section 5.2, which are closely tied to field observations from numerous investigations on both Syncrude's sites, and other relevant sites within the AOSR. Finally, two applications (Sections 5.3 and 5.4) demonstrate how the models can be used to optimize hummock designs and achieve targeted hydrologic functions and to understand the interrelationships between key governing factors.

5.1 Analytical Modelling Framework

Analytical models frequently applied in hydrogeology have been adapted herein to address challenges specifically associated with hummock technology on Syncrude's leases. The analytical models simulate water table configurations and associated groundwater flow patterns as a function of multiple key factors that define hummock morphology, hydrogeological properties, and coversoil characteristics (corresponding to those outlined in Section 3.1).

5.1.1 Steady-State Analytical Models

The analytical models detailed in this section solve for average, long-term (i.e. steady-state) water table configurations. They can also be applied to represent inter-annual climate cycles (i.e. wet, mesic, and dry conditions) because climate cycles are multi-year events in the AOSR (see Section 2.3). The water table configuration relative to hummock morphological and hydrogeological properties can be estimated in the following form:

$$h^2 = H^2 - \frac{R}{K}(L - x)x \quad 5-1$$

where:

- h – the elevation of the water table at all positions x across a hummock cross-section,
- R – recharge,
- K – hydraulic conductivity,
- L – distance between hydrological boundaries, and
- H – saturated aquifer thickness.

This analytical model is a form of the Dupuit-Forchheimer model, a steady-state solution of the water table in an unconfined aquifer. Schematically, it can be visualized as the water table rise measured at the midpoint of a groundwater mound beneath a hummock (Figure 5-1).

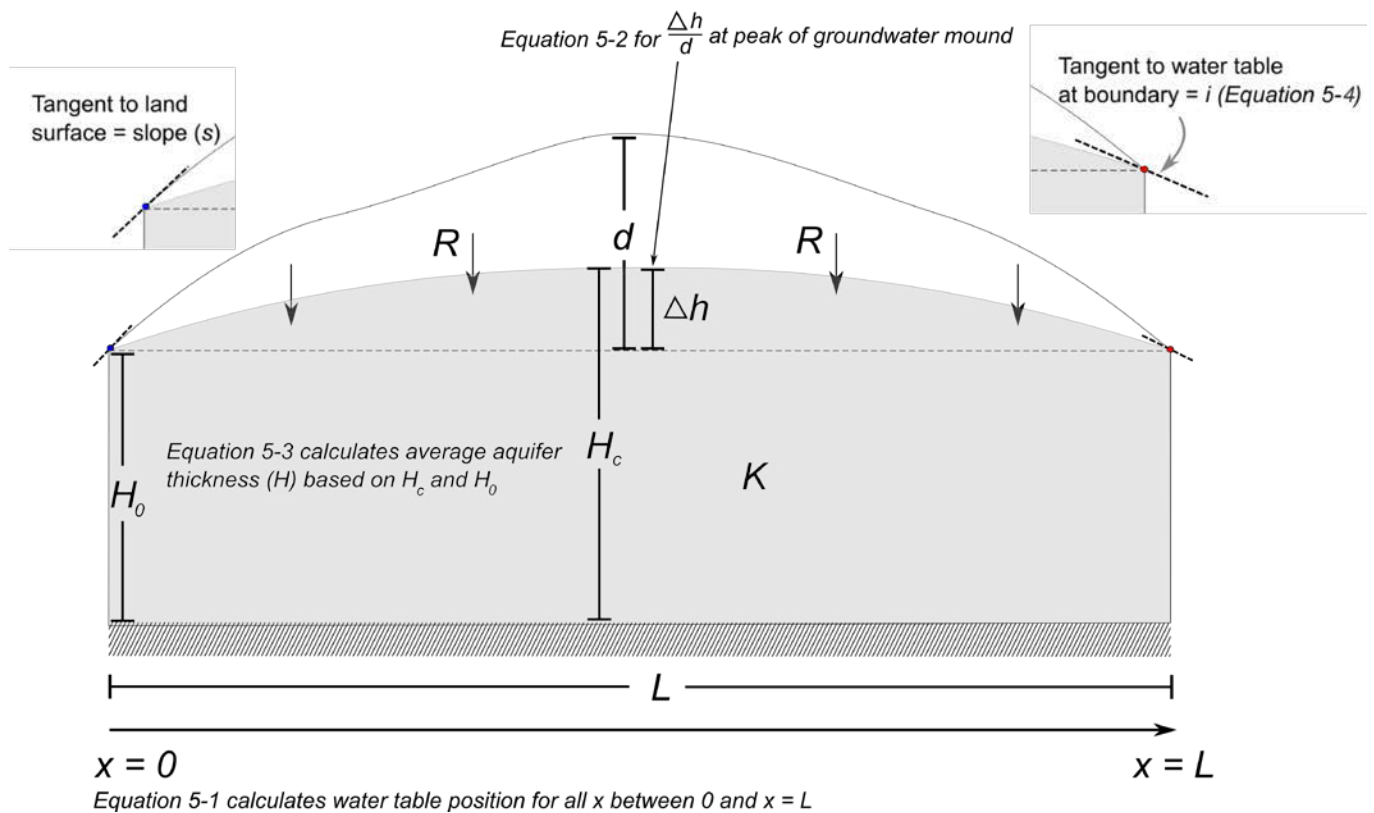


Figure 5-1 Schematic showing how the different analytical models and variables represent the hydrogeological processes and characteristics of hummocks.

The model assumes that the aquifer is dominated by horizontal flow, aligning with the much greater length of hummocks relative to their corresponding aquifer thicknesses. Furthermore, it is generally understood that there is typically limited spatial variability in material properties within an individual constructed hummock; therefore, the model's assumptions of homogeneous and isotropic aquifer properties generally hold true. The model's application is limited to systems that behave as aquifers or are

slightly less permeable than aquifers; put differently, K cannot be so low that horizontal flow is not appreciable (e.g. Hokanson et al. 2020). Additionally, water may discharge or seep to a wetland or body of water at the boundaries shown in Figure 5-1, rather than exit the model domain horizontally as assumed. Note that the model does not explicitly represent the position of the land surface; therefore, if the simulated water table is above the land surface, it indicates the occurrence of seepage and/or overland flow.

Qualizza and McKenna (2007) have previously employed the Dupuit-Forchheimer model for hummock design and analysis. A more general form of the Dupuit-Forchheimer model is detailed in Appendix 1, which can be used if a regional hydraulic gradient/slope is present across a hummock (i.e. different water level elevations at the hydrological boundaries). It is not considered herein because the regional gradient is generally small on capped and reclaimed CT deposits. Additional details and assumptions of the analytical model are outlined in Appendix 1.

Two other relationships, derived from Equation 5-1 (see Appendix 1), are useful measures of the water table configuration at the midpoint and edges of a hummock. At the midpoint, the maximum water table rise at the centre of the groundwater mound can be estimated as (Haitjema and Mitchell-Bruker, 2005):

$$\frac{\Delta h}{d} = \frac{R}{K} \times \frac{L}{H} \times \frac{L}{d} \times \frac{1}{C} \quad 5-2$$

where maximum hummock height (d), aquifer shape factor (C), and the expected rise in the water table (Δh) are related in terms of ratios in Equation 5-2 (Figure 5-1; note same equation as in Section 3.1). In Equation 5-2, H now represents the average saturated aquifer thickness of the groundwater mound, calculated as:

$$H = \frac{H_c + H_0}{2} \quad 5-3$$

where H is the average aquifer thickness, H_c is the saturated aquifer thickness at the centre of the groundwater mound, and H_0 is the aquifer thickness at the edge of the groundwater mound (i.e. at the bounding edges of a hummock). H_0 can also be conceptualized as the aquifer thickness in the absence of recharge.

The second relationship estimates the water table gradient (i) at the boundary/edge of the groundwater mound (Figure 5-1):

$$i = \frac{1}{2} \times \frac{R}{K} \times \frac{L}{H} \quad 5-4$$

Used in conjunction with the land surface slope (s) at the toe of the hummock, the water table gradient can identify when the water table may be near the land surface:

when $i > s$, water table is estimated to reach land surface near the hummock-lowland interface

when $i < s$, water table is estimated not to reach land surface near the hummock-lowland interface

Effectively, the water table gradient (i) is a simple indication of a hummock's shape (as indicated by s) relative to its performance (as indicated by the water table configuration). Hummock shapes near the toes generally range from convex (higher s) to concave (lower s), as detailed in Section 3.1 and Figure 3-2. In Equation 5-4, it is apparent the water table gradient (i) at the hummock toe only depends on two ratios. At the hummock toe, where $x = 0$, i is the greatest, while at the groundwater divide (i.e. where $\Delta h/d$ is calculated), it is zero. The combination of i (Equation 5-4) and $\Delta h/d$ (Equation 5-2) efficiently provides the reclamation practitioner a sense of the potential water table configuration at the edge and middle of a hummock, respectively, for a given design scenario. See Appendix 1 for further details on the models and their derivations.

5.1.2 Transient Analytical Models

The AOSR climate is characterized by large intra-annual precipitation events, the most pertinent being snowmelt and large, infrequent rainfall events. To determine the effect of large precipitation events on water table configurations and corresponding shifts in local-scale groundwater flow, transient analytical solutions were adapted and modified from van de Giesen et al. (1994). These models were also used to examine the applicability of the steady-state models across a range of recharge values representative of inter-annual climate (i.e. the magnitude of water table variations due to intra-annual versus inter-annual events).

The parameters in the transient analytical models are the same as the steady-state analytical models, except for the specific yield (S_y) which is representative of drainable porosity. In the transient analytical models, recharge is instantaneously applied to the water table; therefore, it is assumed that infiltration of water at the land surface results in displacement of water from the unsaturated zone to the groundwater flow system (see assumptions in Appendix 1). Full details for the transient analytical models developed and derived as a part of this modelling framework are provided in Appendix 1.

5.1.3 Model Calibrations

Both steady-state and transient analytical models were calibrated to field observations from SFW. Detailed explanations of model calibration and performance are provided in Appendix 1. Overall, the calibration exercise demonstrated that the models can represent the general hydrologic behaviour of hummocks, as well as their response to dynamic inputs (i.e. precipitation events).

5.2 Parameter Ranges

To understand the potential range of water table configurations associated with different hummock designs and material properties, it is critical to define realistic design parameter ranges. Parameters in the analytical models detailed in Section 5.1 are related to hummock design/morphological characteristics (i.e. L , d , s) and/or reconstruction material properties characteristic of capping (i.e. K , H , and C), while R is related to coversoil prescriptions, vegetation, and inter-annual climate. Ranges for these parameters are informed by Synocrude's practical experience reclaiming and reconstructing hummocks (i.e. L , d), as well as the greater body of research and investigations on oil sands reclamation that helps to inform our understanding of hydrogeologic properties (i.e. K , H , and C) and coversoil prescriptions (i.e. R).

Table 5-1 summarizes parameter bounds/ranges, based on Syncrude’s reclamation experience and other sources. These parameter ranges were subsequently used to calculate the range of key ratios also included in Table 5-1. The basis for each of the parameter ranges is briefly detailed in Sections 5.2.1 to 5.2.4. It is important to note that these parameter ranges also fall within the range of values observed in natural boreal forest landscapes (Devito et al. 2012).

Table 5-1 Parameter ranges considered in modelling framework based on literature values and Syncrude’s reclamation experience.

Parameter or Ratio	Lower Bound	Upper Bound	Controls on Parameter	Basis/References
Hummock Length (<i>L</i>)	100 m	1000 m	Construction method, area available, mining logistics	Syncrude Operational Designs
Hummock Height (<i>d</i>)	2 m	10 m	Construction method, material availability, mining logistics	Syncrude Operational Designs
Hummock Slope Near Toe (<i>s</i>)	0.5 %	25 %	Construction method	Syncrude Operational Designs
Hydraulic Conductivity (<i>K</i>)	1×10^{-7} m/s	1×10^{-4} m/s	Material availability, depositional characteristics	Price (2005) ¹ ; Ketcheson et al. (2017) ³ ; Thompson et al. (2011) ¹ ; Twerdy (2019) ¹
Aquifer Thickness (<i>H</i>)	3 m	20 m	Construction method; mining logistics	Syncrude Operational Designs
Aquifer Shape Factor (<i>C</i>)	8	16	Shape of reclaimed landform	Haitjema and Mitchell-Bruker (2005)
Recharge (<i>R</i>) ⁴	10 mm/yr	150 mm/yr	Coversoil prescription; inter-annual climate	<i>Recharge</i> : Alam et al. (2019) ² ; Dobchuk et al. (2013) ¹ ; Huang et al. (2015) ¹ ; Lukenbach et al. (2019) ¹ ; Sutton and Price (2020) ³ ; WorleyParsons (2013) ¹ <i>Evapotranspiration</i> : Carey (2008) ¹ ; Carey and Humphreys (2019) ¹ ; Moore (2008) ¹ ; Strilesky et al. (2019) ¹
<i>R/K</i>	1×10^{-6}	1×10^{-1}	See above	Calculated

Parameter or Ratio	Lower Bound	Upper Bound	Controls on Parameter	Basis/References
<i>L/H</i>	5	350	<i>See above</i>	Calculated
<i>L/d</i>	10	500	<i>See above</i>	Calculated

¹Studies conducted/based on Syncrude’s Mildred Lake Lease

²Studies conducted/based on Syncrude’s Aurora North Lease

³Studies conducted/based on Suncor sites

⁴Note that negative net recharge values are possible in the AOSR (c.f. Hokanson et al. 2020); however, negative net recharge likely occurs in systems different than constructed hummocks on CT deposits.

5.2.1 Hummock Dimensions (*L, d, and s*)

Practical and logistical limitations bound the potential range of constructed hummock lengths, heights, and slopes. While some hummock analogues on Syncrude leases are quite tall, most constructed hummocks on CT deposits will likely range from 2 m to 10 m tall, based on currently employed construction methods on Syncrude leases. Hummock lengths are likely to range from 100 m to 1,000 m, based on achievable lowland spacings that facilitate landform drainage. The shape and slope (i.e. *s*) of hummocks is largely governed by the construction method, where hydraulic placement typically results in more gradual slopes compared to cell construction or mechanical placement/reworking (see also Section 3.1 and Figure 3-2).

5.2.2 Hydrogeologic Properties (*K, H, C*)

Tailings sand is currently the primary material used to construct the trafficability cap and create the closure topography layer on CT deposits (McKenna Geotechnical 2020). Hydraulic conductivities (i.e. *K*) for tailings sand span a wide range (i.e. 10^{-7} m/s to 10^{-4} m/s), although the likely bulk hydraulic conductivity of landforms and landform elements comprised of tailings sand generally appears closer to 10^{-6} m/s or 10^{-5} m/s (Goddard 2017; Price 2005; Thompson et al., 2011; Twerdy 2019). Tailings sand exhibits variable grain size distributions, compositions, and is deposited by various methods (McKenna 2002), thus hydraulic conductivities can vary substantially between and within landforms. Variability in hydrogeologic properties associated with variation in tailings deposition is analogous to geomorphologically-induced hydrogeologic properties in natural landscapes (i.e. depositional environment).

Alternative materials have been considered for capping CT deposits. However, capping materials must be relatively permeable on CT deposits to support trafficability (McKenna Geotechnical 2020). Therefore, the hydraulic conductivity range of tailings sand is likely representative of many alternative capping materials.

The thickness of the trafficability cap generally represents the minimum saturated thickness of the aquifer (i.e. *H*). Minimum capping thicknesses must be adequate to support a trafficable reclamation surface; accordingly, the minimum trafficability cap is approximately 2 to 5 m (McKenna Geotechnical 2020). In comparison, construction of the closure topography layer is primarily governed by constraints imposed by material availability and deposit-scale factors related to the overall configuration of landforms and the Life of Mine Closure Plan (Syncrude 2016). As such, a maximum capping thickness of approximately 20 m is

reasonable, given that some areas of CT deposits on Syncrude leases exhibit caps that approach this thickness (Barr Engineering 2020).

The shape factor (C) characterizes whether the aquifer is planar or radial in shape. Only two values are proposed for this constant (8 and 16 for planar and radial, respectively; Haitjema and Mitchell-Bruker 2005). Assuming the aquifer is planar results in a greater estimate of water table rise (i.e. more conservative) relative to the hummock land surface. Therefore, a value of 8 for C is assumed throughout the analyses herein. Nevertheless, aquifers in many reclaimed CT deposits are likely more planar than radial in form.

5.2.3 Recharge (R)

Numerous investigations (see Table 5-1) have examined factors controlling water movement through coversoils in the AOSR, which are indicative of recharge ranges. The amount of precipitation partitioned to recharge is largely controlled by inter-annual climate, coversoil design, and vegetation (Lukenbach et al., 2019). Additionally, because recharge is primarily the manifestation of the water not taken up by plants, evapotranspiration estimates also inform estimated recharge ranges (see Table 5-1).

Investigations at Syncrude sites, Suncor sites, and exploratory modelling studies (see Table 5-1) consistently indicate that recharge and evapotranspiration are largely influenced by the texture and thickness of the coversoil, vegetation, as well as the hydraulic conductivity of the underlying substrate (i.e. what the hummock is constructed of). Finer-textured (i.e. less sandy) coversoils, peat-mineral mixtures (not dissimilar from potting soil), and/or thicker coversoils limit recharge compared to coarser and/or thinner coversoils (Alam et al. 2019; Lukenbach et. 2019; Merlin et al. 2018). Evapotranspiration estimates from oil sands reclamation sites align with studies of recharge; reclaimed pine stands (characterizing AB ecosites with generally sandier coversoils) have lower evapotranspiration rates compared to aspen stands (characterizing D ecosites with generally finer-textured coversoils) (Carey 2008; Moore 2008).

Temporal factors, including inter-annual climate cycles and the successional stage of forest vegetation (as indicated by leaf area indexes and vegetation type), are also key determinants of recharge. Mean annual P is approximately 440 mm, but annual precipitation in this sub-humid climate can vary from approximately 300 mm/yr to 700 mm/yr. Given that $PET:P$ ratios reach a minimum of approximately 0.75 during wet cycles and substrate materials generally exhibit large storage capacity (Devito et al. 2012), overland flow remains limited even in wet years. As such, recharge fluctuations between years can be large, on the order of 50 mm/yr to 100 mm/yr (Alam et al. 2019; Lukenbach et al. 2019). Similarly, the successional vegetation trajectory also imparts a transient control on recharge, where recharge is higher for approximately five to ten years during the initial reestablishment of vegetation relative to when mature forest stands are established.

In summary, the potential recharge range presented in Table 5-1 is a reflection of literature findings, encompassing effects associated with controllable design factors (i.e. coversoil texture, thickness) and uncontrollable factors (i.e. climate, successional trajectories).

5.2.4 Correlations Between Factors

Parameters in the analytical models (see Section 5.1) are largely independent of one another. However, two exceptions are worth noting: 1) the relationship between recharge and hydraulic conductivity; and 2)

the relationship between recharge and hummock height. Recharge is generally lower when the material used to construct a hummock on a CT deposit has a lower hydraulic conductivity because percolation through the coversoil is impeded and water is made available to plants for a longer period of time (Alam et al. 2019; Lukenbach et al. 2019). Effectively, although the height of the groundwater mound beneath the hummock increases with decreasing hydraulic conductivity (i.e. Equation 5-1 and 5-2), this effect is offset or moderated to some degree by decreases in recharge associated with a lower hydraulic conductivity value for a given substrate. For example, for identical coversoils prescribed to two hummocks having different material compositions (i.e. higher vs. lower K), it is likely that recharge is lower for the hummock constructed from the lower hydraulic conductivity material.

When the hummock ground surface/coversoil are in closer proximity to the water table, evapotranspiration is higher, resulting in less recharge or possibly negative net recharge (Lukenbach et al. 2019). The overall magnitude of this effect across an entire hummock may be relatively small, depending on the configuration of the hummock (Lukenbach et al. 2019). However, situations may occur where the water table is shallow across much of a hummock, reducing recharge across the entire landform element.

These two observations highlight how some combinations of R and K are less likely to occur than others. For example, the occurrence of high R with low K is less likely because lower K hummock construction materials are generally understood to reduce recharge. Similarly, particularly short, broad hummocks may not foster appreciable R if the water table is close to the ground surface over a large areal extent of a hummock. Analytical modelling herein does not explicitly account for these parameter correlations; however, the reclamation practitioner can qualitatively acknowledge these parameter correlations by carefully considering which parameter combinations are unlikely to occur.

5.3 Sensitivity Analyses

The following applications demonstrate how the analytical models inform our understanding of hummock design. First, the sensitivity of key water table configuration descriptors ($\Delta h/d$ and i) to varying R/K ratios was assessed, assuming constant hummock dimensions (i.e. L and d) and constant aquifer thickness at the edges of a hummock (i.e. H_0 , note that H inherently changes as a function of R/K based on the formation of the groundwater mound, see Section 5.1.1). Second, the effect of simultaneously varying both hummock dimensions (i.e. L and d) and hydrogeological properties (i.e. R/K) on $\Delta h/d$ and i was determined. Third, the effect of simultaneously varying the R/K ratio and L/H ratio (i.e. varying H_0 with constant hummock length) on $\Delta h/d$ and i was assessed. The sensitivity analyses are representative of long-term hummock hydrologic behaviour (i.e. steady-state analytical solutions) and can also be related to wet, mesic, and dry climatic cycles. Equations 5-2 and 5-4 are the basis for these analyses, where $\Delta h/d$ and the i are calculated across a range of realistic parameter combinations.

5.3.1 Variation in R/K

The effect of different R/K ratios on parameters describing the water table configuration (i.e. $\Delta h/d$ and i) is first illustrated by assessing a hummock with specified dimensions (i.e. 300 m long, 4 m high) and specified aquifer thickness at the edge of a hummock (i.e. $H_0 = 10$ m) as described in Table 3-1. The first case represents a specific scenario for one hummock. A broader range of scenarios, defined by the interaction between R/K ratios and a range of hummock sizes, is later considered in Section 5.3.2.

The water table configuration at the middle of the hummock (i.e. $\Delta h/d$) across a range of R/K values (x-axis) is denoted by the black curve on Figure 5-2a, corresponding to the black, y-axis. Similarly, the water table configuration near the toe of the hummock (i.e. i) is denoted by the red curve, corresponding to the red, right y-axis. Both dashed lines correspond to the black y-axis, where $\Delta h/d = 1$ (black dashed line) indicates the cut-off for a topographically-controlled water table (i.e. water table rise estimated to be equal to the crest elevation of hummock, see Section 3.1) and the blue dashed line corresponds to a water table depth 2 m below the crest of the hummock (i.e. $\Delta h/d = 0.5$; half of the crest height). These cutoff values highlight how the models can be used to assess whether separation between the water table and rooting zone is adequate for a given hummock design. Note, however, that $\Delta h/d$ indicates the maximum separation between the water table and rooting zone on the hummock because d represents the maximum hummock height. Overall, the analysis in Figure 5-2a demonstrates how the reclamation practitioner can quickly get a sense of the anticipated water table configuration for a hummock design with known dimensions, but uncertain hydrogeologic properties or a yet to be determined coversoil prescription.

Figure 5-2b shows an alternative visualization of the same sensitivity analysis, demonstrating how discrete R/K values on Figure 5-2a (denoted by black points) are water table realizations on the cross-section of a hypothetical hummock with a prescribed configuration. Note that a wide range of topographic profiles are possible for a 300 m long, 4 m high hummock. The topographic profile of the hummock shown in Figure 5-2b was chosen for illustrative purposes, where two different configurations of the hummock toe result in possible concave (left) or convex (right) shapes (see Section 3.1 and Figure 3-2 as well).

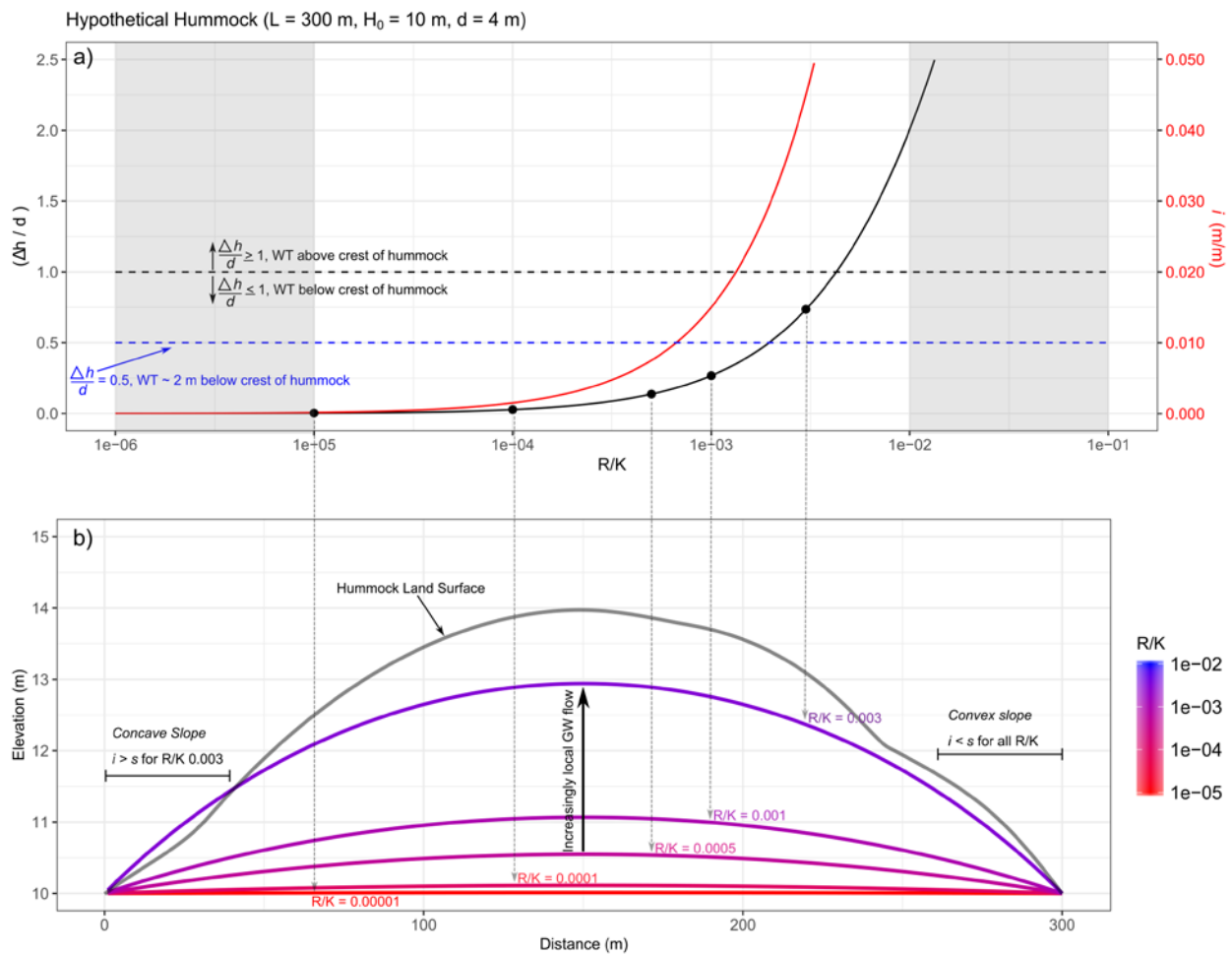


Figure 5-2 a) Sensitivity of parameters $(\Delta h/d, i)$ describing the water table (WT) configuration to the recharge over hydraulic conductivity ratio (i.e. R/K , \log_{10} scale x-axis). The black (red) curve corresponds with the black (red), left (right) y-axis. $\Delta h/d = 1$ (i.e. WT at crest of hummock) and $\Delta h/d = 0.5$ (i.e. WT 2 m below crest of hummock) are denoted with a black and blue dashed line, respectively. Gray shading indicates unlikely R/K ratio ranges. Black points on panel a correspond to WT configurations (coloured lines) associated with specific R/K values (exact values shown in coloured text) in panel b. In b), the gray line denotes the hummock topographic profile, with two differing hummock toe slopes (s): concave slope (left, lower s), convex slope (right, higher s). WT gradient (i) $> s$ for concave slope, and $i < s$ for convex slope. Propensity of local-scale groundwater (GW) flow systems to develop indicated by vertical, black arrow. See Sections 3 and 5.1 for further details and conceptual overview.

Based on the simulated outcomes in Figure 5-2, when the R/K ratio reaches approximately 5×10^{-4} for a hummock with these assumed dimensions, the water table rise at the centre of the hummock starts to be noticeable. This is indicated by $\Delta h/d$ values on Figure 5-2a (black line) and increasingly pronounced groundwater mounds on Figure 5-2b. For $R/K < 5 \times 10^{-4}$, the water table rise is quite modest or not detectable (e.g. R/K value of 10^{-5}), while an R/K value of 3×10^{-3} results in the water table near or at the land surface (Figure 5-2b). A similar effect of R/K on i is observed (red line), although slightly lower R/K values have an appreciable effect on i relative to $\Delta h/d$ for this hummock (as indicated by the earlier rise of

the red curve relative to the black curve in Figure 5-2a). In particular, the value of $i = 0.045$ (4.5% grade) for an R/K value = 3×10^{-3} highlights the contrasting behaviour of concave (left) versus convex (right) slopes. Specifically, for the hypothetical concave slope shown on the left side of Figure 5-2b, $s < i$ for an R/K value = 3×10^{-3} , indicating that the water table is likely to intersect the land surface near the hummock toe. This contrasts with the convex slope on the right side of Figure 5-2b (i.e. $s > i$)

Note that the water table is shown to be above the land surface for $R/K = 3 \times 10^{-3}$ along the concave slope in Figure 5-2b for illustrative purposes only; that is, it indicates the *potential* water table configuration. In other words, an important step in the analytical modelling process is relating the modelled outcomes to the actual hummock topographic profile and determining where the water table is likely to be at the land surface (rather than exceeding the land surface).

The difference in water table configurations between R/K values of 1×10^{-3} versus 3×10^{-3} (illustrated on Figure 5-2b) exemplifies how relatively small changes in R/K can impart large changes on the water table configuration. In practical terms, a change in R/K from 10^{-3} to 3×10^{-3} could correspond to a wet climatic period (~ 95 mm/yr) versus mesic climatic period ($R \sim 30$ mm/yr) for a constructed hummock with a K value of 10^{-6} m/s. Alternatively, this same difference in R could be facilitated by coarse-textured (~ 5 mm/yr) versus fine-textured (~ 30 mm/yr) coversoil prescription (note that this aligns with the recharge contrast found by Lukenbach et al., 2019). Finally, this contrast in R/K (i.e. 10^{-3} vs. 3×10^{-3}) could also represent two constructed hummocks with slightly different K values (i.e. 3×10^{-6} m/s vs. 10^{-6} m/s) that have the same R (assuming recharge of 95 mm/yr). Thus, even smaller changes in K can result in large changes in the proportion of the ground surface in close proximity to the water table (recall Cell 32 vs. 46 at SWSS in Section 4.2).

Water table configurations in the analytical models are also related to groundwater flow patterns, as detailed in Sections 3 and 4 above. As the groundwater mound becomes more pronounced, the propensity for local-scale groundwater flow systems to develop also increases (indicated by black vertical arrow on Figure 5-2b). Thus, the analytical models can also be used to determine the likelihood of local-scale groundwater flow systems forming for different combinations of hydrogeological properties and hummock dimensions.

5.3.2 Covariation in R/K and L/d

Based on the anticipated parameter ranges discussed in Section 5.2 and outlined in Table 5-1, a sensitivity analysis was conducted to examine potential water table configurations associated under both varying hummock dimensions (i.e. L , d) and hydrogeological properties (i.e. K , R). Nine combinations of hummock morphological properties (i.e. L , d) across a continuous range of R/K ratios (assuming a constant $H_0 = 10$ m and $C = 8$) are shown in Figure 5-3. Each panel represents one combination of hummock morphological properties (i.e. L , d). Moving from left to right across the panels, hummock lengths (L) increase, while moving from top to bottom hummock heights (d) decrease. Small, tall hummocks are represented in panel a of Figure 5-3, while large, short hummocks are represented in panel i, aligning with a large range of L/d ratios.

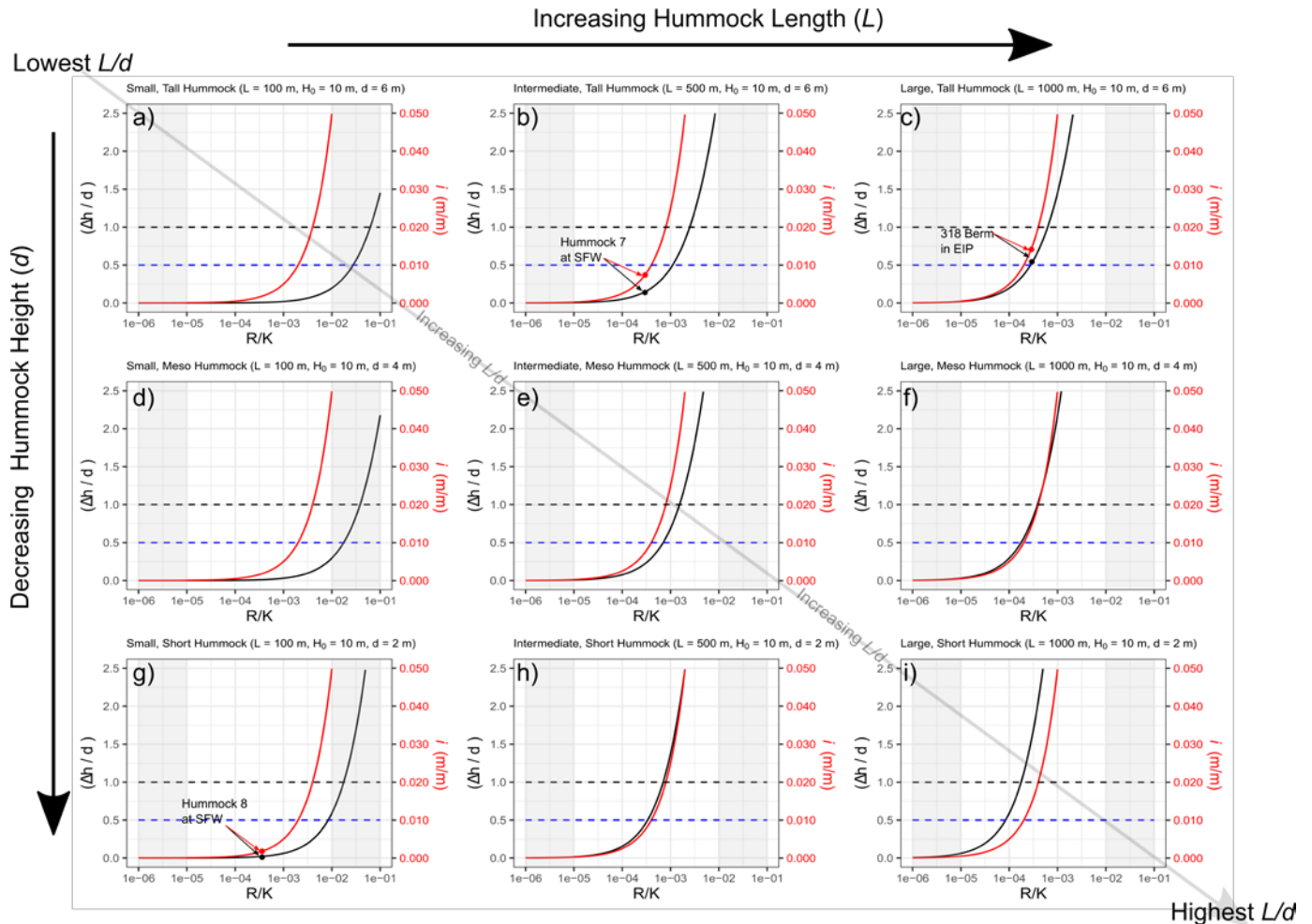


Figure 5-3 Sensitivity analysis of $\Delta h/d$ and i to hummock dimensions (represented by different panels) and R/K values. Hummock length (L) increases from left to right across the diagram, while hummock height (d) decreases from top to bottom. The light gray, diagonal arrow indicates the decreasing trend of L/d across the panels. Select black and red points, corresponding to $\Delta h/d$ and i , respectively, indicate the position actual constructed hummocks (two from SFW, and the 318 Closure Divide in EIP). Layout as in Figure 5-2a (see above).

As hummock length increases from left to right on the panels, the corresponding R/K value that results in the water table reaching the crest of a hummock (i.e. $\Delta h/d = 1$, black dashed line) is lower (Figure 5-3). For example, in panel a versus panel c, the R/K ratio resulting in a water table at the crest of a hummock is approximately two orders of magnitude lower for a 1000 m long hummock (panel c) vs. a 100 m long hummock (panel a). Similarly, as the hummock height decreases from the top of the panels to the bottom, the corresponding R/K values that result in $\Delta h/d = 1$ are lower (Figure 5-3). Nonetheless, across the range of realistic constructed hummock lengths and heights (outlined in Table 5-1), length has a greater influence than hummock height on the distance between the water table and the crest of a hummock.

The leftmost curve (i.e. black vs. red) in Figure 5-3 determines which factor (i.e. $\Delta h/d$ or i) is generally more limiting when designing hummocks. For example, in panel a (i.e. small hummock), s near the hummock toe

would need to be > 0.05 if the R/K value is 0.01 to prevent the water table from intersecting the land surface. Comparatively, for this same R/K value in panel a, the water table depth at the crest of the hummock would be approximately 4.5 m (based on the $\Delta h/d$ value), indicating that separation between the rooting zone and the water table is adequate near the centre of the small hummock. In contrast, for particularly large hummocks (e.g. 1,000 m), the water table rise in the middle of the hummock is likely a greater design consideration, exemplified by relationships on panel i, where the water table is < 1 m below the crest of the hummock for R/K values > 0.0001 . By extension, this means that the water table is also less than 1 m below the land surface on all other parts of the hummock in panel i because calculation of the water table depth at $\Delta h/d$ represents the maximum separation between the water table and the land surface.

Tangible examples of constructed hummocks on Synocrude's leases can be used to more directly relate the sensitivity analysis to existing hummocks. Three constructed hummocks are indicated with black and red points (corresponding to specific values of $\Delta h/d$ and i) in Figure 5-3, spanning a range of constructed hummock dimensions. The interpreted R/K values are based on results from Section 4, based on their coversoil prescriptions and assuming mesic climate conditions. The greater length of the 318 Closure Divide hummock results in a $\Delta h/d$ value of approximately 0.5, indicating that the water table configuration follows the general form of the hummock. Comparatively, Hummock 7 in SFW has a $\Delta h/d < 0.25$, highlighting how the water table configuration does not follow topography and is subject to larger-scale (i.e. deposit-scale) influences (see Section 4.1.2 for further details). In greatest contrast to the 318 Closure Divide hummock is Hummock 8 in SFW, which is a small hummock with a low R/K value that has a water table configuration which does not follow topography and whose behaviour is primarily governed by larger-scale influences. Nevertheless, it is effective at separating the water table from the rooting zone. For all three of these examples, $s > 0.02$ would likely be adequate to prevent the water table from intersecting the land surface at toe of the hummocks (based on values of i).

5.3.3 Covariation in R/K and L/H

The combined effects of varying aquifer thicknesses (i.e. H) and R/K ratios on water table configurations were assessed using the same approach as in Section 5.3.2. Nine combinations of hummock length to aquifer thicknesses (i.e. L/H ratio, assuming a constant $L = 500$ m and $C = 8$) across a continuous range of R/K ratios are shown in Figure 5-4. As aquifer thickness decreases from left to right on the panels, the corresponding R/K value that results in the water table reaching the crest of a hummock (i.e. $\Delta h/d = 1$, black dashed line) is lower (Figure 5-3). Across the range of realistic aquifer thicknesses and hummock heights shown in Figure 5-4, aquifer thickness has a greater influence than hummock height on the distance between the water table and the crest of a hummock. However, by comparing Figure 5-4 to Figure 5-3, it is apparent that hummock length is more influential than aquifer thickness.

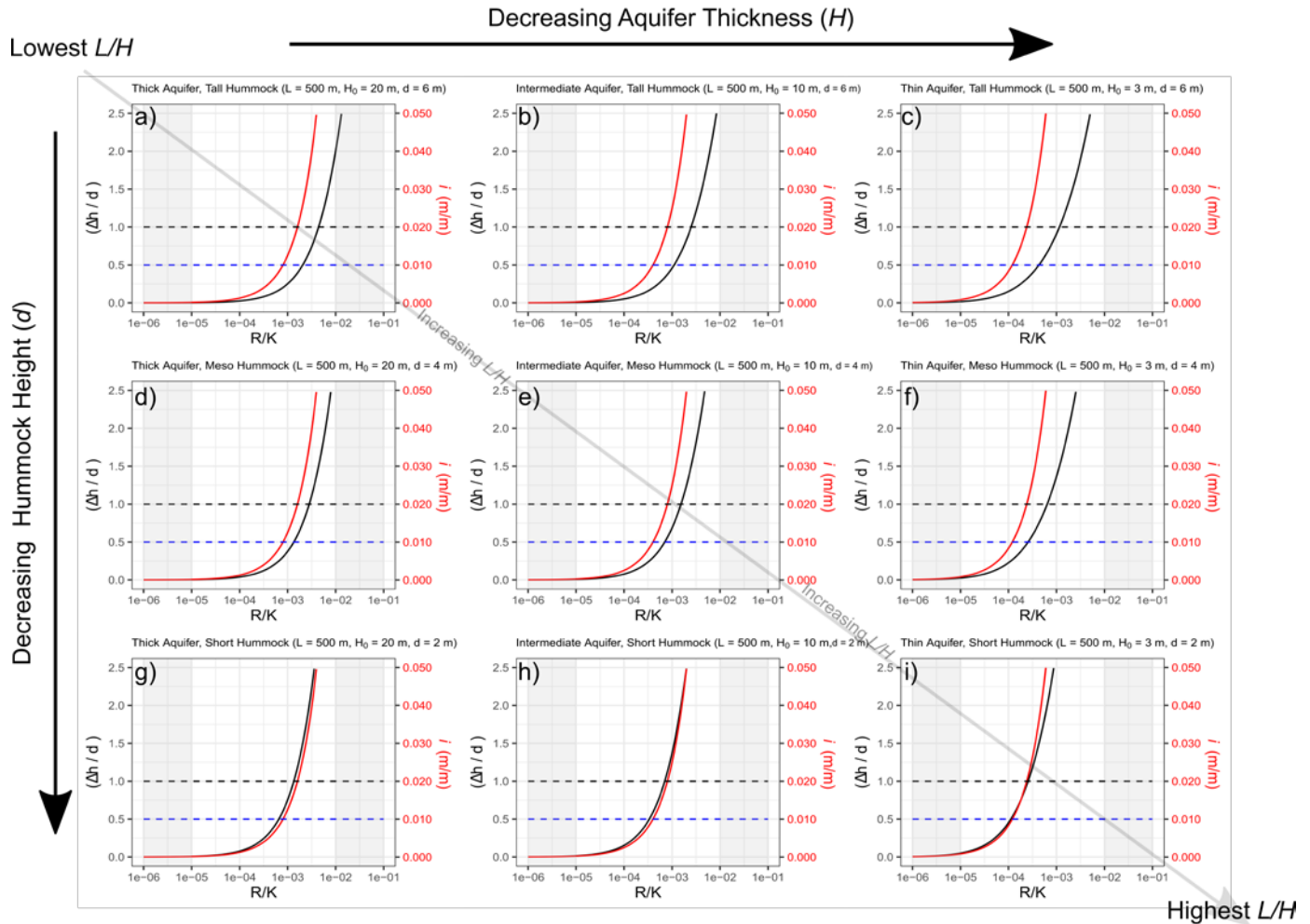


Figure 5-4 Sensitivity analysis of $\frac{\Delta h}{d}$ and i to aquifer thickness (H ; represented by different panels) and R/K values. Aquifer thickness (H) decreases from left to right across the diagram, while hummock height (d) decreases from top to bottom. The light gray, diagonal arrow indicates the decreasing trend of L/H across the panels. Layout as in Figure 5-2a (see above).

Particularly thin aquifers, corresponding to thin caps on CT deposits, increase the likelihood that the water table configuration more closely follows, or intersects, topography (Figure 5-4, assuming constant R/K). Given that cap thicknesses are likely to vary spatially on CT deposits, such an understanding allows reclamation planners to determine the most appropriate hummock designs at a specific location within the landform. Furthermore, particularly small H could result in the displacement of saline, process-affected water by dilute freshwater recharge within the cap beneath constructed hummocks. The occurrence of a freshwater lens overlying process-affected water was observed within SFW (Twerdy 2019; see Section 4.1),

where groundwater flow was primarily characterized by movement within this thin lens. If this freshwater lens represents the “active” groundwater flow system beneath hummocks, aligning with an “effective” aquifer thickness in the modelling framework, it could dictate the water table configuration and associated groundwater mounding (rather than the entire cap thickness).

5.4 Application of Analytical Models to Specific Design Scenarios

To further illustrate the practical applicability of the steady-state analytical models and the usefulness of transient analytical models, specific hummock designs of already constructed hummocks in EIP were evaluated (Figure 5-5). Pairing steady-state and transient models in a unified analysis helps disentangle their relative importance to the water table configuration and, by extension, hummock performance. Field data were not yet available for newly constructed and reclaimed hummocks in EIP. Steady-state models were used to assess the response of three constructed hummocks (i.e. Kingfisher Hummock, Finger Hummock, and East-side Terrace Hummock) to a range of R/K values (see Section 5.4.1). Then, select steady-state outcomes were used to illustrate how large intra-annual precipitation events influenced the water table configurations (see Section 5.4.2).



Figure 5-5 Map of EIP with modelled transects. Transects A, B, and C correspond to the Kingfisher Terrace Hummock, the Finger Hummock, and the East-side Terrace Hummock, respectively. The locations of Sandhill Fen Watershed (SFW), Kingfisher Watershed (KFW), and the 318 Closure Divide are also denoted.

5.4.1 Long-Term Water Table Configurations

True values of recharge and hydraulic conductivity are presently unknown for the three constructed hummocks; therefore, the R/K ratio was varied across a realistic range (10^{-5} to 0.011). Contrasts in

hummock morphological properties (i.e. L , d) between the constructed hummocks in EIP resulted in different simulated water table configurations for the same set of R/K values (Figure 5-6). Aligning with the scenarios in Section 5.3, variability in R/K can represent the effect of multi-year climate cycles (i.e. wet, mesic, dry) and/or different coversoil prescriptions (i.e. coarse versus fine-textured).

Longer hummocks (i.e. terrace hummocks in panels a and c had more elevated water tables than the finger hummock for the same R/K value. R/K scenarios $> 9 \times 10^{-4}$ and $> 3 \times 10^{-4}$ for the Kingfisher and East-side terrace hummock, respectively, were not shown on Figure 5-6, as the simulated water table largely exceeded the land surface, indicating that topography would control the position of the water table under such circumstances. Effectively, the small length of the finger hummock, coupled with its moderate height, allowed it to accommodate a larger range of R/K values and maintain deeper water tables. While the range of simulated R/K values generally did not result in shallow water tables at the crest of the finger hummock (Figure 5-6b), the water table intersected the land surface at the toe of the finger hummock when $R/K > 0.01$ (i.e. $s < i$; Figure 5-6b). Instances of $i > s$ indicate that seepage faces could form at the toe of the finger hummock, depending on R/K .

The analysis of specific design scenarios from EIP also demonstrates how the shape/topographic profiles of actual constructed hummocks may lead to differences in their hydrologic function and behaviour. The shape of the terrace hummocks may lead to the formation seepage faces on the midslope of the hummocks for high R/K values (Figure 5-6). While the modelled water tables beneath the Kingfisher Terrace Hummock, corresponding to the two highest R/K values, were allowed to exceed the land surface in Figure 5-6a for illustrative purposes, they effectively demonstrated how the first break in slope on the Kingfisher hummock would result in the formation of a seepage face at those R/K values. Such spatial variability of the water table configuration across the slope of the terrace hummocks may result in dynamic groundwater interactions under certain circumstances, perhaps not dissimilar from those observed along the benches of Cell 32 at SWSS (see Section 4.2.2).

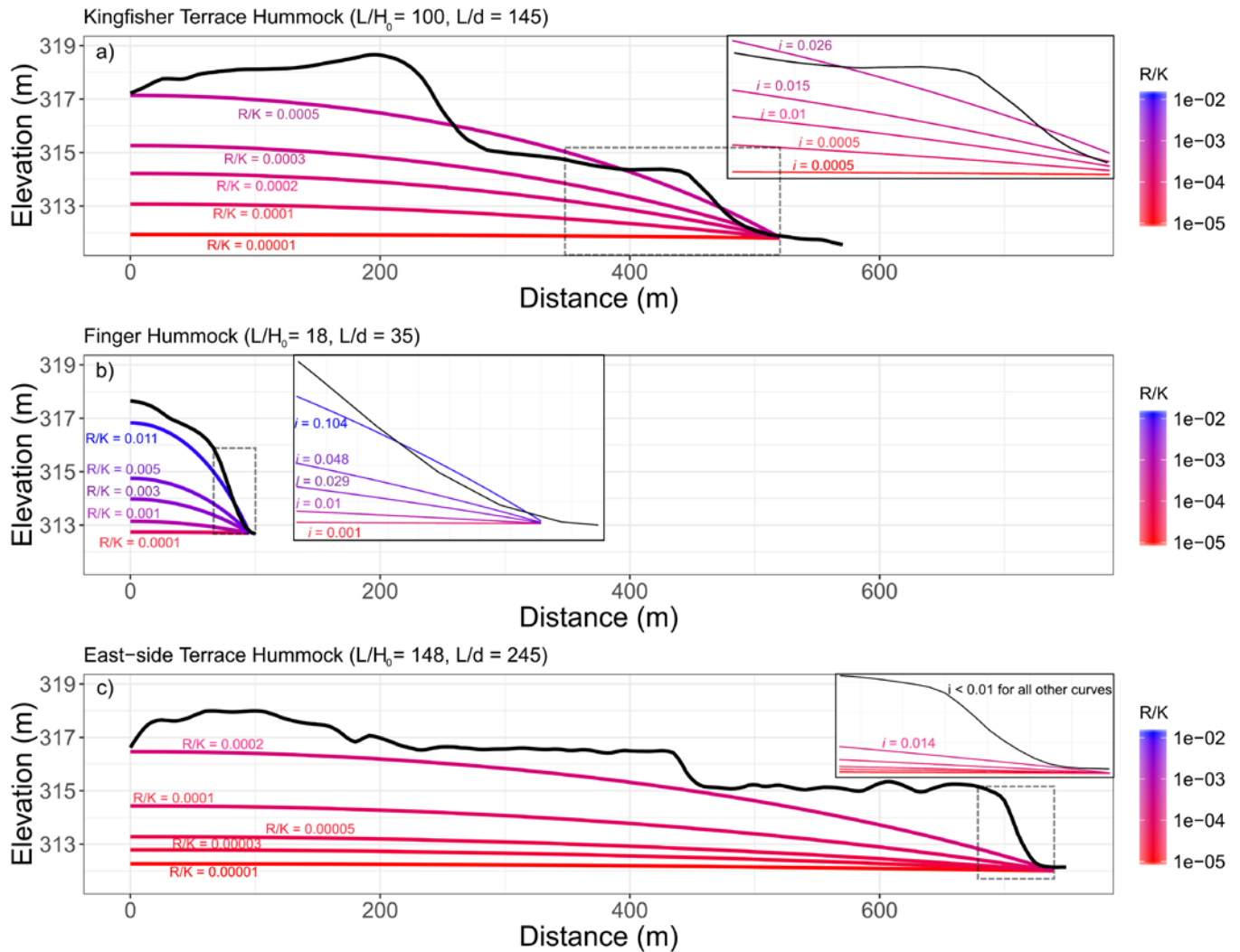


Figure 5-6 Modelled water tables for three constructed hummocks in EIP. Black lines represent the topographic profiles of the hummock transects shown in Figure 5-5. The coloured lines indicate potential water table configurations as a function of R/K values.

Overall, the analyses demonstrate how different water table configurations are a manifestation of the combined effects of design (i.e. L , d , and coversoil effect on R) and hydrogeological properties (i.e. K). If particularly high R/K values are anticipated, smaller hummocks (e.g. like the finger hummock) appear more effective at providing separation between the water table and the rooting zone. Comparatively, larger hummocks may be desirable if R/K values are anticipated to be lower. It should also be noted that hummocks facilitating greater groundwater mounding are also more likely to develop permanent, local-scale groundwater flow systems (and more readily facilitate focused groundwater discharge). Thus, there may be a trade-off between developing local-scale groundwater flow systems that direct water within reclaimed landform elements and ensuring that the water table does not approach the land surface.

5.4.2 Short-Term Transient Influences on Water Table Configurations

The above analyses considered long-term, average water table configurations. Temporal considerations were limited to multi-year climate cycles. Layered on top of the long-term, average behaviour is the effect of intra-annual precipitation events (including snowmelt) that may elevate the water table and affect shallow groundwater flows. Transient analytical models can be used to assess the temporal response of the water table to short-term inputs (i.e. precipitation and snowmelt); see Appendix 1 for further details.

To separate the relative influence of precipitation events (i.e., rain, spring melt) versus mesic/wet climate cycles, scenario tests were conducted for the Kingfisher Terrace Hummock. Similar effects were observed for other hummock types and configurations (results not shown). The influence of short-term, transient events is most relevant during mesic and wet years, when the water table may already be near the land surface. Therefore, a large precipitation event was simulated on top of initial water table configurations corresponding to mesic and wet conditions.

5.4.2.1 Water Table Rise

The initial water table configurations in Figure 5-7 correspond to R/K values of 10^{-4} and 3×10^{-4} for mesic and wet scenarios, respectively (also plotted on Figure 5-6a). Given that these R/K values represent the contrast between mesic and wet cycle cycles, K is constant. Accordingly, a threefold increase in recharge must occur between mesic and wet cycles to achieve this contrast in R/K . It is important to note that this is comparable to variability in recharge generally understood to occur during climate cycles (e.g. 20 mm/yr versus 60 mm/yr; 40 mm/yr versus 120 mm/yr; Devito et al., 2012).

Figure 5-7 shows the effect of a very large, intra-annual precipitation event (100 mm of precipitation over 2 days) on the dynamics of the water table configuration. The size of this event aligns with the largest precipitation events typically observed in the region (Devito et al., 2012). The resultant maximum water tables are dependent on S_y , where lower S_y results in greater water table rises (Figure 5-7). Lower S_y values reflect the fact that there is less available pore space (i.e. storage) to accommodate infiltrating precipitation; therefore, the water table rise is more accentuated.

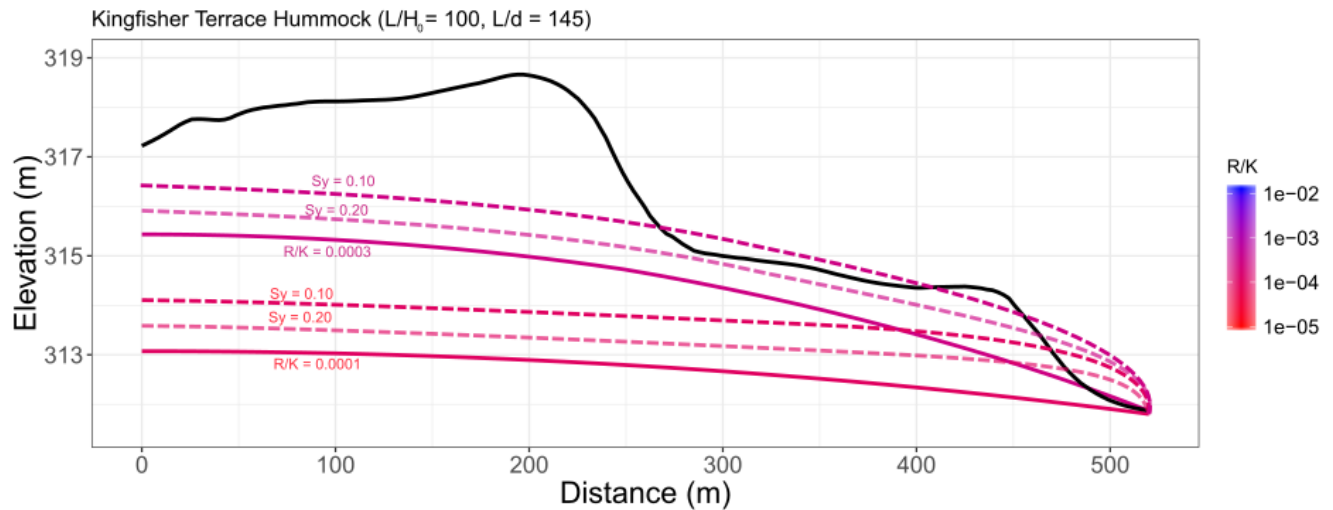


Figure 5-7 Transient scenario tests for the Kingfisher Terrace Hummock. Initial steady-state water tables are indicated by solid lines, while the dashed lines represent different maximum water tables for different S_y values following the addition of 100 mm of precipitation over 2 days.

5.4.2.2 Water Table Recession

In Figure 5-7, R/K ratios represent different recharge values that are used to demonstrate the potential rise in the water table associated with a large precipitation event on top of mesic and wet climatic cycles. However, because the water table recession is primarily controlled by the hydraulic conductivity of the hummock, different hydraulic conductivity values must be used to assess the potential duration of water table recessions. To this end, a second analysis was conducted, shown in Figure 5-8, that assumes a realistic steady-state recharge rate of 30 mm/yr, S_y of 0.10, and the same 100 mm precipitation event occurring over two (2) days. Maintaining R/K values of 10^{-4} and 3×10^{-4} (matching those in Figure 5-7) resulted in corresponding hydraulic conductivities 9×10^{-6} m/s and 3×10^{-6} m/s, respectively.

The more rapid water table recession in Figure 5-8a is due to the higher hydraulic conductivity used in this scenario relative to Figure 5-8b. In both scenarios, however, the recession of the water table is gradual, especially near the centre of the hummock, which is primarily attributable to the relatively long length of the hummock. The relatively long length of the hummock increases the time it takes for water to migrate towards the lowland. Furthermore, the exceptional nature of the precipitation event, being over three times the annual average (i.e. steady-state) recharge rate, also accounts for the slow return of the water table to steady-state conditions. For the $K = 3 \times 10^{-6}$ m/s scenario, the water table configuration rises above the much of the hummock's land surface, indicating the occurrence of seepage and overland flow. Comparatively, the water table remains below the surface across much of the hummock in the $K = 9 \times 10^{-6}$ m/s scenario, although seepage and overland would occur at the hummock toe. Whether 100 mm of recharge can be accommodated by a hummock depends on the hydrogeological properties, initial water table configuration, and size of a hummock. Overall, these scenarios aid in bookending the transient hydrologic behaviour of hummocks and in identifying the potential duration and extent of seepage and overland flow.

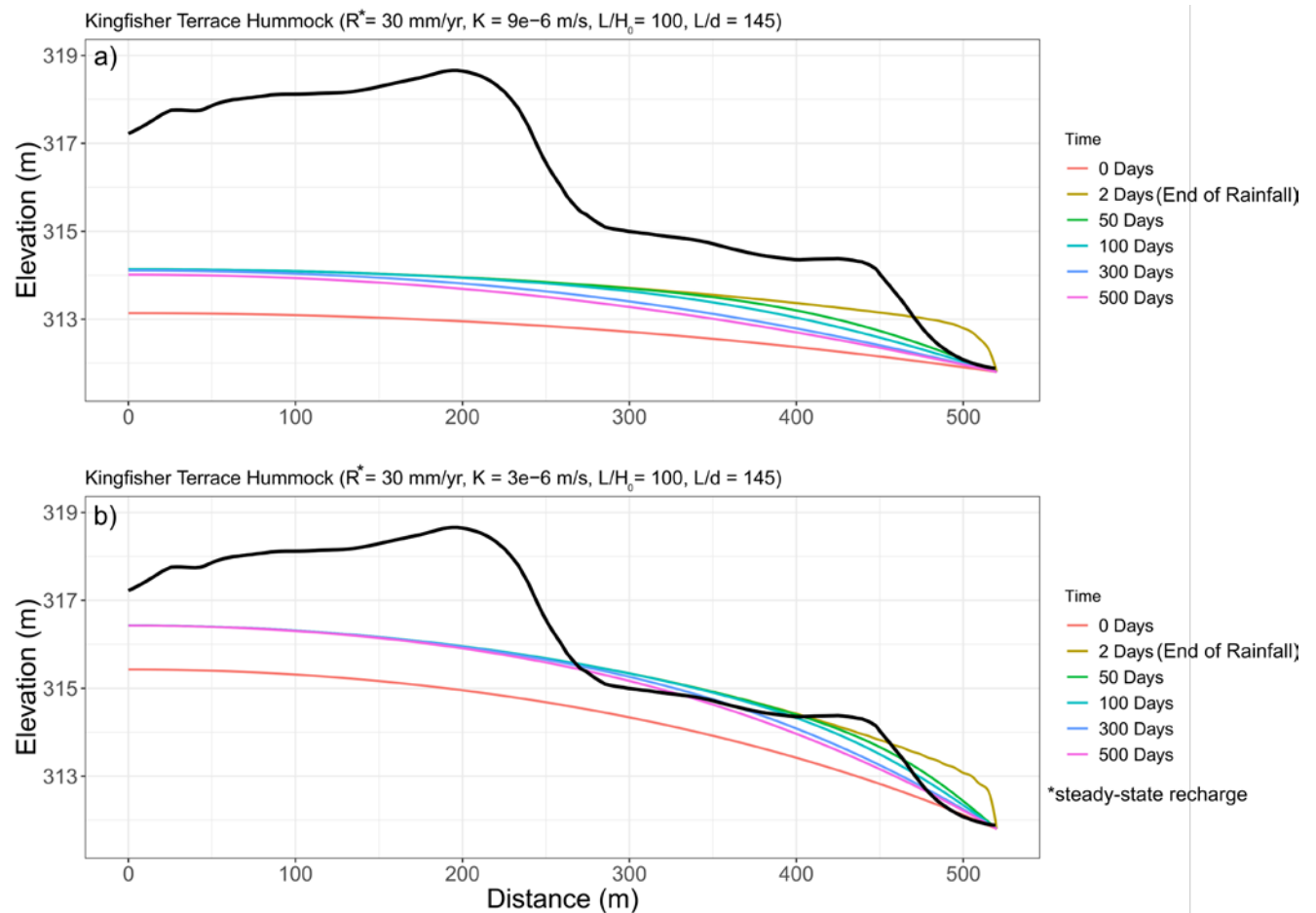


Figure 5-8 Transient scenario tests for the Kingfisher Terrace Hummock for a 100 mm precipitation event over 2 days, showing the rise (Day 0 to Day 2) and fall (50 days, 100 days, 300 days, and 500 days) of the water table (coloured lines). Initial steady-state water table is indicated at Day 0.

5.4.2.3 Comparing Inter-annual and Intra-annual Influences

Results of the transient simulations indicate that inter-annual climate cycles (i.e. mesic versus wet) are likely to impart a greater influence on the water table position than large precipitation events (Figure 5-7). This is further supported by the fact that a 100 mm precipitation event is a very large precipitation event relative to most intra-annual events in the region, and often larger than snowmelt in many years (Devito et al. 2012). However, for particularly low S_y values (i.e. 0.10) or long hummocks with moderate/low hydraulic conductivities (Figure 5-8), the effect of large precipitation events may be appreciable. In the models calibrated to SFW data (detailed in Appendix 1), S_y ranged from 0.20 to 0.25. It is anticipated that SFW has coarser-grained tailings sand than the remainder of EIP, and other constructed hummocks on Syncrude's leases. Therefore, it is possible that S_y values may be as low as 0.10. Overall, the transient analytical models demonstrate that Syncrude can readily evaluate the relative effects of different transient factors (i.e. long-term versus short-term climatic influences) when designing and constructing hummocks to meet targeted hydrologic functions.

5.5 Summary

The demonstrated understanding and developed models show how Syncrude is equipped to analyze hummock performance, as indicated by water table configurations, across a wide range of design scenarios. Analytical models detailed herein not only account for a wide range of static factors (i.e. hummock dimensions and hydrogeological properties), but also dynamic processes associated with the shortest meaningful transient events (i.e. large precipitation events or snowmelt). Depending on the anticipated properties of the capped CT deposit, these models are useful for evaluating how different hummock morphological properties, coversoils, and climatic cycles affect water table configurations. This allows Syncrude to determine suitable hummock designs for a wide range of reclamation scenarios.

The body of oil sands reclamation research and Syncrude's operational designs provide applicable constraints on the potential range of hummock water table configurations. Based on the identified parameter ranges, recharge, hydraulic conductivity, and hummock length exert the largest influence. Furthermore, particularly thin aquifers can have a large effect on water table configurations. To a lesser extent, hummock height can modify the water table configuration; however, more importantly, hummock height and/or morphology generally have a defining role in whether a given water table configuration is useful. Combining this understanding with a general sense of the material properties used to construct hummocks allows Syncrude to assess the feasibility of adjusting different factors during the design process and construction activities to meet targeted hydrologic functions.

Inter-annual climate cycles appear to be a more important design consideration than intra-annual precipitation events. Nevertheless, short-term transient events may be important under certain circumstances. Understanding the variability resulting from these events can help with the design of contingencies and in evaluating risks. Overall, simulating inter-annual climate influences may be sufficient to evaluate whether hummock designs will perform adequately during the "wettest" scenarios (i.e. highest water tables).

Simulated water table configurations not only indicate whether the rooting zone may undergo saturation/salinization, but also the propensity for local-scale groundwater flow systems to develop. As the water table rise increases beneath hummocks, it generally indicates that there is a greater likelihood of local-scale flow. Thus, the analytical models are also a means to assess the general character of groundwater flow systems in reclaimed landform elements.

Applied examples of the analytical models assumed that the water level in lowlands bounding a hummock are the same because the regional gradient is expected to be generally small on capped and reclaimed CT deposits. However, the hydraulic gradient across a hummock may not be flat, as was the case for the largest constructed hummock in SFW (see Section 4.1). Thus, deposit-scale hydrogeological influences may override the influence of hummocks on water table configurations. While not analyzed herein, the models can be adapted to some degree to account for deposit-scale effects (see Appendix 1). Thus, the analytical modelling framework can be extended to account for specific design scenarios where larger-scale, deposit-scale factors are not negligible.

6 Discussion of Uncertainties

Syncrude continues to address uncertainties through its adaptive management framework. Current sources of uncertainty can be broadly categorized as those related to: 1) logistical considerations (e.g. placement techniques, material balances), 2) factors affecting spatial variability, 3) factors affecting temporal variability and/or the timescales currently understood, and 4) limitations of the modelling approaches. Additionally, there may be other factors not considered herein that affect hummock hydrologic functions and performance.

6.1 Logistical Considerations

Tailings sand has been used to construct the trafficability cap and closure topography layer on all Syncrude's CT deposits to date; however, it is likely that alternative materials will be used in the future. Such materials may have different hydrogeological and geochemical properties than tailings sand. The hydrogeological properties of tailings sand are highly variable (see Section 5.2.2), thus the interpretations and modelling herein account for a range of potential behaviours. Nevertheless, until alternative capping materials have been employed at the pilot-scale or field-scale, there will be uncertainty about their implications for hummock hydrologic functions and performance.

Hummocks discussed in Section 4 were constructed using mechanical placement techniques or were mechanically reworked. Alternative hummock construction techniques are being employed by Syncrude, specifically, hydraulic placement. Hydraulically-placed hummocks may exhibit slightly different hydrogeologic properties and hydrologic behaviour than hummocks constructed using mechanical techniques. Additionally, the range of morphological properties characteristic of hydraulically-placed hummocks may be more constrained. For example, achieving abrupt, convex slopes near hummock-lowland interfaces may be challenging because hydraulic placement typically results in more concave slopes and smaller crests. Additionally, hummocks will be initially saturated when hydraulically-placed (versus unsaturated tailings when mechanically constructed), which may affect the temporal trajectory of water table configurations and hummock performance. To address these uncertainties, Syncrude is assessing the performance of hydraulically-placed hummocks through a recently initiated field monitoring program at EIP.

6.2 Factors Affecting Spatial Variability

The influence of deposit-scale factors relative to hummock-scale factors remains a source of uncertainty. Presently, an entire CT deposit has not been reclaimed. Until that occurs, the interaction between deposit-scale factors and hummock-scale factors will remain somewhat uncertain. For example, spatial variability in the hydraulic conductivity and thickness of the trafficability cap/closure topography layer, the CT (e.g. due to deposition and segregation) and/or the combination of CT and coarser tailings will affect how larger-scale groundwater flow systems develop and interact with hummocks (WorleyParsons 2013). Similarly, the spatial organization of hummocks and lowlands across an entire CT deposit (i.e. hummock patterning) are likely to be key controls on the overall hydrologic behaviour of landforms (as detailed in Section 2.2). As Syncrude progresses towards capping and reclaiming entire CT deposits, it aims to evaluate cross-scale interactions between hummock-scale and deposit-scale factors.

Design, construction, reclamation, and monitoring of hummocks on CT deposits remains a relatively new activity. Therefore, additional field data are required to determine how material properties (e.g. hydraulic conductivity) and coversoil placements vary between hummocks. Analyses and modelling demonstrate that such spatial variability can be important to hummock function. Syncrude is addressing this uncertainty by evaluating alternative construction/reclamation techniques and continuing to instrument reclaimed hummocks within EIP and other reclaimed landforms.

An important consideration is the effect of meso- and micro-scale variations in material placement during hummock construction. Spatial variability in material placement is largely uncontrollable at these scales (e.g. hummock toes) but may have an appreciable effect on hydrologic function. For example, finer-grained materials may be more concentrated at hummock toes due to segregation during placement, settlement from compaction or intrusion of lowland construction materials. Such edge effects may have influenced the occurrence of flow reversals at hummock-lowland interfaces in SFW (Spennato et al. 2018). While such variability cannot be explicitly planned for during hummock design, it may create local-scale heterogeneities that diversify hydrologic interactions to the benefit of the entire system.

6.3 Factors Affecting Temporal Variability and Trajectories

Constructed hummocks as well as capped and reclaimed CT deposits are dynamic systems that continue to evolve. Depending on the ratio between recharge and hydraulic conductivity, it may take many years to reach long-term, average hydrologic conditions. Additionally, the coversoil and underlying substrates materials mature over time (Meiers et al. 2011), thereby altering hydraulic properties (e.g. hydraulic conductivities). Possible mechanisms imparting temporal changes in hydraulic properties include freeze-thaw cycles, soil development and root growth (Meiers et al. 2011).

The understanding of hummock temporal trajectories is also currently limited because monitoring data are primarily representative of the effects of the early successional stages of vegetation. Given that hydrologic functions are closely coupled to vegetation assemblages, successional patterns on hummocks will have important consequences for hydrologic functions. For example, modelling studies indicate that the maximum rooting depth eventually reached by upland vegetation is a key control on the partitioning of water between recharge and evapotranspiration (Lukenbach et al., 2019), which could have associated effects on hummock performance. An additional consideration adding uncertainty to the long-term trajectory of constructed hummocks are the potential effects of climate change on the region (Wang et al., 2014). Changes in the magnitude, timing, and phase of precipitation have the potential to alter the temporal trajectories to constructed hummocks. To address these uncertainties, Syncrude has established long-term monitoring networks on hummocks.

6.4 Modelling Limitations

Analytical models employed herein contain simplifying assumptions that may limit their applicability to more complex site scenarios. Additionally, the analytical models were only calibrated to constructed hummocks in SFW. Although data from other constructed hummocks are not yet available, additional calibration data will help refine model applicability. For example, transient analytical models indicate that the water table rise is particularly sensitive to S_y ; further data can help constrain the range of this parameter in constructed hummocks and identify its relationship to measurable quantities (e.g. grain-size distributions).

In circumstances where model outcomes must have greater precision/accuracy, or where site-specific data are known, the application of more advanced numerical models is likely necessary. For example, this is the case when simulating dynamic interactions in the groundwater-soil-plant-atmosphere continuum (c.f., Lukenbach et al. 2019). Likewise, numerical models are also generally required for understanding more complex processes at the scale of entire capped and reclaimed CT deposits (e.g. solute discharge estimates at landform outlets). Syncrude already has experience conducting these types of investigations (e.g. WorleyParsons 2013) and will employ them as needed going forward.

7 Conclusions

The synthesized findings demonstrate Syncrude's current understanding of hummock technology, achieved through extensive applied research programs over the past two decades. Syncrude has an in-depth understanding of hummock design, construction, and performance informed by a variety of investigations, analyses, and interpretations. Syncrude continues to refine its understanding, as evidenced by its continued research and monitoring programs focused on advancing hummock technology.

The sub-humid climate of the region and saline-sodic composition of water associated with capped CT deposits represent key reclamation challenges that hummock technology addresses (see Section 2). By incorporating hummocks into the closure topography layer on capped, reclaimed CT deposits, it is possible to manage water and solute movement. Syncrude's conceptual understanding, founded upon established hydrogeological principles, outlines how hummocks are modifiers of flow and solute movement that can be designed to manage water balance components and water table configurations (see Section 3). Consequently, hummocks can be constructed at appropriate scales and be strategically placed to achieve desirable hydrologic functions within reconstructed landforms.

Hummock performance reflects how effectively hummocks achieve targeted hydrologic functions, including those that are water quantity functions, water quality functions, and landform drainage functions. The water table configuration is a useful and readily measurable metric that can be used to interpret how effective these hydrologic functions are being met by constructed hummocks. Syncrude monitors and evaluates hummock performance relative to these hydrologic functions (see Section 4).

With respect to hydrologic functions, this Synthesis makes the following conclusions:

- Hummocks can be effective at providing separation between the water table and rooting zone.
 - Hummocks prevent saturation and salinization of the rooting zone when water table depths are maintained approximately 2 m below the land surface, aligning with values generally targeted to date by Syncrude (Syncrude, 2016). Note; however, that the necessary separation between the water table and rooting zone is dependent on the specific material properties, coversoil, and vegetation on a hummock.
 - While the available work indicates that an approximate 2 m water table depth is appropriate, hummock shapes also determine the proportion of the land surface close to the water table. Convex hummock shapes/slopes, with abrupt hummock-lowland interfaces, limit the areal extent of shallow water tables across hummocks compared to concave hummock shapes/slopes.
- Constructed hummocks can be used to control the partitioning of precipitation to different water balance components. Given that overland flow is generally rare in the region, precipitation is primarily partitioned between recharge and evapotranspiration. The amount of water partitioned to these two water balance components represents a trade-off between upland vegetation productivity and water for downstream environments. Inter-annual climate cycles, coversoil characteristics (and corresponding vegetation assemblages), and hummock heights determine the magnitude of water partitioned to recharge versus plant water uptake.

- Constructed hummocks can be used to passively manage and flush process-affected water in two ways:
 - Provided hummocks partition adequate amounts of recharge, freshwater percolating into the groundwater system can form freshwater lenses that overlie saline-sodic water. Such solute migration patterns are characteristic of groundwater systems dominated by horizontal flow (i.e. “flow through systems”), where the vertical component of groundwater flow is limited.
 - Hummocks can be used to focus groundwater and solute discharge by facilitating the formation of local-scale groundwater flow systems. Such solute migration patterns occur when the vertical component of groundwater flow is more pronounced.
- The discharge of deeper groundwater associated with the saline-sodic water entrained in the CT deposit appears to be a minor flux of water to the near-surface over the timescales considered; however, consolidation processes may be important (see Figure 2-1).
- Water table configurations beneath hummocks, and associated patterns of flow, are controlled by the ratio of recharge to hydraulic conductivity, hummock lengths, the thickness of the aquifer (related to the thickness of the trafficability cap), and hummock heights. In relative terms, the water table more closely follows the closure topography when there is higher recharge, lower hydraulic conductivity, greater hummock length, shorter hummock height, and lower aquifer thickness.
- Deposit-scale factors may override the influence of hummock morphological and hydrogeological properties, thereby controlling water table configurations and the pattern of groundwater flow/landform drainage. The propensity for hummock-scale factors to dominate over deposit-scale factors is largely dependent on the relative size and configuration of a hummock compared to the influential deposit-scale characteristics (e.g. landform-scale slope, outlet elevations).
- While overland flow tends to be constrained to very wet periods of the climate cycle or high intensity precipitation events on capped and reclaimed CT deposits, the elevated nature of hummocks implies the conveyance of surface water through adjacent lowlands.

SynCrude recognizes that the actual application of hummock technology to reclaimed landforms is still evolving as more experience is gained. To this end, models have been developed to understand hummock performance across a wide range of design scenarios (see Section 5). The models are tools that allow for different combinations of hummock morphological designs and coversoil prescriptions to be assessed when determining their suitability relative to available construction materials and anticipated hydrogeological properties of a capped CT deposit. To complement the models and conceptual understanding, SynCrude is monitoring recently constructed hummocks and landforms in an ongoing effort to better understand and improve hummock technology.

8 References

- Alam, M. S., Barbour, S. L., Huang, M. 2019. Characterizing Uncertainty in the Hydraulic Parameters of Oil Sands Mine Reclamation Covers and its Influence on Water Balance Predictions. *Hydrology and Earth System Sciences Discussion*. DOI: 10.5194/hess-2019-154
- Barr Engineering Inc. 2020. East-in-Pit Deposit Characterization – Revision 1, prepared for Syncrude Canada Ltd, March 2020.
- BGC (BGC Engineering Inc.) 2014a. Construction, Reclamation and Revegetation of Sandhill Fen - As built report, Final Report, prepared for Syncrude Canada Ltd, September 4, 2014.
- BGC (BGC Engineering Inc.) 2014b. Sandhill Fen - As-Built Material Placement Maps, Final Report, prepared for Syncrude Canada Ltd, February 3, 2014.
- Benyon, J. 2014. Characterization of Hydraulic Conductivity Profiles for Sandhill Fen Watershed Reclamation Materials. Undergraduate thesis, Earth and Atmospheric Sciences, University of Alberta, Edmonton, AB.
- Biagi, K. M., Carey, S. K. 2020. The role of snow processes and hillslopes on runoff generation in present and future climates in a recently constructed watershed in the Athabasca oil sands region. *Hydrological Processes*, in press. DOI: 10.1002/hyp.13836
- Biagi, K. M., Oswald, C. J., Nicholls, E. M., & Carey, S. K. 2019. Increases in salinity following a shift in hydrologic regime in a constructed wetland watershed in a postmining oil sands landscape. *Science of The Total Environment*, 653, 1445-1457. DOI: 10.1016/j.scitotenv.2018.10.341
- Booterbaugh A.P., Bentley L.R. & Mendoza C.A. 2015. Geophysical characterization of an undrained dyke containing an oil sands tailings pond, Alberta, Canada. *Journal of Environmental and Engineering Geophysics*, 20: 303-317. DOI: 10.2113/JEEG20.4.303
- Burgers, T.D. 2005. Reclamation of an Oil Sands Tailings Storage Facility: Vegetation and Soil Interactions. M.Sc. thesis, Department of Renewable Resources, University of Alberta, Edmonton, Canada.
- Carey, S. K. 2008. Growing season energy and water exchange from an oil sands overburden reclamation soil cover, Fort McMurray, Alberta, Canada. *Hydrological Processes*, 22(15), 2847–2857. <https://doi.org/10.1002/hyp.7026>
- Carey, S. K., Humphreys, E.R. 2020. The Water and Carbon Balance of the Sandhill Fen Draft Final Report (2013-2018), prepared for Syncrude Canada Ltd, XXXX 2019.
- Devito, K., Mendoza, C., & Qualizza, C. 2012. Conceptualizing water movement in the Boreal Plains. Implications for watershed reconstruction. Synthesis Report Prepared for the Canadian Oil Sands Network for Research and Development. Environmental and Reclamation Research Group. 165. DOI: 10.7939/R32J4H

- Dobchuk, B. S., Shurniak, R. E., Barbour, S. L., O'Kane, M. A., & Song, Q. 2013. Long-term monitoring and modelling of a reclaimed watershed cover on oil sands tailings. *International Journal of Mining, Reclamation and Environment*, 27(3), 180-201. DOI: 10.1080/17480930.2012.679477
- Goddard, M.L. 2017. Material properties and cover options using HYDRUS (2D/3D) for a large undrained sand tailings dam in northern Alberta, Canada. M.Sc. thesis, Faculty of Geosciences, Universiteit Utrecht, Utrecht, Netherlands.
- Haitjema, H. M., & Mitchell-Bruker, S. 2005. Are water tables a subdued replica of the topography? *Groundwater*, 43(6), 781-786. DOI: 10.1111/j.1745-6584.2005.00090.x.
- Hokanson, K. J., Peterson, E.S., Mendoza, C. A., & Devito, K. J. 2020. Forestland-peatland hydrologic connectivity in water-limited environments: hydraulic gradients often oppose topography. *Environmental Research Letters*, 15, 034021. DOI: 10.1088/1748-9326/ab699a
- Huang, M., Barbour, S.L., & Carey, S.K. 2015. The impact of reclamation cover depth on the performance of reclaimed shale overburden at an oil sands mine in Northern Alberta, Canada. *Hydrological Processes*, 29(12), 2840–2854. <https://doi.org/10.1002/hyp.10229>
- Johnson, E. A., & Miyanishi, K. 2008. Creating new landscapes at Alberta oil sands. *Annals of the New York Academy of Sciences*, 1134, 120-145. DOI: 10.1196/annals.1439.007
- Ketcheson, S. J., & Price, J.S. 2016. Comparison of the hydrological role of two reclaimed slopes of different ages in the Athabasca oil sands region, Alberta, Canada. *Canadian Geotechnical Journal*, 53: 1533–1546. DOI: 10.1139/cgj-2015-039
- Ketcheson, S. J., Price, J.S, Sutton, O., Sutherland, G., Kessel, E., Petrone, R.M. 2017. The hydrological functioning of a constructed fen wetland watershed. *Science of The Total Environment*, 603-604, 593-605. DOI: 10.1016/j.scitotenv.2017.06.101
- Lukenbach, M. C., Spencer, C. J., Mendoza, C. A., Devito, K. J., & Landhäuser, S. M. 2019. Evaluating how landform design and soil covers influence groundwater recharge in a reclaimed soft tailings deposit. *Water Resources Research*, 55. DOI: 10.1029/2018WR024298
- Longval, J., & Mendoza, C. 2014. Initial Hydrogeological Instrumentation and Characterization of Sandhill Fen Watershed, Final Report, prepared for Syncrude Canada Ltd, Department of Earth and Atmospheric Science, University of Alberta, Edmonton, Alberta.
- McKenna Geotechnical 2020. Syncrude's Experience with Capping and Trafficking Composite Tailings, prepared for Syncrude Canada Ltd, August 2020.
- McKenna, G.T. 2002. Landscape engineering and sustainable mine reclamation. PhD Thesis, Department of Civil and Environmental Engineering, University of Alberta, Edmonton. 660p
- Meiers, G., Barbour, S.L., Qualizza, C., & Dobchuk, B. 2011. Evolution of the hydraulic conductivity of reclamation covers over sodic/saline mining overburden. *Journal of Geotechnical and Geoenvironmental Engineering*, 137(1): 968–976. [https://doi.org/10.1061/\(ASCE\)GT.1943-5606.0000523](https://doi.org/10.1061/(ASCE)GT.1943-5606.0000523)

- Merlin, M. Leishman, F., Errington, R. C., Pinno, B.D., & Landhäusser, S. M. 2018. Exploring drivers and dynamics of early boreal forest recovery of heavily disturbed mine sites: a case study from a reconstructed landscape. *New Forests*, 50(2), 217-239. DOI: 10.1007/s11056-018-9649-1
- Moore, P.A. 2008. Micrometeorological fluxes and controls on evapotranspiration for a jack pine stand growing on reclamation soil cover, Fort McMurray, Alberta, M.Sc. Thesis, Carleton University, Ottawa, Ontario, Canada, 162 pp.
- Naeth, M.A., Chanasyk, D.S., and Burgers, T.G. 2011. Vegetation and soil water interactions on a tailings storage facility in the Athabasca oil sands region of Alberta Canada. *Physics and Chemistry of the Earth*, 36, 19–30.
- Nichols, E. M., Carey, S. K., Humphreys, E. R., Clark, M. G., & Drewitt, G. B. 2016. Multiyear water balance assessment of a newly constructed wetland, Fort McMurray, Alberta. *Hydrological Processes*, 30(16), 2739-2753. DOI: 10.1002/hyp.10881
- OKC (O’Kane Consultants Inc.) 2007. Instrumented watershed monitoring program at the Southwest Sands Storage facility monitoring data summary report for the period January 2006 to December 2006. Report prepared for Syncrude Canada Ltd.
- Pollard, J., McKenna, G. T. 2018. Design of Landform Elements for Mine Reclamation.
- Qualizza, C. and McKenna, G. 2007. Minimum CT tailings sand capping requirements. Internal Syncrude Canada presentation.
- Schwartz, F. W., Crowe, A. S. 1987. Model Study of Some Factors Influencing the Resaturation of Spoil Following Mining and Reclamation. *Journal of Hydrology*, 44, 121-147. DOI: 10.1016/0022-1694(87)90092-8
- Spennato, H. M., Ketcheson, S. J., Mendoza, C. A., & Carey, S. K. 2018. Water table dynamics in a constructed wetland, Fort McMurray, Alberta. *Hydrological Processes*, 32(26), 3824-3836. DOI: 10.1002/hyp.13308
- Sutton, O.F., Price, J.S. 2020. Modelling the hydrologic effects of vegetation growth on the long-term trajectory of a reclamation watershed. *Science of the Total Environment*, 734, 139323. DOI: 10.1016/j.scitotenv.2020.139323
- Strilesky, S.L., Humphreys, E.R., & Carey, S.K. 2017. Forest water use in the initial stages of reclamation in the Athabasca Oil Sands Region. *Hydrological Processes*, 31(15), 2781–2792. <https://doi.org/10.1002/hyp.11220>
- Syncrude (Syncrude Canada Ltd.) 2016. Syncrude 2016 EPEA Renewal Application.
- Syncrude (Syncrude Canada Ltd.) 2020. Sandhill Fen Watershed: learnings of a reclaimed wetland on a CT deposit.
- Thompson, R. L., Mooder, R. B., Conlan, M. J. W., & Cheema, T. J. 2011. Groundwater flow and solute transport modelling of an oil sands mine to aid in the assessment of the performance of the planned closure landscape. In Fourie A. Tibbett, M., & Beersing A. (Eds.), *Mine Closure 2011*:

Proceedings of the Sixth International Conference on Mine Closure. September 18-21, 2011 Lake Louise, Alberta. Australian Centre for Geomechanics. Nedlands, Western Australia. Volume 2: Post-Closure Monitoring and Responsibilities. 389-398. DOI: 10.36487/ACG_rep/1152_107

- Twerdy, P. 2019 Hydrogeological Considerations for Landscape Reconstruction and Wetland Reclamation in the Sub-humid Climate of Northeastern Alberta, Canada. Alberta, Canada. M.Sc. thesis, Department of Earth and Atmospheric Sciences, University of Alberta, Edmonton, Canada. <https://doi.org/10.7939/r3-zpg2-6p77>
- Vitt, D. H., House, M., & Hartsock, J. 2016. Sandhill Fen, An initial trial for wetland species assembly on in-pit substrates: Lessons after three years. *Botany*, 94, 1015-1025. DOI: 10.1139/cjb-2015-0262
- Wang Y., Hogg, E. H., Price, D. T., Edwards, J., Williamson, T. 2014. Past and projected future changes in moisture conditions in the Canadian boreal forest. *Forestry Chronicle*, 90, 678-91
- Winter, T. C. 2001. The concept of hydrologic landscapes. *Journal of the American Water Resources Association*, 37(2), 335-349. DOI: 10.1111/j.1752-1688.2001.tb00973.x
- Winter, T. C., Rosenberry, D. O., & LaBaugh, J. W. 2003. Where does the ground water in small watersheds come from? *Groundwater*, 41(7), 989-1000. DOI: 10.1111/j.1745-6584.2003.tb02440.x
- WorleyParsons (WorleyParsons Canada Services Ltd.) 2013. Final East-in-Pit Reclamation Landform Design – Hydrological and Hydrogeological Modelling (Project No: 307076-04440), Final Report, prepared for Syncrude Canada Ltd, July 3, 2013.
- Wytrykush, C., Vitt, D., Mckenna, G., & Vassov, R. 2012. Designing landscapes to support peatland development on soft tailings deposits. In D. Vitt & J. Bhatti (Eds.), *Restoration and Reclamation of Boreal Ecosystems: Attaining Sustainable Development*. Cambridge: Cambridge University Press. DOI: 10.1017/CBO9781139059152.011

9 Closure

We trust that this report satisfies your current requirements and provides suitable documentation for your records. If you have any questions or require further details, please contact the undersigned at any time.

Report Prepared by:

Max Lukenbach, Ph.D.
Groundwater Scientist

Pam Twerdy, M.Sc., G.I.T.
Hydrogeologist
Sub-consultant (BGC Engineering Inc.)

Senior Review by:



Trevor Butterfield, M.Sc., P.Geo.
Principal Hydrogeologist



Carl Mendoza, Ph.D., P.Eng., P.Geo.
Principal Hydrogeological Engineer
Sub-consultant (BGC Engineering Inc.)

Water
Advisian Americas

PERMIT TO PRACTICE	
WORLEY CANADA SERVICES LTD.	
RM SIGNATURE:	
RM APEGA ID #:	53315
DATE:	27 Aug 2020
PERMIT NUMBER: P000725	
The Association of Professional Engineers and Geoscientists of Alberta (APEGA)	



Appendix 1
Detailed Description of Analytical Models,
Assumptions, and Calibration

Appendix 1 Detailed Description of Analytical Models, Assumptions, and Calibration

A1.1 Steady-State Analytical Models

A1.1.1 Introduction

Hummocks, which are a component of the closure topography layer, combined with the underlying trafficability cap on Composite Tailings (CT) deposits constitute an unconfined aquifer. The analytical models described in this section solve for the average, long-term (i.e. steady-state) water table configuration in an unconfined aquifer using the Dupuit-Forchheimer approximation. These analytical models are widely applied in hydrogeology (Freeze and Cherry 1979). In the context of hummocks in the Athabasca Oil Sands Region (AOSR), these analytical models can also be applied to represent interannual climate cycles (i.e. wet, mesic, and dry conditions) because climate cycles are multi-year events in the AOSR.

A1.1.2 Solutions

The Dupuit-Forchheimer model of groundwater flow was used to simulate water table configurations (see Figure 5-1 in main report). Detailed derivations and explanations of Equations 1-1, 1-2, and 1-3 are provided by Haitjema (1995) and Haitjema and Mitchell-Bruker (2005). The general form of the Dupuit-Forchheimer solution is:

$$h(x)^2 = H_1^2 - (H_1^2 - H_2^2) \frac{x}{L} + \frac{R}{K} (L - x)x \quad 1-1$$

where water levels (h) for all positions (x) are dependent on recharge (R), hydraulic conductivity (K), and the distance between hydrological boundaries (L). H_1 and H_2 indicate the water levels (and corresponding aquifer thicknesses) in the bounding lowlands. Compared to the main report, the H term has been separated into two variables (H_1 and H_2) to represent how bounding water level elevations and corresponding aquifer thicknesses may differ on either side of a hummock (i.e. in adjacent lowlands; Equation 5-1 in the main report assumes water level elevations are the same). Effectively, this more general equation can represent more complex lowland configurations and landform drainage patterns characterizing hummock landform elements (i.e. deposit-scale influences). Applications of the models in Section 5 of the main report conduct analyses with $H_1 = H_2$.

Equation 1-1 may be rearranged (see Haitjema [1995] for derivation) to relate the maximum height of the groundwater mound to the height of a hummock. This entails solving for the maximum height of the groundwater mound at the groundwater divide (i.e. at $x = L/2$), requiring $H_1 = H_2$, and dividing both sides of the equation by the maximum height of the hummock (d), which yields:

$$\frac{\Delta h}{d} = \frac{R}{K} \times \frac{L}{H} \times \frac{L}{d} \times \frac{1}{C} \quad 1-2$$

where the expected rise in the water table (Δh) is a function of the same parameters defined above and an aquifer shape factor (C). C corresponds to whether the Dupuit-Forchheimer model is derived assuming a planar or radial flow system, where $C = 8$ for planar and $C = 16$ for radial (Haitjema 1995). Additionally, H now represents the average aquifer thickness (Haitjema 1995), which is defined as:

$$H = \frac{H_c + H_0}{2} \quad 1-3$$

where H_c is the aquifer thickness at the centre of the groundwater mound and H_0 is the aquifer thickness at the edge of the groundwater mound (i.e. at bounding edges of a hummock). H_0 can also be conceptualized as the aquifer thickness in the absence of recharge beneath a hummock.

Equation 1-2 represents a useful metric of the water table configuration at the centre of a hummock. To supplement this metric with a measure of the water table configuration at the hummock toe (i.e. edge of a hummock), we derived an expression of the water table gradient (i). This second metric can identify when the water table may be near the land surface, or intersects it, if used in conjunction with the land surface slope (s) at the hummock toe. In Equation 1-1, the slope of the water table at any point x is i , which is greatest at the toe of the hummock and zero at the groundwater divide. To find i at $x = 0$ (i.e. at hummock toe), the slope can be derived by taking the spatial derivative of the Dupuit-Forchheimer model and evaluating for $x = 0$. This procedure yields:

$$i = \frac{1}{2} \times \frac{R}{K} \times \frac{L}{H} \quad 1-4$$

Used in conjunction with the land surface slope (s) at the toe of the hummock, the water table gradient can identify when the water table may be near the land surface:

when $i > s$, water table estimated to reach land surface near the hummock-lowland interface

when $i < s$, water table estimated not to reach land surface near the hummock-lowland interface

A1.1.3 Assumptions

The Dupuit-Forchheimer model assumes that the aquifer is homogeneous, isotropic, and groundwater flow is one-dimensional in a horizontal direction. In general, this is appropriate when L is large relative to H (Haitjema 1995):

$$L \gg \sqrt{\frac{K_h}{K_v}} H$$

1-5

where K_h is the horizontal hydraulic conductivity and K_v is the vertical hydraulic conductivity. In general, the Dupuit-Forchheimer approximation is applicable if L is five times greater than the right side of the above expression. Tailings sands has been observed to range from isotropic (i.e. $K_h = K_v$) to highly anisotropic (Ketcheson et al. 2017; McKenna 2002). A 10:1 anisotropy ratio between K_h and K_v is the most generally assumed ratio. If anisotropy is greater than anticipated in the application of the analytical models, the analytical models will underpredict the water table rise/groundwater mounding height.

A1.1.4 Calibration

The steady-state analytical models were coded in the R programming language. To demonstrate that the analytical models can adequately represent field conditions under long-term, average (i.e., steady-state) conditions, available data from Sandhill Fen Watershed (SFW) were used for calibration (Twerdy 2019). Two transects (Figure A2-1), with different cross-sectional profiles and detailed field data were selected. For both transects, the model boundaries aligned on one side with the lowland in SFW, while the groundwater divide (i.e. symmetry boundary) associated with the 318 Closure Divide represented the other boundary. To represent the groundwater divide at the location shown on the 318 Closure Divide shown on Figure A2-1 in the context of the Equation 1-1, the length of the model domain was doubled with the same head assumed on either side (i.e. $H_1 = H_2$). This allowed us to force a no flow boundary (i.e. symmetry boundary) to occur in the middle of the model domain, aligning with the location of the 318 Closure Divide.



Figure A2-1 Location of modelled transects within SFW used in calibration, aligning with those discussed in detail Twerdy (2019)

Average water table conditions along the two transects were fit to the parameters from Equation 1-1 and are listed in Table A2-1. A comparison between the observed and modelled water table configuration along each transect is shown in Figure A2-2.

Table A2-1 List of parameters used in steady-state calibrations for Transect 1 and Transect 2 in SFW

Parameter (unit)	Transect 1	Transect 2
H ₁ (m)	10	10
H ₂ (m)	10	10
L ^a (m)	970	690
R/K (unitless)	3.2 x 10 ⁻⁵	6.3 x 10 ⁻⁴

^aThis is twice the distance shown in Figure A2-1 because we force the groundwater divide to occur at L/2 (i.e. one end of each transect in Figure A2-1 aligns with the 318 Closure Divide) by doubling the length of the transect and setting H₁ = H₂ (i.e. symmetry boundary).

Water table data were averaged over a four-year collection period (2013 to 2017), during which time the leftmost 190 m and 175 m of Transect 1 and Transect 2, respectively, (i.e. area around 318 Closure Divide) were yet to be reclaimed with coversoils (i.e. recharge was higher than the remainder of the transects). Models were calibrated to R/K values, instead of a single set of recharge and hydraulic conductivity values. This was because a number of parameter combinations of recharge and hydraulic conductivity values adequately fit the observed water table configurations.

Overall, the water table fits for both transects provided confidence in the ability of the models to adequately capture the general configuration of the water table. The fitted R/K values fell within the range of R/K values obtained from a more complex three-dimensional numerical model (i.e. R/K ranged from 9.8 x 10⁻⁵ to 2.2 x 10⁻⁴ in the numerical model) developed by Twerdy (2019). Results may have differed slightly from those in Twerdy (2019) due to the differences in the modelled location of the groundwater divide and/or spatial heterogeneity in material properties between Transects 1 and Transects 2 that necessitated different R/K values for Transect 1 versus Transect 2. Such local-scale variability in material properties between the two transects were averaged out within the three-dimensional numerical model (Twerdy 2019), which may explain why R/K values from Twerdy (2019) fell between those obtained from analytical modelling at the two transects. Given that the bulk hydraulic conductivity of tailings sand within SFW likely falls between 5 x 10⁻⁶ m/s and 5 x 10⁻⁵ m/s (Twerdy 2019), this implies that the absolute values of recharge along the transects likely fall between approximately 30 mm/yr to 150 mm/yr. This recharge range is comparable to that used by Twerdy (2019).

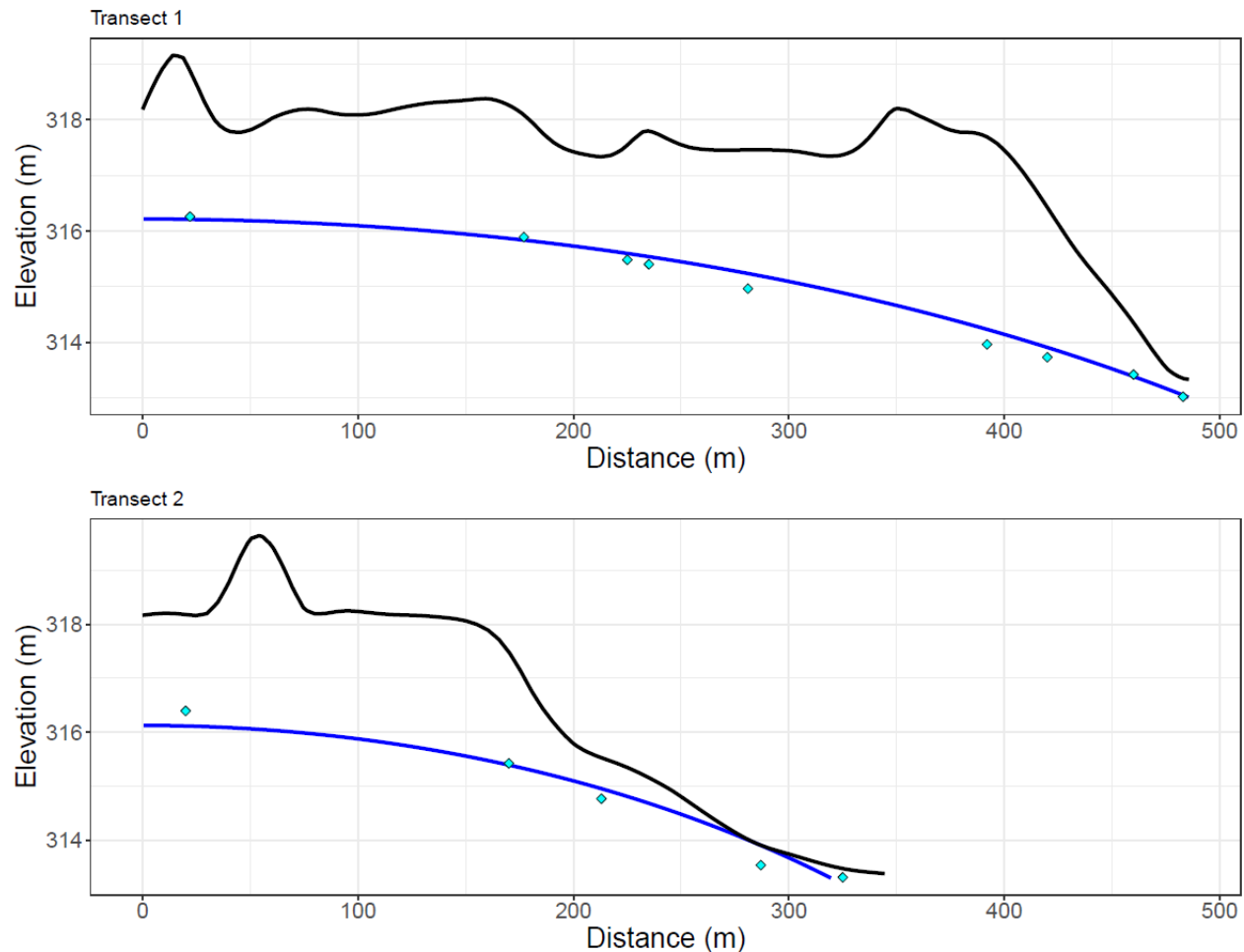


Figure A2-2 Measured (light blue diamonds) and modelled water tables (solid blue lines) along two transects in SFW, aligning with transects detailed by Twerdy (2019). The black line indicates the topographic profile. Note that the left boundary on both modelled transects corresponds to a symmetry boundary (hence L/2 is shown relative to the parameters in Table A2-1).

A1.2 Transient Analytical Models

A1.2.1 Introduction

The AOSR climate is characterized by large intra-annual precipitation events, the most pertinent being snowmelt and large, infrequent rainfall events. To determine the effect of large precipitation events on the rise and fall of the water table beneath a hummock, transient analytical solutions were adapted and modified from van de Giesen et al. (1994). The goal of the transient simulations was to evaluate the response (i.e. rise and subsequent fall) of the water table to a finite, short duration (~1 to 2 days) precipitation event. Steady-state analytical modelling (see above) informed the initial water table positions used as the initial conditions in the transient simulations.

In the equations adapted from van de Giesen et al. (1994), precipitation is applied uniformly across the entire spatial extent of the water table in the model domain and is constant throughout time. Given the duration of the precipitation event (1 to 2 days) and hummock lengths investigated (100 m to 1,000 m), the application of constant and uniform recharge is justifiable as a first-order approximation. The solution's applicability in simulating the effect of precipitation on water tables beneath hummocks is described in greater detail below.

A1.2.2 Boundary and Initial Conditions

For our situation, the aquifer is assumed to overlie an impermeable base, and is bounded on both sides (i.e. at $x = 0$ and $x = L$, where L is the length of the hummock) with two constant head boundary conditions, written as:

$$\begin{aligned}\phi(0, y, t) &= H_1 \\ \phi(L, y, t) &= H_2 \\ \frac{\partial \phi(x, 0, t)}{\partial y} &= 0\end{aligned}\tag{1-6}$$

where ϕ is the hydraulic potential, x and y are the horizontal and vertical coordinates, respectively, and t is time. A diagram of the aquifer is shown in Figure A2-3. For the initial condition, we utilize the general form of the Dupuit-Forchheimer equation (note that this is same as Equation 1-1 except explicitly having the y coordinate equal to 0):

$$h(x, 0) = \sqrt{H_1^2 - (H_1^2 - H_2^2)(x/L) + (R/K)(L - x)x}\tag{1-7}$$

where R is the steady-state recharge when $t < 0$, and K is the hydraulic conductivity of the aquifer.

A1.2.3 Assumptions

The aquifer is assumed to be homogeneous and isotropic, characterized by a single constant hydraulic conductivity K , and a single value for drainable porosity. It is also assumed that the drainable porosity is equal to the specific yield S_y . It is further assumed that there is no contribution from the capillary fringe, and that recharge is constant (within the applied duration), uniform across the domain, and instantaneous applied to the top of the water table.

A1.2.4 Transient Analytical Solution

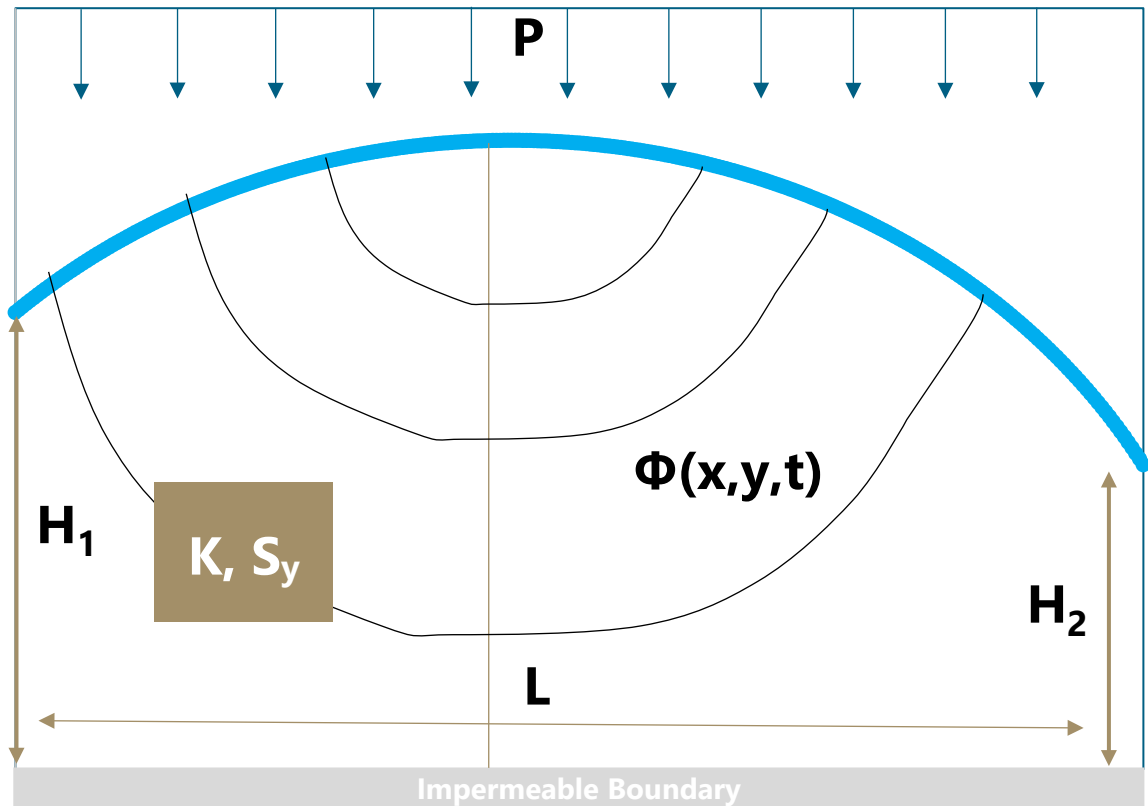


Figure A2-3 Conceptual sketch of the mathematical model

The modelling scenario is shown in Figure A2-3. For the purposes of our analysis, we wanted to obtain generalized equations to simulate the rise and fall of the water table due a recharge event. Expressions in van de Giesen et al. (1994), specifically Equations 40 and 43, were modified for use in our scenario. However, with modification (outlined in detail below), they were successfully applied for our purposes.

For a recharge event of rate P from $t = 0$ to $t = t_0$, which is in addition to average recharge (R), we obtain an expression (Equation 1-8) similar to that derived by van de Giesen et al. (1994; Equation 40 therein).

For $0 \leq t \leq t_0$:

$$\phi_1(x, y, t) = \sqrt{H_1^2 - (H_1^2 - H_2^2)(x/L) + (R/K)(L-x)x} + \sum_{n=1,3,\dots}^{\infty} \frac{4PL}{Kn^2\pi^2} \sin\left(\frac{n\pi x}{L}\right) \frac{\cosh\left(\frac{n\pi y}{L}\right)}{\sinh\left(\frac{n\pi H_1}{L}\right)} \left(1 - \exp\left[-\frac{K}{S_y} \tanh\left(\frac{n\pi H_1}{L}\right) \frac{n\pi}{L} t\right]\right) \quad 1-8$$

In its application herein, the recharge event ceases at $t = t_0$.

Similarly, for the falling limb of the simulation, Equation 43 from van de Giesen et al. (1994) was modified such that the water table position at $t = t_0$ from Equation 1-8 is the starting position for the falling limb (i.e. following cessation of the precipitation event).

For $t > t_0$:¹

$$\phi_2(x, y, t) = \sqrt{H_1^2 - (H_1^2 - H_2^2)(x/L) + (R/K)(L-x)x} + \sum_{n=1,3,\dots}^{\infty} \frac{4PL}{Kn^2\pi^2} \sin\left(\frac{n\pi x}{L}\right) \frac{\cosh\left(\frac{n\pi y}{L}\right)}{\sinh\left(\frac{n\pi H_1}{L}\right)} \left(1 - \exp\left[-\frac{K}{S_y} \tanh\left(\frac{n\pi H_1}{L}\right) \frac{n\pi}{L} t_0\right]\right) \exp\left[-\frac{K}{S_y} \tanh\left(\frac{n\pi H_1}{L}\right) \frac{n\pi}{L} (t - t_0)\right] \quad 1-9$$

At $t = t_0$, Equation 1-9 reduces to the end time in Equation 1-8, and as $t \rightarrow \infty$, Equation 1-9 approaches the Dupuit-Forchheimer solution in Equation 1-7 (i.e. the initial condition).

Evaluating the infinite series required truncating the number of terms to a finite amount. Convergence of the infinite series was shown to have occurred within 100 terms.

A1.2.5 Verification and Calibration

The analytical solutions were coded and evaluated using Octave. To verify that Equation 1-8 and Equation 1-9 were mathematically sound and coded correctly, and that the analytical solutions could predict the response of the water table to a finite, short-term recharge event, results from the analytical solutions were compared to those obtained using a numerical model.

A2.2.5.1 Comparison with Numerical Simulations

The analytical solutions were compared to numerical simulations conducted in FEFLOW. Three values of K were tested ($K = 10^{-5}$, 10^{-6} , and 10^{-7} m/s). Other hydraulic parameters remained consistent between the comparisons; these parameters are listed below in Table A2-2.

¹ Compared to Equation 43, the modified expression (Equation 1-9) differs in that there are now two exponential terms, compared to the original expression, which only had a single exponential term. The original exponential term (the last term in Equation 1-9) has been translated so that the equation is applicable from $t > t_0$. The new exponential term in Equation 1-9 represents (when combined with the previous terms in the infinite series) the position of the water table at the last time step (i.e. $t=t_0$) from Equation 1-8.

Table A2-2 List of parameters used for comparison with numerical simulations^a

Parameter (unit)	Value
H ₁ (m)	10
H ₂ (m)	10
L (m)	200
S _y (-)	0.1
P (mm/day)	100
R (mm/day)	0.25
t ₀ (day)	2

^aSpatial discretization in FEFLOW model included 2 m horizontal nodal spacing, and 10 m vertical spacing. Temporal discretization in FEFLOW was as small as 0.001 days with a maximum time step of 20 days (occurring well after occurrence of precipitation event)

Results of the comparison between the numerical simulation and the analytical solution are presented in Figure A2-4, Figure A2-5, and Figure A2-6. Each of the below figures were taken at the water table maximum, located at $x = 100$ m (i.e. $L/2$).

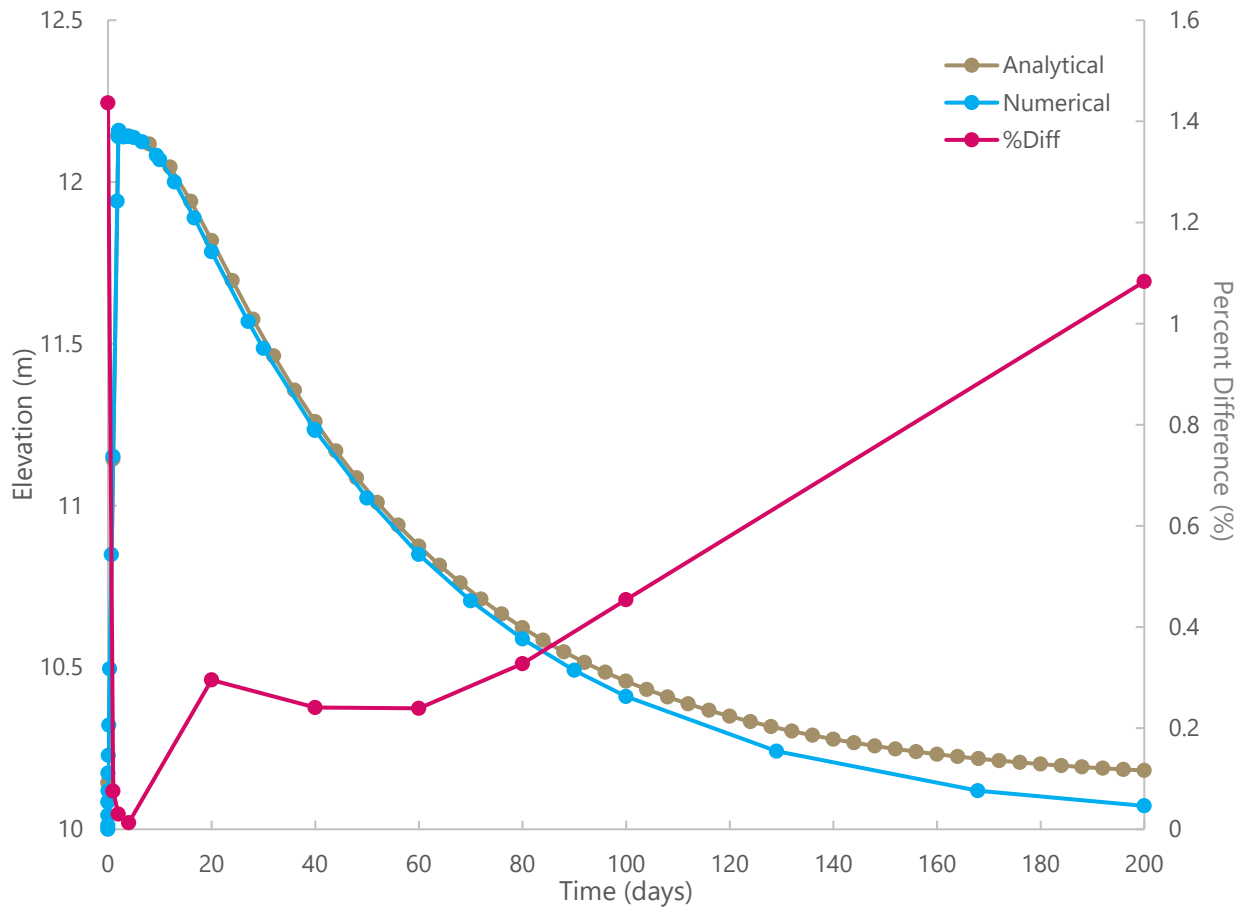


Figure A2-4 Comparison of the water table elevation at $x = 100$ m between numerical and analytical simulations for $K = 10^{-5}$ m/s.

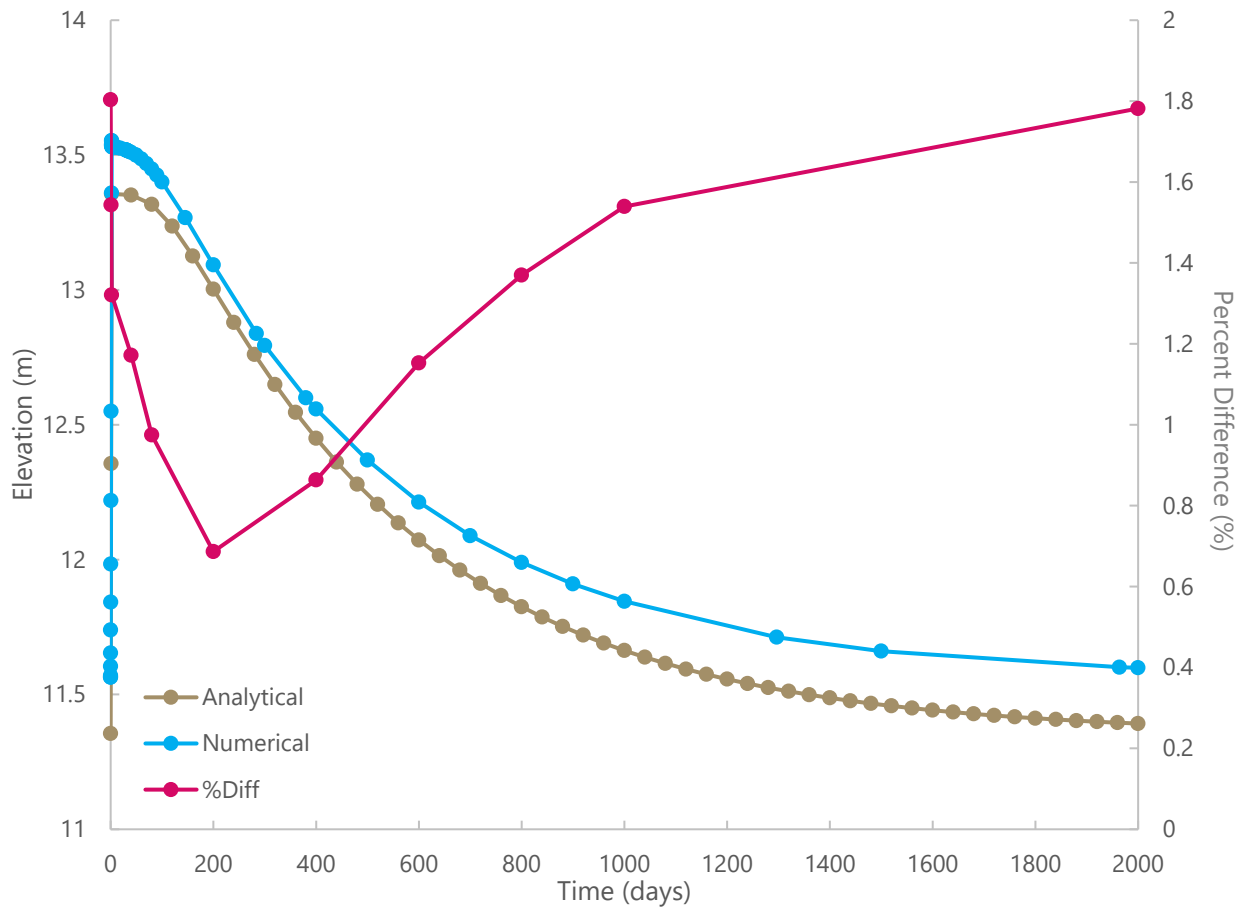


Figure A2-5 Comparison of the water table elevation at $x = 100\text{m}$ between numerical and analytical simulations for $K = 10^{-6} \text{ m/s}$

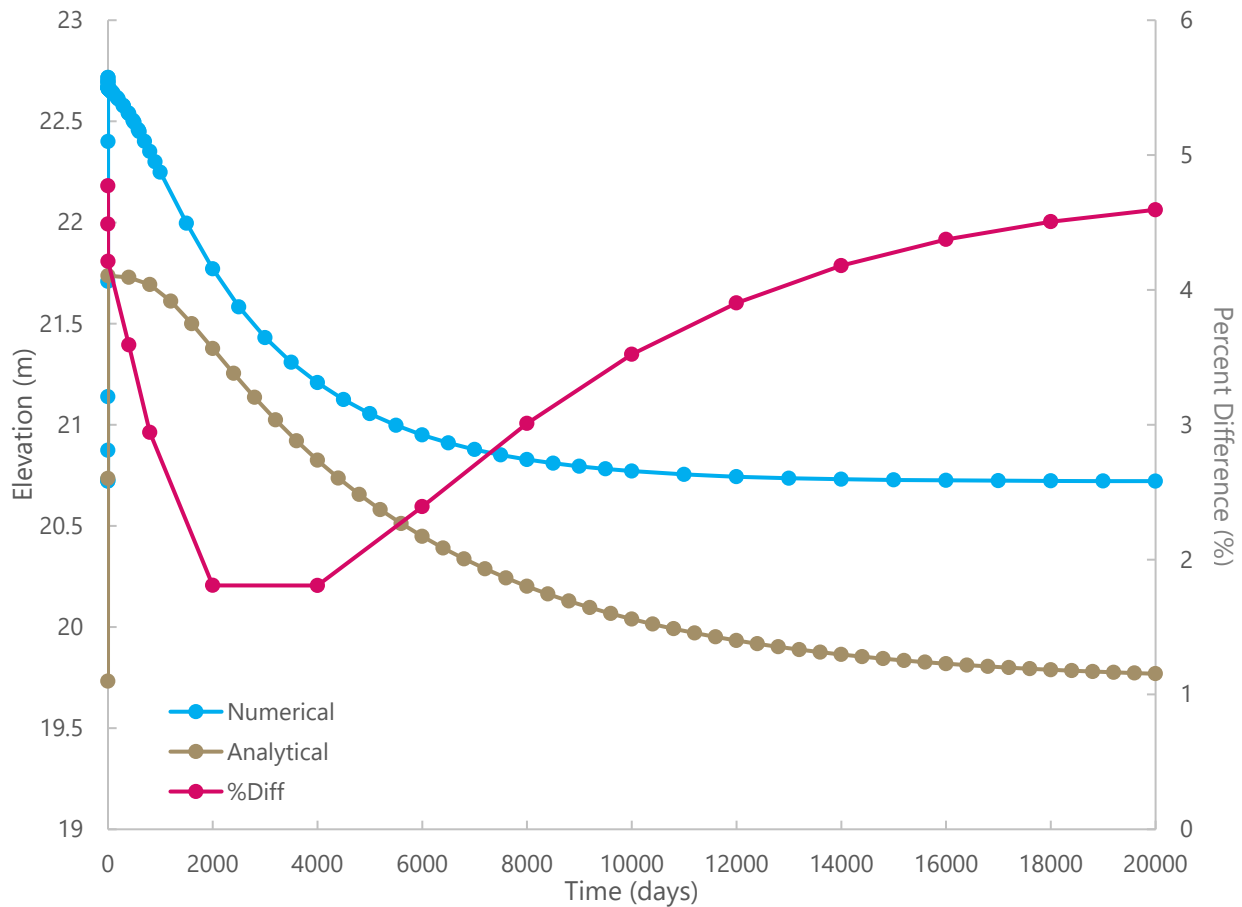


Figure A2-6 Comparison of the water table elevation at $x = 100\text{m}$ between numerical and analytical simulations for $K = 10^{-7}\text{m/s}$

The results show that the analytical solutions closely match those predicted by the numerical simulations. The predicted water table rises due to recharge are similar between the two simulations. Similarly, the duration in which the water table declines back to a steady-state elevation are comparable.

Percent differences between the analytical and numerical simulations were calculated to evaluate their similarity. For $K = 10^{-5}\text{ m/s}$, the absolute magnitude of the percent difference was observed to be no greater than 2% throughout the tested timeframe (Figure A2-4). For $K = 10^{-6}\text{ m/s}$, the analytical solution consistently underpredicted the water table elevation, with the absolute magnitude of the percent differences still no greater than 2% throughout the tested timeframe (Figure A2-5). For $K = 10^{-7}\text{ m/s}$, the analytical solution likewise underpredicted the water table elevation, with the absolute magnitude of the percent differences no greater than 5% within the tested timeframe (Figure A2-6).

The magnitude of deviation (i.e. the percent difference) between the two simulations appears to increase as K decreases. This can mostly be attributed to differences between the initial water table positions. The percent difference, for the falling limb, were generally observed to increase with time as well.

Overall, the comparison between the analytical solution and the numerical simulations are comparable, and suggest that the analytical solutions described by Equation 1-8 and Equation 1-9 can be utilized to predict the behavior of the water table due to a finite, short-term recharge event.

A2.2.5.2 September 3, 2016 Precipitation Event Calibration

To determine whether the analytical model could accurately replicate a real precipitation event, data from water table responses from two wells on Transects 1 and 2 (Figure A2-1) in SFW, SH-GW-26-04 (Transect 1) and SH-GW-40-04 (Transect 2), were used. Pressure transducers (hereafter referred to as levelloggers) continuously measured water levels in the wells. Levellogger data from both wells for the September 3, 2016 rainfall event, in which approximately 60 mm of rainfall was measured in one day, was used for the calibration. For the purposes of the calibration, a half-domain approach was taken, in which only half of the hummock was simulated (i.e. symmetry boundary).

Values for the parameters used in the calibrations for SH-GW-26-04 and SH-GW-40-04 are listed in Table A2-3. The values utilized in the calibrations were based on previous hydrogeologic investigations (Twerdy 2019).

Table A2-3 List of parameters used in calibrations for SH-GW-26-04 and SH-GW-40-04

Parameter (unit)	SH-GW-26-04	SH-GW-40-04
H ₁ (m)	13.2	12.85
H ₂ (m)	10	10
L ^a (m)	485	345
S _y (-)	0.25	0.20
K ^b (m/s)	3 x 10 ⁻⁵	3 x 10 ⁻⁵
P (mm/day)	60	60
R ^b (mm/day)	0.25	0.25
t ₀ (day)	1	1

^aThis is equal to L/2 from the steady-state simulations. In implementing the transient analytical solutions, it was necessary to take the simulated steady-state water level at the 318 Closure Divide and use it as the H₁ value in the transient analytical solutions (i.e. H₁ in transient analytical model was equal to head at L/2 in steady-state analytical model).

^bNote that steady-state solutions (i.e. initial conditions) differed slightly between FEFLOW and analytical models, which accounted for differences in simulated fits. Steady-state water levels predicted by FEFLOW were higher than those in the analytical solutions because the steady-state analytical solutions (i.e. initial condition for transient analytical solutions) had Dupuit assumptions (i.e. no vertical flow; note that vertical flow becomes more influential as K decreases, hence greatest differences for the 10⁻⁷ m/s scenario)

Results of the calibrations are given in Figure A2-7 and Figure A2-8.

The results of the calibrations show that the analytical solutions can reasonably predict the magnitude of the water table rise due to recharge, as well as predict the subsequent water table decline. However, the deviation between the analytical model and the levellogger data were noted at later times in the simulations. This can be most readily seen for well SH-GW-40-04. For the first 14 days of the simulation, the predicted water table elevation is nearly identical to the levellogger data (Figure A2-8). After 14 days, the analytical model consistently overpredicts the elevation of the water table, with the deviation between

the predicted model and the levellogger data increasing with time (Figure A2-8). This may be explained by slight departures from the assumption that equilibrium conditions had been reached prior to the onset of precipitation at the start of the transient analytical models.

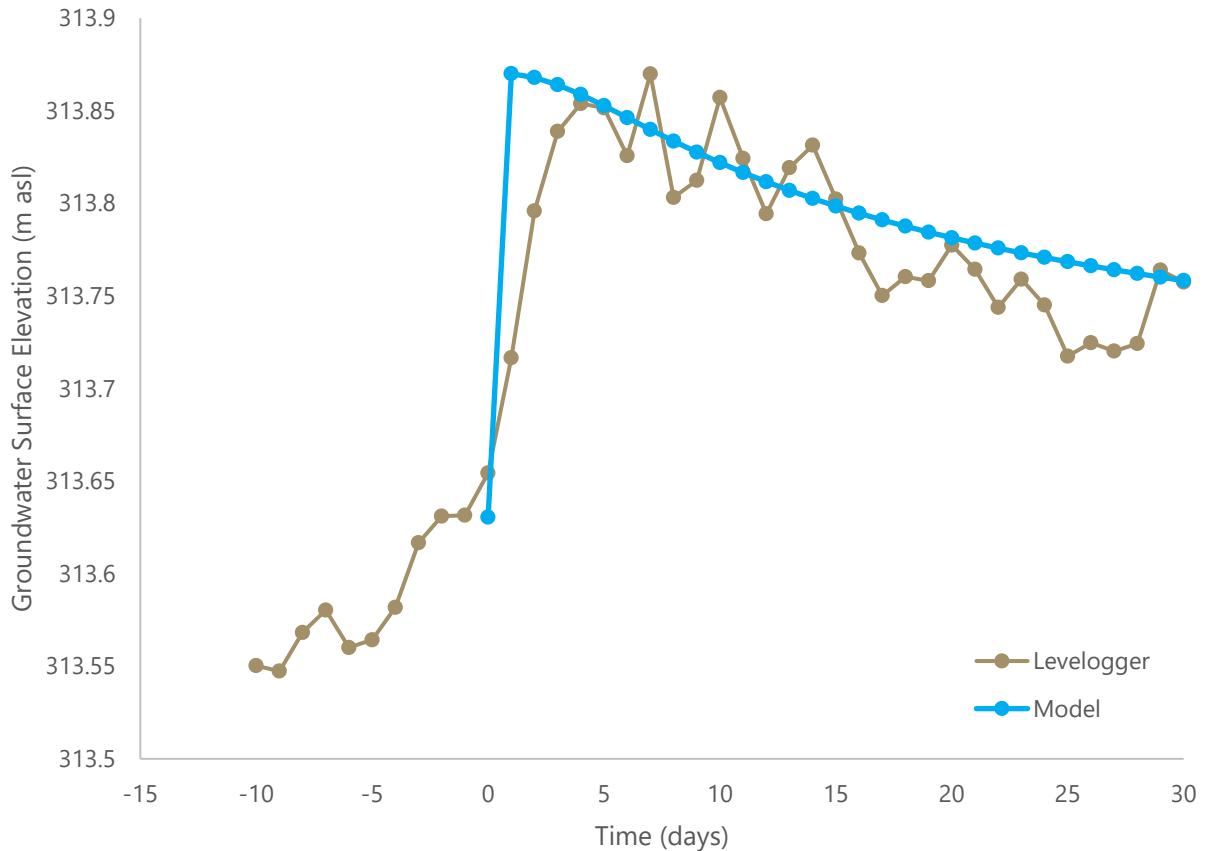


Figure A2-7 September 3, 2016 Calibration for SH-GW-26-04

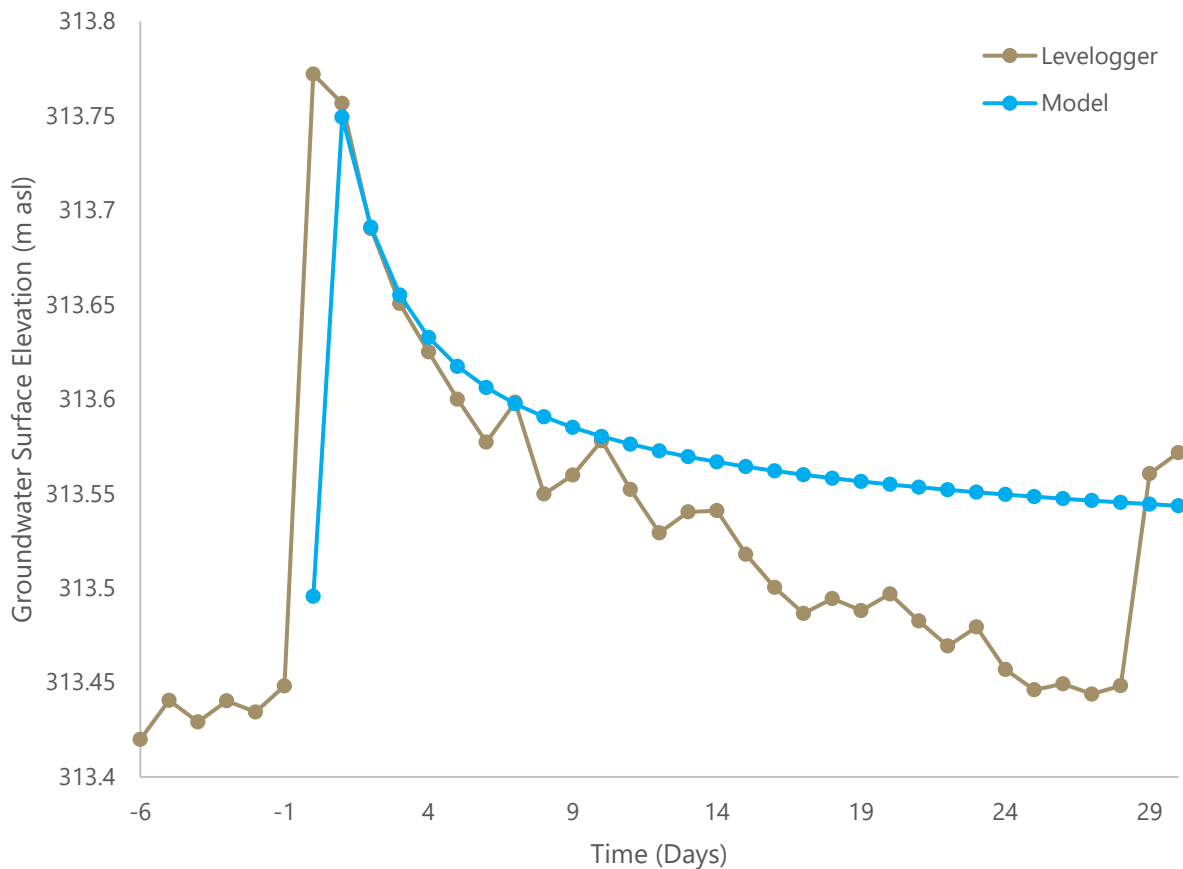


Figure A2-8 September 3, 2016 Calibration for SH-GW-40-04

Overall, the calibrations provide confidence that Equation 1-8 and Equation 1-9 can accurately provide a reasonable representation the behaviour of the water table due to a finite, short-term recharge event (e.g. rainfall).

A1.3 Boundary Conditions for Specific Hummock Design Scenarios in East-in-Pit

Applied scenarios detailed in Section 5.4 of the main report represented a range of hummock types within East-in-Pit (EIP). The modelled transects took advantage of physical boundaries that could be implemented as boundary conditions in the analytical models. The Kingfisher Hummock transect starts near the 318 Closure Divide in EIP and terminates in an adjacent lowland, thus aligning with an assumed symmetry (no flow) boundary at the 318 Closure Divide and a constant head boundary in the lowland. Similarly, the start of the East-side Hummock transect aligns with the edge of the former mining pit, aligning with low permeability material and the location of an assumed no flow boundary, while a constant head is again assumed in the adjacent lowland. The Finger Hummock in the middle of EIP is bounded by lowlands of nearly the same elevation on either side; therefore, half of the hummock can be modelled by taking advantage of a symmetry (no flow) boundary at the midpoint of the hummock.

A1.4 References

- Freeze, R.A., and Cherry, J.A. 1979. Groundwater: Englewood Cliffs, NJ, Prentice-Hall, 604 p.
- Haitjema, H.M. 1995. Analytic Element Modeling of Groundwater Flow. San Diego, California: Academic Press.
- Haitjema, H. M., & Mitchell-Bruker, S. 2005. Are water tables a subdued replica of the topography? Groundwater, 43(6), 781-786. DOI: 10.1111/j.1745-6584.2005.00090.x
- Ketcheson, S. J., Price, J.S, Sutton, O., Sutherland, G., Kessel, E., Petrone, R.M. 2017. The hydrological functioning of a constructed fen wetland watershed. Science of The Total Environment, 603-604, 593-605. DOI: 10.1016/j.scitotenv.2017.06.101
- McKenna, G.T. 2002. Landscape engineering and sustainable mine reclamation. Ph.D. Thesis, Department of Civil and Environmental Engineering, University of Alberta, Edmonton. 660p
- Twerdy, P. 2019. Hydrogeological Considerations for Landscape Reconstruction and Wetland Reclamation in the Sub-humid Climate of Northeastern Alberta, Canada. Alberta, Canada. M.Sc. thesis, Department of Earth and Atmospheric Sciences, University of Alberta, Edmonton, Canada. <https://doi.org/10.7939/r3-zpg2-6p77>.
- van de Giesen, N.C., Parlange, J.-Y., and Steenhuis, T.S. 1994. Transient flow to open drains: Comparison of linearized solutions with and without the Dupuit assumption. Water Resources Research 30(11): 3033 – 3039.

Appendix C

Sandhill Fen Watershed: Learnings from a Reclaimed Wetland on a CT Deposit



SANDHILL FEN WATERSHED:

LEARNINGS FROM A RECLAIMED WETLAND ON A CT DEPOSIT

Syncrude

DISCLAIMER

This report is provided by Syncrude Canada Ltd. To the Alberta Energy Regulator.

The material in this report reflects the judgment of Syncrude in light of the information available at the time of document preparation. Permission for non-commercial use, publication or presentation of excerpts or figures is granted, provided appropriate attribution is cited. Commercial reproduction, in whole or in part, is not permitted without prior written consent from Syncrude. An original copy is on file with Syncrude and is the primary reference with precedence over any other reproduced copies of the document.

Reliance upon third party use of these materials is at the sole risk of the end user. Syncrude accepts no responsibility for damages, if any, suffered by any third party as a result of decisions made or actions based on this document. The use of these materials by a third party is done without any affiliation with or endorsement by Syncrude.

Additional information on the report may be obtained by contacting Syncrude.

The report may be cited as:

Syncrude Canada Ltd. 2020. *Sandhill Fen Watershed: Learnings from a Reclaimed Wetland on a CT deposit*. Syncrude Canada Ltd.

EXECUTIVE SUMMARY

The Sandhill Fen Watershed is located on the northwest corner of the East-In-Pit (EIP) Composite Tailings (CT) deposit at Syncrude Canada Ltd.'s Mildred Lake operation, north of Fort McMurray, Alberta. Sandhill Fen was designed, constructed, reclaimed, and revegetated as an instrumented watershed between late 2007 and 2012, and has had an active research and monitoring program since then. The goals of the project were to design and establish the initial conditions necessary to allow for development of a fen wetland and its watershed over time, and to develop techniques for reclamation of CT deposits.

The Sandhill Fen Watershed design included a primary wetland (the fen) surrounded by an upland area with hummocks constructed from tailings sand, perched wetlands, and supporting infrastructure. The Sandhill Fen Watershed represents the first reclamation of an in-pit tailings deposit in the oil sands industry, and was specifically designed to address research hypotheses. It is also the first attempt to create peatland structure and function on the reclaimed mining landscape. This work is important because a large portion of in-pit tailings deposits are expected to be wetlands. The overarching objectives that drove all activities from design, construction, reclamation, and operation were to: 1) create an instrumented watershed on sand capped soft tailings, 2) to test the viability of practical techniques for soft tailings reclamation and peatland development, and 3) to develop soft tailings reclamation technology to implement operationally. Many of these objectives are transferable to other soft tailings applications.

There are a variety of important outcomes from the design, construction, and research program on the Sandhill Fen Watershed to validate Syncrude's capability to reclaim in-pit CT landforms. Construction activities, reclamation material placement, and revegetation are possible on a sand-capped CT deposit. Even with significant investment in infrastructure to manage water table at the Sandhill Fen Watershed, it was difficult to control water table at a fine scale of resolution. Hummocks formed local-scale groundwater flow systems as predicted, and their water balance is influenced by hummock size, shape and soil texture. Evapotranspiration is an important driver of the water balance, run-off is not. CT deposits will provide groundwater to support wetland development, and Oil Sand Process-affected Water (OSPW) will be present in wetlands. Thresholds of water electrical conductivity for ecological development in wetlands can be as high as 3000-4000 $\mu\text{S}/\text{cm}$.

Sandhill Fen Wetland demonstrates key peatland structural and functional characteristics: typical fen plants, evidence of peat formation, and carbon accumulation. It is unlikely that within the timeframes of closure that any reclaimed wetland will accumulate enough peat (>40cm) to be classified as a peatland according to the Alberta Wetland Classification system. Wetland plant communities are dynamic and respond rapidly to changes in water chemistry and water table fluctuations. Many uncontrollable biotic (e.g. leaf area) and abiotic factors (e.g. climate and weather), influence water availability in reclaimed wetlands and therefore designing wetland types that require tight water table control is unreasonable. Instead, an approach that insures the water quality will be acceptable for a range of outcomes is required.

Knowledge and understanding gained through the instrumented Sandhill Fen Watershed will continue to inform the design, construction and reclamation of other CT deposits, including EIP. Continued performance monitoring of Sandhill Fen Watershed will support understanding and prediction of other in-pit CT deposit reclamation. The work done on Sandhill Fen Watershed is a key component of the adaptive management of EIP and is supporting the design, construction, and reclamation of other CT deposits at Syncrude.

CONTENTS

TABLE OF CONTENTS

DISCLAIMER	I
EXECUTIVE SUMMARY	II
INTRODUCTION	1
RECLAMATION AND CLOSURE	1
DESIGN	3
APPROACH AND OBJECTIVES	3
WATERSHED LOCATION	3
• Key Design Features	5
Area to Perimeter Ratio	6
Hummocks and Topography	6
Water supply	7
Salinity control	7
CONSTRUCTION	8
RECLAMATION	9
COVER SOILS	9
• Wetland Cover soils	9
• Upland Cover soils	9
VEGETATION INTRODUCTION	10
• Wetland Vegetation Introduction	10
• Upland Vegetation Planting	11
OPERATION	13
WATER MANAGEMENT	13
INSTRUMENTATION	13

CONTENTS

- Inflow and Outflow Measurement..... 13
- Weather Stations 13
- Eddy Covariance Stations 13
- Near-surface wells 14
- Hydrogeology wells 14

RESEARCH PROGRAM..... 15

HYDROGEOLOGIC INVESTIGATIONS OF SANDHILL FEN WATERSHED AND PERCHED ANALOGUES- CARL MENDOZA AND KEVIN DEVITO (UNIVERSITY OF ALBERTA) 15

- Key Learnings..... 15
- Hummock Topography and Groundwater Flow Systems 17
- Solute Patterns 17

WATER AND CARBON BALANCE OF THE CONSTRUCTED FEN: SEAN K. CAREY (MCMASTER UNIVERSITY) AND ELYN. R. HUMPHREYS (CARLETON UNIVERSITY)21

- Water Balance Key Learnings.....21
- Water Balance Components21

Snow 21

Rain 22

Water Inflows and Outflows 22

Evapotranspiration (ET) 22

Water Table Dynamics..... 23

Runoff Processes..... 24

Annual Water Balance Components..... 24

- Carbon Balance Key Learnings 25
- Carbon Balance Components 25

Net Ecosystem Productivity (NEP) 25

Methane Flux 26

Dissolved Organic Carbon 27

WETLAND ECOLOGICAL PERFORMANCE: WETLAND PLANT ESTABLISHMENT, COMMUNITY STABILIZATION AND ECOSYSTEM DEVELOPMENT- DALE VITT (SOUTHERN ILLINOIS UNIVERSITY)28

CONTENTS

• Wetland Plant Performance Key Learnings	28
• Plant Responses	29
• Atmospheric Deposition.....	31
• Surface Pore-water Chemistry.....	31
• Soil Dynamics.....	31
WETLAND ECOLOGICAL PERFORMANCE: DEVELOPMENT AND CONTROLS ON ZOOBENTHIC COMMUNITY COMPOSITION AND ABUNDANCE- JAN CIBOROWSKI (UNIVERSITY OF WINDSOR/UNIVERSITY OF CALGARY)	32
• Invertebrate Community Development Key Learnings	32
UPLAND ECOLOGICAL PERFORMANCE: EARLY TREE ESTABLISHMENT AND VEGETATION COLONIZATION OF UPLAND AREAS- SIMON LANDHÄUSSER (UNIVERSITY OF ALBERTA).....	34
• Early Tree Establishment Key Learnings	34
ASSESSING THE SODIUM BUFFERING CAPACITY OF RECLAMATION MATERIALS IN SANDHILL WETLAND- MATT LINDSAY (UNIVERSITY OF SASKATCHEWAN).....	36
• Buffering Capacity of the Clay Layer Key Learnings	36
SANDHILL FEN RESEARCH WATERSHED DISCUSSION AND CONCLUSION	38
SALINITY THRESHOLDS FOR COMMUNITY STRUCTURE	38
SURFACE WATER CHEMISTRY COMPARED TO NATURAL ANALOGUES	38
IS SANDHILL FEN HYDROLOGICALLY SUSTAINABLE?.....	39
WILL SANDHILL FEN BECOME A CARBON SINK?.....	40
DRIVERS OF CHANGES IN SALINITY	40
DID WE BUILD A FEN?	41
CONCLUSION.....	41
REFERENCES CITED	42
BIBLIOGRAPHY OF PUBLICATIONS FROM SANDHILL FEN WATERSHED RESEARCH PROGRAM.....	45
APPENDIX 1: CONSTRUCTION, RECLAMATION AND REVEGETATION OF SANDHILL FEN	49
TERMS OF USE	49

CONTENTS

APPENDIX 2: FINAL SUMMARY REPORT- HYDROGEOLOGIC INVESTIGATIONS OF SANDHILL WATERSHED.....	50
TERMS OF USE	50
APPENDIX 3: THE WATER AND CARBON BALANCE ON THE SANDHILL FEN- DRAFT FINAL REPORT (2012-2018).....	51
TERMS OF USE	51
APPENDIX 4: THE EARLY DEVELOPMENT OF SANDHILL FEN- PLANT ESTABLISHMENT, COMMUNITY STABILIZATION AND ECOSYSTEM DEVELOPMENT.....	52
TERMS OF USE	52
APPENDIX 5: THE ECOLOGY OF SANDHILL FEN YEARS 5-8- MONITORING OF KEY ECOLOGICAL FUNCTIONS AND ESTABLISHMENT OF MARKERS OF SUCCESS FOR PEATLAND RECLAMATION	53
TERMS OF USE	53
APPENDIX 6: THE SANDHILL WATERSHED: EARLY TREE ESTABLISHMENT AND VEGETATION COLONIZATION OF UPLAND AREAS- THE FIRST FIVE YEARS.....	54
TERMS OF USE	54
APPENDIX 7: ASSESSING THE SODIUM BUFFERING CAPACITY OF RECLAMATION MATERIALS IN SANDHILL FEN.....	55
TERMS OF USE	55

FIGURES AND TABLES

LIST OF FIGURES

- **Figure 1: The Sandhill Fen Watershed watershed was constructed on a CT deposit in the northwest corner of a former mine pit, East-In-Pit (EIP), which is located on Syncrude’s Mildred Lake Lease. 4**
- **Figure 2: Hummocks, hummock analogues, and other features in Sandhill Watershed and the associated soil, groundwater, and meteorological monitoring networks. 5**
- **Figure 3: Conceptualized local-scale groundwater flow systems developing beneath hummocks in Sandhill Fen Watershed to meet hummock water functions. Shaded area represents a wetland area. Adapted from Twerdy (2019). 6**
- **Figure 4: Overview of the reclaimed landscape showing upland hummocks capped with either a fine coversoil (solid outline) or a coarse coversoil (dotted outline). 12**
- **Figure 5: Locations of near-surface wells and other instrumentation 14**
- **Figure 6: Topographic site map of SHW (blue outline), piezometers and other instrumentation. Transects 1 (S'-E) and 2(S''-E) correspond to different topographic configurations in the watershed, hummocks to wetlands and slopes to wetlands, respectively. (Figure from Twerdy, 2019.)..... 16**
- **Figure 7: Temporal and spatial evolution of electrical conductivity following a pumping event at Sandhill Fen Watershed, representative of wet, mesic, and dry periods within Sandhill Fen Watershed and in relation to hummocks. 18**
- **Figure 8: Paired plots of $\delta^2\text{H}$ vs $\delta^{18}\text{O}$ (upper) and Na^+ vs $\delta^{18}\text{O}$ (lower) values collected inside the shallowest piezometer from nests (numbers indicate locations) along Transects 1 and 2 (hummock-to-wetland)..... 19**
- **Figure 9: Rainfall at the Sandhill Fen Watershed from 2013-2018. Dashed line is the Ft McMurray 30-year monthly sums for context. 22**
- **Figure 10: Water table as measured at the lowland tower. 24**
- **Figure 11: Net Ecosystem Productivity (NEP), Ecosystem Respiration (ER) and Gross Ecosystem Production for the lowland tower 26**
- **Figure 12: A map of Sandhill Fen with the locations of the 20 wetland vegetation research plots numbered and marked with black dots. 29**
- **Figure 13: Relationship between Zoobenthic Assemblage Conditions Score for Salinity (ZACI-Salinity) and surface water conductivity for samples collected from Sandhill Fen Wetland in 2014 and 2015. 33**

FIGURES AND TABLES

LIST OF TABLES

- *Table 1: Characteristics of cover soils and subsoils placed at the Sandhill Fen Watershed site. 10*
- *Table 2: List of native fen wetland plant species collected and spread throughout the primary wetland and perched wetland footprints..... 10*
- *Table 3: Hummock and upland area tree planting prescriptions..... 11*
- *Table 4: Pumping volume totals and in mm (for lowland area 17 ha) and entire Sandhill Watershed (52 ha) 13*
- *Table 5: Annual water balance components as measured at Sandhill Watershed. NA means not measured, X means analysis in progress..... 25*
- *Table 6: Vascular plant species and recommendation for targeted planting status 30*

The Sandhill Fen Watershed is located on the northwest corner of the East-In-Pit (EIP) Composite Tailings (CT) deposit at Syncrude Canada Ltd.'s Mildred Lake operation, north of Fort McMurray, Alberta. Sandhill Fen was designed, constructed, reclaimed, and revegetated as an instrumented watershed between late 2007 and 2012, and has had an active research and monitoring program since then. The goals of the project were to design and establish the initial conditions necessary to allow for development of a fen wetland and its watershed over time, and to develop techniques for reclamation of CT deposits. A fen is a peat-accumulating wetland with a water table at or near the ground surface, and consisting of mineral-rich water primarily from groundwater.

The Sandhill Fen Watershed design included a primary wetland (the fen) surrounded by an upland area with hummocks constructed from tailings sand, perched wetlands, and supporting infrastructure. The Sandhill Fen Watershed represents the first reclamation of an in-pit tailings deposit in the oil sands industry, and was specifically designed to address research hypotheses. It is also the first attempt to create peatland structure and function on the reclaimed mining landscape. This work is important because a large portion of in-pit tailings deposits are expected to be wetlands. The overarching objectives that drove all activities from design, construction, reclamation, and operation were to: 1) create an instrumented watershed on sand capped soft tailings, 2) to test the viability of practical techniques for soft tailings reclamation and peatland development, and 3) to develop soft tailings reclamation technology to implement operationally. Many of these objectives are transferable to other soft tailings applications.

This report summarizes key components of the design, construction, and research program on the Sandhill Fen Watershed to validate Syncrude's capability to reclaim in-pit CT landforms. The following is a high-level summary of key learnings:

- Construction activities, reclamation material placement, and revegetation are possible on a sand-capped CT deposit.
- Even with significant investment in infrastructure to manage water table at the Sandhill Fen Research, it was difficult to control water table at a fine scale of resolution.
- Hummocks formed local-scale groundwater flow systems as predicted.
- Hummock water balance is influenced by hummock size, shape and soil texture.
- Evapotranspiration is an important driver of the water balance, run-off is not.
- CT deposits will provide groundwater to support wetland development.
- Oil Sand Process-affected Water (OSPW) will be present in wetlands.
- Thresholds of water electrical conductivity for ecological development in wetlands can be as high as 3000-4000 $\mu\text{S}/\text{cm}$.
- Sandhill Fen demonstrates key peatland structural and functional characteristics: typical fen plants, evidence of peat formation, and carbon accumulation.
- It is unlikely that within the timeframes of closure that any reclaimed wetland will accumulate enough peat (>40cm) to be classified as a peatland according to the Alberta Wetland Classification system.
- Wetland plant communities are dynamic and respond rapidly to changes in water chemistry and water table fluctuations.
- Many biotic (e.g. leaf area) and abiotic factors (e.g. climate and weather) influence water availability in reclaimed wetlands and therefore designing wetland types that require tight water table control is unreasonable. Instead, an approach that insures the water quality will be acceptable to a range of outcomes is required.

RECLAMATION AND CLOSURE

Surface mining of oil sands deposits requires disruption of existing landscapes and their processes, and the construction of new landscapes and ecosystems. Syncrude recognizes its responsibility to return disturbed land to that capable of supporting a variety of end land uses similar to pre-disturbance as part of its operating license under the *Alberta Environmental Protection and Enhancement Act* (EPEA). Acceptable performance of newly built landscapes is critical to closure and certification.

Syncrude's approach for closure is to create interconnected landforms that support functioning ecosystems. The availability, quality and distribution of water are critical to the reestablishment of landscape functions. This is achieved by designing landscapes that yield

INTRODUCTION

water at qualities and volumes to both support desired landscape performance, and return water to the environment. The challenge of integrated landform design is to balance these two goals.

A number of different materials (substrates), each with unique physical and chemical challenges, are by-products of mining and extraction activities and are used to recreate the post-mining landscape. These materials include: natural materials (overburden), tailings materials (CT, tailings sand and centrifuged cake) and other process by-products (petroleum coke). Landforms are designed and constructed to optimize the use of these materials to form geotechnically stable hydrologic response areas that control the movement, distribution, and quality of available water for sustainable ecological performance and water quality at the outlet.

Watershed research enables the evaluation of different possible landform design approaches to determine which are best suited to meet closure objectives. Instrumented watersheds are intensively monitored constructed landforms, which provide an opportunity to conduct integrated, multi-disciplinary research programs. This allows the determination of:

Water and energy balances (location, quantity, quality and movement of water in a landscape);

Salt balances (including inorganics, organics, ions, nutrients, metals);

Plant and ecological responses; and

Watershed design and management options to optimize successful reconstruction practices to ensure a sustainable landscape.

Watershed research provides a holistic understanding and assessment of landform performance that cannot be achieved by any individual research activity. These data are used to support overall program objectives of developing best practices (in the areas of landform design, soil cover design, and revegetation) and developing indicators of reclamation success. Uncertainty in future performance can be reduced through the development of predictive models based on the record of performance acquired. Watershed sites are also the benchmark long term research and monitoring sites for Syncrude to demonstrate that the landforms are acceptable for final closure.

Since pioneering the watershed research approach in the oil sands in 1999, Syncrude has established six full scale watershed research areas on each of the dominant substrates at Mildred Lake and Aurora North, including:

- South Bison Hills on saline/sodic overburden (1999)
- Southwest Sand Storage on tailings sand (2000, 2004)
- Mildred Lake Settling Basin Coke Beach (2004)
- Aurora Soil Capping on lean oil sand overburden (2012)
- Sandhill Fen Pilot on tailings sand capped Composite Tailings (2012)
- Base Mine Lake Demonstration of Water Capped Fluid Fine Tailings (2012)

Significant time is required to assess the long term performance of reclamation strategies explored as part of watershed research. Watershed areas transition from comprehensive, high intensity research activities in the first several years followed by a research monitoring phase. The instrumented watershed approach supports adaptive management of landforms to steward to closure outcomes. It is expected that these watershed facilities act as analogues to learn from so that each landform constructed during mine life does not require such intensive work.

The design intent of Sandhill Fen Watershed was to design and establish initial conditions necessary to allow for development of a fen wetland and its watershed over time, and to develop techniques for reclamation of CT deposits. Numerous field and pilot scale screening demonstrations have been conducted to refine our understanding of soft tailings capping (See Appendix A- *Syncrude's Experience with Capping and Trafficking Composite Tailings*). As a result of these investigations, and advice from technical experts, the key CT capping technology advanced in the Sandhill Fen Watershed was mechanical placement of sand hummocks on soft tailings using conventional mine equipment. Syncrude has advanced technology for the creation of sand hummocks, a key feature in all soft tailings closure plans, using conventional tailings pouring technologies (these are described in detail in Appendix B- *Hummock Technology Learnings to Support Water Management on Reclaimed Landforms*). The goal of Sandhill Fen Watershed is to allow Syncrude to gain experience and knowledge through research to guide future CT reclamation, as well as wetland (and watershed) design and reclamation.

APPROACH AND OBJECTIVES

As part of the closure design process, Syncrude undertakes an integrated ground and surface water model of closure landforms. This modelling indicates that significant areas of the reclaimed landscape will have a water table suitable to support wetlands. The underlying stratigraphy, the water balance, and the water chemistry (influenced by fresh and/or OSPW) will influence the wetland type and ecology. The Sandhill Fen Watershed was designed to provide guidance to planners, designers, and reclamation specialists for which areas are likely to become wetlands, how they are interconnected with each other and the surrounding natural and reclaimed upland areas, and how we might promote the development of these wetlands, to achieve Syncrude's end land use goals.

One of the first steps in the design process was to determine the overall objective of the watershed design: **to design and create the appropriate initial conditions to allow the development of a self-sustaining fen wetland and its watershed over time, and to develop techniques for the reclamation of CT deposits.** Because watersheds are complex and include a diverse array of components, and constructing a fen of this size had never been attempted previously anywhere, we commissioned an advisory panel to assist in our design. These experts were from a range of disciplines including civil and geological engineering, peatland ecology, upland revegetation, wetland construction, hydrology and hydrogeology. The advisory panel focused on 3 key tasks: 1) design a watershed appropriate for current environmental conditions; 2) maximize the opportunities for addressing research questions to produce recommendations for future reclamation; 3) maximize probability of success. In the absence of direct experience in peatland reclamation, or specific design guidance, and based on understanding of natural and reclaimed wetlands in the region, the design team recommended a target water electrical conductivity (EC) of 1500 $\mu\text{S}/\text{cm}$ to improve the likelihood of success. Success was defined as: 1) maintaining the water level at +/- 20 cm of the soil surface, 2) vegetation establishment in the wetland area and 3) in the long-term, the wetland becomes carbon accumulating.

Because the physical characteristics of in pit tailings deposit provides opportunity for groundwater recharge, it was decided that East-In-Pit (EIP) sand-capped soft tailings (CT) deposit was an appropriate location for the Sandhill Fen Watershed. This watershed was built to test the viability of practical techniques for soft tailings reclamation and fen development. These techniques were part of the entire process from design to construction, to revegetation, to monitoring performance. This research program would also provide the opportunity to develop soft tailings landform construction and reclamation technology to implement operationally. Syncrude expects wetlands to be a significant component of the closure landscape, especially on soft tailings deposits, and therefore a well-designed, well-constructed, well-monitored research oriented prototype wetland within an instrumented watershed is an important facility that will inform the adaptive management of soft tailings deposits in order to achieve acceptable closure outcomes.

WATERSHED LOCATION

EIP was mined between 1977 and 1999. Deposition of tailings sand and CT into the mined-out pit began in 1999. EIP is filled with approximately 40 m of interbedded CT (Matthews *et al.*, 2002) and tailings sand layers. CT is produced by combining fine tailings, tailings sand and gypsum, to reduce water content and promote dewatering (Kasperski and Mikula, 2011). Calcium derived from gypsum exchanges for sodium at clay-mineral surfaces of FFT solids, thereby promoting dewatering and coagulation. The CT pore-water chemistry is initially derived from OSPW; however, gypsum addition produces elevated SO_4 and Na concentrations. The chemical composition of the CT deposit is spatially heterogeneous (Reid and Warren, 2016). EIP closure topography is nearing completion and remaining sand placement is primarily for landform construction. Progressive reclamation of the deposit is nearing completion.

DESIGN

The Sandhill Fen Watershed is located at the northwestern corner of the EIP CT deposit (Figure 1), and is the first example of CT reclamation. The CT deposit in this area is overlain with nominally 10 m of hydraulically placed tailings sand to produce the closure topography. Hydrogeological modeling predicted vertical migration of CT pore water through the reclamation cover at some locations – particularly at the southern margin of the wetland – within the Sandhill Fen Watershed (see details in Syncrude 2008, Wytrykush *et al.* 2012).

The Sandhill Fen Watershed is approximately 52 ha; about 1000 m long by approximately 500 m wide. Engineered dykes and closure divides define the watershed boundary. The watershed will eventually be connected to the Kingfisher Watershed immediately to the East of Sandhill Fen Watershed, and drain to the north into the Mildred Lake Reservoir. A comprehensive site investigation program was conducted in 2008 to inform design of the watershed. This program included installation of 54 piezometers, two seepage meters, four settlement benchmark anchors, along with soil and water testing. Details of this work can be found in (Syncrude 2008).

The term “watershed” implies that Sandhill Fen Watershed would source water from within the designed boundaries. However, given that the reconstructed watershed was built in the northwestern-most corner of EIP, engineered features beyond the bounds of Sandhill Fen Watershed were anticipated to influence the groundwater system to some degree. Engineered features influencing the hydrogeology of Sandhill Fen Watershed included 318 Closure Divide to the south, as well as the outer limit of EIP to the north that coincided with geotechnically stabilized areas and different materials than those found in the tailings deposit.

The intent of 318 Closure Divide was to serve as a groundwater/surface water divide within the overall reclaimed EIP landform, where precipitation landing south of the closure divide would flow southwards through EIP towards the outlet to Base Mine Lake and precipitation falling north would drain towards Mildred Lake. As such, it was anticipated that 318 Closure Divide would be of adequate size, composition, and configuration to redirect water within the reclaimed EIP landform, thereby influencing groundwater flow in Sandhill Fen Watershed. The outer limit of EIP to the north of Sandhill Fen Watershed coincided with the mining pit wall and was expected to be a low permeability barrier to groundwater flow

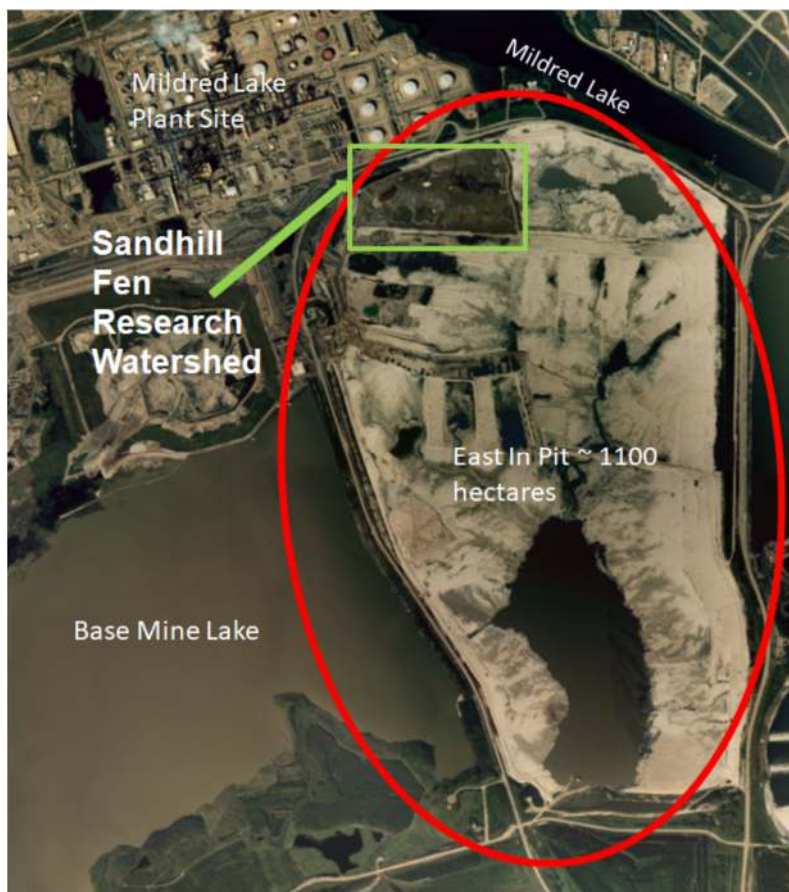


Figure 1: The Sandhill Fen Watershed watershed was constructed on a CT deposit in the northwest corner of a former mine pit, East-In-Pit (EIP), which is located on Syncrude’s Mildred Lake Lease.

Key Design Features

Some of the key design features of the Sandhill Fen Watershed include constructed upland hummocks (hillocks), vegetated swales, a freshwater storage pond, a central wetland, an underdrain system and two perched fens (Figure 2) (Syncrude, 2008, Wytrykush *et al.* 2012). The two perched fens, each ~1.2 ha in area are a test of whether perched wetlands can achieve fen structure and function where water inputs are only from precipitation. There is evidence of perched peatlands in natural areas in the boreal region (Devito and Mendoza, pers. Comm.). Other infrastructure was included in the design to support specific research purposes: paths and boardwalks, instrumentation including piezometers, flow meters, weather stations, and eddy covariance systems (described elsewhere in document), a research trailer, pole-mounted time-lapse camera system, access roads, and a heated weir at the downstream end of the watershed. More instrumentation was added as research programs were developed. Ground and surface water modelling, based on the design, was used to predict the primary wetland extent.

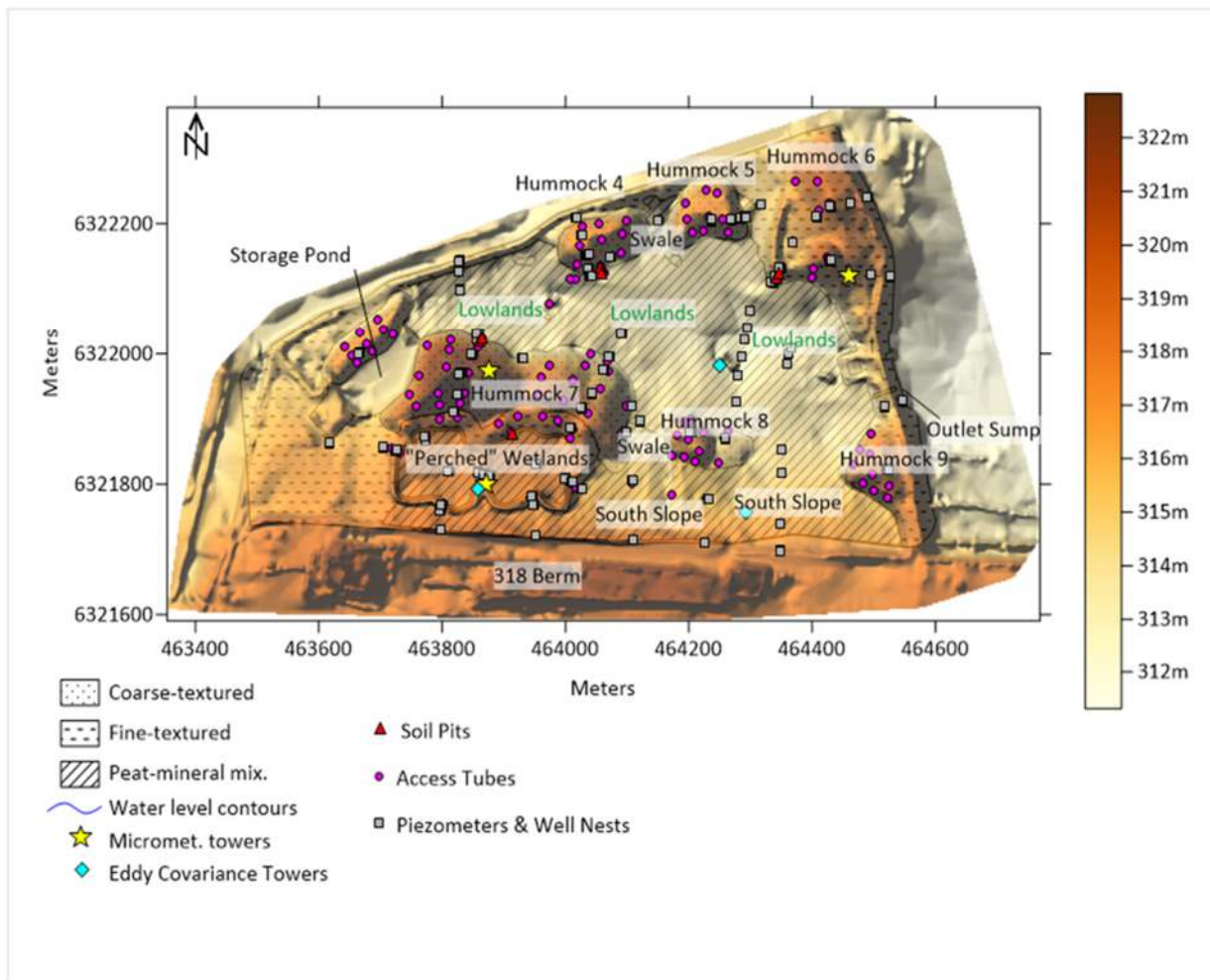


Figure 2: Hummocks, hummock analogues, and other features in Sandhill Watershed and the associated soil, groundwater, and meteorological monitoring networks.

DESIGN

Area to Perimeter Ratio

The area to perimeter ratio for the Sandhill Fen wetland was compared to the average ratios of wetland perimeter and area observed in over 6000 natural fen wetlands (Bloise, unpublished data) to confirm that the planned dimensions of the fen wetland were within the range of natural peatlands in the region.

Hummocks and Topography

The intent of constructed hummocks in Sandhill Fen Watershed was to develop several fresh, shallow, local-scale groundwater flow systems to provide adequate water quantity and quality to the central lowlands in Sandhill Fen Watershed and downstream environments (Figure 3), as well as provide a suitable substrate for upland vegetation growth. Local-scale groundwater flow systems associated with hummocks were a practical and elegant solution to mitigate the expression of process-affected water in the near-surface of the watershed because of their ability to limit the discharge of deeper groundwater associated with process-affected water. By maintaining freshwater at or near the water table through the development of local-scale flow systems, it would ensure adequate freshwater availability to the reclaimed environment within and downstream of Sandhill Fen Watershed. For more details about the conceptual model for hummocks, see Appendix B-*Hummock Technology Learnings to Support Water Management on Reclaimed Landforms*.

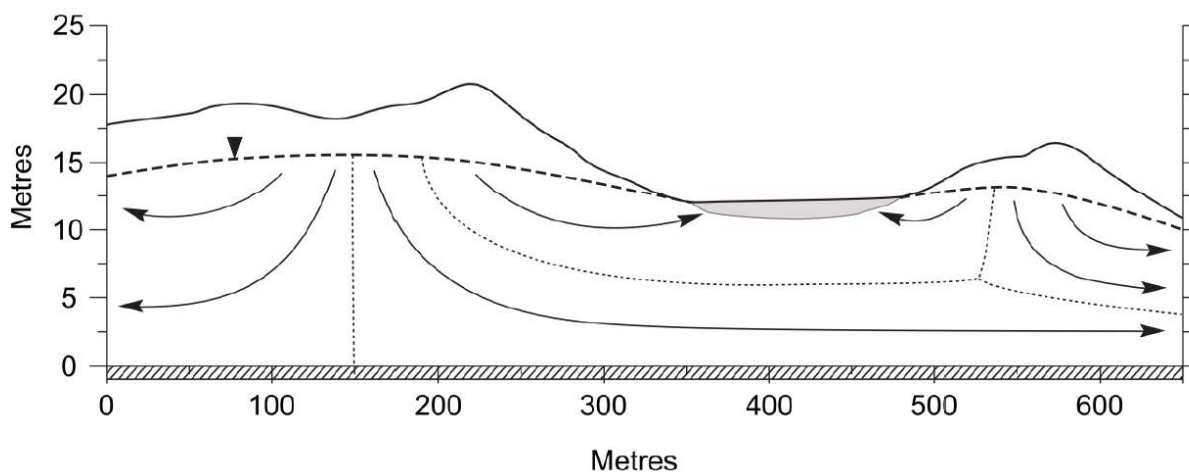


Figure 3: Conceptualized local-scale groundwater flow systems developing beneath hummocks in Sandhill Fen Watershed to meet hummock water functions. Shaded area represents a wetland area. Adapted from Twerdy (2019).

The as-built tailings sand surface in the watershed had low gradients (0.1-0.5%). To create distinct upland recharge areas that provide groundwater supply to the wetland, to provide topographic diversity and support tree growth, uplands in the form of seven hillocks (hummocks) of varying size and configuration were built with mechanically placed tailings sand around the around the wetland perimeter. Tailings sand is a uniform fine grained sand with some fines.

To achieve these hummock water functions, “mounded” hummock forms were chosen during planning and design, with varying heights and sizes that were anticipated to be large enough to redirect groundwater flow towards the lowlands. Hummock design had to balance the partitioning of precipitation between recharge and evapotranspiration. Adequate recharge was necessary to facilitate the formation of groundwater mounds beneath hummocks (i.e., groundwater mounding; see Section 3 of Appendix B-*Hummock Technology Learnings to Support Water Management on Reclaimed Landforms* for conceptual overview). On the other hand, hummocks had to create a substrate for upland vegetation growth, which needed to be sufficiently elevated above the water table to prevent saturation and salinization of the rooting zone. Therefore, the designed separation between ground surface and water table had to strike a balance between these hummock water functions. Dynamic hydrologic and hydrogeologic interactions were anticipated at the toes of the hummocks and at hummock-lowland interfaces, given the proximity of the water table to the ground surface and the potential for local-scale groundwater discharge to these zones (Figure 3).

The hummocks range in size, shape and orientation. The largest hummock is approximately 350 m long and 100 m wide and about 8 m above the ground surface. Most of the hummocks are about 180 x 60 m and 3-4 m high. The long axis of each hummock is

DESIGN

oriented parallel to the wetland to maximize the seepage face contacting the wetland (Syncrude 2008). The geometry of the hummocks was designed to allow for salt flushing over the long term, and lowers the water table in the hummock so that upland tree growth can be supported. Swales were also designed to capture and convey any run-off from the upland areas (i.e. non-wetland) to the main wetland. The swales were designed to be gently sloped areas that are vegetated to limit erosion from run-off. The design included tailings sand in-fill areas to raise the elevation of the swales between hummocks to promote surface drainage to the fen and minimize back-flow into the uplands.

Modelling of the hummocks during the design phase indicated that the phreatic surface within the hummocks would be about 0.5 m above the wetland elevation. Flushing estimates suggest that the upland hummocks will take approximately 20 years to flush tailings pore water (Syncrude 2008). Predictions from the design and modelling of the fen topography indicate that salinity levels in the wetland area are expected to decrease when flushing is completed. For a detailed description of hummock design and performance see (Appendix B-*Hummock Technology Learnings to Support Water Management on Reclaimed Landforms*).

Water supply

Groundwater modeling results of the design showed the water levels in the fen are sustainable from the hummock contribution, but conductivity would increase above the design threshold of 1500 $\mu\text{S}/\text{cm}$ without freshwater import. In order to mitigate this, and to provide a faster trajectory to a fresher water system, it was decided that freshwater should be provided for the wetland. Infrastructure was installed to pump freshwater (EC=500 $\mu\text{S}/\text{cm}$) from Mildred Lake Reservoir (derived from the Athabasca River) across Highway 63 to fill the clay-lined freshwater storage pond and then diffuse to the wetland through a narrow gravel dam. The two perched fens were also initially supplied with freshwater. In the summer of 2012, following reclamation material placement (subsoil and peat material), freshwater from Mildred Lake Reservoir was pumped into the fen area to help saturate the peat and maintain downward seepage gradients to the underdrains to control salinity.

Salinity control

A key driver in the design was to mitigate potential salinity in the wetland. Control of the water table in the tailings sand cap was considered a critical means of limiting salinization of the fen. To facilitate sand cap dewatering, and reduce the influence of tailings pore-water expression to the wetland, an underdrain system (perforated 8-in high density polyethylene (HDPE) covered with a fine-screen geotextile cloth) was ploughed in beneath the wetland footprint in the winter of 2008 prior to placement of reclamation materials. The water collects in the underdrains and flows to a sump at the watershed outlet, where it is pumped out of the watershed, and further south into EIP. Surface water exits the fen through a spill-box and weir structure in the same location as the sump.

3 CONSTRUCTION

Construction of the Sandhill Fen Watershed was carried out from 2009 through 2011. A range of materials were used during the construction of the watershed, including: tailings sand, Pf sand, clay till, and gravel. In order to allow for deeper frost penetration for trafficability, snow clearing was undertaken. During snow clearing a dozer (D6) became mired in an area of standing water and special operational procedures for working in these area were developed so that equipment could avoid areas of standing water.

Hummocks were constructed in the winter of 2009/2010, using a tailings sand stockpile. Tailings sand fill was hauled using 30 and 40T articulated haul trucks, dumped, and then spread using D6 dozers. The hummocks were not landform graded. Trafficability was good in the watershed during winter when a frost cap was present. Further details of the construction timelines and activities can be found in Appendix 1.

4 RECLAMATION

COVER SOILS

Clay till placement began in November of 2010, and was on-going until spring 2012. During winter construction, and into spring, the clay till was often frozen into large lumps (up to 1m in diameter) that were ripped prior to being compacted, where compaction was required. Spreading and compacting (track-packing only) of clay till was done using a D6 dozer. Peat-mineral mix placement was completed in February and March of 2011. The peat mineral mix was hauled by articulated 40T haul trucks from the temporary stockpile and dumped at the edge of the placement area. Operators used several methods to spread the peat. Initial placement in the western end of the fen (the Winter Wet Area) and Perched Fens was spread by numerous passes with a D6 to D8 sized dozer. The final peat mineral mix surface was relatively uniform and flat with several isolated boulder-sized blocks sitting on the surface. Another area of peat mineral mix was placed and spread using a Cat 321 tracked excavator. The final material surface was visibly rough and was 0.6 m to 0.7 m thick, with boulder-sized blocks of peat mineral mix remaining. A third method observed was to spread the peat onto track-packed snow with minimal trafficking in three pushes (one straight, and two at 45° angles) using D6 to D8 sized dozers. This placement method created a somewhat rough surface and minimized compaction from equipment traffic. It was recommended to operators to complete placement using the three-push method. Field observations indicated the eastern portion of the wetland area to be rougher and less compacted than the western end. Details of the reclamation material placement can be found in Appendix 1.

Wetland Cover soils

In the wetland areas, a 0.5m thickness of fine-grained material (clay-till) was placed directly over the tailings sand to provide a mineral base for the wetland, and to slow diffusion of tailings pore-water into the wetland. This was not constructed to be a liner. A 0.5 m layer of recently salvaged peatland material was placed over the clay till providing an organic soil. This peatland material was direct placed from a recently dewatered area of the mine advance. The material was double handled because large haul trucks were unable to access the watershed area to directly place the soil.

One of the perched wetlands was reclaimed with 0.5 m of clay-till overlain with 1.0 m of recently salvaged peatland material (same material as main wetland). The second perched wetland had 0.5 m of clay-till as a base, but overlain with 0.5 m of tailings sand, and then 0.5 m of recently salvaged peatland material (same material as main wetland). Although the conceptual design was that the clay base of the perched systems be compacted as a liner, this was not done. The clay was a mineral base for these wetlands, but did not perform as a true liner.

Upland Cover soils

Different salvaged soil materials were used to recreate soil conditions that are representative of two major forest types of this region (see below). One of the cover soils was reconstructed by placing a 40 cm subsoil layer of salvaged Pleistocene fluvial sand and then covered with 15 cm of salvaged forest floor material. The forest floor material, a mixture of the organic forest floor layer and the underlying mineral soil, had been salvaged to a depth of 15 cm from *Pinus banksiana* forests on coarse-textured Brunisols. The second cover soil type used for some of the hummocks was a 40 cm thick layer of a fine-textured clay-rich subsoil material that was subsequently covered with a 20 cm forest floor material cap salvaged to a depth of 20 cm from mesic upland forest sites dominated by *Populus tremuloides* on fine-textured Luvisols.

All cover soil materials were directly placed without stockpiling to preserve the viability of the propagules bank within. Due to the differences between the two reconstructed soils (mostly driven by soil texture) and the site conditions created by these soils, we can characterize the cover soil as either “coarse” or “fine” soil. More information on the physical and chemical properties of the two soil materials can be found in Appendix 6. Five of the hummocks in the watershed had a coarse soil cap, while three other hummocks received a fine soil cap (Figure 4). Following cover soil placement, coarse woody debris (mainly stems and large branches of white birch and trembling aspen) were placed on all hummocks in volumes ranging from 0.2 m³ ha⁻¹ to 200 m³ ha⁻¹. Reclamation soil placement was primarily completed in 2011.

RECLAMATION

Table 1: Characteristics of cover soils and subsoils placed at the Sandhill Fen Watershed site. Cover soils were salvaged from two forest types, a nutrient poor site with a xeric moisture regime (coarse) and a nutrient rich site with a mesic moisture regime (fine). The cover soil from a coarse forest site was underlain by a sandy subsoil material, and the cover soil from a fine forest site was underlain by a clay loam subsoil material. Data (mean \pm one standard deviation) were collected in 2013.

Soil Material	Coarse-textured cover soil	Sandy subsoil	Fine-textured cover soil	Clay loam subsoil
Soil Texture	Sand	Sand	Clay loam	Sandy clay loam
% Sand (by weight)	90.9 \pm 1.93	97.9 \pm 1.03	41.5 \pm 4.31	55.5 \pm 4.13
% Clay (by weight)	2.7 \pm 1.34	1.2 \pm 0.59	32.1 \pm 4.35	24.6 \pm 4.30
pH	6.3 \pm 0.67	7.4 \pm 0.15	6.9 \pm 0.40	7.5 \pm 0.26
Cation exchange capacity (meq/100 g)	7 \pm 1.38	undetectable	19 \pm 4.45	10 \pm 2.21
Sodium (mg/kg)	32 \pm 12.39	26 \pm 5.38	76 \pm 54.76	116 \pm 79.73
Total organic carbon (% dry weight)	1.6 \pm 0.48	0.2 \pm 0.11	4.3 \pm 4.52	1.4 \pm 0.28
Total nitrogen (% dry weight)	0.08 \pm 0.02	0.03 \pm 0.00	0.28 \pm 0.36	0.04 \pm 0.02
Organic matter (%)	3.3 \pm 0.95	0.4 \pm 0.20	8.5 \pm 9.04	2.8 \pm 0.55
Available Ammonium (μ g/g)	0.8 \pm 0.56	undetectable	2.6 \pm 8.20	undetectable
Available Nitrate (μ g/g)	undetectable	undetectable	5 \pm 2.75	undetectable
Available Phosphorus (μ g/g)	9 \pm 3.42	undetectable	7 \pm 2.90	undetectable
Available Potassium (μ g/g)	39 \pm 9.79	undetectable	100 \pm 27.28	69 \pm 24.79

VEGETATION INTRODUCTION

Wetland Vegetation Introduction

Because the wetland soil was recently salvaged, there were many propagules of a range of wetland plants- seeds, intact roots, rhizome fragments and stem pieces- that all had potential to contribute to wetland plant diversity. However, the primary approach for wetland vegetation was seeding with fen plants. A range of wetland plant seeds were collected during the summer of 2011, and spread throughout the fen footprint during the winter of 2011. A list of the seeds spread across the fen footprint is in Table 2. A range of other wetland plant seedlings were planted in experimental research plots (details in Appendix 4), and seedlings of a range of plants were placed in various areas of the fen over time.

Table 2: List of native fen wetland plant species collected and spread throughout the primary wetland and perched wetland footprints

Seed species	Common name
<i>Beckmannia syzigachne</i> (Steud.) Fernald	American sloughgrass
<i>Betula pumila</i> L. var. <i>glandulifera</i> Regel	bog birch
<i>Carex aquatilis</i> Wahlenb.	water sedge
<i>Carex hystericina</i> Muhl. ex Willd.	bottlebrush sedge
<i>Carex paupercula</i> Michx.	boreal bog sedge
<i>Carex retrorsa</i> Schwein.	knotsheath sedge
<i>Carex utriculata</i> Boott	common beaked sedge
<i>Juncus tenuis</i> Willd.	slender rush
<i>Scirpus lacustris</i> L.	bulrush
<i>Scheuchzeria palustris</i> L.	pod grass
<i>Scirpus cyperinus</i> (L.) Kunth	cottongrass bulrush, woolgrass
<i>Triglochin maritima</i> L.	seaside arrowgrass

Upland Vegetation Planting

The upland areas were planted with several tree prescriptions. These prescriptions were designed to test hypotheses related to both upland revegetation performance, and the effects on wetland hydrology and hydrogeology. The tree planting prescriptions are outlined in Table 3, and shown in Figure 4.

Table 3: Hummock and upland area tree planting prescriptions

Prescription type	Density category	Density (stems/ha)	Tree species
No planting	Control	0	None
a/b ecosite	Medium	5000	10% aspen (<i>Populus tremuloides</i>) 10% white spruce (<i>Picea glauca</i>) 80% jackpine (<i>Pinus banksiana</i>)
	High	10000	
D ecosite	Medium	5000	80% aspen (<i>Populus tremuloides</i>) 10% white spruce (<i>Picea glauca</i>) 10% jackpine (<i>Pinus banksiana</i>)
	High	10000	
Standard		2000	20% aspen (<i>Populus tremuloides</i>) 20% white spruce (<i>Picea glauca</i>) 20% jackpine (<i>Pinus banksiana</i>) 20% white birch (<i>Betula papyrifera</i>) 20% black spruce (<i>Picea mariana</i>)

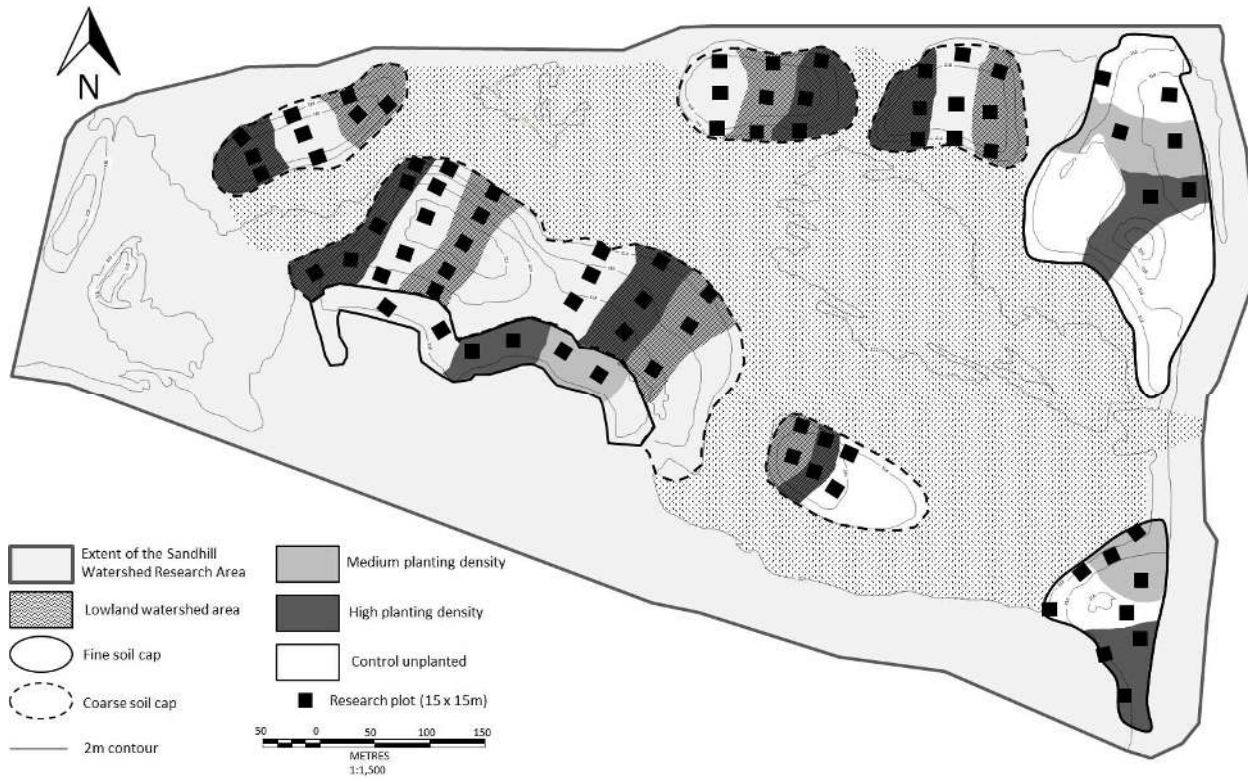


Figure 4: Overview of the reclaimed landscape showing upland hummocks capped with either a fine cover soil (solid outline) or a coarse cover soil (dotted outline). Two seedling planting density prescriptions were applied on the landscape and represented here: a medium planting density (5,000 stems ha⁻¹, light grey) and a high density planting treatment (10,000 stems ha⁻¹, dark grey). Individual research plots are presented on the map as black squares.

WATER MANAGEMENT

The infrastructure to support management of the water fluxes in the fen is described in the Permit Level Design (Syncrude 2008). More details about the water balance are provided in sections 6 and Appendix 3. Management of inflow pumping regimes occurred only in 2013 and 2014. Since 2014, no water has been added to the Sandhill Fen Watershed using the pump management system. Water outflow management also varied among the years. Since 2013, water management has been dramatically reduced, however on several occasions outflow pumps have been turned on to lower the water table in the lowland because excessive inundation was compromising research infrastructure (boardwalks, instruments, and research plots). In 2017 and 2018, large rainfall events contributed to high water tables and pump out was initiated. This proved an effective method to remove water for short time frames (days). A summary of pumping volume totals for each year of operation is provided in Table 4.

Table 4: Pumping volume totals and in mm (for lowland area 17 ha) and entire Sandhill Watershed (52 ha)

Year	Total inflow (m ³)	Total outflow (m ³)	Inflow to lowland-17ha (mm)	Outflow from lowland-17ha (mm)	Inflow to Watershed-52ha (mm)	Outflow from Watershed-52 ha (mm)
2013	147838	150162	970	883	284	289
2014	2470	2907	15	17	5	6
2015	0	9334	0	55	0	18
2016	0	0	0	0	0	0
2017	0	17362	0	102	0	33
2018	0	32655	0	192	0	63

INSTRUMENTATION

A map detailing some of the significant instrumentation to support research and monitoring is shown in Figure 5. The following sections describe some of the key pieces of instrumentation used to support the research and monitoring of the Sandhill Fen Watershed.

Inflow and Outflow Measurement

Inflows and outflows were measured using ultrasonic flowmeters as well as a transducer to measure the level in the water storage pond. Outflow consists of surface flow and underdrain contributions. Surface drainage flowed through a v-notch weir, instrumented with a sensor to continuously record level and then into the sump, where underdrain water is collected and total discharge pumped away from the fen. Flowmeters were installed for both pump inflow and outflow locations.

Weather Stations

Weather stations (3) were installed to collect air temperature, relative humidity, wind speed and direction, net radiation, snow depth, snow water equivalent and rainfall data. Soil moisture and temperature data were collected to a depth of 1 m.

Eddy Covariance Stations

Eddy covariance (ECoV) stations were erected at two principal sites (upland and wetland) and for a short time period (2014-2016) between the 2 perched fens (Figure 5). This instrumentation was used to measure evapotranspiration and ecosystem-scale vertical carbon fluxes. For details of this method please see Appendix 3. The EcoV towers were installed in 2012 (upland), 2013 (lowland), and 2014 (perched fens). The upland and perched fens sites operate from May to October annually. The wetland site is provided power to run year-round.

Near-surface wells

A network of 27 surveyed near-surface wells were installed throughout the fen to measure water table elevation in order to establish depth of the water table from surface and for water quality sampling (Figure 5).

Hydrogeology wells

A total of 223 piezometers, organized into 85 nests (i.e., a nest is monitoring location), were installed in the surficial reclamation materials and tailings sand. Piezometer nest locations were chosen along transects oriented parallel to anticipated flow directions (2) and associated with soil-moisture measurements and vegetation plots (see Figures 5, 6 and Appendix 6). Each nest consists of one to six piezometers screened between 1 and 11 metres below ground surface (m BGS). Within a nest, piezometer standpipes were separated laterally by approximately 1 m and piezometer screens separated vertically by 1 to 4 m intervals. Piezometers were generally installed in augered holes and pushed through caved sand below the water table. Surveys were performed regularly to update, track, and correct piezometer elevations throughout annual freeze/thaw cycles.

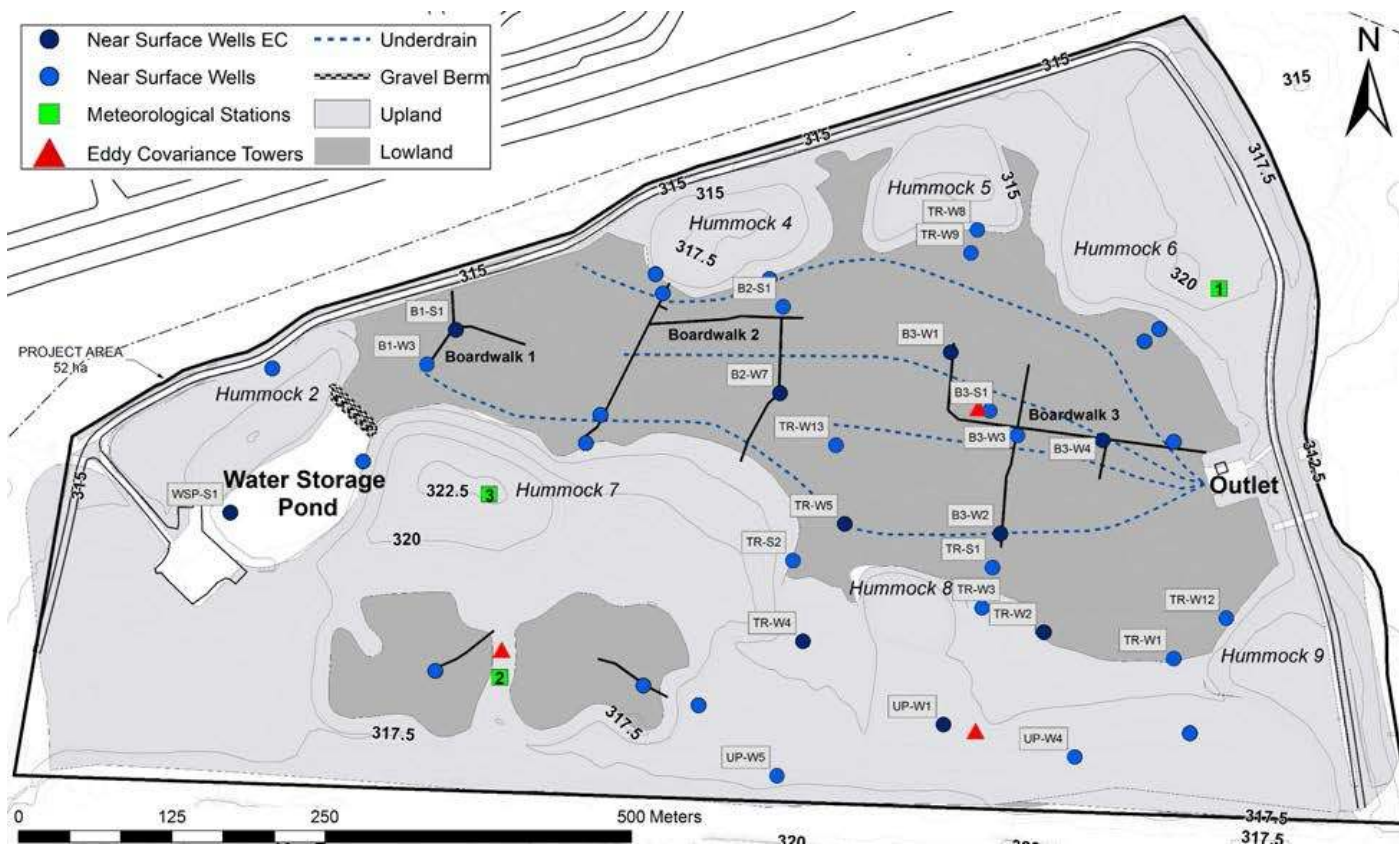


Figure 5: Locations of near-surface wells and other instrumentation

6 RESEARCH PROGRAM

A key objective of the Sandhill Fen Watershed research program is to gain knowledge and provide guidance for future lease development and reclamation. Three key study areas include: understanding the nutrient, salt and water balances, landform design guidance, and wetland reclamation guidance. Research done on the Sandhill Fen Watershed will lead to better reclamation practices and an increased ability to meet our closure commitments.

Core research activities are summarized in the following sections. Other monitoring activities that have been undertaken in the watershed include: wildlife monitoring (songbirds, mammals, rodents and amphibians), macroinvertebrate monitoring, soil monitoring, vegetation monitoring, water quality (inlet and outlet), and time-lapse photography.

HYDROGEOLOGIC INVESTIGATIONS OF SANDHILL FEN WATERSHED AND PERCHED ANALOGUES- CARL MENDOZA AND KEVIN DEVITO (UNIVERSITY OF ALBERTA)

Key Learnings

- A shallow groundwater flow system developed in the watershed. These systems can be designed post-mining landscapes and provide freshwater to downgradient wetlands.
- *Horizontal groundwater flow often results in discharge to the lowlands through seepage faces.*
- *Groundwater within 1.8 m of the water table has a higher proportion of freshwater, indicating groundwater recharge and the development of a freshwater lens.*
- *Groundwater deeper than ~1.8 m below the water table is primarily comprised of oil sands process-affected water (OSPW).*
- *Water discharging through seepage faces may be subject to evapo-concentration during dry periods, leading to a shallow accumulation of water with elevated solute concentrations. Since shallow water tables are highly responsive to inputs of water, areas with shallow water tables and gentle slopes are prone to discharging water with elevated solute concentrations following precipitation events.*
- *Water table configurations respond dynamically to variable recharge rates influenced by depth to the water table, and reclamation prescriptions for soil covers and vegetation.*
- *Recharge varies with soil cover texture (higher in coarser-textured materials) and associated soil hydraulic parameters.*
- *Finer-textured soil covers tend to retain water which is then lost to the atmosphere through evapotranspiration.*
- *Simulation results demonstrate a threshold-like relationship between recharge and upland hummock height, where upland hummocks that are not tall enough to limit root water uptake from the saturated zone exhibit decreased recharge or net upflux.*
- *Recharge is influenced by maximum rooting depths, forest floor placement thicknesses, and leaf area indices on recharge- increased forest development will lead to decreased recharge rates to underlying groundwater systems.*
- *Inter-annual climatic variability is as influential as variation in soil cover texture in determining recharge.*
- *Average recharge rates applied to upland areas ranged from 40 mm/year for wetter ecosites to 88 mm/year for drier ecosites.*
- *Average volumetric groundwater flow through the system was calculated to be 108 m³/d.*

Maintenance of natural and constructed wetlands in the Fort McMurray area is controlled by interactions of local surface and soil water storage and excess water received via surface runoff and groundwater discharge (Devito and Mendoza 2007). This is largely because of the sub-humid climate resulting in long-term soil moisture deficit (Winter and Woo 1990). However, due to the low rainfall in this region, runoff from upland areas is minimal and excess water is derived largely from low-lying ephemeral draws or wetland areas of the landscape where water loss via evapotranspiration is reduced, and fine-grained sediments result in higher water tables (Devito *et al.* 2005). In addition, coarse-grained uplands may provide significant recharge to groundwater, providing excess water in discharge zones for stream base flow and wetlands (Smerdon *et al.* 2005, Winter and Woo 1990). However, the upland topography (depth to water table) and vegetation will have a large control on the amount of recharge, and in upland features with shallow depth to water table, net removal of groundwater may occur (Smerdon *et al.* 2008).

Construction and long-term maintenance of fen wetlands, which require excess water input, may require adequate connection to headwater ephemeral draws or wetlands for surface water inputs and adjacent uplands that provide adequate groundwater discharge.

Alternatively, in many years, the uplands adjacent to wetlands may be a net sink for water because of the vegetation. A better understanding of the total area and spatial orientation of surface flow systems and recharge uplands required to maintain wetlands is required. In addition, the role of groundwater discharge and surface flow networks in diluting, or concentrating salts in wetlands and transition areas is important to understand.

This work comprised hydrologic studies to quantify and generalize landscape and transition zone hydrologic interactions within the Sandhill Fen Watershed at a number of scales. These range from determining the hydrologic role of basin-scale hummocks, to the contributing influence of transition areas and ephemeral draws, to the hydrologic functioning of the two isolated perched fens. The field studies were designed to help develop and refine models that can be used to generalize hydrologic and salt dilution requirements, if any, for future landscape reconstruction.

In terms of hummock technology, this program tested the configuration, height, and size of coarse-grained (tailings sand) hummocks, to maintain wetland and forest ecosystems on reclaimed landscapes. A key focus of understanding the role of hummocks, was to determine the relative contribution to the water balance in the watershed of the potential of the upland hummocks to generate flow, and flush salts, and the uptake of water through upland transpiration.

The purpose of the perched fen research was to test soil layering and the role of storage in layers of different types and thicknesses for generating moisture surplus for wetland and adjacent forest water demands. In particular, the research addressed whether the layering can keep salts below the ground surface and reduce ET to generate surplus freshwater, and whether an un-compacted clay can layer hold enough water and whether enough freshwater can be generated in isolated wetland regions to develop a viable wetland. These perched wetlands were meant to test if we can mimic some natural systems investigated previously (Devito *et al.* 2012) and to do this, required a clay liner. Although a fine-grained, lower conductivity layer was placed, it was not compacted and therefore was too permeable to pond water.

Ephemeral draws were also a component of the watershed design to determine the role of these areas on generating moisture surplus and delivering water to wetlands and adjacent forests. Specifically, the research addressed whether these ephemeral draws can provide intermittent runoff to wetlands, or whether the vegetation utilizes the water instead. It was also important to understand the role of ephemeral draws (and also perched wetlands) in providing moisture to and thus the viability of adjacent forested areas.

Hydrogeological field instrumentation consisted of shallow wells and piezometers, access tubes for soil-moisture measurements, and soil pits with buried devices to measure soil-moisture content and soil-water tension. The network of piezometers is shown in Figure 6. A total of 223 piezometers, organized into 85 nests, were installed in the surficial reclamation materials and tailings sand. Piezometer nest locations were chosen along transects oriented parallel to anticipated flow directions and associated with soil-moisture measurements and vegetation plots (see Appendix 2 and 7).

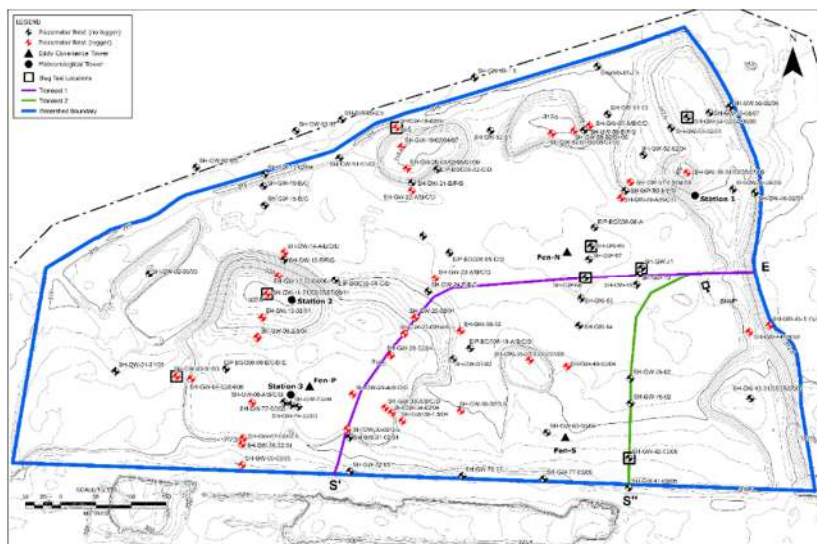


Figure 6: Topographic site map of SHW (blue outline), piezometers and other instrumentation. Transects 1 (S'-E) and 2(S''-E) correspond to different topographic configurations in the watershed, hummocks to wetlands and slopes to wetlands, respectively. (Figure from Twerdy, 2019.)

Hummock Topography and Groundwater Flow Systems

For a detailed description of the Sandhill Fen as a case study for the performance of the hummock topography in establishing flow systems to support wetland and forest vegetation, see Appendix B-*Hummock Technology Learnings to Support Water Management on Reclaimed Landforms*. Some key findings are stated here for context. The hummocks constructed in Sandhill Fen Watershed developed a shallow groundwater flow system. Average vertical hydraulic gradients are generally weak throughout the watershed, including discharge areas, because their directions often fluctuate and are highly transient. Consequently, the horizontal groundwater flow often results in discharge to the lowlands through seepage faces. Where hummocks meet lowlands at an abrupt interface, focused discharge areas tend to arise. Where gentle upland slopes grade into lowlands, these interfaces tend to be broad and discharge is diffuse. That is, water tables may intersect the land surface over a large area, particularly as the water table fluctuates through time, on shallow slopes. Although all of the hummocks in Sandhill Fen Watershed facilitated recharge, none of the constructed hummocks developed groundwater mounds that altered water flow patterns. This held true during average, wet, and dry conditions, and during large precipitation events (e.g. snowmelt and rainfall of ~ 60 mm/day), highlighting the temporal stability of this hummock function currently present within Sandhill Fen Watershed. Recharge facilitated by the hummocks was substantial, upwards of 25% of annual precipitation in some cases, and the design of coarse-textured soil covers on hummocks in Sandhill Fen Watershed was nearly optimal for partitioning water to recharge. Overall, the horizontal component of groundwater flow was dominant and resulted in the formation of flow-through conditions at hummock-lowland interfaces throughout Sandhill Fen Watershed (Twerdy, 2019).

Solute Patterns

One of the objectives of the constructed hummocks in Sandhill Fen Watershed included forming local-scale groundwater flow systems to facilitate solute management and minimize the expression of solutes at the surface. It was anticipated that the hummocks would function to flush and freshen the groundwater system at Sandhill Fen Watershed through recharge. Groundwater mixing was anticipated to occur between the different geochemical end-members comprising the water chemistry at Sandhill Fen Watershed: oil sands process-affected water (residual tailings pore water), Mildred Lake Reservoir water (on-site freshwater reservoir) and meteoric water associated with precipitation (Twerdy, 2019). Although the water table configuration from 2014 to 2017 appeared to be linear, without groundwater mounds beneath hummocks as was anticipated, the solute distribution and movement appears to have developed into a pattern comparable to that expected if groundwater mounds had developed below hummocks. This was largely due to the laterally-dominant, intermediate-scale groundwater flow that developed, where incoming recharge moved horizontally rather than vertically. Furthermore, upward vertical groundwater discharge was variable, but overall negligible, indicating solute movement associated with OSPW has been passively managed in Sandhill Fen Watershed.

Both the hydraulically-placed tailings sand used to construct Sandhill Fen Watershed and the mechanically placed tailings sand used to construct hummocks were entrained with OSPW, having saline-sodic properties (Mikula *et al.*, 1996). Consequently, the initial geochemistry and major ion concentrations of Sandhill Fen Watershed following construction were characterized by process-affected water, with elevated sodium concentrations and sodium adsorption ratios (SAR; Biagi *et al.*, 2019). Immediately following construction, water from Mildred Lake Reservoir, a nearby freshwater reservoir comprised of Athabasca River water and precipitation (lower SAR), was pumped into a storage pond in SHW. Storage pond water was released into the lowlands at Sandhill Fen Watershed to initially freshen the groundwater system (Biagi *et al.*, 2019; Twerdy, 2019). Infiltrating precipitation and associated recharge represented a meteoric flux starting in 2012 after watershed construction was completed. Meteoric water appeared to have a distinct isotopic signature from the other two end-members, even though it was dilute and similar in composition to MLR, aiding in determining recharge patterns between hummocks and other forested upland areas in Sandhill Fen Watershed (Twerdy, 2019).

Overall, the spatial and temporal distribution of solutes underlying hummocks and forested upland areas were an expression of the groundwater flow system and recharge dynamics at Sandhill Fen Watershed. Geochemical data from Sandhill Fen Watershed indicated that there was limited temporal variability in the geochemistry at a given location (i.e. piezometer nest), and that spatial trends were more prominent (Twerdy, 2019). The degree of variability in groundwater geochemistry throughout a field season was notably greater in areas where the water table was near ground surface (i.e. the south slope and hummock-lowland interfaces), compared to areas with water tables deeper below ground surface (i.e., beneath hummocks). Electrical conductivities were responsive to precipitation or pumping events (Figure 7), where peaks occur several days after major flux events (e.g., extreme rainfall in 2016 or pumping in 2017; Twerdy, 2019), although the groundwater quality returned to baseline solute conditions soon thereafter.

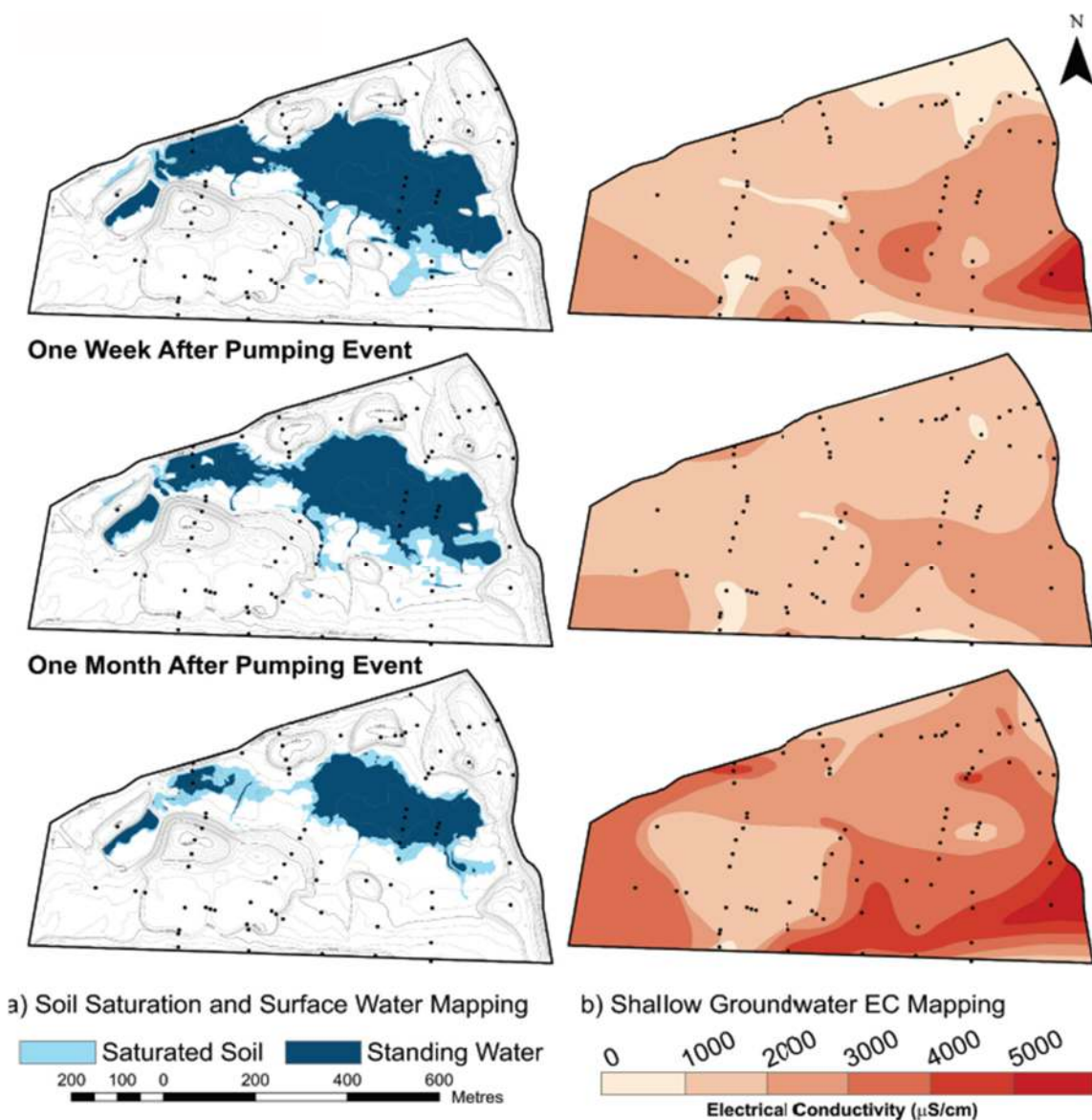


Figure 7: Temporal and spatial evolution of electrical conductivity following a pumping event at Sandhill Fen Watershed, representative of wet, mesic, and dry periods within Sandhill Fen Watershed and in relation to hummocks.

Spatially, elevated sodium concentrations and electrical conductivities were consistently observed at piezometers installed deeper within the saturated zone beneath hummocks (i.e. at depth in the water column), simply reflecting that process-affected water was present at depth in Sandhill Fen Watershed. Sodium concentrations and SAR also tended to be elevated in the near-surface at hummock-lowland interfaces and along the south slope (Biagi *et al.*, 2019; Twerdy, 2019). Biagi *et al.* (2019) hypothesized that elevated sodium concentrations and SAR may be attributable to the discharge of deeper process-affected groundwater. However, data from piezometers indicated that upward vertical gradients were limited in duration and spatial extent along the hummock-lowland and slope-lowland interfaces (Twerdy, 2019; see Appendix 2); therefore, the magnitude of deeper groundwater discharge was likely negligible. As an alternative explanation, Twerdy (2019) proposed that the likely cause of elevated electrical conductivity and sodium in areas with shallow water tables was because recharge was limited in areas like the south slope (i.e. limited freshening) and that the configuration of these areas resulted in the development of broad seepage faces where horizontally-driven groundwater intersected the land surface (i.e. flow-through). Additionally, the south slope and areas with shallow water tables also had thin unsaturated zones that were not flushed by

surface water runoff (as was the case in the lowlands). As a result, high evapotranspiration rates facilitated by root water uptake may have allowed solutes to concentrate in the unsaturated zone that were subsequently mobilized when the water table rose (i.e. evapo-concentration).

Geochemical, EC and stable water isotope data consistently show that groundwater deeper than approximately 1.8 m below the water table is predominantly comprised of OSPW. In areas where the water table is regularly found at depth (>1.8 m BGS), the chemistry of the groundwater within 1.8 m of the water table has a higher proportion of freshwater, indicative of groundwater recharge and the development of a freshwater lens. The chemistry of the groundwater within 1.8 m of the water table becomes more mixed with OSPW solutes as the water table transitions from deep (>1.8 m BGS) to shallow (<1.8 m BGS). However, once the water table regularly fluctuates at, or above, ground surface, which results in intermittent standing water, the water becomes fresher, regardless of the depth where the water was sampled. Geochemical data coupled with isotopic samples indicated that hummocks, and the recharge they facilitated, were freshening a thin zone near the water table in the first years after construction (Figure 8), most notably in areas where the water table was deeper below ground surface (i.e. below hummocks; Twerdy, 2019). The thickness of the freshwater lens was greater for hummocks with coarse-textured soil covers, exemplified by the contrast between Hummock 7 with a coarse-textured soil cover versus Hummock 9 with a fine-textured soil cover (Figure 8). While both of these hummocks have water tables well below the ground surface, Hummock 7 exhibited much lower electrical conductivities than Hummock 9, which was likely associated with the contrast in recharge between these locations (Twerdy, 2019, Appendix 2).

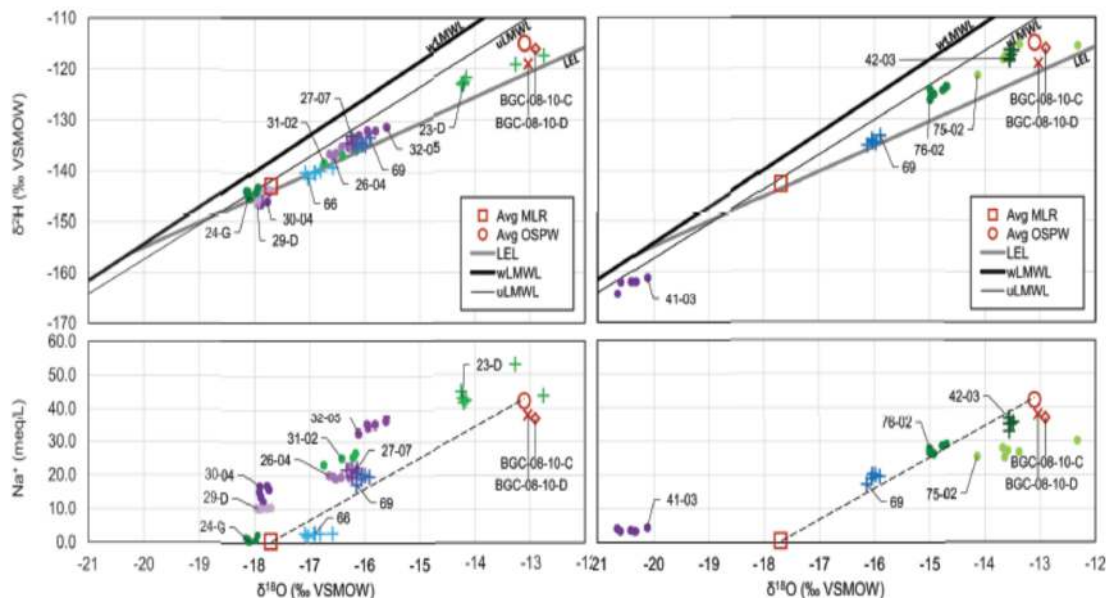


Figure 8: Paired plots of δ^2H vs $\delta^{18}O$ (upper) and Na^+ vs $\delta^{18}O$ (lower) values collected inside the shallowest piezometer from nests (numbers indicate locations) along Transects 1 and 2 (hummock-to-wetland). Average endmember compositions, Mildred Lake Reservoir (MLR) and process-affected water (OSPW) and deep groundwater samples (BGC-##-## piezometers) are plotted in red. Weighted and unweighted meteoric water lines are shown in upper plots. All remaining data are groundwater samples from shallow piezometers in the tailings sand, with shapes and symbols indicating water classes identified by Twerdy (2019). Chemistry data in lower plots were plotted with a theoretical mixing line between the average MLR and average OSPW endmember compositions. Adapted from Twerdy (2019).

To further evaluate the temporal nature of solute flushing through hummocks in Sandhill Fen Watershed, long-term climate simulations were adapted from Lukenbach *et al.* (2019) to determine the progression of pore volume flushing in the hummocks. Several scenarios were considered, including a coarse-textured versus fine-textured soil cover, two porosity values (0.30 versus 0.40), and two hummock heights (4 m vs. 8 m). Over a 53-year period, less than half (0.5) a pore volume had flushed for all scenarios considered. Pore volume flushing facilitated by the coarse-textured soil cover was greater than the fine-textured soil cover by a factor of approximately 2 to 2.5. Comparatively, a difference in porosity of 0.10 resulted in a pore volume flushing that was 1.33 times greater for the low porosity

scenario versus the high porosity scenario. Assuming that process-affected water entrained in the pore spaces behaves conservatively, solutes will continue to be flushed from the unsaturated zone of the hummock for greater than 100 years. This analysis assumed the hummock is homogeneously flushed, whereas spatial variability throughout the unsaturated zone of hummocks likely occurs at the field-scale. Combined with observations of freshening detailed by Twerdy (2019), these results are indicative of how the water quality underneath hummocks may evolve over time.

Transition areas from uplands to lowlands are not always directly adjacent to wetland areas; that is, the transition areas are on the perimeter of the lowlands. Water discharging through seepage faces in these areas may be subject to evapo-concentration during dry periods, leading to a shallow accumulation of water with elevated solute concentrations. Since shallow water tables are highly responsive to inputs of water, areas with shallow water tables and gentle slopes are prone to discharging water with elevated solute concentrations following precipitation events. This phenomenon may explain previous observations of hot spots of high solute concentrations within the wetlands.

Many of the above findings rely on the water table configuration relative to the land surface. Results of coupled unsaturated-saturated modelling, constrained by field observations, demonstrate that water table configurations respond dynamically to variable recharge rates influenced by depth to the water table, and reclamation prescriptions for soil covers and vegetation. Recharge varies with soil cover texture (higher in coarser-textured materials) and associated soil hydraulic parameters. Finer-textured soil covers tend to retain water which is then lost to the atmosphere through evapotranspiration. Simulation results demonstrate a threshold-like relationship between recharge and upland hummock height, where upland hummocks that are not tall enough to limit root water uptake from the saturated zone exhibit decreased recharge or net up-flux.

Based on slug test results and model calibration, the homogeneous, isotropic hydraulic conductivity of the tailings sand was 1.3×10^{-5} m/s. This value is within the range of values provided by Thompson *et al.* (2011) and compares favourably to the value of 3.5×10^{-5} m/s used by Lukenbach *et al.* (2019). Consistent with Lukenbach *et al.* (2019), average recharge rates applied to upland areas ranged from 40 mm/year for wetter ecosites to 88 mm/year for drier ecosites. Average volumetric groundwater flow through the system was calculated to be 108 m³/d.

Scenario tests indicate the general importance and relative influence of maximum rooting depths, forest floor placement thicknesses, and leaf area indices on recharge. These relationships imply that improved forest development will lead to decreased recharge rates to underlying groundwater systems. However, simulations utilizing a historical climate record indicate that inter-annual climatic variability is as influential as variation in soil cover texture in determining recharge to the wetland.

Specific details about hummock performance can be found in section Appendix B-*Hummock Technology Learnings to Support Water Management on Reclaimed Landforms*.

WATER AND CARBON BALANCE OF THE CONSTRUCTED FEN: SEAN K. CAREY (MCMASTER UNIVERSITY) AND ELYN. R. HUMPHREYS (CARLETON UNIVERSITY)

Water Balance Key Learnings

- *The precipitation climate of Sandhill Fen Watershed during 2013-2018 was drier than the climate normal*
- *In the uplands, ET increases in most months as Leaf Area increases*
- *ET does not increase in the same way in the wetland- changes to vegetation and boundary layer properties are modest. ET is driven largely by atmospheric demand.*
- *Water inflows via pumping occurred only in 2013 and 2014.*
- *Water outflow management since 2013 has been used intermittently to prevent critical infrastructure damage*
- *Hummocks can generate freshwater runoff during spring freshet- earlier on south-facing than on north-facing slopes.*
- *In summer, surface runoff from hillslopes will not respond to most rain events, but in cases where high intensity rainfall exceeds infiltration capacity, overland flow will occur.*
- *The water table was always highest in spring, and then declined gradually throughout the summer as evapotranspiration increased. Large rainfall events rapidly increased water table.*
- *There is considerable yearly variability in most components of the water balance, related both to management and to climate variability*

Research on the water and carbon processes at Sandhill Fen Watershed began in 2012, and was led by Dr. Sean Carey and Dr. Elyn Humphreys. The program attempted to understand and quantify the dominant water and carbon flux processes occurring in Sandhill Fen Watershed, and to provide context by comparing to natural boreal systems, and to assess the sustainability of the fen design in terms of developing coupled upland-lowland ecosystems over longer time scales. This project also included preliminary assessments of water chemistry processes.

The specific objectives of this research program are the following:

1. Measure the ecosystem scale annual water and carbon balance and establish their dominant controls.
2. Establish the inter-fen variability in carbon and methane fluxes
3. Characterize the quantity and amount of aqueous carbon leaving the fen through surface pathways.

Details of experimental design, methods, analysis and interpretation can be found in Appendix 3. A summary of research results related to water balance, carbon balance and water quality follows.

Water Balance Components

Although conceptually simple, closing water balances are challenging. Conventionally, rainfall and runoff are measured, change in storage is considered negligible and evapotranspiration is assumed as the difference. For the Sandhill Fen Watershed attempts were made to measure all components of the water balance, which allows for a greater understanding of rates and timing of fluxes, but errors can compound when all components of the water balance are considered together.

For Sandhill Fen Watershed, the water balance is:

Inputs-Outputs = Change in storage

Inputs = Rain + Snow + Pump In + Groundwater In

Outputs = Evapotranspiration + Pump Out + Groundwater Out

Snow

Snowfall was estimated annually via a number of methods, and the best long-term estimate of snow water equivalent was a combination of late-season snow surveys validated against the C725 Snow Water Equivalent (SWE) sensor. In 2018, a more detailed investigation of snow variability was undertaken to more completely assess intra-fen variability. On average, the SWE for the watershed was less than the 30-year mean. In 2014-2017 the SWE was well below normal, with average values between 50 and 60 mm. In 2013 and 2018, the SWE was approximately equal to the Fort McMurray 30 year mean.

RESEARCH

Annual snow surveys indicate moderate variability of snow amount within the fen, and this variability is inconsistent between years. A snow survey during peak SWE in February 2018 indicated modest SWE variability. Hummocks had less SWE than the other upland (i.e. non-wetland) areas.

Rain

Rainfall, measured using 4 tipping bucket gauges across the watershed, showed high variability among seasons and years. Some years (2016-2018) were above the climate normal, and all other years were below. This pattern does not reflect the considerable inter-annual variability which plays a strong role in the hydrology of Sandhill Fen Watershed. As an example, 2018 was a relatively dry to average early growing season, until a very large rainfall event in July (~100 mm). In most years, large periods of dry weather were interrupted by moderate to large rain events in excess of 10mm/day. Overall the precipitation climate of Sandhill Fen Watershed from 2013-2018 was drier than the climate normal (Figure 9)

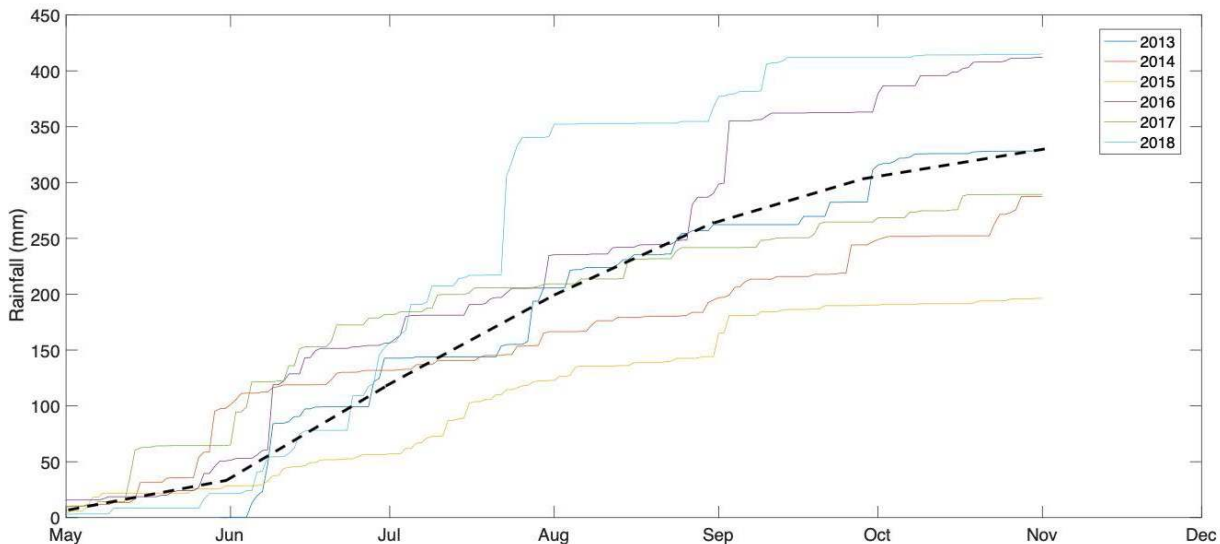


Figure 9: Rainfall at the Sandhill Fen Watershed from 2013-2018. Dashed line is the Ft McMurray 30-year monthly sums for context.

Water Inflows and Outflows

Management of water inflow pumping occurred only in 2013 and 2014. In 2013, inflow began in late May and continued steadily for the growing season, with two periods of no flow (see Nicholls *et al.* 2016 and Spennato *et al.* 2018 for further details). In total for 2013, 1.48×10^5 m³ of freshwater was supplied to the fen. In 2014, inflow began on May 19-20 at maximum pump capacity for about 6 hours only, and then turned off for the rest of 2014. This supplied 2470 m³ of freshwater from May 1 to September 30 2014. After this, no freshwater has been imported to the Sandhill Fen Watershed via the water management system.

Water outflow management also varied among the years. In 2013, pump outflow began in early April, and was active until October. Discharge peaked at 283 m³/h and fluctuated greatly. Total 2013 outflow is estimated as 1.5×10^5 m³. Underdrains remained open during 2013, and this dominated the outflow, contributing over 90% of total discharge. In 2014, the valve connecting the underdrains to the sump was closed, and although there was a small amount of leakage, outflow was dominated by surface contributions in 2014. Since 2013, water management has been dramatically reduced, however on several occasions outflow pumps have been turned on to lower the water table in the lowland because excessive inundation was compromising research infrastructure (boardwalks, instruments, and research plots). In 2017 and 2018, large rainfall events contributed to high water tables and pump out was initiated. This proved an effective method to remove water or short time frames (days). A summary of pumping volume totals for each year of operation is provided in Table 4.

Evapotranspiration (ET)

Evapotranspiration was measured at the upland and wetland eddy covariance sites, over multiple years. ET varied seasonally in response to climate and over shorter timescales, in response to weather. The relative influence of daily weather on ET fluxes is large, and is driven by radiation, vapour pressure deficit and windspeed. In the uplands, the influence of vegetation development on ET is evidenced in an increase in ET in most months as leaf area increases. In 2017, June-August ET rates were ~0.8mm/day greater than in 2013. These

patterns of increasing ET are not apparent in the wetland areas as changes to vegetation and boundary layer properties (turbulence) were modest, and ET was largely driven by atmospheric demand.

ET in the uplands was on average, greater than the lowlands, but not in all years and all seasons. Annual ET estimates are provided in Table 4. It may seem counter-intuitive that the uplands on average had greater annual ET than the lowland, well-watered vegetation surfaces have been reported to have greater total ET than wetlands due to enhanced roughness which decreases atmospheric resistance and enhances turbulent transport.

Water Table Dynamics

Water table was measured throughout the watershed at a number of sampling wells. A single well reported year-round water levels at the wetland eddy covariance site (Figure 10). Near surface wells were distributed throughout the lowland and uplands along pre-defined across and down-gradient transects. Detailed information about water table dynamics can be found in Spennato (2016) and Spennato *et al.* (2018).

Annual water table measured at the lowland tower, in the approximate centre of the lowland area indicates a water table higher than the target water table of ± 20 cm of ground surface. With the exception of 2013, and the onset of 2014, water tables were always above the surface. The water table was always highest in spring, and then declined gradually throughout the summer as evapotranspiration increased. Large rainfall events rapidly increased water table. During the 100 mm event in July 2018, the water table rose 30 cm over 4 days, and in 2016, a wet fall resulted in very wet conditions. The influence of the pump is clearly demonstrated in Figure 10, as continuous operation can rapidly lower the water table.

The Sandhill Fen Watershed has complex longitudinal and lateral hydraulic gradients as represented by the water table surface. The hydrogeological setting of Sandhill Fen Watershed is described in previous sections, and details of the role of upland hummocks on groundwater movement are found in Appendix B-*Hummock Technology Learnings to Support Water Management on Reclaimed Landforms*. Spennato *et al.* (2018) examined differences in water table position for the fen and between the lowland and the upland at several hummock sites. In general, large-scale lateral groundwater flow direction was from the south swale towards the Sandhill Fen Watershed lowland, with more regional groundwater flow system then diverging north-east beyond the topographic boundary of the watershed (see Appendices 2, 3 for more details). While deeper groundwater systems respond slowly to weather conditions, the shallow water table dynamics within the Sandhill Fen Watershed exhibited high-frequency fluctuations. Using 2014 and 2015 as an example, at the beginning of the growing season the lateral hydraulic gradient and near-surface flow was typically from the inlet (B1; west) towards the outlet (B3; east) (Figure 10). However, as drying progressed over the summer, the hydraulic gradient within the lowland reversed by August. During this period of flow reversal, the hydraulic gradient was from the outlet (B3; east) towards the inlet (B1; west). In 2014, weaker and shorter flow reversals occurred, with reversed flow conditions present for a total of 12 days. In contrast, flow was reversed for a total of 52 days in 2015, with stronger horizontal hydraulic gradients in 2015.

Frequent flow reversals were observed between the hummock margins and the lowlands, with the direction of upland-lowland horizontal hydraulic gradients varying as the season progressed. Water flow from the lowland into the margins was more common in 2014 compared with 2015, which was more dynamic and had more frequent flow reversals. Rainfall events elicited a larger water table rise in the margins relative to the lowland area, which resulted in an increase in the lateral hydraulic gradient, indicating a water flux from the margins to the lowland.

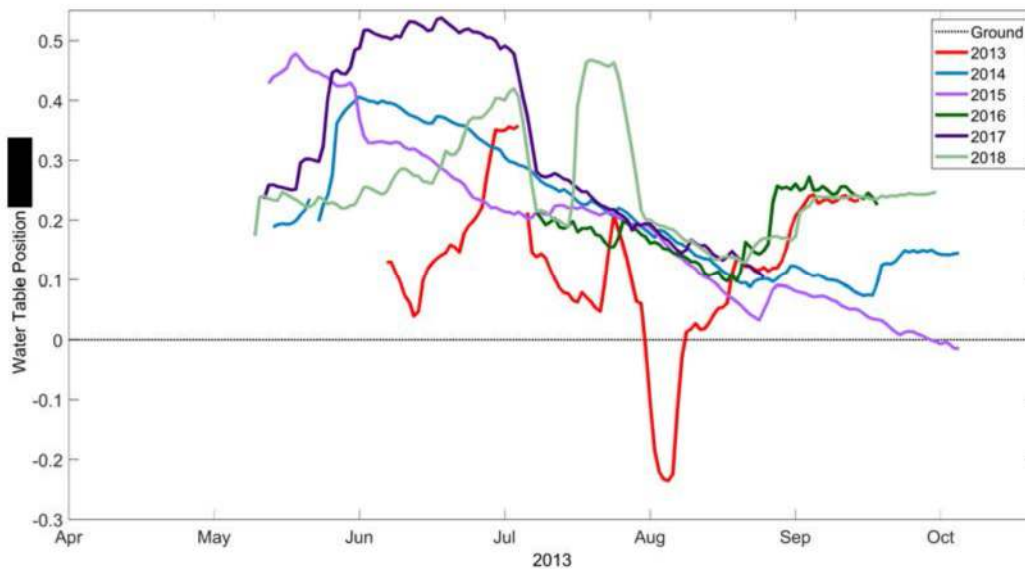


Figure 10: Water table as measured at the lowland tower.

Runoff Processes

The Sandhill Fen Watershed does not have a natural outlet and runoff process that generated outflow from the watershed were not assessed. During summer field activities, no surface runoff was observed during rainstorms and therefore most lateral redistribution within the Sandhill Fen Watershed was considered to occur via subsurface pathways. However, in 2018, a detailed investigation of snowmelt runoff was undertaken on two slopes (north and south facing) during the melt period to identify if lateral runoff occurred during melt. Note that winter 2017/18 was a relatively large snow year and melt was slightly earlier than normal. Details of the runoff assessment can be found in Appendix 3.

Results from runoff collectors on hummocks 5 (south facing) and hummock 8 (north facing) generated runoff during spring freshet. The south-facing slope had meltwater generation approximately one month in advance of the north-facing slope. Through March 15-20 2018, 18 mm of runoff was collected, representing 30% of the snowpack at this site. In contrast, melt on the north-face occurred between April 22-24 and generated 23 mm of water, providing a runoff ratio of ~40%. This suggests that hillslopes have the potential to generate runoff during the snowmelt period. For further details please see Appendix 3.

While runoff was not previously observed during storm events, the continued operation of the collector on the south-facing slope during summer of 2018 allowed for evaluation of whether summer rainfall generated runoff. Unsurprisingly, the 92 mm storm centred on 21 July generated 17 mm of runoff (30% runoff ratio), which was very large. However, all other events, even those of 30 mm, generated almost no runoff (all <0.1 mm). This type of runoff behaviour where large thresholds must be exceeded to generate runoff are widely observed. Surface runoff from hillslopes will not respond to most rain events, but in cases where high intensity rainfall exceeds infiltration capacity, overland flow will occur.

Annual Water Balance Components

Annual water flux totals are shown in Table 5. Note that there is considerable yearly variability in most of the terms, related both to management and to climate variability. In addition, the maximum snow water equivalent is reported in the year that it melts. In certain years, inputs exceed outputs whereas in other years, outputs exceed inputs. It is challenging to ‘close’ the water balance without a distributed measure of storage, which is beyond the scope of this study, yet all fluxes in Table 5 are reported with medium (for pumps) to high (all other) confidence.

RESEARCH

Table 5: Annual water balance components as measured at Sandhill Watershed. NA means not measured, X means analysis in progress

Year	Rain (mm)	Snow (mm)	Inflow to Watershed- 52ha (mm)	Outflow from Watershed- 52 ha (mm)	Upland Evapotranspiration (mm)	Lowland Evapotranspiration (mm)
2013	329	138	284	289	324	381
2014	287	55	5	6	377	370
2015	196	58	0	18	371	373
2016	415	56	0	0	NA	337
2017	289	48	0	33	399	353
2018	415	105	0	63	X	X

Carbon Balance Key Learnings

- The carbon balance of the fen is dynamic:
 - In the beginning, the lowland was a large source of CO₂ to the atmosphere and Gross Ecosystem Productivity (GEP) was low due to limited photosynthesis.
 - Following vegetation establishment GEP and Net Ecosystem Productivity (NEP) increased rapidly.
 - By 2016, the wetland was a C sink.
 - In 2017, CO₂ uptake declined and the fen became a carbon source again.
- Ecosystem respiration at the upland site has increased with time, in part offsetting some of the photosynthetic gains in a net balance. This is a function of increased soil biomass and decomposition of fresh litter.
- The lowland had suppressed respiration in all temperatures and years due to saturated conditions.
- CH₄ emissions in the present study unexpectedly remained very low over the three years despite the establishment of a high water table in the lowland areas of the Sandhill Fen Watershed.
- Vegetation community composition (Typha vs. Carex) has an influence on the carbon dynamics (both NEP, and CH₄ flux)
- DOC varied widely throughout the fen and is exhibiting an increase year-over-year from 2013 to 2018.

Carbon Balance Components

The annual carbon (C) balance of the Sandhill Fen Watershed can be represented as:

$$\Delta C_{org} = NEP + F_{CH_4} + netDOC_{EX} + netPOC_{EX}$$

Where:

ΔC_{org} is the annual change in C,

NEP is the net ecosystem production, equal to the difference between uptake of CO₂ through photosynthesis and loss of CO₂ through aerobic decomposition and respiration integrated over the year,

F_{CH_4} is the loss or gain of C through the annual integrated flux of methane (CH₄),

$netDOC_{EX}$ is the net gain or loss of dissolved organic C, and

$netPOC_{EX}$ is the net gain or loss of particulate organic C.

Most studies of northern peatlands estimate a NEP between -20 to -30 g C m⁻² y⁻² (the negative sign indicates a gain of C), F_{CH_4} = 5 g C m⁻² y⁻², and $netDOC_{EX}$ = 5-10 g C m⁻² y⁻². There are no reported annual rates of $netPOC_{EX}$ from peatlands, and at the onset of the study we realized that these fluxes were minor and were not continued after the first few years.

Net Ecosystem Productivity (NEP)

Net Ecosystem Productivity (NEP) is the reciprocal of Net Ecosystem Exchange (NEE). The two terms are used synonymously. When NEP is positive (negative), the site is as a carbon sink (source). When NEE is positive (negative), it is a carbon source (sink). NEP is the difference between the losses from Ecosystem Respiration (ER) and gains from Gross Ecosystem Production (GEP).

NEP was measured at the lowland tower throughout the entire year via AC power. Figure 11 represents the entire data set. Note that there are some gaps due to instrument malfunction. These gaps are filled in using different standard approaches so that each day has photosynthesis and respiration numbers so that an annual NEP/NEE number can be provided. The upland tower only operated during the growing season.

In the first year before establishment, the lowland was a large source of CO₂ to the atmosphere and GEP was low due to limited photosynthesis. Following the establishment of vegetation, GEP and NEP increased rapidly and by the 2015 growing season, the Sandhill Fen Watershed was likely a net carbon sink or carbon neutral. In 2016, the Sandhill Fen Watershed lowland was a small C sink. However, beginning 2017, CO₂ uptake declined and the fen returned to being a carbon source.

The decline in NEP at the lowland was not a result of climate differences, but likely from changes in vegetation composition in the footprint of the tower. For the lowland site, there was a strong continuous uptake until 2016 and then a marked decline in 2017 with a slight recovery in 2018. Since 2015, there has been an increase in *Typha* and decline in *Carex*, which has greater ecosystem production than other wetland species (see Appendices 4, 5 for details about wetland vegetation development).

The upland tower growing season NEE is distinct from the lowland. Once plants were established in 2013, photosynthesis began to systematically increase and NEE became more negative as vegetation developed. This increase has continued with 2017 and 2018 estimated as the growing season with the greatest carbon uptake. Ecosystem respiration at the upland site has increased with time, in part offsetting some of the photosynthetic gains in a net balance. Increased respiration with time is a function of increased soil biomass and decomposition of fresh litter. In contrast, the lowland had suppressed respiration in all temperatures and years due to saturated conditions.

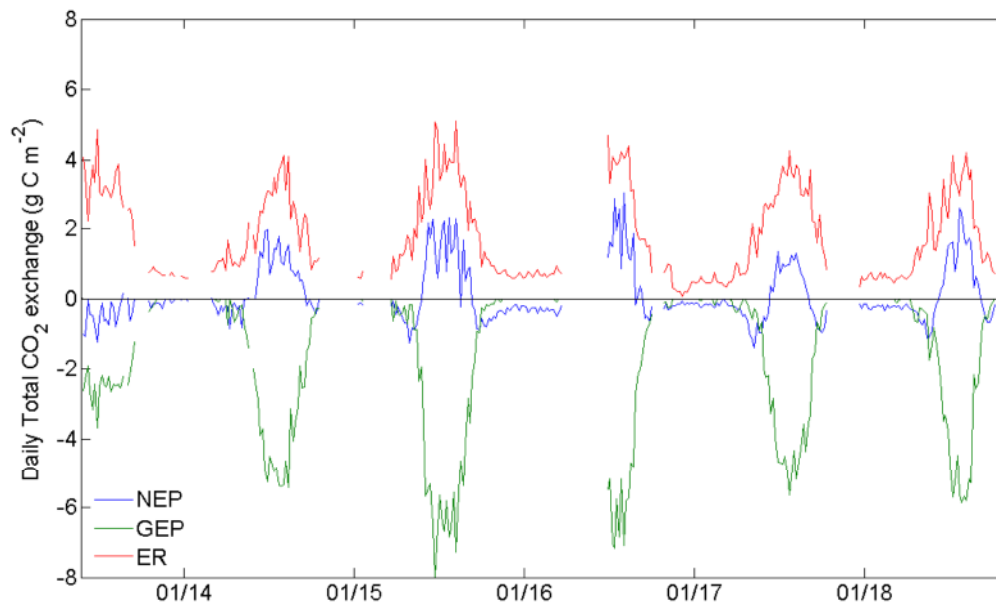


Figure 11: Net Ecosystem Productivity (NEP), Ecosystem Respiration (ER) and Gross Ecosystem Production for the lowland tower

Methane Flux

Methane was measured at a series of chambers which are discussed in detail in Clark (2018). In addition, CH₄ was measured at the lowland tower year-round using the eddy covariance technique. Methane fluxes from the lowland are low compared with those reported in the literature, with some changes seasonally and year-over-year. In natural systems, methane emissions typically increase with increasing water table position within peatlands and among peatlands, and also tend to increase when drained peatlands are restored by flooding. However, CH₄ emissions in the Sandhill Fen Watershed unexpectedly remained very low over the three years despite the establishment of a high water table in the lowland areas of the Sandhill Fen Watershed. Peak CH₄ fluxes from this system are 6 – 30% of the values published from other studies on rewetted peatlands. The fluxes observed in this study are instead similar to those reported from the other constructed wetland in the Alberta Oil Sands region (median CH₄ emissions below 0.08 mg m⁻² h⁻¹) (Murray et al., 2017). These results suggest that although the CH₄ emissions from the Sandhill Fen Watershed are dissimilar from natural wetland systems, the REDOX potentials are low enough to deplete alternative electron acceptors from the substrate, and thus may be favourable to peat formation.

Over the study period, the only plots that showed increasing trends in CH₄ emissions over time were vegetated plots with standing water above the soil surface. The vegetation at these plots was primarily *Carex aquatilis*, and *Typha latifolia*, species with aerenchymatous tissues that enable plant-mediated transport of CH₄ to the surface. These species have been reported in the peatland

RESEARCH

restoration literature to promote CH₄ emissions. However, when examining July methane fluxes (when they would be expected to be greatest), there is no clear trend (Figure 22). In addition, emissions are below the Intergovernmental Panel on Climate Change (IPCC) emission factors for rewetted organic soil (IPCC 2013).

Soil salinity may also have impacted the CH₄ emissions from this wetland. Although the effects of salinity on CH₄ production are not well understood, Poffenbarger et al. (2011) reviewed the literature and found only polyhaline wetlands (18 ppt or ~24000 µS cm⁻¹) had suppressed CH₄ emissions.

Dissolved Organic Carbon

DOC varied widely throughout the fen and is exhibiting an increase year-over-year from 2013 to 2018. Throughout the growing season, DOC increased each month. In addition, DOC increased on average 6 mg/L per year from a baseline level of 14 mg/L in 2013. This increase is associated with a reduction in flushing that occurred during 2013, and an accumulation of organic matter associated with decomposition of new vegetation at Sandhill Fen Watershed. Total export of carbon from DOC is low, ranging from 4 g/m² in 2013 when pumps were exporting large volumes of water to 2.6 g/m² in 2018. Note that this is a relatively small and invariant fraction compared to the GEP fluxes and is largely controlled by pumping volumes.

WETLAND ECOLOGICAL PERFORMANCE: WETLAND PLANT ESTABLISHMENT, COMMUNITY STABILIZATION AND ECOSYSTEM DEVELOPMENT- DALE VITT (SOUTHERN ILLINOIS UNIVERSITY)

Wetland Plant Performance Key Learnings

- *Soil moisture and water table elevation and stability are the key abiotic drivers of plant diversity and abundance.*
- *Water with sodium concentrations below 600 mg/L Na⁺ would allow for a range of wetland plants. Electrical conductivity from a 600mg/L Na solution is ~ 4000 µS/cm.*
- *Conditions (wet vs dry) at time of planting are important for the overall success of plant species.*
- *Scirpus microcarpus, Scirpus atrocinctus, Carex aquatilis, and Carex hystericina are particularly recommended for reclamation: high survival in wet and dry areas, spread quickly, produce considerable biomass.*
- *Beckmannia syzigachne survives well and is a good candidate for a cover crop to reduce weed invasion.*
- *Triglochin maritima survives well regardless of moisture levels, but does not spread as much as other species.*
- *Betula glandulifera performs well in drier wetland areas.*
- *Carex bebbii and Larix laricina survive well in drier sites, Eriophorum angustifolium does better in wetter areas.*
- *Some species are not recommended: Carex limosa, Carex paupercula, Triglochin palustris, and Dasiphora fruticosa.*
- *Fluctuating water tables while plants are establishing may affect survival during early establishment.*
- *Ptychostomum pseudotriquetrum was the most common bryophyte species.*
- *Bryophytes are sensitive to water table. Bryophytes are absent from areas with standing water.*
- *Initial planting of a monoculture allows for higher plant abundance and just as much recruitment of new desirable species as an initial diverse assemblage.*
- *While the peat likely contributed to the development of a soil microbial community similar to established peatlands, the peat likely does not need to be 50 cm deep. A few centimeters of peat may be enough.*
- *If wetland soils become dry, decomposition increases releasing carbon.*

Dr. Vitt and his team have been investigating the soil and water chemistry of the wetland footprint and the dynamics of the developing vegetation community. His earlier work focused on determining native fen plant species that could tolerate the range of salinities expected in the fen (Appendix 4), and the second phase of his effort focused on key ecological functions of wetland performance. Dr. Vitt focuses his interpretation in the context of a fen outcome. He considers desirable species to be fen specific plants and undesirable are those that are not typical of fens, but are still native, regional wetland plants. This must be kept in mind when reading the details of his work (Appendix 4, 5)

Some details of Dr. Vitt's important learnings are shared below, and focus on 4 key areas: plant responses, atmospheric deposition, pore-water chemistry and soil dynamics. To assess these key focus areas, 20 plots were set up throughout the wetland area. Each plot was divided into 4 subplots (quadrants) (Figure 12). One quadrant was planted with a suite of wetland species in 2012, and a second suite in a second quadrant in 2013. The third quadrant was planted in 2013 with a plant community, and the fourth quadrant was left to be vegetated with volunteer species and was used for soil sampling. Surface pore-water sampling and aerial deposition sampling was carried out at all or a subset of these 20 plots. Annual vegetation surveys were undertaken throughout the wetland footprint. Details of methods and results can be found in Appendix 4 and Appendix 5.

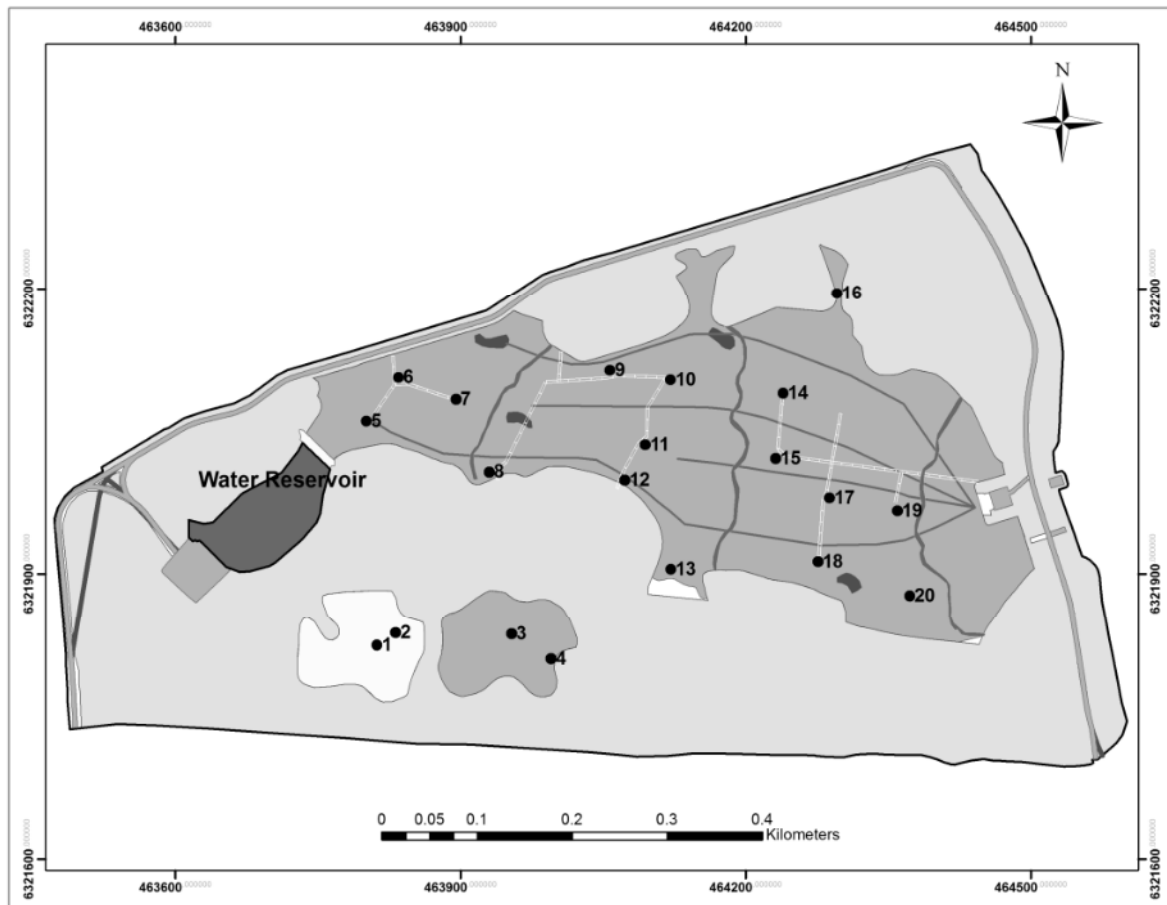


Figure 12: A map of Sandhill Fen with the locations of the 20 wetland vegetation research plots numbered and marked with black dots.

Plant Responses

Seedlings were introduced to research plots (16 species in 2012, and 13 species in 2013). Species survival was good, but variable and closely associated with soil wetness. There are a range of species recommended for fen reclamation, as well as species best suited for wet and dry areas of wetlands (Table 6). 4 Species stand out in particular: *Scirpus microcarpus*, *Scirpus atrocinctus*, *Carex aquatilis*, and *Carex hystericina*. These species exhibited high survival rates in the wetland across dry or wet areas, spread quickly, and produce considerable biomass. Net primary production of *C. aquatilis*, *C. hystericina* and *S. microcarpus*, both above- and below-ground was comparable to those species in natural fens of the region based on literature values. Over 3 years, Gross and Net Photosynthesis for these three species were similar to each other, however, none of these species provide sufficient net CO₂ sinks to make up for CO₂ sources. *Carex aquatilis* was the most efficient in CO₂ exchange.

Research conducted from 2013-2016, indicated a high diversity of native wetland plants, including many that are typical of fens in the region. A vegetation survey conducted in 2016 found 87 vascular plant species, and 23 bryophyte species. Of those 87 vascular plants, 37 (43%) are species naturally present in Alberta peatlands. Overall vegetation cover was 98%. The vegetation was distributed in 3 distinct zones. The first is a zone of relatively low diversity, dominated by *Typha latifolia* and higher water tables. The second zone is dominated by *Carex aquatilis* and a suite of desirable fen species. The third zone is dominated by *Calamagrostis canadensis* and a suite of plants not typical to fens, and generally has the lowest water table. Overall, about half of the wetland footprint is occupied by peat-forming fen plants, and the remaining half contains plants that occupy habitats similar to marshes or riparian areas. Bryophyte diversity was high, but had low overall abundance. Peat initiation was observed. Bryophytes are absent from plots that are too wet or too dry. Bryophyte diversity declined significantly following high water tables in 2017.

RESEARCH

By 2019, eight years post wet-up, the vegetation community has changed greatly, primarily in response to fluctuating water levels. The elevated water table that occurred in 2017 reduced the number of species in the wetlands. Following the flood, the three wetland zones (*Typha*, *Carex aquatilis*, and *Calamagrostis*) appear to have different trajectories in plant community development, suggesting different environmental variables and thresholds are influencing the species assemblages in the three zones. The species present have provided abundant vegetative cover depending on the levels of water occurring at the site level. At sites with low water levels, *Larix laricina* and *Betula glandulifera* have performed extremely well and could be considered for future wetland reclamation.

Table 6: Vascular plant species and recommendation for targeted planting status

Recommended Species	<i>Beckmannia syzigachne</i>
	<i>Carex aquatilis</i>
	<i>Carex hystericina</i>
	<i>Scirpus atrocinctus</i>
	<i>Scirpus microcarpus</i>
	<i>Triglochin maritima</i>
Recommended for DRY areas	<i>Betula glandulifera</i>
	<i>Carex bebbii</i>
	<i>Larix laricina</i>
Recommended for WET areas	<i>Eriophorum angustifolium</i>
Not recommended	<i>Carex diandra</i>
	<i>Carex limosa</i>
	<i>Carex paupercula</i>
	<i>Dasiphora fruticosa</i>
	<i>Eriophorum chamissonis</i>
	<i>Eriophorum vaginatum</i>
	<i>Juncus tenuis</i>
	<i>Scheuchzeria palustris</i>
	<i>Scirpus lacustris</i>
<i>Triglochin palustris</i>	

A comparison of planting species assemblages and monocultures was also undertaken (See appendix 4 for details). After one year, planting diverse assemblages appears to have no influence over the abundance of desirable species, recruitment of new desirable species, nor the limitation of undesirable species establishment. Planting monocultures of desirable species allow for higher abundance with just as much recruitment of new desirable species. This work also validated soil moisture as an important abiotic driver determining the abundance of desirable species.

Greenhouse trials along a salinity gradient indicate that in general most, but not all, wetland plant species show effects above 300 mg/L Na⁺ or about 2,000 μS/cm. Most plant species tested are affected by concentrations above 600 mg/L Na⁺, but some species showed morphological effects at lower concentrations of sodium. At 1,200 mg/L Na⁺ plant survival is strongly impacted. Water with sodium concentrations below 600 mg/L Na⁺ would allow for a range of wetland plants. Electrical conductivity from a 600mg/L Na solution is ~ 4000 μS/cm. This is a much higher threshold for plant community performance than was hypothesized at the start of the watershed design.

Carex aquatilis is recommended as a critical foundation species and has broad tolerances across the fen gradient, especially important is its ability to grow on both mineral and organic substrates and its wide tolerance for water level variation. The performance of this species is reduced at a treatment of 500 mg/L Na⁺ in greenhouse trials, with survival reduced above 500 mg/L Na⁺ [=4,500 µS/cm].

Atmospheric Deposition

There is considerable annual and spatial variation in atmospheric deposition. Nitrogen and sulfur deposition at Sandhill Fen is several times greater than regional means: 20 times higher NH₄⁺ (0.53 kg ha⁻¹ yr⁻¹), 4 times higher NO₃⁻ (0.5 kg ha⁻¹ yr⁻¹), 11 times higher for DIN (1.17 kg ha⁻¹ yr⁻¹), and 1.5 times higher for SO₄²⁻ (7.78 kg ha⁻¹ yr⁻¹) (Wieder *et al.* 2016), these high values could affect plant growth in the future. To date, it appears that there are no negative impacts on vegetation in the wetland.

Surface Pore-water Chemistry

Base cation content of the near surface pore-waters across the fen are highly variable with some portions of the wetland footprint having elevated values of calcium and/or sodium. These areas occur along the southern boundary of the wetland, near the hummock-wetland interface. The sodium levels in the fen have increased over time, and although the mean sodium concentration is above normal rich fen values, it appears to be within the tolerance levels of dominant species currently occupying the fen.

By 2019, Electrical conductivity of surface pore-water in the wetland ranged from about 550-2,500 µS/cm in the central portions and about 2,000 to nearly 5,000 µS/cm along the southern boundaries of the wetland. Based on the Alberta Wetland Classification System (AWCS), this wetland would be classified as slightly brackish (EC=500-2,000 µS/cm) – mostly in the central portions – or moderately brackish (2,000-5,000 µS/cm), mostly along the southern boundaries, and overall the wetland water chemistry can be classified as moderately brackish.

There are areas of the wetland with high cation concentrations, particularly on the margins and especially the southern boundaries and the western wetland. Sodium in particular is higher along the southern boundary. These plots have sodium values up to 600-800 mg L⁻¹. Overall, cation concentrations have little variation with depth. Soil sodium varies across the fen and has increased from 0.77 mg/g in 2017 to 1.36 mg/g in 2019, with the number of plots with concentrations above 1.0 mg/g increasing from 33% in 2017 to 63% in 2019.

Soil Dynamics

An examination of the soil microbial flora in 2014 and 2015 found that the microbial flora did not differ between years, that the microbial communities at Sandhill Fen Wetland are similar to and within the range of some benchmark peatland sites, and that few differences were found along the wet to dry gradient within Sandhill Fen Wetland, indicating that the site has a reasonably homogeneous microbial flora.

WETLAND ECOLOGICAL PERFORMANCE: DEVELOPMENT AND CONTROLS ON ZOOBENTHIC COMMUNITY COMPOSITION AND ABUNDANCE- JAN CIBOROWSKI (UNIVERSITY OF WINDSOR/UNIVERSITY OF CALGARY)

Invertebrate Community Development Key Learnings

- *Threshold of Electrical Conductivity (EC) for invertebrate communities is at least as high as 3000 µS/cm.*
- *Below the salinity threshold, community composition was variable but quickly accumulated a broad diversity of taxa.*
- *At age 3 years, diversity was reduced at sites where conductivity exceeded 3,000 µS/cm. These sites were dominated by larvae of the most tolerant taxa: midges (Diptera: Chironomidae) and biting midges (Diptera: Ceratopogonidae).*

Zoobenthic community composition is influenced by many factors. Previous research on Sandhill Fen Wetland and other natural and constructed wetlands has documented that the most important determinants in young wetlands of the oil sands mine area are water quality (salts and naphthenic acids; both individually and in combination alter attributes), substrate characteristics (mineral vs. organic sediments), and the density and type of aquatic vegetation.

Pilot research over the first three years following creation of Sandhill Fen Wetland demonstrated that most of the invertebrate taxa expected in a typical marsh rapidly colonized wetted areas. Community richness and abundance increased year over year between 2013 and 2015 despite a steady increase in water salinity (measured as electrical conductivity). An unexpected finding was that composition was unaffected by conductivities well above levels initially thought to be a risk to typical marsh fauna (1.5×10^3 µS/cm).

Examination of the relationship between the presence of several dominant taxa and local salinity within the fen suggest that the salinity threshold tolerated was between 2500 and 3000 µS/cm. A multivariate ordination of the Sandhill Fen Wetland invertebrate fauna was conducted to produce an index (Zoobenthic Assemblage Condition Index (ZACI-salinity) that related the relative abundances of zoobenthic taxa to conductivity measured at the point of sampling. A scatterplot of ZACI-salinity vs. conductivity revealed the presence of an apparent threshold value, consistent with a salinity limit of about 3,000 µS (Figure 13). At sample locations with conductivity below the salinity threshold, community composition was variable but consisted of a broad diversity of taxa. Samples collected where conductivity exceeded 3,000 µS/cm were dominated by larvae of midges (Diptera: Chironomidae) and biting midges (Diptera: Ceratopogonidae). An extensive survey conducted in 2019 confirmed that the threshold occurs at or exceeds 3,000 µS/cm. However, record precipitation in that year limited maximum conductivities to approximately 3,000 µS/cm, so that a precise threshold of salinity tolerance remains to be ascertained for Sandhill Fen.

Zoobenthic Assemblage Condition Index vs. Conductivity
(2014 & 2015 data)

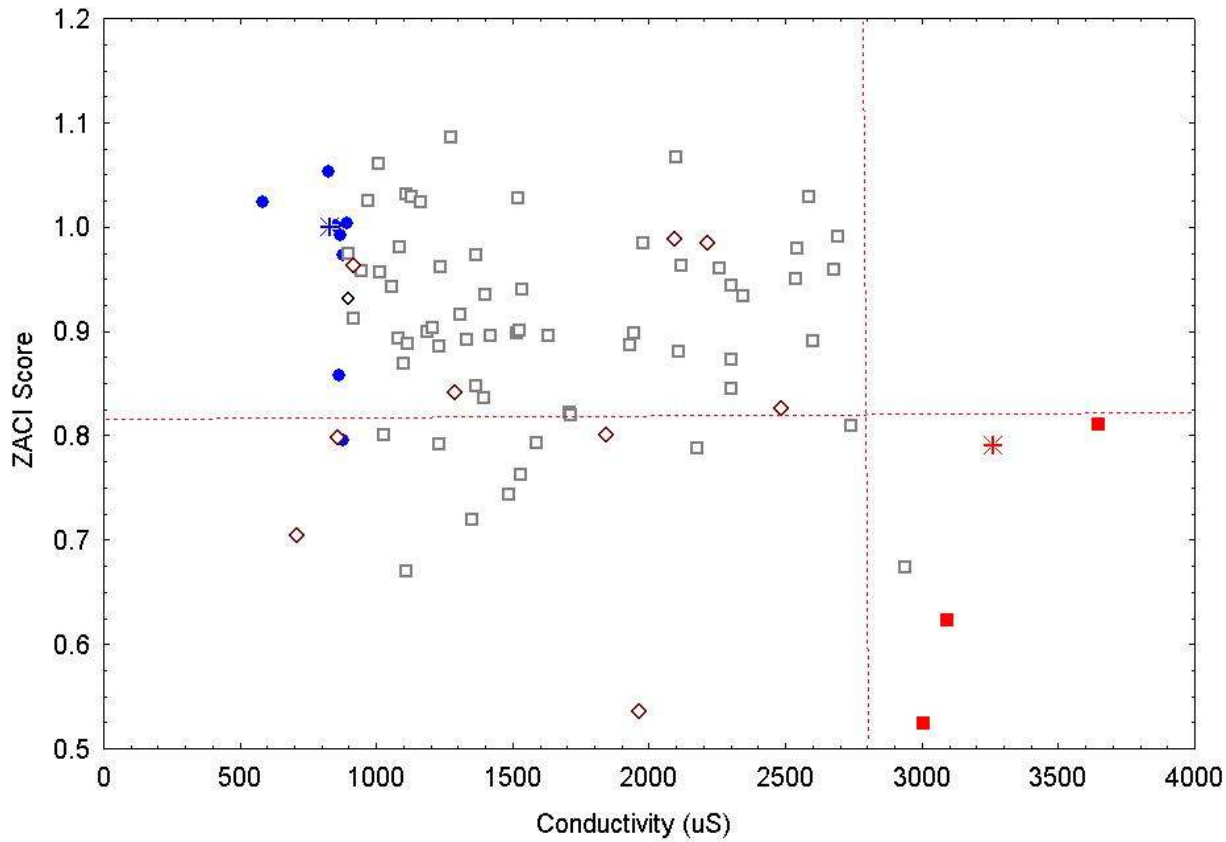


Figure 13: Relationship between Zoobenthic Assemblage Conditions Score for Salinity (ZACI-Salinity) and surface water conductivity for samples collected from Sandhill Fen Wetland in 2014 and 2015. Blue circles and red squares represent reference (lowest conductivity) and “degraded” (highest salinity) sites, respectively. Blue and red asterisks represent the multivariate centroids of those samples. Open squares represent samples containing at least 100 individuals per sample. Red open diamonds represent samples containing over 900 individuals per sample. The horizontal dotted line (fitted by eye) is the preliminary ZACI benchmark score – the highest score observed for a high-saline site. The dotted vertical line (fitted by eye) is the provisional conductivity threshold score – the highest conductivity at which a sample had a ZACI score that exceeded the benchmark value.

UPLAND ECOLOGICAL PERFORMANCE: EARLY TREE ESTABLISHMENT AND VEGETATION COLONIZATION OF UPLAND AREAS- SIMON LANDHÄUSSER (UNIVERSITY OF ALBERTA)

Early Tree Establishment Key Learnings

- *Tree seedlings planted on fine-textured cover soils grow taller than those on coarse-textured cover soils.*
- *In dry years, soil moisture loss was greater on fine-textured hummocks, this is likely due to the higher Leaf Area development*
- *Tree survival was high across all cover soil types.*
- *Reduced survival was evident in trembling aspen, likely associated with stock quality.*
- *Early canopy closure achieved through higher density planting was only achieved on the fine textured cover soils.*
- *There was no difference in seedling performance and understory development between high (10000 stems/ha) and medium (5000 stems/ha) density plantings.*
- *Spatial variability and complexity is achieved through topography, cover soils, tree density and composition, and coarse woody debris placement.*
- *The cover soils salvaged from two very different forest types resulted in the development of two very different plant communities early in site development.*
- *The early response of the colonizing vegetation was most strongly driven by cover soil characteristics and the propagule bank contained within.*
- *Upland areas with cover soil salvaged from a poor-xeric forest site had vegetation communities with a greater proportion of native species, graminoids and shrubs.*
- *Upland areas capped with cover soil salvaged from a rich-mesic forest site had vegetation communities were composed of proportionally more introduced species and forbs.*
- *In both cover soils, metrics of diversity were highest in areas with north facing aspects and higher tree density.*
- *In areas capped with the coarse cover soil from the poor-xeric forest site, the effect of aspect on diversity was modified by coarse woody debris.*
- *Over the whole site, 196 different plant species were detected in the upland areas.*

The overall goal of this research project was to examine the inter-relationships among tree species and density, understory development and its potential on water use on different reclamation ecosites. Tree seedling establishment, early growth and canopy development in response to planting density of jack pine (*Pinus banksiana*) and trembling aspen (*Populus tremuloides*) on substrates salvaged from a/b or d ecosites was assessed. Details about this work can be found in Appendix 6.

All planted tree seedlings grew much taller on the hummocks capped with fine-textured cover soil compared to hummocks capped with the coarse-textured cover soil. However, the hummocks with fine-textured cover soil experienced much greater soil moisture loss during dry years (i.e. 2015) compared to the areas capped with coarse –textured cover soil. Likely the difference in the depletion of soil water is related to the strong differences in leaf area development on these two different site types. Overall, planted tree seedling survival was high across the site, regardless of cover soil material. Some reduced survival was seen in trembling aspen (potentially related to stock quality), while survival in white spruce and pine was consistently high. The variation in survival among species could be related to seedling quality, indicating that planted tree seedlings are capable of establishing on upland reclamation sites over a wide range of site conditions, with early growth rates reflecting the site conditions. Of the three planted tree species, white spruce lacked a strong response to most site conditions and planting regimes, while aspen and pine were much more responsive.

Within the first five years after site construction, soil available nutrients (i.e., cover soil material) and woody debris placement drove early aspen and pine growth responses across the site. Although variables such as topography and planting density appear to play a minor role at this point in time, aspen and pine seedlings responded only to different planting densities and aspects when site condition were more extreme (e.g. less growth on coarse textured soils on south-facing slopes).

Achieving early canopy closure (within five growing seasons) by planting higher seedling density was only achieved on the hummocks that were capped with fine textured soils. There was no significant difference in seedling performance and understory development so far between high (10000 stems/ha) and mid density (5000 stems/ha) plantings. Longer-term impacts of planting densities on other forest ecosystem functions such as understory development and water-use are unknown at this time.

Although not studied in detail across the Sandhill Fen Watershed, the measured and documented variability in topography, cover soils, tree density and species composition, and CWD placement provided significant spatial variability and complexity across this reconstructed landscape feature. This variability is expected to be reflected in greater ecosystem heterogeneity and related ecosystem

functions such as hydrological and soil edaphic processes and successional patterns, which in the long-term is expected to have positive effects on ecosystem responses and recovery to disturbances in these reconstructed landscapes.

As expected, the cover soils salvaged from two very different forest types resulted in the development of two very different plant communities early in site development. The early response of the colonizing vegetation was most strongly driven by cover soil characteristics and the legacies (propagule bank) contained within. In areas capped with cover soil salvaged from a poor-xeric forest site, vegetation communities included a greater proportion of native species, graminoids and shrubs, while in areas capped with cover soil salvaged from a rich-mesic forest site, vegetation communities were composed of proportionally more introduced species and forbs.

After five growing seasons, the colonizing vegetation on the hummocks capped with the two different cover soils continue to be different from each other. However, vegetation communities in areas capped with cover soils salvaged from poor-xeric and rich-mesic forest types became more similar to each other over the years studied. It is not clear from our study whether this trend of convergence will continue. It is possible that, on longer timescales, topographical position, density of planted tree seedlings and coarse woody debris will be more important drivers of vegetation community development than initial cover soil source.

Regardless of cover soil, vegetation diversity was primarily influenced by seedling planting density (canopy cover) and topographical aspect. In both cover soils, metrics of diversity were highest in areas with north facing aspects and higher tree density. North facing aspects, which typically experience less heat and moisture stress, and treatments with higher densities of tree seedlings may have created an environment that was more favourable for the emergence and growth of the largely forest adapted species present in the propagule banks of the cover soils, leading to a more diverse community. Complex interactions between planting density, aspect and coarse woody debris (CWD) impacted metrics of diversity in both cover soils.

In areas capped with the coarse cover soil from the poor-xeric forest site, the effect of aspect on diversity was modified by CWD abundance, suggesting that coarse woody debris may have moderated the harsher environmental conditions present on south facing slopes in areas capped with the poor-xeric material, where water may have been limiting. This indicates that CWD appears to have a beneficial effect on colonizing vegetation and seedling growth. Varying the volumes of CWD at different scales appears to encourage variation in colonizing vegetation cover and correspondingly, heterogeneity of plant communities at different spatial scales.

Changes of the colonizing vegetation community were rapid early on (first two growing seasons) and dominated by few non-native, annual and biannual ruderal species, while plant communities appear to become more stable (perennial species driven) in the subsequent years, where changes are more subtle.

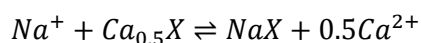
Over the whole site 196 different plant species were detected in the upland areas of the Sandhill Fen Watershed. Increased spatial variability, a result of topographical variation, differences in cover soil materials, and placement of CWD played a significant role in the high species richness, community diversity and heterogeneity across this reclaimed landscape.

ASSESSING THE SODIUM BUFFERING CAPACITY OF RECLAMATION MATERIALS IN SANDHILL WETLAND- MATT LINDSAY (UNIVERSITY OF SASKATCHEWAN)

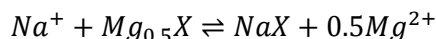
Buffering Capacity of the Clay Layer Key Learnings

- Sodium attenuation in the clay layer is likely limited and short-lived.
- It is unlikely that calcium concentrations in the surface water are derived from ion exchange with sodium as OSPW migrates through the clay layer.
- Calcium concentrations may be associated with background shallow groundwater.
- There is a mixing trend between OSPW-influenced groundwater to the south of the watershed, and background shallow groundwater within the wetland footprint.
- The apparent absence of a vertical Na breakthrough curve within soil pore water vertical trends in pore water composition (i.e., increasing dissolved Na concentrations with depth) at individual sampling locations suggests that ion exchange reactions have limited impact on Na migration.
- Sodium attenuation was controlled by ion exchange reactions, whereas dissolved Ca and Mg concentrations were likely influenced by mineral precipitation-dissolution reactions.
- Results of the field study and column experiments indicated that ion exchange reactions will not effectively limit Na transport over time.

Elevated calcium concentrations were observed in surface waters of the Sandhill Fen shortly after establishment. It was thought that these elevated Ca concentrations may result from ion exchange with Na during migration of OSPW (Allen, 2008) from the underlying CT deposit through the sub-soil (clay-rich Pleistocene till) and peat (salvaged live peat) layers that comprise the reclamation soil cover. Although the clay layer was not designed to buffer ions migrating through the clay, this study was undertaken to investigate any potential buffering capacity of the clay. This reaction is described by the following equation:



Where X represents a single exchange site within the reclamation cover materials. Ion exchange with Mg may also contribute to Na attenuation:



Although elevated Ca or Mg concentrations are not a water quality issue, Na concentrations in ground water and surface waters may increase as Ca and Mg occupied exchange sites become depleted. This study was conducted to provide insight into relationships between ion exchange reactions and water chemistry within Sandhill Fen Wetland and the broader reclamation landscape. The overall project goal was to constrain the current extent of, and capacity for, ion exchange reactions to buffer sodium migration within the reclamation soil cover. More generally, the results of this study improve understanding of the geochemical behaviour of reclamation soil cover materials within wetland reclamation systems.

The field sampling campaign indicated that Na attenuation is likely limited and short-lived. Results of solid-phase and pore-water analyses revealed that elevated Ca concentrations observed in Sandhill Fen Wetland surface waters was unlikely derived from ion exchange with Na during migration of OSPW through the reclamation soil cover. Instead, the chemical and isotopic signatures of soil pore water suggest that the elevated Ca concentrations may be associated with background shallow groundwater typical of Pleistocene tills found in the Canadian Prairies. Analysis of soil pore-water samples obtained along a south to north transect of the Sandhill Fen Wetland revealed a mixing trend between OSPW-influenced groundwater to the south and background shallow groundwater within the wetland area. This distribution of OSPW-type water was generally consistent with previously modeled groundwater discharge zones. The apparent absence of a vertical Na breakthrough curve within soil pore water vertical trends in pore water composition (i.e., increasing dissolved Na concentrations with depth) at individual sampling locations suggests that ion exchange reactions have limited impact on Na migration.

The column experiments demonstrated that substantial Na exchange may be achieved by till and peat during initial pore volumes. However, Na attenuation declined rapidly and breakthrough eventually occurred with continual input of simulated OSPW. Although effluent concentrations decreased by up to one half during the first pore volume, Na concentrations were consistently elevated throughout the experiment. Sodium attenuation was controlled by ion exchange reactions, whereas dissolved Ca and Mg concentrations were likely influenced by mineral precipitation-dissolution reactions.

RESEARCH

Results of the field study and column experiments indicated that ion exchange reactions will not effectively limit Na transport over time. Initial Na attenuation within till and peat was controlled by ion exchange reactions involving Ca and Mg, yet pore-water and effluent Na concentrations remained elevated. These results suggest that decision-making related to soil cover system design should take into consideration the limited influence of till and peat on long-term Na migration. Further details of this work can be found in Appendix 7.

7

SANDHILL FEN RESEARCH WATERSHED DISCUSSION AND CONCLUSION

SANDHILL FEN RESEARCH WATERSHED KEY LEARNINGS

Although the Sandhill Fen Watershed is a newly reclaimed system, there is much that Syncrude has learned through the entire process, from concept, to design, to construction, to reclamation to research and monitoring. Some of the key learnings are summarized below. Many more details are provided in the appendices and can also be found in the published literature (see Chapter 9 for bibliography).

- *Conductivity thresholds for ecological communities can be as high as 3000-4000 $\mu\text{S}/\text{cm}$.*
- *Methylmercury concentrations in the wetland are low, and comparable to other boreal wetlands.*
- *For most substances measured, surface water quality at Sandhill Fen Wetland falls within the range of the results from natural sites (brackish marshes to saline fens) and this is a good indicator of progress towards achieving equivalent wetland function.*
- *Surface runoff represented a small flux (< 10% of annual precipitation) on hummocks and was constrained to extreme high intensity rainfall events (e.g. 92 mm in 30 hours) or the snowmelt period.*
- *The primary controlling factors on hummock recharge in Sandhill Fen Watershed were the soil cover prescription and associated vegetation productivity, the lithological composition and morphology (height, width, convexity, etc.) of the hummocks, and climatic influences.*
- *Next to precipitation, evapotranspiration, primarily transpiration associated with root water uptake, was the largest component of the water balance on hummocks in Sandhill Fen Watershed.*
- *Most of the hummocks in Sandhill Fen Watershed had convex up slopes, resulting in a limited areal extent of shallow water tables at hummock-lowland transition zones. This meant that shallow water tables had a limited effect on the total amount of recharge any one hummock facilitated; a rough estimation suggested that shallow water tables at hummock-lowland interfaces only reduced total recharge on a hummock by 10% to 20%.*
- *The Sandhill Fen Watershed appears to be sustainable hydrologically, in that a saturated lowland area with wetland vegetation occurs that is supplied by flow from upland and regional areas via surface and groundwater pathways.*
- *The Sandhill Fen Wetland has demonstrated potential for carbon sequestration.*
- *Salinity levels have been increasing in the wetland over time, but are still within the range of natural wetlands in the region.*
- *Achieving peatland targets as described in the Alberta Wetland Classification System, are not possible within the timeframes of closure.*
- *Structural and functional aspects of fen wetlands are achievable, even in short timeframes and on CT landforms.*

SALINITY THRESHOLDS FOR COMMUNITY STRUCTURE

In the absence of direct evidence of peatland development potential with OSPW, the design team used a 1500 $\mu\text{S}/\text{cm}$ benchmark for conductivity to guide a design that would maximize probability of success. Evidence from a range of laboratory and field studies indicate that a range of native fen plants, and the macroinvertebrate community are able to tolerate, survive, reproduce and accumulate biomass at much higher levels of EC. Evidence indicates that plant communities may be tolerant of EC as high as 4000 $\mu\text{S}/\text{cm}$ and invertebrate communities as high as 3000 $\mu\text{S}/\text{cm}$.

SURFACE WATER CHEMISTRY COMPARED TO NATURAL ANALOGUES

At Sandhill Fen Wetland, the dominant ions in near-surface water are bicarbonate, sulfate, chloride, sodium, calcium, and magnesium. Since the first growing season, concentrations for these ions have increased annually, causing concurrent increases in electrical conductivity. In year 2019, water chemistry at Sandhill Fen Wetland was most comparable to regional saline fens, systems that exhibit elevated electrical conductivity and high sodicity. In the most recent year of monitoring, near-surface water at the reclamation site exceeded water quality guidelines for two chemical properties (dissolved chloride and total alkalinity). The saline fen natural reference sites also exceeded water quality guidelines for these same chemical properties, suggesting guideline exceedances are a norm for some natural wetland types. Notably, all dissolved organic compounds evaluated at Sandhill Fen Wetland were below detection limits and no exceedances for dissolved heavy metals were detected in near-surface water (Hartssock *et al.* in prep).

DISCUSSION AND CONCLUSIONS

A comparison of the total mercury (THg) and methyl mercury (MeHg) concentration in the Sandhill Fen Watershed to two nearby natural reference sites was implemented to explore the drivers of MeHg production in the sediment and waters of Sandhill Fen Watershed. Results of this work are published in Oswald and Carey (2016).

The concentrations of sediment THg and MeHg in the Sandhill Fen are on the low end of values measured in other constructed wetlands. The relatively low THg concentrations are likely a result of the higher amount of mineral soil incorporated into the Sandhill fen peat; however, the relatively low MeHg concentrations may be due to the high sulfate concentration of the constructed peat package. The majority of pore-water MeHg concentrations measured in the Sandhill Fen fell between 0.02 and 1.0 ng/L with the exception of several samples exceeding 1.0 ng/L to a maximum of 4.3 ng/L. This range in values is similar to the values reported for other natural boreal peatlands and constructed wetlands. Filtered MeHg concentrations draining the wetland through the weir (0.21 ng/L) and the sand aquifer via the underdrains (0.091 ng/L) were on the low end of values from other constructed/created wetlands, but were similar to values from natural boreal systems in northwestern Ontario (Oswald and Carey 2016).

When compared to natural reference wetlands, near-surface water chemistry at Sandhill Fen Wetland was similar to the slightly brackish marsh and saline fens. However, with increased concentrations of anions and cations over time, the chemistry of Sandhill Fen Wetland water is becoming more similar to natural saline fens in the region. In 2019, near-surface water quality at Sandhill Fen Wetland exceeded Alberta surface water quality guidelines for only two substances (dissolved chloride and total alkalinity) and irrigation water quality guidelines for EC levels. The regional saline fens also exceeded guidelines for the same two substances. Other natural sites exceeded up to six Alberta surface water guidelines, demonstrating natural environmental factors in the region can certainly account for variations in water quality, and that generic government issued guidelines are a good starting point, but site-specific water quality targets may need to be developed for Sandhill Fen Wetland and future constructed wetlands on tailings substrates (Hartsock *et al.* in prep).

Evaluation of surface water chemistry at Sandhill Fen Wetland indicates freshwater systems should be carefully targeted for CT tailings deposit reclamation and that suitable conditions exhibited by slightly brackish marshes and saline fens may be likely endpoints. For most substances measured, surface water quality at Sandhill Fen Wetland falls within the range of the results from the natural sites, a good indicator of progress towards achieving equivalent wetland function (Hartsock *et al.* in prep).

IS SANDHILL FEN HYDROLOGICALLY SUSTAINABLE?

The Sandhill Fen Watershed appears to be sustainable hydrologically, in that a saturated lowland area with wetland vegetation occurs that is supplied by flow from upland and regional areas via surface and groundwater pathways.

However, as with any prediction of the future, uncertainties remain. One of these uncertainties is climate and weather. It is well established that the climate of the region has variability that occurs over multiple cycles (~5 years and 15 years or longer) that oscillate between wet and dry. The Sandhill Fen Watershed was constructed in a dry phase. Only two years had precipitation that would be considered above normal. Regardless, in all years, the Sandhill Fen Wetland remained wet and pumping of water was often required due to the lack of a natural outlet. Sandhill Fen Wetland will be connected to its adjacent watershed in the near future.

Another consideration is the effects of upland vegetation development. As upland vegetation increases in density, less rainfall will reach the surface in the summer due to canopy interception. While this was not quantified during this research, aspen and spruce forests can intercept ~30-40% of summer rainfall at canopy closure, which will decrease soil moisture recharge and reduce the rewetting of soils from summer rain. In contrast, increasing forest covers will tend to increase snow retention and snow water equivalent, and delay melt to later in the year so that moisture can be more readily used by plants when demand is there.

Finally, the Athabasca Oil Sands Region (AOSR) is projected to become warmer and wetter as the century advances, with anticipated increases in intense summer convective precipitation. A change in precipitation regimes will influence the hydrology of the fen through a number of potential pathways that can be readily speculated, but difficult to quantify as both warming and wetting have opposite consequences in terms of wetland sustainability. However, even with fluctuations in water table elevation during the early stages of development, the vegetation communities have responded effectively. There are no un-vegetated areas in the watershed. If some areas become wetter or drier over time, we are confident that the vegetation community will adjust.

The greatest loss of water from the Sandhill Fen Watershed now and likely in the future is evapotranspiration. Total ET ranged between 350-400 mm for the Sandhill Fen Watershed in both lowlands and uplands, which compares well to values reported in the literature for boreal landscapes (Brümmer *et al.* 2012). ET for the uplands is slightly greater than the lowlands; an observation which has been reported elsewhere in the Boreal Plains. ET at the uplands site has not reached its peak rate. As Strilesky (2019) reported, ET increased at reclamation upland sites regardless of ecosystem type for approximately 8-10 years, at which point it plateaued and had rates similar to those of reference forests.

The sustainability of wet conditions in the lowland relies on the continuous and intermittent supply of water. The local and regional hydrogeology of the fen indicates a regional hydraulic gradient that brings groundwater from the closure divide to south of the Sandhill Fen Watershed into the watershed and then diverges in the lowland to the east towards Kingfisher watershed and also to the

DISCUSSION AND CONCLUSIONS

north at the upper part of the lowland. A critical consideration is that Sandhill Fen Watershed sits within a broader regional hydrogeological context, which should be considered during landform/wetland design, planning and performance assessment.

In terms of runoff processes within the Sandhill Fen Watershed, snowmelt runoff was observed from both north- and south-facing hummocks during an average snow year in 2018 that provided water to the lowlands. It is unclear whether this runoff occurs in most years. While rainfall-driven surface runoff was not previously observed, during an intense summer rainfall (>90mm, with very high hourly intensity), surface runoff was generated. However, there were numerous other rainfall events in 2018 (~30mm/day) that did not generate appreciable runoff. Surface runoff from closure divides and uplands are not considered a significant source of water for the lowlands over longer terms.

In the western Boreal region, hydrologic connections between landscape units, such as peatlands and uplands, are critical controls on the “eco-hydrologic functionality” of the system (Devito *et al.*, 2005; Devito *et al.*, 2012). In wet years, peatlands typically receive recharge from adjacent uplands, whereas during dry periods, the peatlands can provide water to the adjacent uplands (Lukenbach *et al.*, 2017; Thompson *et al.*, 2015; Wells *et al.*, 2017). Although the Sandhill Fen Watershed is still in the early stages post-construction, preliminary patterns of intermittent wetting have occurred at hummock-lowland transitions (Spennato *et al.*, 2018). The rise in water table at the margins and increasing lateral hydraulic gradients provides evidence that local flow systems are developing and these landforms are supplying localized groundwater flow to the lowland, yet this is restricted to the edges of the hummocks. The small contribution from the hummocks to the lowland may help sustain wetness.

WILL SANDHILL FEN BECOME A CARBON SINK?

As natural uplands and wetlands are weak to moderate carbon sinks, and carbon sequestration is an indicator of plant growth, and a key indicator of peatland function, there is considerable value in tracking the annual carbon budget of reclamation ecosystems. There have been considerable changes in the annual and growing season carbon budgets for both the lowlands and the uplands that reflect the establishment of vegetation, changes in vegetation type, climate and the overall excessive wetness of the lowland portion of the Sandhill Fen Watershed. The magnitude of growing season production and respiration was usually greatest at the upland and lowest at the lowland. Overall, the year-over-year increase in Ecosystem Respiration (ER) throughout the Sandhill Fen Watershed did not keep pace with the increase in GEP at the upland tower, yet NEE continued to increase as the upland forest grew. The Sandhill Fen Watershed lowland NEE is within the wide range of annual NEE observed for northern peatland ecosystems.

DRIVERS OF CHANGES IN SALINITY

The Sandhill Fen Watershed has had changes in salinity detected in a range of research programs. In 2013 when the study began, the combination of freshwater supply, open underdrains and frequent discharge at the outlet kept salinity levels reduced across the lowlands. While there were several heavy rainfall events, the relative volume of water added from the rainfall events (~100 mm over the season) was small compared to the volume of water added and removed from pumping (~800 mm to the lowland), which likely overshadowed atmospheric influences on hydrochemistry. Frequent pumping resulted in large variations in the water table, EC and ion concentrations in response to both inflow and outflow. Outlet water had the highest Na⁺ concentrations and SAR in 2013 due to the active removal of both surface and subsurface waters that contained OSPW. Most sites across Sandhill Fen Watershed exhibited low EC, Na⁺ concentrations and SAR values which indicates the limited influence of OSPW, most of which was discharged through the underdrains, and the addition of fresh water from the water storage pond.

Early evidence of an enriched zone of upwelling OSPW was present in late 2013 when the underdrains were inactive. When the underdrains were active, OSPW was effectively moved to the drains and hydraulic gradients were downward, keeping the wetland water relatively fresh. In May 2014, the underdrains were closed and except for a short inflow event, no water from the storage pond was added past this point. Controlled drainage events occurred in each year except 2016. As a result, the changes in hydrochemistry were largely controlled by vertical atmospheric fluxes as rainfall events increased the water table, which gradually declined throughout the season in response to evapotranspiration. As surface waters became stagnant without any inflow or drainage through the outlet, EC and ion concentrations increased. Despite the overall increase in ion concentrations in the lowlands, most sites had relatively low SAR values, indicating little influence of Na⁺ sources at these sites and suggesting evapo-concentration during dry periods and dissolution of salts in the unsaturated zone as a mechanism for increased salinity during rainfall. This pattern began to change in 2017 when across the fen, the molarity of both Ca²⁺ and Na⁺ began to increase, as well as the ratio of sodium to calcium. Whereas rainfall itself acts to dilute the system, residual salts can complicate the influence of precipitation on salinity.

A notable change under the less managed hydrological regime post 2014 was elevated Na⁺ concentrations at certain sites along the margin between the southern hummocks (hummocks #2, 7, and 8) and the lowlands, where OSPW is presumed to be discharging from depth in the near-surface. These areas exhibited Na⁺ concentrations and SAR values more than two-fold of those observed at all other sites across Sandhill Fen Watershed, indicating they are more active areas of cation exchange between Ca²⁺ and Na⁺ as a result from the

DISCUSSION AND CONCLUSIONS

input of Na⁺-rich waters from OSPW. These increases have occurred through 2018. Vitt (Appendix 5) found that soil sodium varied throughout the fen, and by 2019, 63% of his research plots had concentrations about 1.0 mg/g. Soils are considered saline-sodic when EC and SAR are >4000 $\mu\text{S}/\text{cm}$ and 13, respectively. Reported Na⁺ concentrations in composite tailings and OSPW range between 690 and 1100 mg/L while Ca²⁺ is <100 mg/L (Renault *et al.*, 1998; Renault *et al.*, 1999; Leung *et al.*, 2003; Zubot, 2010; Zubot *et al.*, 2012), indicating OSPW presence in the Sandhill Fen Watershed. Stable isotopes further support the emergence of OSPW in these Na⁺-rich areas, as OSPW has a distinct isotopic signature as a result of the industrial refining process (Baer *et al.*, 2016). In contrast, stable isotopes of surface water in the wetland plot along the local evaporation line, and near-surface groundwater plot along the local meteoric water line and have more negative $\delta^2\text{H}$ and $\delta^{18}\text{O}$ signatures (Biagi *et al.*, 2019). Although there have been increases in sodicity and EC in Sandhill Fen Wetland over time, the water chemistry is comparable to regional slightly brackish marshes and saline fens (Hartssock *et al.* in prep).

DID WE BUILD A FEN?

The objectives of the design were not to construct a fen, but rather was to design and establish initial conditions necessary to allow for development of a fen wetland and its watershed over time, and to develop techniques for reclamation of CT deposits. The Sandhill Fen Wetland does have a range of wetland plants that are typical of fens- including peat forming species, bryophytes are present (where the wetland has stable and appropriate water table), peat initiation was observed, and there is evidence of macrophyte biomass accumulation. There is evidence of Net carbon sequestration. These are all important structural and functional components of fen wetlands. According to the Alberta Wetland Classification System (AWCS, ESRD 2015), peatlands, including fens, should have 40 cm of accumulated peat. Peat accumulation will not happen at a rate to achieve 40 cm of accumulation within the timeframes of closure. According to the AWCS, there are areas of the watershed that could be considered marsh, and other areas that could be considered swamp. Although we have not achieved a fen target, there is evidence that important fen structure and functions can be established on reclaimed landforms, including CT deposits.

CONCLUSION

Although the Sandhill Fen Watershed is a newly reclaimed system, there is much that Syncrude has learned through the entire process, from concept, to design, to construction, to reclamation to research and monitoring. Construction activities, reclamation material placement, and revegetation are possible on a sand-capped CT deposit.

The objective of the Sandhill Fen Watershed was to design and establish initial conditions necessary to allow for development of a fen wetland and its watershed over time, and to develop techniques for reclamation of CT deposits. There were three measures of success for the Sandhill Fen Watershed: 1) maintaining the water level at +/- 20 cm of the soil surface, 2) vegetation establishment in the wetland area and 3) in the long-term, the wetland becomes carbon accumulating. Even with the investment in infrastructure to control the water table, maintaining water table control at this fine scale of resolution was not possible. Results from the research and monitoring indicate that even though this level of control is not achievable, acceptable ecological outcomes are still possible. We were successful with respect to establishing a range of natural fen vegetation in the wetland area. Although the third metric- carbon sequestration- is a long-term metric, there is evidence that the fen can sequester carbon even early on in its development.

An assessment of the ecological performance of the plants and invertebrates indicates that thresholds of salinity are much higher than previously thought, and the OSPW influenced chemistry is similar to natural wetlands in the region. There is evidence that hummock topography has created local-scale groundwater systems as expected, and although there are many drivers in the water balance, the watershed appears to be hydrologically sustainable. Structural and functional aspects of fen wetlands are achievable, even in short timeframes and on CT landforms, however, the wetland cannot be classified as a "fen" using conventional wetland classification. Because of the requirement for 40cm of accumulated peat, achieving peatland targets as described in the Alberta Wetland Classification System, are not possible within the timeframes of closure. Knowledge and understanding gained through the instrumented Sandhill Fen Watershed will continue to inform the design, construction and reclamation of other CT deposits, including EIP. Continued performance monitoring of Sandhill Fen Watershed will support understanding and prediction of other in-pit CT deposit reclamation. The work done on Sandhill Fen Watershed is a key component of the adaptive management of EIP and other CT deposits.

8

REFERENCES CITED

- Alberta Environment and Sustainable Resource Development (ESRD). 2015. *Alberta Wetland Classification System*. Water Policy Branch, Policy and Planning Division, Edmonton, AB.
- Allen, E.W. 2008. Process water treatment in Canada's oil sands industry: I. Target pollutants and treatment objectives. *Journal of Environmental Engineering and Science*, 7, 123–138.
- Baer, T., Barbour, S.L., Gibson, J.J. 2016. The stable isotopes of site wide waters at an oil sands mine in northern Alberta, Canada. *Journal of Hydrology*, 541, 1155–1164
- Biagi, K.M., Oswald, C.J., Nicholls, E.M., Carey, S.K., 2019. Increases in salinity following a shift in hydrologic regime in a constructed wetland watershed in a post-mining oil sands landscape. *Sci. Total Environ.* 653, 1445–1457. <https://doi.org/10.1016/j.scitotenv.2018.10.341>
- Brümmer, C., Black, T., Jassal, R., Grant, N., Spittlehouse, D., Chen, B., Nestic, Z., Amiro, B., Arain, M., Barr, A., et al. 2012. How climate and vegetation type influence evapotranspiration and water use efficiency in Canadian forest, peatland and grassland ecosystems. *Agricultural and Forest Meteorology* 153: 14–30. DOI: 10.1016/j.agrformet.2011.04.008
- Clark, M.G., 2018. The initial biometeorology of the constructed Sandhill Fen Watershed in Alberta, Canada. Carleton University. 192 pp.
- Devito, K., & Mendoza, C. (2007). Appendix C: Maintenance and dynamics of natural wetlands in western boreal forests: Synthesis of current understanding from the Utikuma Research Study Area. Appendices to the Guideline for Wetland Establishment on Reclaimed Oil Sands Leases Revised (2007) Edition.
- Devito, K.J., Creed, I.F., & Fraser, C.J.D. 2005. Controls on runoff from a partially harvested aspen-forested headwater catchment, Boreal Plain, Canada. *Hydrological Processes*, 19, 3-25. <https://doi.org/10.1002/hyp.5776>
- Devito, K., Mendoza, C., Qualizza, C., 2012. Conceptualizing Water Movement in the Boreal Plains: Implications for Watershed Reconstruction. Synthesis report prepared for the Canadian Oil Sands Network for Research and Development, Environmental and Reclamation Research Group; 164 pp.
- Hartsock, J, Piercey, J., House, M. and Vitt, D. *in prep*. A history of water quality at the reclaimed Sandhill Wetlands and comparisons to natural Albertan wetlands and environmental quality guidelines for Alberta surface waters.
- IPCC, 2013. 2013 Supplement to the 2006 IPCC Guidelines for National Greenhouse Gas Inventories: Wetlands. IPCC Switzerland.
- Kasperski, K. and Mikula, R. 2011. Waste Streams of Mined Oil Sands: Characteristics and Remediation. *Elements*, 7:387-392.
- Leung, S.S., MacKinnon, M.D., Smith, R.E.H., 2003. The ecological effects of naphthenic acids and salts on phytoplankton from the Athabasca oil sands region. *Aquat. Toxicol.* 62, 11–26. [https://doi.org/10.1016/S0166-445X\(02\)00057-7](https://doi.org/10.1016/S0166-445X(02)00057-7).
- Lukenbach, M. C., Hokanson, K. J., Devito, K. J., Kettridge, N., Petrone, R. M., Mendoza, C. A., 2017. Postfire ecohydrological conditions at peatland margins in different hydrogeological settings of the Boreal Plain. *Journal of Hydrology*, 548, 741–753. <https://doi.org/10.1016/j.jhydrol.2017.03.034>

REFERENCES CITED

- Lukenbach, M. C., Spencer, C. J., Mendoza, C. A., Devito, K. J., & Landhäusser, S. M. 2019. Evaluating how landform design and soil covers influence groundwater recharge in a reclaimed soft tailings deposit. *Water Resources Research*, 55. DOI:10.1029/2018WR024298
- Matthews, J.G., Shaw, W.H., MacKinnon, M.D., Cuddy, R.G. 2002. Development of Composite Tailings Technology at Syncrude. *International Journal of Surface Mining, Reclamation and Environment*, 16, 24–39.
- Mikula, R. J., Kasperski, K. L., Burns, R. D., & MacKinnon, M. D. 1996. *Nature and Fate of Oil Sands Fine Tailings*. In *Suspensions: Fundamentals and Applications in the Petroleum Industry*, edited by Laurier L. Schramm, 251:677-723. Washington, DC: American Chemical Society. DOI: 10.1021/ba-1996-0251.ch014
- Murray, K.R., Barlow, N., Strack M. 2017. Methane emissions dynamics from a constructed fen and reference sites in the Athabasca Oil Sands Region, Alberta, *Science of The Total Environment*, 583, 369-381. <https://doi.org/10.1016/j.scitotenv.2017.01.076>.
- Nicholls, E. M., Carey, S. K., Humphreys, E. R., Clark, M. G., & Drewitt, G. B. 2016. Multiyear water balance assessment of a newly constructed wetland, Fort McMurray, Alberta. *Hydrological Processes*, 30(16), 2739-2753. DOI: 10.1002/hyp.10881
- Oswald, C. J., Carey, S. K., 2016. Total and methyl mercury concentrations in sediment and water of a constructed wetland in the Athabasca Oil Sands Region. *Environmental Pollution*, 213, 628-637. <https://doi.org/10.1016/j.envpol.2016.03.002>
- Renault, S., Lait, C., Zwiazek, J., MacKinnon, M., 1998. Effect of high salinity tailings waters produced from gypsum treatment of oil sands tailings on plants of the boreal forest. *Environ. Pollut.* 102, 177–184. [https://doi.org/10.1016/S0269-7491\(98\)00099-2](https://doi.org/10.1016/S0269-7491(98)00099-2).
- Renault, S., Paton, E., Nilsson, G., Zwaizek, J.J., MacKinnon, M.D., 1999. Responses of boreal plants to high salinity oil sands tailings water. *J. Environ. Qual.* 28 (6), 1957–1962
- Reid, M.L., Warren, L.A. (2016). S reactivity of an oil sands composite tailings deposit undergoing reclamation wetland construction. *Journal of Environmental Management*, 166, 321–329.
- Smerdon, B. D., Devito, K. J., & Mendoza, C. A. 2005. Interaction of groundwater and shallow lakes on outwash sediments in the subhumid Boreal Plains of Canada. *Journal of Hydrology*, 314(1-4), 246-262. DOI: 10.1016/j.jhydrol.2005.04.001
- Smerdon, B.D., Mendoza, C.A., & Devito, K.J. 2008. Influence of subhumid climate and water table depth on groundwater recharge in shallow outwash aquifers. *Water Resources Research*, 44, W08427. <https://doi.org/10.1029/2007WR005950>
- Spennato, H. MSc Thesis. 2016. An Assessment of the Water Table Dynamics in a Constructed Wetland, Fort McMurray, Alberta. 65 pp. McMaster University.
- Spennato, H.M., Ketcheson, S.J., Mendoza, C.A., Carey, S.K., 2018. Water table dynamics in a constructed wetland, Fort McMurray, Alberta. *Hydrol. Process.* 32, 3824–3836. <https://doi.org/10.1002/hyp.13308>
- Strilesky, S.L. 2019. Functioning of reclaimed oil sands ecosystems and the implications for reclamation certification. Carleton University. 174 pp.
- Syncrude Canada Ltd. 2008. Wetland Construction, Research and Monitoring at Syncrude Canada Ltd. Appendix 2- Permit Level Design for Syncrude’s Sandhill Fen Watershed.

REFERENCES CITED

- Thompson, R.L., Mooder, R.B., Conlan, M.J.W., & Cheema, T.J. 2011. Groundwater flow and solute transport modelling of an oil sands mine to aid in the assessment of the performance of the planned closure landscape. In: Fourie A. Tibbett, M. & Beersing A. (Eds.), *Mine Closure 2011: Proceedings of the Sixth International Conference on Mine Closure*. September 18-21, 2011, Lake Louise, Alberta. Australian Centre for Geomechanics. Nedlands, Western Australia. Volume 2
- Thompson, C., Mendoza, C. A., Devito, K. J., Petrone, R. M., 2015. Climatic controls on groundwater– surface water interactions within the Boreal Plains of Alberta: Field observations and numerical simulations. *Journal of Hydrology*, 527, 734–746. <https://doi.org/10.1016/j.jhydrol.2015.05.027>
- Twedy, P. 2019. *Hydrogeological Considerations for Landscape Reconstruction and Wetland Reclamation in the Sub-humid Climate of Northeastern Alberta, Canada*. M.Sc. thesis, Earth & Atmospheric Sciences, University of Alberta, 204p. <https://doi.org/10.7939/r3-zpg2-6p77>
- Wells, C., Ketcheson, S., Price, J., 2017. Hydrology of a wetland-dominated headwater basin in the Boreal Plain, Alberta, Canada. *Journal of Hydrology*, 547, 168–183. doi.org/10.1016/j.jhydrol.2017.01.052
- Wieder RK, Vile M, Albright CM, Scott K, Vitt DH, Quinn JC, Burke-Scoll M. 2016. Effects of altered atmospheric nutrient deposition from Alberta oil sands development on *Sphagnum fuscum* growth 117 and C, N and S accumulation in peat. *Biogeochemistry*, 129:1-2, DOI 10.1007/s10533-016-0216-6
- Winter, TC, and MK Woo 1990. Hydrology of lakes and wetlands. pp. 159-187 in *Surface Water Hydrology*. MG Wolman and HC Riggs eds. The Geological Society of America. North Dakota. <https://doi.org/10.1130/DNAG-GNA-O1.159>
- Wytrykush, C., Vitt, D.H., McKenna, G., Vassov, R., 2012. Designing landscapes to support peatland development on soft tailings deposits, in: Vitt, D.H., Bhatti, J. (Eds.), *Boreal Ecosystem: Attaining Sustainable Development*. Cambridge University Press, pp. 161–178.
- Zubot, W., 2010. Removal of Naphthenic Acids from Oil Sands Process Water Using Petroleum Coke. M.Sc. Thesis. University of Alberta.
- Zubot, W., MacKinnon, M.D., Chelme-Ayala, P., Smith, D.W., Gamal El-Din, M., 2012. Petroleum coke adsorption as a water management option for oil sands process-affected water. *Sci. Total Environ.* 427–428, 364–372. <https://doi.org/10.1016/j.scitotenv.2012.04.024>.

9

BIBLIOGRAPHY OF PUBLICATIONS FROM SANDHILL FEN WATERSHED RESEARCH PROGRAM

- Benyon, J., 2014. Characterization of Hydraulic Conductivity Profiles for Sandhill Fen Watershed Reclamation Materials. Undergraduate thesis, Earth & Atmospheric Sciences, University of Alberta.
- Biagi, K. MSc Thesis. 2015. Understanding flow pathways, major chemical transformations and water sources using hydrochemical data in a constructed fen, Alberta, Canada. 96 pp. McMaster University.
https://macsphere.mcmaster.ca/bitstream/11375/18047/2/Kelly%20Biagi_MSc%20Thesis_Sept15.pdf
- Biagi, K, C. Oswald, E. Nicholls, S. Carey. 2019. Increases in salinity following a shift in hydrologic regime in a constructed wetland watershed in a post-mining oil sands landscape, *Science of The Total Environment*, 653, 1445-1457.
DOI: <https://doi.org/10.1016/j.scitotenv.2018.10.341>.
- Bradford, L. 2014. Microbial Community Response during Oil Sands Reclamation. M.Sc. Thesis. McMaster University.
- Bradford, L., Ziolkowski, L., Goad, C., Warren, L., and Slater G. 2017. Elucidating carbon sources driving microbial metabolism during oil sands reclamation. *Journal of Environmental Management*. 188:246-254. <https://doi.org/10.1016/j.jenvman.2016.11.029>
- Bowman, D. 2015. Characterization of naphthenic acid methyl esters in Alberta oil sands composite tailings. Ph.D. thesis. McMaster University.
- Bowman, D.T., G.F. Slater, L.A. Warren and B.E. McCarry. 2014. Identification of Individual Thiophene-, Indane-, Tetralin-, Cyclohexane-, and Adamantane-type Carboxylic Acids in Composite Tailings Pore Water from Alberta Oil Sands." *Rapid Communications in Mass Spectrometry* 28(19): 2075-2083. <https://doi.org/10.1002/rcm.6996>
- Cilia, C. 2014. Assessing the occurrence of aqueous intermediate sulfur redox species through combined solution total sulfur, sulfate, and hydrogen sulfide analyses. B.Sc. thesis. McMaster University.
- Clark, M.G., PhD Thesis. 2018. The initial biometerology of the constructed Sandhill Fen Watershed in Alberta, Canada. Carleton University. 192 pp.
- Clark MG, Humphreys ER, Carey SK. 2019. The initial three years of carbon dioxide exchange between the atmosphere and a reclaimed oil sand wetland. *Ecological Engineering*. 135:116-126. <https://doi.org/10.1016/j.ecoleng.2019.05.016>
- Clark MG, Humphreys ER, Carey SK. Downscaling eddy covariance measurements of energy and carbon dioxide fluxes in a constructed boreal wetland. Presented at CGU Annual General Meeting, May 2017. *Award for Best Student Presentation from the Canadian Society for Agriculture and Forest Meteorology*.
- Faubert, J-P., and Carey, S. 2014. Growing season water balance of wetland reclamation test cells, Fort McMurray, Alberta. *Hydrological Processes*. 28(14): 4363-4376. <https://doi.org/10.1002/hyp.10240>
- Glaeser, L. 2015 Established plant physiologic responses and species assemblage development during early fen reclamation in the Alberta oil sands. M.Sc. thesis, Southern Illinois University, 135 pp.
- Glaeser, L.C., Vitt, D.H., and Ebbs, S.E. 2016 Responses of the wetland grass, *Beckmannia syzigachne*, to salinity and soil wetness: Consequences for wetland reclamation in the oil sands area of Alberta. *Ecological Engineering* 86:24-30.

BIBLIOGRAPHY

- Goepfel, A. 2014. Evaluating jack pine seedling characteristics in response to drought and outplanting. MSc Thesis, Department of Renewable Resources, University of Alberta, Edmonton, AB.
- Hamilton, A., 2015. Instrumentation and Characterization of Soil Moisture for the Syncrude Sandhill Fen Watershed. Undergraduate project, Earth & Atmospheric Sciences, University of Alberta.
- Hartsock J (2020). Characterization of key performance measures at reclaimed Sandhill Wetland: Implications for achieving wetland reclamation success in the Athabasca oil sands region. *Ph.D. Dissertation, Southern Illinois University, Carbondale, IL*
- Hartsock, J., House, M., and Vitt, D.H. (2016) Net nitrogen mineralization in boreal fens: A potential performance indicator for peatland reclamation. *Botany*. 94: 1015-1025.
- Hartsock, J.A., and Bremer, E. 2018. Nutrient supply rates in a boreal extreme-rich fen using ion exchange membranes. *Ecohydrology* 11(7): 8. doi: 10.1002/eco.1995.
- Hartsock, J.A., Bremer, E., and Vitt, D. 2019. Nutrient supply patterns across the Sandhill Fen reclamation watershed and regional reference fens in Alberta, Canada: An ion exchange membrane study. *Ecohydrology* 13(2): 8. <https://doi.org/10.1002/eco.2188>
- Hartsock, J, Piercey, J., House, M. and Vitt, D. *in prep*. A history of water quality at the reclaimed Sandhill Wetlands and comparisons to natural Albertan wetlands and environmental quality guidelines for Alberta surface waters
- Hazell, Mallory. 2017. The use of peat applications and *Carex aquatilis* for peatland reclamation on post mined landscapes in northern Alberta, Canada. MSc Thesis. University of Alberta
- Hazen, R.E. 2016. Organic layer inputs from four species of Cyperaceae within an oil-sands reclamation. MSc Thesis. Southern Illinois University Carbondale. USA 135 pp.
- Hodgson, Paul. 2013. Direct Infusion Lipidomics: Profiling the Oil Sands Microbiome. M.Sc. thesis, McMaster University.
- Hoffman, E. 2016. Influence of environmental and site factors and biotic interactions on vegetation development following surface mine reclamation using coversoil salvaged from forest sites. M.Sc. Thesis, Department of Renewable Resources, University of Alberta, Edmonton, AB.
- Kendra, K. 2013. Microbial Sulfur Biogeochemistry of Oil Sands Tailings with Depth. M.Sc. thesis, McMaster University. <https://macsphere.mcmaster.ca/handle/11375/13528>
- Ketcheson, SJ, Price JS, Carey SK, Petrone RM, Mendoza CA, Devito KJ. 2016. Constructing fen peatlands in post-mining oil sands landscapes: Challenges and opportunities from a hydrological perspective. *Earth-Science Reviews*, 161: 103-139. <http://dx.doi.org/10.1016/j.earscirev.2016.08.007>
- Koropchak, S. 2010. *Carex aquatilis* as a pioneer species for boreal wetland reclamation. M.Sc. thesis, Southern Illinois University. <https://opensiuc.lib.siu.edu/theses/267/>
- Koropchak, S. and Vitt. D. 2013. Survivorship and growth of *Typha latifolia* L. across a NaCl gradient: a greenhouse study. *International Journal of Mining, Reclamation and Environment*. 27(2):143-150.
- Koropchak S., Vitt D., Bloise R., and Wieder K. 2012. Fundamental paradigms, foundation species selection, and early plant responses to peatland initiation on mineral soils. *Restoration and Reclamation of Boreal Ecosystems: Attaining Sustainable Development*, Cambridge University Press, Cambridge, UK, pp. 76-100.

BIBLIOGRAPHY

- Kulbaba SP. 2014. Evaluating trembling aspen (*Populus tremuloides* Michx.) seedling stock characteristics in response to drought and out-planting on a reclamation site. M.Sc. Thesis, University of Alberta, 107 pp.
- Longval, J.M., and C. Mendoza, 2014. Initial Hydrogeological Instrumentation and Characterization of Sandhill Fen Watershed. Final report, Hydrogeology Group, Earth & Atmospheric Sciences, University of Alberta. December.
- Lukenbach, M.C., C.J. Spencer, C.A. Mendoza, K.J. Devito, S.M. Landhäusser and S.K. Carey, 2019. Evaluating how landform design and soil covers influence groundwater recharge in a reclaimed soft tailings deposit. *Water Resources Research*, 55(8), 6464-6481. <https://doi.org/10.1029/2018WR024298>
- Melnik K. 2013. Role of aspect and CWD in plant diversity recovery. B.Sc. Honours Thesis, University of Alberta. 23p.
- Menard, K. 2017. Community development of terrestrial and semi-terrestrial Invertebrates in a reclaimed wetland along environmental gradients. M.Sc. Thesis, University of Windsor, Windsor, ON.
- Merlin, M, Leishman, F, Errington, RC, Pinno, B., and Landhäusser SM. 2018. Exploring drivers and dynamics of early boreal forest recovery of heavily disturbed mine sites: a case study from a reconstructed landscape [online]. *New Forests*. doi: .10.1007/s11056-018-9649-1.
- Ngonadi, N. 2012. Using PLFA to constrain microbial distribution related to S-cycling in oil sands composite tailings during reclamation. M.Sc. thesis, McMaster University.
- Nicholls EM. MSc Thesis. 2015. Multi-year water balance dynamics of a newly constructed wetland, Fort McMurray, Alberta. 114 pp. McMaster University.
- Nicholls EM, Carey SK, Humphreys ER, Clark MG, Drewitt GB. 2016. Multi-year water balance assessment of a newly constructed wetland, Fort McMurray, Alberta. *Hydrological Processes*. *Hydrological Processes*, 30: 2739-2753. doi: 10.1002/hyp.10881.
- Oswald CJ, Carey SK. 2016. Total and methyl mercury concentrations in sediment and water of a constructed wetland in the Athabasca Oil Sands Region. *Environmental Pollution*, 213, 629-637. <http://dx.doi.org/10.1016/j.envpol.2016.03.002>
- Overbeeke, G. 2013. Petroleum hydrocarbon distributions in a constructed fen as part of oil sands reclamation. B.Sc. Thesis, McMaster University.
- Rastelli, J. MSc Thesis. 2016. Dissolved organic carbon concentrations, patterns and quality at a reclaimed and two natural wetlands, Fort McMurray, Alberta. 127 pp. McMaster University
- Reid, M. 2014. Biogeochemical Zonation in an Athabasca Oil Sands Composite Tailings Deposit Undergoing Reclamation Wetland Construction. M.Sc. thesis. McMaster University.
- Reid, M. and Warren, L. 2016. S reactivity of an oil sands composite tailings deposit undergoing reclamation wetland construction. *Journal of Environmental Management*, 166:321-329. <https://doi.org/10.1016/j.jenvman.2015.10.014>
- Seuradge, B. 2013. Characterization of organic carbon pools associated with Oil Sands reclamation. B.Sc. Thesis McMaster University.
- Spennato, H. 2016. MSc Thesis. An Assessment of the Water Table Dynamics in a Constructed Wetland, Fort McMurray, Alberta. 65 pp. McMaster University.
- Spennato, H.M., S.J. Ketcheson, C.A. Mendoza and S.K. Carey, 2018. Water table dynamics in a constructed wetland, Fort McMurray, Alberta. *Hydrological Processes*, 32(26), 3824-3836. doi: 10.1002/hyp.13308

BIBLIOGRAPHY

- Stephenson, K. 2012. Seasonal Sulfur Biogeochemistry of Oil Sands Composite Tailings undergoing Fen Reclamation. B.Sc. Thesis, McMaster University.
- Strilesky, S.L. 2019. PhD Thesis. Functioning of reclaimed oil sands ecosystems and the implications for reclamation certification. Carleton University. 174 pp.
- Syncrude Canada Ltd. 2008. Wetland Construction, Research and Monitoring at Syncrude Canada Ltd. Appendix 2- Permit Level Design for Syncrude's Sandhill Fen Watershed.
- Thorne, C. MSc Thesis. 2015. A comparison of soil nitrogen availability for a previously mined reclaimed wetland and two natural wetlands in Fort McMurray, Alberta. 105 pp. McMaster University
- Twedy, P. 2019. *Hydrogeological Considerations for Landscape Reconstruction and Wetland Reclamation in the Sub-humid Climate of Northeastern Alberta, Canada*. M.Sc. thesis, Earth & Atmospheric Sciences, University of Alberta, 204p.
<https://doi.org/10.7939/r3-zpg2-6p77>
- Vessey, C., Lindsay, M., and Barbour, SL. 2019. Sodium transport and attenuation in soil cover materials for oil sands mine reclamation. *Applied Geochemistry* 100 (2019) 42-54.
- Vitt, D.H. and House, M. 2015. Establishment of bryophytes from indigenous sources after disturbance from oil sands mining. *The Bryologist* 118: 123-129.
- Vitt, D. H., House, M., and Hartsock, J. 2016. Sandhill Fen, an initial trial for wetland species assembly on in-pit substrates: lessons after three years. *Botany*. 94: 1027-1040. <https://doi.org/10.1139/cjb-2015-0262>
- Vitt, DH, Glaeser, LC, House, M, Kitchen, S. 2020. Responses of *Carex aquatilis* to a regime of increasing sodium concentrations. *Wetland Management and Ecology* (in review).
- Warren, L., Kendra, K., Brady, A. and Slater G. 2016. Sulfur biogeochemistry of an oil sands Composite Tailings deposit. *Frontiers in Microbiology*, 6: 1533. doi: 0.3389/fmicb.2015.01533
- Wieder, RK, Vile, M, Scott, K, Albright, CM, McMillen, K, Vitt, D, Fenn, M (2016). Differential effects of high atmospheric deposition on bog plant/lichen tissue and porewater chemistry across the Athabasca oil sands region. *Environmental Science and Technology* 50: 12630-12640, DOI: 10.1021/acs.est.6b03109
- Wieder, R.K., Vile, M.A., Albright, C.M., Scott, K.D., Vitt, D.H., Quinn J.C., and Burke-Scoll, M. 2016. Effects of altered atmospheric nutrient deposition from Alberta oil sands development on *Sphagnum fuscum* growth and C, N and S accumulation in peat. *Biogeochemistry* 129: 1-19.
- Wytrykush, C., Vitt, D.H., McKenna, G., Vassov, R., 2012. Designing landscapes to support peatland development on soft tailings deposits, in: Vitt, D.H., Bhatti, J. (Eds.), *Boreal Ecosystems: Attaining Sustainable Development*. Cambridge University Press, pp. 161-178.

APPENDIX 1: CONSTRUCTION, RECLAMATION AND REVEGETATION OF SANDHILL FEN

TERMS OF USE

BGC Engineering Inc. were retained by Syncrude to carry out the studies presented in this publication and the material in this report reflects the judgment of BGC Engineering Inc. in light of the information available at the time of document preparation. Permission for non-commercial use, publication or presentation of excerpts or figures is granted, provided appropriate attribution is cited. Commercial reproduction, in whole or in part, is not permitted without prior written consent from Syncrude. An original copy is on file with Syncrude and is the primary reference with precedence over any other reproduced copies of the document.

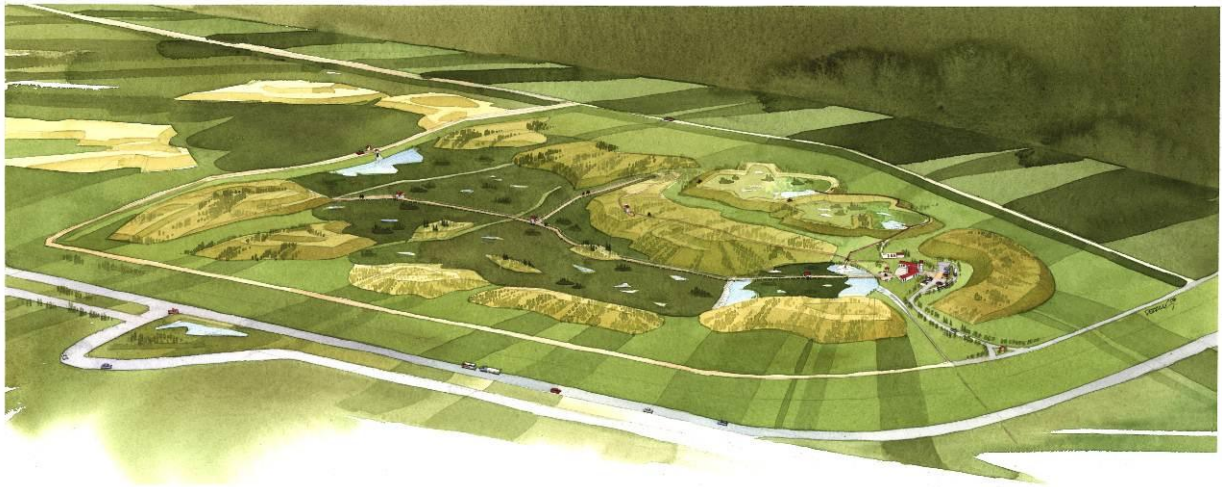
Reliance upon third party use of these materials is at the sole risk of the end user. Syncrude accepts no responsibility for damages, if any, suffered by any third party as a result of decisions made or actions based on this document. The use of these materials by a third party is done without any affiliation with or endorsement by Syncrude.

Additional information on the report may be obtained by contacting Syncrude.

This appendix may be cited as:

BGC Engineering. 2014. Construction, Reclamation, and Revegetation of Sandhill Fen Final Report (Revision 1), Appendix 1, in Syncrude Canada Ltd. *Sandhill Fen Watershed: Learnings from a Reclaimed Wetland on a CT deposit*. Syncrude Canada Ltd. 2020.

SYNCRUDE CANADA LTD.



CONSTRUCTION, RECLAMATION, AND REVEGETATION OF SANDHILL FEN

FINAL REPORT (REVISION 1)

PROJECT NO.: 0534-090
DATE: September 4, 2014

DISTRIBUTION:
RECIPIENT: 2 copies
BGC: 2 copies



BGC ENGINEERING INC.
AN APPLIED EARTH SCIENCES COMPANY

Suite 800 - 1045 Howe Street
Vancouver, BC Canada V6Z 2A9
Telephone (604) 684-5900
Fax (604) 684-5909

September 4, 2014
Project No.: 0534-090

Jessica Piercey, B.Sc.
Syncrude Canada Ltd.
Mail Drop 0078
PO Bag 4009
Fort McMurray AB T9H 3L1

Dear Jessica,

Re: Construction, Reclamation, and Revegetation of Sandhill Fen Report – Final Revision 1

This report describes the construction, reclamation, and revegetation activities of Sandhill Fen undertaken by Syncrude and numerous consultants and contractors. Report content and as-built information provided by several third parties has been summarized but not independently verified by BGC.

This report was issued to Syncrude in draft form on June 14, 2013 and has been finalized based on comments from Syncrude received in October 2013 and February 2014. Revision 1 was prepared based on comments from Syncrude received on August 22, 2014.

We trust this report meets your current needs. Please contact me anytime with questions or comments.

Yours sincerely,

BGC ENGINEERING INC.
per:

ISSUED AS DIGITAL DOCUMENT.
SIGNED HARDCOPY ON FILE WITH
BGC ENGINEERING INC.

Gord McKenna, PhD, PEng, PGeol
Senior Geotechnical Engineer

EXECUTIVE SUMMARY

Sandhill Fen is located on the northwest corner of the East-In-Pit (EIP) at Syncrude Canada Ltd.'s Mildred Lake Operation, north of Fort McMurray, Alberta. The design intent of Sandhill Fen is to create a watershed with the necessary initial conditions for a reconstructed fen to become established, and over time, become self-sustaining. The goal of Sandhill Fen is to allow Syncrude to undertake research to gain additional experience and knowledge regarding wetland (and watershed) design and reclamation. This research will be used to guide future fen wetland design and construction through a technology transfer process.

Sandhill Fen was designed, constructed, reclaimed, and revegetated as an instrumented watershed between 2008 and 2012, and has been operational since January 2013. Sandhill Fen includes a Primary Fen surrounded by an upland area with hummocks, Perched Fens, a Water Storage Pond, and supporting infrastructure. Currently, the conditions for a fen-type wetland have been created but, by definition, a fen is not established. It is expected that a fen-like ecosystem will develop over decades or centuries.

This report is a compilation of information provided by Syncrude and consultants involved with Sandhill Fen construction, reclamation, and revegetation. The objective of this report is to describe the design, construction, reclamation, and revegetation activities using the (unverified) information provided by third-parties to BGC. The package is intended to provide full background information to researchers and to form the major reference for an application for reclamation certification down the road.

Available design, construction, reclamation, and revegetation details are described in this report for the following major Sandhill Fen elements:

- Berms (Sandhill Berm, North-South and East-West Berms, North Containment Berm, and 318 m Spur Dyke)
- Sump Pad and Vault
- Underdrains
- Hummocks
- Primary Fen
- Perched Fens
- Water Storage Pond
- Fresh Water Pipeline
- Coarse Woody Debris (CWD) Berms
- Infrastructure (Perimeter Road, Research Centre Pad, boardwalks, electricity)

Construction and reclamation was completed by the December 2012 deadline set by Syncrude's Environmental Protection and Enhancement Act (EPEA) Operating Approval. Sandhill Fen is currently in the operation, monitoring, and research phase.

TABLE OF CONTENTS

EXECUTIVE SUMMARY	i
TABLE OF CONTENTS.....	ii
LIST OF TABLES	iii
LIST OF FIGURES.....	iii
LIST OF DRAWINGS.....	iv
LIST OF APPENDICES	iv
LIMITATIONS	v
1.0 INTRODUCTION	1
1.1. Scope of Work	2
1.2. Key Personnel and Responsibilities.....	3
1.3. Definitions	4
2.0 BACKGROUND.....	6
2.1. Design intent.....	6
2.2. Peat Transplant Trial – U-Shaped Cell.....	7
2.3. Timeline	7
2.4. Site Selection and Site Investigations	7
2.5. Weather during Construction, Reclamation, and Revegetation Activities.....	8
3.0 CONSTRUCTION, RECLAMATION, AND REVEGETATION MATERIALS	9
3.1. Tailings Sand	9
3.2. Clay Till.....	10
3.3. Pf Sand	11
3.4. Peat Mineral Mix	12
3.5. Litter-Fibric-Humic – A/B Ecosite and D Ecosite.....	13
3.6. Coarse Woody Debris	14
3.7. Gravel	15
3.8. Revegetation	16
4.0 SUMMARY OF ACTIVITIES.....	17
4.1. Berms	17
4.1.1. Sandhill Berm and the North-South and East-West Berms.....	17
4.1.2. North Containment Berm.....	18
4.1.3. 318 m Spur Dyke.....	19
4.2. Sump Pad and Vault.....	19
4.3. Underdrains	20
4.3.1. Design	20
4.3.2. Construction	20
4.4. Hummocks	21
4.4.1. Design	21
4.4.2. Construction	22

4.4.3. Reclamation and Revegetation	22
4.5. Primary Fen	23
4.6. Perched Fens	24
4.7. Uplands and Swales	25
4.8. Water Storage Pond	26
4.9. Freshwater Pipeline	26
4.10. CWD Berms	27
4.11. Infrastructure	27
4.11.1. Perimeter Road	27
4.11.2. Research Centre Pad	28
4.11.3. Boardwalks	28
4.11.4. Electricity	28
5.0 SURVEYS AND INSTRUMENTATION	29
5.1. Placement Surveys	29
5.2. Annual Topographic Surveys and Aerial Photographs	29
5.3. Instrumentation	30
6.0 CONCLUSIONS	31
7.0 CLOSURE	32
REFERENCES	33
LIST OF APPENDED DOCUMENTS	34

LIST OF TABLES

Table 1.1. Responsibility for Personnel Involved with Sandhill Fen	3
Table 3.1. Tree Planting Prescriptions	16
Table 5.1. Sandhill Fen Element Areas	29

LIST OF FIGURES

Figure 3-1. Sonic drilling core of tailings sand from the foundation zone underlying Sandhill Fen (Fall 2008)	9
Figure 3-2. Frozen lumps of clay till in Sandhill Fen (March 2012)	10
Figure 3-3. Pf Sand and tailings sand recovered using hand auger (July 2011)	11
Figure 3-4. Peat mineral mix placed in the Primary Fen (April 2012)	12
Figure 3-5. LFH and coarse woody debris on Hummock 9 (April 2011)	13
Figure 3-6. Coarse woody debris berm (Winter 2011)	14
Figure 3-7. Crushed Gravel used as Sump Vault base (April 2009)	15

LIST OF DRAWINGS

DRAWING 00	SITE LOCATION MAP
DRAWING 01	GENERAL ARRANGEMENT 2012 FINAL CONSTRUCTED SURFACE
DRAWING 02	SANDHILL FEN HISTORY 2008 AERIAL PHOTO
DRAWING 03	SANDHILL FEN HISTORY 2008 TOPOGRAPHY
DRAWING 04	SANDHILL FEN HISTORY 2009 AERIAL PHOTO
DRAWING 05	SANDHILL FEN HISTORY 2009 TOPOGRAPHY
DRAWING 06	SANDHILL FEN HISTORY 2010 AERIAL PHOTO
DRAWING 07	SANDHILL FEN HISTORY 2010 TOPOGRAPHY
DRAWING 08	SANDHILL FEN HISTORY 2011 AERIAL PHOTO
DRAWING 09	SANDHILL FEN HISTORY 2012 AERIAL PHOTO
DRAWING 10	SANDHILL FEN HISTORY 2012 TOPOGRAPHY

**All data for the drawings was supplied to BGC by Syncrude.*

LIST OF APPENDICES

APPENDIX A	PROJECT TIMELINE
APPENDIX B	WEATHER DURING CONSTRUCTION PERIOD (2009 – 2012)
APPENDIX C	DESIGN DRAWINGS
APPENDIX D	FIELD MEMORANDA
APPENDIX E	BGC SITE VISIT REPORTS
APPENDIX F	PHOTOGRAPHIC RECORD DURING CONSTRUCTION
APPENDIX G	DAILY REPORTS AND MEETING MINUTES
APPENDIX H	DESIGN CHANGES
APPENDIX I	AS-BUILT MATERIAL PLACEMENT MAPS
APPENDIX J	INSTRUMENTATION
APPENDIX K	WATER MANAGEMENT PLAN
APPENDIX L	VIDEOS
APPENDIX M	SYNCRUDE DESIGN DECISION RECORDS

**All Appendices are provided in the enclosed CD.*

LIMITATIONS

BGC Engineering Inc. (BGC) prepared this document for the account of Syncrude Canada Ltd. The material in it reflects the judgment of BGC staff in light of the information available to BGC at the time of document preparation. Numerous third parties have contributed content and information for this report and BGC has communicated this information without it being independently verified by BGC. Any use which a third party makes of this document or any reliance on decisions to be based on it is the responsibility of such third parties. BGC accepts no responsibility for damages, if any, suffered by any third party as a result of decisions made or actions based on this document.

As a mutual protection to our client, the public, and ourselves, all documents and drawings are submitted for the confidential information of our client for a specific project. Authorization for any use and/or publication of this document or any data, statements, conclusions or abstracts from or regarding our documents and drawings, through any form of print or electronic media, including without limitation, posting or reproduction of same on any website, is reserved pending BGC's written approval. If this document is issued in an electronic format, an original paper copy is on file at BGC and that copy is the primary reference with precedence over any electronic copy of the document, or any extracts from our documents published by others.

1.0 INTRODUCTION

Sandhill Fen is an instrumented watershed located on the northwest corner of the East-In-Pit (EIP) at Syncrude Canada Ltd.'s (Syncrude's) Mildred Lake Operation north of Fort McMurray, Alberta (Drawing 00). Sandhill Fen was designed, constructed, reclaimed, and revegetated between 2008 and 2012 by Syncrude with the support from a large multi-disciplinary team (see Section 1.2). As part of this team, BGC Engineering Inc. (BGC) provided the Permit Level Design and the Gate 3 Detailed Design, and was retained to compile this Construction, Reclamation, and Revegetation report. This report is based on input and information provided to BGC by Syncrude and third parties.

Design began in 2008. Construction and reclamation was carried out from 2009 through 2012, and since 2013, the Sandhill Fen has been in the operation, monitoring, and research phase. Sandhill Fen was designed and constructed to provide the initial conditions for a fen-type wetland to develop, as recommended by the Technical Advisory Committee (TAC). Currently, the wetland cannot be classified as a fen according to conventional wetland classification schemes, such as the Canadian Wetland Classification System.

Sandhill Fen is approximately 52 ha in area with a 15 ha Primary Fen. The watershed area (based on 2012 LiDAR) is 55 ha. The watershed area is larger than the boundary of Sandhill Fen due to run-off contribution from the 318 m Spur Dyke to the south. As shown in Drawing 01, Sandhill Fen includes a Primary Fen with islands, seven tailings sand hummocks, a Water Storage Pond, and associated infrastructure (Perimeter Road, Research Centre Pad, and boardwalks).

This report is a compilation of the construction, reclamation, and revegetation information provided by Syncrude and involved parties. A list of construction-related reports and memorandums, a log of key activities and milestones, and select photographs is provided. The objective of this report is to describe the construction, reclamation, and revegetation activities. This report is intended to be used by Syncrude and its researchers and consultants as a compendium of information for Sandhill Fen. It will provide a source of information for the design and implementation of future wetland reclamation projects. In the future, it may also be used as a source of information for the preparation of the certification application of the EIP.

Prior to this report, the last comprehensive documentation of Sandhill Fen was the Permit Level Design Report (BGC 2008a).

The design basis for Sandhill Fen was to create an instrumented watershed with a fen-type wetland to facilitate the research objectives set out by Syncrude and the TAC while also constructing a landscape that is aligned with Syncrude's overall closure objectives. The research objective was to create an instrumented watershed with a fen-type wetland in a typical oil sands reclamation setting for reclamation research. Other key research goals included the following:

- Monitoring of site hydrology and hydrogeology to assess water flow regimes which may lead to facilitation of a fen wetland
- Determining salinity tolerance limits for various key fen wetland species
- Evaluating the use of reclamation materials for a wetland reclamation site
- Monitoring to determine ecosystem succession over time.

The Permit Level Design Report (BGC 2008a) provides details regarding the design intent and research goals. The constructed Sandhill Fen is being incorporated into an overall landscape design for the EIP. The Sandhill Fen is permanent reclamation but will require decommissioning of infrastructure prior to closure.

1.1. Scope of Work

BGC initially prepared a proposal dated February 28, 2013 for this summary report which was updated afterwards using feedback on draft versions from Syncrude. Following those discussions, BGC's scope of work included the following main tasks:

- Create a list of documentation prepared by Syncrude and their contractors and consultants pertaining to design, construction, reclamation, and revegetation activities at Sandhill Fen.
- Compile this documentation submitted by Syncrude and their contractors and consultants into appendices.
- Create a comprehensive activity summary report with the documentation included as appendices.

Jessica Piercey and Carla Wytrykush of Syncrude Environmental Research commissioned this work. The objective of this report is to be a compilation of information, therefore recommendations are not provided, as directed by Syncrude.

BGC's scope of work did not include formal monitoring of construction, reclamation, and revegetation activities, nor did BGC receive information from field personnel while these activities were ongoing. The information (reports, photographs, logs) included in this report has been compiled from a variety of third party sources and are in their original formats. The work performed and documents prepared by third parties are communicated by BGC in this report, but have not been independently verified or reviewed by BGC. Syncrude, as the Owner, was responsible for overseeing construction, reclamation, and revegetation activities. BGC provided select technical support to Syncrude and was directed by Syncrude Environmental Research to make site visits on an as-requested basis to make site observations and discuss specific construction queries with Syncrude Base Plant Projects.

Specifically, given this context and the noted limitations on BGC's scope of work and that BGC did not formally monitor construction or provide quality assurance for construction, this report is *not* a typical engineering "as-built" that would typically be provided for other constructed facilities where construction activities and accordance / deviations from design requirements

are documented by the firm that monitored construction as the engineer of record. That said, it is a valuable compilation of the voluminous information already generated by the project.

1.2. Key Personnel and Responsibilities

Syncrude with numerous consultants and contractors were involved with the construction, reclamation, and revegetation at Sandhill Fen. Syncrude Environmental Research led the research phase (2007 – ongoing) and the Permit Level Design phase (2007 – 2008). Syncrude Base Plant Projects led the Gate 3 Detailed Design, construction, reclamation, and revegetation phases (2009 – 2012) with Syncrude Environmental Research providing support. Syncrude Environmental Research currently leads the operation and research phases at Sandhill Fen. Key personnel and their responsibilities are outlined in Table 1.1.

Table 1.1. Responsibility for Personnel Involved with Sandhill Fen

Group	Responsibility
Permit Level / Gate 3 Design (2008 – 2010)	
Syncrude Environmental Research	Lead design process for Syncrude
BGC Engineering Inc.	Lead designers, engineering landform design and groundwater site investigation
CoSyn Technology (Worley Parsons Ltd.)	Detailed design of fresh water pipeline and electrical power supply (Gate 3 only)
Technical Advisory Committee (TAC)	Technical and scientific input / basis for design provided by review of Permit Level Design and Gate 3 Detailed Design Design for research objectives and monitoring
Construction and Reclamation (2009 – 2012)	
Syncrude Base Plant Projects	Lead construction and project management. Supported reclamation and revegetation activities.
Syncrude Environmental Research	Supported construction and reclamation, and lead revegetation activities with Mildred Lake and Aurora Mine Planning-Reclamation.
Bear Slashing Ltd.	Equipment operators / materials salvaging until April 2010
BGC Engineering Inc.	Select design support during construction, reclamation, and revegetation activities
Caldwell Contracting Ltd.	Equipment operators / materials salvaging in 2009 and 2010
Cow Harbour Construction Ltd.	Material salvage and hummock construction, winter of 2009/2010
Global Fabrications Ltd.	Installation of main boardwalks on Primary Fen (summer 2012)
Graham Group Ltd.	Equipment operators / materials salvaging beginning in May 2010

Group	Responsibility
Jacobs Industrial Services Inc.	Equipment operators, underdrain extension and burial
North American Construction Group (NACG)	Equipment operators for material placement
Skocdopole Construction Ltd.	Underdrain construction in April 2009
Construction / Reclamation Monitoring (2009 – 2012)	
Syncrude Base Plant Projects	Construction / reclamation supervision, project management
Terracon Geotechnique Ltd.	Construction / reclamation monitoring April 2010 to April 2011
Navus Environmental Inc.	Construction monitoring in 2012
Survey	
HCS Focus Ltd.	Stockpile surveys
LN Land Development Technologies Inc.	Surveys
Sands Surveys 2000 Ltd.	Scan of Primary Fen area for underground drains prior to material placement in Primary Fen
Other	
ATCO Gas	Provided electrical services to research trailer, Sump Vault, instrumentation, and Mildred Lake Reservoir for pump
AECOM Technology Corporation	Operation and servicing the weir and underdrain

1.3. Definitions

For consistency with previous Sandhill Fen reports, key terms are defined below (see Drawing 01 for polygons of some aerial definitions):

- **Primary Fen** refers to the 15 ha lowland portion of Sandhill Fen where fen-type wetland is predicted to become established.
- **Upland Area** is the non-fen area of Sandhill Fen within the project area. The uplands include the hummocks, Perched Fens, Water Storage Pond, and related infrastructure.
- **Hummocks** are landforms designed to surround the fen to feed groundwater to the Primary Fen and to support upland vegetation.
- **Watershed Boundary** is the surface water divide for water that reports to the Primary Fen. Note that this watershed boundary is not the groundwater divide.
- **Sandhill Fen** refers to the 52 ha area shown in Drawing 01, and includes the design, construction, reclamation, and revegetation activities, and the operation, monitoring, and research program as a whole.
- **Permit Level Design** refers to the Permit Level Design, as submitted to Syncrude by BGC in December 2008 (BGC 2008a).

- **Gate 3 Detailed Design** refers to the detailed design that occurred after the Permit Level Design. The Gate 3 Detailed Design includes the Issued for Construction (IFC) Drawings for hummocks in December 2009, and the Water Storage Pond and reclamation materials in January 2010. Preparation of a formal Gate 3 Detailed Design report was not commissioned, but a risk assessment was conducted where the design deviated from the Permit Level Design.
- **Construction and Reclamation Materials:**
 - Tailings sand is a fine grained sand byproduct of the extraction process (it is the oil sands with the oil (bitumen) removed. Tailings sand can be placed hydraulically or mechanically. The tailings sand beach/foundation underlying Sandhill Fen was placed hydraulically. The tailings sand fill for Sandhill Fen landforms was placed mechanically.
 - Clay till refers to clay till mineral soil, also referred to as Pl/Pg clay.
 - Pf sand refers to Pleistocene fluvial sand.
 - Litter-fibric-humic (LFH) – A/B ecosite refers to organic forest floor materials, A/B ecosite was used to create a drier (xeric to mesic) soil prescription.
 - Litter-fibric-humic (LFH) – D ecosite refers to organic forest floor materials, D ecosite was used to create a wetter (sub-hydric) soil prescription.
 - Peat mineral mix refers to a mixture of peat and mineral soil placed as reclamation cover soil. Peat mineral mix is salvaged from the advancing mine and can be stockpiled or direct hauled to the reclamation area. Peat mineral mix used at Sandhill Fen was direct hauled to a temporary stockpile on the 318 m Spur Dyke and then placed in its final location within several weeks / months.

Terminology used for peat mineral mix has varied between documents prepared throughout the construction and reclamation activities. For consistency with the Permit Level Design, peat mineral mix has been used throughout this document. More detailed descriptions of these units are provided in Section 3.

There are some inconsistencies with these definitions and definitions in previous reports. It is recommended that these definitions be used for consistency in the future.

2.0 BACKGROUND

Sandhill Fen¹ was constructed and reclaimed in response to operating conditions in Synchrude's Environmental Protection and Enhancement Act (EPEA) approval². Additionally, this activity marks the beginning of reclamation activities for the EIP, a significant component in Synchrude's mining closure landscape, and provides the first opportunity to test the Hydrology Ecology and Disturbance of Western Boreal Forest (HEAD) conceptual model on a new hydrologic response area (tailings sand).

2.1. Design intent

The design intent of Sandhill Fen was to create a watershed that could support the initial conditions necessary for a fen-like wetland to become established. The goal of Sandhill Fen is to allow Synchrude to gain experience and knowledge through research and guide future wetland (and watershed) design and reclamation through technology transfer.

Fen wetlands compose a large proportion of the natural wetlands found in the Athabasca oil sands region. From the Canadian Wetland Classification System (National Wetlands Working Group 1997), the primary characteristics of fens are as follows:

- An accumulation of peat
- Surface is level with the water table, with water flow on the surface and through the subsurface
- Fluctuating water table which may be at, or a few centimeters above or below, the surface
- Decomposed sedge or brown moss peat
- Graminoids and shrubs characterize the vegetation cover.

Sandhill Fen is the first instrumented watershed to be designed and reclaimed to support a fen-type wetland on a soft tailings deposit. Knowledge in technology and operations for recreating wetlands on soft tailings deposits will be gained through Sandhill Fen that will be useful for optimizing reclamation of soft tailings areas on Synchrude's leases. Sandhill Fen also provides operational experience for implementing reclamation projects on soft tailings, and provides opportunities to research the hydrologic and upland reclamation performance of tailings sand hummocks.

¹ This section has been adapted from the Permit Level Design report (BGC 2008a).

² Specifically, EPEA Approval Number 26-02-00, dated June 21, 2007 contains two pertinent conditions. Condition 6.1.61 states, "The approval holder shall undertake, or participate in, a study on reclamation techniques specific to all three plants that examines the viability of bog/fen creation for a portion of the final landscape". Condition 6.1.62 states, "The approval holder shall undertake construction of pilot wetlands and their watersheds by December 31, 2012 to provide opportunities for monitoring, model validation, and incorporation of findings into the update of the *Guideline for Wetland Establishment on Reclaimed Oil Sands Leases*, 2000, as amended".

Pollard et al (2012) provide useful overview of the Sandhill Fen design and construction. Some details of the Suncor Nikanotee Fen design and construction are also included in this conference paper.

2.2. Peat Transplant Trial – U-Shaped Cell

To complement Sandhill Fen research, a peat transplant research program was initiated in September 2008 at the U-Shaped Cell on Mildred Lake Settling Basin (MLSB) in partnership with scientists from the Southern Illinois University (SIU). The U-Shaped Cell peat transplant research included twenty-eight 10 by 20 m wetland plots. The program was developed to evaluate wetland revegetation techniques including peat source, placement thickness, degree of compaction, timing of salvage / placement, and water source (freshwater versus process water). The U-Shaped Cell design, as-built report, and operational guidelines are provided in BGC (2009a).

2.3. Timeline

The timeline for design, reclamation, and revegetation of Sandhill Fen has been divided into the following five phases:

- Phase 1: Site selection and investigation (2007 – 2008)
- Phase 2a: Permit Level Design (2008)
- Phase 2b: Gate 3 Detailed Design (2009 – 2010)
- Phase 3a: Construction (2009 – 2011)
- Phase 3b: Reclamation (2011 – 2012)
- Phase 3c: Revegetation (2011 – 2012)
- Phase 4: Operation (2012 onwards)
- Phase 5: Research and monitoring

These project phases are outlined further in an overall project timeline in Appendix A. Though these phases are mainly sequential, there is significant overlap between them. For example, research has been ongoing throughout all phases. Phases 4 and 5 are currently ongoing but this document focuses on Phases 1, 2, and 3. The future Sandhill Fen and EIP reclamation certification phase is not discussed herein.

2.4. Site Selection and Site Investigations

Initially, the Composite Tailings (CT) Prototype, on the north side of the MLSB, was selected as the fen project area in December of 2007. A conceptual design was developed and costs estimated in early 2008. BGC (2010) provides details of this investigation program.

However, in March 2008, the Syncrude Long Range Mine Plan was updated to expand the footprint of the W4 Dump over the CT Prototype. Therefore, proposed location for the Sandhill Fen was relocated to the northwest corner of EIP in April 2008 (Drawing 00).

The EIP is the site of the former Syncrude East Mine (part of the Base Mine) which was mined from 1977 to 1999 and has been backfilled with CT and tailings sand since 1999 for permanent storage and reclamation as part of the Mildred Lake closure landscape. EIP is approximately 5 km north to south and 2.5 km east to west, and occupies an area of 1,153 ha (11.53 km²). Background of the EIP, including bedrock geology, pit dimensions, tailings deposition history, and tailings stratigraphy, is described in BGC (2007).

Site investigations were carried out to confirm the underlying stratigraphy and to investigate the groundwater flow regime of Sandhill Fen (BGC 2008b). In July 2008, four settlement monuments were installed to observe the amount and rate of settlement due to consolidation of the underlying CT. The monuments indicated that consolidation of the underlying CT is largely complete (BGC 2009b). In fall 2008, a follow-up drilling program, that included hollowstem, sonic drilling, and CPT, was conducted to characterize the tailings sand and CT at depth, to observe the deeper groundwater flow regime, and to determine depth to limestone.

The site investigations indicated that Sandhill Fen is underlain with a 10 m thick tailings sand cap over interbedded CT and tailings sand layers to the base of the EIP tailings deposit. The thickness and extents of tailings varied depending on base of feed and pit geometry. The results of the site investigations are presented in a site investigation report (BGC 2008b).

2.5. Weather during Construction, Reclamation, and Revegetation Activities

The weather during construction, reclamation, and revegetation activities of Sandhill Fen is summarized in Appendix B. Figure B-1 presents the temperatures during the construction period and Figure B-2 presents precipitation using data from the Fort McMurray Airport Weather Station. These figures also present the monthly climate norms from 1971 to 2000 for comparison.

The figures indicate that the temperatures from 2009 to 2012 throughout the construction, reclamation, and revegetation activities were similar to the normals for the region. Precipitation was on average lower than normal, especially in summer 2011.

Tabulated daily climate data from the Mildred Lake Climate Station, located 2 km from Sandhill Fen, from September 2009 to May 2012 is provided in Appendix B.

3.0 CONSTRUCTION, RECLAMATION, AND REVEGETATION MATERIALS

This section provides a description of the materials used to construct and reclaim Sandhill Fen. General descriptions and salvage details for the construction and revegetation materials are provided in this section, while revegetation details are provided in Section 3.8. General soil descriptions are according to the Unified Soil Classification System (USCS).

The intended design function and placement details of these materials are described and provided in Section 4 according to individual or grouped Sandhill Fen elements and are shown on the Design Drawings in Appendix C.

3.1. Tailings Sand

Tailings sand is a uniform fine grained sand with some fines. A tailings sand stockpile was constructed hydraulically using cell construction on the 318 m Spur Dyke and used as a tailings sand borrow for Sandhill Fen. An assessment of the moisture content with depth within the tailings sand stockpile and workability / compaction of the tailings sand was completed in June 2009. A memorandum outlining the field program with a plan view drawing showing test pit locations, observations, and results is presented in Appendix D1.

Tailings sand was placed mechanically as fill to construct many Sandhill Fen elements, including the hummocks, Sandhill Berm, North Containment Berm, Sump Pad, and Research Centre Pad. Design tailings sand lift thickness specified in the Gate 3 Detailed Design varied depending on the Sandhill Fen element. For example, hummocks had a design lift thickness of 1 m, while Sandhill Berm and North Containment Berm had a design lift thickness of 0.3m.



Figure 3-1. Sonic drilling core of tailings sand from the foundation zone underlying Sandhill Fen (Fall 2008)

3.2. Clay Till

Clay till, often used as subsoil for reclamation activities, refers to both Pleistocene glacial till (Pg) and Pleistocene glaciolacustrine (PI) clay for this project. Glacial till (Pg) is a sandy silty clay while glaciolacustrine (PI) clay is a low to medium plastic silty / sandy clay and is often identified by its pinkish colour. These Pleistocene units are removed as part of overburden stripping in preparation of mining. Individual units are often combined / blended during overburden removal.

The Gate 3 Detailed Design specified that clay till be glacial till (Pg) or glaciolacustrine (PI) clay with at least 15% fines and be considered fair to good quality material according to Syncrude reclamation material suitability classification. Clay till was specified to be placed throughout the majority of Sandhill Fen at various thicknesses. Placement areas and thicknesses include 1.0 m for clay till islands in the Primary Fen, 0.5 m in the Primary Fen and Water Storage Pond areas, and 0.3 m in the uplands, on Hummocks 6 and 9, on the Sandhill Berm, and as Perimeter Road subgrade.

Clay till was salvaged from the North Wall of the North Mine Advance in the winter of 2009 by Cow Harbour Construction. Due to winter salvage and placement, the clay till was often in frozen lumps (approximate average diameter of 0.3 m and maximum diameter of 1.0 m). As a result, the clay till was often ripped prior to being compacted, as compaction of these aggregated frozen lumps can be ineffective. Compaction of the clay till consisted of a dozer taking several passes over the placed material (track packing).



Figure 3-2. Frozen lumps of clay till in Sandhill Fen (March 2012)

3.3. Pf Sand

Pf sand refers to Pleistocene fluvial sand. It is typically fine to coarse grained sand, poorly to well graded, with trace gravel and fines.

The Gate 3 Detailed Design specified a 0.4 m loose thickness of Pf sand to be placed on Hummocks 2, 4, 5, 7, and 8.

Pf sand was salvaged from T-Pit in December 2009 by Caldwell Contracting. Few details with respect to the description of Pf sand salvaged were provided to BGC. Pf sand recovered using a hand auger in July 2011 to the east of Hummock 5 indicates that the Pf sand placed is a fine to medium grained sand, as shown in Figure 3-3.

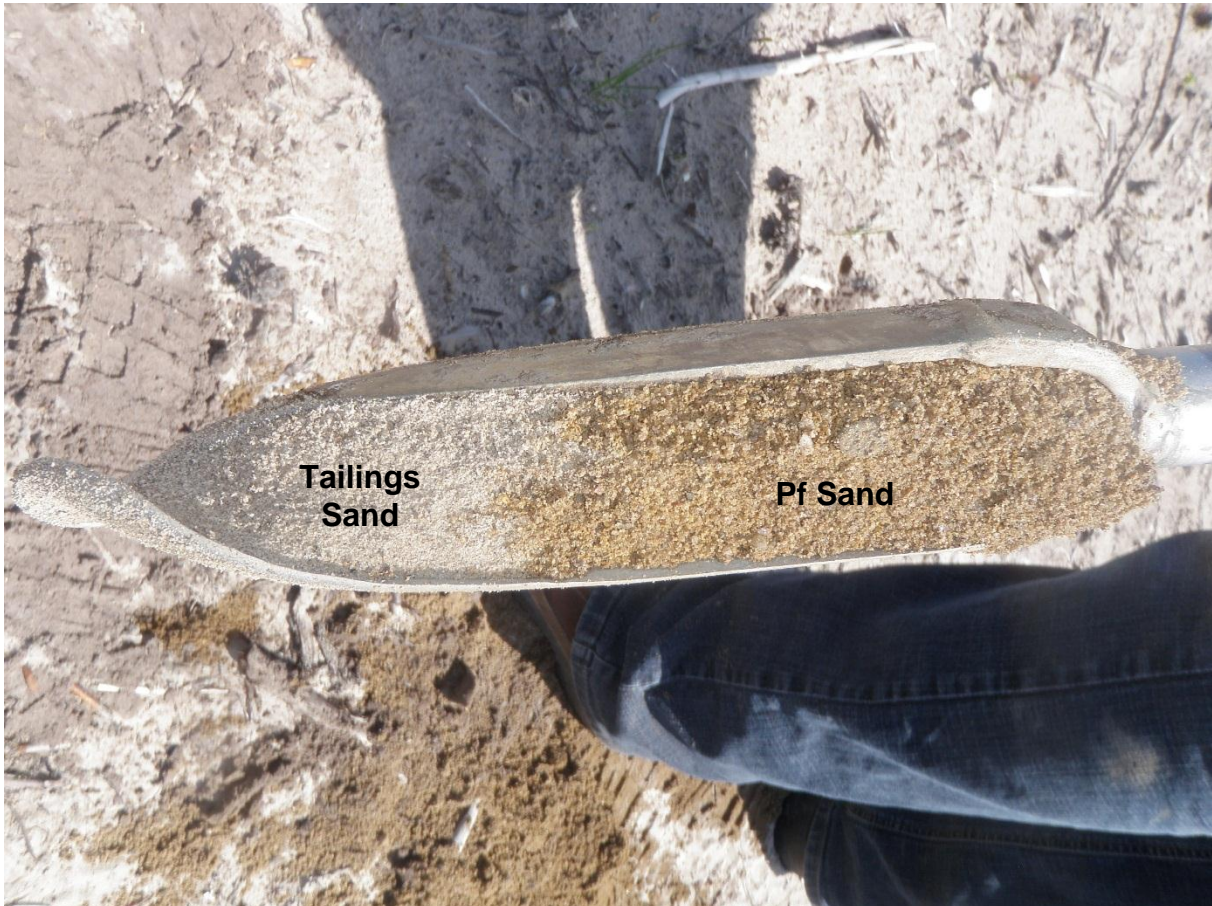


Figure 3-3. Pf Sand and tailings sand recovered using hand auger (July 2011)

3.4. Peat Mineral Mix

Peat mineral mix refers to a combination of Holocene peat and Holocene / Pleistocene mineral soil (Figure 3-4). In-situ peat is usually 0 to 2 m thick at Syncrude. In advance of mining, peat is often salvaged with mineral soil, creating a peat mineral mix, which is hauled to a stockpile or directly to the reclamation material placement area.

The Gated 3 Detailed Design specified that peat mineral mix be fair to good quality material according to Syncrude reclamation material suitability classification and be placed loose and remain uncompacted. Peat mineral was specified to be placed 0.5 m thick in the Primary Fen and Perched Fen 2 and 1.0 m thick in Perched Fen 1.

Peat mineral mix was salvaged from the North Mine Advance in winter of 2010 / 2011 by North American Construction Group. Peat mineral mix was hauled from the salvage location to the 318 m Spur Dyke where it was temporarily stockpiled for several weeks or months while placement was ongoing. More details about methods to spread the peat mineral mix in the Primary Fen are provided in Section 4.5.



Figure 3-4. Peat mineral mix placed in the Primary Fen (April 2012)

3.5. Litter-Fibric-Humic – A/B Ecosite and D Ecosite

LFH is the thin layer of decomposing forest floor organic material – seeds, roots, and decomposing organic materials (Figure 3-5). Its use promotes rapid reestablishment of native species. LFH is salvaged in advance of mining, and direct hauled to upland reclamation placement areas.

The Gate 3 Detailed Design specified use of LFH – A/B ecosite (from lichen / jackpine or blueberry / aspen / spruce ecosites) and LFH – D ecosite (from low bush cranberry / aspen / spruce ecosites). LFH – A/B ecosite was specified to be placed 0.15 m thick over Pf sand on Hummocks 2, 4, 5, 7, and 8 to create a “drier” (xeric to mesic) soil prescription. LFH – D ecosite was specified to be placed 0.2 m thick over clay till on Hummocks 6 and 9, the Perched Fen berm, and the uplands to create a “wetter” (sub-hydric) soil prescription. LFH is not compacted or tracked over (other than during initial spreading).

LFH – A/B ecosite was salvaged from the T-Pit by Bear Slashing, Graham, and Caldwell Contracting from April to May 2010. LFH – D ecosite and additional A/B ecosite materials were salvaged and hauled from N-Pit in June and July 2010 by Caldwell.

The LFH delivered to Sandhill Fen contained large (>1.0 m diameter) pieces of coarse woody debris (CWD). The reclamation prescription for Hummock 2 included 0.15 m of LFH – A/B ecosite, but placement of large CWD pieces was difficult for dozers. LFH thickness was increased in the field on the north side of Hummock 2 to a thickness that simplified placement.



Figure 3-5. LFH and coarse woody debris on Hummock 9 (April 2011)

3.6. Coarse Woody Debris

CWD is freshly fallen or stockpiled trees and large branches with some smaller debris, roots and sticks (Figure 3-6).

The Gate 3 Detailed Design specified that CWD be freshly fallen or stockpiled dead trees and large branches. CWD was specified to be placed in a non-linear configuration approximately 1 m thick and 3 m wide to create three CWD Berms with a general north-south orientation between Hummocks 4 and 7, Hummocks 5 and 8, and Hummocks 6 and 9. CWD Berms were designed to limit the peat mineral mix from shifting downstream with the flow of water.

CWD was salvaged from Cell 31, West Wall / W1, and the 2014 North Mine Advance and hauled to a stockpile on the 318 m Spur Dyke in June and July 2010 by Caldwell Contracting. CWD at Sandhill Fen is relatively coarse, with larger logs up to 12 m long and approximately 0.3 m in diameter while smaller debris having varying lengths and generally less than 0.1 m in diameter. As more CWD was salvaged than required for construction of the CWD Berms, smaller CWD was placed on Hummocks 2 and 9.



Figure 3-6. Coarse woody debris berm (Winter 2011)

3.7. Gravel

Gravel is coarse granular material and is used for road construction, armour, and as fill for infrastructure and foundations (Figure 3-7). The Gate 3 Detailed Design specified 150 mm diameter gravel be used to construct the outlet energy dissipation apron for the Freshwater Pipeline from the Mildred Lake Reservoir and the flow through diffuser, and 19 mm diameter crushed gravel be used for the Sump Vault base and as surfacing for the Perimeter Road, Research Centre Pad, and Sump Pad.

Crushed gravel (approximate median size of 19 to 25 mm diameter) was used for the Sump Vault base and for surfacing roads and pads. There is little information available about the source, grain size, moisture content, or level of compaction of the gravel material used at Sandhill Fen.



Figure 3-7. Crushed Gravel used as Sump Vault base (April 2009)

Clearwater Formation Clay Shale Fill

Clearwater Formation clay shale fill (referred to as Kc material) was used in construction as a subgrade fill for the Perimeter Road, the outlet weir berm, and for the Research Centre Pad. Kc is a saline sodic clay shale that may confound the salt balance of the Sandhill Fen and so had been excluded from the list of design materials. Much of this Kc material was subsequently removed from the outlet weir berm, as noted in the BGC site visit memorandum dated July 18, 2012 in Appendix E. Kc material is likely still present at the subgrade of the Perimeter Road and the Research Centre Pad.

3.8. Revegetation

The uplands were revegetated with several tree planting prescriptions. Trees were not planted on the Perimeter Road, Research Centre Pad, or within the Perched Fens. The tree planting prescriptions are outlined in Table 3.1 and each element is discussed in more detail below in Section 4.

Table 3.1. Tree Planting Prescriptions

Prescription Type (Density)	Tree Species
No Planting (0 stems per hectare)	No trees planted
A/B Ecosite (5,000 or 10,000 stems per hectare)	10% Aspen (<i>Populus tremuloides</i>) 10% White Spruce (<i>Picea glauca</i>) 80% Jack Pine (<i>Pinus banksiana</i>)
D Ecosite (5,000 or 10,000 stems per hectare)	80% Aspen (<i>Populus tremuloides</i>) 10% White Spruce (<i>Picea glauca</i>) 10% Jack Pine (<i>Pinus banksiana</i>)
Standard (2,000 stems per ha)	20% Aspen (<i>Populus tremuloides</i>) 20% White Birch (<i>Betula papyrifera</i>) 20% White Spruce (<i>Picea glauca</i>) 20% Black Spruce (<i>Picea mariana</i>) 20% Jack Pine (<i>Pinus banksiana</i>)

The Primary Fen and Perched Fens were seeded from November 14th to 19th, 2012 by Syncrude, SIU, and BGC. It should be noted that seeding was not a scheduled task for November 2012, but because the freshwater supply was not operational and there was concern for weed development (cattails), Syncrude and the researchers spread wetland seeds on the peat to maximize potential for wetland vegetation to become established from the placed seeds and rhizomes in the fresh peat. The seeds were placed during winter conditions while snow covered the seeding areas, with the intention that seeds would be imbedded within the snow and be in-place during snowmelt in the spring. Seventy kilograms (70 kg) of seeds were harvested from natural fens in the Fort McMurray area in the summer of 2011. The seed mixture was 1:1 ratio of cracked wheat to seed mix. Seeding took place on foot and with Argos. A BGC memorandum that provides as-built details and a map of the fen and Perched Fen seeding is attached in Appendix D.

Numerous revegetation plots were planted in the uplands and sipper-peeper plots were planted in the Primary Fen and Perched Fen as part of the research instrumentation program. The revegetation plots and sipper-peeper plots were planted by Simon Landhausser and Dale Vitt as part of ongoing Sandhill Fen research. See Drawing *01 Updated Sandhill Fen Instrumentation Map to Mar 2013* in Appendix J.

4.0 SUMMARY OF ACTIVITIES

This section provides a summary of the Permit Level and Gate 3 Detailed Designs and the construction, reclamation, and revegetation activities for Sandhill Fen.

The Permit Level Design for Sandhill Fen was completed in 2008 by BGC, in conjunction with input from Syncrude and the TAC. The Gate 3 Detailed Design involved preparation of IFC drawings to support Syncrude Base Plant Projects and construction activities and was completed in December 2009 and January 2010. The BGC IFC Drawings for the Hummocks, Underdrains, Water Storage Pond, and Reclamation material placement are in Appendix C, as well as, the CoSyn IFC Drawings for the freshwater supply, and mechanical, piping, and electrical components associated with Sandhill Fen. This section also provides a summary of the construction, reclamation, and revegetation activities: relevant field memoranda (Appendix D), site visit records (Appendix E), photographic record (Appendix F), daily reports and meeting minutes (Appendix G) and design change documentation (Appendix H).

The 2014 as-built material placement maps (BGC 2014) were developed using soil survey data collected by NorthWind Land Resources Inc. (Appendix I). Syncrude decision records are provided in Appendix M.

4.1. Berms

Sandhill Fen is contained by the Sandhill Berm to the east, the North Containment Berm to the north, the perimeter road to the west, and the 318 m Spur Dyke to the south. Two additional berms, the North-South Berm and East-West Berm, were not designed to contain Sandhill Fen but were constructed to limit ingress of tailings from nearby tailings deposition.

4.1.1. Sandhill Berm and the North-South and East-West Berms

The Sandhill Berm is located between Hummocks 6 and 9 and is designed to be the eastern watershed boundary of Sandhill Fen and separate Sandhill Fen from Kingfisher Wetland to the east. The Sandhill Berm is intended to provide light-vehicle access to the Sump Pad and Outlet Pad. Sandhill Berm was not designed as a dam or to be a water retaining structure.

In the Permit Level Design, the Sandhill Berm was approximately 210 m in length, with a constant height of 3 m, slopes of 4H:1V, a crest width of 5 m, and constructed using tailings sand. This design included an upstream 0.5 m thick clay till seepage blanket to reduce seepage losses from the Primary Fen.

In the Gate 3 Detailed Design, the length of the berm was reduced to approximately 120 m due to extending the southern toe of Hummock 6, and the side slopes were steepened to 3H:1V to reduce material volumes. The crest width was increased to 25 m for haul traffic and equipment access during construction and reclamation. The 0.5 m clay till substrate in the Primary Fen was considered to be sufficient to reduce seepage losses through the Primary Fen, therefore an upstream seepage blanket was not included in the Gate 3 Detailed Design. A spillway with an invert elevation of 313.5 m was included in the design of Sandhill Berm to

allow water to flow into the Kingfisher watershed if the weir outlet became blocked or overwhelmed. The spillway has yet to be constructed.

In late 2008 / early 2009, during preparation for underdrain installation, it was observed that coarse tailings were being deposited within Sandhill Fen project area from a nearby discharge. To limit ingress of this tailings slurry into Sandhill Fen, the North-South Berm and the East-West Berm were constructed as unengineered berms using random Pf sand fill from T-Pit. The Pf sand fill was incorporated into the Gate 3 Detailed Design of Sandhill Berm and Hummock 9. The East-West Berm west of Hummock 9 was shown to be regraded / removed as necessary to allow surface water to flow towards the Primary Fen.

The Sandhill Berm was constructed mechanically during the 2009 / 2010 winter using tailings sand from the 318 m Spur Dyke stockpile. The Sandhill Berm was constructed by Cow Harbour while they were constructing the hummocks. It is assumed that the same equipment was used to construct the Sandhill Berm as the hummocks. See Section 4.4 for hummock construction information.

In September 2010, work was on-going to remove the East-West Berm, and the area west of Hummock 9 was regraded. As-built topography suggests that the East-West Berm was removed and regraded.

Sandhill Berm reclamation design included 0.3 m clay till overlain with 0.2 m LFH – D ecosite. The 2014 as-built placement maps indicate 0.2 to 0.4 m of clay till was placed on the Sandhill Berm and that no LFH – D ecosite was placed on the Sandhill Berm.

4.1.2. North Containment Berm

The North Containment Berm was not included in the Permit Level Design. The North Containment Berm was designed, in parallel with the Sandhill Berm spillway design, during Gate 3 Detailed Design to provide some protection for Highway 63 during extreme storm events. The North Containment Berm was designed to have a constant centreline elevation of 314.4 m to provide freeboard above the level of the Sandhill Berm spillway invert. The North Containment Berm was designed to have a 10.4 m wide crest that slopes at 2% slope towards the Primary Fen and be constructed using tailings sand.

The North Containment Berm was constructed by Cow Harbour during hummock and Sandhill Berm construction. It is assumed that the same equipment used to construct the hummocks was used to construct the North Containment Berm. Field observations indicated Kc material was used as subgrade fill for the Perimeter Road, which suggests that some Kc material may have been used as fill for the North Containment Berm.

The North Containment Berm reclamation design included 0.3 m of clay till overlain with 0.2 m LFH – D ecosite. The 2014 as-built placement maps indicate 0.2 to 0.4 m of clay till was placed on the south edge of the berm or just south of the berm, and do not indicate whether LFH – D ecosite was placed on the berm.

4.1.3. 318 m Spur Dyke

The 318 m Spur Dyke is the southern boundary of Sandhill Fen. The 318 m Spur Dyke was designed and constructed by Tailings Operations as part of the closure design for the EIP.

The Gate 3 Detailed Design indicated that the 318 m Spur Dyke regraded slope was to be field fit with slopes between 4H:1V and 10H:1V. The crest of the 318 m Spur Dyke was used as a laydown for construction materials, reclamation material stockpiles, and a tailings sand cell was poured for use as a borrow stockpile. The north slope of the 318 m Spur Dyke was regraded, reclaimed, and revegetated as part of Sandhill Fen.

The 318 m Spur Dyke slope reclamation design included 0.3 m clay till overlain with 0.2 m LFH – D ecosite. The 2014 as-built placement maps indicate 0.2 to 0.4 m of clay till was placed along the north slope with increased thickness near the toe, overlain by 0.1 to 0.3 m of LFH – D ecosite west of the Perched Fens. In the area south and east of the Perched Fens, the clay till is overlain by 0.2 to 0.4 m of peat mineral. Several areas have less than 0.2 m while some areas have more than 0.4 m peat mineral mix. Due to the size reduction of Hummock 8 during Gate 3 Detailed Design, the upland area behind Hummock 8 was designed to be reclaimed with peat mineral mix, instead of LFH – D ecosite, to manage the risk of salinization from an elevated groundwater table in this area.

4.2. Sump Pad and Vault

The Sump Pad was designed to support outlet infrastructure, allow equipment access to the Sump Vault location to install dewatering wells and install the Sump Vault, and to provide personnel and light-vehicle access to the Sump Vault. The Sump Vault is designed to collect the flow from the underdrains where it can then be pumped from the vault, and to house a valve to open and close the underdrains. An outlet structure adjacent to the Sump Pad houses removable stop logs and a v-notch weir to control and measure surface water outflow.

The Permit Level and Gate 3 Detailed Design of the Sump Pad and Sump Vault were similar with no major design changes. The Sump Vault design includes six 2.6 m outside diameter pre-fabricated concrete rings, with a top slab and bottom slab. Each ring has a wall thickness of 0.2 m and is 1.2 m tall with ladder rungs on the inside of the ring. The rings are connected using a bituminous joint sealant. Custom holes were cored for the underdrain collector pipe and the pump outlet pipe. BGC IFC drawings for the Sump Pad and Sump Vault and CoSyn IFC drawings for the outlet structure and Sump Vault pump details are in Appendix C.

The Sump Pad was constructed in January / February 2009 after completion of the North-South Berm. In February 2009, six dewatering wells and two monitoring wells were installed to lower the water table below the Sump Vault base design elevation to facilitate excavation and Sump Vault installation. The Sump Vault area was dewatered throughout February and March 2009. In early April 2009, the excavation was completed with no sloughing and the base and rings was installed using a crane. Due to concerns regarding potential liquefaction / collapse of the excavation walls, no one was allowed to enter the excavation below a certain

elevation (see BGC IFC Drawings for details). The outlet structure was constructed in March 2012 to house the instrumentation and v-notch weir, but few construction details have been made available to BGC. The Sump Vault is a confined space and special procedures for entry are required.

The Sump Pad reclamation design included 0.3 m clay till overlain with 0.2 m LFH – D ecosite. The 2014 as-built placement maps indicated that 0.3 m of clay till is inferred in the Sump Pad area and do not indicate LFH – D ecosite placement. Field observations indicated that LFH – D ecosite was placed on the Sump Pad, but the thickness is unknown.

4.3. Underdrains

4.3.1. Design

During the site investigation, upward gradients of saline groundwater indicated that water table control within the Primary Fen was required to manage salinization. The TAC recommended attempting to keep the electrical conductivity of surface water and pore water in the wetland below 1000 $\mu\text{S}/\text{cm}$ to increase the probability of successful wetland function. The TAC recognized that many natural fens have much higher electrical conductivities, but the ions responsible for that conductivity are different in natural areas (calcium and magnesium cations in natural areas rather than the sodium cations that dominate tailings systems). Underdrains were designed to intercept the upward saline groundwater beneath the Primary Fen as a method to manage salinization and control sodium, as there was an absence of knowledge with respect to floral and faunal thresholds of sodium salinity for fens.

The Permit Level Design included four 200 mm diameter perforated HDPE underdrains wrapped with a geotextile sock. The underdrains were designed to be installed using a plough train at a nominal depth of 2 m below tailings surface. All four underdrains drain into the Sump Vault. Valves were included in the design to control the underdrains.

The Gate 3 Detailed Design of the underdrains did not include any major revisions from the Permit Level Design. The underdrains converge into a custom collector pipe that drains into the Sump Vault. The custom collector pipe is a 400 mm diameter HDPE pipe with four 200 mm diameter adapters. The collector pipe and underdrains 50 m upstream of the collector pipe are not perforated. Instead of a valve for each underdrain, a single 400 mm butterfly valve within the Sump Vault was included. Due to confined space concerns, a custom valve stem extension was designed and installed to operate the valve from the top of the Sump Vault. The construction drawings for the underdrains can be found in Appendix C.

4.3.2. Construction

Skocdopole Construction installed the underdrains in April 2009 with no major deviations in construction from the Gate 3 Detailed Design. The underdrains were installed using a plough train consisting of a trencher and plough that was tethered to a dozer. A sufficient frost cap was required to support the plough train equipment but was a challenge for the trenching

equipment. The underdrains were installed at a nominal depth of 1 to 2 m below tailings surface to produce positive drainage from the pipe terminus to the Sump Vault. Where underdrains are within 1 m of tailings surface, an exclusion zone for equipment was highlighted (see BGC Underdrain Protection Guidelines memorandum in Appendix H2).

During underdrain installation, the upstream underdrain terminus of each underdrain was laid on the tailings surface to allow for future extension or flushing / maintenance of the underdrain, if required. Guidelines to bury the upstream pipe terminuses in an underdrain protection trench and extend the buried underdrain from the bottom of the trench to the tailings surface using a 90 degree elbow and extension piece were provided in the BGC Underdrain Protection Guidelines memorandum (Appendix H2). Jacobs Industrial Services Inc. completed the underdrain extension and burial in November 2010.

It should be noted that in preparation for underdrain construction, snow clearing was performed to allow for deeper frost penetration. During snow clearing, a dozer, most likely a D6 or similarly sized dozer, became mired in an area of standing water, this area is referenced as the Winter 2008 / 2009 Wet Zone in the IFC drawings. Special operational procedures for working in this area were developed, including keeping equipment on the hummocks rather than on soft wet tailings sand areas.

During dewatering of the Sump Vault / underdrain tie-in area, an H₂S alarm was triggered. The confined space issue was alleviated by moving the dewatering discharge to an open area, as the discharge was originally in a tented structure.

In the summer of 2009, tailings sand ridges were present above the drains. These ridges are most likely spoil windrows from the trenching equipment during installation.

4.4. Hummocks

4.4.1. Design

Hummocks were designed to surround and generate fresh water recharge to the Primary Fen. The hummocks were designed such that there is sufficient depth to the water table and saline capillary fringe that it does not impact revegetation success on the surface of the hummock. Groundwater modeling conducted as part of the Permit Level Design suggested that approximately 20 years of rainfall is required to flush the tailings sand hummocks.

The Permit Level Design included nine hummocks around the perimeter of the Primary Fen. The hydraulic conductivity of the hummock fill material is expected to influence the time for hummock flushing. Therefore, to research these flushing characteristics, six hummocks were designed to be conventional tailings sand and three hummocks were designed to be cycloned (densified) tailings sand. Cycloned tailings sand, that has lower fines and higher hydraulic conductivity than conventional tailings sand, was hypothesized to lower the water table within the hummocks, perhaps increase net percolation, and thus may promote additional flushing compared to conventional tailings sand. Due to availability issues of cycloned tailings sand from the CT Plant, all hummocks were designed to use conventional tailings sand fill.

The Gate 3 Detailed Design included the removal of Hummocks 1 and 3, a redesign of Hummock 8, and height reduction of the other hummocks to reduce fill volume and construction costs. The Gate 3 Detailed Design hummocks are presented in the December 2009 Hummock IFC Drawings (Appendix C). The hummock crests and slopes were simplified to aid construction with the expectation that they would be later landform graded.

Hummocks 2, 4, 5, 7, and 8 are designed to be reclaimed as “drier” hummocks using a 0.4 m thick layer of Pf sand, placed directly onto the hummock tailings sand, overlain by a 0.15 m thick layer of LFH – A/B ecosite. Hummocks 6 and 9 are designed to be reclaimed as “wetter” hummocks using a 0.3 m thick layer of clay till placed directly onto the hummock tailings sand, and be overlain by a 0.2 m thick layer of LFH – D ecosite. The drier hummocks are designed to transmit a greater percentage of rainfall as interflow and groundwater seepage to the Primary Fen, while the wetter hummocks are design to promote surface run-off. Reclamation details for hummocks are shown in the January 2010 Reclamation IFC Drawings (Appendix C).

4.4.2. Construction

Hummocks were mechanically constructed by Cow Harbour during winter 2009 / 2010. The seven hummocks were constructed using conventional tailings sand from the tailings sand stockpile on the 318 Berm. Tailings sand fill was hauled from the 318 m Spur Dyke stockpile to the hummock location using 30 and 40T articulated haul trucks, dumped, and spread and compacted using D6 dozers.

Due to operational constraints, the hummocks were not landform graded. Swale infills to limit water from back-flooding from the Primary Fen into the swales between hummocks were field fit and constructed using tailings sand.

Trafficability was good in areas of Sandhill Fen during winter conditions while a thick frost cap was present. Ice was observed in location of Hummock 9 prior to construction. A BGC site visit memorandum is in Appendix E.

4.4.3. Reclamation and Revegetation

The 2014 as-built placement maps indicate that 0.1 to 0.5 m of Pf sand was placed on Hummocks 2, 4, 5, 7, and 8, with one area being thinner than 0.1 m and several areas being thicker than 0.5 m. The overlying LFH – A/B ecosite was generally placed 0.1 to 0.2 m thick with several areas being thinner than 0.1 m and thicker than 0.2 m. For Hummocks 6 and 9, 0.2 to 0.4 m of clay till was placed, with an area in the depression on Hummock 6 and northwest slope of Hummock 9 being thicker than 0.4 m, and several areas on Hummock 6 and 9 being thinner than 0.2 m. Some CWD was also spread over Hummock 2 and Hummock 9 in April 2011 on top of the LFH material.

Hummocks were revegetated using three tree planting prescriptions at varying stems per hectare density in May 2012: A/B ecosite, D ecosite, and standard upland. The tree planting densities were 5,000, 10,000, and 0 stems per hectare for A/B ecosite and D ecosite, 2,000 stems per hectare for standard uplands, and 0 stems per hectare as a control to monitor

effectiveness of the unplanted LFH materials. See Appendix D for tree planting design details and map. As-built revegetation information is not available for this report.

4.5. Primary Fen

The Primary Fen is the 15 ha lowland area of the watershed that is approximately 700 m long and 250 m at its widest point. The Primary Fen area is designed to be reclaimed to create the conditions required for a fen-type wetland to be established. Tailings sand and clay till islands were included as part of the experimental design to monitor performance of various reclamation prescriptions relative to mineral controls (BGC 2008a).

The Primary Fen area is underlain by tailings sand with a reclamation material prescription comprised of a 0.5 m thick clay till layer overlain by 0.5 m thick peat mineral mix layer. The 0.5 m thickness of peat mineral mix was selected because it provides a reasonable depth against limited erosion and settlement. The 0.5 m of clay till was selected to provide a mineral-rich subsoil to allow root establishment and to provide a buffer layer against salt migration into the fen from underlying tailings pore water; the clay till is not intended to act as a liner.

The Permit Level and Gate 3 Detailed Designs were largely similar, with minor areal differences due to removing and reducing footprints of hummocks in the Gate 3 Detailed Design, although a difference was that the slope of the Primary Fen was reduced from 0.4% to 0.15% in the Gate 3 Detailed Design due to involuntary tailings sand slurry ingress near the Sandhill Berm.

The Permit Level Design included three large tailings sand islands in the Primary Fen: Islands A, B, and C. During Gate 3 Detailed Design, smaller tailings sand and clay till islands, and live peat transplant areas were included in the design and reclamation of the Primary Fen. In 2009, it was decided to not include live peat transplants due to logistical issues during reclamation.

Clay till placement began on November 18, 2010 and was on-going into spring 2012. In March 2012, construction of the clay till islands was complete. During winter construction and into spring, the clay till was often frozen into large lumps (up to 1 m diameter) that were ripped prior to being compacted. Spreading and compacting (track-packing only) of clay till was done using a D6 sized dozer. The 2014 as-built placement maps indicate that 0.4 to 0.6 m of clay till was generally placed in the Primary Fen, with several areas in the central portion of the Primary Fen being 0.6 to 0.9 m thick, and several areas being 0.2 to 0.4 m thick north of Hummock 7 and 8, and south of Hummock 5 and 6.

Peat mineral mix placement, including on the Perched Fens, was completed in February and March 2011. The peat mineral mix was hauled by articulated 40T haul trucks from the 318 m Spur Dyke temporary stockpile and dumped at the edge of the placement area. During a February 2011 BGC site visit, the peat mineral mix was observed to be placed unfrozen on a track packed layer of snow (nominally 0.3 m thick). Peat mineral mix was spread using several methods during Primary Fen reclamation which are described as follows:

- Initial placement in the western end of the fen (the Winter Wet Area) and Perched Fens was spread by numerous passes with a D6 to D8 sized dozer. The final peat mineral mix surface was relatively uniform and flat with several isolated boulder-sized blocks sitting on the surface.
- An area of peat mineral mix, from where the CWD berm meets Hummock 4 to the central instrumentation point SM-02, was placed and spread using a Cat 321 tracked excavator. The final material surface was visibly rough and was 0.6 m to 0.7 m thick, with boulder-sized blocks of peat mineral mix remaining.
- The material near Hummock 4 was then spread onto track-packed snow with minimal trafficking in three pushes (one straight, and two at 45° angles) using D6 to D8 sized dozers. This placement method created a somewhat rough surface and minimized compaction from equipment traffic.

In the March 3, 2011 site visit memorandum, BGC recommended Syncrude place the remaining peat mineral using a D6 to D8 sized dozer and the three-push method described above in the third bullet. The methodology used to place the remaining peat mineral mix was not documented, but the peat mineral mix surface in the eastern end was observed in 2011 to be rougher and less compact compared to the western end.

Additional peat mineral mix was placed in March and April 2012 to the area south of the Perched Fens and Hummock 8 and on the 318 m Spur Dyke. For the 318 m Spur Dyke, peat mineral mix was placed in a 0.3 m lift with a D8 in two pushes from the top of the slope to the bottom of the slope.

The 2014 as-built placement maps indicate that 0.4 to 0.6 m of peat mineral mix was generally placed within the Primary Fen. An area north of Hummock 8 in the central portion of the Primary Fen is shown to have a peat mineral mix thickness of 0.1 to 0.4 m, while several small areas have a thickness greater than 0.6 m.

4.6. Perched Fens

Two circular-shaped Perched Fens were included in the design to test the hypothesis that fen reclamation is not reliant on a large groundwater catchment. The hypothesis assumes that the Perched Fen vegetation is able to 'shut-down' evapotranspiration and use moisture from peripheral bank-storage in times of deficit.

The Permit Level Design included two Perched Fens that tie into the south slope of Hummock 7 and are separate from the Primary Fen. The Perched Fens were designed to have slightly bowl-shaped basins (with 0.5% slopes). Perched Fen 1 is designed to be 1 m of peat mineral mix and Perched Fen 2 is designed to be 0.5 m flushed tailings sand overlain with 0.5 m peat mineral mix. Both Perched Fens are underlain with 0.3 m track-packed clay till placed on an elevated tailings sand pad and are contained with tailings sand berms. The clay till is intended to reduce the rate of downward migration of water from the Perched Fens.

The Gate 3 Detailed Design was similar to the Permit Level Design with no major design revisions. The tailings sand underlying the peat mineral mix in Perched Fen 2 was updated to

conventional tailings sand due to a lack of available material. Freshwater from the Water Storage Pond is piped to the Perched Fens and delivered via a perforated pipe. The IFC Drawings for the Perched Fens are in Appendix C.

Perched Fen construction with tailings sand occurred from July to September 2010. Construction observation records for this area are not available. During construction, a BGC memorandum was prepared to address a construction query whether to place clay till on the inside slopes of the Perched Fens. To provide bank storage and facilitate research, the memorandum indicated that the inside slopes were not to be lined with clay till (Appendix H).

Erosion gullies of the inside slopes of Perched Fen 2 were noted. In September 2010, BGC inspected the slopes and found that the erosion gullies were due to runoff on the highly erodible tailings sand and that there were no global stability issues with the Perched Fens. See Appendix E for a site visit memorandum.

The 2014 as-built placement maps indicate 0.2 to 0.4 m of clay till was placed in the Perched Fens, with an area of 0.5 m thick clay till in Perched Fen 1. In general, the peat mineral mix is 0.6 to 0.7 m thick in Perched Fen 1 and 0.3 to 0.6 m thick in Perched Fen 2.

4.7. Uplands and Swales

The uplands are the non-fen areas of the watershed, hummocks are considered to be part of the uplands but are discussed separate from this section due to significance to design. Swales capture and convey run-off from the uplands and hummocks to the fen.

The swales were designed to be gently sloped areas that are vegetated to limit erosion from run-off. The design included tailings sand in-fill areas to raise the elevation of the swales between hummocks to promote surface drainage to the fen and minimize back-flooding into the uplands.

The reclamation design included 0.3 m of clay till overlain by 0.2 m of LFH – D ecosite material. The as-built placement maps indicate 0.2 to 0.4 m of clay till was placed in the uplands and swale, with an area south of the Perched Fens and Hummock 8 being thicker than 0.4 m and an area to the southwest of the Research Centre Pad being thinner than 0.2 m. LFH – D ecosite was generally placed 0.1 to 0.3 m thick in the uplands south of the Research Centre Pad and LFH – A/B ecosite was thinner than 0.1 m north of Hummocks 4 and 5. As mentioned above, the uplands south of the Perched Fens and Hummock 8 received a variable thickness of peat mineral mix.

The upland area south of the Research Centre Pad and west of the Perched Fens was overcompacted. During tree planting in the summer of 2011, it was noted that there were areas that were too compact to plant trees. During discussions in December 2012, it was decided that these overcompacted areas would be scarified to allow for revegetation. Several areas on Hummock 6 were also found to be overcompacted, and were also to be scarified. Scarification was completed by dozers and graders. Care was taken to avoid scarifying the underlying tailings sand.

4.8. Water Storage Pond

The Water Storage Pond is a 1 ha pond located between Hummocks 1 and 7, and the Research Centre Pad. The pond is supplied freshwater from the Mildred Lake Reservoir via the Freshwater Pipeline. The water in the storage pond diffuses into the Primary Fen through a coarse flow through diffuser, often referred to as the “leaky dam”.

The Permit Level Design included the flow through diffuser between the pond and the Primary Fen, as well as a geosynthetic clay liner (GCL) at the base of the pond to reduce percolation losses to seepage. The GCL was to be covered with Pf sand of variable depth to create diversity and small islands in the pond.

The Gate 3 Detailed Design had a similar areal extent of the pond and flow through diffuser basis, but a major design revision was the GCL was replaced with 0.5 m thick clay till reclamation layer, as the GCL installation is more construction intensive. The flow through diffuser was designed to have a clay till core, a non-woven geotextile separation layer, and a washed gravel / cobble dressing. The freshwater pipe outlet energy dissipation apron is a 10 m long perforated 300 mm diameter pipe buried within washed rock to simulate low-energy, groundwater flow conditions into the water storage pond.

Inlet and perimeter berms were designed to surround the water storage pond to provide 0.5 m of freeboard and to limit back-flooding into the area west of the Perched Fens. The Water Storage Pond was designed to have a wet well and pump house to supply freshwater to the Perched Fens. See Appendix C for Water Storage Pond IFC Drawings.

A temporary watering system was required because the peat mineral mix was placed before the water storage pond, Freshwater Pipeline, and flow through diffuser were constructed and operational. The temporary watering system was installed in the summer of 2011 to provide water to sustain the peat mineral mix throughout the summer. By summer of 2012, the water storage pond, Freshwater Pipeline, and flow through diffuser were constructed and the temporary watering system was no longer required.

Construction of the water storage pond and the flow through occurred in spring 2011.

In July 2012, the Freshwater Pipeline from Mildred Lake Reservoir to the water storage pond was activated (running at 25% capacity), and the water storage pond was filled. A conceptual water management plan is in Appendix K.

4.9. Freshwater Pipeline

A Freshwater Pipeline was included for Sandhill Fen to provide freshwater from the Mildred Lake Reservoir for initial saturation of the peat mineral mix, and to provide control of the water supply and water level in the Primary Fen, and flush salts if salinization becomes an issue. The Freshwater Pipeline supplies water to the freshwater pipe outlet energy dissipation apron in the water storage pond described above.

The Permit Level Design and Gate 3 Detailed Designs are similar with no major changes. The Freshwater Pipeline is a 350 mm diameter HDPE pipe, about 2.6 km in length, and required a horizontal bore under Highway 63. The CoSyn Gate 3 Detailed Design Drawings, including piping and electricity details, are in Appendix C.

Construction of the Freshwater Pipeline began in spring 2011 and was completed and operational by summer 2011. A pipeline to supply the Perched Fens with freshwater from the water storage pond was also constructed.

4.10. CWD Berms

The CWD Berms were designed and built to have a sinuous shape and variable width and height with a parallel alignment of logs. The CWD Berms were built in February 2011. The berms between Hummocks 6 and 9 and between Hummocks 5 and 8 were constructed first, and the third CWD berm between Hummocks 4 and 7 was constructed last.

The berm between Hummocks 4 and 7 stands approximately 1.0 to 1.2 m high. This is a lower height than the CWD Berms between Hummocks 6 and 9 and Hummocks 5 and 8. It is also approximately 30% less material volume than the other two and approximately 1 to 2 m narrower due to the inclusion of freshly broken logs and the exclusion of smaller debris (roots and sticks) for this berm.

In February and March 2011, the CWD Berms were extended 2 m vertically upslope at the abutments of the hummocks to limit erosion.

Refer to BGC Site Visit report from February 16 and February 28, 2011 for more details on CWD berm construction in Appendix E. Refer to a video in Appendix L for an example of CWD placement.

Construction was sequenced such that the CWD berm construction would not limit access to construction equipment. The berms settled considerably over the first year. Though some floating of the CWD from the berms during spring melt / flooding did occur, in general, the berms became more compact and the small amount of material that did float did not cause any problems.

4.11. Infrastructure

Sandhill Fen infrastructure includes a Perimeter Road, a Research Centre Pad, boardwalks, electricity, and instrumentation.

4.11.1. Perimeter Road

A four season Perimeter Road was included in the design to provide access to the research trailer and Sump Vault, as well as the perimeter of Sandhill Fen. The Perimeter Road is on the North Containment Berm along the north of Sandhill Fen, on Hummock 6 and 9 and the Sandhill Berm along the east, the 318 m Spur Dyke to the south, and forms the surface watershed boundary to the west.

The Permit Level and Gate 3 Detailed Designs are similar with no major revisions. The Perimeter Road design includes a 5 m wide flat surface for light vehicles. IFC Drawings for the Perimeter Road are in Appendix C.

Perimeter Road construction began in September 2010 and was completed as of March 2012. Some maintenance (fixing erosion along the Perimeter Road) was carried out in April 2012. Few construction records and material placement details for the Perimeter Road were provided to BGC. Kc fill material was observed in the Perimeter Road subgrade. It is uncertain whether the Kc material remains or was removed. Where the Kc remains, it may impact the Sandhill Fen salt balance.

4.11.2. Research Centre Pad

A Research Centre Pad is included to the west of the water storage pond. The Research Centre Pad design intent was to provide area for a research trailer, parking, and building to house the electricity supply. The Permit Level and Gate 3 Detailed Designs are similar with no major design revisions. The Research Centre Pad is designed to have a 45 m by 48 m pad that sheds water to the south at 0.5%. The pad was designed to be constructed with tailings sand and be surfaced with gravel. IFC Drawings for the Research Centre Pad are in Appendix C.

The Research Centre Pad was constructed in March 2012 with a trailer (Building 1813) being installed shortly afterwards. No construction records or material placement thicknesses were provided to BGC.

4.11.3. Boardwalks

Boardwalks were included in the design to provide access to the Primary Fen for personnel to access research monitoring and instrumentation locations.

Syncrude designed and oversaw construction of the boardwalks. Boardwalks were constructed in July 2012 by Global Fabrications Inc. The boardwalks consist of 100 by 150 mm pressure treated wooden planks and 75 by 300 mm rough sawn decking material (not pressure treated) which were anchored with steel anchors into the fen. Installation of the screw pile anchors was done with a Cat 311 excavator heavy duty auger driver. When installing the boardwalks, materials were carried out to the work area with a tracked skid steer (Cat 299D).

A job hazard assessment for board walk installation is in Appendix H.

4.11.4. Electricity

ATCO electrical power lines were installed by April 2012 to provide A/C power to the research trailer, the weir building, the Sump Vault pump and eddy co-variance research towers. The power lines to the eddy co-variance research towers were strung along the base of the boardwalks.

5.0 SURVEYS AND INSTRUMENTATION

5.1. Placement Surveys

Topographic surveys were carried out on an on-going basis on various elements throughout construction and reclamation. As-built surveys occurred regularly throughout material placement activities. However, several contractors and survey datums were used to survey the material stockpiles and the material placement thickness and extents, which made generating accurate material placement surfaces and isopachs impossible.

Instead, material placement extents and thicknesses were confirmed in 2013 by NorthWind using a shallow hand auger. The as-built material placement maps created using the 2013 soil survey data are provided in BGC (2014), and in Appendix I.

5.2. Annual Topographic Surveys and Aerial Photographs

Drawings 02 through 11 present annual regional topographic surveys and aerial imagery. LiDAR surveys can be used for monitoring and indications of settlement.

Areas of Sandhill Fen elements, based on the 2012 digital elevation model provided by Syncrude, are provided in Table 5.1.

Table 5.1. Sandhill Fen Element Areas

Element	Measured area (ha)
Sandhill Fen	52
Primary Fen	15
Perched Fen #1	1.1
Perched Fen #2	1.2
Surface Water Watershed	55

As shown in Drawing 01, the watershed area (based on 2012 LiDAR) is 55 ha. The watershed area is larger than the boundary of Sandhill Fen due to run-off contribution from the 318 m Spur Dyke to the south. This watershed area, particularly the run-off contribution from the 318 m Spur Dyke, is not well defined and may evolve over time. If Syncrude desires, small watershed berms could be constructed to create a better defined watershed boundary.

Aerial photographs of Sandhill Fen are provided in the Drawings section. Aerial photographs from 2008, 2009, 2010, 2011, and 2012 are shown in Drawings 02, 04, 06, 08, and 09, respectively. The annual aerial photographs may be used to interpret conditions during construction, reclamation, and revegetation activities, and may provide insight into observed conditions, such as showing temporary access roads and construction activities.

5.3. Instrumentation

Instrumentation has been installed to inform design and research of Sandhill Fen. The majority of instrumentation to inform design was installed in 2008. Instrumentation installed included monitoring wells and settlement monuments. Research monitoring wells were installed in 2011 but the majority of instrumentation for research was installed after the summer of 2012, when construction and reclamation activities were substantially complete.

In 2008, monitoring wells were installed in the watershed during the initial site investigations. In January and February of 2010, two surveys were conducted to determine the status of all the existing instrumentation present at Sandhill Fen. In 2010, there were a total of eight nested monitoring wells and 32 single monitoring wells. The results of these two surveys are presented in Appendix J.

Five data loggers that were installed in January 2010 to measure and record groundwater level, temperature, and electrical conductivity (EC) within wells near the underdrains. The research and operational purpose of the program was to monitor the effect of operating the underdrains on the water level in the Primary Fen and to groundwater level and quality. A description of the field program and the two memoranda containing results of the monitoring and logger data from September 2008 and 2010 are presented the in Appendix J.

In July 2011, 47 additional standpipe monitoring wells were installed in Sandhill Fen, 20 monitoring wells were installed in the Primary Fen, 15 monitoring wells were installed in the uplands on or near hummock slope transitions, and 12 were installed in the Perched Fens. The standpipes consisted of 25 mm diameter PVC pipe with a slotted screen. Additional installation details are summarized in memorandums found in Appendix J.

Research instrumentation and research plots were implemented in summer 2012. Sipper peeper plots and wells were implemented in the Primary Fen and Perched Fens and revegetation plots and soil moisture access tubes were implemented on the hummocks. Three cameras were mounted to take photographs of Sandhill Fen. Two eddy covariance towers were installed, one south of Hummock 8 and one in the eastern area of the Primary Fen. Three weather stations were installed, one on the Perched Fen berm that separates Perched Fen 1 and Perched Fen 2, one on Hummock 6, and one on Hummock 7. An instrumentation map, current to March 2013, is included in Appendix J.

Ongoing monitoring is being performed by Syncrude and the researchers. Data collected, such as monitoring well readings and surface water quality measurements, is uploaded to the Sandhill Fen Mapping and Metadata Site (SFMMS), where it is stored and accessible to Syncrude, researchers, and consultants. The SFMMS is also a repository for Sandhill Fen related memorandums and reports.

6.0 CONCLUSIONS

Sandhill Fen was constructed, reclaimed, and revegetated from 2009 to 2012, and is currently (2014) in the operation phase. Though there were some changes to the overall construction schedule, the construction and reclamation of Sandhill Fen was completed by the December 2012 deadline set by Syncrude's EPEA Operating Approval.

Sandhill Fen is the first instrumented watershed and research program designed and reclaimed to support a fen-type wetland on a soft tailings deposit, to facilitate Syncrude and TAC research objectives, and be aligned with Syncrude's overall closure objectives. A great amount of knowledge in technology and operations for recreating wetlands on soft tailings deposits will be gained through Sandhill Fen. This knowledge will be useful for optimizing reclamation of soft tailings areas on Syncrude's leases. Sandhill Fen also provides operational knowhow for implementing various reclamation projects, not only wetland projects, on sand capped soft tailings deposits.

Design, construction, reclamation, and revegetation of Sandhill Fen required a multidisciplinary team of consultants and contractors lead by Syncrude over multiple years. Syncrude Environmental Research led the research phase (2007 – ongoing) and Permit Level Design phase (2007 – 2008). Syncrude Base Plant Projects led the Gate 3 Detailed Design, construction, reclamation, and revegetation phases (2009 – 2012) with Syncrude Environmental Research providing support. Syncrude Environmental Research currently leads the operation and research phases at Sandhill Fen.

Some details related to material source, description, or placement used during construction and reclamation were not provided to BGC, as noted in the report text, it is assumed that these details were not documented or available. If any of these details noted in the report are available, Syncrude should consider providing these details to researchers and consultants, and document the details for future soil audit and certification activities.

Sandhill Fen has successfully moved into the research and operational phases, where it provides the opportunity for Syncrude and its research partners to continue to gain experience, learn, and refine techniques for future fen and watershed reclamation. An extensive research program is currently ongoing.

Using experience from Sandhill Fen, there is opportunity for Syncrude to develop a technology transfer program for future wetland design and implementation at the commercial scale. The information and learnings from each reclaimed wetland can be used by Syncrude, researchers, and consultants to guide future wetland design, reclamation, revegetation, operation, monitoring, and research, and eventually the certification process.

7.0 CLOSURE

We trust the above satisfies your requirements at this time. Should you have any questions or comments, please do not hesitate to contact us.

Yours sincerely,

BGC ENGINEERING INC.

per:

ISSUED AS DIGITAL DOCUMENT.
SIGNED HARDCOPY ON FILE WITH
BGC ENGINEERING INC.

ISSUED AS DIGITAL DOCUMENT.
SIGNED HARDCOPY ON FILE WITH
BGC ENGINEERING INC.

Andy Jamieson, PEng
Geotechnical Engineer

Heather Provost, MSc
Groundwater Specialist

Reviewed by:

ISSUED AS DIGITAL DOCUMENT.
SIGNED HARDCOPY ON FILE WITH
BGC ENGINEERING INC.

Gord McKenna, PhD, PEng, PGeol
Senior Geotechnical Engineer

AJ/GM/jwc/cm

APEGA Permit to Practice: 5366

REFERENCES

- Alberta Environment, 2007. Environmental Protection and Enhancement (EPEA) Act. R.S.A. 2000, c.E-12, as amended. Approval No. 26-02-00 for Syncrude Canada Ltd. June 21, 2007.
- BGC Engineering Inc., 2007. Soft Tailings Geotechnical Investigation Design for Syncrude's East-In-Pit (EIP) Tailings Deposit Final Report. Prepared for Syncrude Canada Ltd., December 2007.
- BGC Engineering Inc., 2008a. Syncrude EIP Instrumented Watershed: Sandhill Fen – Permit Level Design. Prepared for Syncrude Canada Ltd., December 2008.
- BGC Engineering Inc., 2008b. East-In-Pit Instrumented Watershed - Sandhill Fen Permit Level Design: 2008 Hydrogeological Site Investigation Report. Prepared for Syncrude Canada Ltd., December 2008.
- BGC Engineering Inc., 2009a. EIP Instrumented Watershed – U-Shaped Cell As-Built Report and Operational Guidelines Final Report. Prepared for Syncrude Canada Ltd., July 2009.
- BGC Engineering Inc., 2009b. Settlement Monument Closure Memorandum. Prepared for Syncrude Canada Ltd., June 2009.
- BGC Engineering Inc., 2010. CT Prototype Instrumented Watershed – 2008 Geotechnical Site Investigation Final Report. Prepared for Syncrude Canada Ltd., June 2010.
- Pollard J, McKenna GT, Fair J, Daly C, Wytrykush C, Clark J. 2012. Design aspects of two fen wetlands constructed for reclamation research in the Athabasca oil sands. Mine Closure 2012 Symposium. Brisbane. Australian Centre for Geomechanics p815-829.

APPENDIX 2: FINAL SUMMARY REPORT- HYDROGEOLOGIC INVESTIGATIONS OF SANDHILL WATERSHED

TERMS OF USE

University of Alberta was retained by Syncrude to carry out the research presented in this report and the material in this report reflects the judgment of the author(s) in light of the information available at the time of document preparation. Permission for non-commercial use, publication or presentation of excerpts or figures requires the consent of the author(s). Commercial reproduction, in whole or in part, is not permitted without prior written consent from Syncrude. An original copy is on file with Syncrude and is the primary reference with precedence over any other reproduced copies of the document.

Reliance upon third party use of these materials is at the sole risk of the end user. Syncrude accepts no responsibility for damages, if any, suffered by any third party as a result of decisions made or actions based on this document. The use of these materials by a third party is done without any affiliation with or endorsement by Syncrude.

Additional information on the report may be obtained by contacting Syncrude.

This appendix may be cited as:

Mendoza, C., and Devito, K. 2020. Final Summary Report: Hydrogeologic Investigations of Sandhill Watershed. Appendix 2 in Syncrude Canada Ltd. *Sandhill Fen Watershed: Learnings from a Reclaimed Wetland on a CT deposit*. Syncrude Canada Ltd. 2020.

Final Summary Report Hydrogeologic Investigations of Sandhill Watershed

Prepared for:

Jessica Piercey, Carla Wytrykush and Dallas Heisler
Syncrude Canada Limited
Edmonton, Alberta

Prepared by:

Carl Mendoza¹ and Kevin Devito²
2020-06-30

Drawing on the significant work of:

Pam Twerdy, Max Lukenbach, Jean-Michel Longval
and numerous summer students

¹Department of Earth and Atmospheric Sciences

²Department of Biological Sciences

University of Alberta,
Edmonton, AB, Canada



UNIVERSITY OF ALBERTA
HYDROGEOLOGY

Preamble

The summary provided here is largely extracted from Lukenbach et al. (2019) and Twerdy (2019), appended. Further details on methods, observations and data, interpretations and conclusions are included in those publications. Equipment installation details are provided in Longval and Mendoza (2014), appended. Appendix F lists all articles, presentations, reports and theses related to this research program.

Acknowledgements

Primary architects of this work were Jean-Michel Longval, Max Lukenbach and Pam Twerdy. Mika Little-Devito was instrumental for assisting with logistics. Summer students and other helpers included: Thomas Baer, Brendan Guest, Nicole Roberts, Stephane Poitras, Jennifer Benyon, Ashley Hamilton, Quinn Hunter, Nicole Brazzoni, Jordan Pearson, Jon Effa, Chris Spencer and Trevor Moningka. Input from Kelly Hokanson is also appreciated.

Funding, plus field, logistical and analytical support from Syncrude Canada is appreciated. Thank you to Carla Wytrykush, Jessica Piercey, Dallas Heisler, Lori Cyprien, Mohammed Salem, Christopher Beierling and Audrey Lanoue, among others, who contributed to, supported and promoted our work.

The Natural Sciences and Engineering Research Council (NSERC) contributed funding through a Collaborative Research and Development grant (NSERC-CRDPJ477235-14) to Kevin Devito with industry partners Syncrude Canada Ltd. and Canadian Natural Resources Limited, and through a CGS-M scholarship to Pam Twerdy. Pam was further supported by Walter H. Johns graduate fellowships, an Alberta Scholarship for Graduate Students, a Queen Elizabeth II Graduate Scholarship and Teaching Assistantships from the Department of Earth and Atmospheric Sciences, University of Alberta.

We appreciate the continued input from our close collaborators, Sean Carey and Simon Landhäusser, and their students and technicians, Erin Nicholls, Haley Spennato, Kelly Biagi and Fran Leishman, among others.

BGC Engineering staff, including Gord McKenna, June Pollard, Dylan Lee, Vanessa Mann, Heather Provost, Jessica Worley and Joe Champagne, assisted with different aspects of the research program, from design, through implementation, to evaluation. Sophie Kessler, Wendy Kline, Janna Lutz and Richard Kao from O’Kane Consultants assisted with data and field logistics.

Table of Contents

Preamble.....	ii
Acknowledgements.....	ii
1 Introduction	1
2 Methods.....	2
2.1 Field Instrumentation.....	2
2.2 Field Measurements.....	4
2.3 Groundwater and Geochemistry Analyses	6
2.4 Soil-moisture and Recharge Analyses	8
3 Results and Discussion	10
3.1 Groundwater	10
3.1.1 Groundwater Flow Observations.....	10
3.1.2 Numerical Modelling.....	15
3.1.3 Groundwater Flow System	16
3.2 Geochemistry	17
3.2.1 Electrical Conductivity.....	17
3.2.2 Geochemistry	18
3.2.3 Isotopes and Sodium.....	20
3.2.4 Solute Distributions and Dynamics.....	21
3.3 Soil-moisture and Recharge	24
3.3.1 General Observations and Water Balance.....	24
3.3.2 Controls on Recharge.....	24
3.4 Perched wetlands.....	29
4 Conclusions for Sandhill Watershed	30
5 Implications for Practice	32
6 References	35
7 Appendices.....	38
Appendix A – Longval and Mendoza (2014) report.....	38
Appendix B – Lukenbach et al. (2019) paper	38
Appendix C – Twerdy (2019) MSc thesis.....	38
Appendix D – Hydrogeological Research Questions.....	39

Appendix E – Assessing Hydrologic Function..... 41

Appendix F –Articles, Presentations, Reports & Theses..... 45

 Refereed Journal Articles 45

 International Invited Presentations 45

 Selected Regional Invited Presentations 45

 Selected Conference Abstracts 46

 Technical Reports..... 47

 Student Theses and Project Reports..... 47

1 Introduction

Sandhill Watershed (SHW) was constructed on a thick deposit of soft tailings in the former East-in-Pit (EIP) area of Syncrude's Mildred Lake operation. The 52 ha site consists of a 17 ha lowland surrounded by upland hummocks and swales, and a gentle slope in the southeast. The site is bounded by the 318-Berm to the south. Two elevated areas, approximately 1 ha each, were constructed to potentially develop into local perched hydrologic systems. A water reservoir and associated infrastructure were constructed within SHW to supply freshwater; however, minimal water management occurred after the first year of operation. Wytrykush et al. (2012) provides background on the experimental design and construction of SHW, stating it is "designed as an instrumented research watershed in order to develop operational techniques and guide future wetland reclamation at Syncrude".

This final program report summarizes the instrumentation, monitoring, and results associated with hydrogeological aspects of SHW from 2012 to 2017. These include groundwater flow, geochemistry, soil-moisture studies in the unsaturated zone, and groundwater recharge. Sections 2 to 4 focus on SHW; section 5 provides guidance for implementation in practice.

2 Methods

2.1 Field Instrumentation

Hydrogeological field instrumentation consisted of shallow wells and piezometers, access tubes for soil-moisture measurements, and soil pits with buried devices to measure soil-moisture content and soil-water tension. A small number of piezometers (<4 m below ground surface; BGS) were installed in 2011, prior to full reclamation (see BGC, 2011). Most instruments were installed in 2012 (piezometers, <11 m BGS) and 2013 (soil-moisture access tubes and soil pits) by Jean-Michel Longval with the University of Alberta (U of A; see Longval and Mendoza, 2014). Supplementary piezometers were installed by U of A as needed in 2013 and 2014 (Longval and Mendoza, 2014), and in 2017 (Twerdy, 2019). McMaster University personnel installed shallow 2" monitoring wells in 2013 and again thereafter (see Carey and Humphreys, 2019). Several 2" piezometers were installed in the underlying tailings (7 to 74 m BGS) prior to SHW construction (BGC, 2008).

The network of piezometers installed by U of A is shown in Figure 1. A total of 223 piezometers, organized into 85 nests (i.e., a nest is monitoring location), were installed in the surficial reclamation materials and tailings materials. Piezometer nest locations were chosen along transects oriented parallel to anticipated flow directions (Figure 1) and associated with soil-moisture measurements and vegetation plots (see Landhäusser, 2019). Each nest consists of one to six piezometers screened between 1 and 11 metres below ground surface (m BGS). Within a nest, piezometer standpipes were separated laterally by approximately 1 m and piezometer screens separated vertically by 1 to 4 m intervals. Piezometers were generally constructed from threaded polyvinyl chloride (PVC) 1" pipe with a 0.30 m screen and PVC drive point tip at the bottom. Selected piezometers installed in 2011 had modified screen lengths (BGC, 2011). Piezometers were generally installed in augered holes and pushed through caved sand below the water table. Surveys were performed by Syncrude using differential GPS in 2013, 2014 and 2017 (± 0.01 m) to update, track, and correct piezometer elevations throughout annual freeze/thaw cycles.

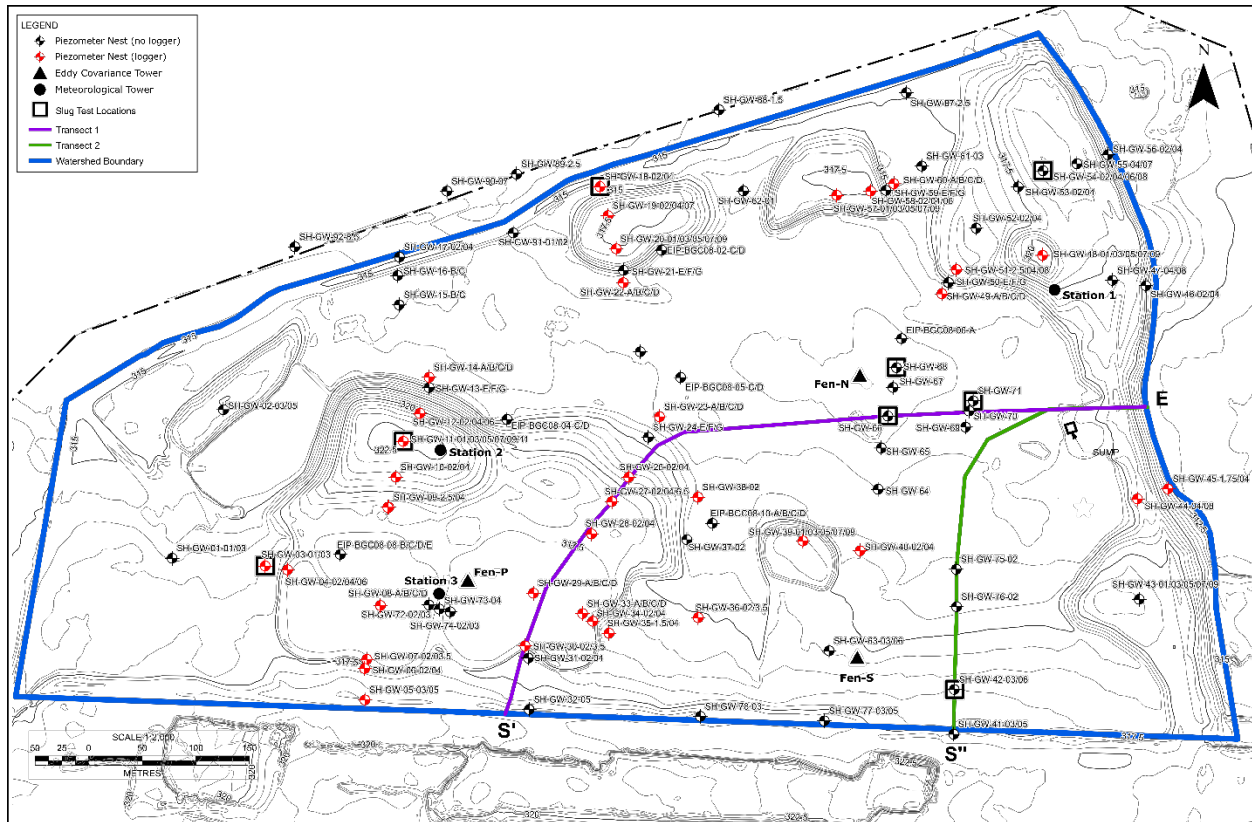


Figure 1 Topographic site map of SHW (blue outline), piezometers and other instrumentation. Transects 1 (S'-E) and 2 (S''-E) correspond to different topographic configurations in the watershed, hummocks to wetlands and slopes to wetlands, respectively. (Figure from Twerdy, 2019.)

Access tubes used to facilitate manual measurements of soil-moisture content were installed at every upland vegetation plot (see Landhäusser, 2019), at every soil-pit (see below) and at selected breaks in-slopes and islands within the anticipated wetland areas (Longval and Mendoza, 2014). A total of 126 access tubes were installed in 2013 as shown in Figure 2. The access tubes, manufactured by Delta-T Devices, are thin, plastic hollow cylinders, approximately 4 ft in length and 1” in diameter, with a sealed, pointed end at the base. The tubes were carefully driven into a hand-augered hole of slightly smaller diameter. A tight fit is required to maximize soil-tube interaction with the soil and minimize leakage of water along the tube.

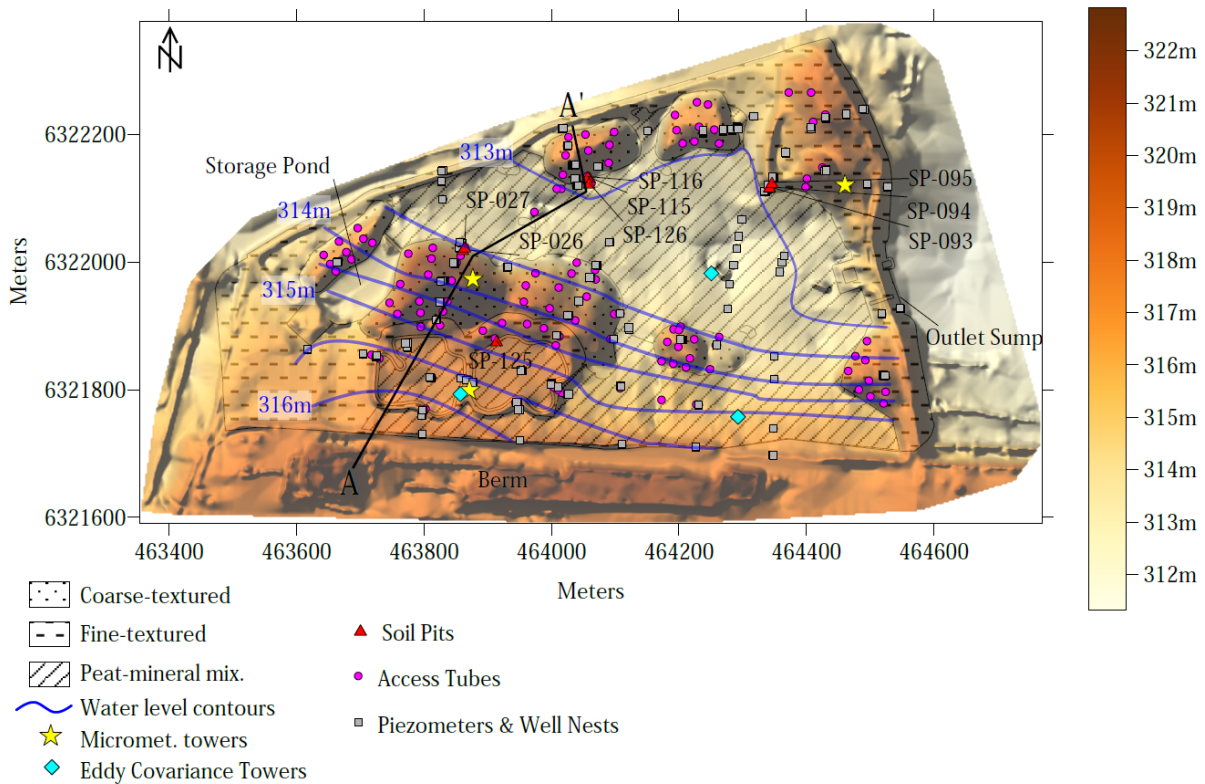


Figure 2 Locations of soil moisture access tubes, soil pits, piezometer/well nests, meteorological stations, and eddy covariance towers in SHW. Surface elevation (colour shading), water level contours (blue lines, May 2015) and 2-D model transect (A–A'). (Figure from Lukenbach et al., 2019.)

Nine soil pits were instrumented in selected wetland-hummock transition zones. Instruments installed in each soil pit consist of paired Decagon MPS-2 Matric Potential and Decagon 5TE Soil Moisture, Temperature and EC sensors (Longval and Mendoza, 2014; Lukenbach et al., 2019). Sensor pairs were installed at depths of 20, 30, 40 and 80 cm BGS. The sensors were connected to Decagon EM50 dataloggers at each pit location. The soil pits were backfilled with excavated material placed in the original lithological order and compacted to a similar density. Soil pits were co-located with soil-moisture access tubes at sites SP-026, SP-027, SP-093, SP-094, SP-095, SP-115, SP-116, SP-125 and SP-126 (Figure 2).

2.2 Field Measurements

Manual soil-moisture content measurements were collected on a weekly to monthly basis throughout the field season, from 2013 to 2016, from the 126 access tubes (Lukenbach et al., 2019). Measurements were obtained at depths of 10, 20, 30, 40, 60 and 100 cm BGS using a PR2 profile probe (Delta-T Devices). Automated measurements of soil-moisture content, soil-water tension, and soil temperature and electrical conductivity were collected hourly from 2013 to 2017.

Manual groundwater measurements were collected from shallow piezometers biweekly to monthly during the field season (May to October) from 2013 to 2017 with a Solinst TLC meter

(Twerdy, 2019). Measurements included depth to water below the top of casing, and water temperature and electrical conductivity at the screen. Where standing water was present adjacent to a piezometer, surface water elevations relative to the top of the casing were also collected. The BGC piezometers completed in underlying tailings were measured once per year in 2013, 2014 and 2017. Groundwater and surface water elevations were calculated using available survey data for top-of-casing elevations.

Automated water level measurements were recorded hourly, ranging from intermittently to year-round, from 44 pressure transducers located in representative piezometer locations from 2013 to 2017 (Twerdy, 2019). Absolute pressure and temperature data were recorded by a pressure transducer with an integrated datalogger (Solinst Levellogger-Edge or Solinst-Levellogger); water pressure was calculated by compensating with barometric data collected on-site (Solinst Barologger-Edge). Groundwater elevations were calculated using manual water level measurements and available survey data.

All shallow piezometers that had enough water were sampled yearly, in midsummer, from 2013 to 2017 (Twerdy, 2019; see also Figure 1). Samples of surface water were obtained adjacent to any pipe when standing water was observed (except for 2016). The deep BGC piezometers were only sampled in 2013, 2014 and 2017. All these samples were analyzed for major and minor ions, EC, and pH (Syncrude Research, Edmonton). Additional groundwater samples were collected six times over the 2017 summer field season, every 2 to 4 weeks, from fifteen piezometers located along the two detailed transects. These samples were analyzed for stable water isotopes (Isobrine Solutions Inc.) and common metals (Alessi Research Group, UofA). Rainwater isotope samples were also collected intermittently during the 2017 field season.

Distributions of areas that were classified as dry, saturated or inundated by water were mapped approximately biweekly to monthly during the field season from 2013 to 2017. Mapping was performed using the squishy-boot method (Devito et al., 2005) and the resulting data are presented in “soil wetness” maps. Mapping was done manually, with a map and a GPS receiver, in 2013 to 2015, and digitally, on an Apple iPad with a Bluetooth-enabled GPS and ArcGIS mapping software, in 2016 and 2017. (BGC, 2013; Twerdy, 2019)

The hydraulic conductivity of materials at the site was determined using several techniques. Slug tests were performed in each shallow piezometer with enough water to obtain representative results (Longval and Mendoza, 2014; Twerdy, 2019). Guelph Permeameter tests were performed in near-surface soils and cover materials (Benyon, 2014). Laboratory permeameter tests were performed on some clay materials (Benyon, 2014).

Meteorological, snow and evapotranspiration data, and vegetation characteristics, were obtained from collaborators (e.g., O’Kane Consultants, Sean Carey, Simon Landhäusser).

2.3 Groundwater and Geochemistry Analyses

Twierdy (2019) reports the details of analysis methods for the groundwater and geochemical system.

Groundwater and geochemical data were analyzed to evaluate the short-term (i.e., single event) to seasonal and long-term (i.e., year to year) influences of climate, vegetation and hydrostratigraphy on the groundwater system dynamics. Water table maps were developed to illustrate the progression of the water table configuration three to five years after watershed construction was completed. Hyetographs (i.e., precipitation vs. time) were paired with hydrographs (i.e., groundwater elevation vs. time) from manual and automated water level data to determine the influence of precipitation and recharge on the water table at various points along two transects (e.g., spring freshet or large precipitation events), and to examine long-term (>1 year) water table dynamics. These data were paired with temporal plots of manual electrical conductivity data (i.e., EC vs. time) to evaluate the spatial and temporal influence of groundwater inputs and outputs on relative solute distributions throughout the watershed. EC maps were also developed to compare spatial and temporal solute distributions. Finally, soil wetness maps were used to evaluate the catchment area in the lowlands and to assist in evaluating the responsiveness of the wetland to large precipitation events and how solutes, represented by EC maps, change in relation to precipitation events.

Two transects were chosen for detailed evaluations of groundwater and geochemical dynamics in different landform configurations (Figure 1). Transect 1 passes through a southern hummock and extends along the lowlands (i.e., wetland). Transect 2 traverses a gentle slope that extends from the southern topographic high into the lowlands. A challenge when evaluating a shallow hydrogeologic system was that the position of a piezometer screen remains constant in space whereas the sampling depth within a water column changes with water level fluctuations. Furthermore, evaluating many groundwater geochemistry samples spatially (horizontally and vertically) and temporally, collected from various depths below the water table and the ground surface, further complicates the analysis. To overcome these challenges, piezometers were generally classified according to, first, the average depth of the water level relative to ground surface and, second, the depth of the midscreen relative to the water level observed in the piezometer (see Figure 3). The transition between shallow vs. deep was interpreted to be 1.8 m.

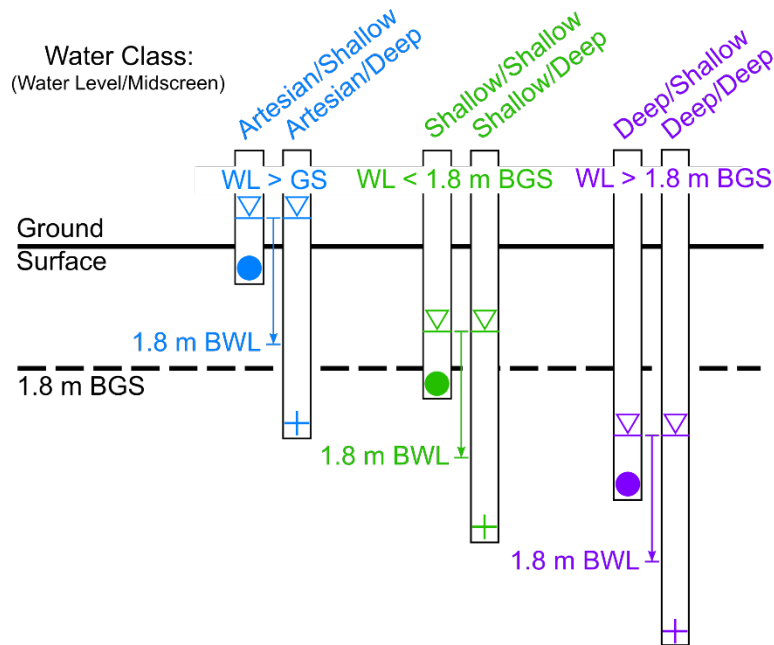


Figure 3 Conceptual diagram outlining six water classes defined by the depth to water level relative to ground surface (symbol color), and the depth of the midscreen relative to the water level (circle = shallow; plus = deep). (Figure from Twerdy, 2019.)

Geochemical and isotope analyses were performed using a qualitative groundwater mixing model with endmember compositions defined from known major inputs to the groundwater system: meteoric water, Mildred Lake Reservoir (MLR) water and oil-sand process water (OSPW). Endmember stable water isotopes, EC, and chemistry were used to evaluate the sources of surface water, shallow groundwater, and deep groundwater samples based on their geochemical and isotope compositions. To facilitate data interpretation, the groundwater samples were grouped into one of four water classes (Figure 3). They were characterized as having shallow water levels (<1.8 m BGS) or deep water levels (>1.8 m BGS) relative to ground surface, and characterized as having shallow midscreens (<1.8 m BWL), or deep midscreens (>1.8 m BWL) relative to the water level. The mixing model utilized these water classes to determine the sources of groundwater at various locations within the watershed and to elucidate solute movement mechanisms along the two transects.

To assist with conceptualizing and quantifying groundwater movement through, and surface-water configurations within, the reconstructed watershed, a 3-D groundwater flow model was developed using Visual MODFLOW (Waterloo Hydrogeologic, 2018). The model incorporated a digital elevation model and reported hydrostratigraphy of the watershed, and recharge fluxes determined from soil-moisture modelling, to simulate steady-state groundwater flow conditions. The calibrated model was also used to explore potential scenarios, such as changes in climate or evapotranspiration (e.g., due to changes in vegetation), that may affect the hydrologic system.

2.4 Soil-moisture and Recharge Analyses

Lukenbach et al. (2019) reports details of the approach to analyzing soil-moisture dynamics and groundwater recharge.

Interpretation of the soil-moisture data obtained from soil pits and access tubes was largely accomplished using numerical models to represent the soil-water and water-table dynamics demonstrated by the field observations. The numerical models were then used to demonstrate how reconstructed landforms (e.g., upland hummocks) with varying heights, geometries, soil covers, and vegetation characteristics may influence recharge.

Fully coupled 2-D saturated-unsaturated flow models were primarily employed to dynamically solve for the position of the water table and to account for its influence on recharge. These analyses were performed for a transect (Transect A-A') that extends from the southern boundary, across the tallest hummock, through the lowland, to a northern hummock, encompassing several soil-moisture and groundwater observation sites (Figure 2). The model domain and assigned geological materials is shown in Figure 4. The 2-D model was calibrated to field observations for 2013 to 2015; performance of the model was then verified by comparing to data from 2016. The 2-D analyses were complemented by 1-D simulations to evaluate the influence of model parameters that represent different soil-cover characteristics at four specific soil-pit locations.

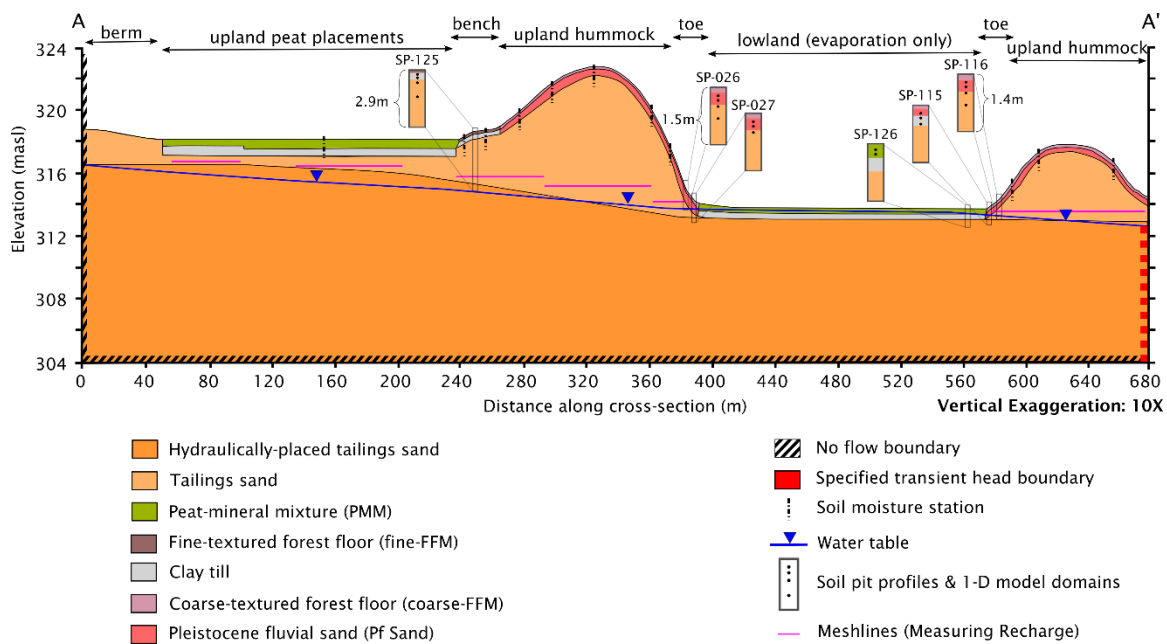


Figure 4 2-D model domain with generalized lithological characteristics, soil covers, boundary conditions, general water table position, and soil profiles corresponding to three (SP-125, SP-026, and SP-116) of the four 1-D soil profile simulation locations (SP-095 not shown). (Figure from Lukenbach et al., 2019.)

Transient simulations were performed using HYDRUS (Šimůnek et al., 2006), which solves for saturated-unsaturated flow with a sink term for root water uptake. Water input was represented by measured precipitation and estimated snowmelt determined from measured

snowpack data. Potential evapotranspiration (PET) was estimated from measured climate data. Measured leaf-area indices were used to estimate interception and partition PET into potential evaporation and potential transpiration. Maximum rooting depths of 0.30 to 0.35 m were assigned to represent the early successional state of the vegetation and to limit root distributions to be within the soil covers.

Scenario testing was used to investigate the influence of a wide range of parameters on recharge within the reconstructed system. Aspects considered include soil hydraulic parameters, vegetation parameters and soil layering characteristics. Soil covers considered included a) coarse-grained soil cover, b) fine-textured soil cover without forest floor material (FFM), c) fine-textured soil cover with FFM, and d) peat-mineral mix (PMM). The scenarios tested with the model included detailed simulations for the study period (i.e., 2013 to 2016) and longer-term simulations using historical climate data (i.e., 1953 to 2006).

3 Results and Discussion

3.1 Groundwater

Twerdy (2019) reports the full analysis of the groundwater system, primarily focussed on results from 2015 to 2017.

3.1.1 Groundwater Flow Observations

A shallow groundwater flow system developed in the upper surficial tailings sand deposits of SHW. Most groundwater flows from the southern boundary of the watershed, beneath the southern hummocks or gentle slope, and toward the eastern (subsurface) outlet to Kingfisher Valley (Figure 5), were similar to the orientation of Transects 1 and 2. The water table configuration indicates groundwater does not mound beneath individually constructed hummocks. During the summer field seasons (May to October), depth to groundwater below the uplands ranged (spatially) from 8.7 m BGS to fluctuating immediately below ground surface near areas transitioning into lowlands. Some piezometers within the lowlands exhibited slightly artesian conditions. Maximum and minimum water levels beneath hummocks showed relatively subdued water level changes through time relative to the notable changes in water levels observed in the slope (Figure 6 and Figure 7). Overall, water levels in piezometers on the southern uplands of Transect 1 were lower in 2016 and 2017 compared to 2015; the water levels in the remaining piezometers fluctuated within the same range year to year (Figure 6). Water levels in piezometers along Transect 2 all fluctuate within the same range, year to year (Figure 7).

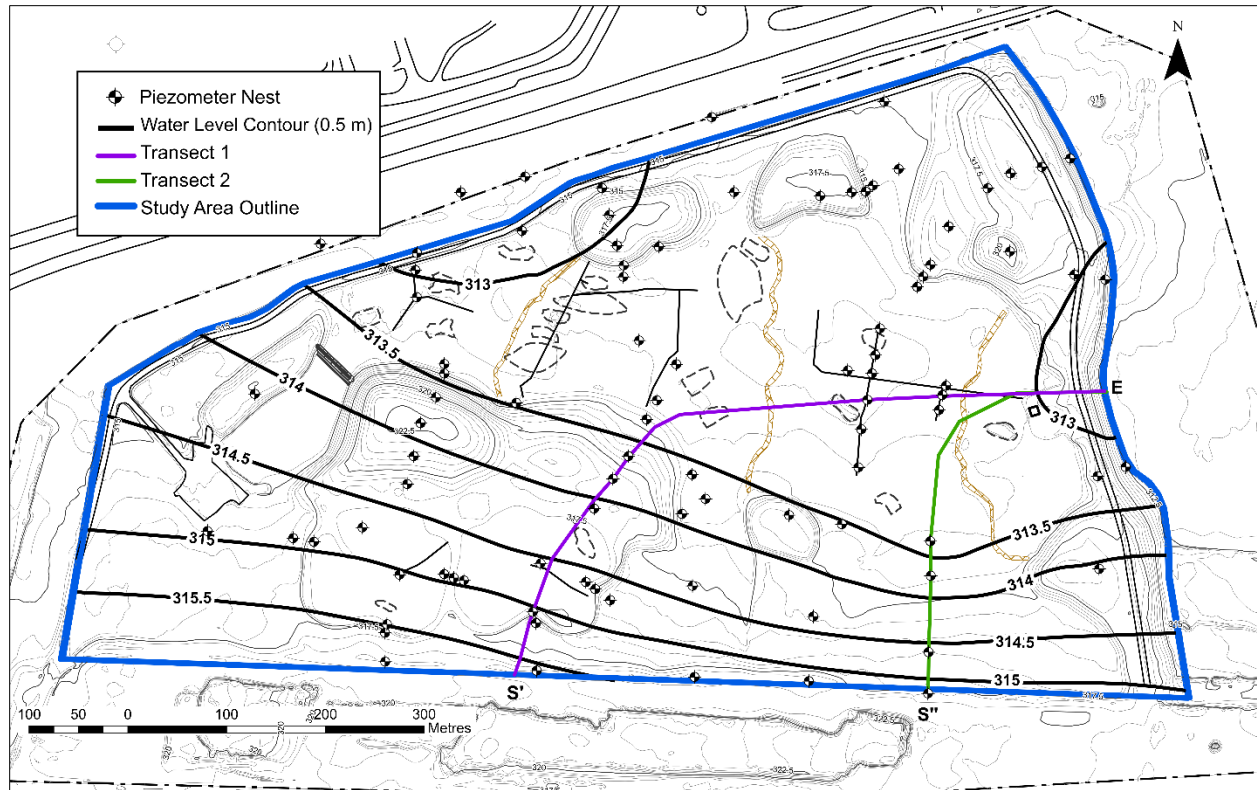


Figure 5 Topographic map of SHW with water table configuration (black contours in m ASL) for July 7, 2017. Transects included for reference for results shown in Figure 6 (Transect 1) and Figure 7 (Transect 2). (Figure from Twerdy, 2019.)

In general, the lowlands had shallow groundwater levels relative to land surface, but some areas had an average standing water level 0.7 metres above ground surface (Figure 6 and Figure 7). Standing water persisted throughout the summer, year to year, in two areas (the east and west wetlands herein; Figure 8). The wetlands are more responsive to snowmelt than areas where the water table is further below ground surface (Figure 6 and Figure 7). The seasonal maximum aerial extent of the standing water and saturated areas in the lowlands may occur early in the field season following snowmelt, although the watershed may wet up appreciably after several sequential large rain events (e.g., in 2016). The least standing water and saturated areas generally occurred later in the field season (i.e., October), except in years with late summer, large precipitation events (i.e., September 2016). Based on soil wetness maps, the wettest days in the lowlands during the study period, correspond to saturated and standing water areas of 17.0 ha and 13.1 ha, respectively, on June 3, 2017; the driest days in the lowlands during the study period corresponded to saturated and standing water areas of 4.9 ha and 1.3 ha on October 25, 2015.

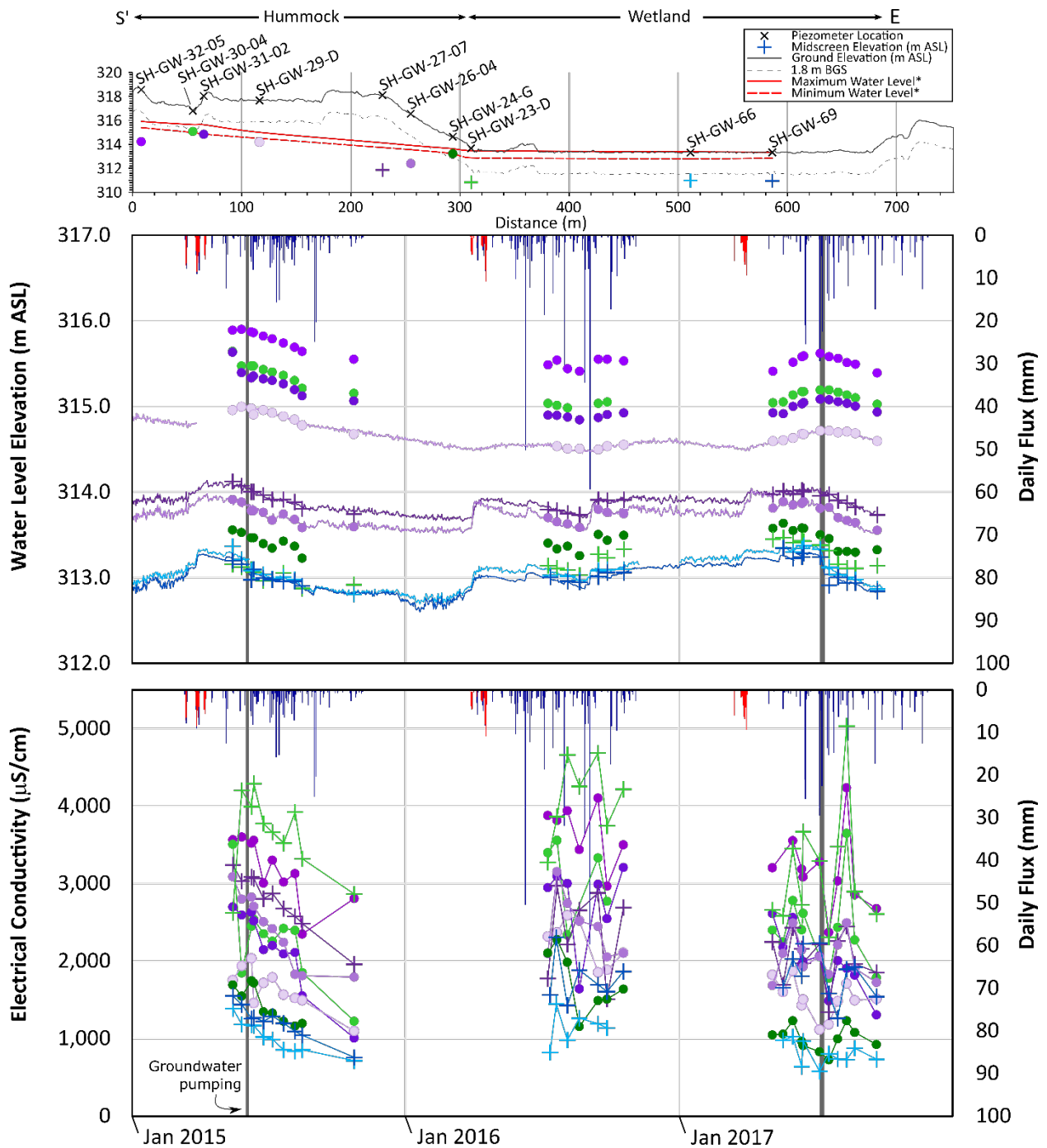


Figure 6 Water level and EC data for Transect 1 (hummock to wetland). Colours and symbols correspond to Figure 3. Points are measured manually. Lines in hydrograph are continuous data; lines in EC plot are only to assist in interpretation. (Figure from Twerdy, 2019.)

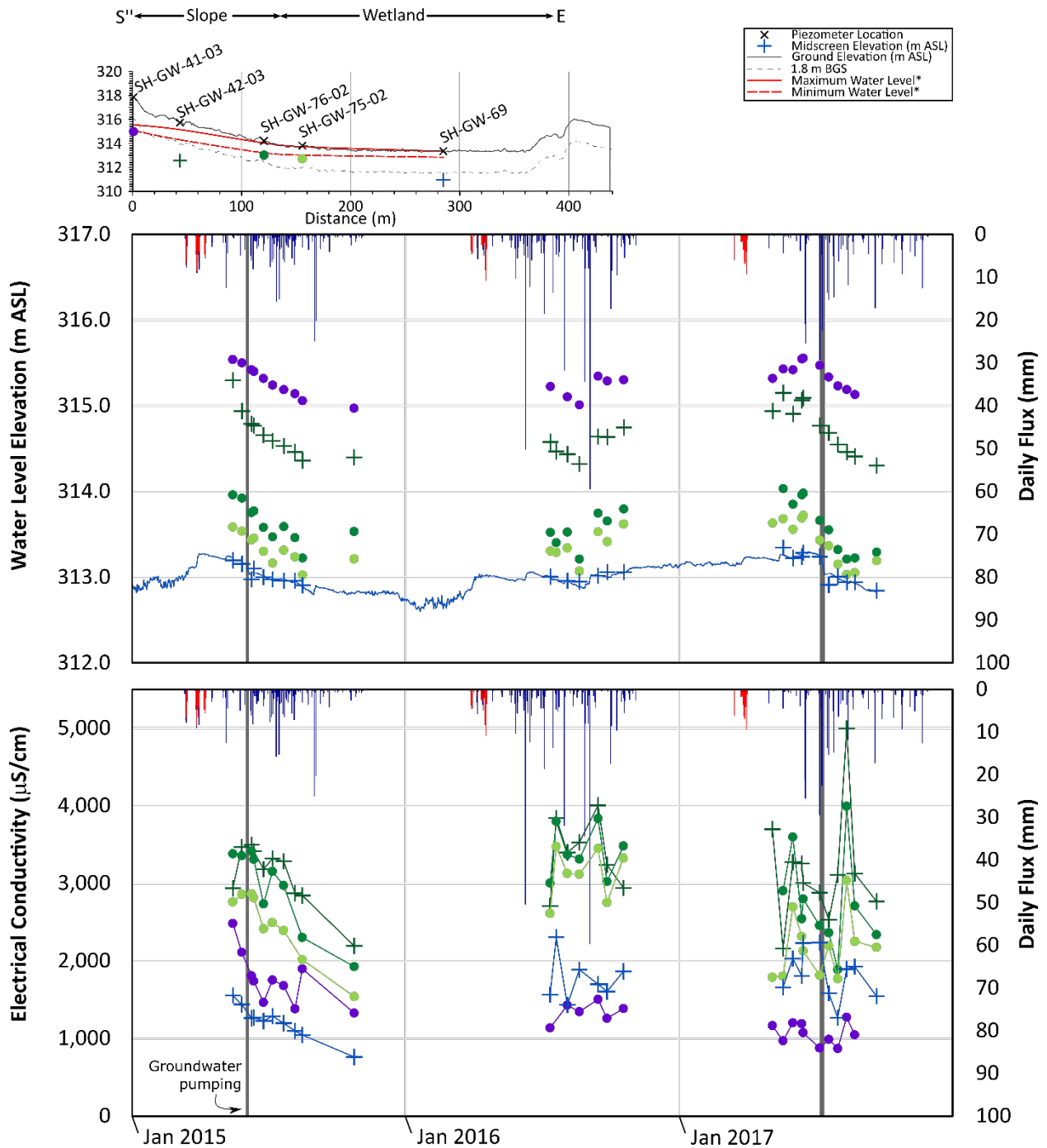


Figure 7 Water level and EC data for Transect 2 (slope to wetland). Colours and symbols correspond to Figure 3. Points are measured manually. Lines in hydrograph are continuous data; lines in EC plot are only to assist in interpretation. (Figure from Twerdy, 2019.)

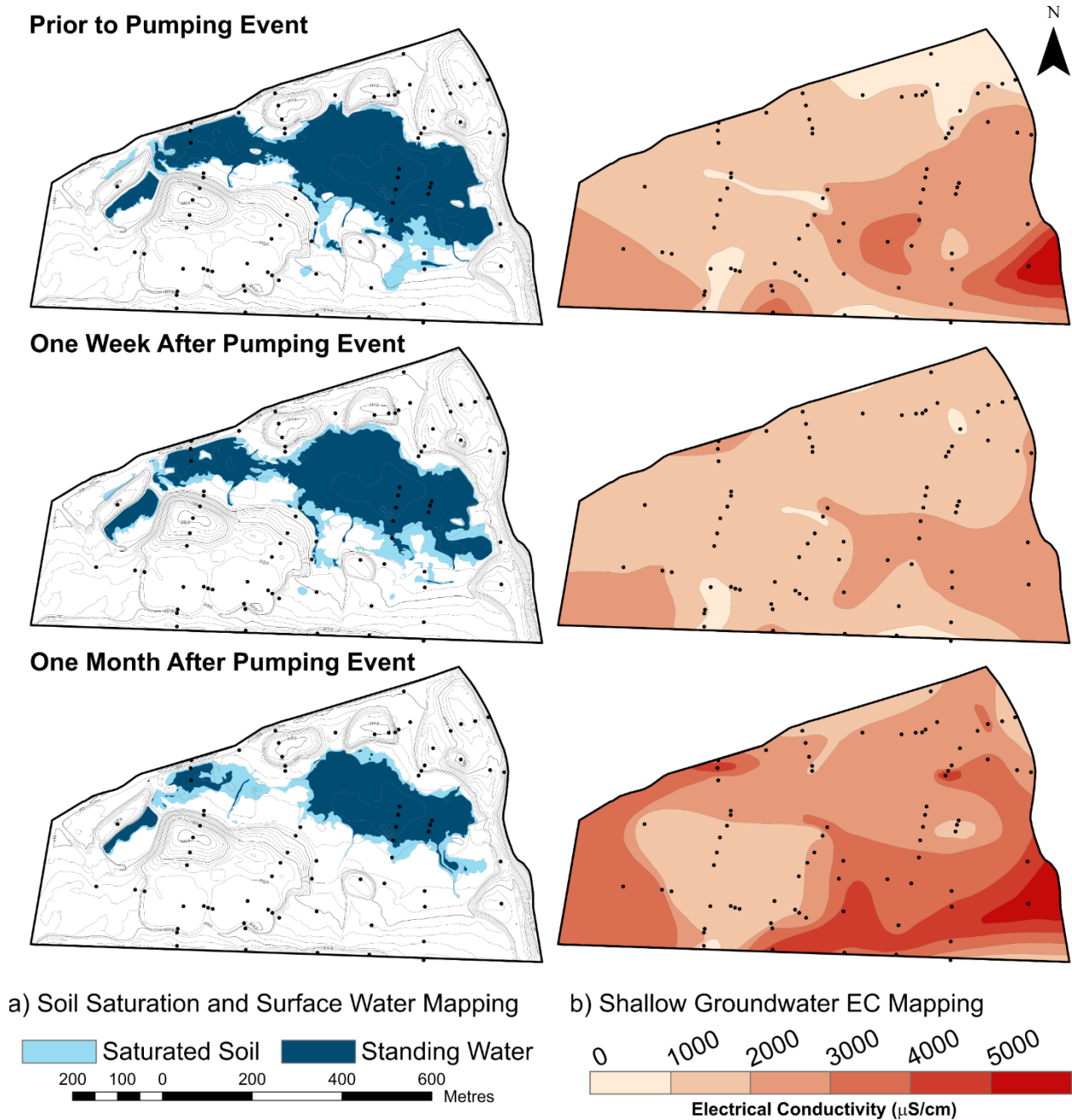


Figure 8 (a) Soil wetness and (b) EC maps from summer 2017. Pumping event removed 101 mm of water from the wetland. EC plotted from the shallowest piezometers (only where the midscreen fell within the uppermost 1.8 m of the water column). East and west wetlands are readily distinguishable in the lower left panel. (Figure from Twerdy, 2019.)

Horizontal hydraulic head gradients were greatest (0.01) below the southern hummocks and decrease ($\ll 0.01$) as the topography transitions into lowlands. Beneath the uplands, intermittent vertical hydraulic gradients ranged from -0.08 to 0.1 (upward and downward flow, respectively); however, average upland vertical gradients were negligible but indicated generally downward flow. Vertical gradients within the lowland were slightly larger, ranging from -0.3 to 0.5 and have greater temporal variability.

Notable examples of watershed response to input (precipitation) or output (pumping) events were observed in the early spring every year (snowmelt events), late in the summer of 2016 (multiple consecutive large precipitation events) and midsummer of 2017 (a 5-day pumping event in July). These responses can be seen in Figure 6 and Figure 7. Influx from spring melt was observed every year in the continuous water level data from piezometers screened in areas with shallow water tables (<1.8 m BGS), or piezometers in standing water in the lowlands. Effects of spring melt were notably less prominent in upland piezometers, where the water table was deep (>1.8 m BGS).

The overall response of the groundwater system to precipitation events is best demonstrated in 2016, where two days with major precipitation events (>30 mm/d) occurred late summer (Aug 27 and Sept 3) between two soil wetness mapping events (Aug 21, pre-event, and Sep 15, post-event). Over the 25-day period between mapping events, 126 mm of rain fell in the watershed, causing a 160 mm increase in standing water levels. Water level responses in piezometers beneath the hummock along Transect 1 were varied (Figure 6); the water level in the southernmost piezometers, where the water table is deep, rose 60 mm; the water level in piezometers closer to the wetland rose 220 mm.

3.1.2 Numerical Modelling

For the steady-state numerical model, the calibrated hydraulic conductivity values fall within an acceptable range of the measured and literature values, the simulated water table resembles the water table configuration observed during summer field seasons, and the calibration statistics indicate calculated heads adequately represent field conditions. Consequently, the model was judged to provide a reasonable representation of the groundwater system in SHW and was used to explore several sensitivity scenarios.

Based on slug test results (Longval and Mendoza, 2014) and model calibration, the homogeneous, isotropic hydraulic conductivity of the tailings sand was 1.3×10^{-5} m/s. This value is within the range of values provided by Thompson et al. (2011) and compares favourably to the value of 3.5×10^{-5} m/s used by Lukenbach et al. (2019). Consistent with Lukenbach et al. (2019), average recharge rates applied to upland areas ranged from 40 mm/year for wetter ecosites to 88 mm/year for drier ecosites. Average volumetric groundwater flow through the system was calculated to be 108 m³/d.

The scenarios evaluated possible impacts of decreasing and increasing recharge rates associated with climate change, vegetation development or extreme climate conditions. In general, the water table elevation decreases as recharge decreases and increases as recharge increases. Overall, areas in the watershed that have previously been described as having shallow water tables (i.e., upland areas adjacent to and transitioning into lowlands), also have the greatest capacity to buffer water level changes through different recharge scenarios. Results of further scenarios, performed using the coupled saturated-unsaturated flow model which allows for incorporation of rigorous detail on a wide range of mechanisms, are discussed below.

3.1.3 Groundwater Flow System

Based on the observed field conditions and simulated groundwater flow system, the horizontal hydraulic gradients in SHW are primarily driven by the up-gradient topographic high, 318 Berm, south of the study area, which is likely coincident with a groundwater divide oriented parallel to, but outside, the southern boundary of SHW. The primary, south to east, groundwater flow path was engineered to curve through SHW towards Kingfisher Valley by utilizing contrasts in hydraulic conductivities between the watershed's tailings sand and the adjacent shale along the western and northern edges of the former mine (EIP). The groundwater system is therefore influenced by the broader, intermediate topography (318 Berm), rather than local hummocks, in conjunction with contrasting hydraulic conductivities between watershed tailings sand and surrounding geology.

The hydraulic gradients in the watershed vary between the uplands and lowlands, both horizontally and vertically (Figure 5). The horizontal gradients in the uplands are laterally planar and steep, relative to the subtle horizontal gradients observed in the lowlands. The abrupt break in the slope of the water table in the southern uplands coincides with the topographic transition from uplands into the lowlands (Figure 5). The water table fluctuated near ground surface in these transition zones throughout the study period, at times intersecting ground surface (Figure 6 and Figure 7). These areas are essentially seepage faces (i.e., discharge areas) across which horizontal hydraulic gradients drive groundwater movement. In hummocky terrain (i.e., at the toes of constructed hummocks) the extent of these discharge areas is limited to where the water table coincides with the toe of the hummock. In areas with gently sloping topography (i.e., on the southeast slope of SHW) the seepage faces are more diffuse; the water table fluctuates near ground surface over a more extensive area.

Although the entire lowland was intended to develop into a wetland, small-scale variations in topography, and potentially outflows through the northern boundary, resulted in the presence of east and west wetlands during lower water levels; the areas between and adjacent to these persistent wetlands may develop into terrestrial environments (Vitt et al., 2016). Overall the seasonal water levels varied among years, details provide below.

The influence of atmospheric and managed fluxes on the water table configuration was observed throughout the study period. In 2015, outfluxes were dominated by AET and groundwater pumping (ignoring groundwater inflows and outflows), resulting in a gradual decline in water levels through fall and the lowest water levels observed in the watershed throughout the study period. During 2016, influxes due to snowmelt and rainfall dominated, leading to higher water levels than the year previous; water levels at the end of the 2016 field season were approximately the same as at the start of the field season. This led to particularly high water levels for the start of the 2017 field season. While outfluxes (i.e., pumping) were greater than influxes in 2017, the fluxes were closely balanced compared to previous years; therefore, water level changes due to pumping were likely buffered by incoming precipitation.

Regardless, following pumping, water levels gradually declined, responding similarly to the pumping event in 2015.

3.2 Geochemistry

Twierdy (2019) reports the full analysis of the geochemical system, primarily focussed on results from 2015 to 2017.

3.2.1 Electrical Conductivity

Electrical conductivity (EC; $\mu\text{S}/\text{cm}$) was used to generalize solute distribution and movement in the watershed. Available manual surface water EC measurements adjacent to piezometers in the wetlands ranged from 600 to 3200 $\mu\text{S}/\text{cm}$ in the 2016 and 2017 summer field season. The average EC of surface water in the wetlands from the 2016 and 2017 field seasons was $1600 \pm 500 \mu\text{S}/\text{cm}$ and $1400 \pm 500 \mu\text{S}/\text{cm}$, respectively, which is lower than average EC values for water measured in 2015 from wetland wells that were screened to surface ($1785 \pm 929 \mu\text{S}/\text{cm}$; Biagi et al., 2018). Spatially, ECs appeared to be lower in the east wetland ($1300 \pm 400 \mu\text{S}/\text{cm}$) than the west wetland ($1800 \pm 600 \mu\text{S}/\text{cm}$) during the 2016 and 2017 field seasons. A small, isolated permanent surface water body, located in a low spot adjacent to Hummock 7, had an average EC of $2300 \pm 500 \mu\text{S}/\text{cm}$ over 2016 and 2017, ranging from 1800 $\mu\text{S}/\text{cm}$ to 3400 $\mu\text{S}/\text{cm}$.

Manual groundwater EC measurements ranged from 100 $\mu\text{S}/\text{cm}$ to 5700 $\mu\text{S}/\text{cm}$ during the summer field seasons of 2015 to 2017. The lowest EC values corresponded to piezometers installed in the wetlands, whereas higher ECs were associated with lowland areas along the periphery of the uplands and beneath the uplands themselves (Figure 6 and Figure 7). In the uplands, EC distributions were more variable than those in the wetlands, as depths to the water table are less consistent, and the piezometers may be screened deeper in the water column.

In general, EC increases with depth through the water column. EC values of water from piezometers installed in areas with shallow or deep water tables (relative to ground surface) and deeper midscreens (relative to the water level), have high EC values (i.e., shallow/deep and deep/deep piezometers, respectively; Figure 6 and Figure 7). Water from piezometers located in areas with deep water tables relative to ground surface, and shallow midscreens relative to the water table (i.e., deep/shallow piezometers) tend to have lower EC values, compared to water from piezometers located in areas with shallow water tables and shallow midscreens relative to the water table (i.e., shallow/shallow piezometers). The latter tend to have higher ECs and larger ranges in ECs overall.

Measured ECs fluctuated throughout each field season (Figure 6 and Figure 7), regardless of water table depth and sampling location (collectively, the piezometer's water class; Figure 3). The EC fluctuations generally aligned with inflow/outflow events, although spring snow melts were not well represented. In 2015, the ECs in the watershed slowly freshened throughout the summer, following a 55 mm outflow event, with temporary increases to several small subsequent rainfall events (Figure 6 and Figure 7). In 2016, the watershed received more precipitation and larger individual rain events compared to 2015; overall, EC values were

elevated throughout the 2016 field season compared to 2015. For example, 126 mm of rain fell in the 25 days between Aug 21 and Sept 15. During which time, upland EC values in Transect 1 piezometers increased in most sampling locations (e.g., up to 1300 $\mu\text{S}/\text{cm}$ in nest 30, a shallow/shallow piezometer), but decreased in others (e.g., down 700 $\mu\text{S}/\text{cm}$ in nest 29, a deep/deep piezometer). However, in Transect 2, ECs in all upland piezometers increased during this time period (200 to 500 $\mu\text{S}/\text{cm}$; Figure 6 and Figure 7). These trends were also observed spatially in EC maps, beyond the transects. In 2017, a 101 mm pumping event, resulted in an average EC decrease of 400 $\mu\text{S}/\text{cm}$ in all upland nests along Transect 1, whereas ECs in upland piezometers along Transect 2 ranged from a 400 $\mu\text{S}/\text{cm}$ increase (nest 75, a shallow/shallow piezometer) to a 400 $\mu\text{S}/\text{cm}$ decrease (nest 42, a shallow/deep piezometer) in the week following pumping. Over the following month, EC values rebounded to be greater than pre-event conditions, increasing up to 1700 $\mu\text{S}/\text{cm}$ in Transect 1 (nest 23, shallow/deep), and greater than 2000 $\mu\text{S}/\text{cm}$ in Transect 2 (nest 42; shallow/deep)

3.2.2 Geochemistry

The annual geochemical samples (major and minor ions) provide a general characterization for groundwater and surface waters located within the watershed across three years; however, it is difficult to evaluate year to year trends given the overall temporal resolution of the data. Major ions are therefore compared spatially, both horizontally and vertically, and by grouping piezometers based on their water classes (Figure 3) and comparing them to groundwater endmember compositions defined by MLR water and OSPW.

Groundwater sampled from artesian piezometers (artesian/shallow and artesian/deep piezos) were similar to surface waters, regardless of the midscreen/sampling depth relative to water level (Figure 9 and Figure 10). Compared to endmember compositions, these waters were well-mixed, enriched with sulphate and calcium, and depleted in sodium. Groundwater sampled from shallow water tables with shallow midscreens (shallow/shallow pipes) ranged from a mixed-cation and chloride-sulphate-enriched water-type ($\text{Cl}^-/\text{SO}_4^{2-}$) to a sodium-chloride-sulphate enriched water-type ($\text{Na}^+ \text{Cl}^-/\text{SO}_4^{2-}$). Samples from piezometers in areas with shallow water tables and deeper midscreens (shallow/deep pipes) were almost exclusively sodium-chloride-sulphate-enriched water ($\text{Na}^+ \text{Cl}^-/\text{SO}_4^{2-}$), overlapping with OSPW endmember compositions. Groundwater from piezometers located in areas with deep water tables and shallow midscreens (deep/shallow pipes) had a similar range of mixed chemistries compared to water from shallow/shallow piezometers. Samples from deeper water tables yielded similar chemistries as shallow/deep piezometers, with few exceptions, overlapping in chemistry with the OSPW endmember (i.e., Na^+ enriched).

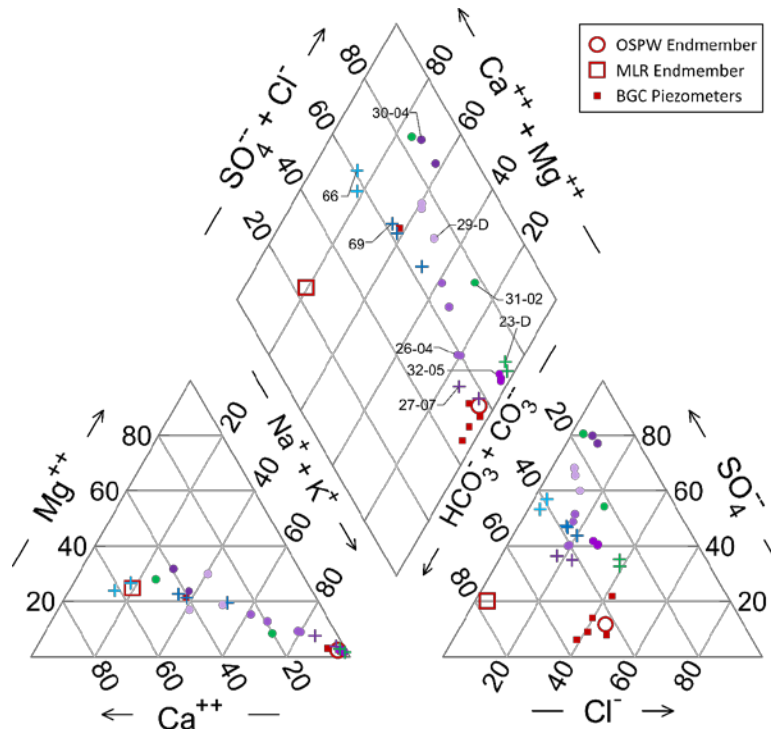


Figure 9 Piper plot of annual (2015-2017) water samples along Transect 1 (hummock to wetland). Composition for one representative piezometer is shown per nest; symbology is consistent with water classes in Figure 3. BGC piezometers correspond to samples from below the sand cap. (Figure from Twerdy, 2019.)

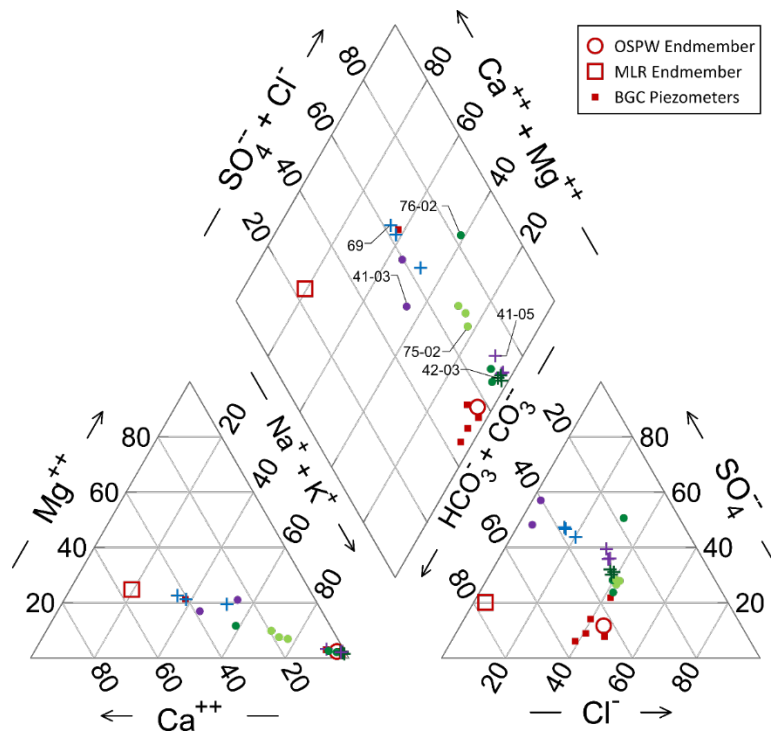


Figure 10 Piper plot of annual (2015-2017) water samples along Transect 2 (slope to wetland). Composition for one representative piezometer is shown per nest; symbology is consistent with water classes in Figure 3. BGC piezometers correspond to samples from below the sand cap. (Figure from Twerdy, 2019.)

3.2.3 Isotopes and Sodium

Analyses of $\delta^2\text{H}/\delta^{18}\text{O}$ isotopic endmembers showed that OSPW was the most isotopically enriched endmember and had the highest sodium concentration, while MLR water is more isotopically depleted than OSPW and has very low sodium concentrations (Figure 11 and Figure 12). Groundwater samples collected from piezometers completed in the tailings sand predominantly plot along a mixing line between OSPW and MLR endmember signatures for both Transect 1 and Transect 2 (Figure 11 and Figure 12). Groundwater samples with depleted $\delta^2\text{H}/\delta^{18}\text{O}$ values (i.e., closer to precipitation and MLR isotope endmember compositions) tend to have lower sodium concentrations. Samples that are more isotopically enriched plot closer to the OSPW isotope endmember composition and have higher concentrations of sodium.

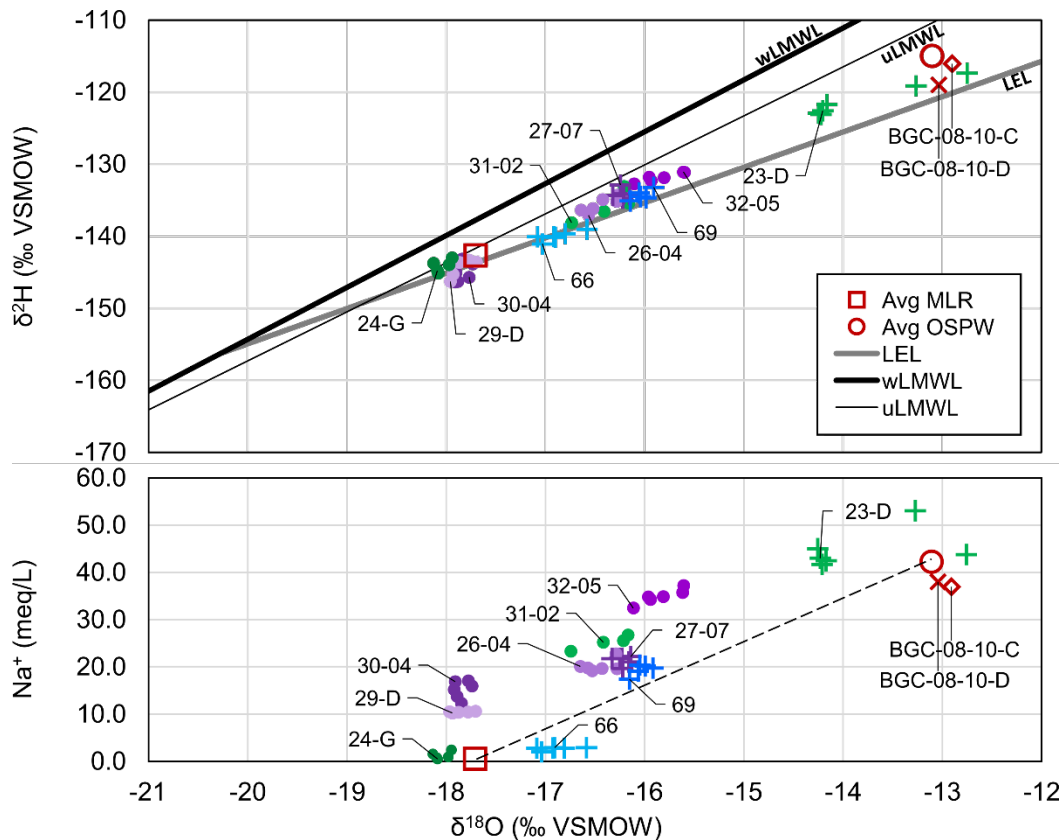


Figure 11 Paired plots of $\delta^2\text{H}$ vs $\delta^{18}\text{O}$ (upper) and Na^+ vs $\delta^{18}\text{O}$ (lower) values collected inside the shallowest piezometer from nests along Transect 1 (hummock to wetland) during the summer field season of 2017. Symbology is consistent with water classes in Figure 3. (Figure from Twerdy, 2019.)

In Transect 1, where the water level is generally deeper below ground surface (i.e., deep/shallow or deep/deep; Figure 11), groundwater isotope signatures tend to plot close to the MLR endmember and up to halfway between MLR and OSPW. Samples that have freshest water compositions, closest to precipitation, were obtained within 1.8 m of the water level (i.e., shallow/shallow and deep/shallow pipes). The groundwater samples that plot closest to OSPW endmembers ($\delta^2\text{H}$, $\delta^{18}\text{O}$ and Na^+) were from the lowlands at the toe of Hummock 7. Samples from this nest also exhibited the greatest variability. Overall, stable water isotope values

obtained along Transect 1 fall neatly along a line between OSPW and MLR endmember compositions; however, the Na^+ data do not.

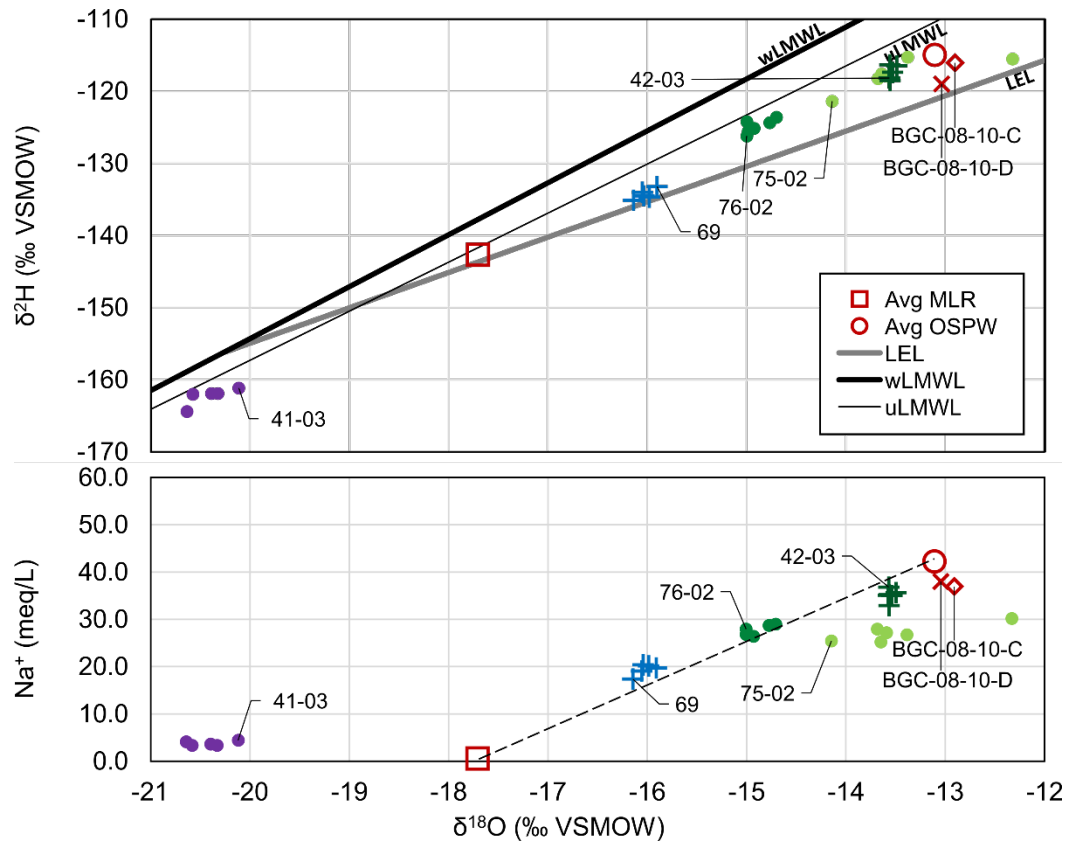


Figure 12 Paired plots of $\delta^2\text{H}$ vs $\delta^{18}\text{O}$ (upper) and Na^+ vs $\delta^{18}\text{O}$ (lower) values collected inside the shallowest piezometer from nests along Transect 2 (slope to wetland) during the summer field season of 2017. Symbology is consistent with water classes in Figure 3. (Figure from Twerdy, 2019.)

Most groundwater samples collected along Transect 2 were more isotopically enriched compared to samples from Transect 1, plotting towards the OSPW isotope endmember composition (Figure 12). These enriched samples also have higher concentrations of Na^+ and subsequently plot near the OSPW Na^+ endmember. These samples were all collected from piezometers in areas with shallow water levels sampled from anywhere within the water column (i.e., shallow/shallow and shallow/deep pipes). Overall, except for the one deep/shallow nest, the isotope and Na^+ data for Transect 2 plot between the OSPW and MLR endmember compositions.

3.2.4 Solute Distributions and Dynamics

The groundwater flow system in SHW is dynamic, rising and falling in response to daily and seasonal fluxes into and out of the watershed, which directly influences the spatial and temporal distribution of solutes in groundwater and surface water (Figure 6 and Figure 7). Interpretation of solute distributions is facilitated by classifying piezometers according to, first, the average depth of the water level relative to ground surface and, second, the depth of the

midscreen relative to the water level observed in the piezometer (see Figure 3). In this context, the transition between shallow vs. deep was interpreted to be approximately 1.8 m.

Since construction 2012, the groundwater system has been exposed to recharge via rainfall and snowmelt and, to a lesser degree, managed freshwater influxes (i.e., pumping). These influences led to development of a shallow groundwater system with a thin freshwater lens overlying, and gradually mixing into, the underlying concentrated OSPW. In general, electrical conductivity increased with depth in the groundwater column, and tended to be higher in uplands compared to the wetlands throughout the study period (Figure 8).

The wetlands in the central lowlands are frequently wetted due to daily and seasonal precipitation; therefore, total dissolved solids (i.e., electrical conductivity) are likely diluted and buffered by rising water levels that frequently result in standing water and saturated soil conditions. This differs from the periphery of the lowlands, where the lowlands transition to the uplands, and upland areas with shallow water tables (WL <1.8 m BGS); the water tables do not frequently rise above ground surface, if at all. Consequently, these peripheral soils are not flushed during rain events like those soils in the centralized areas of the wetlands. Instead, the soil in these areas gradually accumulate solutes, likely through cycles of evapoconcentration due to shallow water table fluctuations. This concentrated water then may be entrained in stagnant pore water during periodically high water levels and mobilized to downgradient areas in the watershed (Hayashi et al., 1998). Finally, in the uplands, where water tables are generally deeper below ground surface (WL >1.8 m BGS), the groundwater at the water table appears to be freshened by recharge.

Temporally, groundwater chemistry (i.e., major ion proportions) remained generally consistent at each location in a given area, across annual sampling campaigns. Spatially, the proportion of major ions varied across sampling locations, ranging from OSPW dominant ($\text{Na}^+ \text{Cl}^-/\text{SO}_4^{2-}$ groundwater), to a mixed water type plotting away from the MLR and OSPW endmembers.

Samples from surface water and artesian piezometers (exclusively located in the wetland) had a mixed groundwater composition. Samples from the deepest groundwater relative to the water table indicated the highest proportion of OSPW in the watershed (i.e., MS >1.8 m BWL), regardless of the water level position relative to ground surface (i.e., shallow/deep and deep/deep groundwater); however, some deep/deep groundwater indicated mixing away from OSPW endmember. The shallowest water sampled relative to the water table (i.e., MS <1.8 m BWL) tended to have the highest variability in ion proportions; this water ranged from OSPW dominant to mixed water, regardless of the depth of the water table below ground surface (i.e., shallow/shallow, deep/shallow).

Given that water sampled near the water table (MS <1.8 m BWL) showed variably mixed water chemistry with OSPW and can have elevated ECs, stable water isotopes were used to determine whether the concentrated solutes in the shallow water table were truly mixed with OSPW, or whether solute distributions were being influenced by other factors (e.g., soil storage,

attenuation, transformations). Stable water isotopes indicated water sampled from the water column, just below the water table (i.e., shallow/shallow and deep/shallow) in hummocks was predominantly comprised of rainwater and was, at most, moderately mixed with OSPW. Any mixing is likely the result of gradually diluting residual OSPW pore water with incoming recharge from precipitation. On the gentle southeast slope, shallow groundwater was predominantly comprised of OSPW (shallow/shallow) with far less recharge than hummocks (except for the water sampled from deeper water tables; deep/shallow).

Areas with elevated EC and Na⁺ have previously been described as “hotspots” attributed to upwelling of OSPW (Biagi et al., 2018); however, vertical hydraulic gradients appear to be negligible overall. The groundwater flow system is predominantly driven by horizontal gradients, as confirmed by the groundwater simulations, which integrates physical processes across the site; therefore, it follows that groundwater with elevated EC, Na⁺ and δ¹⁸O compositions (indicating OSPW endmember mixing), is primarily associated with residual OSPW that was stored in the tailings sand and now discharges laterally across the seepage face. Given that the water table fluctuates within/across these seepage faces, and slowly declines (in general) through the field season, solutes could potentially accumulate in the pore spaces of the intermittently saturated zone through cycles of evapoconcentration. Then, during periods of rainwater influx, rapid water table rises associated with groundwater ridging may force out pre-event water (Gillham, 1984), leading to elevated EC “slugs” moving through the system, entraining concentrated pore water solutes once again through subsequent dissolution (Hayashi et al., 1998). The larger groundwater system will continue to laterally discharge residual OSPW (solute) from the tailings sand to these seepage faces, with negligible relief from incoming recharge due to the rooting zones being close to the water table in these areas (Lukenbach et al., 2019).

The effect of different recharge rates on EC distributions in the uplands, due to various soil prescriptions, was evident when comparing groundwater quality below Hummock 7 and Hummock 9; both of which have water tables further below ground surface over larger areas and similar flow paths, but have different cover prescriptions (i.e., coarse- and fine-textured soils, respectively). Groundwater below Hummock 7 has some of the lowest EC values of the upland areas in the south, whereas Hummock 9 consistently has some of the highest EC values in the entire watershed. These results indicate the watershed is sensitive to recharge, given that EC distributions in shallow groundwater are dynamic throughout the field seasons and across the study period.

The lowlands were specifically developed to have shallow water tables (or standing water) relative to land surface; however, EC, Na⁺ or δ¹⁸O values indicate OSPW is not concentrating in any location specifically within in the wetlands, or at depth; this is only occurring along the periphery of the lowlands. Given that the extent of the standing water and saturated areas in the watershed are highly variable within a single field season (Figure 8) and highly responsive to

fluxes in and out of the watershed, the soils in the lowland show greater potential for dilution and flushing than upland soils that will never be saturated.

3.3 Soil-moisture and Recharge

Lukenbach et al. (2019) report the full results of soil-moisture dynamics and groundwater recharge and document the modelling approach and parameters. Lukenbach et al (2019) discuss some of the uncertainty and limitations of these modelling results.

3.3.1 General Observations and Water Balance

Observed changes in soil-moisture content exhibited a characteristic response to precipitation events, generally defined by amplified responses at shallow depths and damped or absent responses at greater depths (see Lukenbach et al., 2019). The 2-D model was judged to be a good fit to the field observations, particularly given the homogeneous representations of each hydrostratigraphic unit, and to provide reasonable representation of recharge and its key controls at the landform-scale. Supplementary 1-D simulations helped confirm that the representation of boundary conditions was suitable. The 1-D simulation results also confirmed that 2-D simulations are necessary to allow the unsaturated-saturated continuum to better characterize the overall soil water dynamics of upland hummocks and associated water table configurations.

Simulated upland hummock water balance components are documented in Table 4 of Lukenbach et al. (2019); they were also indicative of model performance and characteristics of the reconstructed system. Modelled actual evapotranspiration (AET) for fine-textured soil covers (258 mm/yr to 327 mm/yr) and PMM soil covers (185 mm/yr to 284 mm/yr) were similar to reclaimed boreal forest stands possessing similar LAI and soil texture characteristics (224 mm/yr to ~350 mm/yr; Carey, 2008; Strilesky et al., 2017). Likewise, modelled AET in coarse-textured soil covers ranged from 208 mm/yr to 241 mm/yr, similar to boreal pine stands having similar age, LAI, and PET (165 mm/yr to 210 mm/yr, McCaughey et al., 1997; Moore et al., 2000). Differences in interception between cover types were attributable to differences in leaf area index (LAI) values. LAIs were consistently less than one for the coarse-textured soil cover, while they approached three for the fine-textured soil cover. Surface runoff did not occur during any of the simulations. Lowland AET was estimated to be a larger outflux than either pumping or modelled seepage, although simulated lowland AET (444 mm/yr to 498 mm/yr) was greater than measured lowland AET (310 mm/yr to 392 mm/yr). This discrepancy was largely attributed to model simplifications.

3.3.2 Controls on Recharge

Soil cover characteristics that primarily influenced recharge, indicated by contrasts in calibrated material types and scenario tests, were 1) soil texture and associated soil hydraulic parameters, 2) vegetation parameters (e.g., LAI, maximum rooting depth), and 3) the layering and thickness of reclamation materials conducive to root water uptake (Figure 13). The range of parameters

considered and resulting ranges in groundwater recharge considered for the scenario testing are documented in Table 5 of Lukenbach et al. (2019).

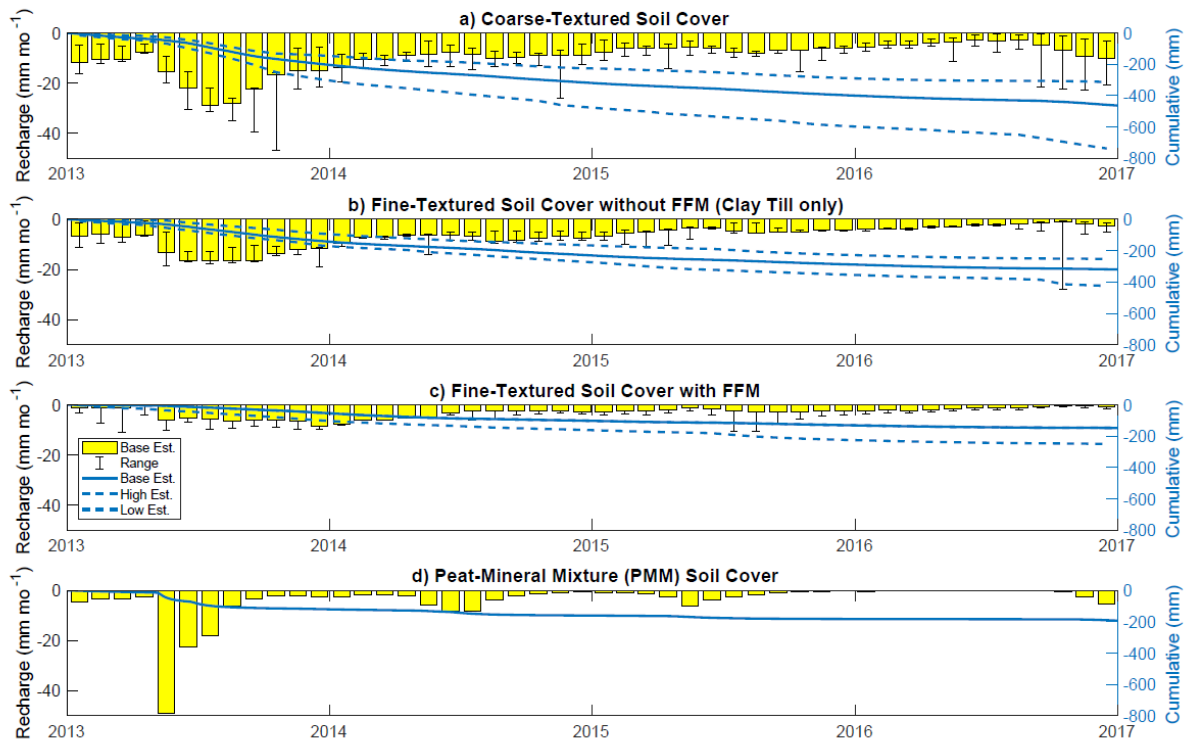


Figure 13 Simulated monthly recharge fluxes and cumulative recharge for the study period. Panels (a) to (c) are for upland hummocks with different soil covers; (d) is only upland PMM area. High/low estimates correspond to extreme results of scenario tests of soil hydraulic parameters. (Figure from Lukenbach et al., 2019.)

Cumulative recharge for the coarse-textured soil cover was ~50% to 100% higher than for fine-textured and PMM soil covers, although temporal trends in recharge were generally similar (Figure 13). A pulse of recharge occurred one to three months after snowmelt in 2013; however, this effect was damped in other years (and absent in 2016) due to lower snowmelt. Below average precipitation in 2015 and spring 2016 resulted in low antecedent moisture conditions, leading to the lowest monthly recharge (Figure 13). Late in 2016, increases in recharge were associated with higher rainfall starting in June 2016 and two events > 50 mm. More dynamic recharge responses for upland peat placements in Figure 13d were an artefact of their flat configuration compared to the variable topography of upland hummocks, where pulse-like effects were masked because recharge was integrated across a range of surface elevations.

The results indicate deeper maximum rooting depths substantially decreased recharge, aligning with results of tritium tracer tests (Li et al., 2018) and prior modelling (Adane et al., 2018). At reclaimed sites, maximum rooting depths can reach or exceed one metre because thicker soil covers are frequently prescribed or roots may penetrate deeper than soil covers (e.g., Lazorko,

2008; Huang et al., 2015; Meiers et al., 2011). Therefore, scenarios with one metre deep soil covers represented a realistic parameter range. Altered root density shape functions had a limited effect on recharge and, for all maximum rooting depth scenarios, only 4% to 6% of the root mass was in the bottom 0.10 m of the rooting zone, similar to Huang et al (2015). The maximum depth eventually reached by roots likely varies with soil cover thickness, as well as the salinity (Duan et al., 2015) and nutrient availability in underlying reclamation materials (Dhar et al., 2018).

Simultaneous perturbations to only soil hydraulic parameters explored the influence of coarsening or fining a soil cover's texture. For example, a coarse-textured soil cover may have coarser/finer grain sizes with more/less pore connectivity (i.e., coarser versus finer sand). Simulated textural variability led to broad recharge ranges for all soil cover types, bounds on Figure 13). Coupling simultaneous perturbations to soil hydraulic parameters with a range of maximum rooting depths and FFM/PMM thicknesses demonstrated how much recharge may vary across a realistic parameter space. However, this was only based on the 2013 to 2016 climatic period. By simultaneously perturbing soil hydraulic parameters under mature vegetation scenarios (i.e., greater maximum rooting depths, LAIs) and with historical climate data Figure 14), the transition of the watershed from an early to late successional state was assessed (i.e., compare Figure 13 and Figure 14. Notably, interannual climatic variability was as influential as variation in soil cover texture (Figure 9), driven by wet (e.g., early 1970s) and dry (e.g., early 2000s) climate cycles (Figure 14). Simulated forest development reduced recharge relative to present day, but high versus low long-term LAI scenarios displayed a <10% difference in cumulative recharge (results not shown).

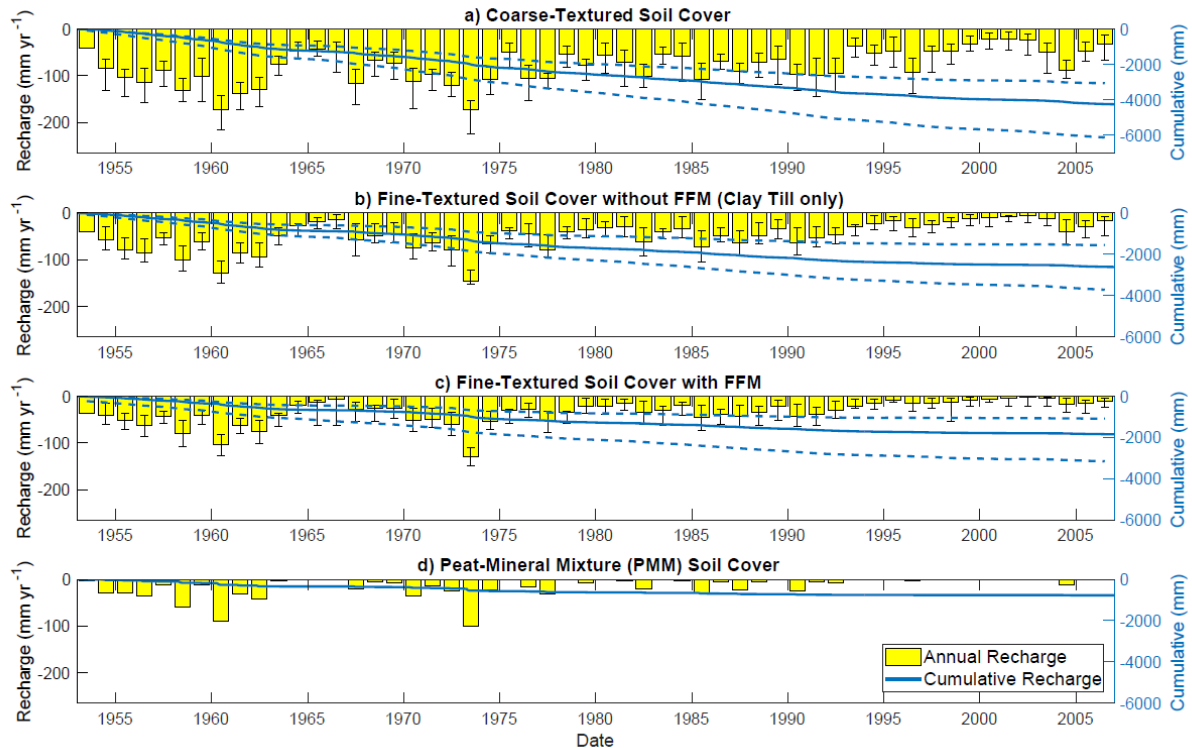


Figure 14 Simulated annual recharge fluxes and cumulative recharge using historical climate data (1953 to 2006) for upland hummocks with different soil covers. Layout and details follow Figure 8. (Figure from Lukenbach et al., 2019.)

Facilitating appreciable recharge in fine-textured/PMM soil covers requires a unique combination of factors, potentially beyond what is operationally feasible. Increased maximum rooting depths had a greater effect on fine-textured/PMM soil covers than coarse-textured ones and, as more of the soil profile comprised layers that effectively store snowmelt and rainwater, roots accessed water later in the growing season. Moreover, underlying reclamation materials with low *saturated* hydraulic conductivity can increase residence time in materials conducive to root water uptake (i.e., low saturated hydraulic conductivity for tailings sand). The reduced ability of PMM soil covers to provide recharge was further exemplified by dual porosity scenario tests, where increased recharge was primarily attributable to differences in PMM porosity between this study and Huang et al. (2015), rather than differences related to dual porosity parameters. This aligns with previous studies, where PMM soil covers facilitated lower recharge (Dobchuk et al., 2013), coinciding with their higher forest productivity (Strilesky et al., 2017).

The ability of upland hummocks to consistently maintain recharge and limit upflux depended on their height, driven by the distance between the water table and maximum rooting depths. Recharge exhibited a threshold-like relationship to upland hummock height (Figure 15a). Above this threshold height, recharge magnitudes varied little between top and mid-slope positions, although the timing of recharge varied, by approximately one to two months, due to differences in travel times through the unsaturated zone Figure 15a). Comparatively, as the

water table became shallower beneath the hummock's ground surface, recharge began to decline and transition to upflux because roots readily accessed water from the saturated zone (Figure 15a). Modelled upflux primarily occurred in summer, often dictated by the difference between potential evapotranspiration and precipitation for a given time interval (Figure 15b and Figure 15c). This is perhaps best exemplified by comparing summer 2016 (wet) to summers 2014 and 2015 (dry) in Figure 15b and Figure 15c. Upflux conditions have been previously reported in sub-humid regions, where shallow water tables decreased net recharge (Dobchuk et al., 2013; Carrera-Hernandez et al., 2011; Smerdon et al., 2008; Soylu et al., 2011).

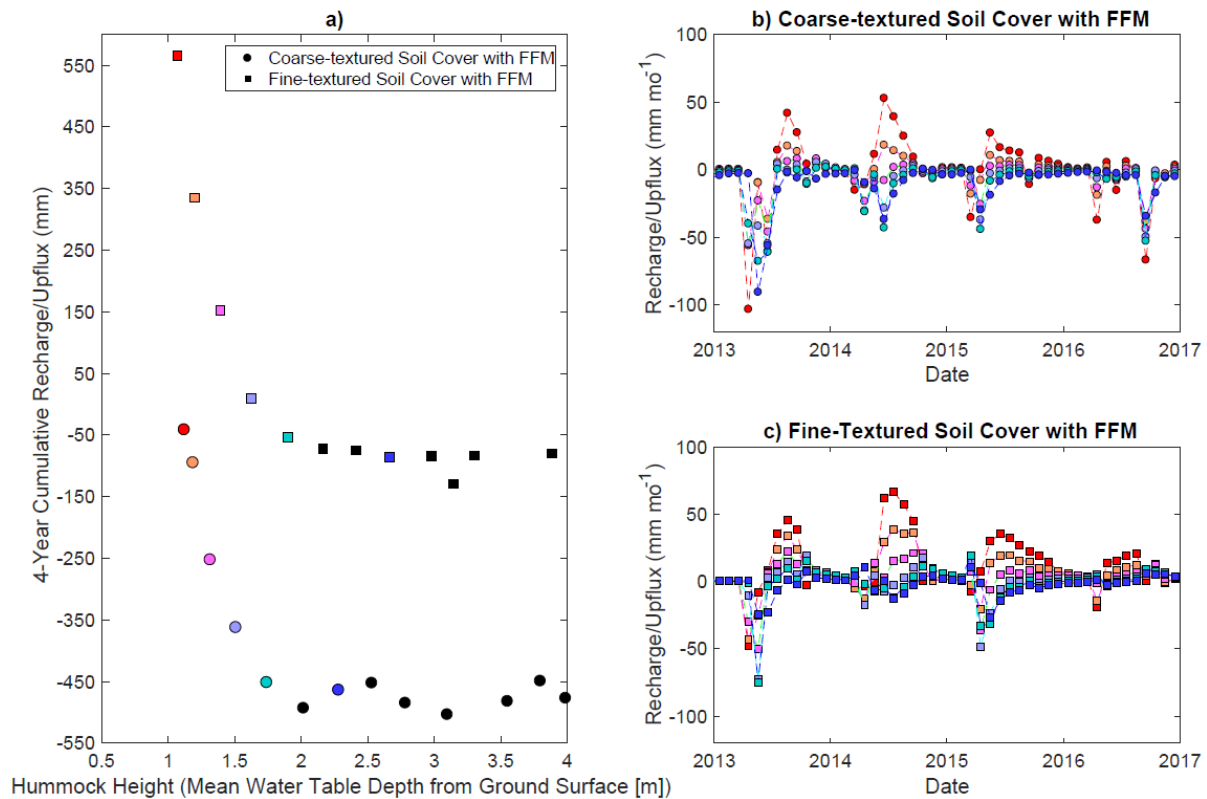


Figure 15 (a) Relationship between mean water table depth (relative to ground surface of upland hummock) and cumulative recharge (negative) or upflux (positive) for coarse- versus fine-textured soil covers (shapes). Monthly recharge for (b) coarse- and (c) fine-textured soil covers. A coloured point in panel (a) is represented by a continuous trace in (b) or (c); black points on (a) are not shown in (b) or (c). (Figure from Lukenbach et al., 2019.)

The potential for lower elevation parts of upland hummocks to reduce total recharge in SHW appears limited because upland hummocks are relatively steep and, thus, have a relatively small areal extent near the water table. Indeed, roughly weighting recharge magnitudes by elevation indicated that low elevation parts of upland hummocks may only decrease recharge in SHW by ~10% to 20%. However, if a large proportion of a constructed landform were close to the water table, upflux might frequently occur over a much larger area. This is typical of many gently sloping riparian areas that enhance AET of groundwater (Schoeneberger and Wysocki, 2005). To limit upflux, the area occupied by shallow depths to groundwater should be

minimized, insofar as is operationally and geotechnically possible. However, particularly tall upland landforms may provide little benefit due to their added cost.

3.4 Perched wetlands

The design of SHW included two areas that were to develop into “perched wetlands”. These areas did not retain enough water to develop into perched wetlands; however, anecdotal observations indicate that vegetation performance in these areas is superior to many other areas within the watershed. The interpreted reasons for these observations are that, although the finer-grained, lower conductivity layer placed within these areas was too permeable to pond water, the surface materials (peat) did retain enough water between precipitation events to promote enhanced plant growth. However, recent anecdotal observations (August 2019) of the western area indicate that decomposition and/or compression of relatively deep (1 m) surface peat has resulted in poorer drainage and near surface saturation. Some wetland species, typical of dry peatlands, were observed. Further research on these dynamics is warranted.

4 Conclusions for Sandhill Watershed

Following construction and reclamation, SHW developed a shallow groundwater flow system that flows northward from a groundwater divide near 318 Berm, through to Sandhill Berm and Kingfisher Valley in the East, with some flow diverging north. The difference between hydraulic heads in 318 Berm and in the lowlands of SHW results in a groundwater flow system dominated by horizontal hydraulic gradients. Average vertical hydraulic gradients are generally weak throughout the watershed, including discharge areas, because their directions often fluctuate and are highly transient. Consequently, the horizontal groundwater flow often results in discharge to the lowlands through seepage faces. Where hummocks meet lowlands at an abrupt interface, focussed discharge areas tend to arise. Where gentle upland slopes grade into lowlands, these interfaces tend to be broad and discharge is diffuse. That is, water tables may intersect the land surface over a large area, particularly as the water table fluctuates through time, on shallow slopes.

Geochemical, EC and stable water isotope data consistently show that groundwater deeper than approximately 1.8 m below the water table is predominantly comprised of OSPW. In areas where the water table is regularly found at depth (>1.8 m BGS), the chemistry of the groundwater within 1.8 m of the water table has a higher proportion of freshwater, indicative of groundwater recharge and the development of a freshwater lens. The chemistry of the groundwater within 1.8 m of the water table becomes more mixed with OSPW solutes as the water table transitions from deep (>1.8 m BGS) to shallow (<1.8 m BGS). However, once the water table regularly fluctuates at, or above, ground surface, which results in intermittent standing water, the water becomes fresher, regardless of the depth where the water was sampled.

Transition areas from uplands to lowlands are not always directly adjacent to wetland areas; that is, the transition areas are on the perimeter of the lowlands. Water discharging through seepage faces in these areas may be subject to evapoconcentration during dry periods, leading to a shallow accumulation of water with elevated solute concentrations. Since shallow water tables are highly responsive to inputs of water, areas with shallow water tables and gentle slopes are prone to discharging water with elevated solute concentrations following precipitation events. This phenomenon likely explains previous observations of hotspots of high solute concentrations within the wetlands.

Many of the above findings rely on the water table configuration relative to the land surface. Results of coupled unsaturated-saturated modelling, constrained by field observations, demonstrate that water table configurations respond dynamically to variable recharge rates influenced by depth to the water table, and reclamation prescriptions for soil covers and vegetation. Recharge varies with soil cover texture (higher in coarser-textured materials) and associated soil hydraulic parameters. Finer-textured soil covers tend to retain water which is then lost to the atmosphere through evapotranspiration. Simulation results demonstrate a threshold-like relationship between recharge and upland hummock height, where upland

hummocks that are not tall enough to limit root water uptake from the saturated zone exhibit decreased recharge or net upflux. For SHW, and similar systems considered through sensitivity analyses, a separation threshold of 2 m between the ground surface and the water table was found to induce consistent recharge. Such recharge should help flush salts over time and produce lenses of freshwater at some water table interfaces, as observed at SHW.

Scenario tests indicate the general importance and relative influence of maximum rooting depths, forest floor placement thicknesses, and leaf area indices on recharge. These relationships imply that improved forest development will lead to decreased recharge rates to underlying groundwater systems. However, simulations utilizing a historical climate record indicate that interannual climatic variability is as influential as variation in soil cover texture in determining recharge to SHW.

Summarized answers to key research questions posed in the original proposal are as follows:

- *Do the constructed upland hummocks generate flow and flush, or do the hummocks take up water through transpiration?* The large uplands extending past the southern margins of SHW generated flow for the hydrogeological system and lowlands.
- *What is the dominant scale of groundwater interaction between the hummocks and wetlands?* The scale of the primary groundwater flow system is on the order of hundreds of metres (i.e., from 318 Berm to the lowlands); weak local-scale flow systems on the order of tens of metres developed on hummocks along the northern edge of SHW.
- *What is the rate of recharge, and so salt flushing, through the sand hummocks?* Average recharge rates for upland areas ranged from 40 mm/year for wetter ecosites to 88 mm/year for drier ecosites; these inputs resulted in an average of approximately 100 m³/d of groundwater flowing through SHW.

5 Implications for Practice

Selected research questions, posed by Syncrude, related to hydrogeological aspects of hummock and wetland design are itemized in Appendix D. Many of the questions concern the impact of hummock height, shape, slope and configuration (including size, orientation and aspect) on water availability, salt movement (including flushing and salinization) and forest development or productivity. Answers to hydrogeological aspects of these questions are provided in the discussion below. Also, Appendix E presents a set of decision trees to assist with conceptualizing the role that hummocks and their features may play in generating groundwater recharge for flow systems and wetlands. Many questions related to linking hydrology and vegetation, plus aspect and orientation, cannot be satisfactorily addressed by this work alone; they will require synthesis with results from studies of upland vegetation (i.e., Simon Landhäusser and team) and meteorological effects (i.e., Sean Carey and team).

Shallow groundwater systems, which can provide freshwater to downgradient wetlands, can be designed to develop in post-mining reconstructed landscapes. Our results indicate that, ideally, coarse-grained uplands should be laterally extensive with enough height to promote infiltration such that recharge dominates over upflux at the water table. Landform heights exceeding this requirement likely result in the placement of excess material; furthermore, additional solute mass will be available for flushing from the tailings sand that forms the thicker unsaturated zone associated with this excess material.

To encourage recharge, landforms should be paired with soil covers comprised of coarser-textured materials and compatible vegetation. If only finer-textured or organic-dominated soil covers are operationally available, thinner prescriptions may compensate for the increased storage, higher evapotranspiration and reduced recharge that is generally associated with finer-grained cover materials and their vegetation (Merlin et al., 2018).

For the materials employed at SHW, a separation of approximately 2 m between the land surface and the water table was found to be adequate. Although this separation distance may vary for other material properties comprising other constructed landforms, such variations are expected to be small and a separation depth of 2 m provides a realistic design guideline. The recharge resulting from this separation results in a lens of freshwater, at depth, near the water table. With predominantly horizontal flow, this freshwater preferentially discharges to lowlands which may form wetlands. Water below the freshwater lens is likely to be dominated by OSPW placed with the underlying tailings materials; the design of the flow system and the interface between uplands and lowlands should minimize discharge of this water.

The interface between the uplands and lowlands should be abrupt (i.e., convex upward) to limit the extent of seepage faces at the interface. If gently sloping interfaces are employed, shallow fluctuating water tables within the rooting zone may have elevated solute concentrations near the water table, especially following precipitation or snowmelt events, due to vertical

groundwater seepage and mixing, groundwater ridging and evapoconcentration. Away from the interface a hummock may have a gentle slope if the water table is deep enough.

The general guidelines for hummock design described above are illustrated for SHW in Figure 16. The conceptual illustration proposes broader hummocks that are laterally extensive, low to moderate in height, but scaled so the water table is approximately 2 m BGS, and with steep slopes near the lowland transition. Broad hummocks are better suited for recharging reclaimed landscapes compared to smaller hummocks or gentle slopes; the steep interfaces limit seepage faces to narrow bands along the toes of slopes.

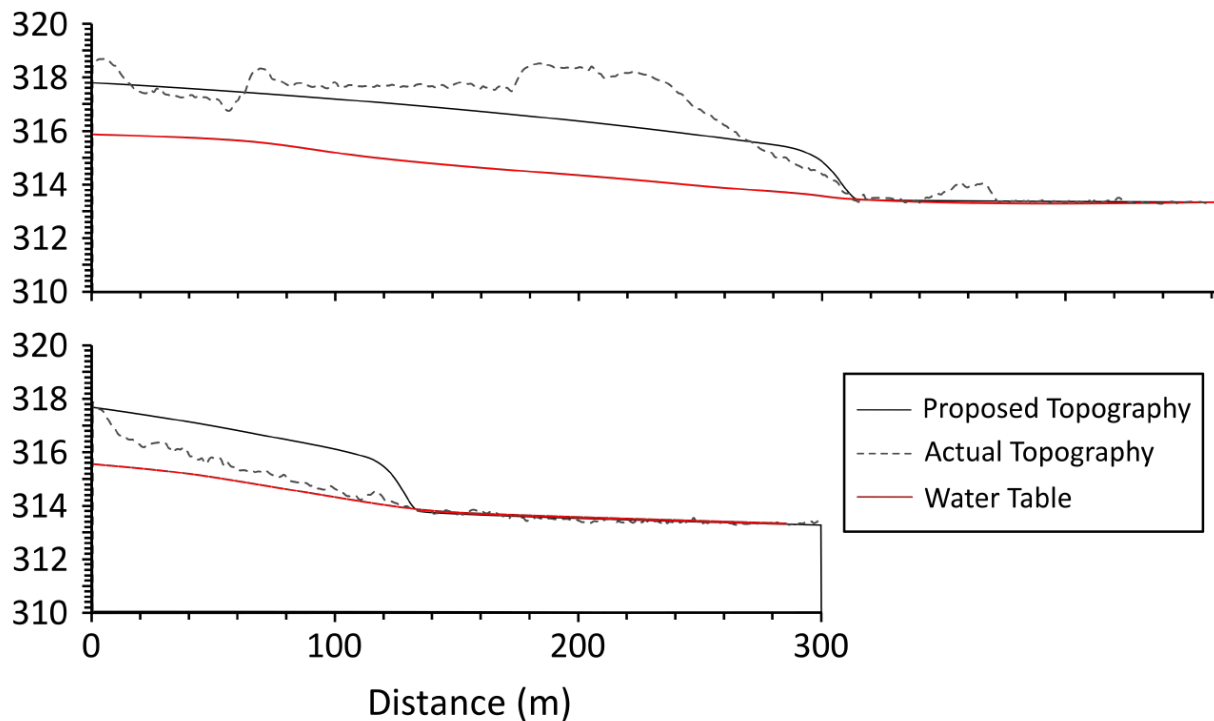


Figure 16 Proposed landform designs for Transect 1 (top) and Transect 2 (bottom) based on groundwater system and solute distributions observed in SHW 5 years post-construction. (Figure from Twerdy, 2019.)

These guidelines may be combined with Dupuit-Forchheimer equations and concepts documented by Haitjema & Michell-Bruker (2005) to help design landforms for other materials. The critical parameters controlling landform height are expected to be the ratio of recharge rate to hydraulic conductivity, the expected lateral extent of the landform and the thickness of the sand cap. Recharge is primarily a function of precipitation minus losses to overland flow (largely during hydrologic events such as snowmelt and large storms) and evapotranspiration (including interception and sublimation); however, evapotranspiration may be modified through cover and vegetation design, and depends on climate. In relative terms, greater hummock heights are necessary for scenarios with increased recharge rate, decreased hydraulic conductivity, increased lateral hummock extent and decreased cap thickness.

It may be possible to encourage the development of perched systems within the reclaimed landscape; however, this has yet to be demonstrated at SHW. The observations indicate that the hydraulic conductivity achieved by placing clay-rich material and packing-by-spreading was insufficient to provide a perching layer. Thus, a base would need to have a greater clay content and/or be compacted to achieve a lower conductivity. Such a layer would need to be protected from cracking due to developing desiccation or freeze/thaw cycles. Alternatively, it may be that peat decomposition may develop the necessary water-holding capacity and hydraulic conductivity to encourage perched conditions over time. Consequently, further monitoring of the perched fen sites at SHW is warranted.

6 References

- Benyon, J. (2014). *Characterization of Hydraulic Conductivity Profiles for Sandhill Fen Watershed Reclamation Materials*. B.Sc. thesis, Earth & Atmospheric Sciences, University of Alberta, 24p.
- BGC Engineering Inc. (2008). *Syncrude EIP Instrumented Watershed: Sandhill Fen – Permit Level Design*. Prepared for Syncrude Canada Ltd., December 2008.
- BGC Engineering Inc. (2011). *Sandhill Fen – Research Monitoring Wells As-built Report*. Project memorandum to Syncrude Canada Ltd., 29 July 2011.
- Biagi, K.M., Oswald, C.J., Nicholls, E.M., & Carey, S.K. (2018). Increases in salinity following a shift in hydrologic regime in a constructed wetland watershed in a post-mining oil sands landscape. *Science of The Total Environment*, 653, 1445-1457. <https://doi.org/10.1016/j.scitotenv.2018.10.341>
- Carey, S.K. (2008). Growing season energy and water exchange from an oil sands overburden reclamation soil cover, Fort McMurray, Alberta, Canada. *Hydrological Processes*, 22(15), 2847-2857. <https://doi.org/10.1002/hyp.7026>
- Carey, S.K. & Humphreys, E.R. (2019). The water and carbon balance of the Sandhill Fen. Draft Final Report (2013-2018) submitted to Syncrude Canada, 43p.
- Carrera-Hernández, J.J., Mendoza, C.A., Devito, K.J., Petrone, R.M., & Smerdon, B.D. (2011). Effects of aspen harvesting on groundwater recharge and water table dynamics in a subhumid climate. *Water Resources Research*, 47. <https://doi.org/10.1029/2010WR009684>
- Devito, K.J., Creed, I.F., & Fraser, C.J.D. (2005). Controls on runoff from a partially harvested aspen-forested headwater catchment, Boreal Plain, Canada. *Hydrological Processes*, 19, 3-25. <https://doi.org/10.1002/hyp.5776>
- Dhar, A., Comeau, P.G., Karst, J., Pinno, B.D., Chang, S.X., Naeth, A., & Vassov, R., Bampfylde, C. (2018). Plant community development following reclamation of oil sands mine sites in the boreal forest: a review. *Environmental Reviews*, 26 (3), 286–298. <https://doi.org/10.1139/er-2017-0091>
- Dobchuk, B.S., Shurniak, R.E., Barbour, S.L., O’Kane, M.A., & Song, Q. (2013). Long-term monitoring and modelling of a reclaimed watershed cover on oil sands tailings. *International Journal of Mining, Reclamation and Environment*, 27, 180-201. <https://doi.org/10.1080/17480930.2012.679477>
- Duan, M., House, J., & Chang, S.X. (2015). Limiting factors for lodgepole pine (*Pinus contorta*) and white spruce (*Picea glauca*) growth differ in some reconstructed sites in the Athabasca oil sands region. *Ecological Engineering*, 75, 323-331. <https://doi.org/10.1016/j.ecoleng.2014.12.010>

- Gillham, R.W. (1984). The capillary fringe and its effect on water-table response. *Journal of Hydrology*, 67(1), 307-324. [https://doi.org/10.1016/0022-1694\(84\)90248-8](https://doi.org/10.1016/0022-1694(84)90248-8)
- Haitjema, H.M., & Mitchell-Bruker, S. (2005). Are water tables a subdued replica of the topography? *Groundwater*, 43(6), 781-786. <https://doi.org/10.1111/j.1745-6584.2005.00090.x>.
- Hayashi, M., van der Kamp, G., & Rudolph, D. L. (1998). Water and solute transfer between a prairie wetland and adjacent uplands 2. Chloride cycle. *Journal of Hydrology*, 207(1-2), 56-67. [https://doi.org/10.1016/S0022-1694\(98\)00099-7](https://doi.org/10.1016/S0022-1694(98)00099-7)
- Huang, M., Barbour, S.L., & Carey, S.K. (2015). The impact of reclamation cover depth on the performance of reclaimed shale overburden at an oil sands mine in Northern Alberta, Canada. *Hydrological Processes*, 29(12), 2840-2854. <https://doi.org/10.1002/hyp.10229>
- Landhäuser, S. (2019). Sandhill Watershed Final report.
- Lazorko, H.M. (2008). *Root distribution, Activity, and Development for Boreal Species on Reclaimed Oil Sand Mine Soils in Alberta, Canada*. M.Sc. thesis, Soil Science, University of Saskatchewan, 177p. <https://doi.org/10388/etd-07042008-160353>
- Li, H., Bincheng, S., & Li, M. (2018). Rooting depth controls potential groundwater recharge on hillslopes. *Journal of Hydrology*, 564, 164-174. <https://doi.org/10.1016/j.jhydrol.2018.07.002>
- Lukenbach, M.C., C.J. Spencer, C.A. Mendoza, K.J. Devito, S.M. Landhäuser and S.K. Carey, 2019. Evaluating how landform design and soil covers influence groundwater recharge in a reclaimed soft tailings deposit. *Water Resources Research*, 55(8), 6464-6481. <https://doi.org/10.1029/2018WR024298>
- McCaughey, J.H., Lafleur, P.M., Joiner, D.W., Bartlett, P.A., Costello, A.M., Jelinski, D.E. & Ryan, M.G. (1997). Magnitudes and seasonal patterns of energy, water, and carbon exchanges at a boreal young jack pine forest in the BOREAS northern study area. *Journal of Geophysical Research*, 102, 28997-29007. <https://doi.org/10.1029/97JD00239>
- Meiers, G., Barbour, S.L., Qualizza, C., & Dobchuk, B. (2011). Evolution of the hydraulic conductivity of reclamation covers over sodic/saline mining overburden. *Journal of Geotechnical and Geoenvironmental Engineering*, 137(1): 968-976. [https://doi.org/10.1061/\(ASCE\)GT.1943-5606.0000523](https://doi.org/10.1061/(ASCE)GT.1943-5606.0000523)
- Merlin, M. Leishman, F., Errington, R.C., Pinno, B.D., & Landhäuser, S.M. (2018). Exploring drivers and dynamics of early boreal forest recovery of heavily disturbed mine sites: a case study from a reconstructed landscape. *New Forests*, 1-23. <https://doi.org/10.1007/s11056-018-9649-1>
- Moore, K.E., Fitzjarrald, D.R., Sakai, R.K. & Freedman, J.M. (2000). Growing season water balance at a boreal jack pine forest. *Water Resources Research*, 36, 483-493. <https://doi.org/10.1029/1999WR900275>

Schoeneberger, P.J., & Wysocki, D.A. (2005). Hydrology of soils and deep regolith: A nexus between soil geography, ecosystems and land management. *Geoderma*, 126(1-2), 117-128. <https://doi.org/10.1016/j.geoderma.2004.11.010>

Šimůnek, J., van Genuchten, M.T., & Sejna, M. (2006). *The HYDRUS software package for simulating two-and three-dimensional movement of water, heat, and multiple solutes in variably-saturated media* (Technical Manual, version, 1, 241p.).

Smerdon, B.D., Mendoza, C.A., & Devito, K.J. (2008). Influence of subhumid climate and water table depth on groundwater recharge in shallow outwash aquifers. *Water Resources Research*, 44, W08427. <https://doi.org/10.1029/2007WR005950>

Soylu, M.E., Istanbuluoglu, E., Lenters, J.D., & Wang, T. (2011). Quantifying the impact of groundwater depth on evapotranspiration in a semi-arid grassland region. *Hydrology & Earth System Sciences*, 15(3), 787-806. <https://doi.org/10.5194/hess-15-787-2011>

Strilesky, S.L., Humphreys, E.R., & Carey, S.K. (2017). Forest water use in the initial stages of reclamation in the Athabasca Oil Sands Region. *Hydrological Processes*, 31(15), 2781-2792. <https://doi.org/10.1002/hyp.11220>

Thompson, R.L., Mooder, R.B., Conlan, M.J.W., & Cheema, T.J. (2011). Groundwater flow and solute transport modelling of an oil sands mine to aid in the assessment of the performance of the planned closure landscape. In: Fourie A. Tibbett, M. & Beersing A. (Eds.), *Mine Closure 2011: Proceedings of the Sixth International Conference on Mine Closure*. September 18-21, 2011, Lake Louise, Alberta. Australian Centre for Geomechanics. Nedlands, Western Australia. Volume 2

Twerdy, P. (2019). *Hydrogeological Considerations for Landscape Reconstruction and Wetland Reclamation in the Sub-humid Climate of Northeastern Alberta, Canada*. M.Sc. thesis, Earth & Atmospheric Sciences, University of Alberta, 204p. <https://doi.org/10.7939/r3-zpg2-6p77>

Vitt, D.H., House, M., & Hartsock, J. (2016). Sandhill Fen, An initial trial for wetland species assembly on in-pit substrates: Lessons after three years. *Botany*, 94, 1015-1025. <https://doi.org/10.1139/cjb-2015-0262>

Wytrykush, C., Vitt, D., Mckenna, G., & Vassov, R. (2012). Designing landscapes to support peatland development on soft tailings deposits. In D. Vitt & J. Bhatti (Eds.), *Restoration and Reclamation of Boreal Ecosystems: Attaining Sustainable Development*. Cambridge: Cambridge University Press. <https://doi.org/10.1017/CBO9781139059152.011>

7 Appendices

Large appendices are provided as separate files.

Appendix A – Longval and Mendoza (2014) report

Longval, J.M., and C.A. Mendoza, 2014. *Initial Hydrogeological Instrumentation and Characterization of Sandhill Fen Watershed*. Hydrogeology Group, Earth & Atmospheric Sciences, University of Alberta, Edmonton, AB. 63p plus electronic appendices. REV_1 issued 24 March 2020.

Filename: Longval+Mendoza_SHW_Hydrogeology_2014-REV_1.pdf

Supplementary electronic appendices available.

Appendix B – Lukenbach et al. (2019) paper

Lukenbach, M.C., C.J. Spencer, C.A. Mendoza, K.J. Devito, S.M. Landhäusser and S.K. Carey, 2019. Evaluating how landform design and soil covers influence groundwater recharge in a reclaimed soft tailings deposit. *Water Resources Research*, 55(8), 6464-6481. <https://doi.org/10.1029/2018WR024298>

Filename: Lukenbach+_2019_WRR.pdf

Electronic supplement and data available; see published paper.

Appendix C – Twerdy (2019) MSc thesis

Twerdy, P., 2019. *Hydrogeological Considerations for Landscape Reconstruction and Wetland Reclamation in the Sub-humid Climate of Northeastern Alberta, Canada*. M.Sc. thesis, Earth & Atmospheric Sciences, University of Alberta, 204p.

Filename: Twerdy_Pamela_201909_MSc_portrait.pdf

Supplementary electronic appendices available.

Appendix D – Hydrogeological Research Questions

Syncrude posed numerous questions to be addressed by the overall research program. Selected questions that pertain to the hydrogeology component of the research program are itemized below. The questions have been grouped into similar themes and emphasis added. These question themes are discussed in Section 5, Implications for Practice.

- Which hummock **height** provides optimal water to support fen?
- Which hummock **height** allows salt flushing more rapidly?
- What is the optimal hummock **height** to maintain thick enough sand cap over salty fines to prevent soil salinization?
- Which hummock **height** allows for development of fully functioning forest, and optimization of forest productivity?

- What is the appropriate hummock **shape** (concave vs convex) to allow water to report to fen wetland?
- What is optimal hummock **shape** to allow salt flushing to improve landscape performance?
- What is the influence of hummock **shape** on salt flushing and water chemistry reporting to fen wetland?
- What is the appropriate hummock **shape** to allow development of fully functioning forest, and optimize forest productivity?

- What is the appropriate hummock **slope** (steep vs. shallow) to allow water to report to fen wetland?
- How does hummock **slope** (steep vs. shallow) affect salt flushing and water chemistry reporting to fen wetland?
- What is the appropriate hummock **slope** (steep vs. shallow) to allow development of fully functioning forest, and optimize forest productivity?

- Effects of thin vs thick **soil cover** on hydrology and forest performance?
- What is the effect of upland **salt flushing** on fen performance?
- Can **perched fens** be sustainable?

Several questions involve hydrogeological components but are intimately connected to vegetation or meteorological factors. They require further integration and synthesis with the remainder of the interdisciplinary research team.

- What is optimal hummock **orientation** to support fen wetland?
- How does **aspect** influence the amount of water reporting to fen?
- How does **aspect** influence the quality of water reporting to fen?

- What is the **soil moisture** capability to support vegetation?
- Does **hydraulic lift** occur on tailings sand hummocks?

- What is the appropriate hummock **size** to optimize water to the fen and allow some level of forest productivity (linking hydrology and vegetation)?
- What is the appropriate hummock **shape** to optimize water to the fen and allow some level of forest productivity (linking hydrology and vegetation)?
- What is the appropriate hummock **orientation** to optimize water to the fen and allow some level of forest productivity (linking hydrology and vegetation)?
- What is the appropriate hummock **configuration** to optimize water to the fen and allow some level of forest productivity (linking hydrology and vegetation)?
- What is the appropriate hummock **configuration extent** to optimize water to the fen and allow some level of forest productivity (linking hydrology and vegetation)?

Appendix E – Assessing Hydrologic Function

Decision Trees for Assessing Hummock Hydrologic Function

Max Lukenbach

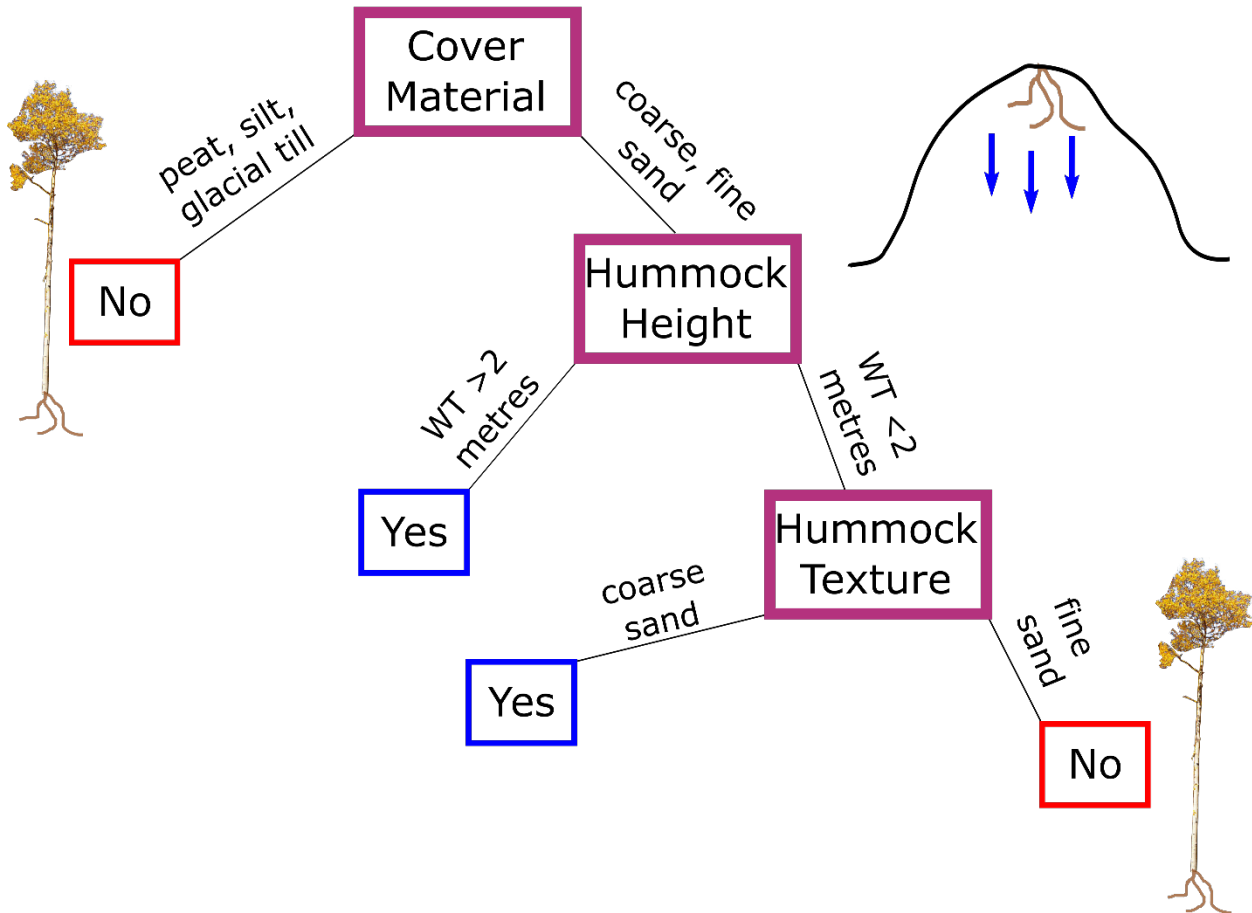
University of Alberta

Decision trees are introduced as a tool to assist with assessing the hydrologic function of hummocks in reclaimed landscapes. This conceptualization focuses on whether hummocks can contribute to groundwater recharge and redirect groundwater flow. In other words, is the water level beneath a hummock likely to be higher than directly adjacent landscape components such as wetlands?

The first two decision trees address the question of whether enough water can infiltrate into a hummock, bypass roots, reach the water table and become groundwater recharge. The third decision tree addresses the question of whether recharge leads to groundwater mounds.

Sufficient Groundwater Recharge?

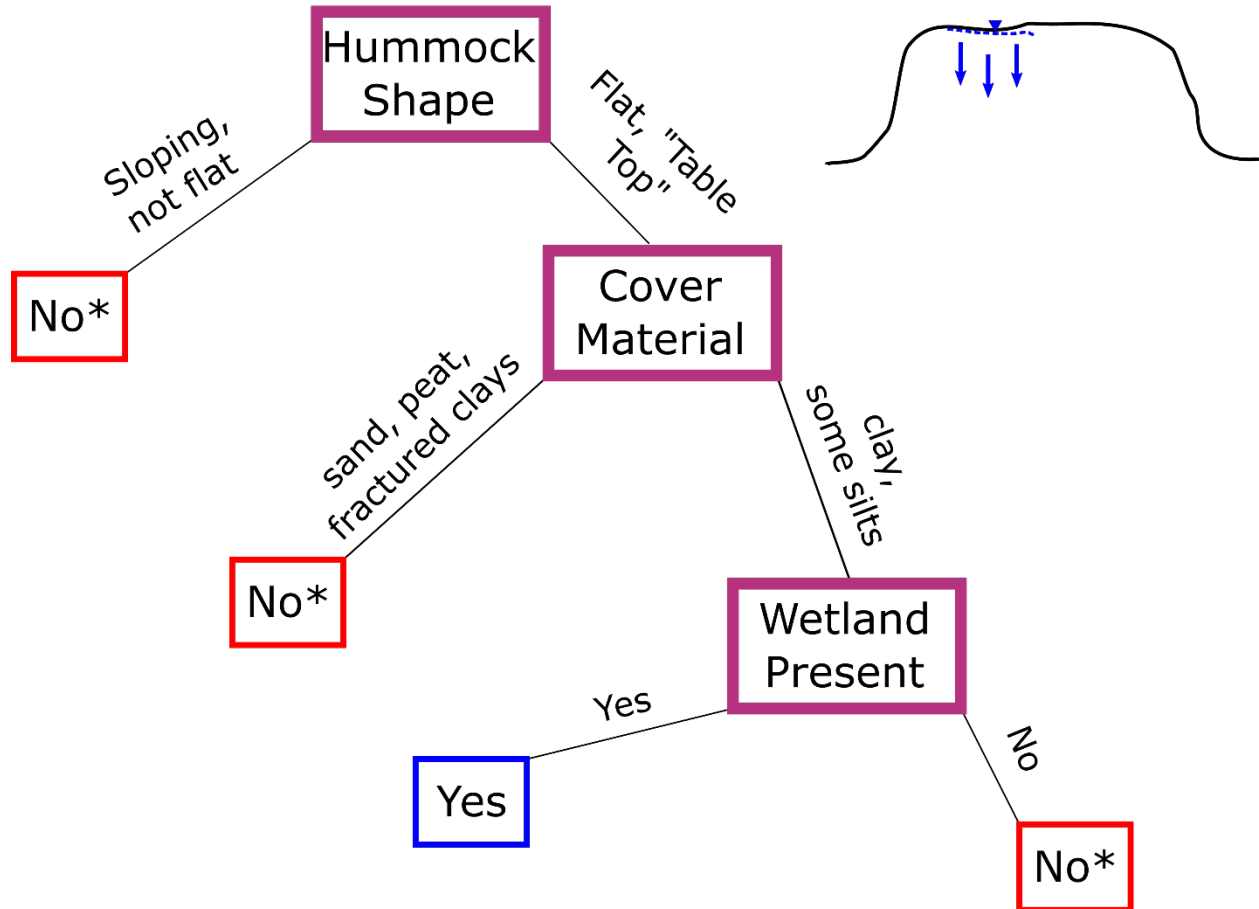
1. Diffuse Groundwater Recharge?



Decision tree 1 corresponds to diffuse recharge, where water from precipitation or snowmelt infiltrates into the unsaturated zone and gradually migrates to the water table.

Sufficient Groundwater Recharge?

2. Focused Groundwater Recharge?

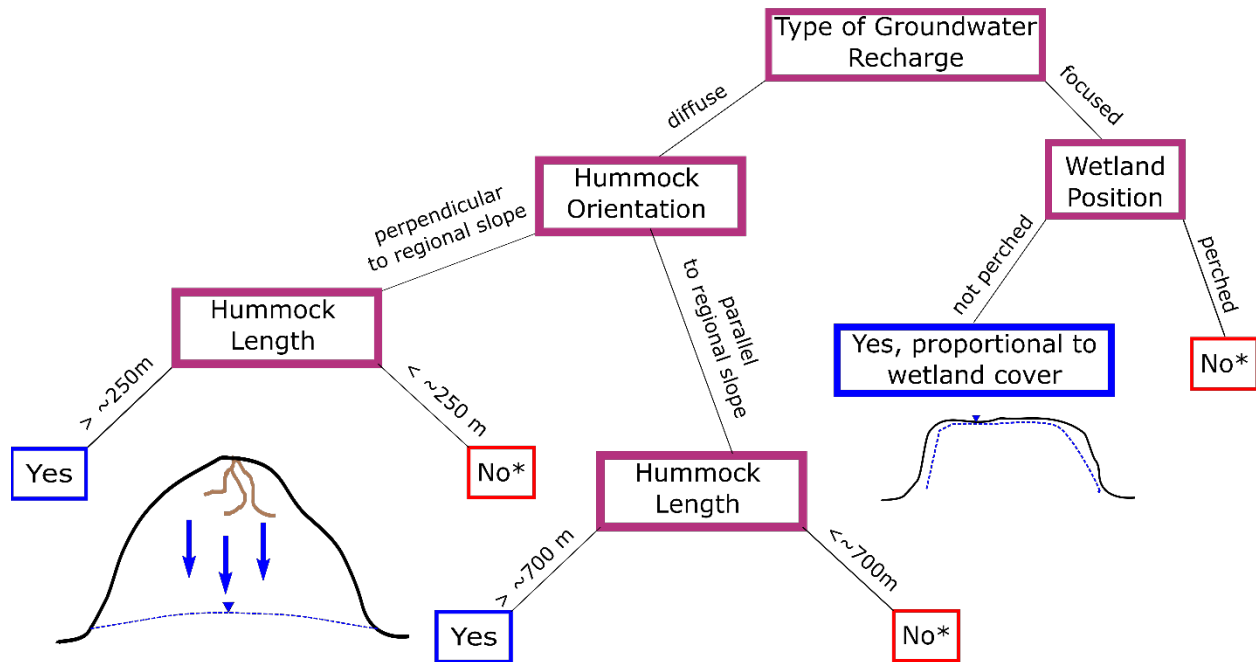


*Start from top of Diffuse Groundwater Recharge

Decision tree 2 corresponds to focused recharge, where water seeps from persistently saturated features on the landform (i.e., wetlands).

Influence of Hummocks on Groundwater Flow

3. Formation of Local Groundwater Flow System (i.e. Mounding)? (assumes #1 or #2 is satisfied)



*Still a source of water to overall landscape

Decision tree 3 corresponds to understanding whether water levels are likely to rise and form persistent groundwater mounds beneath hummocks.

Appendix F –Articles, Presentations, Reports & Theses

Refereed Journal Articles

Lukenbach, M.C., C.J. Spencer, C.A. Mendoza, K.J. Devito, S.M. Landhäusser and S.K. Carey, 2019. Evaluating how landform design and soil covers influence groundwater recharge in a reclaimed soft tailings deposit. *Water Resources Research*, 55(8), 6464-6481. doi: 10.1029/2018WR024298

Spennato, H.M., S.J. Ketcheson, C.A. Mendoza and S.K. Carey, 2018. Water table dynamics in a constructed wetland, Fort McMurray, Alberta. *Hydrological Processes*, 32(26), 3824-3836. doi: 10.1002/hyp.13308

Ketcheson, S.J., J.S. Price, S.K. Carey, R.M. Petrone, C.A. Mendoza and K.J. Devito, 2016. Constructing fen peatlands in post-mining oil sands landscapes: Challenges and opportunities from a hydrological perspective. *Earth-Science Reviews*, 161, 130-139. doi: 10.1016/j.earscirev.2016.08.007

International Invited Presentations

Mendoza, C., P. Twerdy, M. Lukenbach, S. Carey, K. Devito and S. Landhäusser, 2021. Ecohydrogeological interactions between trees, soil moisture, groundwater and wet lowlands in a reconstructed oil-sand mine landscape. *CLRA/SWS/SER RE3 Conference*, Quebec, Jun 19-24. Postponed from 2020.

Biagi, K.M., M.G. Clark, E.R. Humphreys, S.K. Carey and C. Mendoza, 2021. A ecohydrological overview of a constructed peatland in the Athabasca oil sands region, Canada – six years after commission. *CLRA/SWS/SER RE3 Conference*, Quebec, Jun 19-24. Postponed from 2020.

Mendoza, C., M. Lukenbach, P. Twerdy, S. Carey, K. Devito and S. Landhäusser, 2018. Mitigation of environmental impacts through construction of a reclaimed upland-wetland system on soft tailings at an oil-sand mine, NE Alberta, Canada. *Resources for Future Generations 2018*, Abstract 2053, Vancouver, BC, June. **(Session Keynote)**

Mendoza, C., and K. Devito, 2013. Hydrological challenges and opportunities for reconstructing ecosystems after oil-sand mining. *SER 2013: 5th World Conference on Ecological Restoration*, Madison, WI, October.

Selected Regional Invited Presentations

Mendoza, C., and K. Devito, 2016. Designing landscapes for wetlands following oil-sand mining. *Connecting Our Waters, A World Water Day Panel Discussion*, Edmonton, March.

Mendoza, C., 2014. Hydrology, climate and constructed geology for reclaiming oil-sand mining landscapes. *Geological Engineering Seminar Series, University of British Columbia*, Vancouver, April.

Mendoza, C., 2013. Hydrology, constructed geology and reclamation of oil-sand mining landscapes. *Department of Earth Sciences Seminar, Simon Fraser University, Burnaby, November.*

Selected Conference Abstracts

Lukenbach, M.C., P.A. Twerdy, C.A. Mendoza, S.K. Carey, K.J. Devito and T.R. Butterfield, 2020. Hydrological and hydrogeological performance of constructed hummocks at a reclaimed composite tailings deposit. *GeoConvention 2020* (International Association of Hydrogeologists).

Landhäuser, S., S. Carey, K. Devito, F. Leishman, M. Lukenbach, C. Mendoza and M. Merlin, 2019. Early drivers of upland forest development and associated hydrology in a reconstructed landscape on a boreal oil-sands mine site. *Geophysical Research Abstracts*, Vol. 21, EGU2019-11201.

Biagi, K., M.G. Clark, E. Humphreys, C. Mendoza and S.K. Carey, 2019. An evaluation of the hydrological functioning of a constructed wetland in the Athabasca oil sands region, Canada – six years after commission. *Geophysical Research Abstracts*, Vol. 21, EGU2019-12056.

Twerdy, P.A., M.C. Lukenbach and C.A. Mendoza, 2018. Hydrogeological considerations for landscape reclamation on soft tailings deposits in the Athabasca Oil Sands Region. *Proceedings, GeoEdmonton, 71st Canadian Geotechnical and 13th Joint CGS/IAH-CNC Groundwater Conference*, Edmonton, September.

Lukenbach, M.C., C.J. Spencer, C.A. Mendoza, K.J. Devito, S.M. Landhäuser and S.K. Carey, 2018. Groundwater recharge in a reclaimed watershed following oil sands mining: Implications for groundwater flow in reconstructed landscapes. *Proceedings, GeoEdmonton, 71st Canadian Geotechnical and 13th Joint CGS/IAH-CNC Groundwater Conference*, Edmonton, September.

Lukenbach, M., C. Mendoza, K. Devito, K. Hokanson, P. Twerdy and S. Landhäuser, 2018. Landform design influences groundwater recharge and local-scale flow when re-establishing Boreal ecosystems on soft tailings deposits. *Resources for Future Generations 2018*, Abstract 1641, Vancouver, June.

Mendoza, C., M. Lukenbach, P. Twerdy, S. Carey, K. Devito and S. Landhäuser, 2018. Ecohydrological development of a reclaimed upland-wetland system constructed on soft tailings at an oil-sand mine, NE Alberta, Canada. *Geophysical Research Abstracts*, Vol. 20, EGU2018-11843.

Lukenbach, M.C., C.J. Spencer, C.A. Mendoza, K.J. Devito, S.M. Landhäuser and S.K. Carey, 2017. Resolving the need for groundwater recharge versus forest productivity in a

reclaimed watershed. *GSA Abstracts with Programs*, 49(6). doi: 10.1130/abs/2017AM-306440

Lukenbach, M.C., C.J. Spencer, C.A. Mendoza, K.J. Devito, S.M. Landhäusser and S.K. Carey, 2017. Variably saturated flow between constructed upland hummocks and a wetland in a reclaimed watershed following oil sands mining. *CGU/CSAFM Joint Annual Scientific Meeting*, Vancouver, May. Abstract B04-09.

Spennato, H.M., S.K. Carey, E.M. Nicholls and C.A. Mendoza, 2016. An assessment of water table dynamics in a constructed wetland, Fort McMurray, Alberta. *CMOS/CGU Joint Annual Meeting*, Fredericton, June. Abstract 8557.

Biagi, K., S. Carey, E. Nicholls and C. Mendoza, 2015. Understanding flow pathways, major chemical transformations and water sources using hydrochemical and hydrometric data in a constructed fen, Fort McMurray, Alberta. *AGU/CGU Joint Assembly*, Abstract H14A-0187.

Nicholls, E., S. Carey, G. Drewitt, E. Humphreys, M.G. Clark and C. Mendoza, 2015. Multi-year water balance assessment of a constructed wetland, Fort McMurray, Alberta. *AGU/CGU Joint Assembly*, Abstract H13A-05. **(CGU Best Student Paper Award)**

Mendoza, C., S. Carey, K. Devito, S. Landhäusser and J.M. Longval, 2014. Early water dynamics within a wetland complex constructed on tailings at an oil-sand mine. *GSA Abstracts with Programs*, 46(6), p. 816.

Price, J., K. Devito, C. Mendoza and R. Petrone, 2014. Hydrological challenges and opportunities for reconstructing wetland ecosystems after oil-sands mining. Responsible management of peatlands: Involvement of the industrial sector. *Peatland Ecology Research Group (PERG) 20th Symposium, Symposium on responsible management of peatlands: Involvement of the industrial sector*, Quebec, QC, February.

Technical Reports

Provost, H., V. Mann and C. Mendoza, 2015. *Sandhill Fen Numerical Groundwater Modeling – Final*. BGC Report submitted to Environmental and Reclamation Research, Syncrude Canada Ltd., Edmonton. 55p plus 2 appendices.

Longval, J.M., and C.A. Mendoza, 2014. *Initial Hydrogeological Instrumentation and Characterization of Sandhill Fen Watershed*. Hydrogeology Group, Earth & Atmospheric Sciences, University of Alberta, Edmonton, AB. 63p plus electronic appendices. REV_1 issued 24 March 2020.

Student Theses and Project Reports

Twerdy, P., 2019. *Hydrogeological Considerations for Landscape Reconstruction and Wetland Reclamation in the Sub-humid Climate of Northeastern Alberta, Canada*. M.Sc. thesis,

Earth & Atmospheric Sciences, University of Alberta, 204p. <https://doi.org/10.7939/r3-zpg2-6p77>

Hamilton, A., 2015. *Instrumentation and Characterization of Soil Moisture for the Syncrude Sandhill Fen Watershed*. Undergraduate term project, Earth & Atmospheric Sciences, University of Alberta, 51p. [Limited distribution.]

Benyon, J., 2014. *Characterization of Hydraulic Conductivity Profiles for Sandhill Fen Watershed Reclamation Materials*. B.Sc. thesis, Earth & Atmospheric Sciences, University of Alberta, 24p. [Limited distribution.]

Longval, J.M., 2014. [Superseded by Longval and Mendoza, 2014.]

Moningka, T.M., 2013. *Hydrologic Interactions at a Constructed Forestland-Wetland Interface*. M.Eng. Project report, Civil & Environmental Engineering, University of Alberta, 91p. [Limited distribution.]

Effa, J., 2013. *Water Table Dynamics in a Hillslope in the Syncrude Sandhill Reclamation Site During and After Revegetation*. B.A.Sc. thesis, Geological Engineering, UBC, 72p. [Limited distribution.]

APPENDIX 3: THE WATER AND CARBON BALANCE ON THE SANDHILL FEN- DRAFT FINAL REPORT (2012-2018)

TERMS OF USE

McMaster University was retained by Syncrude to carry out the studies presented in this report and the material in this report reflects the judgment of the authors in light of the information available at the time of document preparation. Permission for non-commercial use, publication or presentation of excerpts or figures requires the consent of the authors. Commercial reproduction, in whole or in part, is not permitted without prior written consent from Syncrude. An original copy is on file with Syncrude and is the primary reference with precedence over any other reproduced copies of the document.

Reliance upon third party use of these materials is at the sole risk of the end user. Syncrude accepts no responsibility for damages, if any, suffered by any third party as a result of decisions made or actions based on this document. The use of these materials by a third party is done without any affiliation with or endorsement by Syncrude.

Additional information on the report may be obtained by contacting Syncrude.

This appendix may be cited as:

Carey, S. and Humphreys, E. 2019. The Water and Carbon Balance of the Sandhill Fen- Draft Final Report (2013-2018). Appendix 3 in Syncrude Canada Ltd. *Sandhill Fen Watershed: Learnings from a Reclaimed Wetland on a CT deposit*. Syncrude Canada Ltd. 2020.



The Water and Carbon Balance of the Sandhill Fen

Draft Final Report (2013-2018)

Sean K. Carey¹ and Elyn R. Humphreys²

¹McMaster University, ²Carleton University

Synopsis

Research on water and carbon processes at the Sandhill Fen Watershed (SFW) began in 2012 with the program fully implemented in 2013. As part of a broader R&D program, this project led by Dr. Sean Carey and Dr. Elyn Humphreys sought to understand and quantify the dominant water and carbon flux processes occurring in the SFW and provide context as to how these compare with those in natural boreal systems, and to assess whether the fen design was sustainable in terms of developing coupled upland-lowland ecosystems over longer time scales. This research was carried out through a number of undergraduate, graduate student and post-doctoral scientist projects. In addition, the scope of the initial proposed research was expanded to provide preliminary assessments of water chemistry processes.

Over the course of this program, SFW underwent remarkable changes. Vegetation established in the uplands and lowlands, influencing the rate, timing and magnitude of water and carbon fluxes. Vertical fluxes predominated the water balance (precipitation and evapotranspiration) in most years, yet there were important lateral transfers (runoff, groundwater flow) that sustained lowland wetness. The fen was highly managed in terms of pumping in the year immediately after commissioning, which strongly affected the extent of saturation, water table and water chemistry. There is evidence that the fen is salinizing. The lack of a defined outlet challenged our ability to interpret the sustainability of the fen hydrologically, yet evidence suggests that wet lowlands will occur and be sustainable. In terms of carbon dynamics, the fen began to accumulate carbon in both uplands and lowlands during the growing season rapidly following establishment, yet in the lowlands carbon uptake has declined. We estimate SFW is a weak source of CO₂ to the atmosphere. Methane and dissolved organic carbon fluxes were limited through 2018.

Throughout this program we have achieved notable insights into the SFW and published several peer-reviewed papers on the system, with more in progress. In this report we outline the key findings from the SFW research program provide insights for wetland design and avenues for future research. This report is constructed as a high-level overview. Specific details and additional methods can be found in respective theses and papers that are referenced and amended to this report.

Acknowledgements

We would like to gratefully acknowledge Syncrude Canada Ltd. for supporting this research. Throughout the program, we have had unwavering support for this research in terms of funding, logistics and in the day-to-day personal nature of student-based research. We are forever grateful for supporting this program.

We would like to acknowledge the input to this report from Dr. Mike Treberg, Dr. Gordon Drewitt, Dr. Claire Oswald, Dr. Graham Clark, Erin Nicholls, Kelly Biagi, Haley Spennato, Jessica Rastelli, Chelsea Thorne and Dr. Stacey Strilesky.

Table of Contents

1	INTRODUCTION	- 6 -
2	EXPERIMENTAL DESIGN	- 7 -
2.1	WEATHER STATIONS.....	- 7 -
2.2	SNOW SURVEYS.....	- 8 -
2.3	EDDY COVARIANCE.....	- 8 -
2.4	SOIL CHAMBERS FOR METHANE MEASUREMENT.....	- 9 -
2.5	NEAR-SURFACE WELLS.....	- 10 -
2.6	MANAGED INFLOW AND OUTFLOW	- 10 -
2.7	WATER QUALITY MEASUREMENTS	- 10 -
2.7.1	ELECTRICAL CONDUCTIVITY (EC)	- 10 -
2.7.2	MAJOR IONS	- 11 -
2.7.3	MERCURY	- 11 -
2.7.4	ORGANIC CARBON.....	- 11 -
2.7.5	STABLE ISOTOPES	- 11 -
3	HYDROLOGY.....	- 12 -
3.1	PRECIPITATION AND GENERAL CLIMATE	- 12 -
3.1.1	SNOW	- 12 -
3.1.2	RAIN	- 14 -
3.2	WATER MANAGEMENT FLUXES.....	- 15 -
3.2.1	WATER ADDITIONS.....	- 15 -
3.2.2	WATER EXTRACTIONS	- 15 -
3.3	EVAPOTRANSPIRATION.....	- 16 -
3.4	WATER TABLE DYNAMICS.....	- 17 -
3.5	RUNOFF PROCESSES	- 19 -
3.6	ANNUAL WATER BALANCE COMPONENTS	- 21 -
4	WATER CHEMISTRY	- 22 -
4.1	ELECTRICAL CONDUCTIVITY, MAJOR IONS AND STABLE ISOTOPES	- 22 -
4.2	MERCURY	- 24 -
5	CARBON PROCESSES.....	- 25 -
5.1	NET ECOSYSTEM PRODUCTIVITY.....	- 25 -
5.2	METHANE	- 28 -
5.3	DISSOLVED ORGANIC CARBON.....	- 29 -
6	SYNTHESIS.....	- 30 -

6.1	IS THE SANDHILL FEN WATERSHED HYDROLOGICALLY SUSTAINABLE?	- 30 -
6.2	WHAT IS DRIVING THE CHANGES IN SALINITY?	- 33 -
6.3	WILL THE SANDHILL FEN BECOME A CARBON SINK?	- 35 -
7	<u>FUTURE RESEARCH DIRECTIONS</u>	<u>- 36 -</u>
8	<u>REFERENCES</u>	<u>- 38 -</u>
9	<u>SUPPLEMENTARY INFORMATION</u>	<u>- 41 -</u>
9.1	RESEARCH TEAM	- 41 -
9.2	COMPLETED GRADUATE STUDENT THESES	- 41 -
9.3	COMPLETED PEER REVIEW PUBLICATIONS	- 41 -
9.4	CONFERENCE PRESENTATIONS	- 42 -
	Figure 1 Instrumentation map of SFW. Dark grey areas represent the lowland (wetland) area and lighter grey represent the margins and upland areas. Well locations with a black dot represent sampling locations for water quality.	- 7 -
	Figure 2 Meteorological Tower 3 atop Hummock 7.	- 8 -
	Figure 3 Eddy Covariance tower at Fen Lowland site.	- 9 -
	Figure 4 Soil collars for chamber measurements. One collar has roots excluded to assess soil respiration.	- 9 -
	Figure 5 Snow Water Equivalent at each weather station as measured using the C725. Dashed line is the Ft McMurray A 30-year Mean. Tower locations appear in Figure 1.	- 13 -
	Figure 6 Snow Water Equivalent (SWE) variability in February 2018.	- 14 -
	Figure 7 Rainfall at the Sandhill Fen Watershed from 2013-2018. Dashed line is the Ft McMurray A 30-year monthly sums for context.	- 14 -
	Figure 8 Monthly evapotranspiration (ET) from the lowland and upland eddy covariance towers.	- 16 -
	Figure 9 Water table as measured at the lowland tower.	- 17 -
	Figure 10 Rainfall (top), water table (middle) and pump (bottom) for 2014 and 2015. Note that positions of the lines in m asl change, indicating flow reversals across the fen.	- 18 -
	Figure 11 TOP: Water table level (in m asl) between the toe of a hummock (TR-W8) and the lowland (B3-W1). When above the 1:1 line, the horizontal hydraulic gradient (i.e., water flow) is from the lowland towards the hummock. BOTTOM: Hydraulic gradient (between well B3-W1 and TR-W8) over time during the 2014 and 2015 study periods. Positive values indicate flow towards the lowland, negative values indicate flow toward the hummock (Note the change in x-axis scale).	- 19 -
	Figure 12 Construction and installation of the runoff collector on the Hummock 8 (north facing slope)	- 20 -
	Figure 13 Half hour (grey bars) and total (black lines) runoff observed at the (a) south-facing, and (b) north facing runoff collectors during 2018 melt.	- 21 -
	Figure 14 Rainfall (bars) and cumulative runoff (black dashed lines) during major storm even on 21-22 July 2018.	- 21 -
	Figure 15 Average electrical conductivity at each water sampling site (black dots) for each of the study years.	- 23 -
	Figure 16 Molarity of Calcium and Sodium ions and their respective ratios for each study year.	- 24 -
	Figure 17 Net Ecosystem Productivity (NEP), Ecosystem Respiration (ER) and Gross Ecosystem Production for the lowland tower.	- 26 -
	Figure 18 Cumulative Net Ecosystem production for growing season years at the lowland tower.	- 26 -
	Figure 19 Cumulative growing season Net Ecosystem Exchange (NEE) for the upland and lowland towers. Early 2016 is estimated.	- 27 -

Figure 20 Ecosystem respiration and soil temperature for the upland and lowland towers. Lines of best fit are for individual years.	- 27 -
Figure 21 Median June-August methane flux for the study years.	- 28 -
Figure 22 All half-hour methane fluxes for July over the course of the study. Black dash is IPCC emission factor associated with rewetted organic soils.	- 29 -
Figure 23 Porewater DOC concentration from lowland water during the study years.....	- 29 -
Figure 24 Progression of upland vegetation by year for the upland tower with photos in summer and winter for 2018.....	- 31 -
Figure 25 Figure 24 Progression of upland vegetation by year for the lowland tower with photos in summer and winter for 2018.....	- 32 -
Table 1 Pumping volume totals and in mm (for lowland area 17 ha) and entire SFW area (52 ha).....	- 15 -
Table 2 Annual water balance components as measured at the SFW. NA means not measured and X means analysis in progress.	- 22 -
Table 3 Dissolved organic carbon export from SFW by year.	- 30 -

1 Introduction

The Sandhill Fen Watershed (SFW) is one of two constructed peatlands that exist in the Athabasca Oil Sands Region (AOSR), both of which vary considerably in design (see Daly et al., 2012, Wytrykush et al., 2012, and Ketcheson et al., 2016 for background information). Prior to construction, a former mine area called East-In Pit was filled with 35 m of inter-bedded composite tailings and tailings sand layers followed by a 10 m structural cap of sand. The SFW was then constructed on top of these materials and is approximately 52 ha in area, which includes a 35 ha upland and a 17 ha lowland that was the target area for a fen ecosystem. At construction, SFW was comprised of several landscape units that included swales, perched fens, woody berms, a freshwater storage pond, and an underdrain system. Seven hummocks varying in elevation from three to eight meters above the lowland were constructed through mechanical placement to encourage recharge and direct water to the lowland (Figure 1). Hummocks were capped with fluvial sand and compacted, whereas non-hummock areas were capped with ~0.5 m of peat-mineral mix soils while the lowland comprised of 0.5 m of clay topped with 0.5 m of salvaged organic soil sourced from a poor fen and placed in January 2011. Seeds were spread in the fen November 2011 to encourage vegetation growth. Upland vegetation was planted at different densities at plots throughout the uplands. Details of upland and wetland vegetation can be found in companion reports by Vitt and Landhäusser.

The initial objectives of our research program over a six-year period (2013-2018) were to:

- 1) Measure the ecosystem scale annual water and carbon balance and establish their dominant controls.
- 2) Establish the inter-fen variability in carbon and methane fluxes.
- 3) Characterize the quality and amount of aqueous carbon leaving the fen through surface pathways.

Throughout the course of the program, there were adjustments made that reflected operational and logistical constraints and new emerging issues that supplemented the original objectives. In particular, we increased focus on water chemistry (major ions and salinity) and provided some baseline information on nutrient and mercury dynamics.

This report is divided into sections where key results and findings will be discussed. In the first section, we outline the instrumentation and research design, and then results are presented in terms of water, salinity and carbon dynamics. A final integrates findings and provides guidance for future research. Again, note that this report is a synopsis of the key findings and that additional details can be found in associated theses and peer-reviewed journal papers.

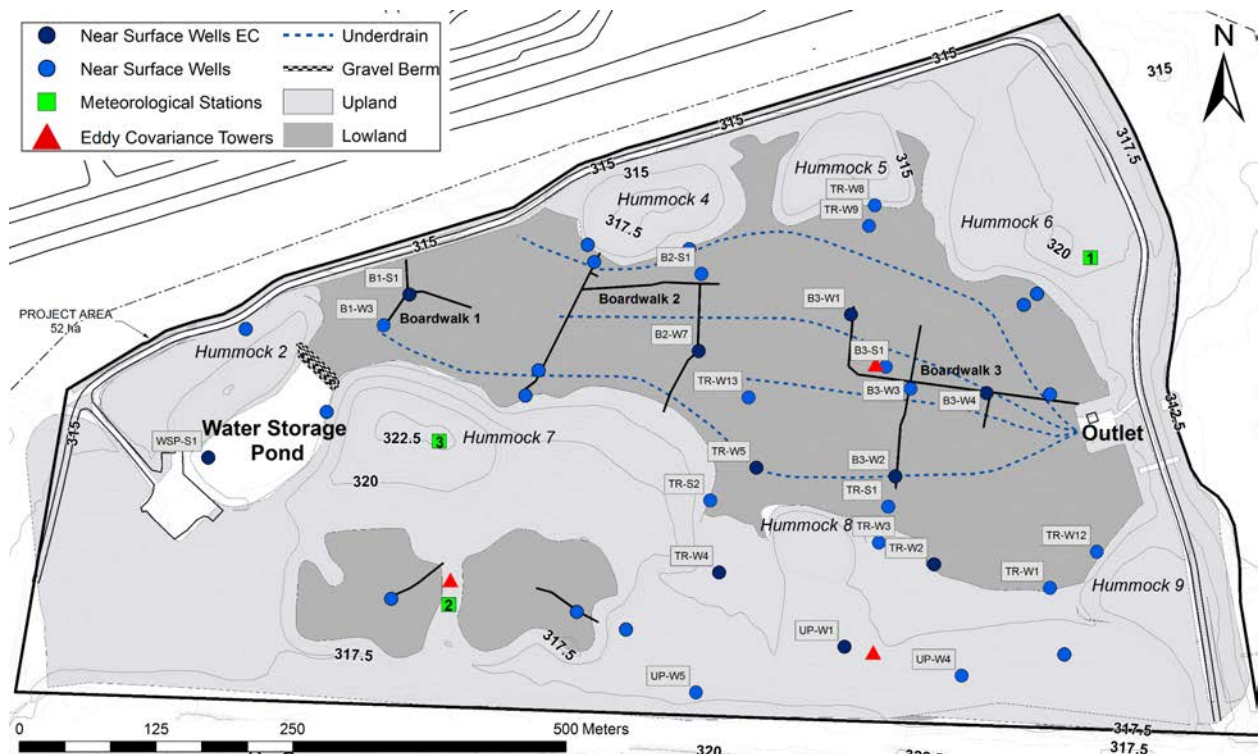


Figure 1 Instrumentation map of SFW. Dark grey areas represent the lowland (wetland) area and lighter grey represent the margins and upland areas. Well locations with a black dot represent sampling locations for water quality.

2 Experimental Design

Beginning in 2013, we implemented a distributed water and carbon flux monitoring program. A map of the locations of the principal hydrometric instrumentation appears in Figure 1.

2.1 Weather Stations

Three weather stations (Figure 1 – green squares) were installed by O’Kane Consultants and this data was utilized by our research team. At these sites, air temperature, relative humidity, wind speed and direction, net radiation, snow depth, snow water equivalent and rainfall were collected. In addition, soil moisture and temperature were collected to a depth of 1 m. Figure 2 shows Meteorological Station 3 on Hummock 7.



Figure 2 Meteorological Tower 3 atop Hummock 7.

2.2 Snow Surveys

Snow surveys were conducted most years by O’Kane Consultants on transects at the approximate time of peak snow water equivalent (SWE). We utilized this data to confirm estimates of snow input to SFW and the data can be found in the respective annual reports.

2.3 Eddy Covariance

For measuring evapotranspiration and ecosystem-scale vertical carbon fluxes, we utilized the eddy covariance (EC) technique at two principal sites (upland and lowland), and for a short period between the perched fens (Figure 3). The EC technique uses micrometeorological theory to directly sample the turbulent exchange of energy and trace gases between a surface and the atmosphere. A review of the use of the EC technique for assessing ecosystem functioning was presented by Baldocchi et al., (2001). The EC technique for the measurement of fluxes of heat, water vapour (H₂O), and carbon (CO₂ and CH₄), involves measuring the concentration of selected entities at high frequency (carried by drafts of air past a sensor) and the concurrent fluctuations in vertical wind speed. The covariance of vertical wind speed and trace gas or temperature fluctuations can be used to compute the flux after addressing instrumentation effects. At each of the eddy covariance sites, complementary meteorological data was collected including all-wave radiation, wind speed, temperature, relative humidity, soil heat flux, soil temperature and soil moisture. The eddy covariance towers were constructed in May of 2012 (upland), 2013 (lowland) and 2014 (perched fen), respectively. The perched fen tower was removed in 2016 as it provided no new information compared with the upland. The upland and perched fen sites operated from May to October, while the lowland site ran year-round. Details on flux processing can be found in Nicholls et al., (2016) and Clark (2018).



Figure 3 Eddy Covariance tower at Fen Lowland site.

2.4 Soil Chambers for methane measurement

While the lowland eddy covariance system measured CH₄ flux on a half-hour basis, plot-scale measurements were used to assess the spatial and temporal variation in CH₄ and the factors that influence their variability. Non-steady state static chambers were placed in the lowland and upland, with a maximum number of plots of 29 in 2015 (Figure 4). Details of the experimental design are found in Clark (2018).



Figure 4 Soil collars for chamber measurements. One collar has roots excluded to assess soil respiration.

2.5 Near-surface wells

Water table elevation was measured using a network of 27 surveyed near-surface wells throughout the SFW (Figure 1). Wells were constructed using 1.6 m long PVC slotted pipe (6.4 cm internal diameter) and were installed to a depth of 0.25 to 1.15 m. Wells were instrumented with Solinst Levellogger Junior Edge pressure transducers and Solinst LTC (level, temperature, conductivity). Note that these wells measure near-surface water table, and were primarily designed to establish the depth of water table from the surface and for water quality sampling.

2.6 Managed Inflow and Outflow

Inflows and outflows were measured using ultrasonic flowmeters as well as a transducer (Rosemount Inc., Chanhassen, MN, USA) measuring the level in the water storage pond. Outflow consists of surface flow and underdrain contributions. Surface drainage flowed through a V-notch weir, instrumented with a sensor to continuously record level and then into the sump, where underdrain water is collected, and total discharge is pumped away from the fen. Flowmeters for inflow and outflow used Model AT868 AquaTrans™ Ultrasonic Flow Transmitter for water (1-Channel and 2-Channel) (General Electric, Fairfield, CT, USA). Measurement error of inflow and outflow was considered within 25% in 2013 and $\pm 10\%$ after 2014. While inflow began on 29 May 2013, dataloggers did not begin functioning until 26 July, 2013. Inflow during this time was inconsistent, and the pumping rate was frequently adjusted; therefore, reported values are based on daily notes taken from the flowmeter as well as corrections developed through water level rise and fall within the storage pond, weir and sump. Outflow data records begin in April 2013.

2.7 Water Quality Measurements

Water quality was measured throughout the course of the program at the network of wells described above and in standing water throughout the fen. In addition, outflow, sump and inflow water were sampled. The frequency of the sampling varied based on the year, but at a minimum monthly samples were taken during the May – October period. All water samples were collected using the standard ‘clean hands, dirty hands’ technique. For the porewater samples, water was collected from the network of water table wells using a peristaltic pump with Teflon sample lines. The pump lines and bottles were environmentalized prior to collecting the sample into pre-cleaned 1 L QCS-grade glass amber Boston round bottles. Field duplicates and field reagent blanks were collected every 10 samples. All water samples were filtered through pre-baked 0.7 μm . Total Hg, MeHg and DOC filtrate splits were stored in glass amber Boston round bottles and ion filtrate splits were stored in HDPE bottles. All samples were stored at 4 °C in the dark prior to analyses. Filters were frozen in petri dishes after filtration for subsequent analysis for particulate organic carbon (POC). Additional details of water sampling protocols can be found in Oswald and Carey (2016) and Biagi et al., (2019).

2.7.1 Electrical Conductivity (EC)

Continuous measures of EC were taken in a series wells using Solinst LTC every 15 min from May to October. Discrete measurements of EC were taken weekly using a YSI Professional Plus Multiparameter instrument at over 50 surface and pore water sampling sites. All EC values, both discrete and continuous, were corrected to 25 °C.

2.7.2 Major Ions

Water samples were analyzed at the Biogeochemistry Laboratory, University of Waterloo, for major ions including Na⁺, K⁺, Mg⁺², Ca⁺², Cl⁻ and SO₄⁻² using a Dionex AS40 Automated Sampler, and alkalinity using a Bran & Luebbe AutoAnalyzer3 (Folio Instruments) with all results reported in mg/L. HCO₃⁻ concentrations were calculated by multiplying the alkalinity values by a conversion factor of 1.22. Minimum detection limits for Na⁺, K⁺, Mg⁺², Ca⁺², Cl⁻, SO₄⁻² and alkalinity were 0.13, 0.1, 0.3, 0.67, 0.02, 0.1 and 5 in mg/L, respectively. A correction curve was built with standards from Thermofisher and 5% of samples are re-run as duplicates for analytical QA/QC procedures.

2.7.3 Mercury

Total Hg concentrations in water samples were determined by cold vapor atomic fluorescence spectrometry (CVAFS) on a Tekran 2600 automated Hg analysis system according to US EPA Method 1631 Revision E (USEPA, 2002). Sediment samples (80-120 mg for MeHg; 100-150 mg for THg) were acid digested (7:3 Nitric Acid:Sulfuric Acid) overnight in a Teflon tube, diluted, and then analyzed in the same manner as water samples. Methyl mercury concentrations in all samples were determined by isotope dilution-gas chromatography-inductively coupled plasma mass spectrometry. The water samples were first distilled at 127°C with the addition of Ammonium 1-Pyrrolidinecarbodithioate (APDC) and Hydrochloric Acid (HCl). The samples were then distilled at 110°C with the addition of APDC and HCl. A known quantity of Me²⁰¹Hg was added to all samples as an internal standard. For the analysis, Ascorbic Acid was added to the distillate, which was then transferred to glass vials where the pH was adjusted with Acetate buffer. Full details can be found in Oswald and Carey (2016).

2.7.4 Organic Carbon

Total organic carbon (TOC) was measured in water samples using a Shimadzu 500A TOC analyzer according to EPA Method 415.3. Particulate carbon and nitrogen concentrations on filter residues were analysed using a CE440 Elemental analyzer with a combustion temperature of 975 °C and a reduction temperature of 690 °C. Total organic carbon was measured in sediment samples using a Leco SC444 analyser with a combustion temperature of 1350 °C. Optical indices of dissolved organic matter quality were obtained from absorbance spectra and fluorescence excitation-emission matrices (EEMs) measured on an Aqualog spectrofluorometer (Jobin Yvon Horiba). Details of EEM analysis can be found in Rastelli (2017).

2.7.5 Stable Isotopes

Stable hydrogen and oxygen isotope samples were collected simultaneously with the pore and surface water samples. Samples were filtered and stored in 20-mL polyethylene scintillation vials at room temperature. Stable isotope ratios of hydrogen and oxygen were determined using a Los Gatos Research DTL-100 Water Isotope Analyzer at the University of Toronto. Five standards of known isotope composition, with δ²H ranging from -154‰ to -4‰, purchased from Los Gatos Research were used for calibration, in addition to periodic checks using the international standards, VSMOW2 and SLAP2. During analytical runs, samples were interweaved with standards at a ratio of 3:1. Details of isotope analysis can be found in Biagi et al., (2019).

3 HYDROLOGY

While conceptually simple, closing water balances are notoriously difficult to complete when measuring all components of the hydrological cycle independently. Typically, rainfall and runoff are measured, change in storage is considered negligible and evapotranspiration is assumed the difference. When fully considering all components of the water balance, errors can compound, yet a more thorough understanding of the rate and timing of fluxes is considered. In this work we do not explicitly try to close the water balance, yet we calculate its components and the processes responsible for their patterns.

For the SFW, we consider the water balance:

Inputs – Outputs = Change in Storage

Inputs = Rain + Snow + Pump In + Groundwater In

Outputs = Evapotranspiration + Pump Out + Groundwater Out

In this report, we do not consider groundwater inputs/outputs to the SFW as they are summarized by the report by Mendoza; although they are discussed in a number of places when examining hummock processes and surface water levels.

3.1 Precipitation and General Climate

Precipitation is challenging to measure, yet this is often not considered in hydrological analysis. Snow falls across the landscape and is redistributed by wind and melts intermittently in space and time. Rainfall while at the scale of the SFW is not highly variable, is difficult to measure during high intensity events and when windy. Direct measurements of snowfall were not taken, and under-catch can be an issue.

For context, we will compare values for the study years against the thirty-year normal climate at Fort McMurray A (1981-2010). Average air temperature at this site is +1.0°C, and total precipitation is 418.6 mm, with 316.3 mm as rainfall. Temperatures between 2013 and 2018 were on average 1°C greater than the climate normal in most of the growing season months. Notable cool months below the climate normal were in May 2014 and September 2018.

3.1.1 Snow

Snowfall was estimated via a number of methods at SFW. The best long-term estimate of snow water equivalent was a combination of snow surveys taken late-season and validated against the C725 Snow Water Equivalent (SWE) sensor that measures passive gamma ray emissions which are attenuated by water (Figure 5). In 2018, a more detailed investigation of snow variability was undertaken to more thoroughly assess intra-fen variance.

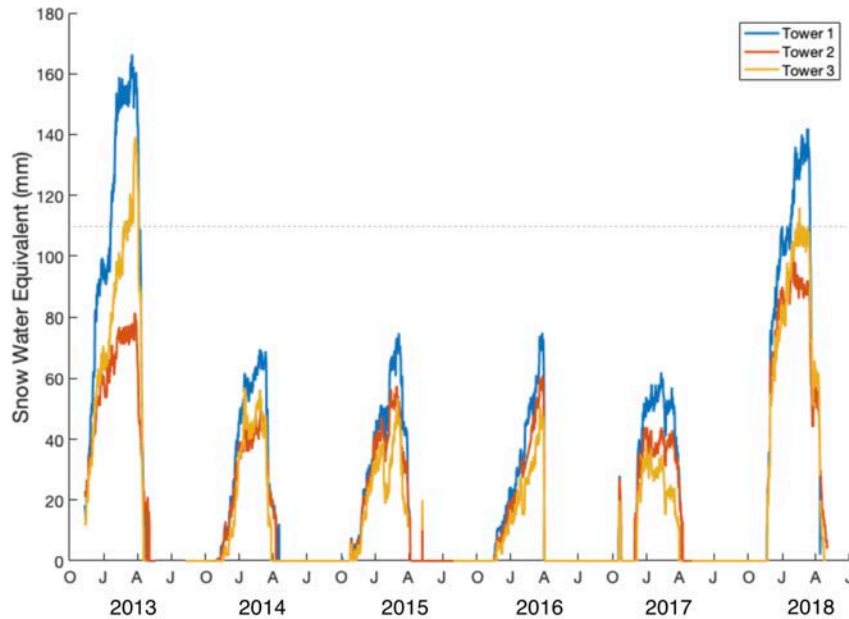


Figure 5 Snow Water Equivalent at each weather station as measured using the C725. Dashed line is the Ft McMurray A 30-year Mean. Tower locations appear in Figure 1.

On average, SWE was less than the 30-year normal in all years except 2013 and 2018 when values were approximately normal. The 2014-2017 years were all well below normal, with average values ranging between 50 and 60 mm.

3.1.1.1 Snow variability

Annual snow surveys suggest that there is moderate variability within the fen, and that this variability changes among years. We have not completed a detailed analysis of the snow survey data collected. However, in 2018 we conducted an extensive set of snow surveys throughout the melt season and identified a number of factors that explain SWE variability at the fen.

A snow survey during peak SWE in February 2018 revealed only modest SWE variability (Figure 6). Hummocks had less SWE than the upland areas which had less than the fen lowland. The influence of vegetation on trapping snow at this point is not apparent and differences in roughness from vegetation are modest. On the hummocks, crests have less SWE than mid and low slope positions like due to wind scour. In terms of aspect, north and east slopes have greater SWE than south and west slopes. This observation is common and often attributed to enhanced solar radiation and sublimation over-winter on south and west slopes. However, the differences are not large. We anticipate additional work evaluating spatial and temporal patterns of SWE once the historical snow survey reports are collated.

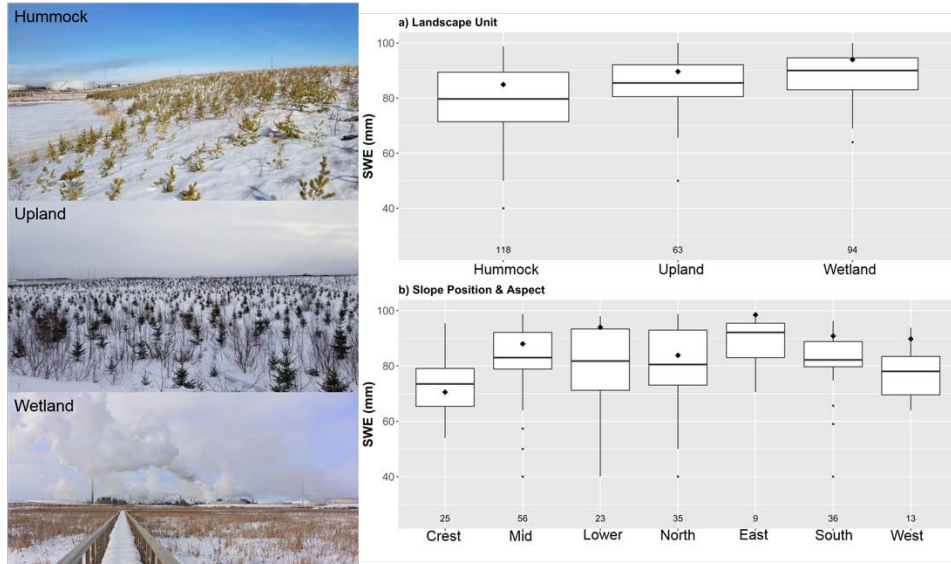


Figure 6 Snow Water Equivalent (SWE) variability in February 2018.

3.1.2 Rain

Rainfall was measured using four tipping bucket gauges across the SFW. There were no appreciable differences in the total among the gauges and Figure 7 is an aggregate daily total of the gauges from May through the end of October. Rainfall was highly variable among seasons and years. 2018 and 2016 were above the climate normal, whereas all other years were below. This pattern however does not reflect the considerable inter-annual variability which plays a strong role in the hydrology of the SFW. For example, 2018 was a relatively dry to average early growing season until a very large rainfall event in July (~100 mm). In most years, large periods of dry weather were interrupted by moderate to large rain events in excess of 10 mm/day. Overall, the precipitation climate of SFW during the 2013-2018 period was drier than the climate normal as represented by the black dashed line in Figure 7.

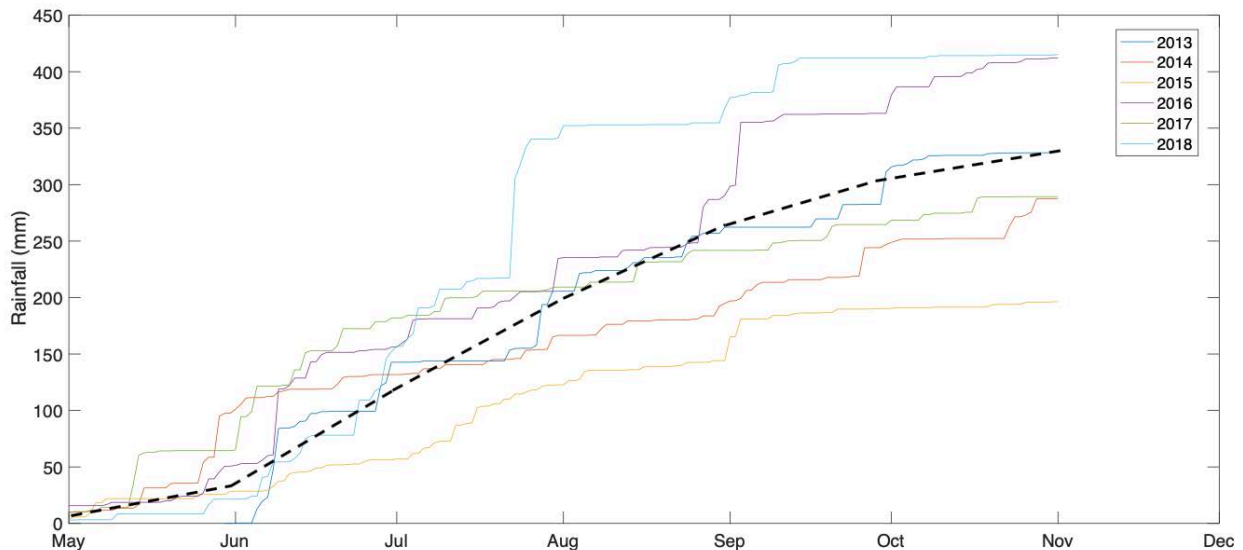


Figure 7 Rainfall at the Sandhill Fen Watershed form 2013-2018. Dashed line is the Ft McMurray A 30-year monthly sums for context.

3.2 Water Management Fluxes

The SFW watershed was designed with a water management system that added and removed water via pumps and underdrains that have been comprehensively described in Wytrykush et al. (2012) and Nicholls et al., (2016). As documented in Nicholls (2015) and Nicholls et al., (2016), there were large uncertainties in the estimation of flux volumes during 2013 due to inconsistencies in operation. Since 2013, reduced usage and improved records provide a better estimate of managed additions and abstractions.

3.2.1 Water Additions

Management of inflow pumping regimes occurred only in 2013 and 2014. In 2013, inflow began in late May and continued steadily for the growing season, with two periods of no flow (see Nicholls et al., 2016 and Spennato et al., 2018 for details). In total, this supplied 1.48×10^5 m³ of water to the fen (870 mm to the lowland and 284 mm total unit area respectively). In contrast, in 2014, inflow began on May 19–20, pumping at a maximum capacity of 260 m³/h for approximately 6 hrs in total and was turned off for the rest of 2014 providing only 2470 m³ (15 mm to the lowland or 5 mm to SFW) from May 1 to September 30. Following 2014, no water has been added to the SFW via the pump management system.

3.2.2 Water Extractions

Management of outflow pumps also varied among the years. In 2013, the pump outflow began early in April and was active until October. Discharge reached 283 m³/h at its peak and fluctuated greatly. Total 2013 outflow values are estimated as 1.5×10^5 m³ or 883 mm over the fen lowland area or 289 mm over 52 ha. Underdrains were left open during 2013, dominating outflow and contributing over 90% of total discharge. In 2014, the valve connecting the underdrains to the sump was closed, and although a small amount of leakage occurred, surface contributions dominated outflow in 2014. There has been dramatically reduced management since 2013, yet on several occasions, outflow pumps have been turned out to lower the water table in the lowland area due to excessive inundation of the boardwalks and research plots and for specific experiments (see Section 3.4). In 2017 and 2018, large rainfall resulting in high water tables were the primary rationale for pumping, which are very effective in removing water over relatively short time frames (days).

Table 1 Pumping volume totals and in mm (for lowland area 17 ha) and entire SFW area (52 ha)

YEAR	Total inflow (m ³)	Total outflow (m ³)	Inflow to lowland – 17ha (mm)	Outflow from lowland – 17 ha (mm)	Inflow to SFW - 52 ha (mm)	Outflow from SFW - 52 ha (mm)
2013	147838	150162	870	883	284	289
2014	2470	2907	15	17	5	6
2015	0	9334	0	55	0	18
2016	0	0	0	0	0	0
2017	0	17362	0	102	0	33
2018	0	32655	0	192	0	63

3.3 Evapotranspiration

Evapotranspiration (ET) was measured at the two eddy covariance sites (upland and lowland) over multiple years and at the perched fen for 2014 and 2015. The perched fen data will not be discussed in this report as it is similar to the upland site yet is reported in Nicholls et al., (2016) and Clark (2018). There were some instrumentation issues in 2018 and data are still being processed and will be later amended to this report. In 2016, the fires affected logistics and limited collection at the upland tower. ET varied seasonally in response to climate and over shorter timescales in response to weather. The relative influence of daily weather on ET fluxes was large, as radiation, vapour pressure deficit and windspeed all played important factors on a daily basis in driving ET (Nicholls et al., 2016; Clark, 2018). The influence of vegetation growth on ET is apparent in the uplands as increasing leaf area over the four years translates to an increase in ET rates during most months, as June-August ET rates were ~ 0.8 mm/d greater in 2017 compared with 2013. These patterns of increasing ET are not apparent in the lowland as changes to vegetation and the boundary layer properties (turbulence) were more modest and ET was largely driven by atmospheric demand.

ET in the uplands was, on average, greater than the lowlands, although not in all years and all seasons. Annual ET estimates are provided in Table 2 when discussing the total water balance fluxes. While it may be counter-intuitive that the uplands on average had a greater annual ET than the lowland, well watered vegetation surfaces have been reported to have greater total ET than wetlands due to enhanced roughness which decreases atmospheric resistance and enhances turbulent transport.

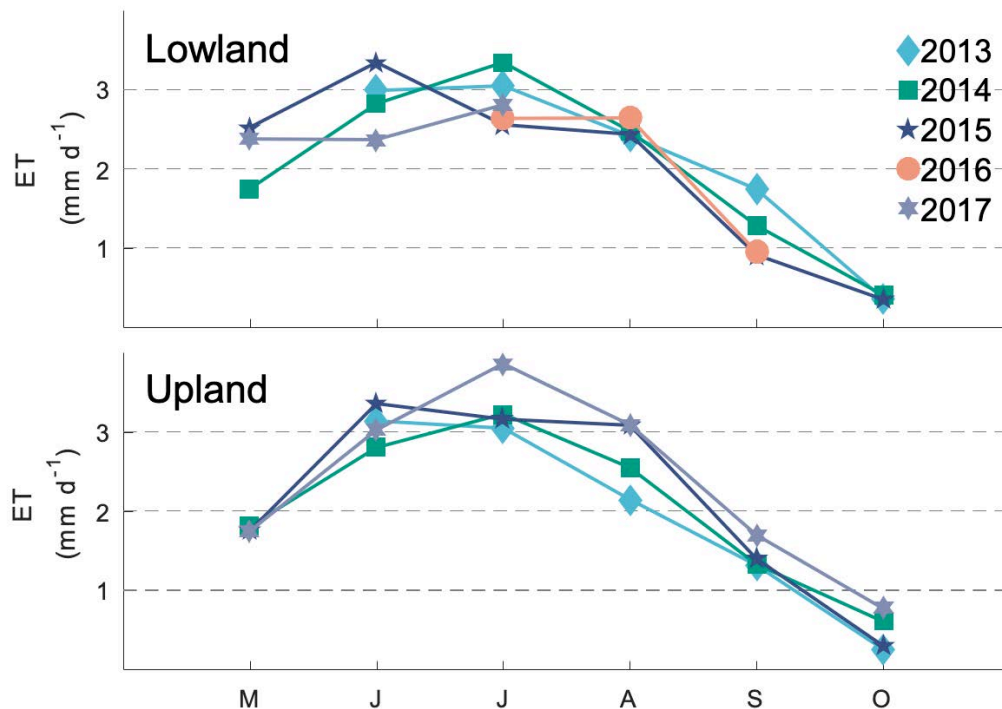


Figure 8 Monthly evapotranspiration (ET) from the lowland and upland eddy covariance towers.

3.4 Water Table Dynamics

Water table was measured in a distributed manner throughout SFW at a number of sampling wells that varied based on student projects and monitoring objectives. A single well reported year-round water levels at the lowland eddy covariance tower (Figure 9). Near surface wells were distributed throughout the lowland and uplands along pre-defined across and down-gradient transects (see Figure 1 for location of wells). For detailed information on water table dynamics, see Spennato (2016) and Spennato et al., (2018).

Annual water table measured at the lowland tower shows that the SFW at the approximate centre of the lowland has a water table that is considerably higher than would be expected at reference wetlands in the AOSR, which are between the surface and 30 cm below ground surface (Wells and Price, 2015; Wells et al., 2017; Elmes and Price, 2019). With the exception of 2013 and the onset of 2014, water tables were always above the surface, with the highest levels in spring and a gradual decline throughout summer with increased evapotranspiration. That said, large rainfall events rapidly increased the water table in the fen as observed in the years from 2015 to 2018. During the 100 mm event in July 2018, the water table rose 30 cm over 4 day and in 2016 a wet fall resulted in very wet conditions. The influence of the pump is clearly demonstrated in Figure 9 as continuous operation can rapidly lower the water table.

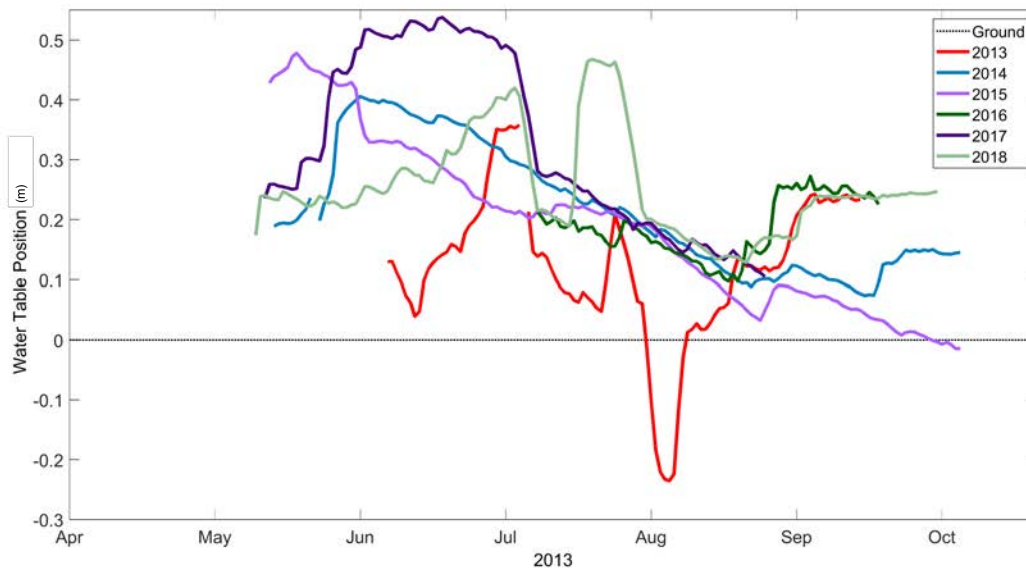


Figure 9 Water table as measured at the lowland tower.

SFW has complex longitudinal and lateral hydraulic gradients as represented by the water table surface. While the report by Mendoza will highlight most of the hydrogeological setting of the SFW, Spennato et al. (2018) examined differences in water table position for the fen and between the lowland and the upland at several hummock sites. In general, large-scale lateral groundwater flow direction was from the south swale towards the SFW lowland, with more regional groundwater flow system then diverging north-east beyond the topographic boundary of the watershed (see Mondoza report). While deeper groundwater systems respond slowly to weather conditions, the shallow water table dynamics within the SFW exhibited high-frequency fluctuations. Using 2014 and 2015 as an example, at the beginning of the growing season the lateral hydraulic gradient and near-surface flow was typically from the inlet (B1; west) towards the outlet (B3; east) (Figure 10). However, as drying progressed over the summer, the hydraulic gradient within the

lowland reversed by August. During this period of flow reversal, the hydraulic gradient was from the outlet (B3; east) towards the inlet (B1; west). In 2014, weaker and shorter flow reversals occurred, with reversed flow conditions present for a total of 12 days. In contrast, flow was reversed for a total of 52 days in 2015, with stronger horizontal hydraulic gradients in 2015.

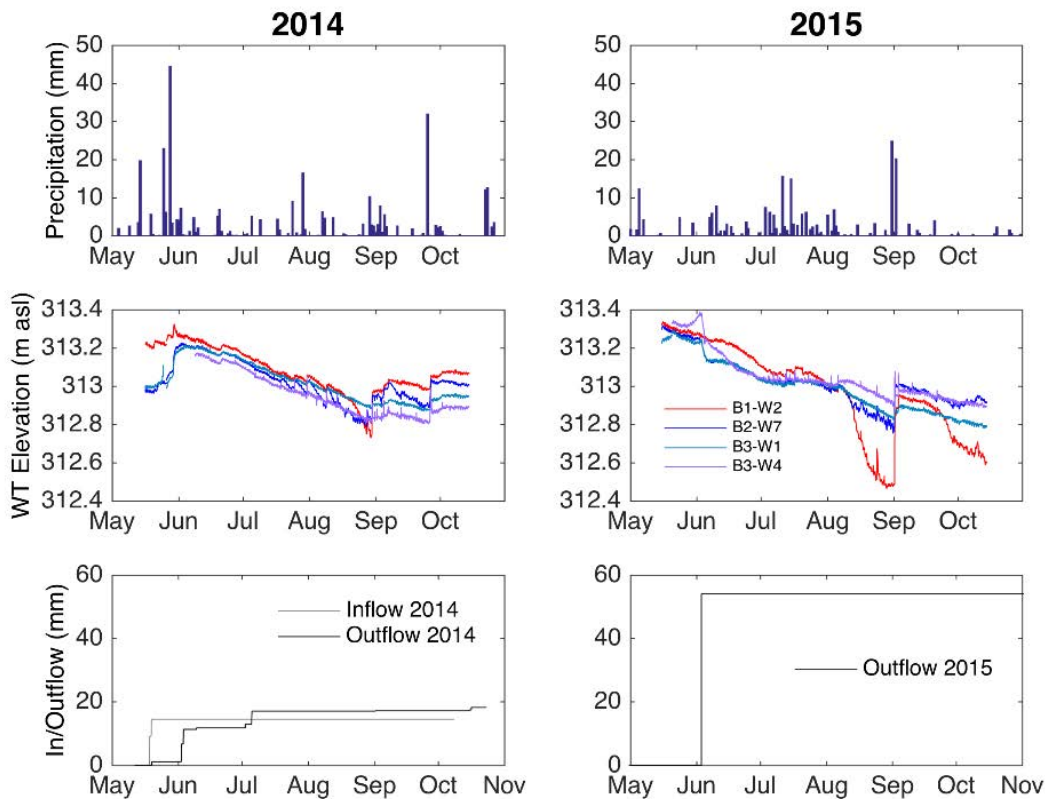


Figure 10 Rainfall (top), water table (middle) and pump (bottom) for 2014 and 2015. Note that positions of the lines in m asl change, indicating flow reversals across the fen.

Frequent flow reversals were observed between the hummock margins and the lowlands, with the direction of upland-lowland horizontal hydraulic gradients varying as the season progressed (Figure 11). Water flow from the lowland into the margins was more common in 2014 compared with 2015, which was more dynamic and had more frequent flow reversals. Rainfall events elicited a larger WT rise in the margins relative to the lowland area, which resulted in an increase in the lateral hydraulic gradient, indicating a water flux from the margins to the lowland.

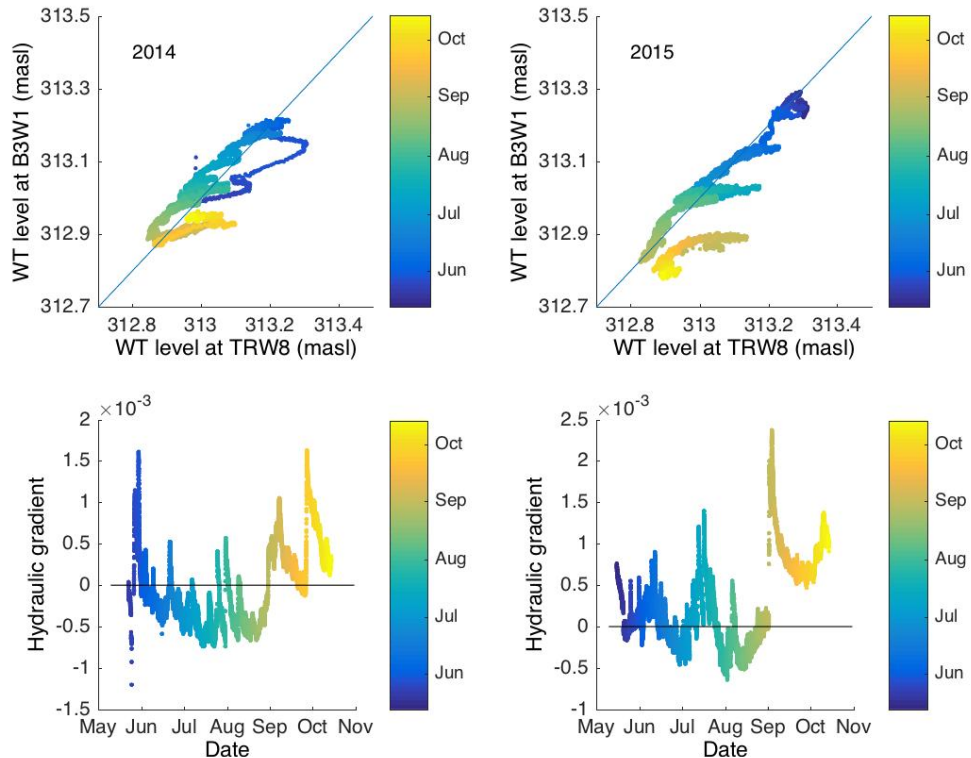


Figure 11 TOP: Water table level (in m asl) between the toe of a hummock (TR-W8) and the lowland (B3-W1). When above the 1:1 line, the horizontal hydraulic gradient (i.e., water flow) is from the lowland towards the hummock. BOTTOM: Hydraulic gradient (between well B3-W1 and TR-W8) over time during the 2014 and 2015 study periods. Positive values indicate flow towards the lowland, negative values indicate flow toward the hummock (Note the change in x-axis scale).

3.5 Runoff Processes

The SFW does not have a natural outlet and runoff process that generated outflow from SFW were not assessed. During the summer season when students were on site, no surface runoff was observed during rainstorms and therefore most lateral redistribution within the SFW was considered via subsurface pathways. However, in 2018, we conducted a detailed investigation of snowmelt runoff on two slopes (north and south facing) during the melt period to identify if lateral runoff occurred during melt. Note that winter 2017/18 was a relatively large snow year and melt was slightly earlier than normal (Figure 5).

Results from runoff collectors (Figure 12) on both collectors on hummocks 5 (south facing) and hummock 8 (north facing) generated runoff during freshet. The south-facing slope had meltwater generation approximately one month in advance of the north-facing slope (Figure 13). Between 15-20 March, 18 mm of runoff was collecting, representing 30% of the snowpack at this site. In contrast, melt on the north-face occurred between 12-24 April and generated 23 mm of water, providing a runoff ratio of ~40%. As will be discussed further, this suggests that hillslopes have the potential to generate runoff during the snowmelt period.

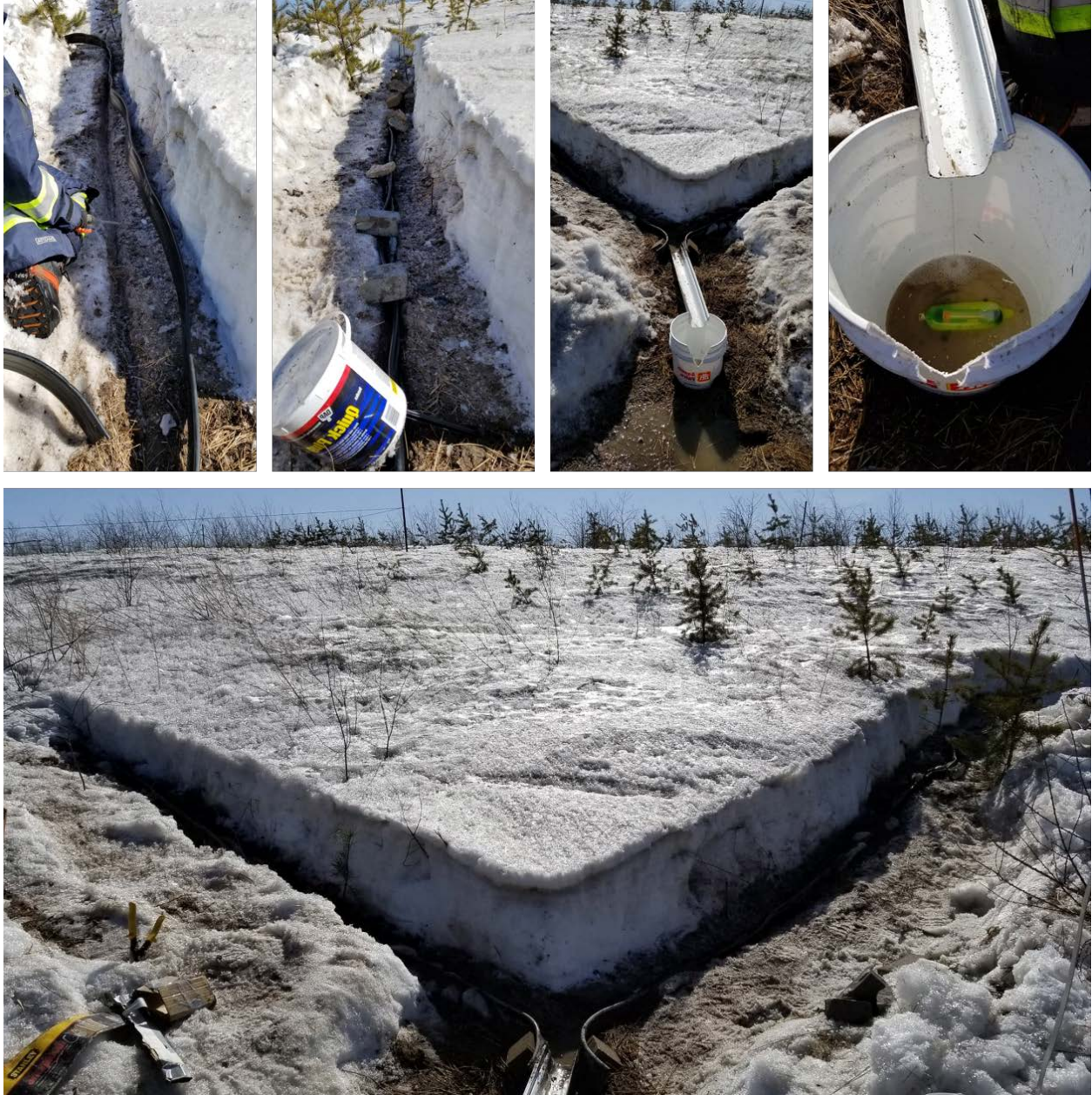


Figure 12 Construction and installation of the runoff collector on the Hummock 8 (north facing slope)

While runoff was not previously observed during storm events, the continued operation of the collector on the south-facing slope during summer of 2018 allowed for evaluation of whether summer rainfall generated runoff. Unsurprisingly, the 92 mm storm centred on 21 July generated 17 mm of runoff (30% runoff ratio), which was very large (Figure 14). However, all other events, even those of 30 mm, generated almost no runoff (all <0.1 mm). This type of runoff behaviour where large thresholds must be exceeded to generate runoff are widely observed. Surface runoff from hillslopes will not respond to most rain events, but in cases where high intensity rainfall exceeds infiltration capacity, overland flow will occur.

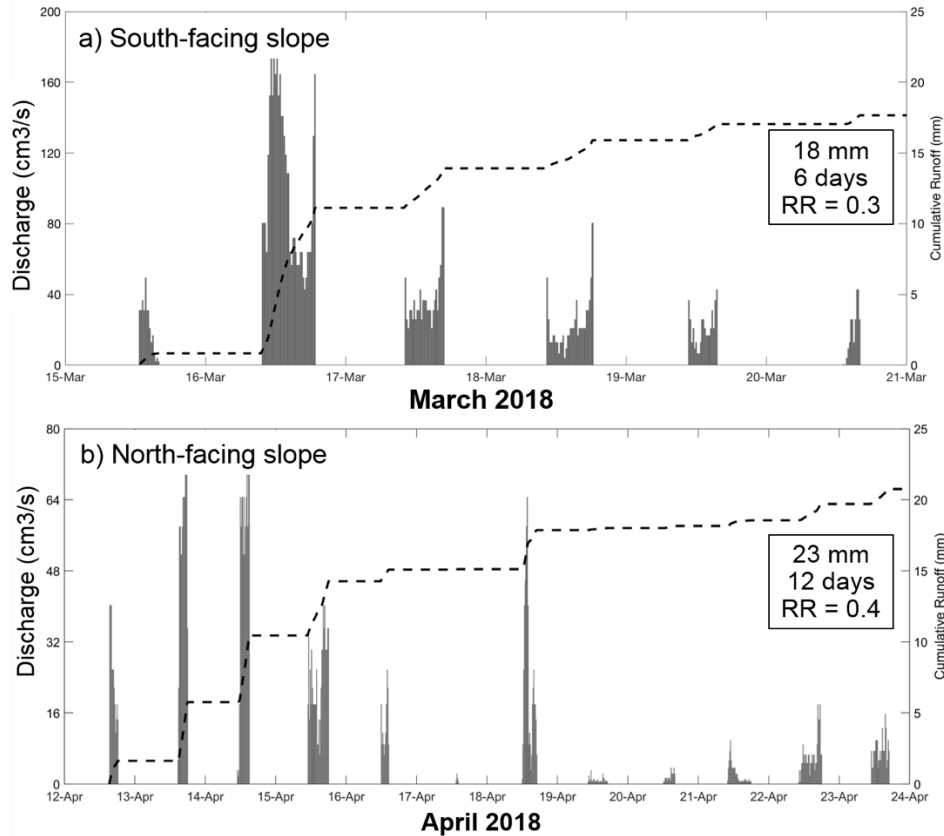


Figure 13 Half hour (grey bars) and total (black lines) runoff observed at the (a) south-facing, and (b) north facing runoff collectors during 2018 melt.

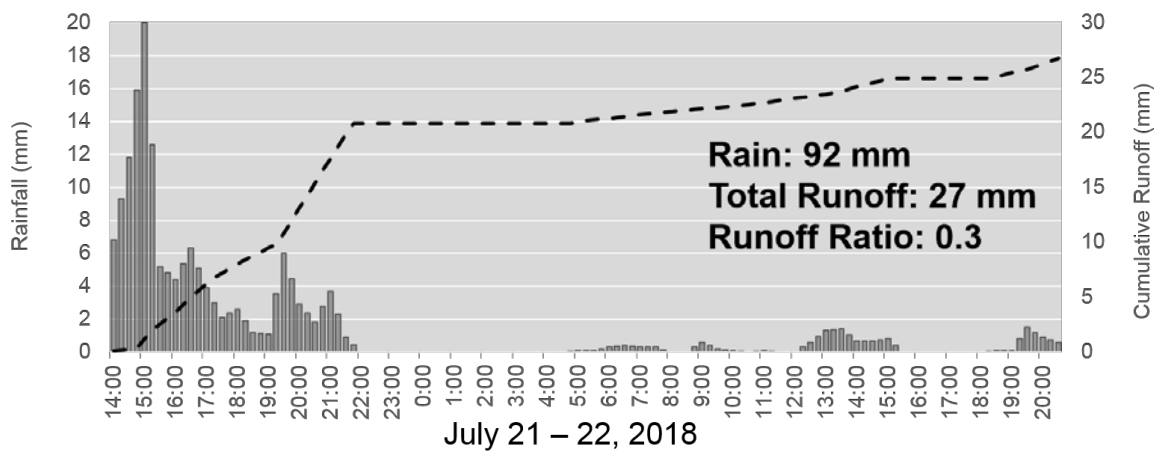


Figure 14 Rainfall (bars) and cumulative runoff (black dashed lines) during major storm even on 21-22 July 2018.

3.6 Annual Water Balance Components

Annual water flux totals are shown in Table 2. Note that there is considerable yearly variability in most of the terms, related both to management and to climate variability. In addition, the maximum snow water

equivalent is reported in the year that it melts. In certain years, inputs exceed outputs whereas in other years, outputs exceed inputs. It is challenging to ‘close’ the water balance without a distributed measure of storage, which is beyond the scope of this study, yet all fluxes in Table 2 are reported with medium (for pumps) to high (all other) confidence.

Table 2 Annual water balance components as measured at the SFW. NA means not measured and X means analysis in progress.

YEAR	Rain (mm)	Snow (mm)	Inflow to SFW - 52 ha (mm)	Outflow from SFW - 52 ha (mm)	Upland Evapotranspiration (mm)	Lowland Evapotranspiration (mm)
2013	329	138	284	289	324	381
2014	287	55	5	6	377	370
2015	196	58	0	18	371	373
2016	415	56	0	0	NA	337
2017	289	48	0	33	399	353
2018	415	105	0	63	X	X

Note that water balance components in Table 2 represent maximum snow water equivalent that would report to SFW in that given year.

4 Water Chemistry

While not part of the original research objectives, we began collecting water quality samples for major ions beginning 2013 to link hydrology and carbon processes to catchment biogeochemical processes. In addition, one MSc theses were completed to assess nutrient dynamics and availability in the SFW (Thorne, 2015), and to compare the DOC and nutrient quality of SFW with natural analogues (Rastelli, 2017). Results indicate that while the nitrogen speciation varies in SFW compared with three natural fens in the region, there is no notable nutrient limitation to plant growth in the SFW. Details on these studies are provided in the appended theses. Additional nutrient studies were completed under the Vitt research program.

4.1 Electrical Conductivity, Major Ions and Stable Isotopes

Major anions and cations along with total water salinity (as inferred by electrical conductivity - EC) were measured between 2013 and 2018 throughout SFW. Results during the first three years and the influence of water management on water salinity were summarized in Biagi (2015) and Biagi et al. (2019). Each month, surveys of EC were completed and interpolated yearly maps of salinity as averaged by monthly samples are shown in Figure 15. Note that there is some variance in sample location among the years. EC patterns varied within the year, largely in response to pumping in the early years, and also subtly in response to precipitation and evapo-concentration (Biagi et al., 2019). Once the water storage pond stopped supplying water to the lowland and outflow management declined, there was a general increase in average salinity at Boardwalks 1 and 2 at the upper part of the lowland with, with values near the outlet and Boardwalk 3 where there was consistent standing water remaining more consistent. Values in the upper lowland reached between 2-3000 $\mu\text{S}/\text{cm}$ by 2018, which is a slight increase from 2015 when management stopped. Value in the lower part of the fen near the outlet were also increasing year-over-year. The margins and uplands were the sites with the greatest salinization over the study period. By 2018, some sites between and adjacent to hummock 7 and 8 had EC > 6000 $\mu\text{S}/\text{cm}$. While there may have been some sample bias due to differences in timing of salinity surveys, these increases are considerable.

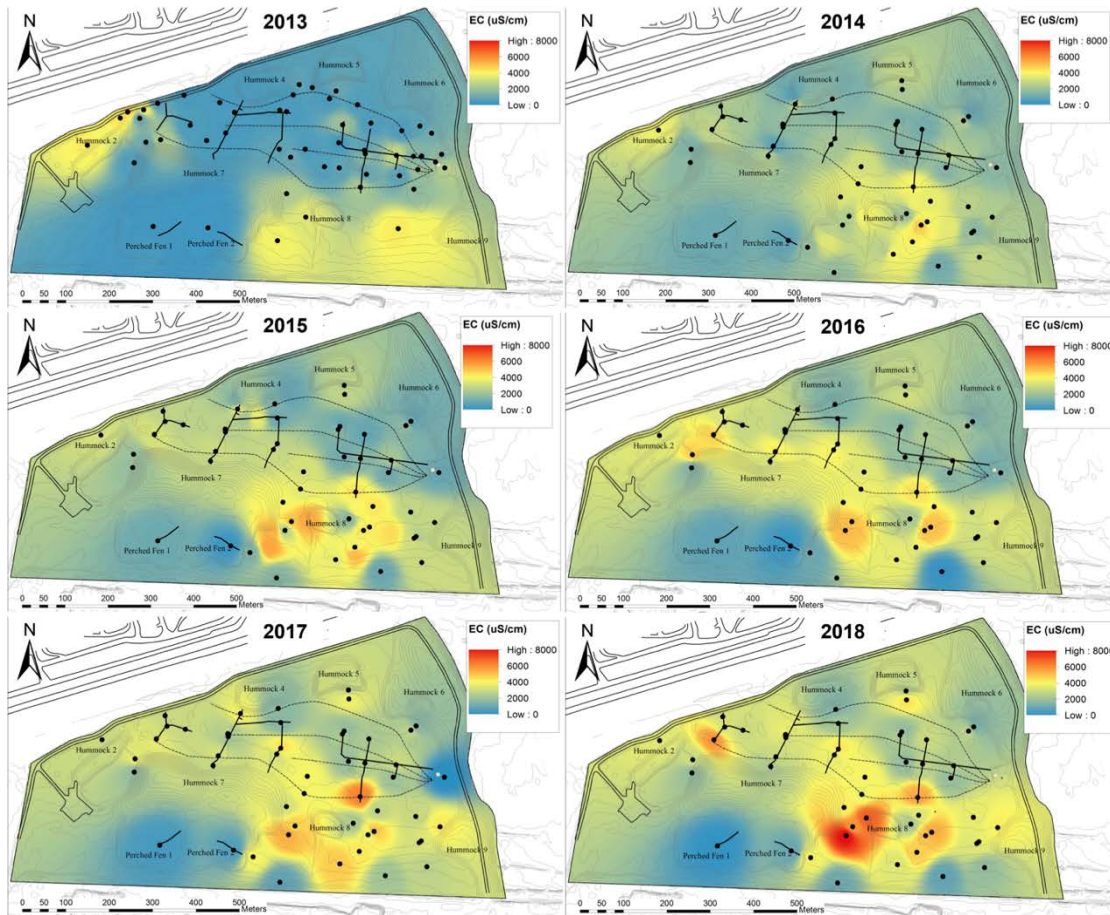


Figure 15 Average electrical conductivity at each water sampling site (black dots) for each of the study years.

Major ion concentrations followed a similar pattern to EC, as concentrations were low at the onset of the study and gradually increased (Biagi et al., 2019). While there is an overall increase in major ions, by focussing on Na^+ and Ca^{+2} , we can infer some of the major exchange processes and hydrological interactions within SFW. In 2013, Ca^{+2} exceeded Na^+ at most sites in the lowland and were relatively low. Following the cessation of water management, there began to form areas of Na^+ enrichment that occurred along the border between the base of the southern hummocks and lowlands where Na^+ was more than double other sites (in excess of 900 mg/L). In addition, sodium absorption ratio (SAR) was much higher at these sites than other areas of the SFW. Figure 16 shows the molar ratio of Ca^{+2} and Na^+ and their molarity in the lowland sampling wells for each year. While there was a slight decline reported in 2016 (likely due to reduced sampling), there has been a gradual increase in both the molarity and the relative ratio of Na^+ to Ca^{+2} with time.

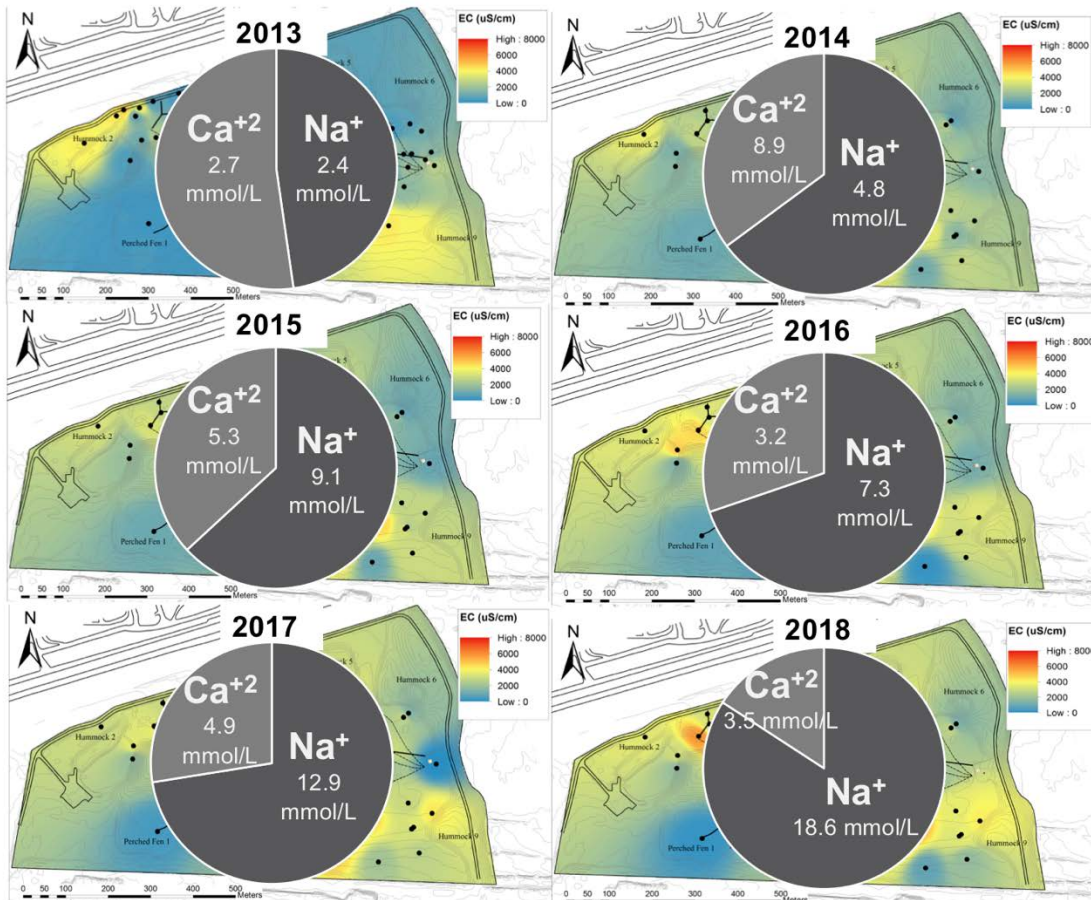


Figure 16 Molarity of Calcium and Sodium ions and their respective ratios for each study year.

4.2 Mercury

Due to the reported concern of mercury (Hg) deposition in the AOSR (Kirk et al., 2014), and downstream elevated Hg concentrations (Kelly et al., 2014), we implemented a study to compare the total mercury (THg) and methyl mercury (MeHg) concentration in the SFW to two nearby natural reference sites and to explore the drivers of MeHg production in the sediment and waters of SFW. Results of this work are published in Oswald and Carey (2016).

The concentrations of sediment THg and MeHg in the Sandhill Fen are on the low end of values measured in other constructed wetlands. The relatively low THg concentrations are likely a result of the higher amount of mineral soil incorporated into the Sandhill fen peat; however, the relatively low MeHg concentrations may be due to the high sulfate concentration of the constructed peat package. The majority of porewater MeHg concentrations measured in the Sandhill Fen fell between 0.02 and 1.0 ng/L with the exception of several samples exceeding 1.0 ng/L to a maximum of 4.3 ng/L. This range in values is similar to the values reported for other natural boreal peatlands and constructed wetlands. Filtered MeHg concentrations draining the wetland through the weir (0.21 ng/L) and the sand aquifer via the underdrains (0.091 ng/L) were on the low end of values from other constructed/created wetlands, but were similar to values from natural boreal systems in northwestern Ontario.

Owsald and Carey (206) found low levels of THg and MeHg in input, output and pore waters; however, the Sandhill Fen could be a source of MeHg to downstream ecosystems, especially during periods of water table fluctuation. The potentially exacerbating effect of elevated sulfate concentrations on MeHg production was not found in the Sandhill Fen. On the contrary, the exceptionally high sulfate levels in the system may be mitigating MeHg production; however, these may become problematic with respect to downstream MeHg production once drainage from the fen to a large wetland network is engineered. Further study of the chemical speciation of MeHg and Hg as it relates to sulphur cycling in this unique ecosystem is warranted

5 Carbon Processes

The annual carbon (C) balance of the SFW can be represented as

$$\Delta C_{\text{org}} = \text{NEP} + F_{\text{CH}_4} + \text{netDOC}_{\text{EX}} + \text{netPOC}_{\text{EX}}$$

Where ΔC_{org} is the annual change in C, NEP is the net ecosystem production, equal to the difference between uptake of CO_2 through photosynthesis and loss of CO_2 through aerobic decomposition and respiration integrated over the year, F_{CH_4} is the loss or gain of C through the annual integrated flux of methane (CH_4), $\text{netDOC}_{\text{EX}}$ is the net gain or loss of dissolved organic C and $\text{netPOC}_{\text{EX}}$ is the net gain or loss of particulate organic C.

Most studies of northern peatlands estimate a NEP between -20 to -30 $\text{g C m}^{-2} \text{y}^{-2}$ (the negative sign indicates a gain of C), $F_{\text{CH}_4} = 5 \text{ g C m}^{-2} \text{y}^{-2}$ and $\text{netDOC}_{\text{EX}} = 5\text{-}10 \text{ g C m}^{-2} \text{y}^{-2}$. There are no reported annual rates of $\text{netPOC}_{\text{EX}}$ from peatlands, and at the onset of the study we realized that these fluxes were minor and were not continued after the first few years.

5.1 Net Ecosystem Productivity

Net Ecosystem Productivity (NEP) is the reciprocal of Net Ecosystem Exchange (NEE). The two terms are used synonymously. When NEP is positive (negative), the site is as a carbon sink (source). When NEE is positive (negative), it is a carbon source (sink). NEP is the difference between the losses from Ecosystem Respiration (ER) and gains from Gross Ecosystem Respiration.

NEP was measured at the lowland tower throughout the entire year via AC power. Figure 17 represents the entire data set. Note that there are some gaps due to instrument malfunction. These gaps are filled in using different standard approaches so that each day, there is a photosynthesis and respiration numbers so that an annual NEP/NEE number can be provided. The upland tower only operated during the growing season because of power.

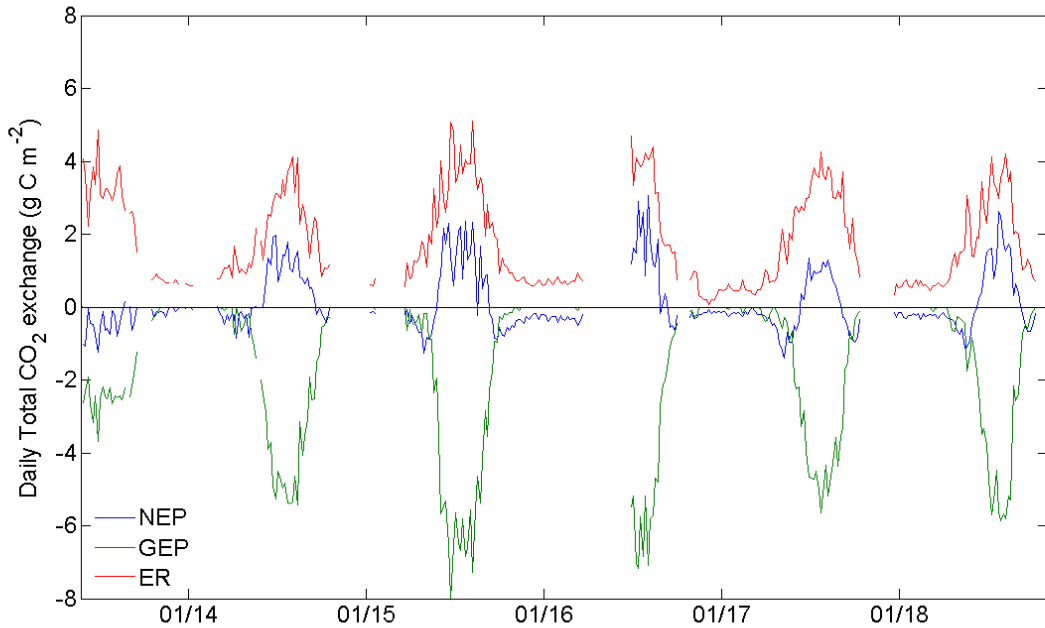


Figure 17 Net Ecosystem Productivity (NEP), Ecosystem Respiration (ER) and Gross Ecosystem Production for the lowland tower.

Gap-filled cumulative NEP at the lowland tower for the study years beginning in May (the onset of growth) is shown in Figure 18. When cumulative values are greater than zero, SFW is a CO₂ sink that year. When values are negative, SFW is a CO₂ source with respect to CO₂. In the first year before establishment, the lowland was a large source of CO₂ to the atmosphere and GEP was low due to limited photosynthesis. Following the establishment of vegetation, GEP and NEP increased rapidly and by the 2015 growing season, the SFW was likely a net carbon sink or carbon neutral. In 2016, the SFW lowland was a small C sink. However, beginning 2017, CO₂ uptake declined and the fen returned to being a carbon source.

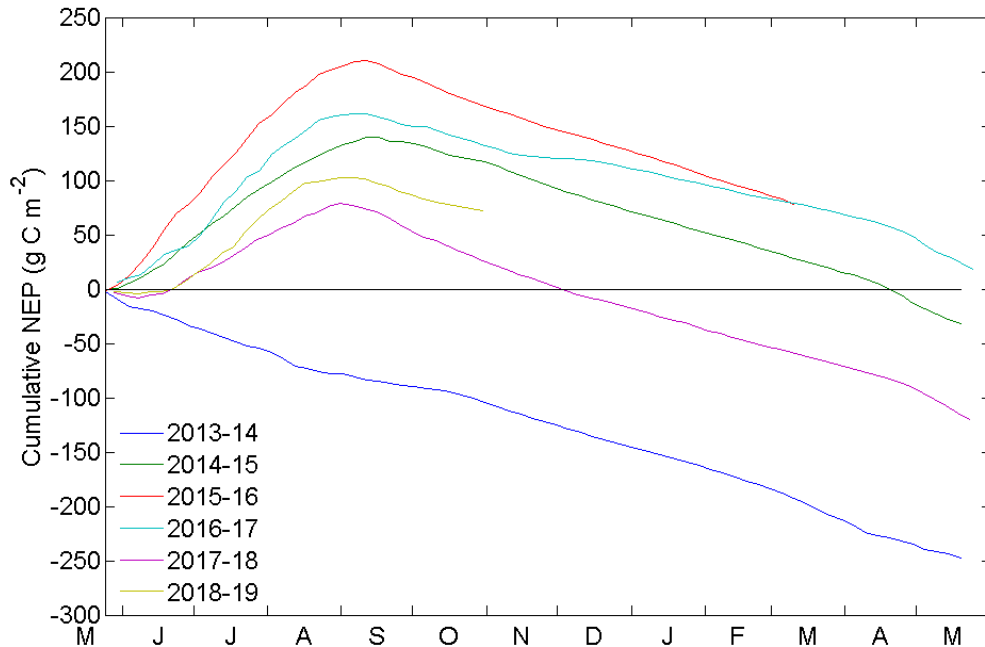


Figure 18 Cumulative Net Ecosystem production for growing season years at the lowland tower.

The decline in NEP at the lowland was not a result of climate differences, but likely from changes in vegetation composition in the footprint of the tower. Figure 19 shows the growing season (June to September) NEE at the lowland and upland towers. For the lowland site, there was a strong continuous uptake until 2016 and then a marked decline in 2017 with a slight recovery in 2018. Since 2015, there has been an increase in *Typha* and decline in *Carex*, which has greater ecosystem production than other wetland species.

The upland tower growing season NEE is distinct from the lowland (Figure 19). Once plants were established in 2013, photosynthesis began to systematically increase and NEE became more negative as vegetation developed. This increase has continued with 2017 and 2018 estimated as the growing season with the greatest carbon uptake.

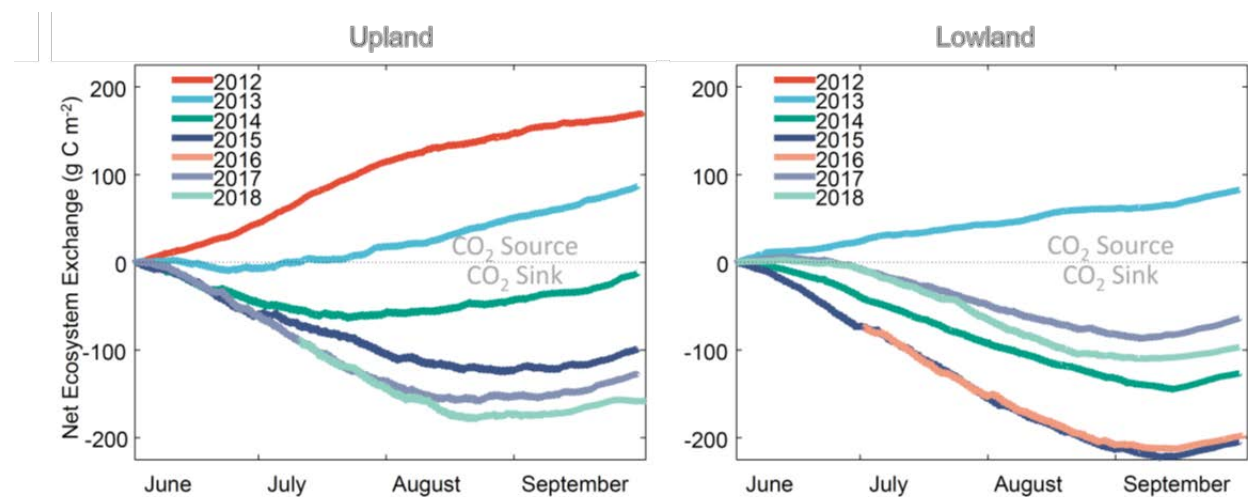


Figure 19 Cumulative growing season Net Ecosystem Exchange (NEE) for the upland and lowland towers. Early 2016 is estimated.

Ecosystem respiration at the upland site has increased with time, in part offsetting some of the photosynthetic gains in a net balance (Figure 20). Increased respiration with time is a function of increased soil biomass and decomposition of fresh litter. In contrast, the lowland had suppressed respiration and all temperatures and years due to saturated conditions.

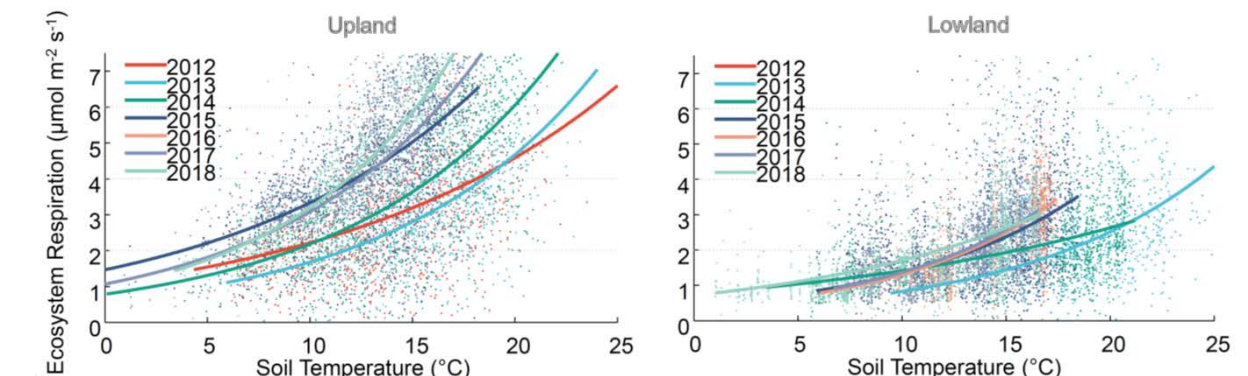


Figure 20 Ecosystem respiration and soil temperature for the upland and lowland towers. Lines of best fit are for individual years.

5.2 Methane

Methane was measured at a series of chambers which are discussed in detail in Clark (2018). In addition, CH₄ was measured at the lowland tower year-round using the eddy covariance technique. Methane fluxes from the lowland are low compared with those reported in the literature, with some changes seasonally and year-over-year. Methane emissions typically increase with increasing water table position within peatlands and among peatlands, and also tend to increase when drained peatlands are restored by flooding. However, CH₄ emissions in the present study unexpectedly remained very low over the three years despite the establishment of a high water table in the lowland areas of the SFW. Peak CH₄ fluxes from this system are 6 – 30% of the values published from other studies on rewetted peatlands. The fluxes observed in this study are instead similar to those reported from the other constructed wetland in the Alberta Oil Sands region (median CH₄ emissions below 0.08 mg m⁻² h⁻¹) (Murray et al., 2017). These results suggest that although the CH₄ emissions from the SFW are dissimilar from natural wetland systems, the REDOX potentials are low enough to deplete alternative electron acceptors from the substrate, and thus may be favourable to peat formation.

Over the study period, the only plots that showed increasing trends in CH₄ emissions over time were vegetated plots with standing water above the soil surface. The vegetation at these plots was primarily *Carex aquatilis*, and *Typha latifolia*, species with aerenchymatous tissues that enable plant-mediated transport of CH₄ to the surface. These species have been reported in the peatland restoration literature to promote CH₄ emissions. However, when examining July methane fluxes (when they would be expected to be greatest), there is no clear trend (Figure 22). In addition, emissions are below the IPCC emission factors for rewetted organic soil (IPCC 2013).

Soil salinity may also have impacted the CH₄ emissions from this wetland. Although the effects of salinity on CH₄ production are not well understood, Poffenbarger et al. (2011) reviewed the literature and found only polyhaline wetlands (18 ppt or ~24000 µS cm⁻¹) had suppressed CH₄ emissions.

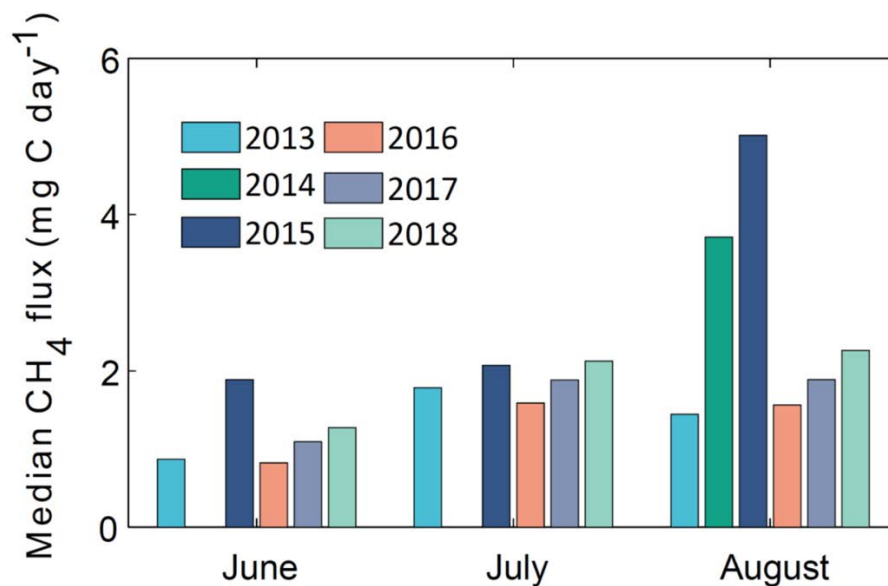


Figure 21 Median June-August methane flux for the study years.

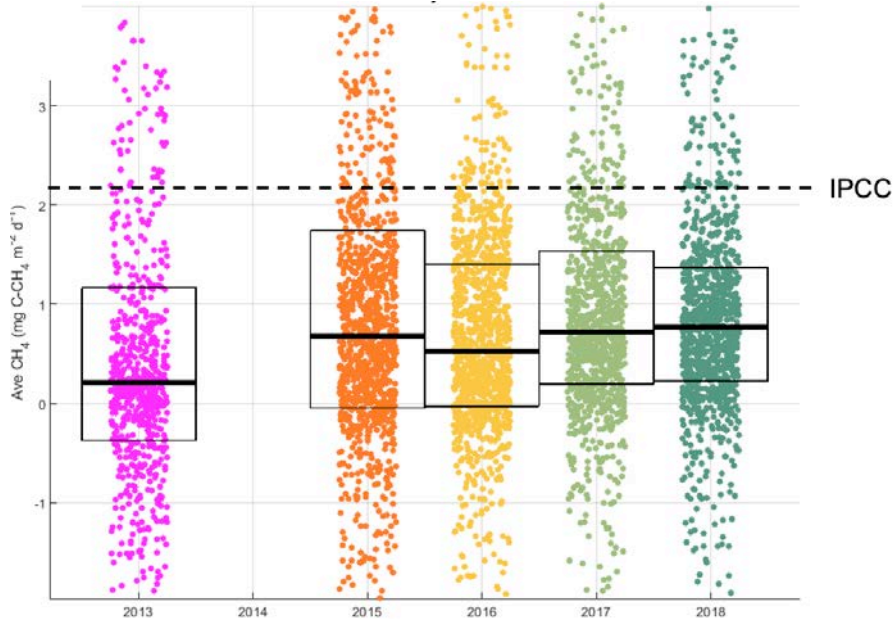


Figure 22 All half-hour methane fluxes for July over the course of the study. Black dash is IPCC emission factor associated with rewetted organic soils.

5.3 Dissolved Organic Carbon

DOC varied widely throughout the fen and is exhibiting an increase year-over-year from 2013 to 2018 (Figure 23). During the growing season, DOC increased each month throughout the growing season. In addition, DOC increased on average 6 mg/L per year from a baseline level of 14 mg/L in 2013. This increase is associated with a reduction in flushing that occurred during 2013, and an accumulation of organic matter associated with decomposition of new vegetation at SFW. Total export of carbon from DOC is low, ranging from 4 g/m² in 2013 when pumps were exporting large volumes of water to 2.6 g/m² in 2018. Note that this is a relatively small and invariant fraction compared to the GEP fluxes and is largely controlled by pumping volumes.

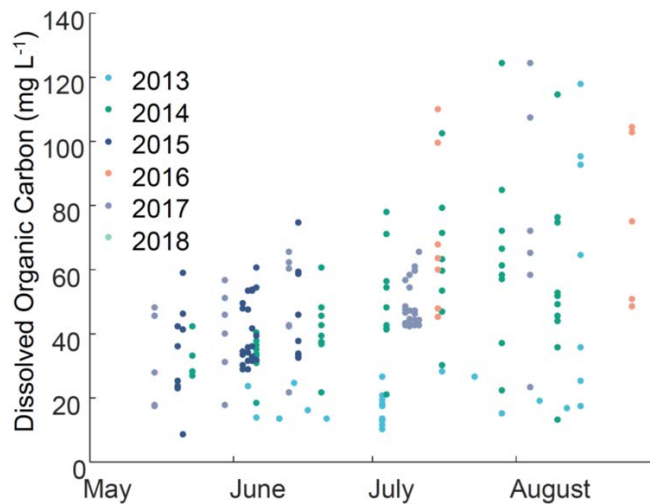


Figure 23 Porewater DOC concentration from lowland water during the study years.

Table 3 Dissolved organic carbon export from SFW by year.

YEAR	DOC Export (g/m ²)
2013	4.0
2014	0.1
2015	0.4
2016	0
2017	1.3
2018	2.6

6 Synthesis

The initial objectives of the SFW program was to test the viability of the technology to build an integrated upland-wetland system of soft tailings. Much of the design for this system, which occurred over a number of years, was the foundational knowledge provided by Drs. Kevin Devito and Carl Mendoza that arose from their findings in natural analog systems (see Devito et al., 2012). However, during the design and construction phase, a number of compromises were made for logistical and financial reasons that resulted in the SFW being ‘under-built’, with fewer and smaller hummock uplands and variances in soil material. Regardless, the SFW was an excellent platform to assess reclamation strategies with regards to upland-wetland systems. It is at a scale where landscape-level hydrological interactions can be observed and understood, it integrates many of the current reclamation practices, and while the heavily managed nature of the system will likely never be repeated, the learnings from this system will provide strong guidance for reclamation planning going forward and provide the information to regulators that demonstrate its success.

6.1 Is the Sandhill Fen Watershed Hydrologically Sustainable?

The SFW appears to be sustainable hydrologically, in that a saturated lowland area with wetland vegetation occurs that is supplied by flow from upland and regional areas via surface and groundwater pathways. However, there are a number of findings from this research program that here we will outline are primary factors that in part place the SFW at risk; the first of which is climate and weather. It is well established that the climate of the AOSR has variability that occurs over multiple cycles (~5 years and 15 years or longer) that oscillate between wet and dry. The SFW was constructed in a somewhat dry phase, as only two years had precipitation that would be considered above normal. Regardless, in all years, the SWF lowland remained wet and pumping of water was often required due to the lack of a natural outlet. While increasing precipitation during wet phases will help sustain wet areas, only with a constructed outlet will management of the system decline. One factor that must be considered is that as upland vegetation increases in density, less rainfall will reach the surface in the summer due to canopy interception. While this was not quantified during this research, aspen and spruce forests can intercept ~30-40% of summer rainfall at canopy closure, which will decrease soil moisture recharge and reduce the rewetting of soils from summer rain. In contrast, increasing forest covers will tend to increase snow retention and snow water equivalent, and delay melt to later in the year so that moisture can be more readily used by plants when demand is there. Finally, the AOSR is projected to become warmer and wetter as the century advances, with anticipated increases in intense summer convective precipitation. A change in precipitation regimes will influence the hydrology of the fen through a number of potential pathways that can be readily speculated, but difficult to truly know as both warming and wetting have opposite consequences in terms of wetland sustainability.

The greatest loss of water from the SFW now and likely in the future is evapotranspiration. Total ET ranged between 350-400 mm for the SFW in both lowlands and uplands, which compares well to values reported in the literature for boreal landscapes (Brümmer et al. 2012). ET for the uplands is slightly greater than the lowlands; an observation which has been reported elsewhere in the Boreal Plains. ET at the uplands site has not reached its peak rate, as Strielsky (2019) reported that ET increased at reclamation upland sites regardless of ecosystem for approximately 8-10 years, at which point it plateaued and had rates similar to those of reference forests. Figures 24 and 25 show the progression of the vegetation at the two towers. Leaf area index (a measure of transpiring area) continues to increase at the upland, which drives increases in transpiration until a relative equilibrium is achieved. In contrast, the fen site which smoother and has less vegetation can suppress ET by limiting turbulent transfer. If the water table is lowered and vegetation increases, ET rates would be expected to increase in the lowland. However, negative feedbacks associated with wetland soils would act to limit excessive drying from ET (Waddington et al., 2014).

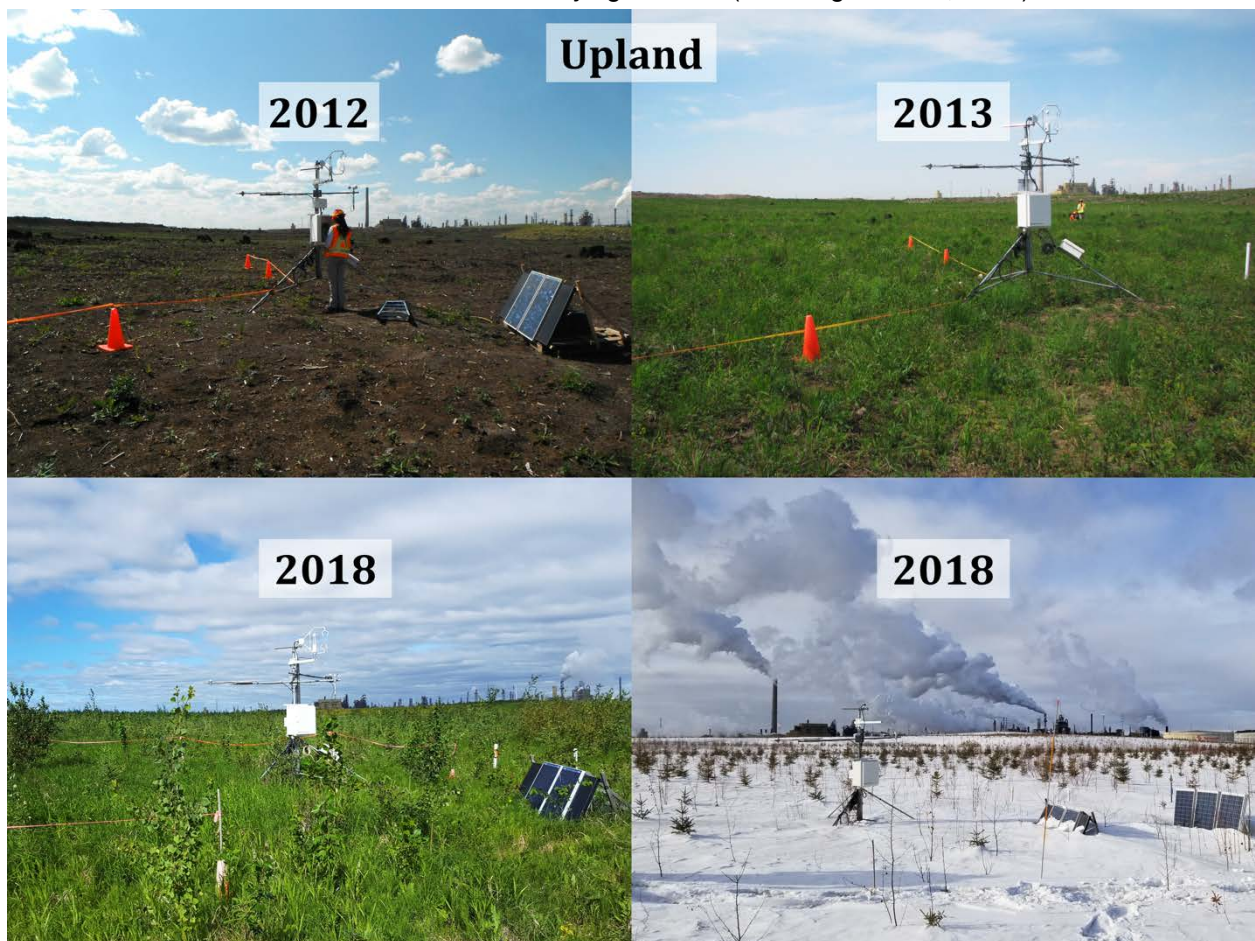


Figure 24 Progression of upland vegetation by year for the upland tower with photos in summer and winter for 2018.



Figure 25 Figure 24 Progression of upland vegetation by year for the lowland tower with photos in summer and winter for 2018.

The sustainability of wet conditions in the lowland relies on the continuous and intermittent supply of water. The Mendoza report outlines the local and regional hydrogeology of the fen, which indicates a regional hydraulic gradient that brings groundwater from the berm to south of the SFW into the watershed and then diverges in the lowland to the east towards Kingfisher watershed and also to the north at the upper part of the lowland near boardwalk 1. A critical consideration is that SFW sits within a broader regional hydrogeological context, and future wetland design, particularly at the landscape scale, must consider this. In terms of runoff processes within the SFW, we did observe snowmelt runoff from both north and south-facing hummocks during an average snow year in 2018 that provided water to the lowlands. It is unclear whether this runoff occurs in most years. The generation of runoff from the reclaimed slopes of the constructed Nikanotee fen was between 70-90% of the snowpack (Ketcheson and Price, 2016), and at this site was an important supplier of water to the lowlands. While rainfall-driven surface runoff was not previously during an intense summer rainfall event (>90mm, with very high hourly intensity), surface runoff was generated (Figure 14). However, there were numerous other rainfall events in 2018 (~30mm/day) that did not generate appreciable runoff. Surface runoff from berms and uplands are not considered a viable source of water for the lowlands over longer terms.

In the western Boreal region, hydrologic connections between landscape units, such as peatlands and uplands, are critical controls on the “eco-hydrologic functionality” of the system (Devito et al., 2005; Devito et al., 2012). In wet years, peatlands typically receive recharge from adjacent uplands, whereas during dry

periods, the peatlands can provide water to the adjacent uplands (Lukenbach et al., 2017; Thompson et al., 2015; Wells et al., 2017). Although the SFW is still in the early stages postconstruction, preliminary patterns of intermittent wetting have occurred at hummock–lowland transitions (Spennato et al., 2018). The rise in WT at the margins and increasing lateral hydraulic gradients provides evidence that local flow systems are developing and these landforms are supplying localized groundwater flow to the lowland yet is restricted to the edges of the hummocks. Although Thompson et al. (2015) indicate that peatlands in the WBP do not necessarily require significant inputs from regional groundwater or adjacent uplands, the small contribution from the hummocks to the lowland may help sustain wetness, yet longer term study is required to assess the importance of this process.

From a management perspective, reclaimed landscapes have hydrophysical properties based on construction materials and placement practice that can influence hydrological fluxes and interactions. At SFW, differing properties, notably the specific yield, of placed organic and mineral materials in combination with rainfall events supported water movement from margin areas to adjacent lowlands to support wetness during dry periods through short-term water storage. Although this influence is more subtle than large-scale engineered aquifers (Ketcheson et al., 2016) and the placement of upland landforms to enhance recharge (Devito et al., 2012; Wytrykush et al., 2012), it suggests that there are alternate approaches that can be utilized to help sustain wetlands and landscape-scale hydrological interactions. Efforts to incorporate a variety of landscape features (e.g., a mosaic of small and large hummocks together with larger scale engineered aquifers) that possess a range of water storage characteristics and timescales might serve to increase constructed wetland resiliency to climatic stressors over both the short- and long-term and warrant further investigation. There is concern, however, that upland areas with thick peat-mineral mixes are overbuilt with respect to soil storage, limiting supply of water for down-gradient ecosystems. In a modelling-based study of South Bison Hill, Huang et al., (2015) suggested that lateral redistribution and runoff can be strongly suppressed as soil covers become > 75 cm.

The size and geometry of the hummocks and the method of placement also influences the interpretation of these results as hummocks were mechanically placed dry whereas future designs are being implemented with hummocks that are hydraulically placed wet with tailings water. The water exchanges and flow reversals along hummock margins observed in this study suggest that aligning smaller hummocks with shorter storage timeframes in close proximity to the lowland boundary can provide a short-term water supply. However, flow reversals (i.e., hydraulic gradients from lowland to margin) suggest that additional longer-term sources of water from aquifers with different properties are advantageous. Further research is required to assess how hummock size, geometry, placement method (wet vs. dry), and water storage timescales can be optimized.

6.2 What is driving the changes in salinity?

The SFW has had large changes in salinity as outlined in Section 3. In 2013 when the study began, the combination of freshwater supply, open underdrains and frequent discharge at the outlet kept salinity levels reduced across the lowlands. While there were several heavy rainfall events, the relative volume of water added from the rainfall events (~100 mm over the season) was small compared to the volume of water added and removed from pumping (~800 mm to the lowland), which likely overshadowed atmospheric influences on hydrochemistry. Frequent pumping resulted in large variations in the water table, EC and ion concentrations in response to both inflow and outflow. Outlet water had the highest Na⁺ concentrations and SAR in 2013 due to the active removal of both surface and subsurface waters that contained OSPW. Most sites across SFW exhibited low EC, Na⁺ concentrations and SAR values which indicates the limited

influence of OSPW, most of which was discharged through the underdrains, and the addition of fresh water from the water storage pond. While sampling was more limited at the margins in 2013, early evidence of an enriched zone of upwelling OSPW was present in late 2013 near Boardwalk 1 when the underdrains were inactive. When the underdrains were active, OSPW was effectively moved to the drains and hydraulic gradients were downward, keeping the wetland water relatively fresh.

In May 2014, the underdrains were closed and except for a short inflow event, no water from the storage pond was added past this point. Controlled drainage events occurred in each year except 2016. As a result, the changes in hydrochemistry were largely controlled by vertical atmospheric fluxes as rainfall events increased the water table, which gradually declined throughout the season in response to evapotranspiration. As surface waters became stagnant without any inflow or drainage through the outlet, EC and ion concentrations increased. Despite the overall increase in ion concentrations in the lowlands, most sites had relatively low SAR values, indicating little influence of Na⁺ sources at these sites and suggesting evapo-concentration during dry periods and dissolution of salts in the unsaturated zone as a mechanism for increased salinity during rainfall. This pattern began to change in 2017 when across the fen, the molarity of both Ca⁺² and Na⁺ began to increase, as well as the ratio of sodium to calcium. Whereas rainfall itself acts to dilute the system, residual salts can complicate the influence of precipitation on salinity. A notable change under the less managed hydrological regime post 2014 was elevated Na⁺ concentrations at certain sites along the margin between the southern hummocks (hummocks #2, 7, and 8) and the lowlands, where OSPW is presumed to be discharging from depth in the near-surface. These areas exhibited Na⁺ concentrations and SAR values more than two-fold of those observed at all other sites across SFW, indicating they are more active areas of cation exchange between Ca⁺² and Na⁺ as a result from the input of Na⁺-rich waters from OSPW. These increases have occurred through 2018. Soils are considered saline-sodic when EC and SAR are >4000 $\mu\text{S}/\text{cm}$ and 13, respectively. Reported Na⁺ concentrations in composite tailings and OSPW range between 690 and 1100 mg/L while Ca⁺² is <100 mg/L (Renault et al., 1998; Renault et al., 1999; Leung et al., 2003; Zubot, 2010; Zubot et al., 2012), indicating OSPW presence in the SFW. Stable isotopes further support the emergence of OSPW in these Na⁺-rich areas, as OSPW has a distinct isotopic signature as a result of the industrial refining process (Baer et al., 2016). In contrast, stable isotopes of surface water in the wetland plot along the local evaporation line, and near-surface groundwater plot along the local meteoric water line and have more negative $\delta^2\text{H}$ and $\delta^{18}\text{O}$ signatures (Biagi et al., 2019).

The overall hydrogeological flow pattern transports OSPW in deeper groundwater moving from the south to northeast in the 10-m sand cap which emerges along the margins of hummocks 2, 7 and 8 via a combination of advection and diffusion (BGC Engineering Inc., 2015). These hummocks (2, 7 and 8) provide a preferential pathway for the transport of OSPW to the surface, as they are constructed of tailings sand material that has a high horizontal and vertical saturated hydraulic conductivity ($K_h = 10^{-4}$ m/s, $K_v = 10^{-5}$ m/s) and are the only areas without a clay layer present. As the tailings sand in the hummocks is two to three orders of magnitude greater than the clay layer ($K_{h,v} = 10^{-7}$ m/s), the deep groundwater that transports OSPW can emerge at the base of the hummocks between the tailings sand material in the hummock and the clay-underlain areas. There is some evidence that OSPW may be occurring at the base of hummock 5 and becoming more widespread and mixed throughout surface based on results in 2017 and 2018. Based on the results of Lindsay, we do not believe this increase is from diffusion in the clay layer at the base of the lowland.

There are a number of factors that may influence the salinity of SFW that were not assessed in this study. (1) When the SFW was initially saturated in 2013, solubility reactions would result in a sitewide increase in

water salinity, yet the rate of these reactions is uncertain. The rapid pumping did not allow for an observation in salinity changes associated with this initial wetting, yet we assume by 2014 a relative measure of equilibrium was achieved. (2) There were differences in weather among the years, which although in 2013 had a reduced influence on salinity patterns, may exert an important role over longer-term as the Western Boreal Plain undergoes considerable long-term cycles in climate that strongly influence the presence of water on the landscape. (3) The vegetation within SFW continues to change rapidly (Vitt et al., 2016), and although their influence on system chemistry it has been documented in natural systems (Chee and Vitt, 1989; Vitt and Chee, 1990), the influence of vegetation assemblages on salinity at SFW is unknown.

6.3 Will the Sandhill Fen become a carbon sink?

The carbon balance of the SFW is an integrated indicator of its overall health and sustainability. As natural uplands and wetlands are weak to moderate carbon sinks, and carbon sequestration is an indicator of plant growth, there is considerable value in tracking the annual carbon budget of reclamation ecosystems. There have been considerable changes in the annual and growing season carbon budgets for both the lowlands and the uplands that reflect the establishment of vegetation, changes in vegetation type, climate and the overall excessive wetness of the lowland portion of the SFW. The magnitude of growing season production and respiration was usually greatest at the upland and lowest at the lowland. Overall, the year-over-year increase in ER throughout the SFW did not keep pace with the increase in GEP at the upland tower, yet NEE continued to increase as the upland forest grew.

The SFW lowland NEE is within the wide range of annual NEE observed for northern peatland ecosystems. For example, NEE ranged from $-88 \text{ g C m}^{-2} \text{ y}^{-1}$ to $-14 \text{ g C m}^{-2} \text{ y}^{-1}$ in a recent review of 11 northern peatlands by Petrescu et al., (2015). In another example, the range was -101 to $+98 \text{ g m}^{-2} \text{ y}^{-1}$ in minerotrophic peatlands and 85 to $+67 \text{ g C m}^{-2} \text{ y}^{-1}$ in ombrotrophic peatlands in a review of eight boreal peatlands by Saarnio et al., (2007). In 12 northern peatland and tundra sites reviewed by Lund et al. (2010), annual NEE was $-103 \pm 103 \text{ g C m}^{-2}$. Many of these annual rates of net CO₂ uptake exceed the apparent long-term accumulation of $19.4 \pm 2.1 \text{ g C m}^{-2} \text{ y}^{-1}$ based on an assessment of peat age-depth models for western Canadian boreal peatlands (Vitt et al., 2000). This may occur in part because the peat core records would represent the full long-term C budgets including C lost through aquatic pathways, CH₄ emissions and disturbances (i.e. fire). However, NEE is typically the largest term in a northern peatland's C budget.

Because of the difficulty in monitoring NEE over the winter months, the majority of studies report seasonal NEE. NEE at an extreme-rich fen in northern Alberta was -35 , -154 and -42 g C m^{-2} per growing season (May-Oct) over 3 years (2004 - 2006) while NEE at a poor fen in the same region was similar in all 3 years with an average of 110 g C m^{-2} (Adkinson et al., 2011). NEE at the SFW lowland during the same months in year 3 was -155 g C m^{-2} . Cai et al., (2010) reported a seasonal (June-September) NEE of -282 and -207 g C m^{-2} over 2 growing seasons at a treed fen in northern Alberta which is comparable to the lowland's -212 g C m^{-2} in 2015 for the same months. However, GEP and ER at this Alberta treed fen was greater than at the SFW lowland. Greater GEP and ER were likely due to a greater abundance of vegetation at the treed fen where LAI was 2.6 ± 0.2 compared to 2.1 ± 0.9 at the SFW lowland in year 3. Humphreys et al. (2006) compared midsummer (July and August) NEE for seven Canadian peatlands including the Alberta peatlands discussed above. The mean midsummer NEE was $-1.5 \pm 0.2 \text{ g C m}^{-2} \text{ d}^{-1}$ for all seven peatlands in that study, which is within the range observed at SFW. The SFW lowland nighttime ER was at the lower range of values presented by Humphreys et al., (2006).

Whereas the SFW has a CO₂ budget that is comparable to reference ecosystems, methane and DOC fluxes were low. The causes for reduced methane fluxes are discussed in section 5.2 and are likely due to REDOX potentials and high sulfate concentrations. Further details are also reported in Clark (2018), yet low CH₄ fluxes are a characteristic of constructed wetlands elsewhere in the AOSR (Murray et al., 2017).

Dissolved organic carbon (DOC) fluxes were also low compared with natural wetlands (Nilsson et al., 2008; Roulet et al., 2007). While DOC concentrations are reaching levels that are similar to natural wetlands, the lack of an outflow and reduced discharge limit the export of DOC from the SFW. It is expected in the future that this flux will increase with time. The quality of the DOC in the SFW is also changing as plant decomposition increases (see Rastelli 2017 for details), and is similar to reference sites.

7 Future Research Directions

The Sandhill Fen Watershed is a unique and outstanding research facility that should continue to be a focus of environmental and reclamation research going forward. It has 7 years of data through 2019, which places it in an unprecedented position as one of the longest-monitored constructed watersheds in the world. It will continue to provide peer-reviewed scientific findings that form the basis for certification. As has been demonstrated previously, long-term research and monitoring provide unprecedented knowledge above that which is obtained from shorter target-specific questions because as ecosystems evolve, new insights are obtained opportunistically. This is particularly important considering the nature of climate variability and projected change in this region.

Hydrologically, it is important to understand the changes to the SFW as it is tied into the surrounding landscape. With a defined outlet into the down-gradient Kingfisher watershed, and ongoing reclamation in East-in Pit, the boundary conditions that control the drainage of surface water and hydrogeological flow field will be altered. It is anticipated that with a defined outlet, water levels in the lowland will decline, reducing the ubiquitous standing water. The opportunity that a defined outlet (sill) provide to alter SFW are numerous. Lowering the water table will alter vegetation species, potentially reducing the presence of *Typha* and provide a shift to more carbon-accumulating wetland species. A sill will also change the timing and volume of water discharge, influencing the overall chemistry of the fen through enhanced drainage potentials.

As the SFW changes, vegetation will shift, influencing hydrological partitioning as outlined earlier. Whereas there has been considerable research understanding how ET trajectories change with time in upland forests (Strilesky 2019; Strilesky et al., 2017), similar information does not exist for wetlands and how different species influence ET. In addition, we do not have a clear understanding of how changing vegetation influences recharge processes, particularly on hummocks which are thought to be critical for recharge provision of water. It is recommended that additional research on the role of vegetation and interception on recharge be completed.

We have nascent understanding of the role the hummocks play. While not as large as originally intended, it is important to more thoroughly understand what role hummocks and other uplands play over time. We recommend instrumenting in more detail a number of transects to more carefully observe upland-lowland hydrological interactions. It is interesting to observe that construction practice alone may have the greatest influence on the generation of surface runoff. For the constructed Nikanotee watershed, snowmelt runoff

ratios were between 0.7-0.9 (Ketcheson and Price, 2016), compared with 0.3-0.4 observed in 2018. As new uplands are being built, fundamental research on hillslope hydrology and its relation to construction practice and soil placement should occur.

Perhaps the greatest risk to the SFW as a functioning ecosystem is salinization, resulting in plant mortality. Ongoing monitoring of water quality is essential, as is research identifying the source, transformation and fate of salts within the system. As salt movement is related to hydrological flow pathways, an integrated fully-coupled research program is recommended. Note that we anticipate the salinity to change in response to the creation of a sill.

In terms of carbon, it is still unresolved as to whether the SFW will evolve into a peat-forming ecosystem. At present, the system is too wet to promote peat-forming wetland species and is a weak carbon source, yet we anticipate that this will change in the future. At present, methane and DOC fluxes are low, limiting carbon loss, yet it is uncertain as to whether these low fluxes will continue in the future.

Finally, Waddington et al., (2015) outline the negative feedbacks that allow wetlands to be sustainable, and one of the most important is the development of a characteristic organic soil profile with regards to physical properties. While peat was salvaged and placed in the wetland, the soil profile does not mirror natural ecosystems, and it is important to assess once drier if reclamation soils are effective in promoting wetland sustainability.

8 References

- Adkinson, A.C., Syed, K.H., Flanagan, L.B., 2011. Contrasting responses of growing season ecosystem CO₂ exchange to variation in temperature and water table depth in two peatlands in northern Alberta, Canada. *J. Geophys. Res.* 116, G01004. <https://doi.org/10.1029/2010JG001512>
- Amiro, B.D., Barr, A.G., Barr, J.G., Black, T.A., Bracho, R., Brown, M., Chen, J., Clark, K.L., Davis, K.J., Desai, A.R., Dore, S., Engel, V., Fuentes, J.D., Goldstein, A.H., Goulden, M.L., Kolb, T.E., Lavigne, M.B., Law, B.E., Margolis, H.A., Martin, T., McCaughey, J.H., Misson, L., Montes-Helu, M., Noormets, A., Randerson, J.T., Starr, G., Xiao, J., 2010. Ecosystem carbon dioxide fluxes after disturbance in forests of North America. *J. Geophys. Res. Biogeosciences* 115. <https://doi.org/10.1029/2010JG001390>
- Baer, T., Lee Barbour, S., Gibson, J.J., 2016. The stable isotopes of site wide waters at an oil sands mine in northern Alberta, Canada. *J. Hydrol.* <https://doi.org/10.1016/j.jhydrol.2016.08.017>.
- Baldocchi, D., Falge, E., Gu, L., Olson, R., Hollinger, D., Running, S., ... & Fuentes, J., 2001. FLUXNET: A new tool to study the temporal and spatial variability of ecosystem-scale carbon dioxide, water vapor, and energy flux densities. *Bulletin of the American Meteorological Society*, 82(11), 2415-2434.
- BGC Engineering Inc., 2015. Sandhill Fen Numerical - Numerical Groundwater Modeling (DOI: Project No: 0534135).
- Biagi, K.M., 2015. Understanding flow pathways, major chemical transformations and water sources using hydrochemical data in a constructed fen, Alberta, Canada. 96 pp. McMaster University.
- Biagi, K.M., Oswald, C.J., Nicholls, E.M., Carey, S.K., 2019. Increases in salinity following a shift in hydrologic regime in a constructed wetland watershed in a post-mining oil sands landscape. *Sci. Total Environ.* 653, 1445–1457. <https://doi.org/10.1016/j.scitotenv.2018.10.341>
- Brümmer C, Black TA, Jassal RS, Grant NJ, Spittlehouse DL, Chen B, Nesic Z, Amiro BD, Arain MA, Barr AG, et al. 2012. How climate and vegetation type influence evapotranspiration and water use efficiency in Canadian forest, peatland and grassland ecosystems. *Agricultural and Forest Meteorology* 153: 14–30. DOI: 10.1016/j.agrformet.2011.04.008
- Cai, T., Flanagan, L.B., Syed, K.H., 2010. Warmer and drier conditions stimulate respiration more than photosynthesis in a boreal peatland ecosystem: Analysis of automatic chambers and eddy covariance measurements. *Plant, Cell Environ.* 33, 394–407. <https://doi.org/10.1111/j.1365-3040.2009.02089.x>
- Chee, W.-L.L., Vitt, D.H., 1989. The vegetation, surface-water chemistry and peat chemistry of moderate-rich fens in Central Alberta, Canada. *Wetlands* 9 (2), 227–261.
- Clark, M.G., 2018. The initial biometeorology of the constructed Sandhill Fen Watershed in Alberta, Canada. Carleton University. 192 pp.
- Daly, C., Price, J., Rezanezhad, F., Pouliot, R., Rochefort, L., Graf, M.D., 2012. Initiatives in oil sand reclamation: considerations for building a fen peatland in a post-mined oil sands landscape. *Restoration and Reclamation of Boreal Ecosystems: Attaining Sustainable Development*. Cambridge University Press, Cambridge, pp. 179–198.
- Devito, K., Creed, I., Gan, T., Mendoza, C., Petrone, R., Silins, U., Smerdon, B., 2005. A framework for broad-scale classification of hydrologic response units on the Boreal Plain: is topography the last thing to consider?, *Hydrological Processes*, 19, 1705–1714. <https://doi.org/10.1002/hyp.5881>
- Devito, K., Mendoza, C., Qualizza, C., 2012. Conceptualizing Water Movement in the Boreal Plains: Implications for Watershed Reconstruction. Synthesis report prepared for the Canadian Oil Sands Network for Research and Development, Environmental and Reclamation Research Group; 164 pp.
- Elmes, M. C., Price, J. S., 2019. Hydrologic function of a moderate-rich fen watershed in the Athabasca Oil Sands Region of the Western Boreal Plain, northern Alberta. *Journal of Hydrology*, 570, 692-704.
- Huang, M., Barbour, S.L., Carey, S.K., 2015. The impact of reclamation cover depth on the performance of reclaimed shale overburden at an oil sands mine in Northern Alberta, Canada. *Hydrol. Process.* 29, 2840–2854. DOI: 10.1002/hyp.10229
- Humphreys, E.R., Lafleur, P.M., Flanagan, L.B., Hedstrom, N., Syed, K.H., Glenn, A.J., Granger, R., 2006. Summer carbon dioxide and water vapor fluxes across a range of northern peatlands. *J. Geophys. Res. Biogeosciences* 111. <https://doi.org/10.1029/2005JG000111>

- IPCC, 2013. 2013 Supplement to the 2006 IPCC Guidelines for National Greenhouse Gas Inventories: Wetlands. IPCC Switzerland.
- Kelly, E.N., Schindler, D.W., Hodson, P.V., Short, J.W., Radmanovich, R., Nielsen, C.C., 2010. Oil sands development contributes elements toxic at low concentrations to the Athabasca river and its tributaries. *Proc. Natl. Acad. Sci. U. S. A.* 107 (37), 16178e16183.
- Ketcheson, S. J., Price, J. S., 2016. Comparison of the hydrological role of two reclaimed slopes of different ages in the Athabasca oil sands region, Alberta, Canada. *Canadian Geotechnical Journal*, 53(9), 1533-1546.
- Ketcheson, S.J., Price, J.S., Carey, S.K., Petrone, R.M., Mendoza, C.A., Devito, K.J., 2016. Constructing fen peatlands in post-mining oil sands landscapes: challenges and opportunities from a hydrological perspective. *Earth Sci. Rev.* 161, 130–139. <https://doi.org/10.1016/j.earscirev.2016.08.007>.
- Kirk, J., Muir, D.C.G., Gleason, A., Wang, X., Frank, R., Lehnher, I., Wrona, F., 2014. Atmospheric deposition of mercury and methylmercury to landscapes and waterbodies of the Athabasca oil sands region. *Environ. Sci. Technol.* 48, 7374e7383.
- Leung, S.S., MacKinnon, M.D., Smith, R.E.H., 2003. The ecological effects of naphthenic acids and salts on phytoplankton from the Athabasca oil sands region. *Aquat. Toxicol.* 62, 11–26. [https://doi.org/10.1016/S0166-445X\(02\)00057-7](https://doi.org/10.1016/S0166-445X(02)00057-7).
- Lukenbach, M. C., Hokanson, K. J., Devito, K. J., Kettridge, N., Petrone, R. M., Mendoza, C. A., 2017. Post-fire ecohydrological conditions at peatland margins in different hydrogeological settings of the Boreal Plain. *Journal of Hydrology*, 548, 741–753. <https://doi.org/10.1016/j.jhydrol.2017.03.034>
- Lund, M., Lafleur, P.M., Roulet, N.T., Lindroth, A., Christensen, T.R., Aurela, M., Chojnicki, B.H., Flanagan, L.B., Humphreys, E.R., Laurila, T., Oechel, W.C., Olejnik, J., Rinne, J., Schubert, P., Nilsson, M.B., 2010. Variability in exchange of CO₂ across 12 northern peatland and tundra sites. *Glob. Chang. Biol.* 16, 2436–2448. <https://doi.org/10.1111/j.1365-2486.2009.02104.x>
- Moreno-Mateos, D., Power, M.E., Comín, F.A., Yockteng, R., 2012. Structural and functional loss in restored wetland ecosystems. *PLoS Biol.* 10. <https://doi.org/10.1371/journal.pbio.1001247>
- Murray, K.R., Barlow, N., Strack M. 2017. Methane emissions dynamics from a constructed fen and reference sites in the Athabasca Oil Sands Region, Alberta, *Science of The Total Environment*, 583, 369-381. <https://doi.org/10.1016/j.scitotenv.2017.01.076>.
- Nicholls, EM. 2015. Multi-year water balance dynamics of a newly constructed wetland, Fort McMurray, Alberta. McMaster University. 115 pp.
- Nicholls, E.M., Carey, S.K., Humphreys, E.R., Clark, M.G., Drewitt, G.B., 2016. Multi-year water balance assessment of a newly constructed wetland, Fort McMurray, Alberta. *Hydrol. Process.* <https://doi.org/10.1002/hyp.10881>.
- Nilsson, M., Sagerfors, J., Buffam, I., Laudon, H., Eriksson, T., Grelle, A., Klemmedtsson, L., Weslien, P., Lindroth, A., 2008. Contemporary carbon accumulation in a boreal oligotrophic minerogenic mire - A significant sink after accounting for all C-fluxes. *Glob. Chang. Biol.* 14, 2317–2332. <https://doi.org/10.1111/j.1365-2486.2008.01654.x>
- Oswald, C. J., Carey, S. K., 2016. Total and methyl mercury concentrations in sediment and water of a constructed wetland in the Athabasca Oil Sands Region. *Environmental Pollution*, 213, 628-637. <https://doi.org/10.1016/j.envpol.2016.03.002>
- Petrescu, A.M.R., Lohila, A., Tuovinen, J.-P., Baldocchi, D.D., Desai, A.R., Roulet, N.T., Vesala, T., Dolman, A.J., Oechel, W.C., Marcolla, B., Friborg, T., Rinne, J., Matthes, J.H., Merbold, L., Meijide, A., Kiely, G., Sottocornola, M., Sachs, T., Zona, D., Varlagin, A., Lai, D.Y.F., Veenendaal, E., Parmentier, F.-J.W., Skiba, U., Lund, M., Hensen, A., van Huissteden, J., Flanagan, L.B., Shurpali, N.J., Grünwald, T., Humphreys, E.R., Jackowicz-Korczyński, M., Aurela, M. a, Laurila, T., Grüning, C., Corradi, C. a R., Schrier-Uijl, A.P., Christensen, T.R., Tamstorf, M.P., Mastepanov, M., Martikainen, P.J., Verma, S.B., Bernhofer, C., Cescatti, A., 2015. The uncertain climate footprint of wetlands under human pressure. *Proc. Natl. Acad. Sci. U. S. A.* 112, 4594–9. <https://doi.org/10.1073/pnas.1416267112>
- Poffenbarger, H. J., Needelman, B.A., Megonigal, J.P., 2011. Salinity Influence on Methane Emissions from Tidal Marshes, *Wetlands*, (31), 831–842, doi:10.1007/s13157-011-0197-0.
- Rastelli J. 2016. Dissolved organic carbon concentration, patterns and quality at a reclaimed and two natural wetlands, Fort McMurray, Alberta. McMaster University. 114 pp.

- Renault, S., Lait, C., Zwiazek, J., MacKinnon, M., 1998. Effect of high salinity tailings waters produced from gypsum treatment of oil sands tailings on plants of the boreal forest. *Environ. Pollut.* 102, 177–184. [https://doi.org/10.1016/S0269-7491\(98\)00099-2](https://doi.org/10.1016/S0269-7491(98)00099-2).
- Renault, S., Paton, E., Nilsson, G., Zwaizek, J.J., MacKinnon, M.D., 1999. Responses of boreal plants to high salinity oil sands tailings water. *J. Environ. Qual.* 28 (6), 1957–1962.
- Roulet, N.T., Lafleur, P.M., Richard, P.J.H., Moore, T.R., Humphreys, E.R., Bubier, J., 2007. Contemporary carbon balance and late Holocene carbon accumulation in a northern peatland. *Glob. Chang. Biol.* 13, 397–411. <https://doi.org/10.1111/j.1365-2486.2006.01292.x>
- Spennato, H.M., Ketcheson, S.J., Mendoza, C.A., Carey, S.K., 2018. Water table dynamics in a constructed wetland, Fort McMurray, Alberta. *Hydrol. Process.* 32, 3824–3836. <https://doi.org/10.1002/hyp.13308>
- Strilesky, S.L. 2019. Functioning of reclaimed oil sands ecosystems and the implications for reclamation certification. Carleton University. 174 pp.
- Strilesky, S. L., Humphreys, E. R., Carey, S. K., 2017. Forest water use in the initial stages of reclamation in the Athabasca Oil Sands Region. *Hydrological processes*, 31(15), 2781-2792.
- Thompson, C., Mendoza, C. A., Devito, K. J., Petrone, R. M., 2015. Climatic controls on groundwater–surface water interactions within the Boreal Plains of Alberta: Field observations and numerical simulations. *Journal of Hydrology*, 527, 734–746. <https://doi.org/10.1016/j.jhydrol.2015.05.027>
- Thorne, C. 2015. A comparison of soil nitrogen availability along hillslopes for a previously mined reclaimed wetland and two natural wetlands in Fort McMurray, Alberta. McMaster University. 105 pp.
- Vitt, D.H., Chee, W.L., 1990. The relationships of vegetation to surface-water chemistry and peat chemistry in fens of Alberta, Canada. *Vegetation* 89 (2), 87–106. <https://doi.org/10.1007/BF00032163>.
- Vitt, D.H., Halsey, L.A., Bauer, I.E., Campbell, C., 2000. Spatial and temporal trends in carbon storage of peatlands of continental western Canada through the Holocene. *Can. J. Earth Sci.* 37, 683–693. <https://doi.org/10.1139/cjes-37-5-683>
- Vitt, D.H., House, M., Hartsock, J.A., 2016. Sandhill Fen, An Initial Trial for Wetland Species Assembly on In-pit Substrates: Lessons after Three Years. *Botany* 94. <https://doi.org/10.1139/cjb-2015-0262>
- Waddington, J. M., P. J. Morris, N. Kettridge, G. Granath, D. K. Thompson, Moore, P.A., 2014. Hydrological feedbacks in northern peatlands, *Ecohydrology*, 8(1), 113-127. doi:10.1002/eco.1493.
- Wells, C., Ketcheson, S., Price, J., 2017. Hydrology of a wetland-dominated headwater basin in the Boreal Plain, Alberta, Canada. *Journal of Hydrology*, 547, 168–183. doi.org/10.1016/j.jhydrol.2017.01.052
- Wells, C. M., Price, J. S., 2015.. A hydrologic assessment of a saline-spring fen in the Athabasca oil sands region, Alberta, Canada - a potential analogue for oil sands reclamation. *Hydrological Processes*, 29, 4533–4548. <https://doi.org/10.1002/hyp.10518>
- Wytrykush, C., Vitt, D.H., McKenna, G., Vassov, R., 2012. Designing landscapes to support peatland development on soft tailings deposits, in: Vitt, D.H., Bhatti, J. (Eds.), *Boreal Ecosystem: Attaining Sustainable Development*. Cambridge University Press, pp. 161–178.
- Zubot, W., 2010. Removal of Naphthenic Acids From Oil Sands Process Water Using Petroleum Coke. (M.Sc. Thesis). University of Alberta.
- Zubot, W., MacKinnon, M.D., Chelme-Ayala, P., Smith, D.W., Gamal El-Din, M., 2012. Petroleum coke adsorption as a water management option for oil sands process-affected water. *Sci. Total Environ.* 427–428, 364–372. <https://doi.org/10.1016/j.scitotenv.2012.04.024>.

9 Supplementary Information

9.1 Research Team

Sean Carey	McMaster University	Professor
Elyn Humphreys	Carleton University	Associate Professor
Michael Treberg	McMaster University	Research Technician
Gordon Drewitt	McMaster University	Research Technician
Claire Oswald	McMaster University	Post-Doctoral Fellow
Scott Ketcheson	McMaster University	Post-Doctoral Fellow
Graham Clark	Carleton University	PhD Student
Kelly Biagi	McMaster University	PhD Student
Stacey Strilesky	Carleton University	PhD Student
Erin Nicholls	McMaster University	MSc Student
Chelsea Thorne	McMaster University	MSc Student
Jessica Rastelli	McMaster University	MSc Student
Haley Spennato	McMaster University	MSc Student
Arthur Szybalski	McMaster University	BSc Student
Hannah Ponsonby	McMaster University	BSc Student

9.2 Completed Graduate Student Theses

Biagi, K. MSc Thesis. 2015. Understanding flow pathways, major chemical transformations and water sources using hydrochemical data in a constructed fen, Alberta, Canada. 96 pp. McMaster University.

Clark, M.G., PhD Thesis. 2018. The initial biometeorology of the constructed Sandhill Fen Watershed in Alberta, Canada. Carleton University. 192 pp.

Nicholls EM. MSc Thesis. 2015. Multi-year water balance dynamics of a newly constructed wetland, Fort McMurray, Alberta. 114 pp. McMaster University.

Thorne, C. MSc Thesis. 2015. A comparison of soil nitrogen availability for a previously mined reclaimed wetland and two natural wetlands in Fort McMurray, Alberta. 105 pp. McMaster University

Rastelli, J. MSc Thesis. 2016. Dissolved organic carbon concentrations, patterns and quality at a reclaimed and two natural wetlands, Fort McMurray, Alberta. 127 pp. McMaster University

Spennato, H. MSc Thesis. 2016. An Assessment of the Water Table Dynamics in a Constructed Wetland, Fort McMurray, Alberta. 65 pp. McMaster University.

Strilesky, S.L. 2019. PhD Thesis. Functioning of reclaimed oil sands ecosystems and the implications for reclamation certification. Carleton University. 174 pp.

9.3 Completed Peer Review Publications

Biagi, K.M., Oswald, C.J., Nicholls, E.M., Carey, S.K., 2019. Increases in salinity following a shift in hydrologic regime in a constructed wetland watershed in a post-mining oil sands landscape. *Sci. Total Environ.* 653, 1445–1457. <https://doi.org/10.1016/j.scitotenv.2018.10.341>

Clark, M.G., Humphreys, E.R. Carey, S.K. Accepted. The initial three years of carbon dioxide exchange between the atmosphere and a reclaimed oil sand wetland. *Ecological Engineering*.

- Ketcheson, S.J., Price, J.S., Carey, S.K., Petrone, R.M., Mendoza, C.A., Devito, K.J., 2016. Constructing fen peatlands in post-mining oil sands landscapes: challenges and opportunities from a hydrological perspective. *Earth Sci. Rev.* 161, 130–139. <https://doi.org/10.1016/j.earscirev.2016.08.007>.
- Nicholls, E.M., Carey, S.K., Humphreys, E.R., Clark, M.G., Drewitt, G.B., 2016. Multi-year water balance assessment of a newly constructed wetland, Fort McMurray, Alberta. *Hydrol. Process.* <https://doi.org/10.1002/hyp.10881>.
- Oswald, C. J., Carey, S. K., 2016. Total and methyl mercury concentrations in sediment and water of a constructed wetland in the Athabasca Oil Sands Region. *Environmental Pollution*, 213, 628-637. <https://doi.org/10.1016/j.envpol.2016.03.002>
- Spennato, H.M., Ketcheson, S.J., Mendoza, C.A., Carey, S.K., 2018. Water table dynamics in a constructed wetland, Fort McMurray, Alberta. *Hydrol. Process.* 32, 3824–3836. <https://doi.org/10.1002/hyp.13308>

9.4 Conference Presentations

- Cark MG, Biagi K, Humphreys EH, Carey SK. The carbon budget of a constructed boreal plains wetland. Presented at the European Geosciences Union Meeting, Vienna, Austria, April 2019.
- Biagi K, Cark MG, Humphreys EH, Carey SK. An overview of a constructed peatland in the Athabasca oil sands region, Canada: six years after commission. Presented at the European Geosciences Union Meeting, Vienna, Austria, April 2019.
- Biagi K, Clark MG, Humphreys EH, Carey SK. The role of winter processes in the hydrological development of a constructed wetland in the Athabasca Oil Sands Region, Alberta, Canada. Presented at the American Geophysical Union Meeting, Washington, DC, December 2018.
- Biagi K, Nicholls EM, Clark G, Humphreys H, Carey SK. The influence of winter processes on the hydrology of a constructed wetland in the Athabasca Oil Sands Region, Alberta: six years after construction. Presented at the Canadian Geophysical Union Annual General Meeting, June 2018, Niagara Falls, ON.
- Clark MG, Humphreys EH, Carey SK. The initial biometeorological development of a constructed watershed. Presented at the Canadian Geophysical Union Annual General Meeting, June 2018, Niagara Falls, ON.
- Irvine S, Rastelli J, Biagi K, Carey SK. Temporal and spatial variability in the DOC dynamics of a constructed wetland in the Athabasca Oil Sands Region. Presented at the Canadian Geophysical Union Annual General Meeting, June 2018, Niagara Falls, ON.
- Mendoza C, Lukenbach M, Twerdy P, Carey SK, Devito K, Landhausser S. Ecohydrological development of a reclaimed upland-wetland system constructed on soft tailings at an oil-sand mine, NE Alberta, Canada. Presented at the European Geosciences Union Meeting, June 2018, April, Vienna, Austria.
- Biagi KM, Oswald CJ, Nicholls EM, Carey SK. The influence of managed versus natural hydrologic regimes on the hydrochemical patterns in a constructed wetland in the Athabasca oil sands region, Canada. Presented at the American Geophysical Union Annual General Meeting, New Orleans, USA. December 2017.
- Lukenbach MC, Spencer CS, Mendoza CA, Devito KJ, Landhausser SM, Carey SK. Resolving the need for groundwater recharge versus forest productivity in a reclaimed watershed using numerical modelling. Presented at: Geological Society of American Annual Meeting. Seattle, October 2017.
- Lukenbach MC, Spencer CS, Mendoza CA, Devito KJ, Landhausser SM, Carey SK. Variably saturated flow between constructed upland hummocks and a wetland in a reclaimed watershed

following oil sands mining. Presented at the Canadian Geophysical Union Annual General Meeting, Vancouver, Canada. May 2017.

Strilesky SL, Carey SK, Humphreys ER, Petrone RM, Drewitt GB, Sutherland G. Filling in a forest patchwork: A multi-site analysis of conventional and constructed patches of the Canadian boreal forest. Presented at the Canadian Geophysical Union Annual General Meeting, Vancouver, Canada. May 2017.

Clark MG, Humphreys ER, Carey SK. Downscaling eddy covariance measurements of energy and carbon dioxide fluxes in a constructed boreal wetland. Presented at the Canadian Geophysical Union Annual General Meeting, Vancouver, Canada. May 2017.

Clark MG, Humphreys ER, Carey SK. Low methane fluxes from a constructed boreal wetland. Presented at American Geophysical Union Annual Fall Meeting, December 2016.

Biagi K, Oswald C, Carey SK, Nicholls EM. Understanding the hydrochemical evolution and patterns of a constructed wetland in the Athabasca oil sands region, Canada. Presented at CGU Annual General Meeting, May 2016.

Spennato H, Carey SK. An assessment of water table dynamics within a constructed reclaimed fen, Fort McMurray, Alberta. Presented at CGU Annual General Meeting, May 2016.

Rastelli J, Carey SK, Oswald C. Evaluating the composition of dissolved organic carbon (DOC) with the use of fluorescence indices between a reclaimed and two natural wetlands, Fort McMurray, Alberta. Presented at CGU Annual General Meeting, May 2016.

Biagi K, Carey SK, Nicholls EM, Mendoza CA. Understanding Flow Pathways, Major Chemical Transformations and Water Sources Using Hydrochemical and Hydrometric Data in a Constructed Fen, Fort McMurray Alberta. Presented at Canadian Geophysical Union Annual General Meeting, Montreal, Qc, May 2015.

Clarke MG, Humphreys ER, Carey SK. Evolution of function in a constructed wetland over the first two years. Presented at Canadian Geophysical Union Annual General Meeting, Montreal, Qc, May 2015.

Nichols EM, Carey SK, Drewitt GM, Humphreys ER, Clarke MG. Multi-Year Water Balance Assessment of a Constructed Wetland, Fort McMurray, Alberta. Presented at Canadian Geophysical Union Annual General Meeting, Montreal, Qc, May 2015.

Thorne C, Carey SK, Humphreys EM, Macrae ML, Petrone RM. A Comparison of Soil Nitrogen Availability Between a Post Mined Reclaimed Wetland and Two Natural Wetlands in Fort McMurray, Alberta. Presented at Canadian Geophysical Union Annual General Meeting, Montreal, Qc, May 2015.

Mendoza C, Carey SK, Devito K, Landhausser S, Longval J-M. Early water dynamics within a wetland complex constructed on tailings at an oil-sand mine. Presented at Geological Society of America AGM, Vancouver BC. October 2014.

Nicholls EM, Carey SK, Drewitt GB, Humphreys ER, Clark MG. Towards a water balance of a constructed wetland, Fort McMurray, Alberta. Presented at CGU Annual General Meeting, May 2014.

Thorne CE, Carey SK, Oswald C. A comparison of nutrient availability in reclaimed wetland soils, Fort McMurray, Alberta. Presented at CGU Annual General Meeting, May 2014.

APPENDIX 4: THE EARLY DEVELOPMENT OF SANDHILL FEN- PLANT ESTABLISHMENT, COMMUNITY STABILIZATION AND ECOSYSTEM DEVELOPMENT

TERMS OF USE

Southern Illinois University was retained by Syncrude to carry out the studies presented in this report and the material in this report reflects the judgment of author(s) in light of the information available at the time of document preparation. Permission for non-commercial use, publication or presentation of excerpts or figures requires the consent of the author(s). Commercial reproduction, in whole or in part, is not permitted without prior written consent from Syncrude. An original copy is on file with Syncrude and is the primary reference with precedence over any other reproduced copies of the document.

Reliance upon third party use of these materials is at the sole risk of the end user. Syncrude accepts no responsibility for damages, if any, suffered by any third party as a result of decisions made or actions based on this document. The use of these materials by a third party is done without any affiliation with or endorsement by Syncrude.

Additional information on the report may be obtained by contacting Syncrude.

This appendix may be cited as:

Vitt, D. 2017. The early development of Sandhill Fen: plant establishment, community stabilization, and ecosystem development. Appendix 4 in Syncrude Canada Ltd. *Sandhill Fen Watershed: Learnings from a Reclaimed Wetland on a CT deposit*. Syncrude Canada Ltd. 2020.

The Early Development of Sandhill Fen: Plant Establishment, Community stabilization, and Ecosystem Development

FINAL REPORT – May 2017

Principle Investigators:

Dr. Dale H. Vitt
Dr. Stephen Ebbs†
Southern Illinois University

Senior Technical Support

Melissa House

Graduate Student Participants

Lilyan Glaeser
Jeremy Hartsock
Renee Hazen

Table of Contents

Executive Summary & Acknowledgements	3
Introduction and Background – Section 1	5
Plant Responses – Section 2	8
Atmospheric Deposition – Section 3	52
Porewater Chemistry – Section 4	54
Soil Dynamics – Section 5	59
References	68
Publications from Sandhill Fen	70

Executive Summary

Between 2011 and 2016 we provide results and recommendations for 1) plant responses, 2) atmospheric deposition, 3) porewater chemistry, and 4) soil dynamics for Sandhill Fen. These results are for the first four years after wet-up in August 2012. In 2012, we set up 20 research plots from which much of our data were obtained. Other data came from the fen as a whole.

1. **Plant Responses:** We introduced seedlings from 16 species in 2012 and 13 species in 2013. Species survival varied from 67% in 2012 to 41% in 2013. Species survival was varied and closely associated with soil wetness. We provide a list of species that we recommend for fen reclamation in general, as well as species best suited for wet and dry areas of the fen. In particular, four species stood out: *Scirpus microcarpus*, *Scirpus atrocinctus*, *Carex aquatilis*, and *Carex hystericina*. In 2015 and 2016 we used 83 plots evenly distributed within the fen to examine species occurrence and vegetation patterns on the fen. The fen has a high diversity of both desirable and undesirable species distributed in three vegetation zones. Zone one is dominated by *Typha latifolia* and has low diversity, occupying 9.6% of the fen in 2016. Zone 2 is dominated by *Carex aquatilis* and a suite of desirable fen species – it occupied 50.6% in 2016. Zone 3 is dominated by *Calamagrostis canadensis* and a suite of undesirable species and occupied 39.8%. Overall, about half of the fen is occupied by peat-forming fen plants, whereas the remaining half has either plants of riparian areas or plants that occupy habitats similar to marshes. Bryophytes have high diversity in the fen, but overall low abundance; however, bryophyte species occurrences in 2016 were 17% lower than in 2015. Our greenhouse study of sodium tolerance of *Beckmannia syzigachne* revealed that the species had reduced physiological performance at a sodium level of $850 \text{ mg}^{-1} \text{ L}^{-1}$. We also examined whether planting a number of species yielded more species diversity compared to planting monocultures and concluded that there was no advantage to planting more than one species (as far as species diversity is concerned). Our study of net primary production, both above- and belowground, revealed that three species *Carex aquatilis*, *Carex hystericina*, and *Scirpus microcarpus* all had production levels comparable to natural fens of the region based on literature values. Gross and net photosynthesis for these three species were similar to one another, however when CO_2 exchange is considered for the entire year, none of these species provide sufficient net sinks in CO_2 to make up for overall sources of CO_2 derived from the decomposing peat layer. Of the three species, *C. aquatilis* appears to be the most efficient in CO_2 exchange.
2. **Atmospheric deposition:** Nitrogen and sulfur deposition at Sandhill Fen is several times greater than regional means: 20 times higher NH_4^+ ($0.53 \text{ kg ha}^{-1} \text{ yr}^{-1}$), 4 times higher NO_3^- ($0.5 \text{ kg ha}^{-1} \text{ yr}^{-1}$), 11 times higher for DIN ($1.17 \text{ kg ha}^{-1} \text{ yr}^{-1}$), and 1.5 times higher for SO_4^{2-} ($7.78 \text{ kg ha}^{-1} \text{ yr}^{-1}$ (Wieder et al. 2016), these high values could affect plant growth in the future.
3. **Porewater chemistry:** Base cation content of porewaters across the fen are highly variable with areas of the fen having areas with high values of calcium and/or sodium. These areas with high values occur along the southern boundary of the fen and are increasing for sodium (mean 2015 value about 270 mg l^{-1}).
4. **Soil dynamics:** We examined the microbial flora in 2014 and 2015 (using phospholipid fatty acid extractions). We found that the microbial floras did not differ between years, that the microbial communities at Sandhill Fen are similar to and within the range of some benchmark peatland sites, and that few differences were found along the wet to dry gradient within Sandhill Fen, indicating that the site has a reasonably homogeneous microbial flora. We utilized net N-mineralization as an indicator of site performance. Comparing natural analogues, we found that rates are faster in some fen types than others and that net N mineralization rates across wet and dry plots at Sandhill Fen (SHF) were equivalent to several benchmark sites, suggesting the amount of plant available inorganic N remaining at SHF following microbial immobilization should not limit NPP rates at the current stage of

reclamation. In general, plots localized in wet areas at SHF were most similar to natural fen benchmark sites, while dry areas at SHF, however exhibited few fen characteristics, and net N mineralization was dominated by nitrification, a situation characteristic of upland systems. Likewise, dry sites at SHF have greater rates of decomposition compared to wet areas of the fen.

Acknowledgments. We dedicate this report to Dr. Stephen Ebbs, who inspired us to add our work on physiological performance of plants at Sandhill Fen. Stephen was a delight to work with and we shall miss him greatly.

Section 1: Introduction and Background

Sandhill Watershed is located on an in-pit of Syncrude Canada, Ltd. oil sands lease located at 57-02'16.10"N, 111-36'06.09"W and 57-02'29.03"N, 111-35'06.37"W at 312 m elevation. In 2007, Syncrude Canada, Ltd. initiated design of the experimental watershed in order to determine procedures for reclamation of future expansive in-pit features (Wytrykush et al. 2012). This watershed, named Sandhill Watershed, is 52 ha in area and contains a central 17 ha wetland (Sandhill Fen), two 'perched wetlands' each 1.2 ha, all contained within an upland of designed hills and valleys draining into Sandhill Fen. Over the tailings sand cap, a 0.5 m layer of fine-grained clay till was placed followed by a 0.5 m layer of freshly harvested peat. This peat was from a peatland complex with both minerotrophic and ombrotrophic areas where the entire peat column was harvested, resulting in variable peat characteristics (degree of decomposition and chemistry). This peat was harvested in the autumn of 2010 and spread on Sandhill Fen in January 2011. Peat was placed by bulldozer leaving some microtopography.

In November 2011, a native seed mix was spread on the fen using commercial seed spreaders. Seeds were collected for the mix in late summer of 2011 from a number of natural sites dominated by *Carex aquatilis*, a species thought to be critical in oil sands peatland reclamation (Koropchak et al. 2012); however, small amounts (1-5%) of typical rich fen species were also included in the mix (Vitt et al. 2016). The fen remained dry until wet-up in August 2012 when water was introduced through a system of pipes and a holding pond (Wytrykush et al. 2012). In 2013, water continued to be supplied to the fen in order to complete wet-up and maintain water levels. Beginning in 2014, water levels were maintained without additional water. Our study was designed to evaluate the early establishment of Sandhill Fen. We posed the following questions.

Questions:

Section 2: Plants

- 1) Will seedlings of native wetland species of the region survive and establish?
- 2) What is the flora throughout the fen?
- 3) Do the introduced wetland species function physiologically similarly to benchmark sites?
- 4) Is there an advantage to planting diverse communities compared to monocultures?
- 5) Are sedge species producing biomass and sequestering carbon?

Section 3: Air

- 1) What is the atmospheric deposition rate of nitrogen and sulfur?

Section 4: Water

- 1) What is the pH and electrical conductivity (EC) of the water in Sandhill Fen?
- 2) What are the porewater concentrations of base cations (calcium, magnesium, potassium, and sodium)?
- 3) Does water chemistry change with depth within the peat profile (0-50 cm)?

Section 5: Soil Dynamics

- 1) Does decomposition vary across the fen?
- 2) Have soil microbial communities established? Are they comparable to benchmark sites?
- 3) What are the rates of nitrogen mineralization within the fen and do they match the range of rates at benchmark sites?

To answer these questions, we set up 20 plots throughout Sandhill Fen (Figure 1.1). Each plot was divided into 4 subplots (quadrants) (Figure 1.2). One quadrant was planted with a suite of wetland species in 2012, a second suite of species was planted in a second quadrant in 2013, plant community plots were planted in the third quadrant in 2013, and the fourth was left to be vegetated by volunteer species and was used for soil sampling. Water sampling and aerial deposition sampling was carried out at all or a subset of these 20 plots. Throughout this report, these 20 plots will be referred to in the methods used to answer our research questions.

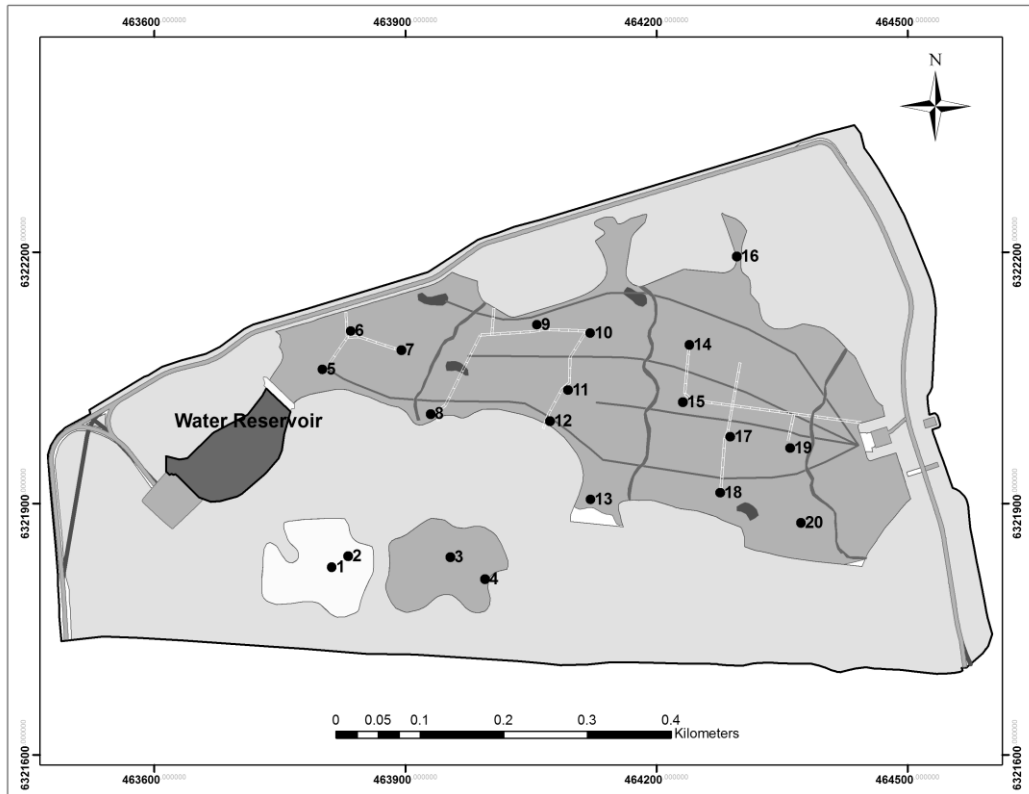


Figure 1.1 A map of Sandhill Fen with the locations of our 20 plots numbered and marked with black dots.

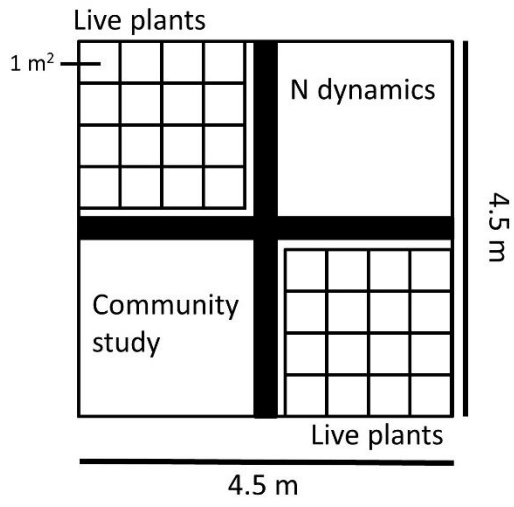


Figure 1.2 Diagram of experimental plot set-up.

Section 2: Plant Responses

Seedling survival by species

A suite of wetland plants was selected for introduction to Sandhill Fen. Selection was based on their occurrence in disturbed, early successional fens, or in high conductivity, sodium rich systems. We wanted to determine if these species could survive and establish within the environmental gradients present at Sandhill Fen.

Methods: In 2012, we planted 16 species in 20 plots, 16 plots in the lower fen and 2 plots in each of 2 perched fens. Another planting of 13 species took place in 2013 using a different subplot within our 20 plots. Some plants were planted and/or survived in such low numbers that those species could not be included in statistical analysis. Results are shown for 10 plant species introduced in 2012 and 11 species introduced in 2013 (Table 2.1). In 2014, survival of species planted in both 2012 and 2013 were recorded, and the results for each planting were analyzed separately. A 2-way ANOVA was used to test for differences between species and moisture class of the plots: wet or dry. Plots were split into two groups: wet plots (n=10), those plots with standing water for at least part of the growing season of 2014, and dry plots (n=10, includes perch fen plots), with the water table always beneath the soil surface.

Species Planted - First Year	Number Planted	Species Planted - Second Year	Number planted
<i>Beckmannia syzigachne</i>	24	<i>Beckmannia syzigachne</i>	20
<i>Betula glandulifera</i>	24	<i>Carex aquatilis</i>	20
<i>Carex aquatilis</i>	7	<i>Carex canescens</i>	20
<i>Carex bebbii</i>	15	<i>Carex diandra</i>	20
<i>Carex diandra*</i>	3	<i>Carex limosa</i>	17
<i>Carex hystericina</i>	17	<i>Carex pauciflora</i>	10
<i>Carex paupercula</i>	18	<i>Carex paupercula</i>	20
<i>Dasiphora fruticosa</i>	20	<i>Eriophorum angustifolium</i>	20
<i>Eriophorum vaginatum*</i>	2	<i>Eriophorum chamissonis*</i>	2
<i>Juncus tenuis*</i>	3	<i>Eriophorum vaginatum*</i>	2
<i>Scheuchzeria palustris*</i>	3	<i>Larix laricina</i>	12
<i>Scirpus atrocinctus</i>	19	<i>Triglochin maritima</i>	20
<i>Scirpus lacustris*</i>	2	<i>Triglochin palustris</i>	12
<i>Scirpus microcarpus</i>	24		
<i>Triglochin maritima</i>	11		
<i>Triglochin palustris*</i>	2		

Table 2.1 List of species and number of each planted per plot for 2012 and 2013 planting events.

* Indicates species that could not be included in statistical analysis due to low introduction and/or low survival.

Results: Plants Introduced in 2012 – First Planting

Overall, the majority of plants survived. Across all the plots in the fen, mean survival for all species planted was 67%. There was a significant interaction of moisture and species indicating that some species survived better in wet plots, other survived better in dry plots, and other species exhibited no difference in survival rates.

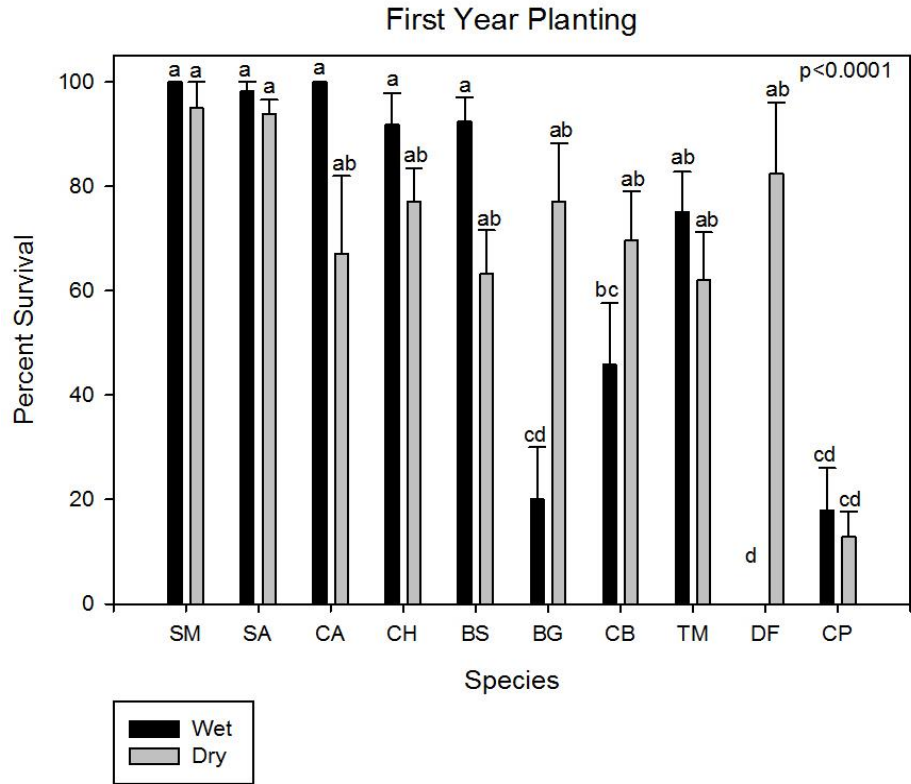


Figure 2.2. Species names are listed in Table 2.2. Black bars are mean percent survival for wet pots; grey bars are mean percent survival for dry plots. Different letters are the result of Tukey's HSD pairwise comparisons.

Species	Wet Plots	Dry Plots
<i>Scirpus microcarpus</i>	100	95 ± 5
<i>Scirpus atrocinctus</i>	98 ± 2	94 ± 3
<i>Carex aquatilis</i>	100	67 ± 15
<i>Carex hystericina</i>	92 ± 5	77 ± 11
<i>Beckmannia syzigachne</i>	92 ± 5	63 ± 8
<i>Betula glandulifera</i>	20 ± 10	77 ± 11
<i>Carex bebbii</i>	46 ± 12	70 ± 10
<i>Triglochin maritima</i>	75 ± 8	62 ± 9
<i>Dasiphora fruticosa</i>	0	83 ± 14
<i>Carex paupercula</i>	18 ± 8	13 ± 5

Table 2.2 Mean percent survival with the standard error for wet plots and dry plots in Sandhill Fen. Species are listed from highest survival rates to lowest.

Some species survived well in both wet and dry plots. *Scirpus microcarpus* survival in wet plots was 100% and 95% in dry plots. *Scirpus atrocinctus* survival in wet plots was 98% and 94% in dry plots. *Carex aquatilis* survival in wet plots was 100% and in dry plots 67%. *Carex hystericina* survival was 92% in wet plots and 77% in dry plots. *Beckmannia syzigachne* survival in wet plots was 92% in wet plots and 63% in dry plots. While *Carex aquatilis*, *Carex hystericina* and *Beckmannia syzigachne* seem to have higher survival in wet plots, it is not statistically significant.

Similarly, *Triglochin maritima* survival did not differ based on moisture: 75% in wet plots and 62% in dry plots. *Carex bebbii* survival was not different for wet plots (46%) and dry plots (70%). *Carex paupercula* had lower survival rates, but no difference between wet plots (18%) and dry plots (13%).

Two species were affected by the moisture of the plots. *Betula glandulifera* survival was lower in wet plots (20%) and higher in dry plots (77%). *Dasiphora fruticosa* did not survive in wet plots (0%) but survived well in dry plots (83%).

These plants were also surveyed and analyzed in 2013. Results from the 2013 field season are available in the 2013 Annual Report submitted to Syncrude.

Plants Introduced in 2013- Second Planting

Across the fen, the overall survival of species planted in 2013 was 41%. This lower survival rate, compared to 2012, was due to some additional 2013 species with poor survival rates in either dry or wet plots, long with no individuals of the *Scirpus* species being planted. There is a significant interaction of moisture of the plots and the species on survival rates. This significant interaction indicates that some species survive better in wet plots, other species survive better in dry plots, and other species survival rates are not affected by the moisture of the plots.

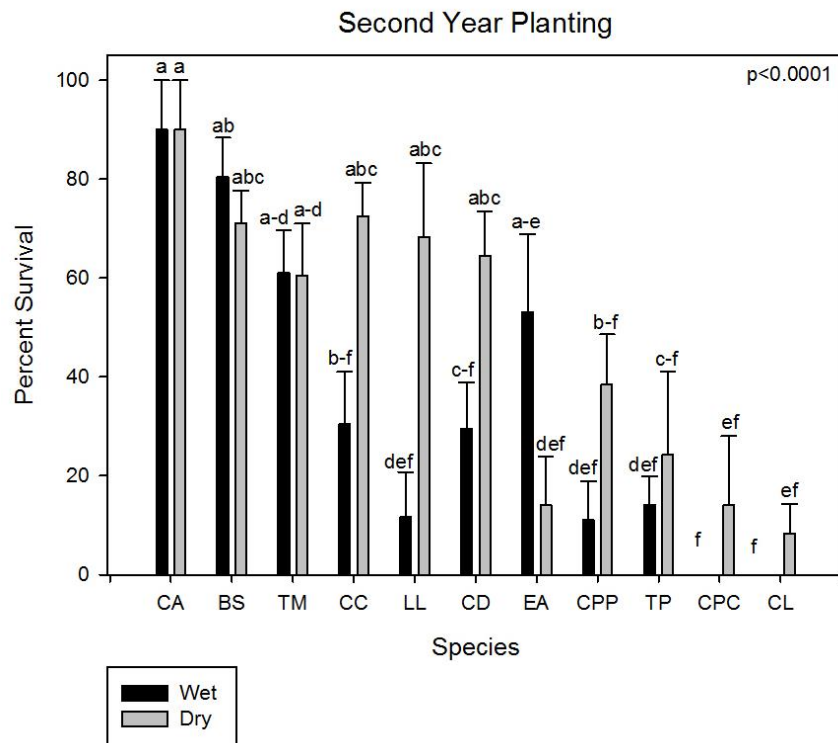


Figure 2.3 Species names are listed in Table 2.3 Black bars are mean percent survival for wet pots; grey bars are mean percent survival for dry plots. Different letters are the result of Tukey's HSD pairwise comparisons.

Species	Wet Plots	Dry Plots
<i>Carex aquatilis</i>	90 ± 10	90 ± 10
<i>Beckmannia syzigachne</i>	81 ± 8	71 ± 7
<i>Triglochin maritima</i>	61 ± 9	61 ± 11
<i>Carex canescens</i>	31 ± 11	73 ± 7
<i>Larix laricina</i>	12 ± 9	68 ± 15
<i>Carex diandra</i>	30 ± 9	65 ± 9
<i>Eriophorum angustifolium</i>	53 ± 16	14 ± 10
<i>Carex paupercula</i>	11 ± 8	39 ± 10
<i>Triglochin palustris</i>	14 ± 6	24 ± 17
<i>Carex pauciflora</i>	0	14 ± 14
<i>Carex limosa</i>	0	8 ± 6

Table 2.3 Mean percent survival with the standard error for wet plots and dry plots in Sandhill Fen. Species are listed from highest survival rates to lowest.

A set of species exhibited high survival rates (>60%) with no effect from moisture. *Carex aquatilis* survival in wet plots was 90% in both wet and dry plots. *Beckmannia syzigachne* survival is 81% in wet plots and 71% in dry plots. *Triglochin maritima* survival was 61% in both wet and dry plots.

Carex canescens survival was 31% in wet plots and 73% in dry plots. Due to high variability between plots within moisture classes (wet and dry), there was no statistical difference between the mean survival.

Larix laricina survival was significantly lower in wet plots (12%) than in dry plots (68%).

Another set of species had lower survival (<66%), but were not significantly affected by the moisture of the plots. *Carex diandra* survival was not different for wet plots (30%) than dry plots (65%). *Eriophorum angustifolium* survival was 53% in wet plots and 14% in dry plots. *Carex paupercula* survival in wet plots was 11% and 39% in dry plots. *Triglochin palustris* survival was low in both wet plots (14%) and dry plots (24%). *Carex pauciflora* did not survive in wet plots (0%), but had 14% survival in dry plots. *Carex limosa* also senesced in wet plots (0% survival), and had only 8% survival in dry plots.

Discussion and Recommendations for Reclamation: From the results of this study, we can recommend plants for reclamation purposes at sites similar to Sandhill Fen. We have also learned the conditions at the time of planting are important for the overall success of the plants.

We highly recommend *Scirpus microcarpus*, *Scirpus atrocinctus*, *Carex aquatilis*, and *Carex hystericina* for planting in fen reclamations. These species exhibited high survival rates across the fen in both dry and wet areas. These species also tend to spread quickly and produce considerable biomass (as discussed in detail later in this report), which would likely help to reduce weed colonization.

Beckmannia syzigachne also survives well and is a good candidate for a cover crop to reduce weed invasion, however, results from the U-Cell study indicated that *B. syzigachne* dies out within 4-5 years. Another desirable species should be introduced during that time.

Triglochin maritima survives well at Sandhill Fen regardless of moisture levels. We recommend this species for reclamation planting, but due to its caespitose growth form, it does not spread as much as the *Carex* and *Scirpus* species discussed above.

Betula glandulifera is a good species to introduce after the water regime at a reclamation has been determined as it performs better in drier areas. Similarly, *Carex bebbii* prefers drier conditions and could be introduced in these areas especially if increasing plant diversity is a goal of the reclamation. *Larix laricina* also survived well at the drier sites.

Eriophorum angustifolium could be introduced once wet areas of the reclamation have been identified; there is a trend toward lower survival at dry plots.

There is a suite of species that do not survive well in either wet or dry plots at Sandhill Fen. The cost and effort of planting these species does not result in abundance of these species. *Carex limosa*, *Carex paupercula*, and *Triglochin palustris* did not survive well, and thus are not recommended. *Dasiphora fruticosa* is not recommended for planting in wetland reclamations. It does not survive in wet plots, and is not typically found in fens or other wetlands in the region.

There are other species we do not recommend. These species had low greenhouse stock from the seed likely due to low germination and low survival in the field making it impossible to provide statistics on their survival. Included in this group are *Carex diandra*, *Eriophorum chamissonis*, *Eriophorum vaginatum*, *Juncus tenuis*, *Scheuchzeria palustris* and *Scirpus lacustris*.

Plants planted in 2012 survived better overall than plants introduced in 2013. The fen was dry in 2012, which made planting logistically easier. Plants planted in 2013 were planted in much wetter conditions, and the water table fluctuated from flooded to very dry due to pump failures and problems with the watering system. These fluctuations likely contributed to the lower survival rates for plants introduced in 2013. Younger plants are generally more susceptible to environmental stresses than established plants. Considering what we've learned, we recommend planting in dry conditions then a slow introduction of water until the water is just at or slightly below the soil surface.

Recommended Species
<i>Beckmannia syzigachne</i>
<i>Carex aquatilis</i>
<i>Carex hystericina</i>
<i>Scirpus atrocinctus</i>
<i>Scirpus microcarpus</i>
<i>Triglochin maritima</i>
Recommended for Dry Areas
<i>Betula glandulifera</i>
<i>Carex bebbii</i>
<i>Larix laricina</i>
Recommended for Wet Areas
<i>Eriophorum angustifolium</i>
Not Recommended
<i>Carex diandra</i>
<i>Carex limosa</i>
<i>Carex paupercula</i>
<i>Dasiphora fruticosa</i>
<i>Eriophorum chamissonis</i>
<i>Eriophorum vaginatum</i>
<i>Juncus tenuis</i>
<i>Scheuchzeria palustris</i>
<i>Scirpus lacustris</i>
<i>Triglochin palustris</i>

Table 2.4 Table of species and summary of recommendation status.

Sandhill Fen Vegetation

Introduction: We were requested to sample the vegetation and soils at Sandhill Fen in summer of 2016. We compared the vegetation results to those from summer 2015. In both years, we were tasked with evaluating the composition and distribution of vegetation of the wetland area of Sandhill Fen Watershed. We identified the vascular plant species as well as the bryophytes using similar methods in both years. Site design and construction of the watershed were described in detail by Wytrykush *et al.* (2012).

Methods: In early August of 2015 and 2016, we conducted a plant survey of Sandhill Fen. We used 93 plot locations originally placed by Acden Navus in 2012; locations of these plots are available in the 2013 Navus vegetation report. These plots were systematically located at the center of a 40 x 40 m grid. Plots were circular with an area of 8.0 m². Presence of all species was recorded and abundance of vascular plants (as % cover to 5%) was estimated. In 2016, stem counts of *Populus balsamifera* were recorded in surrounding 80 m² circular plots. In 2015, six plots were excluded, and in 2016 exclusions increased to eight plots because they were considered upland. Nomenclature follows Johnson *et al.* (1995) for vascular plants, BFNA (2007, 2014) for mosses and Stotler and Crandall-Stotler (1977) for liverworts.

Species abundances along with bryophyte presence/absence were utilized in a non-Metric Multi-Dimensional Scaling (NMDS) ordination and in a group average cluster analysis with 40% similarity cut levels using Primer (Clarke & Gorley 2006); the cut level was determined by a SIMPROF test indicating that all groups formed at the 40% similarity level are significantly different; further splitting would result in clusters that are not actually different. Species richness was evaluated through three measures (Whittaker 1972): alpha species richness is the number of species within a single plot, gamma species diversity is the total number of species within all plots of a group, and beta diversity is species turnover between plots calculated as gamma divided by alpha. In 2015, spatial patterns on Sandhill Fen were developed by University of Windsor / GLIER GIS team, which we used for comparison in 2016. We will discuss the results from 2016 highlighting any shifts that occurred between 2015 and 2016.

Results: The 2016 survey of 85 plots distributed evenly across the fen revealed 87 vascular plant species and 23 bryophyte species. The second order jackknife estimate of total diversity is 153.4 (PC-ORD; McCune & Mefford 1999). Of the 108 species recorded, 28 [26%] (21 vascular plant and 7 bryophytes) were found only one time. Currently, the fen has both peat-forming species - species found in natural fens of the region (here termed desirable species) along with species of uplands, marshes (non-peat-forming wetlands), and noxious weeds (together termed undesirable species). Of the 28 locally rare species, 16 are desirable and 12 are undesirable species. Of the 87 vascular plant species found in the fen, 37 (43%) are desirable species naturally found in Albertan peatlands. Overall plant cover across the fen is 98%. The two most abundant species are *Carex aquatilis* and *Calamagrostis canadensis*.

The 23 species of bryophytes occurred 260 times, averaging 3.1 occurrences (species) per plot. However, 25 plots had no bryophytes (either submerged plots or dry plots), so for the 60 plots for which bryophytes occurred, the mean number of bryophyte occurrences was 4.4. *Ptychostomum pseudotriquetrum* was the most common species, occurring in all 60 plots.

As in 2015, we used group average cluster analysis, with similarity cut levels of 45% in 2015 and 40% in 2016, to recognize significantly different plant assemblages (Primer 6; Clarke & Gorley 2006) – In 2016, three of these are represented by more than one plot, two plots are outliers having only one plot. We ordinated the 85 plots using NMDS, recognizing these three major clusters as ‘species groups’ that are organized into distinct assemblages (Figure 2.4). For each of these 3 major species groups we plotted the abundance of the dominant species over the ordination and provide data on species abundance patterns (Table 2.4) and richness parameters (Tables 2-3). These three species groups from the 2016 field surveys are quite similar to the three major species groups in 2015.

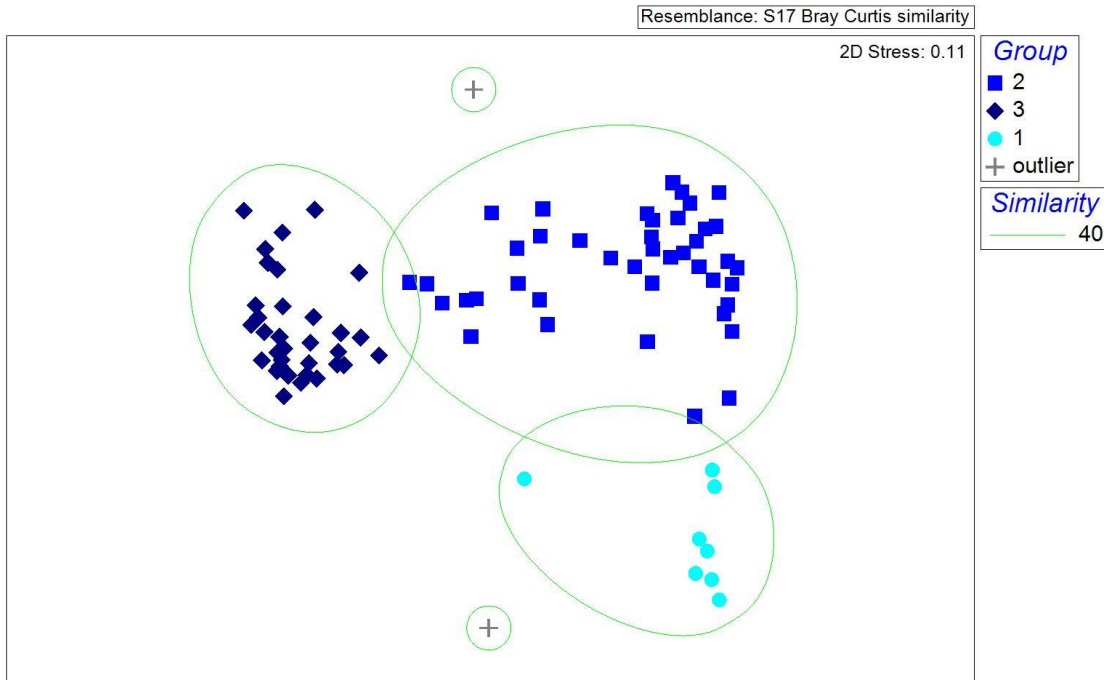


Figure 2.4 NMDS ordination of 2016 species abundance data. The three major vegetation groups (Group 1 – circles, group 2 – squares, group 3 – diamonds) and 2 minor outliers (plus signs) as defined at 40% similarity by group average cluster analysis.

2016

Abundant Species	Group 1	Group 2	Group 3	Group 1	Group 2	Group 3
<i>Calamagrostis canadensis</i>	0.0	12.8	55.6	3.8	13.9	66.8
<i>Carex aquatilis</i>	31.5	51.5	3.2	10.1	52.6	3.3
<i>Carex utriculata</i>	4.5	6.5	1.0	1.6	8.2	0.9
<i>Populus balsamifera</i>	0.0	0.3	5.2	0.0	0.9	6.7
<i>Salix petiolaris</i>	0.0	0.8	5.6	0.0	1.0	5.6
<i>Typha latifolia</i>	34.1	4.8	0.1	51.9	7.9	0.2

Table 2.4 Abundant species found across Sandhill Fen; mean abundance for the three vegetation groups from the 2016 survey compared to that from 2015.

Group 1 (Figure 2.5): Dominated by *Typha latifolia* (52% cover) and *Carex aquatilis* (3%) and occurring in the center of the fen (Figure 2.6). This group of plots has very few occurrences of bryophytes (gamma diversity=3.0). Mean alpha (plot) diversity of both desirable species (3.0) and undesirable species (2.0) is low. Overall gamma diversity is also low (15 species). Overall vascular plant abundance (71% cover) is lowest amongst the 3 groups, with desirable species cover 14% of the total.

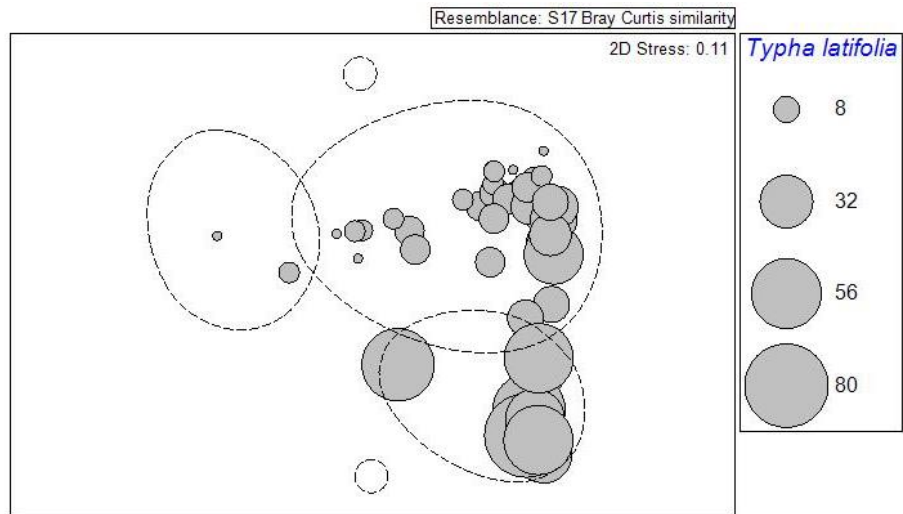


Figure 2.5 NMDS ordination of 2016 species abundance data with abundance (as percent cover) of *Typha latifolia* overlain. Dotted circles are bounds of species groups.

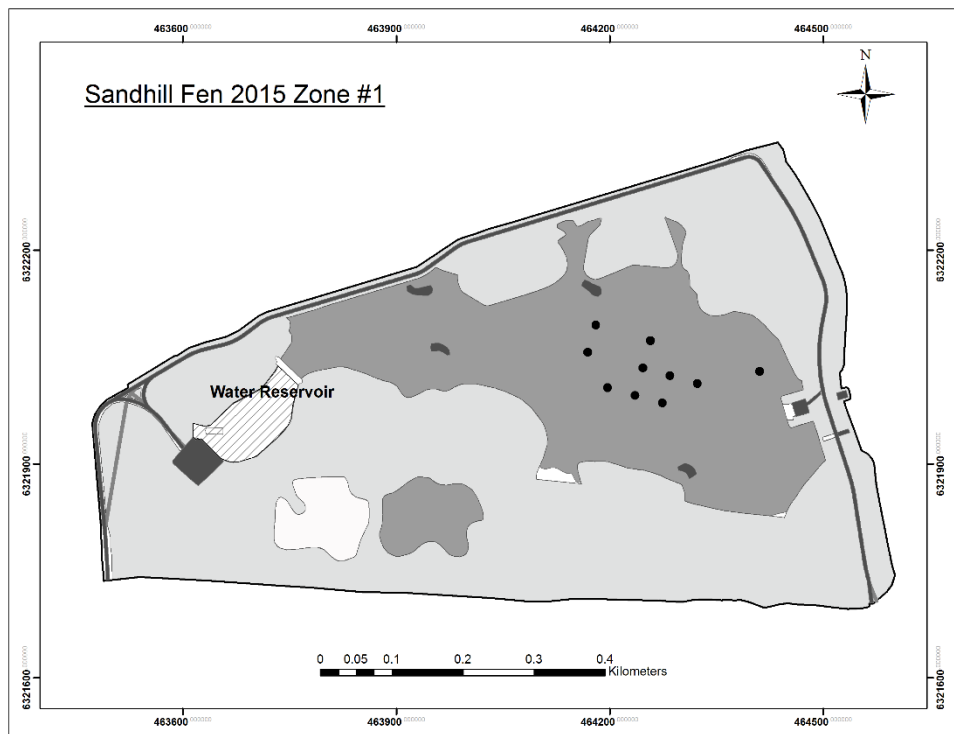


Figure 2.6 Spatial Distribution of Group 1 plots (2015) within Sandhill Fen.

Group 2 (Figure 2.7): Dominated by *Carex aquatilis* (53% cover) and occurring throughout the fen tending toward the northern edge (Figure 2.8), this group of plots has mean alpha diversity of 1.3 for bryophytes, 4.6 for desirable vascular plant species, and 3.1 for undesirable species.

Gamma diversity is high with 17 bryophytes and 64 vascular plant species of which 34 (53%) are desirable. Overall vascular plant abundance (97% cover) is high, with desirable species cover 67% of the total. Shrubs and trees are not common, with stem counts of *Populus balsamifera* ranging from 0-29 individuals/80m² (mean=3.6).

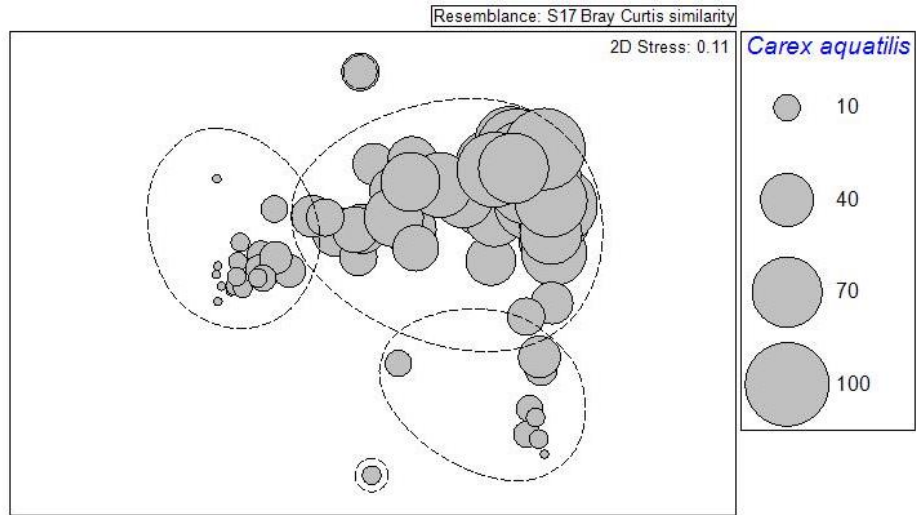


Figure 2.7 NMDS ordination of 2016 species abundance data with abundance (as percent cover) of *Carex aquatilis* overlain. Dotted circles are bounds of species groups.

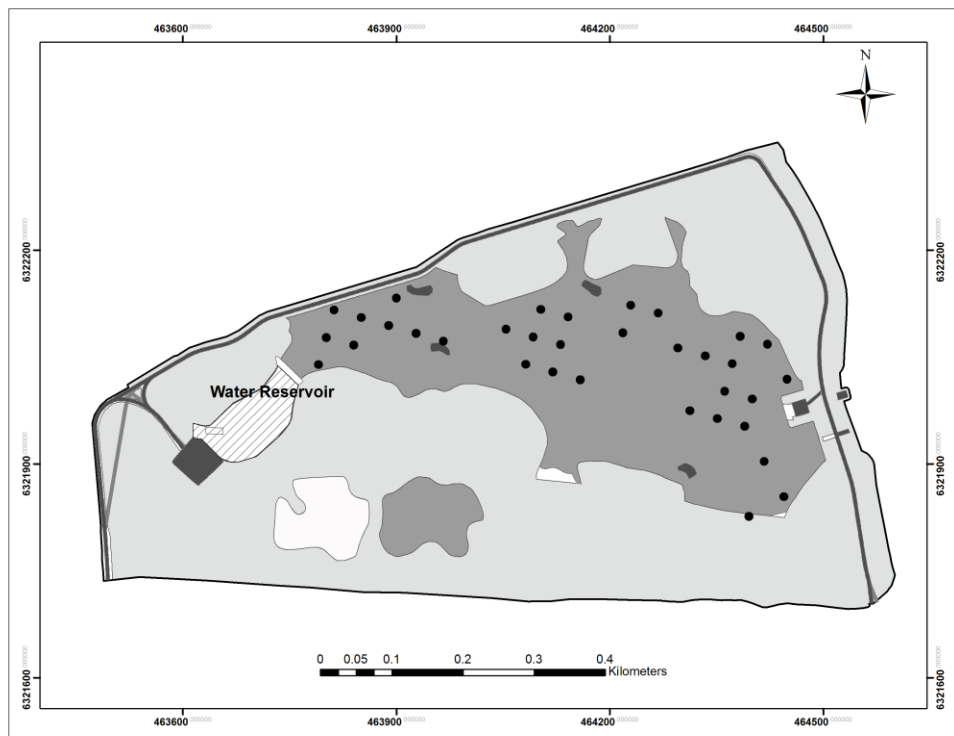


Figure 2.8 Spatial Distribution of Group 2 plots (2015) within Sandhill Fen.

Group 3 (Figure 2.9): Dominated by *Calamagrostis canadensis* (53% cover) and occurring along the southern edge (Figure 2.10), this group of plots has mean alpha diversity of 3.2 for bryophytes, 3.6 for desirable vascular plant species, and 9.9 for undesirable species. Gamma diversity is high with 16 bryophytes and 60 vascular plant species of which 20 (33%) are desirable. Overall vascular plant abundance (106% cover) is highest amongst the three groups, with desirable species cover 14% of the total. *Populus balsamifera* and *Salix lutea* are most abundant in this group. Stem counts for *P. balsamifera* were estimated to range from 2-81 individuals/80m² (mean=22.5).

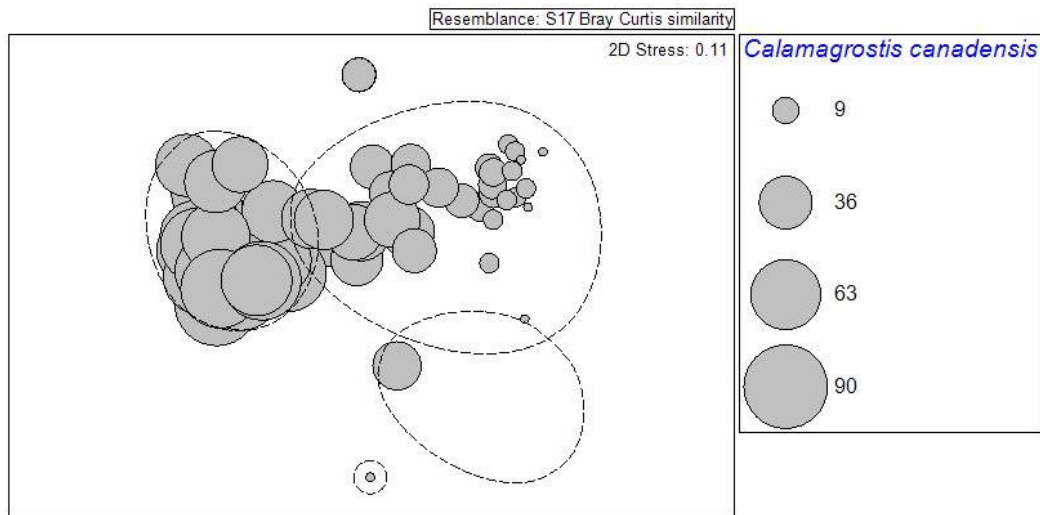


Figure 2.9 NMDS ordination of 2016 species abundance data with abundance (as percent cover) of *Calamagrostis canadensis* overlain. Dotted circles are bounds of species groups.

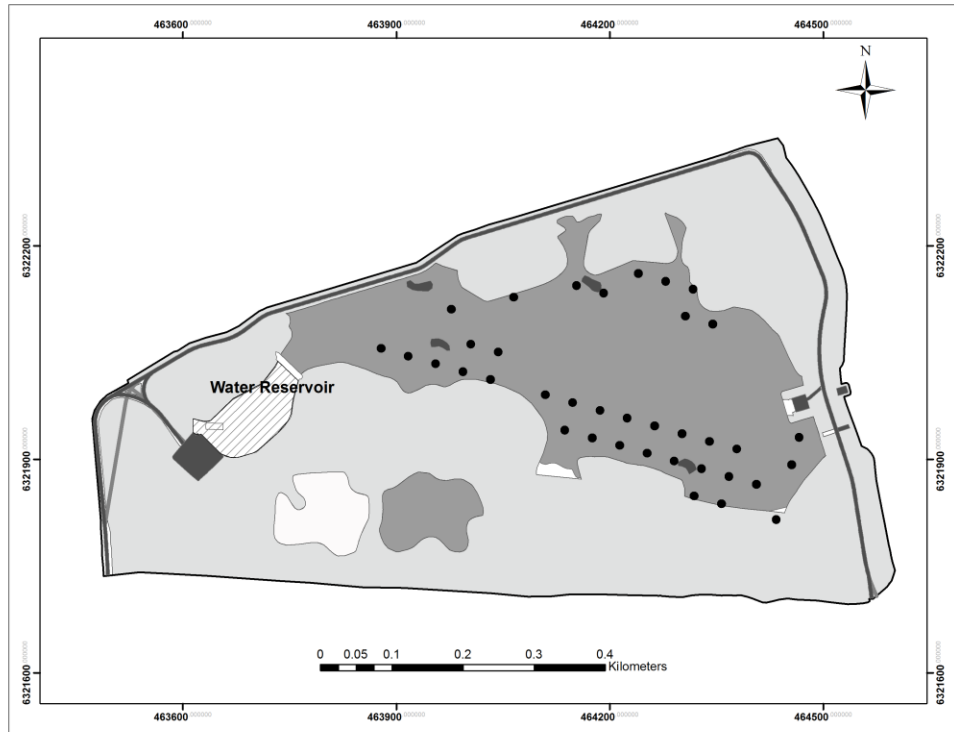


Figure 2.10 Spatial distribution of Group 3 plots (2015) within Sandhill Fen.

Patterns in Species Abundances and Richness: Desirable vascular plant species abundances (cover) are highest in group 2 and decrease in groups 1 and 3 (Figure 2.11), in contrast, undesirable vascular plant abundances are much higher in groups 1 and 3 and lowest in group 2 (Figure 2.12). Thus, species naturally found in peat-forming habitats (fens) in the region are most abundant in group 2 while upland species and weeds are most abundant in group 3, while marsh species are abundant in group 1. Species richness follows a similar pattern – with greatest number of desirable vascular plant species in Species group 2 and less in groups 1 and 3 (Table 2.5, Figure 2.12). In contrast undesirable, vascular plant species have greatest richness in species group 3 (Table 2.5, Figure 2.12).

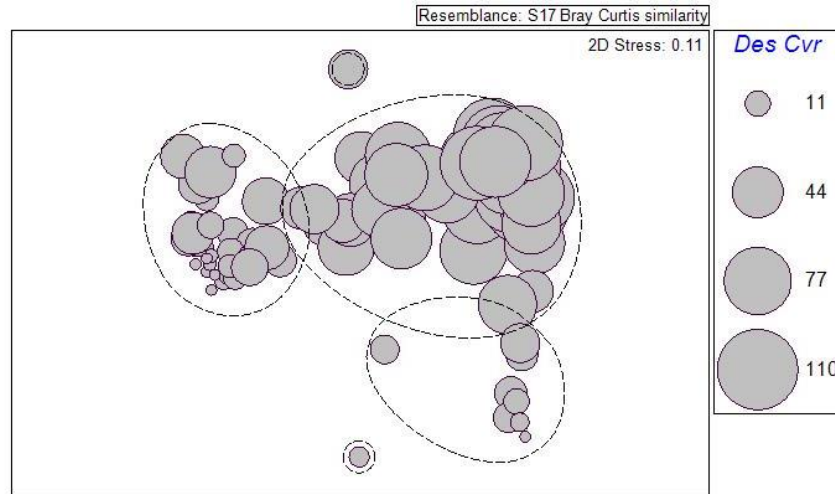


Figure 2.11 NMDS ordination of 2016 abundance data with abundance (as percent cover) of desirable vascular plant species overlain. Dotted circles are bounds of species groups.

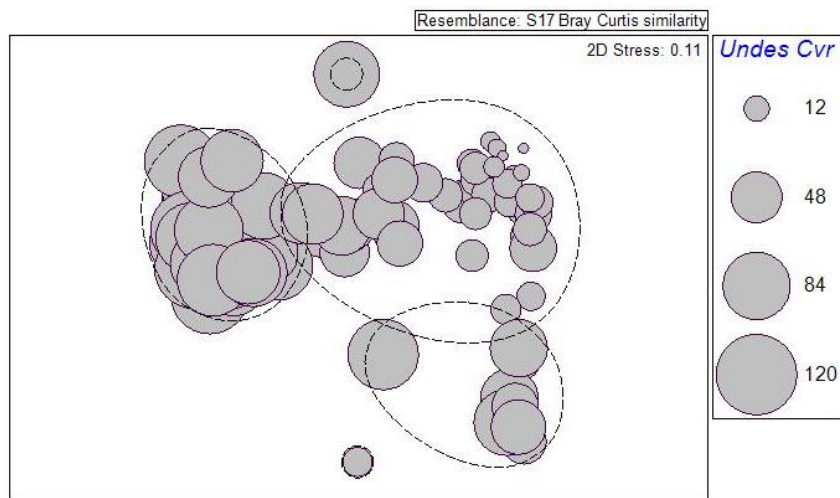


Figure 2.12 NMDS ordination of 2016 abundance data with abundance (as percent cover) of undesirable vascular plant species overlain. Dotted circles are bounds of species groups.

2015	Undesirable Species			Desirable Species		
Group	Alpha	Beta	Gamma	Alpha	Beta	Gamma
1	1.1	1.8	2.0	2.2	3.7	8.0
2	5.9	6.4	38.0	5.5	5.8	32.0
3	11.5	4.6	53.0	3.9	6.2	24.0
2016	Undesirable Species			Desirable Species		
Group	Alpha	Beta	Gamma	Alpha	Beta	Gamma
1	2.0	4.0	8.0	3.0	2.3	7.0
2	3.1	11.0	34.0	4.6	6.5	30.0
3	9.9	4.0	40.0	3.6	5.5	20.0

Table 2.5 Mean alpha and beta, and gamma diversity for desirable and undesirable vascular plant species as found in the four species groups in based on the 2105 survey and the three species groups from the 2016 survey.

Patterns in Bryophyte Diversity: In 2016, both ‘all bryophytes’ and ‘peat-forming bryophytes’ occur very infrequently in group 1 and are consistently diverse across groups 2 and 3 (Figures 2.13-2.14).

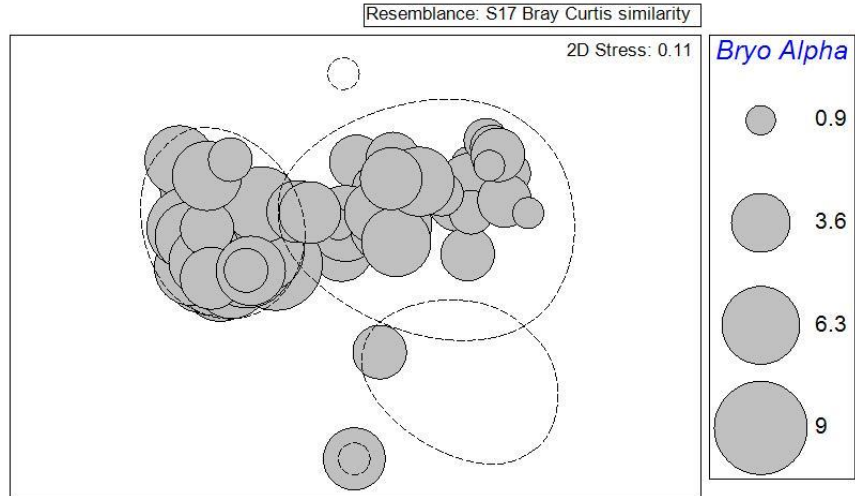


Figure 2.13 NMDS ordination of 2016 abundance data with alpha diversity of bryophyte species at each plot overlain. Dotted circles are bounds of species groups.

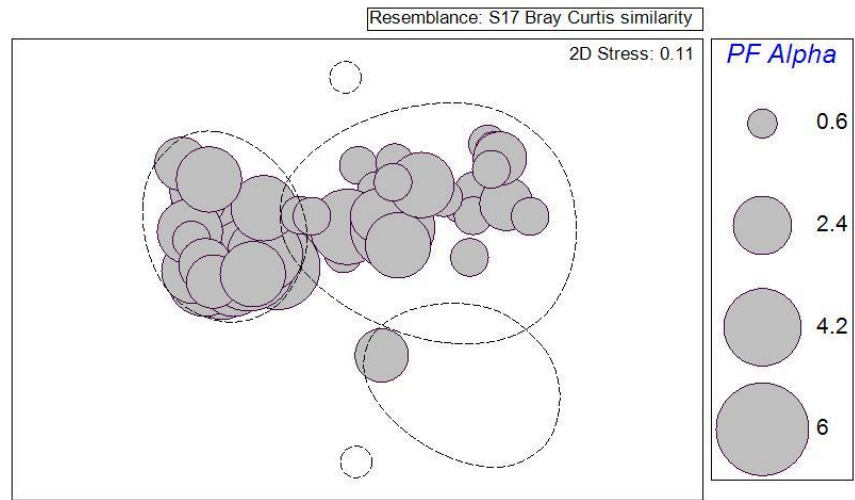


Figure 2.14 NMDS ordination of 2016 abundance data with alpha diversity of peat-forming bryophyte species at each plot overlain. Dotted circles are bounds of species groups.

Spatial Patterns Across Sandhill Fen (Figure 2.15): As in 2015, the 85 plots are uniformly distributed across Sandhill Fen, and we can determine the spatial extent of the three species groups. In 2015, we mapped the occurrences of the three species groups across Sandhill Fen, and each of the three groups had a unique distribution across the fen (Figure 2.6, 2.8, and 2.10). Group 1 occurred in the eastern-center portion of the fen, group 2 in the center and northern portion of the fen, and group 3 along the edges especially along the southern edge. A fourth group occurred in a small area to the northwest in 2015, but did not persist into 2016 (not shown). In 2016, Comparing the three major groups in 2015 with those in 2016 yields the following changes: Overall 12 plots changed species group (2 in group 4 were considered upland in 2016). Five plots changed from group 3 to group 2; 4 plots from group 1 to group 2 – thus group 2 gained 9 plots. Also, one plots changed from group 2 to group 1 and one plots changed from group 2 to 3 – thus here group two lost 2 plots. In 2016, 9.6% of the fen is occupied by group 1, 50.6% by group 2, and 39.8% by group 3. Changes from 2015 include a decrease in group 1 (13.2% to 9.6%) an increase in group 2 (39.8% to 50.6%) and a decrease in group 3 (47% to 39.8%).

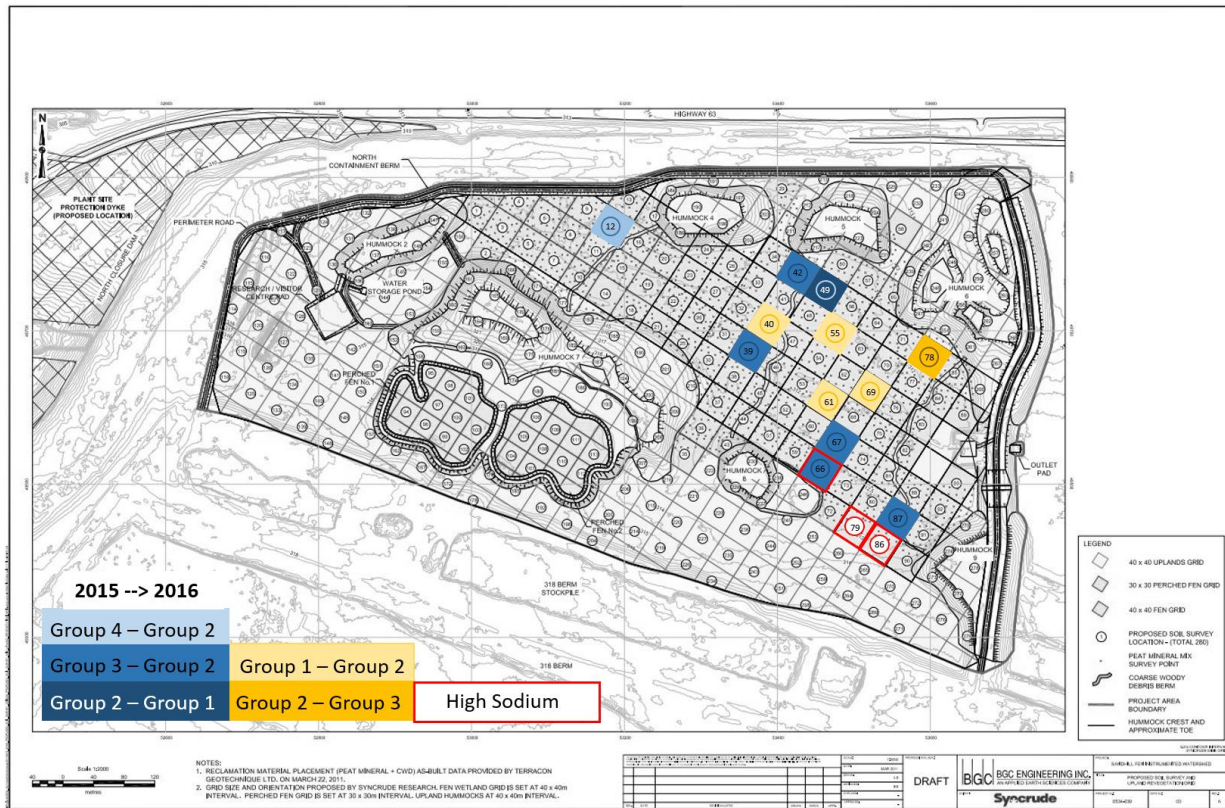


Figure 2.15 Map of Sandhill Fen with plots (color coded; see key) that changed their species group from 2015 to 2016; plots with high extractable sodium values are outlined in red.

Further Comparisons Between 2015 and 2016: Overall the three species groups remain stable, each characterized by the same dominant species; however, a few changes seem important and may indicate trends.

- 1) *Calamagrostis canadensis* increased in abundance in group 3 by 11.2%.
- 2) Vascular plant species abundances in group 2 remained stable.
- 3) *Typha latifolia* increased in abundance in group 1 by 65.7% (43% to 52% cover), with a decrease in *Carex aquatilis* from 32% to 10% cover.
- 4) Total occurrences of vascular plants decreased from 1,087 in 2015 to 852 in 2016 – a decrease of 235 occurrences or 22%; likewise, total number of vascular plant species decreased from 100 to 87. This decrease was most evident in a decrease in undesirable species in group 3. Bryophyte occurrences decreased from 312 in 2015 to 260 in 2016, a decrease of 17%, but total number of species remained nearly stable 24 vs. 23).
- 5) Alpha (plot) diversity of bryophytes decreased markedly in group 2 (3.2 to 1.3; Table 2.6) yet gamma (overall) diversity remained high in group 2 indicating fewer occurrence in the species group – perhaps in association with the 9% overall increase in cover of the major vascular plant species.
- 6) Desirable vascular plant cover is clearly associated with group 2 (Figure 2.11), while undesirable vascular plant cover is associated with group 1 and 3 (Figure 2.12), these patterns remained unchanged from 2015 (Table 2.5).

2015	All Bryophytes			Peat Forming Bryophytes		
Group	Alpha	Beta	Gamma	Alpha	Beta	Gamma
1	0.0	0.0	0.0	0.0	0.0	0.0
2	3.2	5.7	18.0	2.1	7.1	15.0
3	4.9	3.9	19.0	2.8	5.4	15.0
2016	All Bryophytes			Peat Forming Bryophytes		
Group	Alpha	Beta	Gamma	Alpha	Beta	Gamma
1	0.4	8.0	3.0	0.3	8.0	2.0
2	1.3	12.8	17.0	0.6	21.2	12.0
3	3.2	5.0	16.0	2.1	5.7	12.0

Table 2.6 Mean alpha and beta, and gamma diversity for ‘all bryophytes’ and for bryophyte species that contribute to peat formation as found in the four species groups in based on the 2015 survey and the three species groups from the 2016 survey.

Conclusions and Recommendations: From a survey of 85 plots we found 87 vascular plant species and 23 bryophyte species (combining both groups - 11% fewer than 2015). The most common species were *Carex aquatilis* and *Calamagrostis canadensis*, similar to that in 2015. We used cluster analysis and NMDS ordination to define three species groups. These groups are arranged along a moisture gradient with marsh species dominating one group, peat-forming species the second group, and upland/weedy species (undesirable species) the third group. These three species groups are similar to the three dominant groups in 2015. Changes from 2015 include a decrease in area of occurrence in group 1 (12% to 9.4%) an increase in group 2 (40% to 48.2%) and a decrease in group 3 (40% to 34%). In 2015, these groups all had distinctive spatial distributions across Sandhill Fen, and in 2016 most of the changes between groups was in the lower (weir) region. Species canopy cover varies from 45 to 100%, thus there is abundant plant cover throughout the fen, however, only species group 2 has high abundance and high diversity of desirable peat-forming plants. In contrast, and similar to 2015, species group 1 has abundance of an undesirable species (*Typha latifolia*), whereas group 3 has high species diversity of undesirable species.

We conclude that there are both abundant and diverse vascular plants and bryophytes on Sandhill Fen, and that these species are clearly distributed into species assemblages (groups). These

assemblages occupy discrete areas of the fen; however, peat-forming species characteristic of natural fen habitats in the region form only a portion of the diversity and abundance on the fen; these desirable species are most abundant in only one of the species groups and this group of species occupies about 48.2% of the fen, an increase in 8.2% from 2015 - suggesting that this area has similarities to natural fens of the region. Species groups dominated by upland and weedy species occupy 34% of the fen (6% lower than 2015), while the species group of marsh plants occupies 9.4% of the fen (2.6% lower than 2015) - suggesting that these areas may not be on a trajectory to peat-forming fens, but represent early stages of either marsh or riparian plant communities (the latter with high numbers of *Populus balsamifera*). Bryophytes, as major peat-forming species, occur frequently in two of the three species groups, but are less frequent in 2016 than in 2015 (17% fewer occurrences). Likewise, the frequency of occurrence of vascular plants decreased 22% in 2016, and in this case, contribute to a decrease in species diversity. These decreases in occurrences and/or diversity may be attributed in part to an increase in abundance of the dominant species.

Physiological Performance of Target Species

Here we provide a summary of key findings from Lilyan Glaeser's Master's thesis, *Established plant physiological responses and species assemblage development during early fen reclamation in the Alberta oil sands area*. The full thesis document is available through the SFMMS web tool or by request. The Master's study set out to answer: 1) At what sodium concentration does *Beckmannia syzigachne* show a negative physiological response and 2) what are the physiological parameters for *Carex aquatilis*, *Scirpus atrocinctus*, and *Triglochin maritima* and how do they compare to benchmark sites?

***Beckmannia syzigachne* physiological response to sodium and water level**

(Please see Glaeser et al. [2016] for detailed methods and analysis.)

To determine the sodium tolerance of *Beckmannia syzigachne*, a greenhouse study was designed and carried out. Seedlings were exposed to two water levels, 2.5 cm below the soil surface and 7.5 cm below the soil surface, and six sodium levels: 5 mg⁻¹ L⁻¹, 400 mg⁻¹ L⁻¹, 850 mg⁻¹ L⁻¹, and 1,250 mg⁻¹ L⁻¹, 1850 mg⁻¹ L⁻¹, and 2700 mg⁻¹ L⁻¹. The plants were maintained for 5 months. Net photosynthesis, evapotranspiration, and stomatal conductance of the plants was measured at 83 days, 118 days, and 146 days from the start of the experiment. At the end of the experiment, the plants were rinsed and dried; root and shoot biomass were weighed.

Results: Water level did have an affect on *Beckmannia syzigachne* biomass (Figure 2.16); higher water table position led to significantly lower biomass. Sodium treatment did affect physiological processes and biomass. *Beckmannia syzigachne* plant biomass was reduced at the 1,250 mg⁻¹ L⁻¹ Na treatment level (Figure 2.17), and a reduced physiological performance was observed at the 850 Na treatment level, the lowest level of sodium that would cause an effect is between 400 and 850 mg⁻¹ L⁻¹ Na, but the exact point could not be detected by this study. At 850, stomatal conductance, evapotranspiration, and photosynthetic rate decline. *Beckmannia syzigachne* plants survive all treatments levels up to 2,700 mg⁻¹ L⁻¹. Currently, sodium levels at Sandhill Fen are approximately 200 mg⁻¹ L⁻¹. *Beckmannia syzigachne* is a good reclamation candidate for this system, and other reclamations in which sodium levels are a concern. *B. syzigachne* has potential survive rising sodium levels.

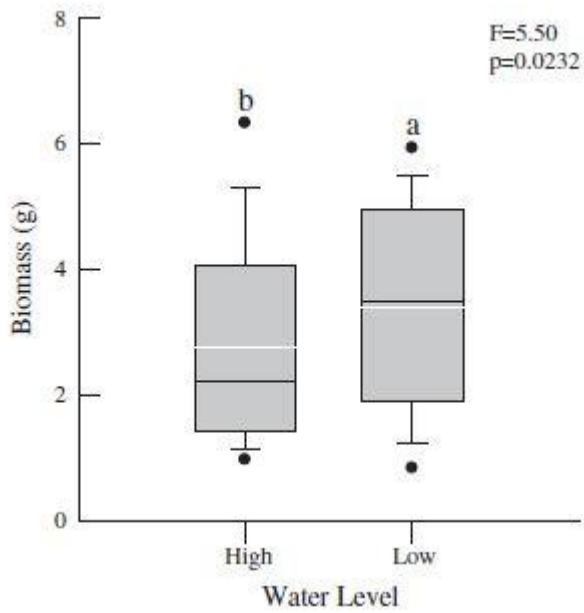


Figure 2.16 Influence of water level on total dry weight biomass of *Beckmannia syzigachne* plants. The white line represents the mean, the black line represents the median, the error bars show the minimum and maximum values of the data set, the box below the median represents the first quartile and the box above the median represents the third quartile. Significant differences are indicated by different letters.

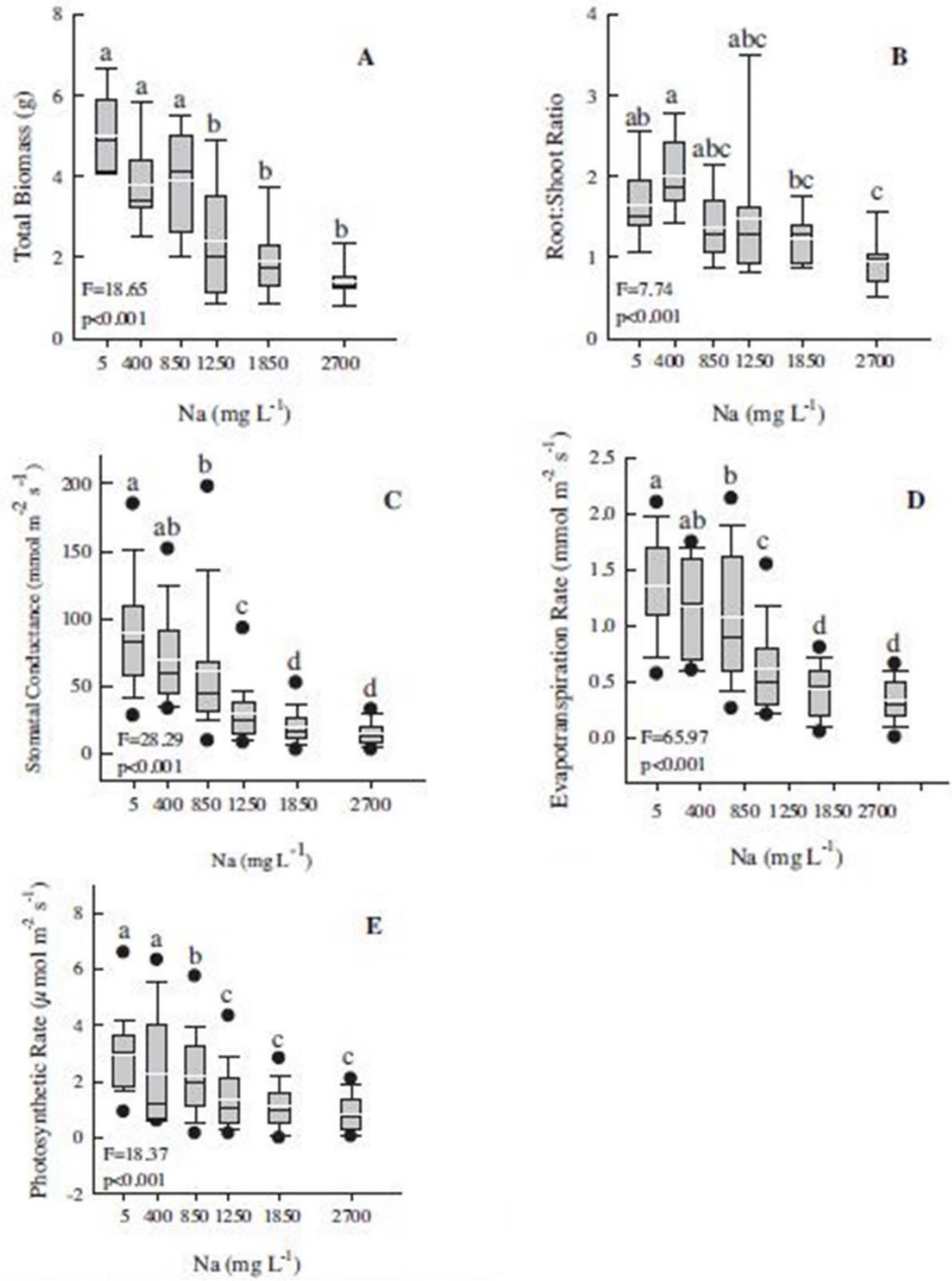


Figure 2.17 Influence of sodium (Na) treatment on total dry weight biomass (A), root:shoot ratio (B), stomatal conductance (C), evapotranspiration (D), and photosynthetic rate (E) of *Beckmannia syzigachne* plants. For panels A-E, the white line represents the mean, the black line represents the median, the error bars show the minimum and maximum values of the data set, the box below the median represents the first quartile and the box above the median represents the third quartile.

Physiological response of three reclamation species to soil moisture

As a gradient of soil moisture and sodium concentration became clear across Sandhill Fen, a study was designed to test the physiological performance of three planted species that exhibited high survivorship rates (>80%) in our 20 research plots spatially distributed across the fen. We wanted to know, as soil electrical conductivity (EC) and soil sodium concentrations increase, will there be a physiological response in the target plant species? Will increased soil moisture elicit a positive physiological response from these wetland species?

Methods: To answer these questions, Lilyan Glaeser measured the photosynthetic rate and evapotranspiration of *Carex aquatilis*, *Scirpus atrocinctus*, and *Triglochin maritima* plants across Sandhill fen in 2014. In addition, benchmark sites were established for each species to determine if the plants were performing similarly at Sandhill Fen as compared to natural sites. To assess soil moisture, soil EC, and soil sodium content, soil samples were collected from all plots.

Benchmark Sites

Physiology of the three species was compared within the environmental gradients of Sandhill Fen and compared to naturally occurring sites, at varying ages of disturbances.

Anzac roadside consists of three sites (56°22.585 N, 111°01.174 W; 56°22.563 N, 111°01.327 W; 56°22.574 N, 111°01.312 W): a poorly drained ditch (Anzac Ditch) where *C. aquatilis* is abundant, a mineral soil (Anzac Mineral) where *S. atrocinctus* and *C. aquatilis* grow with weedy mosses and other graminoids, and a transitional peatland (Anzac Bog Transition), where *C. aquatilis* grows in dense populations of *Sphagnum angustifolium*. The most recent disturbance of this site was in 2006 when the road was paved.

Engstrom Lake (56°12.023 N, 110°53.476 W) is a poorly drained area where *S. atrocinctus* grows with several other sedges. The most recent disturbance to this area is unknown, but occurred within the past 30 years, when the area was heavily populated and construction began for access roads to recreational areas.

High-test fen (56°57.036 N, 111°31.818 W) is a millennial old rich wet fen where *T. maritima* grows sparsely, not in dense monocultures. The most recent disturbance to this area occurred over one hundred or possibly thousands of years ago.

Mariana Lake is a marshlike environment along an access road, where *S. atrocinctus* grows. The most recent disturbance to this area occurred over one hundred or possible thousands of years ago.

U-Cell is an experimental site, where peat was placed into cells and wetland species were planted and different water regimes were implemented. *Carex aquatilis*, *Triglochin maritima*, and *Scirpus atrocinctus* is found throughout the site. This site was initiated in 2009, and has the least time since disturbance of the benchmark sites.

Here we will discuss the effect of soil moisture on photosynthetic rate because this presented the strongest relationship of those sampled. Additional methods and results are available in her thesis.

To determine soil moisture content, a sample was taken from the rooting zone (0-10 cm depth), the fresh sample was weighed, then dried at 55° C for 48 hours, a final weight was recorded, and percent soil moisture calculated.

Photosynthesis rates were measured using a CI-340 handheld photosynthesis system. In 2014, all measurements were taken between 10:00 am and 3:00 pm MDT, June 20 – June 22. The CI-340 determines the photosynthetic rate by measuring the difference between carbon dioxide levels in air coming into and going out of a closed chamber clamped onto leaf tissue. To reduce variability in measurements, an external light source emitting 750 nm was placed on top of the chamber containing the leaves.

Results: *Carex aquatilis* photosynthetic rates at Sandhill Fen ranged from 1.4 – 18.3 $\mu\text{mol m}^{-2} \text{s}^{-1}$, and there was no relationship between photosynthetic rate and percent soil moisture (Figure 2.18). The range of photosynthetic rates in benchmark sites (n=4) performed within the range of Sandhill Fen measurements (2.5 – 14.4 $\mu\text{mol m}^{-2} \text{s}^{-1}$).

For *Scirpus atrocinctus*, there was no relationship between photosynthetic rate and percent soil moisture. The photosynthetic rate recorded in Sandhill Fen was 3 – 16 $\mu\text{mol m}^{-2} \text{s}^{-1}$. Plants from one benchmark site, the least disturbed, performed outside of this range (10.8 – 17.4 $\mu\text{mol m}^{-2} \text{s}^{-1}$). The remaining benchmark sites (n=3) fell within the range recorded at Sandhill Fen ($\mu\text{mol m}^{-2} \text{s}^{-1}$).

Triglochin maritima photosynthetic rates at Sandhill Fen ranged from 2 – 29.5 $\mu\text{mol m}^{-2} \text{s}^{-1}$, and there was a weak positive relationship between photosynthetic rate and increasing percent soil moisture. Photosynthetic rates (2.7 – 15.6 $\mu\text{mol m}^{-2} \text{s}^{-1}$) from benchmark sites (n=2) fell within the range recorded at Sandhill Fen.

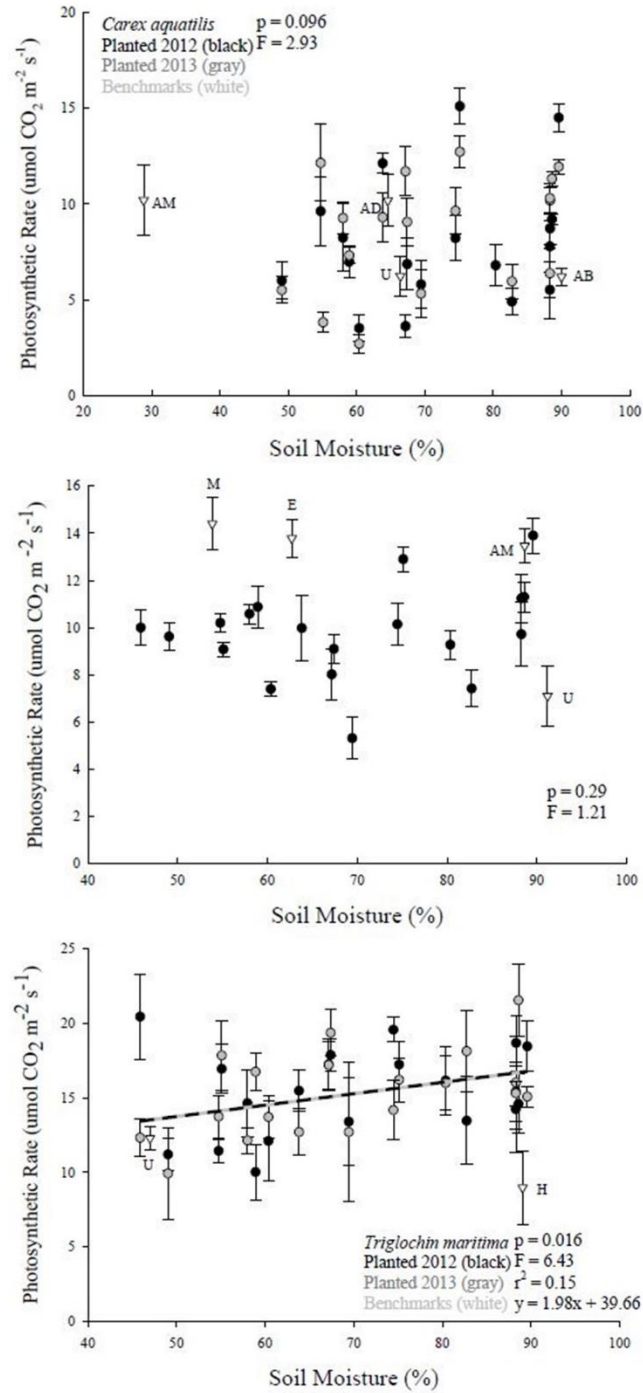


Figure 2.18 Regression line for photosynthetic rate response as percent soil moisture increases for *Carex aquatilis* (top), *Scirpus atrocinctus* (middle), and *Triglochin maritima* (bottom). Black circles are monocultures planted in SHF in 2012; white circles or triangles (for *S. atrocinctus*) are benchmark sites.

Conclusions: *Beckmannia syzigachne* shows reduced physiological performance in response to sodium concentrations exceeding $850 \text{ mg}^{-1} \text{ L}^{-1}$, but survives in sodium levels up to $2,700 \text{ mg}^{-1} \text{ L}^{-1}$; 2) *Carex aquatilis*, *Scirpus atrocinctus*, and *Triglochin maritima* physiological parameters are within the range observed at benchmark sites, and performance within Sandhill Fen is tied to soil moisture.

All three species, *C. aquatilis*, *S. atrocinctus*, and *T. maritima* exhibit similar physiological performance at Sandhill Fen as at benchmark sites. Soil sodium levels at Sandhill Fen as of 2014, had no adverse effects on plant performance. Higher soil moisture resulted in higher photosynthetic rates for *T. maritima*.

We would recommend all four species for open pit mine reclamation. *Scirpus atrocinctus* appears to be the least sensitive to inherent abiotic factors of a reclamation site, however, all three responded favorably to increased soil moisture. Thus, we conclude that soil moisture and the management of site moisture appears to be the most important factor especially during the first few years of plant establishment.

A comparative study of planting species assemblages vs. monocultures

Introducing plants to a reclamation is a challenge made more difficult when the site is designed to be a wetland with a water table at or near the soil surface. Low seed viability of many wetland plant species further complicates plant introduction. Planting seedlings is labor intensive and costly. Planting a monoculture of a desirable species that spreads by rhizomes is an appealing option, but does it come at a cost to overall plant diversity?

This study was designed to answer: 1) does planting diverse species rich assemblages assist in the proliferation of desirable species, 2) does planting diverse species rich assemblages assist in recruitment of desirable species, and 3) does soil moisture play a role in species assemblage composition?

Results:

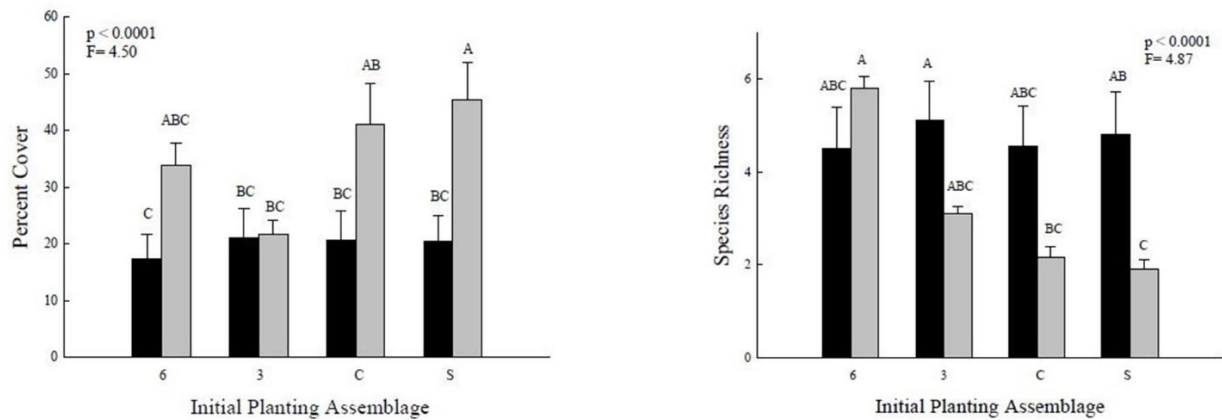


Figure 2.19 Abundance (left) and species richness (right) of undesirable (black bars) and desirable species (gray bars) one year after four different plant assemblages were planted in Sandhill Fen. Bars are means of abundance (n=20), lines are plus standard error. Different letters indicate significant differences (p<0.05). C: *Carex aquatilis* monoculture, S: *Scirpus microcarpus* monoculture, 3: trios plots, 6: sextet plots.

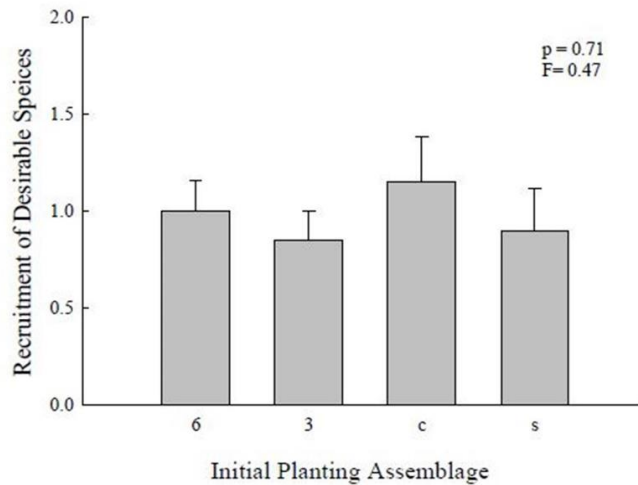


Figure 2.20 Recruitment of new desirable species among the four plant assemblages. Bars are means of species richness (n=80), lines above the bars are plus standard error. Different letters indicate significant differences ($p < 0.05$). C: *Carex aquatilis* monoculture, S: *Scirpus microcarpus* monoculture, 3: trios plots, 6: sextet plots.

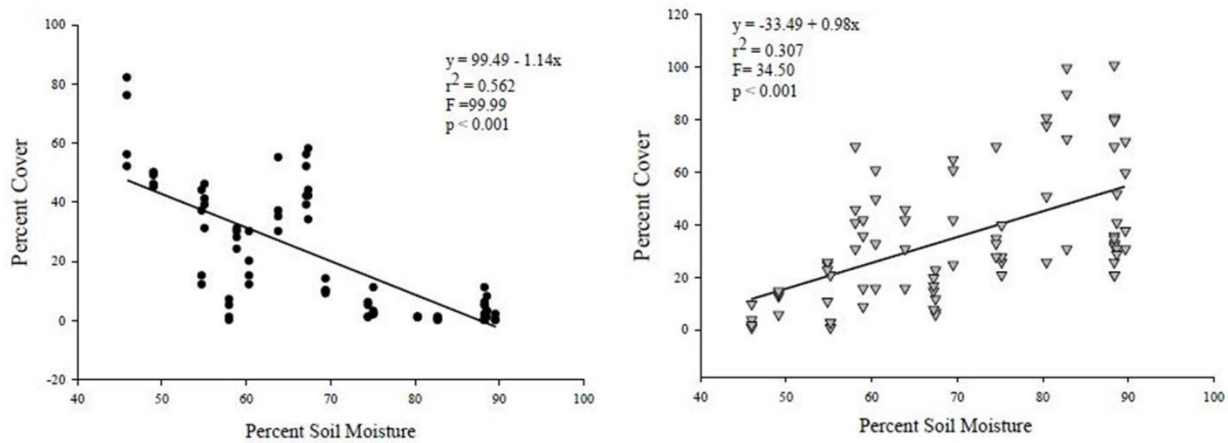


Figure 2.21 Linear regression of abundances of undesirable species (left) and desirable species (right) in planting assemblage plots in relation to percent soil moisture.

Conclusions : After one year, planting diverse assemblages appears to have no influence over the abundance of desirable species (Figure 2.19), recruitment of new desirable species (Figure 2.20), nor the limitation of undesirable species establishment (Figure 2.19). Planting monocultures of desirable species allow for higher abundance with just as much recruitment of new desirable species. Here again, we find that soil moisture is an important abiotic driver determining the abundance of desirable species (Figure 2.21).

These conclusions are after one year of growth, and recruitment of new species could take more time. We recommend that these plots be reevaluated to determine if the trajectories differences occur over a longer time span than one year.

Aboveground and belowground net primary production of four Cyperaceae at the Sandhill Fen reclamation site

The objective of this study was to compare four sedge species (*Carex aquatilis*, *Carex canescens*, *Carex hystericina* and *Scirpus microcarpus*), with differing structural attributes, in terms of net primary production (NPP) and carbon-to-nitrogen ratios (CN) of the aboveground and belowground tissues. Comparing these traits helps determine each species' influence on organic layer development and gives further insight into tolerances of conditions in a recent oil-sands reclamation or a similar scenario.

Carex aquatilis, *Carex canescens*, *Carex hystericina*, and *Scirpus microcarpus* were chosen for comparison due to their differing morphologies. *Carex hystericina* and *S. microcarpus* are larger species, with wide leaf blades. The four sedge species not only differ in size, but also in growth form. *Carex aquatilis* and *S. microcarpus* are rhizomatous growth forms, while *C. canescens* and *C. hystericina* are considered caespitose, or clumpy, growth forms. All the species are perennials, apart from *C. aquatilis*, which is a biennial. Biennial species often produce more biomass (shoots, roots, and seed) in the second year of life, which may influence this species net ecosystem exchange rate.

Methods: Twelve 10 m² research plots were chosen from the twenty set up across Sandhill Fen. These plots were chosen due to varying hydrologic conditions, such as consistently dry, fluctuating water levels, or consistently saturated. *Carex hystericina* and *S. microcarpus* were planted in 2012. *Carex aquatilis* and *Carex canescens* were planted in 2013. The four sedge species chosen to be studied over the 2014 and 2015 growing seasons (*Carex aquatilis*, *Carex hystericina*, *Carex canescens*, and *Scirpus microcarpus*) were chosen based on high species survival (>50%) over the last two years and because of their common use in reclamation scenarios.

Aboveground Net Primary Production

At the beginning of the growing season, 30 cm diameter rings were placed around randomly selected sedges from each of the four species at each of the twelve research plots. At the end of the growing season in late fall, aboveground biomass was clipped, and then dried at 60 °C until the weight stabilized. The weights of each aboveground sample were recorded and the biomass was returned to the plant, minus a small subsample for CN analyses.

Belowground Net Primary Production

In 2014, belowground biomass was collected by taking 7.6 cm diameter by 30 cm deep cores as close to each of the four sedge species as possible, without damaging the plant. After the removal of cores, root in-growth bags made from tulle and filled with clean, moist peat were immediately placed in the holes (Polomski and Kuhn 2002). Initial soil cores were removed and root in-growth bags were placed in late spring, May 26 - July 7, 2014. Root in-growth bags were removed at the beginning of the 2015 field season, June 7 - June 11. To preserve roots and limit decomposition, samples were kept in cold storage until roots could be sorted from the substrate.

In the lab, soil cores were sieved to remove clay and other fine particles. Each sample was sorted for roots for one hour. It was determined that after an hour of root sorting, any increases in biomass retrieved were negligible. Wet root biomass was dried at 60°C until dry weight had stabilized. Annual belowground NPP was calculated from the root dry weight divided by the volume of the core or root in-growth bag.

Carbon-to-Nitrogen Ratios

Biomass subsamples of aboveground and belowground tissue was dried, ground, and weighed with a microbalance before being analyzed with a Flash 2000 Series CHN/CHNS/Oxygen Automatic Elemental Analyzer.

Statistical Analysis

One-way ANOVAS were run with SigmaPlot software (Windows Version 11.0 Build 11.1.0.102) on aboveground NPP, belowground NPP, total NPP and shoot CN data to test for differences between species (*C. aquatilis*, *C. canescens*, *C. hystericina*, and *S. microcarpus*). All data passed the equal variance test, except for belowground NPP ($P < 0.050$). Datasets for root CN and whole plant CN were missing a large number of samples, therefore statistical analyses could not be run on these sets. Data for CN was normally distributed; however, aboveground NPP was not normally distributed. In order to achieve normality for further analyses, major outliers were removed, square root transformations were applied to aboveground NPP data.

Results:

Net Primary Production

Aboveground, belowground, and total NPP had a consistent pattern across 2014 and 2015. *Carex aquatilis* and *C. hystericina* were quite similar producers in all categories, while *C. canescens* was on the lower end of production and *S. microcarpus* was on the high. Here we present combined data to highlight the differences between species.

Scripus microcarpus produces more aboveground biomass ($302.9 \text{ g m}^{-2} \text{ yr}^{-1}$) than *C. hystericina* ($184.2 \text{ g m}^{-2} \text{ yr}^{-1}$), *C. aquatilis* ($187.6 \text{ g m}^{-2} \text{ yr}^{-1}$), and *C. canescens* ($123.4 \text{ g m}^{-2} \text{ yr}^{-1}$). When it comes to belowground biomass, however, *Carex canescens* produces less ($210 \text{ g m}^{-2} \text{ yr}^{-1}$) than *S. microcarpus* ($356 \text{ g m}^{-2} \text{ yr}^{-1}$), *C. aquatilis* ($349.6 \text{ g m}^{-2} \text{ yr}^{-1}$), and *C. hystericina* ($382.8 \text{ g m}^{-2} \text{ yr}^{-1}$). In some cases, these sedges produce nearly double belowground biomass compared to the amount of aboveground biomass. As a result, total biomass (aboveground and belowground biomass combined) is higher in *C. aquatilis* ($546.9 \text{ g m}^{-2} \text{ yr}^{-1}$), *C. hystericina* ($554.4 \text{ g m}^{-2} \text{ yr}^{-1}$), and *S. microcarpus* ($663.4 \text{ g m}^{-2} \text{ yr}^{-1}$) than in *C. canescens* ($327 \text{ g m}^{-2} \text{ yr}^{-1}$; Figure 2.22).

This study was conducted at Sandhill Fen without benchmark sites for comparison, but the values can be compared to those found in the literature. Thormann and Bayley (1977) found that sedge dominated fens produce an average of $266 \text{ g OM m}^{-2} \text{ yr}^{-1}$ in aboveground biomass, and the mean value for aboveground NPP of $204.1 \text{ g m}^{-2} \text{ yr}^{-1}$. For total biomass, an open fen was found to produce between 209.1 and $413.7 \text{ g m}^{-2} \text{ yr}^{-1}$ (Graham 2012); at Sandhill Fen, total NPP was $535.0 \text{ g m}^{-2} \text{ yr}^{-1}$. Not many species specific NPP studies have been done, but for *Carex aquatilis*, we found annual aboveground NPP to be an average of $187.5 \text{ g m}^{-2} \text{ yr}^{-1}$, and Campbell et al. (2000) measured aboveground NPP to range from 164 to $240 \text{ g m}^{-2} \text{ yr}^{-1}$. Sedge NPP varies depending on site conditions and species present, but sedge biomass production at Sandhill Fen is comparable to that found in natural sites.

Carbon to Nitrogen Ratios

Shoot CN ratios were higher for *C. hystericina* and *S. microcarpus* than for *C. aquatilis* and *C. canescens*. There were no differences between species for belowground or total CN ratios (Figure 2.23).

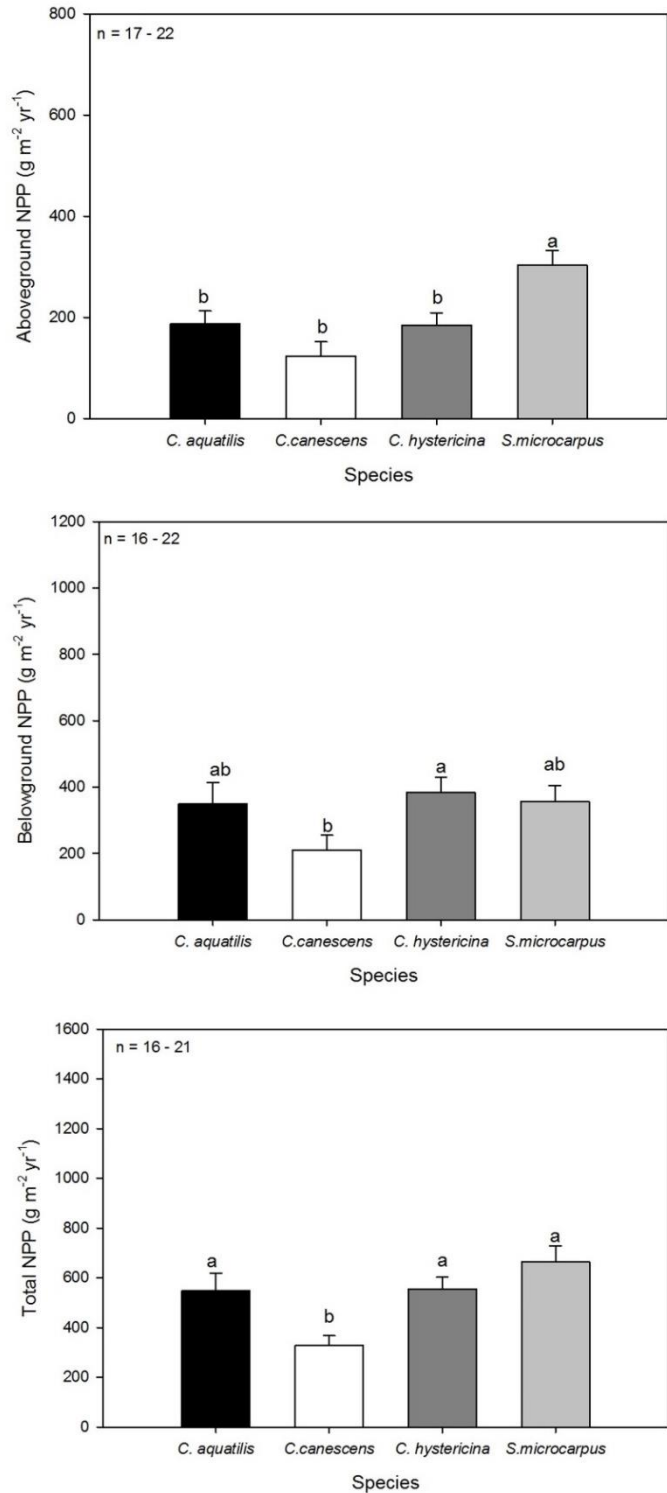


Figure 2.22 Mean aboveground (top), belowground (middle), and total biomass (bottom) $\text{g m}^{-2} \text{yr}^{-1}$ in 2014 and 2015 combined for *Carex aquatilis*, *C. canescens*, *C. hystericina*, and *Scirpus microcarpus*. Differences between aboveground NPP of *S. microcarpus* and all other species were significant ($P < 0.05$).

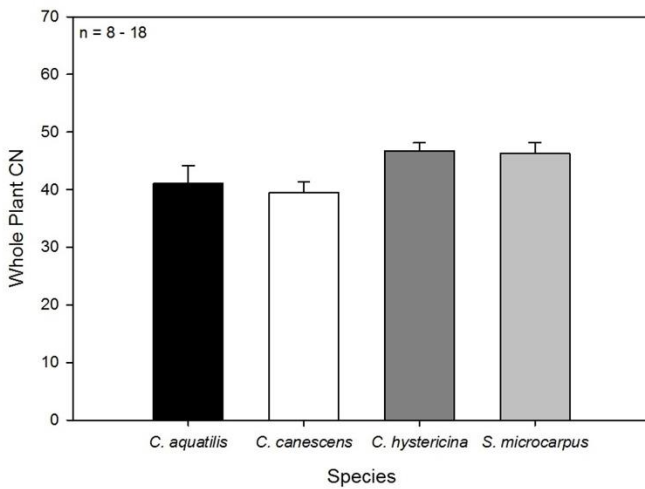
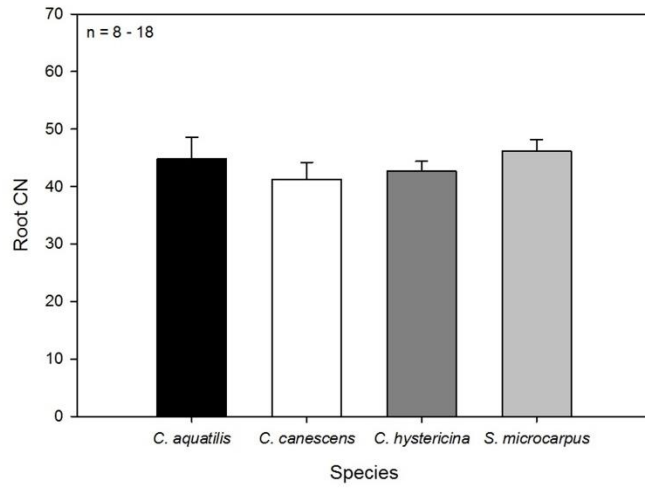
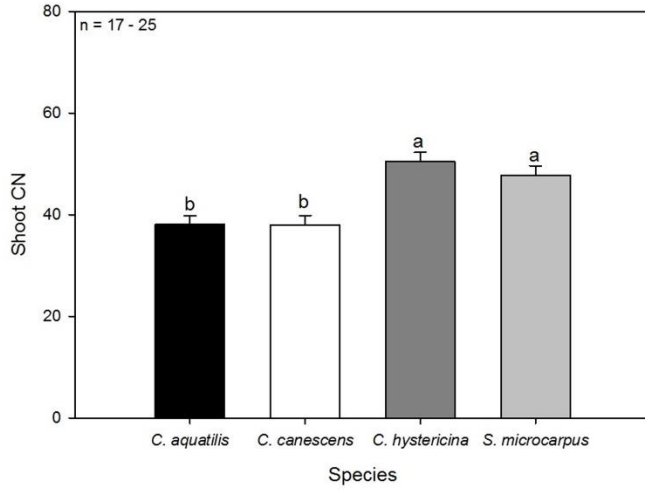


Figure 2.23 Shoot biomass (top), root biomass (middle), and total biomass (bottom) mean carbon-to-nitrogen ratios in 2014 and 2015 combined for *Carex aquatilis*, *C. canescens*, *C. hystericina*, and *S. microcarpus*. Differences between shoot carbon-to-nitrogen ratios of each species were significant ($P < 0.05$).

Conclusions: Aboveground, belowground, and total NPP had a consistent pattern across 2014 and 2015. *Carex aquatilis* and *C. hystericina* were quite similar producers in all categories, while *C. canescens* was on the lower end of production and *S. microcarpus* was on the high.

Simply through observing *S. microcarpus* through the study period, this species appeared to be more robust. *Scirpus microcarpus* had wide leaf blades and produced many ramets, which created a seemingly weed-resistant mat. *Carex hystericina* had thick leaf blades, but the clumpy growth form appeared to restrict this species ability to compete with nearby weedy or native propagules. *Carex aquatilis* is a narrow-bladed sedge, but has a rhizomatous growth form similar to *S. microcarpus*. The rhizomatous growth form may be advantageous for species in a reclamation scenario, where belowground development of the organic layer is desired. However, the biennial nature of *C. aquatilis* may be why this species had NPP values comparable to the often larger, *C. hystericina*. *Carex canescens* had the lowest NPP and appeared to be losing the competition for the root column based on the NPP data and root-to-shoot ratios (data not shown; available in Hazen 2016).

Three of the sedge species, excluding *C. canescens*, are recommended for oil sands reclamation. The root systems of each of the species are establishing within the organic layer, net primary production is increasing through time, and the CN of these plants is within moderate levels necessary for building an organic layer. These three species will also add to plant diversity within the site, due to their differing sizes and growth forms. Finally, it may be advisable for site managers to develop practices which will ensure the aboveground NPP is not lost through events such as wind and water erosion. The development of the organic layer is very important within peatland ecosystems, so it is imperative that every bit of plant biomass remain at the Sandhill Fen reclamation site.

Carbon dioxide net ecosystem exchange of four Cyperaceae species

Quantifying carbon dioxide flux of a monoculture of plant species may be beneficial in comparing efficiency of CO₂ sequestration of individual plant species within that site. Net ecosystem exchange (NEE, $\mu\text{mol m}^{-2} \text{s}^{-1}$) can be used to describe the carbon budget of a local area of an ecosystem by combining the rates of photosynthesis and respiration (both autotrophic plant respiration and heterotrophic respiration of soil fauna). Positive NEE values signify that a system is functioning as a carbon sink, and negative NEE values mean that it is a source of carbon to the atmosphere.

The objectives of this study are: 1) to determine the differences in NEE of carbon dioxide of four sedge species: *Carex aquatilis*, *Carex canescens*, *Carex hystericina*, and *Scirpus microcarpus*, all common across Sandhill Fen, and 2) to determine if the four species of interest are acting as annual source or sink for carbon.

Methods: This study was carried out in subset of 12 of our 20 research plots across Sandhill Fen, excluding the perched fens. Plots were chosen from across the hydrologic gradient. To measure CO₂ flux, collars were installed around a plant of each species so that a transparent plastic chamber could be attached with an air-tight seal. An infrared gas analyzer (IRGA, PP Systems) with an additional probe for reading photosynthetically active radiation (PAR) was attached to the chamber. The IRGA measures the concentration of CO₂ entering the chamber, and the concentration leaving the chamber after 2 minutes. A decrease in outgoing CO₂ vs. in the intake is the result of carbon fixed by the plant within the chamber; an increase in CO₂ would be the result of respiration exceeding the photosynthetic rate. Readings were taken in full ambient light, and then with shade cloths that reduced the light entering the chamber by 30, 50, 70, and 100%), and the PAR probe recorded the PAR value within the clear chamber. Additionally, temperature of the chamber was recorded. Chamber readings on the plant species across the fen were carried out every day that weather allowed in 2014 and 2015 throughout June and July; daily measurements began no earlier than 9:00 and ended no later than 15:00.

The recorded values of CO₂, light (PAR), and temperature were then used to calculate the monthly and annual carbon budgets of the monocultures using hourly data from a weather station in Sandhill Fen.

Detailed methods, including equations used for calculations can be found in Renee Hazen's thesis (Hazen 2016).

Results:

Gross Photosynthesis

Overall, gross photosynthesis increases with increasing PAR until a point of light saturation is reached and the curve levels off (Figure 2.25). Through the 2014 and 2015 growing seasons, mean gross photosynthesis when PAR equals 1500 $\mu\text{mol m}^{-2} \text{s}^{-1}$ for all species combined was 10.3 $\mu\text{mol m}^{-2} \text{s}^{-1}$. In the 2014 and 2015 growing seasons combined, *C. canescens* had a lower gross photosynthetic rate of 5.2 $\mu\text{mol m}^{-2} \text{s}^{-1}$ compared to the other three sedge species, which had rates ranging from 10.3 to 12.6 $\mu\text{mol m}^{-2} \text{s}^{-1}$ (Figure 2.26, $P < 0.001$). *Scirpus microcarpus* had a higher gross photosynthesis rate than *C. hystericina* and *C. aquatilis* when comparing species over both growing seasons combined, but differences between the gross photosynthesis rates of these three species were not statistically significant.

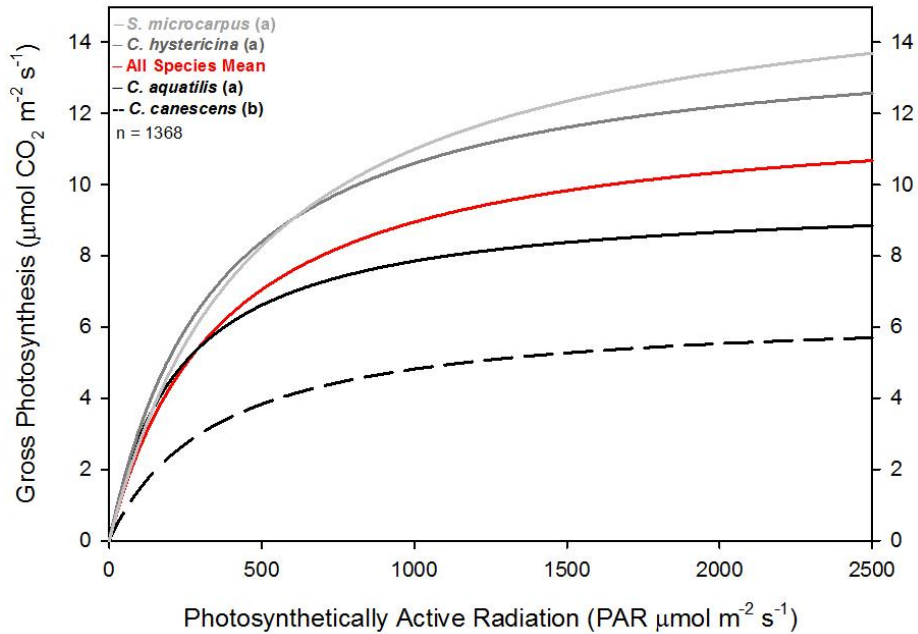


Figure 2.25 Mean gross photosynthesis represented as a function of PAR through the 2014 and 2015 growing seasons for *Carex aquatilis*, *C. canescens*, *C. hystericina*, *Scirpus microcarpus*, bare soil plots and the four sedge species combined at each of the twelve study plots across the Sandhill Fen site. Species names are color-coordinated with CO₂ flux curves, with the exception of *C. canescens*, which has a black dashed CO₂ flux curve. Differences in gross photosynthesis between species were significant ($P < 0.0001$, lowercase letters).

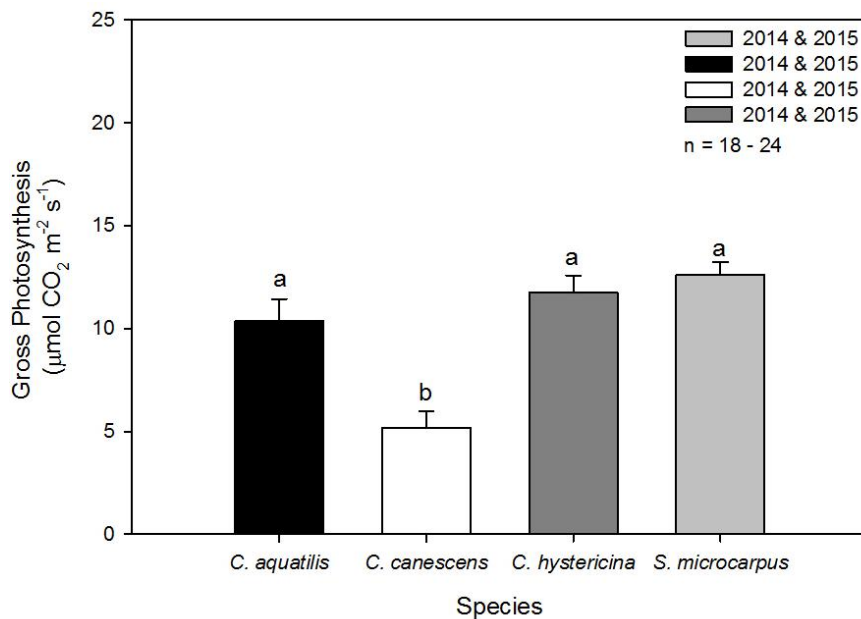


Figure 2.26 Mean gross photosynthesis when PAR is 1500 $\mu\text{mol m}^{-2} \text{s}^{-1}$ through the 2014 and 2015 growing seasons for *Carex aquatilis*, *C. canescens*, *C. hystericina*, and *Scirpus microcarpus*. Differences between gross photosynthesis of *C. canescens* and all other species were significant ($P < 0.001$). Bars are means; lines above are + standard error.

Dark Respiration

When interpreting dark respiration, dark respiration increases as the value for the rate becomes more negative. Through both 2014 and 2015 growing seasons, all species combined had a mean dark respiration rate of $-5.5 \mu\text{mol m}^{-2} \text{s}^{-1}$, when the temperature was 30°C (Figure 2.27). Between seasons, the difference in mean dark respiration of all sedges combined was slight, with $-5.5 \mu\text{mol m}^{-2} \text{s}^{-1}$ in 2014 and $-5.6 \mu\text{mol m}^{-2} \text{s}^{-1}$ in 2015.

Curve fitting of dark respiration for the entire study period demonstrated that each species showed an increase in respiration as temperatures increase. Bare soil respiration shows the same trend. Over both growing seasons, *C. hystericina* had the greatest amount of CO_2 release, with a dark respiration rate of $-7.2 \mu\text{mol m}^{-2} \text{s}^{-1}$ when the temperature was set equal to 30°C ($P < 0.001$, Figure 2.28). During this same time frame, dark respiration values of the other three species were not different from one another ($P > 0.05$). *Carex canescens* had the lowest dark respiration rate among this group, at $-4.9 \mu\text{mol m}^{-2} \text{s}^{-1}$, followed by *S. microcarpus* at $-6.3 \mu\text{mol m}^{-2} \text{s}^{-1}$ and then *C. aquatilis* at $-7.7 \mu\text{mol m}^{-2} \text{s}^{-1}$.

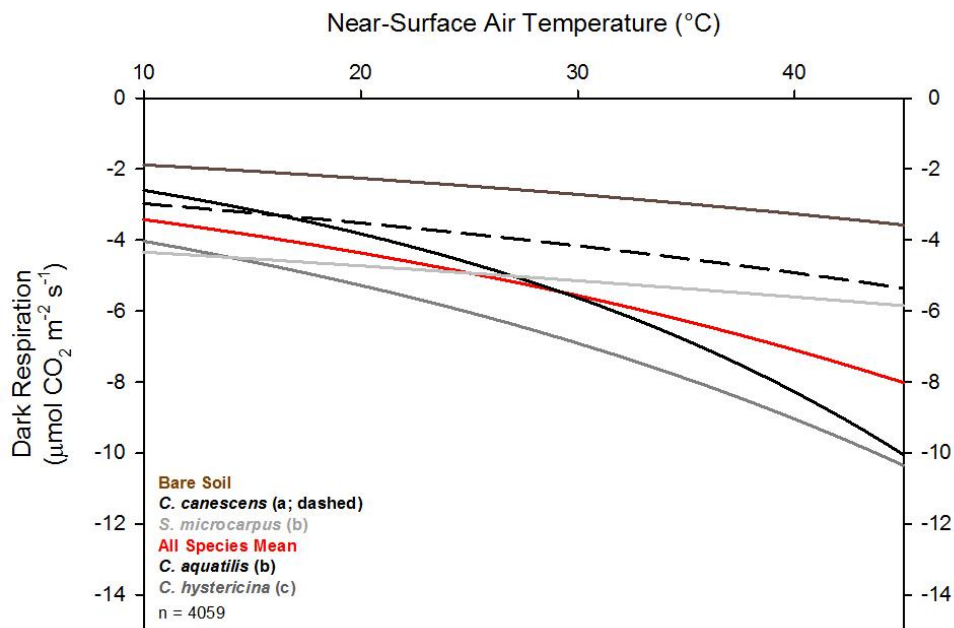


Figure 2.27 Mean dark respiration represented as a function of net ecosystem exchange (NEE) and near surface temperature through the 2014 and 2015 growing seasons for *Carex aquatilis*, *C. canescens*, *C. hystericina*, *Scirpus microcarpus*, and the four sedge species combined at each of the twelve study plots across the Sandhill Fen site. Bare soil respiration is considered the baseline respiration rate of the underlying soil column and not dark respiration. Differences in dark respiration between species were significant ($P < 0.0001$, lowercase letters).

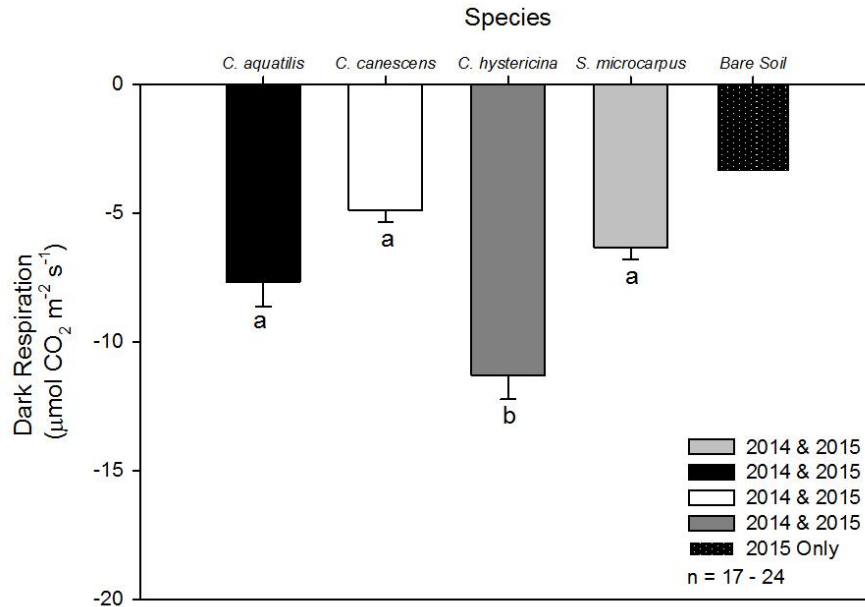


Figure 2.28 Mean dark respiration of CO₂ at 30°C (µmol m⁻² s⁻¹) through the 2014 and 2015 growing seasons for *Carex aquatilis*, *C. canescens*, *C. hystericina*, and *Scirpus microcarpus*. Bare soil respiration is considered the baseline respiration rate of the underlying soil column and not dark respiration. Differences between total respiration of *C. hystericina* and the other three species were significant ($P < 0.001$). Bars are means; lines below are minus standard error

Net Ecosystem Exchange

Curve fitting NEE of each species demonstrates that three of the four species reach peak NEE at similar levels of PAR, needed for it to become a carbon dioxide sink (Figure 2.29). The order of the species, from the lowest to highest amount of PAR needed for each plant to become a carbon dioxide sink, follows: *S. microcarpus* < *C. hystericina* < *C. aquatilis* < *C. canescens*. Bare soil plots, lacking any plant-life, were always sources of carbon dioxide (Figure 2.29).

Through 2014 and 2015 growing seasons, mean NEE for all four sedges combined was 5.6 µmol m⁻² s⁻¹ when PAR equals 1500 µmol m⁻² s⁻¹ (Figure 2.30). In the combined 2014 and 2015 growing seasons, *C. canescens* had the lowest mean NEE when PAR equals 1500 µmol m⁻² s⁻¹ ($P < 0.001$, Figure 2.30), while differences among mean NEE rates of the other three sedge species were negligible ($P = 0.3$).

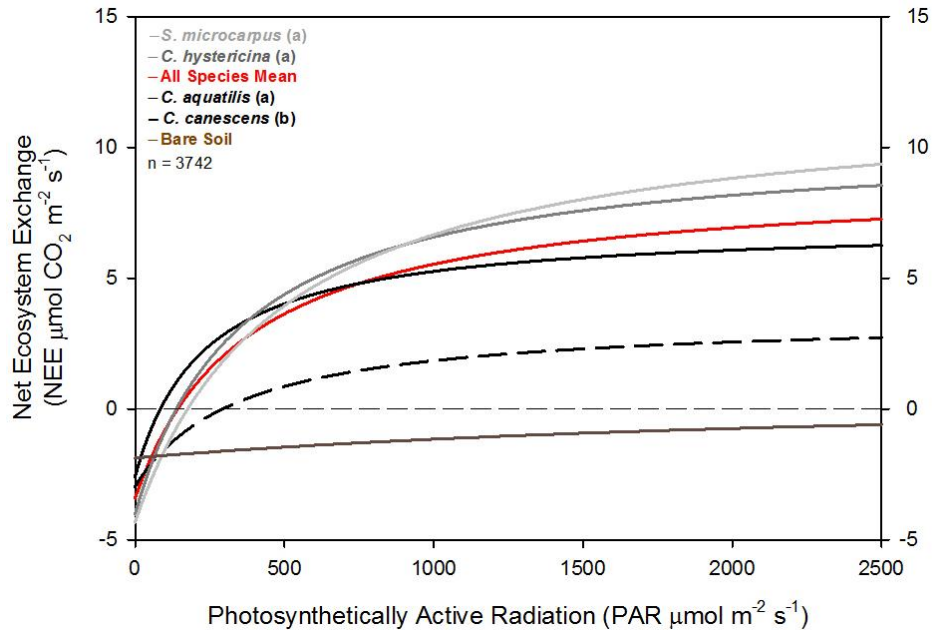


Figure 2.29 Mean net ecosystem exchange (NEE) as a function of PAR through the 2014 and 2015 growing seasons for *Carex aquatilis*, *C. canescens*, *C. hystericina*, *Scirpus microcarpus*, bare soil plots and the four sedge species combined at each of the twelve study plots across the Sandhill Fen site. Species names are color-coordinated with CO₂ flux curves, except *C. canescens* has a black dashed CO₂ flux curve. Differences in NEE between species were significant ($P < 0.0001$, lowercase letters).

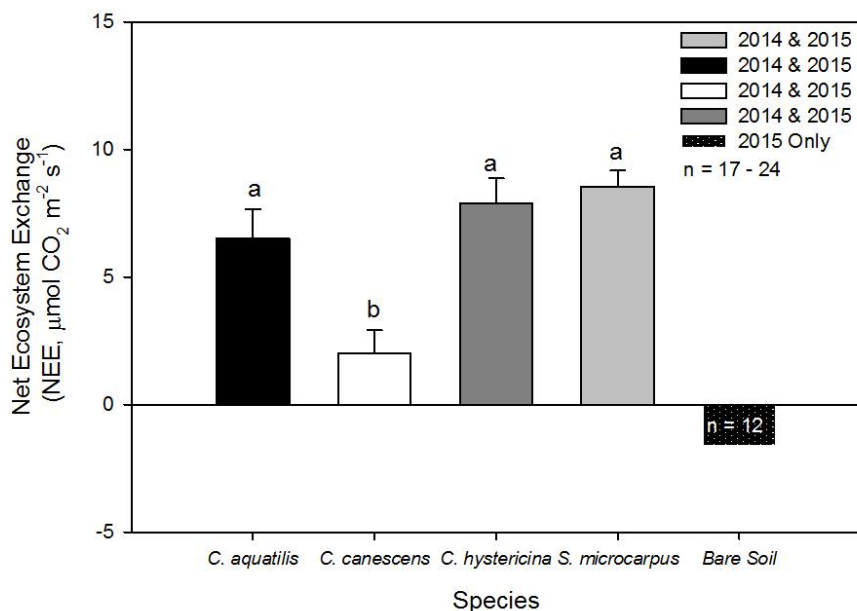


Figure 2.30 Mean net ecosystem exchange (NEE, $\mu\text{mol m}^{-2} \text{ s}^{-1}$) when PAR is $1500 \mu\text{mol m}^{-2} \text{ s}^{-1}$ through the 2014 and 2015 growing seasons for *Carex aquatilis*, *C. canescens*, *C. hystericina*, *Scirpus microcarpus* and bare soil plots. Differences between NEE of *C. canescens* and all other species were significant ($P < 0.001$). Bars are means; lines above are + standard error.

Annual Carbon Exchange

The mean annual cumulative carbon exchange for all four species combined in 2014 and 2015 was $-86.5 \mu\text{mol m}^{-2} \text{ yr}^{-1}$ (Figure 2.31). Bare soil respiration serves as a baseline for soil respiration. Therefore, the difference between annual bare soil respiration and the mean annual cumulative carbon exchange value represents the amount of carbon sequestration by these sedge species. The difference between respiration and annual cumulative carbon change can also be interpreted as total NPP in $\text{g C m}^{-2} \text{ yr}^{-1}$. Therefore, the four sedge species as a whole had an estimated total NPP of $336.8 \text{ g C m}^{-2} \text{ yr}^{-1}$. Separately, *C. aquatilis* had the highest mean annual cumulative carbon exchange at $-10.2 \mu\text{mol m}^{-2} \text{ yr}^{-1}$ (Figure 2.32), meaning this species had an estimated total NPP of $414.1 \text{ g C m}^{-2} \text{ yr}^{-1}$. *Carex hystericina* and *S. microcarpus* were similar, with mean annual cumulative carbon exchange values of $-82.7 \mu\text{mol m}^{-2} \text{ yr}^{-1}$ and $-76.9 \mu\text{mol m}^{-2} \text{ yr}^{-1}$, respectively. Estimates of total NPP from the annual cumulative carbon exchange rate of *C. hystericina* and *S. microcarpus* are $341.6 \text{ g C m}^{-2} \text{ yr}^{-1}$ and $347.4 \text{ g C m}^{-2} \text{ yr}^{-1}$, respectively. The lowest mean annual cumulative carbon exchange value belonged to *C. canescens*, making this species the largest carbon source among all four sedges, with a mean annual cumulative carbon exchange rate of $-269.9 \mu\text{mol m}^{-2} \text{ yr}^{-1}$. Estimates of total NPP for *C. canescens* equate to $154.4 \text{ g C m}^{-2} \text{ yr}^{-1}$.

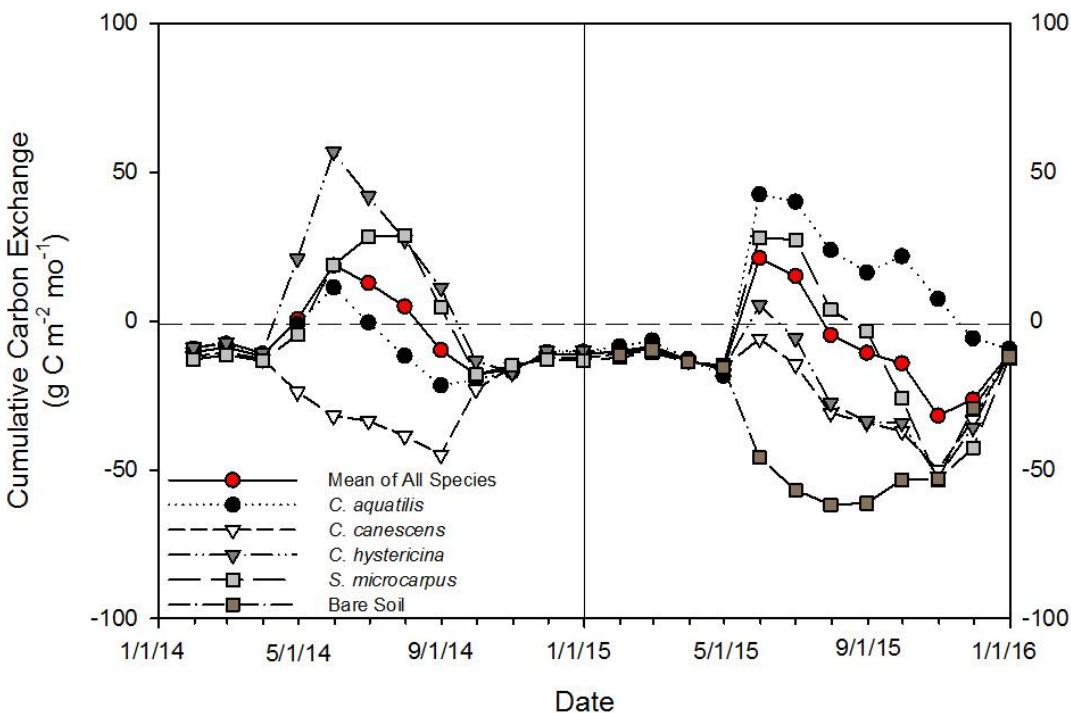


Figure 2.31 Cumulative monthly carbon exchange in 2014 and 2015 estimated from hourly PAR and temperature readings taken at the Mildred Lake weather station located near Sandhill Fen. The 2014 growing season occurred between April 14th and September 8th, and is indicated by the increase in cumulative carbon exchange. In 2015, the growing season occurred from May 6th to late September. The steep declines bracketing the 2014 and 2015 growing seasons indicate periods when the ground is covered by snow at a depth of at least 1cm.

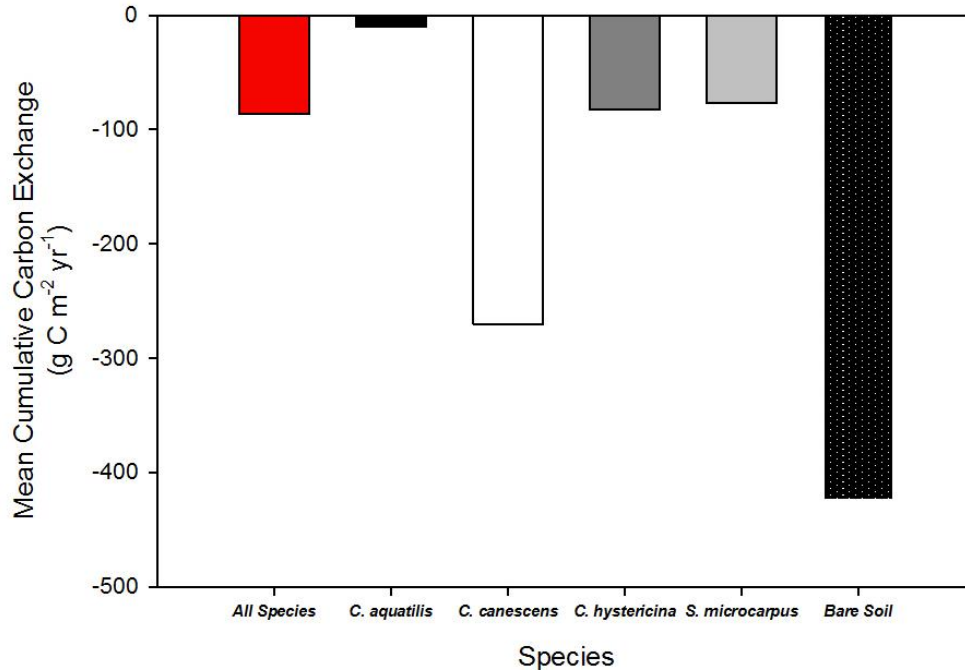


Figure 2.32 Mean annual cumulative carbon exchange for each sedge species and the mean of all sedge species combined through 2014 and 2015. Data for bare soil plots was only collected in 2015. Annual cumulative carbon exchange is estimated from hourly photosynthetically active radiation and temperature readings taken at the Mildred Lake weather station located near the Sandhill Fen.

Conclusions: *Carex hystericina* is the second most efficient in terms of growing season net ecosystem exchange, with the greatest dark respiration rate. This suggests that in a scenario of increasing temperatures, *C. hystericina* would be a less efficient carbon sink, but possibly more able to continue physiological processes. This may be a species-specific trait and not related to morphology, as the other caespitose species (*C. canescens*) had the lowest (less negative) dark respiration rate and the dark respiration rate of the other large species, *S. microcarpus*, was much lower than *C. hystericina*. The low dark respiration rate of *C. canescens* also might be due to the limited amount of net primary production, making this species a poor comparison to other caespitose plant species.

Moving onto annual cumulative carbon exchange, *C. aquatilis* appears to be the smallest source of annual carbon compared to the three other sedge species. This is surprising because the NEE

of *C. hystericina* and *S. microcarpus* are among the highest rates, and it would be suspected that these species would have a higher annual cumulative carbon exchange than *C. aquatilis*. Compared to NEE results, the estimation of annual carbon exchange for each species may provide a more accurate description of carbon sequestration and release. However, whether this hypothesis could be validated would not become clear until the winter dark respiration rates of each individual species were measured, to determine if there were great differences between these four species.

The larger sedge species, *C. hystericina* and *S. microcarpus*, had the greatest NEE exchange rates. However, these rates were only significantly greater than one of the small sedges, *C. canescens*. Dark respiration did not appear to have any relationship with the growth form of each species. *Carex hystericina*, had the greatest dark respiration rate among the four species.

The carbon sequestration rates of *C. aquatilis*, *C. hystericina*, and *S. microcarpus* species across the reclamation site are unable to overcome the rates of autotrophic and heterotrophic respiration. The recently disturbed substrate at the site may be releasing carbon dioxide as it continues to settle and decompose. This coupled with establishing plant life may indicate that it will take some time before the reclamation site can return to acting as a carbon sink. It is promising, however, that the total NPP estimated from annual carbon exchange (336.8 g C m⁻² yr⁻¹), is very similar to estimated peatland carbon exchange value of 370 g C m⁻² yr⁻¹ from previous literature (Gorham 1990, 1991, and 1995). This indicates that the plants are sequestering carbon as they would at a natural site, but decomposition is still too great for accumulation of carbon to occur.

Of the four sedge species, *C. canescens* is the least efficient at carbon sequestration. The other three sedges have greater gross photosynthesis rates, lower dark respiration rates, and greater NEE rates. Overall, *C. aquatilis*, *C. hystericina*, and *S. microcarpus* can sequester large amounts of carbon to the Sandhill Fen reclamation site during the growing season, and as of 2015, *C. aquatilis* is the biggest carbon sink among the four species.

Section 3: Atmospheric Deposition

Deposition of nitrogen and sulfur is historically low for northern Alberta, less than $1 \text{ kg ha}^{-1} \text{ yr}^{-1}$ for N and less than $2 \text{ kg ha}^{-1} \text{ yr}^{-1}$ for sulfur (Vitt et al. 2003; Wieder et al. 2016), and fen species that have persisted in low nitrogen may be nitrogen limited. Increased nitrogen availability may lead to changes in interspecific competition, and vascular plants, such as shrubs and herbaceous perennials, could crowd out other desirable fen species. Likewise, increased sulfur deposition could be detrimental to some desirable fen species by lowering pH. We set out to determine the rates of nitrogen and sulfur atmospheric deposition at Sandhill Fen and compare them to regional deposition rates.

Methods

Atmospheric deposition of inorganic nitrogen (NO_3^- and NH_4^+) and SO_4^{2-} was measured using ion exchange resin collectors (Fen and Poth 2004). Six resin collectors and a control, sealed at both ends, were installed across Sandhill Fen starting in late May 2013 and retrieved in September 2013, at which time a new set of resin tubes is placed in the field and one- m snow tubes were attached to collect snow over the winter until it melts and flows through the attached resin tube. Resin tubes were shipped back to the lab at SIU, where they were extracted using 1 M KI. The extracted resin solution was frozen, sent to Villanova University, where it was analyzed colorimetrically (Seal AA3 AutoAnalyzer) for NO_3^- , NH_4^+ and SO_4^{2-} . One-way ANOVA (JMP 7.0) was used to test for differences between years for NH_4^+ , NO_3^- , DIN, and SO_4^{2-} .

Results

There is considerable annual and spatial variation, but there are no differences in atmospheric deposition of DIN (NO_3 or NH_4) or SO_4 between 2013, 2014, and 2015 ($p > 0.05$, ANOVA; JMP 7.0). Dissolved inorganic nitrogen deposition over the three years averaged $13.1 \pm 3.5 \text{ Kg ha}^{-1} \text{ yr}^{-1}$. More ammonium ($10.7 \pm 3.7 \text{ kg ha}^{-1} \text{ yr}^{-1}$) falls on Sandhill Fen than nitrate (2.3 ± 0.7). Sulfate deposition ($11.9 \pm 2.1 \text{ kg ha}^{-1} \text{ yr}^{-1}$) is less than DIN deposition.

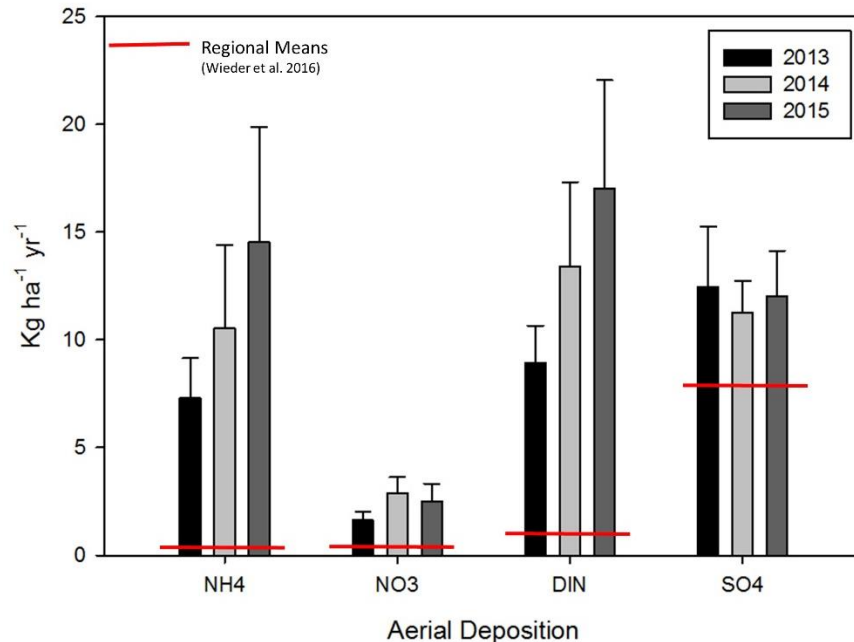


Figure 3.1 Mean values of atmospheric deposition (NH_4^+ , NO_3^- , DIN, and SO_4^{2-}) at 6 plots within Sandhill Fen for 2013, 2014, and 2015. Bars are means; lines above are plus the standard error. Red lines are regional means from Wieder et al. 2016.

Nitrogen and sulfur deposition at Sandhill Fen is several times greater than regional means: 20 times higher NH_4^+ ($0.53 \text{ kg ha}^{-1} \text{ yr}^{-1}$), 4 times higher NO_3^- ($0.5 \text{ kg ha}^{-1} \text{ yr}^{-1}$), 11 times higher for DIN ($1.17 \text{ kg ha}^{-1} \text{ yr}^{-1}$), and 1.5 times higher for SO_4^{2-} ($7.78 \text{ kg ha}^{-1} \text{ yr}^{-1}$; Wieder et al. 2016; Figure 3.1). To date, it appears that there are no negative impacts on vegetation at Sandhill Fen, but our study is not designed to examine impacts (we have no control sites). Since atmospheric deposition is so high compared to the regional inputs, it should continue to be monitored. As late successional species, such as shrubs, establish in the fen, plant community composition should be evaluated. Increased nitrogen availability could allow species that are nitrogen limited in fens to become dominant; this could change the carbon storing potential of Sandhill Fen.

Recommendations for Reclamation

Atmospheric deposition of nitrogen and sulfur are much higher at Sandhill Fen than the surrounding region. This should continue to be monitored. Furthermore, the plant community should be evaluated for potential response to increased nitrogen availability or negative responses to increased sulfur. Nutrient cycling and allocation could also be impacted, and this may warrant monitoring as well.

Section 4: Porewater Chemistry

During the planning stage of Sandhill Fen, a committee of experts recommended that electrical conductivity be maintained below 1000 $\mu\text{S}/\text{cm}$ for the health of the plants and invertebrates (Wytrykush et al. 2012). This was a challenging notion considering the seepage water in the fen contained high Na^+ and Cl^- , characteristic of tailings water. High sodium concentrations can be problematic for plant species, especially since the plant species introduced to Sandhill Fen were from regional peatlands with low pore water sodium concentration. We set out to monitor electrical conductivity and base cations, with an emphasis on sodium, concentrations across the fen and throughout the depth profile of the peat (50 cm). We wanted to be able to identify when and where in the fen this threshold was crossed so that closer monitoring of the biotic components could be established.

Methods

Sipper-peepers were installed at the 20 plots throughout the fen in 2011. The sipper-peepers consist of a 5-cm diameter and 50 cm long slotted pvc pipe; each 10 cm section is separated and has a tube that runs to the surface. Using the tubes from the different sections, we can collect water from specific depths: 0-10, 11-20, 21-30, 31-40, and 41-50. Fen wet-up occurred in August of 2012, revealing some plots were always dry including the perched fen plots. These sippers yielded no water and were removed (plots 1, 2, 3, 4, 16). The following data are from the remaining 15 sippers, all located in the main fen. Sippers were sampled 3 times each field season: June, July, and September. Samples were taken back to the laboratory at Southern Illinois University. Cations were quantified using a Varian 220 FS atomic absorption spectrometer. Electrical conductivity (EC) was measured using Orion 4 Star EC meter and pH using an Accumet AB15 pH meter.

Results

Mean EC in 2013 was $1133 \pm 210 \mu\text{S}/\text{cm}$, increasing to $1807 \pm 100.9 \mu\text{S}/\text{cm}$ in 2014 and $2076.9 \pm 84 \mu\text{S}/\text{cm}$ in 2015. Annual variation is significant with 2013 less than 2015 and 2014, while 2014 and 2015 values did not differ (Figure 4.1). Spatial variation was significant, with values varying from a low of 1000 to values approaching 4000 $\mu\text{S}/\text{cm}$; low EC plots are located in areas with deep (> 20 cm) standing water (Fig 4.1). EC did not vary with depth (Fig 4.2).

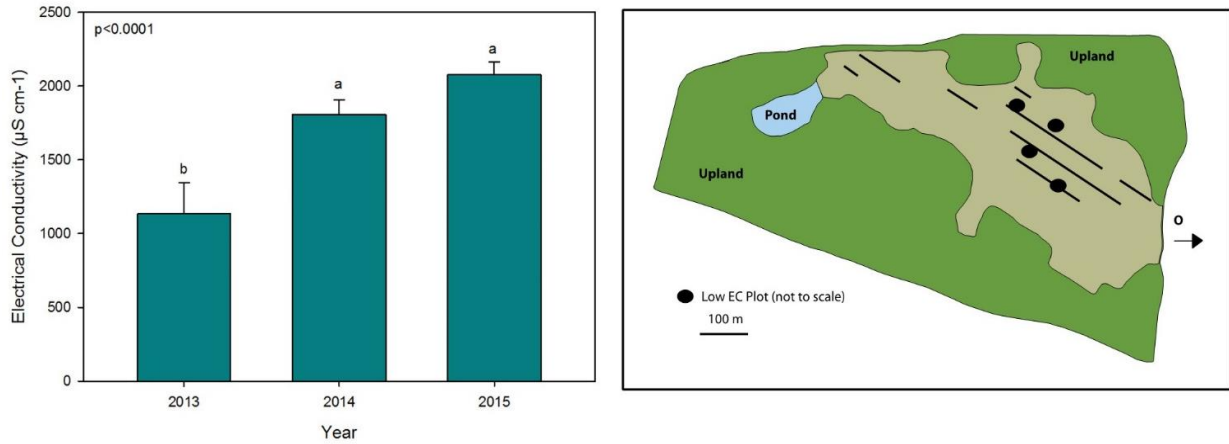


Figure 4.1 Electrical conductivity (EC) mean values from across Sandhill fen for 2013, 2014, and 2015 (left). Bars are means; lines are plus the standard error. Letters show significant differences in values (Tukey's HSD). On the right, is a map of Sandhill Fen, with low EC plots marked with black circles.

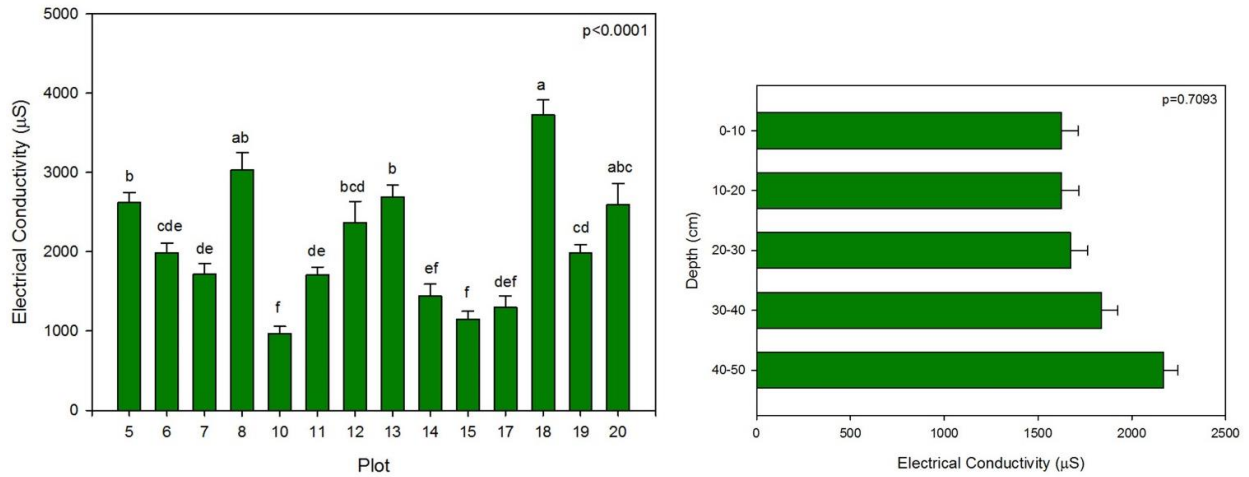


Figure 4.2 Electrical conductivity for plots across Sandhill Fen (left); EC values at depth (mean from all plots). Bars are means; lines are plus the standard error. Letters show significant differences in values (Tukey's HSD).

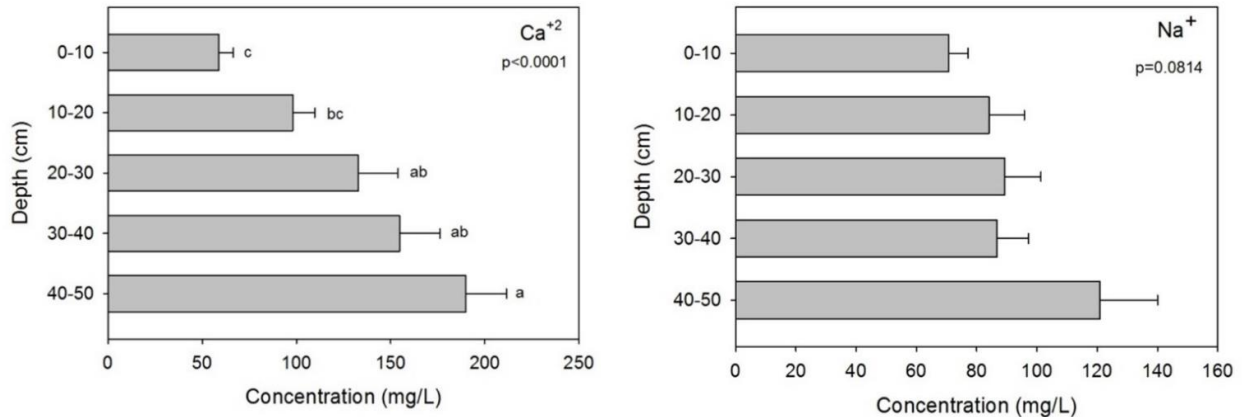


Figure 4.3. Data from 2013, calcium concentrations at depth (left; mean from all plots), and sodium concentrations at depth (right). Bars are means; lines are plus the standard error. Letters show significant differences in values (Tukey's HSD).

In 2013, sodium did not vary significantly with depth, however higher concentrations of calcium were found at depth (Figure 4.3). This indicated possible upwelling from beneath the peat layer. By 2014, there was no depth effect for calcium or sodium (Figure 4.4), but calcium increased significantly. Comparing 2015 with 2014, calcium values decreased and sodium increased significantly (Figure 4.6). Spatial variability in sodium and calcium concentration across the fen were both significant in 2015 (Figure 4.5), with four plots having higher calcium values located along the southern boundary of the fen, while five plots had high sodium values, all located along the southeastern margin of the fen. Only two of these plots with high values had both high contents of both elements.

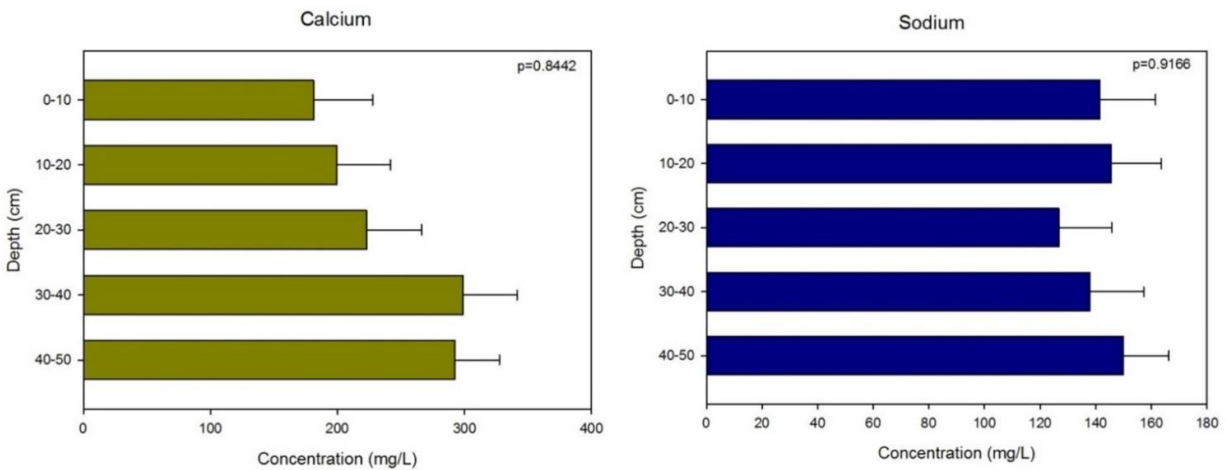


Figure 4.4. Data from 2014, calcium concentrations at depth (left; mean from all plots), and sodium concentrations at depth (right). Bars are means; lines are plus the standard error. Letters show significant differences in values (Tukey's HSD).

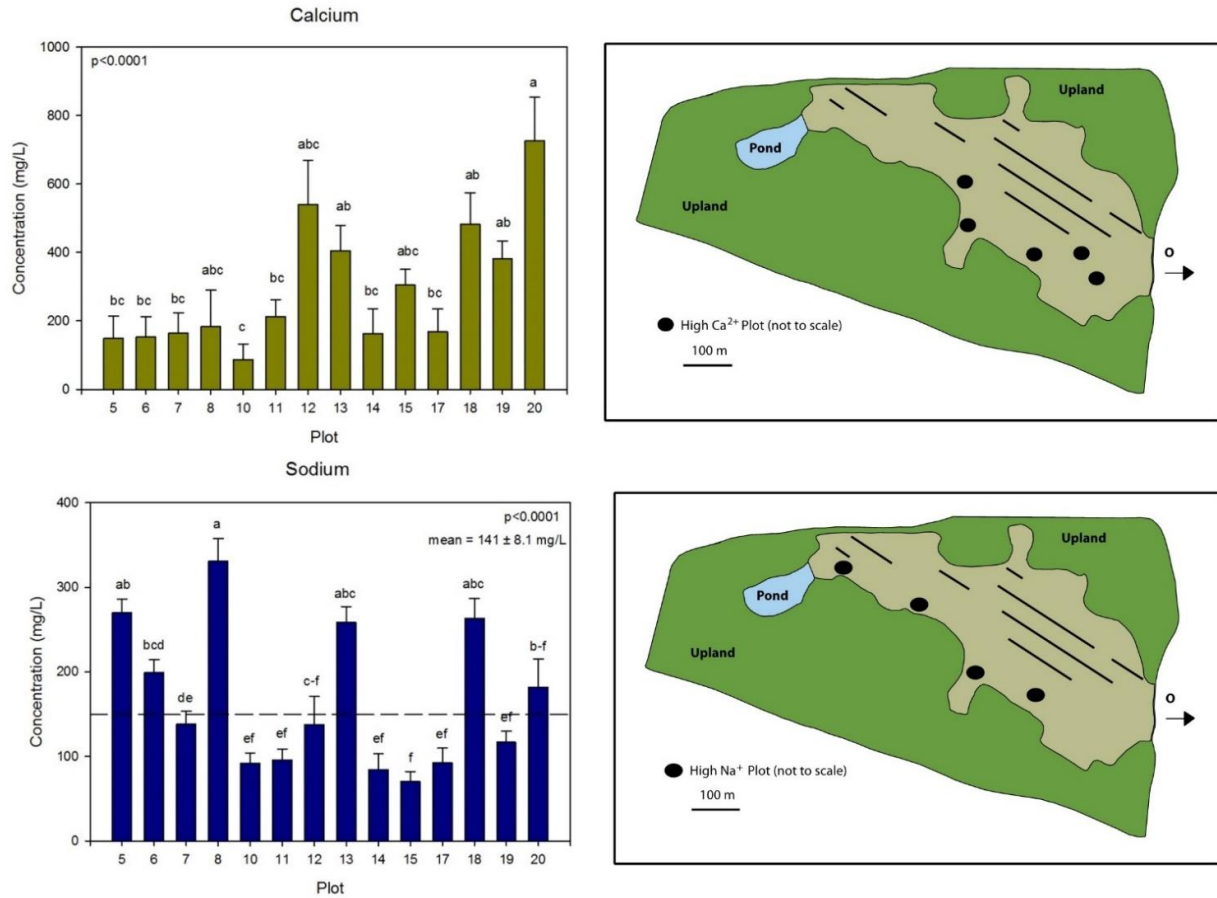


Figure 4.5 Calcium concentrations (top, left) and sodium concentrations (bottom, left) from plots across Sandhill Fen. Bars are means; lines are plus the standard error. Letters show significant differences in values (Tukey’s HSD). Maps of high calcium (top, right) and high sodium (bottom, right) locations in Sandhill Fen.

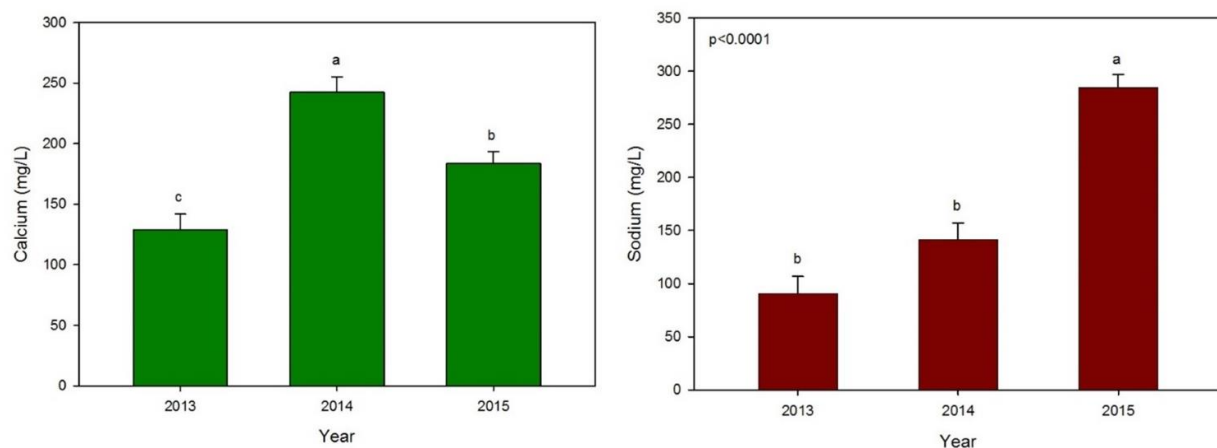


Figure 4.6 Calcium (left) and sodium (right) concentrations for all plots and depths for 2013, 2014, and 2015. Bars are means; lines are plus the standard error. Letters show significant differences in values (Tukey’s HSD).

The sodium hot spots should be closely monitored for continued increase in sodium, and possible negative effects on biotic processes, including sedge photosynthesis. Greenhouse trials have shown a negative response in *Carex utriculata*, a common species in SHF, survival and biomass of surviving plants occurring between 600 and 1200 mg⁻¹L⁻¹ of sodium in porewater (Vitt et al. 2013 – U-cell Report).

Recommendations for Reclamation

The continued rise in sodium concentrations is worrying. The current mean value of 284.5 mg⁻¹L⁻¹ is beyond normal rich fen values, but seemingly within tolerance levels for the dominant species currently occupying Sandhill Fen. Plant species, including sedges, are tolerating the current sodium conditions. No diebacks have been observed. As sodium levels continue to rise, we recommend setting up a study to test for a physiological response, i.e. change in photosynthetic rate, of sedges in sodium hot spots as compared to areas of Sandhill Fen with much less sodium.

Section 5: Soil Dynamics

To assess the health of soil microbial community and microbe mediated decomposition and nutrient cycling, we set out to assess the soil microbial community, nitrogen mineralization rates, and decomposition rates of Sandhill Fen. To determine if what we observed in Sandhill Fen was typical for the region, we also tested a suite of Benchmarks sites for soil microbial and nitrogen mineralization analysis.

Benchmark sites

The six regional benchmark fens monitored in this study are located within a 100 km driving radius of Fort McMurray, AB. Benchmark sites were selected based on indicators that captured the full range of chemical and floristic variability characteristic of fens in the AOSR (with the exception of saline fens).

High-Test Rich Fen (abbreviation: ERF) (56.950 N, -111.531 W; 314 m elevation) is an open patterned extreme rich fen with a ground layer dominated by the moss *Scorpidium scorpioides*, and by the *Carex* species *C. chordorrhiza*, and *C. lasiocarpa*. The site contains sporadic populations of *Triglochin maritima*, and *Campylium stellatum*. Hummocks are absent from the fen interior.

Anzac Rich Fen (abbreviation: MRF1) (56.382 N, -111.026 W; 466 m elevation) is an open moderate rich fen closely flanked by an ombrotrophic bog to the west, and by Highway 881 to the east (repaved in 2006). The site recently has developed over the last 8 years following road construction disturbance, and accumulated peat deposits are quite shallow (< 20 cm). The site is dominated by an especially dense cover of the early successional sedge *Carex aquatilis*. Within the fen main body are sporadic occurrences of mosses within the genera *Calliergon*, and *Drepanocladus*. Along the western edge nearest to the bog, *Sphagnum* becomes increasingly abundant. Hummocks are absent from the fen main body.

Stoney Mountain Rich Fen (abbreviation: MRF2) (56.365 N, -111.276 W; 726 m elevation) is a shrubby moderate rich fen dominated by several species of *Salix*, *Carex aquatilis*, *Carex utriculata*, and *Calamagrostis canadensis*. Hummocks are colonized by *Aulacomnium palustre* and *Sphagnum teres*, hollows are colonized by mosses within the genera *Calliergon* and *Drepanocladus*.

Beaver Pond Rich Fen (abbreviation: MRF3) (56.378 N, -111.253 W; 763 m elevation) is an open moderate rich fen with a floating mat. The site is dominated by *Carex* species, namely *C. aquatilis* and *C. utriculata*, and a ground layer composed largely of *Sphagnum squarrosum*. The site receives water inputs from a spillover culvert that drains a beaver pond. Over the 2014 growing season, a trench developed below the outflow culvert, and water was diverted away from the site. Consequently, the water table in 2014 was markedly lower compared to year 2013.

Stoney Mountain Poor Fen (abbreviation: PF1) (56.364 N, -111.276 W; 725 m elevation) is dominated by a ground layer of *Sphagnum* species (*S. angustifolium*, *S. magellanicum*, *S. fuscum*, and *S. majus*). *Carex aquatilis* is the dominant sedge present at the site. Other vascular plants include *Andromeda polifolia*, *Kalmia polifolia*, and *Oxycoccus microcarpus*.

Mariana Lake Poor Fen (abbreviation: PF2) (55.898 N, -112.095 W; 695 m elevation) is an oligotrophic site dominated by a ground layer of *Sphagnum* species, namely, *S. angustifolium*, *S. fuscum*, and *S. magellanicum*. The dominant vascular species include *Carex aquatilis*, *Kalmia polifolia*, *Andromeda polifolia*, *Scheuchzeria palustris*, *Eriophorum angustifolium* and *Oxycoccus microcarpus*.

Phospholipid Fatty Acid (PLFA) Extraction

Soil microbes are key to decomposition and nutrient cycling in all ecosystems. The establishment of a diverse, functioning soil microbiome is important to the success of a reclaimed system. At Sandhill fen, 50 cm of stockpiled peat was placed over 50 cm of mineral soil. The peat placed on Sandhill Fen contained remnants of both rich fen and bog components (D. Vitt pers. comm.) and could contain all the components needed to provide a microbial community similar to natural peatlands of the area.

Would soil microbes thrive in the moisture, pH, and nutrient conditions of Sandhill Fen? To answer this question, we collected soil from across Sandhill fen and six benchmark sites: 2 rich fens, 2 poor fens, 2 disturbed fens, and 1 bog. Phospholipid fatty acids were extracted, and functional groups of bacteria and fungi were quantified.

Methods:

Field sampling

Samples were collected in mid-July and September from each of eight plots in the 6 benchmark sites and the 20 research plots at Sandhill Fen. The samples were kept frozen until the time of analysis. A subsample of the fresh (not dried) material was weighed. The phospholipid fatty acids extracted following a modified Bligh and Dyer extraction technique (Quideau et al. 2012), and analyzed on a GC-FID. Microbial biomass was corrected based on surrogate recovery for ANOVA statistical analysis.

Statistical Analysis

Soil microbial communities (μmol extracted) were analyzed for similarities between sites using cluster analysis, cut level was determined at the highest percent similarity that yields significantly different groups as determined by a SIMPROF test, and graphed in an MDS ordination. Differences between *a priori* site types were tested using PERMANOVA. Differences between microbial functional groups were tested for using ANOVA; these data were corrected μg per g soil corrected for by surrogate recovery.

Results:

Community Analysis

There was no difference between the microbial communities found across our sites between 2014 and 2015 (Figure 5.1). Microbial communities were stable within the benchmark sites between the 2 years as was Sandhill Fen.

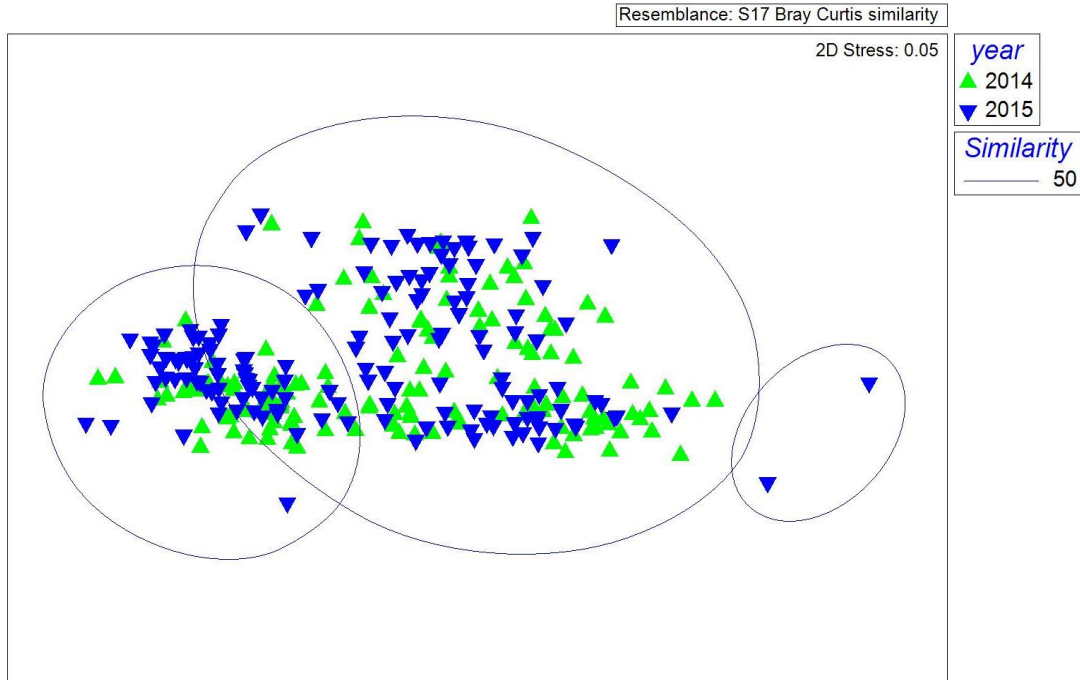


Figure 5.1 Ordination of all plots from Sandhill Fen and benchmark sites from 2014 and 2015. There was no difference between years for any of the sites, which can be seen here as 2014 (green triangles) are intermixed with 2015 (blue triangles). Circles are the result of group average cluster analysis, cut level of 50 (SIMPROF test).

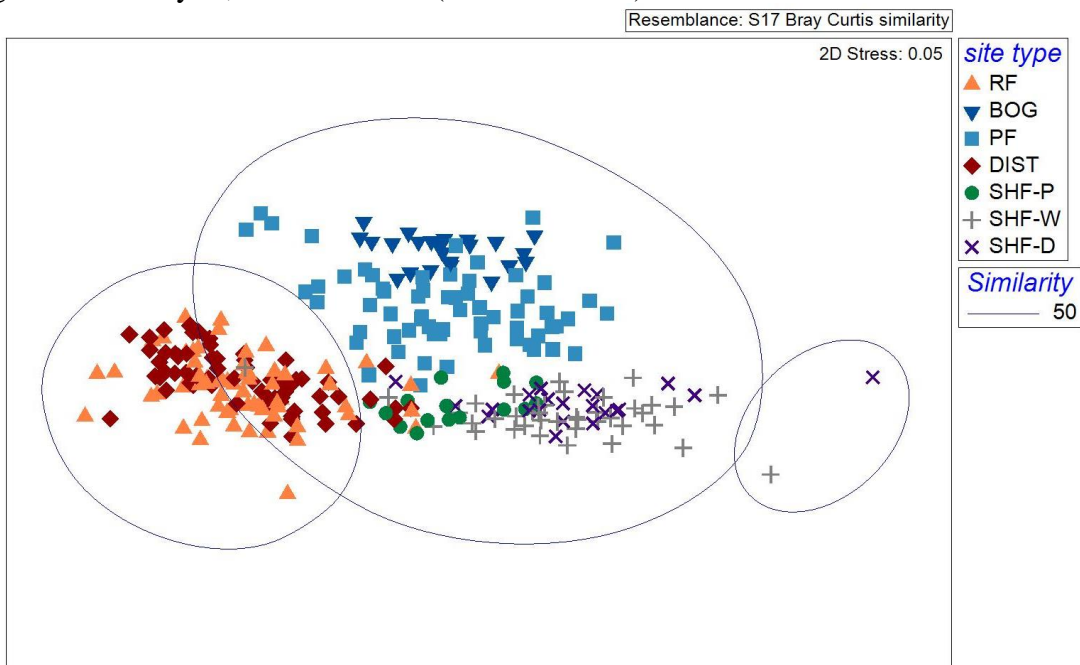


Figure 5.2 Ordination of plots from benchmark sites and Sandhill Fen. Circles are the result of group average cluster analysis, cut level of 50 (SIMPROF test). Benchmarks site types are shown, RF = rich fens, bogs, PF = poor fens, DIST = disturbed fens, SHF-P are Sandhill Fen perch plots, SHF-D are dry plots, and SHF-W are wet plots.

Cluster Analysis

Soil microbial communities form two main groups in ordination space: one comprised of rich fens and disturbed fens (left portion of ordination; Figure 5.2) and the other of poor fen, bog, and Sandhill Fen plots (center portion of ordination - 50% similarity significance; result of SIMPROF test). Two Sandhill Fen plots are outliers to the right on the ordination.

PERMANOVA and ANOVA Results

There are differences between all a priori site types: bog, poor fens, disturbed fens, rich fens, and Sandhill Fen perch fens. Sandhill Fen wet and dry plots do not differ from one another, but differ from all other site types ($p < 0.05$; PERMANOVA results). Microbial communities differ between all of the site types. Overall, more microbial biomass was extracted from more disturbed sites (Figure 5.3). To further determine the differences between site types, fatty acids were sorted into functional groups and the contribution of the functional groups to the microbial communities was analyzed.

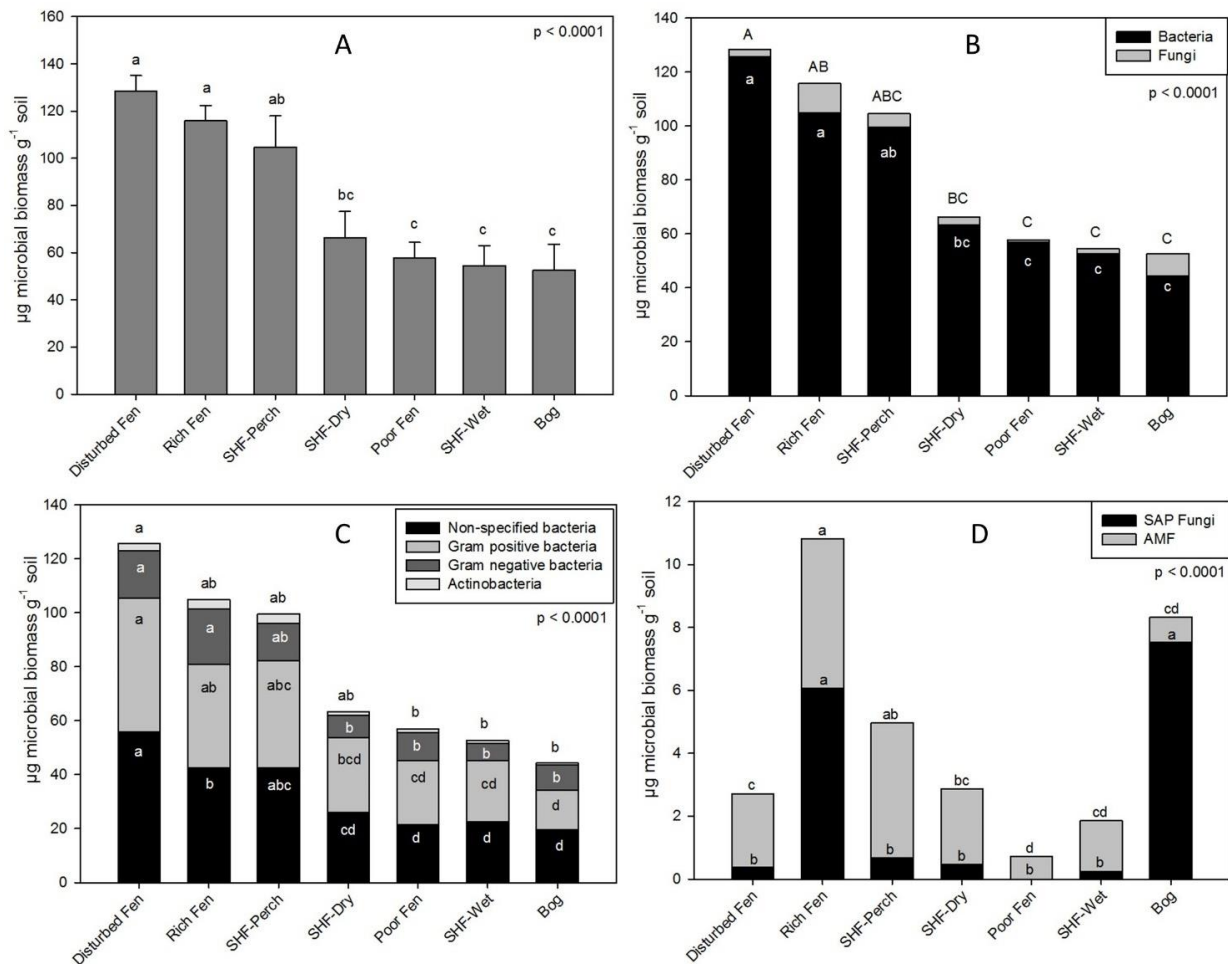


Figure 5.3 Microbial biomass (A), bacterial and fungal biomass (B), bacterial biomass broken down into groups: non-specified bacteria, gram positive, gram negative, and actinobacteria (C), and saprophytic and arbuscular mycorrhizae (D) biomass extracted from soil of the benchmark

sites and Sandhill Fen wet, dry, and perch areas. Bars are means; lines in panel A are plus standard error. Within panels, letters are significant differences (Tukey's HSD).

Total microbial biomass was highest in the disturbed fens, rich fens, and Sandhill Fen perch plots. Less biomass was extracted from Sandhill Fen dry plots, poor fens, Sandhill Fen wet plots, and bog plots (Figure 5.3a). More bacterial than fungal biomass was extracted from all site types (Figure 5.3b). Non-specified bacteria and gram positive bacteria make up the majority of the bacterial biomass from all sites. Gram negative bacteria are a smaller component of the bacterial community, and actinobacteria are the least abundant (Figure 5.3c). Fungal biomass is much less abundant than bacterial, and saprophytic fungi and arbuscular mycorrhizal fungi (AMF) biomass were variable across sites. No saprophytic fungal biomass was found in the poor fens (Figure 5.3d).

Recommendations for Reclamation

Currently, the soil microbial community at Sandhill Fen is similar to and within the range of some peatland sites that were sampled. The soil amendments used at Sandhill Fen, 50 cm mineral soil, covered by 50 cm of peat have developed and support a soil microbial community comparable to some peatlands of the region. Few differences were found along the wet to dry gradient within Sandhill Fen, indicating that the site has a reasonably homogeneous microbial flora.

While the peat likely contributed to the development of a soil microbial community similar to established peatlands, the peat likely does not need to be 50 cm deep. A few centimeters of peat may be enough.

We would recommend sampling the soil and analyzing the soil microbial community during the early years of future reclamation projects. Decomposition and nutrient cycling rely on a diverse, functioning soil microbial flora.

Nitrogen Mineralization

Experimental Design

Across the six benchmark fen sites, in years 2013, 2014 and 2015, research plots (n=8 for each site) were established randomly along transects bisecting the interior of each peatland. At SHF, to account for within-site moisture gradient differences, the twenty research plots were separated into 'wet' and 'dry' groupings (n=10 for each group), and treated as two independent sites (SHF wet and SHF dry), thereby capturing potential consequences of low soil moisture levels on ecosystem processes during the early stages of wetland reclamation. The presence or absence of standing water across SHF research plots was assessed in June, July and September of each year. Wet plots were those that remained submerged for at least one month each growing season, and for dry plots the soil surface was exposed above the water table throughout the entirety of the growing season.

Net N mineralization rates were quantified using the *in situ* buried polyethylene bag technique (Robertson 1999; Bayley et al. 2005). In mid-June (2013 - 2015), soil cores (0-10 cm) were collected with a cylindrical aluminum corer (6.5 x 10 cm), halved longitudinally with a serrated

bread knife, and placed into separate polyethylene Whirl Pak[®] bags (hereafter referred to as initial extractable N core, and final extractable N core) at field moisture content. Live plants were removed from each soil core prior to placement into Whirl Pak[®] bags. Immediately after collection from the field, initial extractable N cores were taken to a laboratory for processing and extraction (60 min per extraction) with 1.0 molar KCl to displace initial extractable ammonium and nitrate contents (modified from Verhoeven et al. 1990). For the final extractable N cores, after being placed into polyethylene Whirl Pak[®] bags, samples were reburied in the same peat profile location from which they were removed. Incubation cores remained in the peat matrix for approximately 30 days. Following the field incubation period, final extractable N cores were collected and immediately taken to a laboratory for processing and extraction. Net N mineralization was calculated from the difference between final extractable ammonium + nitrate contents (obtained from the field incubation cores) and initial extractable ammonium + nitrate contents (obtained from the initial cores) (Robertson 1999). Net nitrification was calculated from the difference between final extractable nitrate contents and initial extractable nitrate contents (Robertson 1999). Extractable ammonium and nitrate concentrations were measured on a N autoanalyzer using the alkaline phenol and cadmium reduction methods, respectively.

Statistical Analyses

Differences across study sites were assessed using a one-way analysis of variance (ANOVA) design, pooling all values across sites for 2013, 2014 and 2015. Where datasets failed to meet normality assumptions, non-parametric Kruskal-Wallis tests were performed. Significance was assigned at $\alpha = 0.05$. Post hoc comparisons were made using Tukey's test. All ANOVA tests were conducted using JMP version 7.0.

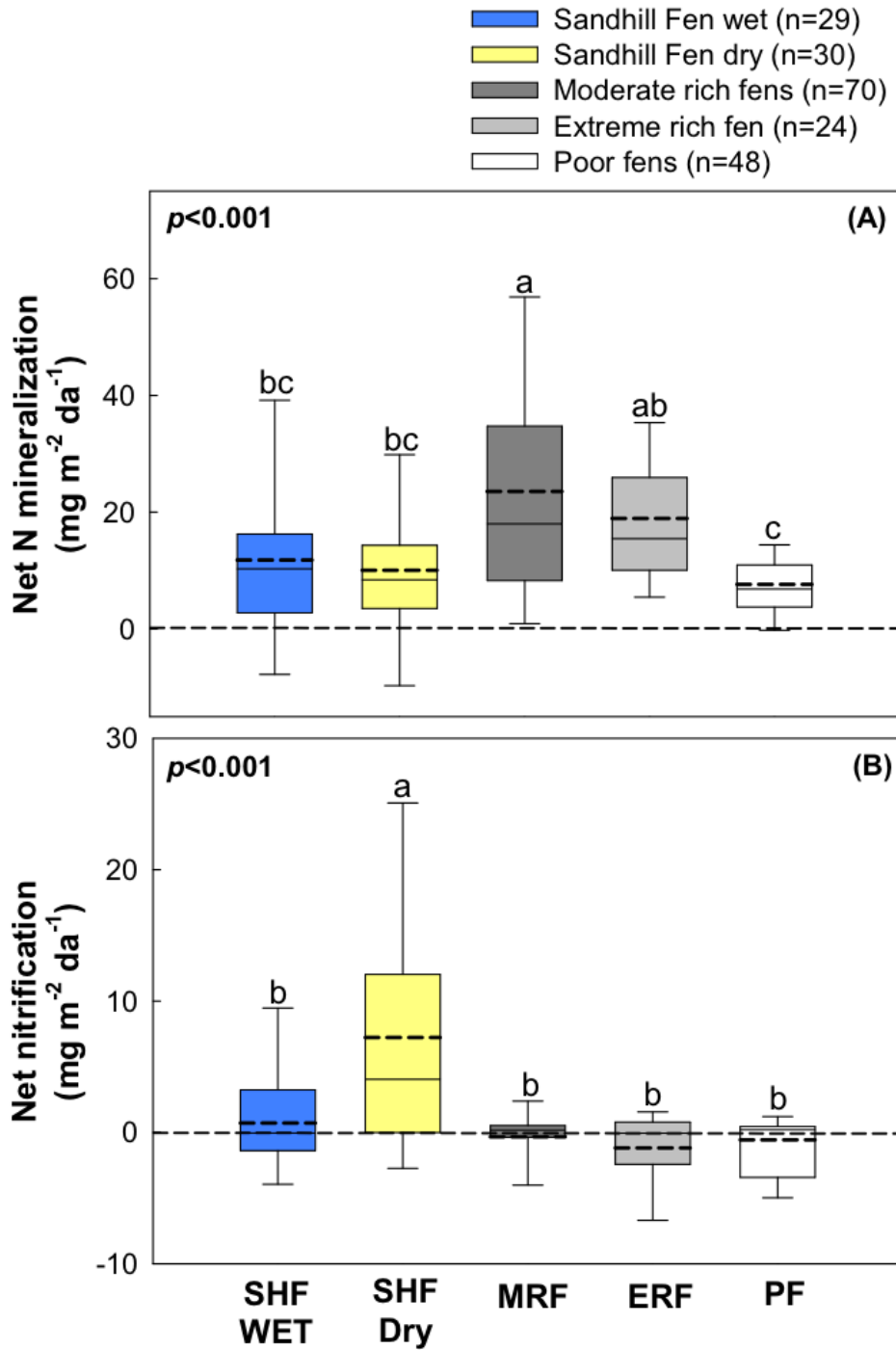


Figure 5.4 Box and whisker plots for Net N mineralization (panel A) and net nitrification (panel B) rates across Sandhill Fen (Wet and Dry plots) and benchmark sites (MRF = moderate rich fens; ERF = extreme rich fens; PF = poor fens). Solid horizontal lines are the median, and dashed horizontal lines are the mean. Differences across study sites were assessed using a one-way analysis of variance (ANOVA) design, pooling all values across sites for 2013 – 2015, $\alpha = 0.05$, Tukey's post hoc test.

Results and Discussion: Overall, the key characteristics observed across benchmark sites are 1) mean net N mineralization rates were faster in rich fens than poor fens, and 2) net nitrification was slow across all benchmark sites (Figure 5.4 a-b). At SHF, net N mineralization rates across wet and dry plots were equivalent to several benchmark sites (Figure 5.4a). This observation suggests the amount of plant available inorganic N remaining at SHF following microbial immobilization should not limit NPP rates at the current stage of reclamation, and the return of microbial activity at the reclamation site was quite resilient. In general, plots localized in wet areas at SHF were most similar to ERF and PF sites. Dry areas at SHF, however, exhibited few fen characteristics, and net N mineralization was dominated by nitrification, a situation characteristic of upland systems.

Reclamation recommendation: Utilizing net N mineralization as an indicator for site performance can be a useful tool for evaluating the overall ‘health’ of the belowground environment, and provides useful information to improve future wetland reclamations.

To improve the probability of success for future wetland reclamations on previously mined in-pits, and to facilitate microbial-mediated processes to fall within an acceptable range of variation comparable to undisturbed Albertan fens, managing water tables at appropriate levels (i.e., < +15 cm above the water table and > -5 cm) during the early the stages of fen reclamation is key.

Decomposition

Peat accrual in peatlands of northeastern Alberta is the result of very slow decomposition. It is within the peat that large carbon pools are stored, making peatlands global carbon sinks. If Sandhill Fen is to develop peat, then decomposition rates should be low, comparable to peatlands of the region.

Methods: Decomposition rates were measured across Sandhill Fen from 2013 to 2015 in the 20 research plots. Decomposition rates were measured using nylon bags stuffed with 5 Whatman 42 filters. Bags were dried for a minimum of 48 hours, and dry weight recorded. Decomposition bags were buried in September and retrieved the following September. The bags were cleaned, dried, and final weight recorded. The percent of decomposition was calculated and served as a relative measure for the plots across Sandhill Fen. Sandhill Fen plots were sorted into 3 vegetation zones (See Section 2 of this report). Decomposition differences between zones and years were tested for using a 2-way ANOVA (JMP 7.0).

Results:

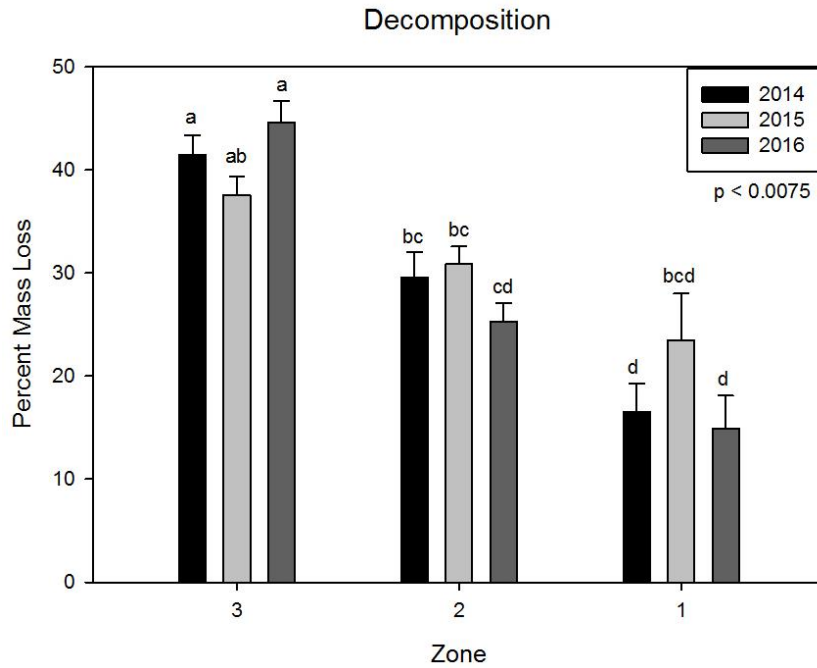


Figure 5.5 Decomposition (% mass loss) for 2013-2015 across vegetation zones (see Section 2 of this report). Results of Two-way ANOVA; letters indicate significant differences (Tukey's HSD). Bars are means; lines are plus the standard error.

Decomposition rates were highest in the driest plots, lowest in the wettest plots, and intermediate in the zone 2 plots (Figure 5.5). There is annual variability in the decomposition rates, but the driving factor is zone, closely associated with depth of the water table.

Reclamation recommendation: Maintaining the water table is very important. If fen soils become dry, then decomposition increases and carbon is released rather than stored in the fen.

References

- BFNA. 2007, 2014. Flora of North America North of Mexico, Volume 27 Bryophyta, part 1 (2007), Volume 28 Bryophyta, part 2 (2014). Oxford University Press, New York, Oxford.
- McCune, B., and Mefford, M. 1999. Multivariate Analysis of Ecological Data. Version 4.0. MjM Software. Gleneden Beach, OR.
- Campbell C, Vitt DH, Halsey DH, Campbell ID, Thormann MN, and Bayley SE. 2000. Net primary production and standing biomass in northern continental wetlands. North For Centre Inf Rep NOR-X-369.
- Clarke, K.R., and Gorley, R.N. 2006. PRIMER v6: User Manual/Tutorial. PRIMER-E, Plymouth.
- Fenn, M.E., Poth, M.A. 2004. Monitoring nitrogen deposition in through fall using ion exchange resin columns: a field test in the San Bernardino Mountains. *Journal of Environmental Quality* 33:2007–2014.
- Glaeser, L. 2015. Established plant physiological responses and species assemblage development during early fen reclamation in the Alberta Oil Sands Area. MSc Thesis. Southern Illinois University Carbondale. USA.
- Glaeser, L.C., Vitt, D.H., and Ebbs, S.E. 2016. Responses of the wetland grass, *Beckmannia syzigachne*, to salinity and soil wetness: consequences for wetland reclamation in the oil sands area of Alberta. *Ecological Engineering* 86: 24-30.
- Gorham E. 1990. Biotic impoverishment in northern peatlands. In: *The earth in transition: patterns and processes of biotic impoverishment*. Cambridge University Press. Cambridge, UK. 65–98.
- Gorham E. 1991. Northern peatlands: role in the carbon cycle and probable responses to climatic warming. *Ecological Applications* 1: 182–195.
- Gorham E. 1995. The biogeochemistry of northern peatlands and its possible response to global warming. In Woodwell GM and Mackenzie FT. Eds. *Biotic Feedback in the Global Climatic System*. Oxford University Press. New York, NY. 169–187.
- Graham J. 2012. Patterns in environmental drivers of wetland functioning and species composition in a complex peatland. MSc Thesis. Southern Illinois University Carbondale. USA.
- Hartsock, J.A., House, M., and Vitt, D.H. 2016. Net nitrogen mineralization in boreal fens: a potential performance indicator for peatland reclamation. *Botany* 94: 1027-1040.
- Hazen, R.E. 2016. Organic layer inputs from four species of Cyperaceae within an oil-sands reclamation. MSc Thesis. Southern Illinois University Carbondale. USA.
- JMP®, Version 7. SAS Institute Inc., Cary NC, 1989-2007.
- Johnson, D., L. Kershaw, A. MacKinnon, and Pojar, J. 1995. *Plants of the western boreal forest and aspen parkland*. Lone Pine Publishing and the Canadian Forest Service, Edmonton, AB.
- Koropchak, S., Vitt, D.H., Bloise, R, and Wieder R.K. 2012. Fundamental paradigms, foundation species selection, and early plant responses to peatland initiation on mineral soils. In *Restoration*

- and reclamation of boreal ecosystems. *Edited by* D.H. Vitt and J. Bhatti. Cambridge University Press, Cambridge. pp. 76-100.
- Polomski, J., and Kuhn, N. 2002. Root research methods. *In* Plant roots: The hidden half. 295–321.
- Quideau, S. A., Das Gupta, S., Mackenzie, M.D., and Landhäusser, S.M. (2012) Microbial response to fertilization in contrasting soil materials used during oil sands reclamation. *Soil Biology & Biochemistry* 77: 145-154.
- Robertson, G.P., Wedin, D., Groffman, P.M., Blair, J.M., Holland, E.A., Nadelhoffer, K.J., and Harris, D. 1999. Soil carbon and nitrogen availability — nitrogen mineralization, nitrification and soil respiration potentials. *In* Standard soil methods for long-term ecological research. Vol. 2. pp. 258–271.
- Stotler, R., and Crandall-Stotler, B. 1977. A checklist of the liverworts and hornworts of North America. *Bryologist*, 80:405–428. doi:10.2307/3242017.
- Thorman, M.N. and Bayley, S.E. 1977. Aboveground plant production and nutrient content of the vegetation in six peatlands in Alberta, Canada. *Plant Ecology* 131: 1–16.
- Verhoeven, J.T.A., Maltby, E., and Schmitz, M.B. 1990. Nitrogen and phosphorus mineralization in fens and bogs. *Journal of Ecology* 78: 713–726. doi:10.2307/2260894.
- Vitt D.H., Wieder R.K., Halsey L.A., Turetsky M.R. 2003. Response of *Sphagnum fuscum* to nitrogen deposition: a case study of ombrogenous peatlands in Alberta, Canada. *The Bryologist* 106:235–246.
- Vitt, D.H., House, M., and Koropchak, S. Report to Syncrude: CT Fen Construction: Water Chemistry, Peat Compaction, Peatland Plant Establishment, Vegetation Scale-up, and Monitoring. Syncrude Canada Internal Report, Syncrude Research Center, Edmonton, Alberta.
- Vitt, D.H., House, M., and Hartsock, J.A. 2016. Sandhill Fen, an initial trial for wetland species assembly on in-pit substrates: lessons after three years. *Botany* 94: 1015-1025.
- Whittaker, R.H. 1972. Evolution and measurement of species diversity. *Taxon* 21: 213–251.
- Wieder, R.K., Vile, M.A., Albright, C.M., Scott, K.D., Vitt, D.H., Quinn J.C., and Burke-Scoll, M. 2016. Effects of altered atmospheric nutrient deposition from Alberta oil sands development on *Sphagnum fuscum* growth and C, N and S accumulation in peat. *Biogeochemistry* 129: 1-19.
- Wytrykush, C., Vitt, D.H., McKenna, G., and Vassov, R. 2012. Designing landscapes to support peatland development on soft tailings deposits. *In* Restoration and reclamation of boreal ecosystems. *Edited by* D.H. Vitt and J. Bhatti. Cambridge University Press, Cambridge. pp. 161-178.

Publications from Sandhill Fen:

Ebbs, S., House, M., Glaeser, L., Hazen, R., Vitt, D.H. (2014) Plant establishment, community stabilization, and ecosystem development on oil sands soft tailings. 11th Annual Meeting, International Phytotechnologies Society, Heraklion, Crete. 1-4 October.

Glaeser, L. 2015. Established plant physiological responses and species assemblage development during early fen reclamation in the Alberta Oil Sands Area. MSc Thesis. Southern Illinois University Carbondale. USA.

Glaeser, L.C., Vitt, D.H., and Ebbs, S.E. 2016. Responses of the wetland grass, *Beckmannia syzigachne*, to salinity and soil wetness: consequences for wetland reclamation in the oil sands area of Alberta. *Ecological Engineering* **86**: 24-30.

Hartsock, J.A., House, M., and Vitt, D.H. 2016. Net nitrogen mineralization in boreal fens: a potential performance indicator for peatland reclamation. *Botany* **94**: 1027-1040.

Hazen, R.E. 2016. Organic layer inputs from four species of Cyperaceae within an oil-sands reclamation. MSc Thesis. Southern Illinois University Carbondale. USA.

Vitt, D.H., and House, M. 2015. Establishment of bryophytes from indigenous sources after disturbance from oil sands mining. *Bryologist*, **118**: 123–129.

Vitt, D.H., House, M., and Hartsock, J.A. 2016. Sandhill Fen, an initial trial for wetland species assembly on in-pit substrates: lessons after three years. *Botany* **94**: 1015-1025.

Publications featuring data from Sandhill Fen:

Wieder, R.K., Vile, M.A., Albright, C.M., Scott, K.D., Vitt, D.H., Quinn J.C., and Burke-Scoll, M. 2016. Effects of altered atmospheric nutrient deposition from Alberta oil sands development on *Sphagnum fuscum* growth and C, N and S accumulation in peat. *Biogeochemistry* **129**: 1-19.

APPENDIX 5: THE ECOLOGY OF SANDHILL FEN YEARS 5-8- MONITORING OF KEY ECOLOGICAL FUNCTIONS AND ESTABLISHMENT OF MARKERS OF SUCCESS FOR PEATLAND RECLAMATION

TERMS OF USE

Southern Illinois University was retained by Syncrude to carry out the studies presented in this report and the material in this report reflects the judgment of author(s) in light of the information available at the time of document preparation. Permission for non-commercial use, publication or presentation of excerpts or figures requires the consent of the author(s). Commercial reproduction, in whole or in part, is not permitted without prior written consent from Syncrude. An original copy is on file with Syncrude and is the primary reference with precedence over any other reproduced copies of the document.

Reliance upon third party use of these materials is at the sole risk of the end user. Syncrude accepts no responsibility for damages, if any, suffered by any third party as a result of decisions made or actions based on this document. The use of these materials by a third party is done without any affiliation with or endorsement by Syncrude.

Additional information on the report may be obtained by contacting Syncrude.

This appendix may be cited as:

Vitt, D., House, M. and Hartsock, J. 2020. The ecology of Sandhill Fen- years 5-8 (Dec 2016- May 31 2020): Monitoring of key ecological functions and establishment of markers of success for peatland reclamation. Appendix 5 in Syncrude Canada Ltd. *Sandhill Fen Watershed: Learnings from a Reclaimed Wetland on a CT deposit*. Syncrude Canada Ltd. 2020.

Final Report – April 2020

The Ecology of Sandhill Fen - years 5-8 (Dec.2016-May 31, 2020): Monitoring of key ecological functions and establishment of markers of success for peatland reclamation

Dale H. Vitt, (PI), Melissa House, and Jeremy Hartsock

School of Biological Sciences, Southern Illinois University, Carbondale, IL

dvitt@siu.edu

Table of Contents

Executive Summary

1 Background

2 Summary of 2016 proposal

3 Project 1. Continued monitoring of key ecological functions at Sandhill Wetland

3 Project 1. Continued monitoring of key ecological functions at Sandhill Wetland

3.1 Chemistry

3.1.1 Atmospheric Deposition at Sandhill Wetland

3.1.2 Porewater chemistry-base cations – 2019

3.1.3 Spatial patterns of base cation - 2019

3.1.4 Temporal patterns in base cations - 2016-2019

3.1.5 Porewater chemistry-pH and EC – 2019

3.1.6 Soil chemistry-sodium – 2017-2019

3.2 Vegetation

3.2.1 2012-2013 Plant introductions in Sandhill Wetland research plots: Status in 2019

3.2.2 Plant species assemblages, diversity, and distribution at Sandhill Wetland – 2016-2019

4 Project 2. Plant performance in response to variable and increasing salinity at

Sandhill Wetland

4.1 Responses of *Carex aquatilis* to a regime of increasing sodium concentrations under control conditions

4.2 Responses of *Carex aquatilis* to varying concentrations of sodium at Sandhill Wetland – 2019

4.3 Net primary production of *Carex aquatilis* (2017-2019)

5 Project 3. Identification and quantification of markers of success for fen reclamation

5.1 Nutrient supply patterns across Sandhill Wetland and regional reference fens utilizing ion exchange membranes

5.2 Nutrient supply rates in a boreal extreme-rich fen using ion exchange membranes

5.3 A history of water quality at Sandhill Wetland and comparisons to regional natural wetlands

5.4 Comparison of plant communities, water quality, and soil characteristics at Sandhill Wetland to regional natural peatlands and marshes

5.5 A wetland monitoring approach for evaluating reclamation performance and guiding adaptive management

6 Conclusions

7 Acknowledgments

8 References

9 Appendices

3.1 Ebbs, SE, Glaeser, L, House, M, Vitt, D (2015) A plant physiological approach to assess the performance and potential success of mine revegetation. In. Fourie, AB, Tibbett, L, Sawartsky, L, van Zyl, D (eds.). Mine Closure 2915: Proceeding of the 10th International Conference on Mine Closure: June 1-3, 2015, Vancouver, Canada. Infomine Inc., Vancouver BC. 14 pp

5.1 Phase 1 wetland target selection scorecard

5.2 Species occurring in Acid Fens

5.3 Species occurring in Circumneutral Fens

5.4 Species occurring in Alkaline Fens

5.5 Species occurring in Sodic Fens

5.6 Species occurring in Marshes

5.7 Species occurring at Sandhill Wetland from survey in 2018 (Hartsock (2020))

10 Publications

List of Figures

3.1.1 Atmospheric Deposition at Sandhill Wetland

Fig. 3.1 Mean ($\text{kg ha}^{-1} \text{yr}^{-1}$) and standard error for deposition of $\text{NH}_4^+\text{-N}$, $\text{NO}_3^-\text{-N}$, DIN (Dissolved Inorganic Nitrogen), and $\text{SO}_4^-\text{-S}$ in $\text{kg N/S ha}^{-1} \text{yr}^{-1}$ for the years 2013-2019 at Sandhill Wetland

3.1.2 Porewater Chemistry- base cations – 2019

Figure 3.2 Map of sodium concentrations from vegetation grid surface waters across SHW

Figure 3.3 Map of sodium concentrations from sipper samples across SHW in May 2019

Figure 3.4 Map of sodium concentrations from sipper samples across SHW in July 2019

Figure 3.5 Map of sodium concentrations from sipper samples across SHW in September 2019

Figure 3.6 Map of calcium concentrations from vegetation grid surface waters across SHW

Figure 3.7 Map of calcium concentrations from sipper samples across SHW in May 2019

Figure 3.8 Map of calcium concentrations from sipper samples across SHW in July 2019

Figure 3.9 Map of calcium concentrations from sipper samples across SHW in September 2019

Figure 3.10 Map of magnesium concentrations from vegetation grid surface water across SHW

Figure 3.11 Map of magnesium concentrations from sipper samples across SHW in May 2019

Figure 3.12 Map of magnesium concentrations from sipper samples across SHW in July 2019

Figure 3.13 Map of magnesium concentrations from sipper samples across SHW in September 2019

Figure 3.14 Sodium concentrations from sippers across SHW from 2016 to 2019

Figure 3.15 Calcium concentrations from sippers across SHW from 2016 to 2019

3.1.3 Porewater Chemistry-pH and electrical conductivity – 2019

Figure 3.16 pH across SHW from vegetation grid point surface water

Figure 3.17 pH measurements from sipper samples across SHW from May 2019

Figure 3.18 pH measurements from sipper samples across SHW from July 2019

Figure 3.19 pH measurements from sipper samples across SHW from September 2019

Figure 3.20 Electrical conductivity of surface water (sampled from the grid in August 2019) across SHW

Figure 3.21 Electrical conductivity across SHW May 2019

Figure 3.22 Electrical conductivity across SHW July 2019

Figure 3.23 Electrical conductivity across SHW September 2019

3.1.4 Soil Chemistry-Sodium 2017-2019

Figure 3.24 Sodium concentrations in surface water plotted against sodium concentrations in 0-10 cm of soil column in July 2019

Fig 3.25 Concentration of sodium from 0-10 cm soil column for samples taken in July 2017, 2018, and 2019 plotted against ranked plots

3.2.2 Sandhill species assemblages and species distributions on Sandhill Wetland - 2016-2019

Figure 3.26 Map of Sandhill Wetland with vegetation plot locations

Figure 3.27 NMDS ordination of Sandhill Wetland vegetation plots from years 2015-2019

Figure 3.28 Map showing plots in each species assemblage zone in 2015; zones differentiated by color

Figure 3.29 NMDS ordination of plots with *Typha latifolia* abundance overlain

Figure 3.30 Map of *Typha latifolia* abundance across SHW

Figure 3.31 NMDS ordination of plots with *Carex aquatilis* abundance overlain

Figure 3.32 Map of *Carex aquatilis* abundance across SHW

Figure 3.33 NMDS ordination of *Calamagrostis canadensis* abundance overlain

Figure 3.34 Map of *Calamagrostis* abundance across SHW

Figure 3.35 NMDS ordination of species assemblage centroids

Figure 3.36 Map of 2016 SHW water levels

Figure 3.37 Map of 2017 SHW water levels

Figure 3.38 Map of 2018 SHW water levels

Figure 3.39 Map of 2019 SHW water levels

Figure 3.40 Total plant cover across the zones and years

Figure 3.41 *Calamagrostis canadensis* abundance across zones and years

Figure 3.42 *Carex aquatilis* abundance across SHW zones and years

Figure 3.43 *Typha latifolia* abundance across SHW zones and years

Figure 3.44 Undesirable species occurrences by zone and year

Figure 3.45 Desirable species occurrences by zone and year

Figure 3.46 Bryophyte occurrences by zone and year

Figure 3.47 Undesirable alpha diversity by year

Figure 3.48 Undesirable alpha diversity abundance across zones and years

Figure 3.49 Map of change in undesirable species diversity

Figure 3.50 Desirable species alpha diversity by zone and year

Figure 3.51 Map of change in desirable species diversity

Figure 3.52 Bryophyte species alpha diversity by zone and year

Figure 3.53 Map of change in bryophyte species diversity

Figure 3.54 Gamma diversity of undesirable species by zone and year

Figure 3.55 Gamma diversity of desirable species by zone and year

Figure 3.56 Gamma diversity of bryophyte species by zone and year

Figure 3.57 Ordination of centroids for benchmark sites and SHW zones by year

Figure 3.58 Map of *Populus balsamifera* individual counts at vegetation plots across SHW

4.1 Responses of *Carex aquatilis* to a regime of increasing sodium concentrations under control conditions

Figure 4.1 Regression of *Carex aquatilis* aboveground biomass as a function of sodium treatment (df = 1, F = 14.85, n = 72)

Figure 4.2 Regression of *Carex aquatilis* belowground biomass as a function of sodium treatment (df = 1, F = 77.62, n = 72)

Figure 4.3 Regression of *Carex aquatilis* aboveground/belowground biomass ratio as a function of sodium treatment (df = 1, F = 33.59)

Figure 4.4 Regression of *Carex aquatilis* longest leaf length as a function of sodium treatment (df = 1, F = 16.58) and was measured in the final month (April) of the experiment

Figure 4.5 Regression of *Carex aquatilis* photosynthetic rate as a function of sodium treatment (df = 1, F = 22.04) and was measured in the final month (April) of the experiment

Figure 4.6 Regressions of *Carex aquatilis* transpiration rate as a function of sodium treatment (df = 1, F = 18.96) and was measured in the final month (April) of the experiment

Figure 4.7 Regressions of *Carex aquatilis* stomatal conductance as a function of sodium treatment (df = 1, F = 24.80) and was measured in the final month (April) of the experiment

Figure 4.8 Regressions of *Carex aquatilis* sodium concentration in aboveground biomass as a function of sodium treatment (df = 1, F = 49.77)

Figure 4.9 Regressions of *Carex aquatilis* sodium concentration in belowground biomass as a function of sodium treatment (df = 1, F = 123.07)

Figure 4.10 Regressions of *Carex aquatilis* sodium concentration in root:shoot tissue as a function of sodium treatment (df = 1, F = 17.44)

5.1 Nutrient supply patterns across Sandhill Wetland and regional reference fens utilizing ion exchange membranes

Figure 5.1 Plant root simulator (PRS) probe locations across the spatial extent of Sandhill Wetland

Figure 5.2 Plant Root Simulator (PRS) probe deployment protocol across three reference peatlands with different vegetation structure

Fig. 5.3 Grouped bar plots of Plant Root Simulator (PRS) probe nutrient supply rates

5.2 Nutrient supply rates in a boreal extreme-rich fen using ion exchange membranes

Figure 5.4 Plant Root Simulator (PRS) probes inside a poly-vinyl-chloride cylinder

Figure 5.5 Plant Root Simulator (PRS) probe supply rates for (A) ammonium, (B) nitrate, (C) phosphorus, (D) calcium, (E) magnesium, (F) potassium, (G) sulfate, (H) iron, and (I) manganese in the surface layer of extreme-rich fen peat

5.3 A history of water quality at Sandhill Wetland and comparisons to regional natural wetlands

Figure 5.6 Bar plots of temporal porewater cation concentrations at Sandhill Wetland

Figure 5.7 Bar plots of temporal porewater anion concentrations at Sandhill Wetland

5.4 A comparison of plant communities, water quality, and soil characteristics at Sandhill Wetland to regional natural peatlands and marshes

Figure 5.8 Reference wetland photographs

Figure 5.9 Vegetation survey locations across Sandhill Wetland

Figure 5.10 Percent plant cover (as canopy cover) \pm standard errors across reference wetlands and Sandhill Wetland

Figure 5.11 (a) NMDS ordination of 140 sampling units and (b) significant environmental vectors ($p < 0.05$)

5.5 A wetland monitoring approach for evaluating reclamation performance and guiding adaptive management

Figure 5.12 Threshold cubes for two marshes that include a slightly brackish marsh (Mb) and a fresh marsh (Mf) compared against Sandhill Wetland (SHW) using 20 research plots

Figure 5.13 Performance assessment research plot locations across Sandhill Wetland superimposed above 3 distinct plant assemblage zones (Zones 1 – 3) from Vitt et al. (2016)

Figure 5.14 Threshold cubes for two marshes that include a moderately brackish marsh (Mb) and a fresh marsh (Mf) compared against the alternative Sandhill Wetland (SHW) threshold cube (following removal of six survey plots exhibiting water table position below the soil surface that included a single Zone 2 plot in yellow, and five Zone 3 plots in red). Zones 1–3 correspond to sampling areas previously established by Vitt et al., (2016)

List of Tables

3.1.1 Atmospheric Deposition at Sandhill Wetland

Table 3.1 Mean (\pm SE) for deposition of nitrogen and sulfur for 2013-2019 at Sandhill Wetland

3.1.2 Porewater Chemistry – base cations – 2019

Table 3.2 p-values from one-way ANOVA and Kruskal-Wallis tests for Na, Mg, and Ca over three time periods for five sampling depths

Table 3.3 Mean (mg L^{-1}) and Standard Error (SE) for Na, Mg, and Ca at Sandhill Wetland for 2019, for the three sampling times. Significant differences indicated by letters

Table 3.4 p-values from one-way ANOVA for three elements at 9 sipper locations from the top 20 cm

Table 3.5 Mean (mg L^{-1}) and Standard Error (SE) for Na, Mg, and Ca at 9 sipper locations with highest Na concentrations for the three sampling times

3.1.3 Porewater Chemistry-pH and electrical conductivity – 2019

Table 3.6. p-values for pH depth profiles over the three sampling periods (May, July, and September) (one-way ANOVA).

Table 3.7. Differences in pH over the depth profile for July (Dunn's Method for Joint Ranking)

Table 3.8. Differences in pH over the depth profile for September (Tukey's post-hoc test)

Table 3.9. Differences in pH for the three sampling periods (Tukey's post-hoc test)

Table 3.10. Mean (SE) pH for the three sampling periods (all depths combined)

Table 3.11. Means and SE for EC sippers

Table 3.12. p-values for EC depth profiles over the three sampling periods (May, July, and September) (one-way ANOVA)

3.2.1 2012-2013 Plant Introductions in Sandhill Research Plots: Status in 2019

Table 3.13 Survival (2019) of graminoid species planted in 2012/2013 in 16 sandhill wetland plots

Table 3.14 Survival (2019) of *Betula glandulosa*, *Larix laricina*, and *Dasiphora fruticosa* planted in 2012/2013

3.2.2 Sandhill species assemblages and species distributions on Sandhill Wetland - 2016-2019

Table 3.15 Undesirable species alpha \pm standard error, beta diversity, and gamma diversity

Table 3.16 Desirable species alpha \pm standard error, beta diversity, and gamma diversity

Table 3.17 Bryophyte species alpha \pm standard error, beta diversity, and gamma diversity

Table 3.18 List of species found in SHW and the zone(s) that they occur

Table 3.19 Species not recorded from the 86 grid plots between 2016-2017, 2017-2018, and 2018-2019

4.1 Responses of *Carex aquatilis* to a regime of increasing sodium concentrations under control conditions

Table 4.1 Mean concentrations of sodium, calcium, magnesium, potassium, and electrical conductivity at the beginning of the experiment and after every 2 weeks for each treatment

4.2 Responses of *Carex aquatilis* to varying concentrations of sodium at Sandhill Wetland

Table 4.2 Means (SE) for photosynthesis, stomatal conductance, and transpiration from plants at 12 sites

4.3 Net Primary production of *Carex aquatilis* (2017-2019)

Table 4.3 Means and standard errors for 2017-2019 NPP (g m^{-2})

5.1 Nutrient supply patterns across Sandhill Wetland and regional reference fens utilizing ion exchange membranes

Table 5.1 Plant Root Simulator (PRS) probe summary table for nutrient adsorption patterns, and p-values from 2-way analysis of variance tests ($p \leq 0.05$)

Table 5.2 Adsorption of nutrients by PRS probes in two days compared to twenty days

5.3 A history of water quality at Sandhill Wetland and comparisons to regional natural wetlands

Table 5.3 Organic compounds analyzed at Sandhill Wetland and reference wetlands for year 2019

Table 5.4 Porewater concentrations at Sandhill Wetland. Values are means with standard deviations in parenthesis

Table 5.5 Porewater concentrations among reference wetland classes

5.4 A comparison of plant communities, water quality, and soil characteristics at Sandhill Wetland to regional natural peatlands and marshes

Table 5.6 Wetland site locations and elevation

Table 5.7 Porewater properties across wetland sites

Table 5.8 Physical properties across wetland sites

Table 5.9 Total species cover at reference wetlands vs desirable species cover at Sandhill Wetland for specific wetland types

Table 5.10 Diversity indices across wetland sites

Table 5.11 Mean similarity between/ within groups

5.5 A wetland monitoring approach for evaluating reclamation performance and guiding adaptive management

Table 5.12 Wetland characteristics by site type for completing Phase I reclamation target endpoint selections. Values are site means \pm standard deviations.

Table 5.13 Phase 1 assessment scorecard demonstrating performance measure overlap between Sandhill Wetland test site and natural wetlands

Table 5.14. Total species cover at reference wetlands and desirable species cover at Sandhill Wetland for specific wetland types

Executive Summary. Syncrude Canada, Ltd. provided funding for research carried out by D. H. Vitt and colleagues (Southern Illinois University, Carbondale, IL USA) within a project entitled The Ecology of Sandhill Fen - years 5-8 (Dec.2016-May 31, 2020): Monitoring of key ecological functions and establishment of markers of success for peatland reclamation. The document below is the final report from research carried out between 2016 and 2019 under three project headings: 1) Continued monitoring of key ecological functions at Sandhill Wetland; 2) Plant performance in response to variable and increasing salinity at Sandhill Wetland; and 3) Identification and quantification of markers of success for wetland reclamation. A summary of significant findings is as follows:

1. Atmospheric deposition of nitrogen is high compared to the region and proposed critical loads. The deposition of nitrogen on the wetland has been relatively stable over the past four years and provides high amounts of this nutrient for the plant growth; however, the deposition is about double of recently recommended critical load levels.

2. Electrical conductivity of porewaters ranged from about 550-2,500 $\mu\text{S cm}^{-1}$ in the central portions and about 2,000 to nearly 5,000 $\mu\text{S cm}^{-1}$ along the southern boundaries. Based on the currently accepted Alberta Wetland Classification System (AWCS), Sandhill Wetland would be classified as slightly brackish ($\text{EC}=500\text{-}2,000 \mu\text{S cm}^{-1}$) - mostly the central portions – or moderately brackish ($2,000\text{-}5,000 \mu\text{S cm}^{-1}$) -

mostly along the southern boundaries, and overall classified as moderately brackish. Water chemistry should continue to be monitored especially regarding its effects on biota, including plants. There are areas of the wetland with high cation concentrations, particularly on the margins and especially the southern boundaries and the western wetland. Sodium in particular is higher along the southern boundary. These plots have sodium values up to 600-800 mg L⁻¹. Overall, cation concentrations have little variation with depth. Some (9) plots have high sodium concentrations (varying from 571 to 971 mg L⁻¹) in the rooting zone: 0-20 cm.

3. Soil sodium varies across the fen and has increased from 0.77 mg g⁻¹ in 2017 to 1.36 mg g⁻¹ in 2019, with the number of plots with concentrations above 1.0 mg g⁻¹ increasing from 33% in 2017 to 63% in 2019.

4. Eight years post wet-up, most species of plants that were introduced to the wetland in 2012 have not survived; however, those that did have provided abundant vegetative cover depending on the levels of water occurring at the site level. At sites with low water levels, *Larix laricina* and *Betula glandulifera* have performed extremely well and should be considered for future reclamation designs.

5. Our comprehensive vegetation/water chemistry/water level study provided a detailed look at the current status of Sandhill Wetland. We summarize our program as follows: the vegetation at Sandhill Wetland has changed dramatically over the past 5 years, with the 2017 high water event making a lasting and quite negative impact on the species distributions and diversity on the Wetland. Currently, all three species assemblages at the Wetland have different trajectories suggesting different environmental variables and thresholds are influencing the species assemblages in the three zones. None of the Sandhill Wetland zones overlaps with the reference sites, indicating that the species assemblages found at Sandhill do not closely resemble reference site plant communities and at the present time can be considered to possess sets of unique characteristics. The demise of bryophyte diversity and lowered desirable species richness, along with the increasing abundance of *Carex aquatilis* and *Typha latifolia* and select undesirable species (e.g., *Populus balsamifera*) are all of concern.

6. A phytotron experimental study of the response of *Carex aquatilis* to increasing sodium regimes found that both structural and functional attributes of *C. aquatilis* decrease linearly with increases in sodium concentrations. Belowground components have greater decreases compared to aboveground components, including both biomass and photosynthesis. These greater aboveground decreases are associated with exclusion of sodium from the aboveground components by the belowground components. Reduction in photosynthesis is strongly correlated with reduced stomatal conductance and lower transpiration. *Carex aquatilis* survived all treatment concentrations of sodium – up to 2,354 mg L⁻¹; however, performance was reduced above treatments of 1,079 mg L⁻¹. These decreases in performance in our greenhouse trials are at a similar level to those currently present at Sandhill Wetland and careful assessment of sodium concentrations in the near future needs to be continued.

7. Net primary production of *Carex aquatilis* varied from 192.3 g m⁻² in 2018 to 311.7 g m⁻² in 2017 and compares well with values from natural sites of the region.

8. An investigation of nutrients, divalent base cations, and associated anions show that Sandhill Wetland had low nutrients, high base cation and high sulfur compared to natural sites. Sandhill Wetland is not a eutrophic system in the sixth growing season, and supply for most nutrients are within the ranges of natural systems.

9. A second study of PRS probes demonstrated that ion exchange membranes contained in the probes reach equilibrium shortly after 24 hours, and in ion-rich wetlands such as Sandhill Wetland and natural rich fens,

these probes should only be used for burial periods of one to three days. Incubation times longer than this will result in divalent ions replacing monovalent ones.

10. We compared Sandhill Wetland to 12 natural sites that included the entire range of wetland site-types of the region. Evaluation included floristic, plant community, physical, and chemical characteristics. Sandhill Wetland plant communities present across high and intermediate water table position areas (SH-Z1 and SH-Z2 plots, respectively) are most closely associated with the fresh and slightly brackish marshes surveyed. Plots located in areas exhibiting low water table position (SH-Z3 plots) were quite dissimilar from the natural sites monitored. Furthermore, all plant communities across Sandhill Wetland were quite dissimilar from the reference fens; with maximum similarity scores ranging from 0–5%. Porewater chemistry and water table position across SH-Z1 and SH-Z2 sampling zones were most similar to conditions at the two marshes. Porewater chemistry patterns were additionally comparable to the saline fens. Overall, Sandhill Wetland remains spatially heterogenous in terms of plant community composition, physical characteristics, and site chemistry. Future tailings reclamations should either embrace elevated salinity conditions and seek to create regionally uncommon sodium-dominated systems (e.g., slightly brackish/sodic marshes or saline/sodic fens) or develop more effective methods of preventing ion intrusion into wetland areas.

11. We demonstrate the practicality of using a novel, ‘threshold cube’ approach for appropriately guiding adaptive management and evaluating reclamation performance at sites undergoing reclamation. Based upon our Phase I assessment protocol, environmental aspects at Sandhill Wetland are most similar to marshes at its current developmental stage, however; about 94% of the reclamation site’s threshold cube volume falls outside of typical marsh conditions and demonstrates the many unique attributes of the site.

We conclude: Currently, the plant communities and porewater chemistry of Sandhill Wetland present a largely unique set of conditions and plant communities that largely do not match natural wetland site-types of region. Increasing salinity, especially sodicity, and changing water levels provide a background of environmental conditions that make predicting a future site trajectory impossible, and continued assessment of these changing drivers and the plant responses is highly recommended.

1 Background. The 52 ha Sandhill Watershed was constructed on infill of a formerly mined-out open pit located on Syncrude Canada, Ltd. oil sands lease at 57.040°N; 111.596°W and 310 m elevation (Wytrykush et al. 2012). The 60-100 m deep open pit was infilled with composite tailings and pure sand tailings between 1999 and 2008. Ten meters of sand were placed mechanically and form the present-day topography of the watershed. Site construction of the 17 ha central wetland was completed by adding a 0.5 m of clay sediments designed to reduce hydraulic conductivity and covered by 0.5-1.0 m of salvaged fresh peat obtained from a nearby peatland with a variety of peatland site-types. The wetland was seeded in winter 2011 with a seed mix of characteristic rich fen plant species but composed largely of *Carex aquatilis* (Vitt et al. 2016). Water was introduced to the fen in late summer 2012. Over the first three years, Sandhill Wetland changed considerably, proceeding from having an open, unvegetated surface to one richly covered with a variety of plant species. Currently, the fen has a nearly complete plant cover. Three years after wet-up, Vitt et al. (2016) recognized three plant species assemblages, arranged as zones across a wetness gradient – Zone 1: *Typha latifolia*-dominated community; Zone 2: *Carex aquatilis*-dominated community; Zone 3: *Calamagrostis canadensis*-dominated community, (a Zone 4 was also present; however, comprised of a small number of survey plots). At that time (2016), the area of Zone 2 contained water table position and plant species assemblages most representative of those in moderate-rich fens (Vitt and Chee 1990). However, subsequent changes at Sandhill Wetland have been unpredictable with changing water levels and increasing salinity and sodicity, all affecting the existing plant communities; and which will have an effect on animal communities and ecosystem functions. These rapidly changing environmental conditions and concurrent vegetative responses require assessment in order to project possible future outcomes.

2 Summary of 2016 proposal. Our proposal from 2016 outlined three projects to be carried out over the course of four field seasons (2016, 2017, 2018, and 2019) with a final report in early 2020. We identified a suite of important variables at Sandhill Wetland that have been assessed over this time frame. We also proposed to identify a set of comparative benchmark sites from which parameters comparing structure, function, and species diversity can be standardized for comparison to those at Sandhill Wetland. We proposed a program divided into three parts:

1. Continued monitoring of four aspects (water chemistry, plant community, net ecosystem productivity, and flora of Sandhill Wetland) in order to determine key changes over the next four years.
2. Establish a new experimental project to examine plant responses to developing salinity regimes.
3. A program to determine the most efficient markers of success for fen (or wetland) reclamation.

3 Project 1. Continued monitoring of key ecological functions at Sandhill Wetland

Deliverables (revised from 2016 proposal): 1. Determine areas of salinization within Sandhill Wetland and their subsequent effects on reclamation success. Demonstrate how plants can serve as passive biomonitors for salinity within Sandhill Wetland*. 2. Supply a recommendation of how plant diversity affects plant community development and how these would affect peat-forming species. 3. Determine rates of net productivity and organic matter accumulation of four sedges that have successfully established at Sandhill Wetland. 4. Provide a complete species list, list of wetland vascular plants, bryophytes, and how they associate in communities within the spatial variation the fen.

* The untimely death of Dr. Stephen Ebbs, who was leading this project, has curtailed our efforts for this deliverable; however, we have made significant progress in 2014-15 that addresses this issue and it is available in published form and copied in Appendix 1 (Ebbs et al. 2015).

3.1 Chemistry

3.1.1 Atmospheric Deposition at Sandhill Wetland

Methods: Five ion exchange resin tube collectors (plus blank control) of atmospheric deposition were installed throughout Sandhill Wetland in 2013 and maintained through 2019. Collectors consist of a 20 cm long 1" PVC pipe containing mixed bed of cation/anion exchange resin (Amberlite IRN 150; DuPont, Wilmington, Delaware, USA). A plastic funnel with a collection area of 400 cm² channeled precipitation into the resin tubes. We affixed 1-m extension tubes to each collection funnel to capture snowfall that upon melt drains into the resin tubes. Resins are collected in late May and mid-September annually and analyzed for NH₄⁺-N, NO₃⁻-N, SO₄⁻-S and DIN (total inorganic N). We extracted retrieved resins with 1 M KI and analyzed the extract solutions for NH₄⁺-N (phenate method) on a Seal AA3 AutoAnalyzer (Seal Analytical, Madison, Wisconsin, USA) and for NO₃⁻-N, SO₄⁻-S by ion chromatography (Dionex ICS 1500; Thermo Fisher Scientific, Waltham, Massachusetts, USA). We subtracted volume weighted concentrations in blank resin tube extracts from concentrations in extracts from exposed resin tubes and corrected deposition values for laboratory-determined extraction efficiencies (96.9% and 98.2% for NH₄⁺-N and NO₃⁻-N, respectively (Wieder et al. 2016a, 2016b).

Data failed the Shapiro-Wilks test for normality ($p < 0.05$). Significant differences were examined through a non-parametric Kruskal-Wallis test with Dunn's pairwise post-hoc comparison to determine differences between years.

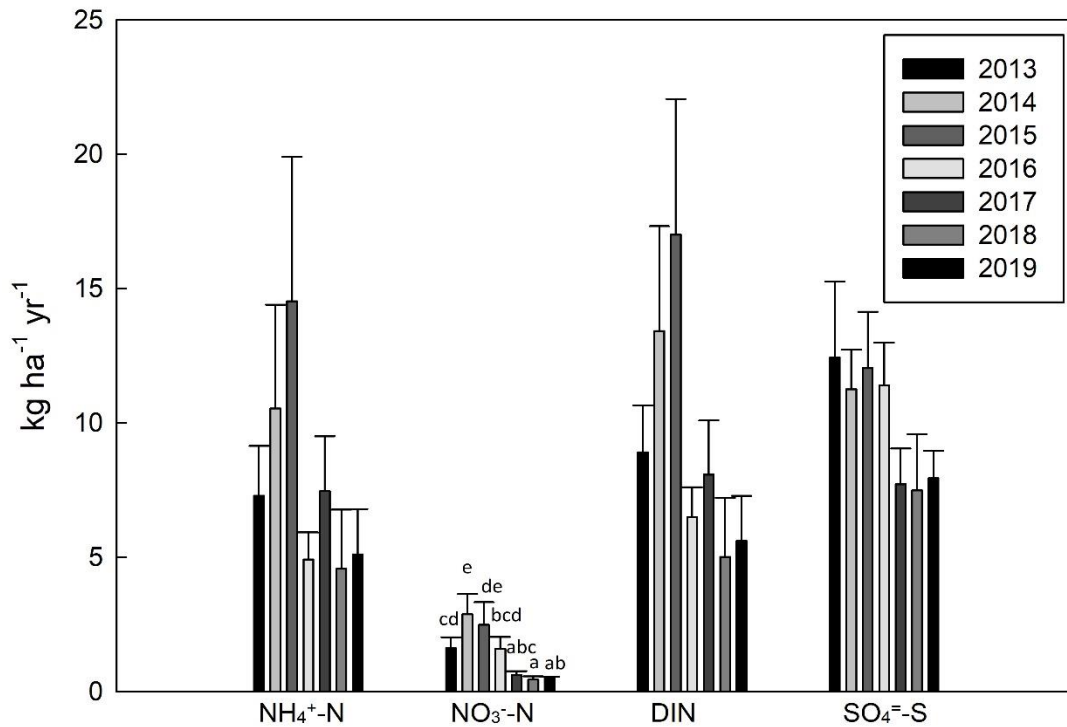
Results: Over the seven years of measurement, mean values were (as kg N/S ha⁻¹ yr⁻¹): NH₄⁺-N=7.77; NO₃⁻-N=1.45; DIN=9.21, and SO₄⁻-S=10.03. Deposition peaked in 2015 with DIN=17.01 kg N ha⁻¹ yr⁻¹ and SO₄⁻-S=12.00 kg S ha⁻¹ yr⁻¹. However, over the last four years (2016-2019) average DIN was 6.3 kg N ha⁻¹

yr^{-1} and $\text{SO}_4^{2-}\text{-S}=8.63 \text{ kg S ha}^{-1} \text{ yr}^{-1}$. $\text{NH}_4^+\text{-N}$ was on average 5.3 times as abundant as $\text{NO}_3^-\text{-N}$ (Table 3.1). In comparison, deposition at a pristine site (Mariana Lakes - 2011-2015) $\text{NH}_4^+\text{-N}$ averaged $0.68 \text{ kg N ha}^{-1} \text{ yr}^{-1}$; $\text{NO}_3^-\text{-N}$ averaged $0.87 \text{ kg N ha}^{-1} \text{ yr}^{-1}$, and DIN averaged $1.55 \text{ kg N ha}^{-1} \text{ yr}^{-1}$ (Wieder et al. 2019). In addition, data from 2009-2014 from six bog sites located from 11 to 251 km from the mid-point of Syncrude/Suncor stacks yielded the following average deposition (as $\text{kg N/S ha}^{-1} \text{ yr}^{-1}$): $\text{NH}_4^+\text{-N}=0.53$; $\text{NO}_3^-\text{-N}=0.65$; $\text{DIN}=1.17$, and $\text{SO}_4^{2-}\text{-S}=7.78$ (Wieder et al. 2016b). A critical load for N deposition of $3 \text{ kg N ha}^{-1} \text{ yr}^{-1}$ has been recommended for northern bogs (Wieder et al. 2019).

Only $\text{NO}_3^-\text{-N}$ deposition was significant between years ($\text{df}=6$, $F=6.18$, $p<0.0001$); $\text{NH}_4^+\text{-N}$ ($\text{df}=6$, $F=0.59$, $p=0.736$), DIN ($\text{df}=6$, $F=1.44$, $p=0.213$), and $\text{SO}_4^{2-}\text{-S}$ ($\text{df}=6$, $F=2.13$, $p=0.062$) were not significant between years (Fig. 3.1).

Table 3.1 Mean (\pm SE) for deposition of nitrogen and sulfur for 2013-2019 at Sandhill Wetland

Year	2013	2014	2015	2016	2017	2018	2019
$\text{NH}_4^+\text{-N}$	7.29 \pm 1.85	10.54 \pm 3.85	14.53 \pm 5.37	4.91 \pm 1.02	7.46 \pm 2.05	4.57 \pm 2.20	5.11 \pm 1.68
$\text{NO}_3^-\text{-N}$	1.62 \pm 0.41	2.87 \pm 0.76	2.48 \pm 0.85	1.59 \pm 0.44	0.62 \pm 0.15	0.45 \pm 0.12	0.50 \pm 0.05
DIN	8.90 \pm 1.75	13.42 \pm 3.90	17.01 \pm 5.05	6.51 \pm 1.10	8.08 \pm 2.01	5.01 \pm 2.20	5.61 \pm 1.67
$\text{SO}_4^{2-}\text{-S}$	12.43 \pm 2.83	11.25 \pm 1.48	12.04 \pm 2.10	11.40 \pm 1.59	7.72 \pm 1.33	7.49 \pm 2.08	7.94 \pm 1.02



Aerial Deposition

Fig. 3.1 Mean (kg ha⁻¹ yr⁻¹) and standard error for deposition of NH₄⁺-N, NO₃⁻-N, DIN (Dissolved Inorganic Nitrogen), and SO₄⁼-S in kg N/S ha⁻¹ yr⁻¹ for the years 2013-2019 at Sandhill Wetland. Different letters indicate significant differences (Dunn’s pairwise post-hoc comparison - p<0.05)

Significant Findings: Nitrogen deposition at Sandhill Wetland has been stable over the past four years and is twice the recommended level for bogs and poor fens (3 kg N ha⁻¹ yr⁻¹- Wieder et al. 2019). These deposition levels provide large amounts of N for plant growth and site decomposition. Wieder et al. (2016a) produced a map of inorganic N deposition in a 3,255 km² sampling area centered at the midpoint between the Syncrude and Suncor upgrader stacks. Within this area, 1,506 km² currently receives N deposition in excess of 3 kg N ha⁻¹ yr⁻¹, of which 104 km² and 355 km² are bogs and fens, respectively, based on the Alberta Wetland Inventory (Halsey et al. 2003) (fens are not differentiated between poor, rich, and shrubby fens). Thus, it appears that bogs and poor fens are being negatively impacted by N deposition related to oil sands development in northern Alberta (Wieder et al. 2020).

3.1.2 Porewater Chemistry-Base Cations – 2019

Porewater variation – Depth (2019)

Methods: Sipper-peepers were installed at 20 plots throughout the fen in 2011. The sipper-peepers consist of a 5-cm diameter and 50 cm long slotted PVC pipe; each 10 cm section is separated and has a tube that runs to the surface. Using the tubes from the different sections, pristine water can be collected from specific depths: 0-10, 11-20, 21-30, 31-40, and 41-50. Fen wet-up occurred in August of 2012, revealing some plots were always dry including the perched fen plots. Five sippers yielded no water and were removed. The following data are from the remaining 15 sippers, all located in the main fen. Additional sippers were

installed in 2015 (total of 30 sippers). Sippers were sampled 3 times each field season: May, July, and September. Samples were taken back to the laboratory at Southern Illinois University. Cations were quantified using a Varian 220 FS atomic absorption spectrometer.

Concentrations (mg L^{-1}) of each element (for all depths and months combined) were log transformed to normalize the data set. When data were successfully normalized, a one-way ANOVA was used to test for significant differences between months. When the data set failed the Shapiro-Wilk test for normalization ($p < 0.05$), a non-parametric Kruskal-Wallis test was used. Means were compared using an all pairs Tukey's post-hoc test when a one-way ANOVA was performed. When a Kruskal-Wallis test was performed, a Dunn's all-pairwise comparisons test was used to compare differences between the means.

Results: Calcium concentrations did not differ in the top 50 cm ($n=5$) for the three sampling periods (May, July, September). Magnesium (both ANOVA and Kruskal-Wallis) and Sodium (Kruskal-Wallis) concentrations differed only in September (Table 3.2).

Table 3.2 p-values from one-way ANOVA and Kruskal-Wallis tests for Na, Mg, and Ca over three time periods for five sampling depths

Element	Month	ANOVA	Kruskal-Wallis
Na	May	0.686	0.696
Na	July	0.344	0.636
Na	September	0.195	0.0005
Mg	May	0.244	0.148
Mg	July	0.344	0.616
Mg	September	0.002	0.0005
Ca	May	0.191	0.237
Ca	July	0.177	0.143
Ca	September	0.399	0.152

Porewater variation – Season

When all 30 sipper locations are considered together, there were no seasonal differences for Calcium (ANOVA, $p=0.733$) and Sodium (ANOVA, $p=0.507$), whereas Magnesium concentrations were different (ANOVA, $p=0.0001$) between May and July (Tukey's post-hoc Test) 125 mg L^{-1} in May and 75 mg L^{-1} in July, with September intermediate (119 mg L^{-1}).

Mean values (for all depths combined) for the overall site ranged from 312-317 for Calcium, 75-125 for Magnesium, and 470-546 for Sodium (Table 3.3). For sampling times with significant differences in concentrations with depth -- in September, Mg concentrations ranged from 12 at 20-30 cm to 335 at 30-40 cm, while Na concentrations varied from 71 at 40-50 cm to 1353 at 20-30 cm in September.

Table 3.3 Mean (mg L^{-1}) and Standard Error (SE) for Na, Mg, and Ca at Sandhill Wetland for 2019, for the three sampling times. Significant differences indicated by letters

Element	Month	Mean	SE
Na	May	546.150	33.890
Na	July	522.449	30.743
Na	September	470.957	25.926
Mg	May	124.502(A)	5.735

Mg	July	74.6163(B)	1.043
Mg	September	118.527(A)	6.099
Ca	May	310.619	9.484
Ca	July	316.552	10.346
Ca	September	317.364	12.524

We separated the 9 sipper locations having the highest Na concentrations in the top 20 cm (rooting zone). Seasonal comparisons for these nine locations were: Ca concentrations were not different ($p=0.825$), whereas both Mg ($p=0.0002$) and Na ($p=0.0000$) were different (Table 3.4). Calcium varied little, from 326 to 343 mg L⁻¹, whereas Mg varied from 75 mg L⁻¹ in July to 129 mg L⁻¹ in May. Sodium varied from 571 mg L⁻¹ in September to 971 mg L⁻¹ in May – a 1.7-fold difference (Table 3.5).

Table 3.4 p-values from one-way ANOVA for three elements at 9 sipper locations from the top 20 cm

Element	ANOVA p-value
Na	0.0000
Mg	0.0002
Ca	0.8225

Table 3.5 Mean (mg L⁻¹) and Standard Error (SE) for Na, Mg, and Ca at 9 sipper locations with highest Na concentrations for the three sampling times

Element	Month	Mean	SE
Na	May	971.139(A)	75.558
Na	July	721.878(B)	58.057
Na	September	570.679(B)	37.119
Mg	May	128.857(A)	14.181
Mg	July	75.075(B)	2.580
Mg	September	110.217(AB)	14.527
Ca	May	341.297	24.029
Ca	July	320.905	24.027
Ca	September	325.881	22.961

When concentrations for the three base cations (using data from the grid, collected in early August) are considered by vegetation zone (see below), only calcium has differences (Kruskal-Wallis $p=0.013$), with zone 1 different from zone 3.

3.1.3 Spatial Patterns in Base Cations – 2019

Methods: Surface water was collected during the 2019 vegetation survey from each of the 87 plots that had water above 30 cm below the soil surface. These samples were analyzed in the lab as the methods described above (Section 3.1.2).

Results: Sodium has highest concentrations along the southern boundary of the wetland and lowest in the center (Fig. 3.2). Seasonal variation is present between May (Fig. 3.3), July (Fig. 3.4), and September (Fig. 3.5). September has more plots (3) with lowest values (small yellow circles) compared to May and July (each with 1) and fewer plots (1) with highest values (large purple circles) compared to May (4) and July (3).

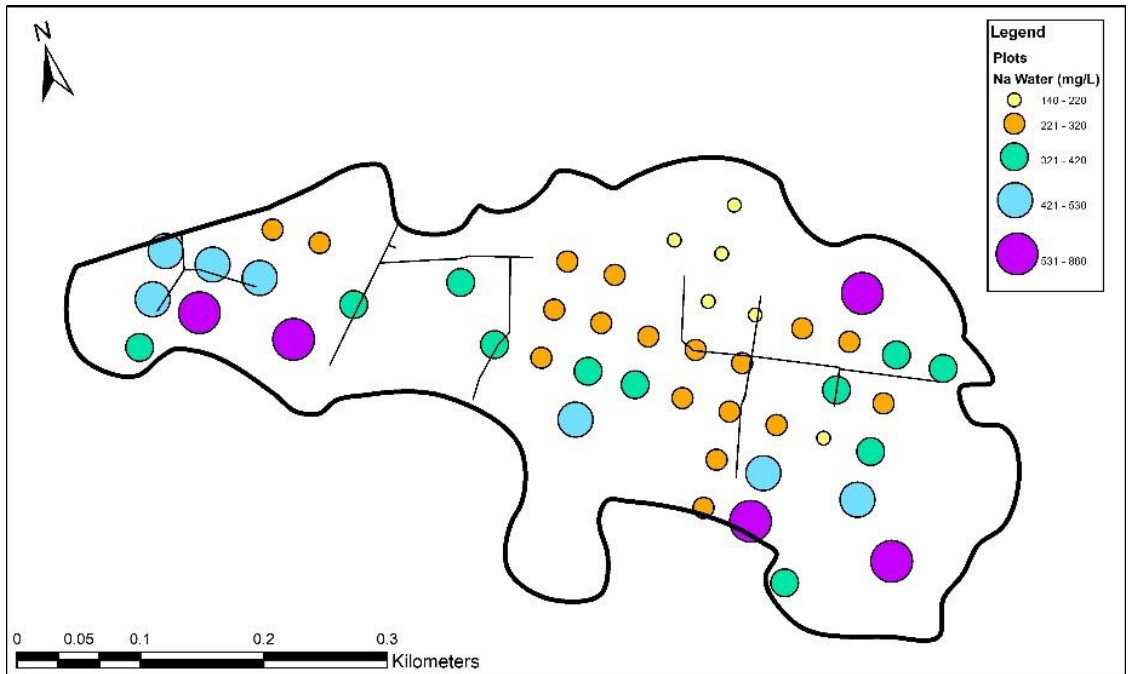


Figure 3.2 Map of sodium concentrations from vegetation grid surface waters across SHW. Larger circles indicate larger sodium concentrations; different colors are classes of sodium concentrations

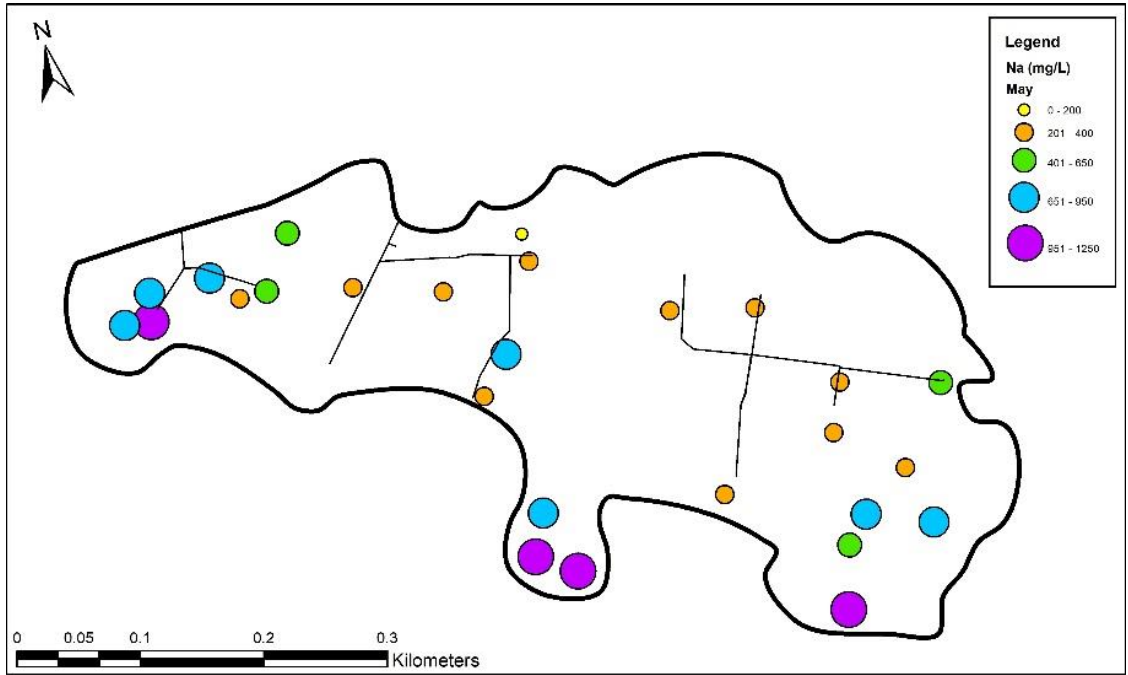


Figure 3.3 Map of sodium concentrations from sipper samples across SHW in May 2019. Larger circles indicate larger sodium concentrations; different colors are classes of sodium concentrations

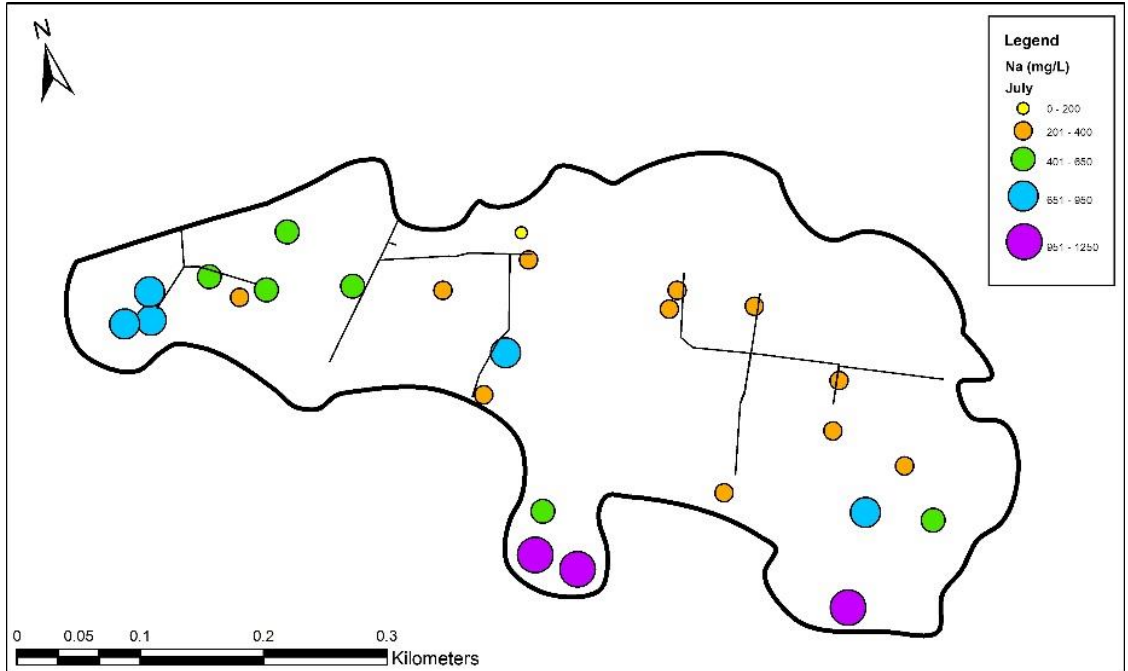


Figure 3.4 Map of sodium concentrations from sipper samples across SHW in July 2019. Larger circles indicate larger sodium concentrations; different colors are classes of sodium concentrations

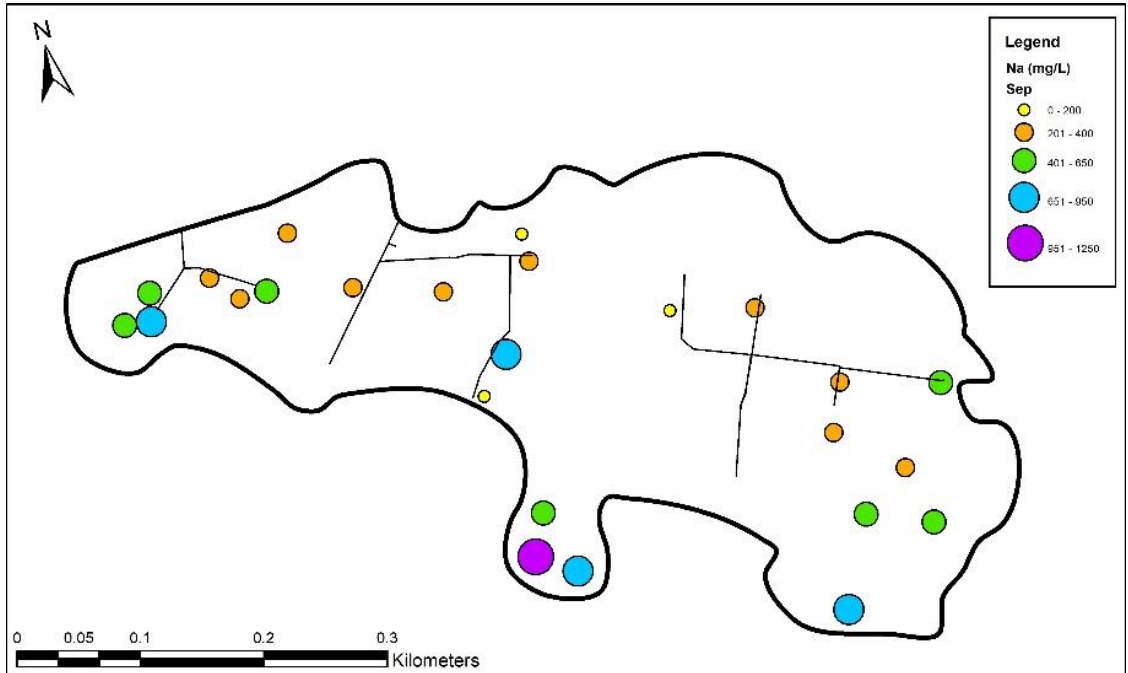


Figure 3.5 Map of sodium concentrations from sipper samples across SHW in September 2019. Larger circles indicate larger sodium concentrations; different colors are classes of sodium concentrations

Calcium is more generally distributed, but with most plots having high concentrations found to the western end of the wetland (plus two on the north boundary -Fig. 3.6). Seasonal variation is low with little change in number of plots with smallest and largest concentrations - staying the same or changing by only one plot (Figs. 3.7-3.9).

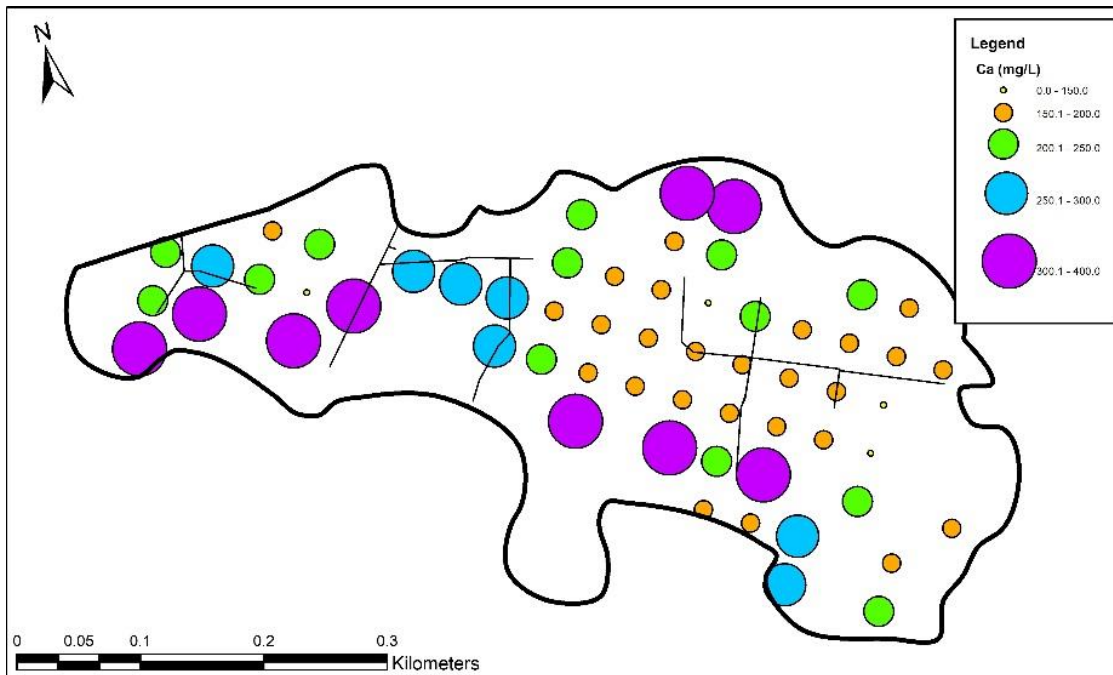


Figure 3.6 Map of calcium concentrations from vegetation grid surface waters across SHW. Larger circles indicate larger calcium concentrations; different colors are classes of calcium concentrations

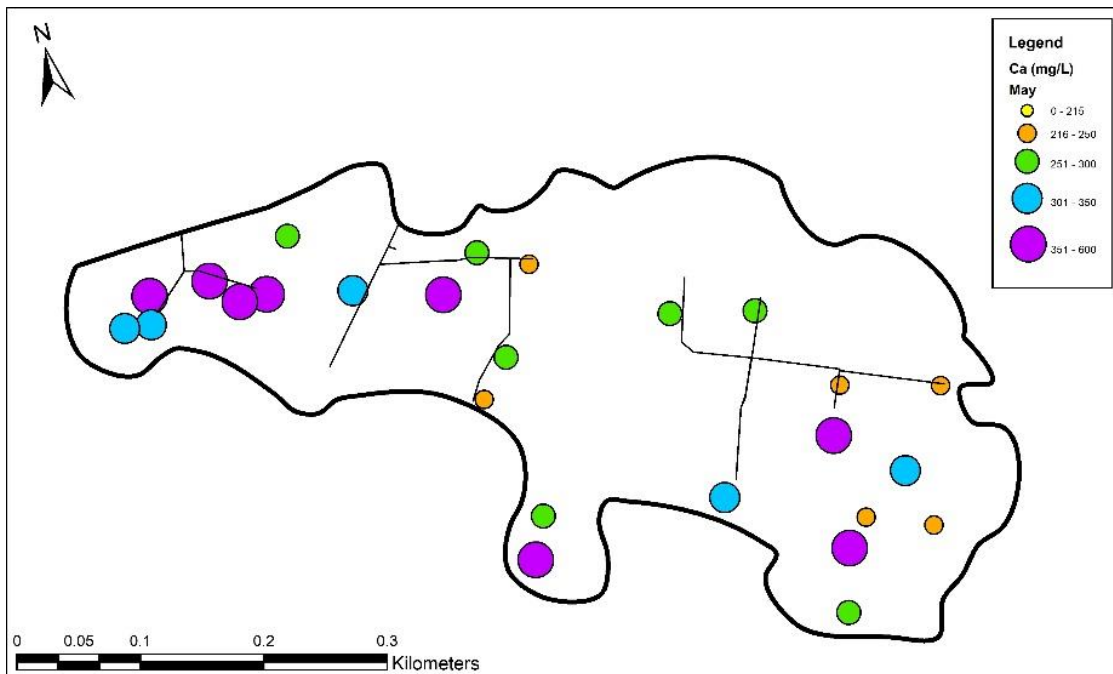


Figure 3.7 Map of calcium concentrations from sipper samples across SHW in May 2019. Larger circles indicate larger calcium concentrations; different colors are classes of calcium concentrations

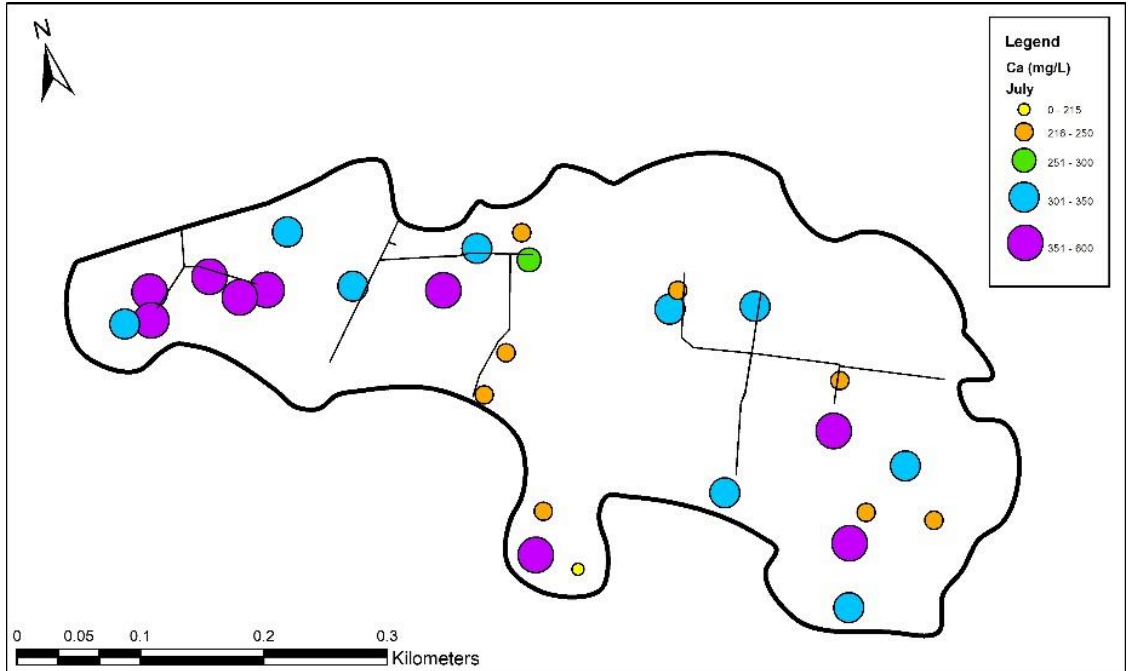


Figure 3.8 Map of calcium concentrations from sipper samples across SHW in July 2019. Larger circles indicate larger calcium concentrations; different colors are classes of calcium concentrations

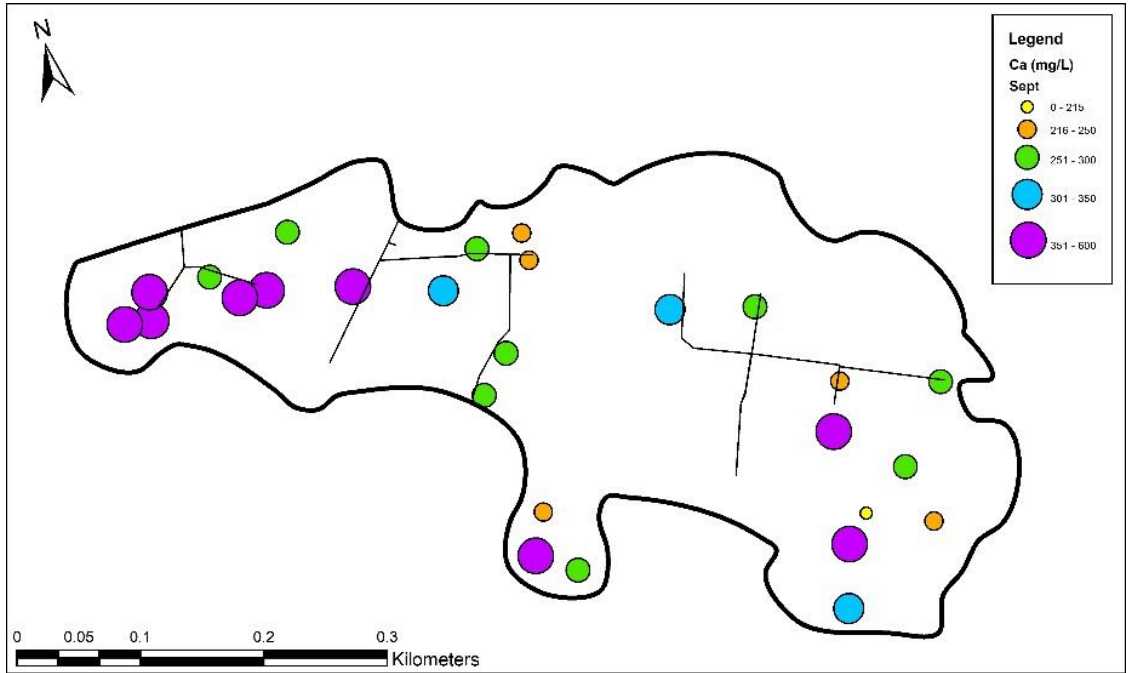


Figure 3.9 Map of calcium concentrations from sipper samples across SHW in September 2019. Larger circles indicate larger calcium concentrations; different colors are classes of calcium concentrations

Magnesium concentrations mirror those of calcium (Fig. 3.10) but have less variation (Figs. 3.11-3.13). Seasonal variation is minimal between May and September; however, the consistently low July readings are suspect (Fig. 3.12). These July Magnesium analyses should be reviewed in the future.

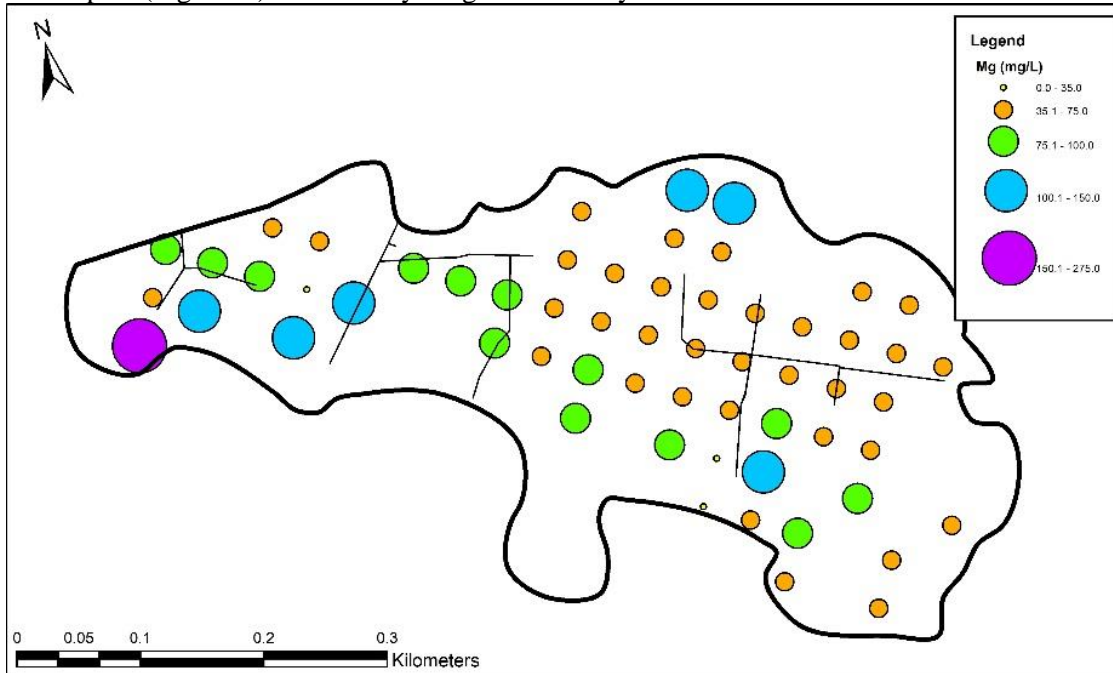


Figure 3.10 Map of magnesium concentrations from vegetation grid surface water across SHW. Larger circles indicate larger magnesium concentrations; different colors are classes of magnesium concentrations

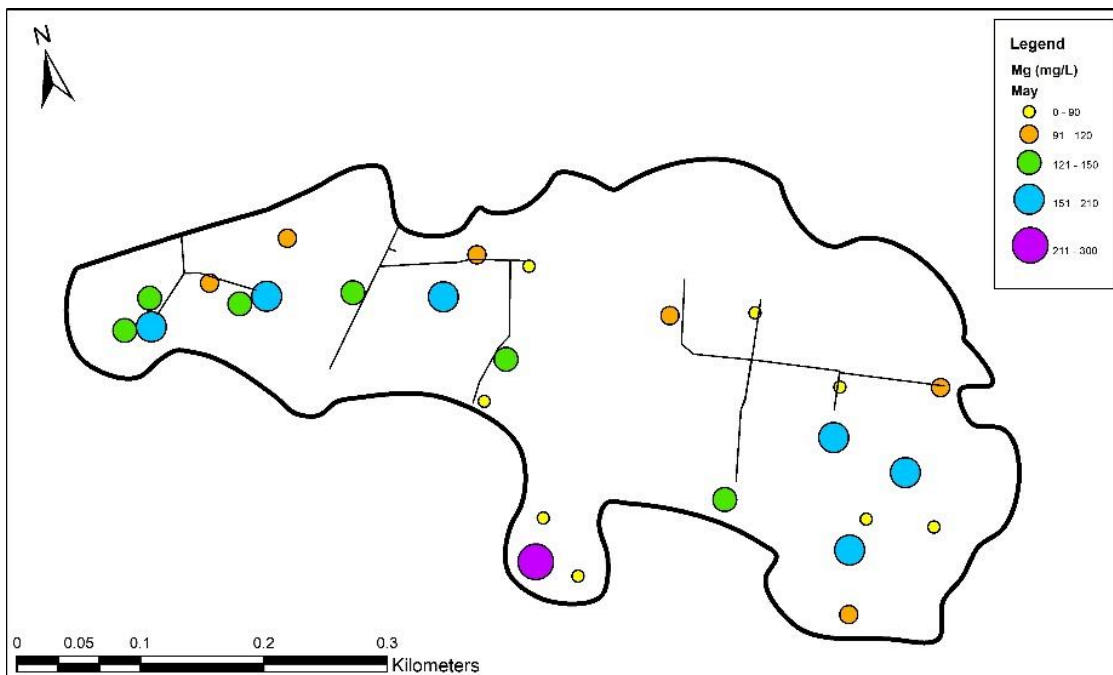


Figure 3.11 Map of magnesium concentrations from sipper samples across SHW in May 2019. Larger circles indicate larger magnesium concentrations; different colors are classes of magnesium concentrations

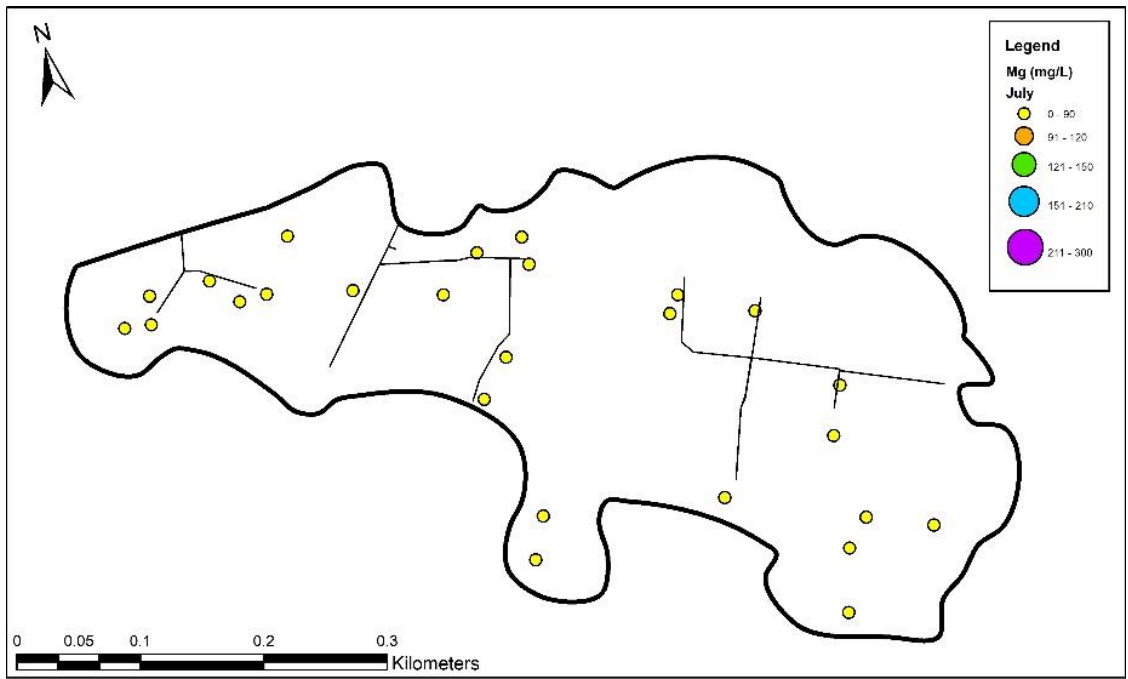


Figure 3.12 Map of magnesium concentrations from sipper samples across SHW in July 2019. Larger circles indicate larger magnesium concentrations; different colors are classes of magnesium concentrations

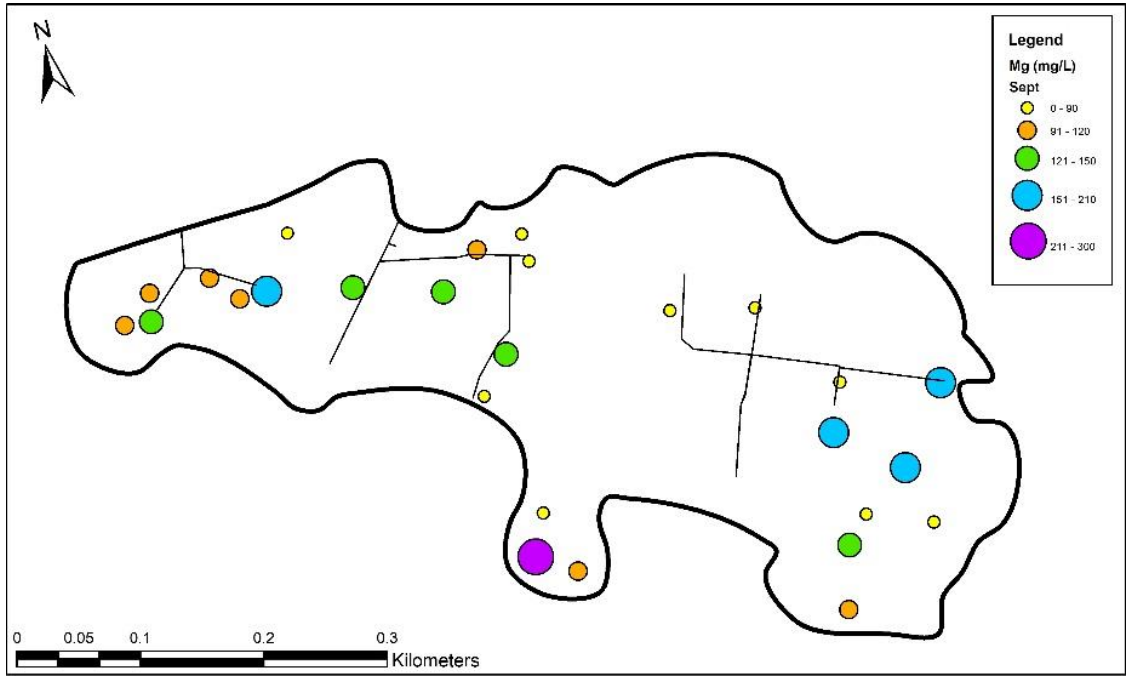


Figure 3.13 Map of magnesium concentrations from sipper samples across SHW in September 2019. Larger circles indicate larger magnesium concentrations; different colors are classes of magnesium concentrations

3.1.4 Temporal Patterns in base Cations – 2016 to 2019

Methods: Samples were collected from sipper-peepers as described above (Section 3.1.2). Data were not normal and were analyzed using Kruskal-Wallis test followed by a Dunn's pairwise test ($p < 0.05$).

Results: Sodium increased over the years ($p < 0.0001$). Sodium increased from 2016 to 2017 and again in 2018. Sodium in 2019 is not different from 2017 or 2018 (Fig. 3.14). Likewise, calcium increased ($p < 0.0001$) from 2016 to 2017, but no increase was observed in subsequent years (Fig. 3.15).

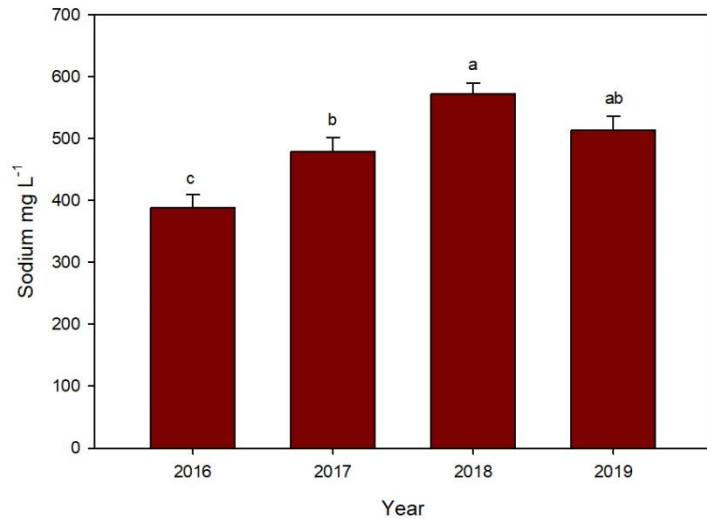


Figure 3.14 Sodium concentrations from sippers across SHW from 2016 to 2019. Letters indicate significant Dunn's test result ($p < 0.05$)

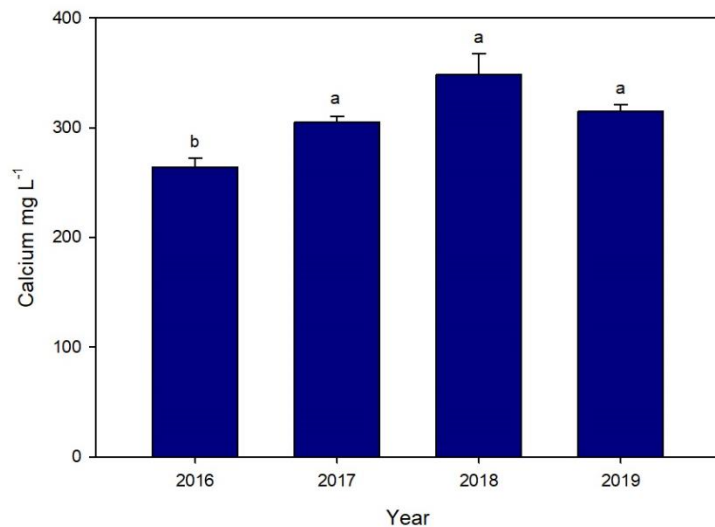


Figure 3.15 Calcium concentrations from sippers across SHW from 2016 to 2019. Letters indicate significant Dunn's test result ($p < 0.05$)

3.1.5 Porewater Chemistry-pH and Electrical Conductivity – 2019

Methods: The same water samples as those collected above were analyzed for pH and EC at SIUC using an Accumet AB15 pH meter and an Orion 4 Star EC meter. One-way ANOVA's were performed on the data sets with pH and electrical conductivity if they were normally distributed; if not normally distributed, data were log transformed. When the data set could not be transformed to a normal distribution, a nonparametric Kruskal-Wallis test was used followed by a Dunn's test to show differences between month,

depth, pH, and electrical conductivity. A Tukey's post-hoc test was performed after an ANOVA to show differences between groups.

pH sampled in the top 50 cm of the peat profile varied significantly for depth in the July and September sampling periods (Table 3.6), with depths of 10-30 differing from the remainder in July and 40-50 differing in September (Tables 3.7-3.8). Mean pH varied significantly over the three sampling periods (Table 3.9), varying from 7.3 in September to 7.4 in July, and 7.6 in May (Table 3.10). Even though there was significantly different values for some depths and over the season, there was overall very little variation (7.3 to 7.6).

pH is highest in the central portions of the wetland (Fig. 3.14). Differences in seasonal variation in pH (Figs. 3.15-3.17) is driven by the plots with highest values (large purple circles) - 4 in May, 0 in July and 0 in September) and by the plots having lowest values (small orange circles) - 3 in May, 9 in July, and 12 in September.

Table 3.6. p-values for pH depth profiles over the three sampling periods (May, July, and September) (one-way ANOVA)

Month	p-value for depth	p-value for sipper
May	0.064	0.0001
July	0.032*	0.0017*
September	0.0007	0.0150

Table 3.7. Differences in pH over the depth profile for July (Dunn's Method for Joint Ranking)

Month	Group
Surface	AB
0-10	AB
10-20	B
20-30	B
30-40	AB
40-50	A

Table 3.8. Differences in pH over the depth profile for September (Tukey's post-hoc test)

Depth	Group
0-10	AB
10-20	B
20-30	B
30-40	AB
40-50	A

Table 3.9 Differences in pH for the three sampling periods (Tukey's post-hoc test).

p-value=0.0001

Month	Group
May	A
July	B
September	C

Table 3.10. Mean (SE) pH for the three sampling periods (all depths combined)

Month	Mean	SE
May	7.58	0.025
July	7.39	0.035
September	7.32	0.027

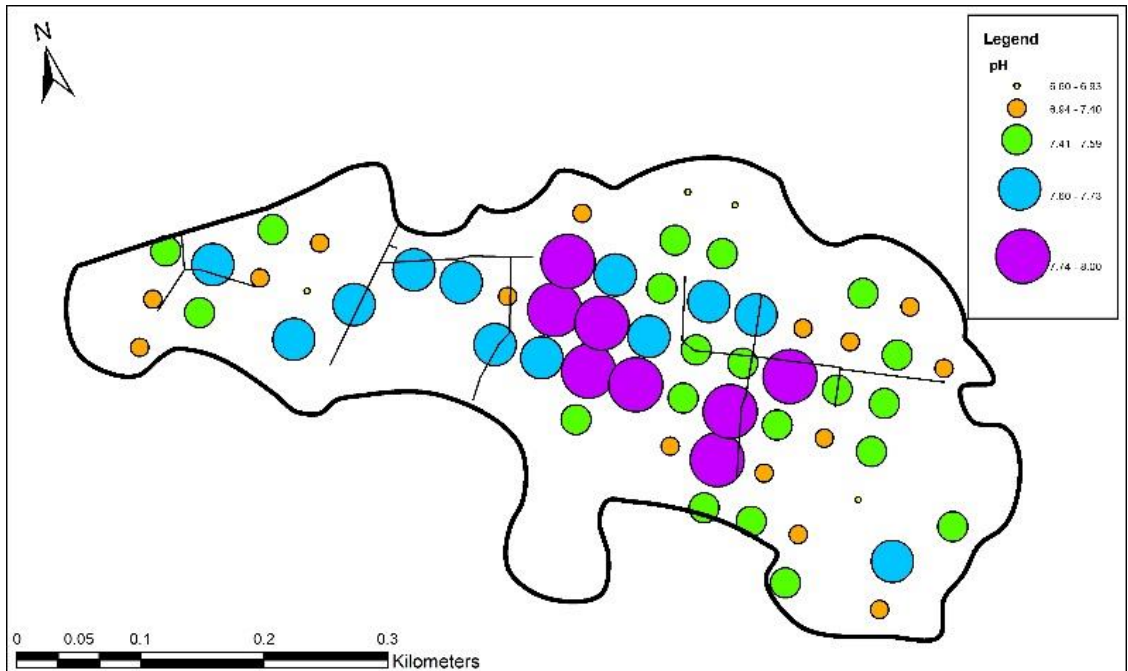


Figure 3.16 pH across SHW from vegetation grid point surface water. Larger circles indicate higher pH; colors indicate different levels of pH

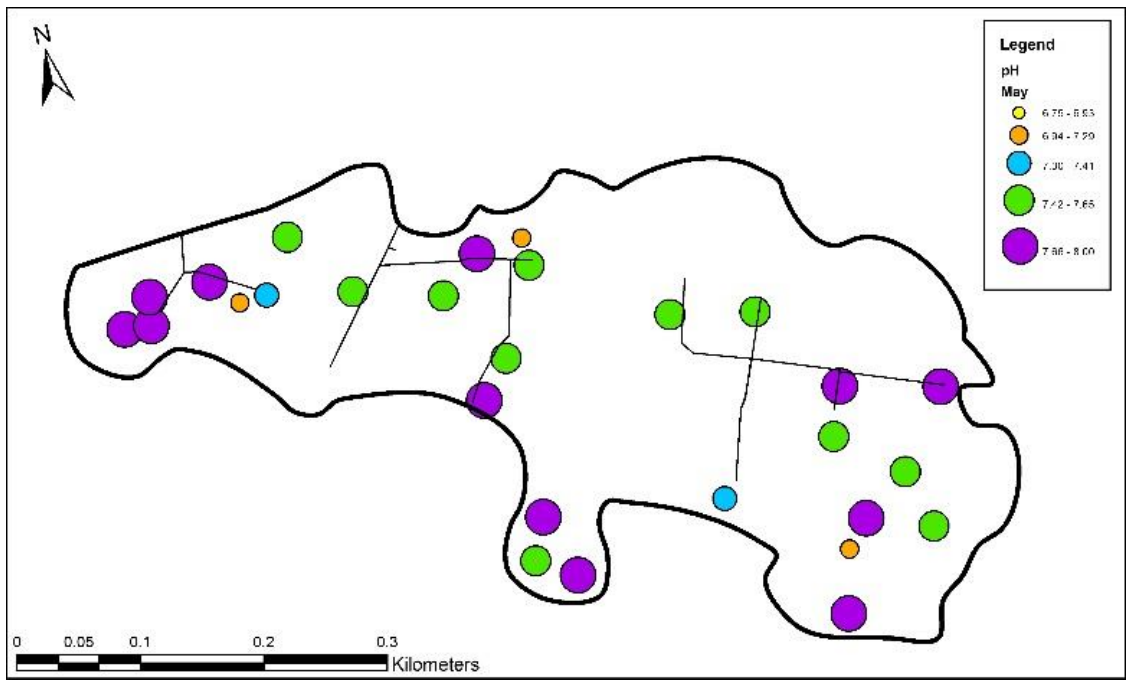


Figure 3.17 pH measurements from sipper samples across SHW from May 2019. Larger circles indicate higher pH values; different colors are different level of pH

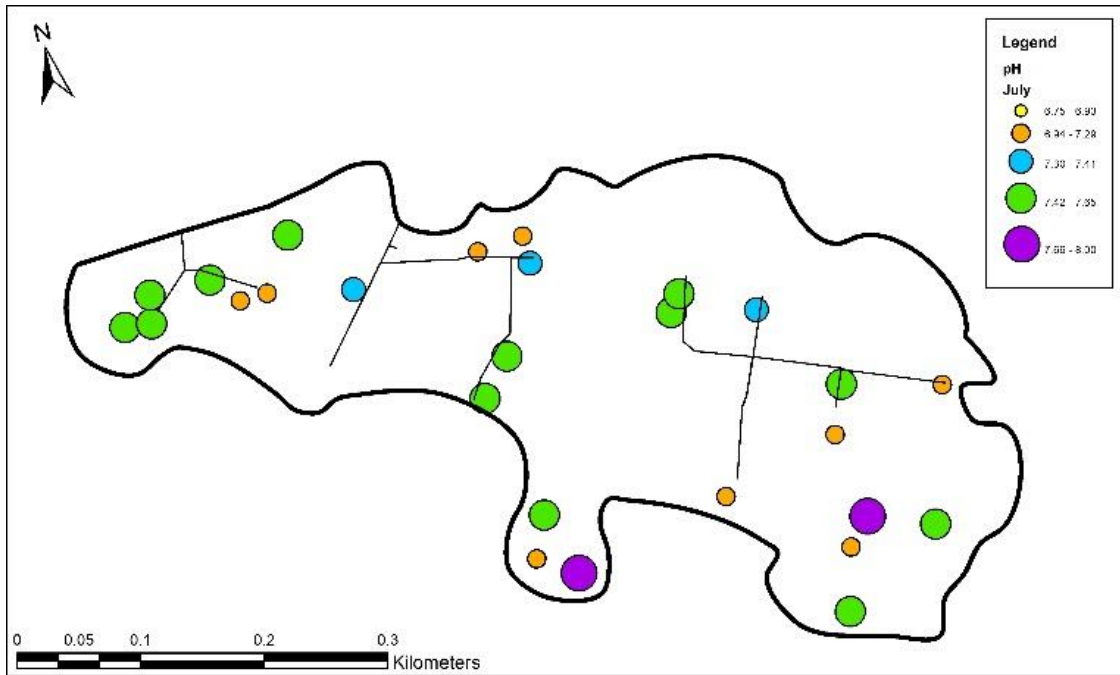


Figure 3.18 pH measurements from sipper samples across SHW from July 2019. Larger circles indicate higher pH values; different colors are different levels of pH

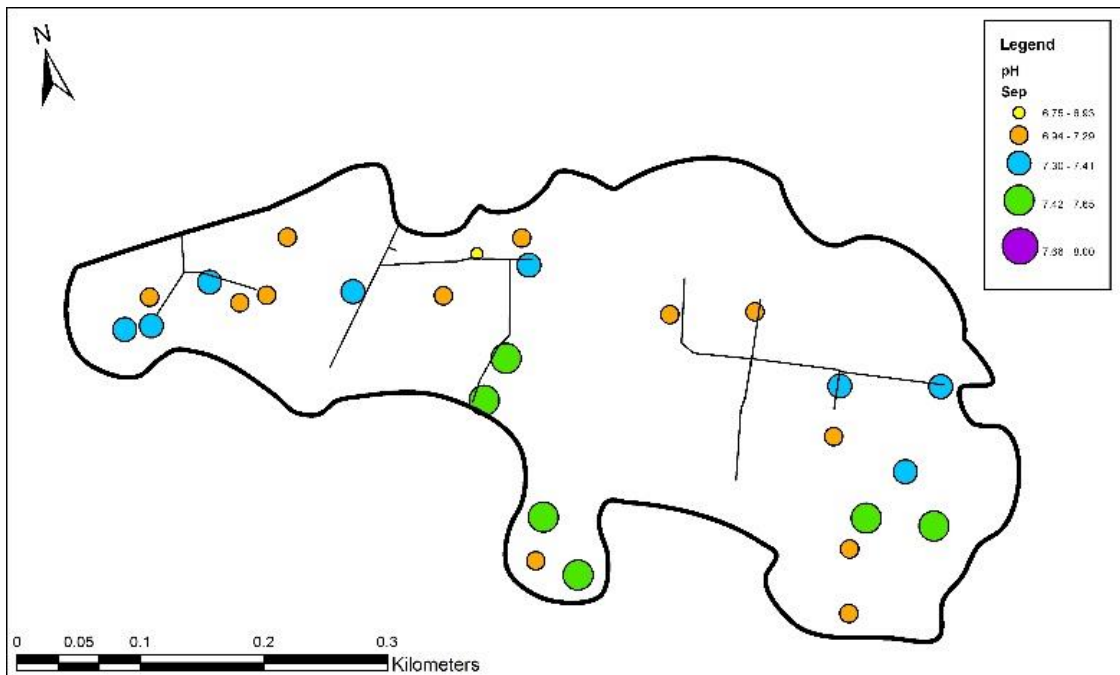


Figure 3.19 pH measurements from sipper samples across SHW from September 2019. Larger circles indicate higher pH values; different colors are different levels of pH

Mean electrical conductivity (EC - as a measure of total ions - salinity) for the three sampling periods varied from 3,888.1 to 3,804.3 $\mu\text{S cm}^{-1}$ (Table 3.11) (with no significant differences (Tukey's) along the depth profile (Table 3.12) nor over the three sampling periods (when all depths are combined - Kruskal-Wallis $p=0.834$).

Table 3.11. Means and SE for EC sippers

Month	Mean	SE
May	3888.1	141.45
July	3804.3	132.71
September	3875.3	150.34

Table 3.12. p-values for EC depth profiles over the three sampling periods (May, July, and September) (one-way ANOVA)

Month	p-value for depth	p-value for sipper
May	0.1653*	0.0001*
July	0.0445 (A,A,A-Tukey's)	0.0001
September	0.0384 (A,A,A-Tukey's)	0.0001

*indicates a Kruskal-Wallis test was used

EC is highest along the southern boundary of the wetland, with lowest values throughout the interior (Fig. 3.18). The lack of seasonal variation in EC is evident in Figs. 3.19-3.21, where the number of plots with highest values (large purple circles) vary from 1 in May to 0 in July to 1 in September; comparably, the number of plots with lowest EC values (small yellow circles) consistently are 6 in number.

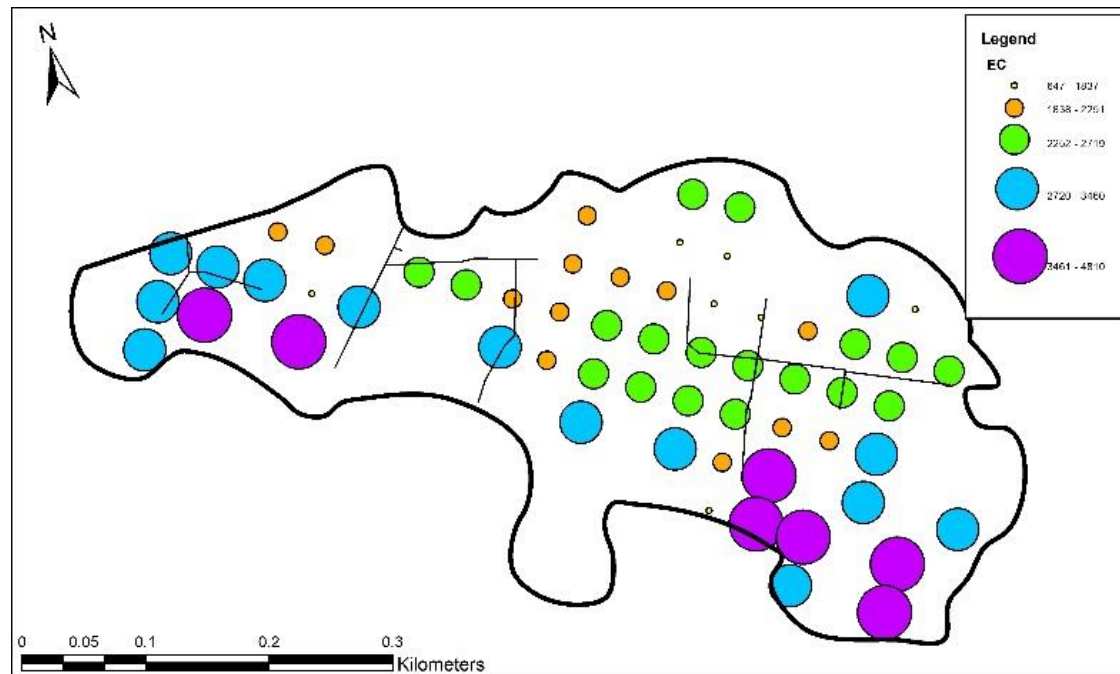


Figure 3.20 Electrical conductivity of surface water (sampled from the grid in August 2019) across SHW. Larger circles indicate higher conductivity; colors indicate different classes of EC measurement ($\mu\text{S cm}^{-1}$)

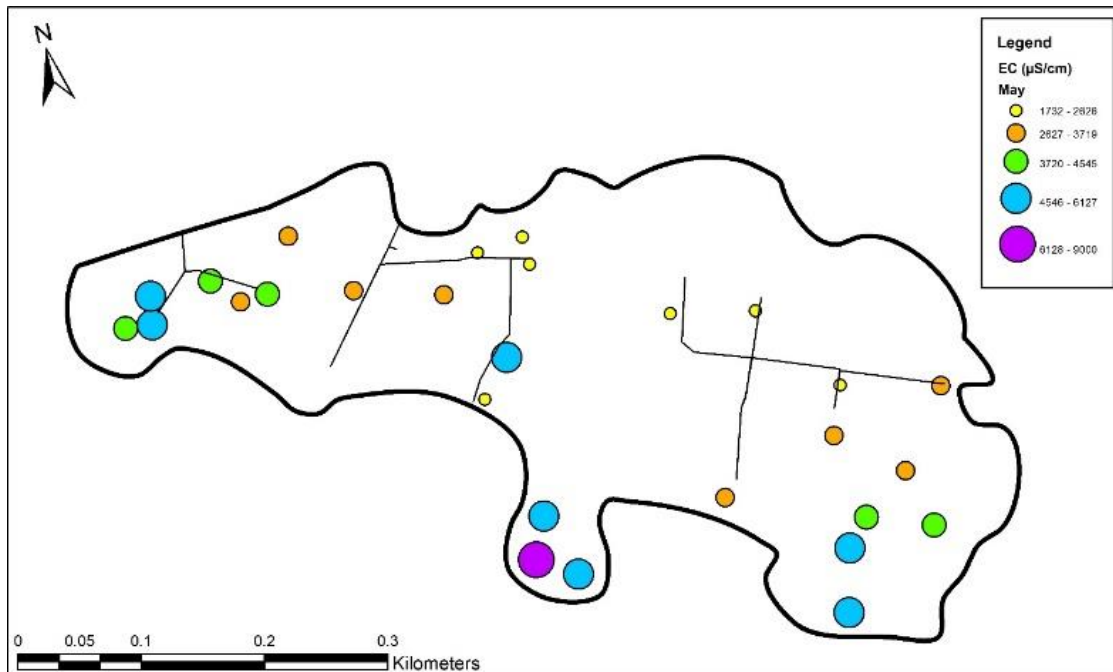


Figure 3.21 Electrical conductivity across SHW. Larger circles indicate higher conductivity; colors indicate different classes of EC measurement ($\mu\text{S cm}^{-1}$) in May 2019

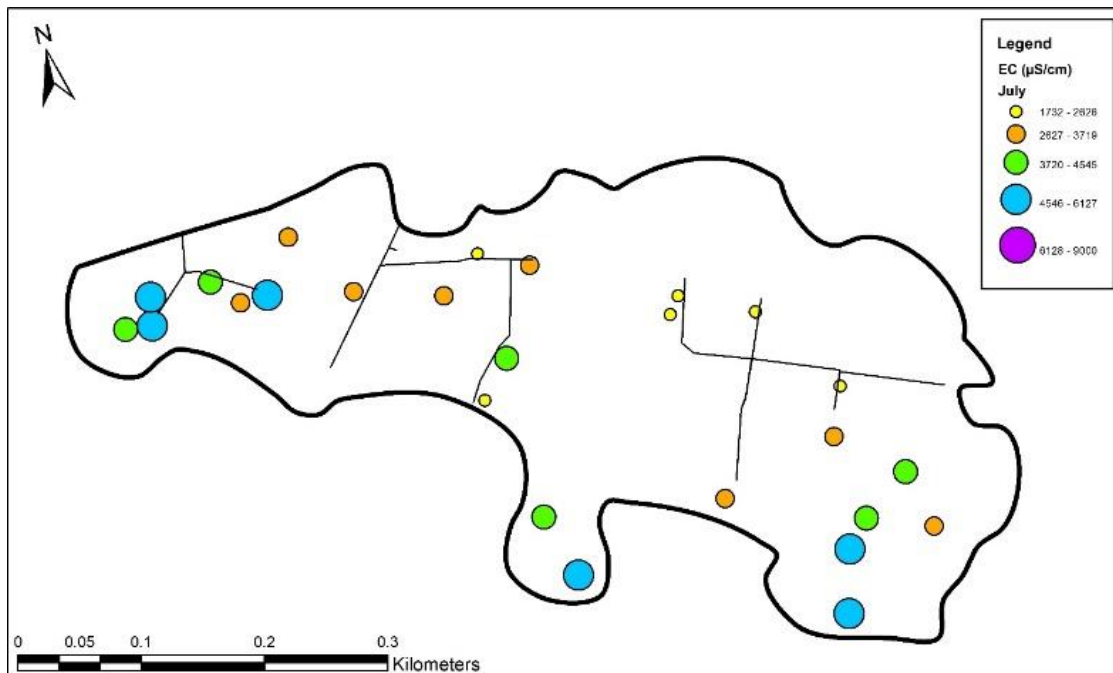


Figure 3.22 Electrical conductivity across SHW. Larger circles indicate higher conductivity; colors indicate different classes of EC measurement ($\mu\text{S cm}^{-1}$) in July 2019

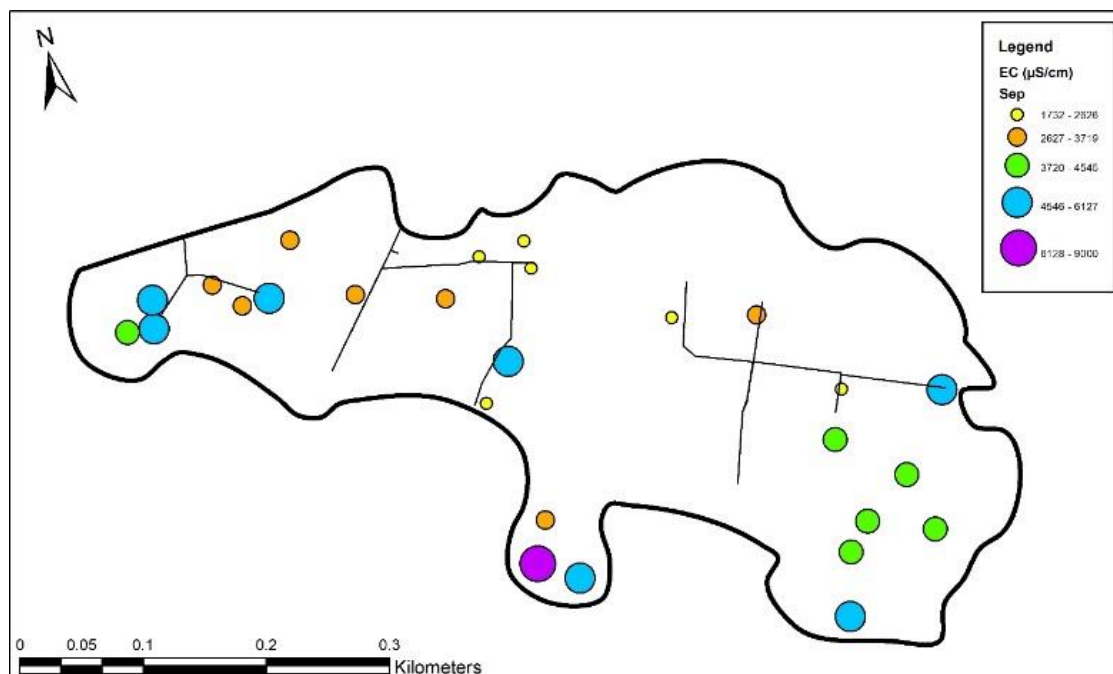


Figure 3.23 Electrical conductivity across SHW. Larger circles indicate higher conductivity; colors indicate different classes of EC measurement ($\mu\text{S cm}^{-1}$) in September 2019

Significant Findings: Overall there were few differences in concentrations with depth. The patterns of seasonal variation differ among the three elements; when all locations are considered calcium and sodium do not differ seasonally, Mg is lowest in midseason (July). When locations with high sodium in the upper porewater column are considered separately, calcium remains consistent over the seasons; however, both sodium and magnesium concentrations differ over the seasons - high in May and low in July and September. Although there is considerable spatial variation across the wetland for all three base cations, only calcium varies across the vegetation zones.

There are areas of the wetland with high cation concentrations, particularly on the margins and especially the southern boundaries and the western wetland. Sodium, in particular is higher along the southern boundary. These plots have sodium values up to 600-800 mg L^{-1} . Overall, cation concentrations have little variation with depth. Some (9) plots have high sodium concentrations (varying from 571 to 971 mg L^{-1}) in the rooting zone: 0-20 cm.

Electrical conductivity ranged from about 550-2,500 $\mu\text{S cm}^{-1}$ in the central portions and about 2,000 to nearly 5,000 $\mu\text{S cm}^{-1}$ along the southern boundaries. Based on the currently accepted Alberta Wetland Classification System (AWCS), Sandhill Wetland would be classified as slightly brackish ($\text{EC}=500\text{-}2,000 \mu\text{S cm}^{-1}$) - mostly the central portions - or moderately brackish (2,000-5,000 $\mu\text{S cm}^{-1}$) - mostly along the southern boundaries, and overall classified as moderately brackish. Water chemistry should continue to be monitored especially regarding its effects on biota, including plants.

3.1.6 Soil Chemistry-Sodium - 2017-2019

Methods: We sampled 71 grid plots for soil sodium (top 10 cm) in July/August of 2017-2019. Several grid plots with water depth over +30 cm were not sampled. Samples were dried at 55°C for at least five days. Samples were homogenized using a Wiley Mill. Sodium was extracted using a 1:10 ratio of soil to 0.5 M ammonium acetate + 0.02 M EDTA, shaken for 16 hours at 200 rpm, and filtered through Whatman 1 filter

paper, then Whatman 40 filter paper, and lastly 0.22 μm filter paper. The filtered sample was then acidified and analyzed through AAS for Na^+ concentration.

Results: There is a significant correlation ($p < 0.001$, $r^2 = 0.420$) between sodium in the water and that in the soil (Fig. 3.22).

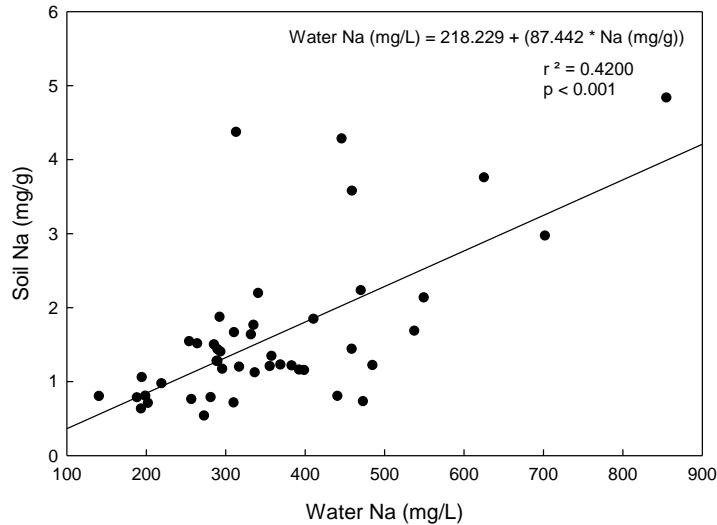


Figure 3.24 Sodium concentrations in surface water plotted against sodium concentrations in 0-10 cm of soil column in July 2019

In 2017, mean sodium concentration was 0.77 mg g^{-1} (median- 0.59), and sodium concentrations varied from 0.35 mg g^{-1} to 2.21 mg g^{-1} with 33.3% of the plots having values above 1.0 mg g^{-1} . In 2018, mean sodium concentration was 1.07 mg g^{-1} (median- 0.61) and plots varied from 0.21 mg g^{-1} to 5.99 mg g^{-1} , with 50.6% of the plots above 1 mg g^{-1} . Comparatively, in 2019 the mean concentration was 1.36 mg g^{-1} (median 0.73) varying from 0.22 to 4.83 mg g^{-1} with 62.5% of the plots above 1.0 mg g^{-1} . Sodium concentrations were different between 2017 and 2019 ($p=0.025$). Average sodium concentration was 177% higher in 2019 compared to 2017, but the increase was not uniform across the fen. Figures 3.23 illustrates the patterns of concentrations of sodium for each year. Across the board, sodium did increase each year; however, the greatest increases were in plots with the highest concentrations. The high average values are largely due to higher increases in plots with high sodium. As a result, the distribution of sodium and the annual increases in concentration are not uniform across the wetland.

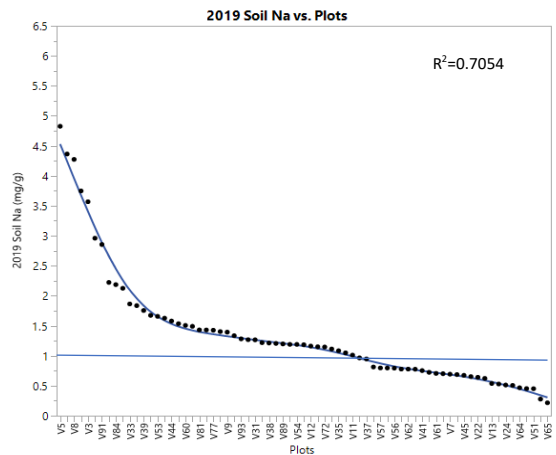
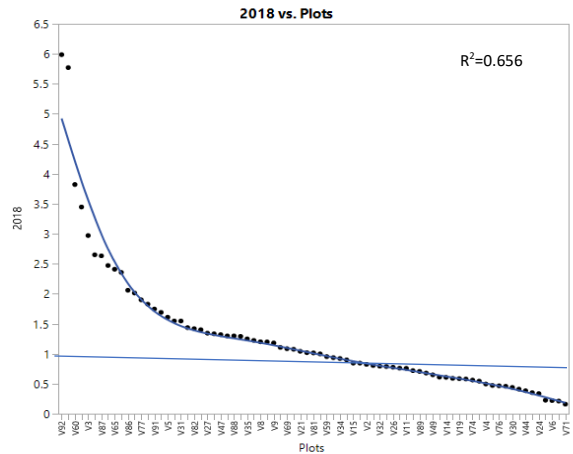
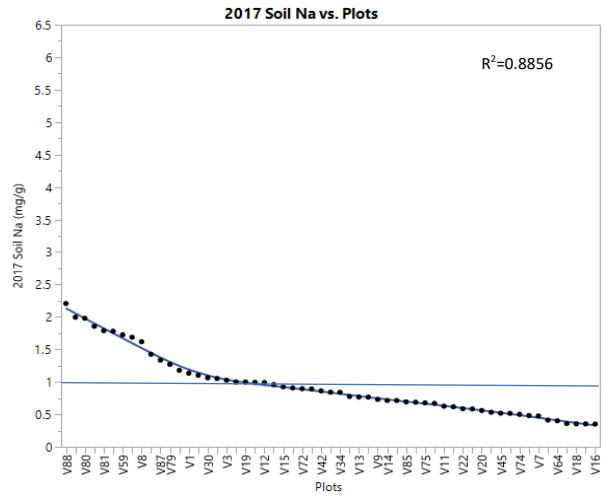


Fig 3.25 Concentration of sodium from 0-10 cm soil column for samples taken in July, 2017, 2018, and 2019 plotted against ranked plots. Horizontal line is placed at 1.0 mg/g⁻¹

Significant Findings: Soil sodium varies across the fen and has increased from 0.77 mg g⁻¹ in 2017 to 1.36 mg g⁻¹ in 2019, with the number of plots with concentrations above 1.0 mg g⁻¹ increasing from 33% in 2017 to 63% in 2019. However, the increase has not been uniform across the wetland, with the greatest increases in plots having the highest concentrations, resulting in the high average values largely due to higher

increases in plots with high sodium. In addition, the strong positive relationship between concentrations of sodium in the soil and in the water suggests that monitoring soil sodium where water is not available is an option.

3.2 Vegetation

3.2.1 2012-2013 Plant Introductions in Sandhill Research Plots: Status in 2019

Methods: In the spring of 2012 and again in 2013 we introduced seedlings of 25 wetland plant species to our 20 research plots in Sandhill Wetland. We planted from 2-24 individuals grown at Smoky Lake nursery in 1m² plots. In July 2019, we resurveyed 15 of these plots (1-4 and 16 excluded from survey) and recorded presence/absence of each species.

Results: After 7-8 years these interactions can be summarized as follows:

Graminoids (Table 3.13): 13 species (52%) are no longer present in the plots and include the following species:

Carex bebbii
Carex paupercula
Carex limosa
Carex canescens
Carex pauciflora
*Carex retrorsa**
*Carex atherodes**
*Carex utriculata**
Triglochin palustris
Scirpus lacustris
Scheuchzeria palustris
Juncus tenuis
*Eriophorum vaginatum**

*only 2-5 individuals introduced

Species present in 2019 (with number of plots [out of 15] with occurrence in 2019).

Scirpus validus (7)
Scirpus microcarpus (8)
Carex aquatilis (6)
Carex hystericina (2)
Carex diandra (1)
Eriophorum chamissonis (7)
Eriophorum angustifolium (2)
Triglochin maritima (5)
Beckmannia syzigachne (1)

Woody plants (Table 3.14): (with number of plots [out of 15] with occurrence in 2019).

Betula glandulifera (6)
Larix laricina (5)
Dasiphora fruticosa (5)

In 2019, water levels varied from 0 (at surface) to +40 cm above the peat surface. Five plots (10, 14, 15, 17, 19) all with water levels greater than 35 cm above the surface contained no original introductions. Five plots with levels near the peat surface (0) all contained the three woody species, with *Larix* having from 42-92% survival, *Betula* from 29-100% survival, and *Dasiphora* from 21-100% survival. None of these three species survived in the wet plots.

Significant Findings: Many species (13 of the 25 introduced) are not present in the plots in 2019. Of those that are present in the plots in 2019, 7 of the 9 graminoids are present outside of the plots and occur commonly on the fen (*B. syzigachne* and *C. diandra* are rare in the fen). Likewise, two of the species no longer present in plots occur elsewhere in the fen (*C. atherodes* and *C. utriculata*). The three woody species had good survival in plots with water levels near to the surface, but are not common or not present outside of the plots. Of importance is the survival and growth (see Table 3.14) of *Larix*, a species typical of swamps and wooded fens)

Table 3.13 Survival (2019) of graminoid species planted in 2012/2013 in 16 sandhill wetland plots; 1=present, 0=absent

Plot No.	Water Level (cm)	<i>S. validus</i>	<i>B. syzigachne</i>	<i>E. angustifolium</i>	<i>C. aquatilis</i>	<i>S. microcarpus</i>	<i>T. maritima</i>	<i>C. hystericina</i>	<i>C. diandra</i>
5	10	1	0	0	0	1	1	0	0
6	30	1	0	0	0	1	0	0	0
7	20	0	0	0	0	0	0	0	0
8	0	0	0	0	1	1	0	1	0
9	0	1	1	0	1	1	1	0	1
10	35	0	0	0	0	0	0	0	0
11	30	1	0	0	0	0	0	0	0
12	0	1	0	0	0	1	0	1	0
13	10	1	0	0	1	1	1	0	0
14	40	0	0	0	0	0	0	0	0
15	40	0	0	0	0	0	0	0	0
16	-	-	-	-	-	-	-	-	-
17	40	0	0	0	0	0	0	0	0
18	0	0	0	1	1	1	1	0	0
19	40	1	0	0	0	0	0	0	0
20	0	0	0	1	1	1	1	0	0

Notes: *Scirpus validus*, *Beckmannia syzigachne*, *Eriophorum angustifolium*, *Carex aquatilis*, *Scirpus microcarpus*, *Triglochin maritima*, *Carex hystericina*, *Carex diandra*

Table 3.14 Survival (2019) of *Betula glandulosa*, *Larix laricina*, and *Dasiphora fruticosa* planted in 2012/2013

Plot No.	Water Level (cm)	<i>Betula</i> (No. plants/24)	<i>Larix</i> (No. plants/12)	<i>Larix</i> (mean height (m) \pm S.E.M.)	<i>Dasiphora</i> (No. plants/24)
5	10	0	0	0	0
6	30	0	0	0	0
7	20	6	0	0	0
8	0	10	10	1.8 \pm 0.09	20
9	0	24	11	1.4 \pm 0.06	16
10	35	0	0	0	0
11	30	0	0	0	0
12	0	7	11	1.3 \pm 0.06	5
13	10	0	0	0	0
14	40	0	0	0	0
15	40	0	0	0	0
16	-	-	-	-	-
17	40	0	0	0	0
18	0	24	7	0.7 \pm 0.07	7
19	40	0	0	0	0
20	0	24	5	0.5 \pm 0.03	24

3.2.2 Sandhill Wetland Plant Species Assemblages, Diversity, and Distribution at Sandhill Wetland - 2016-2019

Using a grid system, we surveyed the vegetation of Sandhill Wetland (SHW) each year beginning in 2015 and continuing through 2019. The 2015 survey resulted in a publication (Vitt et al. 2016) that proposed three distinct plant communities (=species assemblages) that are spatially arranged at SHW. The resulting three spatial areas were termed ‘zones.’ Zone 1 was the wettest zone, dominated by *Typha latifolia*. Zone 2 had intermediate water levels and was dominated by *Carex aquatilis*. Zone 2 most closely resembled rich fen site-types, particularly in areas with water levels just below the soil surface allowing for bryophyte establishment. Zone 3, the driest of the zones, was dominated by *Calamagrostis canadensis*. Furthermore, within each zone, we identified ‘desirable’ and ‘undesirable’ species. Desirable species are native plants found in peat-forming systems. Undesirable species are not found in peat-forming plant communities, and include upland species, weeds, and exotic species. In 2015, the greatest abundance and diversity of desirable species was found in Zone 2.

Four years after the identification of the zones (2019), we asked: 1) Do the zones persist? 2) Has the vegetation of the zones changed? 3) Have the dominant species changed? 4) Has diversity changed? 5) Have species occurrences changed?

Methods: Using a grid of 86 plots centered at 40 m intervals across SHW, we conducted a vegetation survey. At each grid point, we identified all plants (vascular plants and bryophytes) within a circular 8 m² plot (Fig. 3.26). In addition, we measured water level position relative to the soil surface (a hole was dug to determine water table position if the water table was below the soil surface - up to 30 cm below). If water was available, a water sample from the top 2-3 cm was taken. Soil samples (0-10 cm depth) were collected from each grid point. Water and soil chemistry results are reported in sections 3.1.2-3.1.4.

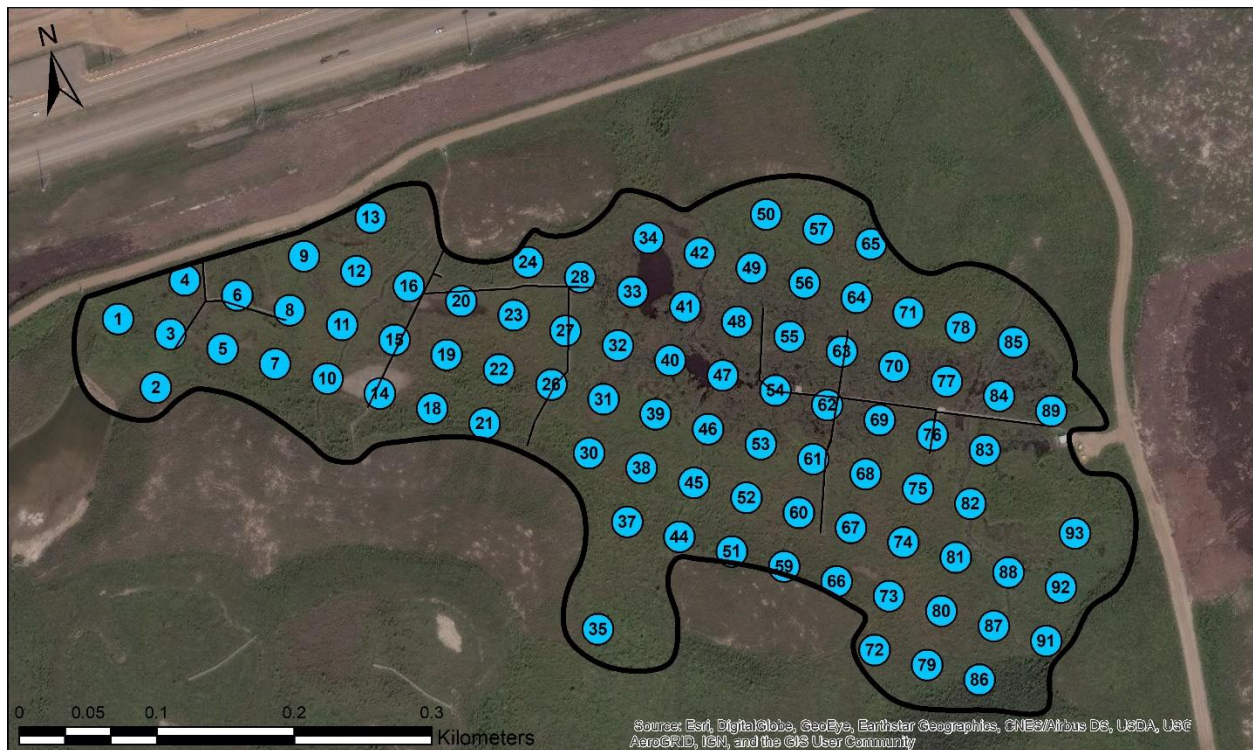


Figure 3.26 Map of Sandhill Wetland with vegetation plot locations

Data analysis - Plant community data were analyzed using non-metric dimensional scaling (NMDS) based on Bray-Curtis similarity using raw abundance data. To test for differences in year and zone a 2-way and pair-wise permutational multivariate analysis of variance (PERMANOVA) was used. Centroids of vegetation zones and overlay trajectory function were used to show differences between years in ordination space (Primer 7; Clarke & Gorley 2006). Species richness was evaluated through three measures (Whittaker 1972): alpha diversity, beta diversity, and gamma diversity. Alpha diversity is the number of species recorded in individual plots. Gamma diversity is the total number of species in a group. Beta diversity is species turnover between plots (gamma/alpha). Two-way analysis of variance (ANOVA) was used to test for effect of year and zone on total plant cover, abundance of dominant species, alpha diversity, and species occurrences (JMP Pro 14). When data were not normal and transformation did not yield a normal distribution, raw data were analyzed. ArcGIS was used to map plots in zones, plot level species abundances, species diversity change, water chemistry, and water level.

Results: Species assemblage groups (Fig. 3.27) differed ($p=0.001$), but there were no differences between years ($p=0.291$) for overall SHW vegetation. Pair-wise comparisons found all three species assemblages (1, 2, and 3) to be different from one another ($p<0.05$). Thus, those identified by Vitt et al. (2016) persist today (Fig. 3.28). Spatial distributions of the species assemblages are shown in Fig. 3.28, and these spatial areas are referred to as zones.

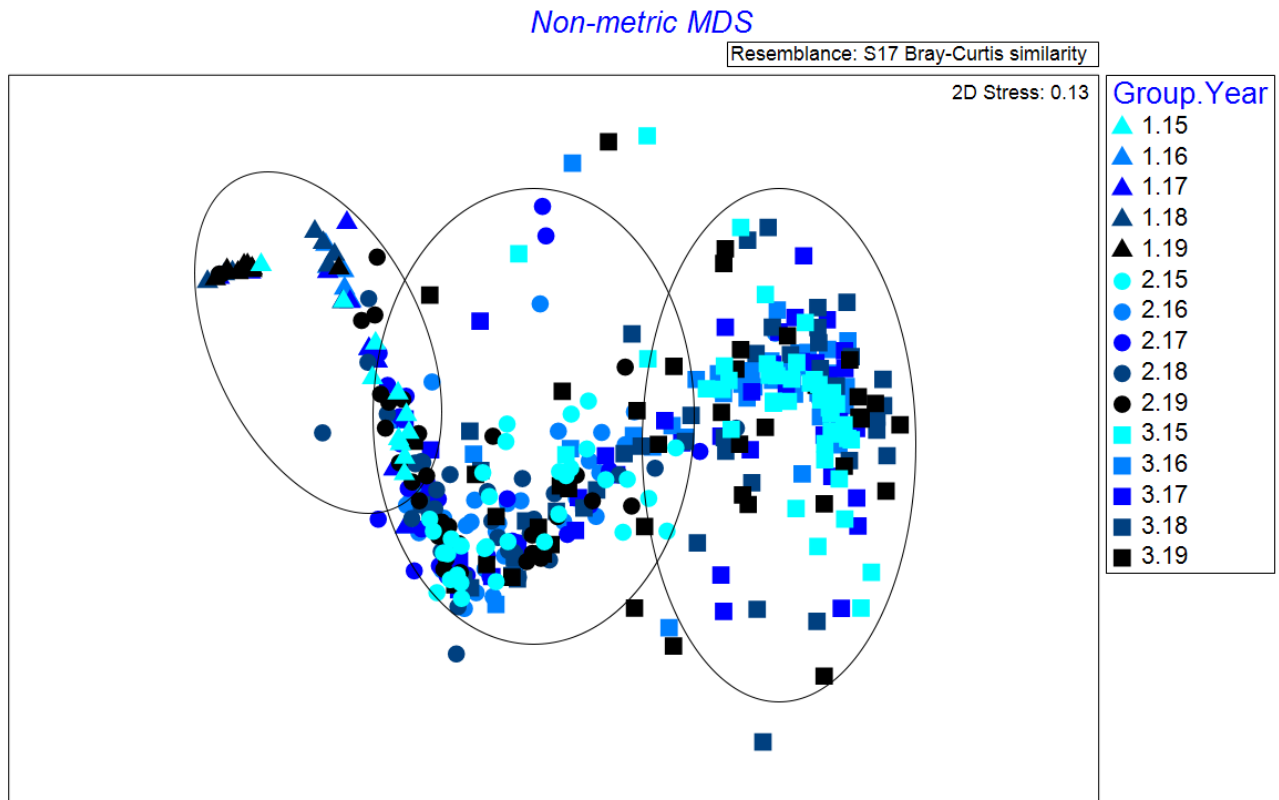


Figure 3.27 NMDS ordination of Sandhill Wetland vegetation plots from years 2015-2019. Species assemblages are differentiated by shape, and year by color

Typha latifolia dominates zone 1 (Figs. 3.29 and 3.30), but it is also found in zone 2 in lower quantities, and sporadically in zone 3. *Carex aquatilis* is the dominant species in zone 2 (Figs. 3.31 and 2.32); it is found in lower quantities in zones 1 and 3. *Calamagrostis canadensis* is dominant in zone 3, and found in lower abundances in zone 2, and is absent in zone 1 (Figs. 3.33 and 3.34).

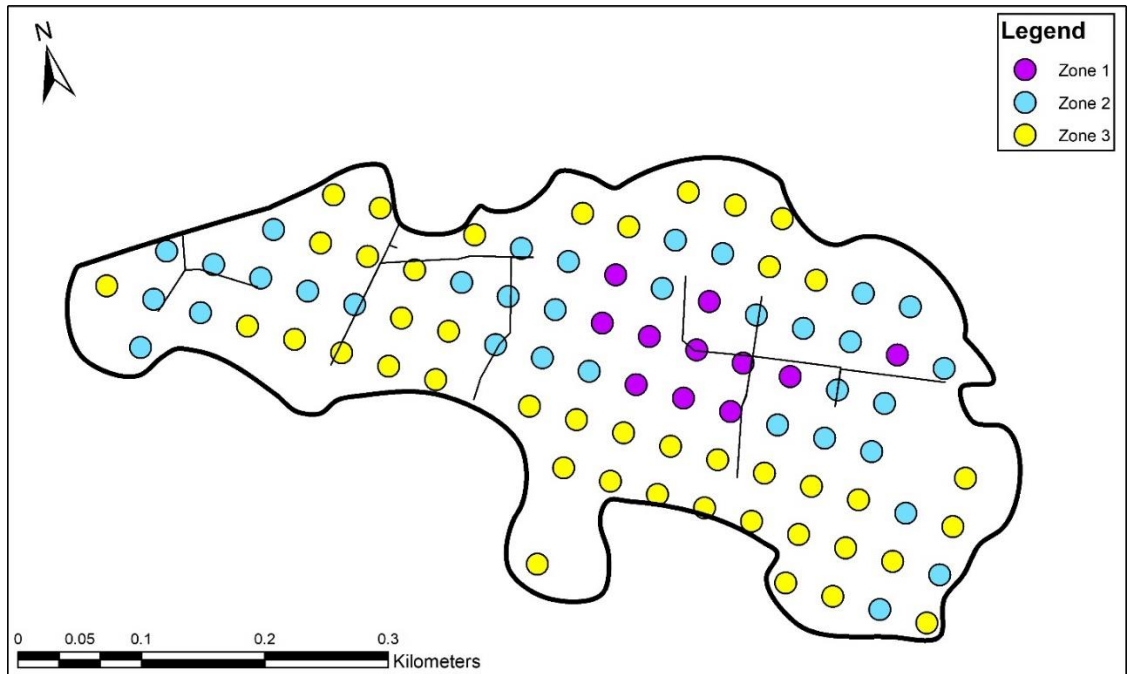


Figure 3.28 Map showing plots in each species assemblage zone in 2015; zones differentiated by color

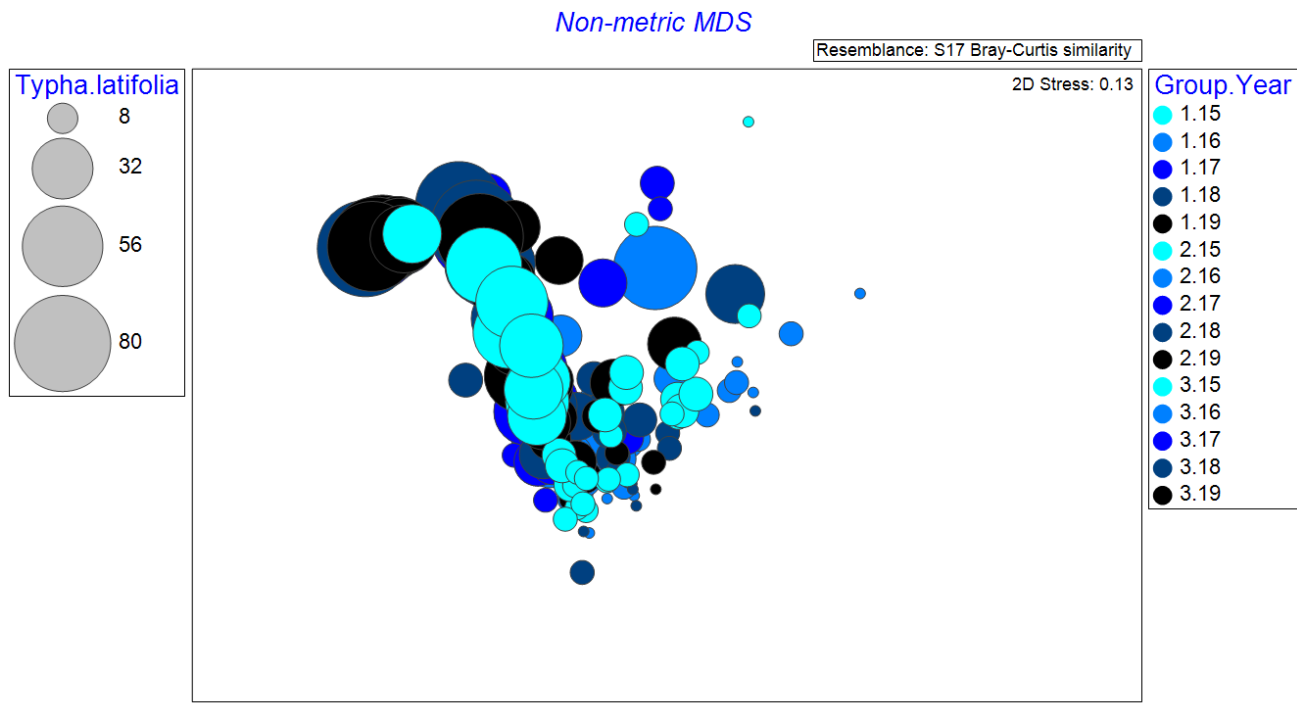


Figure 3.29 NMDS ordination of plots with *Typha latifolia* abundance overlain. Size of the circles represents the abundance at each plot. Years are indicated by color

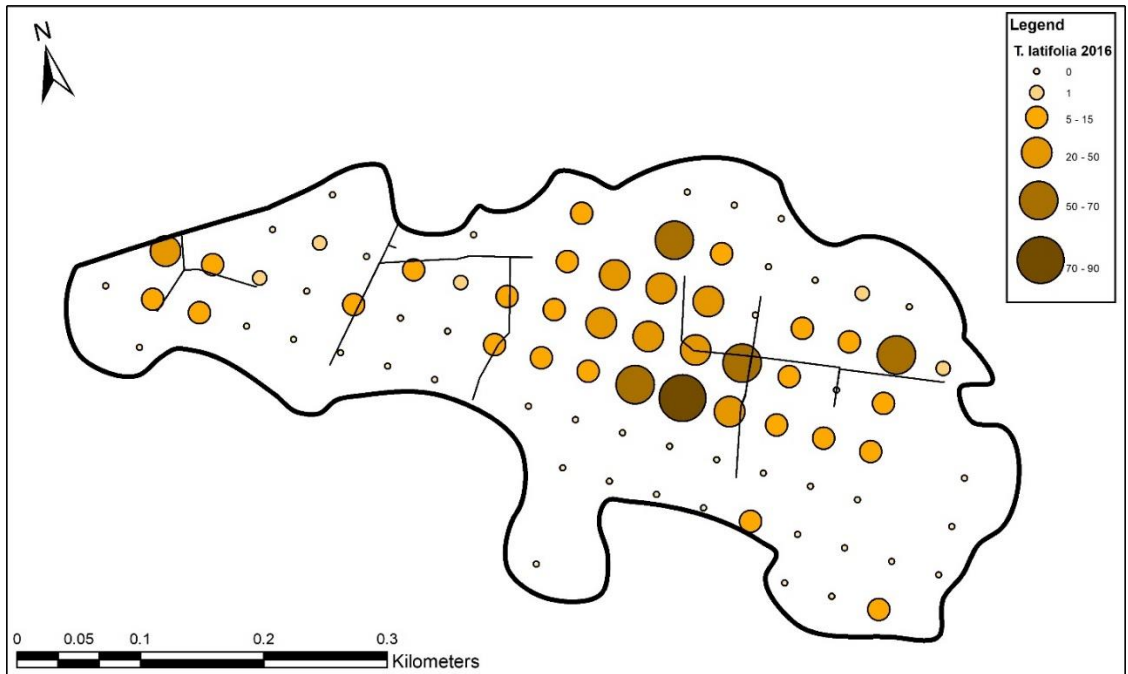


Figure 3.30 Map of *Typha latifolia* abundance across SHW

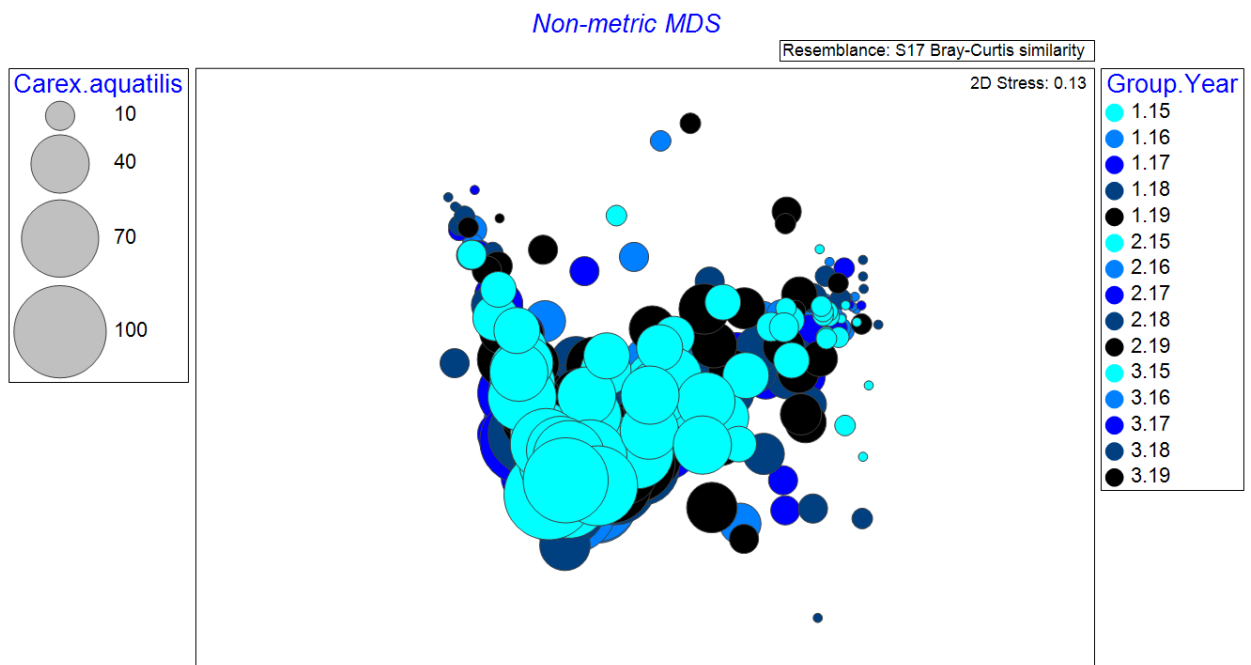


Figure 3.31 NMDS ordination of plots with *Carex aquatilis* abundance overlain. Size of the circles represents the abundance at each plot. Years are indicated by color

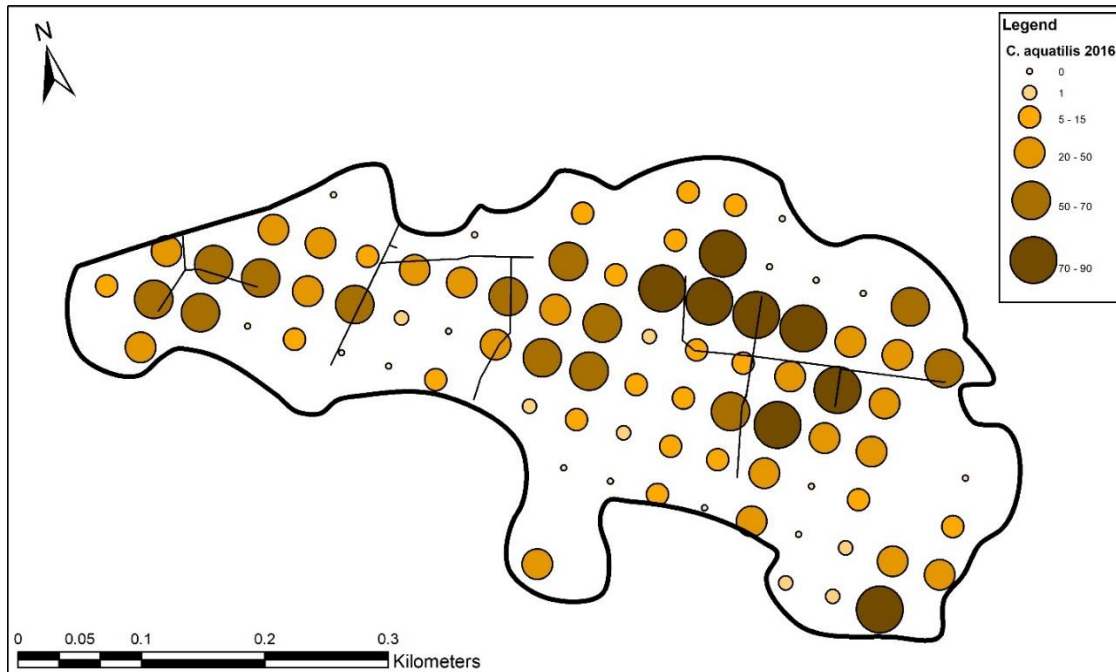


Figure 3.32 Map of *Carex aquatilis* abundance across SHW

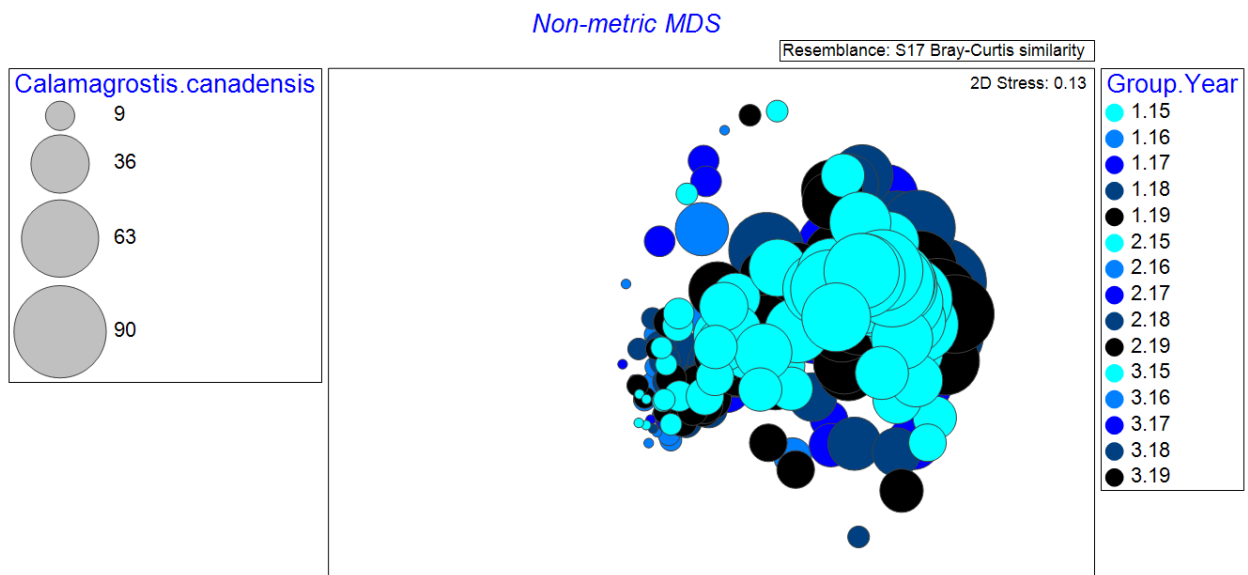


Figure 3.33 NMDS ordination of *Calamagrostis canadensis* abundance overlain. Size of the circles represents the abundance at each plot. Years are indicated by color

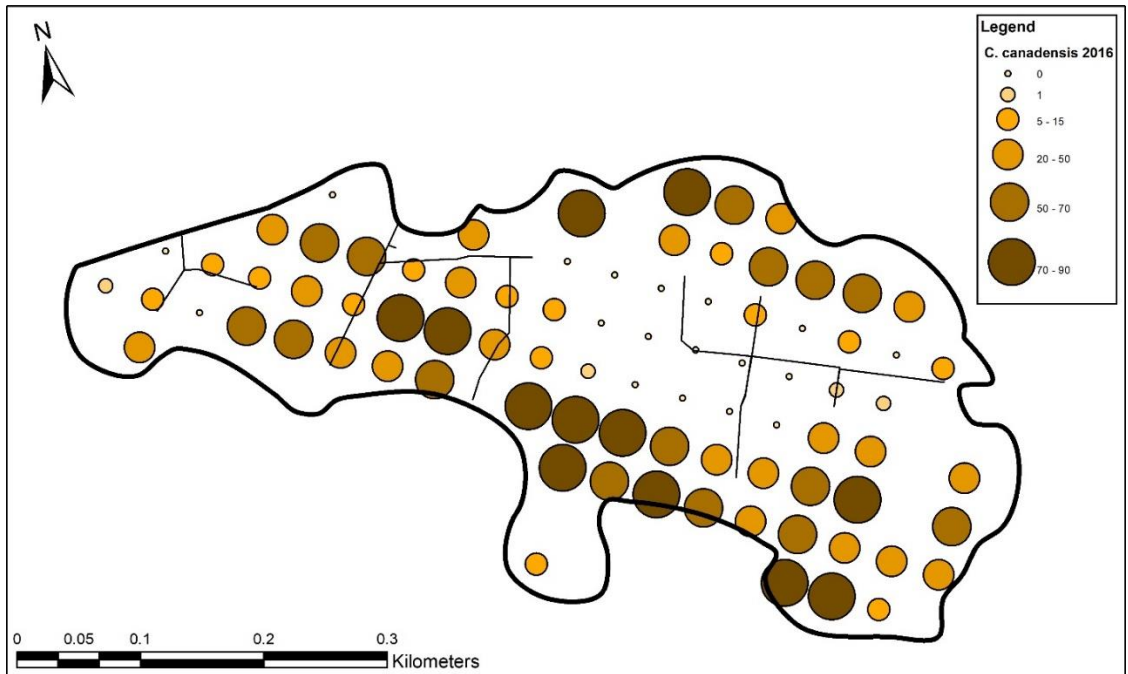


Figure 3.34 Map of *Calamagrostis* abundance across SHW

Non-metric MDS

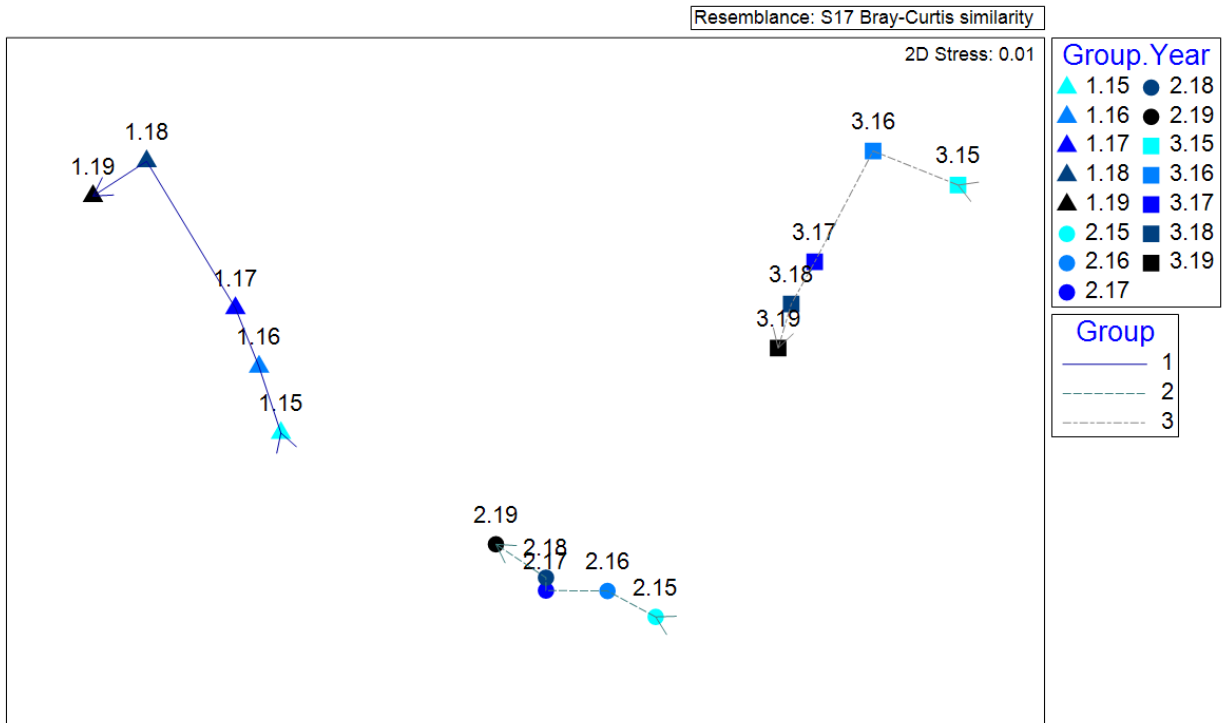


Figure 3.35 NMDS ordination of species assemblage centroids. Groups differentiated by shape, year by color. Arrows indicate shift of the group centroid through time: 2015-2019

While differences between years were not detected by PERMANOVA, using group centroids and year trajectories, it is clear that directional shifts occurred within the three species assemblages (Fig. 3.35). The

dominant species remained the same; however, large shifts occurred in Group 1 following the 2017 high water table. In Groups 2 and 3, shifts occurred between 2016 and 2017 in response to the elevated water table.

In nearly all parts of the wetland, the water table increased between 2016 and 2017 (Figs. 3.36 & 3.37). In 2017, the water table was so high that some plots in the central portion of the fen could not be accessed or measured (Fig. 3.37). In 2018 and 2019, the water table returned to near 2016 levels (Figs. 3.38 & 3.39); however, the 2017 shifts in the species assemblages mostly did not return to pre-2017 status (Fig. 3.36). These large shifts in all three of the species assemblages may indicate a regime shift after perturbation that may lead to an alternative stable state within Sandhill Wetland.

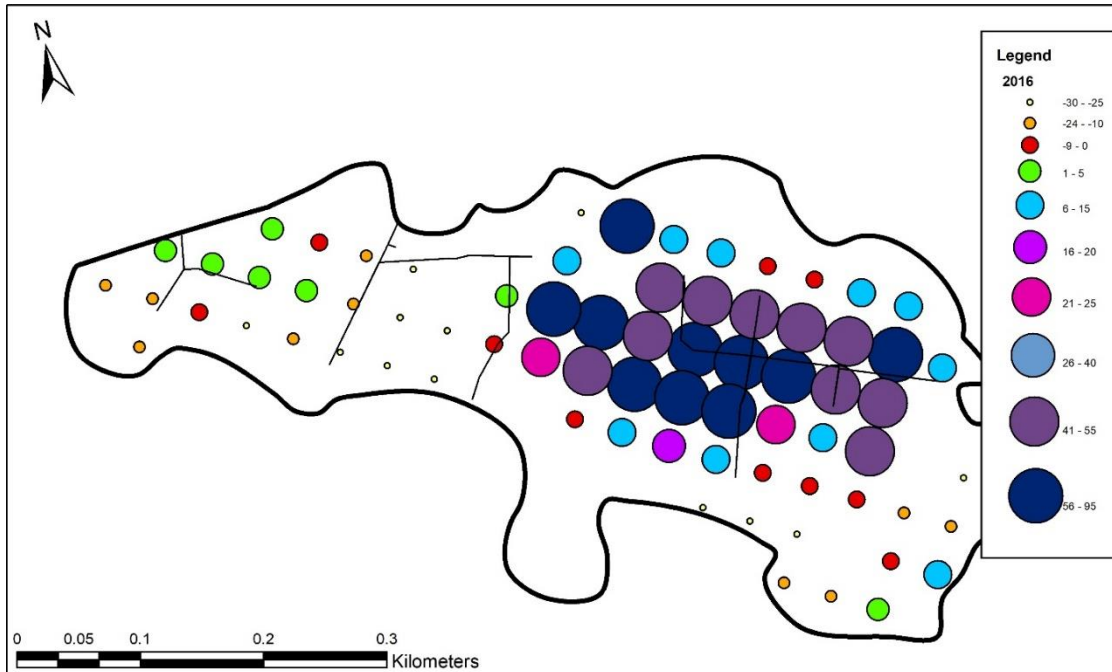


Figure 3.36 Map of 2016 SHW water levels

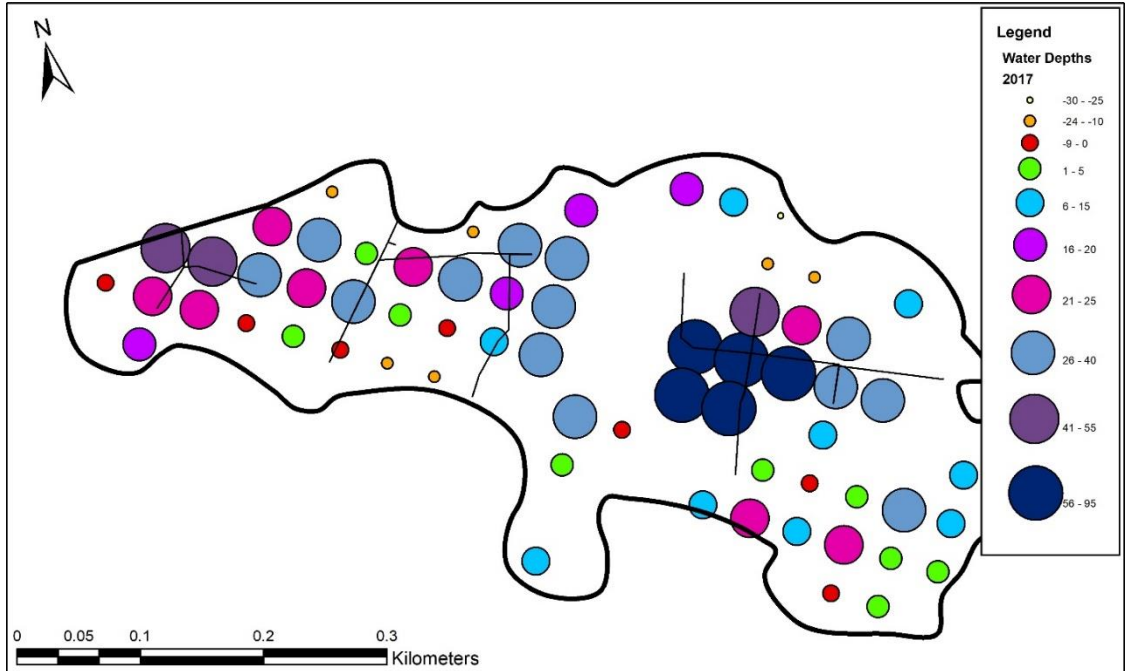


Figure 3.37 Map of 2017 SHW water levels

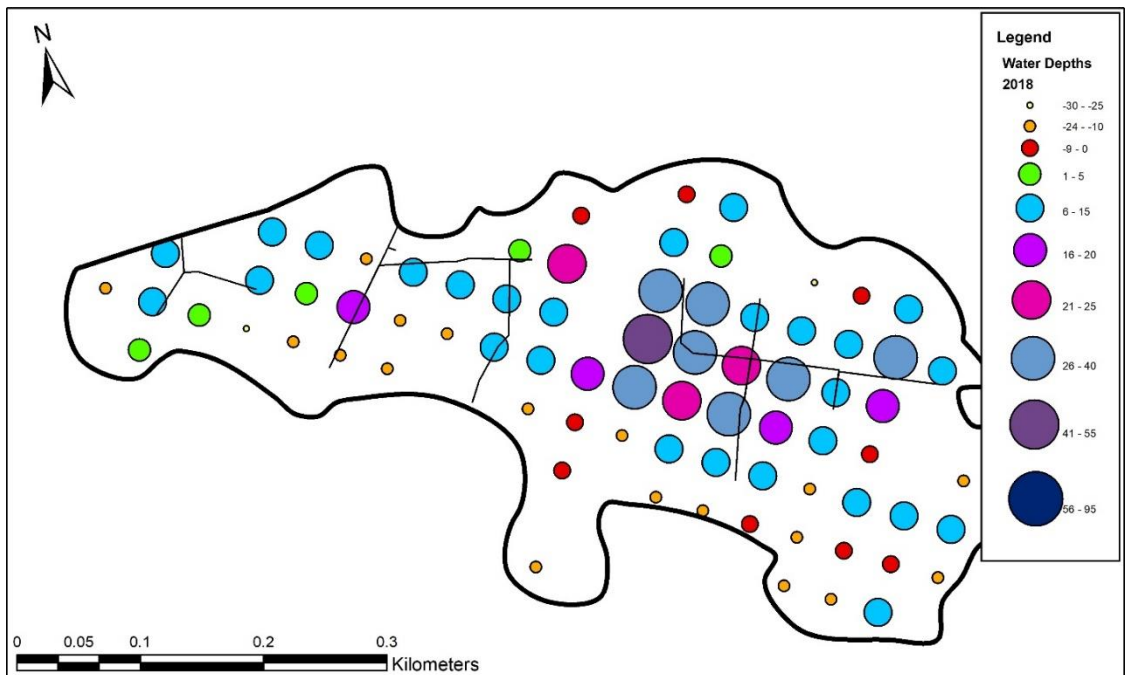


Figure 3.38 Map of 2018 SHW water levels

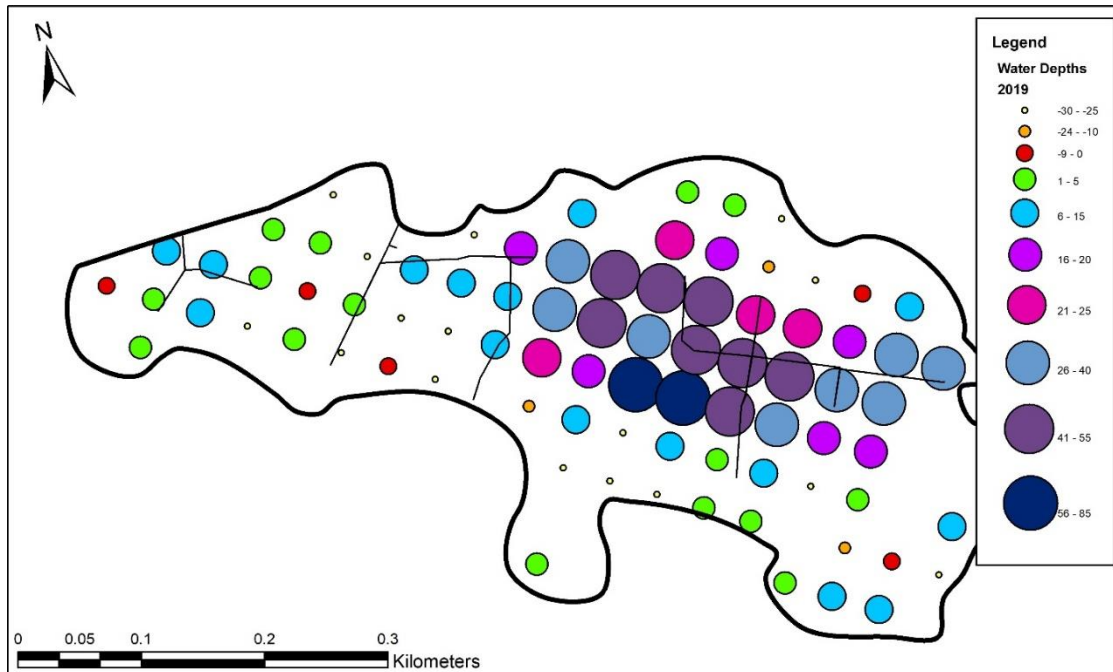


Figure 3.39 Map of 2019 SHW water levels

As a result of the 2017 water level increase, total plant cover decreased in zone 2 (from 100% to 70%) with some return of plant cover in 2018 (83%) and 2019 (86%). Overall plant cover increased in zone 3 in 2018 (from 103% in 2017 to 133% in 2018, Fig.3.40), associated with areas in this zone having wetter substrates, and in 2017 a decrease in *Calamagrostis canadensis* abundance and a slight increase in *Carex aquatilis*.

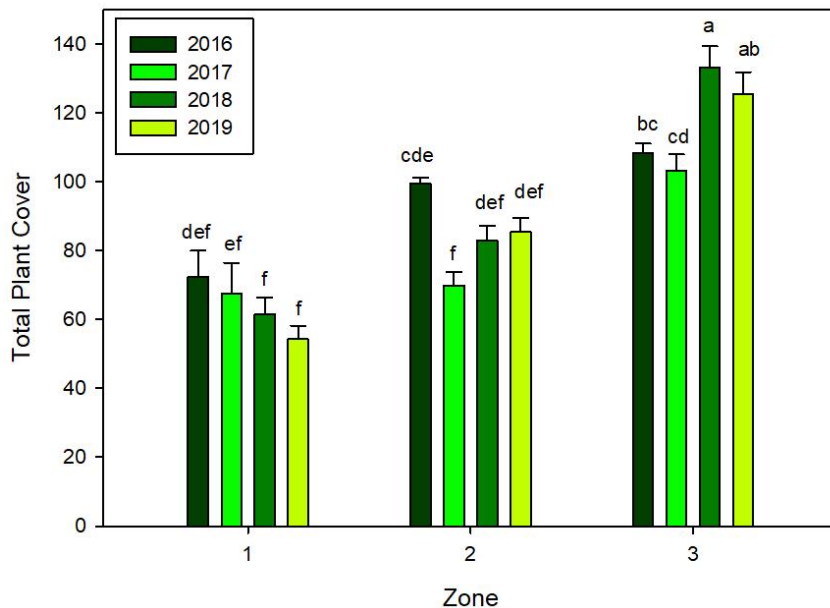


Figure 3.40 Total plant cover across the zones and years. Different letters indicate significant differences (from Tukey's HSD test $-p < 0.05$). A significant interaction between zone and year ($p < 0.0001$) was present (two-way ANOVA)

Calamagrostis canadensis abundance differed between years ($p = 0.026$) and zone ($p < 0.0001$, two-way ANOVA), with no interaction, with differences in years within zone 3 ($p = 0.0003$), but not zone 2 ($p = 0.054$,

one-way ANOVA). Especially noteworthy is the decrease in *Calamagrostis canadensis* abundance in zone 3 following the elevated water table of 2017 (Fig. 3.41).

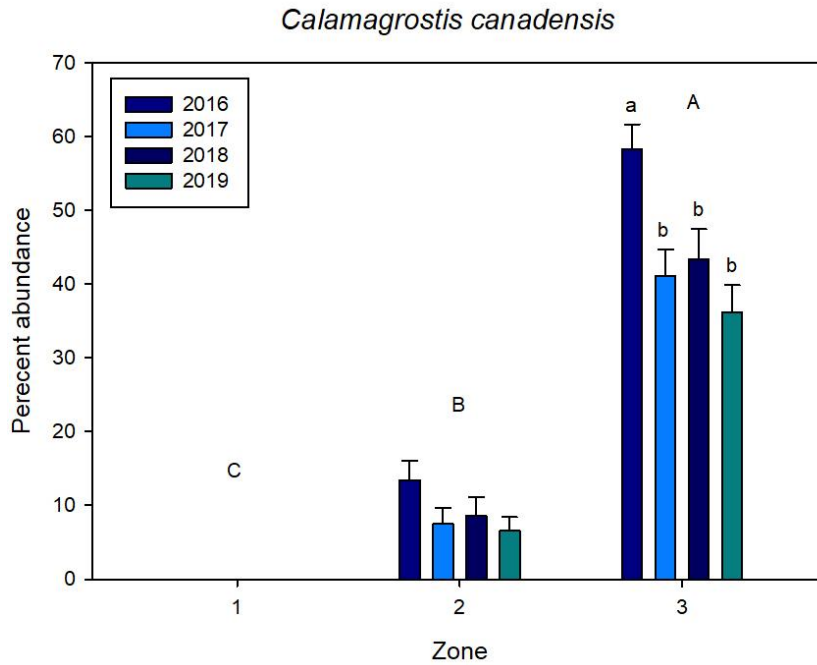


Figure 3.41 *Calamagrostis canadensis* abundance across zones and years. Different capital letters indicate significant differences in zones based on a two-way ANOVA. Different lower-case letters indicate differences in years based on a Tukey’s HSD test ($p < 0.05$)

Carex aquatilis abundance differed between zone and year (two-way ANOVA interaction $p = 0.0001$). Although not significant, there were some noteworthy trends - Within zone 1, *C. aquatilis* decreased substantially in 2018. There were slightly lower abundances in zone 2 in 2017-2019 compared with 2016. In zone 3; however, there was an upward trend in *C. aquatilis* abundance (Fig. 3.42).

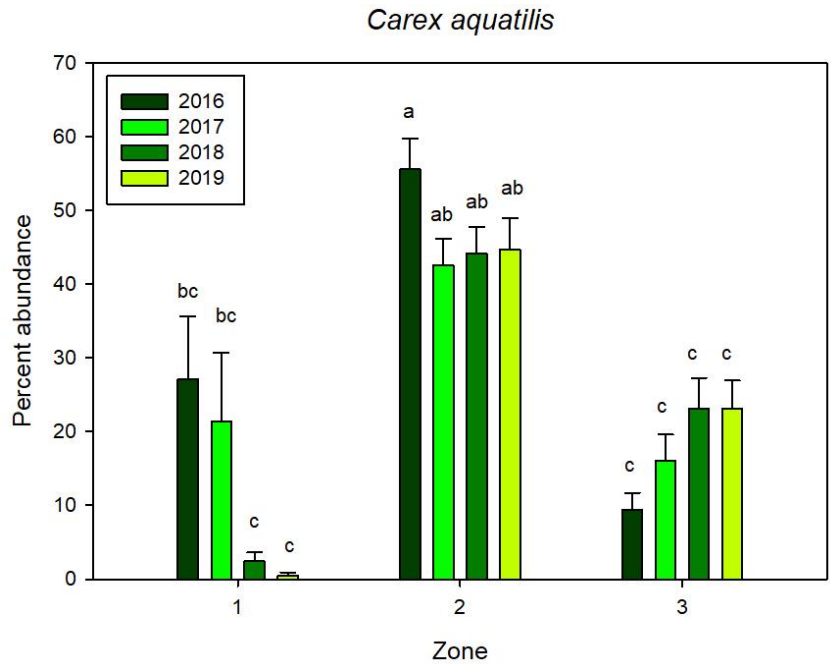


Figure 3.42 *Carex aquatilis* abundance across SHW zones and years. Letters indicate result of Tukey's HSD test ($p < 0.05$)

Typha latifolia differed by zone and year (two-way ANOVA interaction $p = 0.020$). In zone 1, *T. latifolia* increased between 2016 and 2018, with a slight decrease in 2019. In zone 2, abundance of *T. latifolia* remained the same through the years (with slight increases in 2018 and 2019). In zone 3, *T. latifolia* abundance remained consistently low for all four years (Fig. 3.43).

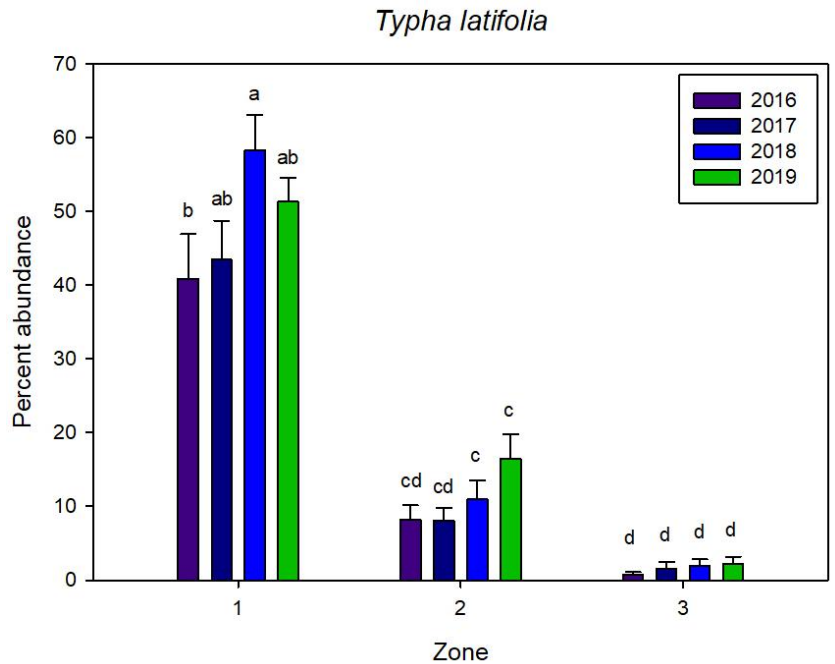


Figure 3.43. *Typha latifolia* abundance across SHW zones and years. Letters indicate result of Tukey's HSD test ($p < 0.05$)

Plant occurrences (number of times a species was recorded in the gridded plots): Undesirable species occurrences were much higher in zone 3 than in zones 1 and 2. They were stable in zone 1, ranging from 10 in 2018 to 16 in 2016. In zone 2, there was a notable decrease between 2016 (136) and 2017 (58), with little resurgence in 2018 (77) and 2019 (65). In zone 3, undesirable species occurrences decreased between 2016 (353) and 2017 (263). Then in 2018, undesirable species increased (316), but a decrease in 2019 (263) also was observed (Fig. 3.44). Undesirable species declined 33% between 2016 and 2019.

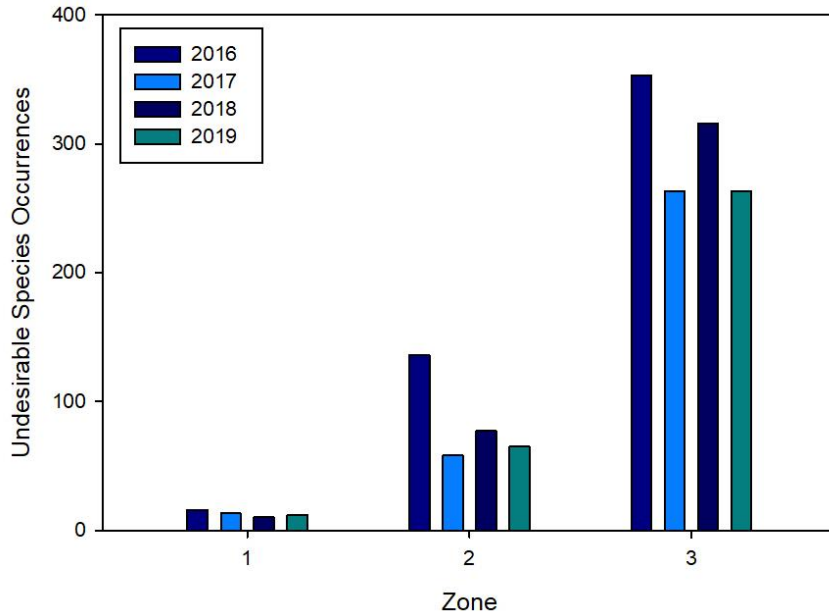


Figure 3.44 Undesirable species occurrences by zone and year

Desirable species occurrences were higher in zones 2 and 3 than in zone 1. They declined in zone 1 each year: 2016 (30) 2017 (24) and 2018 (11) and 2019 (8). Zone 2 experienced a large decline (54%) in desirable species occurrences between 2016 (163) and 2017 (75). While a slight increase was observed in 2018 (101), 2019 (84) showed another decrease in desirable species occurrences. In zone 3, desirable species occurrences decreased between 2016 (127) and 2017 (84). There was an increase in 2018 (112), and a slight decrease in 2019 (101). Across all three zones, desirable species occurrences decreased after the 2017 flooding event and have not returned to pre-2017 values (Fig. 3.45). Overall, across the Wetland, desirable species have decreased 40% between 2016 and 2019, with the ratio of undesirable to desirable increasing from 1.58 in 2016 to 1.75 in 2019.

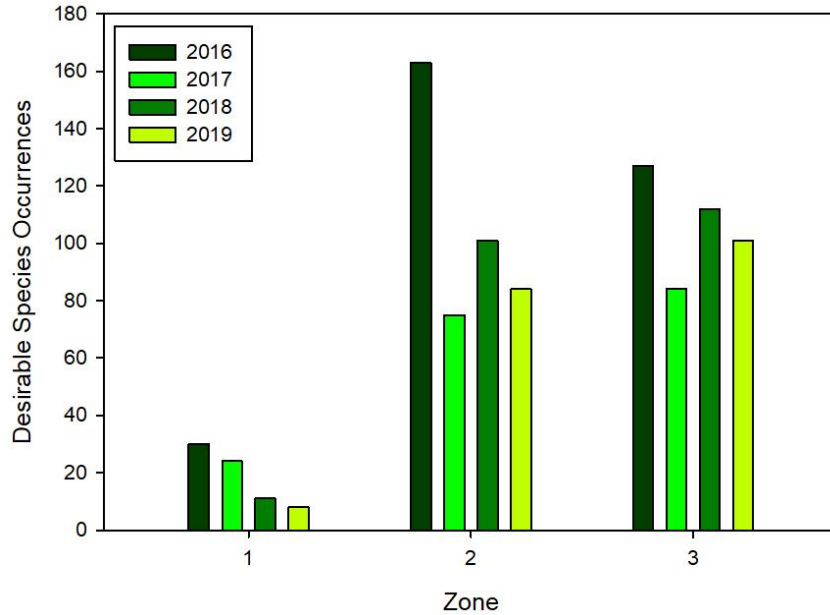


Figure 3.45 Desirable species occurrences by zone and year

Bryophytes do not occur in zone 1 due to the water level well over the soil surface. In zone 2, bryophyte species occurrences declined slightly between 2017 (14) and 2018 (10), with a subsequent slight increase in 2019 (15). In zone 3, bryophyte species occurrences decreased each year: 2016 (181), 2017 (164), 2018 (114) and 2019 (96) (Fig. 3.46), with an overall 4-year decrease of 47%

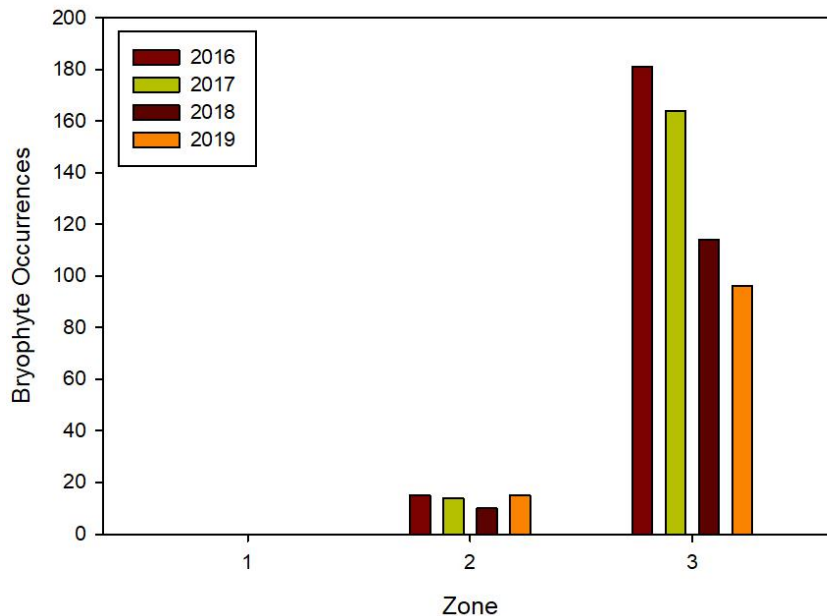


Figure 3.46 Bryophyte occurrences by zone and year

Diversity across the SHW Zones: Between 2016 and 2019, we recorded a total of 75 plants at the wetland, including 34 undesirable vascular plants, 26 desirable vascular plants, and 15 bryophytes (Table 3.18). Seven percent of the species occur in zone 1, 59% in zone 2, and 87% in zone 3.

Undesirable alpha diversity differed across years and zones (Figs. 3.47-3.48), with no interaction between the zone and year. In 2017 and 2019, undesirable alpha diversity was lower than 2016; 2018 diversity was

in between and did not differ from any other year. Overall, in 2019, SHW undesirable alpha diversity is 33% lower compared with 2016 (Fig. 3.48, Table 3.15), with richness in zone 2 having the greatest decline (ca. 50%). Overall, all zones lost undesirable species over the 4-year time period.

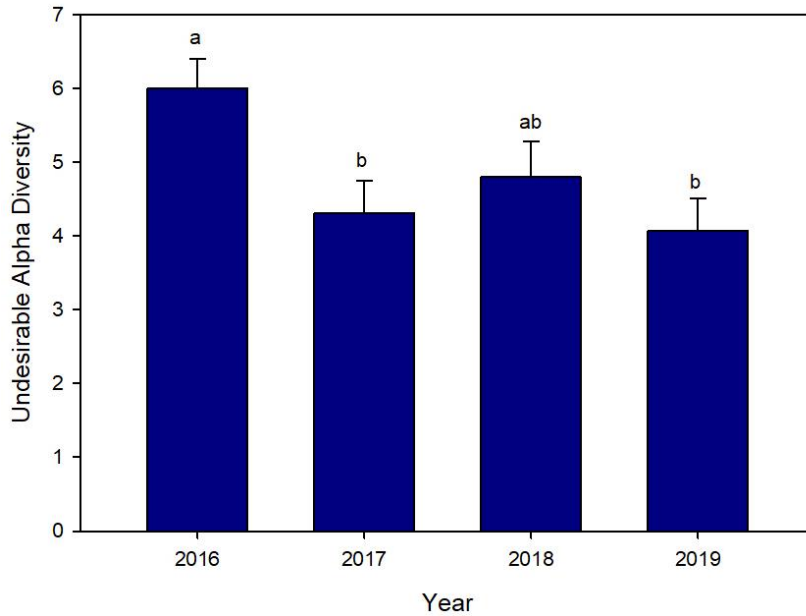


Figure 3.47 Undesirable alpha diversity by year; letters indicate significant Tukey’s HSD result ($p<0.05$)

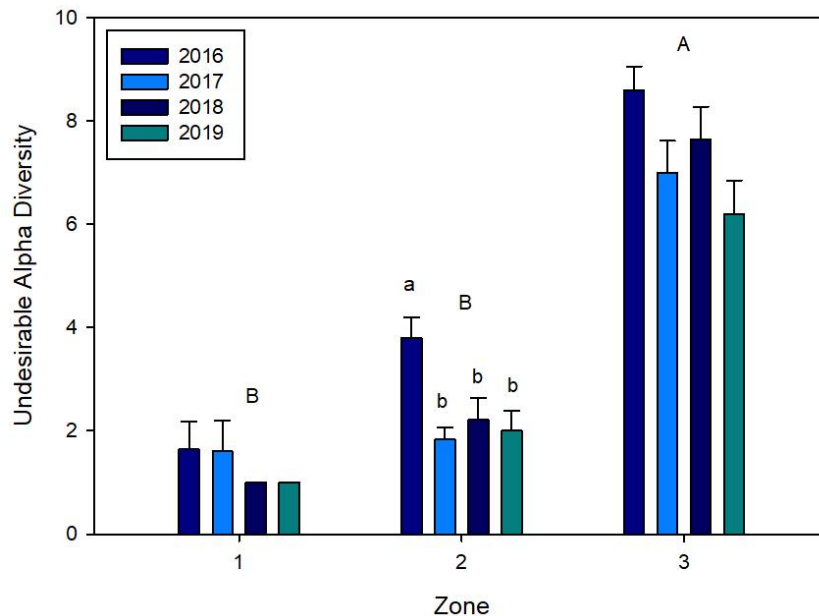


Figure 3.48 Undesirable alpha diversity abundance across zones and years. Capital letters are result of a two-way ANOVA. Lower case letters are result of a one-way ANOVA’s. Different letters indicate a significant Tukey’s HSD result ($p<0.05$)

Between 2016 and 2019, 76% of the plots had a decrease in undesirable species. Spatially, undesirable species diversity (alpha) was a decrease in eight plots mostly along the eastern, southern boundary of SHW. Smaller decreases occurred in the central fen, the southeastern corner and a few plots in the west of SHW. Increases in undesirable alpha diversity occurred in eight plots in the western portion of the wetland. Two

northern plots also had a decrease in undesirable species along with ten scattered in the southeastern portion (Fig 3.49).



Figure 3.49 Map of change in undesirable species diversity. Green circles indicate decrease; purple represent increase. Larger circles indicate larger changes

Overall desirable alpha diversity decreased across the wetland over the 4-year time period. In zone 1, desirable alpha diversity decreased between 2016 and 2019 (but not significantly), remaining low in 2019. In zone 2, desirable alpha diversity decreased between 2016 and 2017 (by ca. 50%) and remained low in 2017, 2018, and 2019. In zone 3, there was a trend of decreasing desirable alpha diversity (Fig. 3.50, Table 3.16). The loss of alpha diversity in zone 2, the zone previously resembling rich fen flora, is notable.

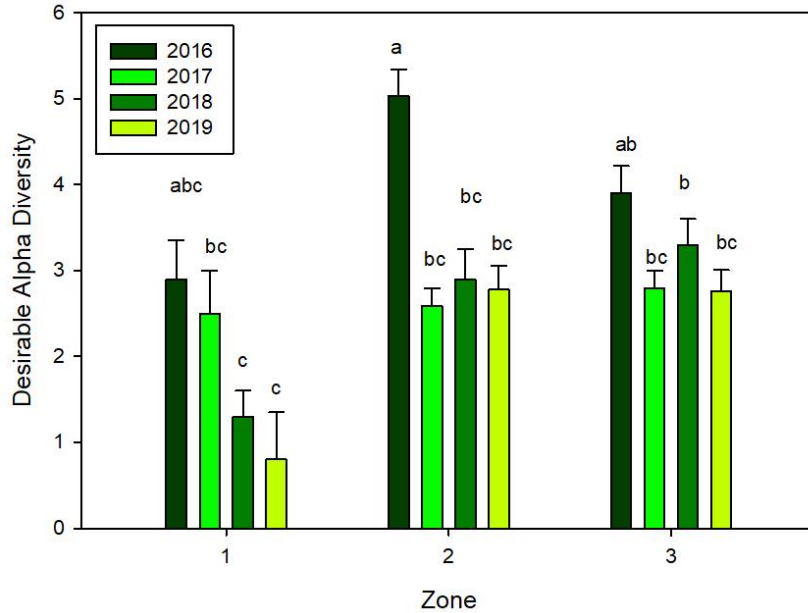


Figure 3.50 Desirable species alpha diversity by zone and year; letters indicate significant Tukey's HSD result ($p < 0.05$)

Spatially, 81% of the plots showed a decrease in desirable species diversity, with increases in desirable alpha from 2016 to 2019 occurring sporadically in a few plots, mostly in the southern portion of the Wetland (Fig. 3.51).



Figure 3.51 Map of change in desirable species diversity. Green circles indicate decrease; purple represent increase. Larger circles indicate larger changes

Bryophytes do not occur in zone 1 due to the presence of standing water throughout the growing season. In Zone 2, there was a loss of bryophyte diversity (from 2.0 to less than 0.5 species per plot) between 2016 and 2017, remaining low through 2019. In Zone 3, there was a (nearly 50%) decrease in bryophyte alpha diversity between 2017 and 2018 (Fig. 3.52, Table 3.17).

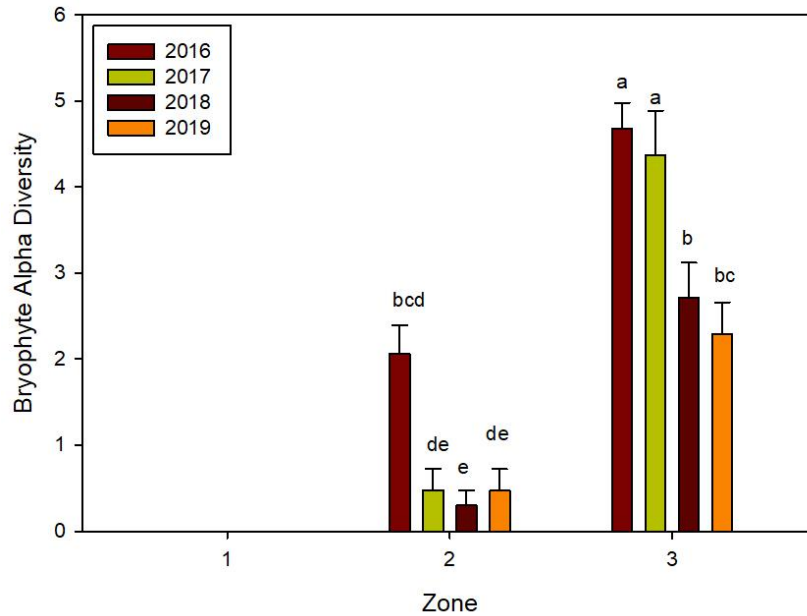


Figure 3.52 Bryophyte species alpha diversity by zone and year; letters indicate significant Tukey's HSD result ($p < 0.05$)

Spatially, bryophyte diversity decreased in 84% of the plots. Increases (2016 to 2019) were observed in four plots on the west end of the wetland, a line of plots through the southern center of the fen, and three plots on the margins of the southern end (Fig. 3.53).

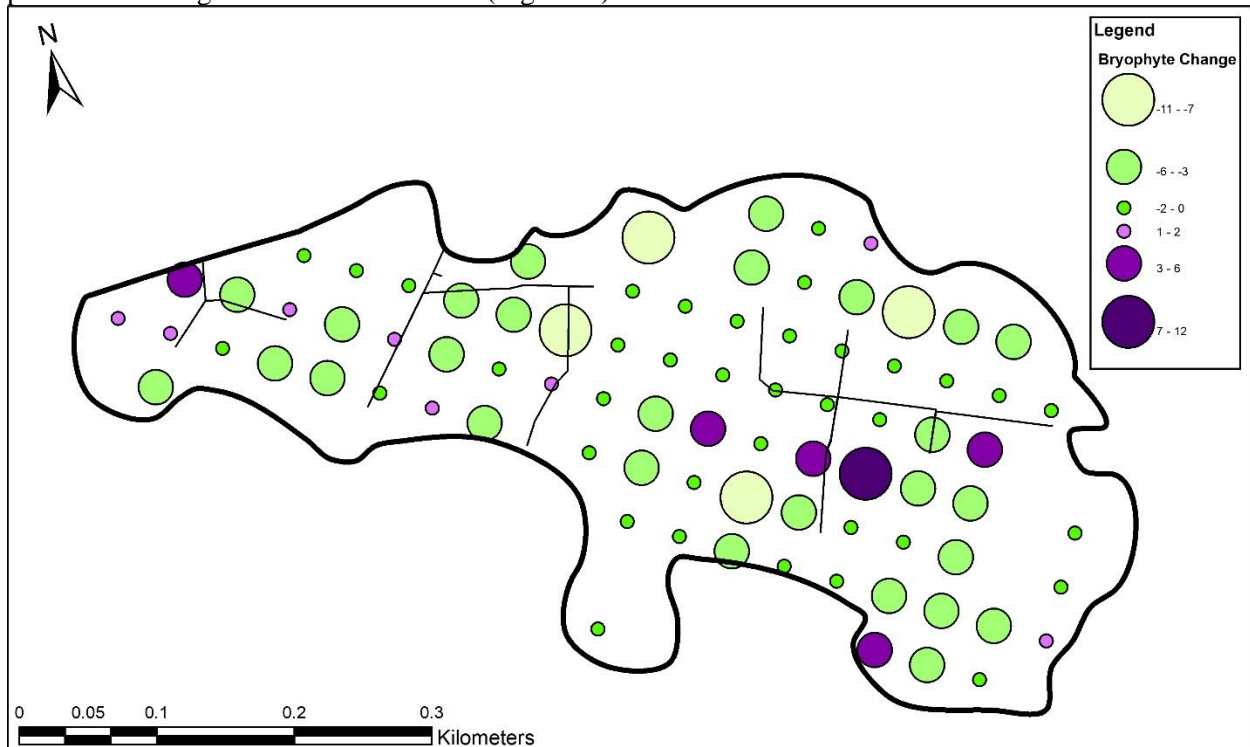


Figure 3.53 Map of change in bryophyte species diversity. Green circles indicate decrease; purple represent increase. Larger circles indicate larger changes

Similar to alpha diversity, undesirable gamma diversity decreased from 2016 to 2019. Thus, across all of zone 1, 3 species were lost. In zone 2, 15 undesirable species were lost between 2016 and 2017 with a slight increase in 2018. In zone 3, 15 undesirable species were lost (Fig. 3.54, Table 3.15).

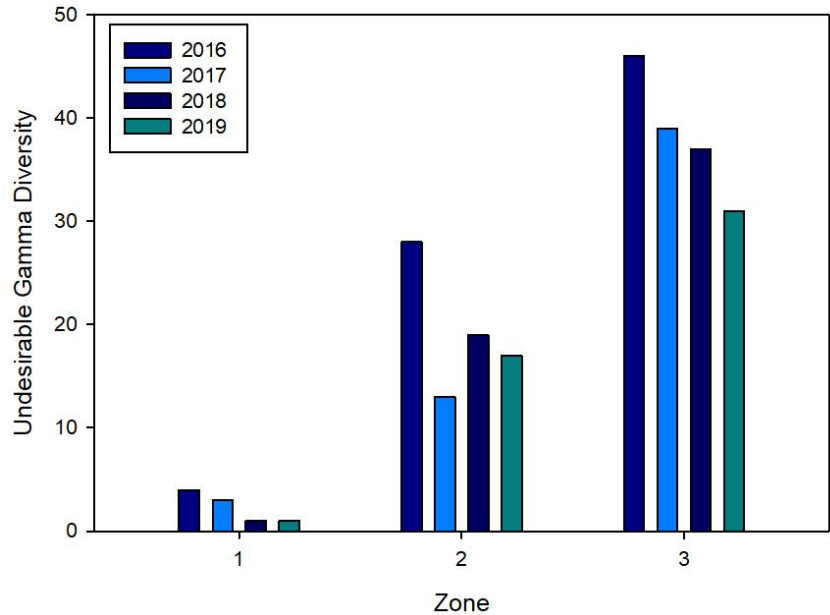


Figure 3.54 Gamma diversity of undesirable species by zone and year

Desirable gamma diversity decreased in zone 1 from 2017 to 2018 (2 species lost), remaining steady in 2019. Across zone 2, 16 desirable species were lost between 2016 to 2017, with only a slight increase in 2018 and 2019. In zone 3, gamma diversity decreased between 2016 to 2017, a loss of 6 species; in 2018 an increase of 4 species was observed followed by another decrease in 2019 of 6 species. Overall, the loss of desirable species in zone 2 after the 2017 water table change is of concern (Fig. 3.55, Table 3.16).

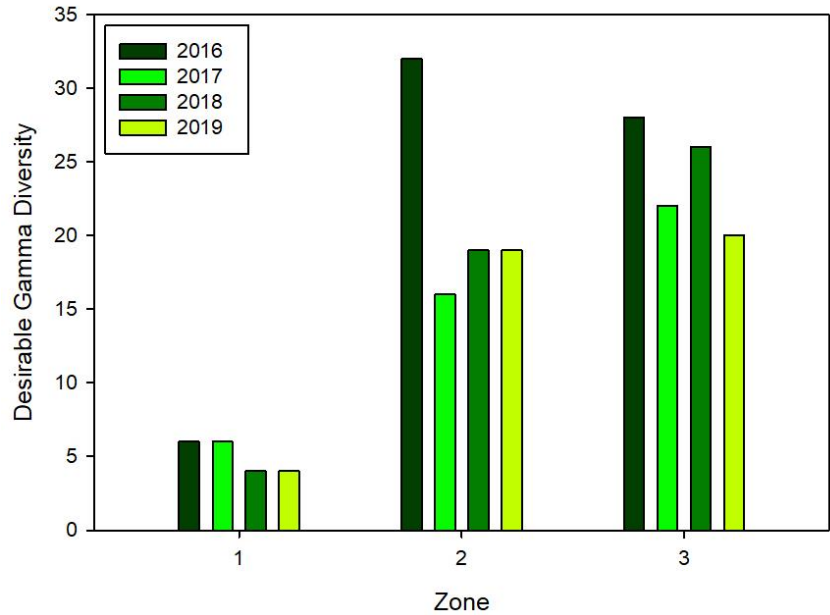


Figure 3.55 Gamma diversity of desirable species by zone and year

Bryophyte gamma diversity declined in zone 2 from 2016 to 2017 (7 species lost). In zone 3, bryophytes increased from 2017 to 2018 (3 species gained) but then decreased in 2018 (6 less species) and 2019 (3 less species). Across zones 2 and 3, bryophyte gamma decreased substantially from 2016 to 2019 (Fig. 3.56, Table 3.19). A list of species found at SHW is found in Table 3.18. A list of species lost between years is found in Table 3.19. Some species were lost and returned. Overall, 34 species were lost entirely between 2016 and 2019.

Beta diversity (turnover between plots) was highest in zone two for undesirable species (7.3-9.5, Table 3.15), while desirable species beta diversity was highest in zone 3 (7.2-7.9, Table 3.16). Bryophyte beta diversity was highest in zone 2, there increasing from 7.1 in 2016 to between 16.0 and 23.3 in the subsequent years (Table 3.17). These very high betas reflect the strong differences in species presence between plots.

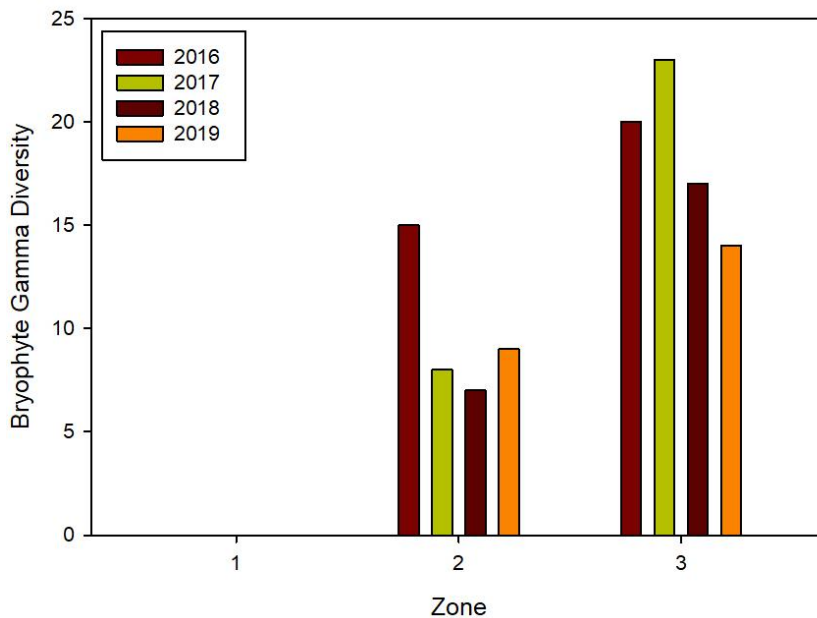


Figure 3.56 Gamma diversity of bryophyte species by zone and year

We ordinated data from our five years of vegetation surveys of the 86 gridded plots at Sandhill Wetland together with vegetation data collected from the 12 reference sites (Hartsock 2020). Reference sites ordinate as peatland site-types (poor fens to the bottom right, rich fens to the right, saline wetlands to the top, and marshes to bottom left). All three Sandhill Wetland zones from separate clusters, these positioned left central on the ordination. All three SHW zones have different trajectories over the five year time period (i.e., zone 1 moving to the left, zone 2 to the top, and zone 3 to the bottom of the ordination) suggesting different environmental variables and thresholds are influencing the species assemblages in the three zones. None of the Sandhill Wetland zones overlaps with the reference sites, indicating that the species assemblages found at Sandhill do not closely resemble reference site plant communities and at the present time can be considered to possess sets of unique characteristics. Zone 2 comes nearest to the brackish marsh (BMAR) and the fresh marsh (FMAR), but its trajectory is moving away from these communities. Zone 3 is moving toward the marsh communities, and zone 1 is moving away from all reference site types (Fig. 3.57).

Populus balsamifera is aggressively establishing around the boundaries of the wetland mostly in zone 3 adding to the undesirable set of species occurring in the Wetland (Fig. 3.58).

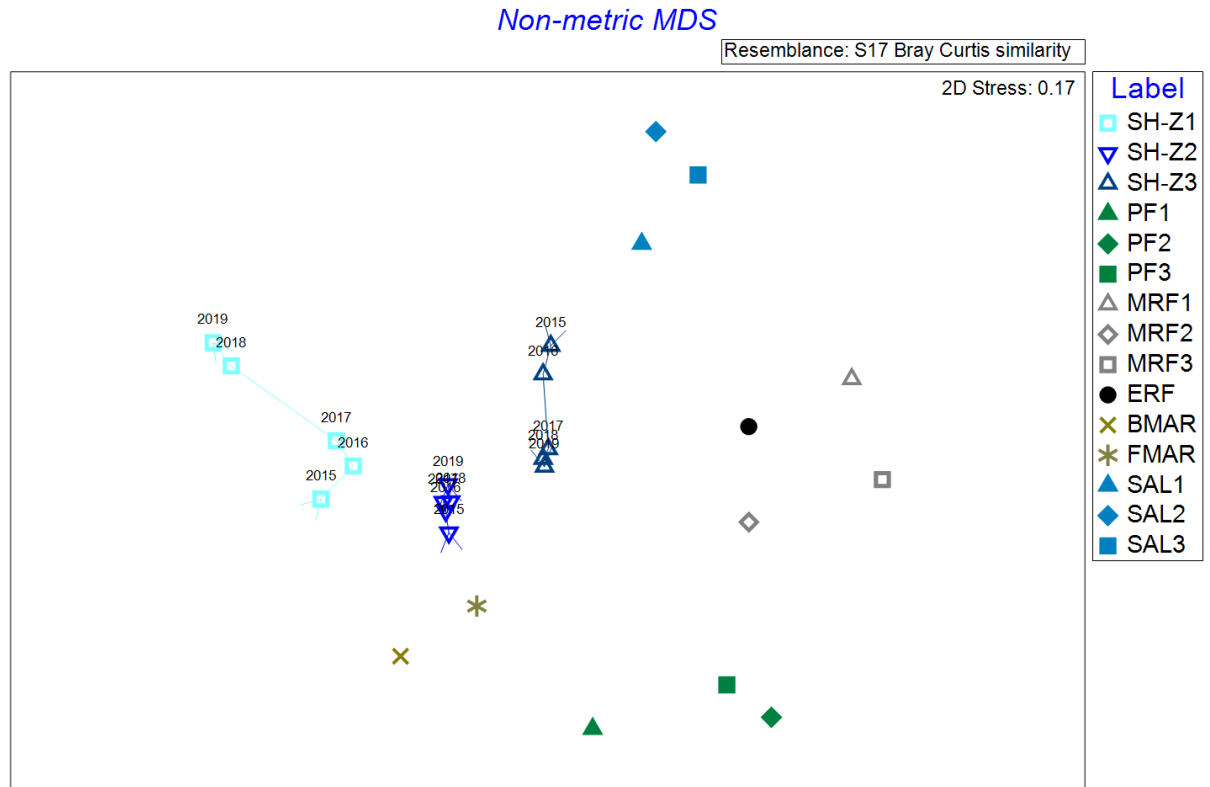


Figure 3.57 Ordination of centroids for benchmark sites and SHW zones by year. Arrows indicate shift in zone centroids through time. Labels are SHW Zones 1-3 (SH-Z1-3), poor fens 1-3 (PF1-3), moderate-rich fens 1-3 (MRF 1-3), extreme-rich fen (ERF), brackish marsh (BMAR), fresh marsh (FMAR), and saline fens 1-3 (SAL 1-3). SHW species abundance data taken from the 86 gridded plots; species abundance data for reference sites taken from data in Hartsock (2020)

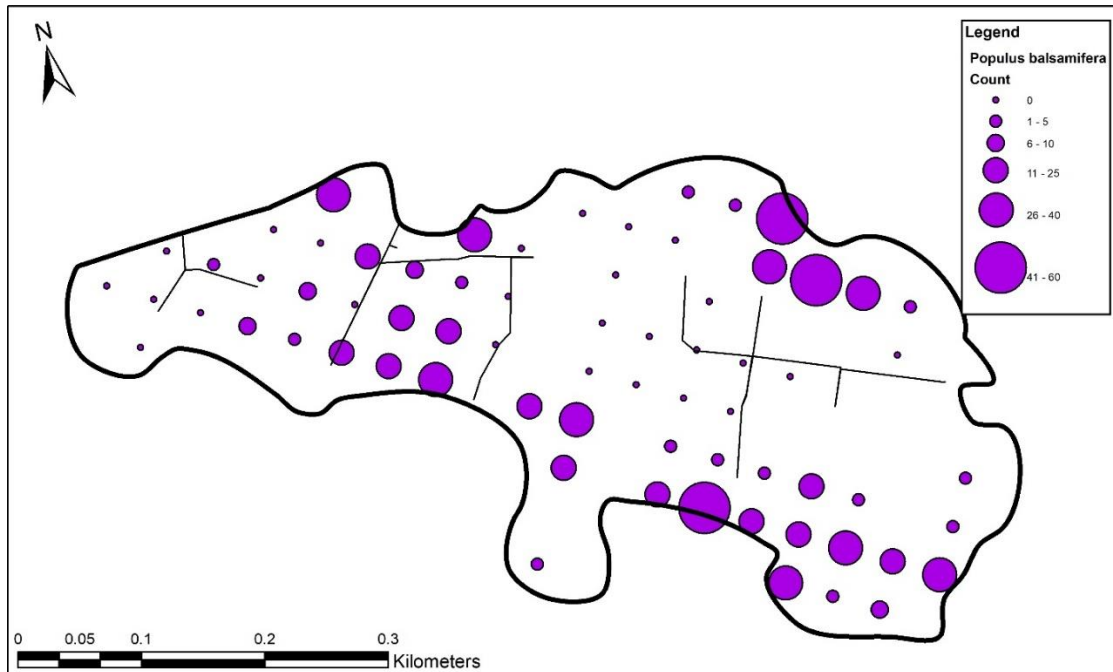


Figure 3.58 Map of *Populus balsamifera* individual counts at vegetation plot across SHW. Larger circles indicate larger counts

Table 3.15 Undesirable species alpha \pm standard error, beta diversity, and gamma diversity
Undesirable species

Year	Zone	Alpha	Beta	Gamma
2016	1	1.6 \pm 0.5	2.5	4
2016	2	3.8 \pm 0.4	7.4	28
2016	3	8.6 \pm 0.4	5.3	46
2017	1	1.6 \pm 0.6	1.9	3
2017	2	1.8 \pm 0.2	7.2	13
2017	3	7.0 \pm 0.6	5.6	39
2018	1	1.0 \pm 0.0	1.0	1
2018	2	2.0 \pm 0.4	9.5	19
2018	3	7.6 \pm 0.6	4.9	37
2019	1	1.0 \pm 0.0	1.0	1
2019	2	2.0 \pm 0.4	8.5	17
2019	3	6.2 \pm 0.7	5.0	31

Table 3.16 Desirable species alpha \pm standard error, beta diversity, and gamma diversity
Desirable Species

Year	Zone	Alpha	Beta	Gamma
2016	1	2.9 \pm 0.4	2.1	6
2016	2	5.0 \pm 0.3	6.4	32
2016	3	3.9 \pm 0.3	7.2	28

2017	1	2.5 ± 0.5	2.4	6
2017	2	2.6 ± 0.2	6.2	16
2017	3	2.8 ± 0.2	7.9	22
2018	1	1.3 ± 0.3	3.1	4
2018	2	2.9 ± 0.4	6.6	19
2018	3	3.3 ± 0.2	7.9	26
2019	1	0.8 ± 0.2	5.0	4
2019	2	2.7 ± 0.2	7.0	19
2019	3	2.7 ± 0.2	7.4	20

Table 3.17 Bryophyte species alpha ± standard error, beta diversity, and gamma diversity
Bryophyte species

Year	Zone	Alpha	Beta	Gamma
2016	1	0.0 ± 0.0	0.0	0
2016	2	2.1 ± 0.3	7.1	15
2016	3	4.7 ± 0.3	4.3	20
2017	1	0.0 ± 0.0	0.0	0
2017	2	0.5 ± 0.2	16.0	8
2017	3	4.4 ± 0.5	5.2	23
2018	1	0.0 ± 0.0	0.0	0
2018	2	0.3 ± 0.2	23.3	7
2018	3	2.7 ± 0.4	6.3	17
2019	1	0.0 ± 0.0	0.0	0
2019	2	0.5 ± 0.3	18.0	9
2019	3	2.3 ± 0.4	6.1	14

Table 3.18 List of species found in SHW and the zone(s) that they occur. Species occurrences are based on assessment of the 86 grid plots assessed annually between 2016 and 2019

2019 Vascular Species		Zone 1	Zone 2	Zone 3
<i>Achillea millefolium</i>	U			X
<i>Agrostis scabra</i>	U		X	
<i>Aster conspicuus</i>	U		X	X
<i>Aster puniceus</i>	U			X
<i>Astragalus alpinus</i>	U			X
<i>Astragalus canadensis</i>	U			X
<i>Betula pumila</i>	D			X
<i>Calamagrostis canadensis</i>	U		X	X
<i>Carex aquatilis</i>	D	X	X	X
<i>Carex atherodes</i>	D		X	X
<i>Carex canescens</i>	D		X	X
<i>Carex utriculata</i>	D	X	X	X
<i>Cicuta maculata</i>	D		X	
<i>Cirsium arvense</i>	U		X	X
<i>Dasiphora fruticosa</i>	U			X
<i>Deschampsia caespitosa</i>	U			X
<i>Epilobium angustifolium</i>	U		X	X
<i>Equisetum arvense</i>	U		X	X
<i>Equisetum fluviatile</i>	D		X	
<i>Equisetum pratense</i>	U			X
<i>Equisetum sylvaticum</i>	D		X	X
<i>Fragaria vesca</i>	U		X	X
<i>Geum rivale</i>	D		X	X
<i>Glyceria borealis</i>	U			X
<i>Glyceria striata</i>	U			X
<i>Hieracium umbellatum</i>	U			X
<i>Hippuris vulgaris</i>	U	X		
<i>Juncus tenuis</i>	D			X
<i>Lotus corniculatus</i>	U		X	X
<i>Myrica gale</i>	D			X
<i>Parnassia palustris</i>	D			X
<i>Petasites palmatus</i>	U			X
<i>Petasites sagittatus</i>	U		X	X
<i>Poa palustris</i>	U		X	X
<i>Populus balsamifera</i>	U		X	X
<i>Populus tremuloides</i>	U		X	X
<i>Ribes lacustre</i>	U			X
<i>Rosa acicularis</i>	U			X
<i>Rubus idaeus</i>	U		X	X
<i>Rubus pubescens</i>	U		X	X

<i>Rumex occidentalis</i>	U			X
<i>Salix exigua</i>	D		X	X
<i>Salix monticola</i>	D		X	X
<i>Salix petiolaris</i>	D		X	X
<i>Schoenoplectus acutus</i>	D		X	
<i>Scirpus atrocinctus</i>	D		X	
<i>Scirpus microcarpus</i>	D		X	
<i>Scutellaria galericulata</i>	D		X	X
<i>Sium suave</i>	D		X	
<i>Solidago canadensis</i>	U			X
<i>Sonchus arvensis</i>	U		X	X
<i>Stellaria longifolia</i>	D			X
<i>Stellaria longipes</i>	D			X
<i>Taraxacum officinale</i>	U		X	X
<i>Trientalis borealis</i>	U		X	X
<i>Triglochin maritima</i>	D		X	X
<i>Triglochin palustris</i>	D			X
<i>Typha latifolia</i>	U	X	X	X
<i>Utricularia minor</i>	D	X	X	
<i>Vaccinium myrtilloides</i>	D			X
Bryophytes				
<i>Aneura pinguis</i>	D			X
<i>Aulacomnium palustre</i>	D		X	X
<i>Brachythecium acutum</i>	D			X
<i>Campylium stellatum</i>	D		X	X
<i>Ceratodon purpureus</i>	D			X
<i>Drepanocladus aduncus</i>	D		X	X
<i>Drepanocladus polygamus</i>	D		X	X
<i>Funaria hygrometrica</i>	D			X
<i>Hypnum pratense</i>	D		X	X
<i>Leptobryum pyriforme</i>	D		X	X
<i>Marchantia polymorpha</i>	D		X	
<i>Plagiomnium ellipticum</i>	D			X
<i>Polytrichum strictum</i>	D			X
<i>Ptychostomum pseudotriquetrum</i>	D		X	X
<i>Tomentypnum nitens</i>	D			X

Table 3.19 Species not recorded from the 86 grid plots between 2016-2017, 2017-2018, and 2018-2019. Desirable species labeled ‘D,’ undesirable species labeled ‘U,’ and bryophyte species labeled ‘B’

2016 to 2017		2017 to 2018		2018 to 2019	
<i>Aster borealis</i>	D	<i>Eleocharis palustris</i>	D	<i>Carex aurea</i>	D
<i>Beckmannia syzigachne</i>	D	<i>Geum aleppicum</i>	D	<i>Carex bebbii</i>	D
<i>Betula occidentalis</i>	D	<i>Lemna minor</i>	D	<i>Carex hystericina</i>	D
<i>Carex diandra</i>	D	<i>Agropyron trachycaulum</i>	U	<i>Juncus alpinus</i>	D
<i>Galium trifidum</i>	D	<i>Agrostis scabra</i>	U	<i>Rhododendron groenlandicum</i>	D
<i>Juncus tenuis</i>	D	<i>Galeopsis tetrahit</i>	U	<i>Spiranthes romanzoffiana</i>	D
<i>Potentilla palustris</i>	D	<i>Melilotus officinalis</i>	U	<i>Picea glauca</i>	U
<i>Ranunculus gmelinii</i>	D	<i>Bryum argenteum</i>	B	<i>Pinus contorta</i>	U
<i>Rubus chamaemorus</i>	D	<i>Calypogeia sphagnicola</i>	B	<i>Polygonum amphibium</i>	U
<i>Salix glauca</i>	D	<i>Helodium blandowii</i>	B	<i>Barbula unguiculata</i>	B
<i>Scirpus cyperinus</i>	D	<i>Lophozia ventricosa</i>	B	<i>Brachythecium campestre</i>	B
<i>Sium suave</i>	D	<i>Marchantia polymorpha</i>	B	<i>Cephalozia connivens</i>	B
<i>Triglochin palustris</i>	D	<i>Plagiomnium ellipticum</i>	B	<i>Mylia anomala</i>	B
<i>Betula papyrifera</i>	U	<i>Pohlia nutans</i>	B		
<i>Bromus inermis</i>	U	<i>Polytrichum juniperinum</i>	B		
<i>Crepis tectorum</i>	U	<i>Riccardia multifida</i>	B		
<i>Fragaria virginiana</i>	U				
<i>Glyceria grandis</i>	U				
<i>Lysimachia thyrsiflora</i>	U				
<i>Polygonum lapathifolium</i>	U				
<i>Ribes oxycanthoides</i>	U				
<i>Rorippa islandica</i>	U				
<i>Rumex occidentalis</i>	U				
<i>Brachythecium salebrosum</i>	B				
<i>Campylium stellatum</i>	B				
<i>Climacium dendroides</i>	B				
<i>Warnstorfia fluitans</i>	B				

Significant Findings: We provide the following answers to our original five questions:

Do the zones persist? Yes – Three zones still persist, and each are characterized by a different suite of species. The 2017 water level increase had a dramatic effect on the wetland vegetation, both in terms of species abundances, distributions, and number of species. We suggest that after this hydrological event these large shifts in all three of the species assemblages may indicate a regime shift after perturbation that may lead to an alternative stable state within Sandhill Wetland.

Has the vegetation of the zones changed? Yes – Both undesirable and desirable species have decreased by between 37-43%. *Populus balsamifera* has invaded the drier portion of the wetland, producing more shade. The dominant species in all three zones have increased in relative abundance to the exclusion of less abundant species; this is especially evident in the bryophyte component.

Have the dominant species changed? No – Each zone continues to be dominated by one species, abundances have decreased in some zones, but overall, the dominant species remain the same.

Has diversity changed? Yes – Species richness - in terms of species occurrences, number of species at the plot level, and at the landscape level have all changed dramatically. Significant losses of species have occurred over the past four years, with between 13 and 27 species lost between individual years.

Have species occurrences changed? Yes – Over the four years the species assemblages have become more uniform with less diversity, illustrated by species occurrences decreasing from 33-47%, with bryophyte occurrences decreasing by 47%.

In summary, the vegetation at Sandhill Wetland has changed dramatically over the past 5 years, with the 2017 high water event making a lasting and quite negative impact on the species distributions and diversity on the Wetland. Currently, all three species assemblages at the Wetland have different trajectories suggesting different environmental variables and thresholds are influencing the species assemblages in the three zones. None of the Sandhill Wetland zones overlaps with the reference sites, indicating that the species assemblages found at Sandhill do not closely resemble reference site plant communities and at the present time can be considered to possess sets of unique characteristics. The demise of bryophyte diversity and lowered desirable species richness, along with the increasing abundance of *Carex aquatilis* and *Typha latifolia* and select undesirable species (e.g., *Populus balsamifera*) are all worrying attributes.

4 Project 2. Plant Performance in Response to Variable and Increasing Salinity at Sandhill Wetland

Deliverables (revised from 2016 proposal): Responses and tolerances of key species to salinity within the natural setting of Sandhill Wetland, including parameters that are most responsive to and predictive of salinity in the rooting zone.

4.1 Responses of *Carex aquatilis* to a Regime of Increasing Sodium Concentrations Under Control Conditions

Background: Water sedge (*Carex aquatilis* Wahlenb., Cyperaceae) has a circumboreal distribution with extensions southward in the Western Cordillera of North America and the Kamchatka Peninsula, and is abundant in boreal peatlands (Hultén 1968; Gignac et al. 2004). It has a wide range of tolerance for pH (3.0-8.5), electrical conductivity (0-8,820 $\mu\text{S cm}^{-1}$ and Ca^{+2} concentrations (0.2-146.6 mg L^{-1}) and is common in all fen site-types as well as some marshes and shallow open waters (Koropchak et al. 2012). The species is also highly tolerant of differing water levels and can be abundant at levels between -80 and +36 cm from the soil surface. *Carex aquatilis* occurs in brackish marshes (Hartsock 2020) and may be a dominant species in reclaimed mine pits (Purdy et al. 2005), often colonizing disturbed areas (Bliss and Gruelke 1988). The species also occurs on wet sandy or clay soils (Chapin and Chapin 1981) and is one of the first colonizers of disturbed roadsides on both organic and mineral soils. *Carex aquatilis* is an aggressive colonizer producing rhizomatous shoots twice a year (Bernard and Somers 1973), with flowering in May to June and seed maturity in August to September (Gorham and Somers 1973). Seeds are abundant and readily germinate (Koropchak et al. 2012). These attributes make *C. aquatilis* a candidate as an effective species for establishing wetland plant communities on post-mined substrates (Vitt et al. 2011); however, few data describing limitations to survival from extreme pH, salinity, and Na^{+} concentrations are available.

In this study, we used a variable and increasing sodium regime set around water chemistry similar to that at Sandhill Wetland – and similar to many natural wetlands of the region. Our primary objective was to determine the responses of *Carex aquatilis* to increasing Na^{+} concentrations using a set of structural

(biomass, chlorophyll, plant tissue concentrations) and functional (photosynthesis, stomatal conductance, transpiration) attributes. We formulated three questions – for *Carex aquatilis*: 1) is there a threshold response of performance to increasing sodium, 2) if so, does it occur in the range of sodium that is present at current reclamation programs, and 3) is *Carex aquatilis* resistant to high concentrations of sodium?

In 2019, mean sodium concentrations measured from the water in the top 0-20 cm of the substrate across Sandhill fen were 578 mg L⁻¹ in early season to 431 mg L⁻¹ in late season ($n = 28$) – a 1.3 fold difference between spring and fall. Additionally, mean seasonal variation in Na⁺ varied 1.7 fold for those areas with highest Na⁺ concentrations (July – 971 mg L⁻¹ to September – 571 mg L⁻¹, $n = 9$, ANOVA $p=0.0000$). Sodium concentrations have also increased 1.3 times over the past four years averaging 389 (± 21.7 SE) mg L⁻¹ in 2016, 489 (± 20.4 SE) mg L⁻¹ in 2017, and 573 (± 22.8 SE) mg L⁻¹ in 2018 and 513 (± 17.6 SE) in 2019.

Experimental design: To determine responses of *Carex aquatilis* to increasing levels of sodium, we conducted a greenhouse experiment from December 13, 2018 to April 3, 2019 (112 days) using germinated *C. aquatilis* seeds collected from Sandhill Wetland (SHW). We exposed fully grown plants of *C. aquatilis* to solutions initially containing one of six sodium concentrations: 5, 75, 150, 300, 600, and 1,200 mg L⁻¹ Na⁺. The 5 mg L⁻¹ Na⁺ was used as a control, matching natural rich fen waters (Vitt and Chee 1990).

Carex aquatilis seeds were collected in July 2018 at SHW from six locations with differing levels of sodium, ranging from 0.56 – 5.99 mg g⁻¹ of extracted soil sodium. From dried soil samples, sodium was extracted using a 1:10 ratio of soil to 0.5 M ammonium acetate + 0.02 M EDTA, shaken for 16 hours at 200 rpm, and filtered through Whatman 1 filter paper, then Whatman 40 filter paper, and lastly 0.22 μ m filter paper. The filtered sample was then acidified and analyzed through AAS for Na⁺ concentration. Seeds were wet stratified at 2°C on moist paper towels enclosed in plastic bags for 30 days and germinated on moist peat at 20°C. Seedlings (2-4 cm high) were transplanted to 10 cm square pots with a mixture of 2/3 perlite - 1/3 vermiculite. To maintain soil moisture, each pot was placed in individual 18.4 cm round polypropylene containers that were consistently filled to 400 mL of distilled water containing Jack's Professional® Water-Soluble Fertilizer (20-3-19 Petunia Feed PlusMg, Allentown, PA; 140.3125 ppm N). Plants were left to adjust to their transplant for one month prior to the start of the experiment.

The experiment was performed in the Southern Illinois University Carbondale (37°42'51.9"N; 89°13'21.7"W) phytotron facility with natural, ambient sunlight and ambient daytime temperatures ranging from 23 to 36°C in full sunlight. Seventy-two *C. aquatilis* plants were randomly assigned to one of six sodium treatments each with twelve replicates. Plants were randomly rearranged and moved to different locations within the phytotron every two weeks. In order to emulate natural seasonal variation at Sandhill Wetland, during each two-week period we maintained consistent water levels in each container by replacing evaporated water with that from the original stock solutions and at two-week intervals water was completely replaced in each container. Stock water solutions were prepared for each sodium treatment and contained 7 mg L⁻¹ magnesium, 4 mg L⁻¹ potassium, and 10 mg L⁻¹ calcium to mimic natural fen water conditions. Cations were added to the stock solutions using magnesium sulfate (MgSO₄), potassium bicarbonate (KHCO₃), calcium oxide (CaO), and sodium sulfate (Na₂SO₄) as well as 1/8 teaspoon of the 20-3-19 fertilizer (140.3125 ppm N). Due to calcium oxide's water-insoluble nature, we added hydrochloric acid and MES buffer to the CaO solution in order to bring pH of the stock solution to neutral (average: 7.38 \pm 0.03 SE). We added the sodium to the treatment solutions using sulfate as the anion owing to its dominance at Sandhill Wetland (Hartsock et al. 2019). Water samples from the round polypropylene containers were collected every two weeks and Na⁺, K⁺, Mg²⁺, and Ca²⁺ concentrations determined on an atomic absorption spectrometer (Varian SpectrAA 220 FS). Water samples were also analyzed for electrical conductivity (EC) and pH.

For each *C. aquatilis* plant within each treatment, we quantified: 1) longest leaf length of plant, 2) number of ramets produced (genetically identical new shoots produced from rhizomes), 3) chlorophyll content, 4) stomatal conductance (defined as overall water loss of the leaf, determined using transpiration rate and leaf surface temperature, 5) transpiration rate (defined as rate at which water vapor accumulates on a leaf over time, 6) photosynthesis rate (defined as rate at which a known area of leaf assimilates CO₂ over time), 7) dry aboveground and belowground biomass, and 8) sodium tissue concentrations (aboveground and belowground). Longest leaf lengths and ramet count were recorded every two weeks. Chlorophyll content was determined with a Minolta SPAD 502 chlorophyll meter (Konica Minolta Sensing, Inc., Osaka) every two weeks. A CI-340 handheld photosynthesis system (CID Bio-Science, Inc., Camas, WA) was used at 46, 82, and 104 days post-start date to quantify stomatal conductance, transpiration rate, and photosynthesis rate, with three measurements taken for each plant at each of the three time periods. After the breakdown of the experiment, plants were rinsed with DI water and dried at 60°C for at least 72 hours to quantify aboveground and belowground biomass. Sodium uptake levels in *C. aquatilis* roots and shoots were determined using a plant sodium extraction protocol described by Iseki et al. (2017). Roots and shoots were air dried, then ground, and 15-25 mg of sample was weighed. Samples were collected in 2-mL tubes and 500 µL of DI water and dry metal beads were added before shaking samples for 2 hrs. at 200 rpm. Samples were centrifuged for 5 minutes and 200 µL of the supernatant was measured using a Na⁺ ion meter (Horiba).

Statistical analyses: We characterized the responses to sodium concentrations using linear and polynomial regression. We assessed curvi-linear regressions by comparing R² values. In these regression analyses, Na⁺ treatment values were 14 mg L⁻¹, 108 mg L⁻¹, 274, mg L⁻¹, 522 mg L⁻¹, 1,079 mg L⁻¹, and 2,354 mg L⁻¹, derived as the mean values at the start and end of each two-week watering regime. All statistical analyses were performed in SigmaPlot (SigmaPlot Version 11.0). Leaf length (longest leaf length of original plant at the end of the experiment), total ramet count, aboveground and belowground biomass, chlorophyll content, and sodium tissue concentrations were tested against sodium treatment levels using a linear regression (polynomial regression for sodium tissue concentrations). Outliers were removed from physiological data sets if one of the three measurement reading was irregular using the Quartile method (Benhadi-Marín 2018). Stomatal conductance, transpiration rates, and photosynthetic rates were tested against sodium treatment levels using linear regression.

Results: Water chemistry: Electrical conductivities within each two-week period increased between 1.3 and 2.2 times (Table 1). This increase was manifested in sodium concentrations increasing between 2.1 and 3.2 times, calcium concentrations increasing by 1.7 – 2.3 times, magnesium 4.2 – 14.8 times, and potassium by 2.8 – 4.4 times. Mean concentrations for the two highest Na⁺ treatments during the two-week intervals (Table 4.1) were 1,100 mg L⁻¹, similar to the higher values currently at Sandhill Wetland and 2,400 mg L⁻¹, similar to those from sodic fens in the area (Hartsock et al. 2019). Seasonal variation in sodium concentrations at Sandhill Wetland in 2019 for areas with high sodium varied 1.70 fold, while when all areas are considered together, seasonal variation was somewhat less (1.34 fold).

Table 4.1 Mean concentrations of sodium, calcium, magnesium, potassium, and electric conductivity at the beginning of the experiment and after every 2 weeks for each treatment

Na ⁺ Treatment	5 mg L ⁻¹	75 mg L ⁻¹	150 mg L ⁻¹	300 mg L ⁻¹	600 mg L ⁻¹	1200 mg L ⁻¹
Day 1	6.8 ± 0.1	62.8 ± 0.7	126.5 ± 1.2	331.5 ± 4.0	593.9 ± 5.4	1109.1 ± 9.3
[Na ⁺] mg L ⁻¹ ± SE	(n=18)	(n=9)	(n=18)	(n=9)	(n=18)	(n=18)
Day 14	21.2 ± 1.3	153.4 ± 4.0	422.5 ± 14.7	712.5 ± 13.9	1564.3 ± 34.9	3599.4 ± 96.0
[Na ⁺] mg L ⁻¹ ± SE	(n=48)	(n=48)	(n=48)	(n=48)	(n=48)	(n=48)
Day 1	20.6 ± 0.2	27.9 ± 1.1	34.5 ± 1.1	31.8 ± 0.3	35.9 ± 0.4	38.9 ± 0.6
[Ca ²⁺] mg L ⁻¹ ± SE	(n=18)	(n=9)	(n=18)	(n=9)	(n=18)	(n=18)

Day 14 [Ca ²⁺] mg L ⁻¹ ± SE	46.6 ± 2.9 (n=27)	54.4 ± 2.2 (n=30)	61.2 ± 2.4 (n=29)	68.2 ± 2.0 (n=32)	73.7 ± 2.3 (n=28)	64.6 ± 2.6 (n=28)
Day 1 [Mg ²⁺] mg L ⁻¹ ± SE	4.6 ± 0.1 (n=18)	4.2 ± 0.1 (n=9)	4.5 ± 0.1 (n=18)	4.2 ± 0.1 (n=9)	4.2 ± 0.1 (n=18)	4.0 ± 0.1 (n=18)
Day 14 [Mg ²⁺] mg L ⁻¹ ± SE	19.4 ± 2.4 (n=30)	25.0 ± 2.2 (n=31)	34.7 ± 3.1 (n=24)	49.5 ± 5.0 (n=32)	50.0 ± 6.9 (n=28)	59.3 ± 9.8 (n=28)
Day 1 [K ⁺] mg L ⁻¹ ± SE	7.5 ± 0.3 (n=18)	8.9 ± 0.5 (n=9)	9.3 ± 0.4 (n=18)	10.4 ± 0.7 (n=9)	11.7 ± 0.4 (n=18)	13.7 ± 0.7 (n=18)
Day 14 [K ⁺] mg L ⁻¹ ± SE	21.2 ± 3.1 (n=27)	25.4 ± 2.7 (n=31)	30.8 ± 3.9 (n=27)	39.9 ± 3.4 (n=32)	45.9 ± 2.7 (n=28)	60.0 ± 3.4 (n=28)
Day 1 EC μS cm ⁻¹ ± SE	221 ± 4.0 (n=16)	548 ± 6.0 (n=8)	894 ± 6.5 (n=16)	1542 ± 7.7 (n=8)	2791 ± 6.9 (n=16)	5156 ± 43.7 (n=16)
Day 14 EC μS cm ⁻¹ ± SE	288 ± 15.1 (n=22)	1035 ± 42.6 (n=26)	1787 ± 58.9 (n=22)	3326 ± 97.3 (n=26)	6123 ± 211.3 (n=22)	10611 ± 300.8 (n=22)

Ramet count: *Carex aquatilis* produced the fewest number of ramets (5.3 ± 0.51 SE) per individual plant in the highest sodium treatment, ($2,354 \text{ mg L}^{-1}$). The other treatments produced more ramets on average- 14 mg L^{-1} : 7.8 ± 0.64 SE, 108 mg L^{-1} : 6.4 ± 0.57 SE, 274 mg L^{-1} : 7.7 ± 0.83 SE, 522 mg L^{-1} : 7.4 ± 0.80 SE, and $1,079 \text{ mg L}^{-1}$: 7.8 ± 0.84 SE. The slope of ramet count as a function of treatment was significant, but with very weak R^2 (DF=1, F=4.52, p=0.037, $R^2=0.061$).

Biomass: Both aboveground biomass (Fig. 4.1) and belowground biomass (Fig. 4.2) decreased with increasing sodium treatment, with a steeper slope for belowground biomass. Aboveground biomass decreased on average 45% between the two end points of treatments (from 2.4 to 1.3 g), while belowground biomass decreased 68% (from 2.5 to 0.8 g). The ratio of aboveground to belowground biomass in the control treatment was 1.05 decreasing to 0.65 at the highest treatment (Fig. 4.3). Over the spectrum of treatments, there was a gradual decline in aboveground/belowground biomass ratios, with the ratio of aboveground to belowground biomass decreasing 38% overall.

Longest leaf length: Longest leaf lengths for plants in the control (14 mg L^{-1}) averaged 71 cm (± 2.39 SE), decreasing to 53 cm (± 1.68 SE) for the highest Na^+ treatment. Over the six treatments the longest leaf lengths decreased 25% (Fig. 4.4).

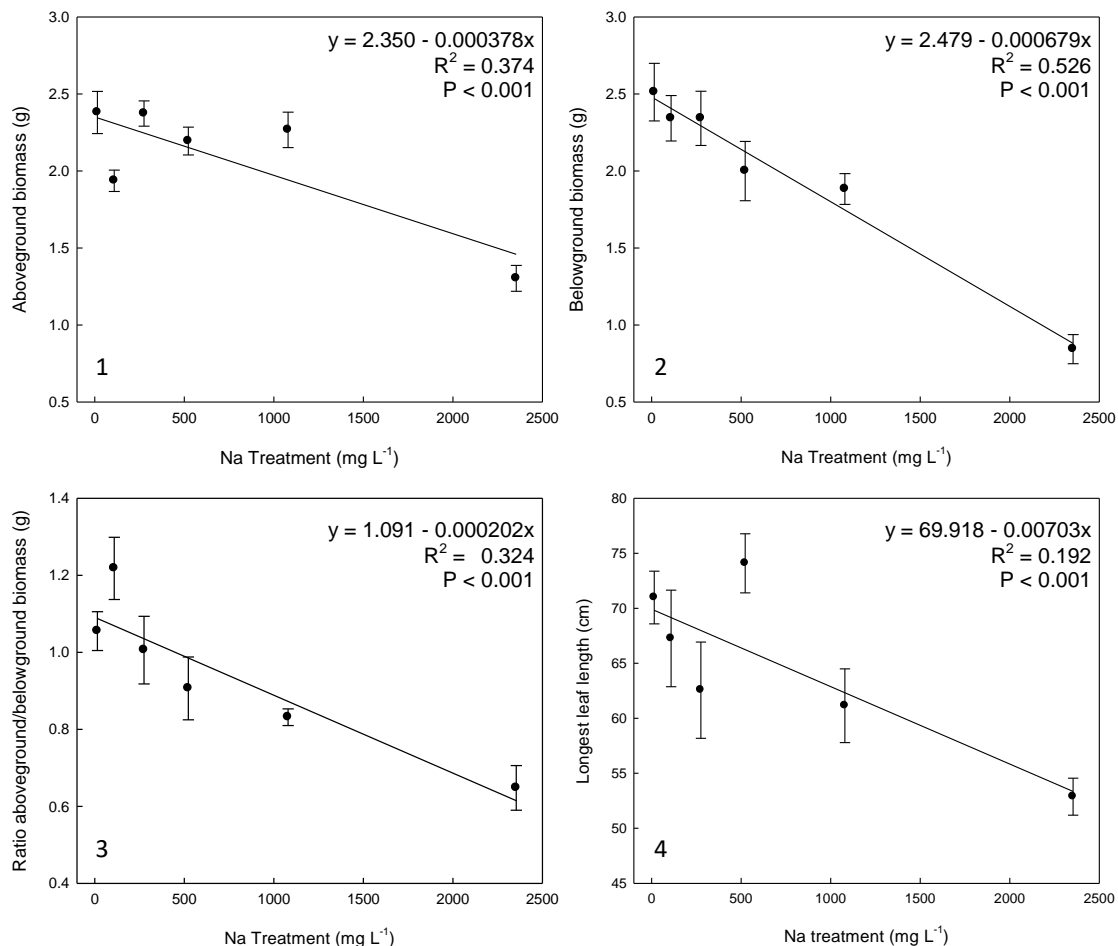


Figure 4.1 Regression of *Carex aquatilis* aboveground biomass as a function of sodium treatment (df=1, F=14.85, n=72). Values are mean \pm SE; n=72. **Figure 4.2** Regression of *Carex aquatilis* belowground biomass as a function of sodium treatment (df=1, F=77.62, n=72). Values are mean \pm SE; n=72. **Figure 4.3** Regression of *Carex aquatilis* aboveground/belowground biomass ratio as a function of sodium treatment (df=1, F=33.59). Values are mean \pm SE; n=72. **Figure 4.4** Regression of *Carex aquatilis* longest leaf length as a function of sodium treatment (df=1, F=16.58) and was measured in the final month (April) of the experiment. Values are mean \pm SE; n=72

Chlorophyll content: The slope for chlorophyll content at the end of the study as a function of treatment was not significant (DF=1, F=0.091, p=0.764).

Photosynthetic rate: Collectively, photosynthetic rates for *C. aquatilis* were higher, on average, on day 46 than on days 82 (1.4 times higher) and 104 (1.3 times higher). On day 104 (at the end of the experiment), there was a decline in photosynthetic rate, decreasing by 41% among the six treatments, but particularly noticeable in the 2,354 mg L⁻¹ treatment compared to the lower treatments (Fig. 4.5).

Transpiration rate: The mean transpiration rate decreased by 47% from 1.35 mmol m⁻² s⁻¹ (\pm 0.12 SE) in the 14 mg L⁻¹ treatment to 0.71 mmol m⁻² s⁻¹ (\pm 0.06 SE) in the 2354 mg L⁻¹ treatment (Fig. 4.6).

Stomatal conductance: Stomatal conductance decreased substantially from a mean of 43 mmol m⁻² s⁻¹ (\pm 3.69 SE) in the control to 19 mmol m⁻² s⁻¹ (\pm 1.65 SE) at the highest Na⁺ treatment, a decrease of 55% (Fig.

4.7). Stomatal conductance was correlated to transpiration rate ($p=1.047E-052$, $R^2=0.908$) and photosynthesis rate ($p=2.106E-018$, $R^2=0.566$ - Pearson Product Moment Correlation).

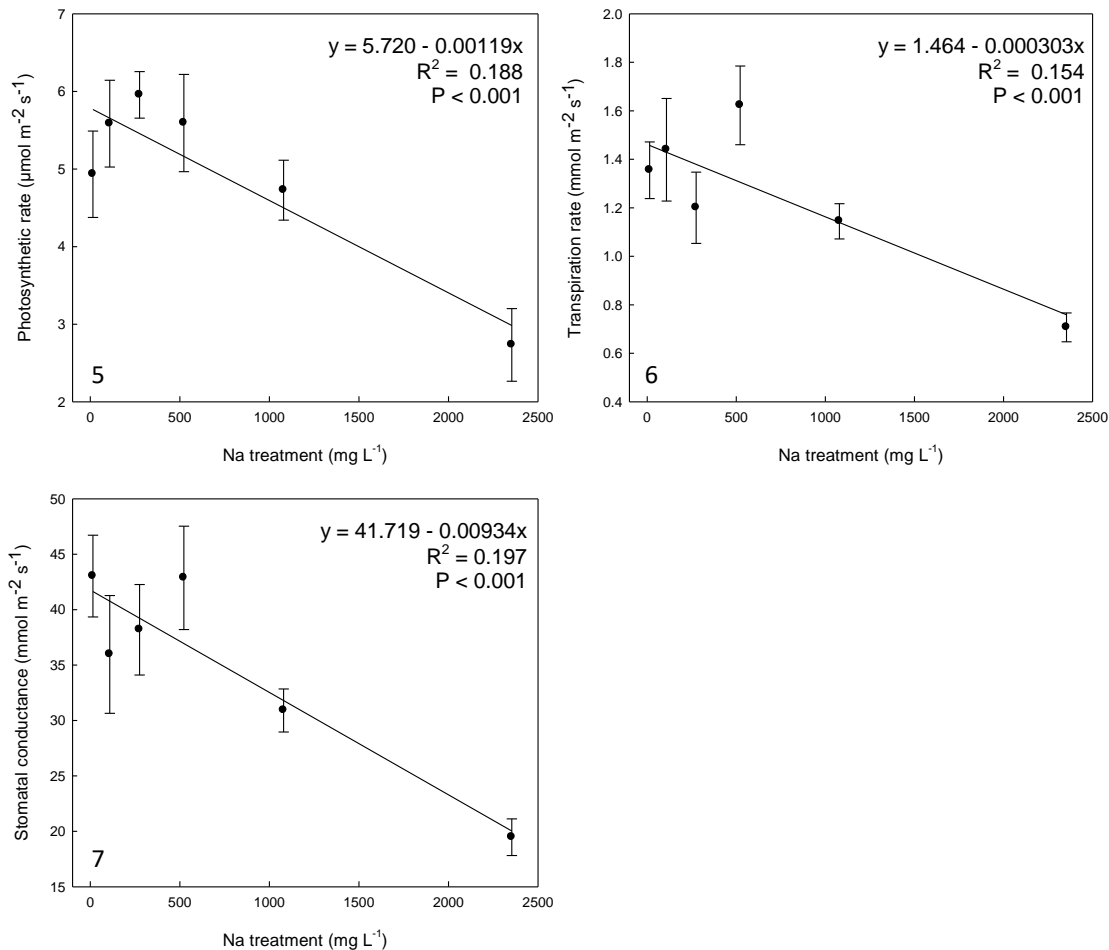


Figure 4.5 Regression of *Carex aquatilis* photosynthetic rate as a function of sodium treatment ($df=1$, $F=22.04$) and was measured in the final month (April) of the experiment. Values are mean \pm SE, $n=97$. **Figure 4.6** Regressions of *Carex aquatilis* transpiration rate as a function of sodium treatment ($df=1$, $F=18.96$) and was measured in the final month (April) of the experiment. Values are mean \pm SE, $n=106$. **Figure 4.7** Regressions of *Carex aquatilis* stomatal conductance as a function of sodium treatment ($df=1$, $F=24.80$) and was measured in the final month (April) of the experiment. Values are mean \pm SE, $n=103$

Sodium concentrations in above- and belowground biomass: The concentration of sodium present in plant tissues increased in both aboveground (Fig. 4.8) and belowground (Fig. 4.9) biomass of *Carex aquatilis*. In aboveground tissues, sodium increased from 0.9 mg g^{-1} to 3.6 mg g^{-1} , whereas in belowground tissues the increase was more dramatic, from 1.5 mg g^{-1} to 9.5 mg g^{-1} . This large increase in sodium in belowground tissues contributed to the ratio of sodium (aboveground/belowground) increasing as well (Fig. 4.10).

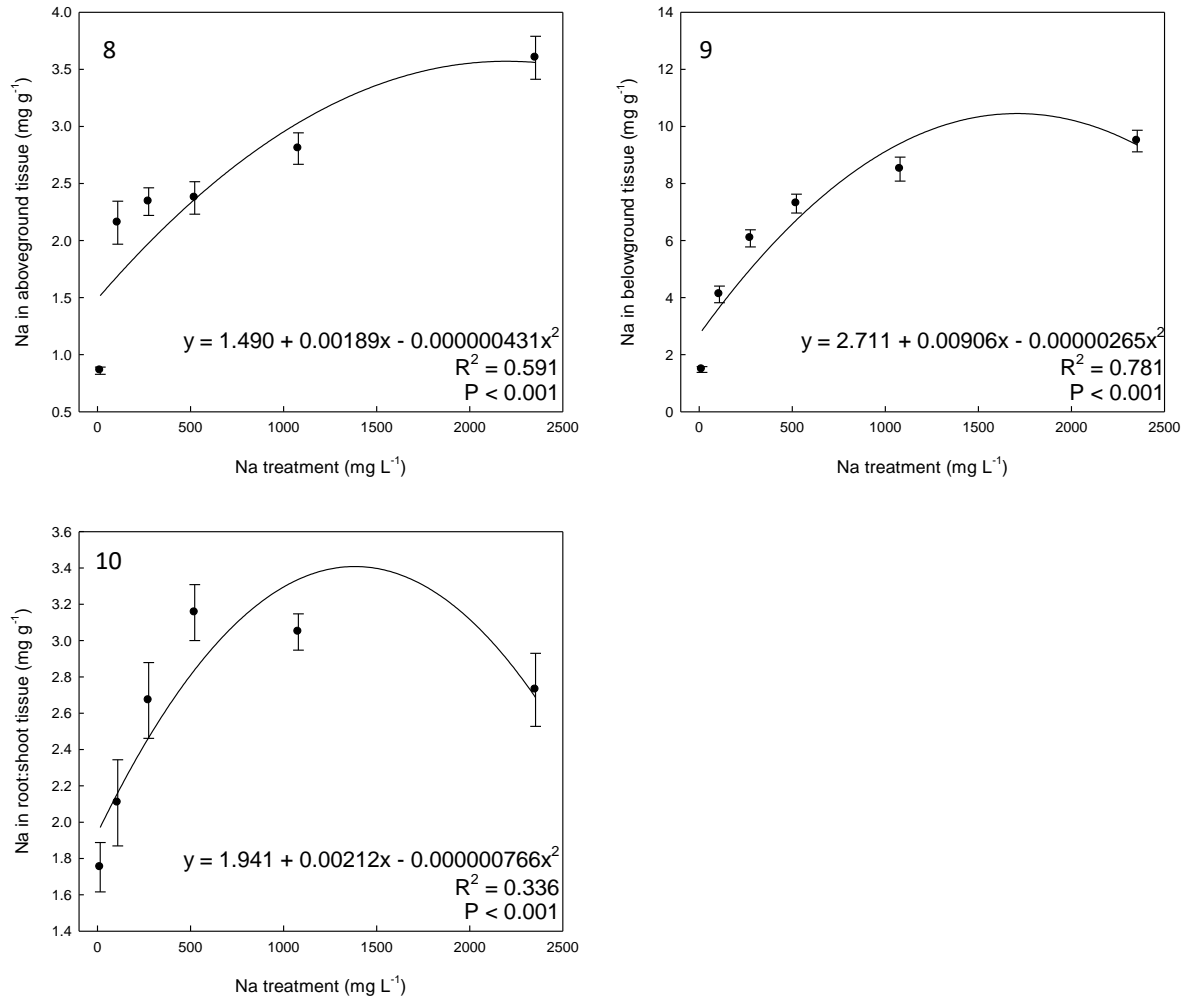


Figure 4.8 Regressions of *Carex aquatilis* sodium concentration in aboveground biomass as a function of sodium treatment (df=1, F=49.77). Values are mean \pm SE; n=72. Figure 4.9 Regressions of *Carex aquatilis* sodium concentration in belowground biomass as a function of sodium treatment (df =1, F=123.07). Values are mean \pm SE; n=72. Figure 4.10 Regressions of *Carex aquatilis* sodium concentration in root:shoot tissue as a function of sodium treatment (df =1, F=17.44). Values are mean \pm SE; n=72

Discussion: After three years, plant communities were largely influenced by water levels (Vitt et al. 2016); however, increasing cation concentrations, especially sodium, have become more important over the past several years (years 5-8 –Biagi et al. 2019). In 2019, sodium concentrations were variable over the fen. Overall mean values were near 500 mg L⁻¹; however, some sites had values as high as 1,420 mg L⁻¹. These high sodium concentrations are unlike those of natural rich fens of the region (Vitt and Chee 1990) and resemble values found in brackish marshes (Hartsock 2020). *Carex aquatilis* is abundant in fens and marshes of Alberta, but does not occur in sodic fens with sodium concentration above 1,900 mg L⁻¹ (Hartsock 2020). It is not known whether cation concentrations will continue to rise at Sandhill Wetland, but if they do, they could reach a point affecting the growth and occurrences of *C. aquatilis*, the dominant species on the wetland at the present time.

We addressed our initial question of whether there is a threshold response of *C. aquatilis* to increasing concentrations of sodium through linear regression. Regressions for all components of biomass

and rates of photosynthesis, stomatal conductance, and transpiration showed significant linear decreases. Biomass components were especially noteworthy, with R^2 ranging between 0.324 and 0.526. Belowground biomass was more strongly affected by higher concentrations of sodium, with the ratio of above to belowground biomass increasing from about one in the control treatment to more than 2.5 in higher treatments. Comparably, functional attributes of photosynthesis, transpiration, and stomatal conductance were more variable, especially within the treatments having lower sodium concentrations, (R^2 ranging between 0.154 and 0.197). The nearly identical slopes and correlative decrease ($R^2=0.566$) in stomatal conductance and photosynthetic rates provide a clear indication that the latter is strongly affected by the former. Likewise, the rate of transpiration is highly correlated with stomatal conductance ($R^2=0.908$). These results demonstrate that increased sodium concentrations affect photosynthetic rates by reduction in stomatal conductance and consequent restriction of availability of CO_2 .

Many non-halophytes maintain salt tolerance by exclusion of sodium by the roots from the shoots (Greenway and Munns 1980; Munns and Tester 2008) and this appears to be the case for *C. aquatilis*. Belowground/aboveground ratios of sodium tissue concentrations increased dramatically (from 1:1 to more than 2.5:1) as sodium treatments increased, and may be, at least in part, the reason for the high tolerance of *C. aquatilis* to increasing sodium concentrations. However, at the higher sodium treatment concentrations the ratios of sodium tissue concentrations (belowground/aboveground) level off and decrease at the highest treatment suggesting saturation of the below ground biomass that has decreased as well.

Significant Findings: Both structural and functional attributes of *C. aquatilis* decrease linearly with increases in sodium concentrations. Belowground components have greater decreases compared to aboveground components, including both biomass and photosynthesis. These greater aboveground decreases are associated with exclusion of sodium from the aboveground components by the belowground components. Reduction in photosynthesis is strongly correlated with reduced stomatal conductance and lower transpiration. *Carex aquatilis* survived all treatment concentrations of sodium – up to 2,354 mg L⁻¹; however, performance was reduced above treatments of 1,079 mg L⁻¹. These decreases in performance in our greenhouse trials are at a similar level to those currently present at Sandhill Wetland and careful assessment of sodium concentrations in the near future need to be continued.

4.2 Responses of *Carex aquatilis* to Varying Concentrations of Sodium at Sandhill Wetland

Background: We reported earlier that sodium concentrations (in upper 10 cm of the soil column) have increased over the past three years (averaging 0.77 mg g^{-1} in 2017, 1.07 mg g^{-1} in 2018 and 1.36 mg g^{-1} in 2019. Also the percent of sites with annual increases greater than 1.0 mg g^{-1} was 33.3% in 2017, 50.6% in 2018, and 62.5% in 2019.

Methods: We chose 12 sites along the increasing sodium regime at Sandhill Wetland and assessed photosynthesis, stomatal conductance, and transpiration. We used a CI-340 portable photosynthesis system (CID Bioscience, Camas, WA) with the 6.25 cm^2 flat rectangular chamber and a light module, which emitted light at a wavelength of 750 nm, between 1400-1500 ppfd to measure from July 10th–12th, 2019. Four plants from each site was measured three times, using a different leaf each time, giving a least a minute between each reading. If a leaf was not large enough to fill the width of the chamber, two or more leaves were placed without overlap in the chamber. No measurements were taken if leaf temperature exceeded 40°C .

We explored the results through analysis of variance [Kruskal-Wallis followed by Dunn's test] as follows: 1. Tested for differences between sites having high ($3.6\text{-}6.0 \text{ mg g}^{-1}$) vs. low ($0.45\text{-}0.70 \text{ mg g}^{-1}$) concentrations of sodium ($n=3$). 2. We tested for differences between sites have low ($0.45\text{-}0.70 \text{ mg g}^{-1}$) medium ($1.15\text{-}1.63 \text{ mg g}^{-1}$) and high ($3.60\text{-}5.99 \text{ mg g}^{-1}$) concentrations of sodium ($n=3, 6$ and 3).

Results: Mean values for each of the three measured parameters are given in Table 4.2.

Photosynthesis varied from 1.9 to $4.6 \mu\text{mol m}^{-2} \text{ s}^{-1}$ (mean 3.6). When the 12 sites are divided into those with high and low sodium concentrations, photosynthesis is not different between the two groups ($p=0.872$); likewise, when sites are assigned to groups of high, medium, and low sodium concentrations, there are no differences in photosynthesis ($p=0.311$), however these values are much lower than those from the control in the controlled experiment (see above).

Stomatal conductance varied from 43.1 to $78.8 \text{ mmol m}^{-2} \text{ s}^{-1}$ (mean 54.6) among plants from the 12 sites. These values are somewhat higher than those from the controlled experiment (see above). Comparison of sites with high and low sodium concentrations show no differences ($p=0.704$), nor are there differences in stomatal conductance among plants from the three groups (high, medium, low) ($p= 0.073$). Although not significant in this case, stomatal conductance correlated significantly with transpiration ($r^2=0.29$).

Transpiration varied from 0.8 to $2.6 \text{ mmol m}^{-2} \text{ s}^{-1}$ (mean 2.1) among plants from the 12 sites. Plants from sites with high sodium differed from those from sites with low sodium ($p=0001$). When plants from sites with high, medium and low sodium concentrations are compared, low (A) differed from medium (B), and from high (C). Also, when Sandhill transpiration rates are compared to those from the controlled experiment, the higher values at Sandhill are somewhat higher than the experimental control, while those from the sites with high sodium compare well to those at the highest experimental levels.

Table 4.2 Means (SE) for photosynthesis , stomatal conductance, and transpiration from plants at 12 sites. Sites ranked by soil sodium concentration (lowest to highest) soil sodium concentration

Plot	Photosynthesis ($\mu\text{mol m}^{-2} \text{s}^{-1}$)	Stomatal Conductance ($\text{mmol m}^{-2} \text{s}^{-1}$)	Transpiration ($\text{mmol m}^{-2} \text{s}^{-1}$)	Soil Na Concentration (mg/g)
14	4.4 ± 0.339	72.8 ± 5.349	2.6 ± 0.122	0.454
16	4.0 ± 0.878	46.7 ± 2.984	2.0 ± 0.144	0.654
75	2.9 ± 0.831	54.7 ± 10.456	1.9 ± 0.236	0.702
26	3.7 ± 0.693	67.7 ± 4.552	1.5 ± 0.112	1.151
80	4.5 ± 0.911	62 ± 9.03	1.9 ± 0.160	1.191
23	3.4 ± 0.732	52.1 ± 9.111	1.4 ± 0.162	1.219
60	2.3 ± 0.341	43.3 ± 3.307	1.5 ± 0.100	1.507
76	4.1 ± 0.914	43.1 ± 1.990	1.5 ± 0.082	1.628
78	1.9 ± 0.527	78.8 ± 3.420	0.9 ± 0.073	1.675
3	4.6 ± 0.979	68 ± 10.268	0.9 ± 0.096	3.569
8	3.4 ± 0.559	59.3 ± 4.555	0.8 ± 0.054	4.275
92	3.9 ± 0.599	52.7 ± 6.219	1.5 ± 0.110	5.988
Grand Mean	3.6 ± 0.111	54.6 ± 1.071	1.5 ± 0.020	2.001

4.3 Net Primary Production of *Carex aquatilis* (2017-2019)

Methods. In plots across Sandhill Wetland, a 0.25 m² quadrat was used to clip above ground *Carex aquatilis* biomass. In September, scissors were used to clip all green living tissue occurring above the soil surface from the quadrat. Tissue was bagged and sent back to SIU where samples were dried at 55° C for at least five days. The dried biomass was weighed, and biomass was calculated for a 1 m² area. In 2017, 12 plots were used, in 2018, 28 plots, and 12 plots in 2019.

Results. Net primary production of *Carex aquatilis* varied from 192.3 g m⁻² in 2018 to 311.7 g m⁻² in 2017, with no relationship to photosynthesis (p=0.994) or transpiration (p=0.114 – both n=12). We reported NPP for 2014-15 as 187.6 g m⁻² (2017 Syncrude report) and these values compare well with those from natural sites that average 204.1 g m⁻² yr⁻¹ (Thormann and Bayley 1977). The high value in 2017 was associated high water levels (see above).

Table 4.3 Means and standard errors for 2017-2019 NPP (g/m²). Letters indicate significant differences (p<0.05; Tukey’s HSD test)

Year	Mean	Standard Error
2017	311.72 A	38.88
2018	192.34 B	24.65
2019	217.35 AB	35.37

5 Project 3. Identification and Quantification of Markers of Success for Fen Reclamation

Deliverables (revised from 2016 proposal): 1). Characterizes species richness (i.e., number of different species present in a plant community) and species diversity indices (i.e., quantitative measures reflecting species richness/ abundance/ density/ evenness), 2) identifies 5 or less ground layer species that identify the various peatland types, and 3) identifies the key vascular plant species that compose the dominant vegetation of the peatland site types. These indicators will be chosen after surveys of 10 benchmark peatlands in the AOSR and after comparison to important past literature. Sandhill Fen will be used as the test case.

5.1 Nutrient Supply Patterns across Sandhill Wetland and Regional Reference Fens Utilizing Ion Exchange Membranes

Introduction: Plant root simulator (PRS®) probes (ion exchange membranes in a rigid plastic housing) are a widely used tool designed for quantifying nutrient supply rates to plants and could serve a future role for evaluating wetland reclamation performance. However, because both natural and reclaimed wetlands have been shown to exhibit considerable chemical and functional variation, knowledge is required to assess how ion exchange membranes behave (e.g., as ion-sinks or ion-exchangers) during short and long-term incubations. Using Plant Root Simulator (PRS®) probes, we evaluated nutrient supply rates at Sandhill Wetland across a gradient of increasing water table position and compared observations to three reference fens (a poor, moderate-rich, and saline fen). Our objectives were three-fold 1) determine the behavior of PRS probes across multiple peatland classes, 2) determine which type of peatland the Sandhill Wetland is most analogous to in terms of nutrient supply patterns, and 3) attempt to provide a repeatable approach for assessing nutrient supply in peatlands.

Methods: Four research plots were established at random locations within the interior of each reference fen. At Sandhill Wetland, plot locations were selected across three spatially distinct vegetation zones described by Vitt et al. (2016) (four research plots per zone). Fig. 5.1 displays the plot locations at Sandhill Wetland. For each burial treatment (initial 2 day, final 2 day, 20 days), three pairs of PRS probes (Western Ag Innovations, Saskatoon, SK) were installed at each plot (Fig. 5.2). Each PRS probe pair consisted of one anion probe with a positively charged membrane and one cation probe with a negatively charged membrane. For long-term burial treatments, PRS probes incubated in the peat profile for 20 days starting on June 13, 2018 at the reference fens, and at Sandhill Wetland on June 14, 2018. To assess whether ion-exchange membranes were acting as ion sinks or exchangers (stable or dynamic), PRS probes were also buried for two days at the beginning and the end (starting on day 18) of the 20-day period. Following removal from the field, all PRS probes were cleaned with a test-tube brush and distilled deionized water, placed into labeled plastic bags, and sent for analysis in accordance with the Western Ag sample return protocol. PRS probes were eluted with 0.5 M HCl and eluents were analyzed for nitrate and ammonium colorimetrically using an automated flow injection analysis system (Skalar San⁺⁺ Analyzer, Skalar Inc., NL) and for P, S, Fe, Mn, K, Ca and Mg using inductively coupled plasma (ICP) spectrometry (Optima ICP-OES 8300, PerkinElmer Inc., USA).

Results and Significant findings: PRS probes had low ammonium, nitrate, and phosphorus at all sites, high calcium and magnesium at all sites (except the poor fen), and much higher sulfur at Sandhill Wetland than natural fens (Table 5.1, Fig. 5.3). PRS-probe measurements at Sandhill Wetland were most similar to the moderate-rich and saline fens except for sulfur supply, which was considerably elevated (Fig. 5.3). Site differences in PRS probe measurements were smaller for 20- than 2-day burial periods due to displacement of elements that are less strongly held (e.g., ammonium, potassium, and manganese) in fens with high ion activity and continued accumulation in fens with low ion activity (Table 5.2). We recommend reclamation assessments over a range of natural and reclaimed fen types should use a relatively short burial period of one to three days. Burial periods of one to four weeks or more may be necessary for monitoring of nutrients

focusing on poor fens. However, burial period is not critical for ions that are strongly held in fens with elevated ion activities, which facilitates comparison among other studies that used longer burial periods. Of note, sodium and chloride supply were not measured because sodium is used as the counterion on cation PRS probes and HCl is used for displacing adsorbed ions for analysis. Alternative methods should be used (Greer and Schoenau 1996) to evaluate these key ions abundant at Sandhill Wetland and regional saline fens. Overall, we showed that Sandhill Wetland is not a eutrophic system in the sixth growing season, and supply for most nutrients are within the ranges of natural systems.

Table 5.1 Plant Root Simulator (PRS) probe summary table for nutrient adsorption patterns, and p-values from 2-way ANOVA ($p \leq 0.05$)

Nutrient	Median adsorption (range)		p-value		
	mg m ⁻²	% of capacity	Site	Burial Treatment	Interaction
<i>Nutrients adsorbed primarily on cation PRS probes</i>					
Calcium	1507 (5 to 2529)	32 (0.1 to 53)	<0.001	<0.001	<0.001
Magnesium	330 (1 to 451)	11 (0.0 to 16)	<0.001	<0.001	<0.001
Potassium	15 (7 to 129)	0.2 (0.1 to 1.4)	<0.001	0.020	<0.001
Ammonium	4 (1 to 21)	0.11 (0.02 to 0.62)	<0.001	<0.001	0.016
<i>Nutrients adsorbed primarily on anion PRS probes</i>					
Sulfur	131 (6 to 1071)	5 (0.3 to 45)	<0.001	0.170	0.170
Phosphorus	1.2 (0.5 to 6.3)	0.03 (0.01 to 0.14)	<0.001	0.020	0.600
Nitrate	0.2 (0.0 to 1.6)	0.01 (0.00 to 0.08)	<0.001	0.530	0.005
Iron	48 (1 to 248)	1.2 (0.0 to 5.9)	<0.001	0.240	<0.001
Manganese	4 (0 to 270)	0.1 (0.0 to 6.6)	<0.001	0.180	<0.001

Table 5.2 Adsorption of nutrients by PRS probes in two days compared to twenty days. Values are means of 2-day burial periods conducted at start and end of the 20-day burial period. Site abbreviations: Sandhill fen low (SHFL), intermediate (SHFI), and high-water table position (SHFH), poor fen (PF), moderate rich fen (MRF), and saline fen (SF)

Site	Nutrient adsorption in 2 days (percent of 20 days)						
	Calcium	Magnesium	Potassium	Phosphorus	Sulfur	Iron	Manganese
SHFL	66bc	81ab	183b	121	67	320a	379a
SHFI	79ab	86ab	163b	90	102	250a	373a
SHFH	74bc	91a	170b	78	104	197a	230a
PF	31d	13c	30c	82	111	14c	16c
MRF	41cd	46bc	583a	87	64	29bc	54b
SF	109a	100a	126b	86	109	94ab	194a
p-value	<0.01	<0.01	<0.01	0.38	0.33	<0.01	<0.01

Values within columns followed by the same lower-case letter are not significantly different from each other ($p \leq 0.05$, Tukey-Kramer test).

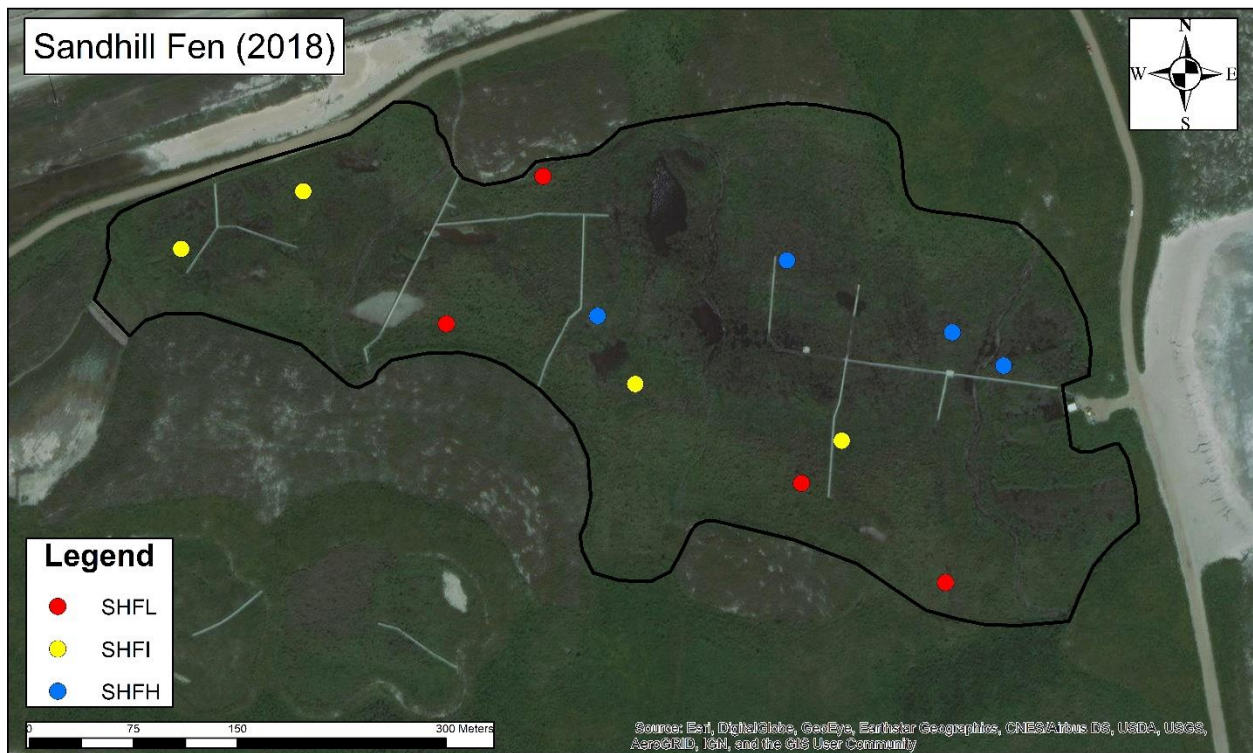


Figure 5.1 Plant root simulator (PRS) probe locations across the spatial extent of Sandhill Wetland. Red dots=Sandhill Wetland low water table position plots (SHFL); Yellow dots = Sandhill Wetland intermediate water table position plots (SHFI); Blue dots = Sandhill Wetland high water table position plots (SHFH). The bold black border indicates the wetland boundary within the constructed watershed

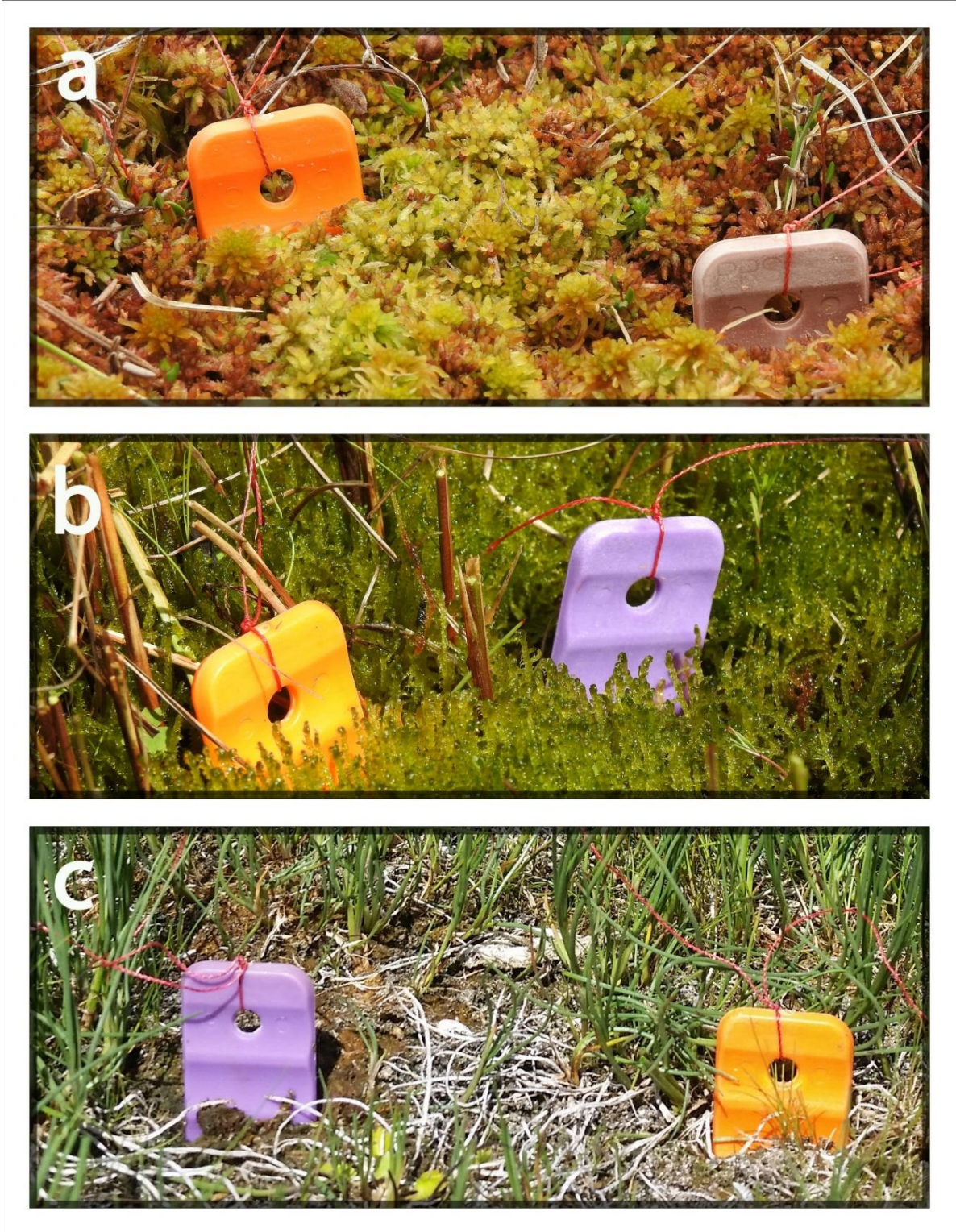


Figure 5.2 Plant Root Simulator (PRS) probe deployment protocol across three reference peatlands with different vegetation structure: Poor fen (a), moderate-rich fen (b), and a saline fen (c). *Following image capture, PRS probes were further inserted into the peat profile until plastic tops were flush with the peat surface

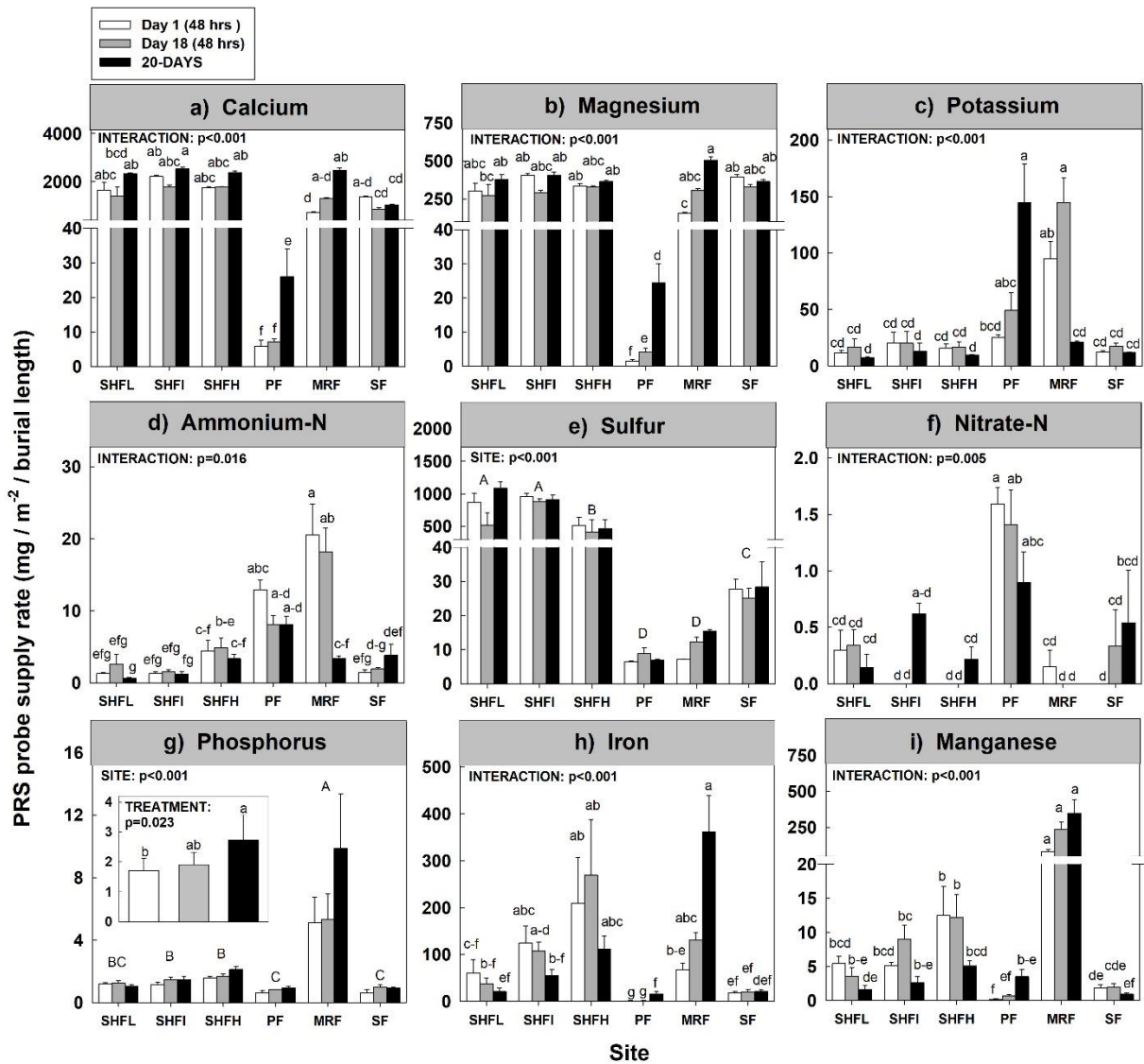


Fig. 5.3 Grouped bar plots of Plant Root Simulator (PRS) probe nutrient supply rates. Differing letters indicate significantly different groups determined by a 3×6 full factorial ANOVA ($\alpha=0.05$, Tukey's post hoc tests). Capital letters indicate significant effects of site and lower-case letters indicate a significant interaction. Site abbreviations: Sandhill Wetland low (SHFL), intermediate (SHFI), and high-water table position (SHFH), Poor fen (PF), moderate-rich fen (MRF), and saline fen (SF)

5.2 Nutrient Supply Rates in a Boreal Extreme-rich Fen Using Ion Exchange Membranes

Plant Root Simulator (PRS[®]) probes have been widely used to assess soil nutrients in the Athabasca Oil Sands Region (AOSR), but their optimum method of use and functionality in natural boreal fens and reclaimed wetlands needs to be determined. We assessed nutrient adsorption by PRS probes over three incubation periods (2-hours, 24-hours and 384-hours) in a boreal extreme-rich fen, a system with moderately high porewater electrical conductivity (EC) and a potential reclamation endpoint target. To

ensure appropriate implementation and interpretation of PRS probe or other ion exchange resin membranes, knowledge is required on whether the membranes are functioning as a sink (i.e., initial membrane counterions are exchanged by other ions in the medium), dynamic exchanger (i.e., once the initial counterions are exchanged, proportions of ions on the membrane are controlled by the concentrations of ions in the medium), or combination of these functions during the study period (Skogley and Dobermann 1996). In addition, there is concern that ion exchange membranes may be rapidly saturated with ions in some natural fens and oil sands reclamation sites that have porewaters with EC values exceeding $300 \mu\text{S cm}^{-1}$, potentially leading to interpretation errors during long incubations. Here, our primary goal was to determine the ideal incubation period for PRS probes at a fen with high EC. Our objectives were 1) assess nutrient supply rates in an extreme-rich fen using PRS probes, and 2) determine the appropriate incubation period for PRS probes in a system with high porewater EC.

Methods: The sedge-moss-dominated extreme-rich fen is located approximately 26 kilometers north of Fort McMurray, Alberta, Canada (56.950°N , 111.531°W ; 314 m elevation). The site is patterned and dominated (95-100% cover) by a ground layer of true mosses, namely, *Scorpidium revolvens*, *Scorpidium scorpioides*, and a sparse field layer of *Carex lasiocarpa* and *C. chordorrhiza*.

Three pairs of PRS probes (Western Ag Innovations, Saskatoon, SK) were placed inside 24 polyvinyl chloride (PVC) cylindrical-shaped collars (15 cm diameter x 15 cm deep) that were installed randomly within the fen interior (Fig. 5.4). The PVC collars were intended to limit nutrient immobilization by adjacent roots, and thus provide a better measure of processes such as net nitrogen mineralization. Each PRS probe pair consisted of one anion probe with a positively charged membrane and a cation probe with a negatively charged membrane. Within each PVC collar, PRS probe resin membranes penetrated into the peat profile approximately 3-8 cm, resin membranes were below the green moss tissues (i.e., below apparent photosynthetic regions), and all resin membranes were below the water table. Half of the 24 PVC collars were covered with plastic lids to control for potential atmospheric deposition of nitrogen and sulfate emanating from surrounding oil sands mining operations and to maintain consistent moisture levels. PRS probe treatments were incubated in collars over three differing time periods to assess ion exchange membrane sink or dynamic exchanger capacities: 2-hours, 24-hours, or 384-hours (16-days) ($n=4$ for each covered and non-covered treatment). Additionally, following PRS probe removal from the 2-hour and 24-hour treatments, PVC collars remained vacant for 14-days. New PRS probes ('final placements') subsequently were re-installed inside these collars and incubated for 2-hours and 24-hours; providing insight whether nutrient levels remained constant or varied in collars during the 14-days between placements. After removal from the field, all PRS probes were cleaned with a test-tube brush and distilled deionized water, placed into labeled plastic bags, and sent for analysis in accordance with the Western Ag sample return protocol. Analytes measured included ammonium, nitrate, phosphate, calcium, magnesium, potassium, sulfate, iron, and manganese (refer to www.westernag.ca for PRS probe methodology).

Results and Significant findings: Preliminary studies with PRS probes in wetlands can be important to ensure ion exchange membranes meet the function desired by the researcher. For ammonium and nitrate, PRS supply rates were quite low, which agrees with low net nitrogen mineralization and low nitrification characteristic of peatland systems (Hartsock et al. 2016). Calcium and magnesium were the dominant base cations on PRS probes, consistent with concentrations in porewater, and were likely at equilibrium on PRS probes shortly after 24-hours, given the negligible change occurring after 24-hours (Fig. 5.5). The increasing ratio of calcium to potassium on PRS probes and the decline in potassium after 24-hours is consistent with preferential selectivity of resins for divalent rather than monovalent ions (Skogley and Dobermann 1996). Divalent cations are held more strongly than monovalent cations on exchange sites, and thus calcium and magnesium likely displaced potassium from the PRS probes over the course of the 384-hour incubation. Sulfate supply was intermediate between poor and rich fens studied by Wood et al. (2016) and considerably lower than observations in a constructed fen (i.e., $45 \mu\text{g S}/10\text{cm}^2/\text{day} \times 30 \text{ days burial period} = 1,350 \mu\text{g S}/10\text{cm}^2/\text{burial period}$) (Nwaishi et al. 2016b). High sulfate levels may displace more

weakly held anions over time, as observed for manganese on anion PRS probes in a lab study with a saline-sodic riparian soil (Miller et al. 2016).

The only elements that clearly failed to reach a stable equilibrium in the study were iron and manganese. High iron and manganese in long-term burials either reflect gradual accumulation inside the PVC cylinders and (or) a very high iron and manganese activity at the end of the incubation period. The latter explanation is supported by the similarly high iron and manganese supply in the final 24-hour and 384-hour incubation treatments, which was attributed to conditions becoming more anaerobic due to increasing temperatures in the peat profile (data not shown).

Overall, the findings here are useful to indicate if PRS probe data from long-term burials (several days to weeks) in extreme-rich fens reflects diffusion-limited adsorption or equilibrium conditions (dynamic or stable), and whether dominant ions are displacing weakly held ions that were adsorbed initially. For the majority of ions measured, nutrient adsorption by PRS probes was at or close to a stable or dynamic equilibrium with the extreme-rich fen porewater within 24-hours of incubation and there was little change in the supply rates between incubation periods of 24 or 384-hours. Thus, burial periods of one to three days should be used for characterization of ion supply across wetlands exhibiting high EC levels.



Figure 5.4 Plant Root Simulator (PRS) probes inside a poly-vinyl-chloride cylinder

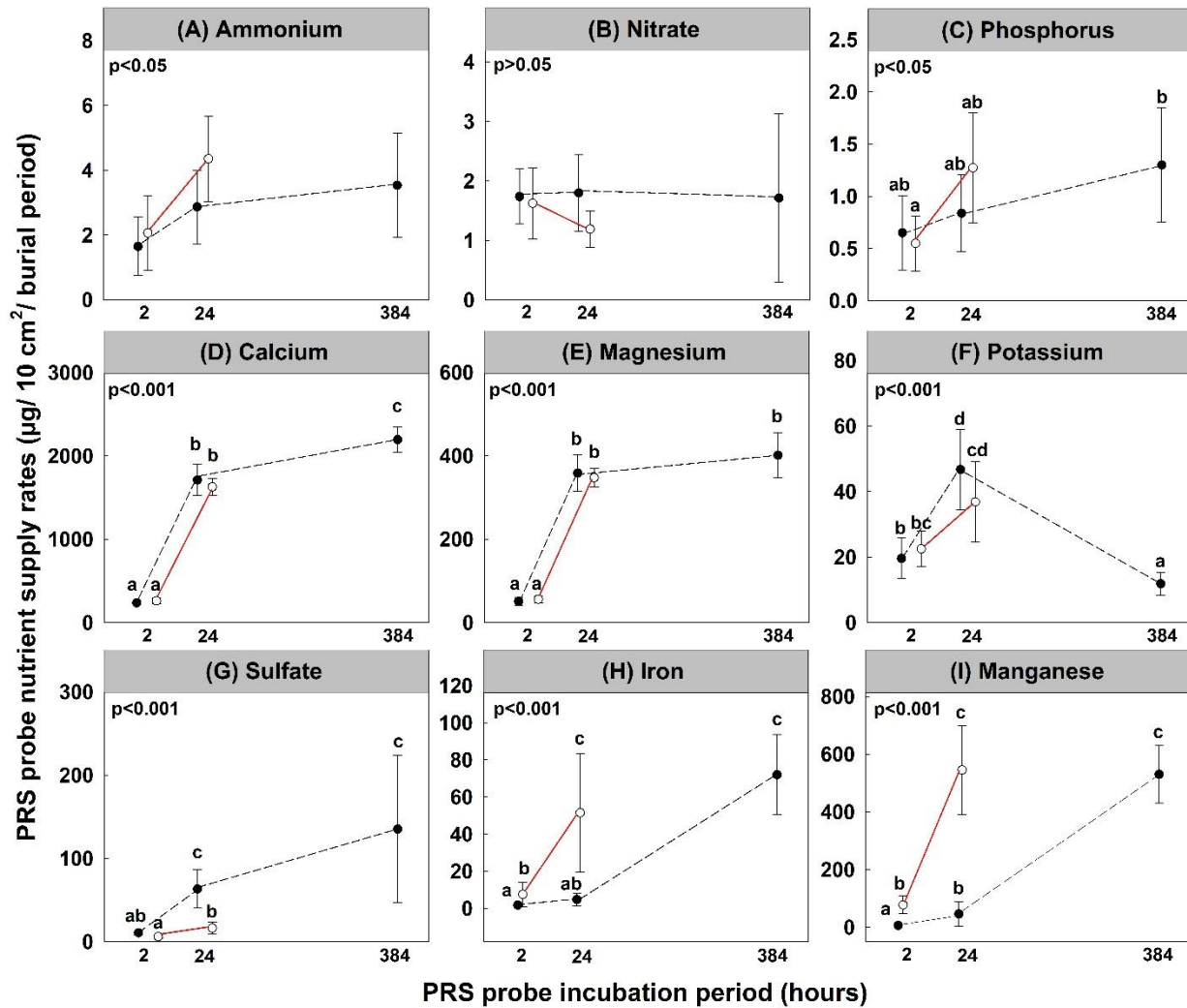


Figure 5.5 Plant Root Simulator (PRS) probe supply rates for (A) ammonium, (B) nitrate, (C) phosphorus, (D) calcium, (E) magnesium, (F) potassium, (G) sulfate, (H) iron, and (I) manganese in the surface layer of extreme-rich fen peat. Differing letters indicate significantly different groups determined by a 2 (covered vs. open cylinders) \times 5 (2-hours initial, 2-hours final, 24-hours initial, 24-hours final, or 384-hour incubation periods) factorial ANOVA, $\alpha=0.05$, Tukey's post hoc tests. Plotted values are means \pm 95% confidence intervals. Dashed lines represent PRS probe initial placements and solid lines represent final placements. Because covered vs. open cylinder treatment effects were not observed (i.e., $p>0.05$), values were pooled, and plotted values represent incubation period treatments only ($n=8$ for each point)

5.3 A history of water quality at Sandhill Wetland and comparisons to regional natural wetlands

Introduction: Here, we present water chemistry data obtained from several water collection campaigns at Sandhill Wetland spanning each growing season from 2013–2019. We also present data obtained from sub-surface monitoring wells installed four years prior to site construction completion (years 2009, 2011, and 2012) in order to highlight baseline conditions of water residing below Sandhill Watershed/Wetland. For all analytes measured, we compared observations at the reclamation site to 12 mature reference wetlands (10 fens and 2 marshes). Our primary objectives are three-fold: 1) present a summary of ion concentrations at Sandhill Wetland, 2) determine whether ion concentrations at the Sandhill Wetland are comparable to observations among natural reference wetlands, and 3) provide a near complete characterization of the chemical composition of water at Sandhill Wetland and regional wetlands to be utilized as a reference for government, industry, university, and public interests.

Methods: *Reference sites.* In total, 12 reference wetlands were monitored to determine the type of wetland (or wetlands) that Sandhill Wetland was most analogous to during its early developmental stages (from a water chemistry standpoint). The reference wetlands monitored include 3 poor fens, 1 open moderate-rich fen, 2 wooded moderate-rich fens, 1 extreme-rich fen, 3 saline fens, 1 fresh marsh, and 1 slightly brackish marsh.

Reference site water collection. At reference sites, near surface water samples were obtained from 2–4 random locations within the interior of each site in July 2018 and 2019 (except for one saline fen that was sampled in 2018 only). Characterization of organic compounds in water was completed in year 2019 only. Water samples from the natural reference sites were analyzed by the commercial laboratory MAXXAM Analytics, Inc. and concentrations are expressed in mg L⁻¹ or µg L⁻¹.

Sandhill Wetland Water collection (monitoring). Surface water quality sampling has been carried out at Sandhill Wetland annually. Water quality samples are taken during open water months from the eastern edge of the wetland area where the weir is located, coinciding with the only surface drainage point from the site. The annual surface water quality monitoring started when the research watershed was commissioned in 2012. Prior to 2012 water quality was also monitored, albeit less regularly, to gain baseline water quality at the site prior to reclamation. This baseline sampling included ground water. All monitoring samples discussed above have been included in this work (surface water and ground water). Water samples from the site were analyzed by accredited commercial laboratories EXOVA Canada, Inc. and later MAXXAM Analytics, Inc. For years 2009, 2011, and 2012, water was collected intermittently during the ice-free months (May–September) from a subset of sub-surface wells installed across Sandhill Watershed spatial extent (n=15, 6, and 14, for years 2009, 2011, and 2012, respectively). Water samples were pulled from depths ranging from 1.5–39.3 meters below the ground surface, with a mean sampling depth of 12.4 meters. Collection of water from sub-surface wells ceased after year 2012. For years 2013–2019, near-surface water samples were obtained from a myriad of locations across Sandhill Wetland, but primarily from locations near the weir building. For the first five growing seasons (2013–2017), water samples (for years 2013–2017, n=11, 12, 10, 3, and 10, respectively) were obtained solely, or in combination from either the weir intake pond, the physical weir (located inside the weir building), or the fen sump. Because of the intimate connectivity between the weir intake pond, the physical weir, and fen sump (especially after closing of the underdrain valve in May 2014), we hereafter refer to these three locations collectively as the “outlet”. Because of clear artifacts associated with winter sampling indoors at the weir, we only report data from sampling during the ice-free growing season months (May–October). For year 2018, near-surface water was collected from the outlet and additionally from areas along the three boardwalks distributed across Sandhill Wetland (n= 10). For year 2019, water was obtained from areas near the three boardwalks only (n=5). Characterization of organic compounds in water was completed in year 2019 only. A complete list of the organic chemicals measured are shown in Table 5.3.

Sandhill Wetland water collections (research): In addition to water collections carried out by Syncrude, characterization of water chemistry across the Sandhill Wetland has also been completed by academic research groups. These other studies are of great benefit, because much of the water obtained by Syncrude personal was collected from one area (i.e., the outlet), and the data are insufficient to provide spatial patterns of ions across the site. Thus, from a review of three previous studies that better characterized spatial patterns of ions at Sandhill Wetland, we also present their findings (means) along with our unpublished observations obtained during years 2017 and 2018. For published works, we display results from Hartsock et al. (2016), Vitt et al. (2016), and Biagi et al. (2019). In general, Hartsock et al. (2016) and Biagi et al. (2019) presented water chemistry patterns of near-surface water, whereas Vitt et al. (2016) presented observations from depths ranging from 5- 50 cm below the placed peat surface. The majority of water samples in all three studies were obtained from locations within close proximity to the three boardwalks. For the unpublished water collections that we report (years 2016–2018 for reduced electrical conductivity (EC), and 2017–2018 for base cations), near-surface water samples again were obtained from sampling locations near the three boardwalks (n=15–20 for each parameter). Water collections for years 2016-2018 followed methods modified from Hartsock et al. (2016). In brief, near-surface water samples were collected by hand in 60 mL plastic bottles, frozen within 24-hours of collection, and subsequently filtered with 0.4 μm Millipore filters in a laboratory. Cations were measured with a SpectrAA 220FS Atomic Absorption Spectrometer using US EPA protocols. Temperature corrected EC reduced for H^+ ions (Sjörs 1950) were also measured in the laboratory following filtering.

Results and Discussion: *Sandhill Wetland sub-surface water.* For sub-surface EC, values ranged from 2,500 to 5,290 $\mu\text{S cm}^{-1}$ over years 2009–2012, with a mean EC of 4,213 $\mu\text{S cm}^{-1}$ over the four-year period (Fig. 5.6 and Table 5.4). Sub-surface EC was markedly higher than near-surface water observations. For dissolved base cations, sodium was the dominant ion. Sodium concentrations in sub-surface water were markedly higher than near-surface water observations, which again was expected due to previously reported findings of high sodium contents in OSPW. Interestingly, dissolved calcium and magnesium concentrations in sub-surface water were lower than near-surface water. One possible source of calcium and magnesium in near surface is the clay till layer placed below the peat in the wetland portion of the constructed watershed. Dissolved potassium concentrations in sub-surface water were slightly higher than near-surface water, but only by a small margin. For dissolved sub-surface anions, bicarbonate and chloride were dominant. Sulfate concentrations generally were 2-fold lower than bicarbonate and chloride, yet surprisingly similar to near-surface water observations, namely in years 2017–2019. Of potential importance, we show sub-surface water observations generally were higher than near-surface water for the following properties/dissolved elements: total alkalinity, total dissolved solids (TDS), ammonium, lithium, barium, boron, aluminum, chromium, cobalt, molybdenum, nickel, arsenic, titanium, uranium, and vanadium (Table 5.4).

Sandhill Wetland near-surface water. For near-surface water collections at Sandhill Wetland, our primary objective centered on summarizing results obtained over a seven-year period from select sampling locations. We are forthright and acknowledge that consequent of obtaining samples primarily from the outlet and boardwalks, the data presented do not represent the true spatial patterns of ions distributed across the wetland.

Since initial site flooding, the behavior of EC at Sandhill Wetland has been quite erratic (Fig. 5.6 and Table 5.4). Because of mixing of freshwater being pumped into the wetland and water being pulled from the underdrain system into the fen sump (OSPW affected water), EC levels of near-surface water collected at the outlet in years 2013–2014 were quite high. Closure of the underdrain valve in May 2014 resulted in marked EC decreases at the outlet in 2015. Since the 2015 growing season, EC levels have increased by approximately 283 $\mu\text{S cm}^{-1}$ each year to current levels of 2,560 $\mu\text{S cm}^{-1}$ measured in 2019. For years 2013–2015, our observations closely correspond with findings from Biagi et al. (2019) who also sampled water at the outlet. However, other studies monitoring near-surface water across the Sandhill Wetland spatial

extent, namely in year 2013, reveal EC levels at the outlet far exceeded observations across the entire wetland area, which generally were below $1,000 \mu\text{S cm}^{-1}$ (cf. Vitt et al. 2016; Hartsock et al. 2016; Biagi et al. 2019). Overall, all studies monitoring near-surface water EC at Sandhill Wetland show levels have increased since the first growing season.

The base cation calcium historically has been the second most abundant dissolved ion at Sandhill Wetland, followed by magnesium; and calcium: magnesium ratios have rarely strayed from 1:4. Since year 2013, calcium and magnesium concentrations have increased annually by approximately 15 and 5 mg/L, respectively. A positive aspect of annual increases in dissolved calcium and magnesium; however, centers on potential amelioration of some negative effects caused by increasing sodium concentrations on established wetland plants (Greenway and Munns 1980).

For dissolved anions, sulfate and bicarbonate were both dominant in near-surface water over the first five growing seasons (Fig. 5.7 and Table 5.4); exhibiting sulfate: bicarbonate ratios near 1:1. However, for years 2018–2019, sulfate concentrations have notably increased, raising sulfate: bicarbonate ratios to 1.5:1. We are unsure of the mechanisms responsible for marked sulfate concentration increases at Sandhill Wetland over the last two years. For the anion chloride, although concentrations were lower than sulfate and bicarbonate, the anion was quite prevalent at the Sandhill Wetland exhibiting concentrations exceeding those of calcium for most years. Disregarding sampling at the outlet in years 2013 and 2014 (prior to underdrain valve closure), chloride, bicarbonate, and sulfate concentrations appear to increase annually in the wetland. Since year 2015, chloride, bicarbonate, and sulfate, concentrations have increased by 30, 26, and 73 mg/L, respectively, each year to current levels of 246, 398, and 622, respectively. Overall, with few exceptions, the dominant anions and cations present in near-surface water at Sandhill Wetland have increased each growing season in a linear fashion. These patterns by dominant ions cumulatively are responsible for annual increases in EC, total alkalinity, and total dissolved solids at the site. Of note, for the growth limiting nutrients nitrogen and phosphorus, near-surface water concentrations are low (Table 5.4). In contrast to sub-surface water observations, all metals exhibiting high concentrations in sub-surface water were not abundant in near-surface water. Moreover, for all organic compounds analyzed, measured values for both sub-surface and near-surface areas were below detection limits.

Sandhill Wetland vs natural wetlands. For base cation concentrations, Sandhill Wetland overall was most similar to the saline fens and slightly brackish marsh, and somewhat comparable to the extreme-rich fen for select ions (Figs. 5.6-5.7 and Table 5.5). During the first years, sodium concentrations at the reclamation site were most similar to the slightly brackish marsh. However, following the 2016 growing season, sodium concentrations increased a great deal at Sandhill Wetland, rising beyond slightly brackish marsh levels. Current sodium concentrations at Sandhill Wetland fall in a unique range between the slightly brackish marsh and saline fens. We put forward that sodium concentrations at the Sandhill Wetland will likely continue increasing, and levels will soon resemble those of OSAA saline fens. For calcium, since the first growing season, concentrations at Sandhill Wetland have been comparable to the saline fens. If calcium concentrations continue increasing in the wetland, they potentially may exceed levels characteristic of regional saline fens. For magnesium, during the first years, Sandhill Wetland was most comparable to the slightly brackish marsh and extreme-rich fen. However, due to annual increases in dissolved magnesium, concentrations currently are becoming more similar to saline fens. For potassium, concentrations at Sandhill Wetland generally exceeded observations at reference sites, yet values were most similar to the slightly brackish and fresh marshes. Based on the data available, it appears potassium may not be increasing annually at Sandhill Wetland, which does not conform with the behavior exhibited by the other base cations. Potassium is perhaps serving as a limiting nutrient for plant growth.

For anions, excluding the first years (due to mixing with underdrain water at the outlet), bicarbonate concentrations at Sandhill Wetland were similar to the extreme-rich fen in year 2016 only. However, over subsequent growing seasons, bicarbonate levels have annually increased, and current levels are most similar

to the slightly brackish marsh and saline fens. Similar patterns also occurred for sulfate, and concentrations currently are most similar to the slightly brackish marsh and saline fens. Interestingly, dissolved chloride concentrations at the reclamation site fall in a unique range. For all years monitored, chloride concentrations at Sandhill Wetland have exceeded all reference sites except for the saline fens, which are markedly higher than concentrations observed at the reclamation site. As was previously mentioned, annual increases in dominant anions and cations have influenced total alkalinity and dissolved solids at the reclamation site. Currently, total alkalinity levels at Sandhill Wetland are most comparable to the slightly brackish marsh and saline fens, yet total dissolved solids are within a unique range falling between the aforementioned natural sites.

For trace metals, heavy metals, dissolved nitrogen, dissolved phosphorus, and dissolved organics, Sandhill Wetland was quite comparable to all the reference wetlands. Overall, concentrations for all the aforementioned analytes were quite low. Considering many previous studies have voiced concerns regarding high levels of naphthenic acids and polycyclic hydrocarbons present in OSPW, these compounds currently appear to be under control at the reclamation site. However, we do suggest continued monitoring of near-surface water over subsequent years to ensure potential increases in dissolved metals and (or) organic compounds are not overlooked.

Significant findings: In year 2019, marking the seventh full growing season at Sandhill Wetland, the six dominant ions dissolved in near-surface water are bicarbonate, sulfate, chloride, sodium, calcium, and magnesium. From a water chemistry standpoint, Sandhill Wetland currently shares the most attributes with the saline fen and the slightly brackish marsh reference sites. Although we cannot be certain, we suspect dominant ions will continue increasing in the wetland over subsequent years. If our predictions manifest, site conditions at Sandhill Wetland will become even more analogous to regional saline fens in the relative near future. Near-surface water concentrations for trace metals, heavy metals, dissolved nitrogen, dissolved phosphorus, and dissolved organics were low at the reclamation site, which overall is quite promising given the concerns surrounding potential interactions with OSPW. Sandhill Wetland has provided valuable insights for future reclamation efforts on oil sands land leases. Intensive monitoring of environmental conditions should continue at Sandhill Wetland to track further changes in water chemistry patterns, and consequent changes in plant community composition attributable to elevated sodicity at the site.

Table 5.3 Organic compounds analyzed at Sandhill Wetland and reference wetlands for year 2019

F1 (C6-C10)	Perylene
Benzene	Acenaphthylene
m & p-Xylene	Indeno(1,2,3-cd)pyrene
Toluene	Dibenz(a,h)anthracene
Ethylbenzene	2-Methylnaphthalene
o-Xylene	Acenaphthene
F1 (C6-C10) – BTEX	Fluorene
Xylenes (Total)	1-Methylnaphthalene
F2 (C10-C16 Hydrocarbons)	Benzo(a)anthracene
F3 (C16-C34 Hydrocarbons)	Phenanthrene
F4 (C34-C50 Hydrocarbons)	Anthracene
B[a]P TPE Total Potency	
Equivalents	Benzo(c)phenanthrene
Quinoline	Fluoranthene
Naphthalene	Benzo(g,h,i)perylene
Chrysene	Benzo(b&j)fluoranthene
Benzo(k)fluoranthene	Acridine
Benzo(e)pyrene	Pyrene
Benzo(a)pyrene	

Table 5.4 Porewater concentrations at Sandhill Wetland. Values are means with standard deviations in parenthesis. In cases where means could not be calculated b/c values were below detection limit, the highest concentration observed was reported

Year:	2009	2011	2012	2013	2014	2015	2016	2017	2018	2019
Sampling location:	BGC	BGC	BGC	Outlet	Outlet	Outlet	Outlet	Outlet	Outlet +	FEN
Replicate no:	n = 15	n = 6	n = 14	n = 11	n = 12	n = 10	n = 3	n = 10	n = 20	n = 5
<u>Property</u>										
pH	8.1 (0.1)	8.1 (0.1)	7.9 (0.4)	8.0 (0.2)	8.1 (0.1)	7.9 (0.2)	7.9 (0.2)	7.8 (0.1)	7.9 (0.2)	7.9 (0.1)
EC ($\mu\text{S cm}^{-1}$)	4456 (454)	4152 (328)	3978 (534)	1779 (769)	1692 (439)	1143 (275)	1380 (100)	1858 (219)	2310 (961)	2560 (305)
T-Alkalinity	923 (198)	819 (144)	843 (283)	365 (122)	280 (93)	219 (60)	266 (26)	302 (29)	307 (118)	362 (55)
TDS (calculated)	2878 (365)	2647 (158)	2805 (338)	1117 (501)	1111 (273)	728 (204)	879 (39)	1177 (158)	1505 (698)	1640 (305)
Bicarbonate	1126 (241)	999 (178)	(347)	445 (149)	342 (113)	267 (73)	324 (32)	369 (35)	374 (143)	398 (67)
Ammonium - NH ₄	n.d.	5.24 (2.40)	8.22 (4.09)	2.54 (1.75)	<5.92	0.05 (0.04)	0.10 (0.13)	<0.17	n.d.	n.d.
TKN	n.d.	n.d.	n.d.	n.d.	n.d.	n.d.	n.d.	n.d.	1.89 (0.82)	2.14 (0.29)
Nitrate – N	<0.10	<0.14	<1.80	<0.54	<0.47	<0.18	<0.05	<0.08	<0.061	<0.010
Nitrite – N	<0.05	<0.02	<0.07	<0.14	<0.01	<0.005	<0.02	<0.02	<0.010	<0.010
Phosphorus (P)	n.d.	n.d.	n.d.	n.d.	n.d.	n.d.	n.d.	n.d.	<0.10	<0.10
DOC (mg/L)	n.d.	66 (10)	79 (14)	n.d.	n.d.	n.d.	n.d.	n.d.	56 (24)	58 (13)
Sulfate	351 (156)	341 (111)	627 (381)	346 (170)	413 (69)	258 (74)	275 (13)	357 (50)	566 (296)	622 (205)
Chloride	849 (169)	790 (145)	608 (228)	161 (86)	154 (41)	95 (34)	142 (19)	224 (38)	247 (145)	246 (53)
Sodium	1065 (152)	985 (83)	965 (178)	260 (139)	206 (104)	105 (45)	135 (7)	253 (78)	301 (185)	344 (60)
Calcium	34 (37)	15 (9)	53 (50)	97 (26)	131 (14)	109 (19)	125 (10)	152 (27)	162 (52)	184 (38)
Magnesium	13 (8)	8 (3)	23 (21)	24 (7)	34 (4)	27 (7)	33 (2)	41 (6)	44 (16)	53 (7)
Potassium	13.0 (2.3)	11.3 (1.7)	17.4 (5.5)	7.0 (2.5)	4.6 (1.7)	3.2 (1.3)	8.2 (0.4)	9.0 (2.1)	7.0 (2.8)	6.9 (1.8)
Cadmium ($\mu\text{g/L}$)	0.05 (0.01)	<0.05	<0.2	<0.01	<0.02	<0.05	<0.01	<0.02	<0.18	<0.02
Iron	<0.05	<0.05	<0.83	<0.35	<0.84	0.07 (0.03)	0.06 (0.050)	0.16 (0.14)	<1.30	0.39 (0.29)

Lithium	0.28 (0.03)	0.28 (0.01)	0.33 (0.06)	0.09 (0.01)	0.07 (0.04)	0.04 (0.01)	0.04 (0.00)	0.08 (0.03)	0.09 (0.05)	0.13 (0.06)
Manganese	0.09 (0.04)	<0.07	0.57 (1.05)	<1.25	<0.74	<0.54	<0.25	<1.72	0.39 (0.49)	0.28 (0.38)
Strontium	0.9 (0.4)	0.6 (0.1)	1.2 (0.8)	0.8 (0.1)	0.8 (0.1)	0.6 (0.2)	0.7 (0.1)	0.8 (0.2)	0.8 (0.3)	1.0 (0.3)
Barium (µg/L)	169 (65)	142 (83)	118 (110)	77 (9)	59 (5)	52 (7)	51 (3)	64 (17)	44 (20)	28 (8)
Silicon	5.5 (1.0)	4.4 (0.9)	5.9 (1.3)	3.8 (0.6)	2.6 (0.7)	1.2 (1.0)	0.8 (0.2)	5.1 (1.5)	5.9 (2.5)	5.5 (1.7)
Boron	3.07 (0.29)	3.07 (0.37)	3.06 (0.41)	0.86 (0.14)	0.5 (0.37)	0.21 (0.09)	0.20 (0.01)	0.29 (0.21)	0.40 (0.21)	0.48 (0.35)
Aluminum (µg/L)	11 (11)	<20	<1780	<14	14 (7)	6 (3)	<2	<9	<18	<5
Chromium (µg/L)	<13	7 (2)	<4	<1	<1	<1	<1	<1	<1	<1
Cobalt (µg/L)	<0.8	0.8 (0.9)	<136.0	10.7 (8.7)	3.7 (5.0)	<12.1	<0.5	<1.0	<1.7	<1.3
Copper (µg/L)	<7	<5	<10	<2	<6	3 (2)	<1	<5	<3	4 (4)
Lead	<0.0009	<0.0005	0.0048	<0.0002	<0.0002	<0.0001	<0.0001	<0.0002	<0.0002	<0.00020
Antimony	<0.0010	<0.0010	<0.001	<0.0004	<0.0004	<0.0003	<0.0002	<0.0004	<0.0006	<0.00060
Molybdenum	<120	79 (49)	<13	11 (2)	<20	<4	<1	<2	<2	<1
Nickel (µg/L)	<5.6	4.7 (2.8)	<144.0	22.3 (4.6)	11.3 (8.1)	3.6 (30.2)	1.4 (0.1)	2.3 (0.7)	2.5 (1.7)	2.5 (0.7)
Selenium (µg/L)	0.9 (0.2)	<1.0	<1.0	<0.4	<0.4	<0.2	<0.2	<0.4	<250.0	<0.2
Silver	<0.00050	<0.00005	<0.00005	<0.00002	<0.00002	<0.00001	<0.00001	<0.00002	<0.00010	<0.00010
Arsenic (µg/L)	3.9 (2.9)	4.9 (4.2)	<5	1.7 (0.4)	2.1 (0.7)	1.0 (0.2)	1.0 (0.3)	1.2 (0.3)	1.1 (0.5)	0.9 (0.2)
Thallium	<0.0010	<0.0002	<0.0002	<0.0001	<0.0001	<0.0001	<0.0001	<0.0001	<0.0002	<0.00020
Tin	<0.007	<0.005	<0.005	<0.002	<0.002	<0.001	<0.001	<0.002	<0.001	<0.0010
Titanium (µg/L)	6 (4)	9 (3)	10 (14)	<1	<1	<1	<1	<1	<2	<1
Uranium (µg/L)	2.8 (1.5)	<6.0	<9.0	1.6 (0.5)	<3.7	<1.1	<0.5	<1.0	<1.0	<0.9
Vanadium (µg/L)	4.6 (1.7)	6.5 (1.8)	<16	0.2 (0.1)	<0.5	<0.2	<0.1	<0.8	<1.0	<1.0
Zinc (µg/L)	<10	<8	13 (10)	9 (3)	11 (6)	27 (36)	<1	<3	<84	n.d.
Beryllium	<0.0008	<0.0005	<0.0005	<0.0002	<0.0002	<0.0001	<0.0001	<0.0002	<0.0010	n.d.

Table 5.5 Porewater concentrations among reference wetland classes. Values are means with standard deviations in parenthesis. In cases where means could not be calculated b/c values were below detection limit, the highest concentration observed was reported

Wetland Type:	Mb	Mf	SAL	MRF	ERF	PF
Replicate no:	n=5	n=6	n=15	n=19	n=7	n=15
Property						
pH	7.78 (0.24)	7.12 (0.11)	7.40 (0.58)	7.06 (0.22)	7.92 (0.09)	3.99 (0.26)
EC ($\mu\text{S cm}^{-1}$)	717 (158)	216 (35)	8808 (5930)	134 (53)	329 (69)	38 (68)
T-Alkalinity	504 (157)	90 (16)	496 (415)	62 (23)	180 (24)	<1
TDS (calculated)	562 (145)	130 (28)	6323 (4514)	71 (25)	227 (20)	32 (34)
Bicarbonate	616 (188)	111 (21)	613 (513)	77 (29)	220 (31)	<1
Ammonium - N	0.11 (0.07)	0.11 (0.08)	0.40 (0.37)	0.05 (0.03)	0.06 (0.03)	0.04 (0.03)
TKN	3.50 (0.63)	3.63 (1.26)	5.65 (3.95)	0.95 (0.50)	0.77 (0.24)	0.98 (0.42)
Nitrate - N	1.78 (2.30)	<0.20	<0.26	<1.20	<0.17	<2.20
Nitrite - N	0.26 (0.33)	<0.20	<0.18	<0.20	<0.010	<0.010
Phosphorus	0.59 (0.48)	0.84 (0.41)	0.04 (0.03)	0.01 (0.00)	<0.01	0.11 (0.11)
DOC	62 (14)	72 (26)	63 (38)	26 (7)	17 (2)	32 (9)
Sulfate	616 (188)	111 (21)	613 (513)	77 (29)	220 (31)	<1
Chloride	8 (5)	4 (1)	3245 (3112)	3 (2)	16 (5)	5 (11)
Sodium	144 (38)	10 (2)	1979 (1372)	4 (2)	22 (2)	2 (4)
Calcium	59 (16)	27 (6)	144 (120)	16 (6)	53 (4)	1 (1)
Magnesium	19 (4)	10 (2)	62 (56)	7 (2)	15 (1)	< 2
Potassium	4.9 (2.9)	4.9 (5.2)	2.9 (1.9)	1.3 (1.3)	1.9 (0.8)	0.7 (0.4)
Cadmium ($\mu\text{g/L}$)	<0.020	<0.020	<0.040	<0.15	<0.15	<0.18
Iron	0.92 (0.95)	3.15 (2.01)	<3.00	<0.32	<0.068	<1.1
Lithium	0.06 (0.02)	<0.04	<0.48	<0.020	<0.020	<0.020
Manganese	3.18 (2.34)	1.33 (1.11)	<2.20	<2.60	0.059 <1.80	(0.061)
Strontium	0.35 (0.08)	0.23 (0.05)	4.89 (5.16)	<0.14	0.10 (0.01)	<0.023
Barium	0.12 (0.07)	0.04 (0.02)	<0.60	<0.076	0.05 (0.01)	<0.18
Silicon	12.48 (4.23)	3.05 (1.28)	9.15 (6.49)	3.38 (0.83)	3.00 (1.58)	<3.90
Boron	0.07 (0.01)	0.05 (0.01)	0.51 (0.17)	<0.020	0.04 (0.01)	<0.10
Aluminum	0.006 (0.002)	0.024 (0.015)	0.030 (0.033)	<0.011	<0.0067	0.070 (0.047)
Chromium	<0.0010	<0.0010	<0.0020	<0.012	<0.0010	<0.013
Cobalt	<0.0022	<0.0031	<0.0013	<0.0004	<0.00030	<0.0015
Copper	<0.00023	<0.00024	<0.0016	<0.0035	<0.0012	<0.078
Lead	<0.00020	<0.00020	<0.00069	<0.00035	<0.00020	<0.00020
Antimony	<0.00060	<0.00060	<0.0087	<0.00060	<0.00060	<0.00060

Molybdenum (µg/L)	<0.81	<0.20	<0.40	<0.20	<0.20	<0.20
Nickel (µg/L)	1.9 (0.9)	2.2 (0.8)	<2.7	<0.8	<2.3	<2.6
Selenium	<0.00044	<0.00020	<0.0076	<0.00020	<0.00020	<0.00020
Silver	<0.00010	<0.00010	<0.00020	<0.00010	<0.00010	<0.00010
Arsenic (µg/L)	1.4 (0.7)	1.0 (0.2)	0.7 (0.3)	1.5 (2.2)	<0.67	<0.4
Thallium	<0.00020	<0.00020	<0.00040	<0.00020	<0.00020	<0.00020
Tin	<0.0010	<0.0010	<0.0020	<0.0010	<0.0022	<0.002
Titanium	<0.0010	<0.0010	<0.0035	<0.015	<0.0010	<0.016
Uranium	<0.0017	<0.00010	<0.00020	<0.00010	<0.00010	<0.00010
Vanadium	<0.0010	<0.0010	<0.0020	<0.018	<0.0010	<0.018
Zinc (µg/L)	<9.1	<3.0	<18.0	<9.9	<7.5	11.1 (5.8)
Beryllium	<0.0010	<0.0010	<0.0020	<0.0010	<0.0010	<0.0010

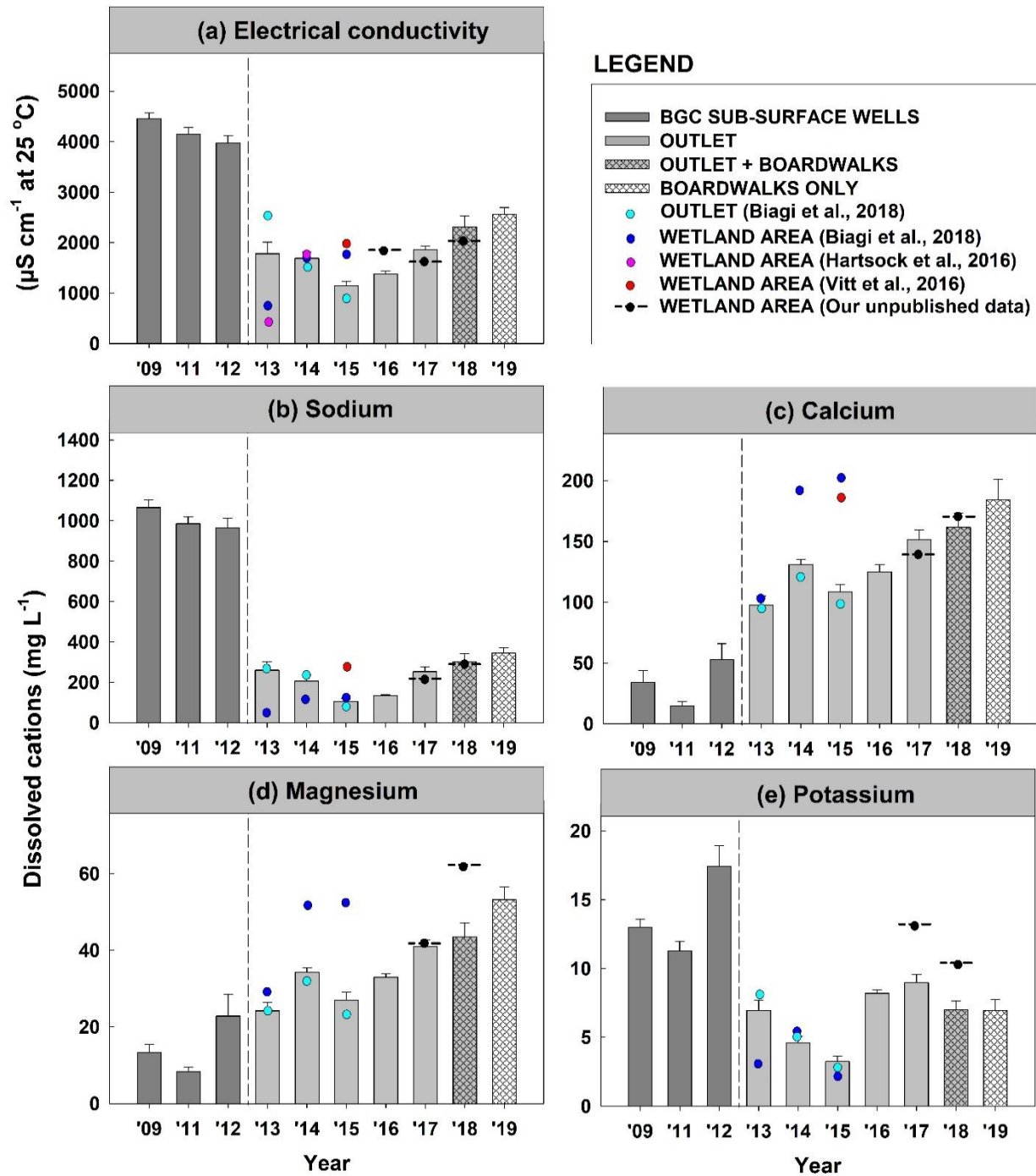


Figure 5.6 Bar plots of temporal porewater cation concentrations at Sandhill Wetland

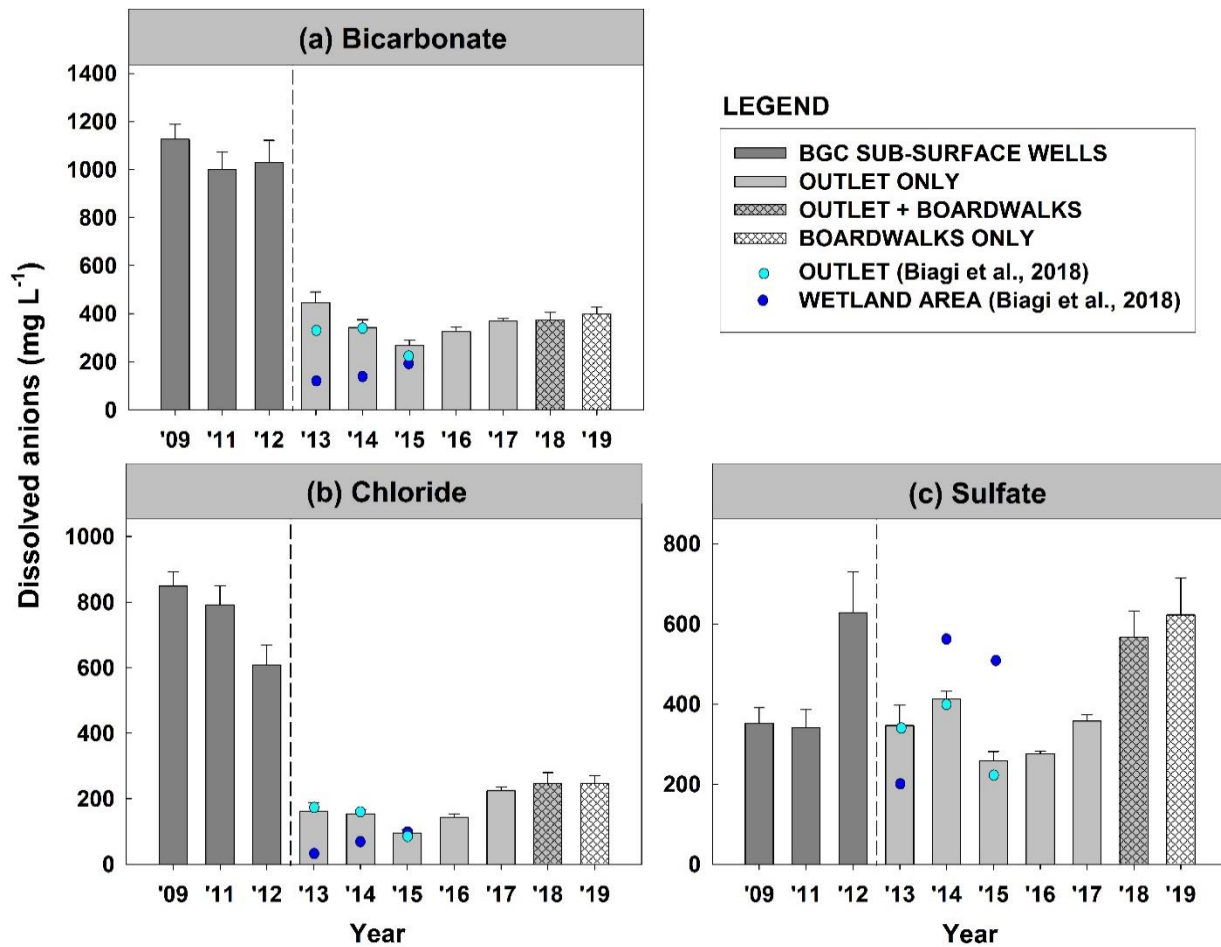


Figure 5.7 Bar plots of temporal porewater anion concentrations at Sandhill Wetland

5.4 A Comparison of Plant Communities, Water Quality, and Soil Characteristics at Sandhill Wetland to Regional Natural Peatlands and Marshes

Introduction: At the onset, Sandhill Wetland was projected to mature into a moderate-rich fen based on seed mix composition and a fresh water source. In the third growing season, findings from Vitt et al. (2016) revealed some areas in the wetland area contained high abundances of moderate-rich fen species, while other areas with especially high or low water table position contained high abundances of non-fen species. After six growing seasons, there has been little effort made to objectively determine which type or types of wetlands the reclaimed site is most comparable to through direct comparisons with reference sites. Here, we compare plant community composition, along with associated water quality and physical characteristics of soil at Sandhill Wetland to a number of mature natural wetlands. We also identify specific environmental factors driving vegetation assemblages. We aim to provide a holistic assessment of the reclaimed wetland in the sixth growing season, and moreover, answer our key question, does Sandhill Wetland exhibit attributes resembling those of regional fens or marshes?

Methods: *Reference sites.* In total, 12 reference sites were assessed to evaluate the type of wetland to which Sandhill Wetland was most analogous. The reference sites (3 poor fens, 3 moderate-rich fens (2 of which are wooded-moderate-rich fens), 1 extreme-rich fen, 3 saline fens, 1 fresh marsh, and 1 brackish

marsh) are located along highways 881 and 63, the Clearwater River, and within Elk Island National Park (Fig. 5.8 and Table 5.6).

Environmental and vegetation sampling. At reference sites, transects were established through the interior of each wetland. At approximate equidistant intervals, ten environmental monitoring plots were established at random distances 2–5 meters left or right of the transect. At Sandhill Wetland, 20 research plots were established within the spatially distinct vegetation zones (zones 1-3) previously described by Vitt et al. (2016). In this study, zones 1-3 are abbreviated as SH-Z1 (n=5), SH-Z2 (n=10), and SH-Z3 (n=5), respectively. The spatial distribution of research plots across Sandhill Wetland are presented in Fig. 5.9. The plot placements additionally capture a gradient of water table position present at the reclamation site, whereby water table position decreases from SH-Z1 to SH-Z3. At all sites, porewater samples, volumetric soil cores (0-10 cm depths), and water table position measurements (distance from the ground layer) were recorded at each plot. Porewater samples were collected by hand in 60 mL plastic bottles near the water table surface, frozen within 48-hours of collection, and subsequently filtered with 0.4 μm Millipore filters in a laboratory. Porewater samples were analyzed for primary nutrients, base cations, temperature adjusted pH and reduced EC. Soil cores were dried in an oven at 55°C and dry weights were obtained for bulk density calculations. Sub-samples from each soil core were analyzed for carbon and nitrogen content. In late July, plant surveys were conducted across all wetland sites. Circular 8.0 m² vegetation monitoring plots were established randomly 5–10 meters away from the environmental monitoring plots. Composition of the ground, field, shrub, and overstory layers was assessed by percent cover estimates (as canopy cover) to the nearest 5%. For instances where moss cover was especially low and for the discovery of single species occurrences, a value of 1% was used.

Results and Discussion: *Environmental properties.* In comparison to the 12 reference wetlands, porewater chemistry at Sandhill Wetland in year 2018 was most similar to the marshes and saline fens, and most different from the poor fens (Table 5.7). Reduced EC levels were highly variable among sites, with the highest levels occurring at the saline fens (combined range=586–20,760 $\mu\text{S cm}^{-1}$) and the lowest at the poor fens (combined range=5–188 $\mu\text{S cm}^{-1}$). Apart from the saline fens, EC levels at Sandhill Wetland exceeded all other reference sites, ranging from 1,263–5,140 $\mu\text{S cm}^{-1}$ across the three predefined zones. Porewater calcium and magnesium concentrations were spatially variable at Sandhill Wetland, with SH-Z1 and SH-Z2 plots exhibiting lower concentrations than SH-Z3 plots. Porewater potassium concentrations were highest among SH-Z1 and SH-Z2 plots (combined range=1.2–14.9 mg L^{-1}), yet similar to the fresh marsh (range=0.9–9.0 mg L^{-1}). For porewater sodium, the highest concentrations were observed at saline fens 1 and 2 (combined range=888.1–4,597.4 mg L^{-1}). At Sandhill Wetland, porewater sodium concentrations were quite high as well (combined range=65–972) and most comparable to the slightly brackish marsh (range=92–134) and saline fen 3 site (range=541–899). Lastly, dissolved inorganic nitrogen and phosphate concentrations were quite low across all wetlands with concentrations rarely exceeding 1.0 mg L^{-1} .

Water table position among the reference sites was highly variable, ranging from -39 cm below the peat surface at the saline fen 3 to 39 cm above the peat surface at the fresh marsh (Table 5.8). However, within site variation for water table position was quite low at the natural sites. At Sandhill Wetland, spatial differences in water table position was apparent between the three zones ($p < 0.001$). SH-Z2 plots exhibited water levels ranging from -30–+30 cm that overlapped with many reference sites, whereas SH-Z1 water levels (range=15–51 cm) were most comparable to the fresh marsh only. The lowest water tables were observed across SH-Z3 plots (mean=-41 cm), which were comparable to the saline fen 3 site. Within site water table position variation for SH-Z1 and SH-Z2 plots (standard deviation=15 cm and 17 cm, respectively) exceeded reference sites by a considerable margin.

Clear differences emerged among wetlands for soil bulk density patterns ($p < 0.001$). In general, sites dominated by a ground layer of peatland mosses (e.g., poor fens, moderate-rich fens, and extreme-rich fens) exhibited low soil bulk densities (combined range=17–87 mg cm^{-3}). For reference sites exhibiting low (or

no) moss cover (e.g., marshes and saline fens), soil bulk density was markedly higher, ranging from 60–217 mg cm⁻³. Bulk density observations across all zones at Sandhill Wetland were higher than reference sites (combined range=171–535 mg cm⁻³) and no differences emerged between the three zones.

Loss on combustion total soil nitrogen (TN) concentrations were lowest at the *Sphagnum*-dominated poor fens and also at wooded moderate-rich fen 1. TN concentrations at the extreme-rich fen, wooded moderate-rich fen 2, open moderate-rich fen, fresh marsh, and brackish marsh were higher than the aforementioned wetlands (combined range=0.7–3.1 mg g⁻¹), yet, generally lower than TN concentrations across the saline fens (combined range=2.2–4.0 mg g⁻¹). No differences were detected among the spatial zones at the reclamation site for soil TN concentrations, and values were quite similar to the poor fens and wooded moderate-rich fen 1. Total soil carbon (TC) concentrations generally were similar among reference sites ranging from 30–50 mg g⁻¹. The Sandhill Wetland plots exhibited the lowest TC concentrations by a large margin (range=7–42 mg g⁻¹) ($p < 0.001$), and further within site variation was markedly higher than reference sites. Soil CN ratios generally were inverse of TN observations, whereby the highest CN ratios were observed across the poor fens and wooded moderate-rich fen 1, and the saline fens exhibited the lowest CN ratios. At Sandhill Wetland, soil CN ratios were quite comparable to many reference sites. Overall, because the lag-times required for some soil composition changes to occur may operate on decadal timescales. We put forward that current physical properties of soil evaluated in this study are satisfactory and not threatening reclamation success within Sandhill Wetland.

Plant abundance. This survey across 140 plots recorded 91 vascular plant species and 44 bryophyte species. Of the 135 plant species, 18 (12 vascular plant and 6 bryophytes) were found only one time. At Sandhill Wetland, the predefined zones, SH-Z1, SH-Z2, and SH-Z3, were dominated by *Typha latifolia*, *Carex aquatilis*, and *Calamagrostis canadensis*, respectively. Across the two marshes, *Carex aquatilis* was most abundant at the fresh marsh, whereas the brackish marsh was dominated by both *Carex aquatilis* and *Carex atherodes*. For the saline fens, the rush *Juncus balticus* and forb *Triglochin maritima* were dominant species. *Carex lasiocarpa* and the true moss *Drepanocladus aduncus* was common at the open moderate-rich fen, whereas the wooded moderate-rich fens contained high abundances of the shrub *Betula glandulifera*, the sedge *Carex lasiocarpa* and the true mosses *Hamatocaulis vernicosus* and *Tomentypnum nitens*. Mosses in the genus *Scorpidium* and the vascular plant *Menyanthes trifoliata* were common at the extreme-rich fen. Lastly, the poor fens were dominated by a ground layer of mosses in the genus *Sphagnum* (e.g., *Sphagnum angustifolium*, *S. fuscum*, or *S. magellanicum*) and also by the shrub *Andromeda polifolia*.

Total plant abundance (as percent cover) among reference sites was variable (Fig. 5.10). Total cover (vascular plants + bryophytes) was highest at the wooded moderate-rich fens by a large margin (mean=265%). Total cover among SH-Z1 and SH-Z2 plots were comparable to the fresh marsh and saline fens, whereas SH-Z3 plots were most similar to the open moderate-rich fen, brackish marsh, and extreme-rich fen. However, many SH-Z3 plots exhibited high cover of undesirable or non-fen species (Tables 5.9 and 5.10). Total bryophyte cover was highest at the poor fens (101%), the extreme-rich fen (91%), and at both wooded moderate-rich fens (101%) (Fig. 3b). Among the remaining wetlands, including the reclamation site, bryophyte cover was quite low (less than 50%), especially at the two marshes. Vascular plant cover for SH-Z3 plots were higher than SH-Z1 and SH-Z2 plots due to an overstory stratum comprised of the tree *Populus balsamifera* and the shrub *Salix lutea* (Fig. 3c).

Diversity indices. At reference sites, mean alpha diversity was highest at the wooded moderate-rich fens and lowest at the saline fens and marshes (Table 5.10). SH-Z2 and SH-Z1 sampling areas exhibited especially low mean alpha diversity values (4.8 and 3.4, respectively), whereas alpha diversity across SH-Z3 plots (14.4) was surpassed only by the wooded moderate-rich fens. However, as previously mentioned, many SH-Z3 plots exhibited high cover of undesirable or non-fen species, which affected diversity scores subsequent to omitting undesirable species from the analysis. Beta diversity at reference sites was quite low (1.5–2.7), with the highest mean beta diversity occurring at saline fen 1. Across SH-Z1, SH-Z2 and

SH-Z3 plots, beta diversity (2.7, 4.6, and 2.4, respectively) generally was higher than the reference wetlands, highlighting that plant community composition at Sandhill Wetland was quite variable between survey plots. Gamma diversity was highest at the wooded moderate-rich fens (41–44 species), and similar between the open moderate-rich fen, poor fens, brackish marsh, extreme-rich fen, and saline fen 1 reference sites, ranging from 18–25 species. The fresh marsh, saline fen 2 and saline fen 3 exhibited the lowest gamma diversity (15, 9, and 11, respectively). At Sandhill Wetland, gamma diversity across SH-Z1, SH-Z2, and SH-Z3 plots was 9, 22, and 34, respectively. However, gamma diversity was 6, 13, and 19, respectively, following omission of undesirable species.

Multivariate analyses. All 140 vegetation plots were ordinated using NMDS techniques, and predefined groups (poor fen, open moderate-rich fen, fresh marsh, brackish marsh, wooded moderate-rich fen, extreme-rich fen, saline fen, SH-Z1, SH-Z2, and SH-Z3) were coded appropriately to view sampling units in ordination space (Fig. 5.11). Wetlands of the same type showed a high degree of association. PERMANOVA output revealed plant community composition was different among all ten predefined groupings (pseudo $F = 29.998$, $p < 0.001$). However, SH-Z2 plots were most similar to the fresh and brackish marshes, but only moderately, with mean similarity of 50% and 42%, respectively (Table 5.11). SH-Z1 sampling units were also somewhat comparable to the fresh and slightly brackish marshes; however, with lower mean similarity scores of 26% and 19%, respectively. The three predefined vegetation zones at Sandhill Wetland were at maximum only 5% similar to the reference fens. The sedge *Carex aquatilis* was the primary link causing SH-Z1 and SH-Z2 plots to exhibit the closest associations in ordination space.

Significant findings: Out of 20 plots surveyed across a gradient of increasing water table position at Sandhill Wetland, total plant cover was quite high averaging 95% in the sixth year. Across areas with water table position above the soil surface, the sedge *Carex aquatilis* and the forb *Typha latifolia* were abundant. Across the wetland periphery, where water table position was below the soil surface, plant communities were dominated by the grass *Calamagrostis canadensis*, a species not common in fens. Based on NMDS ordination, we show Sandhill Wetland plant communities present across high and intermediate water table position areas (SH-Z1 and SH-Z2 plots, respectively) are most closely associated with the fresh and slightly brackish marshes surveyed. Plots located in areas exhibiting low water table position (SH-Z3 plots) were quite dissimilar from the natural sites monitored. Furthermore, all plant communities across Sandhill Wetland were quite dissimilar from the reference fens; with maximum similarity scores ranging from 0–5%. Porewater chemistry and water table position across SH-Z1 and SH-Z2 sampling zones were most similar to conditions at the two marshes. Porewater chemistry patterns were additionally comparable to the saline fens. Overall, Sandhill Wetland remains spatially heterogeneous in terms of plant community composition, physical characteristics, and site chemistry.

While the reclamation has been successful in terms of creating a wetland that has persisted, and moreover, resembles natural sites in the region across some areas, fundamental concerns at Sandhill Wetland center on site salinization, namely, by means increasing sodium concentrations that appear to increase annually. Sodium-tolerant plant species such as *Carex atherodes* and the forb *Triglochin maritima* fortunately are present across the wetland. Over subsequent growing seasons, there is potential for these desirable species to replace current flora should sodium levels cause declines in plant performance. We recommend future reclamation attempts should maintain water table position at consistent and appropriate depths over large areas to promote more homogenous plant communities comprised of desirable wetland plant species. Additionally, future tailings reclamations should either embrace elevated salinity conditions and seek to create regionally uncommon sodium-dominated systems (e.g., slightly brackish/sodic marshes or saline/sodic fens) or develop more effective methods of preventing ion intrusion into wetland areas.

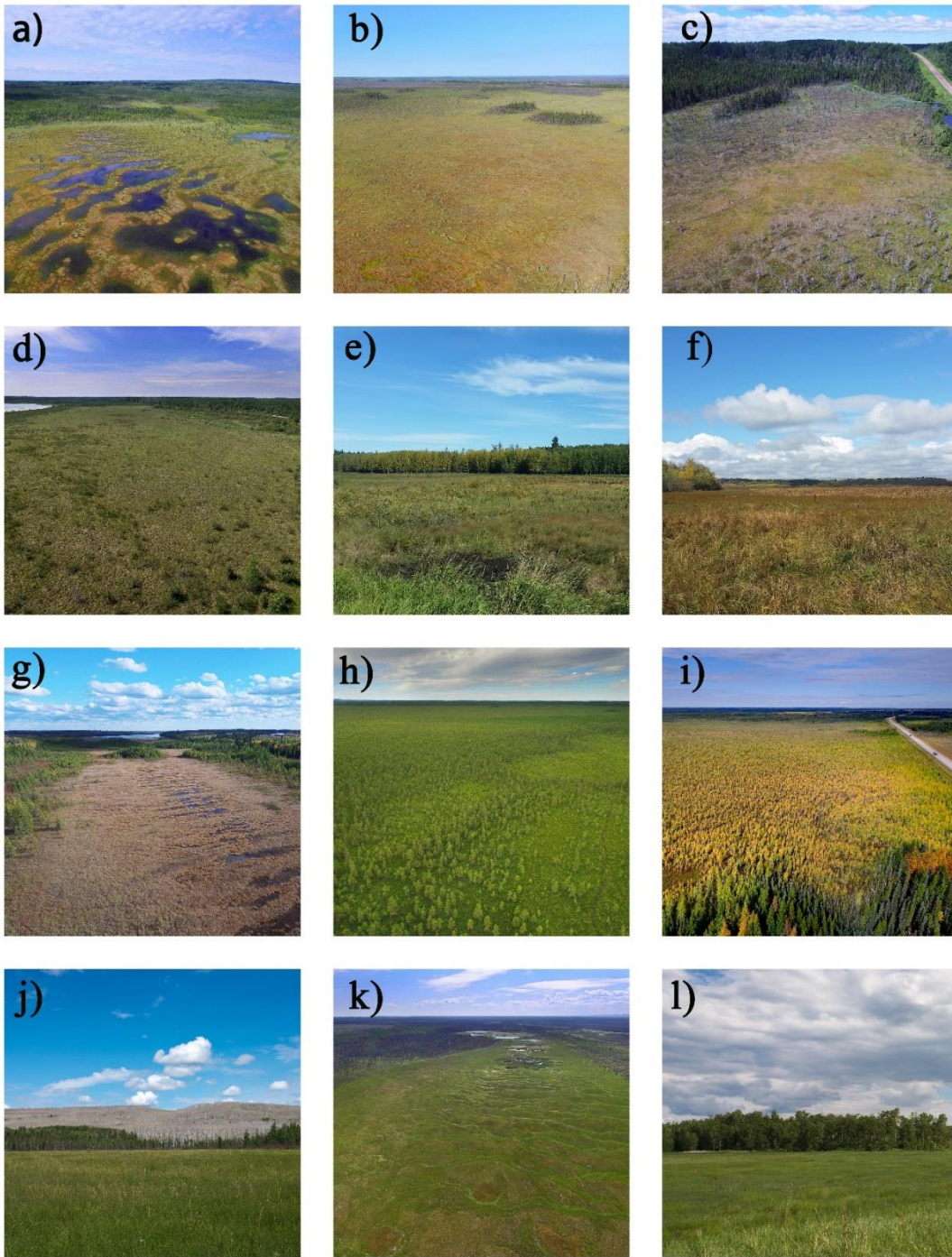


Figure 5.8 Reference wetland photographs. (a) Poor fen 1 [abbrev: PF1], (b) Poor fen 2 [abbrev: PF2], (c) Poor fen 3 [abbrev: PF3], (d) Open moderate-rich fen [abbrev: MRFo], (e) Fresh marsh [abbrev: Mf], (f) brackish marsh [abbrev: Mb], (g) Extreme-rich fen [abbrev: ERF], (h) Wooded moderate-rich fen 1 [abbrev: MRFw1], (i) Wooded moderate-rich fen 2 [abbrev: MRFw2], (j) Saline fen 1 [abbrev: SAL1], (k) Saline fen 2 [abbrev: SAL2], (l) Saline fen 3 [abbrev: SAL3]

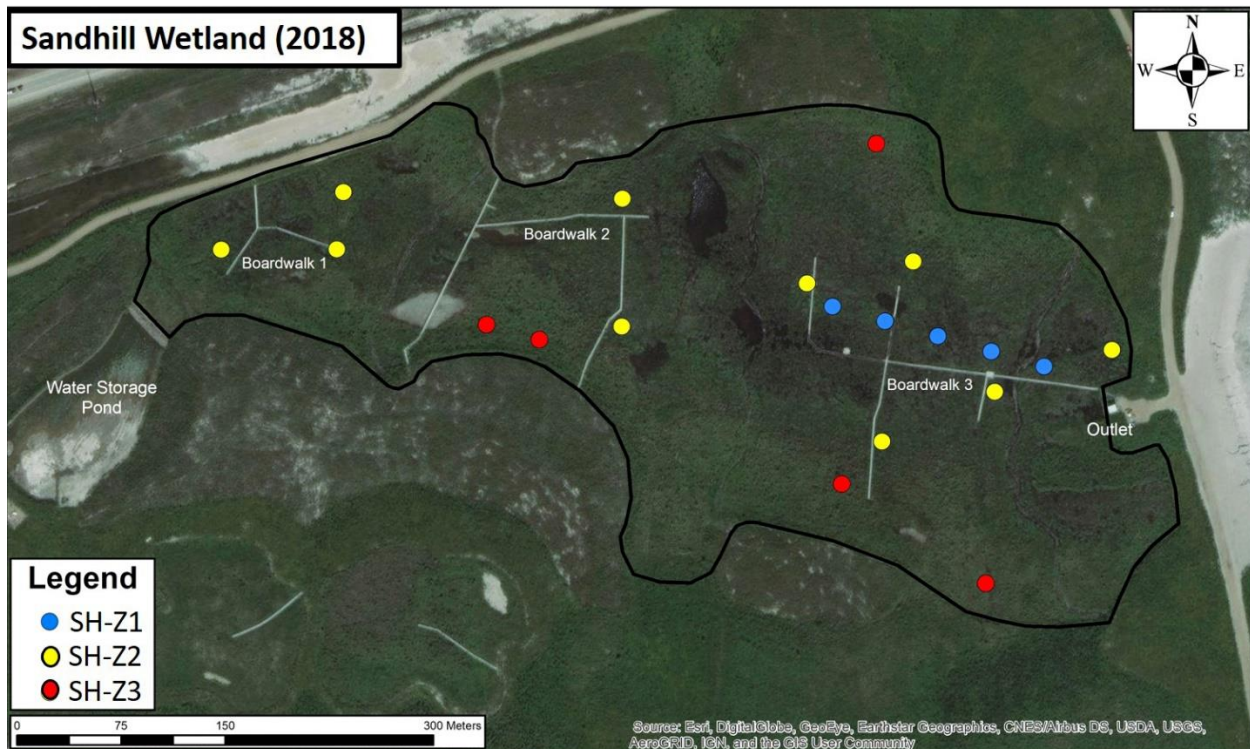


Figure 5.9 Vegetation survey locations across Sandhill Wetland. Research plots were placed across three spatially distinct vegetation assemblages, called zones, previously delineated by Vitt et al., (2016). Abbreviations: SH-Z1 = Sandhill Wetland Zone 1, SH-Z2 = Sandhill Wetland Zone 2, SH-Z3 = Sandhill Wetland Zone 3. The bold black border indicates the wetland area boundary

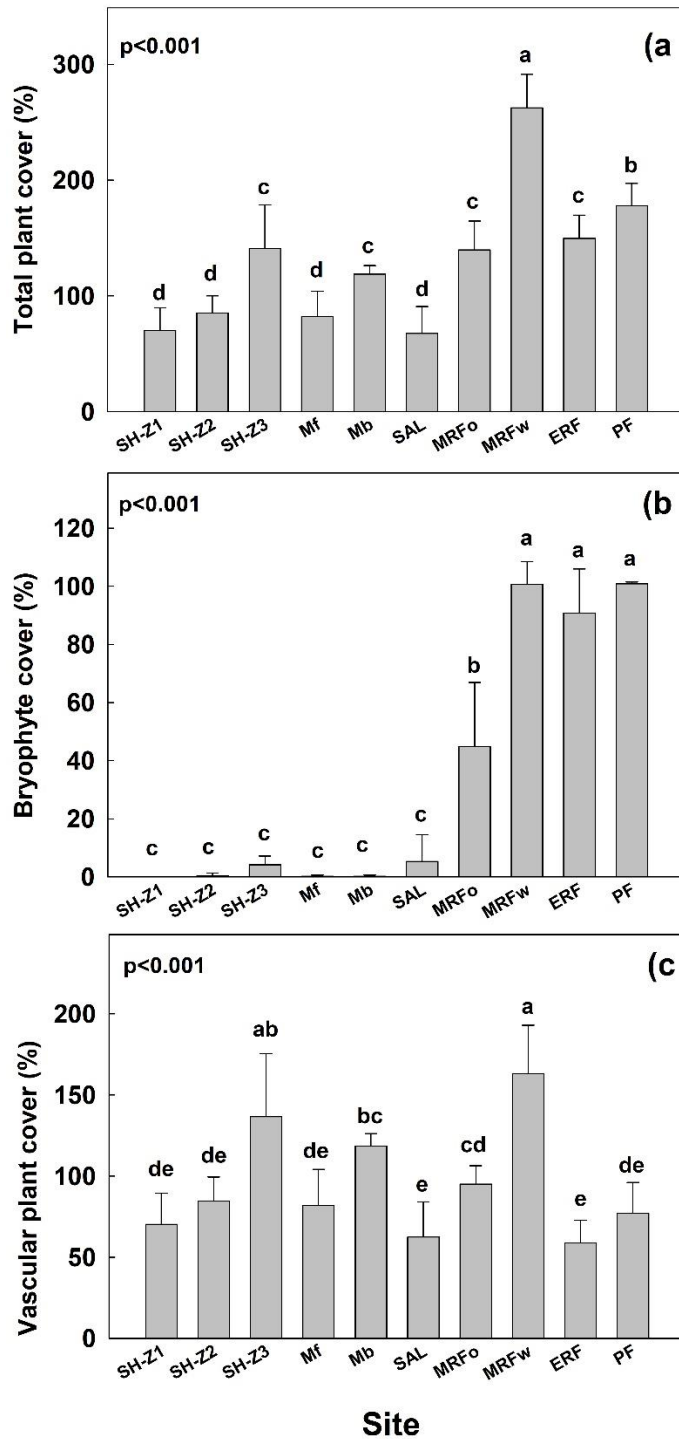


Figure 5.10 Percent plant cover (as canopy cover) \pm standard errors across reference wetlands and Sandhill Wetland. (a) Total cover (vascular plants + bryophytes), (b) total bryophyte cover, (c) total vascular plant cover. Abbreviations: SH-Z1 = Sandhill Wetland Zone 1, SH-Z2 = Sandhill Wetland Zone 2, SH-Z3 = Sandhill Wetland Zone 3, Mf = fresh marsh, Mb = brackish marsh, SAL = saline fen, MRFo = open moderate-rich fen, MRFw = wooded moderate-rich fen, ERF = extreme-rich fen, PF = poor fen

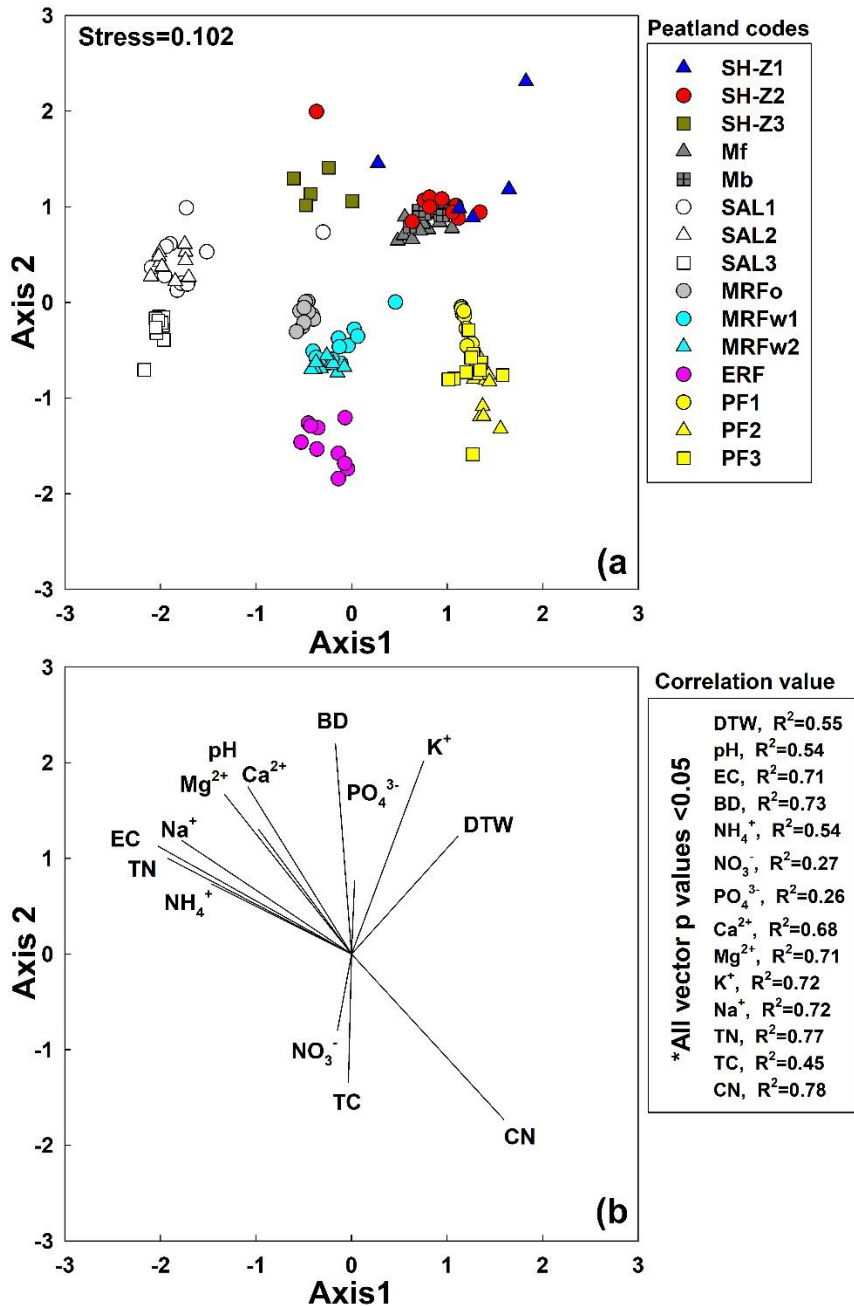


Figure 5.11 (a) NMDS ordination of 140 sampling units and (b) significant environmental vectors ($p < 0.05$). For vector analysis, initial vector segment lengths (i.e., < 1.0 graphing unit) were scaled by a factor of three to match the ordination axes (i.e., 3.0 graphing units). Abbreviations: SH-Z1 = Sandhill Wetland Zone 1, SH-Z2 = Sandhill Wetland Zone 2, SH-Z3 = Sandhill Wetland Zone 3, Mf = fresh marsh, Mb = brackish marsh, SAL = saline fen, MRFo = open moderate-rich fen, MRFw = wooded moderate-rich fen, ERF = extreme-rich fen, PF = poor fen, WTP = water table position (cm^{-1}), BD = bulk density (mg cm^{-3}), TN = total nitrogen, TC = total carbon, CN = carbon/nitrogen ratio. EC = electrical conductivity reduced for H^+ ions (expressed in $\mu\text{S cm}^{-1}$)

Table 5.6 Wetland site locations and elevation. Abbreviations: SH = Sandhill Wetland, PF = poor fen, MRFo = open moderate-rich fen, MRFw = wooded moderate-rich fen, ERF = extreme-rich fen, Mf = fresh marsh, Mb = brackish marsh, SAL = saline fen

Site name	Wetland type	Location	Elevation (meters)
SH	Sandhill Wetland	57°02'25.32" N 111°35'22.61" W	311
PF1	Poor fen	56°22'35.21" N 111°14'09.82" W	743
PF2	Poor fen	55°53'50.14" N 112°05'38.15" W	695
PF3	Poor fen	55°32'17.78" N 112°20'09.48" W	727
MRFo	Moderate-rich fen (non-Wooded)	54°28'28.93" N 113°19'27.80" W	669
MRFw1	Moderate-rich fen (Wooded)	55°40'25.85" N 110°53'35.45" W	565
WMRw2	Moderate-rich fen (Wooded)	55°14'56.96" N 111°19'42.70" W	569
ERF	Extreme-rich fen	56°56'56.52" N 111°31'41.05" W	314
Mf	Fresh marsh	53°39'35.05" N 112°50'54.24" W	720
Mb	Brackish marsh	53°31'25.40" N 112°56'15.93" W	726
SAL1	Saline fen	56°40'45.25" N 111°09'19.72" W	255
SAL2	Saline fen	56°34'24.97" N 111°16'34.14" W	398
SAL3	Saline fen	53°31'21.38" N 112°56'05.73" W	729

Table 5.7 Porewater properties across wetland sites. Data are site means with standard deviations in parenthesis. For nutrients and base cations, units are expressed in mg L⁻¹. Different letters indicate significantly different groups from ANOVA (Tukey's Honest Significant Difference test; p<0.05). Abbreviations: SH-Z1 = Sandhill Wetland Zone 1, SH-Z2 = Sandhill Wetland Zone 2, SH-Z3 = Sandhill Wetland Zone 3, Mf = fresh marsh, Mb = brackish marsh, SAL = saline fen, MRFo = open moderate-rich fen, MRFw = wooded moderate-rich fen, ERF = extreme-rich fen, PF = poor fen, EC = electrical conductivity reduced for H⁺ ions (expressed in μS cm⁻¹)

	pH	EC	Ca	Mg	K	Na	NH₄⁺-N	NO₃⁻-N	P
SH-Z1	8.8 (0.1)a	1674 (84)b	66 (16)de	57.8 (3.0)b	11.1 (1.5)a	220 (38)cd	0.12 (0.05)bc	0.02 (0.02)b	0.02 (0.00)bc
SH-Z2	8.3 (0.3)a	2449 (1248)b	107 (78)cd	66.9 (13.4)b	10.0 (3.8)a	379 (271)bc	0.11 (0.09)c	0.02 (0.007)b	0.04 (0.03)bc
SH-Z3	7.3 (0.4)fg	2825 (866)b	321 (65)a	138.7 (50.3)a	4.7 (3.7)bc	266 (146)cd	0.03 (0.01)c	0.01 (0.00)b	0.03 (0.00)bc
Mf	8.5 (0.4)ab	211 (35)d	37 (11)ef	18.2 (2.1)cd	10.3 (1.0)a	8 (5)f	0.06 (0.02)c	0.01 (0.005)b	0.15 (0.06)ab
Mb	8.4 (0.4)abc	638 (73)c	55 (11)de	27.6 (4.5)c	6.2 (3.1)b	108 (14)d	0.17 (0.06)bc	0.01 (0.005)b	0.22 (0.29)a
SAL1	7.9 (0.4)de	10665 (3301)a	224 (82)ab	162.3 (39.1)a	0.4 (0.2)ef	1918 (535)a	0.12 (0.04)c	0.03 (0.031)b	0.06 (0.04)bc
SAL2	6.9 (0.1)g	12601 (4209)a	159 (50)bc	164.5 (43.6)a	1.5 (0.5)def	2831 (877)a	0.69 (0.24)a	0.02 (0.006)b	0.06 (0.02)bc
SAL3	8.0 (0.2)cde	2093 (733)b	35 (11)ef	5.3 (3.8)f	1.7 (1.1)c-f	654 (102)b	0.29 (0.28)b	0.02 (0.007)b	0.12 (0.04)abc
MRFo	7.7 (0.2)ef	172 (16)de	26 (3)f	14.3 (1.2)d	3.4 (0.4)cd	7 (3)f	0.06 (0.02)c	0.01 (0.005)b	0.02 (0.00)bc
MRFw1	8.1 (0.4)b-e	81 (9)f	7 (4)gh	6.4 (0.7)eg	0.4 (0.3)ef	6 (2)fg	0.04 (0.02)c	0.01 (0.004)b	0.02 (0.01)bc
MRFw2	8.3 (0.5)a-d	93 (11)ef	9 (2)g	7.9 (0.4)e	0.1 (0.0)f	6 (1)fg	0.03 (0.01)c	0.01 (0.003)b	0.01 (0.00)c
ERF	8.6 (0.3)a	302 (40)d	28 (7)f	17.5 (1.6)cd	2.5 (0.6)cde	26 (3)e	0.06 (0.04)c	0.07 (0.064)a	0.01 (0.00)c
PF1	4.1 (0.1)h	12 (4)h	7 (1)gh	1.2 (0.4)g	1.2 (0.4)def	3 (1)g	0.03 (0.01)c	0.01 (0.003)b	0.08 (0.04)bc
PF2	4.0 (0.1)h	9 (4)h	4 (1)gh	0.3 (0.2)h	0.9 (0.8)ef	4 (1)fg	0.05 (0.04)c	0.03 (0.029)b	0.04 (0.01)bc
PF3	4.1 (0.1)h	55 (64)g	7 (1)gh	2.0 (1.5)g	0.8 (0.4)ef	11 (14)fg	0.03 (0.01)c	0.01 (0.004) b	0.02 (0.00)bc

Table 5.8 Physical properties across wetland sites. Data are site means with standard deviations in parenthesis. Different letters indicate significantly different groups from ANOVA (Tukey's Honest Significant Difference test; $p < 0.05$). Abbreviations: SH-Z1 = Sandhill Wetland Zone 1, SH-Z2 = Sandhill Wetland Zone 2, SH-Z3 = Sandhill Wetland Zone 3, Mf = fresh marsh, Mb = brackish marsh, SAL = saline fen, MRFo = open moderate-rich fen, MRFw = wooded moderate-rich fen, ERF = extreme-rich fen, PF = poor fen, WTP = water table position (cm^{-1}), BD = bulk density (mg cm^{-3}), TN = total nitrogen, TC = total carbon, CN = carbon/nitrogen ratio

	WTP	BD	TN	TC	CN
SH-Z1	32 (15)a	264 (115)a	1.1 (0.5)gh	28 (10)d	25 (2)de
SH-Z2	9 (17)bc	285 (104)a	1.1 (0.3)h	25 (8)d	23 (3)de
SH-Z3	-41 (4)h	317 (50)a	1.2 (0.4)fgh	29 (10)d	23 (2)def
Mf	31 (6)a	85 (16)cde	2.5 (0.1)cd	47(1)ab	19 (1)def
Mb	15 (7)b	150 (28)b	2.9 (0.2)bc	42 (2)abc	15 (1)ef
SAL1	-4 (4)def	145 (34)bc	3.2 (0.7)ab	39 (7)c	12 (1)f
SAL2	-15 (3)fg	103 (16)bcd	3.2 (0.2)ab	45 (1)abc	14 (1)ef
SAL3	-30 (8)h	143 (23)bc	3.4 (0.3)a	43 (1)abc	13 (1)f
MRFo	4 (7)bcd	66 (10)def	2.1 (0.2)de	47 (1)ab	23 (2)de
MRFw1	-17 (7)g	29 (5)ef	1.1 (0.3)h	40 (4)c	38 (11)c
MRFw2	0 (7)cde	22 (4)f	1.8 (0.5)ef	43 (2)abc	27 (9)d
ERF	-4 (2)def	53 (10)def	1.7 (0.2)efg	41 (3)bc	34 (3)de
PF1	-10 (4)efg	41 (8)ef	0.9 (0.2)h	47 (1)ab	54 (8)b
PF2	-11 (5)efg	29 (5)ef	0.7 (0.2)h	48 (1)a	67 (13)a
PF3	-6 (4)def	29 (6)ef	0.8 (0.1)h	47 (1)ab	64 (10)a

Table 5.9 Total species cover at reference wetlands vs desirable species cover at Sandhill Wetland for specific wetland types. Values are means with standard deviations in parenthesis

REFERENCE WETLANDS	AVG TOTAL SP. COVER	AVG DESIRABLE SP. COVER
Acid fen	178 (19)	32 (26)
Circumneutral fen	223 (66)	63 (25)
Alkaline fen	150 (20)	0 (1)
Sodic fen	69 (23)	1 (3)
Marsh	101 (25)	74 (17)

Table 5.10 Diversity indices across wetland sites. Reported values are means and standard deviations in parenthesis where applicable. Abbreviations: SH-Z1 = Sandhill Wetland Zone 1, SH-Z2 = Sandhill Wetland Zone 2, SH-Z3 = Sandhill Wetland Zone 3, Mf = fresh marsh, Mb = brackish marsh, SAL = saline fen, MRFo = open moderate-rich fen, MRFw = wooded moderate-rich fen, ERF = extreme-rich fen, PF = poor fen. Values in red represent diversity indices for desirable species only at Sandhill Wetland

SITE	Alpha	Beta	Gamma
SH-Z1	3.4 (1.1)	2.7	9
SH-Z2	4.8 (2.1)	4.6	22
SH-Z3	14.4 (3.4)	2.4	34
Pooled SH	6.9 (5.1)	6.5	44
<i>SH-Z1</i>	<i>3.0 (0.7)</i>	<i>2.0</i>	<i>6</i>
<i>SH-Z2</i>	<i>2.9 (1.0)</i>	<i>4.5</i>	<i>13</i>
<i>SH-Z3</i>	<i>7.8 (2.0)</i>	<i>2.4</i>	<i>19</i>
<i>Pooled SH</i>	<i>4.0 (2.7)</i>	<i>6.3</i>	<i>25</i>
Mf	6.7 (1.5)	2.2	15
Mb	5.4 (1.8)	2.4	19
SAL1	6.6 (1.3)	2.7	18
SAL2	4.6 (0.8)	2.0	9
SAL3	5.0 (0.7)	2.2	11
Pooled SAL	5.4 (1.3)	5.7	31
MRFo	12.2 (1.9)	1.8	22
MRFw1	21.3 (3.2)	1.9	41
MRFw2	22.1 (2.6)	2.0	44
Pooled MRF	21.7 (2.8)	2.7	58
ERF	12.1 (2.4)	2.1	25
PF1	10.8 (1.6)	2.0	22
PF2	12.1 (1.1)	1.5	18
PF3	10.9 (1.4)	1.8	20
Pooled PF	11.3 (1.5)	2.8	31

Table 5.11 Mean similarity between/ within groups. Within group similarity in bold text. Abbreviations: SH-Z1 = Sandhill Wetland Zone 1, SH-Z2 = Sandhill Wetland Zone 2, SH-Z3 = Sandhill Wetland Zone 3, Mf = fresh marsh, Mb = brackish marsh, SAL = saline fen, MRFo = open moderate-rich fen, MRFw = wooded moderate-rich fen, ERF = extreme-rich fen, PF = poor fen

SITE	SH-Z1	SH-Z2	SH-Z3	Mf	Mb	SAL	MRFo	MRFw	ERF	PF
SH-Z1	38.15									
SH-Z2	34.14	50.35								
SH-Z3	13.14	14.30	54.47							
Mf	25.91	49.62	7.13	61.69						
Mb	19.03	42.44	4.23	52.70	74.79					
SAL	0.65	1.14	1.43	1.33	1.18	41.42				
MRFo	0.00	0.02	0.36	5.91	0.60	1.11	56.29			
MRFw	1.37	2.23	1.43	5.81	2.55	1.11	26.88	48.53		
ERF	0.00	0.05	0.67	0.07	0.05	0.65	3.85	13.61	46.25	
PF	3.66	5.37	1.35	5.85	5.36	0.18	0.01	6.54	2.79	48.98

5.5 A Wetland Monitoring Approach for Evaluating Reclamation Performance and Guiding Adaptive Management

Introduction: Since initial site flooding in year 2012, the wetland portion of the constructed watershed (i.e., Sandhill Wetland) has persisted, albeit requiring management to maintain a desired water table position . While after six growing seasons Sandhill Wetland exhibits many aspects resembling those of regional natural wetlands in some areas (Hartsock et al. 2016; Vitt et al. 2016; Biagi et al. 2019; Clark et al. 2019; Hartsock et al. 2019 in review), no officially recognized protocols exist for evaluating the success of the reclamation. Officially recognized assessment protocols that inform reclamation success are greatly needed. Further, evaluation protocols that inform adaptive management also are necessary to prevent succession towards undesirable outcomes. While multivariate analyses are arguably the most effective for organizing and visualizing multidimensional attributes of wetlands (González and Rochefort 2019), disadvantages of utilizing multivariate techniques for wetland evaluations and for guiding adaptive management are apparent. Notably, complications with results interpretation (primarily amongst non-academic personal) diminish the effectiveness of implementing multivariate protocols for wetland performance evaluations often conducted and (or) interpreted by individuals having limited statistical background. Relying on multivariate tools for wetland evaluations may ultimately provide greater value to academics, rather than oil sands operators and stakeholders charged with managing reclaimed lands.

Here, using Sandhill Wetland as a test site, we propose a novel, user-friendly, non cost prohibitive approach for evaluating site performance of a recently reclaimed wetland. From a relatively easy to obtain suite of environmental performance measures obtained from 12 mature reclamation relevant wetlands (3 poor fens, 3 moderate-rich fens, 1 extreme-rich fen, 3 saline fens, and 2 marshes), we capture the ranges of key environmental thresholds that drive plant community structure and infer ecosystem functioning. Based on overlap of key environmental thresholds between the natural sites and Sandhill Wetland, our early diagnostic monitoring strategy will reveal the type of wetland to which Sandhill Wetland is most equivalent, infer wetland performance, and moreover assist guiding adaptive management to increase chances of reclaiming towards an attainable target.

Methods: Phase I – Selecting realistic reclamation endpoint target. In order to expedite succession towards wetlands that perform equivalently to natural systems, it makes logical sense to reclaim towards attainable wetland targets based upon early evaluation of initial site conditions (e.g., physical and chemical aspects). However, protocols that clearly inform the type of wetland to reclaim towards are lacking for some reclamation relevant systems. Early works from pioneer peatland ecologists G. E. DuRietz and Hugo Sjörs were among the first to delineate between boreal fen types using vegetation indicators and porewater properties, respectively. Moreover, it was demonstrated that peatland plant communities and porewater chemistry patterns are fundamentally linked peatland aspects (Vitt and Chee 1990). It is difficult to dispute that for many wetland types (e.g., acid, circumneutral, and alkaline fens) porewater pH and vegetation indicators remain the most useful for discerning between systems and inferring ecosystem functioning. For some reclamation relevant wetlands such as marshes and sodic fens; however, porewater pH can overlap with circumneutral and alkaline fens (Hartsock and Bremer 2018; Hartsock et al. 2019), thereby convoluting the decision-making process for deciding which type of wetland to reclaim towards. To ensure an appropriate reclamation target analogue is selected, additional porewater properties besides pH alone must be considered. In addition to porewater pH levels, our endpoint target selection protocol incorporates porewater nutrient concentrations (NPK) and sodium concentrations to accommodate marsh and sodic fens into the wetland target selection process, respectively. We also utilize water table position as a physical performance measure and wetland delineation factor (due to the importance water table position on several wetland functions) to provide further resolution for making endpoint target decisions. Cumulatively, our proposed protocol for establishing reclamation endpoint targets incorporates evaluating key aspects of water chemistry, plant community structure, and water table position to make logical reclamation outcome decisions.

Environmental sampling methods. In year 2018, the Sandhill Wetland test site and 12 mature reference wetlands were surveyed to characterize important performance measures necessary for conducting our proposed reclamation site performance assessment. At each reference site ten environmental monitoring plots were established randomly along transects at approximate equidistant intervals. At Sandhill Wetland, 20 research plots were established within the wetland area (Fig. 5.12). Efforts were made to capture clear variation along a previously established high to low water table position continuum (Vitt et al. 2016; Hartsock et al. 2019 in review). At all sites, porewater samples and water table position measurements (distance from the vegetation ground layer) were obtained at each plot. Porewater samples were analyzed for primary nutrients, base cations, temperature adjusted pH and reduced EC (Sjörs 1950). In order to assess plant community structure, and moreover, determine bryophyte abundance (an important criterion for wetland delineations) plant surveys were conducted across all wetlands in late July (year 2018).

Phase I protocol. Using descriptive statistics, we present means (\pm standard deviations) for our nine measured performance and wetland delineation indices obtained at natural reference sites and Sandhill Wetland (Table 5.12). A reclamation target endpoint should be selected based upon the natural analogue to which a reclaimed area shares the most environmental overlap with (see Table 5.13). Lastly, for instances where reclaimed areas exhibit minimal overlap with natural wetlands, professional judgement should determine whether alternative endpoint targets (such as upland/riparian systems) should be considered as more realistic reclamation outcomes. *Appendix 5.1 provides a blank scorecard template for completing Phase I reclamation target selections.

Phase II – Assessing reclamation performance through “threshold cube” modeling. Following Phase I endpoint target selection, Phase II assessments place more weight on the presence and abundance of desirable wetland plant species at a reclamation site. The structural attributes characteristic of specific wetland types are disproportionally important, and largely responsible for influencing wetland functions. Overall, reestablishing desirable plant species assemblages characteristic of the selected endpoint target (in addition to restoring other key performance parameters) will be necessary to achieve reclamation success.

In Phase II, our protocol is built upon interpreting overlap between ‘threshold cubes’ generated from key environmental performance measures obtained at the reclamation site being evaluated and from the endpoint target selected. For acid, circumneutral, and alkaline fen targets, the key x, y, z performance measures used to generate threshold cubes include: Porewater pH, percent desirable species cover, and water table position, as these parameters are critical for restoring ecosystem functions among the aforementioned systems. For sodic fens, porewater sodium concentration was substituted for pH. For marshes, due to elevated porewater nutrient and sodium concentrations in select cases, porewater (NPK + Na) concentrations were substituted for pH. The rationale for substituting alternative porewater parameters for sodic fen and marsh wetland targets centers on incorporating properties that we deem more important than pH for influencing succession trajectories in these systems. Of note, desirable plant species lists specific to each wetland type (for regional wetlands) are displayed in Appendices 5.2–5.6 and plant species encountered at Sandhill Wetland are shown in Appendix 5.7.

Performing the evaluation. In practice, in order to view the range of variation exhibited by the measured x, y, z performance measures, 3-D scatter plots firstly were generated using the program SigmaPlot. Environmental threshold cubes subsequently were generated by calculating the mean $\pm 2x$ standard deviation for each x, y, z wetland performance measure (specific to each wetland type) (Gonzalez and Rochefort 2019). At the intersections of each calculated maximum and minimum value for each x, y, z environmental performance parameter, threshold cubes were superimposed around the measured x, y, z variables. In cases where calculated thresholds fell outside of ‘real-world’ observations (i.e., desirable plant cover <0.0 %) we adjusted threshold cubes to remain ecologically relevant. Calculation of threshold cube overlap and lack of overlap (overlapping volume expressed as a percent) between the natural reference analogue and reclamation site provided an encompassing inference of reclamation site performance, and moreover could serve as an index of equivalent land capability. Lastly, reclamation site sampling locations falling outside of reference analogue threshold cube space should be noted for guiding adaptive management in areas exhibiting properties dissimilar from the reference condition. In extreme cases, outlier plots should be omitted from the analyses (using professional judgement) to prevent incorporating non-wetland areas into the performance evaluation model.

Results: Sandhill Wetland performance evaluation - Phase I assessment. In the sixth growing season, of the nine performance metrics measured, environmental overlap occurred most frequently between Sandhill Wetland and the marsh-type wetlands (8 of 9), followed by the sodic and circumneutral fens (5 of 9), alkaline fen (4 of 9), and lastly the acid fens (3 of 9) (Table 5.13). Based upon our Phase I assessment protocol, environmental aspects at Sandhill Wetland are most representative of marshes in the sixth year since initiation, and therefore a marsh-like analogue should be considered as the most realistic endpoint target based upon current site conditions.

Phase II assessment. Following completion of Phase I endpoint target selections, Phase II comparisons should only occur between the reclamation site being evaluated and the selected endpoint target - a marsh in our case. Phase II evaluations between Sandhill Wetland and marshes (a slightly brackish marsh (abbreviation: **mb**) and a fresh marsh (abbreviation: **mf**)) displayed a relatively high degree of threshold cube volume overlap. Extant environmental conditions at Sandhill Wetland (across all 20 research plots) overlapped with 57% of the marsh threshold cube (Fig. 1). Marsh plant species exhibiting the highest cover at Sandhill Wetland include the sedge *Carex aquatilis*, the forb *Typha latifolia*, and the grass *Calamagrostis canadensis*. We acknowledge that *Typha latifolia* and *Calamagrostis canadensis* are less desirable than peat-forming sedges; however, the aforementioned species are indeed present within some regional marshes (see Bayley and Mewhort 2004; Whitehouse and Bayley 2005). Of note, the total volume of Sandhill Wetland threshold cube is approximately tenfold larger than the marsh cube. Out of 4,871,704 cubic units making up the Sandhill Wetland threshold cube volume, only 272,832 cubic units overlap with the marshes. Thus, although Sandhill Wetland is most similar to marshes at its current developmental stage, about 94% of the reclamation site’s threshold cube volume falls outside of typical marsh conditions. The key area of

environmental dissimilarity between the reclamation site and the marshes centers on low water table position across select sampling areas at Sandhill Wetland.

In the methods section, we discussed the potential need for removing extreme outliers that may affect wetland performance interpretations. In a previous study at Sandhill Wetland, Vitt et al. (2016) revealed four distinct plant species assemblages, or zones, that sorted differently across the projected wetland area boundaries. Because marshes exhibit relatively high water levels, based on our professional knowledge of boreal wetlands we amended our original Phase II assessment of the Sandhill Wetland threshold cube by removing six survey plots with water tables below the soil surface; a general characteristic of wetland meadows or uplands (*water tables among the six plots omitted ranged from -7.0->-40.0 cm). For a spatial reference, we superimposed our wetland performance survey plot localities above the distinct zones from Vitt et al. (2016) (Fig. 5.13). In short, five of the six plots omitted from our amended Phase II assessment were localized in areas categorized as upland/riparian-like (Zone 3 plots) whereas the sixth omitted plot was located in slightly disturbed circumneutral-fen-like area (Zone 2 plots). Our alternative assessment based upon a reduced sample size showed that areas at Sandhill Wetland with water tables above the soil surface were quite similar to the marsh reference sites (Fig 5.14). The alternative Sandhill Wetland environmental threshold cube using 14 plots occupied only 28% of the original volume generated from using 20 survey plots. Moreover, the amended threshold cube boundaries reside considerably nearer to the marsh threshold conditions. Although 85% of the remodeled Sandhill Wetland threshold cube volume remains outside of marshes, less extreme management adjustments are likely required to assist succession towards a marsh target endpoint. Overall, here we show two general landform types exist within the originally projected wetland area boundaries of the reclamation site, a marsh-like analogue in the central area with water table position above the soil surface surrounded by an upland/riparian/wetland meadow environment. Based on the amended Phase II assessment using appropriate survey plots to remove potentially confounding areas, we show succession towards a slightly brackish marsh endpoint target is potentially achievable.

Evaluation of the threshold cube performance assessment protocol- Pros and cons. While the restoration of all wetland functions may require several decades, some important wetland attributes can recover quickly such as reestablishment of desirable peatland plants, water chemistry characteristics, and important functions such as carbon sequestration. The reclamation protocol presented here is to be used for evaluating reclamation performance at relatively recently reclaimed sites, for guiding adaptive management, and deciding whether a site is on a trajectory to meet equivalent land capability. We acknowledge our reclamation performance protocol indeed has many positive qualities for making meaningful site evaluations, yet, the protocol is far from perfect.

Beginning with the positive aspects, here we provide a comprehensive compilation of important environmental characteristics (and their ranges) exhibited by several reclamation relevant regional wetlands. Using the information provided in Tables 5.12-5.14; Appendices 5.1-5.7 other researchers will be able to perform reclamation assessments using our suggested protocol. Our site evaluation protocol is not based on multivariate analyses, and thereby should be straightforward to repeat, and easily comprehended by individuals having minimal background in statistics. Apart from conducting vegetation surveys at future reclamation sites, all properties required to complete the threshold cube wetland evaluation protocol are relatively simple and non-cost prohibitive parameters to measure.

Inadequacies of our evaluation protocol perhaps center on researcher bias towards the performance measures selected, yet all selected wetland performance parameters have been used previously for delineating between wetland types and inferring ecosystem functioning (Vitt et al. 2011; Environment and Parks 2015). It is impossible and counterproductive to measure every wetland property for characterizing performance, and we feel our chosen parameters are adequate for making meaningful performance evaluations. The 2x standard deviation values used for threshold cube modeling are controversial; however,

similar protocols were used by Gonzelez and Rochefort (2019) for evaluating restoration success at several cut-over peatland sites. Major shortcomings of our protocol include 1) many wetland researchers are not skillful at identifying wetland plants (especially bryophytes) and 2) our threshold cube procedure relies on additive abundance of desirable plant species. Thus, even species poor reclamation sites have potential to exhibit high desirable species cover scores. For example, the Sandhill Wetland exhibited high cover of the sedge *Carex aquatilis* (a desirable species for acid fens, circumneutral fens, and marshes), thus, although species composition dissimilarities between acid fens and the reclamation site were quite apparent during the vegetation survey, Sandhill Wetland appeared to exhibit high cover of desirable acid fen species due to the presence and high abundance of *C. aquatilis* cover. Nevertheless, combining other environmental aspects for threshold cube construction was successful for demonstrating Sandhill Wetland is indeed highly dissimilar (0.0% threshold cube overlap) from acid fens. Some reclamation efforts may require spatial splitting should select areas exhibit markedly different properties (i.e., areas of OSPW upwelling). Professional judgement should be used for the spatial splitting of reclamation sites, which clearly benefited our performance evaluation at Sandhill Wetland following removal of six plots located in areas exhibiting low water table position.

Importance of early adaptive management - what we already know. No matter how much foresight and effort are directed towards reclaiming landscapes on mineral surface leases, even the most thorough watershed design plans will likely require some management during early reclamation stages, namely, soil moisture management across areas slated for wetland development. In the wetland restoration/reclamation literature consequences resultant from failing to manage hydrologic aspects are discussed ad nauseum. At the experimental Sandhill Wetland, considerable management efforts have centered on stabilizing water tables and maintaining water table position at appropriate levels. Despite management efforts; however, spatial water table patterns are not uniform across the wetland boundaries. In general, areas exhibiting exceptionally high and low water tables are dominated plant species uncommon in peatlands. Areas at Sandhill Wetland exhibiting water table position more representative of reference wetlands contain species assemblages comprised of more desirable species, many of which are peat-forming. The importance of establishing stable water tables at appropriate levels early on in the reclamation process is vital to facilitate succession towards desirable wetland outcomes. Further, due to inevitable interactions with OSPW, mitigating or simply allowing intrusion of OSPW into reclaimed areas should be considered. As demonstrated from our analysis, sodium concentrations are quite high at Sandhill Wetland; however, halophytic species fortunately are present sporadically across some areas of the wetland. Should salinity continue increasing to reach threshold levels that affect glycophytic plant species performance, there is potential for halophytic species to replace these sodium sensitive plants in later years. Coping with OSPW affected materials will likely remain a challenge at future reclamations on oil sands mineral surface leases.

Significant findings: The challenges of developing standardized reclamation performance evaluation protocols are numerous. Further, the overall perception of reclamation success may vary considerably among specific parties. Because of conflicting viewpoints among oil sands operators, academic consultants, and governmental agencies regarding how similar reclaimed lands should reflect natural wetlands, reaching a consensus on the standards required to achieve reclamation certification is also a hot button issue. Nevertheless, here we demonstrate the practicality of using a novel, threshold cube approach for appropriately guiding adaptive management and evaluating reclamation performance at a recently reclaimed wetland. Based upon our Phase I assessment protocol, environmental aspects at Sandhill Wetland are most representative of marshes in the sixth year since initiation, and therefore a marsh-like analogue should be considered as the most realistic endpoint target based upon current site conditions. From structural and chemical standpoints, the reclamation site was clearly different from acid, and alkaline fens, yet moderately different from circumneutral and sodic fens. For Phase II assessments, following omission of sampling areas exhibiting water table position below the soil surface where plant assemblages are more indicative of mesic uplands, riparian systems or wetland meadows, environmental conditions at Sandhill Wetland test site were about 15% equivalent to two regional marsh reference sites (based on

threshold cube overlap). In general, characteristic marsh plant species were present, often at relatively high abundances. In addition, many areas across the reclamation site exhibited water table position quite similar to regional marshes. The majority of environmental dissimilarity between Sandhill Wetland and marshes was attributed to elevated porewater sodium concentrations at the reclamation site. Whether porewater sodium levels will attenuate over subsequent years is uncertain. Overall, select areas across the reclamation site, namely in the center of the projected wetland area appear to be performing quite well. Performance of the peripheral areas; however, are tracking towards endpoint targets dissimilar from the reference wetlands monitored here. The threshold cube wetland performance protocol was effective for providing a holistic assessment of Sandhill Wetland test site.

Table 5.12 Wetland characteristics by site type for completing Phase I reclamation target endpoint selections. Values are site means ± standard deviations. All porewater values are in mg/L units unless specified otherwise. Abbreviations: EC = electrical conductivity, N = nitrogen, P = phosphorus, K = potassium, Na = sodium, WTP = water table position, positive values indicate water levels above the soil surface whereas negative values are below the soil surface

Peatland Type	ACID FEN (n=30)	CIRCUM-NEUTRAL FEN (n=30)	ALKALINE FEN (n=10)	SODIC FEN (n=30)	MARSH (n=20)	SANDHILL WETLAND (n=20)
<i>Porewater properties</i>						
pH	4.0 (0.01)	8.0 (0.4)	8.6 (0.3)	7.6 (0.5)	8.5 (0.4)	8.3 (0.7)
Reduced EC (µS/cm)	25.2 (41.6)	115.4 (42.8)	301.7 (40.3)	8317 (5580) 1801	424.6 (225.9)	2260 (987.5) 288.6
Sodium Inorganic nitrogen	5.7 (8.3) 0.05 (0.04)	6.2 (1.9) 0.05 (0.02)	25.5 (2.7) 0.13 (0.10)	(1075) 0.39 (0.32)	57.7 (52.3) 0.13 (0.07)	(192.2) 0.10 (0.08)
Phosphorus	(0.04)	0.02 (0.00)	0.01 (0.00)	0.08 (0.04)	0.18 (0.21)	0.03 (0.03)
Potassium	1.0 (0.6)	3.2 (2.4)	2.5 (0.6)	1.2 (0.9) 1802	8.2 (3.1)	9.0 (4.2) 288.8
NPK + Na	5.8 (8.3)	6.3 (1.9)	25.6 (2.6)	(1075)	58.0 (52.4)	(192.2)
<i>Physical characteristics</i>						
WTP (cm)	-9.1 (4.8)	-4.6 (11.6)	-4.0 (2.2)	-16.2 (12.0)	22.6 (10.5)	3.9 (30.4)
Moss cover	>90% cover of Sphagnum mosses	>90% cover of True mosses	>90% cover of mosses	>10% cover of True mosses	>10% cover of True mosses	>10% cover of True mosses

*Reduced electrical conductivity has been corrected to remove the influence of H⁺ ions.

Table 5.13 Phase 1 assessment scorecard demonstrating performance measure overlap between Sandhill Wetland test site and natural wetlands. Sandhill Wetland values are site means ± standard deviations. All porewater values are in mg/L units unless specified. Abbreviations: EC = electrical conductivity, N = nitrogen, P = phosphorus, K = potassium, Na = sodium, WTP = water table position. EC = electrical conductivity, N = nitrogen, P = phosphorus, K = potassium, Na = sodium, WTP = water table position

Peatland Type	ACID FEN	CIRCUM-NEUTRAL FEN	ALKALINE FEN	SODIC FEN	MARSH	SANDHILL WETLAND Performance measure ranges
<i>Porewater properties</i>						
pH		X	X	X	X	8.3 (0.7)
Reduced EC (µS/cm)				X		2260 (987.5)
Sodium					X	288.6 (192.2)
Inorganic nitrogen	X	X	X		X	0.10 (0.08)
Phosphorus	X	X	X	X	X	0.03 (0.03)
Potassium		X			X	9.0 (4.2)
NPK + Na					X	288.8 (192.2)
<i>Physical characteristics</i>						
WTP (cm)	X	X	X	X	X	3.9 (30.4)
Moss cover				X	X	>10% cover of True mosses
TOTALS	3	5	4	5	8	

*Reduced electrical conductivity has been corrected to remove the influence of H⁺ ions.

Table 5.14. Total species cover at reference wetlands and desirable species cover at Sandhill Wetland for specific wetland types. Values are means with 2x standard deviations in parenthesis

REFERENCE WETLANDS	AVG TOTAL SP. COVER	AVG DESIRABLE SP. COVER
Acid fen	178 (39)	32 (52)
Circumneutral fen	223 (131)	63 (49)
Alkaline fen	150 (40)	0 (2)
Sodic fen	69 (45)	1 (5)
Marsh	101 (50)	74 (33)

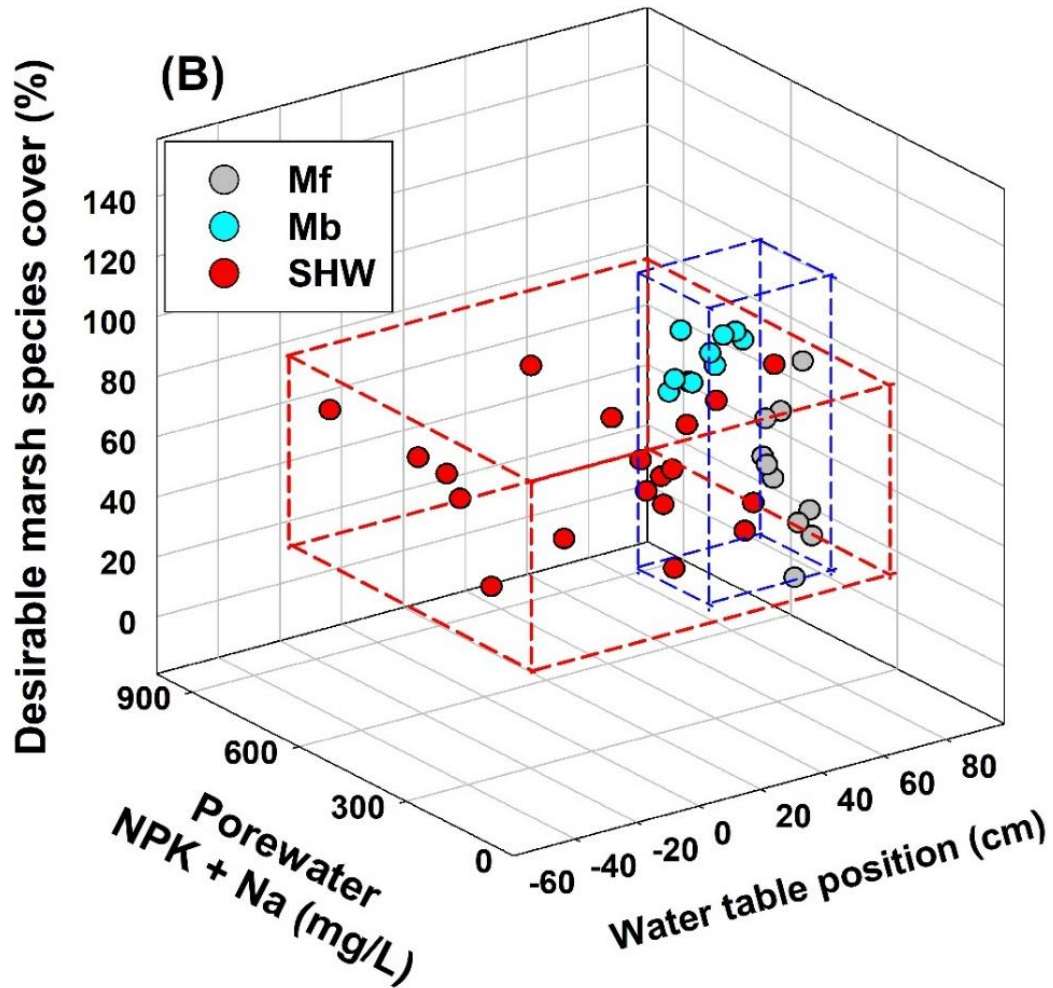


Figure 5.12 Threshold cubes for two marshes that include a slightly brackish marsh (Mb) and a fresh marsh (Mf) compared against Sandhill Wetland (SHW) using 20 research plots

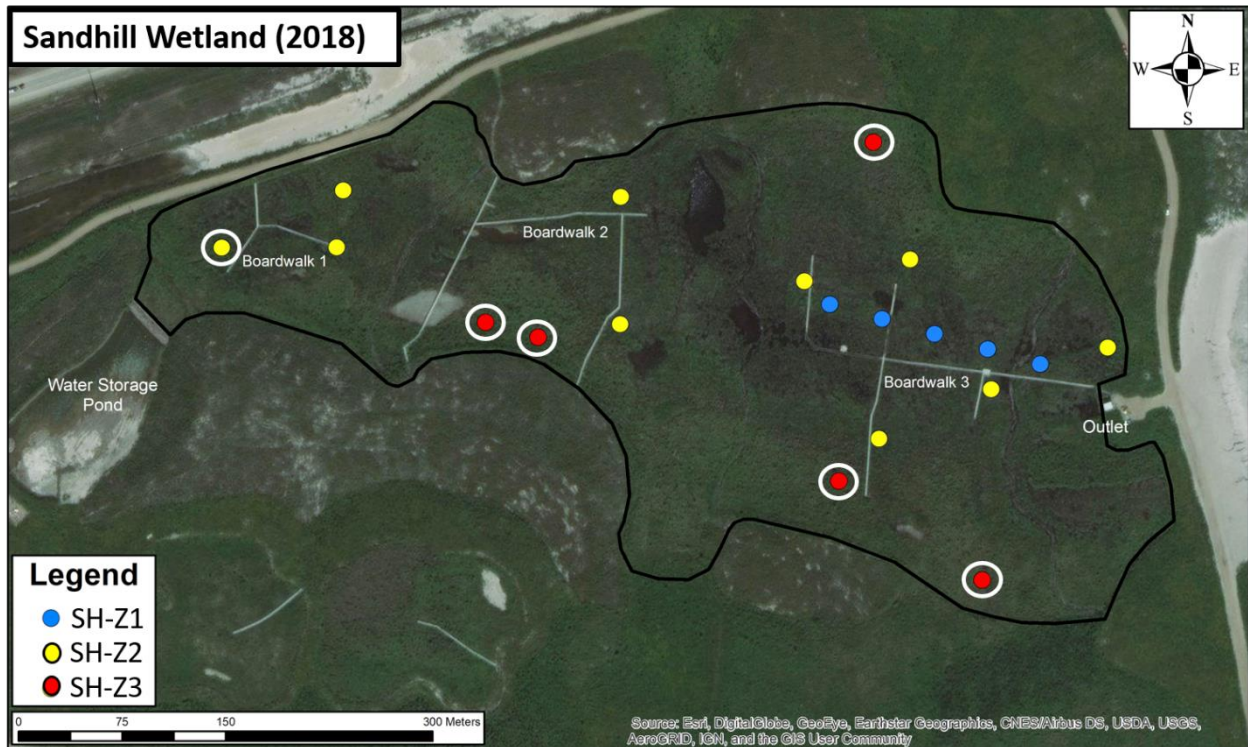


Figure 5.13 Performance assessment research plot locations across Sandhill Wetland superimposed above 3 distinct plant assemblage zones (Zones 1 – 3) from Vitt et al. (2016). Abbreviations: SH-Z1 = Sandhill Wetland Zone 1 (high water table position areas characterized by high abundance of the forb *Typha latifolia* and open water), SH-Z2 = Sandhill Wetland Zone 2 (intermediate water table position areas characterized by circumneutral fen species), SH-Z3 = Sandhill Wetland Zone 3 (low water table position areas with mesic upland plant species). The bold black border indicates the originally projected wetland area boundaries. For amended Phase II assessments, circled plots were removed from the analysis

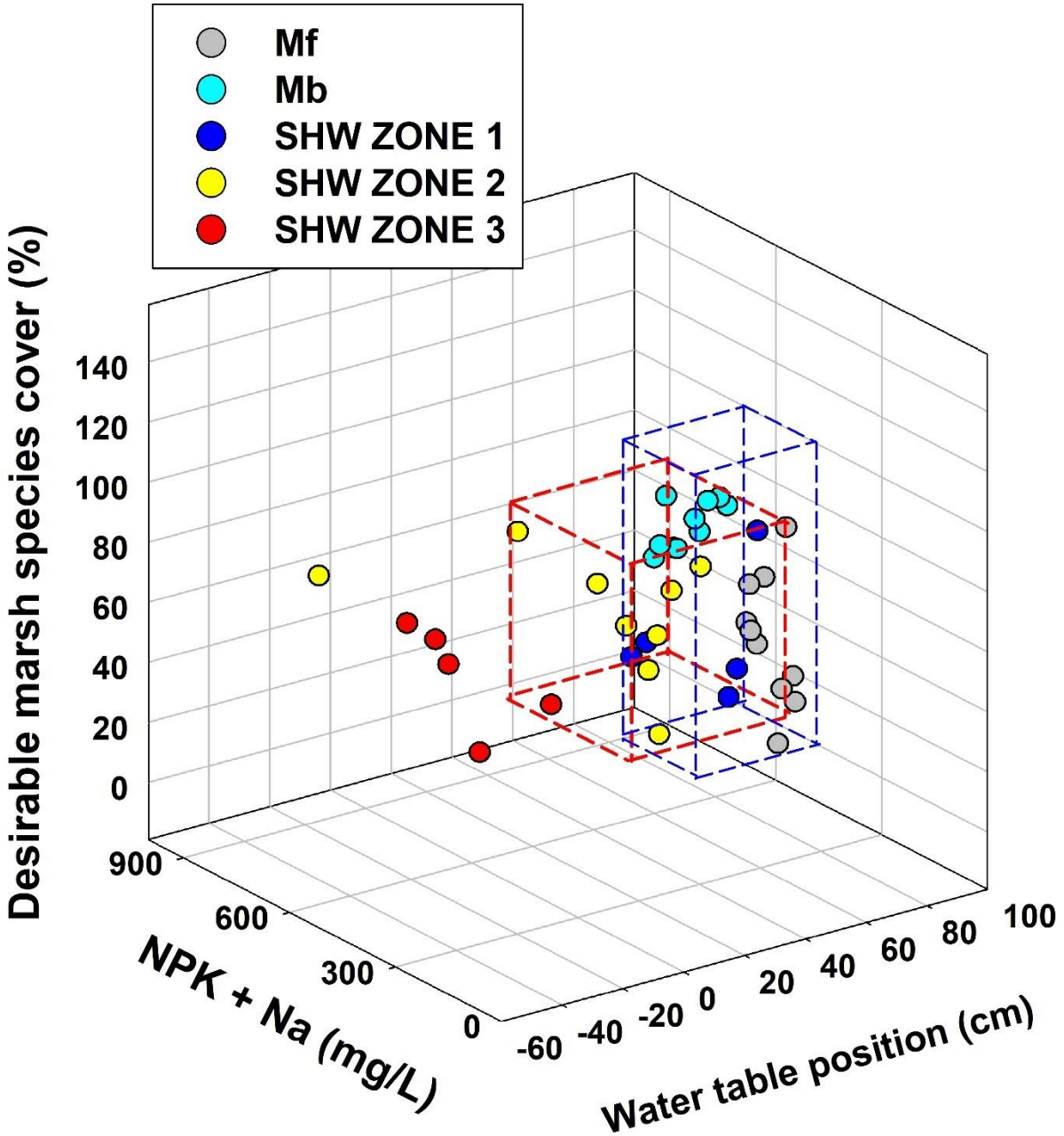


Figure 5.14 Threshold cubes for two marshes that include a moderately brackish marsh (Mb) and a fresh marsh (Mf) compared against the alternative Sandhill Wetland (SHW) threshold cube (following removal of six survey plots exhibiting water table position below the soil surface that included a single Zone 2 plot in yellow, and five Zone 3 plots in red). Zones 1 – 3 correspond to sampling areas previously established by Vitt et al., (2016). In short, Zones 1 – 3 correspond to areas with plant species assemblages that sorted differently consequent of changes in spatial water table position, which decreased from Zone 1 → .

6 Conclusions Between 2016 and 2019 (4 field seasons) we sampled a variety of environmental and vegetative characteristics at Sandhill Wetland. We concentrated our sampling on base cation and water level variation across the fen and over the four year time period. We also sampled 12 natural wetlands that included examples of all peatland site-types in the region and proposed a method to compare Sandhill Fen to these natural sites. We examined the responses to increasing sodium of the most abundant plant species occurring at the Wetland through a controlled growth experiment.

We summarize our significant findings as follows. 1) Atmospheric deposition of nitrogen at Sandhill Wetland is high compared to the region and proposed critical loads. The deposition of nitrogen on the wetland has been relatively stable over the past four years and provides high amounts of this nutrient for the plant growth; however, the deposition is about double of recently recommended critical load levels. 2) Electrical conductivity of porewaters ranged from about 550-2,500 $\mu\text{S cm}^{-1}$ in the central portions and about 2,000 to nearly 5,000 $\mu\text{S cm}^{-1}$ along the southern boundaries. Based on the currently accepted Alberta Wetland Classification System (AWCS), Sandhill Wetland would be classified as slightly brackish ($\text{EC}=500\text{-}2,000 \mu\text{S cm}^{-1}$) - mostly the central portions – or moderately brackish (2,000-5,000 $\mu\text{S cm}^{-1}$) - mostly along the southern boundaries, and overall classified as moderately brackish. Water chemistry should continue to be monitored especially regarding its effects on biota, including plants. There are areas of the Wetland with high cation concentrations, particularly near the margins and especially along the southern boundaries and the western portion of the wetland. Sodium, in particular is higher along the southern boundary. These plots have sodium values up to 600-800 mg L^{-1} . Overall, cation concentrations have little variation with depth. Some (9) plots have high sodium concentrations (varying from 571 to 971 mg L^{-1}) in the rooting zone: 0-20 cm. 3) Soil sodium varies across the fen and has increased from 0.77 mg g^{-1} in 2017 to 1.36 mg g^{-1} in 2019, with the number of plots with concentrations above 1.0 mg g^{-1} increasing from 33% in 2017 to 63% in 2019.

4) Eight years post wet-up, most species of plants that were introduced to the wetland in 2012 have not survived; however, those that did have provided abundant vegetative cover depending on the levels of water occurring at the site level. At sites with low water levels, *Larix laricina* and *Betula glandulifera* have performed extremely well and should be considered for future reclamation designs. 5) Our comprehensive vegetation/water chemistry/water level study provided a detailed look at the current status of Sandhill Wetland. We summarize our program as follows: the vegetation at Sandhill Wetland has changed dramatically over the past five years, with the 2017 high water event making a lasting and quite negative impact on the species distributions and diversity on the Wetland. Currently, all three species assemblages at the Wetland have different trajectories suggesting that different environmental variables and thresholds are influencing the species assemblages in the three zones. None of the Sandhill Wetland zones overlaps with the reference sites, indicating that the species assemblages found at Sandhill do not closely resemble reference site plant communities, and at the present time can be considered to possess sets of unique characteristics. It is possible that most of the plant communities at Sandhill have reached an alternative stable state and may exhibit strong resistance for return to those present before 2018. The demise of bryophyte diversity and lowered desirable species richness, along with the increasing abundance of *Carex aquatilis* and *Typha latifolia* and select undesirable species (e.g., *Populus balsamifera*) are all worrying attributes.

6) A phytotron experimental study of the response of *Carex aquatilis* to increasing sodium regimes found that both structural and functional attributes of *C. aquatilis* decrease linearly with increases in sodium concentrations. Belowground components have greater decreases compared to aboveground components, including both biomass and photosynthesis. These greater aboveground decreases are associated with exclusion of sodium from the aboveground components by the belowground components. Reduction in photosynthesis is strongly correlated with reduced stomatal conductance and lower transpiration. *Carex aquatilis* survived all treatment concentrations of sodium – up to 2,354 mg L^{-1} ; however, performance was reduced above treatments of 1,079 mg L^{-1} . These decreases in performance in our greenhouse trials

are at a similar level to those currently present at Sandhill Wetland and careful assessment of sodium concentrations in the near future need to be continued. 7.) Net primary production of *Carex aquatilis* varied from 192.3 g m⁻² in 2018 to 311.7 g m⁻² in 2017 and compares well with values from natural sites of the region.

8). An investigation of nutrients, divalent base cations, and associated anions show that Sandhill Wetland had low nutrients, high base cations, and high sulfur compared to natural sites. Sandhill Wetland is not a eutrophic system in the sixth growing season, and supply for most nutrients are within the ranges of natural systems. 9) A second study of PRS probes demonstrated that ion exchange membranes contained in the probes reach equilibrium in shortly after 24 hours, and in ion-rich wetlands such as Sandhill Wetland and natural rich fens, these probes should only be used for burial periods of one to three days. Incubation times longer than this will result in divalent ions replacing monovalent ones. 10) We compared Sandhill Wetland to 12 natural sites that included the entire range of wetland site-types of the region. Evaluation included floristic, plant community, physical, and chemical characteristics. Sandhill Wetland plant communities present across high and intermediate water table position areas (SH-Z1 and SH-Z2 plots, respectively) are most closely associated with the fresh and slightly brackish marshes surveyed. Plots located in areas exhibiting low water table position (SH-Z3 plots) were quite dissimilar from the natural sites monitored. Furthermore, all plant communities across Sandhill Wetland were quite dissimilar from the reference fens; with maximum similarity scores ranging from 0–5%. Porewater chemistry and water table position across SH-Z1 and SH-Z2 sampling zones were most similar to conditions at the two marshes. Porewater chemistry patterns were additionally comparable to the saline fens. Overall, Sandhill Wetland remains spatially heterogeneous in terms of plant community composition, physical characteristics, and site chemistry. Future tailings reclamations should either embrace elevated salinity conditions and seek to create regionally uncommon sodium-dominated systems (e.g., slightly brackish/sodic marshes or saline/sodic fens) or develop more effective methods of preventing ion intrusion into wetland areas. 11) We demonstrate the practicality of using a novel, ‘threshold cube’ approach for appropriately guiding adaptive management and evaluating reclamation performance at site undergoing reclamation. Based upon our Phase I assessment protocol, environmental aspects at Sandhill Wetland are most similar to marshes at its current developmental stage, however; about 94% of the reclamation site’s threshold cube volume falls outside of typical marsh conditions and demonstrate the many unique attributes of the site.

We conclude: Currently, the plant communities and porewater chemistry of Sandhill Wetland present a largely unique set of conditions and plant communities that largely do not match natural wetland site-types of region. Increasing salinity, especially sodicity, and changing water levels provide a background of environmental conditions that make predicting a future site trajectory impossible, and continued assessment of these changing drivers and the plant responses is highly recommended.

7 Acknowledgments

We would like to thank Lilyan Glaeser and Alexandra Tsalickis for their assistance preparing this document. For help in the field we would like to thank Samantha Kitchen, Derek Tollette, Brian Widmer, Kemar Jones, and Ava Alford. For ongoing collaborative efforts, we would like to thank Dr. Andrea Borkenhagen and Dr. David Cooper. For help in the laboratory, we thank Amanda Rotherth of the SIU CORE Facility. We thank Dr. R. Kelman Wieder and Kimberli Scott for analyzing our atmospheric deposition resins. Finally, we thank the Syncrude Environmental Research team for their tremendous help in the field and Syncrude lab: Carla Wytrykush, Jessica Piercey, Chris Beierling, Mohamed Salem, John Arnold, Wendy Kline, and Richard Kao.

8 References

- Bayley SE, Mewhort RL (2004). Plant community structure and junctional differences between marshes and fens in the southern boreal region of Alberta, Canada. *Wetlands*, 24:277-294
- Bernard JM, Gorham E (1978). Life history aspects of primary production in sedge wetlands. *Freshwater Wetlands*, Academic Press, New York, pp. 39-51
- Biagi KM, Oswald CJ, Nicholls EM, Carey SK (2019). Increases in salinity following a shift in hydrologic regime in a constructed wetland watershed in a post-mining oil sands landscape. *The Science of the Total Environment*, 653:1445-1457
- Bliss LC, Grulke, NE (1988). Revegetation in the High Arctic: its role in reclamation of surface disturbance. Northern environmental disturbances. *Boreal Institute of Northern Studies, University of Alberta, Edmonton Occasional Publication*, 14:43-55
- Chapin FS, Chapin, MC (1981). Ecotypic differentiation of growth processes in *Carex aquatilis* along latitudinal and local gradients. *Ecology*, 62:1000–1009
- Gignac LD, Gauthier R, Rochefort L, Bubier, J (2004). Distribution and habitat niches of 37 peatland Cyperaceae species across a broad geographic range in Canada. *Canadian Journal of Botany*, 82:1292-1313
- Gorham E, Somers, ME (1973). Seasonal changes in the standing crop of two montane sedges. *Canadian Journal of Botany*, 51:1097-1108
- Government of Alberta (2015). Oil sands. Reclamation. Government of Alberta. <http://oilsands.alberta.ca/FactSheets/FactSheet-Reclamation-2015.pdf>
- Greenway H, Munns R (1980). Mechanisms of salt tolerance in non-halophytes. *Annual Review of Plant Physiology and Plant Molecular Biology*, 31:149-190
- Greer KJ, Schoenau JJ (1996). A rapid method for assessing sodicity hazard using a cation exchange membrane. *Soil Technology*, 8(4):287-292
- Halsey, LA, Vitt, DH, Beilman, D, Crow, S, Mehelicic, S, Wells, R, (2003). Alberta Wetland Inventory Classification System, Version 2.0. Alberta Sustainable Resource Development, Edmonton, Alberta, Canada.
- Hartsock JA, House M, Vitt DH (2016). Net nitrogen mineralization in boreal fens: a potential performance indicator for peatland reclamation. *Botany*, 94:1027-1040
- Hartsock J (2020). Characterization of key performance measures at reclaimed Sandhill Wetland: Implications for achieving wetland reclamation success in the Athabasca oil sands region. *Ph.D. Dissertation, Southern Illinois University, Carbondale, IL*
- Hultén E (1968). *Flora of Alaska and Neighboring Territories*. Vol 2193. Stanford University. Press, Stanford, 1008 pp

- Koropchak S, Vitt DH, Bloise R, Wieder RK (2012). Fundamental paradigms, foundation species selection, and early plant responses to peatland initiation on mineral soils. *Restoration and Reclamation of Boreal Ecosystems: Attaining Sustainable Development*, Cambridge University Press, Cambridge, UK, pp. 76-100
- Miller, JJ, Bremer E, Curtis T (2016). Influence of organic amendment and compaction on nutrient dynamics in a saturated saline-sodic soil from the riparian zone. *Journal of Environmental Quality*, 45(4):1437-1444
- Munns R, Tester M (2008). Mechanisms of salinity tolerance. *Annual Review of Plant Biology*, 59:651-681
- Nwaishi F, Petrone RM, Macrae ML, Price JS, Strack M, Slawson R, Andersen R. (2016). Above and below-ground nutrient cycling: a criteria for assessing the biogeochemical functioning of a constructed fen. *Applied Soil Ecology*, 98: 77-194
- Purdy BG, Macdonald E, Lieffers VJ (2005). Naturally saline boreal communities as models for reclamation of saline oil sand tailings. *Restoration Ecology*, 13:667-677
- Skogley, EO, Dobermann A. (1996). Synthetic ion-exchange resins: Soil and environmental studies. *Journal of Environmental Quality*, 25(1):13-24.
- Sjörs H (1950). On the relation between vegetation and electrolytes in North Swedish mire waters. *Oikos*, 2:241-258
- Thorman, MN and Bayley, SE (1977). Aboveground plant production and nutrient content of the vegetation in six peatlands in Alberta, Canada. *Plant Ecology* 131:1–16
- Vitt DH, Chee WL (1990). The relationships of vegetation to surface-water chemistry and peat chemistry in fens of Alberta, Canada. *Journal of Vegetation Science*, 89:87-106
- Vitt DH, Wieder RK, Xu B, Kaskie M, Koropchak S (2011). Peatland establishment on mineral soils: Effects of water level, amendments, and species after two growing seasons *Ecological Engineering*, 37:354-363, doi.org/10.1016/j.ecoleng.2010.11.029
- Vitt DH, House M, Hartsock JA (2016). Sandhill Fen, an initial trial for wetland species assembly on in-pit substrates: lessons after three years. *Botany*, 94:1015-1025
- Western Ag Innovations (2014). <https://www.westernag.ca/innovations/customer/interpretation>
- Whitehouse HE, Bayley SE (2005). Vegetation patterns and biodiversity of peatland plant communities surrounding mid-boreal wetland ponds in Alberta, Canada. *Canadian Journal of Botany-Revue Canadienne De Botanique*, 83:621-637
- Wieder RK, Vile M, Scott K, Albright CM, McMillen K, Vitt D, Fenn M (2016a). Differential effects of high atmospheric deposition on bog plant/lichen tissue and porewater chemistry across the Athabasca oil sands region. *Environmental Science and Technology*, 50:12630-12640
- Wieder RK, Vile M, Albright CM, Scott K, Vitt DH, Quinn JC, Burke-Scoll M (2016b). Effects of altered atmospheric nutrient deposition from Alberta oil sands development on *Sphagnum fuscum* growth

and C, N and S accumulation in peat. *Biogeochemistry*, 129:1-2, DOI 10.1007/s10533-016-0216-6, 12630-12640, DOI: 10.1021/acs.est.6b03109

Wieder RK, Vitt DH, Vile MA, Graham JA, Hartsock JA, Fillingim H, House M, Quinn JC, Scott KD, Petix M, McMillen KJ (2019). Experimental nitrogen addition alters structure and function of a boreal bog: Critical loads and thresholds revealed. *Ecological Monographs*, 00(00):e01371.10.1002/ecm.1371

Wieder, RK, Vitt, DH, Vile, MA, Graham, JA, Hartsock, JA, House, M, Popma, JM, Fillingim, H, Quinn, JC, Scott, KD, Petix, M, McMillen KJ (2020). Experimental nitrogen addition alters structure and function of a boreal poor fen: Implications for critical loads. *Science of the Total Environment*. doi.org/10.1016/j.scitotenv.2020.138619

Wood ME, Macrae ML, Strack M, Price JS, Osko TJ, Petrone RM (2016). Spatial variation in nutrient dynamics among five different peatland types in the Alberta oil sands region *Ecohydrology*, 9:688-699

Wytrykush C, Vitt, DH, McKenna G, Vassov R (2012). Designing landscapes to support peatland development on soft tailings deposits. In Vitt DH, Bhatti J (eds) *Restoration and Reclamation of Boreal Ecosystems: Attaining Sustainable Development*. Cambridge University Press, Cambridge, UK pp.161-

9 Appendices

Appendix 3.1 Ebbs, SE, Glaeser, L, House, M, Vitt, D (2015) A plant physiological approach to assess the performance and potential success of mine revegetation. In. Fourie, AB, Tibbett, L, Sawartsky, L, van Zyl, D (eds.). *Mine Closure 2915: Proceeding of the 10th International Conference on Mine Closure: June 1-3, 2015, Vancouver, Canada*. Infomine Inc., Vancouver BC. 14 pp

A plant ecophysiological approach to assess the performance and potential success of mine revegetation

S. Ebbs *Southern Illinois University, USA*

L. Glaeser *Southern Illinois University, USA*

M. House *Southern Illinois University, USA*

D. Vitt *Southern Illinois University, USA*

Abstract

The Canadian oil sands industry is actively engaged in the revegetation and reclamation of sites associated with bitumen mining. One current reclamation research effort sponsored by Syncrude Canada Ltd., referred to as the Sandhill Fen Research Watershed (SFRW) project, is taking place on a former open pit mine in northern Alberta. One aspect of this project involves the establishment of a wetland on the former mine, which has since been back filled with soft tailings. A component of the active research taking place at the SFRW is the evaluation of using plant ecophysiological parameters as markers of success. The parameters being used include rates of photosynthesis, transpiration, stomatal conductance, and additional derived parameters (e.g., water use efficiency). These ecophysiological measures provide quantitative information on the physiological status of the plants and a potential assessment tool for plant performance

*during the early stages of reclamation. Additionally, this approach could provide insight into the trajectory of the plants in the reclaimed vegetation community, and the potential success/stability of the reclamation long term. Comparable data from the same plant species growing on disturbed and undisturbed benchmark sites is being collected. These sites can provide a frame of reference for predicting reclamation trajectories, as well as expectations for plant physiological performance as a function of time. Ecophysiological data collected one year after the initiation of the project demonstrated that plants in the wetland were showing similar performance to plants on the benchmark sites, suggesting that the reclamation was on a comparable ecological trajectory to those reference sites. For example, an array of ecophysiological parameters was monitored for water sedge (*Carex aquatilis*), a key species planted in the pilot wetland. Photosynthesis rates for water sedge in the Sandhill Fen pilot ranged from 2.2 – 20.5 $\text{mmoles CO}_2 \text{ m}^{-2} \text{ min}^{-1}$ as compared to values ranging from 1.4 – 14.2 $\text{mmoles CO}_2 \text{ m}^{-2} \text{ min}^{-1}$ for plants on the benchmark sites. Water use efficiency values ranged from 0.9 to 6.1 for water sedge in the pilot site as compared to 0.6 to 4.8 on the benchmark sites. Across the SFRW, there is a gradient of soil moisture from dry to inundated. Plant performance relative to this moisture was monitored closely to offer guidance on how water levels influence plant establishment. The results thus far illustrate the value of this ecophysiological approach in providing markers of success for wetland reclamation efforts. The results also suggest that this same approach might be applicable to other mine closure scenarios, providing a means to relate the ecological trajectory of reclamation to relevant benchmark sites.*

1 Introduction

During mine site reclamation, natural vegetation communities are commonly used as references. Appropriate reference communities can represent a general or specific assemblage of plant species or a community that provides one or more desired ecosystem functions. The progress of the reclaimed vegetation community over time can be compared to the natural reference community to assess whether the reclamation is moving on a trajectory towards the reference community structure or on an altered trajectory (White and Walker, 1997). Reference communities have been used in a variety of ecological contexts, including forest, grassland, and wetland restoration. Reference communities have also been used to assist in recent mine closure and/or revegetation efforts (e.g., Gravina et al., 2011; Rooney and Bayley, 2011; Vickers et al., 2012). The progress and potential success of the reclamation relative to the reference community has been tracked by monitoring parameters such as species richness, species density, or net primary production. Often the potential stability and trajectory of the restored community does not become evident for several years. Early markers of success may be measureable in terms of structural aspects of the plant community, such as the recruitment of foundation species, survival of naturally recruited or introduced plants, percent cover achieved by the community or indices such as the community structure integrity or higher abundance indices (Jaunatre et al., 2013). Another approach to evaluate the early progress of a reclamation effort is to take a functional approach by measuring ecophysiological parameters of target or representative plant species to assess their performance relative to the same species in a reference community. This ecophysiological approach has been used to monitor establishment and performance of native, introduced, or exotic plants in some ecological restorations (e.g., Lambert et al., 2011; Ostertag et al., 2008; Rovai et al., 2013), but has not been applied as widely during mine closure reclamation scenarios.

The extraction of mineable surface deposits of bitumen from the oil sands in Alberta can take place through open pit mining. When the bitumen deposit is exhausted, the resulting pit (referred to as an in-pit) is often utilised for tailings storage and backfilled with mine waste materials such as salty sand (Wytrykush et al., 2012). The current government mandate to the oil sands industry (Alberta Environment, 1999) is that the mined areas must be replaced with self-sustaining and maintenance-free ecosystems that provide land capabilities equivalent or superior to the pre-disturbance conditions. Those ecosystems should consist of an integrated landscape of uplands and wetlands. Pre-disturbance land capabilities include ecosystem services such as wildlife habitat, wetland and watershed functions,

sources of timber, traditional foods, medicinal plants, or recreational use (Oil Sands Reclamation Committee, 1998). Achieving these endpoints have been described as the engineering of new ecosystems over a time scale of >100 years (Johnson and Myanishi, 2008). There are still many years of oil sands extraction planned for most mining leases, and therefore mine closure has not been completed to date in Alberta's oil sands industry. The industry is, however, executing progressive reclamation. Many operational scale revegetation efforts have been completed, for example Syncrude Canada Ltd has over 3000 hectares of permanently reclaimed uplands. Wetland reclamation is relatively new and has only been attempted at the pilot or small scale.

Syncrude Canada, Ltd. initiated an experimental watershed in 2008, referred to as the "Sandhill Fen Research Watershed", to establish an integrated upland-wetland landscape on a former open pit mine. The total area of this watershed is 52 ha, 17 ha of which is a central wetland (Sandhill Fen). The project aimed to understand the initial conditions needed for a stable wetland to develop over time, particularly if the trajectory of establishment leads to a boreal rich fen. Rich fens have a relatively high abundance in the natural northern Alberta boreal region where Syncrude operations are located. Rich fens are dominated by true mosses and include a diversity of vascular plant species (Vitt and Chee, 1990). Establishment of a fen represents a particular challenge as there have been no prior efforts to create a peat-forming wetland. Examination of cores from existing fens in the region indicate that the presence of vascular plants are critical to the early establishment of these peat-forming wetlands, most likely as nurse plants to facilitate the establishment of the underlying moss layers. To aid in the development of future revegetation plans for soft tailings reclamation, experimental plots were established in the experimental wetland in order to evaluate the growth and performance of an array of fen vascular plant species. One year after the plots were established, the performances of three species were evaluated across the wetland area using ecophysiological parameters. Reference communities in northern Alberta for each plant species were also identified and included sites ranging from either recently disturbed or have been undisturbed for millennia. The same ecophysiological parameters were measured to assess performance of plants in the experimental watershed relative to those from the reference sites. Another reference site used was a nearby, smaller scale reclamation effort.

The first objective of the research was to establish the range of values for each ecophysiological parameter across the reference sites and the range of values across a moisture gradient that developed on Sandhill Fen. The second objective was to compare the ranges of values obtained to assess the physiological performance of the species in the experimental watershed to the reference sites. The final objective was to demonstrate the utility of these ecophysiological parameters for assessing the early performance of plants in a wetland reclamation scenario. The more general application of this monitoring approach to the success of mine closure and revegetation efforts is discussed.

2 Methods and materials

2.1 Study sites

2.1.1 Sandhill Watershed

A complete description of the construction of the Sandhill Watershed (SW) can be found in Wytrykush et al. (2012). The Sandhill Fen Research watershed project is located in the north section of East In-pit on Syncrude Canada's oil sands lease. The former mine was used as a tailings storage facility and filled with composite tailings. Before construction of the Sandhill Fen research project the site location was a relatively flat, soft tailings sand feature. Above-grade landform construction components of the watershed (hummocks) were mechanically constructed with heavy equipment. Construction started in the winter of 2009 and was completed in the fall of 2012 and summer of 2013. The watershed consists of seven small upland hills on the northern and southern borders with water flowing into a central wetland (i.e., "Sandhill

Fen”) approximately 800 m in length and 350 m in width at its widest point (Figure 1). For the central wetland, 0.5 m of peat was spread over the 17 ha area. The peat was collected from a peatland complex on the oil sands lease in the fall/winter of 2010 and stored in piles until fall/winter 2011, at which point it was spread across the wetland area. Mixed with the peat were small amounts (<5% w/w) of the underlying clay mineral soil beneath the peat deposit. Some physicochemical parameters for the peat are shown in Table 1. Some initial water for the wetland was pumped from a nearby natural lake (Mildred Lake) into a small holding pond separated from the wetland by a rocky dam. Water was released into the wetland area through the dam throughout the summer and fall of 2012 and 2013.

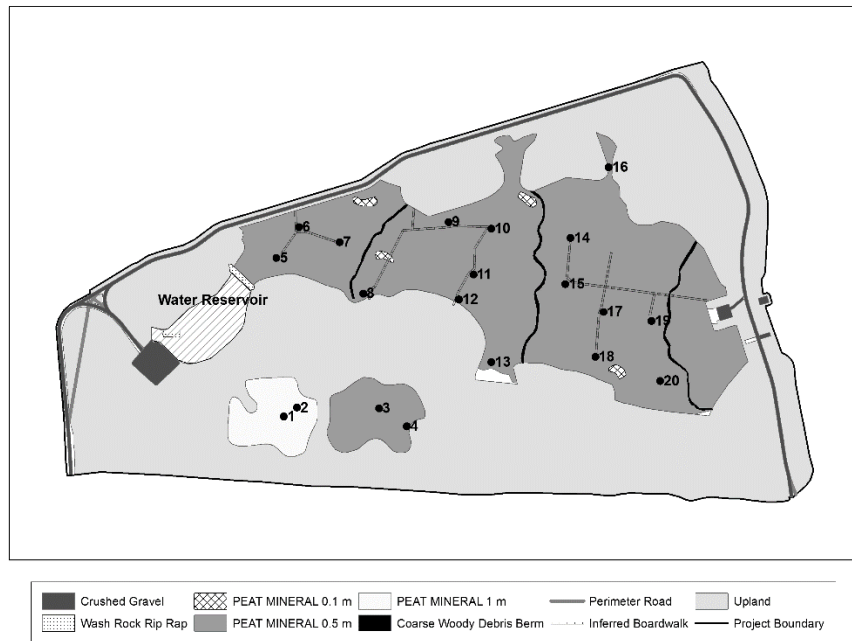


Figure 1 Schematic diagram of the Sandhill Fen Research Watershed. The wetland areas are those that are associated with the layers of peat mineral mix that were placed within the watershed

Notes: the positions of the twenty research plots within the wetland area associated with this study are indicated. The water reservoir that provided the initial water supply for the watershed is shown to the west of the main wetland area

Table 1 Physicochemical parameters of the peat substrate comprising the surface layer of the Sandhill Fen Research Watershed. Data reflect the mean and standard error for each parameter based on samples collected from each of the 20 research plots

Parameter	
Bulk density (g cm ⁻³)	246.9 ± 63.5
Organic matter (%)	36.5 ± 6.4
Moisture content (%)	69.0 ± 10.1
pH (substrate)	5.3a ± 0.3
pH (pore water)	7.0 ± 0.4
Carbon (%)	28.5 ± 9.3
Nitrogen (%)	1.4 ± 0.4
C:N ratio	20.5 ± 2.8
Extractable nitrate (mg g ⁻¹)	19.0 ± 9.0
Extractable ammonium (mg g ⁻¹)	1.4 ± 0.2
Extractable phosphorus (mg g ⁻¹)	28.0 ± 12.0

During spring 2012, experimental plots were established within the wetland area (Figure 1). Twenty research plots were positioned across the fen; 16 are located in the main fen watershed and four plots (referred to hereafter as the perched plots) were positioned on one of the southern upland hills approximately 25 m above the wetland. All 20 plots were positioned to span the environmental gradients of moisture that were expected in the watershed. The perched plots were isolated from the fen watershed to create a separate hydrology and moisture regime. The 20 research plots are 10 m x 10 m and divided into four equal quadrants. Within one of the quadrants, monocultures of native wetland species were planted in 1 m x 1 m subplots.

Three of the species established in those subplots were examined here: water sedge (*Carex aquatilis*), black-girdle bulrush *Scirpus atrocinctus*, and seaside arrowgrass (*Triglochin maritima*). The first two species are monocotyledonous sedges while seaside arrowgrass is also monocotyledonous but a member of its own taxonomic family (Juncaginaceae), closely related to the Liliaceae. All three species are indigenous to fens and marshes of Alberta. All three plant species utilise the C3 photosynthetic pathway (Bruhl and Wilson, 2007; Wang et al., 2006). The plants were grown in 2011 at the Smoky Lake Forest Nursery (Smoky Lake, AB) using seed collected from fens across northern Alberta. Seed was germinated in standard nursery trays in a peat-mineral soil mix watered as needed. The plants were grown under ambient greenhouse conditions and then transplanted in spring 2012 as plugs into the subplots at a density of twenty-four plants m⁻² for *Scirpus atrocinctus* and *Triglochin maritima* and seven plants m⁻² for *Carex aquatilis* seedlings. The plugs were planted directly into the peat layer.

By summer 2013, at the initiation of the study reported here, there was 100% survival of each of the three species across the 20 plots. The wetting of the fen was not uniform or continuous, but four discrete categories of soil moisture could be distinguished. There were 5 plots that had been under continuous standing water of at least 10 cm (inundated plots). An additional 5 plots were continually saturated with water at or within 10 cm below the substrate surface but had not been inundated (saturated plots). A total of 6 plots were well hydrated with water due to past inundation but at the time the measurements were made were not fully saturated (soil moisture >50%, unsaturated plots). The four perched fens received water predominantly from snow melt, but augmented with some water pumped to these areas. These plots

(perched plots) also experienced variable levels of soil hydration as for the unsaturated plots but at the time of measurement were more similar to upland conditions than the wetland conditions in the watershed.

2.1.2 Reference communities

The plants in plots from the Sandhill Fen were compared to plants growing on naturally occurring reference communities in northern Alberta, each with varying ages of disturbance.

2.1.2.1 Anzac sites

The Anzac sites include three sites at a roadside locality disturbed in 2006 owing to road expansion.

Anzac Roadside 1 (“Anzac ditch”): A poorly drained ditch on organic soil with abundant sedges (56°22.56’N, 111°01.32’W). Sampled: Water sedge (*C. aquatilis*).

Anzac Roadside 2 (“Anzac mineral”): A site with wet mineral soil and abundant mosses and graminoids (56°22.59’N, 111°01.17’W). Sampled: Water sedge (*C. aquatilis*).

Anzac Roadside 3 (“Anzac fen”): A fen with populations of *Sphagnum angustifolium* and various sedges (56°22.57’N, 111°01.31’W). Sampled: Water sedge (*C. aquatilis*).

2.1.2.2 Engstrom Lake

Along the access road to Engstrom Lake is a poorly drained wetland with sedges. The most recent disturbance to this area is unknown, but it must have occurred within the past 30 years when construction began for access roads to nearby recreational areas (56°12.02’N, 110°53.47’W). Sampled: black-girdle bulrush (*S. atrocinctus*).

2.1.2.3 Mariana Lake

An undisturbed minerotrophic wetland is located near an access road to the east of Mariana Lake. No disturbance to this area is evident (55°54.01’N, 112°03.88’W). Sampled: black-girdle bulrush (*S. atrocinctus*).

2.1.2.4 Extreme rich fen

This reference site is a mature open sedge/moss-dominated rich fen with abundant scorpidium moss (*Scorpidium scorpioides*). No disturbance to this area is evident (56°57.04’N, 111°31.82’W). Sampled: Seaside arrowgrass (*T. maritima*).

2.1.2.5 U-cell Experimental Area

The U-cell Experimental Area is located on the Syncrude Canada Ltd. production facility and served in this study as reference reclamation plots. U-cell is a set of 28 cells (10 x 20 m) with different substrate and water chemistry treatments (Wytrykush et al., 2012). In 2008, a variety of water and substrate treatments were established. These included a set of 14 cells filled with stockpiled peat at 15, 50, and 100 cm depth. Seedlings of a variety of wetland plants propagated as described above were established in the cells and their survival and growth monitored. Some cells received fresh water while other cells received mine process water. In 2010, process waters in U-cell treatments had electrical conductivities ranging from 388 to 1,360 $\mu\text{S cm}^{-1}$ (Wytrykush et al., 2012). Individuals of water sedge, black-girdle bulrush, and seaside arrowgrass were among the species planted in the cells. Measurements were taken from cells with large populations of these species. (57° 03'01.00" N, 111°39'20.33"W). Sampled: Water sedge (*C. aquatilis*), on peat substrate with fresh water from 2009-2011, mine process water in 2012, and rain-fed in 2013-2014 (Cell 8); Black-girdle bulrush (*S. atrocinctus*) on peat substrate receiving fresh water until it was rain fed in 2013 to 2014 (Cell 6); Seaside arrowgrass (*T. maritima*) on mineral substrate receiving fresh water from 2009 to 2010, process water from 2011-2012, and rain fed in 2013-2014 (Cell 16). U-Cell was included as a reference site to illustrate a recent reclamation scenario with highly variable conditions over the years since establishment.

2.2 Measurement of ecophysiological parameters

Ecophysiological parameters were measured for the three plant species using a CI-340 portable photosynthesis system (CID Bioscience, Camas, WA) under ambient humidity, temperature, and light intensity using an open system configuration with a 6.25 cm² flat rectangular chamber. All measurements of plants on the Sandhill watershed and the reference sites were made in summer 2013 between 9 AM and noon from mid-June to the end of July (18 June – 31 July). Leaves selected for measurement were fully expanded and free from damage. Once enclosed in the chamber and after an acclimation period of 5 min, photosynthetic rate, evapotranspiration, stomatal conductance, and photosynthetically active radiation (PAR) were measured. Measurements were taken on five plants from each plot on Sandhill Fen and from each reference site. All three parameters are common indicators of plant physiological status. Photosynthesis and evapotranspiration are highly responsive parameters and their rate drops quickly if plants are experiencing stress. Stomatal conductance is an indicator of the degree to which the stomatal pores on the leaves are open to allow for gas exchange and evapotranspiration. The diameter of the pore can be biologically controlled to balance the entry of CO₂ for photosynthesis against the loss of water. Stomatal conductance is highest when plants have fully open stomates and an adequate supply of water and decreases under water-limiting conditions or in response to other stresses.

2.3 Data analysis

The data were subjected to a one-way ANOVA analysis with Tukey's HSD used to provide post hoc comparisons. In addition to the ecophysiological parameters measured directly, two additional parameters were derived from the data recorded. Radiation use efficiency (RUE), a representation of the efficiency to which the light available was used to drive photosynthesis, was calculated as the ratio of photosynthetic rate to photosynthetically active radiation (Sinclair and Horie, 1989). Water use efficiency (WUE) is a common parameter used to relate the amount of water expended per unit of photosynthesis achieved and was calculated as the ratio of photosynthetic rate to evapotranspiration.

3 Results

3.1 Water sedge

Water sedge (*Carex aquatilis*) has a wide distribution across Canada and the United States (south to Arizona, Missouri, and Virginia) and has been classified as a native and obligate wetland plant (FNA, 2002). This species can be found throughout the boreal wetlands of Canada. Water sedge is also resilient to disturbance and can naturally colonise disturbed soils, road side ditches, and mining pads (Koropchak et al., 2012). Water sedge has been included in a variety of reclamation and revegetation efforts, including revegetation efforts on oil pads and mined peatlands (Vitt et al., 2011). The plants are capable of growing on mineral soils although the species shows more robust growth on organic soils and under wetland conditions (Koropchak et al., 2012). In the study here, the rate of photosynthesis by water sedge was significantly lower on the mineral soil from the Anzac site as compared to the undisturbed Mariana Lake wetland site, but did not differ significantly from any of the other reference sites (Figure 2). The rate of evapotranspiration on the mineral soil differed significantly only from the U-cell site and there was no significant difference across the reference sites for stomatal conductance. Aside from the differences displayed by plants from the mineral soil, there was no significant difference in any of these parameters as a function of time from the disturbed sites to the undisturbed Mariana Lake site. The range of values for three ecophysiological parameters across all the reference sites was no more than three-fold. The water sedge plants in the Sandhill Fen experienced a range of soil moisture regimes from inundated plots to the more mesic terrestrial conditions of the perched fens and the unsaturated plots, but did not show any significant differences in the parameters as a function of soil moisture. More importantly, after only one year of growth in the Sandhill Fen plots, the only significant differences observed were between the

Sandhill Fen plots and the Anzac mineral soil and this was limited to rates of photosynthesis and evapotranspiration for the wetter Sandhill Fen plots. The values for three parameters across this moisture gradient did not differ significantly from the organic substrates from any of the reference sites. This demonstrates that within one year of planting, the water sedge plants were performing as well as plants on the other reference sites with organic substrates, including the undisturbed Mariana Lake site. This was also evident when the individual ecophysiological parameters were integrated into either the radiation use efficiency (RUE) or water use efficiency (WUE). The range of RUE values across the reference sites was from 1.2 to 9.2 and for WUE was from 0.58 to 4.8. By comparison, the corresponding ranges across all the plots from the Sandhill Fen were 1.2 to 13.2 and 0.86 to 6.1, respectively. The ranges overlap with one another, with some plants in the Sandhill Fen demonstrating even greater efficiency than plants on the reference sites.

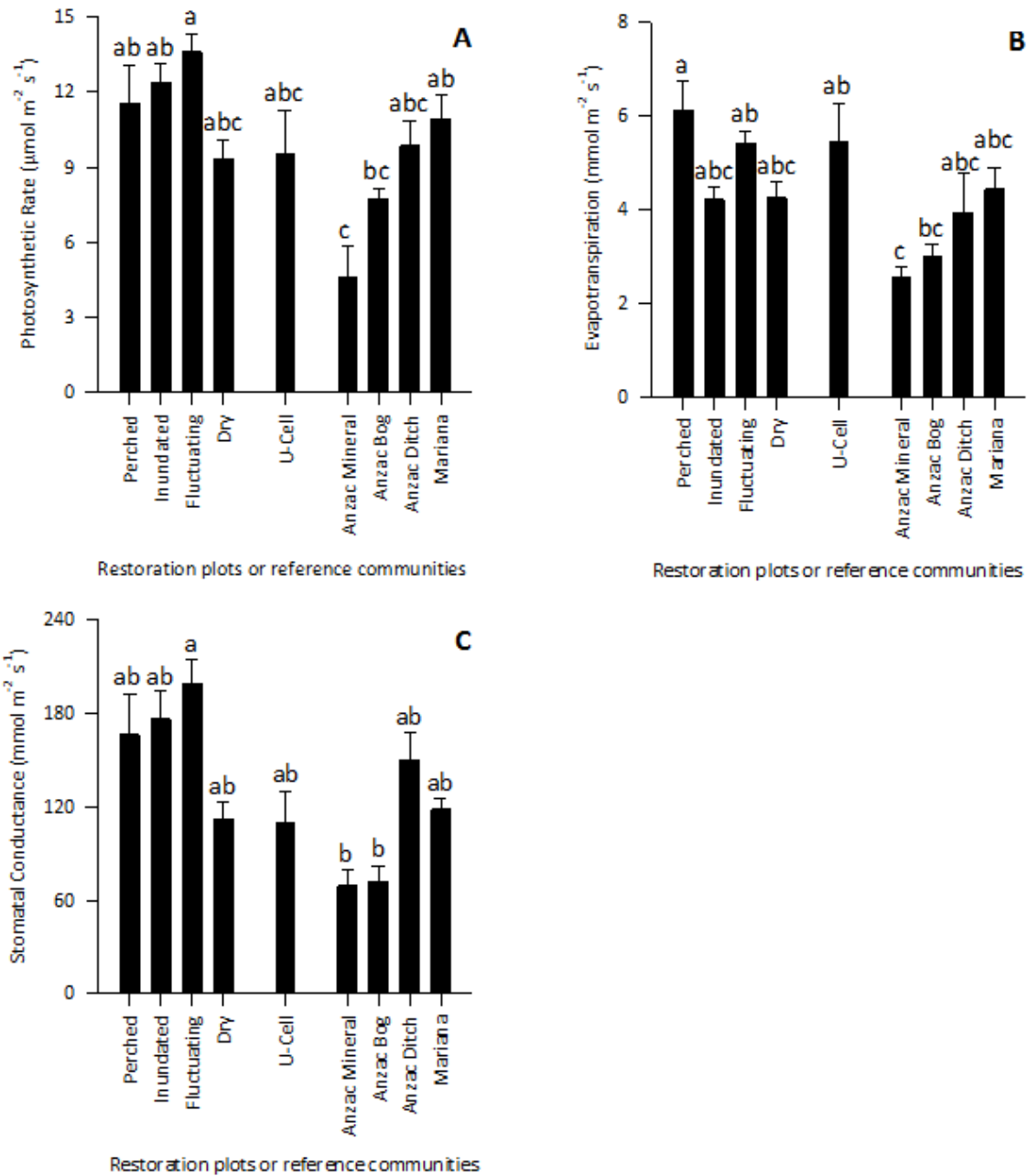


Figure 2 Net photosynthesis rate (A), transpiration rate (B), and stomatal conductance (C) for water sedge (*Carex aquatilis*) growing in plots on the Sandhill Fen Watershed (restoration plots) and on five reference communities

Notes: data represent the mean and standard error. Bars with different letters are significantly different from each other ($\alpha=0.05$)

3.2 Black-girdle bulrush

Black-girdle bulrush (*Scirpus atrocinctus*) is distributed in the United States in New England, West Virginia, and the states bordering the upper Mississippi river valley and Great Lakes (e.g., Iowa, Wisconsin, Michigan, Illinois) and across Canada (FNA, 2002). The species is classified as a native species and as either an obligate or facultative wetland plant. Black-girdle bulrush is most often associated with wetlands or wet soils and has been found in abundance on some disturbed peatland sites (Mahmood and Strack, 2011; Sottocornola et al., 2007). Across the three reference sites utilised for this species, significant differences were observed only for the rates of photosynthesis and evapotranspiration between the more recently disturbed plots (i.e., U-cell and/or Engstrom Lake) and the undisturbed Mariana Lake site (Figure 3). The range in the data was less than two-fold for the two parameters. The only significant differences observed for this plant species on the Sandhill Fen plots was that the rate of stomatal conductance was significantly higher on the two groups of wetter plots as compared to the two groups drier plots. This rate was significantly higher than what was observed for any of the reference sites. The rates of photosynthesis and evapotranspiration were not significantly different between the Sandhill Fen plots and all the reference sites with the values for each parameter falling within the narrow range of variability between the reference sites. The same trends were observed for the RUE and WUE. The range of RUE values on the reference sites was 0.26 to 10.0 as compared to a range of 0.68 to 12.4 for the Sandhill Fen plots. The ranges for WUE were 0.06 to 4.2 and 0.71 to 3.8, respectively. The ranges for both parameters correspond well between the reference sites and the Sandhill Fen sites.

3.3 Seaside arrowgrass

Seaside arrowgrass (*Triglochin maritima*) has a distribution similar to water sedge and is a native and obligate wetland species. This species frequently co-occurs with water sedge in extreme rich fens. Because arrowgrass shows some tolerance to disturbance and is a halophyte (Cody, 1996), this species has also been considered for revegetation scenarios, including those associated with the oil sands industry. The only parameter that differed significantly between the two reference sites was the rate of evapotranspiration (Figure 4), which was higher for plants at the U-cell site as compared to the rich fen site. The U-cell site is situated on a hilltop above the refinery complex and is considerably windier than the other sites examined. This greater wind velocity may be partially responsible for this difference, and also the higher rates observed for the other two species. Across the moisture gradients identified in the Sandhill Fen, the pattern in the ecophysiological data was the same as that observed for black-girdle bulrush. The only significant difference observed was for stomatal conductance between the wetter and drier groups of plots, which likely represents a response of this wetland species to the mesic conditions in these plots. The range observed in the values for each parameter for the plants on the Sandhill Fen, particularly for the wetter groups of plots, corresponds closely to both the recent disturbance at the U-Cell site and the undisturbed rich fen. As for the other two species, there was clear overlap in the range of values for RUE (5.0 to 19.6 reference sites; 0.26 to 43.1 Sandhill Fen) and WUE (3.3 to 26.0 reference sites; 0.67 to 25 Sandhill Fen) although the ranges were wider for plants from the Sandhill Fen.

4 Conclusions

Mine closure and reclamation are ongoing endeavours for the oil sands industry in Alberta. The prescriptions needed to guide those efforts are continually evolving. Incorporating large scale wetland complexes into the reclamation landscape is fundamental to Syncrude's future reclamation efforts. The

Sandhill Fen project is a wetland restoration but is also exploring opportunities to create a wetland with healthy and diverse set of plant species. The terrain in northern Alberta has extensive networks of peat-forming wetlands (i.e., fens and bogs) which could be impacted by oil sands mining. Successful wetland reclamation could return the landscape function provided by natural peat-forming wetlands, thereby fulfilling the mandate established by Alberta Environment to restore the ecosystem with equivalent ecological capacity (Alberta Environment, 1999). Peat-forming fens and bogs are highly effective carbon sinks, and globally have stored an estimated 436 Gt of carbon (Loisel et al., 2014).

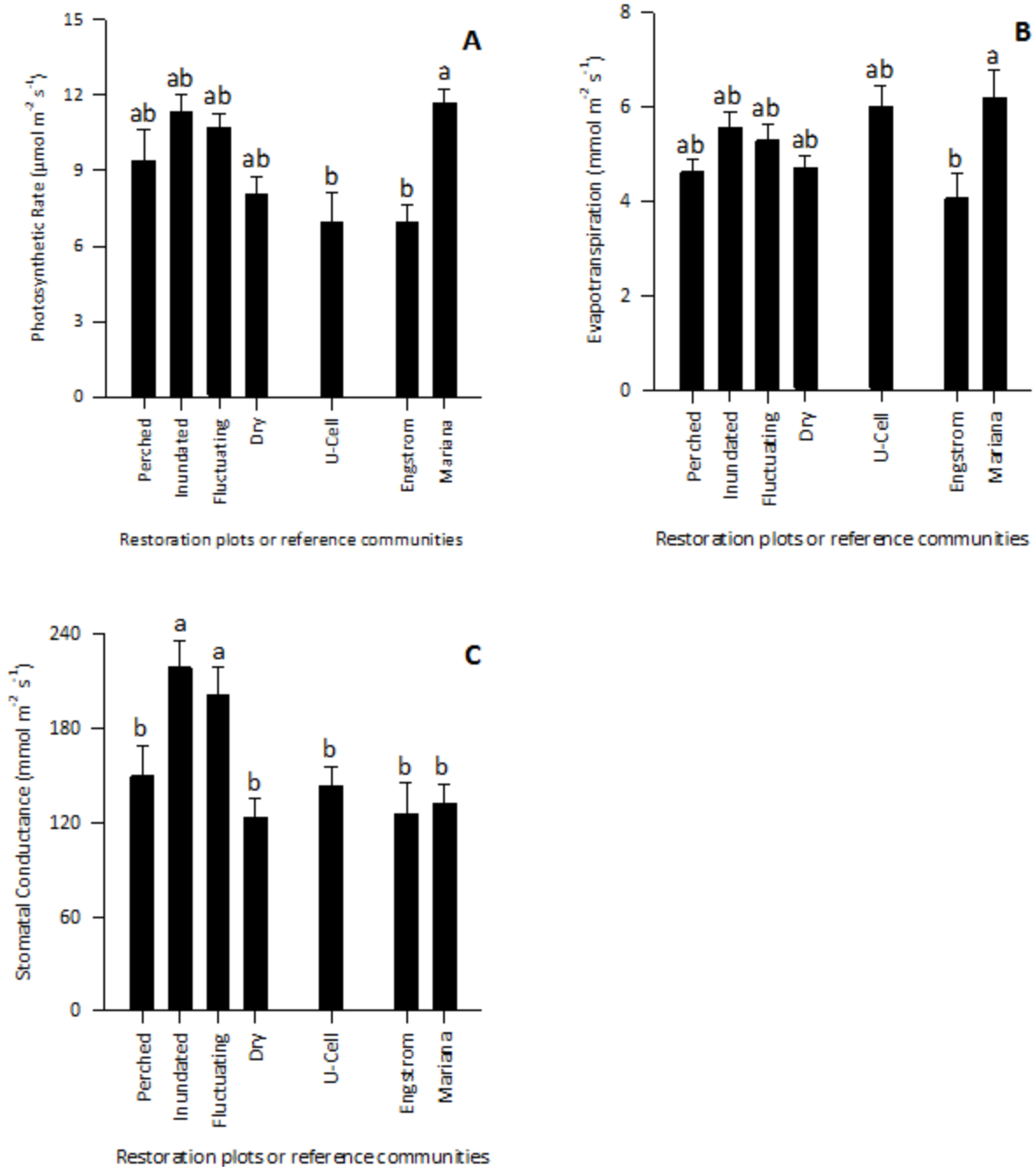


Figure 3 Net photosynthesis rate (A), transpiration rate (B), and stomatal conductance (C) for black-girdle bulrush (*Scirpus atrocinctus*) growing in plots on the Sandhill Fen Watershed (restoration plots) and on three reference communities

Notes: data represent the mean and standard error. Bars with different letters are significantly different from each other ($\alpha=0.05$)

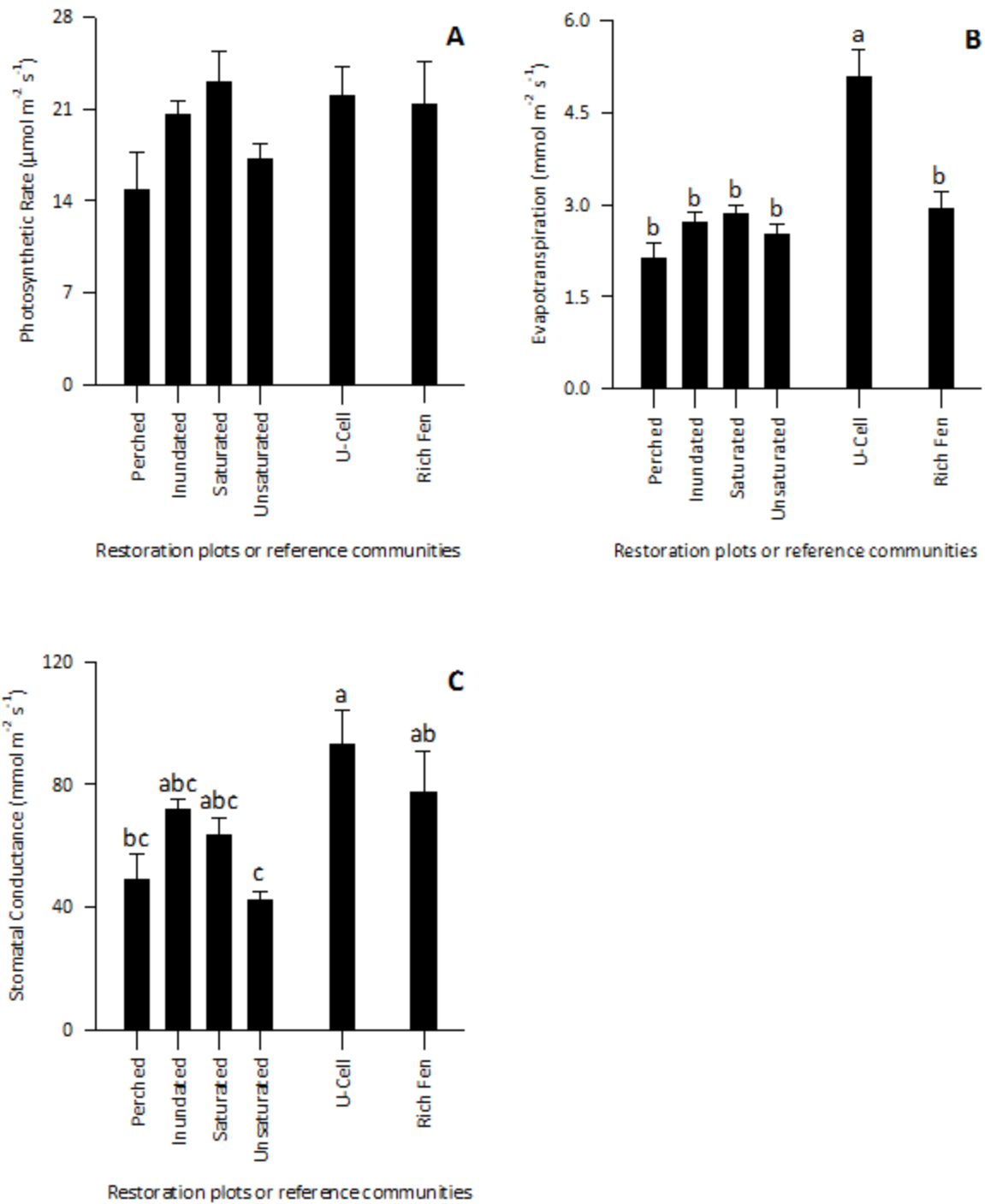


Figure 4 Net photosynthesis rate (A), transpiration rate (B), and stomatal conductance (C) for seaside arrowgrass (*Triglochin maritima*) growing in plots on the Sandhill Fen

Watershed (restoration plots) and on two reference communities

Notes: data represent the mean and standard error. Bars with different letters are significantly different from each other ($\alpha=0.05$)

Successful reclamation of wetlands, including those that may form peat, is a priority for the oil sands industry and could have the benefit of reducing the carbon footprint of the industry. There has been some success with peatland restoration in Europe (Timmermann et al., 2006; Vasander et al., 2003; Zerbe et al., 2013) and Canada (Rochefort and Lode, 2006). Peatland reclamation had not been attempted at this scale prior to the Sandhill Fen research project, yet represents one of the more likely mine closure scenarios. Site managers and regulatory agencies are interested in early markers of success for vegetation establishment during reclamation efforts in order to evaluate reclamation progress and suitability for certification. The ecophysiological approach demonstrated here offers a set of markers that can provide such information.

The selection of reference communities for this study included both recently disturbed and undisturbed sites with the intention of bracketing the most likely range of values. Establishing these ranges was part of the first objective of this study. This strategy provided at least two points along a vector describing the performance of these vascular plants between the sites. As expected, more recent disturbance generally resulted in lower values for the ecophysiological parameters as compared to the undisturbed sites. For water sedge, the results from the Anzac sites illustrated that substrate type was also a determining factor in the performance of this plant species. These results for water sedge underscore prior research (Mollard et al., 2012; Raab and Bayley, 2013, Vitt et al., 2011) that has demonstrated the robustness of this species for reclamation on disturbed sites, including mineral soils. The constraints that substrate type places on physiological performance of water sedge, and potentially early establishment of this species during reclamation efforts, are also evident. Nonetheless, the range of values observed for this species varied by no more than three-fold for the parameters measured. A similar range of values was also observed for the parameters measured for the other two species. The U-cell site provided another type of reference community for this study, one that is highly disturbed, but also an experimental reclamation with some similarity to the reclamation projected for Sandhill Fen. The results for all three species from the U-Cell site consistently fell within the observed ranges, providing additional evidence that the ranges established are representative for each ecophysiological parameter and for each plant species.

The topography of Sandhill Fen resulted in a variable distribution of water, creating the four distinct soil moisture conditions described here. The advantage that arose from this soil moisture variability is that it allowed for the range of values for each parameter to be established (an aspect of the first objective of this research) and for that factor to be considered in evaluating the performance of these three species one year after establishment. In any revegetation effort, the availability of water is critical to initial plant establishment, particularly for wetland plants. Wetland plant species able to withstand periods of water deficit while maintaining their physiological performance would be highly desirable for reclamation efforts in general, as well as for the specific reclamation efforts that would take place on disturbed sites associated with oil sands mining. The three plant species examined in this study are obligate wetland plants and their physiological performance clearly declined on the drier plots associated with Sandhill Fen, but all three species were able to survive these conditions and sustain their physiological performance. The range observed in the parameters across this moisture gradient aligned well with the range of values associated with the corresponding reference sites. This specific comparison was the second objective of this research. Each plant species after one year of growth was performing as well as plants on the undisturbed sites. Such information provided a clear indication of successful initial establishment of the plants across the Sandhill Fen plots. It is particularly remarkable that these wetland plants were able to establish themselves in less than ideal areas of the fen watershed under drier conditions than would normally be considered unsuitable for these species. The planning of a reclamation effort might presume that these plants could not be established successfully without the necessary wetland

conditions. The evidence here suggests that establishment is possible without such conditions, but that physiological performance would be less than optimal. This sub-optimal performance still fell within the ranges that were established from the reference communities, showing that the dry conditions in areas of the Sandhill Fen represented in the first year of this project a disturbance no more stressful than that in the disturbed reference sites.

The use of the ecophysiological parameters to assess physiological performance and early establishment of plants in the Sandhill Fen provides industry with a potential set of markers to evaluate the initial success of the planned reclamation restoration efforts as compared to benchmark performance of each species. Here we demonstrate that performance of individual species differs and species must be treated individually. The ecophysiological parameters described here have been used in subsequent years at Sandhill Fen on the same plots and reference communities to extend the monitoring of these plant species. The results (data not shown) are the same as what has been reported here. The plants established in the plots in 2012 continue to thrive and consistently produce biomass each year as indicated by the appearance of litter. There is also evidence from other areas within Sandhill Fen that multiple species of bryophytes associated with peat-forming wetlands have become established across the fen (Vitt and House, 2015) with the plant species associated with this study serving as nurse plants to create the necessary microclimate for moss establishment. The first year results presented here offered early insight into the trajectory of establishment, which aligned with the later successful performance and establishment that was observed. While not observed here, a scenario where there was poor ecophysiological performance outside the range of values early in a reclamation effort, relative to the range of values from reference sites, would indicate conditions where establishment could be in jeopardy or might proceed more slowly than expected. Such information would allow site managers the opportunity to intervene earlier to correct the conditions that are limiting performance. For example, in the case of Sandhill Fen, the non-uniform wetting was an initial cause for concern as it was expected that the drier conditions would limit plant performance. The first year data reported here reduced that concern, contributed to later discussions about the design of wetland reclamations, and provided insight into the type of wetland that would likely develop.

By extension, the same framework could be applied to mine closure scenarios. Once an array of foundation species suitable for reclamation have been selected, the next step would be the identification of an array of regional reference communities to establish the range of values for these parameters exhibited by these plant species. Any threshold values below which physiological performance of reference plants decreased could be noted, particularly if an association with a particular disturbance or stress could be assigned. Empirical studies could also be conducted with those species to determine the limits of tolerance to a disturbance or stress expected during the reclamation. For example, given that elevated concentrations of sodium might intrude into the growth substrate during reclamation efforts above in-pit tailings, greenhouse studies with water sedge and American sloughgrass (*Beckmania syzigachne*) were performed to identify the threshold for sodium toxicity to these two species (Glaeser et al., 2015; Koropchak, 2010). The ranges of values then form a rubric against which performance of the plants in the reclamation could be compared. Alignment with, or deviation outside, this range could be an early signal to industry that could guide subsequent management of the reclamation or inform future reclamation plans. The decision structure could also integrate any other site-specific factors that might influence plant establishment. An additional value of these measurements is that it could allow industry to provide stakeholders and regulatory agencies with early results on the progress of plant establishment. These results would provide *functional* information on the status of the foundation species that could complement any additional descriptive data that was collected. As the reclamation progresses, and even after certification, the continued use of these ecophysiological parameters offers a strategy to monitor key plant species in the reclaimed area and assess its long-term stability.

Acknowledgments

This research was supported by a grant from Syncrude Canada Ltd. The authors would like to offer special thanks to Jessica Piercey and Carla Wytrykush of Syncrude Canada Ltd. for their assistance with the development and implementation of this research in the Sandhill Watershed. The authors would also like to thank Alice Grgicak-Mannion for providing the schematic diagram of the Sandhill Fen Research Watershed. Jessica Piercey provided valuable revisionary suggestions for the manuscript for which we are grateful.

References

- Alberta Environment (1999) Regional Sustainable Development Strategy for the Athabasca Oil Sands Area, Alberta Environment, Government of Alberta, Report no. 1/754.
- Bruhl, J.J. and Wilson, K.L. (2007) Towards a comprehensive survey of C3 and C4 photosynthetic pathways in Cyperaceae, *Aliso: A Journal of Systematic and Evolutionary Botany*, Vol. 23(1), pp. 99–148.
- Clarke, K.R., and Gorley, R.N. 2006. PRIMER v6: User Manual/Tutorial. PRIMER-E, Plymouth.
- Cody, W.J. (1996) *Flora of the Yukon Territory*, 2nd ed, Ottawa: NRC Research Press.
- FNA (2002) *Magnoliophyta: Commelinidae (in part): Cyperaceae*, New York: Oxford University Press.
- Glaeser, L.C., Vitt, D.H. and Ebbs, S.D. (2015) Responses of the wetland grass, *Beckmannia syzigachne*, to salinity and soil wetness: Consequences for wetland reclamation in the oil sands area of Alberta, *Canada Ecological Engineering* (in review).
- Gravina, A., McKenna, P. and Glenn, V. (2011) Evaluating the success of mineral sand mine rehabilitation on North Stradbroke Island, Queensland: comparisons with reference eucalypt communities, *Proceedings of the Royal Society of Queensland*, Vol. 117, pp. 419–435.
- Jaunatre, R., Buisson, E., Muller, I., Morlon, H., Mesléard, F. and Dutoit, T. (2013) New synthetic indicators to assess community resilience and restoration success, *Ecological Indicators*, Vol. 29(0), pp. 468–477.
- JMP®, Version Pro 14.3.0 SAS Institute Inc., Cary NC, 1989-2018.
- Johnson, E.A. and Myanishi, K. (2008) Creating new landscapes and ecosystems: the Alberta oil sands, *Annals of the New York Academic of Sciences*, Vol. 1134, pp. 120–145.
- Koropchak, S. (2010) *Carex aquatilis* as a pioneer species for boreal wetland reclamation in northern Alberta, Southern Illinois University, Carbondale, IL.
- Koropchak, S., Vitt, D.H., Bloise, R. and Wieder, R.K. (2012) Fundamental paradigms, foundation species selection, and early plant responses to peatland initiation on mineral soils, In Vitt, D. and Bhatti, J. (Eds.), *Restoration and Reclamation of Boreal Ecosystems*, Cambridge University Press, Cambridge, pp. 76–100.
- Lambert, A.M., Baer, S.G. and Gibson, D.J. (2011) Intraspecific variation in ecophysiology of three dominant prairie grasses used in restoration: cultivar versus non-cultivar population sources, *Restoration Ecology*, Vol. 19(101), pp. 43-52.
- Loisel, J., Yu, Z., Beilman, D.W., Camill, P., Alm, J., Amesbury, M.J., Anderson, D., Andersson, S., Bochicchio, C. and Barber, K. (2014) A database and synthesis of northern peatland soil properties and Holocene carbon and nitrogen accumulation, *the Holocene*, Vol. 24(9), pp. 1028–1042.
- Mahmood, M.S. and Strack, M. (2011) Methane dynamics of recolonized cutover minerotrophic peatland: implications for restoration, *Ecological Engineering*, Vol. 37(11), pp. 185–1868.
- Mollard, F.P.O., Roy, M.-C., Frederick, K. and Foote, L. (2012) Growth of the dominant macrophyte *Carex aquatilis* is inhibited in oil sands affected wetlands in Northern Alberta, Canada, *Ecological Engineering*, Vol. 38(1), pp. 11–19.
- Oil Sands Reclamation Committee (1998) *Guidelines for Reclamation to Forest Vegetation in the Athabasca Oil Sands Region*, Alberta Environmental Protection, Report no. ESD/LM/99-1.

- Ostertag, R., Giardina, C.P. and Cordell, S. (2008) Understory colonization of Eucalyptus plantations in Hawaii in relation to light and nutrient levels, *Restoration Ecology*, Vol. 16(3), pp. 475–485.
- Raab, D. and Bayley, S.E. (2013) A *Carex* species-dominated marsh community represents the best short-term target for reclaiming wet meadow habitat following oil sands mining in Alberta, Canada, *Ecological Engineering*, Vol. 54(0), pp. 97–106.
- Rocheffort, L. and Lode, E. (2006) Restoration of degraded boreal peatlands, In Wieder, R.K. and Vitt, D.H. (Eds.), *Boreal Peatland Ecosystems*, Springer Berlin Heidelberg, pp. 381–423.
- Rooney, R.C. and Bayley, S.E. (2011) Setting reclamation targets and evaluating progress: submersed aquatic vegetation in natural and post-oil sands mining wetlands in Alberta, Canada, *Ecological Engineering*, Vol. 37(4), pp. 569–579.
- Rovai, A.S., Barufi, J.B., Pagliosa, P.R., Scherner, F., Torres, M.A., Horta, P.A., Simonassi, J.C., Quadros, D.P.C., Borges, D.L.G. and Soriano-Sierra, E.J. (2013) Photosynthetic performance of restored and natural mangroves under different environmental constraints, *Environmental Pollution*, Vol. 181(0), pp. 233–241.
- Sinclair, T.R. and Horie, T. (1989) Leaf nitrogen, photosynthesis, and crop radiation use efficiency: a review, *Crop Science*, Vol. 29(1), pp. 90–98.
- Sottocornola, M., Boudreau, S. and Rocheffort, L. (2007) Peat bog restoration: effect of phosphorus on plant re-establishment, *Ecological Engineering*, Vol. 31(1), pp. 29–40.
- Thorman, M.N. and Bayley, S.E. 1977. Aboveground plant production and nutrient content of the vegetation in six peatlands in Alberta, Canada. *Plant Ecology* Vol. 13(0), pp. 1–16.
- Timmermann, T., Margóczy, K., Takács, G. and Vegelin, K. (2006) Restoration of peat-forming vegetation by rewetting species-poor fen grasslands, *Applied Vegetation Science*, Vol. 9(2), pp. 241–250.
- Vasander, H., Tuittila, E.S., Lode, E., Lundin, L., Ilomets, M., Sallantausta, T., Heikkilä, R., Pitkänen, M.L. and Laine, J. (2003) Status and restoration of peatlands in northern Europe, *Wetlands Ecology and Management*, Vol. 11(1-2), pp. 51–63.
- Vickers, H., Gillespie, M. and Gravina, A. (2012) Assessing the development of rehabilitated grasslands on post-mined landforms in north west Queensland, Australia, *Agriculture, Ecosystems & Environment*, Vol. 163(0), pp. 72–84.
- Vitt, D.H. and Chee, W.-L. (1990) The relationships of vegetation to surface water chemistry and peat chemistry in fens of Alberta, Canada, *Vegetatio*, Vol. 89, pp. 87–106.
- Vitt, D.H., Wieder, R.K., Xu, B., Kaskie, M. and Koropchak, S. (2011) Peatland establishment on mineral soils: effects of water level, amendments, and species after two growing seasons, *Ecological Engineering*, Vol. 37(2), pp. 354–363.
- Vitt, D.H. and House, M. (2015) Reclaiming peatlands after disturbance from oil sands mining: establishment of bryophytes from indigenous sources, *The Bryologist*, Vol. In review, pp.
- Wang, R.Z., Liu, X.Q. and Bai, Y. (2006) Photosynthetic and morphological functional types for native species from mixed prairie in Southern Saskatchewan, Canada, *Photosynthetica*, Vol. 44(1), pp. 17–25.
- White, P.S. and Walker, J.L. (1997) Approximating nature's variation: selecting and using reference information in restoration ecology, *Restoration Ecology*, Vol. 5(4), pp. 338–349.
- Wytrykush, C., Vitt, D.H., McKenna, G. and Vassov, R. (2012) Designing landscapes to support peatland development on soft tailings deposits, In Vitt, D.H. and Bhatti, J. (Eds.), *Restoration and Reclamation of Boreal Ecosystems*, Cambridge University Press, Cambridge, pp. 161–178.
- Zerbe, S., Steffenhagen, P., Parakenings, K., Timmermann, T., Frick, A., Gelbrecht, J. and Zak, D. (2013) Ecosystem service restoration after 10 years of rewetting peatlands in NE Germany, *Environmental Management*, Vol. 51(6), pp. 1194–1209.

Appendix 5.1 PHASE 1 WETLAND TARGET SELECTION SCORECARD

Peatland Type	ACID FEN	CIRCUM-NEUTRAL FEN	ALKALINE FEN	SODIC FEN	MARSH	RECLAMATION SITE RANGES
<i>Porewater properties</i>						
pH						
Reduced EC (µS/cm)						
Sodium						
Inorganic nitrogen						
Phosphorus						
Potassium						
NPK + Na						
<i>Physical characteristics</i>						
WTP (cm)						
Moss cover						
TOTALS						

*Reduced electrical conductivity has been corrected to remove the influence of H⁺ ions.

Appendix 5.2 Peatland Type - Acid Fen; *Indicates a bog species that is also found in ombrotrophic microsites in poor fens; **Indicates a rich fen species found in minerotrophic transition areas in poor fens. Species lists generated from Environment and Parks 2015 and our personal data collections

Structural Layer	Species	Characteristic Species
Tree	<i>Larix laricina</i>	
	<i>Picea mariana</i>	x
Shrub	<i>Andromeda polifolia</i>	x
	<i>Betula glandulosa</i>	x
	<i>Betula pumila</i>	x
	<i>Chamaedaphne calyculata</i>	x
	<i>Rhododendron groenlandicum</i>	
	<i>Oxycoccus microcarpus</i>	
	<i>Vaccinium uliginosum*</i>	
Herb/ forb/ misc.	<i>Calla palustris**</i>	
	<i>Carex aquatilis</i>	x
	<i>Carex limosa</i>	x
	<i>Carex oligosperma</i>	x
	<i>Carex pauciflora</i>	
	<i>Drosera rotundifolia</i>	
	<i>Equisetum fluviatile**</i>	
	<i>Eriophorum chamissonis</i>	
	<i>Eriophorum vaginatum*</i>	

	<i>Juncus stygius</i>	
	<i>Kalmia polifolia</i> *	
	<i>Menyanthes trifoliata</i>	
	<i>Pedicularis labradorica</i> **	
	<i>Rubus chamaemorus</i> *	
	<i>Sarracenia purpurea</i> **	
	<i>Scheuchzeria palustris</i>	
	<i>Vaccinium vitis-idaea</i>	
	<i>Maianthemum trifolium</i>	x
Bryophytes	<i>Aulacomnium palustre</i>	
	<i>Cladopodiella fluitans</i>	
	<i>Mylia anomala</i>	
	<i>Pohlia nutans</i> *	
	<i>Polytrichum strictum</i> *	
	<i>Sphagnum angustifolium</i>	x
	<i>Shpagnum fallax</i>	
	<i>Sphagnum jensenii</i>	
	<i>Sphagnum lindbergii</i>	
	<i>Sphagnum magellanicum</i>	x
	<i>Sphagnum majus</i>	
	<i>Sphagnum riparium</i>	
	<i>Sphagnum russowii</i>	
	<i>Tomentypnum falcifolium</i>	x
	<i>Warnstorfia exannulata</i>	

Appendix 5.3 Peatland Type – Circumneutral Fen Species lists generated from Environment and Parks 2015 and our personal data collections

Structural Layer	Species	Characteristic Species
Tree	<i>Larix laricina</i>	x
	<i>Picea marina</i>	
Shrub	<i>Betula pumila</i>	x
	<i>Betula glandulifera</i>	x
	<i>Chamaedaphne calyculata</i>	
	<i>Ledum groenlandicum</i>	x
	<i>Myrica gale</i>	
	<i>Salix pedicellaris</i>	x
	<i>Salix petiolaris</i>	
	<i>Salix planifolia</i>	x
Herb/ forb/ misc.	<i>Andromeda polifolia</i>	
	<i>Calamagrostis canadensis</i>	
	<i>Callitriche verna</i>	
	<i>Caltha palustris</i>	

<i>Carex atherodes</i>	
<i>Carex aquatilis</i>	x
<i>Carex canescens</i>	
<i>Carex chordorrhiza</i>	
<i>Carex diandra</i>	x
<i>Carex disperma</i>	
<i>Carex flava</i>	
<i>Carex interior</i>	
<i>Carex lasiocarpa</i>	x
<i>Carex leptolea</i>	
<i>Carex limosa</i>	
<i>Carex paupercula</i>	x
<i>Carex tenuiflora</i>	
<i>Carex utriculata</i>	x
<i>Cicuta maculata</i>	
<i>Deschampsia caespitosa</i>	
<i>Drosera rotundifolia</i>	
<i>Epilobium palustre</i>	
<i>Eriophorum angustifolium</i>	
<i>Eriophorum vaginatum</i>	
<i>Equisetum fluviatile</i>	
<i>Gallium trifidum</i>	
<i>Geum rivale</i>	
<i>Juncus stygius</i>	
<i>Menyanthes trifoliata</i>	x
<i>Muhlenbergia glomerata</i>	
<i>Parnassia palustris</i>	
<i>Pinguicula vulgaris</i>	
<i>Potentilla palustris</i>	x
<i>Rubus arcticus</i>	
<i>Rumex occidentalis</i>	
<i>Sarracenia purpurea</i>	
<i>Scirpus caespitosus</i>	
<i>Scirpus hudsonianus</i>	
<i>Maianthemum trifolia</i>	
<i>Stellaria longifolia</i>	
<i>Tofieldia glutinosa</i>	
<i>Vaccinium vitis-idaea</i>	
<i>Utricularia intermedia</i>	

Bryophytes

<i>Amblystegium serpens</i>	
<i>Aulacomnium palustre</i>	
<i>Brachythecium acutum</i>	x
<i>Calliergonella cuspidata</i>	

<i>Campylium stellatum</i>	
<i>Dicranum undulatum</i>	
<i>Drepanocladus aduncus</i>	x
<i>Drepanocladus polygamus</i>	x
<i>Drepanocladus sordidus</i>	
<i>Hamatacaulis vernicosus</i>	x
<i>Helodium blandowii</i>	
<i>Hypnum lindbergii</i>	
<i>Hypnum pratense</i>	
<i>Mesoptychia ruthiana</i>	
<i>Plagiomnium ellipticum</i>	x
<i>Pleurozium schreberi</i>	
<i>Pseudocalliergon trifarium</i>	
<i>Pseudobryum cinclidioides</i>	
<i>Ptilium crista-castrensis</i>	
<i>Ptychostomum pseudotriquetrum</i>	x
<i>Sanionia uncinata</i>	
<i>Scapania paludicola</i>	
<i>Scorpidium revolvens</i>	
<i>Sphagnum contortum</i>	
<i>Sphagnum fimbriatum</i>	
<i>Sphagnum obtusum</i>	
<i>Sphagnum subsecundum</i>	
<i>Sphagnum teres</i>	x
<i>Sphagnum warnstorffii</i>	x
<i>Tomentypnum falcifolium</i>	
<i>Tomentypnum nitens</i>	x

Appendix 5.4 Peatland Type – Alkaline Fen; *Indicates a species that occurs in oligotrophic microsites. Species lists generated from Slack et al., 1980; Environment and Parks 2015 and our personal data collections

Structural Layer	Species	Characteristic Species
Tree	<i>Larix laricina</i>	x
Shrub	<i>Andromeda polifolia</i> *	
	<i>Betula glandulifera</i>	x
	<i>Betula pumila</i>	x
	<i>Rhododendron groenlandicum</i>	
	<i>Oxycoccus microcarpus</i> *	
	<i>Salix pedicellaris</i>	x
	<i>Vaccinium vitis-idaea</i> *	
Herb/ forb/ misc.	<i>Carex atrofusca</i>	
	<i>Carex chordorrhiza</i>	x

	<i>Carex diandra</i>	x
	<i>Carex flava</i>	
	<i>Carex heleonastes</i>	
	<i>Carex lasiocarpa</i>	x
	<i>Carex limosa</i>	
	<i>Carex microglochin</i>	
	<i>Carex paupercula</i>	
	<i>Carex tenuiflora</i>	
	<i>Drosera anglica</i>	
	<i>Epilobium palustre</i>	
	<i>Epipactis palustris</i>	
	<i>Equisetum fluviatile</i>	x
	<i>Eriophorum angustifolium</i>	
	<i>Eriophorum chamissonis</i>	
	<i>Habenaria hyperborea</i>	
	<i>Juncus stygius*</i>	
	<i>Liparis loeselii</i>	
	<i>Menyanthes trifoliata</i>	
	<i>Muhlenbergia glomerata</i>	
	<i>Parnassia palustris</i>	
	<i>Pinguicula vulgaris</i>	
	<i>Potentilla palustris</i>	x
	<i>Sarracenia purpurea</i>	x
	<i>Schoenus ferrugineus</i>	
	<i>Scirpus cespitosus</i>	
	<i>Scirpus hudsonianus</i>	
	<i>Tofieldia glutinosa</i>	
	<i>Tofieldia pusilla</i>	
	<i>Triglochin maritima</i>	x
	<i>Triglochin palustre</i>	x
	<i>Utricularia minor</i>	
<hr/>		
Bryophytes	<i>Aneura pinguis</i>	
	<i>Aulacomnium palustre</i>	
	<i>Calliergon giganteum</i>	x
	<i>Calliergon richardsonii</i>	
	<i>Campylium stellatum</i>	x
	<i>Cinclidium stygium</i>	x
	<i>Drepanocladus sordidus</i>	
	<i>Hamatocaulis vernicosus</i>	x
	<i>Hypnum pratense</i>	x
	<i>Mesoptychia ruthiana</i>	
	<i>Meesia triquetra</i>	
	<i>Paludella squarrosa</i>	

<i>Plagiomnium ellipticum</i>	x
<i>Pseudocalliergon trifarium</i>	
<i>Pseudocalliergon turgescens</i>	
<i>Ptychostomum pseudotriquetrum</i>	x
<i>Sarmentypnum tundrae</i>	
<i>Scopidium cossonii</i>	
<i>Scopidium revolvens</i>	x
<i>Scopidium scorpioides</i>	x
<i>Tomentypnum nitens</i>	x

Appendix 5.5 Peatland Type – Sodic Fen. Species lists generated from Trites and Bayley 2009; Environment and Parks 2015 and our personal data collections

Structural Layer	Species	Characteristic Species
Herb/ forb/ misc.	<i>Achillea millefolium</i>	
	<i>Aster puniceus</i>	
	<i>Beckmannia syzigachne</i>	
	<i>Calamagrostis stricta</i>	x
	<i>Carex aquatilis</i>	
	<i>Carex atherodes</i>	x
	<i>Carex lasiocarpa</i>	
	<i>Carex prairea</i>	
	<i>Carex utriculata</i>	
	<i>Epilobium palustre</i>	
	<i>Gallium trifidum</i>	
	<i>Hordeum jubatum</i>	
	<i>Juncus alpino-articulatus</i>	
	<i>Juncus balticus</i>	x
	<i>Leymus innovatus</i>	
	<i>Muhlenbergia glomerata</i>	
	<i>Parnassia palustris</i>	
	<i>Puccinellia nuttaliana</i>	
	<i>Plantago maritima</i>	
	<i>Potentilla anserina</i>	
	<i>Ranunculus cymbalaria</i>	
	<i>Rubus pubescens</i>	
	<i>Salicornia europa</i>	
	<i>Scirpus maritimus</i>	
	<i>Scirpus pungens</i>	
	<i>Sium suave</i>	
	<i>Sonchus arvensis</i>	
	<i>Stellaria longifolia</i>	

	<i>Suaeda calceoliformis</i>	
	<i>Triglochin maritima</i>	x
	<i>Trichochochin palustris</i>	x
	<i>Tofieldia glutinosa</i>	
Bryophytes	<i>Amblystegium serpens</i>	
	<i>Aulacomnium palustre</i>	
	<i>Brachythecium acutum</i>	
	<i>Ptychostomum pseudotriquetrum</i>	x
	<i>Campylium stellatum</i>	x
	<i>Drepanocladus aduncus</i>	
	<i>Drepanocladus polygamus</i>	
	<i>Leptobryum pyriforme</i>	

Appendix 5.6 Wetland Type – Marsh. Species lists generated from Bayley and Mewhort, 2004; Whitehouse and Bayley, 2005 and our personal data collections

Structural Layer	Species	Characteristic Species
Shrub	<i>Salix pedicellaris</i>	
Herb/ forb/ misc.	<i>Agrostis scabra</i>	
	<i>Alopecurus aequalis</i>	
	<i>Barbarea orthoceras</i>	
	<i>Bidens cernua</i>	
	<i>Calamagrostis canadensis</i>	x
	<i>Callitriche verna</i>	
	<i>Calla palustris</i>	
	<i>Caltha palustris</i>	
	<i>Carex aquatilis</i>	x
	<i>Carex atherodes</i>	x
	<i>Carex lasiocarpa</i>	
	<i>Carex utriculata</i>	x
	<i>Cicuta maculata</i>	x
	<i>Epilobium leptophyllum</i>	
	<i>Equisetum arvense</i>	
	<i>Galium boreale</i>	
	<i>Galium trifidum</i>	
	<i>Geum rivale</i>	
	<i>Hordeum jubatum</i>	
	<i>Lemna minor</i>	x
	<i>Mentha arvensis</i>	
	<i>Menyanthes trifoliata</i>	
	<i>Petasites sagittatus</i>	

	<i>Polygonum amphibium</i>	x
	<i>Polygonum lapathifolium</i>	
	<i>Potentilla norvegica</i>	
	<i>Potentilla palustris</i>	x
	<i>Rumex crispus</i>	
	<i>Rumex occidentalis</i>	
	<i>Scutellaria galericulata</i>	
	<i>Senecio congestus</i>	
	<i>Sium suave</i>	
	<i>Sparganium eurycarpum</i>	
	<i>Typha latifolia</i>	x
Bryophytes	<i>Amblystegium serpens</i>	
	<i>Brachythecium acutum</i>	
	<i>Drepanocladus aduncus</i>	
	<i>Marchantia polymorpha</i>	
	<i>Ptychostomum pseudotriquetrum</i>	

Appendix 5.7 Wetland Type – Sandhill Wetland (year 2018 vegetation survey data from 20 survey plots; sixth full growing season since inception)

Structural Layer	Species	Characteristic Species
Tree	<i>Populus balsamifera</i>	x
	<i>Populus tremuloides</i>	
Shrub	<i>Betula glandulifera</i>	
	<i>Salix exigua</i>	
	<i>Salix lutea</i>	x
Herb/ forb/ misc.	<i>Achillea millefolium</i>	
	<i>Aster conspicuus</i>	
	<i>Aster puniceus</i>	
	<i>Bromus ciliatus</i>	
	<i>Calamagrostis canadensis</i>	x
	<i>Carex aquatilis</i>	x
	<i>Carex canescens</i>	
	<i>Carex utriculata</i>	x
	<i>Cirsium arvense</i>	
	<i>Epilobium angustifolium</i>	
	<i>Equisetum arvense</i>	
	<i>Equisetum pratense</i>	
	<i>Fragaria vesca</i>	
	<i>Glyceria borealis</i>	
	<i>Lotus corniculatus</i>	
	<i>Parnassia palustris</i>	
	<i>Poa palustris</i>	

	<i>Polygonum amphibium</i>	
	<i>Ribes lacustre</i>	
	<i>Rubus idaeus</i>	x
	<i>Rubus pubescens</i>	x
	<i>Scirpus atrocinctus</i>	
	<i>Scirpus lacustris</i>	
	<i>Sonchus arvensis</i>	
	<i>Taraxacum officinale</i>	
	<i>Trientalis borealis</i>	x
	<i>Triglochin maritima</i>	
	<i>Typha latifolia</i>	x
	<i>Utricularia intermedia</i>	x
	<i>Vicia americana</i>	
<hr/>		
Bryophytes	<i>Aneura pinguis</i>	
	<i>Aulacomnium palustre</i>	
	<i>Campylium stellatum</i>	
	<i>Cephalozia connivens</i>	
	<i>Ceratodon purpureus</i>	
	<i>Drepanocladus polygamus</i>	
	<i>Funaria hygrometrica</i>	
	<i>Leptobryum pyriforme</i>	
	<i>Ptychostomum pseudotriquetrum</i>	
<hr/>		

10 Publications

Published during tenure of this grant or not previously reported:

Ebbs, SE, Glaeser, L, House, M, Vitt, D (2015) A plant physiological approach to assess the performance and potential success of mine revegetation. In: Fourie, AB, Tibbett, L, Sawartsky, L, van Zyl, D (eds.). Mine Closure 2915: Proceeding of the 10th International Conference on Mine Closure: June 1-3, 2015, Vancouver, Canada. Infomine Inc., Vancouver BC. 14 pp.

Hartsock JA, House M, Vitt DH (2016). Net nitrogen mineralization in boreal fens: a potential performance indicator for peatland reclamation. *Botany*, 94:1027-1040.

Vitt DH, House M, Hartsock JA (2016). Sandhill Fen, an initial trial for wetland species assembly on in-pit substrates: lessons after three years. *Botany*, 94:1015-1025.

Published from research during this grant:

Hartsock JA, Bremer E (2018). Nutrient supply rates in a boreal extreme-rich fen using ion exchange membranes. *Ecohydrology* 11:8 doi:10.1002/eco.1995.

Hartsock, JA, E Bremer, E, Vitt DH (2019). Nutrient supply patterns across the Sandhill Fen reclamation watershed and regional reference fens in Alberta, Canada: An ion exchange membrane study. *Ecohydrology* Doi: 10.1002/eco.2188.

Hartsock, JA, Piercey, J, House, MK, Vitt, DH (2020). Comparing water quality at Sandhill Wetland to natural reference wetlands and environmental quality guidelines for Alberta surface waters. *Wetland Ecology and Management* (in review).

Vitt, DH, Glaeser, LC, House, M, Kitchen, S (2020). Responses of *Carex aquatilis* to a regime of increasing sodium concentrations. *Wetland Management and Ecology* (in review).

Publications utilizing data from Sandhill Wetland (atmospheric deposition):

Wieder, RK, Vile, M, Scott, K, Albright, CM, McMillen, K, Vitt, D, Fenn, M (2016). Differential effects of high atmospheric deposition on bog plant/lichen tissue and porewater chemistry across the Athabasca oil sands region. *Environmental Science and Technology* 50: 12630-12640, DOI: 10.1021/acs.est.6b03109.

Wieder, RK, Vile, M, Albright, CM, Scott, K, Vitt, DH, Quinn, JC, Burke-Scoll, M (2016). Effects of altered atmospheric nutrient deposition from Alberta oil sands development on *Sphagnum fuscum* growth and C, N and S accumulation in peat. *Biogeochemistry* DOI 10.1007/s10533-016-0216-6.

Dissertation

Hartsock, J. 2020. Characterization of key performance measures at the reclaimed Sandhill Wetland: Implications for achieving wetland reclamation success in the Athabasca oil sands region. Ph.D. thesis, 224 pp.

APPENDIX 6: THE SANDHILL WATERSHED: EARLY TREE ESTABLISHMENT AND VEGETATION COLONIZATION OF UPLAND AREAS- THE FIRST FIVE YEARS

TERMS OF USE

University of Alberta was retained by Syncrude to carry out the studies presented in this report and the material in this report reflects the judgment of author(s) in light of the information available at the time of document preparation. Permission for non-commercial use, publication or presentation of excerpts or figures requires the consent of the author(s). Commercial reproduction, in whole or in part, is not permitted without prior written consent from Syncrude. An original copy is on file with Syncrude and is the primary reference with precedence over any other reproduced copies of the document.

Reliance upon third party use of these materials is at the sole risk of the end user. Syncrude accepts no responsibility for damages, if any, suffered by any third party as a result of decisions made or actions based on this document. The use of these materials by a third party is done without any affiliation with or endorsement by Syncrude.

Additional information on the report may be obtained by contacting Syncrude.

This appendix may be cited as:

Landhäusser, S. 2019. The Sandhill Watershed: early tree establishment and vegetation colonization of upland areas, the first five years. Appendix 6 in Syncrude Canada Ltd. *Sandhill Fen Watershed: Learnings from a Reclaimed Wetland on a CT deposit*. Syncrude Canada Ltd. 2020.

The Sandhill Watershed: Early tree establishment and vegetation colonization of upland areas

The First Five Years

Version: January 8, 2019

Prepared for Syncrude Canada Ltd
Syncrude Canada Ltd – Research
9421 17 Ave NW
Edmonton, AB T6N 1H4

Prepared by the Landhäuser Research Group
4-42 Earth Sciences Building
Department of Renewable Resources
University of Alberta
Edmonton, AB T6G 2E3

Information contained in this report should not be published without the consent of the authors.

Acknowledgements

Preparation of this report was led by Simon Landhäusser and Fran Leishman with the data and help of members of the Landhäusser Research Group, Department of Renewable Resources, University of Alberta, and members of the Pinno Research Group, Natural Resources Canada, Canadian Forest Service, Northern Forestry Centre. This report includes data summarizing tree and vegetation development over the first five growing seasons at the Sandhill Watershed.

Individuals who contributed significantly to this report include Ruth Errington, Shaun Kulbaba, Alexander Goeppel, Elizabeth Hoffman, Katherine Melnik, Morgane Merlin and Caren Jones.

Support is acknowledged from the countless summer research assistants and staff at the University of Alberta and Syncrude. In particular, we thank Eckehart Marenholtz, Jessica Piercey and Carla Wytrykush for their support. This research was financially supported by Syncrude Canada Ltd.

List of publication, theses, and presentations related to the research project

Refereed publication:

Merlin, M, Leishman, F, Errington, RC, Pinno, BD & Landhäusser SM. 2018. Exploring drivers and dynamics of early boreal forest recovery of heavily disturbed mine sites: a case study from a reconstructed landscape [online]. *New Forests*. doi: .10.1007/s11056-018-9649-1.

Theses

Goeppel AE. 2014. Evaluating Jack Pine Seedling Characteristics in Response to Drought and Outplanting. M.Sc. Thesis, University of Alberta, 96 pages

Hoffman E. 2016. Influence of Environmental and Site Factors and Biotic Interactions on Vegetation Development Following Surface Mine Reclamation Using Coversoil Salvaged From Forest Sites. M.Sc. thesis, University of Alberta. 118 pages.

Kulbaba SP. 2014. Evaluating trembling aspen (*Populus tremuloides* Michx.) seedling stock characteristics in response to drought and out-planting on a reclamation site. M.Sc. Thesis, University of Alberta, 107 pages.

Melnik K. 2013. Role of aspect and CWD in plant diversity recovery. B.Sc. Honours Thesis, University of Alberta. 23p.

Presentations and Reports

2017

Leishman F, Errington R, Merlin M, Pinno B and Landhäusser SM. 2017. Developing an upland forest on a reconstructed watershed after oil sands mining in northern Alberta, Canada. 3rd Restoring Forests Conference, Lund, Sweden. Oral presentation.

Lukenbach M, Spencer C, Mendoza C, Devito K, Carey S and Landhäusser SM. 2017. Resolving the Need for Groundwater Recharge versus Forest Productivity in a Reclaimed Watershed. Geological Society of America Annual Meeting, Seattle, Washington. Oral presentation.

Merlin M, Leishman F, Errington R, Pinno B and Landhäusser SM 2017. Drivers affecting tree performance on upland areas of a reconstructed watershed. North American Forest Ecology Workshop, Edmonton, AB, Canada. Oral presentation.

Pinno B, Merlin M, Leishman F, Errington R, and Landhäusser SM. 2017. Upland forest development in a reconstructed watershed after oil sands mining in northern Alberta, Canada, National Meeting of the American Society of Mining and Reclamation, Morgantown, WV. <https://wvmdtaskforce.files.wordpress.com/2017/05/2017-pinno-monday-130.pdf>. Oral presentation.

2016

Merlin, M, Hoffman, E, Leishman, FG, Landhäusser SM, Errington, R, and Pinno, BD. 2016. Syncrude Sandhill Fen tree establishment data. Sandhill Fen Technical Advisory Meeting 2016, December 8-9, 2016, Edmonton. Oral presentation.

2015

Hoffman, E, Landhäusser, SM, and Macdonald, E. 2015. Temporal and spatial development of vegetation community patterns on reclaimed boreal forest sites using salvaged forest floor material. North American Forest Ecology Workshop, June 15, 2015, Veracruz, Mexico. Oral presentation.

Hoffman, E, Landhäusser, SM, and Macdonald, E. 2015. Vegetation pattern development on reclaimed mine sites using salvaged forest floor material. SER Conference, August 23-27, 2015, Manchester, UK. Poster presentation.

Merlin, M, Leishman, FG, Landhäusser SM, Errington, R, and Pinno, BD. 2015. Syncrude Sandhill Fen tree establishment data. Sandhill Fen Technical Advisory Meeting 2014, December 8-9, 2015, Edmonton. Oral presentation.

2014

Hoffman, E. 2014. Spatial interactions between weeds and forest species in response to donor materials from different forest ecosites. Ren R 604 Presentation, March 6, 2014, Edmonton. Oral Presentation.

Hoffman, E, and Landhäusser SM. 2014. Weed population dynamics in response to donor materials from different forest ecosites. Forestry Industry Lecture Series, March 27, 2014, Edmonton. Poster presentation.

Leishman, FG, Landhäusser SM, Errington, R, and Pinno, BD. 2014. Upland vegetation on the Sandhill Fen: Summer 2014. Sandhill Fen Technical Advisory Meeting 2014, December 8, 2014, Edmonton. Oral presentation.

2013

Kulbaba, S, Goepfel, A, and Landhäusser SM. 2013. Evaluating seedling stock characteristics in response to drought. CONRAD Environmental Reclamation Research Group (ERRG) Research Symposium, January 28-29, 2013, Edmonton. Oral presentation.

Leishman, FG, Errington, R, Landhäusser SM, and Pinno, BD. 2013. Landhäusser Research Group Summary 2012: Forest reconstruction on upland sites in the Sandhill Fen Watershed. Summary Report presented to Syncrude Canada Ltd.

Melnik, K, Cahill, JF, Landhäusser SM, Leishman, FG. 2013. Impacts of aspect and coarse woody debris on biodiversity of reclaimed sites. Biology 499 Final Presentation, April 11, 2013, Edmonton. Oral Presentation.

Melnik, K, Landhäusser SM, and Leishman, FG. 2013. Boreal plants prefer shelter in close proximity to coarse woody debris on reclamation sites. CONRAD Environmental Reclamation Research Group (ERRG) Research Symposium, January 28-29, 2013, Edmonton. Poster presentation.

2012

Errington, R, Leishman, FG, Landhäusser SM, and Pinno, BD. 2012. Upland vegetation on the Sandhill Fen: Summer 2012. Sandhill Fen Technical Advisory Meeting 2012, December 11, 2012, Edmonton. Oral Presentation.

Table of Contents

Acknowledgements	ii
List of publication, theses, and presentations related to the research project	iii
Refereed publication:.....	iii
Theses.....	iii
Presentations and Reports	iii
Summary and Implications	ix
Terminology and Abbreviations	xiv
List of Tables	xvi
General Introduction	xvi
Part I.....	xvi
Project 1	xvii
Part II.....	xvii
Project 2	xix
Project 3	xix
List of Figures	xx
General Introduction	xx
Part I.....	xx
Project 1	xx
Part II.....	xxii
Project 2	xxii
Project 3	xxiii
List for Appendix A	xxiv
List for Appendix B	xxv
List for Appendix C	xxvi
List for Appendix D	xxviii
List for Appendix E	xxix
Introduction	1
Part I: Seedling growth response to planting density and site conditions, and identifying drivers and dynamics of these responses.....	2
Project 1: Evaluating jack pine and trembling aspen seedling characteristics to water availability impact of aspect and hydrogel amendment	3
Part II: Factors and drivers affecting early colonizing vegetation development on reclaimed boreal upland sites	4

Project 2: Role of slope aspect and coarse woody debris in plant colonization	5
Project 3: Spatial variation, seedbank and soil type driving vegetation colonization on reclaimed upland sites	5
General Site Description and Measurements	6
Reclaimed landscape description.....	6
Plot layout and measurements.....	8
Seedling performance measurements	9
Measurement of CWD and colonizing vegetation	9
Measurements of edaphic variables.....	10
General Statistical Analyses	13
Linear models.....	13
Structural equation models	13
Part I: Seedling growth response to planting density and site conditions, and identifying drivers and dynamics of these responses.....	17
Capping soil characteristics	17
Climatic and edaphic conditions	17
Seedling survival.....	21
Seedling growth and foliar nutrition.....	22
Environmental drivers of seedling growth	25
Project 1: Evaluating jack pine and trembling aspen seedling characteristics to water availability impact of aspect and hydrogel amendment.....	28
Methods.....	28
Initial seedling characteristics	28
Outplanting and hydrogel amendments	32
Seedling measurements	34
Data analysis for pine.....	35
Data analysis for aspen.....	36
Results.....	37
Climatic conditions (2012) after outplanting	37
Soil moisture and temperature conditions	38
Soil nutrient supply.....	40
Seedling growth and physiological response on north and south-facing plots	41
Impact of hydrogel amendment.....	45
Part II Factors and drivers affecting early colonizing vegetation development on reclaimed boreal forest upland sites	50
Methods.....	50

Plot establishment.....	50
Vegetation measurements	50
Statistical analysis.....	51
Results.....	52
Coversoil material type.....	52
Vegetation diversity and cover in areas capped with coarse coversoil.....	54
Vegetation diversity and cover in areas capped with fine coversoil	58
Vegetation community composition.....	61
Vegetation community change from 2012 to 2015.....	63
Project 2: Role of slope aspect and coarse woody debris in plant establishment	66
Methods.....	66
Plot establishment and field measurements.....	66
Greenhouse seedbank study	66
Statistical analyses.....	67
Results.....	68
Project 3: Spatial variation, seedbank and soil type driving vegetation	
colonization on reclaimed upland sites	72
Methods.....	72
Field sites.....	72
Experimental design.....	73
Vegetation and environmental variable measurements	73
Statistical analyses.....	75
Results.....	77
Literature Cited.....	82
Appendix A: Supplemental material for seedling growth response to planting	
density and site conditions, and identifying drivers and dynamics of these	
responses (Part I).....	87
Appendix B: Supplemental material for evaluating jack pine seedling	
characteristics in response to aspect and hydrogel amendment (Project 1)	91
Appendix C: Supplemental material for factors and drivers affecting early	
colonizing vegetation development on reclaimed boreal upland sites (Part II).....	93
Appendix D: Supplemental material for role of slope aspect and coarse woody	
debris in plant colonization (Project 2)	111
Appendix E: Supplemental material for spatial variation, seedbank and soil type	
driving vegetation colonization on reclaimed upland sites (Project 3)	113

Summary and Implications

Part I Seedling growth response to planting density and site conditions, and identifying drivers and dynamics of these responses:

- All planted tree seedlings grew much taller on the hummocks capped with fine-textured coversoil compared to hummocks capped with the coarse-textured coversoil. However, the hummocks with fine-textured coversoils experienced much greater soil moisture loss during dry years (i.e. 2015) compared to the areas capped with coarse-textured coversoil. Likely the difference in the depletion soil water is related to the stark differences in leaf area development on these two different site types. To explore these responses in more detail, these leaf area-soil water relationship will require further attention as forest stands and their associated leaf area develop on the hummocks.
- Overall, planted tree seedling survival was high across the site, regardless of coversoil material. Some reduced survival was seen in trembling aspen (potentially related to stock quality), while survival in white spruce and pine was consistently high. The variation in survival among species could be related to seedling quality, indicating that planted tree seedlings are capable of establishing on upland reclamation sites over a wide range of site conditions, with early growth rates reflecting the site conditions. Of the three planted tree species, white spruce lacked a strong response to most site conditions and planting regimes, while aspen and pine were much more responsive.
 - Within the first five years after site construction, soil available nutrients (i.e. coversoil material) and woody debris placement drove early aspen and pine growth responses across the site.
 - Although variables such as topography and planting density appear to play a minor role at this point in time, aspen and pine seedlings responded only to different planting densities and aspects when site condition were more extreme (e.g. less growth on coarse textured soils on south-facing slopes).
 - Structural Equation Modeling (SEM) was used to explore this complex data set of biotic and abiotic variables. This modeling approach allowed for a more detailed exploration of the data, exposing relationships and interaction

that linear modeling alone would not be able to detect and potentially identifying indirect causal pathways. Due to lack of plots in some of our treatments, we were able to do this only for planted jack pine seedlings on the coarse coversoils. Using this analysis we uncovered temporal shifts in the variables that governed seedling performance, indicating a pronounced shift from seedling stock quality variables early in the recovery to biotic (competition), edaphic (soil nutrients), and climatic variables (water availability) later in the development.

- Achieving early canopy closure (within 5 growing seasons) by planting higher seedling density was only achieved on the hummocks that were capped with fine textured soils. Planting at 10000 vs. 5000 did not result in much greater benefits to seedling performance and understory development in the short-term; however, more monitoring is required to explore longer-term impacts of planting densities on other forest ecosystem functions such as understory development and water-use.
- Although not studied in detail across the Sandhill fen watershed, the measured and documented variability in topography, coversoils, tree density and species composition, and CWD placement provided significant spatial variability and complexity across this reconstructed landscape feature. This variability is expected to be reflected in greater ecosystem heterogeneity and related ecosystem functions such as hydrological and soil edaphic processes and successional patterns, which in the long-term is expected to have positive effects on ecosystem responses and recovery to disturbances in these reconstructed landscapes.

Project 1: Evaluating jack pine and trembling aspen seedling characteristics to water availability impact of aspect and hydrogel amendment

- It appears that a larger pine seedling stock type was more suitable for reclamation sites, this planting stock grew taller in height while developing larger root systems. There was some indication that shorter pine seedling stock with higher root to shoot ratios (RSR) may also be suitable, particularly in coarse-textured reclamation coversoils, where the threat from above- and below-ground competition is low.
- Aspen seedling stock with high root to shoot ratios (RSR) established and grew more regardless of field conditions. It appears that higher non-structural carbon

reserve (NSC) concentrations in the roots may also have been beneficial to outplanting success. High NSC reserve content (i.e. the reserve pool size, which is related to initial seedling size) did not appear to directly improve growth or outplanting success. Tall aspen seedlings, which have higher NSC content, but often have low RSR, appear to have reduced growth, leaf area and root development, particularly on stressed sites.

- Amending coarse textured soils exposed to a high heat load index (i.e. coarse soils on a south facing aspect) with materials that hold water (i.e. hydrogel) could be beneficial for establishing trees; however, in our study hydrogel did not increase the soil water availability or improve seedling water status, most likely the result of a wet growing season during our experiment. Despite the lack of drought conditions, the potential for hydrogel to help retain soil moisture during less favorable conditions should not be ignored, as aspen seedling height and root growth was increased with hydrogel amendment,. This response might be driven by other edaphic conditions that indicated increased phosphorous and potassium availability in soils amended with hydrogel.

Part II Factors and drivers of early colonizing vegetation development on reclaimed boreal forest upland sites:

- As was expected the cover soils salvaged from two very different forest types resulted in the development of two very different plant communities early in site development. The early response of the colonizing vegetation was most strongly driven by coversoil characteristics and the legacies (propagule bank) contained within. In areas capped with coversoil salvaged from a poor-xeric forest site, vegetation communities included a greater proportion of native species, graminoids and shrubs, while in areas capped with coversoil salvaged from a rich-mesic forest site, vegetation communities were composed of proportionally more introduced species and forbs.
- After five growing season the colonizing vegetation on the hummocks capped with the two different cover soils continue to be different from each other. However, vegetation communities in areas capped with coversoils salvaged from poor-xeric and rich-mesic forest types became more similar to each other over the years studied. It is not clear from our study whether this trend of convergence will continue. It is possible that, on longer timescales, topographical position, density

of planted tree seedlings and coarse woody debris will be more important drivers of vegetation community development than initial coversoil source.

- Regardless of coversoil, vegetation diversity was primarily influenced by seedling planting density (canopy cover) and topographical aspect. In both coversoils metrics of diversity were highest in areas with north facing aspects and higher tree density. North facing aspects, which typically experience less heat and moisture stress, and treatments with higher densities of tree seedlings may have created an environment that was more favourable for the emergence and growth of the largely forest adapted species present in the propagule banks of the coversoils, leading to a more diverse community. Complex interactions between planting density, aspect and coarse woody debris (CWD) impacted metrics of diversity in both coversoils.
- In areas capped with the coarse coversoil from the poor-xeric forest site, the effect of aspect on diversity was modified by CWD abundance, suggesting that coarse woody debris may have moderated the harsher environmental conditions present on south facing slopes in areas capped with the poor-xeric material, where water may have been limiting. This indicates that CWD appears to have a beneficial effect on colonizing vegetation and seedling growth. Varying the volumes of CWD at different scales appears to encourage variation in colonizing vegetation cover and with that heterogeneity of plant communities at different spatial scales (see also Projects 2 and 3).
- Changes of the colonizing vegetation community were rapid early on (first two growing seasons) and dominated by few non-native, annual and biannual ruderal species, while plant communities appear to become more stable (perennial species driven) in the subsequent years, where changes are more subtle.
- Over the whole site we found 196 different plant species in the upland areas of the Sandhill Watershed and we believe that the increased spatial variability, a result of topographical variation, differences in coversoil materials, and placement of CWD played a significant role in the high species richness, community diversity and heterogeneity across this reclaimed landscape.

Projects 2 and 3: Role of slope aspect and coarse woody debris in plant colonization; and spatial variation, seedbank and soil type driving vegetation colonization on reclaimed upland sites

- Variation in topography at different scales ranging from the microtopographical (one meter or less in height) scale to the landscape level has significant effects on colonizing vegetation and the expression of the legacy seedbank contained in the coversoil material. At the microscale, CWD enhanced the expression of this seedbank allowing more forest specific species to establish. At the hummock scale, slope and aspect impact seedling growth and plant community development. Providing variability at different scales is expected to further enhance microsite availability for colonizing vegetation and with that future species richness and diversity.
- Increasing tree planting density (aspen and pine) had a positive effect on maintaining the initial diversity of native and forest associated species contained in the salvaged forest floor material.
- Coarse woody debris (CWD) can help ameliorate harsh conditions (such as the high heat load index on south-facing slopes capped with coarse-textured cover soils) and increase diversity and cover of native and forest associated vegetation. However, there is a trade-off with space occupied by CWD and site availability for plant establishment and growth. This points to a need for potentially prioritizing deployment of CWD, particularly when supply is limited.
- As spatial patterns of the vegetation on reclamation sites change over time, the importance of introduced annual and biannual species currently considered weedy species in the community may decline. However, the long-term effects of canopy development on both native and non-native non-forest perennial grasses and forbs and their effect on forest-associated species are not clear. Therefore, until the effects of these species types on forest-associated species are better understood, management interventions such as non-selective herbicide use to control introduced vegetation should be viewed with caution, as with closing tree canopy conditions further shifts in plant communities can be expected.

Terminology and Abbreviations

AOSR	Athabasca Oil Sands Region
Aspen highNSC stocktype	An aspen seedling stocktype that was developed by germinating seeds under greenhouse conditions in early spring, applying paclobutrazol after seven weeks and then transferring seedlings outside for the rest of the growing season after 15 weeks
Aspen highRSR stocktype	An aspen seedling stocktype that was developed by germinating seeds under greenhouse conditions in early spring and then transferring seedlings outside for the rest of the growing season after five weeks
Aspen large stocktype	An aspen seedling stocktype that was developed by germinating seeds under greenhouse conditions in early spring and then transferring seedlings outside for the rest of the growing season after 17 weeks
Coversoil	Soil material placed at the soil surface of reconstructed soil profiles
CWD	Coarse woody debris
Coarse-textured coversoil	A mixture of the organic forest floor layer and the underlying mineral soil layers typically found on poor-xeric uplands sites dominated by <i>Pinus banksiana</i> and Brunisolic soil types. This coversoil type may also be referred to interchangeably as a “poor-xeric” coversoil
Fine-textured coversoil	A mixture of the organic forest floor and the upper underlying mineral soil layers typically found in rich-mesic upland forest sites dominated by <i>Populus tremuloides</i> and Luvisolic soil types This coversoil type may also be referred to interchangeably as a “rich-mesic” coversoil.
FFM	Salvaged surface soil layers containing the organic forest floor plus the upper underlying A and portion of the b horizon
HLI	Head load index
NSC	Non-structural carbohydrates
Pine G stocktype	A jack pine stocktype that was developed by germinating seeds under greenhouse conditions in early spring (April 11)

	and seedlings continued development under greenhouse conditions for the rest of the growing season
Pine O stocktype	A jack pine stocktype that was developed by germinating seeds under greenhouse conditions in early spring (April 11), and then moving seedlings outside eight weeks later (June 7), where they continued development for the rest of the growing season
Pine OL stocktype	A jack pine stocktype that was developed by germinating seeds under greenhouse conditions mid-spring (May 8), and then moving seedlings outside four weeks later (June 7), where they continued development for the rest of the growing season
RSR	Root to shoot ratio
PRS ^{RTM} probes	Plant root simulator probes
SEM	Structural equation modeling
Subsoil	Soil material placed below the coversoil, but above the overburden material of reconstructed soil profiles

List of Tables

General Introduction

Table 1: Summary of types of measurements taken at each research plot in upland areas of the Sandhill Watershed, the unit in which they are expressed, and when measurements were taken between the 2012 and 2016 growing seasons (May 1 to September 30). “Aw” indicates trembling aspen, “Pj” indicates jack pine and “Sw” indicates white spruce.	12
Table 2: Theoretical constructs (see Figure 2), observed variables and their properties used for the structural equation modeling. The variables labels used in the results are shown in parenthesis and between quotes in the second column.	16
Table 3: Characteristics of coversoils and subsoils placed at the Sandhill Watershed site. Coversoils were salvaged from two forest types, a nutrient poor site with a xeric moisture regime (coarse) and a nutrient rich site with a mesic moisture regime (fine). The coversoil from a coarse forest site was underlain by a sandy subsoil material, and the coversoil from a fine forest site was underlain by a clay loam subsoil material. Data (mean \pm one standard deviation) were collected in 2013 (Syncrude Canada Ltd. 2014).	18
Table 4: Growing season (May 1 – September 30) mean temperature ($^{\circ}$ C) and total precipitation (mm). 2012 data was obtained from AgroClimatic Information Service (2018), all remaining data was obtained from McMaster University (Hamilton, ON, Canada).	18

Part I

Table 1.1: Foliar nutrient (nitrogen, potassium and phosphorus) concentrations of planted trembling aspen and jack pine seedlings planted on coarse or fine coversoils in 2013 and 2016. Mean values and standard deviation for each species, year and coversoil are presented for foliar nitrogen, potassium and phosphorus. All values are presented in mg g^{-1} . The letters between parentheses in the mean columns for each foliar nutrient indicate a statistical difference between the years and soil, “ns”: not significant.	25
Table 1.2: Linear models of the environmental and seedling-specific variables that affected height of trembling aspen on the fine soil and white spruce on both soils for the time periods of 2012-2013 and 2012-2016. For each significant variable or interaction of variables, the slope (linear relationship), or difference (factor levels differences) is presented with its associated p -value. The marginal R^2 for each model is presented. Label: “ns”: non-significant.	26

Project 1

Table 1.1.1: Pre-outplanting average (\pm SE) of morphological and carbon reserve characteristics of seedling stock types (G, O, OL). RSR is root:shoot ratio and NSC is nonstructural carbohydrates. Different letters signify statistical differences among means based on comparisons using Tukey-Kramer adjustment (n=24 with the exception of NSC content and concentrations: n=15). 30

Table 1.1.2: Initial morphological (height, tissue masses and RSR; n=24) and carbohydrate reserve (n=8) characteristics (average \pm SE) of the three trembling aspen seedling stock types prior to the experiment. Different letters signify statistical differences among means based on comparisons using Tukey-Kramer adjustment. ... 32

Table 1.1.3: Average available nutrients (\pm SE) of north-facing, south-facing, and hydrogel plots. Units are expressed as $\mu\text{g } 10 \text{ cm}^{-2} 32 \text{ days}^{-1}$ and different letters signify statistical differences between means based on Tukey-Kramer adjustment (n=10) (Syncrude Canada Ltd. 2014). 40

Part II

Table 2.1: Results of linear mixed effects models testing for the effects of tree planting density (PD), heat load index (HLI; reflecting slope and aspect), and coarse woody debris volume (CWD) on vegetation diversity (overall species richness (Hill number N_0), Hill numbers N_1 (e^x , where x=Shannon's index) and N_2 (the inverse of Simpson's index), and native, introduced, forb and graminoid species richness) and cover (all species, native species, introduced species, forb species, and graminoid species) in areas capped with a coarse-textured coversoil salvaged from a poor-xeric site (see Table C.2 for a complete species list). *P*-values are bolded when significant. Interaction terms are shown when significant; interactions were removed from models when not significant. 54

Table 2.2: Summary of least squared means (\pm standard error) showing all significant effects of planting density on metrics of vegetation diversity for sites capped with coarse-textured coversoils. N_1 is e^x , where x=Shannon's index, and N_2 is the inverse of Simpson's index. Letters in rows indicate significant differences between treatments. Unplanted=0 stems per hectare, Medium Density=5000 stems per hectare, High Density=10000 stems per hectare. See also Table 2.1 56

Table 2.3: Summary of estimates (\pm standard error) showing all significant effects of heat load index on metrics of vegetation diversity for sites capped with coarse-textured coversoils. N_1 is e^x , where x=Shannon's index, and N_2 is the inverse of Simpson's index. See also Table 2.1 56

- Table 2.4: Summary of estimates (\pm standard error) showing all significant effects of coarse woody debris volume on metrics of vegetation diversity for sites capped with coarse-textured coversoils. N_1 is e^x , where x =Shannon's index, and N_2 is the inverse of Simpson's index. See also Table 2.1. 56
- Table 2.5: Results of linear mixed effects models testing for the effects of tree planting density (PD), heat load index (HLI; reflecting slope and aspect), and coarse woody debris amount (CWD) on vegetation diversity (overall species richness (Hill number N_0), Hill numbers N_1 (e^x , where x =Shannon's index) and N_2 (the inverse of Simpson's index), and native, introduced, forb and graminoid species richness) and cover (all species, native species, introduced species, forb species, and graminoid species) in areas capped with a fine-textured coversoil salvaged from a rich-mesic site(see Table C.2 for a complete species list). *P*-values are bolded when significant. Interaction terms are shown when significant; interactions were removed from models when not significant. 58
- Table 2.6: Summary of least squared means (\pm standard error) showing all significant effects of planting density on metrics of vegetation diversity for sites capped with fine-textured coversoils. N_1 is e^x , where x =Shannon's index, and N_2 is the inverse of Simpson's index. Letters in rows indicate significant differences between treatments. Unplanted=0 stems per hectare, Medium Density=5000 stems per hectare, High Density=10000 stems per hectare. See also Table 2.5..... 60
- Table 2.7: Summary of estimates (\pm standard error) showing all significant effects of heat load index on metrics of vegetation diversity for sites capped with fine-textured coversoils. N_1 is e^x , where x =Shannon's index, and N_2 is the inverse of Simpson's index..... 60
- Table 2.8: Summary of estimates (\pm standard error) showing all significant effects of coarse woody debris volume on metrics of vegetation diversity for sites capped with fine-textured coversoils. N_1 is e^x , where x =Shannon's index, and N_2 is the inverse of Simpson's index. 61
- Table 2.9: Results of permutational multivariate analysis of variance (PERMANOVA) models testing for the effects of tree planting density (PD), heat load index (HLI; reflecting slope and aspect) and coarse woody debris (CWD) volume on community composition in areas capped with a coarse-textured or fine-textured coversoil. *P*-values are bolded when significant. Interaction terms are shown when significant; interactions were removed from models when not significant. 62
- Table 2.10: Results of permutational multivariate analysis of variance (PERMANOVA) models testing for the effects of coarse woody debris (CWD) volume, heat load index (HLI; reflecting slope and aspect) and an interaction between the two (CWD x HLI) on community composition at each level of planting density treatment, when a significant

interaction of planting density, coarse woody debris and heat load index was found (Table 2.9) in areas capped with a coarse-textured or fine-textured coversoil. *P*-values are bolded when significant. Interaction terms are shown when significant; interactions were removed from models when not significant. Unplanted=0 stems per hectare, Medium Density=5000 stems per hectare, High Density=10000 stems per hectare. 62

Project 2

Table 2.2.1: Species unique to north and south-facing slopes and their species classification. Species highlighted in light gray are classified as boreal forest species, those highlighted in dark gray as ruderal native species and those highlighted in white as ruderal introduced species. 70

Project 3

Table 2.3.1: Mean concentrations of selected nutrients in *Populus tremuloides* leaves from each of three site types. All concentrations are µg/g except nitrogen, which is a percentage. Letters indicate significant differences between site types ($\alpha= 0.05$) (n=5). Significant differences were determined using one-way ANOVA followed by Tukey HSD tests..... 74

Table 2.3.2: Mean values (\pm SD) of variables describing community complexity (number of community types, number of indicator species per grid, number of quadrats per community type, number of indicator species per community type), spatial complexity (number of significant RDA axes, PCNM variables, and PCNM drivers (number of species driving spatial patterns)), and variation partitioning (proportion variation explained by the PCNM/spatial component, environmental variable component, tree canopy component, microtopography component, linear trend component, and residual component).(....) 78

Table 2.3.3: Results (*P* values) of Fisher’s exact tests comparing the three site types (young – poor-xeric, young – rich-mesic and older – rich-mesic) in terms of the proportions of forest associated *versus* non-forest associated and native *versus* introduced species that were indicator species or drivers of spatial patterns. 80

List of Figures

General Introduction

- Figure 1: Overview of the reclaimed landscape showing upland hummocks capped with either a fine coversoil (solid outline) or a coarse coversoil (dotted outline). (...) 7
- Figure 2: Theoretical structural equation model used for years 2013 and 2016. (...).... 14
- Figure 3: Average soil water potential (MPa) over the growing season (May 1st-September 30th) from 2013 to 2016 for two soils (coarse and fine) (a) and two seedling density treatments in 2016 (b): medium (M, 5,000 stems ha⁻¹), and high (H, 10,000 stems ha⁻¹). (...) 19
- Figure 4: Daily average of soil water potential measured at 20 cm depth (in MPa) combined with the daily cumulative precipitation data from 2013 to 2016 (growing season is defined from the 30th of April to the 30th of September of each year when the data is available). (...) 20
- Figure 5: Soil nutrient availability ($\mu\text{g } 10\text{cm}^2$ per burial length) for 2013 (white) and 2016 (dark grey) on both coarse and fine soils as determined with PRS^{RTM} probes (...) 21

Part I

- Figure 1.1: Mean survival of the three tree seedling species (trembling aspen, jack pine and white spruce) on coarse and fine coversoils five years after site construction. (...) 22
- Figure 1.2: Mean height of the three planted species (trembling aspen, jack pine and white spruce) on coarse coversoil at medium and high planting densities (medium density=5000 stems per hectare, high density=10000 stems per hectare) five years after site construction (2016). (...) 23
- Figure 1.3: Mean annual total height of the three planted species (a: trembling aspen, b: jack pine and c: white spruce) on the coarse (black points, solid line) and fine coversoil (black triangles, dotted line). (...) 24
- Figure 1.4: Final structural equation models for jack pine total height assessed in 2013 (a) and 2016 (b) on coarse soils. R² values for each of the response variables are displayed. (...) 27

Project 1

- Figure 1.1.1: Growing conditions and growing season duration for each stock type (greenhouse (G), outside (O) and outside late-germination (OL)) before frozen storage. 29

Figure 1.1.2: Timeline of growing conditions and treatment applications for aspen seedling stock types used in the aspect and soil amendment studies.	31
Figure 1.1.3: Daily (a) average temperature, (b) precipitation, and (c) average relative humidity during the growing season at Mildred Lake (AgroClimatic Information Service 2013).	38
Figure 1.1.4: Daily average (a) temperature, (b) soil water content, and (c) soil water potential of north-facing, south-facing, and hydrogel plots at 10 cm depth (n=7) from June, 2012 to August, 2012.	39
Figure 1.1.5: Average (a) height growth, (b) height growth relative to initial height, and (c) root growth of different pine stock types(n=20) as well as average (d) new needle mass of north and south-facing aspects (n=30) over one growing season. Error bars represent one standard error, and different letters indicate statistical differences among means based on comparisons using Tukey-Kramer adjustment.	41
Figure 1.1.6: Average RSR percent change of (a) pine stock types (n=20) and (b) north and south-facing aspects (n=30) over one growing season. Error bars represent one standard error, and different letters indicate statistical differences among means based on comparisons using Tukey-Kramer adjustment.	42
Figure 1.1.7: Average stomatal conductance of pine growing on north and south-facing aspects. Error bars represent one standard error (n=30), and different letters indicate statistical differences among means based on comparisons using Tukey-Kramer adjustment.	43
Figure 1.1.8: Average height growth after the first growing season of three aspen seedling stock types planted on north and south-facing slopes. Error bars represent one standard error of the mean and different letters indicate differences among means (n=10).	44
Figure 1.1.9: Average change in root to stem ratio (RSR without leaves) from initial conditions after the first growing season for three aspen seedling stock types planted on a north and south-facing slope. Error bars represent one standard error of the mean and different letters indicate differences among means (n=10).	45
Figure 1.1.10: Average (a) stem growth (n=10) as well as average (b) root growth and (c) RSR changes (n=20) of pine in hydrogel-amended and non-amended plots on a south-facing aspect over one growing season. Error bars represent one standard error, and different letters indicate statistical differences among means based on comparisons using Tukey-Kramer adjustment.	46

Figure 1.1.11: Average leaf area (A), and leaf mass (B) production during the first growing season of aspen seedlings (all three stock types combined) planted in different soil amendments. Error bars represent one standard error of the mean and different letters indicate differences between means (n=30).	47
Figure 1.1.12: Average root volume growth following one growing season of three aspen seedling stock types planted in different soil amendment treatments. Error bars represent one standard error of the mean (n= 10) and different letters indicate differences among means.	48
Figure 1.1.13: Average total seedling mass following one growing season of three aspen seedling stock types planted in different soil amendment treatments. Error bars represent one standard error of the mean (n= 10) and different letters indicate differences among means.	49

Part II

Figure 2.1: Vegetation cover (%) (A) and species richness per vegetation subplot (B) of native and introduced forb, graminoid and shrub species per subplot in areas capped with cover soil salvaged from poor-xeric (coarse-textured) and rich-mesic (fine-textured) forest sites. Error bars show one standard error.	53
Figure 2.2: NMDS ordinations of (A) areas capped with coarse-textured coversoils salvaged from poor-xeric a forest site and fine-textured coversoils from a rich-mesic forest site in 2012, 2013 and 2015; (B) only areas capped with a poor-xeric coversoil over three years; and (C) only areas capped with a rich-mesic coversoil over the same three years. (...)	65

Project 2

Figure 2.2.1: Plots set up on the north facing slope of the hill structure. Each plot was 2x2 m ² , with 8 debris pieces in each half of the plot. Debris pieces were arranged in “T”-shapes, comprising of one log oriented in a north-south direction, and the other log oriented in an east-west direction.	67
Figure 2.2.2: NMDS ordination depicting soil from the north-facing slope (blue) of the study area, and from south-facing slope of the study area (red).	69
Figure 2.2.3: Average number of (a) seedlings and (b) species per plot on north (N) and south (S) facing slopes. Error bars represent 95% confidence intervals.	69
Figure 2.2.4: Average number of plants per plot in split plots with and without coarse woody debris (CWD). Error bars represent 95% confidence intervals.	70

Figure 2.2.5: Average number of plants per plot as a function of direction from the closest log. Error bars represent 95% confidence intervals..... 71

Figure 2.2.6: Number of seedlings as a function of distance from logs. Green bars represent the plants common to a mature boreal forest stand, red bars represent ruderal introduced plants, and yellow bars represent ruderal plants that are native to Alberta, Canada. Error bars represent 95% confidence intervals. 71

Project 3

Figure 2.3.1: Proportions of four functional types (forb, graminoid, shrub, non-vascular (moss) of native and introduced and forest associated and non-forest associated species at the three site types (YPX: young – coarse-textured, YRM: young – fine-textured, ORM: older – fine-textured). Plots show proportions of: A) indicator species; B) species driving spatial patterns; and C) total species of each functional type. Error bars show one standard error. 79

Figure 2.3.2: Mean numbers of species per grid plot by four functional types (forb, graminoid, shrub, non-vascular (moss) that were native *versus* introduced or forest associated *versus* non-forest associated for the three site types (YPX: young – coarse-textured, YRM: young – fine-textured, ORM: older – fine-textured). Error bars show one standard error..... 80

List for Appendix A: Supplemental material for seedling growth response to planting density and site conditions, and identifying drivers and dynamics of these responses (Part I)

Figure A.1: Code for the 2013 total height SEM on jack pine seedlings on the coarse-textured soil. Used with the statistical software R (R Development Core Team 2015) and WinBUGS (Lunn et al. 2000)..... 87

Figure A.2: Code for the 2013 total height SEM on jack pine seedlings on the coarse-textured soil. Used with the statistical software R (R Development Core Team 2015) and WinBUGS (Lunn et al. 2000)..... 89

List for Appendix B: Supplemental material for evaluating jack pine seedling characteristics in response to aspect and hydrogel amendment (Project 1)

Table B.1: Range of soil measures of forest floor material taken from north and south-facing hummocks in close proximity to plots. Soil samples were taken by NorthWind Land Resources Inc. and sent to Exova Laboratories in Edmonton, AB, Canada for analysis	91
Table B.2: Aspect, slope, and location of different hydrogel (H), North-facing (N), and South-facing (S) plots.....	92

List for Appendix C: Supplemental material for factors and drivers affecting early colonizing vegetation development on reclaimed boreal upland sites (Part II)

Table C.1: Mean height (cm) of tree seedlings of three species (<i>Populus tremuloides</i> , <i>Pinus banksiana</i> , <i>Picea glauca</i>) in areas capped with the two coversoil materials in 2012, 2013 and 2014 (seedling height was not measured in 2015).....	93
Table C.2: Species found at the Sandhill Watershed and W1 Dump research sites, including areas capped with coversoil from poor-xeric and rich-mesic sites. Species were identified and classified according to original range (native or introduced) and functional type (Tree, Shrub, Forb, Graminoid or Non-vascular) according to Moss (1983) and USDA (2016).....	93
Figure C.1: Growing season (May 1 – September 30) mean monthly temperature (°C) and total monthly precipitation (mm) for 2012, 2013 and 2015, collected at Mildred Lake, Alberta. Data from Environment Canada (2015).	100
Figure C.2: Interaction of heat load index (HLI; reflecting slope and aspect) and coarse woody debris volume on species richness per vegetation subplot in 2015 in areas reclaimed with coversoil salvaged from a coarse (poor-xeric) site. (...)	101
Figure C.3: Interaction of heat load index (HLI; reflecting slope and aspect) and coarse woody debris volume on total vegetation cover (%) in 2013 in areas reclaimed with coversoil salvaged from a coarse (poor-xeric) site. (...)	102
Figure C.4: Interaction of heat load index (HLI; reflecting slope and aspect) and coarse woody debris volume on cover by forb species (%) in 2013 in areas reclaimed with coversoil salvaged from a coarse (poor-xeric) site. (...)	103
Figure C.5: Interaction of planting density, heat load index (HLI; reflecting slope and aspect) and coarse woody debris volume on species richness per vegetation subplot in 2012 in areas reclaimed with coarse coversoil salvaged from a poor-xeric site. (...) ..	104
Figure C.6: Interaction of planting density, heat load index (HLI; reflecting slope and aspect) and coarse woody debris volume on native species richness per vegetation subplot in 2012 in areas reclaimed with coarse coversoil salvaged from a poor-xeric site. (...).....	105
Figure C.7: Interaction of planting density, heat load index (HLI; reflecting slope and aspect) and coarse woody debris volume on forb species richness per vegetation subplot in 2012 in areas reclaimed with coarse-textured coversoil salvaged from a poor-xeric site. (...)	106

Figure C.8: Interaction of planting density, heat load index (HLI; reflecting slope and aspect) and coarse woody debris volume on species richness per vegetation subplot in 2013 in areas reclaimed with coarse-textured coversoil salvaged from a poor-xeric site. (...)	107
Figure C.9: Interaction of planting density, heat load index (HLI; reflecting slope and aspect) and coarse woody debris volume on species richness per vegetation subplot in 2012 in areas reclaimed with fine-textured coversoil salvaged from a rich-mesic site. (...)	108
Figure C.10: Interaction of planting density, heat load index (HLI; reflecting slope and aspect) and coarse woody debris volume on graminoid species richness per vegetation subplot in 2012 in areas reclaimed with fine-textured coversoil salvaged from a rich-mesic site. (...)	109
Figure C.11: Interaction of planting density, heat load index (HLI; reflecting slope and aspect) and coarse woody debris volume on native species richness per vegetation subplot in 2015 in areas reclaimed with fine-textured coversoil salvaged from a rich-mesic site. (...)	110

List for Appendix D: Supplemental material for role of slope aspect and coarse woody debris in plant colonization (Project 2)

Table D.1: Classification of species found on both north and south-facing slopes of a hill structure capped with fine-textured coversoil at the Sandhill Watershed during the 2012 growing season. Species highlighted in light gray are classified as boreal forest species, those highlighted in dark gray as ruderal native species, wetland native species and unclassified, and those highlighted in white as ruderal introduced species..... 111

List for Appendix E: Spatial variation, seedbank and soil type driving vegetation colonization on reclaimed upland sites (Project 3)

Figure E.1: Results of cluster analysis of young – coarse-textured site type grids (1-5) showing community types for each quadrat in the grid plot.....	113
Figure E.2: Results of cluster analysis of young fine-textured site type grids (6-10) showing community types for each quadrat in the grid plot.....	114
Figure E.3: Results of cluster analysis of older – fine-textured site type grids (11-15) showing community types for each quadrat in the grid plot.....	115
Figure E.4: Results of PCNM analysis (right) and variation partitioning (left) for grid 1, which was a young – coarse-textured site type. (...)	116
Figure E.5 : Results of PCNM analysis (right) and variation partitioning (left) for grid 2, which was a young – coarse-textured site type. (...)	117
Figure E.6: Results of PCNM analysis (right) and variation partitioning (left) for grid 3, which was a young – coarse-textured site type. (...)	118
Figure E.7: Results of PCNM analysis (right) and variation partitioning (left) for grid 4, which was a young – coarse-textured site type. (...)	119
Figure E.8: Results of PCNM analysis (right) and variation partitioning (left) for grid 5, which was a young – coarse-textured site type. (...)	120
Figure E.9: Results of PCNM analysis (right) and variation partitioning (left) for grid 6, which was a young – fine-textured site type. (...)	121
Figure E.10: Results of PCNM analysis (right) and variation partitioning (left) for grid 7, which was a young – fine-textured site type. (...)	122
Figure E.11: Results of PCNM analysis (right) and variation partitioning (left) for grid 8, which was a young – fine-textured site type. (...)	123
Figure E.12: Results of PCNM analysis (right) and variation partitioning (left) for grid 9, which was a young – fine-textured site type. (...)	124
Figure E.13: Results of PCNM analysis (right) and variation partitioning (left) for grid 10, which was a young – fine-textured site type. (...)	125
Figure E.14: Results of PCNM analysis (right) and variation partitioning (left) for grid 11, which was an older – fine-textured site type. (...)	126

Figure E.15: Results of PCNM analysis (right) and variation partitioning (left) for grid 12, which was an older – fine-textured site type. (...) 127

Figure E.16: Results of PCNM analysis (right) and variation partitioning (left) for grid 13, which was an older – fine-textured site type. (...) 128

Figure E.17: Results of PCNM analysis (right) and variation partitioning (left) for grid 14, which was an older – fine-textured site type. (...) 129

Figure E.18: Results of PCNM analysis (right) and variation partitioning (left) for grid 15, which was an older – fine-textured site type. (...) 130

Introduction

The restoration of forest ecosystems is a complex, multi-step process that is subject to topographic and climatic conditions that drive the redevelopment of soils, hydrology, and biota (Macdonald et al. 2012). Sites subject to severe industrial disturbance have pedogenetically young soils; thus, the conditions for forest reclamation correspond more closely to the early stages of primary succession which only slowly reestablishes ecosystem development and functions. However, a priority in the reclamation and certification of disturbed lands is the redevelopment of forested landscapes, including the rapid re-establishment of tree cover.

Capturing a disturbed site through the early development of a tree canopy is an important aspect of quickly moving disturbed landscapes towards forested ecosystems. A rapidly established tree canopy will allow for: (a) the exclusion of non-desirable early successional species such as invasive grasses and non-native weedy species which are common on highly disturbed areas and have the potential to lengthen the non-treed periods during the reclamation process; (b) the creation of understory conditions which support the establishment of desirable forest understory species; and (c) the development of soil processes through organic matter input. As the forest canopy develops, it begins to regulate the availability of resources including light, water, and nutrients for the understory as well as the environmental conditions, such as understory microclimate, forest floor litter quality, and soil pH which influence resource availability. Plants growing on recently reclaimed soils will initially rely on the organic matter and nutrients supplied during the reclamation process for their growing needs, but these resources must eventually be replaced by inputs from litter fall and fine root turnover. Additional knowledge is needed to understand the site factors, such as soil properties and topography, involved in supporting rapid tree canopy development on reclaimed sites.

The understory plant community plays a critical role in providing ecosystem processes such as nutrient and water cycling and biodiversity. The understory plant community association for reclaimed forests of northern Alberta should be similar to that typically found on other upland boreal sites. However, reclamation activities control the initial suite of propagules on the site and impact the environmental conditions that will facilitate the development of an early successional forest community. Reclaimed sites, for which ecosite types and their characteristics serve as the model, are currently being characterized by their natural plant communities and successional trends (Alberta Environment, 2010; e.g. Beckingham and Archibald, 1996). Additions of forest floor

material from those ecosite types could offer advantages to forest development by providing native plant propagules, stimulating microbial activity, and facilitating mycorrhizal associations (Macdonald et al. 2012).

The reciprocal relationship between plants and soil water is critically important in understanding the landscape water cycle. For plants, soil water availability often controls potential productivity while for soil, the leaf area of plants is strongly related to potential water use and evapotranspiration. Combining precipitation and evapotranspiration also gives an indication of potential deep soil drainage. However, on reclaimed sites this relationship between plants and water is not yet well understood. Previous studies have shown that different boreal tree species have differing transpiration rates per unit of leaf area and plants can respond to changes in soil moisture availability by changing their transpiration rates (Bladon et al. 2006; Carey 2008). Evaporation of water from the soil is another important component of evapotranspiration in young reclaimed sites with exposed soil and little vegetation cover (Carey 2008). Soil properties, such as texture and organic matter, have a large influence on soil water holding capacity (Huang et al. 2011) which can then influence evapotranspiration rates. However, most previous studies of water use on reclaimed sites have only examined landscape level relationships or relied on models which greatly simplify the role of vegetation. Therefore, there is a need to better understand the direct link between plants and water on reclaimed sites with different soil properties.

The overall goal of this research project was to examine the inter-relationships among tree species and density, understory development and its potential on water use on different reclamation ecosites.

Part I: Seedling growth response to planting density and site conditions, and identifying drivers and dynamics of these responses

Planting trees remains one of the most effective strategies in rehabilitating boreal forest affected by industrial disturbance to functioning forest ecosystems. The quick development of a continuous tree canopy on a site helps suppress establishment of weedy forb and grass species, which can significantly hinder tree survival and growth (Landhäusser and Lieffers, 1998; Maundrell and Hawkins, 2004). A method to speed up forest canopy development is to increase the planting density of trees. In Canada, planting densities in reclamation areas have generally been based on forestry standards

ranging from 1,500-2,500 stems per hectare. In other jurisdictions, however, densities of greater than 10,000 stems per hectares are common.

As in the natural boreal forest, site conditions such as soil and topography are important factors regulating vegetation development in reclaimed landscapes, particularly in northern latitudes. Topographic factors, such as slope and aspect, affect energy input, microclimate, and other processes, and are therefore significant drivers of vegetation establishment and growth in reclaimed mining landscapes. Soil properties which are known to influence tree development are generally related to soil water and nutrient availability. This includes direct measures of resource availability as well as indirect measures such as soil pH and texture. Since soil and topography play a large role in the design of reconstructed landscapes after mining (Badia et al., 2007), the potential for plant resource limitations means that deep soils and rapid root expansion are critically important in maintaining these forest ecosystems into the future.

To evaluate tree seedling establishment, early growth and canopy development in response to planting density of jack pine (*Pinus banksiana*) and trembling aspen (*Populus tremuloides*) on substrates salvaged from a/b ecosite or d ecosites, the following questions were identified:

There were two main objectives to this part: 1) to assess individual planted tree species growth and survival (*Populus tremuloides*, *Pinus banksiana*, *Picea glauca*) in relation to soil characteristics and competing vegetation, and 2) to explore direct and indirect relationships that could link reclamation practices, soil properties, and vegetation development with *Pinus banksiana* seedling growth the second and fifth growing season after site construction using a network model.

Project 1: Evaluating jack pine and trembling aspen seedling characteristics to water availability impact of aspect and hydrogel amendment

In this project, we explored what role initial seedling stock characteristics have in the first year of establishment of jack pine (*Pinus banksiana* Lamb.) and aspen (*Populus tremuloides* Michx.) seedlings. Seedling stock can display reduced growth and survival from transplant shock following outplanting, particularly on moisture limiting sites (i.e. planting check). We investigated the role of non-structural carbohydrates (NSC) reserves, seedling size, and root:shoot ratio (RSR) in aspen and pine planting stock. We hypothesized that the size of the root system relative to the leaf area (shoot) and the

reserve status of the seedlings might vary in their role with pine and aspen. To alleviate potential drought conditions on sites that could pose extreme soil moisture conditions, we also tested hydrogel as a possible soil amendment.

Part II: Factors and drivers affecting early colonizing vegetation development on reclaimed boreal upland sites

Little is known about floristic seral pathways in a post-mining landscape and thus planning for natural, diverse communities is difficult. Understanding the factors that contribute to the succession of understory vegetation following mining disturbance is central to assess how boreal forests respond to altered disturbance regimes, and enhance reclamation programs. Providing safe microsites that are conducive to seedling establishment and survival is essential. Variations in microtopography, substrate type, and cover such as coarse woody debris can lead to a diversity of regeneration microsites. The surface roughness created allows for the capture of moisture and litter and is important for the natural ingress of plant species.

In areas impacted by intense industrial disturbance there is little or no legacy of the previous plant community (Macdonald et al. 2012). In oil sands reclamation, the peat materials typically used to enrich reclaimed soils with organic matter may contain some legacy of plant propagules; however, since these materials are derived from low-lying wet forest ecosystems, the species they carry may not be suited to conditions on reclaimed upland sites and do not represent the natural understory plant communities of mesic or dry forests (Mackenzie and Naeth, 2010). Recently, the stripping of surface soil materials (including the LFH layer) from pre-mining upland forest areas and placing them directly on the reclamation site has become a viable option in reclamation (Mackenzie and Naeth, 2010, Fair 2011). Application of forest floor material as a surface soil amendment during reclamation can result in greater plant species richness and higher occurrence of native plant species (Mackenzie and Naeth, 2010); however, there can also be dramatic losses of reproductive propagules and the forest floor propagule bank can often be quite dissimilar to the established understory plant community of the original forest (Fair 2011). In addition, the natural establishment of boreal forest tree species through direct seeding on reclamation sites is rare and irregular, as reclaimed sites may fall short of providing a seed source (particular for species with short-distance seed dispersal), an appropriate growing medium, and/or microsite conditions (Schott et al. 2014). Provision of safe microsites could allow for the natural ingress of forest species, which could prove beneficial in reclamation, as it may decrease the risk of failure and increase diversity and

resiliency of the plant community after subsequent natural disturbances such as insects, diseases, and fire.

To investigate the understory vegetation development in response to different site conditions and forest floor substrates salvaged from a/b ecosite or d ecosites, we explored the changes in diversity, cover, and composition of the colonizing upland vegetation in the same reconstructed landscape. We determined how diversity, cover and community composition of the colonizing vegetation is related to soil and plant propagule properties of coversoil salvaged from two forest types and how aspect, coarse woody debris volume, and the planting density of the associated tree species affects the outcome. The roles of edaphic and biotic variables on plant community development were examined by further exploring the interaction of these drivers.

Project 2: Role of slope aspect and coarse woody debris in plant colonization

In this project, we assessed the effectiveness and usefulness of coarse woody debris (CWD) in supporting the early colonization of reclamation areas with native boreal forest species derived from the soil propagule bank contained in the salvaged forest floor material. Further we determined whether the conditions found on different aspects of the upland structures resulted in distinct expressions of a common propagule bank contained in the capping material.

Project 3: Spatial variation, seedbank and soil type driving vegetation colonization on reclaimed upland sites

In this project, we explored how plant community complexity and spatial patterns (spatial complexity) change in time and with variation in salvaged coversoil material. We also assessed how proportions of different functional plant types (i.e. shrub, forb, graminoid) changed temporally and with coversoil type. We identified indicator species for plant communities, species that drove spatial vegetation patterns. Further, we determined how much of the variation in the plant community can be explained by environmental factors versus by spatial variables (which reflect biotic interactions such as competition and dispersal limitations).

General Site Description and Measurements

Unless described otherwise, all research presented was carried out at the same research area, the Sandhill Watershed, a landscape reconstructed after oil sands mining. Measurements and data analyses used for this research are described below. A list of all measurements and when they were conducted over the span of the research program is presented in Table 1. Measurements and analyses specific to a project are described in more detail in each respective section.

Reclaimed landscape description

Research plots were located within a larger reclamation area of East In-Pit (the former mine, and later tailings deposit) in the Athabasca Oil Sands Region near Fort McMurray, Alberta, Canada (57° 2"N, 111° 35'W). During reconstruction, a local watershed (~57 ha) was created using features of dry upland hills (hummocks) and wet lowland areas between the hummocks (Figure 1). The reconstructed watershed (Sandhill Watershed) is situated on Syncrude Canada Ltd.'s Mildred Lake lease. The watershed was constructed on a nominally 10 m thick cap of tailings sand that is underlain by approximately 35 m of interbedded composite tailings and tailings sand layers created during the extraction process of bitumen from the ore (Wytrykush et al. 2012). The upland area of the watershed has eight hummocks (small hill structures) that vary in size and height (Figure 1).

Hummocks were created by mechanically placing tailings sand, which were then capped with different salvaged soil materials to recreate soil conditions that are representative of two major forest types of this region (see below). A more detailed description of the construction of the watershed is provided in Pollard et al. (2012) and Wytrykush et al. (2012). One of the cover soils was reconstructed by placing a 40 cm subsoil layer of salvaged Pleistocene fluvial sand and then covered with 15 cm of salvaged forest floor material (FFM). The FFM material, a mixture of the organic forest floor layer and the underlying mineral soil, had been salvaged to a depth of 15 cm from *Pinus banksiana* forests on coarse-textured Brunisols. The second cover soil type used for some of the hummocks was a 40 cm thick layer of a fine-textured clay-rich subsoil material that was subsequently covered with a 20 cm FFM material cap salvaged to a depth of 20 cm from mesic upland forest sites dominated by *Populus tremuloides* on fine-textured Luvisols. All cover soil materials were directly placed without stockpiling to preserve the viability of the propagules bank within. Due to the differences between the two reconstructed soils

(mostly driven by soil texture) and the site conditions created by these soils, we characterized the coversoil as either “coarse” or “fine” soil from here on to assess planted tree seedling and colonizing vegetation performance. More information on the physical and chemical properties of the two soil materials can be found in Table 3. Five of the hummocks in the watershed had a coarse soil cap, while three other hummocks received a fine soil cap (Figure 1). Following coversoil placement, coarse woody debris (mainly stems and large branches of white birch and trembling aspen) were placed on all hummocks in volumes ranging from $0.2 \text{ m}^3 \text{ ha}^{-1}$ to $200 \text{ m}^3 \text{ ha}^{-1}$. Construction of the reclamation area was completed in the spring of 2012.

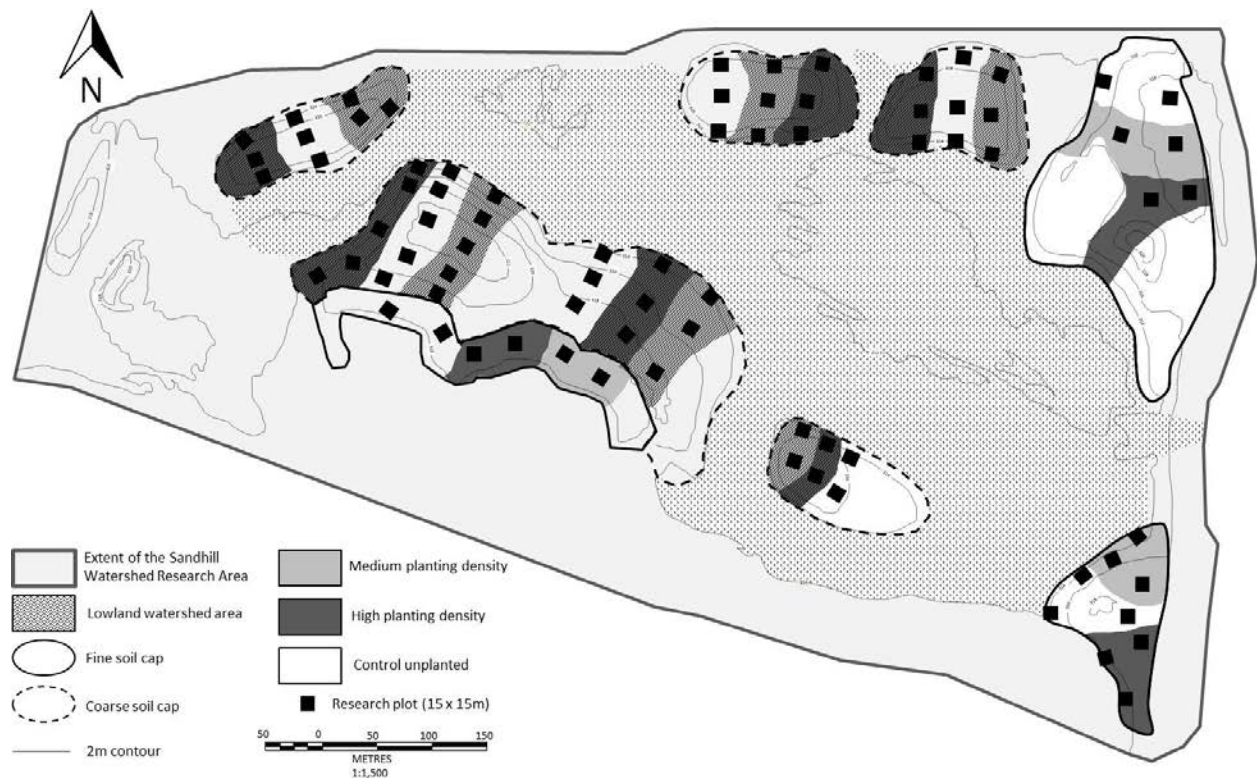


Figure 1: Overview of the reclaimed landscape showing upland hummocks capped with either a fine coversoil (solid outline) or a coarse coversoil (dotted outline). Two seedling planting density prescriptions were applied on the landscape and represented here: a medium planting density ($5,000 \text{ stems ha}^{-1}$, light grey) and a high density planting treatment ($10,000 \text{ stems ha}^{-1}$, dark grey). Individual research plots are presented on the map as black squares.

In the first week of June 2012, upland areas were planted with one-year-old container grown tree seedlings. Seedlings were grown commercially at nurseries from open pollinated local seed sources. Trembling aspen and white spruce seedlings were grown in 515A (250 ml, 5.1 cm diameter, 15.2 cm deep) styroblock (BeaverPlastic, Edmonton,

AB) containers, while jack pine seedlings were grown in 412A (125 ml, 4.6 cm diameter, 11.7 cm deep) styroblock containers. To assess the impact of planting density on forest recovery, each hummock was partitioned into three roughly equal sections and planted to either high density (10,000 stems ha⁻¹), medium density (5,000 stems ha⁻¹) or stayed unplanted as a control (Figure 1). The composition of planted tree species on the different hummocks was based on the two dominant forest types that naturally can be found in this region. Hummocks with coarse-textured coversoil were planted predominantly with jack pine (*Pinus banksiana* Lamb.) (80%) and a mixture of aspen (*Populus tremuloides* Michx.) (10%) and white spruce (*Picea glauca* (Moench) Voss.) (10%). The fine-textured coversoil hummocks on the other hand were planted predominately with *P. tremuloides* (80%) and 10% each of *P. glauca* and *P. banksiana*. Upland areas other than the hummocks that were not part of our measurements were planted at an operational density of 2,000 stems.ha⁻¹ and included various mixtures of tree and shrub species: aspen, white birch (*Betula papyrifera* Marsh.), white spruce, jack pine, dogwood (*Cornus sericea* L.), and green alder (*Alnus viridis* ssp. *crispa* (Chaix.) D.C.).

Plot layout and measurements

Plots (15 × 15m) were established within each planting density treatment at each of the hummocks and kept free of any foot traffic. Depending on the size of the hummocks, between two and five plots were established per tree planting treatment. Across the site a total of 78 plots were established, 57 of these plots were in areas covered with surface soil material salvaged from a coarse site type and 21 plots were in areas covered with surface soil material salvaged from a fine site type. The plots were spatially arranged across the landscape to capture the range of planting prescription and topographical positions present in the reconstructed landscape, i.e. aspect and slope position. As such, the 57 plots that were established on the coarse soils were distributed over five hummocks on level, north and south-facing areas, while the 21 plots were established on fine soils on three hummocks on level and west-facing slopes (Figure 1). Based on the topographical position, a heat load index was calculated for each research plot following McCune and Keon (2002) to convert the factorial variable “aspect” into a continuous variable combining both aspect and slope. To minimize disturbance impacts through foot traffic, a measurement plot (7 × 7m) was nested within the center of each research plot. All seedlings and vegetation were measured in each measurement plot. While seedling growth was measured on all seedlings present in the measurement plot, vegetation

recovery was assessed in four 1 m² vegetation plots established in each corner of the measurement plot.

Seedling performance measurements

Planted seedling performance was assessed in all high and medium density planting plots. Natural tree seedling ingress was also monitored in all of the measurement plots. Survival of planted seedlings was assessed in each measurement plot for each species at the end of the fifth growing season (i.e. at the end of the 2016 growing season). Ten individuals of the dominant tree species in each plot and all seedlings of the other two planted tree species (up to ten) were selected for growth measurements (a seedling was considered a subsample). Mortality across the site contributed to lowering the number of seedlings available for measurement for white spruce (n = 18 plots across the landscape). Seedling height was measured yearly at the end of the 2012, 2013, 2014 and 2016 growing seasons. For all further analysis, survival and height were averaged per measurement plot. As part of the planted seedling assessment, foliar nutrient concentrations were determined in August 2013 and 2016 on foliar samples of trembling aspen and jack pine collected from each measurement plot. Nitrogen concentration was determined using the Dumas Combustion Method (Dumas 1831) on a TruSpec CN Carbon Nitrogen Determinator (©2010 LECO Corporation). Concentrations of P and K were determined by inductively coupled plasma optical emission spectrometry (ICP-OES) after microwave-assisted nitric acid digestion. To compare relative changes in leaf nutrition between years, leaf nutrient concentrations were used. Leaf nutrient concentration rather than content was used, as leaf samples are routinely collected during performance surveys (Alberta Environment and Sustainable Resource Development 2013) and do not require a knowledge of the total size of the pool, needed to estimate nutrient content.

Measurement of CWD and colonizing vegetation

Coarse woody debris presence and volume was assessed in each measurement plot using a line intercept method adapted from Van Wagner (1982), Marshall et al. (2000) and Natural Resources Canada (2008). For the structural equation models for pine on the coarse soils (see below), the distribution of the coarse woody debris volume was strongly bimodal, thus coarse woody debris was used as a categorical variable with two levels: “presence” (volume > 20 m³ ha⁻¹) and “absence” (volume < 20 m³ ha⁻¹). On the fine soil (see below), coarse woody debris volume was much more evenly distributed, and

consequently it was used as continuous variable “coarse woody debris volume” for assessing trembling aspen growth.

Ocular estimation of plant cover – distinguished into vascular vegetation and bryophytes – was conducted in each vegetation plot during July of 2012, 2013 and 2015. Bryophyte cover was separated from other colonizing vegetation cover to take into account the development of vertical structure in the colonizing vegetation community. Percent cover was estimated to the closest 1% below 10%, and to the closest 5% for greater cover. If cover was considered to be less than 1%, it was assigned a cover of either 0.5% or trace (0.05%).

Measurements of edaphic variables

Precipitation and temperature data from 2013 to 2016 were obtained from climate stations present on site that are maintained by O’Kane and by McMaster University, Hamilton, ON, Canada. The 2012 growing season temperature and precipitation averages (prior to the establishment of the onsite weather stations) were obtained from AgroClimatic Information Service (2018). Soil water availability was measured in the center of each measurement plot using MPS-2 matric water potential sensors (Decagon Devices Inc. Pullman, WA, USA). Data was recorded by an EM50 datalogger (Decagon Devices Inc. Pullman, WA, USA). One sensor was installed at a depth of 10 cm (midway through the forest floor material, hereafter referred to as “Water potential at 10 cm”) and the other sensor was installed at a depth of 15 or 20 cm (at the interface of the FFM cover and the subsoil, hereafter referred to as “Water potential at 20 cm”). Collection of soil matric water potential data began only in May 2013 in order to allow sensors to calibrate to the soil conditions throughout the winter since installation occurred in August 2012. Soil water potential was averaged over the growing season (May 1st to September 30th) for each plot and each year.

Soil available nutrient supply rate was assessed using PRS^{RTM} probes (Plant Root Simulator probes, Western Ag. Innovations, Saskatoon, Canada), which are ion exchange resin membranes measuring cation and anion supply rates in situ. The quantity of soil ions adsorbed is a function of soil properties (physical, chemical and biological), soil moisture, and burial time, which control the soil nutrient availability to plants. Four pairs of anion and cation probes were installed in the top 10 cm soil layer from mid-July to end of August in each measurement plot for 42 days during each of the 2013 and 2016 growing seasons. The four anion and four cation probes were pooled for one analysis per

measurement plot. Inorganic nitrogen supply rate was determined colorimetrically using an automated flow injection analysis system. Inductively-coupled plasma spectrometry was used for other nutrient ion supply rates (K^+ , $H_2PO_4^-$).

To accurately represent the soil environment of fine roots, both the soil water potential sensors and the PRS probes were installed at soil depths where the majority of fine roots from the seedling and the colonizing vegetation can be found (following recommendation by Landhüsser et al. 2012b; Laclau et al. 2013; Bockstette et al. 2017). Additionally, sensors and probes were located within or at the boundary between the cover soil layer and the subsoil, providing relevant information on the cover soil characteristics.

Table 1: Summary of types of measurements taken at each research plot in upland areas of the Sandhill Watershed, the unit in which they are expressed, and when measurements were taken between the 2012 and 2016 growing seasons (May 1 to September 30). “Aw” indicates trembling aspen, “Pj” indicates jack pine and “Sw” indicates white spruce.

Measurement	Unit of measure	When conducted
Soil temperature at 10 cm and 20cm	°C	Continuous since May 1, 2013
Soil water potential at 10 cm and 20cm	MPa	Continuous since May 1, 2013
Available soil nutrients (PRS ^{RTM} probes)	µg 10cm ⁻² burial period ⁻¹	Mid July to end of August 2012, 2013 and 2016
Woody debris volume	m ³	June 2012
Woody debris cover	m ²	July 2013 and 2015
Seedling density of planted treatments (site-level)	stems ha ⁻¹	June 2012
Seedling density of planted treatments (research plot-level)	stems ha ⁻¹	August 2012, 2013, 2014 and 2015
Seedling height (Aw, Pj, Sw)	cm	August 2012, 2013, 2014 and 2015
Root collar diameter (Aw, Pj, Sw)	mm	August 2012, 2013, 2014 and 2015
Survival (Aw, Pj, Sw)	%	August 2012, 2013, 2014 and 2015
Foliar nutrient concentrations (Aw, Pj)	mg g ⁻¹	August 2013 and 2016
Leaf area of planted seedlings (Aw, Pj)	cm ²	August 2013 and 2014
Above-ground biomass (Aw, Pj)	g	August 2013 and 2014
Below-ground biomass (Aw, Pj)	g	August 2013
Stomatal conductance (Aw, Pj)	mmol m ⁻² s ⁻¹	Multiple times 2013, 2014 and 2015
Colonizing vegetation cover	%	July 2012, 2013 and 2015
Colonizing vegetation biomass	g	July 2012 and 2013
Leaf area index (LAI)	m ² _{Leaf} m ² _{Ground}	Multiple times 2012, 2013, 2014 and 2015

General Statistical Analyses

Linear models

General statistical analyses were conducted using the statistical R software (R Development Core Team 2015). All models were mixed effects models with Hummock as a random effect unless otherwise stated for individual projects. Each variable was checked for normality assumptions using the Shapiro-Wilk test and appropriate transformations were done for any non-normal variable. Heteroscedasticity was checked for using the Breusch-Pagan test and when significant, variance was allowed to change per hummock to fit the model's assumptions. Plots were treated as independent replicates within each hummock. Non-significant interactions were dropped from the model when necessary. Post-hoc tests were conducted using the package "emmeans" using estimated marginal means and the Tukey method for p -value adjustment. The effects of soil, planting density and year on soil water potential and nutrients supply rates were assessed using a three-way ANOVA. An additional model assessing the effects of Aspect and Year in a two-way ANOVA was used on the coarse soil only for soil water potential. Survival of each planted species was analyzed using binomial generalized linear mixed effects models to assess for the effects of soil, planting density and aspect in 2016 (survival at the end of the fifth growing season).

Cumulative yearly growth for each planted tree species was analyzed for the effect of soil type using linear mixed effects models, as was final height at the end of the growing season in 2016. Mean planted seedling height in 2013 and 2016 was analyzed for each species on their target soil (jack pine on coarse soil, trembling aspen on fine soil and white spruce across the landscape) separately using linear mixed effects models on each species to assess for the effects planting density and aspect, coarse woody debris placement and/or volume, heat load index, soil water potential at 20 cm, foliar nutrition (seedling nitrogen, potassium and phosphorus), colonizing vegetation cover and initial seedling characteristics. The interactions between coarse woody debris and heat load index as well as soil water potential at 20 cm were assessed and removed if not significant.

Structural equation models

To further explore relationships among initial seedling characteristics, environmental and site variables, seedling height and year since planting, structural equation modeling

(SEM) was applied to the multivariate data following the guidelines by Grace et al. (2010 and 2012). Initially the study aimed to use the SEM technique to assess seedling performance for each tree species on their target soil. However, the low number of measured seedlings per plot across the landscape and measurement plots on fine soil (for trembling aspen, $n = 14$, for white spruce, $n = 18$) prevented the use of the SEMs for these two species. This modelling technique was thus only applied to jack pine on the coarse soil. The working meta-model presented in Figure 2 shows the underlying conceptual structure used to build the models following the example of Grace et al. (2010).

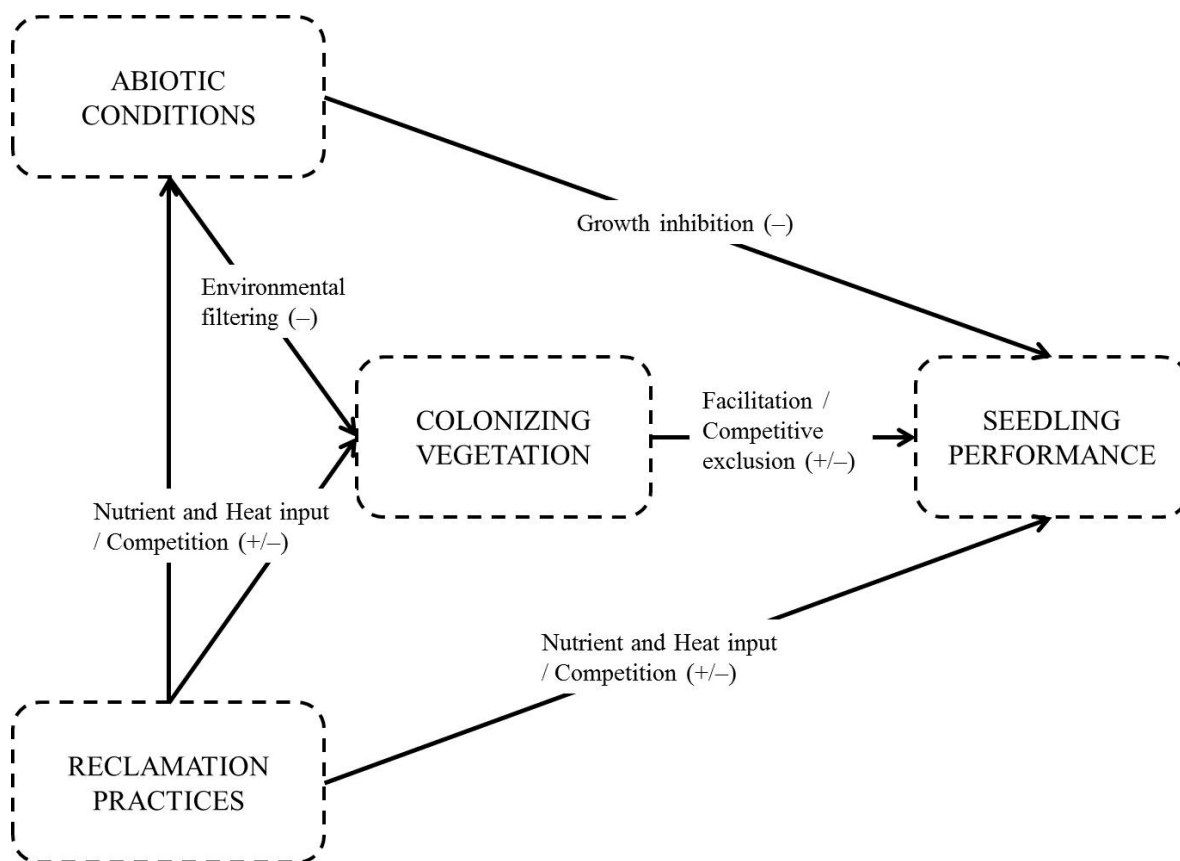


Figure 2: Theoretical structural equation model used for years 2013 and 2016. The theoretical constructs are represented in dotted boxes and are as follows: 1) "Abiotic conditions" encompasses environmental conditions of the system limiting biological productivity, 2) "Reclamation practices" describes the degree to which reclamation practices have modified the site after cover soil placement, 3) "Colonizing vegetation" refers to colonizing vegetation covers and 4) "Seedling performance" refers to measures of foliar nutrition and seedling growth. The hypothesized pathways linking the constructs are labelled with the expected processes and their direction (+: positive, -: negative). The pathway directions and labels demonstrate the expected processes between constructs based on theory and previous observations.

Extrinsic or environmental factors are represented by the abiotic conditions, reclamation practices and colonizing vegetation concepts in Figure 2. Intrinsic factors are represented by seedling characteristics in Figure 2. The observed variables behind the theoretical constructs in the model are presented in Table 2. Links between the observed variables in the structural equation model were based on existing knowledge of relationships between them, and thus are referred to as “drivers” for the seedling responses. The measurement plot was used as the experimental unit, with the observed variables averaged when multiple values per measurement plot were available. Although the use of latent variables – composite variables encompassing observed variables of similar nature – is often recommended for ecological studies (Grace and Bollen 2007; Grace et al. 2010), the low number of samples in our study as well as our goal to identify specific drivers motivated our choice to keep observed variables as individual variables in the model. As our sample size was small (36 measurement plots – experimental units – sampled per year as two plots had to be excluded from all 38 coarse-textured soil plots), a Bayesian approach using a Monte Carlo Markov Chain (MCMC) procedure (Lee 2007) was selected instead of common maximum likelihood procedures that rely on large sample sizes. All links between the observed variables were represented with linear relationships to limit model complexity, resulting initially in 17 pathways and a ratio of 2.2 of samples per pathways. The use of a Bayesian approach was supported due to the low ratio of samples to pathways. Estimation was performed using WinBUGS (Lunn et al. 2000) implemented through the R package “R2winbugs” (Sturtz et al. 2005). Three independent chains were used in the MCMC estimation process, with 500,000 iterations per chain, with a burn-in of 100,000. A thinning of 50 was used to ensure no autocorrelation among estimates. Results reported are repeatable based on independent estimation runs and all parameters were evaluated to determine whether there was basis for model simplification based on assessments of 95% credible intervals and no loss of explanatory power. Links that could be ignored were then removed and a new simplified model was built and assessed. Pearson’s correlations were calculated for relationships between residuals for the endogenous variables and the exogenous variables to quantify linear relationships. The ultimate decision to include additional linkages in a revised model was based on evaluation of parameter significance for included links. We used a query approach to estimate quantities equivalent to classical standardized coefficients (Grace et al. 2012). Each year was modelled separately to investigate the changes in the potential drivers of jack pine height. The equation specifications for the final structural equation models for each year are available in Appendix C.

Table 2: Theoretical constructs (see Figure 2), observed variables and their properties used for the structural equation modeling. The variables labels used in the results are shown in parenthesis and between quotes in the second column.

Theoretical construct	Observed variables related to construct	Properties of variables
Abiotic conditions	Soil water potential at 20 cm ("WP20")	Very low to close to zero (-2,500 to 0); continuous
	Heat Load Index ("HLI")	Continuous
	Soil N supply rate ("Total N")	Continuous
	Soil K supply rate ("K")	Continuous
	Soil P supply rate ("P")	Continuous
Reclamation practice	Presence of woody debris ("CWD")	Categorical with two levels: presence-absence
	Density of planted jack pine seedlings ("Density")	Categorical with two levels: medium/high
Colonizing vegetation	Vascular vegetation cover ("Vegcover")	0-100%; semi-continuous
	Bryophyte cover ("moss")	0-100%; semi-continuous
Seedling performance	Height	Continuous
	Leaf N concentration ("Seedling N")	Continuous
	Leaf K concentration ("Seedling K")	Continuous
	Leaf P concentration ("Seedling P")	Continuous

Part I: Seedling growth response to planting density and site conditions, and identifying drivers and dynamics of these responses*

Capping soil characteristics

Soil characteristics, including texture, conductivity and nutrient availability, differed between the two coversoils and the two subsoils. Coversoil salvaged from the coarse forest site was largely composed of sand, while coversoil salvaged from the fine forest site had a larger clay component (Table 3). Total organic carbon, total nitrogen and total organic matter were greater in coversoil from the fine forest type compared to the coarse forest type. Available ammonium, nitrate, and potassium were higher in the fine-textured coversoil compared to the coarse-textured coversoil, while available phosphorus was higher in the coarse-textured coversoil. Soil pH, sodium and cation exchange capacity were higher in the fine-textured coversoil. Characteristics of the sandy subsoil that underlay areas capped with the coarse coversoil differed substantially from the clay loam subsoil that underlay areas capped with coversoil from the fine forest type. The sandy subsoil included much more sand and less clay and had a lower cation exchange capacity and lower levels of sodium, total organic carbon and organic matter compared to the clay loam subsoil. Both subsoils had few available nutrients; available ammonium, nitrate, and phosphorus were below the detectable limit. However, the clay loam subsoil had a fairly high level of available potassium while this nutrient was undetectable in the sandy subsoil.

Climatic and edaphic conditions

Between the 2012 and 2016 growing seasons (May 1 – September 30), mean temperature ranged between 14.8 and 16.0 °C. Total precipitation during the growing seasons ranged from 195.3 mm to 321.8 mm, with 2015 having the least amount of precipitation and 2013 having the highest amount of precipitation (Table 4).

* More detailed information on the context, objectives and interpretation of the study and its results can be obtained from *Merlin, M, Leishman, F, Errington, RC, Pinno, BD & Landhäusser SM. 2018. Exploring drivers and dynamics of early boreal forest recovery of heavily disturbed mine sites: a case study from a reconstructed landscape [online]. New Forests. doi: .10.1007/s11056-018-9649-1.*

Table 3: Characteristics of coversoils and subsoils placed at the Sandhill Watershed site. Coversoils were salvaged from two forest types, a nutrient poor site with a xeric moisture regime (coarse) and a nutrient rich site with a mesic moisture regime (fine). The coversoil from a coarse forest site was underlain by a sandy subsoil material, and the coversoil from a fine forest site was underlain by a clay loam subsoil material. Data (mean \pm one standard deviation) were collected in 2013 (Syncrude Canada Ltd. 2014).

Soil Material	Coarse-textured coversoil	Sandy subsoil	Fine-textured coversoil	Clay loam subsoil
Soil Texture	Sand	Sand	Clay loam	Sandy clay loam
% Sand (by weight)	90.9 \pm 1.93	97.9 \pm 1.03	41.5 \pm 4.31	55.5 \pm 4.13
% Clay (by weight)	2.7 \pm 1.34	1.2 \pm 0.59	32.1 \pm 4.35	24.6 \pm 4.30
pH	6.3 \pm 0.67	7.4 \pm 0.15	6.9 \pm 0.40	7.5 \pm 0.26
Cation exchange capacity (meq/100 g)	7 \pm 1.38	undetectable	19 \pm 4.45	10 \pm 2.21
Sodium (mg/kg)	32 \pm 12.39	26 \pm 5.38	76 \pm 54.76	116 \pm 79.73
Total organic carbon (% dry weight)	1.6 \pm 0.48	0.2 \pm 0.11	4.3 \pm 4.52	1.4 \pm 0.28
Total nitrogen (% dry weight)	0.08 \pm 0.02	0.03 \pm 0.00	0.28 \pm 0.36	0.04 \pm 0.02
Organic matter (%)	3.3 \pm 0.95	0.4 \pm 0.20	8.5 \pm 9.04	2.8 \pm 0.55
Available Ammonium (μg/g)	0.8 \pm 0.56	undetectable	2.6 \pm 8.20	undetectable
Available Nitrate (μg/g)	undetectable	undetectable	5 \pm 2.75	undetectable
Available Phosphorus (μg/g)	9 \pm 3.42	undetectable	7 \pm 2.90	undetectable
Available Potassium (μg/g)	39 \pm 9.79	undetectable	100 \pm 27.28	69 \pm 24.79

Table 4: Growing season (May 1 – September 30) mean temperature ($^{\circ}$ C) and total precipitation (mm). 2012 data was obtained from AgroClimatic Information Service (2018), all remaining data was obtained from McMaster University (Hamilton, ON, Canada).

Year	Mean Temperature ($^{\circ}$C)	Total Precipitation (mm)
2012	16.0	301.2
2013	16.6	375.1
2014	15.2	299.1
2015	15.5	231.3
2016	15.6	264.9

Average soil water potential decreased from 2013 to 2016 across the whole landscape with a more pronounced drop in the fine-textured coversoil (Figure 3a). Soil water potential on the fine coversoil was lower than on the coarse coversoil in 2015 for the 10 cm depth, and in both 2015 and 2016 for the 20 cm depth (p -value < 0.03). High density plots had lower soil water potential in 2016 than medium density plots on the fine soil for

both depths (p -value < 0.03) whereas no difference was found on the coarse soil (Figure 3b). No difference was found between plot aspect for either depth or soil type. For more detailed annual patterns of soil water potential and precipitation see Figure 4. These differences were likely associated with the much greater leaf area produced by the vegetation and trees on the fine coversoil type (see also below).

Soil nitrogen supply rate as measured by the PRS probes was lower in 2016 compared to 2013, but was not different between the two soil types in either year (Figure 5a). Soil potassium and phosphorus supply rates were lower on the fine soil than on the coarse soil in both 2013 and 2016. No differences among planting density treatments were found for the supply rate of any nutrients.

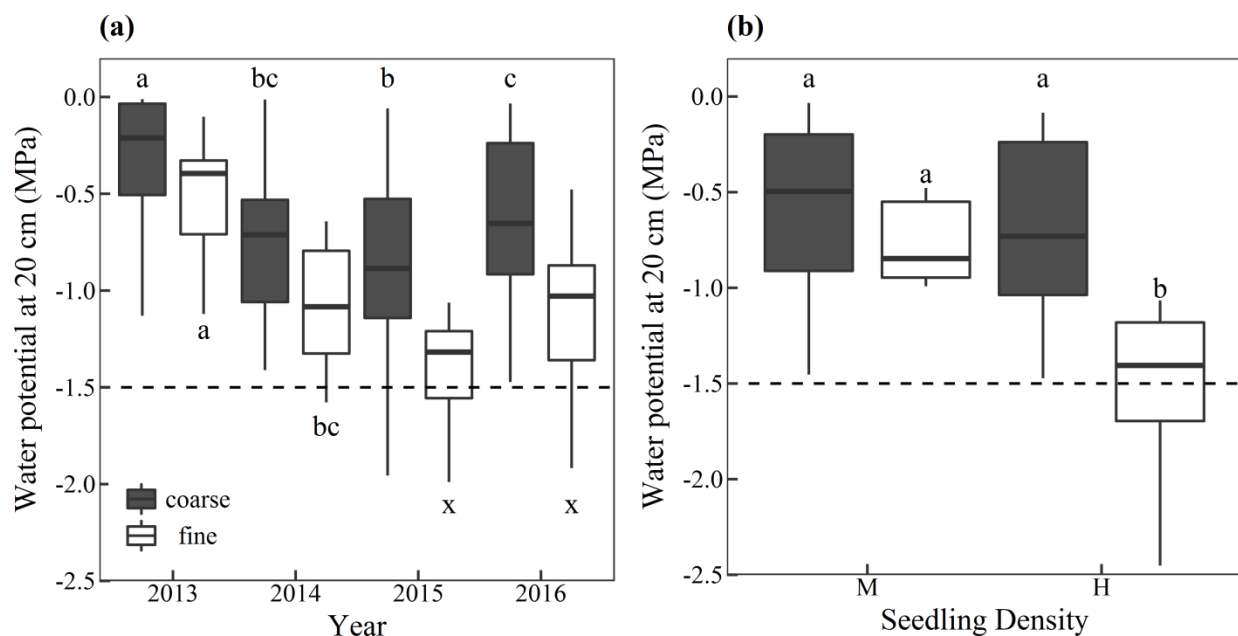


Figure 3: Average soil water potential (MPa) over the growing season (May 1st-September 30th) from 2013 to 2016 for two soils (coarse and fine) (a) and two seedling density treatments in 2016 (b): medium (M, 5,000 stems ha⁻¹), and high (H, 10,000 stems ha⁻¹). Significant statistical differences between soils and years for each year are represented by letters. The dotted line at -1.5 MPa represents the universally accepted wilting point for plants.

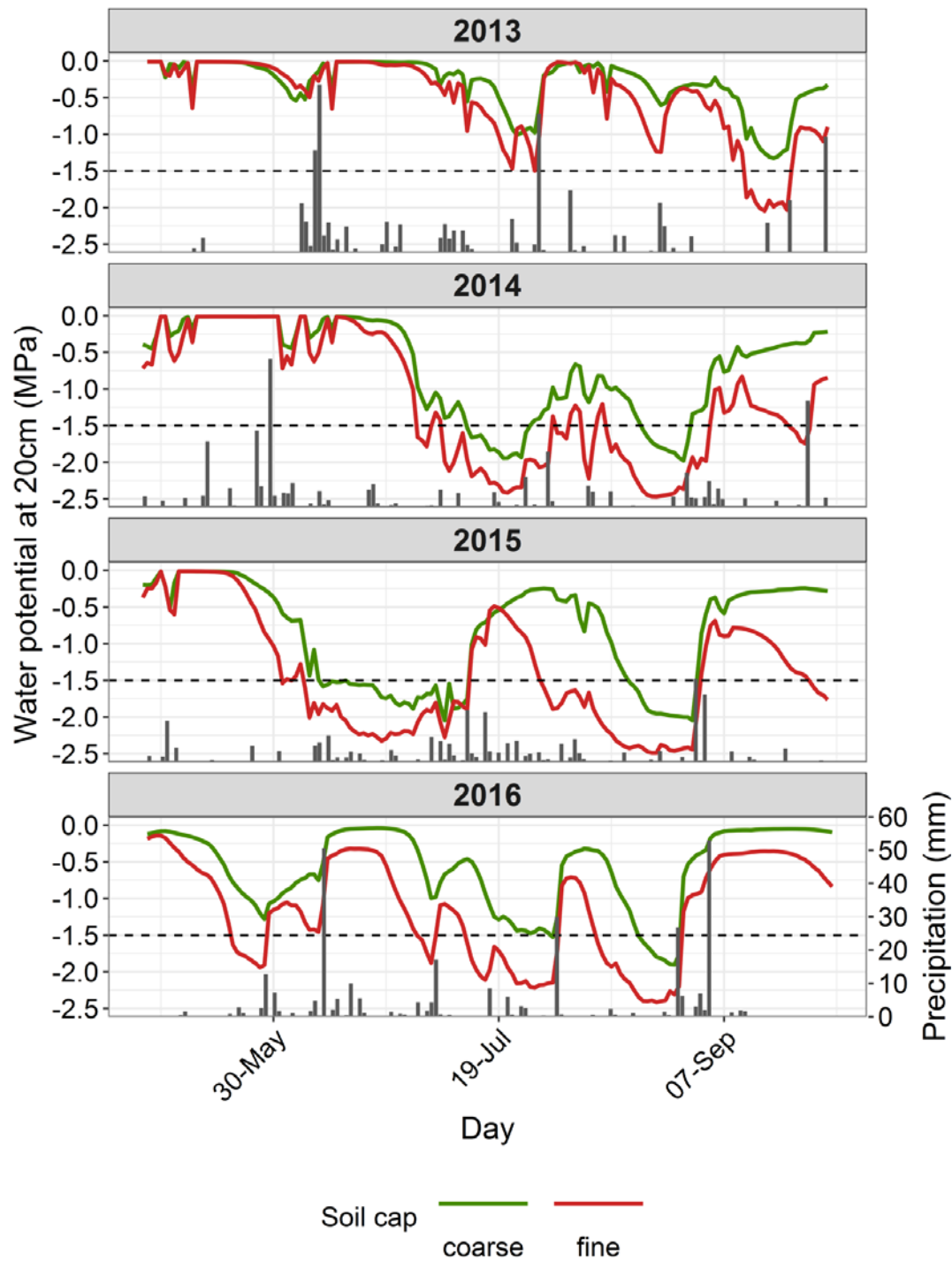


Figure 4: Daily average of soil water potential measured at 20 cm depth (in MPa) combined with the daily cumulative precipitation data from 2013 to 2016 (growing season is defined from the 30th of April to the 30th of September of each year when the data is available). The two different cover soils are presented here: coarse-textured soil in green, fine-textured soil in red. Daily precipitation data was obtained from McMaster University (Hamilton, ON, Canada).

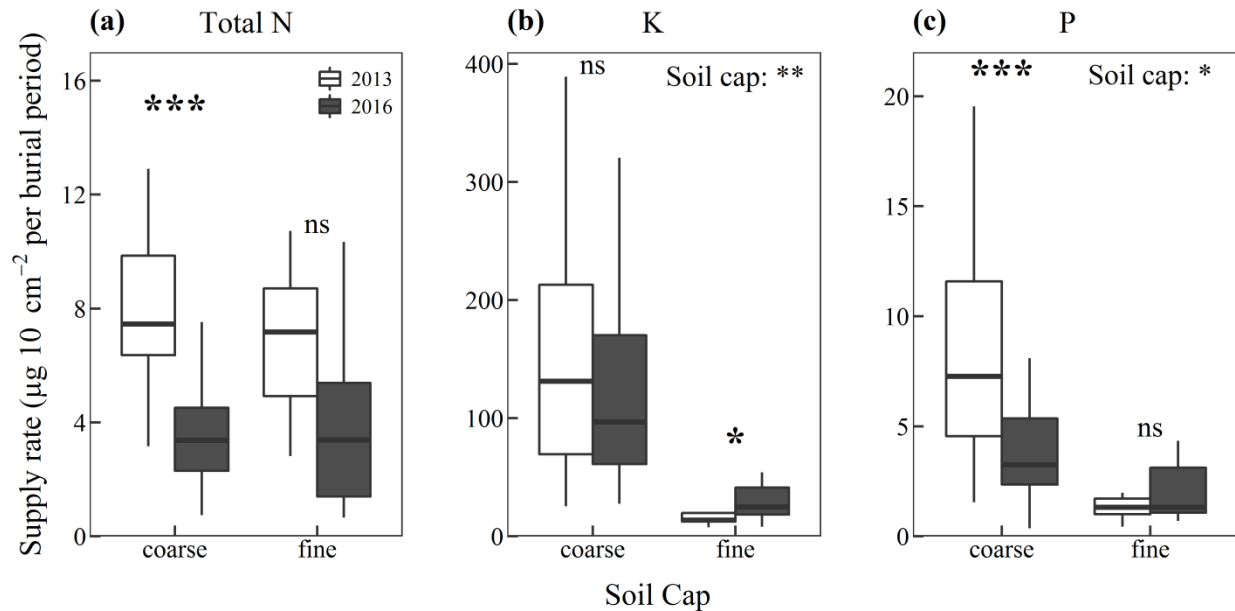


Figure 5: Soil nutrient availability ($\mu\text{g } 10\text{cm}^2$ per burial length) for 2013 (white) and 2016 (dark grey) on both coarse and fine soils as determined with PRS^{RTM} probes (a: total nitrogen (N), b: potassium (K), c: phosphorus (P)). The statistical differences labelled here are from log-transformed data. Labels: “***”: p -value < 0.05 , “**”: p -value < 0.01 , “****”: p -value < 0.001 , “ns”: not significant. Cover soil was a main effect across years for K and P.

Seedling survival

Survival at the end of the fifth growing season was different among species and varied depending on species, planting density, coversoil and topography. Regardless of species or implemented reclamation practice, tree seedling survival was 84.7% after five years. Survival was lowest in trembling aspen (62.5%) followed by jack pine (86.3%) and white spruce (94.5%) on both coversoils combined. While coversoil had no impact on the survival of jack pine (Figure 1.1), trembling aspen and white spruce survival was lower when planted at high density on the coarse coversoil only (trembling aspen: p -value < 0.05 , mortality odds ratio of high versus medium planting density = 3.3, white spruce: p -value < 0.06 , mortality odds ratio of high versus medium planting density = 10.5). Jack pine mortality was marginally higher in the high density planting treatment (p -value < 0.06 , mortality odds ratio of high versus medium planting density treatment = 2.6) and on the south-facing plots (p -value < 0.05 , mortality odds ratio of south versus north-facing plots = 9.6).

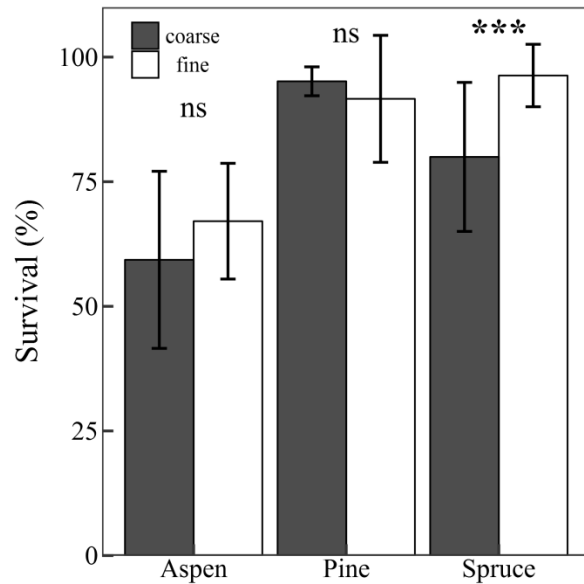


Figure 1.1: Mean survival of the three tree seedling species (trembling aspen, jack pine and white spruce) on coarse and fine coversoils five years after site construction. Statistical differences between coversoil are indicated by asterisks (p -value < 0.05). Error bars represent 95% confidence intervals.

Seedling growth and foliar nutrition

For all three planted tree species, seedling height in 2016 was significantly greater on the fine coversoil compared to the coarse coversoil (all species, p -value < 0.001, Figure 1.3). Trembling aspen seedlings growing on the fine coversoil did not show any differences in response to planting density and aspect. On the coarse coversoil, aspen seedlings were taller in flat areas compared to south-facing aspects when planted at high density (Figure 1.2). Moreover, aspen seedlings planted at high density in flat areas were taller than their medium density counterparts (Figure 1.2). In comparison to aspen, jack pine seedlings growing on the coarse coversoil were taller when growing on north-facing slopes compared to all other aspects (p -value < 0.01) and planting density did not affect jack pine height. On both coversoils white spruce height was unaffected by planting density or aspect.

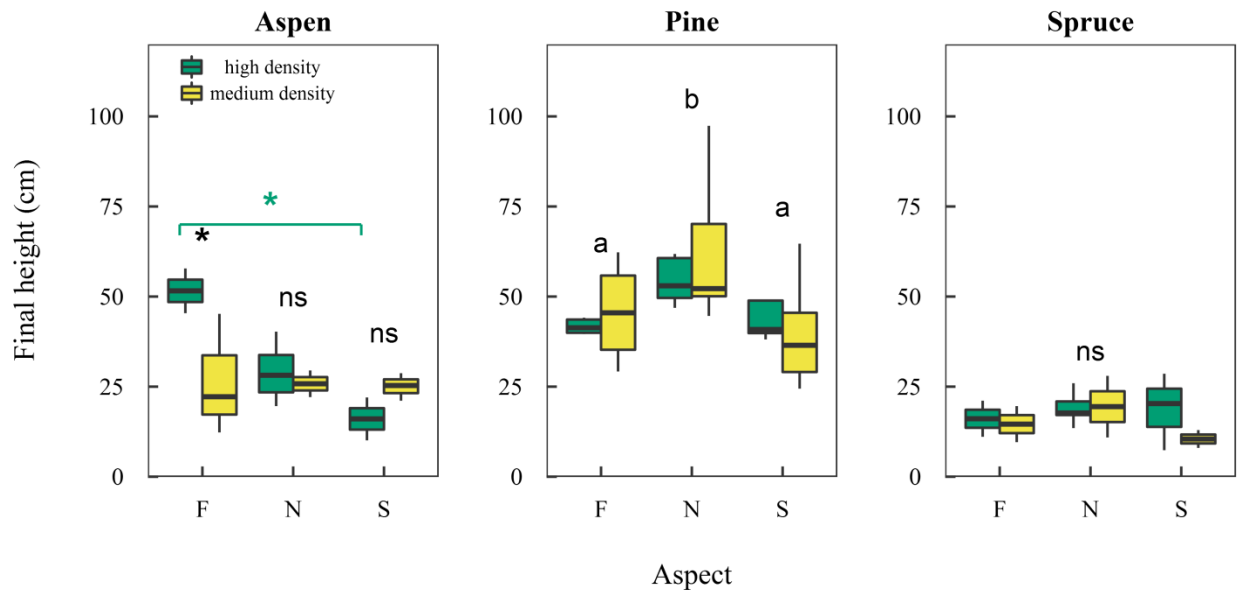


Figure 1.2: Mean height of the three planted species (trembling aspen, jack pine and white spruce) on coarse coversoil at medium and high planting densities (medium density=5000 stems per hectare, high density=10000 stems per hectare) five years after site construction (2016). Tree seedlings were planted on three different aspects: F (flat), N (north-facing) and S (south-facing). Statistical differences between treatment combinations are indicated by an asterisk, whereas statistical differences between aspects are indicated by letters (p -value < 0.05).

Changes in seedling height over time between the two coversoils followed different patterns among species (Figure 1.3); trembling aspen height diverged in 2013 between the coarse and fine coversoils, while this did not happen for the conifers until 2014. In 2015 and 2016 aspen seedlings grew very little in both coversoils, while spruce in the fine coversoil and pine in both coversoils continued to grow. For all species, lowest annual height growth was observed in 2015 (results not shown).

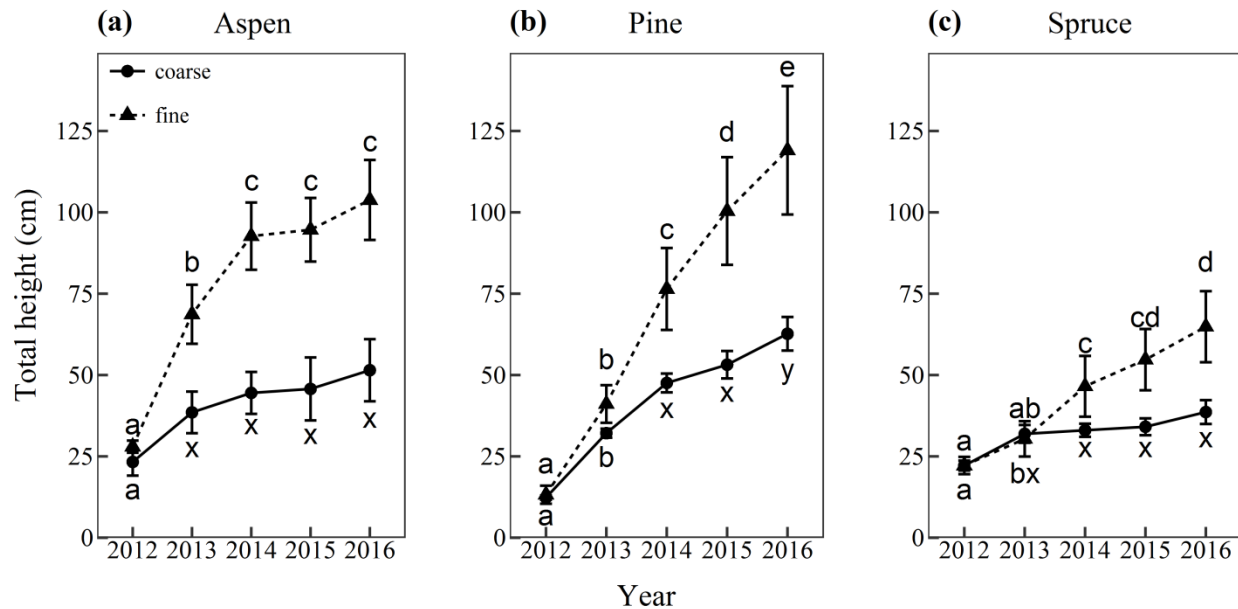


Figure 1.3: Mean annual total height of the three planted species (a: trembling aspen, b: jack pine and c: white spruce) on the coarse (black points, solid line) and fine coversoil (black triangles, dotted line). Statistical differences between years and coversoil have been evaluated for each species separately. The letters indicate a statistical difference for which p -value < 0.05 between the years and coversoil. Error bars represent 95% confidence intervals.

Jack pine foliar nitrogen concentration was higher in 2013 than in 2016 for both coversoil types (Table 1.1, p -value < 0.001) and was higher on the fine soil than the coarse soil in 2013 but not in 2016 (year \times soil interaction, p -value < 0.05). Trembling aspen foliar nitrogen concentration was similar between coversoil types and years. Jack pine foliar potassium concentration was higher on the fine coversoil compared to the coarse coversoil in 2013 but not in 2016 (year \times soil interaction, p -value < 0.05) while there were no differences in trembling aspen foliar potassium between coversoil types. Foliar phosphorus concentrations were similar between coversoil types for both species. For both coversoils and species, foliar potassium and phosphorus concentrations were higher in 2013 compared to 2016 (p -value < 0.05).

Table 1.1: Foliar nutrient (nitrogen, potassium and phosphorus) concentrations of planted trembling aspen and jack pine seedlings planted on coarse or fine coversoils in 2013 and 2016. Mean values and standard deviation for each species, year and coversoil are presented for foliar nitrogen, potassium and phosphorus. All values are presented in mg g⁻¹. The letters between parentheses in the mean columns for each foliar nutrient indicate a statistical difference between the years and soil, “ns”: not significant.

Year	Soil	Nitrogen (mg g ⁻¹)		Potassium (mg g ⁻¹)		Phosphorus (mg g ⁻¹)	
		Mean	SD	Mean	SD	Mean	SD
Trembling aspen							
2013	Coarse	19.36 (ns)	2.81	6.64 (a)	1.49	1.71 (a)	0.28
	Fine	19.94 (ns)	2.35	7.33 (a)	1.63	1.62 (a)	0.21
2016	Coarse	19.06 (ns)	2.45	5.50 (b)	1.64	1.49 (b)	0.26
	Fine	19.25 (ns)	1.99	4.42 (b)	0.72	1.37 (b)	0.15
Jack pine							
2013	Coarse	17.32 (a)	2.47	4.66 (a)	0.85	1.32 (a)	0.15
	Fine	19.50 (b)	2.09	3.73 (b)	0.48	1.31 (a)	0.12
2016	Coarse	13.92 (c)	1.15	3.09 (c)	0.41	1.12 (b)	0.12
	Fine	13.53 (c)	0.80	2.90 (c)	0.38	1.08 (b)	0.07

Environmental drivers of seedling growth

Trembling aspen height in 2013 was negatively related to foliar nitrogen concentration and coarse woody debris volume, but positively related to foliar potassium and phosphorus concentrations (Table 1.2). Trembling aspen height in 2016 was positively related to foliar potassium concentrations only. There were no environmental or seedling-related variables related to white spruce height in 2013, but initial seedling height negatively correlated to white spruce height on the fine soil in 2016.

Structural equation models (SEMs) were only developed for jack pine on the coarse coversoil, as the number of replicates was limited for trembling aspen and white spruce on the fine coversoil. Jack pine seedling height in 2013 and 2016 was used as the response variable for the SEMs. The SEMs for 2013 and 2016 indicate a significant shift in factors that appear to influence seedling height, from intrinsic seedling-based variables in 2013 to extrinsic environmental-based variables in 2016 (Figure 1.4). In 2013 (Figure 1.4a), foliar nitrogen concentration reflective of initial planting stock characteristics, was the only factor that could be directly correlated to seedling total height. Soil nitrogen and potassium appears to indirectly influence pine height through a positive effect on foliar

nitrogen concentration. Presence of coarse woody debris was positively associated with higher levels of foliar nitrogen and potassium, whereas heat load index was negatively associated with foliar potassium. The cover of colonizing vegetation, including the bryophyte cover, was not correlated with any of the measured pine performance variables in 2013.

Table 1.2: Linear models of the environmental and seedling-specific variables that affected height of trembling aspen on the fine soil and white spruce on both soils for the time periods of 2012-2013 and 2012-2016. For each significant variable or interaction of variables, the slope (linear relationship), or difference (factor levels differences) is presented with its associated p -value. The marginal R^2 for each model is presented. Label: "ns": non-significant.

Species	Response variable	Significant variables	R^2
2012-2013			
Trembling aspen	Total height	Coarse woody debris volume (slope = -0.52, $p = 0.002$) Foliar K (slope = 5.44, $p = 0.012$) Foliar P (slope = 54.61, $p = 0.018$) Foliar N (slope = -23.94, $p = 0.059$)	0.82
White spruce	Total height	No model	
2012-2016			
Trembling aspen	Total height	Foliar K (high versus low concentration = 26.88, $p = 0.012$)	0.49
White spruce	Total height	Soil * Initial Height (slope fine soil = -2.07 $p = 0.019$, coarse soil ns)	0.66

Environmental factors had higher significance for explaining seedling height in 2016. Jack pine height was directly and positively correlated to soil potassium supply rates, foliar potassium and to a lesser extent coarse woody debris presence (Figure 1.4). Presence of coarse woody debris was positively associated with higher levels of foliar phosphorus and potassium whereas heat load index was negatively associated with foliar potassium. Similarly, vegetation cover was positively linked with soil potassium supply rate as well as coarse woody debris presence. Soil water potential was positively correlated to vascular vegetation and negatively to bryophyte cover. Bryophyte cover was dominated by the early successional mosses *Ceratodon purpureus* (Hedw.) Brid. and *Bryum argenteum* Hedw. Jack pine height was associated with decreased soil water potential. Linear models confirmed the findings of the structural models on total height for jack pine but failed to identify the network relationships involving soil water potential and vegetation.

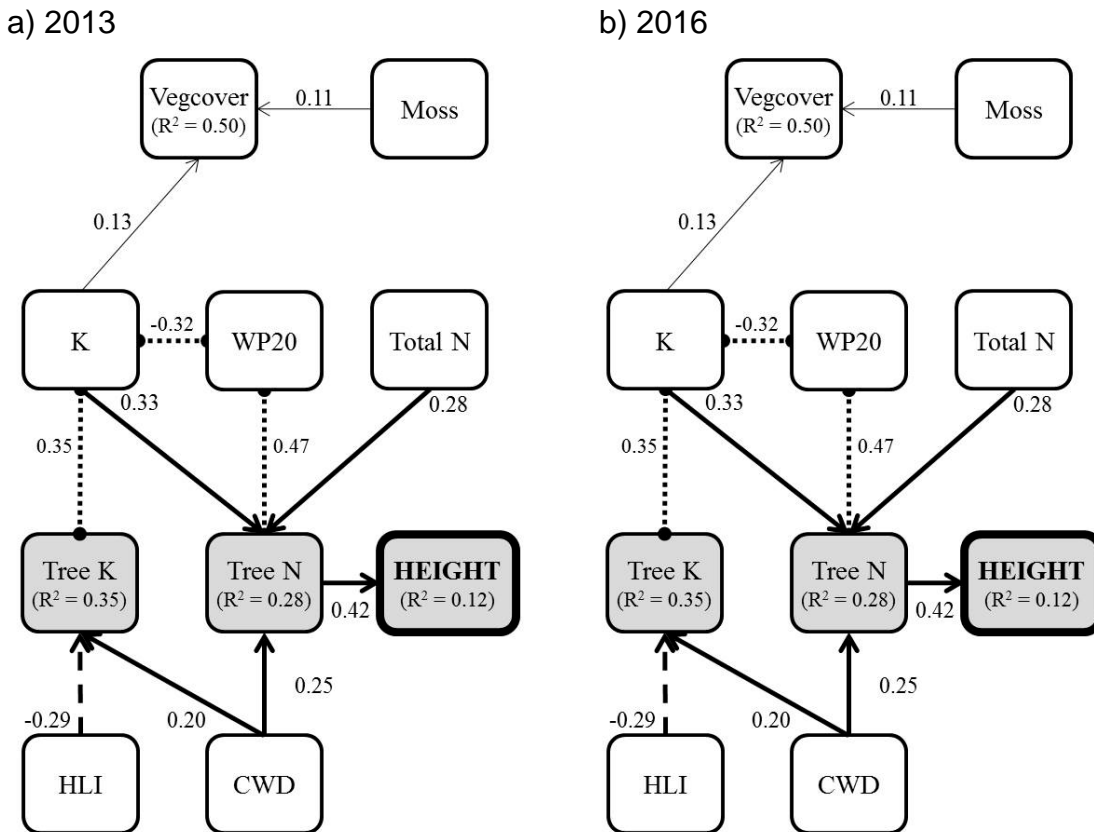


Figure 1.4: Final structural equation models for jack pine total height assessed in 2013 (a) and 2016 (b) on coarse soils. R² values for each of the response variables are displayed. Black solid and dashed arrows represent theorized links between response and predictor variables. The numbers associated with the arrows are queries; they represent the percentage of variation of the response variable relative to its range when the predictor variable varies between its minimum and maximum value. The thickness of the arrow represents the strength of the link, with thicker arrows for queries above 0.2 and thinner arrows for queries below 0.2. The dotted line represents residual correlation between response variables, and its associated Pearson’s moment of correlation. These correlations could not be included in the models as they were either not the focus of the study or their estimation was not strong enough. Please refer to Table 2 (p. 16) for the abbreviations of variables.

Project 1: Evaluating jack pine and trembling aspen seedling characteristics to water availability impact of aspect and hydrogel amendment[†]

Methods

Initial seedling characteristics

Pine

Jack pine seed for this experiment was collected from open pollinated populations located near Fort McMurray, AB, Canada (56.72° N, 111.39° W). All seedlings were cultivated at the Crop Diversification Centre North (CDC North) in Edmonton, AB, Canada (53.64° N, 113.36° W) in styroblock containers (4-12A; Beaver Plastics Ltd, Edmonton, AB, Canada). Each styroblock has a total of 77 cavities (4 cm wide and 12 cm deep; 125 ml) which were filled with growing substrate (Professional Growing Mix, Sun Gro Horticulture Canada Ltd., Seba Beach, AB, Canada) composed of 60-75% sphagnum peat moss, perlite, and dolomite limestone. Two weeks after germination, all seedlings were fertigated twice a week with a commercial nursery blend used for pine seedlings of 96 ppm of N, 76 ppm of P, and 164 ppm of K, supplemented with a blend of chelated micronutrients. At other times seedlings were watered daily or more often when needed. The greenhouse conditions were maintained at 50% relative humidity with natural temperatures, and when needed, natural light was supplemented with fluorescent lights to extend the day period to 16 hours.

To create seedling stock types with different characteristics we grew pine seedlings under different growing conditions. For the greenhouse (G) stock type, seeds were germinated on April 11, 2011, and seedlings were grown under greenhouse conditions through the entire growing season (Figure 1.1.1). For the outside (O) stock type, seeds were also germinated on April 11 under greenhouse conditions, but seedlings were moved outside

[†] More detailed information on the justification, objectives and interpretation of the study and its results can be obtained from Goepfel AE 2014. *Evaluating Jack Pine Seedling Characteristics in Response to Drought and Outplanting*. M.Sc. Thesis, University of Alberta, 96 pages **AND** Kulbaba SP. 2014. *Evaluating trembling aspen (Populus tremuloides Michx.) seedling stock characteristics in response to drought and out-planting on a reclamation site*. M.Sc. Thesis, University of Alberta, 107 pages.

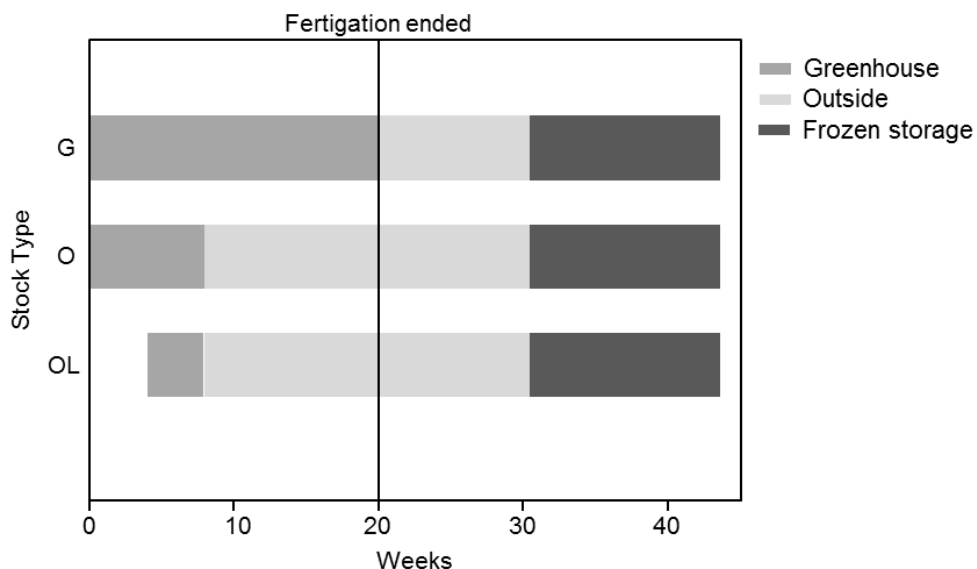


Figure 1.1.1: Growing conditions and growing season duration for each stock type (greenhouse (G), outside (O) and outside late-germination (OL)) before frozen storage.

eight weeks later (June 7), where they continued their growth and development for the rest of the growing season (Figure 1.1.1). For the outside late- germination stock type (OL), seeds were germinated four weeks later (May 8), and seedlings were grown under greenhouse conditions for four weeks and moved outside on the same day as the O seedlings (Figure 1.1.1). During the growth phase all seedlings were fertigated twice a week until August 13, using the nutrient solution described above. During the last two weeks of August the seedlings were fertigated with only half the nitrogen concentration, and after August 31, all fertilization was suspended. At that time, the seedlings of the G stock type were moved outside to naturally harden and induce dormancy in preparation for frozen storage. Prior to frozen storage, 24 seedlings from each stock type were destructively harvested and initial seedlings characteristics such as stem height, root collar diameter, needle dry mass, stem dry mass, and root dry mass were measured (Table 1.1.1). On November 11, the remaining seedlings were lifted and placed into plastic bags and waxed cardboard boxes and put into frozen storage at -3°C for 13 weeks. Applying these different growing regimes during the nursery conditions clearly affected the measures of seedling size and leaf area with a few differences in NSC reserve status. For a summary of the seedling characteristics see Table 1.1.1.

Table 1.1.1: Pre-outplanting average (\pm SE) of morphological and carbon reserve characteristics of seedling stock types (G, O, OL). RSR is root:shoot ratio and NSC is nonstructural carbohydrates. Different letters signify statistical differences among means based on comparisons using Tukey-Kramer adjustment (n=24 with the exception of NSC content and concentrations: n=15).

	Stock type		
	G	O	OL
Height (cm)	11.0 \pm 0.5 A	5.0 \pm 0.3 C	6.8 \pm 0.3 B
Root collar diameter (mm)	2.6 \pm 0.05 A	2.3 \pm 0.07 B	1.9 \pm 0.06 C
Needle mass (g)	1.524 \pm 0.056 A	0.666 \pm 0.045 B	0.482 \pm 0.046 C
Stem mass (g)	0.415 \pm 0.022 A	0.177 \pm 0.013 B	0.143 \pm 0.009 B
Root mass (g)	1.142 \pm 0.040 A	1.186 \pm 0.067 A	0.661 \pm 0.038 B
Total mass (g)	3.080 \pm 0.111 A	2.030 \pm 0.110 B	1.286 \pm 0.078 C
RSR (g g⁻¹)	0.601 \pm 0.022 C	1.458 \pm 0.071 A	1.128 \pm 0.061 B
Whole seedling NSC (g)	0.457 \pm 0.032 A	0.330 \pm 0.018 B	0.203 \pm 0.016 C
Whole seedling NSC (%)	14.03 \pm 0.33	14.47 \pm 0.27	14.85 \pm 0.21
Needle NSC (%)	16.80 \pm 0.32 B	16.84 \pm 0.30 B	18.34 \pm 0.38 A
Stem NSC (%)	14.26 \pm 0.58 B	16.92 \pm 0.59 A	17.60 \pm 0.44 A
Root NSC (%)	10.33 \pm 0.57 B	12.14 \pm 0.46 A	12.00 \pm 0.39 A

Aspen

The trembling aspen seedling stock used in this experiment was also grown at the Crop Diversification Centre North in Edmonton, Alberta from open-pollinated seed sources collected in the Fort McMurray, Alberta area. 192 aspen seedlings were grown in 615A styroblocks (5 total; Beaver Plastics Ltd., Alberta, Canada), which housed 45 cavities containing one seedling each. Each cavity measured 60 mm in diameter and 150 mm depth (340 mL volume). Cavities were filled with a mixture of 10 % perlite, 90 % Sphagnum sp. peat moss (Rich Grow, Sungro Horticulture Ltd., British Columbia, Canada) and treated with lime and soap to increase pH levels and water absorption capacity. Cavities were watered to field capacity, seeded and covered with plastic sheathing. Germination occurred after one week. Germinants were regularly misted and kept at soil field capacity (approximately 0.6 g g⁻¹ gravimetric soil water content). After two weeks, when the first mature pair of leaves was expanded, seedlings were given a single fertilization of 2 g L⁻¹ 5-15-5 (N-P-K) containing chelated micronutrients (Plants Products Co. Ltd., Ontario, Canada). Similarly, a single fertilization event occurred during the third week using a 1 g L⁻¹ 10-52-10 NPK fertilizer (Plants Products Co. Ltd., Ontario, Canada) in order to stimulate root growth. After initial establishment (four weeks),

seedlings were fertilized twice weekly using a nursery blend of liquid 91-77-161 N-P-K water soluble fertilizer with chelated micronutrients (Smoky Lake Nursery Ltd., Alberta, Canada).

After 5 weeks, when seedlings had reached approximately 20 cm height, seedlings were separated into three groups and exposed to different growing conditions known to create different seedling characteristics (Landhäusser et al. 2012a) (Figure 1.1.2). These stock types included: (1) a seedling with highNSC reserves, (2) a seedling with highRSR, and (3) a large seedling. To produce the first stock type (highNSC), seedlings were grown under greenhouse conditions (50 % relative humidity, 16-17 hours of light, ambient greenhouse temperature) for a total of 15 weeks following germination and subjected to a 5 g L⁻¹ application of a paclobutrazol-based shoot growth inhibitor (“Bonzi,” 0.4 % paclobutrazol; Evergro Canada Inc., British Columbia, Canada) during the seventh growing week. These seedlings were subsequently transferred outdoors for hardening (Figure 1.1.2). The second stock type (highRSR) was established under the aforementioned greenhouse conditions but was transferred outdoors after five growing weeks. The final seedling stock used in the experiment, large, was established under the same greenhouse conditions as the highNSC stock type but was not treated with a stem growth inhibitor and was grown under greenhouse conditions for 17 weeks. Following 27 weeks of growth, all seedlings were lifted and packaged into bags and waxed boxes, and were placed into frozen storage (-2 °C) until the commencement of the experiments in May 2012 (approximately 55 weeks) (Figure 1.1.2). On May 25, 2012, one week prior to out-planting, seedlings were lifted from frozen storage and were slowly thawed in a refrigerator at 4 °C.

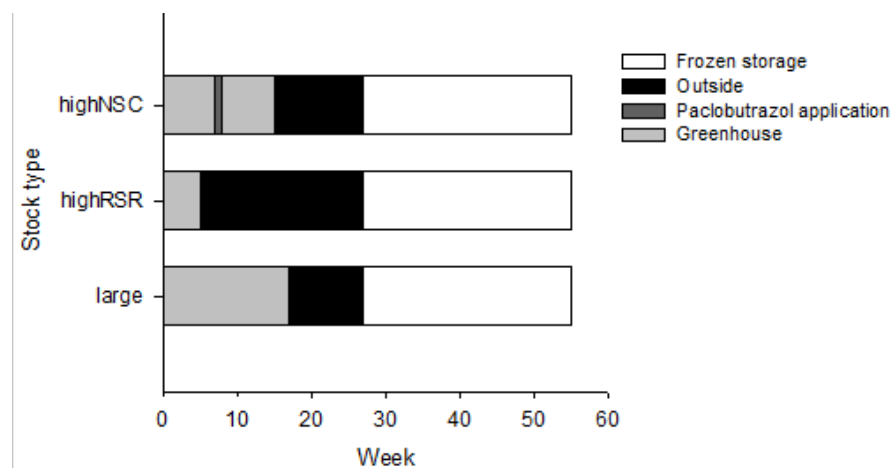


Figure 1.1.2: Timeline of growing conditions and treatment applications for aspen seedling stock types used in the aspect and soil amendment studies.

Relative to the other two stock types produced for this study, the highNSC stock type was characterized by being medium sized in height, total mass and root to stem ratio (RSR, without leaves) (32.3 cm, 3.9 g and 3.2 g g⁻¹, respectively); however, it had high root volume and mass with both the highest NSC content (1.20 g) and concentration (29.6 %) of the three stock types (Table 1.1.2). The highRSR stock type differed from the two other stock types by having the highest RSR (4.9 g g⁻¹), despite being the smallest in terms of height and mass. This stock type also had high NSC concentration (27.0 %); however, it had the lowest NSC content overall (Table 1.1.2). The large stock type was characteristically tall with high root and stem mass, high root volume, low RSR, and low total NSC reserves (concentration) in relation to the other two stock types (Table 1.1.2).

Table 1.1.2: Initial morphological (height, tissue masses and RSR; n=24) and carbohydrate reserve (n=8) characteristics (average \pm SE) of the three trembling aspen seedling stock types prior to the experiment. Different letters signify statistical differences among means based on comparisons using Tukey-Kramer adjustment.

	Stock type		
	highNSC	highRSR	large
Height (cm)	32.3 \pm 0.8 B	15.9 \pm 0.6 C	51.8 \pm 1.3 A
Root collar diameter (mm)	3.9 \pm 0.1 B	3.0 \pm 0.1 C	4.8 \pm 0.1 A
Shoot mass (g)	0.9 \pm 0.04 B	0.3 \pm 0.01 C	1.9 \pm 0.1 A
Root volume (mL³)	7.8 \pm 0.4 A	4.9 \pm 0.4 B	8.0 \pm 0.6 A
Root mass (g)	2.9 \pm 0.1 A	1.6 \pm 0.1 B	2.9 \pm 0.2 A
Total mass (g)	3.9 \pm 0.1 B	2.0 \pm 0.1 C	4.8 \pm 0.2 A
RSR (g g⁻¹)	3.2 \pm 0.1 B	4.9 \pm 0.2 A	1.6 \pm 0.1 C
Whole seedling NSC (g)	1.20 \pm 0.15 A	0.54 \pm 0.20 C	0.90 \pm 0.17 B
Whole seedling NSC (%)	29.6 \pm 0.8 A	27.0 \pm 1.2 A	19.7 \pm 1.1 B

Outplanting and hydrogel amendments

After 29 weeks of frozen storage (-3 °C), all pine and aspen seedlings were outplanted on hummocks with coarse-textured coversoils at the Sandhill Watershed reclamation site. The coversoil material had a sandy texture where sand constituted 89-94 % of the material's dry weight with the remaining weight mostly composed of silt (Table B.1). The coversoil had negligible amounts of available NO₃⁻ while available NH₄⁺ varied from <0.3 to 1 µg g⁻¹. Available P and K ranged from 8 to 18 and <25 to 56 µg g⁻¹, respectively. Total organic carbon varied from 1.3 to 2 % based on dry weight which translated to a C:N ratio of 17 to 20; pH ranged from 5.5 to 7.2 (Table B.1). Daily weather data for this region during the time frame of this particular project was obtained from an Environment Canada

weather station near Mildred Lake (57.03 °N, 111.57 °W) which was approximately 2 km away from the outplanting location (AgroClimatic Information Service, 2013).

A week prior to outplanting, seedlings were removed from frozen storage and thawed slowly. On June 1 and 2, 2012, seedlings were outplanted in 1m × 2 m plots cleared of all vegetation. There were a combined total of 30 north-facing, south-facing, and hydrogel plots (10 plots each) distributed on four hummocks with slopes around 22.5° (Table B.2). Each south-facing plot was paired with a hydrogel plot, as we anticipated warmer temperatures and greater water limitations on the south-facing aspect. Hydrogel plots were amended with granular hydrogel (Stockosorb 660 XL, Stockhausen GmbH, Krefeld, Germany) that was composed of cross-linked potassium polyacrylate, and it varied from one to four millimeters in size. Hydrogel was mixed in the top 15 cm of soil with trowels at a rate of 4.8 kg m⁻³ of soil. Each plot had six rows of either 10 pine or 10 aspen seedlings, and each row was comprised of one stock type (pine G, pine O, pine OL, aspen highNSC, aspen highRSR, and aspen large). Rows were separated by 30 cm, and seedlings within a row were 20 cm away from each other. A 5TM soil moisture sensor probe (Decagon, Pullman, WA, USA) and a MPS-2 dielectric water potential sensor probe (Decagon, Pullman, WA, USA) were installed at a 10 cm depth to measure volumetric soil water content, soil water potential, and soil temperature in seven of the ten north-facing, south-facing, and hydrogel plots. Soil temperature, soil water content, and soil water potential were logged hourly and summarized as daily averages.

Plant Root Simulator (PRS^{RTM}) probes (Western Ag Innovations Inc., Saskatoon, SK, Canada)—ion exchange resin membranes used to measure bioavailable nutrients—were placed in each of the four corners of all plots on July 20, 2012. At each plot corner a pair of PRS^{RTM} probes that captures anion and cation separately was pressed into the ground vertically while ensuring the membrane of the probes was below the soil surface. All probes were removed after 32 days (August 21), placed in Ziploc bags which were then placed in a cooler with icepacks, and transferred to a refrigerator. Probes were cleaned later that day with toothbrushes and de-ionized water to remove any remaining soil. Afterwards, probes were placed in new bags and shipped to Western Ag Innovation for nutrient analysis. For analyses, the four pairs of anion and cation probes from each plot were pooled. The membranes of the PRS^{RTM} probes were placed in a 0.5 N HCl solution for 1 hour before analysis. Nitrate (NO₃⁻) and Ammonium (NH₄⁺) was analyzed colormetrically with automated flow injection analysis system while total N was calculated by adding NO₃⁻ and NH₄⁺ values together. Other nutrients including Ca, Mg, K, P, Fe,

Mn, Cu, Zn, B, S, Pb, Al, and Cd were analyzed with inductively-coupled plasma spectrometry.

Seedling measurements

Growth variables

To determine initial seedling characteristics prior to cold storage and the outplanting experiment, 24 seedlings from each stock type and each species were destructively sampled. Stem height from the root collar to the base of the terminal bud was measured for each seedling, and dry mass was determined for needles, stems, and roots by oven drying samples at 70 °C for at least 72 hours (Table 1.1.1, Table 1.1.2). Prior to drying and weighing, roots were carefully washed to remove growing substrate (Professional Growing Mix, Sun Gro Horticulture Canada Ltd., Seba Beach, AB, Canada) -. Thirteen weeks after outplanting (August 26 and 31, 2012), the same root and shoot measurements were taken on three randomly selected seedlings from each stock type within each plot.

Seedling growth was assessed in several ways. Height growth of each seedling was measured from the bud scar of the previous growing season to the base of the terminal bud. Relative height growth of each seedling was calculated by dividing height growth by the initial seedling height to measure how much a seedling grew relative to initial height over one growing season. Leaf (needle), stem, and root dry mass growth as well as change in RSR were calculated by subtracting the average initial dry mass or ratio for each stock type from the final dry mass or ratio of each outplanted seedling. RSR was calculated as root dry mass divided by needle and stem dry mass, and relative change in RSR was estimated by dividing RSR change by the average initial RSR. These growth measurements were then averaged for each stock type per plot.

Physiological variables

Thirteen weeks after outplanting (August 26 and 31, 2012) and prior to destructive sampling, a leaf porometer (AP4, Delta-T Devices Ltd, Burwell, Cambridge, England) was used to measure stomatal conductance on six seedlings of each species and stock type growing in four north-facing, south-facing, and hydrogel plots each between 09:00 and 16:00 hours. Measurements were blocked in time and space. The same seedlings were destructively sampled afterwards for growth measurements. A slotted cup on the sensory

head was used for measuring stomatal conductance on recently formed pine needles situated near the terminal bud. Comparatively, a circular cup was used to measure stomatal conductance of recently formed but fully expanded aspen leaves so that the cup was entirely covered with the leaf blade. All measured pine needles were marked with a permanent marker. Marked needles were cut after shoot water potentials were taken and placed into paper bags within a Ziploc bag. These bags were kept in a cooler with icepacks until transported to a freezer (-20 °C). The projected leaf area of the cut pine needles was then calculated using winSEEDLE software (winSEEDLE 2006 Régent Instruments Inc., Sainte-Foy, QC, Canada) after being scanned. Stomatal conductance of pine seedlings was subsequently scaled by needle surface area to account for differences in leaf area placed inside the cup of the porometer. Aspen stomatal conductance measurements did not need to be scaled given the porometer cup was fully covered by leaf blade during measurement.

Just after measuring stomatal conductance, shoot water potential was measured in the field on two of the six seedlings measured per species for stomatal conductance. Shoot water potential was measured by cutting the seedlings just above the root collar and placing the stem in a Scholander pressure chamber (PMS Instrument Company, Albany, OR, USA). Both stomatal conductance and shoot water potential measurements among the treatment combinations were blocked by time, so that after measuring a G seedling within a plot, one seedling of each O and OL stock type was measured before proceeding to the next G seedling. The same precautions were taken for each of the three aspen stocktypes. In addition, after completing measurements on a north-facing plot, a south-facing and hydrogel plot was completed before proceeding to the next north-facing plot.

Data analysis for pine

One-way ANOVA was used to compare initial seedling measurements of the three stock types (G, O, and OL) and soil available nutrients between north and south-facing plots and between hydrogel and non-amended south-facing plots. Differences in soil temperature, water content, and water potential between north and south-facing plots and between hydrogel and south-facing plots were compared using repeated measures with plot included as a random variable. Stock type and aspect effects on growth and physiological variables were analyzed using a two-way ANOVA. Because growth variables were calculated as an average for each stock type per plot, a plot was not included as a variable in the analysis. However, as stomatal conductance and shoot water

potential measurements were blocked by time, time block was included as a random variable. Hydrogel effects on growth and physiological responses were analyzed as a split-plot design comparing non-amended south-facing and hydrogel plots. PROC MIXED (SAS 9.2, SAS Institute, Cary, North Carolina, USA) was used for all analyses. Prior to all statistical analyses, tests for normality (Shapiro-Wilk and Kolmogorov-Smirnov) and equal variance (Levene's) of the residuals were performed. Initial measurements such as height, stem mass, root mass, RSR, NSC content had unequal variance. Total N, S, new needle mass, root growth, RSR change, stomatal conductance, shoot water potential had unequal variance in the aspect analysis while K, relative height growth, shoot growth, new needle mass, and RSR change had unequal variance in the soil amendment analysis. For variables with unequal variance, ANOVA models that assume unequal variance were used, and the unequal variance model with the best fit was determined using Bayesian information criterion (BIC) (Littell et al. 2006). BIC was also used to determine which variance covariance structure provides the best fit to soil temperature, water content, and water potential data. Treatment and stock type averages were compared using Tukey-Kramer adjustment with $\alpha=0.05$ as the significance level.

Data analysis for aspen

All data was analyzed using the PROC MIXED function in SAS (SAS 9.2, SAS Institute, North Carolina, U.S.A). North-facing and south-facing aspect impacts on aspen physiological and morphological growth responses were analyzed using a two-way ANOVA with a 3 x 2 factorial design. In the soil amendment study, physiological and morphological growth responses were analyzed using a split plot design to compare non-amended south-facing and hydrogel plots. Time blocks were used as random variables for the analysis of stomatal conductance and shoot water potential in both experiments.

Prior to any statistical analysis, the residuals of each response variable were tested for normality and homogeneity of variance. Residuals were visually examined for normality, while homogeneity of variance was analyzed using Levene's test. In the analysis of nutrient availability, total N, NO_3^- , and K^+ had unequal variance. Height growth, stem mass growth, leaf area, leaf mass, stomatal conductance and shoot water potential had unequal variance in the aspect experiment, while in the soil amendment experiment height growth, stem mass growth, leaf area, leaf mass, root mass, root mass growth, and total seedling mass had unequal variance. Variables with unequal variance were not transformed and were instead analyzed using ANOVA models with covariance structures that account for

unequal variance. The ANOVA model with the best fit was then selected based on Akaike's Information Criterion (AIC) (Milliken and Johnson 2011). Following ANOVA analysis, the least square means for response variables with significant interactions were compared using a Tukey-Kramer adjustment with significance set at $\alpha=0.05$. Least square means for response variables with only significant main effects were compared using an LSD test with a Bonferroni adjustment and significance set at $\alpha=0.017$.

Results

Climatic conditions (2012) after outplanting

Weather conditions during the 2012 growing season were characterized by relatively warm temperatures with ample rainfall throughout most of the growing season. June 2012 was cooler compared to the rest of the growing season with average daily temperatures rarely above 20 °C until the end of the month (Figure 1.1.3a and b). June had an average temperature of 17 °C and accumulated 60 mm of precipitation compared to an average of 45 mm over the previous six year (AgroClimatic Information Service 2013). The beginning of July was characterized by heavy rainfalls, followed by the warmest temperatures during the growing season. Through the rest of July and into August, average temperatures remained between 14 and 23 °C, and rain events were regular but smaller. July and August 2012 had 88 and 35 mm of precipitation and average temperatures of 20 and 18 °C, respectively. In the previous six years, July and August had 61 and 69 mm of precipitation and average temperatures of 19 and 16 °C, respectively (AgroClimatic Information Service 2013). Relative humidity peaked during rain events and lower temperatures (Figure 1.1.3c).

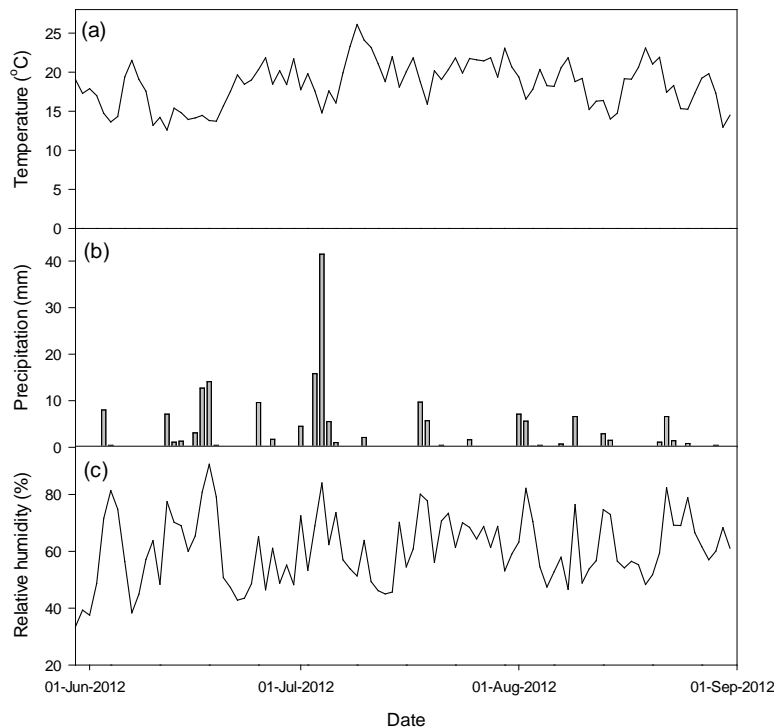


Figure 1.1.3: Daily (a) average temperature, (b) precipitation, and (c) average relative humidity during the growing season at Mildred Lake (AgroClimatic Information Service 2013).

Soil moisture and temperature conditions

North-facing plots were cooler (aspect: p -value <0.001 , Figure 1.1.4a) and wetter (aspect: p -value <0.001 , Figure 1.1.4b) than south-facing plots at a 10 cm depth of soil in 2012. No difference in soil water potential was detected between aspects (aspect: p -value $=0.210$), but there was a difference later in the growing season where south-facing plots had more negative soil water potentials compared to north-facing plots (aspect \times day: p -value <0.001 , Figure 1.1.4c).

Hydrogel plots were also wetter throughout the growing season (treatment: p -value $=0.032$), and water content tended to not fluctuate as much as non-amended plots (Figure 1.1.4B). There was no difference in soil water potentials between hydrogel and non-amended plots (treatment: p -value $=0.543$), but non-amended plots tended to have more negative water potentials than hydrogel plots at the end of the growing season (treatment \times day: p -value <0.001 , Figure 1.1.4c). Soils of the hydrogel plots were generally cooler compared to non-amended plots (treatment: p -value <0.001), although this difference in soil temperature was only apparent at warmer temperatures (Figure 1.1.4a). These

differences are likely related to the higher water content which might have allowed for more evaporative cooling during hot days.

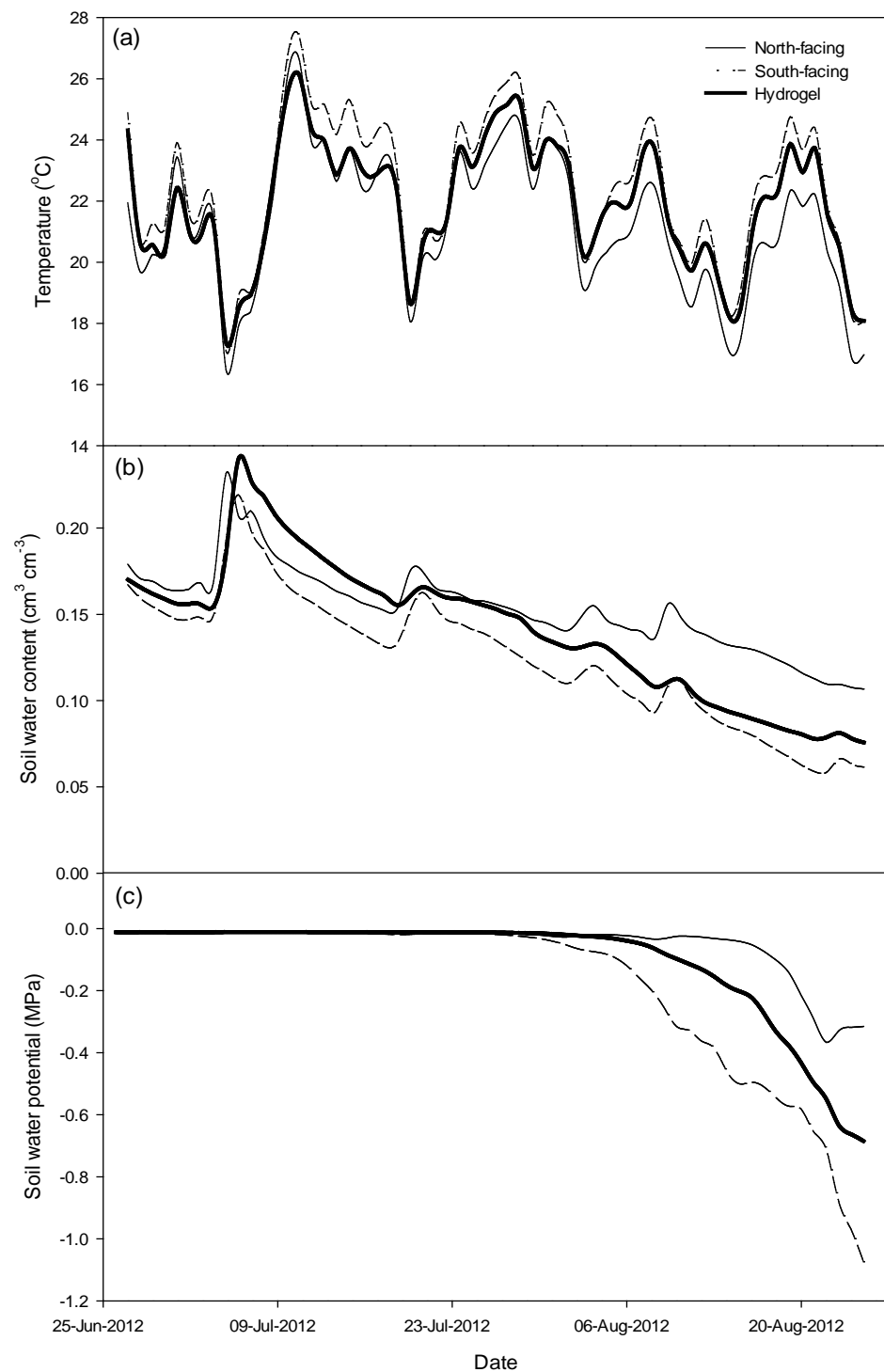


Figure 1.1.4: Daily average (a) temperature, (b) soil water content, and (c) soil water potential of north-facing, south-facing, and hydrogel plots at 10 cm depth (n=7) from June, 2012 to August, 2012.

Soil nutrient supply

North and south-facing plots had slightly different rates of available nutrients in the soil. Both north and south-facing plots had similar available total N, NO_3^- , NH_4^+ , and Mg (Table 1.1.3). However, south-facing plots had twice as much K and P whereas north-facing plots had more than twice as much S and 1.7 times as much Ca which might be related to greater microbial activity related to warmer soil temperatures (Table 1.1.3).

Hydrogel plots generally had more available soil nutrients than non-amended plots. Hydrogel did not affect available NH_4^+ , Ca, or S (Table 1.1.3), but plots amended with hydrogel had 4.6 times more NO_3^- , resulting in roughly 2.7 times more total available N. In addition, hydrogel plots also had 7.8 and 1.7 times more K and P, respectively, than non-amended plots, while the non-amended south-facing plots had 1.4 times more Mg, which similarly to the observations could be related to increased microbial activity driven by less limiting conditions such as water and temperature.

Table 1.1.3: Average available nutrients (\pm SE) of north-facing, south-facing, and hydrogel plots. Units are expressed as $\mu\text{g } 10 \text{ cm}^{-2} \text{ 32 days}^{-1}$ and different letters signify statistical differences between means based on Tukey-Kramer adjustment ($n=10$) (Syncrude Canada Ltd. 2014).

	North-facing	South-facing	Hydrogel
Total N	14.39 \pm 1.25	14.59 \pm 0.80 Y	38.58 \pm 6.86 Z
NO_3^-	9.23 \pm 1.18	6.90 \pm 1.04 Y	31.52 \pm 6.77 Z
NH_4^+	7.06 \pm 1.08	7.70 \pm 1.01	7.06 \pm 1.08
P	3.66 \pm 0.42 B	6.32 \pm 0.83 A Y	11.09 \pm 0.99 Z
K	125.25 \pm 17.84 B	251.52 \pm 29.35 A Y	1972.45 \pm 213.30 Z
Ca	2168.18 \pm 115.29 A	1279.44 \pm 118.96 B	1056.51 \pm 141.15
Mg	253.37 \pm 21.02	272.40 \pm 14.78 Z	189.42 \pm 8.72 Y
S	608.05 \pm 113.72 A	264.82 \pm 34.39 B	381.69 \pm 71.71

Seedling growth and physiological response on north and south-facing plots

Pine

Stock type had a strong influence on height, relative height, and root growth (stock type: all $p = 0.001$) whereas aspect had a strong influence on new needle mass (aspect: $p = 0.003$). The O stock type had 21 % more height growth than both the G and OL stock types which were not different from each other (Figure 1.1.5a). The O stock type, which had initially the highest RSR, had the highest relative height growth while the G stock type had the least (Figure 1.1.5b). Root growth showed the opposite trend, G stock type with initially the smallest RSR had the most root growth (Figure 1.1.5c). In contrast, new needle mass was influenced by aspect rather than stock type, with south-facing plots having 47 % greater needle mass (Figure 1.1.5d). These responses might be related to the storage and availability of NSC reserves in these seedlings. Indicating that shoot size plays a significant role in pine seedlings as significantly more NSC reserves are stored in the needles compared to the other organs.

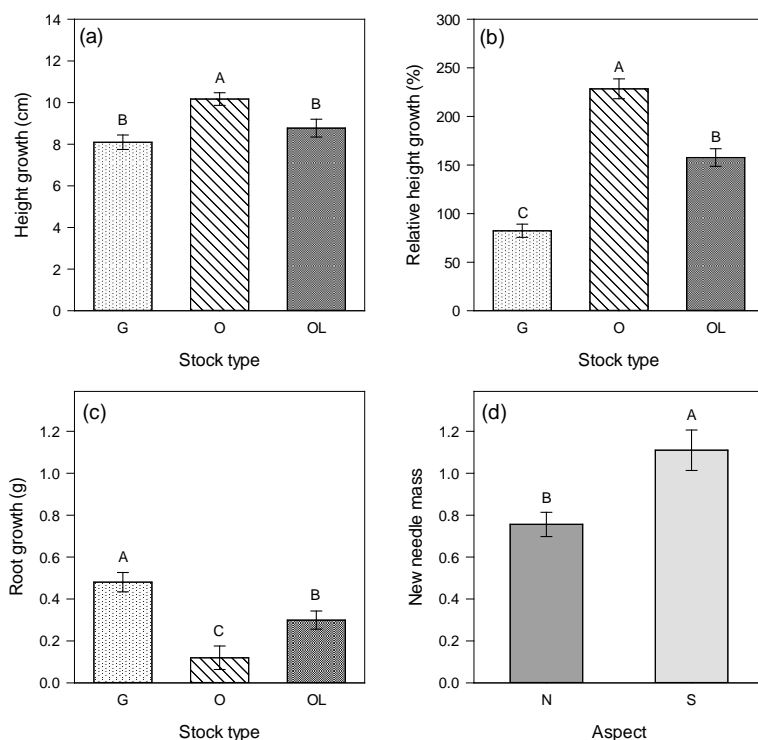


Figure 1.1.5: Average (a) height growth, (b) height growth relative to initial height, and (c) root growth of different pine stock types ($n=20$) as well as average (d) new needle mass of north and south-facing aspects ($n=30$) over one growing season. Error bars represent one standard error, and different letters indicate statistical differences among means based on comparisons using Tukey-Kramer adjustment.

Changes in RSR from initial conditions were influenced by both stock type and aspect, but stock types responded similarly to change in aspect (stock type \times aspect: p -value = 0.901). The G stock type did not change in RSR from initial conditions whereas both the O and OL stock types reduced RSR by 47 % (Figure 1.1.6a). Across pine stock types, seedlings growing in north-facing plots had a smaller reduction in RSR from initial conditions compared to seedlings growing in south-facing plots, most likely due to the proportionally greater reduction in shoot growth (Figure 1.1.6b).

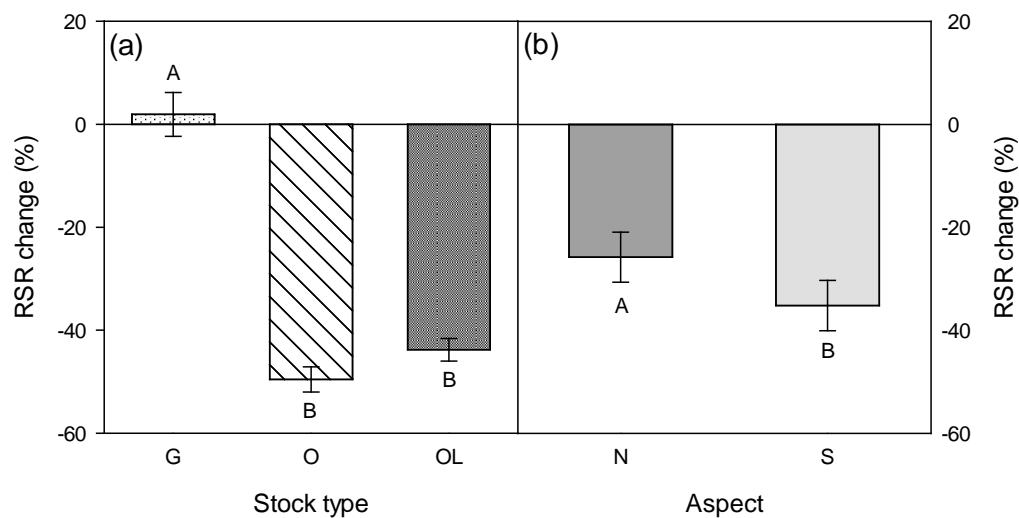


Figure 1.1.6: Average RSR percent change of (a) pine stock types ($n=20$) and (b) north and south-facing aspects ($n=30$) over one growing season. Error bars represent one standard error, and different letters indicate statistical differences among means based on comparisons using Tukey-Kramer adjustment.

Unlike most of the growth responses, stomatal conductance was influenced by aspect rather than stock type (aspect: p -value = 0.001). Seedlings in north-facing plots had approximately 50% lower stomatal conductance than seedlings in south-facing plots (Figure 1.1.7). Seedlings in north-facing plots had average shoot water potentials of -1.4 MPa whereas seedlings in south-facing plots had -1.2 MPa.

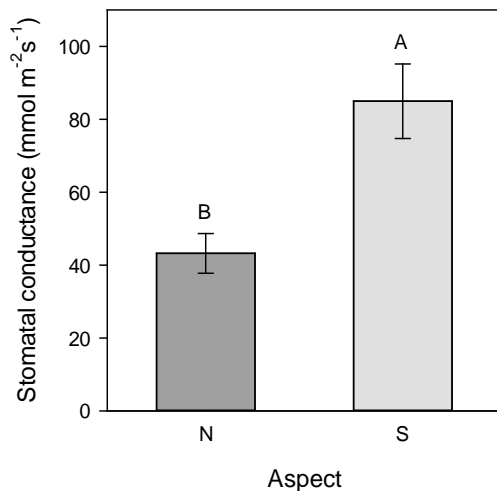


Figure 1.1.7: Average stomatal conductance of pine growing on north and south-facing aspects. Error bars represent one standard error ($n=30$), and different letters indicate statistical differences among means based on comparisons using Tukey-Kramer adjustment.

Aspen

No mortality was observed in any stock type or aspect/soil amendment treatment (100% survival). The pattern of height growth and shoot mass growth (data not shown) in response to stock type and aspect were the same for both response variables. All stock types experienced greater stem growth (height and mass) on south-facing plots compared to north-facing plots (both p -values < 0.001). However, the difference in height and stem mass growth between seedlings growing on the north-facing and on the south-facing plots was greater in the highRSR stock type (difference of 13.0 cm and 0.7 g) compared to the highNSC (4.9 cm and 0.2 g) and large (4.0 cm and 0.2 g) stock types. This resulted in significant stock type by aspect interaction terms for height growth (p -value = 0.055) and new stem mass growth (p -value = 0.005) (Figure 1.1.8). Regardless of aspect, the highRSR stock type had overall the greatest height growth compared to the other two stock types with the large stock type having the lowest height growth (p -value < 0.001). While height growth was similar between large and highNSC seedlings on south-facing plots, highNSC seedlings had greater height growth when grown on north-facing plots (Figure 1.1.8).

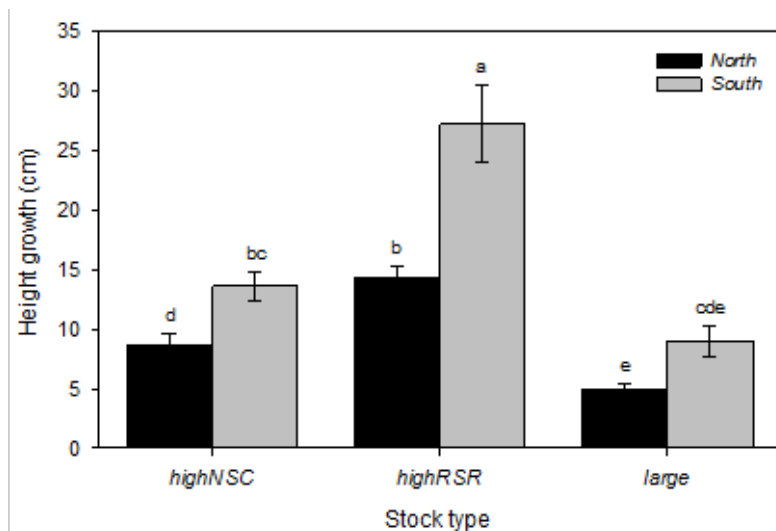


Figure 1.1.8: Average height growth after the first growing season of three aspen seedling stock types planted on north and south-facing slopes. Error bars represent one standard error of the mean and different letters indicate differences among means ($n=10$).

Both leaf area and leaf mass during the first growing season after outplanting were 83 % and 73 % greater in seedlings growing on south-facing slopes than on north-facing slopes (both p -value < 0.001) (data not shown). The highRSR stock type produced the highest leaf area (183.18 cm^2) compared to both the the highNSC (133.74 cm^2) and large (140.62 cm^2) stock types (p -value = 0.0153). HighNSC seedlings had less leaf mass (2.1 g) than both the highRSR (2.5 g) and large seedlings (2.6 g), which did not differ (p -value = 0.047) (data not shown).

There was a slight trend of greater root volume growth of aspen seedlings grown on a south aspect (p -value = 0.052) (data not shown). Overall, highNSC (10.8 mL^3) and large (11.1 mL^3) seedlings had greater root volume compared to the HighRSR seedlings (6.76 mL^3) (data not shown). However, all stock types added similar amounts of root volume to their root systems (data not shown).

Overall, seedling root to stem ratio (RSR, without leaves) declined more from initial conditions on the south-facing treatment than on the north-facing treatment (p -value < 0.001; Figure 1.1.9). This decline was driven by high stem growth on south-facing plots (Figure 1.1.9). Within the highNSC and large stock types, change in RSR was similar between aspect treatments, while highRSR seedlings showed a larger decrease in RSR from initial conditions on the south-facing plots (-3.1 g g^{-1}) than the north-facing plots (-1.8 g g^{-1}); this resulted in a significant interaction effect (p -value = 0.029) (Figure 1.1.9).

RSR decreased the most in the highRSR stock type in both aspect treatments, which can be attributed to their greater stem growth over the first growing season. Root to stem ration of highNSC seedlings also decreased slightly in both aspect treatments. In contrast, RSR of large seedlings increased slightly in both treatments, though this change was minimal (Figure 1.1.9).

Stomatal conductance did not differ among the three stock types and the north and south aspects (p -value = 0.746 and p = 0.303, respectively), but seedlings grown on south aspects had lower shoot water potentials (-1.79 MPa) than those grown on north aspects (-1.55 MPa) (p -value = 0.016). However, shoot water potential did not differ among the three stock types (p -value = 0.550).

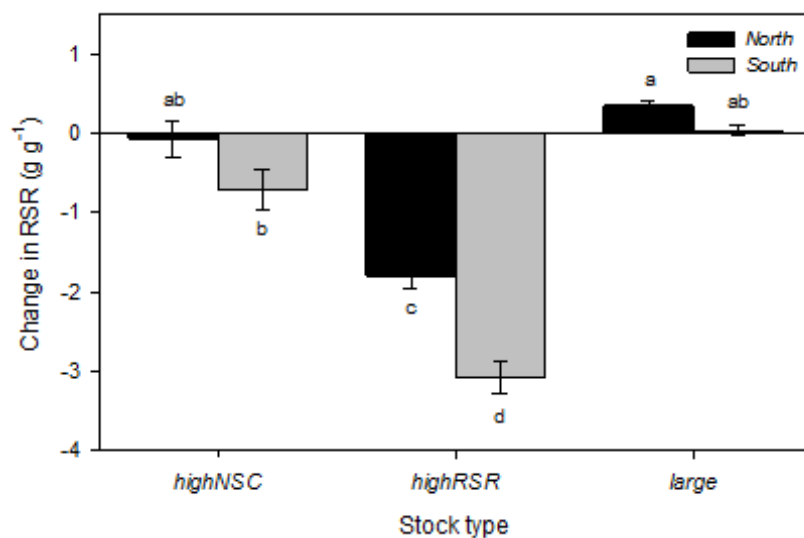


Figure 1.1.9: Average change in root to stem ratio (RSR without leaves) from initial conditions after the first growing season for three aspen seedling stock types planted on a north and south-facing slope. Error bars represent one standard error of the mean and different letters indicate differences among means (n=10).

Impact of hydrogel amendment

Pine

Hydrogel amendment had no effect on pine seedling height and relative height growth regardless of stock type (stock type: p -value = 0.012 and p -value < 0.001, respectively). Trends were the same as height and relative height growth of north and south-facing plots (Figure 1.1.5a and b).

Stem growth had an interaction between stock type and hydrogel amendment (stock type \times treatment: p -value = 0.037). While there was no effect of hydrogel on stem growth for O and OL seedlings, hydrogel did increase stem growth of G seedlings so that they had greater growth than the other stock types (Figure 1.1.10a).

Similar to height and relative height growth, hydrogel had no influence on root growth (stock type: p -value < 0.001; Appendix 5). Trends were similar to root growth of north and south-facing plots (Figure 1.1.5c), but O and OL stock types did not differ significantly (Figure 1.1.10b). Since there was no difference in needle production, root growth drove differences in RSR. The G stock type experienced no change, but the O and OL stock types had approximately 50 % smaller RSR than their initial levels (Figure 1.1.10c).

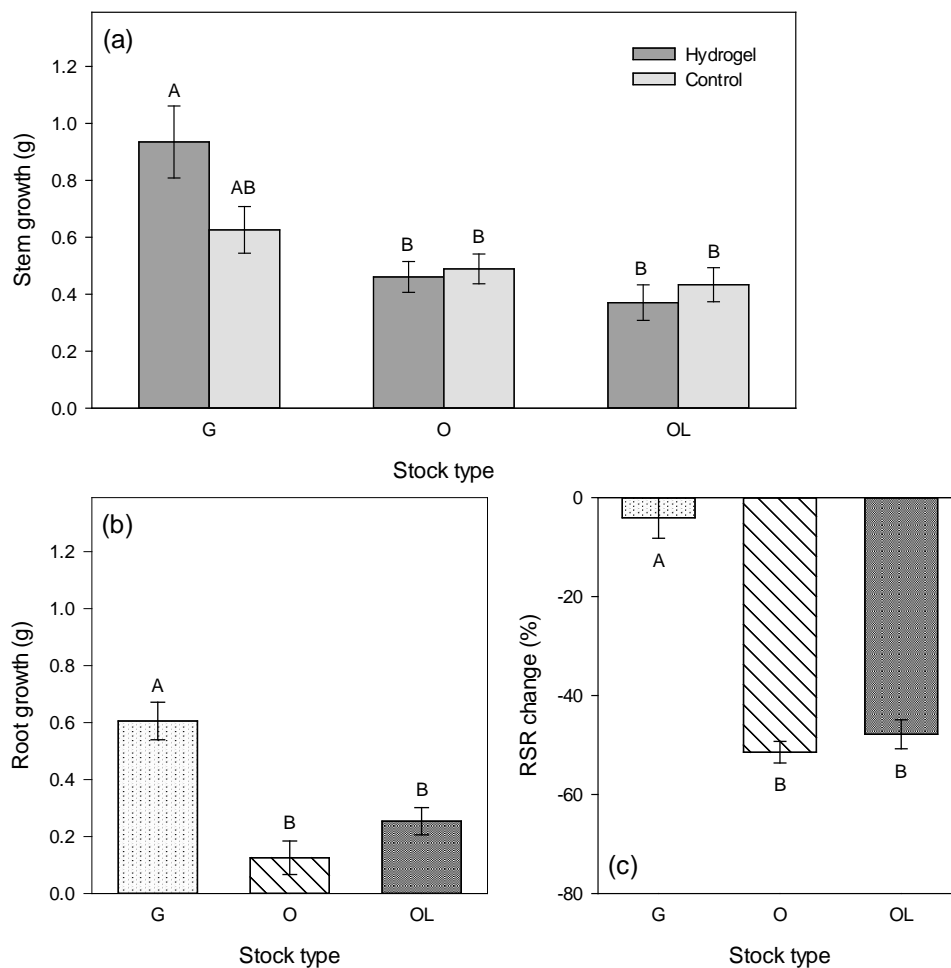


Figure 1.1.10: Average (a) stem growth ($n=10$) as well as average (b) root growth and (c) RSR changes ($n=20$) of pine in hydrogel-amended and non-amended plots on a south-facing aspect over one growing season. Error bars represent one standard error, and different letters indicate statistical differences among means based on comparisons using Tukey-Kramer adjustment.

Aspen

Height growth and stem mass growth were 78 % and 74 % greater in seedlings that grew in soil amended with hydrogel (both p -value < 0.045) (data not shown). Overall, the highRSR stock type had greater stem growth (29.4 cm height growth and 1.3 g stem mass growth) than both the highNSC (13.8 cm and 0.7 g) and large (12.6 cm and 0.7 g) stock types (both p -values < 0.001) (data not shown). Total leaf area and leaf mass also did not differ among the three stock types (p -value \geq 0.211) (data not shown); however, leaf area and leaf mass in the hydrogel treatment increased by 40 % and 30 %, respectively, (330.5 cm² and 2.8 g) relative to the Control treatment (197.4 cm² and 2.0 g) (both p -values < 0.023) (Figure 1.1.11).

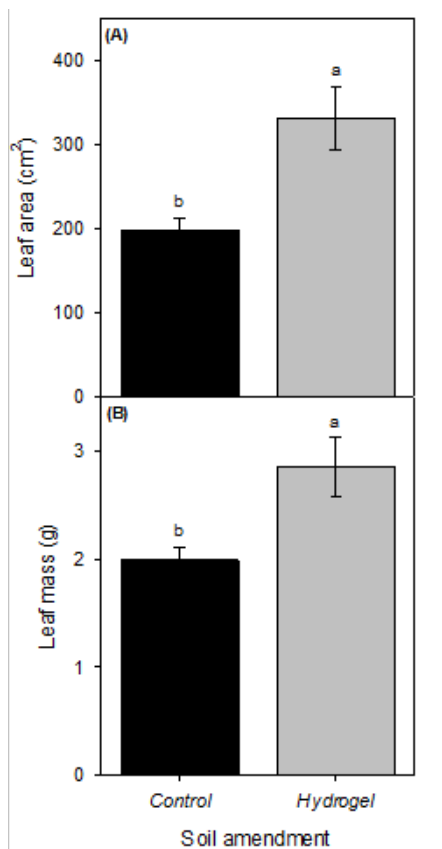


Figure 1.1.11: Average leaf area (A), and leaf mass (B) production during the first growing season of aspen seedlings (all three stock types combined) planted in different soil amendments. Error bars represent one standard error of the mean and different letters indicate differences between means ($n=30$).

Hydrogel application resulted in increased root volume growth (p -value = 0.012); however this was dependent on the stock type. While hydrogel application increased root volume growth by 80 % and 104 % in the highNSC and large stock types, respectively, it did not

affect root volume growth in highRSR seedlings. This response resulted in a significant hydrogel by stock type interaction effect (p -value = 0.015) (Figure 1.1.12). Large seedlings had the most root volume growth in both hydrogel and non-amended south-facing plots (control), while highRSR seedlings had the least root volume growth in both soil treatments (Figure 1.1.12).

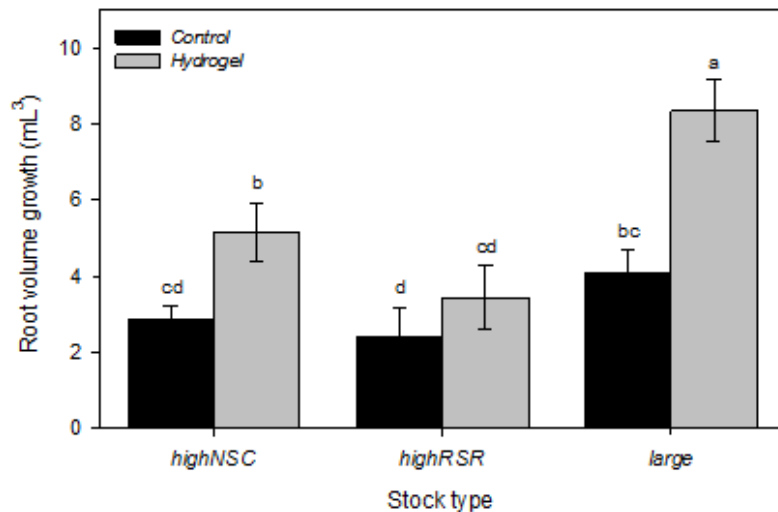


Figure 1.1.12: Average root volume growth following one growing season of three aspen seedling stock types planted in different soil amendment treatments. Error bars represent one standard error of the mean ($n=10$) and different letters indicate differences among means.

Total seedling size (mass) of the highNSC and highRSR stock types was unaffected by the hydrogel application, while the hydrogel amendment increased total seedling mass by 4.3 g in the large stock type (hydrogel \times stock type p -value = 0.043) (Figure 1.1.13). Similar to initial conditions, the large seedlings were still the largest in terms of total mass in both treatments, while highRSR seedlings had the lowest total mass (Figure 1.1.13).

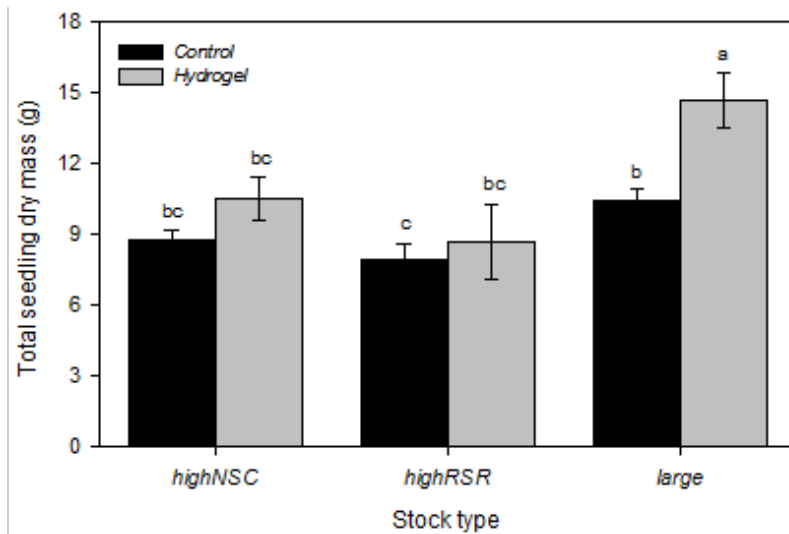


Figure 1.1.13: Average total seedling mass following one growing season of three aspen seedling stock types planted in different soil amendment treatments. Error bars represent one standard error of the mean ($n=10$) and different letters indicate differences among means.

Overall, hydrogel application had no effect on the RSR of all seedling stock types (p -value = 0.889) (data not shown). After the first growing season the highRSR stock type had the largest decrease from initial conditions, 4.9 g g^{-1} to 2.0 g g^{-1} , followed by the highNSC stock type, which decreased from 3.2 g g^{-1} to 2.5 g g^{-1} , and the large stock type (from 1.62 g g^{-1} to 1.56 g g^{-1}) (p -value < 0.001). After one growing season the RSR continued to be higher in the highNSC seedlings compared to large seedlings (p -value < 0.001); however, the RSR in highRSR seedling was intermediate between the highNSC and the large seedlings (data not shown).

Hydrogel application had no effect on stomatal conductance or shoot water potential across all three aspen stock types (p -value = 0.172 and p -value = 0.188, respectively). Similarly, there were no differences in stomatal conductance (p -value = 0.504) or shoot water potential (p -value = 0.733) among stock types.

Part II Factors and drivers affecting early colonizing vegetation development on reclaimed boreal forest upland sites[‡]

Methods

Plot establishment

All 78 measurement plots (planted and unplanted) were used for this part of the study (Figure 1, p. 7). Fifty-seven plots were located in areas covered with coarse coversoil material salvaged from a poor-xeric site type and 21 plots in areas covered with fine coversoil material salvaged from a rich-mesic site type. Within a treatment, plots were located to capture the different aspects present on each hummock; north and south aspects, as well as flat areas, which were all well represented, while only a smaller number of plots were located on west aspects and none on east aspects. In each vegetation plot four 1 × 1 m subplots were laid out in the corners of the plot to assess vegetation cover.

Vegetation measurements

In mid to late August of 2012, 2013 and 2015 vegetation community composition was surveyed. Plant species were identified and their percent cover was visually estimated as described in the general methods. Covers were estimated to the nearest percentage up to 10% and to the nearest 5% after; if less than 1%, cover was either determined to be 0.5% or as a trace (0.05%). Cover by bare ground was also visually estimated. Each species was subsequently classified into functional types (forb, graminoid, shrub, (unplanted) tree and non-vascular) and vascular plants were classified as native or introduced (Moss 1983; USDA 2016).

Planting density (see previous section) of planted tree seedlings was used to explore the effect of planted trees on the colonizing vegetation. Moreover, heat load index (reflecting

[‡] More detailed information on the justification, objectives and interpretation of the study and its results can be obtained from *Hoffman E. 2016. Influence of Environmental and Site Factors and Biotic Interactions on Vegetation Development Following Surface Mine Reclamation Using Coversoil Salvaged From Forest Sites. M.Sc. thesis, University of Alberta. 118 pages.*

slope and aspect), and coarse woody debris (CWD) volume (see previous section) impacts on the colonizing vegetation were also explored.

Statistical analysis

All analyses were carried out in R version 3.1.2 (R Core Team 2014). Areas capped with coversoils salvaged from different forest types (coarse materials from poor-xeric forest sites and fine materials from rich-mesic forest sites) were analyzed separately. Species richness and total vegetation cover per sample plot in areas capped with the two coversoils were compared using two sample t-tests; otherwise responses of the plant communities arising from the two different material types to the treatment variables were only qualitatively compared. Since we also expected significant variation between years due to colonization and climate differences between growing seasons (Figure C.1), separate analyses were also run for each year. Alpha was set at 0.05 for all models.

Linear mixed effects models

Linear mixed-effects models were constructed to assess the effect of planting density, coarse woody debris volume and heat load index on univariate response variables describing vegetation cover and diversity. Measured response variables used to assess vegetation cover included total vegetation cover and cover by native, introduced, forb and graminoid species. Richness and cover of shrubs, non-planted tree species and non-vascular species were not analyzed statistically as these were very low across the site. Vegetation diversity was assessed using Hill's diversity numbers N_0 (species richness), N_1 (e^x , where x =Shannon's index) and N_2 (the inverse of Simpson's index). Hill's numbers measure effective numbers of species; rare species are weighted most heavily in N_0 and have decreasing weight in calculating N_1 and N_2 (Hill 1973). In addition to total species richness (Hill number N_0), richness of functional groups (i.e. native, introduced, forb and graminoid species) was modelled in the same manner.

For all linear mixed effect models, seedling planting density, coarse woody debris volume (CWD) and heat load index (HLI) were used as independent variables. Scatterplots of residuals were assessed for all models to ensure that assumptions of linearity, homoscedasticity and normality were met. Statistically significant effects of continuous variables (coarse woody debris volume and heat load index) were determined to be either positive or negative. Statistically significant effects of the categorical variable (planting density) were followed up using pairwise comparisons of least squares means among the

three planting densities. Interactions were removed from the model when non-significant. Statistically significant interactions were assessed by plotting the effect of one continuous variable on the response variable at different levels of the (continuous or categorical) moderating variable. When the moderating variable was also continuous, the response variable was plotted at the mean and at one standard deviation above and one standard deviation below the mean of the moderating variable. When the moderating variable was categorical (planting density), the response variable was plotted at the three levels of the treatment. To assess a three-way interaction between the categorical (planting density) and two continuous (coarse woody debris, heat load index) variables, the interaction between the continuous variables was plotted separately for each level of planting density.

Permutational multivariate analysis of variance models

Permutational multivariate analysis of variance (PERMANOVA) models were constructed to assess the effects of three independent variables (planting density, coarse woody debris, heat load index) and their interactions on community composition. A random term was included as in the linear mixed effects models. Interactions were removed from the model when non-significant. Statistically significant interactions between categorical (planting density) and continuous (coarse woody debris, heat load index) variables were assessed by creating models of the effect of the continuous variable separately for each level of the categorical variable and determining at which levels the continuous variable was significant. To assess interactions between the categorical (planting density) and two continuous (coarse woody debris, heat load index) variables, the interaction between the continuous variables was assessed separately for each level of planting density to determine significance.

NMDS ordinations

NMDS ordinations were used qualitatively to examine vegetation community change from 2012 to 2015 in the whole site and in each coversoil type.

Results

Coversoil material type

A total of 172 species were identified across the site, with 67 species identified in areas capped with coversoil from a coarse-textured site and 138 species identified in areas

capped with coversoil from a fine-textured site (adjusted for the unequal sample sizes in areas capped with the two coversoils) (Table C.2). Species richness per vegetation subplot was significantly higher in areas capped with fine-textured coversoil than coarse-textured coversoil (p -value < .05). Considering per subplot species richness, a greater proportion of species were native in areas capped with coarse-textured coversoil compared to areas capped with fine-textured coversoil. Relatively more species in the coarse coversoil were graminoids and shrubs, while in the fine coversoil more species were forbs (Figure 2.1a). Vegetation cover per subplot was not significantly different between the two site types and followed a similar pattern to species richness, with proportionally greater cover by native species, graminoids and shrubs in areas capped with coarse coversoils than fine coversoils (Figure 2.1b).

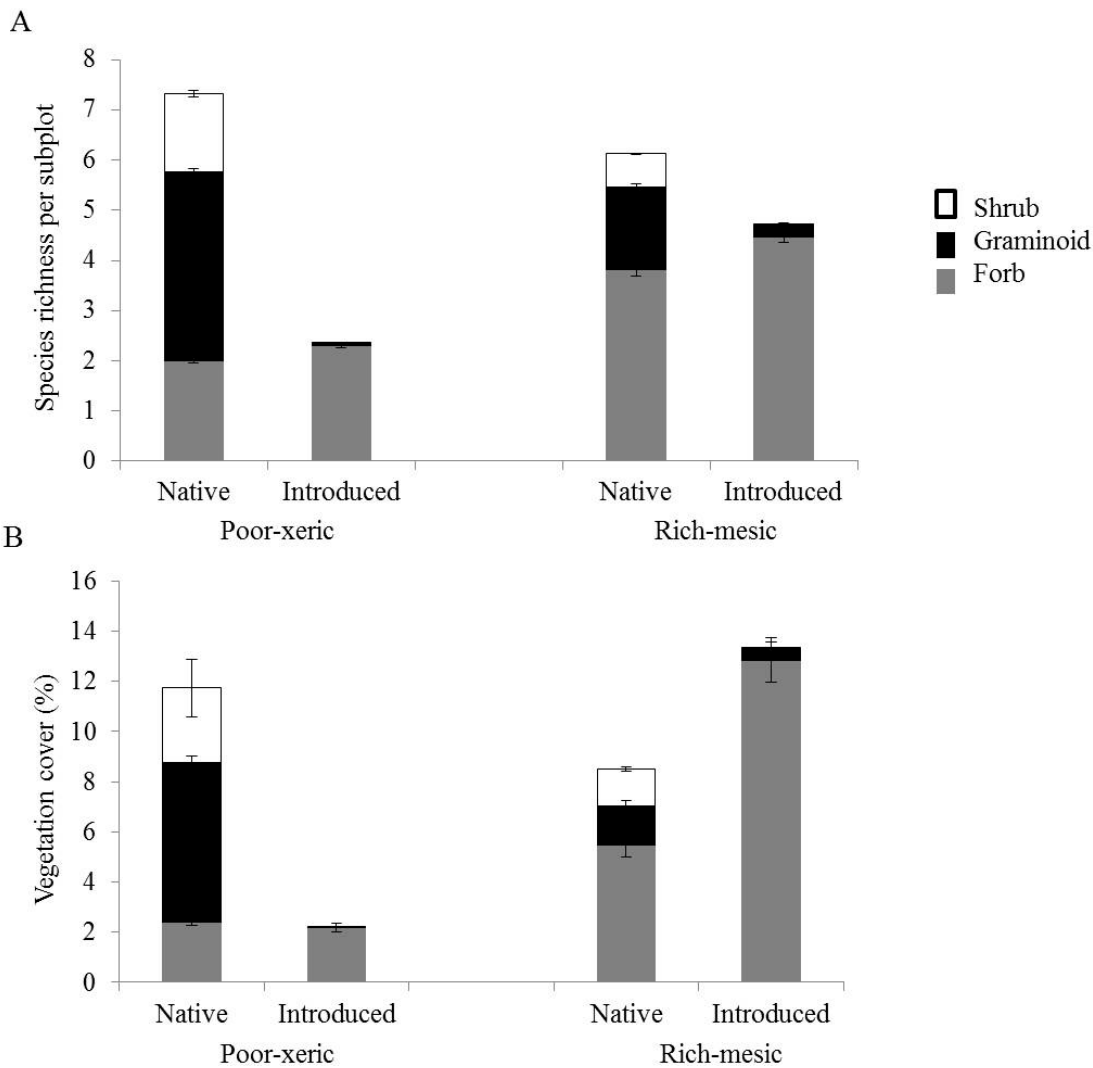


Figure 2.1: Vegetation cover (%) (A) and species richness per vegetation subplot (B) in 2015 of native and introduced forb, graminoid and shrub species per subplot in areas capped with cover soil salvaged from poor-xeric (coarse-textured) and rich-mesic (fine-textured) forest sites. Error bars show one standard error.

Vegetation diversity and cover in areas capped with coarse coversoil

In sites capped with the coarse coversoil, planting density had no effect on the measured vegetation cover variables (data not shown); however, planting density significantly affected a number of diversity measures (total and native species richness, Hill numbers N_1 and N_2). In all cases, diversity was higher in the high and/or medium planting density compared to the unplanted treatment (Table 2.1 and Table 2.2). Species richness (Hill number N_0) was only significantly affected in 2015 when N_0 (richness) was higher in the medium and high density treatments than in the unplanted treatment. Diversity measure N_1 (e^x , where x =Shannon's index) was higher in 2012 for both the high and medium than the unplanted planting density treatments while in 2013, N_1 was only significantly higher in the high density planting treatment. The inverse of Simpson's index (Hill number N_2) was significantly higher in 2012 in the medium density planting treatment than in the unplanted treatment; the high density treatment was intermediate between the two. In 2013, native species richness was significantly higher in the high density compared to the unplanted treatment, while the medium density treatment was intermediate. However, this effect was not detectable in 2012 or 2015.

Table 2.1: Results of linear mixed effects models testing for the effects of tree planting density (PD), heat load index (HLI; reflecting slope and aspect), and coarse woody debris volume (CWD) on vegetation diversity (overall species richness (Hill number N_0), Hill numbers N_1 (e^x , where x =Shannon's index) and N_2 (the inverse of Simpson's index), and native, introduced, forb and graminoid species richness) and cover (all species, native species, introduced species, forb species, and graminoid species) in areas capped with a coarse-textured coversoil salvaged from a poor-xeric site (see Table C.2 for a complete species list). *P*-values are bolded when significant. Interaction terms are shown when significant; interactions were removed from models when not significant.

Response Variable	Planting Density	Heat load Index	Coarse Woody Debris	PDxHLI	PDxCWD	CWDxHLI	PD x CWD x HLI
Species richness 2012	0.0722	0.8678	0.2791	0.2929	0.8794	0.5439	0.0021
Species richness 2013	0.0145	0.2558	0.5401	0.6968	0.1240	0.1017	0.0428
Species richness 2015	0.0374	0.8234	0.1298			0.0480	
N_1 2012	0.0387	0.7549	0.1573				
N_1 2013	0.0161	0.0659	0.3053				
N_1 2015	0.3165	0.0138	0.1996				
N_2 2012	0.0494	0.6085	0.2393				
N_2 2013	0.0523	0.0522	0.3976				

N₂ 2015	0.3283	0.0047	0.4138				
Native sp. richness 2012	0.0463	0.5528	0.3210	0.4290	0.7738	0.4710	0.0062
Native sp. richness 2013	0.0209	0.0923	0.9179				
Native sp. richness 2015	0.1024	0.1916	0.1281				
Introduced sp. richness 2012	0.5770	0.0889	0.6117				
Introduced sp. richness 2013	0.9475	0.1349	0.2998				
Introduced sp. richness 2015	0.3236	0.0077	0.6358				
Forb sp. richness 2012	0.5225	0.4410	0.4373	0.1537	0.6724	0.8870	0.0195
Forb sp. richness 2013	0.4496	0.7893	0.6960				
Forb sp. richness 2015	0.6204	0.1849	0.2799				
Graminoid sp. richness 2012	0.8322	0.4248	0.4274				
Graminoid sp. richness 2013	0.4142	0.5716	0.0900				
Graminoid sp. richness 2015	0.3359	0.7554	0.2266				
Total cover 2012	0.1456	0.8852	0.0314				
Total cover 2013	0.2275	0.3091	0.0207			0.0432	
Total cover 2015	0.3776	0.8030	<0.0001				
Native sp. cover 2012	0.7177	0.9742	0.2518				
Native sp. cover 2013	0.1905	0.3159	0.0512				
Native sp. cover 2015	0.3489	0.7276	<0.0001				
Introduced sp. cover 2012	0.2377	0.9337	0.2229				
Introduced sp. cover 2013	0.7748	0.9819	0.1779				
Introduced sp. cover 2015	0.3879	0.1278	0.0695				
Forb sp. cover 2012	0.1978	0.8702	0.1907				
Forb sp. cover 2013	0.6983	0.7727	0.9410			0.0004	
Forb sp. cover 2015	0.8296	0.0545	0.0687				
Gram. sp. cover 2012	0.8794	0.4972	0.2627				
Gram. sp. cover 2013	0.3967	0.2867	0.0084				
Gram. sp. cover 2015	0.8863	0.7763	0.0453				

Table 2.2: Summary of least squared means (\pm standard error) showing all significant effects of planting density on metrics of vegetation diversity for sites capped with coarse-textured coversoils. N_1 is e^x , where x =Shannon's index, and N_2 is the inverse of Simpson's index. Letters in rows indicate significant differences between treatments. Unplanted=0 stems per hectare, Medium Density=5000 stems per hectare, High Density=10000 stems per hectare. See also Table 2.1.

Response Variable	Year	Unplanted	Medium Density	High Density
Species richness	2015	13.15 \pm 0.49 a	14.51 \pm 0.49 b	14.53 \pm 0.48 b
N_1	2012	4.32 \pm 0.25 a	5.19 \pm 0.25 b	4.92 \pm 0.25 b
N_1	2013	5.27 \pm 0.25 a	5.77 \pm 0.25 ab	6.33 \pm 0.25 b
N_2	2012	3.44 \pm 0.21 a	4.12 \pm 0.21 b	3.88 \pm 0.21 ab
Native sp. richness	2013	7.83 \pm 0.51 a	8.57 \pm 0.51 ab	9.88 \pm 0.51 b

In 2015, heat load index (HLI; reflecting aspect) had a significant negative relationship with Hill numbers N_1 and N_2 and a significant, positive relationship with introduced species richness; there were no effects of HLI in 2012 or 2013 (Table 2.1 and Table 2.3).

Table 2.3: Summary of estimates (\pm standard error) showing all significant effects of heat load index on metrics of vegetation diversity for sites capped with coarse-textured coversoils. N_1 is e^x , where x =Shannon's index, and N_2 is the inverse of Simpson's index. See also Table 2.1.

Response Variable	Year	Heat load Index Estimate
N_1	2015	-0.82 \pm 0.32
N_2	2015	-0.73 \pm 0.25
Introduced sp. richness	2015	1.08 \pm 0.39

Coarse woody debris volume affected measures of vegetation cover but not of diversity; the effects, when significant, were negative but in some cases also interacted with HLI (Table 2.1 and Table 2.4). In both 2012 and 2015, coarse woody debris had significant, negative effects on total vegetation cover. In 2015, coarse woody debris also had significant, negative effects on cover by native species and graminoids. The negative effect of coarse woody debris on graminoid cover was also significant in 2013.

Table 2.4: Summary of estimates (\pm standard error) showing all significant effects of coarse woody debris volume on metrics of vegetation diversity for sites capped with coarse-textured coversoils. N_1 is e^x , where x =Shannon's index, and N_2 is the inverse of Simpson's index. See also Table 2.1.

Response Variable	Year	Coarse Woody Debris Estimate
Total cover	2012	-0.13 \pm 0.06
Total cover	2015	-0.81 \pm 0.17
Native sp. cover	2015	-0.78 \pm 0.17
Graminoid sp. cover	2013	-0.11 \pm 0.04
Graminoid sp. cover	2015	-0.07 \pm 0.04

In two of the three years studied, the effect of heat load index on vegetation diversity and cover differed depending on coarse woody debris volume (HLI x CWD interaction; Table 2.1). In 2015, CWD and HLI influenced species richness; when coarse woody debris volume was low, species richness decreased as heat load index increased, but where coarse woody debris volume was high, species richness increased as heat load index increased (Figure C.2). In 2013, there was a significant interaction between heat load index and coarse woody debris on total vegetation cover and on forb cover. In areas where coarse woody debris volume was low, total vegetation cover decreased strongly as heat load index increased (Figure C.3 and Figure C.4). Where coarse woody debris volume was moderate, total vegetation cover decreased less strongly with increasing heat load index, and where coarse woody debris volume was high, there was a slight increase in total vegetation cover as heat load index increased. The changes in total cover with HLI and CWD were likely driven by the forb cover as it followed a similar pattern in response to these factors.

In the first two years, diversity measures were also affected by the interaction between coarse woody debris volume and heat load index and this interaction was further impacted by planting density (Table 2.1). In 2012, in unplanted areas total species richness, native species richness and forb species richness decreased strongly as heat load index increased and when coarse woody debris volume was high, while species richness decreased weakly when CWD volume was moderate and increased when volume was low (Figure C.5 to Figure C.7). In the medium density treatment, however, total and native species richness declined with heat load index regardless of woody debris cover, while forb species richness decreased more strongly with heat load index when coarse woody debris volume was lower. In the high density planting treatment, all three measures of richness increased with heat load index when coarse woody debris volume was high, increased more weakly when volume was moderate and either increased or decreased very weakly when volume was low. In 2013, there was a significant interaction of all three factors on total species richness. In the unplanted areas, species richness decreased as heat load index increased while coarse woody debris volume had very little impact (Figure C.8). In the medium density planting treatment, species richness again decreased as heat load index increased; however, this effect was stronger when coarse woody debris volume was high. In the high density treatment, species richness decreased as heat load index increased when coarse woody debris volume was low but increased with heat load index when coarse woody debris volume was high.

Vegetation diversity and cover in areas capped with fine coversoil

In areas capped with coversoil salvaged from a rich-mesic forest site, planting density significantly affected both vegetation diversity (Hill numbers N_1 and N_2 , native species richness, forb species richness) and cover (native species cover) measures. Measures of diversity and cover were, in all cases, higher in the high and/or medium planting density than in the unplanted treatment (Table 2.5 and Table 2.6). In 2012, Hill number N_1 , was significantly affected by planting density. N_1 was significantly higher in the high density treatment than the unplanted treatment, while the medium density treatment was intermediate. Hill number N_2 was significantly affected by planting density in 2015. N_2 was significantly higher in both the high and medium density treatments than in the unplanted treatment. Native species richness, forb species richness and native species cover were significantly affected by planting density in 2012. Native species richness was significantly higher in the high density treatment than in the medium or unplanted treatments. Forb species richness was significantly higher in the high density than the medium density treatment. Native species cover was significantly higher in the high density treatment than in the unplanted treatment, while cover in the medium density treatment was intermediate.

Table 2.5: Results of linear mixed effects models testing for the effects of tree planting density (PD), heat load index (HLI; reflecting slope and aspect), and coarse woody debris amount (CWD) on vegetation diversity (overall species richness (Hill number N_0), Hill numbers N_1 (e^x , where x =Shannon's index) and N_2 (the inverse of Simpson's index), and native, introduced, forb and graminoid species richness) and cover (all species, native species, introduced species, forb species, and graminoid species) in areas capped with a fine-textured coversoil salvaged from a rich-mesic site(see Table C.2 for a complete species list). *P*-values are bolded when significant. Interaction terms are shown when significant; interactions were removed from models when not significant.

Response Variable	Planting Density	Heat load Index	Coarse Woody Debris	PDxHLI	PDxCWD	CWDxHLI	PD x CWD x HLI
Species richness 2012	0.0025	0.9943	0.0362	0.8379	0.7805	0.7187	0.0288
Species richness 2013	0.1447	0.1834	0.2057				
Species richness 2015	0.1719	0.3756	0.7302				
N_1 2012	0.0430	0.5855	0.9906				
N_1 2013	0.3179	0.1072	0.3352				
N_1 2015	0.0991	0.0362	0.0066				
N_2 2012	0.1711	0.6257	0.9570				
N_2 2013	0.4581	0.1878	0.4943				

N₂ 2015	0.0444	0.0477	0.0052				
Native sp. richness 2012	0.0027	0.0298	0.5149				
Native sp. richness 2013	0.1420	0.0099	0.2644				
Native sp. richness 2015	0.0524	0.1708	0.7682	0.1827	0.9067	0.6202	0.0417
Introduced sp. richness 2012	0.3608	0.0319	0.0843				
Introduced sp. richness 2013	0.4971	0.0167	0.7110				
Introduced sp. richness 2015	0.8314	0.6694	0.1759				
Forb sp. richness 2012	0.0152	0.5803	0.1483				
Forb sp. richness 2013	0.3044	0.0808	0.3036				
Forb sp. richness 2015	0.3567	0.2008	0.3159				
Graminoid sp. richness 2012	0.4588	0.9002	0.5427	0.9832	0.8237	0.9099	0.0359
Graminoid sp. richness 2013	0.6909	0.7433	0.8180				
Graminoid sp. richness 2015	0.3225	0.6215	0.9823				
Total cover 2012	0.3734	0.3100	0.1280				
Total cover 2013	0.0929	0.5711	0.0041				
Total cover 2015	0.6044	0.7983	0.0005				
Native sp. cover 2012	0.0474	0.9618	0.6680				
Native sp. cover 2013	0.3521	0.0102	0.0215				
Native sp. cover 2015	0.4763	0.8049	0.0074				
Introduced sp. cover 2012	0.4263	0.2859	0.1469				
Introduced sp. cover 2013	0.2313	0.5219	0.0292				
Introduced sp. cover 2015	0.7986	0.2826	0.2283				
Forb sp. cover 2012	0.3904	0.2985	0.1326				
Forb sp. cover 2013	0.1187	0.6402	0.0059				
Forb sp. cover 2015	0.8667	0.9070	0.0984				
Gram. sp. cover 2012	0.1732	0.5730	0.1966				
Gram. sp. cover 2013	0.9045	0.4124	0.0530				
Gram. sp. cover 2015	0.4928	0.7551	0.1558				

Table 2.6: Summary of least squared means (\pm standard error) showing all significant effects of planting density on metrics of vegetation diversity for sites capped with fine-textured coversoils. N_1 is e^x , where x =Shannon's index, and N_2 is the inverse of Simpson's index. Letters in rows indicate significant differences between treatments. Unplanted=0 stems per hectare, Medium Density=5000 stems per hectare, High Density=10000 stems per hectare. See also Table 2.5.

Response Variable	Year	Unplanted	Medium Density	High Density
N_1	2012	2.93 \pm 0.28 a	3.42 \pm 0.29 ab	3.97 \pm 0.27 b
N_2	2015	2.66 \pm 0.26 a	3.49 \pm 0.27 b	3.89 \pm 0.25 b
Native sp. richness	2012	2.99 \pm 0.59 a	3.71 \pm 0.60 a	5.15 \pm 0.58 b
Forb sp. richness	2012	5.23 \pm 0.97 ab	4.21 \pm 0.98 a	6.21 \pm 0.97 b
Native sp. cover	2012	0.46 \pm 0.22 a	0.64 \pm 0.23 ab	1.26 \pm 0.22 b

In 2015, heat load index (HLI; reflecting aspect) had a significant, negative effect on Hill numbers N_1 and N_2 (Table 2.5 and Table 2.7). In 2012, heat load index had a significant, negative effect on native species richness and a significant, positive effect on introduced species richness, and in 2013, HLI had significant, negative effects on native species richness, introduced species richness and native species cover.

Table 2.7: Summary of estimates (\pm standard error) showing all significant effects of heat load index on metrics of vegetation diversity for sites capped with fine-textured coversoils. N_1 is e^x , where x =Shannon's index, and N_2 is the inverse of Simpson's index.

Response Variable	Year	Heat load Index Estimate
N_1	2015	-1.82 \pm 0.79
N_2	2015	-1.38 \pm 0.64
Native sp. richness	2012	-2.24 \pm 0.93
Native sp. richness	2013	-4.90 \pm 1.66
Introduced sp. richness	2012	2.14 \pm 0.90
Introduced sp. richness	2013	-0.57 \pm 0.77
Native sp. cover	2013	-8.89 \pm 3.03

As in areas capped with coarse coversoil, coarse woody debris primarily affected vegetation cover on fine coversoils, and the effects, when significant, were negative (Table 2.5 and Table 2.8). Coarse woody debris also had a limited number of significant effects on diversity; in 2015 coarse woody debris had significant, positive effects on Hill numbers N_1 and N_2 . In 2013, coarse woody debris had significant, negative effects on total vegetation cover, native species cover, introduced species cover and forb cover and in 2015 woody debris had significant, negative effects on total vegetation cover and native species cover.

Table 2.8: Summary of estimates (\pm standard error) showing all significant effects of coarse woody debris volume on metrics of vegetation diversity for sites capped with fine-textured coversoils. N_1 is e^x , where x =Shannon's index, and N_2 is the inverse of Simpson's index.

Response Variable	Year	Coarse Woody Debris Estimate
N_1	2015	0.03 \pm 0.01
N_2	2015	0.03 \pm 0.01
Total cover	2013	-0.43 \pm 0.14
Total cover	2015	-0.84 \pm 0.23
Native sp. cover	2013	-0.14 \pm 0.05
Native sp. cover	2015	-0.65 \pm 0.23
Introduced sp. cover	2013	-0.30 \pm 0.14
Forb sp. cover	2013	-0.41 \pm 0.14

In two of the years studied, diversity measures on fine-textured coversoils were affected by the interaction of planting density, coarse woody debris volume and heat load index (Table 2.5). In 2012 there was a significant interaction of the three factors on total and graminoid species richness, and in 2015 on native species richness. In unplanted areas, total, graminoid and native species richness responded similarly to coarse woody debris and heat load index; richness increased with heat load index when woody debris volume was high and decreased when volume was low (Figure C.9 to Figure C.11). In the medium density treatment, total species richness and graminoid species richness responded similarly; richness increased with heat load index when woody debris volume was high, decreased weakly when volume was moderate and decreased more strongly when volume was low (Figure C.9 and Figure C.10). Native species richness responded differently; richness increased with heat load index at all levels of woody debris volume and the increase was strongest when volume was high (Figure C.11). In the high density planting treatment, all three measures of richness responded similarly. Richness decreased with heat load index when coarse woody debris volume was high and increased when volume was low; richness was intermediate when volume was moderate.

Vegetation community composition

In areas that were capped with a coarse coversoil, planting density, heat load index and coarse woody debris volume all significantly affected vegetation community composition in 2012 and 2013 (Table 2.9). In 2015, only coarse woody debris volume had a significant effect on community composition. There was also a significant interaction in 2013 between coarse woody debris and heat load index, and a significant three-way interaction between coarse woody debris, heat load index and planting density (Table 2.10). In the

unplanted treatment, coarse woody debris and heat load index interacted significantly to affect community composition, while in the medium and high density planting treatments, coarse woody debris and heat load index both significantly affected composition but there was not a significant interaction between the two.

Table 2.9: Results of permutational multivariate analysis of variance (PERMANOVA) models testing for the effects of tree planting density (PD), heat load index (HLI; reflecting slope and aspect) and coarse woody debris (CWD) volume on community composition in areas capped with a coarse-textured or fine-textured coversoil. *P*-values are bolded when significant. Interaction terms are shown when significant; interactions were removed from models when not significant.

Coversoil Type	Response year	Planting Density	Heat load Index	Coarse Woody Debris	PD x HLI	PD x CWD	CWD x HLI	PD x CWD x HLI
Coarse	2012	0.001	0.008	0.001				
Coarse	2013	0.052	0.002	0.001	0.364	0.071	0.012	0.004
Coarse	2015	0.218	0.246	0.001				
Fine	2012	0.017	0.039	0.026	0.023	0.265	0.690	0.022
Fine	2013	0.522	0.021	0.242	0.005	0.124	0.205	0.041
Fine	2015	0.173	0.098	0.001				

Table 2.10: Results of permutational multivariate analysis of variance (PERMANOVA) models testing for the effects of coarse woody debris (CWD) volume, heat load index (HLI; reflecting slope and aspect) and an interaction between the two (CWD x HLI) on community composition at each level of planting density treatment, when a significant interaction of planting density, coarse woody debris and heat load index was found (Table 2.9) in areas capped with a coarse-textured or fine-textured coversoil. *P*-values are bolded when significant. Interaction terms are shown when significant; interactions were removed from models when not significant. Unplanted=0 stems per hectare, Medium Density=5000 stems per hectare, High Density=10000 stems per hectare.

Coversoil Type	Year	Planting Density	CWD	HLI	CWD x HLI
Coarse	2013	Unplanted	0.006	0.025	0.001
		Medium	0.006	0.030	
		High	0.001	0.022	
Fine	2012	Unplanted	0.031	0.051	
		Medium	0.371	0.286	
		High	0.203	0.025	
Fine	2013	Unplanted	0.043	0.005	0.025
		Medium	0.142	0.031	
		High	0.710	0.259	

In areas capped with fine coversoil salvaged from a rich-mesic site, planting density, coarse woody debris and heat load index all had significant effects on community composition in 2012 (Table 2.9). There were also significant interactions between planting density and heat load index, and between planting density, coarse woody debris, and heat load index in 2012 (Table 2.10). In the unplanted treatment, both coarse woody debris and heat load index significantly affected community composition, but there was

no significant interaction between these factors. In the medium density planting treatment, neither of the factors or the interaction was significant. In the high density treatment, only heat load index had a significant effect. In 2013, heat load index had a significant effect on the community, and there was a significant interaction between planting density and heat load index, and between planting density, heat load index and coarse woody debris. In the unplanted treatment, coarse woody debris and heat load index significantly affected community composition. In the medium density planting treatment, heat load index significantly affected community composition and there was a significant interaction between heat load index and coarse woody debris. In the high density planting treatment, neither of the factors significantly affected community composition. As in areas capped with coarse-textured coversoil, in 2015 only coarse woody debris had a significant effect on community composition in areas capped with a fine-textured coversoil.

Vegetation community change from 2012 to 2015

A clear separation in community composition is evident between areas capped with coversoil from poor-xeric versus rich-mesic forest types (Figure 2.2a). The species most strongly associated with the first ordination axis were a native lichen (*Cladonia mitis*) and an introduced forb (*Lepidium densiflorum*). The species most strongly associated with the second axis were a native grass (*Festuca rubra*) and an introduced forb (*Trifolium pratense*). There was some evidence of convergence between communities of the two coversoil types over time with greater similarity in 2015 than in the two earlier years, although PERMANOVA models showed that in all three years studied, community composition differed significantly between the two coversoil types (p -value < .001).

An NMDS ordination contrasting vegetation communities by year for sites capped with coarse coversoil showed greater similarity between 2012 and 2013 than 2015 (Figure 2.2b). Further, there was lower variability among plots in 2015 than in 2012 or 2013. In this coarse material type, the species most strongly associated with the first axis were *Achillea millefolium*, a native forb and a native moss (*Dicranum* sp.). The species most strongly associated with the second axis were two introduced forbs (*Chenopodium album* and *Lotus corniculatus*).

In areas capped with fine-textured coversoil, an NMDS ordination contrasting years showed that variability decreased over time (Figure 2.2c). The community in 2015 was more similar to the community in 2013 than in 2012. In this fine-textured material, the species most strongly associated with the first axis were a native shrub (*Amelanchier*

alnifolia) and a native forb (*Astragalus canadensis*). The species most strongly associated with the second axis were a native forb (*Ranunculus scleratus*) and an introduced forb (*Polygonum convolvulus*).

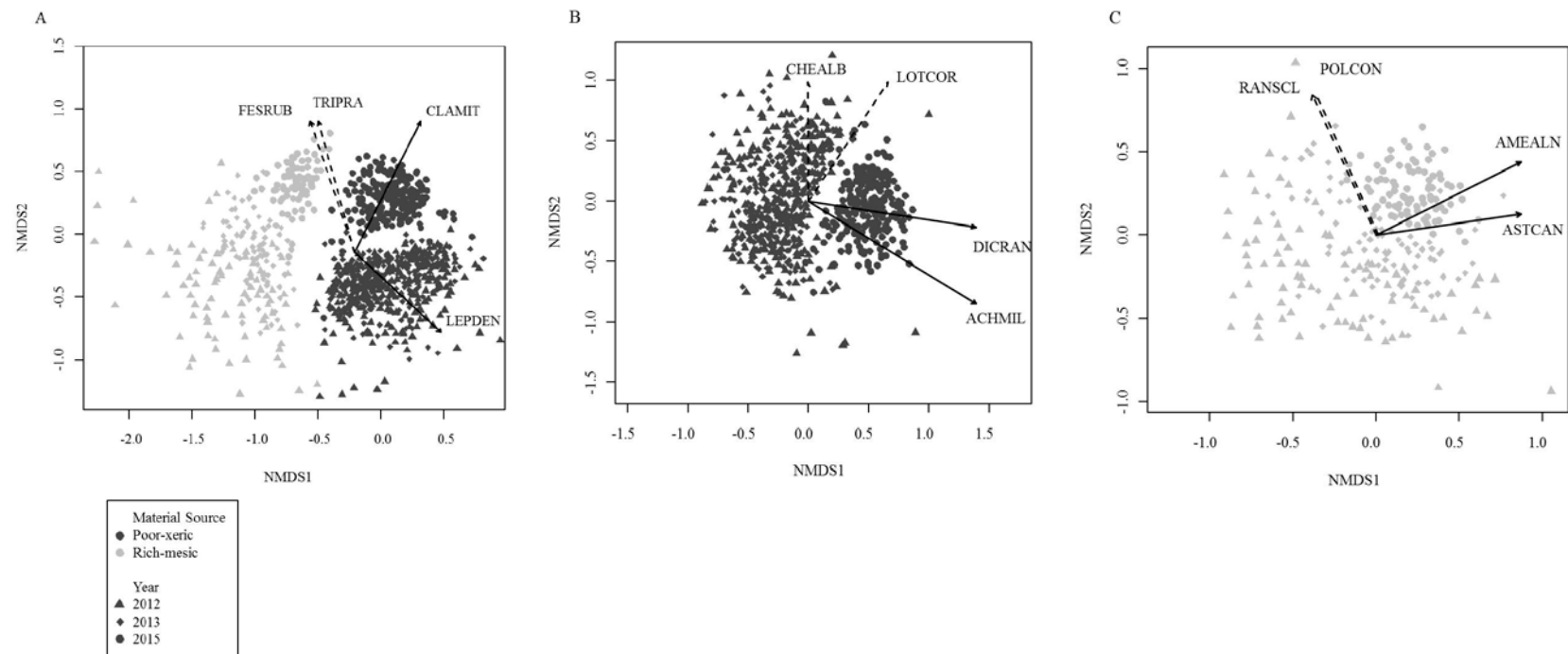


Figure 2.2: NMDS ordinations of (A) areas capped with coarse-textured coversoils salvaged from poor-xeric a forest site and fine-textured coversoils from a rich-mesic forest site in 2012, 2013 and 2015; (B) only areas capped with a poor-xeric coversoil over three years; and (C) only areas capped with a rich-mesic coversoil over the same three years. The two species most positively associated with the first two ordination axes are shown in each panel. Species strongly associated with the first axis (NMDS 1) are shown with solid arrows, and species strongly associated with the second axis (NMDS 2) are shown with dashed arrows. CLAMIT= *Cladonia mitis*, LEPDEN= *Lepidium densiflorum*, TRIPRA= *Trifolium pratense*, FESRUB= *Festuca rubra*, ACHMIL= *Achillea millefolium*, DICRAN= *Dicranum* sp., CHEALB= *Chenopodium album*, LOTCOR= *Lotus corniculatus*, ASTCAN= *Astragalus canadensis*, AMEALN= *Amelanchier alnifolia*, POLCON= *Polygonum convolvulus*, RANSCL= *Ranunculus scleratus*.

Project 2: Role of slope aspect and coarse woody debris in plant establishment[§]

Methods

Plot establishment and field measurements

Measurement plots were established mid-May 2012 immediately after site construction on a hummock in the Sandhill Watershed that stretched east to west providing extensive areas facing south and north. The hummock was capped with a fine-textured material as described in the general methods. This was a split-plot experiment, with a total of twenty 2x2 m² plots. Ten plots were located on the north-facing slope and ten on the south-facing slope of the hummock. Each plot was divided in half and similar-sized pieces of coarse woody debris (CWD) (with a diameter of 8 to 9 cm and a length of 35 cm) were placed in half of the plot, orienting them in either a north-to-south or an east-to-west direction, resulting in four “T”-shaped pairs in each treated plot-half (Figure 2.2.1). To assess soil nutrient availability, four cation and four anion Plant Root Simulator (PRS^{RTM}) probes (Western Ag Innovations Inc., Saskatchewan, Canada) were deployed from July 20 to August 24, 2012 in order to compare the available nutrients of the soils on north-facing slopes with those on the south-facing slopes.

At the end of August 2012, all seedlings in the CWD treatment were identified, and for each seedling, the distance and direction from the nearest log was recorded. In the other plot-half lacking the CWD treatment, the number of seedlings by species was recorded. Greenhouse seedling stakes were used to mark identified seedlings in order to avoid recording the same plant twice.

Greenhouse seedbank study

To assess the potential propagules bank (legacy) of the capping material, 15 soil cores (equivalent to a volume of 1.77 L) were collected every five meters along several 25 m long transects on the north and south-facing slopes of the hill structure. The samples were then transported to Edmonton and temporarily stored in a walk-in cooler (4°C). Each

[§] More detailed information on the justification, objectives and interpretation of the study and its results can be obtained from *Melnik K. 2013. Role of aspect and CWD in plant diversity recovery. B.Sc. Thesis, University of Alberta. 23p.*

sample was then spread on the surface of a Sunshine LA4 mix potting soil (55-65% sphagnum, perlite, dolomitic limestone, gypsum, wetting agent) placed in a 51 cm x 26 cm tray. The trays were kept in a greenhouse under ideal growing conditions, with a 16 hour (from 6:00 to 22:00) photoperiod, at 21°C during the day and 15°C during the night. The trays were watered with an automated sprinkler system every second day to keep soil from drying out and the humidity in the greenhouse ranged from 50% to 75%.

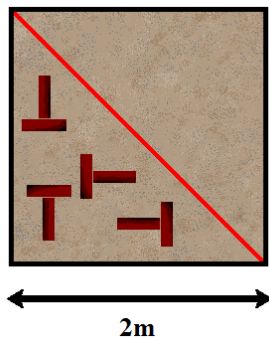


Figure 2.2.1: Plots set up on the north facing slope of the hill structure. Each plot was 2x2 m², with 8 debris pieces in each half of the plot. Debris pieces were arranged in “T”-shapes, comprising of one log oriented in a north-south direction, and the other log oriented in an east-west direction.

Statistical analyses

All the analyses were conducted with R 2.15.1 software. The ‘`ddply()`’ command from the “plyr” package was used in order to obtain the total number of seedlings and species per treatment per plot. The data in the output tables was visualized using the ‘`bargraph.CI()`’ command from the “sciplot” package. Subsequently the data in the output tables was divided into treatments, and the distribution of each treatment was checked for normality and equal variances of the residuals. Since the residual distributions were normal and variances were similar, no transformations were required. Welch two sample t-tests were performed to compare the number of seedlings and the number of species between the two aspects, and the number of seedlings and species between the CWD treatments. To compare the number of seedlings on different sides of the CWD pieces, we ran an

ANOVA. In order to obtain the NMDS ordination from the greenhouse data, the 'metaMDS()' and 'envfit()' commands were used from the "vegan" package.

Results

The ordination of greenhouse data show that the propagules bank composition was not different between the capping materials collected on the north-facing and south facing slopes (Figure 2.2.2). However, the expression of the vegetation found on the north and south-facing slopes on the reclamation site was markedly different. The average number of seedlings per plot was much higher on the north-facing slope compared to the south-facing slope (p -value < 0.001, Figure 2.2.3a). Similarly, the average number of species per plot was higher on the north-facing slope (p -value < 0.001, Figure 2.2.3b). The total number of seedlings and species was also higher on the north-facing slope: 2175 seedlings of 56 species established on the north-facing slope, compared to 742 seedlings of 48 species on the south-facing slope. Although the initial propagule bank was the same between both aspects, both aspects had species that were unique (Table 2.2.1). The north-facing slope had a higher proportion of unique native boreal forest species compared to the species unique to the south-facing slope. Understory species such as *Actaea rubra* (Ait.) Wilkl., *Trientalis borealis* Raf. and *Viola adunca* Sm. dominated the north-facing slope, while species typically found along forest edges such as *Fragaria virginiana* Duchesne, and *Campanula rotundifolia* L. occurred on south-facing slopes.

At a plot level, there were no significant differences in seedling and species numbers observed between treatments with and without coarse woody debris (Figure 2.2.4). Also, the orientation of CWD did not have much impact on the number of plants establishing, (p -value = 0.7748, Figure 2.2.5). However, the distance to CWD affected the germination and establishment success of native boreal species, while invasive and weedy species were unaffected by distance (Figure 2.2.6). Species native to the boreal forest such as *Cornus canadensis* L., *Equisetum arvense* L., *Fragaria virginiana* Duchesne, *Galium boreale* L., *Ledum groenlandicum* L., *Petasites palmatus* (Aiton) A. Gray, *Rosa acicularis* Lindl., *Populus tremuloides* Michx., *Rubus idaeus* L., and *Vicia americana* Muhl. (see Table D.1 for a complete list of species and how they were classified) were predominantly found in close proximity to CWD.

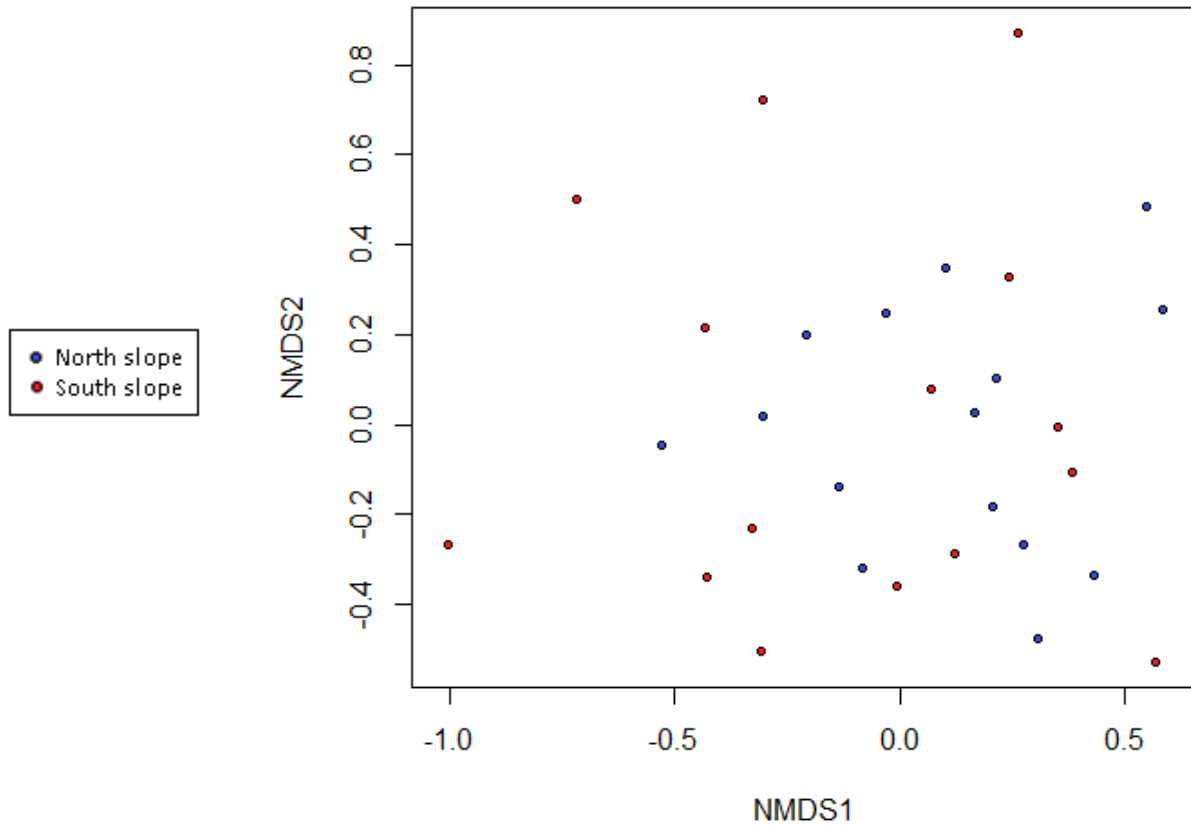


Figure 2.2.2: NMDS ordination depicting soil from the north-facing slope (blue) of the study area, and from south-facing slope of the study area (red).

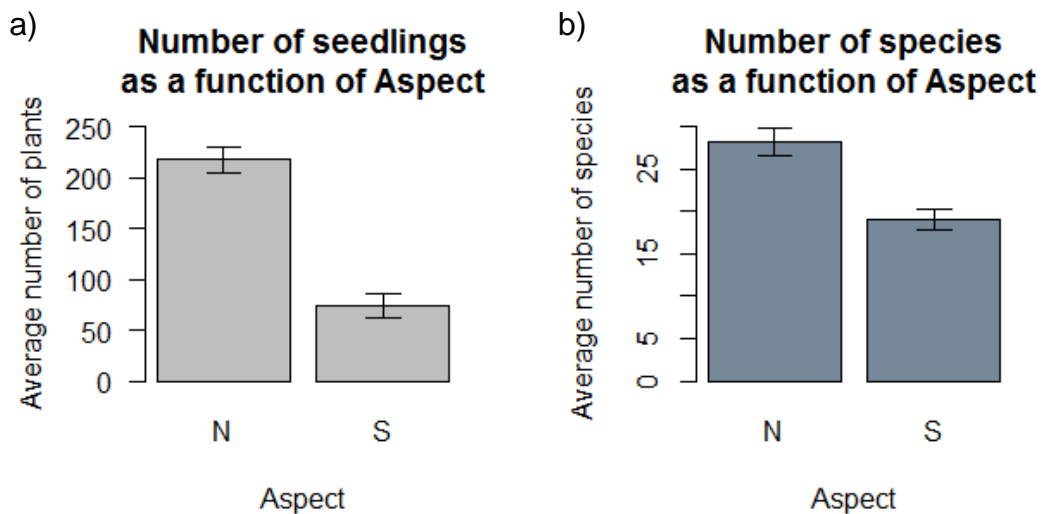


Figure 2.2.3: Average number of (a) seedlings and (b) species per plot on north (N) and south (S) facing slopes. Error bars represent 95% confidence intervals.

Table 2.2.1: Species unique to north and south-facing slopes and their species classification. Species highlighted in light gray are classified as boreal forest species, those highlighted in dark gray as ruderal native species and those highlighted in white as ruderal introduced species.

Slope position	Species	Species classification
Unique to north-facing slopes	<i>Actaea rubra</i>	Boreal forest species
	<i>Chenopodium gigantospermum</i>	Boreal forest species
	<i>Ledum groenlandicum</i>	Boreal forest species
	<i>Prunus virginiana</i>	Boreal forest species
	<i>Trientalis borealis</i>	Boreal forest species
	<i>Urtica dioica</i>	Boreal forest species
	<i>Viola adunca</i>	Boreal forest species
	<i>Mentha arvensis</i>	Wetland native species
	<i>Bidens cernua</i>	Wetland native species
	<i>Achillea millefolium</i>	Ruderal native species
	<i>Epilobium angustifolium</i>	Ruderal native species
	<i>Polygonum arenastrum</i>	Ruderal introduced species
	<i>Plantago major</i>	Ruderal introduced species
	<i>Polygonum convolvulus</i>	Ruderal introduced species
<i>Trifolium hybridum</i>	Ruderal introduced species	
Unique to north-facing slopes	<i>Campanula rotundifolia</i>	Boreal forest species
	<i>Fragaria vesca</i>	Boreal forest species
	<i>Carex</i> sp.	Ruderal native species
	<i>Chenopodium berlandieri</i>	Ruderal native species
	<i>Erigeron canadensis</i>	Ruderal native species
	<i>Galeopsis tetrahit</i>	Ruderal introduced species
<i>Melilotus officinalis</i>	Ruderal introduced species	

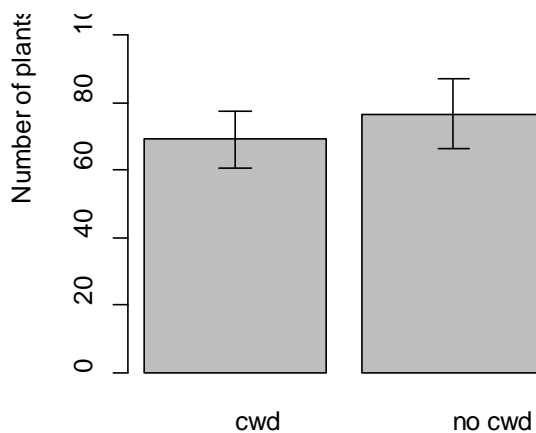


Figure 2.2.4: Average number of plants per plot in split plots with and without coarse woody debris (CWD). Error bars represent 95% confidence intervals.

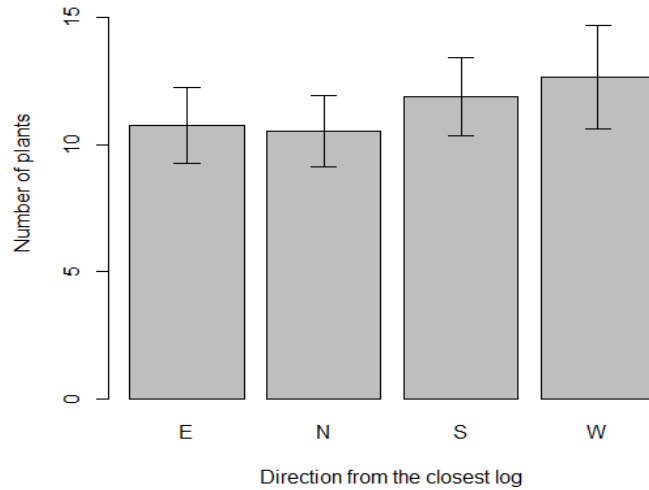


Figure 2.2.5: Average number of plants per plot as a function of direction from the closest log. Error bars represent 95% confidence intervals.

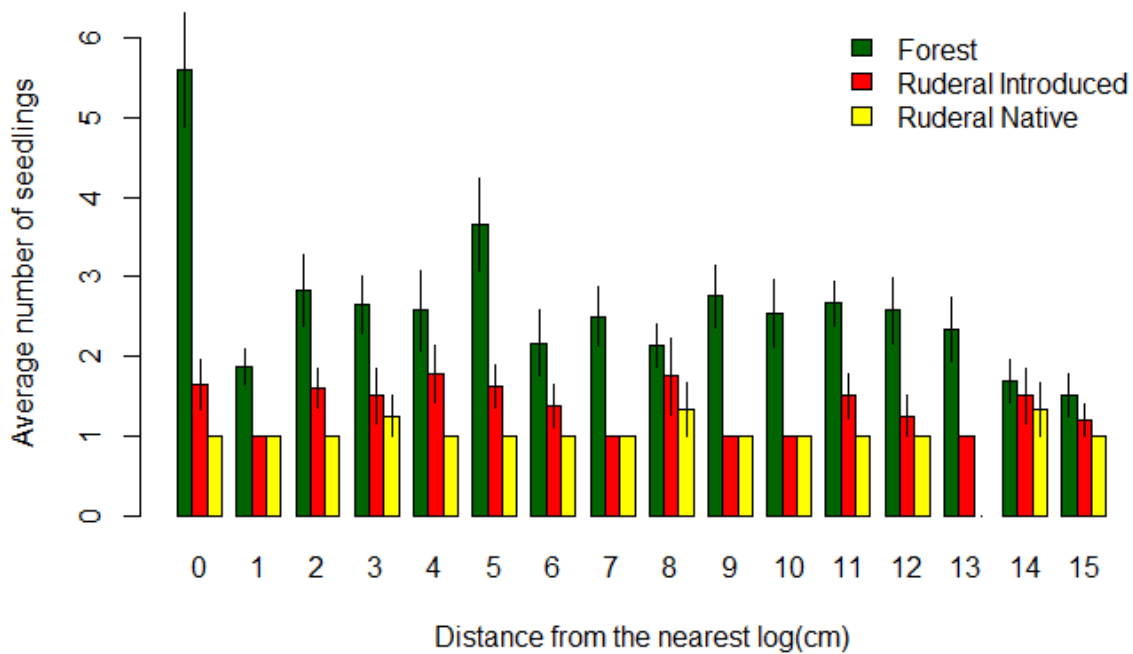


Figure 2.2.6: Number of seedlings as a function of distance from logs. Green bars represent the plants common to a mature boreal forest stand, red bars represent ruderal introduced plants, and yellow bars represent ruderal plants that are native to Alberta, Canada. Error bars represent 95% confidence intervals.

Project 3: Spatial variation, seedbank and soil type driving vegetation colonization on reclaimed upland sites**

Methods

Field sites

Young field reclamation site

Plots measured in the young field site were located in upland areas of the Sandhill Watershed. For more information on the site, please refer to the general methods section at the beginning of the document. Only the unplanted areas of the Sandhill Watershed in either the coarse- or the fine-textured coversoil were used for this study.

Older field reclamation site

This field site was located on the W1 Dump at Syncrude Basemine. The site was part of a cover soil study site constructed on an overburden dump built with saline-sodic overburden (Clearwater formation). The reclamation site was completed in early 2004 (Mackenzie 2006). Coversoil had been salvaged from a rich-mesic donor forest site, similar to the one used for the young site. Coversoil material was placed in early 2004 at a depth of 20 cm and is underlain by 90 cm of fine textured subsoil (Mackenzie 2006). After salvage and prior to placement, the coversoil material had been stored in windrows for three months in the winter (November 2003-February 2004) (Mackenzie and Naeth 2010). In the fall of 2005, *Picea glauca* and *Populus tremuloides* seedlings were planted at a density of 1200 stems ha⁻¹ at the site. No coarse woody debris was placed at this site, although small amounts were included with the salvaged coversoil when it was placed. Initial vegetation community composition on this site was surveyed during the first and second growing season after site construction (Mackenzie 2006), and comparing species lists and abundances the early community was found to have a species composition very similar to the one we found on the young field site constructed with the fine-textured coversoil.

** More detailed information on the justification, objectives and interpretation of the study and its results can be obtained from Hoffman E. 2016. *Influence of Environmental and Site Factors and Biotic Interactions on Vegetation Development Following Surface Mine Reclamation Using Coversoil Salvaged From Forest Sites*. M.Sc. thesis, University of Alberta. 118 pages.

Experimental design

Five grid plots were established in each of the three site types (young – coarse-textured, young – fine-textured and older – fine-textured). Grid plots were located in areas representative of the site that were generally flat, although some micro-topographical variation was present in plots. Each grid plot was a 5 × 5 m square composed of 100 contiguous 50 × 50 cm quadrats. The grid plots were 50 to 800 m apart within a site.

Vegetation and environmental variable measurements

Data on several variables describing vegetation communities and environmental factors were collected from each grid plot. Within each quadrat, individual vascular plant species were identified and their percent cover visually estimated. Total cover of bryophytes, coarse woody debris (CWD), and bare soil were also determined at the quadrat level. Cover by bryophytes was divided into ‘mature’ and ‘immature’ mosses; mature mosses had well developed vegetative and reproductive structures while immature mosses did not. Covers were estimated to the nearest percentage up to 10% and to the nearest 5% after; if less than 1%, cover was either determined to be 0.5% or as a trace (0.05%). To ensure consistency of the cover estimates, researchers performing the task calibrated estimate assessments several times a day, and used coroplast cut-outs (1% and 5% of the plot size) to help estimate cover more accurately.

Grid plot microtopography was mapped using the individual quadrats as guides to hand-draw an overlay of various features onto the grid plot. These maps included high and low areas in the plots, as well as features such as ridges, mounds and depressions (25-100 cm range), along with approximate heights (20-50 cm) of some of those features. For each grid, the map of topographical features was converted into a matrix of binary ‘dummy variables’ indicating whether a feature – for example, a ridge – was present or absent within each quadrat in the grid. Additionally, for the older – fine-textured site type, the area of the plot covered by the crown of a planted *P. tremuloides* or *P. glauca* individual was measured. For all trees for which the crown was covering the grid plot we recorded: species, stem location (according to grid plot coordinates), height, and crown radius. The data on tree crown dimensions were then overlain onto the grid plot using ArcGIS 10.2.2 (ESRI 2014). The Fishnet tool was used to create a reference grid, onto which the tree stem locations were mapped. Each stem location was then buffered by the crown diameter measurement of that tree. Using the ‘Intersect tool’, the area of each quadrat

covered by tree canopies was calculated, and then converted into values for percent cover by each tree species.

To estimate differences in available nutrients between the site types, leaf samples of *Populus tremuloides* were collected in grid plots in late July, as aspen was present on all sites. At the two young site types 20 *P. tremuloides* leaves were collected from five seedlings adjacent to each grid plot, as no planted seedlings were present within the plots; values for the five seedlings per grid plot were pooled. The leaf samples were oven dried at 70°C for three days and then ground to pass through a #40 (0.4 mm) mesh using a Wiley Mini-Mill (Thomas Scientific, New Jersey, USA). The samples were then analyzed for a selection of common elements (N, P, K, S, Al, B, Ca, Cu, Fe, Mg, Mn and Zn) measured using microwave digestion followed by ICP-OES (optical emission spectrometry). N was measured by combustion using a Costech Model EA 4010 Elemental Analyzer (Costech International Strumatzione, Florence, Italy, 2003). All analyses were carried out at the University of Alberta Natural Resources Analytical Laboratory.

Differences between site types in concentrations of selected nutrients were analyzed using one-way ANOVA followed by post-hoc Tukey HSD tests. The similar percentage of nitrogen and concentrations of phosphorus, potassium, manganese and sulphur in *P. tremuloides* leaves at the older and young fine-textured site type suggest that available soil nutrients at these sites were similar (Table 2.3.1). Although not significantly different, concentrations of nitrogen and potassium tended to be lower at the young – coarse-textured site type than at either fine-textured site type. Concentrations of manganese and sulphur were significantly higher for the young – coarse-textured site type than the older – fine-textured site type; concentrations for the young – fine-textured site type were intermediate. These differences suggest that available soil nutrients in the coarse-textured material were likely different than in the fine-textured material.

Table 2.3.1: Mean concentrations of selected nutrients in *Populus tremuloides* leaves from each of three site types. All concentrations are µg/g except nitrogen, which is a percentage. Letters indicate significant differences between site types ($\alpha= 0.05$) (n=5). Significant differences were determined using one-way ANOVA followed by Tukey HSD tests.

	Young – coarse-textured	Young – fine-textured	Older – fine-textured
Nitrogen (%)	1.95 a	2.24 a	2.18 a
Phosphorus	1404.83 a	1357.16 a	1545.74 a
Potassium	7964.20 a	8418.84 a	8486.97 a
Manganese	131.80 a	59.61 ab	56.94 b
Sulphur	3044.40 a	2332.75 ab	1922.64 b

Statistical analyses

All analyses were carried out in R version 3.1.2 (R Core Team 2014). Analyses were conducted for each of the 15 grid plots separately; community and spatial complexity were determined for each grid and these measures were compared between the three site types.

Complexity of plant community composition was measured as the number of unique community types within a grid, the total number of indicator species for each grid, the mean number of quadrats per community type and the mean number of indicator species per community type.

Cluster analysis was used to classify vegetation communities within each grid plot. The Average (UPGMA) method was selected as the best clustering method based on examination of the Cophenetic correlation and Gower distances (Borcard et al. 2011). The R function 'hclust()' was used for the cluster analysis. The optimal number of clusters to be interpreted for each grid plot was selected using silhouette widths; this is a measure of how well an object 'fits' with its assigned cluster (in this case the objects are quadrats within a grid plot) (Borcard et al. 2011). The R function 'silhouette()' was used to determine silhouette widths for each quadrat within a grid (Maechler et al. 2014).

Indicator Species Analysis was used to identify indicator species for each community type that was identified by the cluster analyses. The analysis was done using the R function 'multipatt()', which compares combinations of input clusters to the species in the input vegetation matrix, selects species with the highest association value, and tests for statistical significance (De Caceres and Legendre 2009). The total number of indicator species selected for each grid was interpreted as a measure of community complexity at the grid level. The mean number of indicator species selected for each community type within a grid was interpreted as a measure of complexity at the within-grid level. The species identified in each grid as indicator species were subsequently categorized by four functional types: forbs, graminoids, shrubs and non-vascular (moss classified as 'mature' and 'immature'). Species were then classified as either native or introduced, and as either 'forest' or 'non-forest' species. Forest species were native species commonly found in the understory of the target forest types. Proportions of indicator species of each functional type and original range or forest association were compared between the three site types; these proportions were calculated as the number of indicator species of a functional type

and original range or forest association (i.e. forb and native) as a proportion of all indicator species selected for the site type.

To assess complexity of spatial pattern we used principal coordinates of neighbour matrices (PCNM) analysis. The technique used a truncated matrix of sampling locations (quadrats) within a grid plot to generate a large number of spatial pattern variables; these were then used as explanatory variables in a redundancy analysis (RDA) (Borcard and Legendre 2002). The R function 'PCNM()' was used to create the spatial pattern variables used in the analysis (Legendre et al. 2013).

Spatial complexity was quantified as the number of significant axes produced during the RDA and the number of significant PCNM variables; for both, higher values indicated greater complexity. Additionally, PCNM analysis was used to identify which species were important in driving spatial patterns; a greater number of species driving the patterns was interpreted as greater spatial complexity. This gave insight into both complexity present in the grid plots and spatial relationships among species. Species with scores on RDA axis 1 (the first axis explained the most variation) greater than or equal to 0.1 were considered to be drivers of spatial pattern. As in the community complexity analysis, the species identified as drivers of spatial patterns in each grid were categorized by functional type, original range and forest association and proportions were compared between the site types (see above).

Variation partitioning was used to assess the relative influence of different environmental and site factors on vegetation community composition in the grid plots. The variation partitioning was performed using the R function 'varpart()' (Oksanen et al. 2015). This function partitioned variation in a vegetation community composition response matrix with respect to a series of explanatory environmental variable components: microtopography, CWD abundance, tree canopy (at the older – rich-mesic site type only), PCNM patterns (a surrogate for space to represent dispersal limitations and competition), and a linear trend component, which accounted for variation explained by trends at scales larger than the grid plots. At the young – fine-textured and young – coarse-textured site types, microtopography and CWD variables were considered together as one 'environmental variable' component. For each explanatory component, a matrix containing all possible variables was constructed; the PCNM matrix included all positively spatially correlated PCNM variables, the tree canopy matrix included variables for cover by *P. tremuloides*, *P. glauca* and both species combined, and the microtopography matrix included all

microtopography variables created from the microtopography field maps. Forward selection (using R function `forward.sel()` (Miller and Farr 1971)) was used to select the variables from each initial component matrix to be used in the variation partitioning analysis. In grid 6, none of the environmental variables were selected, and in grid 11 none of the tree canopy variables were selected; these components were excluded from the analyses of these grids.

Differences between site types in mean values for the results of the community complexity, spatial complexity and variation partitioning analyses were analyzed using one-way ANOVA followed by post-hoc Tukey HSD tests, except in cases where the results for one site type had no variation. In these cases, results for the remaining two site types were analyzed using Wilcoxon signed-rank tests because of non-normality. Differences between site types of proportions of indicator species and species driving spatial patterns of species types (native and introduced, forest associated and non-forest associated species) were analyzed using Fisher's exact tests.

Results

The young – coarse-textured site type had an average of two community types per grid plot, while the young – fine-textured site type had an average of 2.4 community types and the older – fine-textured site type had an average of 7.8 community types. In addition, for the young – coarse-textured site type an average of 50 quadrats per grid represented each community type while the community types were represented by 45 and 14 grid plots on average for the young and old – fine-textured site types, respectively. Because there was no variation among grid plots in number of community types and number of quadrats per community type for the young – coarse-textured site type, this site type was not included in the statistical analysis for these measures (Table 2.3.2, Figure E.1 to Figure E.3). The number of indicator species per grid and per community type did not differ between the two young site types, but was significantly greater at the older site type than at either young site type.

The number of significant RDA axes, and of PCNM variables, was significantly lower at the young – coarse-textured site type than at the young and older - fine-textured site types, which did not differ from one another (Table 2.3.2). The average number of species that drove spatial patterns was significantly greater at the older site type than at either of the young site types, which did not differ from one another.

Table 2.3.2: Mean values (\pm SD) of variables describing community complexity (number of community types, number of indicator species per grid, number of quadrats per community type, number of indicator species per community type), spatial complexity (number of significant RDA axes, PCNM variables, and PCNM drivers (number of species driving spatial patterns)), and variation partitioning (proportion variation explained by the PCNM/spatial component, environmental variable component, tree canopy component, microtopography component, linear trend component, and residual component). At the two young site types, the environmental variables consisted of coarse woody debris and microtopography and at the older – fine-textured site type, of microtopography and tree canopy cover. Letters indicate significant differences between site types ($\alpha = 0.05$) ($n=5$). Significant differences were determined using one-way ANOVA followed by Tukey HSD tests except in cases (indicated by *) where one site type had no variation; in these cases, non-parametric Wilcoxon signed-rank tests were used to compare the remaining two site types.

	Young – coarse-textured	Young – fine-textured	Older – fine-textured
Community Types (CT)*	2.0 \pm 0 -	2.4 \pm 0.8 a	7.8 \pm 1.9 b
Indicator species (IS) per grid	1.8 \pm 1.2 a	3.4 \pm 1.0 b	9.8 \pm 1.6 b
Quadrats per CT*	50.0 \pm 0 -	45.0 \pm 10 a	13.8 \pm 3.9 b
IS per CT	0.9 \pm 0.6 a	1.6 \pm 0.3 a	4.2 \pm 1.3 b
Significant RDA Axes	7.2 \pm 0.7 a	11.2 \pm 1.9 b	11.4 \pm 0.8 b
Significant PCNM Variables	19.6 \pm 2.2 a	27.6 \pm 4.8 b	26.6 \pm 4.6 b
PCNM Drivers (# species)	4.6 \pm 2.3 a	5.2 \pm 1.7 a	9.6 \pm 2.3 b
PCNM (Space)	0.34 \pm 0.020 a	0.52 \pm 0.065 b	0.58 \pm 0.025 b
Environmental Variables	0.053 \pm 0.020 a	0.051 \pm 0.050 a	0.16 \pm 0.027 b
Tree Canopy	-	-	0.055 \pm 0.0046
Microtopography	-	-	0.14 \pm 0.021
Linear Trend	0.066 \pm 0.019 a	0.12 \pm 0.045 ab	0.16 \pm 0.056 b
Residuals	0.64 \pm 0.040 a	0.47 \pm 0.065 b	0.41 \pm 0.022 b

Proportions of native *versus* introduced and forest associated *versus* non-forest associated species selected as indicator species and as drivers of spatial pattern, and that were present in the community, did not show significant differences between the site types (Table 2.3.3). When compared to the young – fine-textured site type, however, relatively more of both the indicator species and drivers of spatial pattern were native and forest-associated for the young – coarse-textured site type, and relatively fewer were non-forest grass and non-forest forb species (Figure 2.3.1). In the plant community, more introduced and non-forest associated species were present at the young – fine-textured than the young – coarse-textured site type (Figure 2.3.2). For the older – fine-textured site type, relatively more indicator species and species driving spatial pattern of the plant community were forest-associated and native than at the young – fine-textured site type. Relatively more of the non-forest species selected as indicator species and drivers of spatial patterns at the older – fine-textured site type were grasses, and relatively fewer

were forbs, when compared to the young – fine-textured site type. More native and forest-associated species were present in the community at the older than the young – fine-textured site type (Figure 2.3.2).

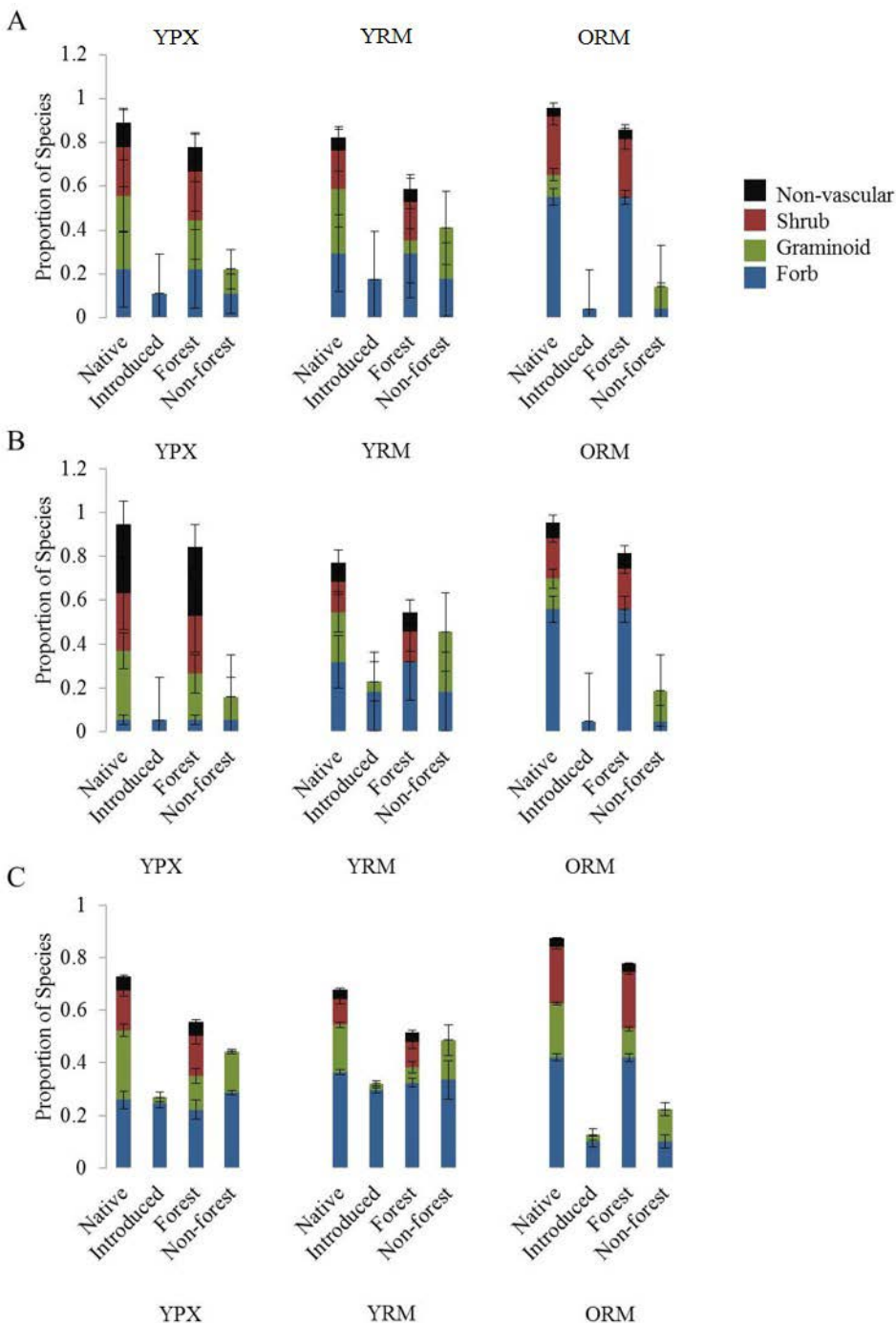


Figure 2.3.1: Proportions of four functional types (forb, graminoid, shrub, non-vascular (moss)) of native and introduced and forest associated and non-forest associated species at the three site types (YPX: young – coarse-textured, YRM: young – fine-textured, ORM: older – fine-textured). Plots show proportions of: A) indicator species; B) species driving spatial patterns; and C) total species of each functional type. Error bars show one standard error.

Table 2.3.3: Results (*P* values) of Fisher’s exact tests comparing the three site types (young – poor-xeric, young – rich-mesic and older – rich-mesic) in terms of the proportions of forest associated *versus* non-forest associated and native *versus* introduced species that were indicator species or drivers of spatial patterns.

	P value
Proportion of forest associated to non-forest associated indicator species	0.539
Proportion of native to introduced indicator species	0.4
Proportion of forest associated to non-forest associated drivers of spatial pattern	0.783
Proportion of native to introduced drivers of spatial pattern	0.5

For all three site types the variance partitioning showed that the vast majority of the explained variation was explained by spatial variation. Significantly more variation was explained by space at the young – fine-textured site type than at the young – coarse-textured site type (Table 2.3.2, Figure E.4 to Figure E.10). The amount of variation explained by the environmental component was not different between the two young site types.

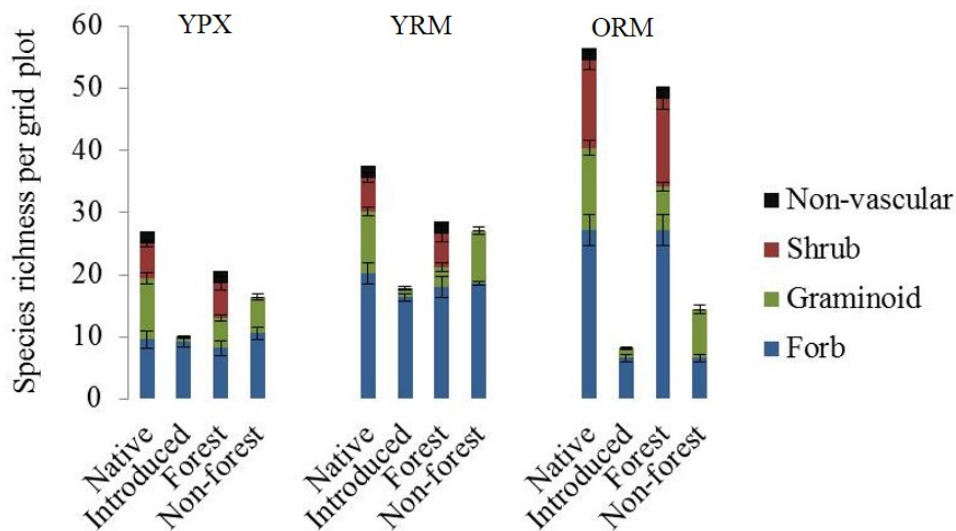


Figure 2.3.2: Mean numbers of species per grid plot by four functional types (forb, graminoid, shrub, non-vascular (moss) that were native *versus* introduced or forest associated *versus* non-forest associated for the three site types (YPX: young – coarse-textured, YRM: young – fine-textured, ORM: older – fine-textured). Error bars show one standard error.

Due to the different site conditions at the older site type (i.e. tree cover, greater variability in topography) the variation was partitioned into a slightly different set of components than at the young site types. The components used were: the PCNM (space) component, a microtopography component, a tree canopy component and a linear trend component.

Coarse woody debris and size of large ant hills were also considered but were not selected during the variable selection process. At the older fine-textured site, as at the two young site types, space explained a much greater proportion of total variation than environmental variables (Table 2.3.2, Figure E.11 to Figure E.15). The majority of the variation explained by environmental factors at the older site type was explained by microtopography, with a smaller amount explained by the tree canopy.

Literature Cited

- AgroClimatic Information Service. 2013. Current and historical Alberta weather station data viewer. Agriculture and Rural Development, Government of Alberta, Canada. <http://agriculture.alberta.ca/acis/alberta-weather-data-viewer.jsp>. Accessed 26 Aug 2013.
- AgroClimatic Information Service. 2018. Current and historical Alberta weather station data viewer. Agriculture and Rural Development, Government of Alberta, Canada. <https://agriculture.alberta.ca/acis/township-data-viewer.jsp>. Accessed 19 July 2018.
- Alberta Environment. 2010. Guidelines for Reclamation to Forest Vegetation in the Athabasca Oil Sands Region, 2nd edn. Prepared by the Terrestrial Subgroup of the Reclamation Working Group of the Cumulative Environmental Management Association, Fort McMurray, AB. December 2009.
- Alberta Environment and Sustainable Resource Development. 2013. Criteria and Indicators Framework for Oil Sands Mine Reclamation Certification. Fort McMurray, AB. September 18, 2012.
- Badia D, Valero R, Gracia A, Marti C and Molina F. 2007. Ten-year growth of woody species planted in reclaimed mined banks with different slopes. *Arid Land Research and Management*, 21, 67-79
- Beckingham, J.D. and Archibald, J.H. 1996. Field Guide to Ecosistemas of northern Alberta. Edmonton, AB: Canadian Forest Service, Northwest Region, Northern Forestry Centre. Special Report 5. [ISBN 0-660-16369-1]
- Bladon, K.D., Silins, U. Landhäusser, S.M. & Lieffers, V.J. 2006. Differential transpiration by three boreal tree species in response to increased evaporative demand after variable retention harvesting. *Agricultural and Forest Meteorology*, 138, 104-119.
- Bockstette S.W., Pinno B.D., Dyck M.F., and Landhäusser S.M. 2017. Root competition, not soil compaction, restricts access to soil resources for aspen on a reclaimed mine soil. *Botany*. 95:685–695. doi: 10.1139/cjb-2016-0301.
- Borcard, D. and Legendre, P. 2002. All-scale spatial analysis of ecological data by means of principal coordinates of neighbour matrices. *Ecological Modelling* 153: 51–68.
- Borcard, D., Gillet, F. and Legendre, P. 2011. *Numerical Ecology with R*. Springer New York.

- Carey, S.K. 2008. Growing season energy and water exchange from an oil sands overburden reclamation soil cover, Fort McMurray, Alberta, Canada. *Hydrological Processes*, 22, 2847-2857.
- De Caceres, M. and Legendre, P. 2009. Associations between species and group of sites: indices and statistical inference. *Ecology*.90 (12): 3566-3574.
- Dumas, J.B.A. 1831. Procédés de l'Analyse Organique. *Annals de Chimie et Physique*. 247:198–213.
- Environment Canada. December 2015. Monthly Climate Summaries. Retrieved from http://climate.weather.gc.ca/prods_servs/cdn_climate_summary_e.html.
- Environmental Systems Research Institute (ESRI). 2014. ArcGIS Release 10.2.2. Redlands, CA.
- Fair J.M. (2011). The potential of forest floor transfer for the reclamation of boreal forest understory communities. M.Sc. thesis 140p.
- Grace J.B., Anderson T.M., Olff H., and Scheiner S.M. 2010. On the specification of structural equation models for ecological systems. *Ecology Monographs*. 80:67–87. doi: 10.1890/09-0464.1.
- Grace J.B., and Bollen K.A. 2007. Representing general theoretical concepts in structural equation models: the role of composite variables. *Environmental and Ecological Statistics*. 15:191–213. doi: 10.1007/s10651-007-0047-7.
- Grace, J.B., Schoolmaster, D.R., Guntensergen, G.R., Little, A.M., Mitchell, B.R., Miller, K.M., and Schweiger, E.W. 2012. Guidelines for a graph-theoretic implementation of structural equation modeling. *Ecosphere* 3(73). doi: 10.1890/ES12-00048.1
- Hill, M. O. 1973. Diversity and evenness: a unifying notation and its consequences. *Ecology*. 54(2): 427-432.
- Huang, M., Barbour, S.L., Elshorbagy, A., Zettl, J.D. and Si, B.C. 2011. Water availability and forest growth in coarse-textured soils. *Canadian Journal of Soil Science*. 91, 199-210.
- Laclau J-P., da Silva E.A., Rodrigues Lambais G., Bernoux, M., le Maire, G., Stape, J.L., Bouillet, J-P., de Moraes Goncalves, J.L., Jourdan, C., and Nouvellon, Y. 2013. Dynamics of soil exploration by fine roots down to a depth of 10 m throughout the entire rotation in *Eucalyptus grandis* plantations. *Frontiers in Plant Science*. 4(243). doi: 10.3389/fpls.2013.00243.

- Landhäusser S.M., B.D. Pinno, V.J. Lieffers, and Chow, P.S. 2012a. Partitioning of carbon allocation to reserves or growth determines future performance of aspen seedlings. *Forest Ecology and Management*. 275: 43-51.
- Landhäusser S.M., Rodriguez-Alvarez J., Marenholtz E.H., Lieffers V.J. 2012b. Effect of stock type characteristics and time of planting on field performance of aspen (*Populus tremuloides* Michx.) seedlings on boreal reclamation sites. *New Forests*. 43:679–693. doi: 10.1007/s11056-012-9346-4.
- Landhäusser, S.M., and Lieffers, V.J. 1998. Growth of *Populus tremuloides* in association with *Calamagrostis canadensis*. *Canadian Journal of Forest Research* 28, 396-401.
- Lee S-Y. 2007. *Structural Equation Modeling: A Bayesian Approach*, 1st edn. John Wiley & Sons, Inc., Chichester, England.
- Legendre, P., Borcard, D., Blanchet, F.G. and Dray S. 2013. PCNM: MEM spatial eigenfunction and principal coordinate analyses. R package version 2.1-2/r109. <http://R-Forge.R-project.org/projects/sedar/>.
- Littell, R.C., Milliken, G.A., Stroup, W.W., Wolfinger, R.D., and Schabenberger, O. 2006. *SAS for mixed models*, 2nd ed. SAS Institute Inc., Cary, NC.
- Lunn D.J., Thomas A., Best N., and Spiegelhalter D. 2000. WinBUGS - A Bayesian modelling framework: Concepts, structure, and extensibility. *Statistical Computing*. 10:325–337. doi: 10.1023/A:1008929526011.
- Macdonald SE, Quideau SA, and Landhäusser SM. 2012. Rebuilding boreal forest ecosystems after industrial disturbance (pp123-161). In: Vitt D & Bhatti J, *Restoration and Reclamation of Boreal Ecosystems, Attaining Sustainable Development*. Cambridge University Press pp 424 ISBN:9781107015715
- Mackenzie, D.D. 2006. *Assisted Natural Recovery Using a Forest Soil Propagule Bank in the Athabasca Oil Sands*. M.Sc. thesis, Department of Renewable Resources, University of Alberta, Edmonton, Alberta, Canada.
- Mackenzie, D.D. and Naeth, M.A. 2010. The Role of the Forest Soil Propagule Bank in Assisted Natural Recovery after Oil Sands Mining. *Restoration Ecology* 18(4): 418–427.
- Maechler, M., Rousseeuw, P., Struyf, A., Hubert, M. and Hornik, K. 2014. *Cluster: Cluster Analysis Basics and Extensions*. R package version 1.15.3.

- Maundrell, C. & Hawkins, C. (2004). Use of an aspen overstory to control understory herbaceous species, bluejoint grass (*Calamagrostis canadensis*), and Fireweed (*Epilobium angustifolium*). *Northern Journal of Applied Forestry*, 21, 74-79.
- Marshall, P. L., Davis, G., and LeMay, V. M. 2000. Using line intersect sampling for coarse woody debris. [Research Section], Vancouver Forest Region.
- McCune B, and Keon D. 2002. Equations for potential annual direct incident radiation and heat load. *Journal of Vegetation Science* 13:603–606. doi: 10.1111/j.1654-1103.2002.tb02087.x.
- Miller, J.K. and Farr, S.D. 1971. Bimultivariate redundancy: A comprehensive measure of interbattery relationship. *Multivariate Behavioral Research*. 6(3): 313-324. doi: 10.1207/s15327906mbr0603_4.
- Milliken, G.A., and Johnson, D.E. 2001. Analysis of covariance models with heterogeneous errors. In: *Analysis of messy data volume III: analysis of covariance*. Chapman and Hall, London.
- Moss, E.H. 1983. *Flora of Alberta*. In 2nd Edi. University of Toronto Press, Scholarly Publishing Division, Toronto, ON.
- Natural Resources Canada. 2008. Canada's National Forest Inventory ground sampling guidelines: specifications for ongoing measurement. Canadian Forest Service, Pacific Forestry Centre, Victoria, BC
- Oksanen, J., Blanchet F.G., Kindt, R., Legendre, P., Minchin, P.R., O'Hara, R.B., Simpson, G.L., Solymos, P., Henry, M., Stevens, H. and Wagner, H. 2015. *vegan: Community Ecology Package*. R package version 2.2-1. <http://CRAN.R-project.org/package=vegan>.
- Pollard, J., McKenna, G. T., Fair, J., Daly, C., Wytrykush, C. and Clark, J. 2012. Design aspects of two fen wetlands constructed for reclamation research in the Athabasca oil sands. *Mine Closure*. 815-829.
- R Core Team. 2014. *R: A language and environment for statistical computing*. R Foundation for Statistical Computing, Vienna, Austria. URL <http://www.R-project.org/>.
- R Development Core Team. 2015. *R: A Language and Environment for Statistical Computing*, Vienna, Austria. URL <http://www.R-project.org/>.

- Schott KM, Karst J, and Landhäusser SM. 2014. The role of microsite conditions in restoring trembling aspen (*Populus tremuloides* Michx) from seed. *Restoration Ecology* 22: 292-295.
- Soil Classification Working Group. 1998. The Canadian System of Soil Classification. Agriculture. and Agri-Food Canada. Publ. 1646 (Revised). 187 pp.
- Sturtz S, Ligges U, Gelman A. 2005. R2WinBUGS: A Package for Running WinBUGS from R.
- Syncrude Canada Ltd. 2014. Sandhill Fen – 2013 Soil Sampling Program Report. Prepared by NorthWind Land Resources Inc. for Syncrude Canada Ltd. (Project number 13-328).
- USDA. 2016. Welcome to the PLANTS Database| USDA PLANTS.
<http://plants.usda.gov/java/>.
- Van Wagner, C. E. 1982. Practical aspects of the line intersect method (Vol. 12). Chalk River, Canada: Petawawa National Forestry Institute.
- Wytrykush C, Vitt DH, McKenna G, and Vassov R. 2012. Designing landscapes to support peatland development on soft tailings deposits: Syncrude Canada Ltd's Sandhill Fen Research Watershed initiative (pp 161–178). In: Vitt D, Bhatti J (eds) *Restoration and Reclamation of Boreal Ecosystems - Attaining Sustainable Development*. Cambridge University Press, Cambridge, UK.

Appendix A: Supplemental material for seedling growth response to planting density and site conditions, and identifying drivers and dynamics of these responses (Part I)

Figure A.1: Code for the 2013 total height SEM on jack pine seedlings on the coarse-textured soil. Used with the statistical software R (R Development Core Team 2015) and WinBUGS (Lunn et al. 2000).

```

sink("MODEL2013_JP.txt")
cat("
MODEL LR1 {
# Likelihoods
for(i in 1:N) {
vegcover[i] ~ dbin(vegcoverp.hat[i], n.vegcover)
logit(vegcoverp.hat[i]) <- b2.0 + b2.4*K[i] + b2.6*moss[i]
tN[i] ~ dnorm(tNp.hat[i], tau.tN)
tNp.hat[i] <- b3.0 + b3.1*K[i] + b3.3*cwdf[i] + b3.4*totN[i]
tK[i] ~ dnorm(tKp.hat[i], tau.tK)
tKp.hat[i] <- b4.0 + b4.3*cwdf[i] + b4.4*HLI[i]
height[i] ~ dnorm(heightp.hat[i], tau.height)
heightp.hat[i] <- b6.0 + b6.1*tN[i]
}
# Priors
b2.0 ~ dnorm(0, 0.00001); b2.4 ~ dnorm(0, 0.00001); b2.6 ~ dnorm(0, 0.00001);
b3.0 ~ dnorm(0, 0.00001); b3.1 ~ dnorm(0, 0.00001); b3.3 ~ dnorm(0, 0.00001);
b3.4 ~ dnorm(0, 0.00001);
tau.tN ~ dgamma(0.001, 0.001);
b4.0 ~ dnorm(0, 0.00001); b4.3 ~ dnorm(0, 0.00001); b4.4 ~ dnorm(0, 0.00001);
tau.tK ~ dgamma(0.001, 0.001);
b6.0 ~ dnorm(0, 0.00001); b6.1 ~ dnorm(0, 0.00001);
tau.height ~ dgamma(0.001, 0.001);
}", fill = T)
sink()

N=36; n.vegcover=100;
data= list("N", "n.vegcover", "K", "moss",
"totN", "vegcover", "tK", "cwdf", "HLI",
"tN", "height")
parameters <- c("b2.0", "b2.4", "b2.6",
"b3.0", "b3.1", "b3.3", "b3.4",
"b4.0", "b4.3", "b4.4",

```

```
"b6.0", "b6.1")
inits <- function(){list(b2.0 = 0, b2.4 = 0, b2.6 = 0,
  b3.0 = 0, b3.1 = 0, b3.3 = 0, b3.4 = 0,
  tau.tN = 100,
  b4.0 = 0, b4.3 = 0, b4.4 = 0,
  tau.tK = 100,
  b6.0 = 0, b6.1 = 0,
  tau.height = 100)}

# MCMC settings
nc <- 3 # number of chains
ni <- 500000 # number of samples for each
nb <- 100000 # number of samples to discard for burn in
nt <- 50 # thinning rate

MODEL2013_JP.out <- bugs(data, inits, parameters.to.save=parameters,
model.file="MODEL2013_JP.txt", n.chains=nc, n.iter=ni, n.burnin=nb, n.thin=nt,
debug=TRUE, DIC=TRUE, working.directory = getwd(), bugs.directory =
'c:/WinBUGS14')
```

Figure A.2: Code for the 2013 total height SEM on jack pine seedlings on the coarse-textured soil. Used with the statistical software R (R Development Core Team 2015) and WinBUGS (Lunn et al. 2000).

```

sink("MODEL2016_JP.txt")
cat("
MODEL LR1 {
# Likelihoods
for(i in 1:N) {
WP20[i] ~ dnorm(WP20p.hat[i], tau.WP20)
WP20p.hat[i] <- b1.0 + b1.1*height[i] + b1.2*vegcover[i] + b1.3*moss[i]
vegcover[i] ~ dbin(vegcoverp.hat[i], n.vegcover)
logit(vegcoverp.hat[i]) <- b2.0 + b2.2*K[i] + b2.3*moss[i] + b2.4*cwdf[i]
tP[i] ~ dnorm(tPp.hat[i], tau.tP)
tPp.hat[i] <- b3.0 + b3.1*K[i] + b3.2*cwdf[i]
tK[i] ~ dnorm(tKp.hat[i], tau.tK)
tKp.hat[i] <- b4.0 + b4.2*cwdf[i] + b4.3*HLI[i]
height[i] ~ dnorm(heightp.hat[i], tau.height)
heightp.hat[i] <- b6.0 + b6.1*tK[i] + b6.2*K[i] + b6.3*cwdf[i]
}
# Priors
b1.0 ~ dnorm(0, 0.00001); b1.1 ~ dnorm(0, 0.00001); b1.2 ~ dnorm(0, 0.00001);
b1.3 ~ dnorm(0, 0.00001);
tau.WP20 ~ dgamma(0.001, 0.001);
b2.0 ~ dnorm(0, 0.00001); b2.2 ~ dnorm(0, 0.00001); b2.3 ~ dnorm(0, 0.00001);
b2.4 ~ dnorm(0, 0.00001);
b4.0 ~ dnorm(0, 0.00001); b4.2 ~ dnorm(0, 0.00001); b4.3 ~ dnorm(0, 0.00001);
tau.tK ~ dgamma(0.001, 0.001);
b3.0 ~ dnorm(0, 0.00001); b3.1 ~ dnorm(0, 0.00001); b3.2 ~ dnorm(0, 0.00001);
tau.tP ~ dgamma(0.001, 0.001);
b6.0 ~ dnorm(0, 0.00001); b6.1 ~ dnorm(0, 0.00001); b6.2 ~ dnorm(0, 0.00001);
b6.3 ~ dnorm(0, 0.00001);
tau.height ~ dgamma(0.001, 0.001);
}", fill = T)
sink()

N=36; n.vegcover=100;
data = list("N", "n.vegcover", "moss", "WP20", "tP", "HLI", "vegcover", "tK",
"cwdf", "K", "height")
parameters <- c("b1.0", "b1.1", "b1.2", "b1.3",
"b2.0", "b2.2", "b2.3", "b2.4",
"b4.0", "b4.2", "b4.3",

```

```
"b3.0", "b3.2", "b3.1",
"b6.0", "b6.1", "b6.2", "b6.3")
inits <- function(){list(b1.0 = 0, b1.1 = 0, b1.2 = 0, b1.3 = 0,
tau.WP20 = 100,
b2.0 = 0, b2.2 = 0, b2.3 = 0, b2.4 = 0,
b3.0 = 0, b3.2 = 0, b3.1 = 0,
tau.tP = 100,
b4.0 = 0, b4.2 = 0, b4.3 = 0,
tau.tK = 100,
b6.0 = 0, b6.1 = 0, b6.2 = 0, b6.3 = 0,
tau.height = 100)}
# MCMC settings
nc <- 3 # number of chains
ni <- 500000 # number of samples for each chain
nb <- 100000 # number of samples to discard for burn in
nt <- 50 # thinning rate

MODEL2016_JP.out <- bugs(data, inits, parameters.to.save=parameters,
model.file="MODEL2016_JP.txt", n.chains=nc, n.iter=ni, n.burn=n.nb, n.thin=nt,
debug=TRUE, DIC=TRUE, working.directory = getwd(), bugs.directory
= 'c:/WinBUGS14')
```

Appendix B: Supplemental material for evaluating jack pine seedling characteristics in response to aspect and hydrogel amendment (Project 1)

Table B.1: Range of soil measures of forest floor material taken from north and south-facing hummocks in close proximity to plots. Soil samples were taken by NorthWind Land Resources Inc. and sent to Exova Laboratories in Edmonton, AB, Canada for analysis

Variable	Unit	Aspect	
		North-facing	South-facing
Available NO ₃ ⁻	µg g ⁻¹	<2	<2
Available NH ₄ ⁺	µg g ⁻¹	<0.3-0.6	<0.3-1
Available P	µg g ⁻¹	9-10	8-18
Available K	µg g ⁻¹	32-56	<25-55
C:N		20	17-20
Total organic C	% dry weight	1.53-1.76	1.3-2
Total N	% dry weight	0.07-0.08	0.07-1
Texture		sand	sand
Sand	% dry weight	88.8-90.8	89.6-94
Silt	% dry weight	5.4-7.2	4.6-9
Clay	% dry weight	3.8-4	<0.1-2.6
pH		6.4-7.2	5.5-6.9

Table B.2: Aspect, slope, and location of different hydrogel (H), North-facing (N), and South-facing (S) plots.

Plot	Aspect ($^{\circ}$)	Slope ($^{\circ}$)	UTM N	UTM W
H1*	192	32	57 02.503	111 35.355
H2*	177	19	57 02.477	111 35.562
H3*	210	19	57 02.478	111 35.583
H4	221	22	57 02.480	111 35.590
H5*	139	25	57 02.412	111 35.883
H6	144	26	57 02.410	111 35.889
H7*	150	22	57 02.407	111 35.896
H8*	160	23	57 02.401	111 35.912
H9	150	24	57 02.399	111 35.918
H10*	147	20	57 02.397	111 35.922
N1*	33	22	57 02.405	111 35.712
N2	33	23	57 02.404	111 35.712
N3*	33	23	57 02.400	111 35.710
N4*	32	24	57 02.400	111 35.705
N5*	32	24	57 02.400	111 35.706
N6*	37	22	57 02.399	111 35.702
N7	38	23	57 02.397	111 35.697
N8*	38	21	57 02.396	111 35.694
N9	39	26	57 02.395	111 35.692
N10*	39	22	57 02.392	111 35.689
S1*	188	27	57 02.504	111 35.351
S2*	171	15	57 02.475	111 35.560
S3*	208	18	57 02.479	111 35.581
S4	210	23	57 02.479	111 35.587
S5*	135	24	57 02.414	111 35.880
S6	140	21	57 02.411	111 35.885
S7*	149	24	57 02.409	111 35.892
S8*	158	20	57 02.402	111 35.908
S9	151	22	57 02.399	111 35.914
S10*	149	19	57 02.398	111 35.921

*Plots that had 5TM soil moisture and MPS-2 dielectric water potential sensor probes

Appendix C: Supplemental material for factors and drivers affecting early colonizing vegetation development on reclaimed boreal upland sites (Part II)

Table C.1: Mean height (cm) of tree seedlings of three species (*Populus tremuloides*, *Pinus banksiana*, *Picea glauca*) in areas capped with the two coversoil materials in 2012, 2013 and 2014 (seedling height was not measured in 2015).

(a) Coarse-textured coversoil

Species	2012	2013	2014
<i>Populus tremuloides</i>	36.63	39.43	44.94
<i>Pinus banksiana</i>	25.96	31.60	46.93
<i>Picea glauca</i>	29.83	33.50	32.53

(b) Fine-textured coversoil

Species	2012	2013	2014
<i>Populus tremuloides</i>	34.37	65.59	89.63
<i>Pinus banksiana</i>	22.34	39.81	76.44
<i>Picea glauca</i>	29.03	32.54	45.65

Table C.2: Species found at the Sandhill Watershed and W1 Dump research sites, including areas capped with coversoil from poor-xeric and rich-mesic sites. Species were identified and classified according to original range (native or introduced) and functional type (Tree, Shrub, Forb, Graminoid or Non-vascular) according to Moss (1983) and USDA (2016).

Species	Original Range	Functional Type
<i>Achillea millefolium</i> L.	Native	Forb
<i>Achillea sibirica</i> Ledeb.	Native	Forb
<i>Actaea rubra</i> (Ait) Willd.	Native	Forb
<i>Agropyron trachycaulum</i> var. <i>glaucum</i> (Pease & Moore) Matte	Native	Graminoid
<i>Agropyron trachycaulum</i> var. <i>trachycaulum</i> (Link) Malte	Native	Graminoid
<i>Agropyron trachycaulum</i> var. <i>unilaterale</i> (Cassidy) Malte	Native	Graminoid
<i>Agrostis scabra</i> Willd.	Native	Graminoid
<i>Alnus crispa</i> (Ait) Pursh	Native	Shrub

<i>Alnus tenuifolia</i> Nutt.	Native	Shrub
<i>Alopecurus aequalis</i> Sobol.	Native	Graminoid
<i>Amelanchier alnifolia</i> Nutt.	Native	Shrub
<i>Apocynum androsaemifolium</i> L.	Native	Forb
<i>Apocynum cannabinum</i> L.	Native	Forb
<i>Aquilegia brevistyla</i> Hook.	Native	Forb
<i>Arabis lyrata</i> ssp. <i>kamchatica</i> (Fisch.) Hult.	Native	Forb
<i>Aralia nudicaulis</i> L.	Native	Forb
<i>Arctostaphylos uva-ursi</i> (L.) Spreng.	Native	Shrub
<i>Arnica chamissonis</i> Less.	Native	Forb
<i>Aster ciliolatus</i> Lindl.	Native	Forb
<i>Aster puniceus</i> L.	Native	Forb
<i>Aster</i> sp. L.	Native	Forb
<i>Astragalus canadensis</i> L.	Native	Forb
<i>Astragalus cicer</i> L.	Introduced	Forb
<i>Astragalus</i> sp. L.	Native	Forb
<i>Aulacomnium palustre</i> (Hedw.) Schwaegr.	Native	Non-vascular
<i>Beckmannia syzigachne</i> (Steud.) Fern.	Native	Graminoid
<i>Betula papyrifera</i> Marsh.	Native	Tree
<i>Betula pumila</i> L.	Native	Shrub
<i>Bidens cernua</i> L.	Native	Forb
<i>Brachythecium</i> sp. BSG.	Native	Non-vascular
<i>Bromus ciliatus</i> L.	Native	Graminoid
<i>Bromus inermis</i> Leyss.	Introduced	Graminoid
<i>Bromus</i> sp. L.	Native	Graminoid
<i>Bryum argenteum</i> Hedw.	Native	Non-vascular
<i>Calamagrostis canadensis</i> spp. <i>canadensis</i> (Michx.) Beauv.	Native	Graminoid
<i>Calamagrostis inexpansa</i> A. Gray	Native	Graminoid
<i>Campanula rotundifolia</i> L.	Native	Forb
<i>Carex aenea</i> Fern.	Native	Graminoid
<i>Carex atherodes</i> Spreng.	Native	Graminoid
<i>Carex aurea</i> Nutt.	Native	Graminoid
<i>Carex bebbii</i> Olney ex. Fern.	Native	Graminoid
<i>Carex deflexa</i> Hornem.	Native	Graminoid

<i>Carex lasiocarpa</i> Ehrh.	Native	Graminoid
<i>Carex praticola</i> Ryed.	Native	Graminoid
<i>Carex rossii</i> Boott.	Native	Graminoid
<i>Carex rostrata</i> Stokes	Native	Graminoid
<i>Carex siccata</i> Dewey	Native	Graminoid
<i>Carex</i> spp. L.	Native	Graminoid
<i>Carex trisperma</i> Dewey	Native	Graminoid
<i>Carex umbellata</i> Schk.	Native	Graminoid
<i>Ceratodon purpureus</i> (Hedw.) Brid.	Native	Non-vascular
<i>Chamaesaracha grandifolia</i> (Hook.) Fern.	Native	Forb
<i>Chenopodium album</i> L. (berlandieri)	Introduced	Forb
<i>Chenopodium capitatum</i> (L.) Aschers.	Native	Forb
<i>Chenopodium gigantospermum</i> Aellen	Native	Forb
<i>Chenopodium rubrum</i> L.	Native	Forb
<i>Cirsium arvense</i> (L.) Scop.	Introduced	Forb
<i>Cladonia mitis</i> Sandst.	Native	Non-vascular
<i>Cladonia</i> sp. P. Browne	Native	Non-vascular
<i>Comandra umbellata</i> (L.) Nutt.	Native	Forb
<i>Cornus canadensis</i> L.	Native	Forb
<i>Cornus stolonifera</i> Michx.	Native	Shrub
<i>Corydalis aurea</i> Willd.	Native	Forb
<i>Corydalis sempervirens</i> (L.) Pers.	Native	Forb
<i>Corylus cornuta</i> Marsh.	Native	Shrub
<i>Crepis tectorum</i> L.	Introduced	Forb
<i>Danthonia spicata</i> (L.) Beauv.	Native	Graminoid
<i>Dicranum</i> sp. Hedw.	Native	Non-vascular
<i>Dracocephalum parviflorum</i> Nutt.	Native	Forb
<i>Drepanocladus uncinatus</i> (Hedw.) Warnst.	Native	Non-vascular
<i>Elymus canadensis</i> L.	Native	Graminoid
<i>Elymus innovatus</i> ssp. <i>Innovatus</i> Beal.	Native	Graminoid
<i>Epilobium angustifolium</i> L.	Native	Forb
<i>Epilobium ciliatum</i> Raf.	Native	Forb
<i>Equisetum arvense</i> L.	Native	Forb
<i>Equisetum hymale</i> L.	Native	Forb
<i>Equisetum pratense</i> Ehrh.	Native	Forb

<i>Equisetum scirpoides</i> Michx.	Native	Forb
<i>Equisetum sylvaticum</i> L.	Native	Forb
<i>Equisetum variegatum</i> Schleich.	Native	Forb
<i>Erigeron canadensis</i> L.	Native	Forb
<i>Erysimum cheiranthoides</i> L. ssp. <i>Altum</i> Ahti.	Introduced	Forb
<i>Festuca rubra</i> L.	Native	Graminoid
<i>Festuca saximontana</i> Rydb.	Native	Graminoid
<i>Fragaria vesca</i> L.	Native	Forb
<i>Fragaria virginiana</i> Duchesne	Native	Forb
<i>Fumaria hygrometrica</i> Hedw.	Native	Forb
<i>Galeopsis tetrahit</i> L.	Introduced	Forb
<i>Galium aparine</i> L.	Native	Forb
<i>Galium boreale</i> L.	Native	Forb
<i>Galium trifidum</i> L.	Native	Forb
<i>Galium triflorum</i> Michx.	Native	Forb
<i>Geranium bicknellii</i> Britt.	Native	Forb
<i>Geum aleppicum</i> Jacq.	Native	Forb
<i>Geum macrophyllum</i> Willd.	Native	Forb
<i>Glyceria pulchella</i> (Nash) K. Schum	Native	Graminoid
<i>Halenia deflexa</i> (Sm.) Griseb.	Native	Forb
<i>Hieracium umbellatum</i> L.	Native	Forb
<i>Hierochloe odorata</i> (L.) Beauv.	Native	Graminoid
<i>Hippophae rhamnoides</i> L.	Introduced	Forb
<i>Hordeum jubatum</i> L.	Native	Graminoid
<i>Hylocomium splendens</i> (Hedw.) BSG	Native	Non-vascular
<i>Impatiens capensis</i> Meerb.	Native	Forb
<i>Juncus</i> (c.f.) <i>balticus</i> Willd.	Native	Graminoid
<i>Larix laricina</i> (Du Roi) K. Koch	Native	Tree
<i>Lathyrus ochroleucus</i> Hook.	Native	Forb
<i>Lathyrus venosus</i> Muhl.	Native	Forb
<i>Lepidium densiflorum</i> Schrad.	Introduced	Forb
<i>Lilium philadelphicum</i> L.	Native	Forb
<i>Lonicera dioica</i> L.	Native	Forb
<i>Lotus corniculatus</i> L.	Introduced	Forb
<i>Lysimachia thrysiflora</i> L.	Native	Forb

<i>Maianthemum canadense</i> Desf.	Native	Forb
<i>Matricaria matricarioides</i> (Less.) Porter	Introduced	Forb
<i>Medicago sativa</i> L.	Introduced	Forb
<i>Melilotus alba</i> Desr.	Introduced	Forb
<i>Melilotus officinalis</i> (L.) Lam.	Introduced	Forb
<i>Melilotus</i> sp. Mill.	Introduced	Forb
<i>Mentha arvensis</i> L.	Native	Forb
<i>Mertensia paniculata</i> (Ait.) G. Don	Native	Forb
<i>Moehringia lateriflora</i> (L.) Fenz.	Native	Forb
<i>Oryzopsis asperifolia</i> Michx.	Native	Graminoid
<i>Oryzopsis pungens</i> (Torr.) A.S. Hitchc.	Native	Graminoid
<i>Peltigera</i> sp. Willd.	Native	Non-vascular
<i>Petasites palmatus</i> (Ait) A. Gray	Native	Forb
<i>Petasites sagittatus</i> (Pursh) A. Gray	Native	Forb
<i>Phalaris arundinacea</i> L.	Native	Graminoid
<i>Phleum pratense</i> L.	Introduced	Graminoid
<i>Picea glauca</i> (Moench) Voss	Native	Tree
<i>Pinus banksiana</i> Lamb.	Native	Tree
<i>Plantago major</i> L.	Introduced	Forb
<i>Pleurozium schreberi</i> (Brid.) Mitt.	Native	Non-vascular
<i>Poa palustris</i> L.	Native	Graminoid
<i>Poa pratensis</i> L.	Introduced	Graminoid
<i>Poa</i> sp. L.	Native	Graminoid
<i>Polygonum arenastrum</i> Jord. ex. Bor.	Introduced	Forb
<i>Polygonum convolvulus</i> L.	Introduced	Forb
<i>Polygonum erectum</i> L.	Native	Forb
<i>Polygonum lapathifolium</i> L.	Introduced	Forb
<i>Polygonum</i> spp. L.	Introduced	Forb
<i>Polytrichum juniperinum</i> Hedw.	Native	Non-vascular
<i>Polytrichum pilferum</i> Hedw.	Native	Non-vascular
<i>Populus balsamifera</i> L.	Native	Tree
<i>Populus tremuloides</i> Michx.	Native	Tree
<i>Potentilla norvegica</i> L.	Introduced	Forb
<i>Potentilla tridentata</i> Ait.	Native	Forb
<i>Prunus pensylvanica</i> L.f.	Native	Shrub

<i>Prunus virginiana</i> L.	Native	Shrub
<i>Puccinella pauciflora</i> (Presl.) Munz	Native	Graminoid
<i>Pyrola</i> sp. L.	Native	Forb
<i>Ranunculus abortivus</i> L.	Native	Forb
<i>Ranunculus macounii</i> Britt.	Native	Forb
<i>Ranunculus sceleratus</i> L.	Native	Forb
<i>Ranunculus</i> spp. L.	Native	Forb
<i>Ribes</i> cf. <i>triste</i> Pall.	Native	Shrub
<i>Ribes glandulosum</i> Grauer	Native	Shrub
<i>Ribes lacustre</i> (Pers.) Poir.	Native	Shrub
<i>Ribes oxyacanthoides</i> L.	Native	Shrub
<i>Rorippa palustris</i> ssp. <i>hispida</i> (L.) Besser	Native	Forb
<i>Rosa acicularis</i> Lindl.	Native	Shrub
<i>Rosa woodsii</i> Lindl.	Native	Shrub
<i>Rubus acaulis</i> Michx.	Native	Forb
<i>Rubus arcticus</i> L.	Native	Forb
<i>Rubus idaeus</i> L.	Native	Shrub
<i>Rubus pubescens</i> Raf.	Native	Forb
<i>Salix</i> cf. <i>planifolia</i> Pursh	Native	Shrub
<i>Salix</i> cf. <i>bebbiana</i> Sarg.	Native	Shrub
<i>Salix lucida</i> ssp. <i>lasiandra</i> Muhl. (Benth)	Native	Shrub
<i>Salix</i> sp. L.	Native	Shrub
<i>Salsola kali</i> L.	Introduced	Forb
<i>Schizachne purpurascens</i> ssp. <i>purpurascens</i> (Torr.) Swallen	Native	Graminoid
<i>Scutellaria galericulata</i> L.	Native	Forb
<i>Senecio pauperculus</i> Michx.	Native	Forb
<i>Shepherdia canadensis</i> (L.) Nutt.	Native	Shrub
<i>Sisyrinchium montanum</i> Greene	Native	Forb
<i>Sium suave</i> Walt.	Native	Forb
<i>Solidago canadensis</i> L.	Native	Forb
<i>Solidago</i> sp. L.	Native	Forb
<i>Solidago spathulata</i> DC.	Native	Forb
<i>Sonchus arvensis</i> L.	Introduced	Forb
<i>Sonchus asper</i> L.	Introduced	Forb

<i>Sonchus uliginosus</i> Bieb.	Introduced	Forb
<i>Stachys palustris</i> L.	Introduced	Forb
<i>Stellaria longifolia</i> Muhl.	Native	Forb
<i>Stellaria longipes</i> Goldie.	Native	Forb
<i>Symphoricarpos albus</i> (L.) Blake	Native	Shrub
<i>Symphoricarpos occidentalis</i> Hook.	Native	Shrub
<i>Taraxicum officinale</i> Weber	Introduced	Forb
<i>Tragopogon dubius</i> Scop.	Introduced	Forb
<i>Trientalis borealis</i> Raf.	Native	Forb
<i>Trifolium hybridum</i> L.	Introduced	Forb
<i>Trifolium pratense</i> L.	Introduced	Forb
<i>Trifolium repens</i> L.	Introduced	Forb
<i>Trifolium</i> sp. L.	Introduced	Forb
<i>Typha latifolia</i> L.	Native	Graminoid
<i>Urtica dioica</i> L.	Native	Forb
<i>Vaccinium myrtilloides</i> Michx.	Native	Shrub
<i>Vicia americana</i> Muhl.	Native	Forb
<i>Viola adunca</i> J.E. Smith	Native	Forb
<i>Viola canadensis</i> L.	Native	Forb
Unidentifiable vascular plant sp.		
Unidentifiable moss sp.		

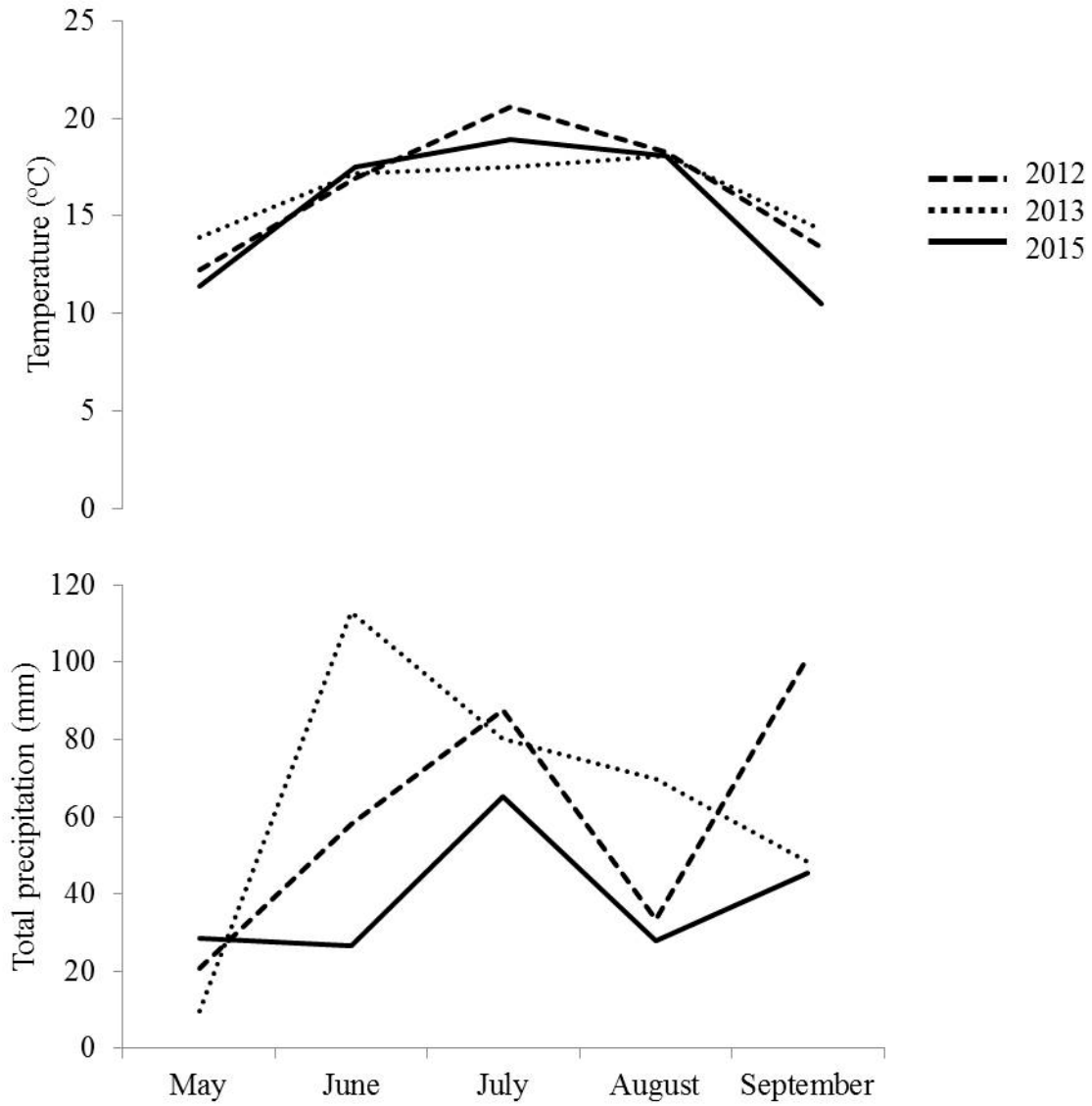


Figure C.1: Growing season (May 1 – September 30) mean monthly temperature (°C) and total monthly precipitation (mm) for 2012, 2013 and 2015, collected at Mildred Lake, Alberta. Data from Environment Canada (2015).

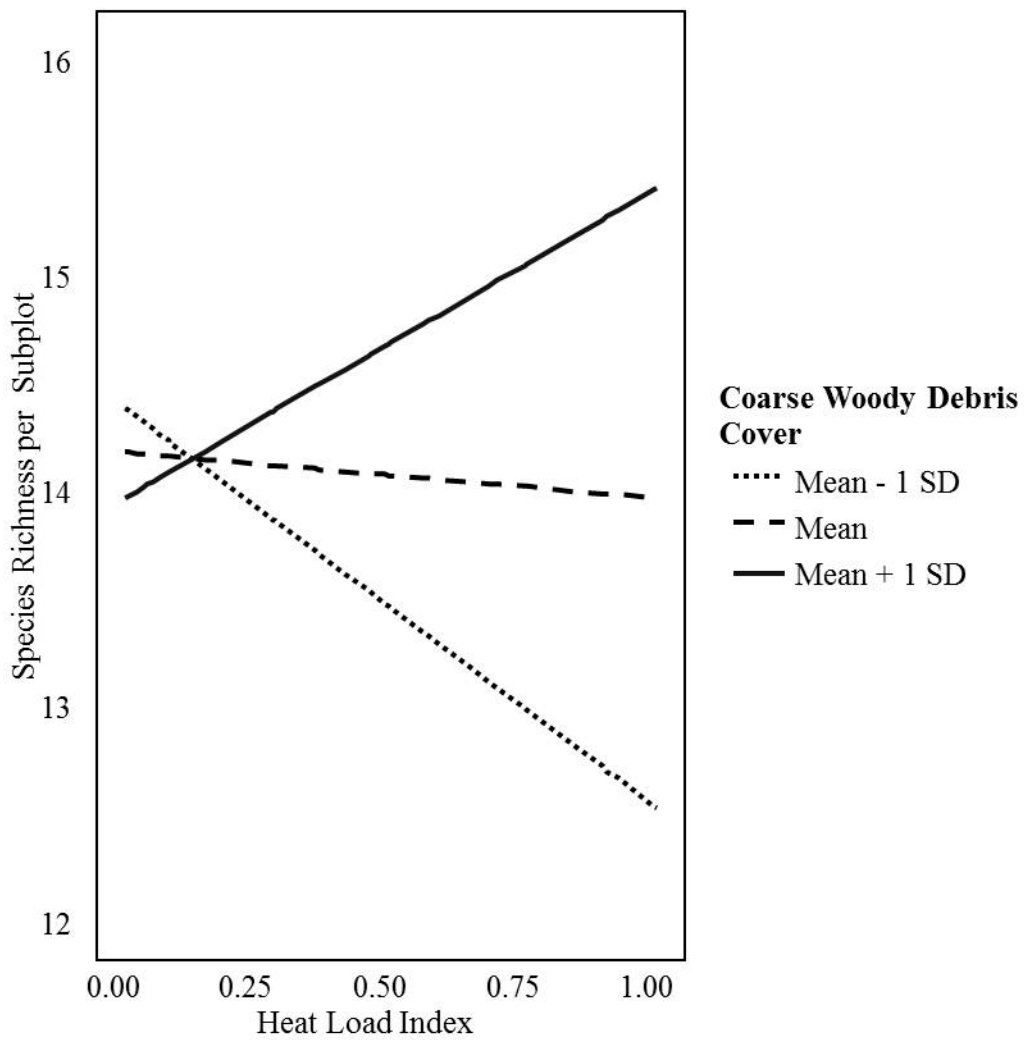


Figure C.2: Interaction of heat load index (HLI; reflecting slope and aspect) and coarse woody debris volume on species richness per vegetation subplot in 2015 in areas reclaimed with coversoil salvaged from a coarse (poor-xeric) site. The influence of HLI on vegetation cover is shown at three levels of coarse woody debris cover (mean, mean – 1 standard deviation and mean + 1 standard deviation). See also Table 2.1.

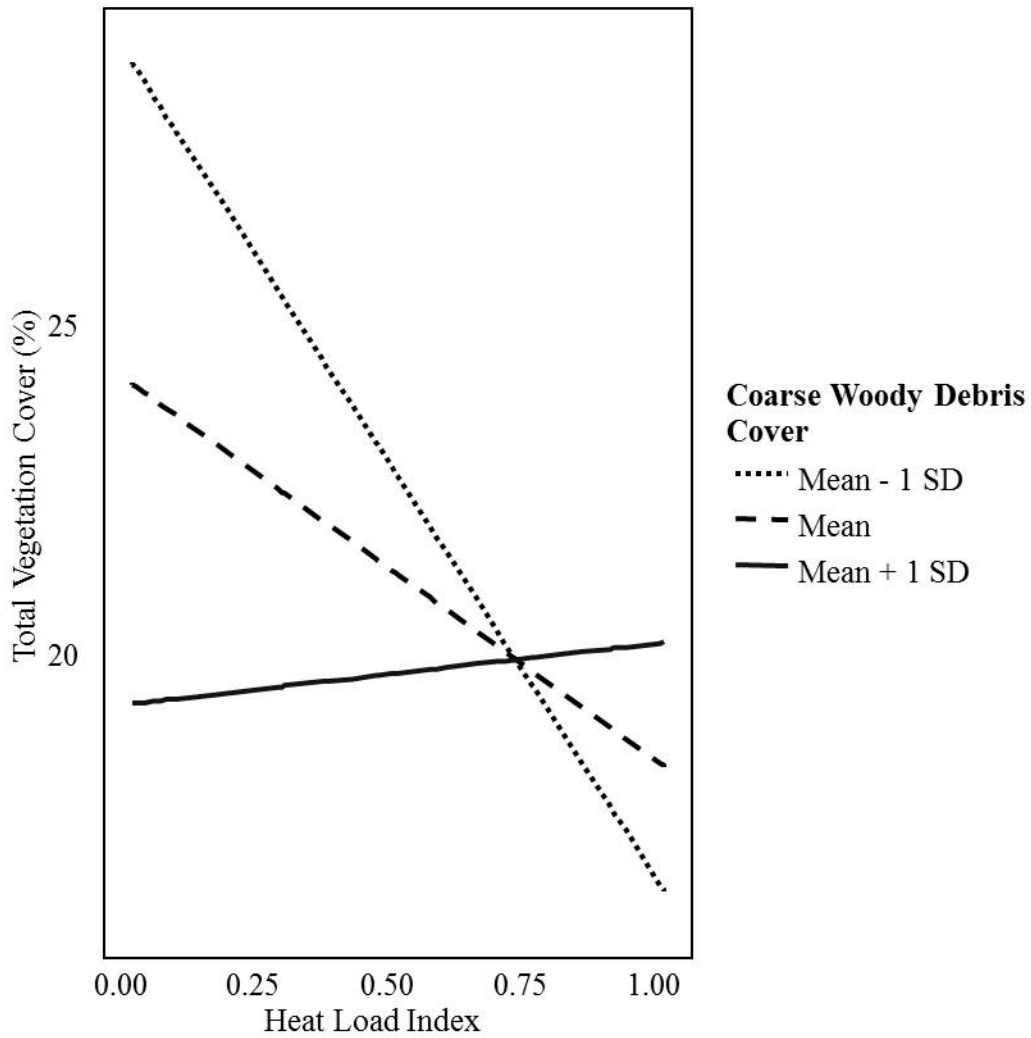


Figure C.3: Interaction of heat load index (HLI; reflecting slope and aspect) and coarse woody debris volume on total vegetation cover (%) in 2013 in areas reclaimed with coversoil salvaged from a coarse (poor-xeric) site. The influence of HLI on vegetation cover is shown at three levels of coarse woody debris cover (mean, mean – 1 standard deviation and mean + 1 standard deviation). See also Table 2.1.

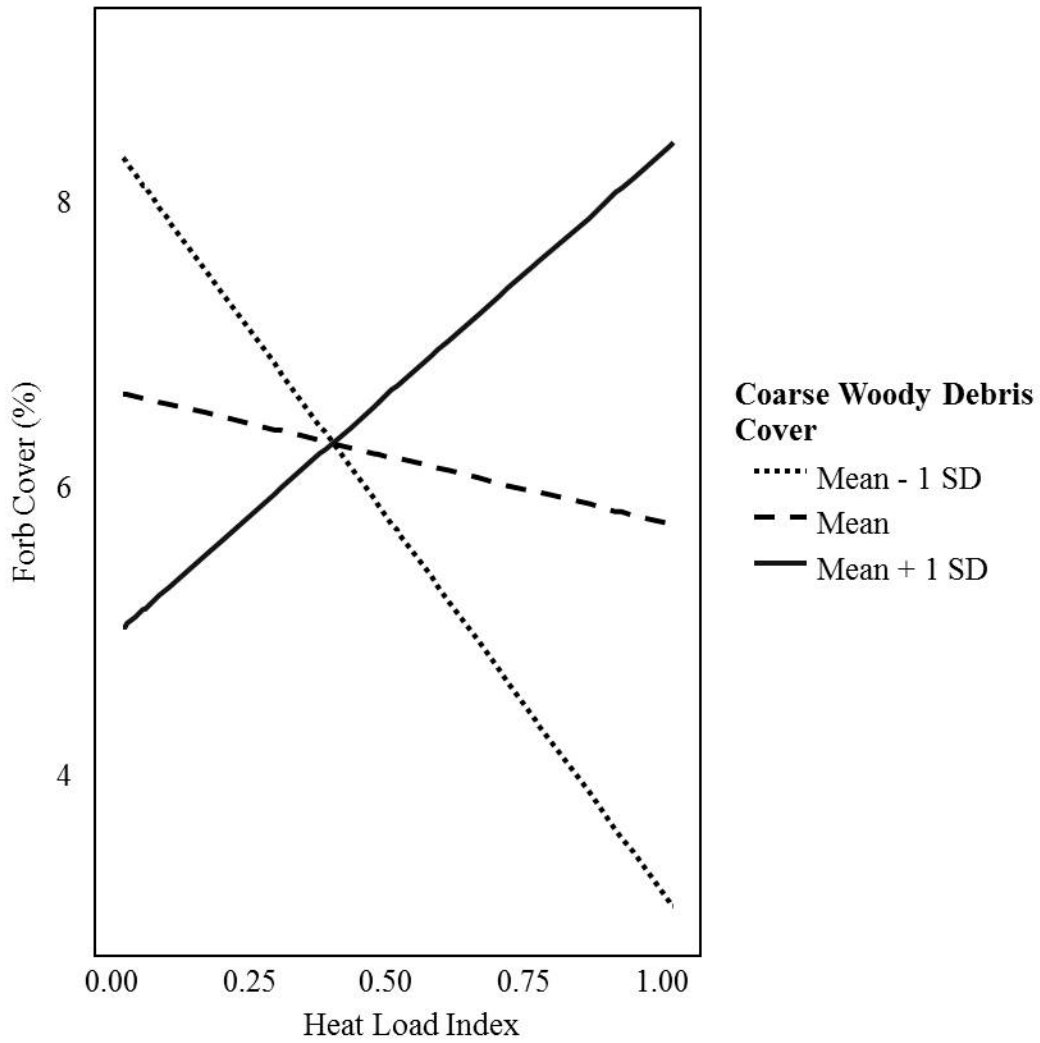


Figure C.4: Interaction of heat load index (HLI; reflecting slope and aspect) and coarse woody debris volume on cover by forb species (%) in 2013 in areas reclaimed with coversoil salvaged from a coarse (poor-xeric) site. The influence of HLI on vegetation cover is shown at three levels of coarse woody debris cover (mean, mean – 1 standard deviation and mean + 1 standard deviation). See also Table 2.1.

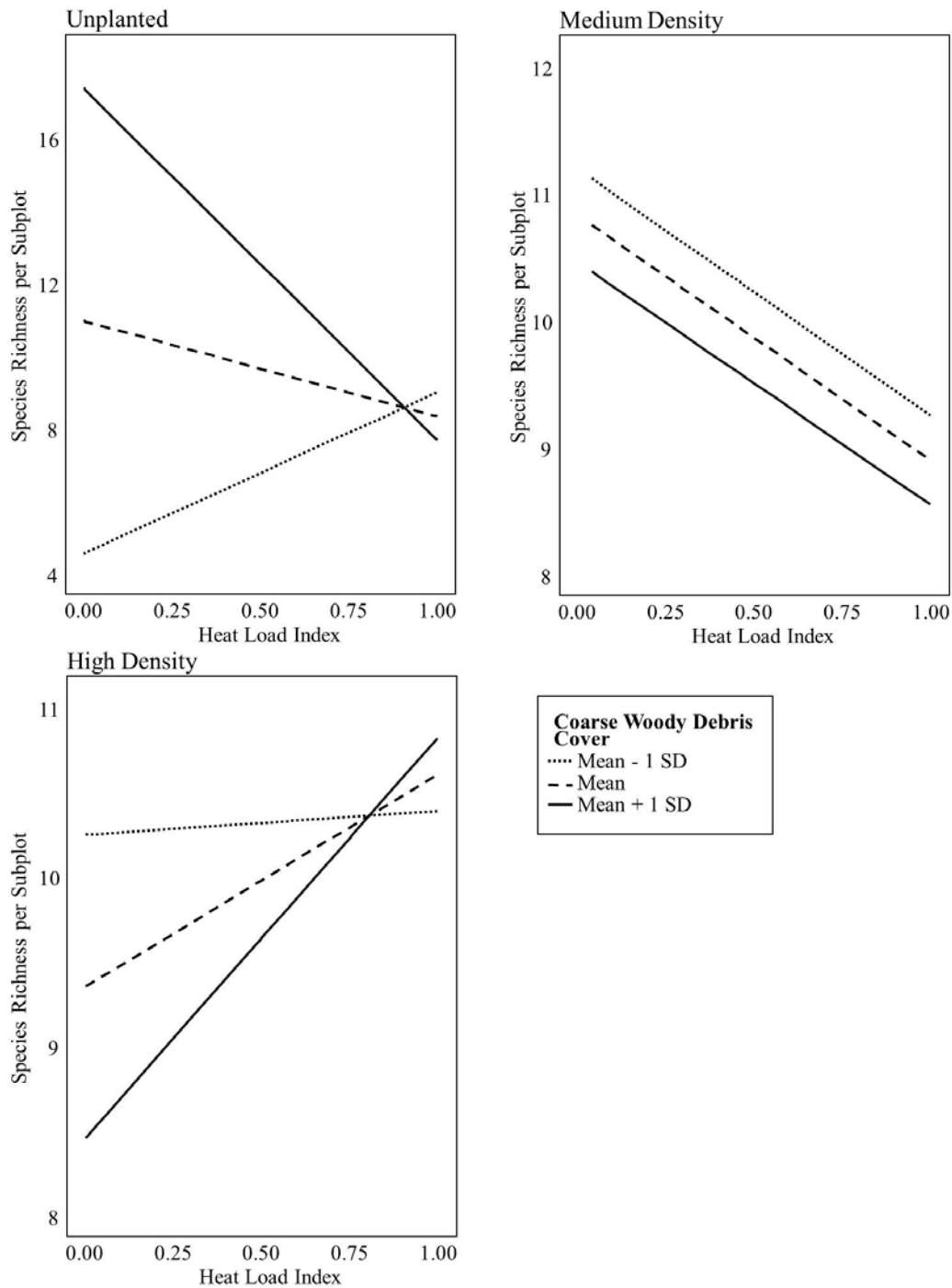


Figure C.5: Interaction of planting density, heat load index (HLI; reflecting slope and aspect) and coarse woody debris volume on species richness per vegetation subplot in 2012 in areas reclaimed with coarse coversoil salvaged from a poor-xeric site. In each of the three planting density treatments (unplanted = 0 stems per hectare (sph), medium density = 5 000 sph, high density = 10 000 sph) the influence of heat load index on species richness is shown at three levels of coarse woody debris cover (mean, mean – 1 standard deviation and mean + 1 standard deviation). See also Table 2.1.

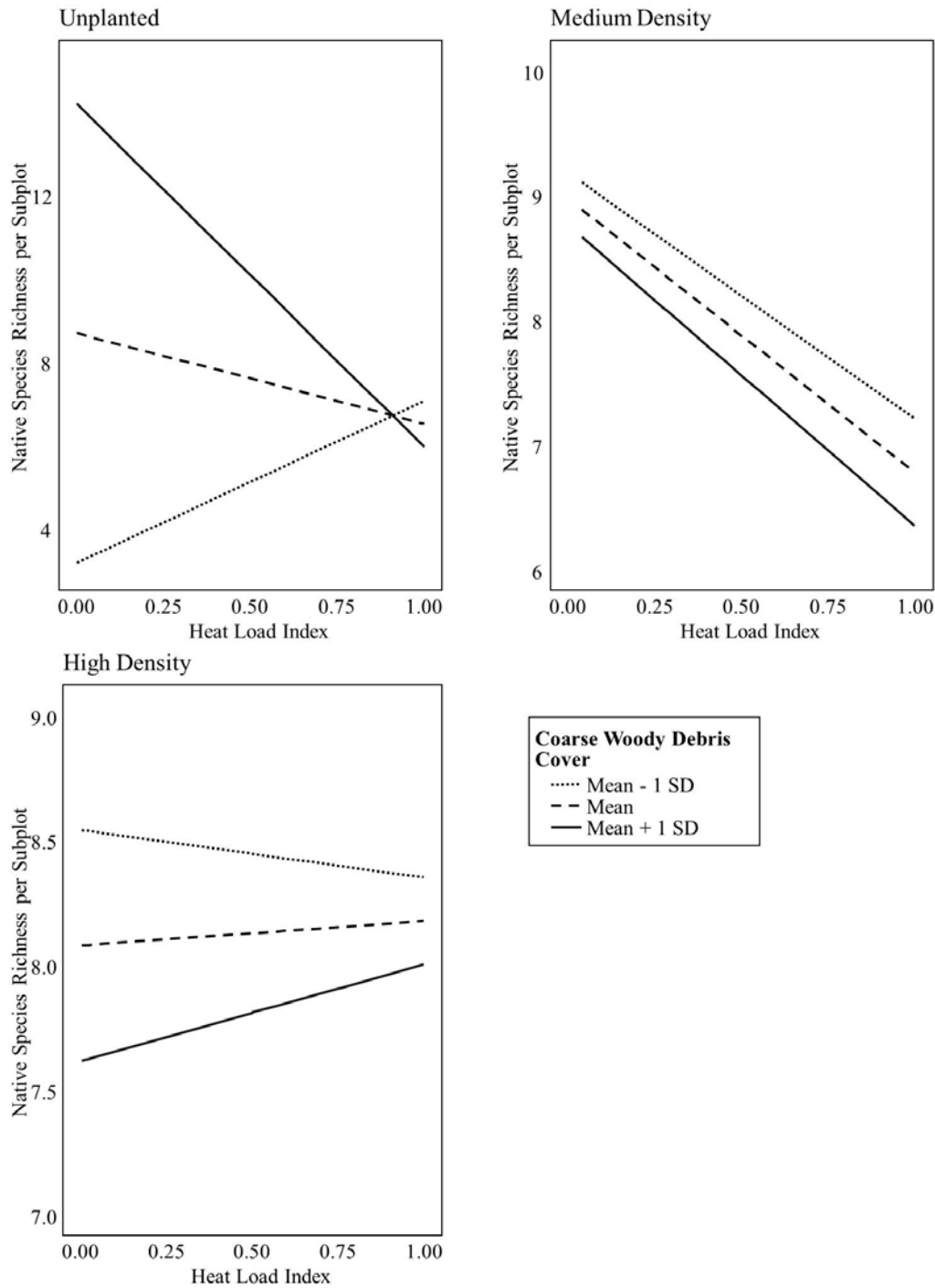


Figure C.6: Interaction of planting density, heat load index (HLI; reflecting slope and aspect) and coarse woody debris volume on native species richness per vegetation subplot in 2012 in areas reclaimed with coarse coversoil salvaged from a poor-xeric site. In each of the three planting density treatments (unplanted = 0 stems per hectare (sph), medium density = 5 000 sph, high density = 10 000 sph) the influence of heat load index on species richness is shown at three levels of coarse woody debris cover (mean, mean – 1 standard deviation and mean + 1 standard deviation). See also Table 2.1.

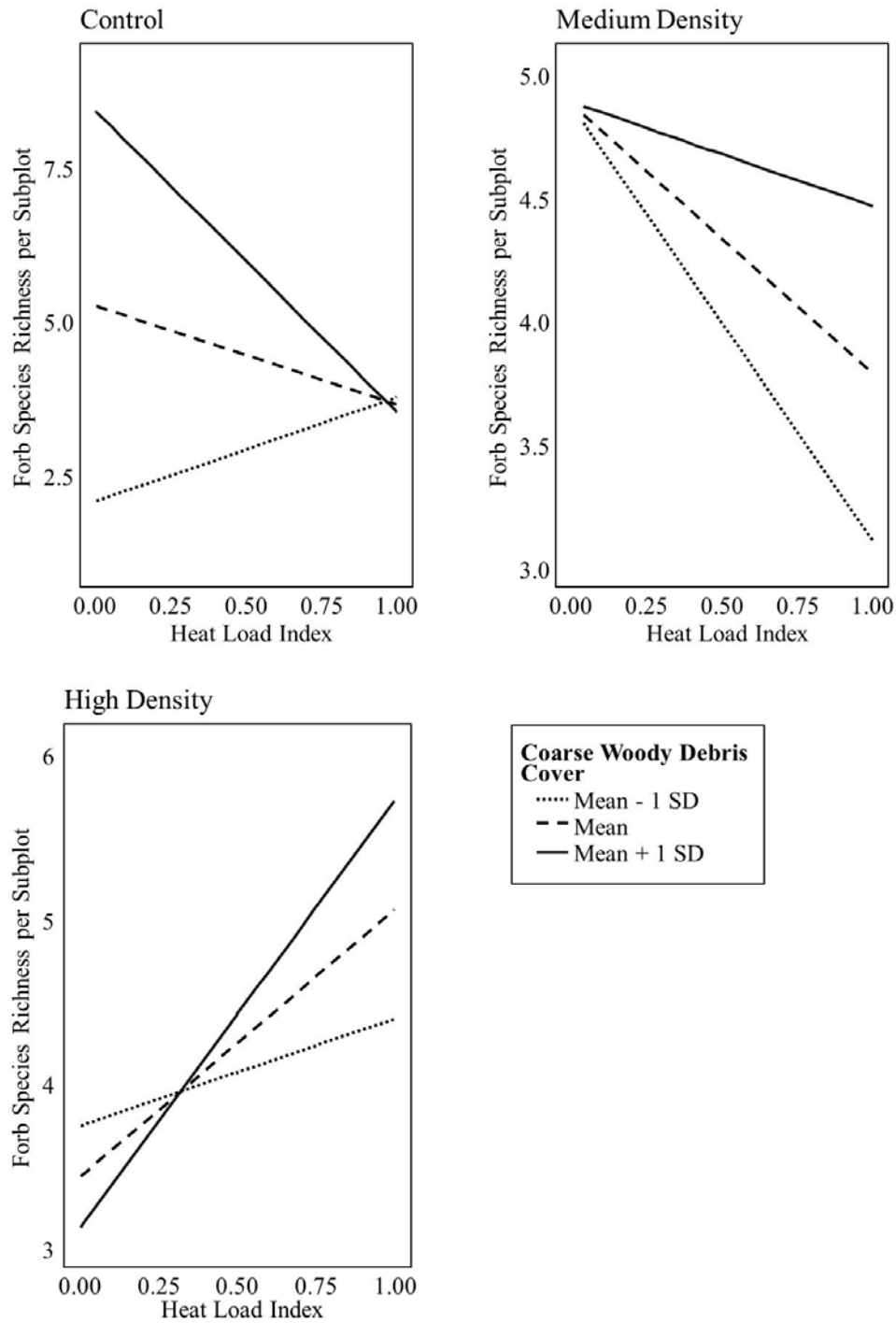


Figure C.7: Interaction of planting density, heat load index (HLI; reflecting slope and aspect) and coarse woody debris volume on forb species richness per vegetation subplot in 2012 in areas reclaimed with coarse-textured coversoil salvaged from a poor-xeric site. In each of the three planting density treatments (unplanted = 0 stems per hectare (sph), medium density = 5000 sph, high density = 10000 sph) the influence of heat load index on species richness is shown at three levels of coarse woody debris cover (mean, mean – 1 standard deviation and mean + 1 standard deviation). See also Table 2.1.

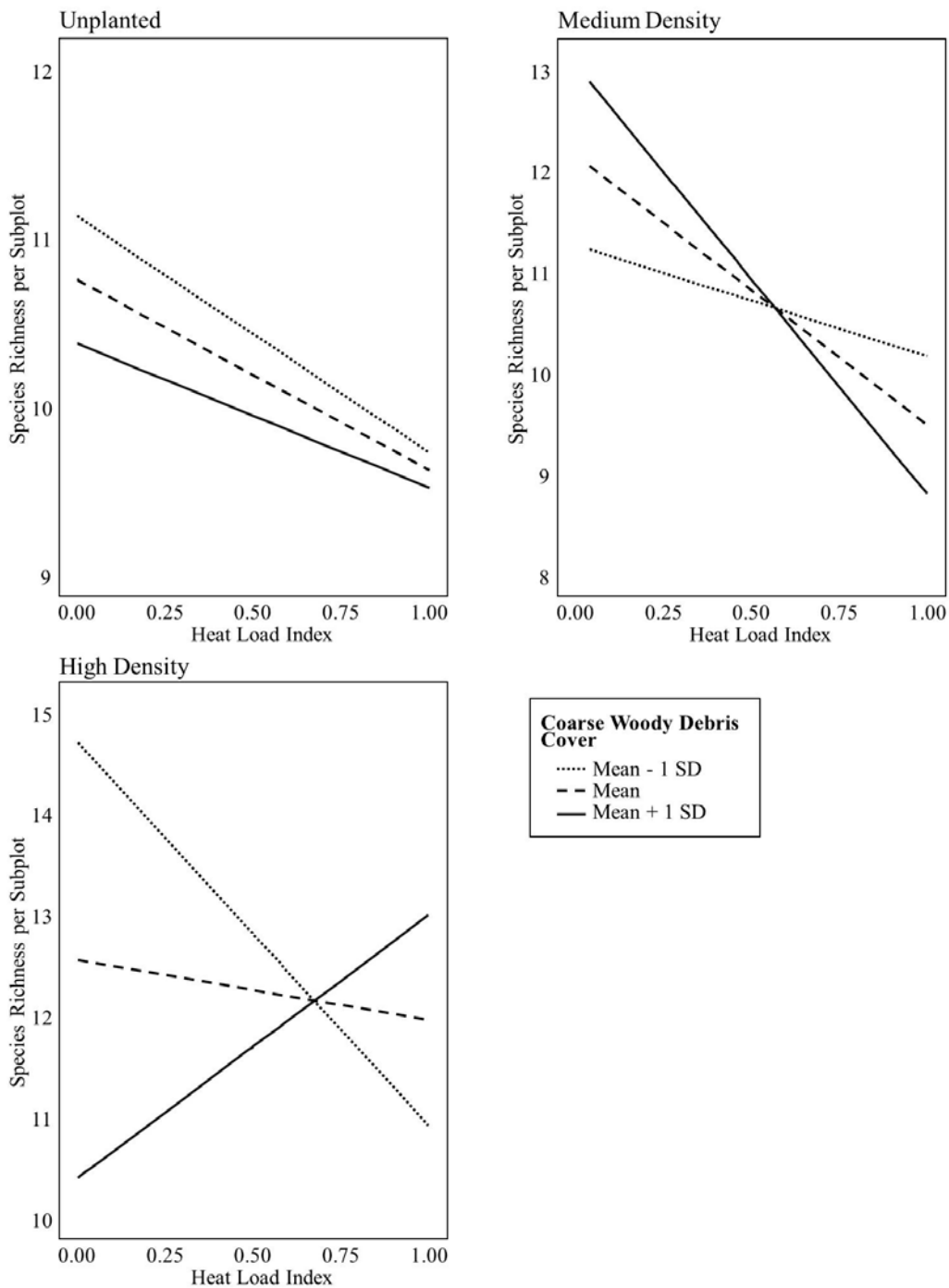


Figure C.8: Interaction of planting density, heat load index (HLI; reflecting slope and aspect) and coarse woody debris volume on species richness per vegetation subplot in 2013 in areas reclaimed with coarse-textured coversoil salvaged from a poor-xeric site. In each of the three planting density treatments (unplanted = 0 stems per hectare (sph), medium density = 5000 sph, high density = 10000 sph) the influence of heat load index on species richness per subplot is shown at three levels of coarse woody debris cover (mean, mean – 1 standard deviation and mean + 1 standard deviation). See also Table 2.1.

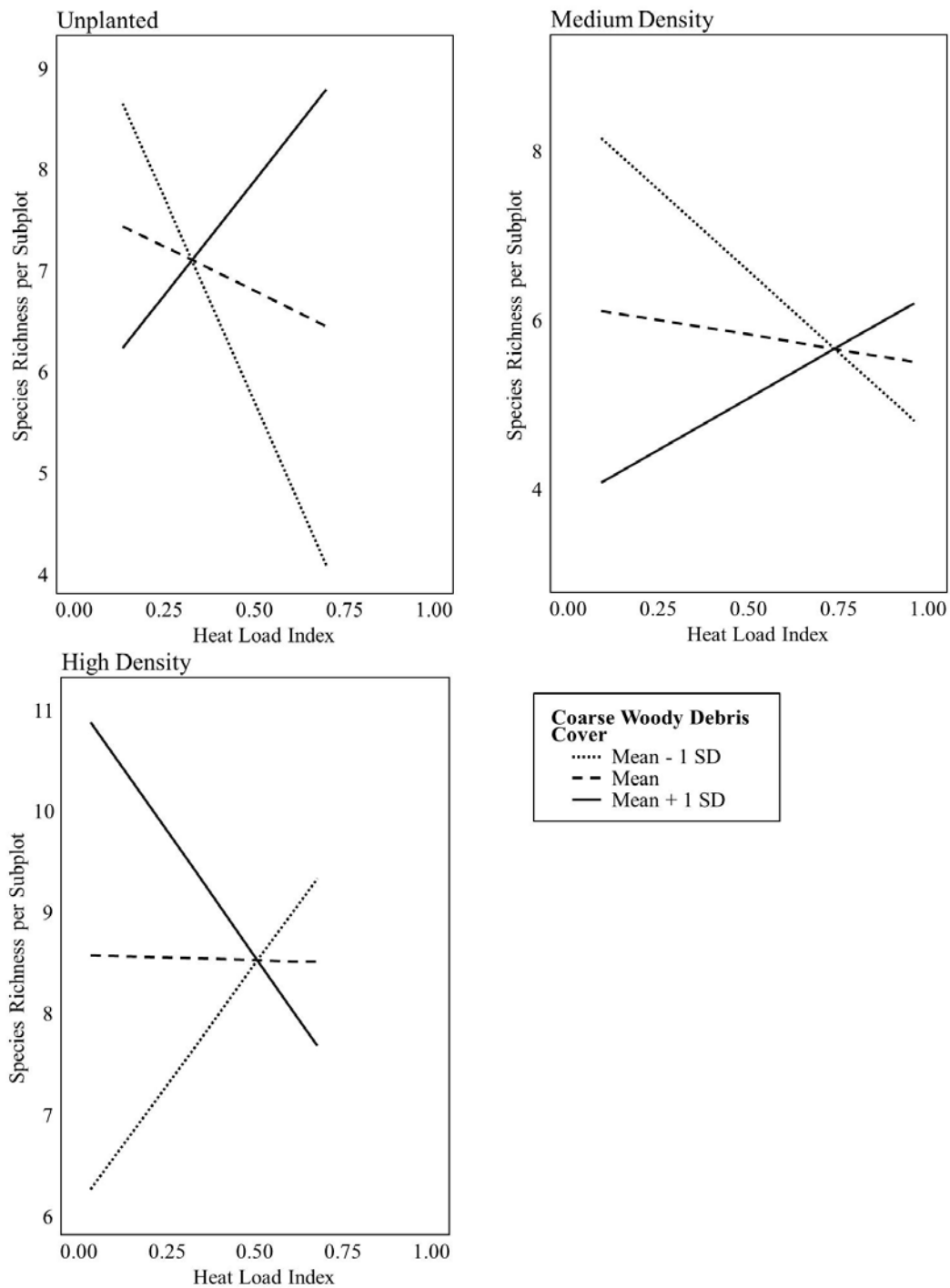


Figure C.9: Interaction of planting density, heat load index (HLI; reflecting slope and aspect) and coarse woody debris volume on species richness per vegetation subplot in 2012 in areas reclaimed with fine-textured coversoil salvaged from a rich-mesic site. In each of the three planting density treatments (unplanted = 0 stems per hectare (sph), medium density = 5000 sph, high density = 10000 sph) the influence of heat load index on species richness is shown at three levels of coarse woody debris cover (mean, mean – 1 standard deviation and mean + 1 standard deviation). See also Table 2.1.

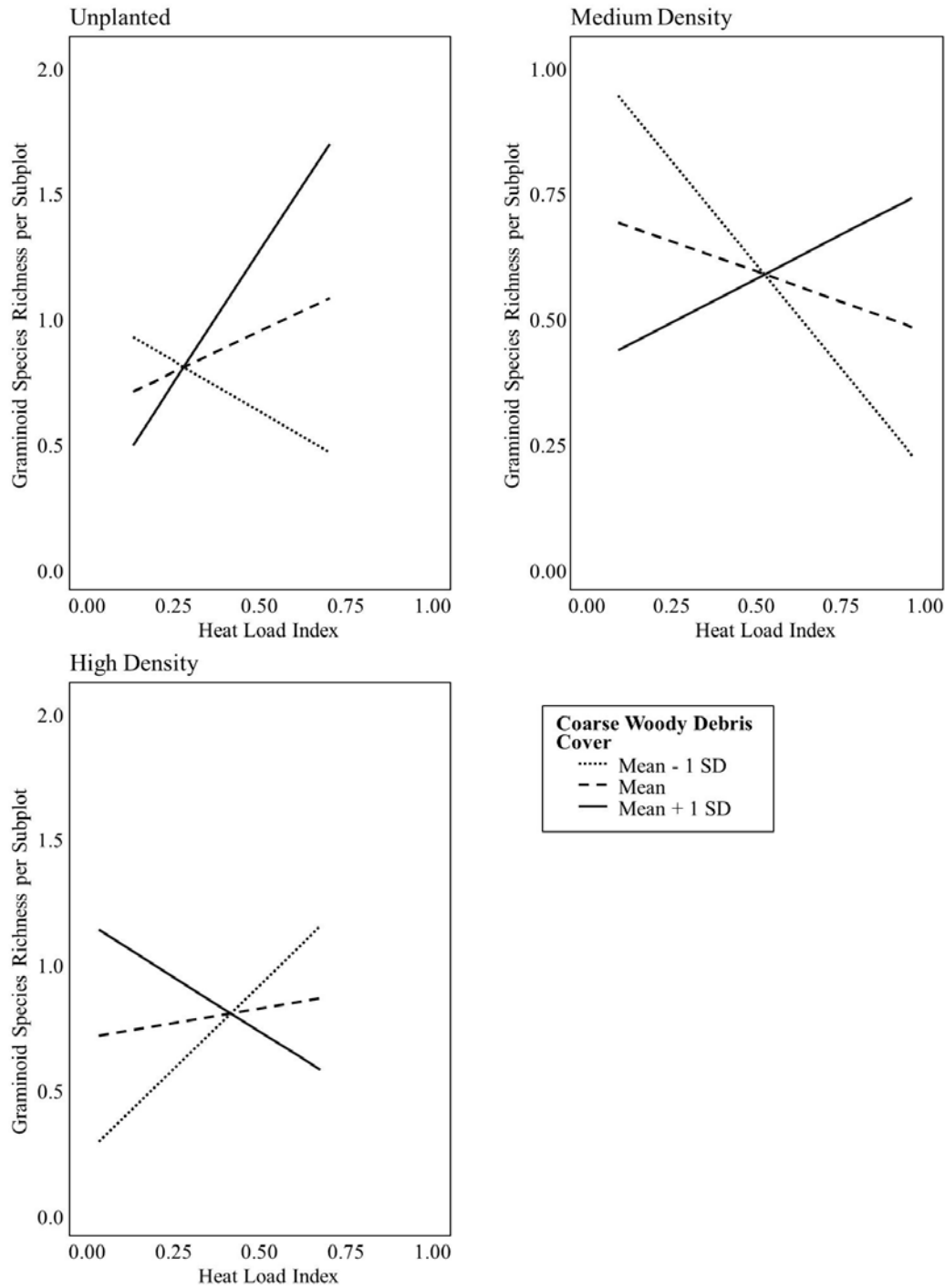


Figure C.10: Interaction of planting density, heat load index (HLI; reflecting slope and aspect) and coarse woody debris volume on graminoid species richness per vegetation subplot in 2012 in areas reclaimed with fine-textured coversoil salvaged from a rich-mesic site. In each of the three planting density treatments (unplanted = 0 stems per hectare (sph), medium density = 5 000 sph, high density = 10 000 sph) the influence of heat load index on species richness is shown at three levels of coarse woody debris cover (mean, mean – 1 standard deviation and mean + 1 standard deviation). See also Table 2.5.

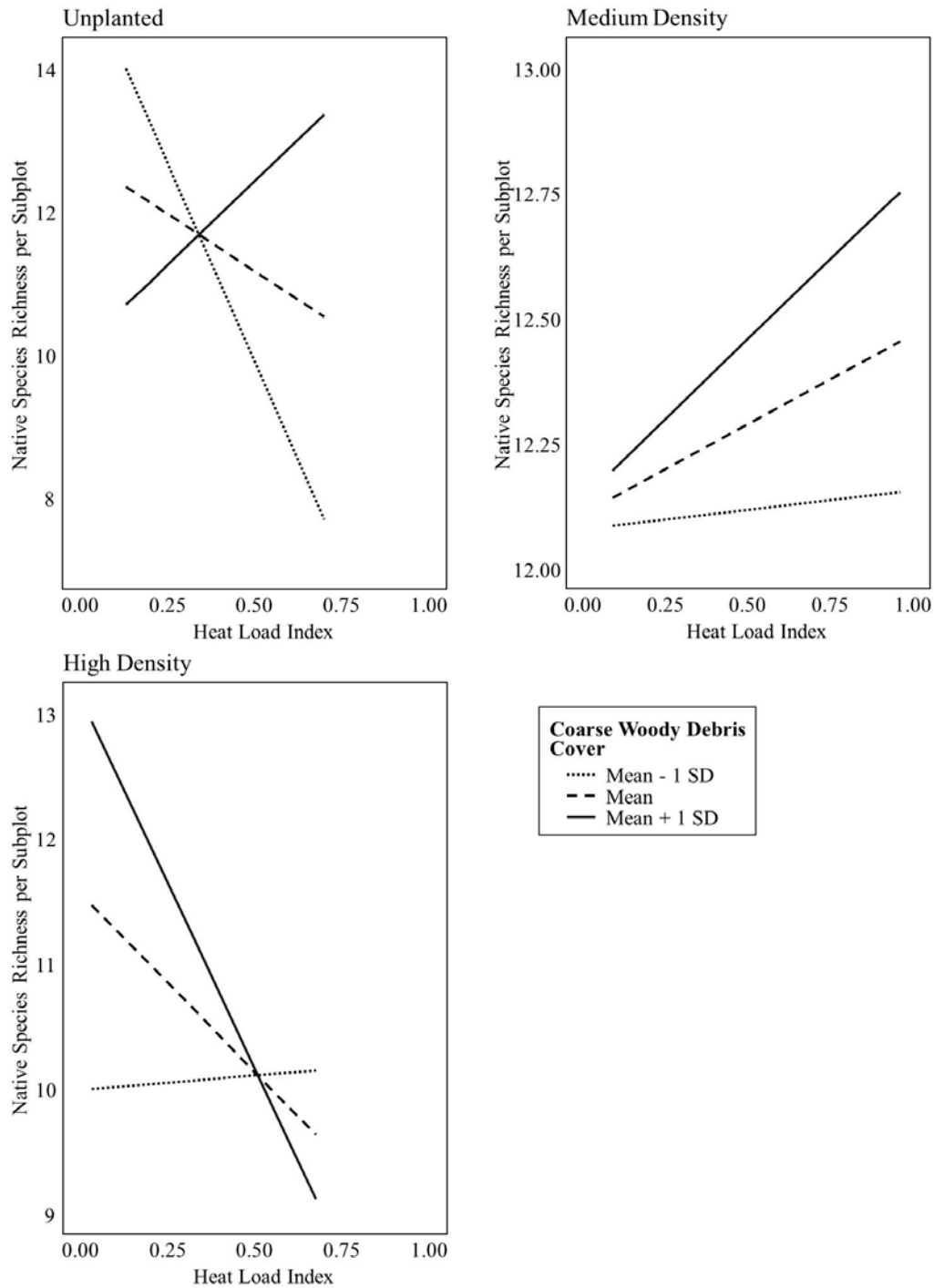


Figure C.11: Interaction of planting density, heat load index (HLI; reflecting slope and aspect) and coarse woody debris volume on native species richness per vegetation subplot in 2015 in areas reclaimed with fine-textured coversoil salvaged from a rich-mesic site. In each of the three planting density treatments (unplanted = 0 stems per hectare (sph), medium density = 5 000 sph, high density = 10 000 sph) the influence of heat load index on species richness is shown at three levels of coarse woody debris cover (mean, mean – 1 standard deviation and mean + 1 standard deviation). See also Table 2.5.

Appendix D: Supplemental material for role of slope aspect and coarse woody debris in plant colonization (Project 2)

Table D.1: Classification of species found on both north and south-facing slopes of a hill structure capped with fine-textured coversoil at the Sandhill Watershed during the 2012 growing season. Species highlighted in light gray are classified as boreal forest species, those highlighted in dark gray as ruderal native species, wetland native species and unclassified, and those highlighted in white as ruderal introduced species.

Boreal forest species	Ruderal introduced species	Ruderal native species	Wetland native species	Unclassified species
<i>Actaea rubra</i>	<i>Chenopodium album</i>	<i>Achillea millefolium</i>	<i>Bidens cernua</i>	<i>Carex</i> spp.
<i>Agrostis scabra</i>	<i>Crepis tectorum</i>	<i>Chenopodium berlandieri</i>	<i>Mentha arvensis</i>	Graminoids
<i>Astragalus canadensis</i>	<i>Galeopsis tetrahit</i>	<i>Epilobium ciliatum</i>	<i>Rorippa palustris</i>	<i>Salix</i> spp.
<i>Calamagrostis canadensis</i>	<i>Lotus corniculatus</i>	<i>Erigeron canadensis</i>	<i>Scutellaria galericulata</i>	
<i>Campanula rotundifolia</i>	<i>Medicago sativa</i>			
<i>Chenopodium gigantospermum</i>	<i>Melilotus alba</i>			
<i>Cornus canadensis</i>	<i>Melilotus officinalis</i>			
<i>Corydalis</i> sp.	<i>Plantago major</i>			
<i>Dracocephalum parviflorum</i>	<i>Polygonum arenastrum</i>			
<i>Epilobium angustifolium</i>	<i>Polygonum convolvulus</i>			
<i>Equisetum arvense</i>	<i>Polygonum lapathifolium</i>			
<i>Equisetum sylvaticum</i>	<i>Sonchus arvensis</i>			
<i>Fragaria vesca</i>	<i>Taraxacum officinale</i>			
<i>Fragaria virginiana</i>	<i>Trifolium hybridum</i>			
<i>Galium boreale</i>				
<i>Galium triflorum</i>				
<i>Geranium bicknellii</i>				

Lathyrus ochroleucus

Ledum groenlandicum

Maianthemum canadense

Mertensia paniculata

Petasites palmatus

Poa palustris

Populus balsamifera

Populus tremuloides

Prunus virginiana

Rosa acicularis

Rubus idaeus

Rubus pubescens

Shepherdia canadensis

Stachys palustris

Trientalis borealis

Vivia americana

Urtoica dioica

Viola adunca

Appendix E: Supplemental material for spatial variation, seedbank and soil type driving vegetation colonization on reclaimed upland sites (Project 3)

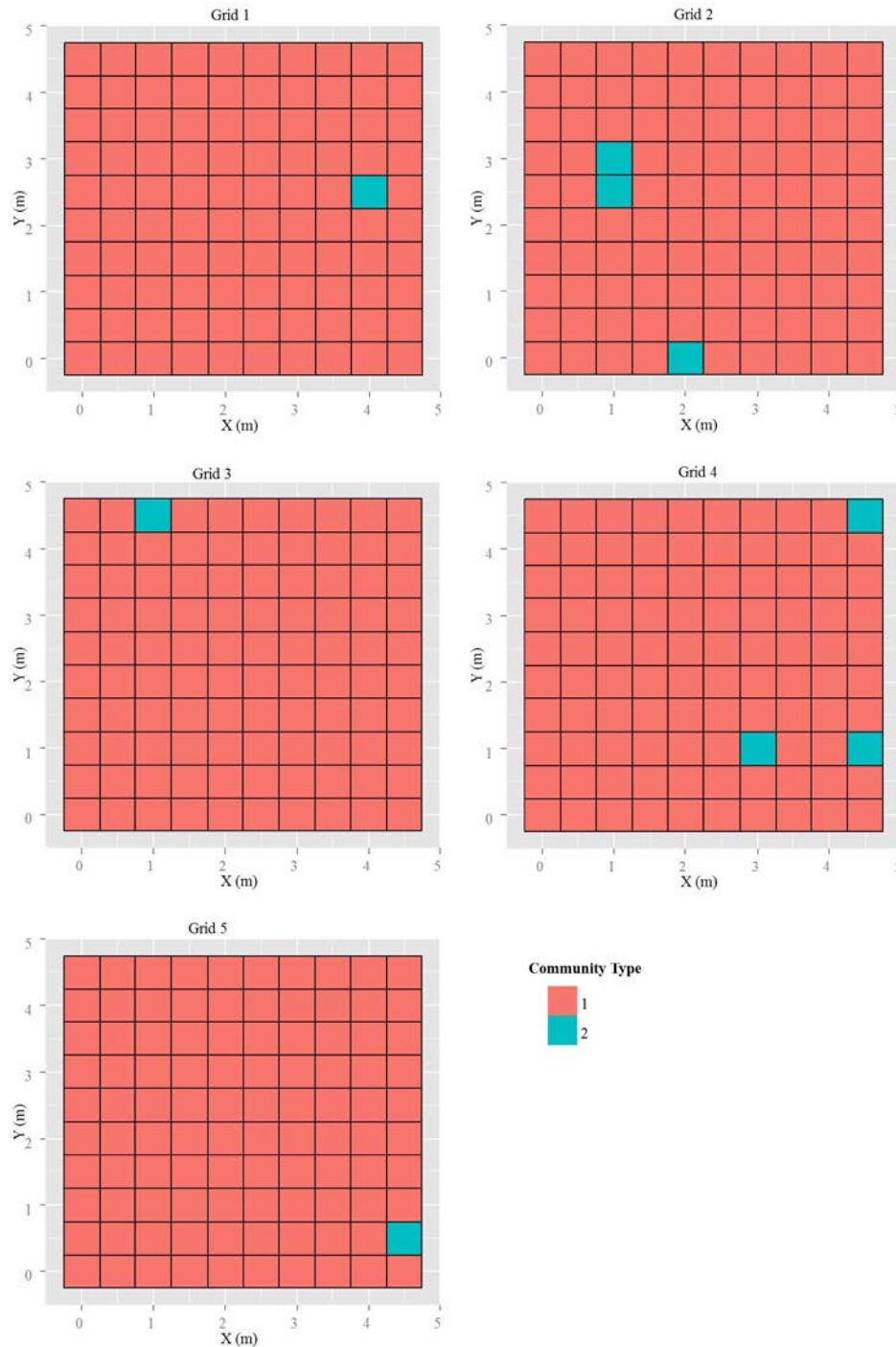


Figure E.1: Results of cluster analysis of young – coarse-textured site type grids (1-5) showing community types for each quadrat in the grid plot.

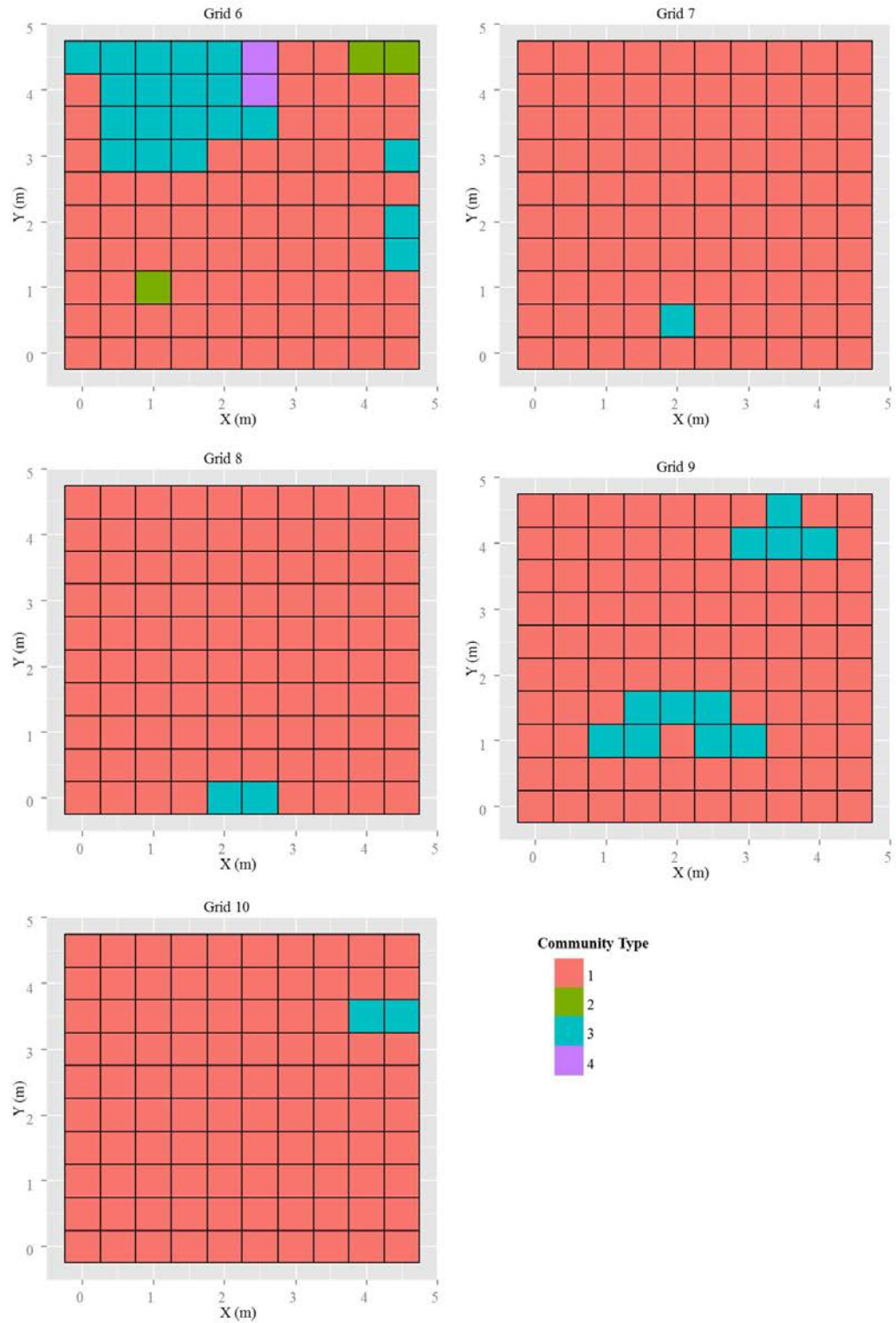


Figure E.2: Results of cluster analysis of young fine-textured site type grids (6-10) showing community types for each quadrat in the grid plot.

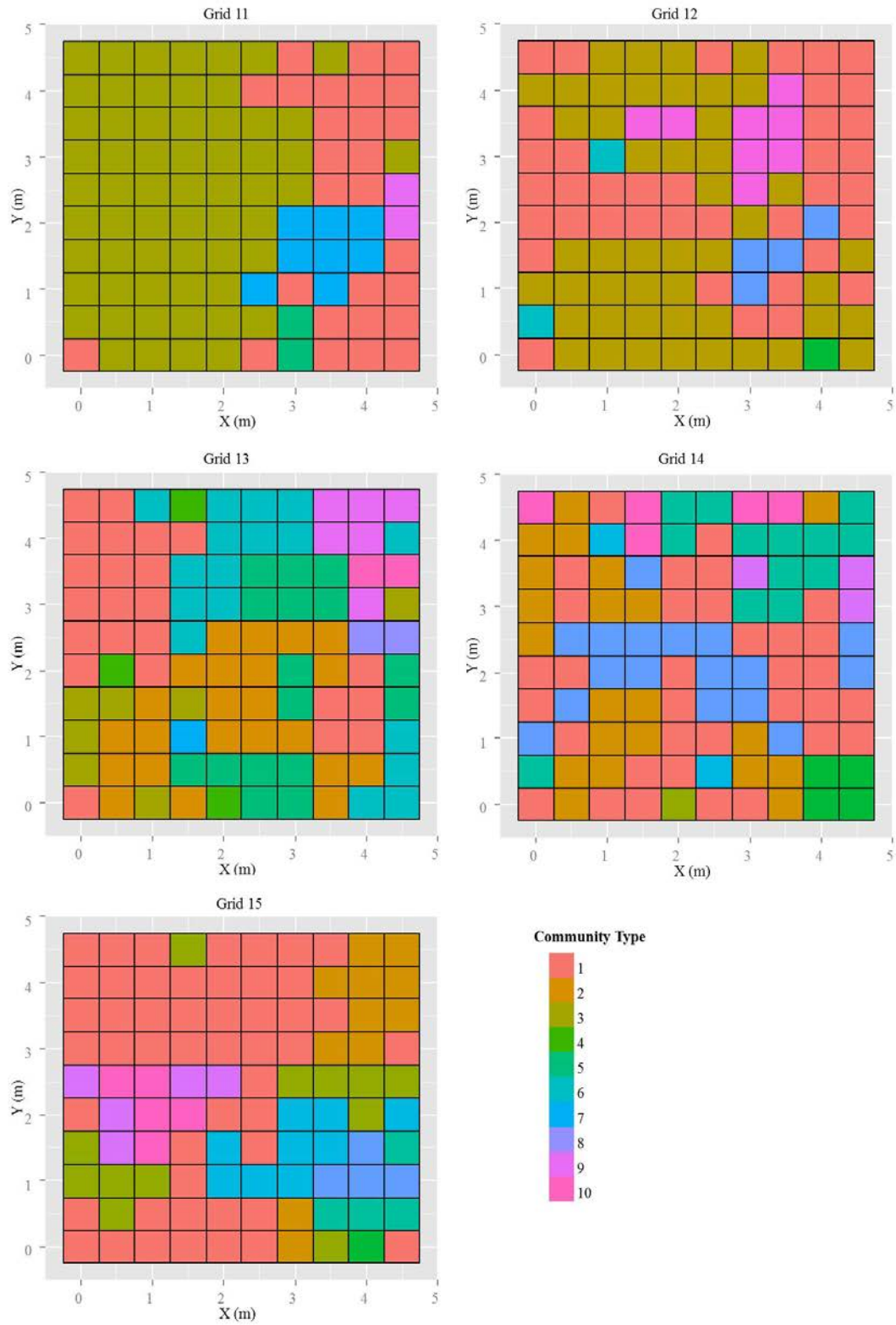


Figure E.3: Results of cluster analysis of older – fine-textured site type grids (11-15) showing community types for each quadrat in the grid plot.

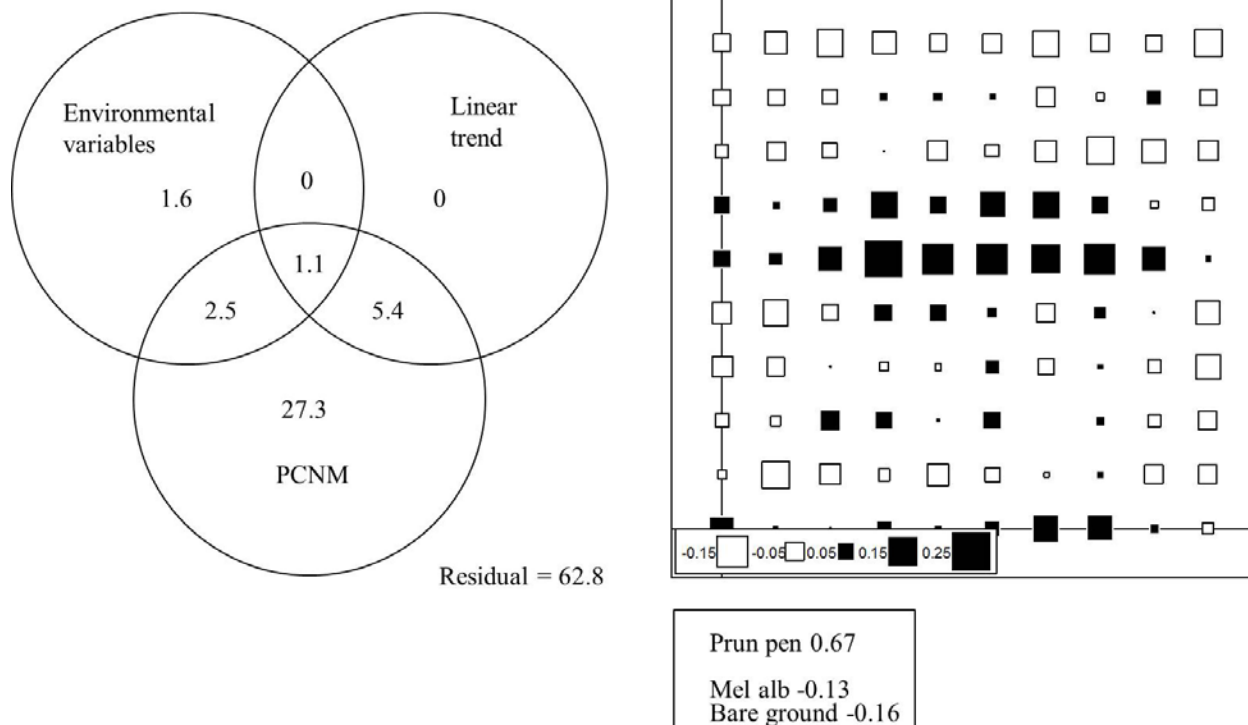


Figure E.4: Results of PCNM analysis (right) and variation partitioning (left) for grid 1, which was a young – coarse-textured site type. The variation partitioning included linear trend, PCNM (spatial) and environmental variable components; the percent variation for each is given and the value in overlapping sections of the diagram indicates the percent of variation shared by the two. Residual indicates the unexplained variation. The PCNM diagram shows the results for correlation of species with the first RDA axis; the diagram is representative of the layout of the grid plot. Species driving the spatial pattern are shown below it (Prun pen = *Prunus pensylvanica*, Mel alb = *Mellilotus alba*). Species with positive scores were associated with the positive (black) pattern and species with negative scores are associated with the negative (white) pattern. The magnitude of the species score, indicating the strength of the association, is shown by the symbol size.

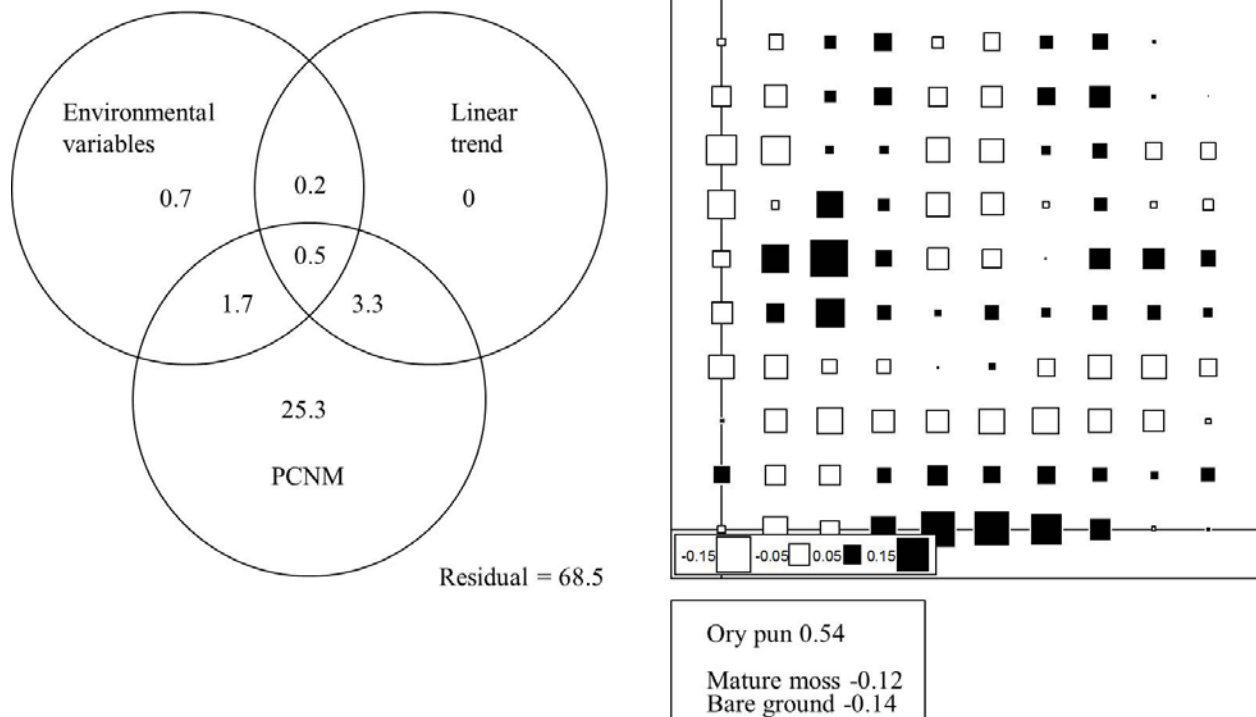


Figure E.5 : Results of PCNM analysis (right) and variation partitioning (left) for grid 2, which was a young – coarse-textured site type. The variation partitioning included linear trend, PCNM (spatial) and environmental variable components; the percent variation for each is given and the value in overlapping sections of the diagram indicates the percent of variation shared by the two. Residual indicates the unexplained variation. The PCNM diagram shows the results for correlation of species with the first RDA axis; the diagram is representative of the layout of the grid plot. Species driving the spatial pattern are shown below it (*Ory pun* = *Oryzopsis pungens*). Species with positive scores were associated with the positive (black) pattern and species with negative scores are associated with the negative (white) pattern. The magnitude of the species score, indicating the strength of the association, is shown by the symbol size.

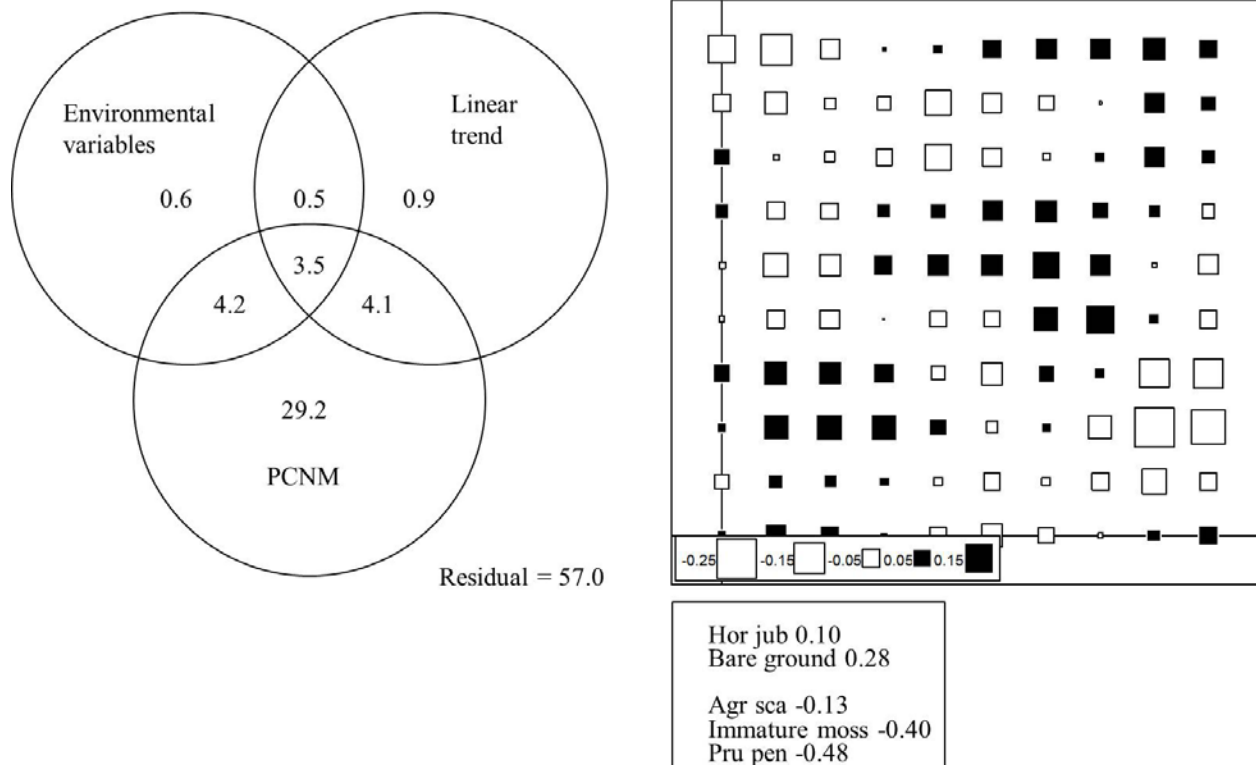


Figure E.6: Results of PCNM analysis (right) and variation partitioning (left) for grid 3, which was a young – coarse-textured site type. The variation partitioning included linear trend, PCNM (spatial) and environmental variable components; the percent variation for each is given and the value in overlapping sections of the diagram indicates the percent of variation shared by the two. Residual indicates the unexplained variation. The PCNM diagram shows the results for correlation of species with the first RDA axis; the diagram is representative of the layout of the grid plot. Species driving the spatial pattern are shown below it (Hor jub = *Hordeum jubatum*, Agr sca = *Agrostis scabra*, Pru pen = *Prunus pensylvanica*). Species with positive scores were associated with the positive (black) pattern and species with negative scores are associated with the negative (white) pattern. The magnitude of the species score, indicating the strength of the association, is shown by the symbol size.

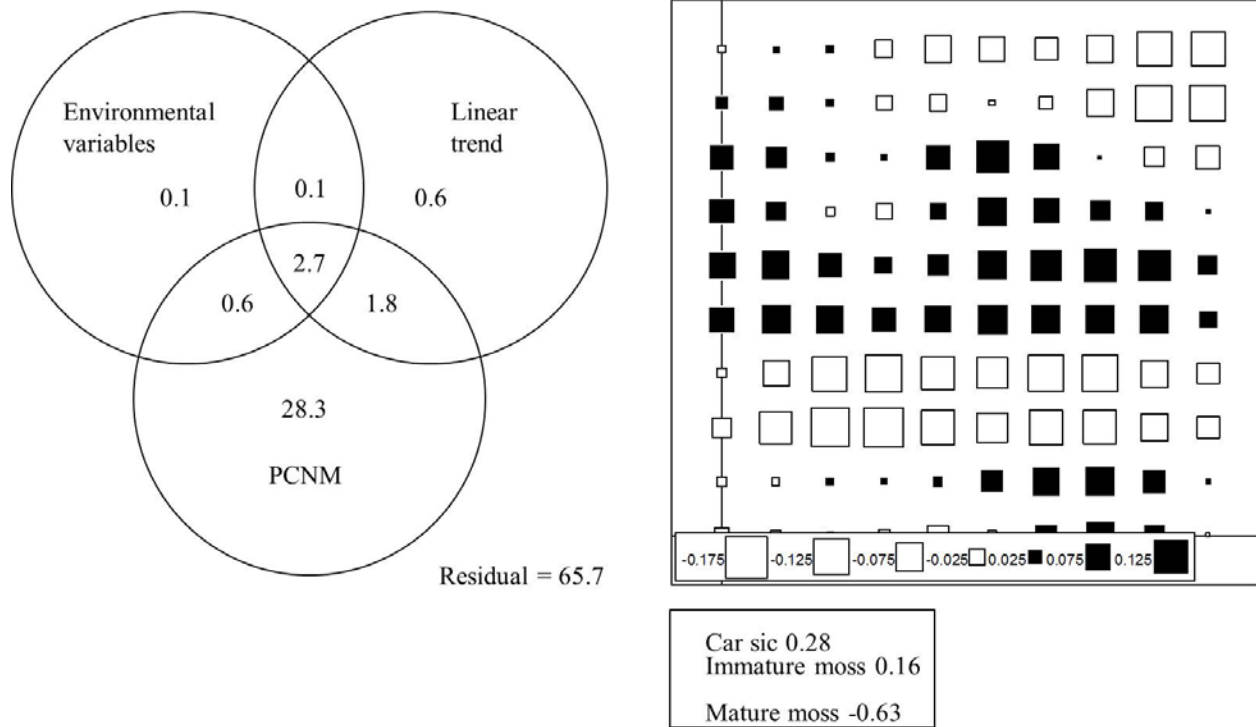


Figure E.7: Results of PCNM analysis (right) and variation partitioning (left) for grid 4, which was a young – coarse-textured site type. The variation partitioning included linear trend, PCNM (spatial) and environmental variable components; the percent variation for each is given and the value in overlapping sections of the diagram indicates the percent of variation shared by the two. Residual indicates the unexplained variation. The PCNM diagram shows the results for correlation of species with the first RDA axis; the diagram is representative of the layout of the grid plot. Species driving the spatial pattern are shown below it (Car sic = *Carex siccata*). Species with positive scores were associated with the positive (black) pattern and species with negative scores are associated with the negative (white) pattern. The magnitude of the species score, indicating the strength of the association, is shown by the symbol size.

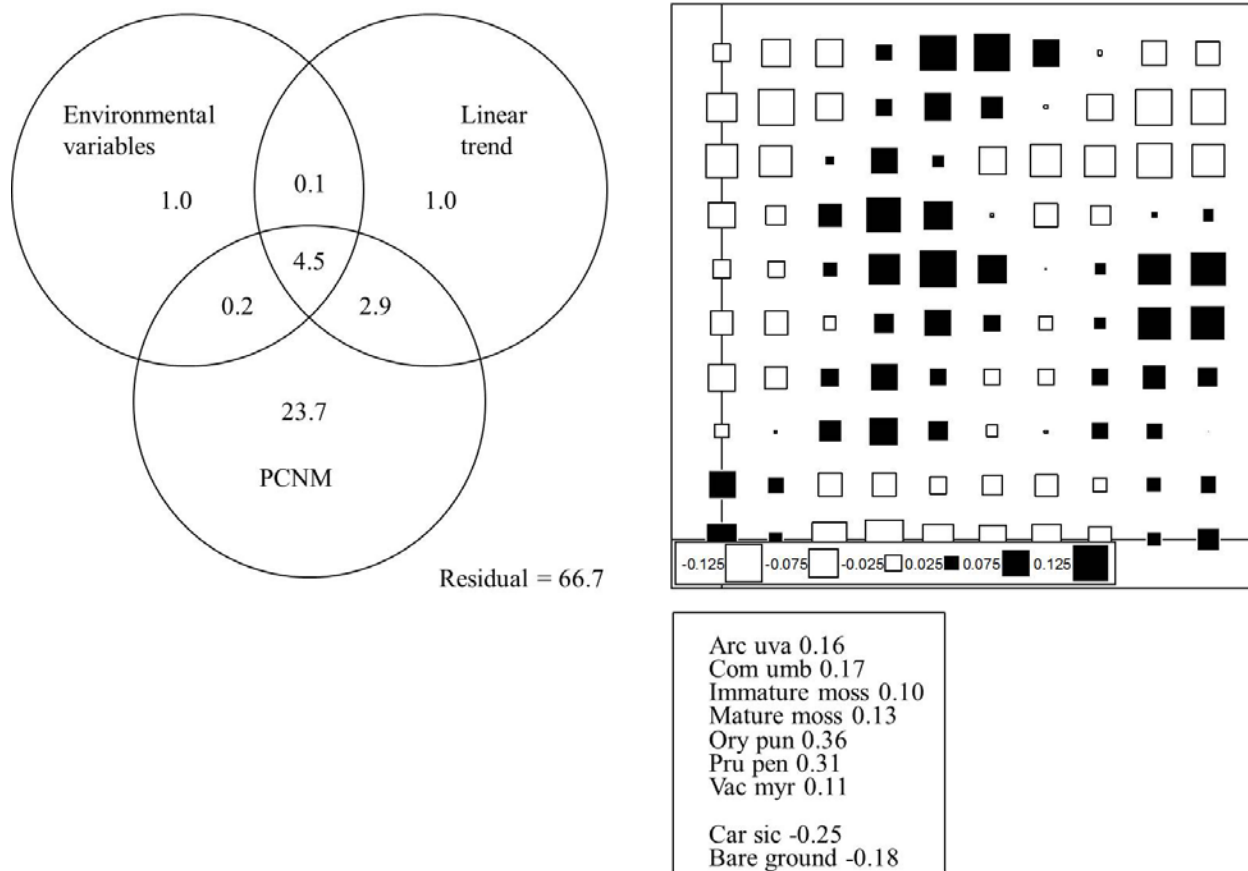


Figure E.8: Results of PCNM analysis (right) and variation partitioning (left) for grid 5, which was a young – coarse-textured site type. The variation partitioning included linear trend, PCNM (spatial) and environmental variable components; the percent variation for each is given and the value in overlapping sections of the diagram indicates the percent of variation shared by the two. Residual indicates the unexplained variation. The PCNM diagram shows the results for correlation of species with the first RDA axis; the diagram is representative of the layout of the grid plot. Species driving the spatial pattern are shown below it (*Arc uva* = *Arctostaphylos uva-ursi*, *Com umb* = *Commandra umbellata*, *Ory pun* = *Oryzopsis pungens*, *Pru pen* = *Prunus pensylvanica*, *Vac myr* = *Vaccinium myrtilloides*, *Car sic* = *Carex siccata*). Species with positive scores were associated with the positive (black) pattern and species with negative scores are associated with the negative (white) pattern. The magnitude of the species score, indicating the strength of the association, is shown by the symbol size.

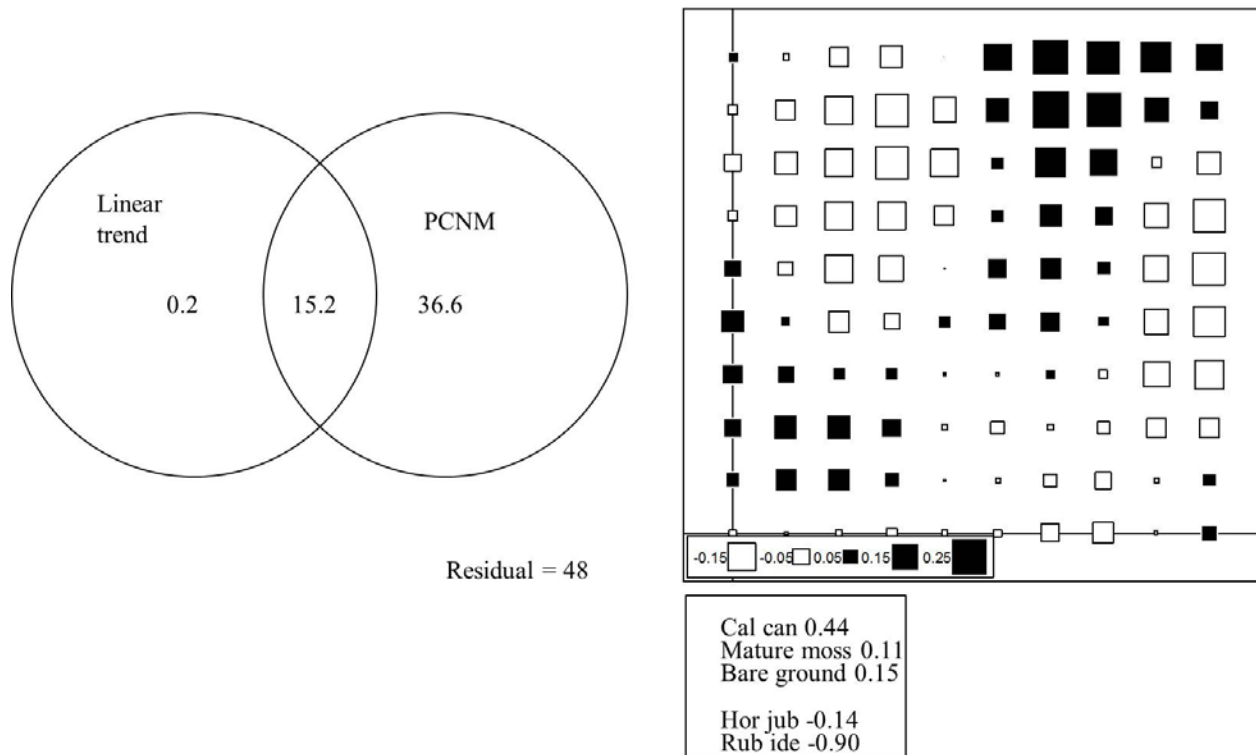


Figure E.9: Results of PCNM analysis (right) and variation partitioning (left) for grid 6, which was a young – fine-textured site type. The variation partitioning included linear trend and PCNM (spatial) components; the percent variation for each is given and the value in overlapping sections of the diagram indicates the percent of variation shared by the two. None of the environmental variables were chosen in the forward selection process so were not included in the variation partitioning. Residual indicates the unexplained variation. The PCNM diagram shows the results for correlation of species with the first RDA axis; the diagram is representative of the layout of the grid plot. Species driving the spatial pattern are shown below it (Cal can = *Calamagrostis canadensis*, Hor jub = *Hordeum jubatum*, Rub ide = *Rubus idaeus*). Species with positive scores were associated with the positive (black) pattern and species with negative scores are associated with the negative (white) pattern. The magnitude of the species score, indicating the strength of the association, is shown by the symbol size.

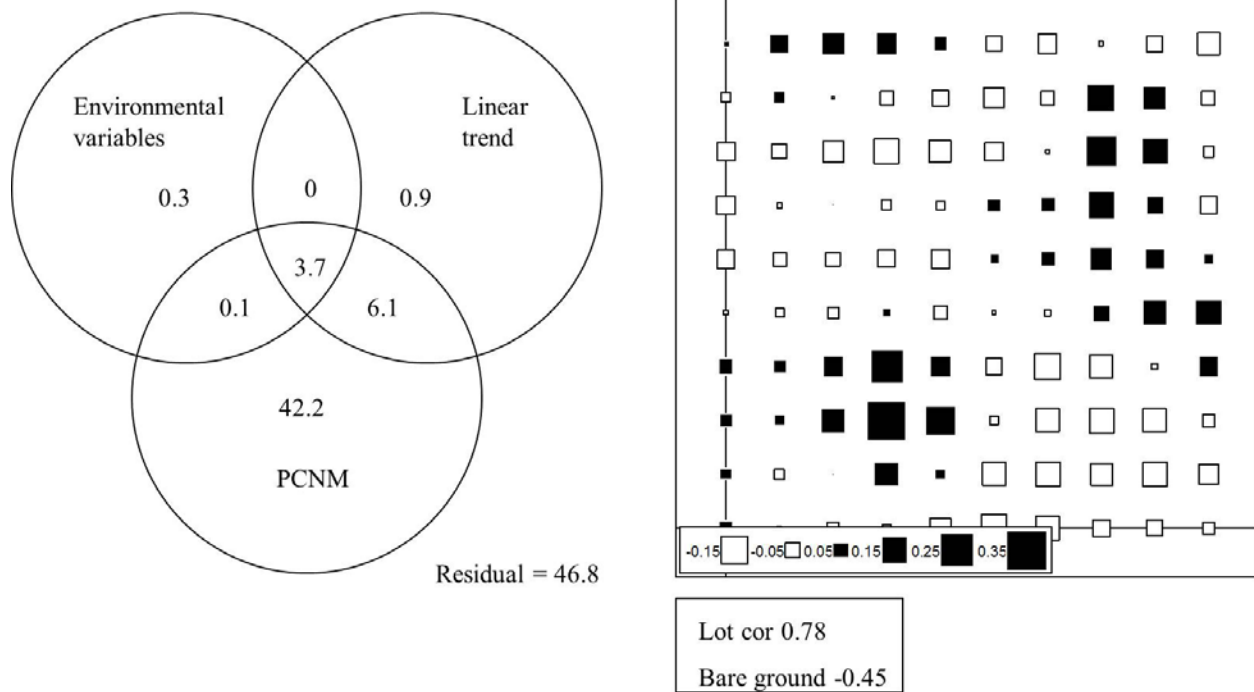


Figure E.10: Results of PCNM analysis (right) and variation partitioning (left) for grid 7, which was a young – fine-textured site type. The variation partitioning included linear trend, PCNM (spatial) and environmental variable components; the percent variation for each is given and the value in overlapping sections of the diagram indicates the percent of variation shared by the two. Residual indicates the unexplained variation. The PCNM diagram shows the results for correlation of species with the first RDA axis; the diagram is representative of the layout of the grid plot. Species driving the spatial pattern are shown below it (Lot cor = *Lotus corniculatus*). Species with positive scores were associated with the positive (black) pattern and species with negative scores are associated with the negative (white) pattern. The magnitude of the species score, indicating the strength of the association, is shown by the symbol size.

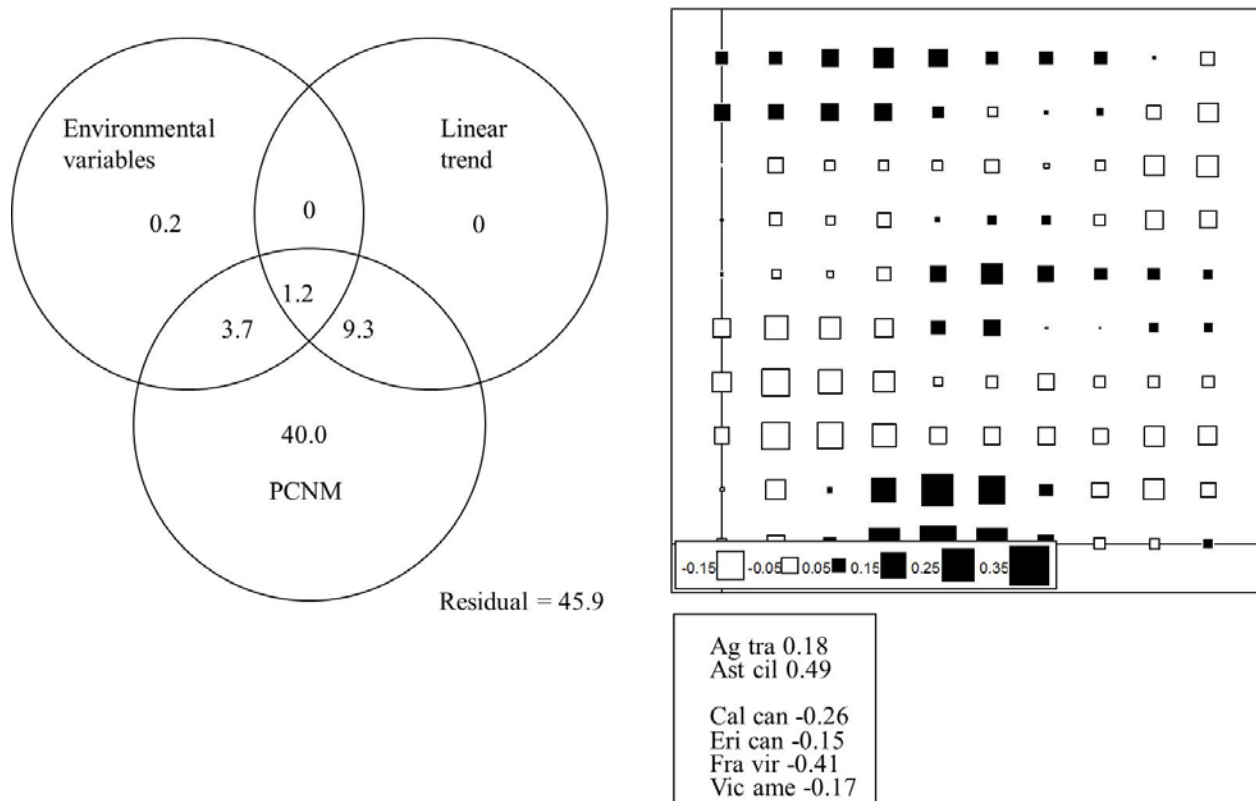


Figure E.11: Results of PCNM analysis (right) and variation partitioning (left) for grid 8, which was a young – fine-textured site type. The variation partitioning linear trend, PCNM (spatial) and environmental variable components; the percent variation for each is given and the value in overlapping sections of the diagram indicates the percent of variation shared by the two. Residual indicates the unexplained variation. The PCNM diagram shows the results for correlation of species with the first RDA axis; the diagram is representative of the layout of the grid plot. Species driving the spatial pattern are shown below it (Ag tra = *Agropyron trachycaulum* var. *trachycaulum*, Ast cil = *Aster ciliolatus*, Cal can = *Calamagrostis canadensis*, Eri can = *Erigeron canadensis*, Fra vir = *Fragaria virginiana*, Vic ame = *Vicia americana*). Species with positive scores were associated with the positive (black) pattern and species with negative scores are associated with the negative (white) pattern. The magnitude of the species score, indicating the strength of the association, is shown by the symbol size.

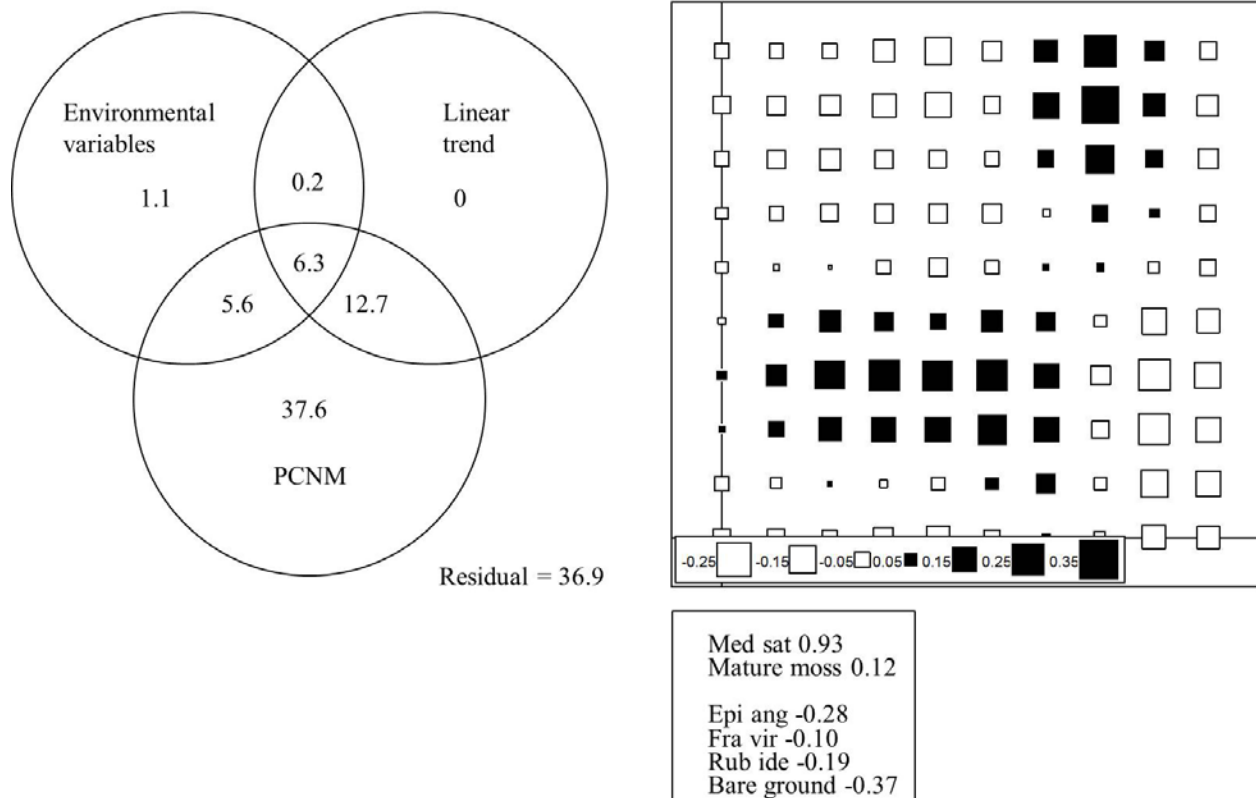


Figure E.12: Results of PCNM analysis (right) and variation partitioning (left) for grid 9, which was a young – fine-textured site type. The variation partitioning included linear trend, PCNM (spatial) and environmental variable components; the percent variation for each is given and the value in overlapping sections of the diagram indicates the percent of variation shared by the two. Residual indicates the unexplained variation. The PCNM diagram shows the results for correlation of species with the first RDA axis; the diagram is representative of the layout of the grid plot. Species driving the spatial pattern are shown below it (Med sat = *Medicago sativa*, Epi ang = *Epilobium angustifolium*, Fra vir = *Fragaria virginiana*, Rub ide = *Rubus idaeus*). Species with positive scores were associated with the positive (black) pattern and species with negative scores are associated with the negative (white) pattern. The magnitude of the species score, indicating the strength of the association, is shown by the symbol size.

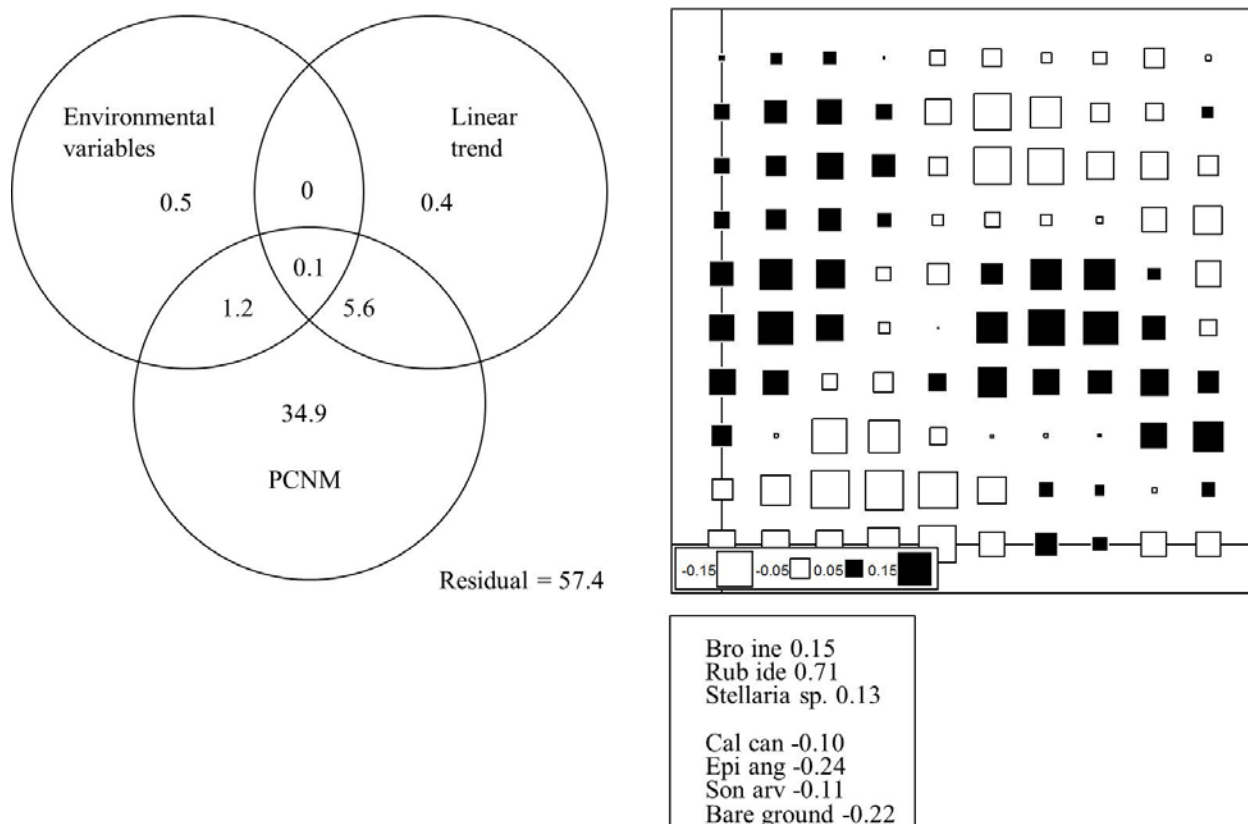


Figure E.13: Results of PCNM analysis (right) and variation partitioning (left) for grid 10, which was a young – fine-textured site type. The variation partitioning included linear trend, PCNM (spatial) and environmental variable components; the percent variation for each is given and the value in overlapping sections of the diagram indicates the percent of variation shared by the two. Residual indicates the unexplained variation. The PCNM diagram shows the results for correlation of species with the first RDA axis; the diagram is representative of the layout of the grid plot. Species driving the spatial pattern are shown below it (Bro ine = *Bromus inermis*, Rub ide = *Rubus idaeus*, Cal can = *Calamagrostis canadensis*, Epi ang = *Epilobium angustifolium*, Son arv = *Sonchus arvensis*). Species with positive scores were associated with the positive (black) pattern and species with negative scores are associated with the negative (white) pattern. The magnitude of the species score, indicating the strength of the association, is shown by the symbol size.

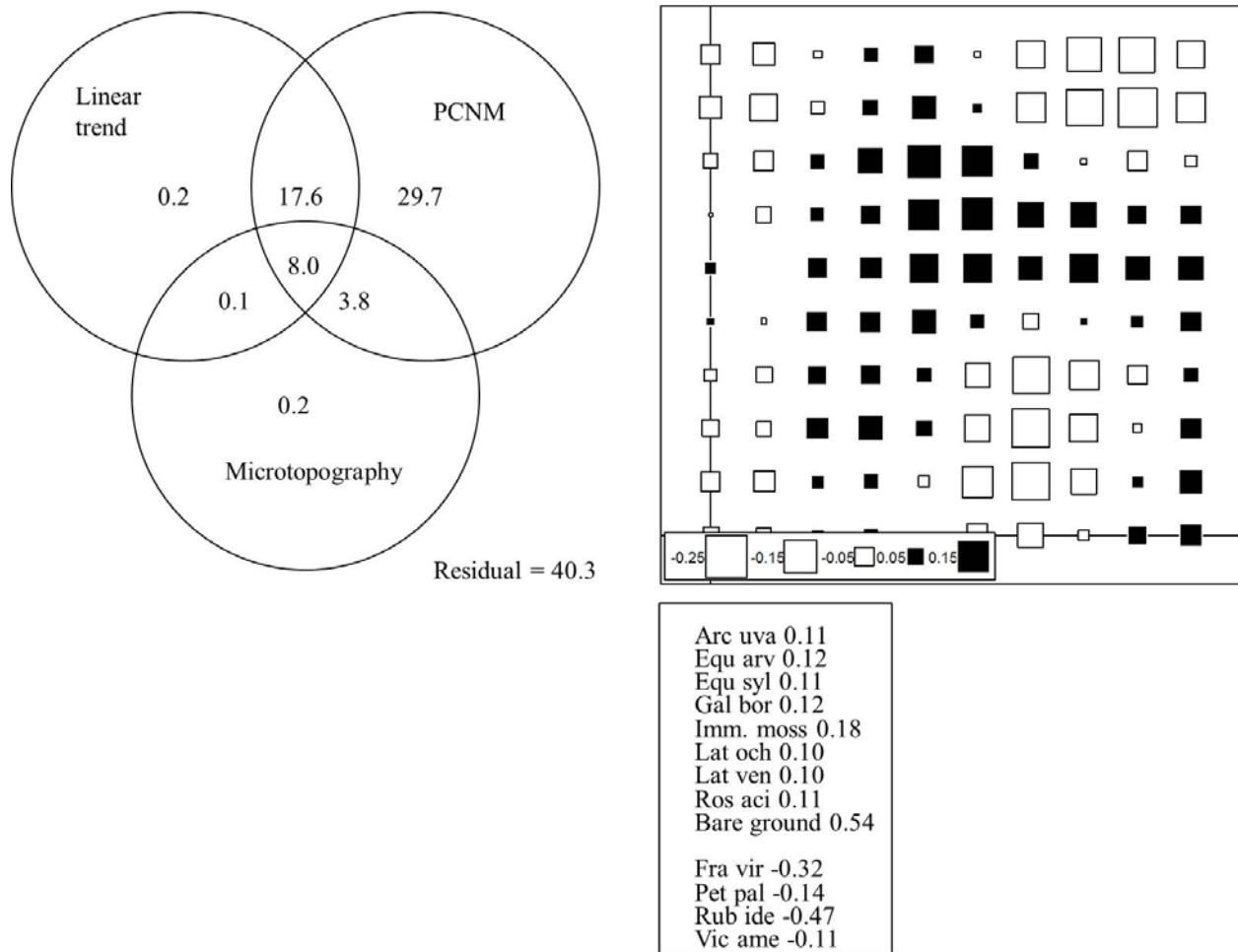


Figure E.14: Results of PCNM analysis (right) and variation partitioning (left) for grid 11, which was an older – fine-textured site type. The variation partitioning included linear trend, PCNM (spatial) and microtopography components; the percent variation for each is given and the value in overlapping sections of the diagram indicates the percent of variation shared by the two. None of the tree canopy variables were chosen in the forward selection process so were not included in the variation partitioning. Residual indicates the unexplained variation. The PCNM diagram shows the results for correlation of species with the first RDA axis; the diagram is representative of the layout of the grid plot. Species driving the spatial pattern are shown below it (*Arc uva* = *Arctostaphylos uva-ursi*, *Equ arv* = *Equisetum arvense*, *Equ syl* = *Equisetum sylvaticum*, *Gal bor* = *Galium boreale*, *Lat och* = *Lathyrus ochroleucus*, *Lat ven* = *Lathyrus venosus*, *Ros aci* = *Rosa acicularis*, *Fra vir* = *Fragaria virginiana*, *Pet pal* = *Petasites palmatus*, *Rub ide* = *Rubus idaeus*, *Vic ame* = *Vicia americana*). Species with positive scores were associated with the positive (black) pattern and species with negative scores are associated with the negative (white) pattern. The magnitude of the species score, indicating the strength of the association, is shown by the symbol size.

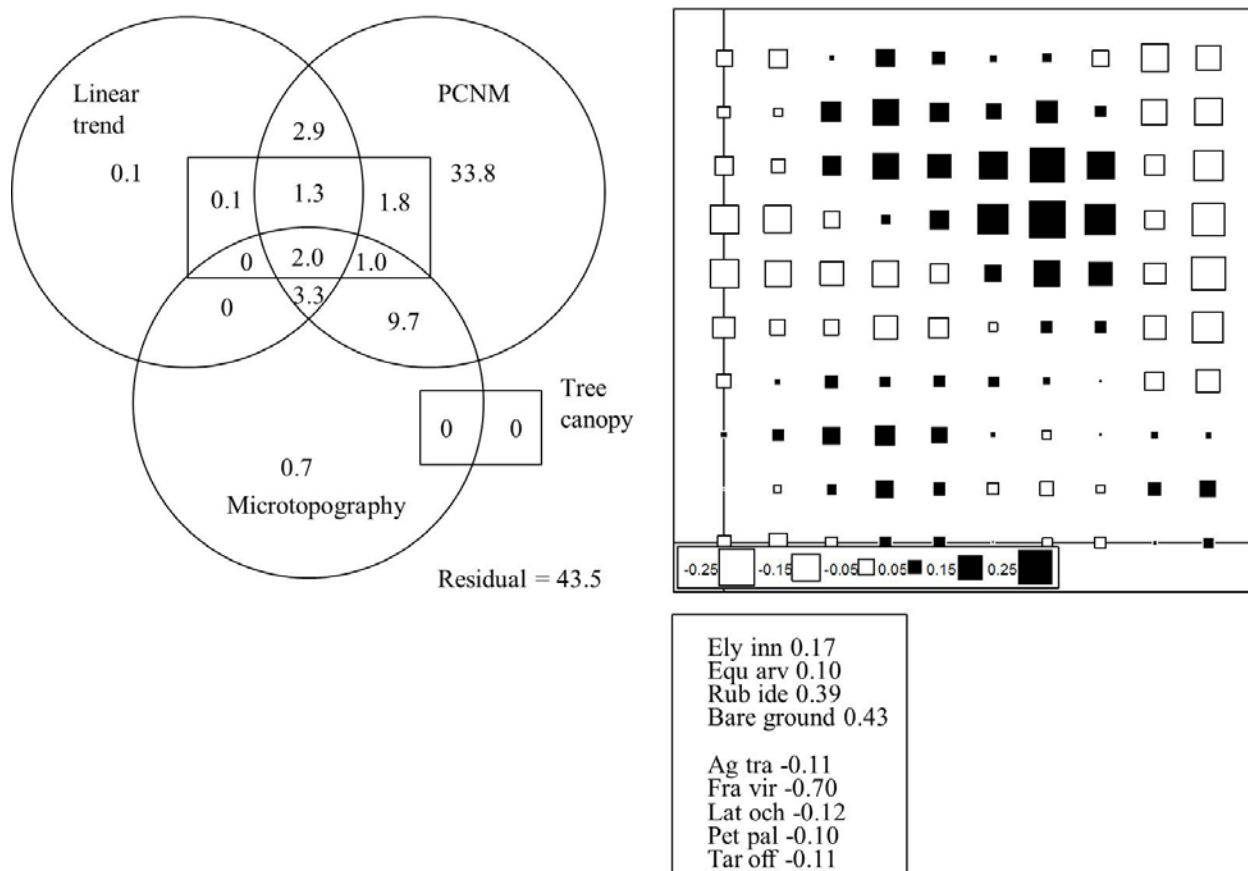


Figure E.15: Results of PCNM analysis (right) and variation partitioning (left) for grid 12, which was an older – fine-textured site type. The variation partitioning included linear trend, PCNM (spatial), microtopography and tree canopy components; the percent variation for each is given and the value in overlapping sections of the diagram indicates the percent of variation shared by the two. Residual indicates the unexplained variation. The PCNM diagram shows the results for correlation of species with the first RDA axis; the diagram is representative of the layout of the grid plot. Species driving the spatial pattern are shown below it (Ely inn = *Elymus innovatus*, Equ arv = *Equisetum arvense*, Rub ide = *Rubus idaeus*, Ag tra = *Agropyron trachycaulum* var. *trachycaulum*, Fra vir = *Fragaria virginiana*, Lat och = *Lathyrus ochroleucus*, Pet pal = *Petasites palmatus*, Tar off = *Taraxacum officinale*). Species with positive scores were associated with the positive (black) pattern and species with negative scores are associated with the negative (white) pattern. The magnitude of the species score, indicating the strength of the association, is shown by the symbol size.

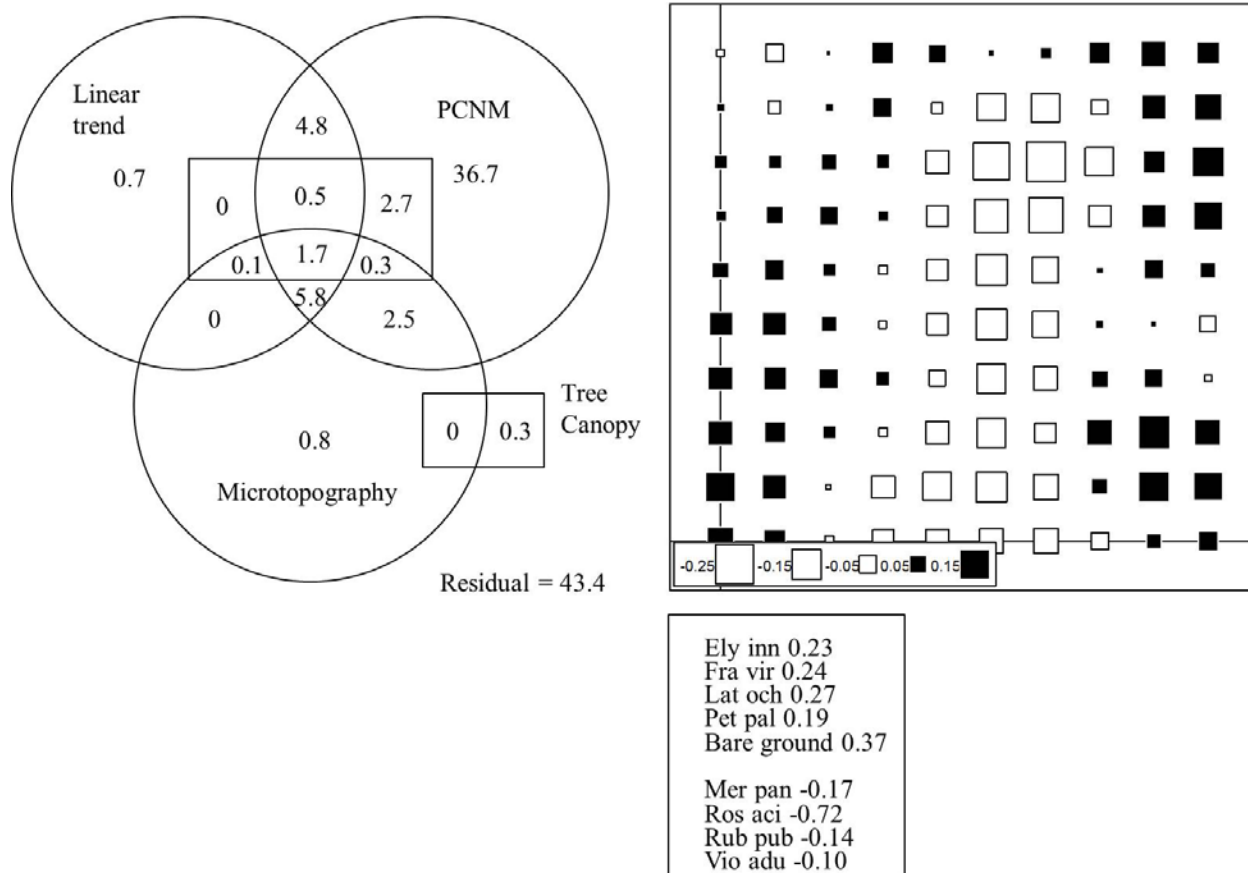


Figure E.16: Results of PCNM analysis (right) and variation partitioning (left) for grid 13, which was an older – fine-textured site type. The variation partitioning included linear trend, PCNM (spatial), microtopography and tree canopy components; the percent variation for each is given and the value in overlapping sections of the diagram indicates the percent of variation shared by the two. Residual indicates the unexplained variation. The PCNM diagram shows the results for correlation of species with the first RDA axis; the diagram is representative of the layout of the grid plot. Species driving the spatial pattern are shown below it (Ely inn = *Elymus innovatus*, Fra vir = *Fragaria virginiana*, Lat och = *Lathyrus ochroleucus*, Pet pal = *Petasites palmatus*, Mer pan = *Mertensia paniculata*, Ros aci = *Rosa acicularis*, Rub pub = *Rubus pubescens*, Vio adu = *Viola adunca*). Species with positive scores were associated with the positive (black) pattern and species with negative scores are associated with the negative (white) pattern. The magnitude of the species score, indicating the strength of the association, is shown by the symbol size.

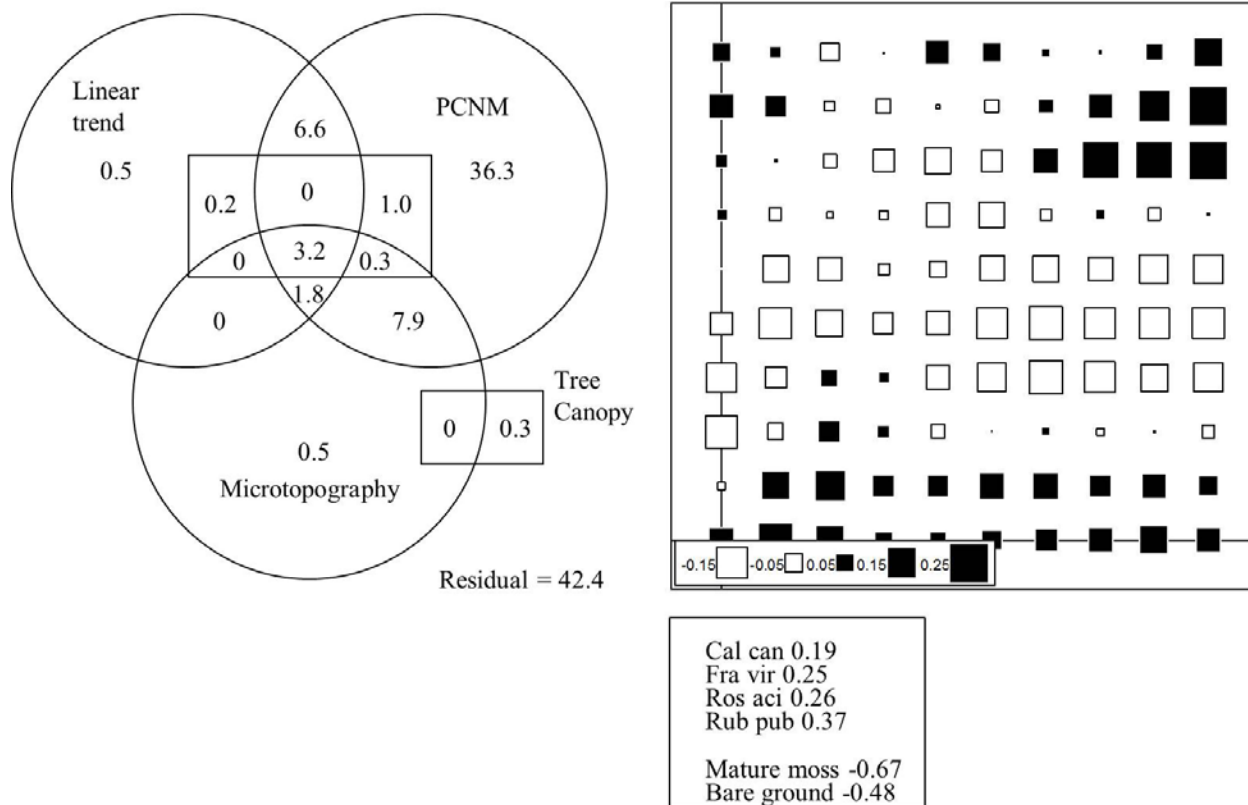


Figure E.17: Results of PCNM analysis (right) and variation partitioning (left) for grid 14, which was an older – fine-textured site type. The variation partitioning included linear trend, PCNM (spatial), microtopography and tree canopy components; the percent variation for each is given and the value in overlapping sections of the diagram indicates the percent of variation shared by the two. Residual indicates the unexplained variation. The PCNM diagram shows the results for correlation of species with the first RDA axis; the diagram is representative of the layout of the grid plot. Species driving the spatial pattern are shown below it (Cal can = *Calamagrostis canadensis*, Fra vir = *Fragaria virginiana*, Ros aci = *Rosa acicularis*, Rub pub = *Rubus pubescens*). Species with positive scores were associated with the positive (black) pattern and species with negative scores are associated with the negative (white) pattern. The magnitude of the species score, indicating the strength of the association, is shown by the symbol size.

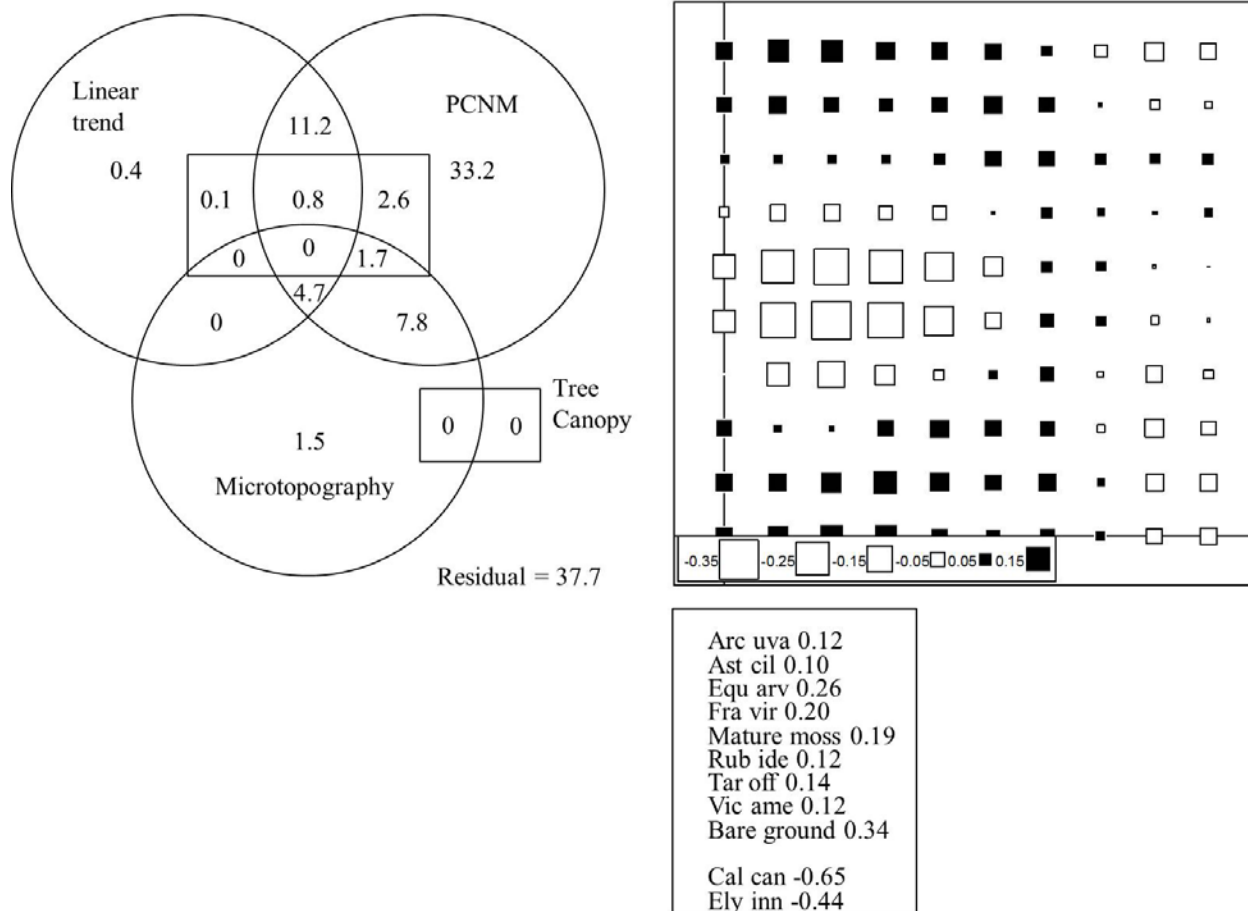


Figure E.18: Results of PCNM analysis (right) and variation partitioning (left) for grid 15, which was an older – fine-textured site type. The variation partitioning included linear trend, PCNM (spatial), microtopography and tree canopy components; the percent variation for each is given and the value in overlapping sections of the diagram indicates the percent of variation shared by the two. Residual indicates the unexplained variation. The PCNM diagram shows the results for correlation of species with the first RDA axis; the diagram is representative of the layout of the grid plot. Species driving the spatial pattern are shown below it (Arc uva = *Arctostaphylos uva-ursi*, Ast cil = *Aster ciliolatus*, Equ arv = *Equisetum arvense*, Fra vir = *Fragaria virginiana*, Rub ide = *Rubus idaeus*, Tar off = *Taraxacum officinale*, Vic ame = *Vicia americana*, Cal can = *Calamagrostis canadensis*, Ely inn = *Elymus innovatus*). Species with positive scores were associated with the positive (black) pattern and species with negative scores are associated with the negative (white) pattern. The magnitude of the species score, indicating the strength of the association, is shown by the symbol size.

APPENDIX 7: ASSESSING THE SODIUM BUFFERING CAPACITY OF RECLAMATION MATERIALS IN SANDHILL FEN

TERMS OF USE

University of Saskatchewan was retained by Syncrude to carry out the studies presented in this report and the material in this report reflects the judgment of author(s) in light of the information available at the time of document preparation. Permission for non-commercial use, publication or presentation of excerpts or figures requires the consent of the author(s). Commercial reproduction, in whole or in part, is not permitted without prior written consent from Syncrude. An original copy is on file with Syncrude and is the primary reference with precedence over any other reproduced copies of the document.

Reliance upon third party use of these materials is at the sole risk of the end user. Syncrude accepts no responsibility for damages, if any, suffered by any third party as a result of decisions made or actions based on this document. The use of these materials by a third party is done without any affiliation with or endorsement by Syncrude.

Additional information on the report may be obtained by contacting Syncrude.

This appendix may be cited as:

Lindsay, M., and Vessey, C. 2017. Assessing the sodium buffering capacity of reclamation materials in Sandhill Fen Final Project Report. Appendix 7 in Syncrude Canada Ltd. *Sandhill Fen Watershed: Learnings from a Reclaimed Wetland on a CT deposit*. Syncrude Canada Ltd. 2020.

Final Project Report

Assessing the sodium buffering capacity of reclamation materials in Sandhill Fen

Prepared for: Reclamation and Closure Research
Syncrude Canada Ltd.

Submitted: July 18, 2017

Prepared by: Matthew Lindsay, Ph.D.
Assistant Professor

Colton Vessey, B.Sc.
Research Assistant

Department of Geological Sciences
University of Saskatchewan

EXECUTIVE SUMMARY

This report summarizes the findings of a University of Saskatchewan research project to examine potential for ion exchange reactions to limit sodium (Na) migration within soil reclamation cover materials at Sandhill Fen. Field sampling was conducted in July 2015 to assess the potential for, and extent of, Na attenuation within the soil reclamation cover. Laboratory column experiments were then conducted to assess the Na attenuation capacity of individual reclamation soil cover materials under controlled conditions. The results of this research indicated that Na attenuation is controlled by ion exchange reactions with calcium (Ca) and, to a lesser extent, magnesium (Mg). Analysis of field samples indicated that oil sands process water (OPSW) from underlying composite tailings (CT) deposit has migrated upward through the reclamation soil cover in an area immediately south of the wetland. The apparent absence of vertical concentration gradients at these locations suggested that the remaining Na attenuation capacity of the reclamation cover soil materials was limited. Results of the laboratory column experiments indicated that ion exchange reactions within till and peat initially can support substantial Na attenuation. However, dissolved Na concentrations remained elevated and the Na attenuation capacity of these materials was quickly consumed. Overall, this research indicated Na attenuation by peat and till used in soil reclamation covers will likely be both limited and short-lived.

TABLE OF CONTENTS

EXECUTIVE SUMMARY	II
LIST OF TABLES.....	IV
LIST OF FIGURES.....	V
LIST OF ABBREVIATIONS	VI
1. INTRODUCTION	1
2. RESEARCH HYPOTHESES AND OBJECTIVES.....	1
3. SITE DESCRIPTION.....	2
4. METHODS.....	2
4.1. Field sampling.....	2
<i>4.1.1. Core sample collection.....</i>	<i>2</i>
<i>4.1.2. Pore-water extraction and analyses.....</i>	<i>3</i>
<i>4.1.3. Solid-phase analyses.....</i>	<i>3</i>
4.2. Laboratory columns.....	4
<i>4.2.1. Setup.....</i>	<i>4</i>
<i>4.2.2. Input Solutions.....</i>	<i>5</i>
<i>4.2.3. Sample collection and analysis.....</i>	<i>5</i>
4.3. Geochemical modeling.....	5
5. RESULTS AND DISCUSSION.....	6
5.1. Field sampling.....	6
<i>5.1.1. Solid-phase characteristics.....</i>	<i>6</i>
<i>5.1.2. Pore-water chemistry.....</i>	<i>7</i>
5.2. Laboratory columns.....	10
<i>5.2.1. Column Solids.....</i>	<i>10</i>
<i>5.2.2. Flow characteristics.....</i>	<i>10</i>
<i>5.2.3. Effluent geochemistry.....</i>	<i>10</i>
<i>5.2.4. Mass Balance Calculations.....</i>	<i>12</i>
6. CONCLUSIONS.....	13
7. REFERENCES.....	14
APPENDIX: DATA SUMMARY.....	37

LIST OF TABLES

Table 4.1. Locations and corresponding depth to FFT-water interface for geochemical samples..... 17

Table 4.2. Target input solution chemistry for column experiments..... 18

Table 5.1. Cation exchange capacity determined by the methylene blue method for soil core samples collected along transect B – B' 19

DRAFT

LIST OF FIGURES

Figure 3.1. Satellite image of Sandhill Fen showing sampling transects A – A’ and B – B’ .	20
Figure 4.1. Satellite image of Sandhill Fen showing soil core locations.	21
Figure 4.2. Photograph of experimental setup used for the column experiments.	22
Figure 5.1. X-ray diffraction patterns obtained for soil core samples collected along transect B – B’ .	23
Figure 5.2. Exchangeable ion concentrations determined by LiCl extraction and normalized per unit mass of dry soil sample.	24
Figure 5.3. Pore-water pH, alkalinity (Alk) and electrical conductivity (EC) for soil core samples collected along transect B – B’ .	25
Figure 5.4. Depth profiles of pore-water calcium (Ca), magnesium (Mg), sodium (Na) and potassium (K) concentrations for soil core samples collected along transect B – B’ .	26
Figure 5.5. Plot of $\delta^2\text{H}$ versus $\delta^{18}\text{O}$ for pore-water from soil core samples collected along transect B – B’ . Local meteoric water line (LMWL) from Baer et al (2016) and linear regression line.	27
Figure 5.6. Principal component analysis (PCA) diagram showing statistical relationships between the major cations and anions.	28
Figure 5.7. Piper diagram of pore-water chemistry from soil core samples collected along transect B – B’ .	29
Figure 5.8. Depth profiles of pore-water chloride (Cl), sulfate (SO_4) and oxygen-18 ($\delta^{18}\text{O}$) concentrations for soil core samples collected along transect B – B’ .	30
Figure 5.9. Depth profiles of pore-water calcium (Ca), magnesium (Mg), sodium adsorption ratio (SAR), chloride (Cl) and sulfate (SO_4) in milliequivalents for soil core samples collected along transect B – B’ .	31
Figure 5.10. Values of pH, alkalinity (Alk.), electrical conductivity (EC), and chloride (Cl) in column effluent (symbols) and input solutions (dashed lines) over time.	32
Figure 5.11. Dissolved concentrations of total iron (Fe), total manganese (Mn), sulfate (SO_4) and strontium (Sr) in column effluent (symbols) for input solutions (dashed lines) over time.	33
Figure 5.12. Dissolved concentrations of sodium (Na), calcium (Ca), magnesium (Mg), and potassium (K) in column effluent (symbols) for input solutions (dashed lines) over time.	34
Figure 5.13. Cumulative masses of sodium (Na), calcium (Ca), magnesium (Mg) and potassium (K) calculated for column effluent (symbols) for input solutions (dashed lines) over time.	35
Figure 5.14. Cumulative mass storage versus cumulative volume calculated in milliequivalents for sodium (Na), calcium (Ca), magnesium (Mg) and potassium (K) from modeled free ion activities in column effluent.	36

LIST OF ABBREVIATIONS

AOSR	Athabasca Oil Sands Region
CBE	Charge Balance Error
CEC	Cation Exchange Capacity
CRDS	Cavity Ring-Down Spectroscopy
CT	Composite Tailings
DI	Deionized
EC	Electrical Conductivity
HDPE	High Density Polyethylene
IC	Ion Chromatography
ICP-MS	Inductively Coupled Plasma – Mass Spectrometry
ICP-OES	Inductively Coupled Plasma – Optical Emission Spectrometry
LMWL	Local Meteoric Water Line
OSPW	Oil Sands Process-Affected Water
PES	Polyethersulfone
Pf	Pleistocene fluvial
PP	Polypropylene
PTFE	Polytetrafluoroethylene
PVC	Polyvinylchloride
XRD	X-Ray Diffraction

1. INTRODUCTION

Elevated calcium concentrations were observed in surface waters of the Sandhill Fen shortly after establishment. Concerns were raised that these elevated Ca concentrations may result from ion exchange with Na during migration of oil sands process-affected water (OSPW; Allen, 2008) from the underlying composite tailings deposit through the sub-soil (clay-rich Pleistocene till) and peat (salvaged live peat) layers that comprise the reclamation soil cover. This reaction is described by the following equation:



where X represents a single exchange site within the reclamation cover materials. Ion exchange with Mg may also contribute to Na attenuation:



Although elevated Ca or Mg concentrations are not a water quality issue, increasing Na concentrations in ground water and surface waters may increase as Ca and Mg occupied exchange sites become depleted. Elevated Na concentrations can degrade soil structure by causing clay dispersion and swelling, which in turn reduces infiltration capacity, hydraulic conductivity and plant-available water. Additionally, elevated sodium concentrations can have detrimental impacts on the health of plants and aquatic organisms. Ongoing research – by others – at Sandhill Fen has demonstrated that the electrical conductivity of surface waters and shallow groundwater has steadily increased steadily over the past few years. These observations are indicative of OSPW migration through the reclamation soil cover materials and subsequent discharge to SHF surface waters. This study was conducted to provide insight into relationships between ion exchange reactions and water chemistry within Sandhill Fen and the broader reclamation landscape.

2. RESEARCH HYPOTHESES AND OBJECTIVES

This study was developed based upon the hypotheses that: (1) elevated calcium concentrations were derived from ion exchange with sodium within reclamation soil cover materials; and (2) ion exchange reactions will have limited influence on Na migration through reclamation soil cover materials. Therefore, the overall project goal was to constrain the current extent of, and capacity for, ion exchange reactions to buffer sodium migration within the reclamation soil cover. This overall goal will be achieved through the following objectives:

- assess the distribution of dissolved ions in pore waters of the reclamation cover;

- determine cation exchange capacity (CEC) of the reclamation materials; and
- evaluate the Na buffering capacity of these materials under dynamic flow conditions.

By accomplishing these research objectives, both research hypotheses were tested and the overall project goal was realized. More generally, the results of this study improve understanding of the geochemical behaviour of reclamation soil cover materials within wetland reclamation systems.

3. SITE DESCRIPTION

Sandhill Fen is a 50-ha experimental reclamation watershed located approximately 35 km north of Fort McMurray, Alberta (57.057°N 111.600°W) at the Mildred Lake mine. The watershed, which contains a 17-ha wetland, was constructed in a decommissioned open pit that was filled with approximately 40 m of interbedded composite tailings (CT; Matthews et al., 2002) and tailings sand layers. Composite tailings are produced by combining fine tailings, tailings sand and gypsum [CaSO₄•2H₂O], to reduce water content and promote dewatering (Kasperski and Mikula, 2011). Calcium derived from gypsum acts exchanges for Na at clay-mineral surfaces of FFT solids, thereby promoting dewatering and coagulation. The CT pore-water chemistry is initially derived from OSPW; however, gypsum addition produces elevated SO₄ and Na concentrations.

The CT deposit is overlain by 10 m of processed tailings sand and a 1 m thick reclamation cover comprised of 0.5 m of salvaged live peat overlying 0.5 m of clay-rich Pleistocene till. The chemical composition of the CT deposit is spatially heterogeneous (Reid and Warren, 2016). Hydrogeological modeling predicted vertical migration of CT pore water through the reclamation cover at some locations – particularly at the southern margin of the wetland – within the Sandhill Fen watershed (BGC, 2015).

4. METHODS

4.1. Field sampling

Core samples of the reclamation soil cover were collected from Sandhill Fen in July of 2015. These cores were used for examining pore-water geochemistry, solid-phase geochemistry, and mineralogy.

4.1.1. Core sample collection

Soil cores were collected from 10 locations along two principle transects (Table 4.1). These transects, A – A' and B – B', were selected based upon results of hydrogeological modeling (BGC, 2014) to capture locations where upward vertical groundwater migration and discharge to surface water was predicted. Samples were collected into polyvinyl chloride (PVC) liners using a soil core sampler that was

advanced using a slide hammer. Sequential cores were collected over 0.15 m intervals a maximum depth of 0.9 m, which approached the lower boundary of the reclamation soil cover. Upon retrieval, the cores were capped and sealed, refrigerated (4°C), and transported to the University of Saskatchewan for analysis.

4.1.2. Pore-water extraction and analyses

Pore-water samples were extracted and analyzed for a total of 38 samples collected at seven locations (i.e., US-SHF-04, US-SHF-05, US-SHF-06, US-SHF-07, US-SHF-08, US-SHF-09, US-SHF-10). Extraction utilized a mechanical squeezing method similar to that described by Moncur et al. (2013). Briefly, sub-samples collected from each core were packed into stainless steel cylinders between a porous stainless-steel plate (bottom) and piston (top). The piston was fitted with O-rings to create a water-tight seal against the cylinder wall. Viton tubing was connected to an outlet at the bottom of the cylinder to facilitate sample collection. A hydraulic press was used to advance the piston and compress the sample; displaced water was collected into polypropylene (PP) syringes (Norm-Ject, HSW) connected to Viton tubing with a polycarbonate Luer-Lok valve.

Measurements of pH, electrical conductivity (EC) and alkalinity were made immediately following sample collection. The pH electrode (Orion 9678BNWP, Thermo Scientific, USA) was calibrated to NIST-traceable pH 4, 7 and 10 buffers. The conductivity cell (Orion 013010MD, Thermo Scientific, USA) was calibrated to NIST-traceable conductivity standards. Calibrations were checked before each measurement and recalibration was performed as required. Remaining pore water was passed through 0.2 µm polyether sulfone (PES) filter membranes. Alkalinity was determined by titration with 1.6 N H₂SO₄ to the bromocresol green methyl red endpoint (i.e., 4.5). Samples were collected into high density polyethylene (HDPE) bottles, preserved according to standard methods, and stored at 4°C until chemical analysis. Inorganic anion concentrations were determined by ion chromatography (IC). Stable isotopes of water ($\delta^2\text{H-H}_2\text{O}$, $\delta^{18}\text{O-H}_2\text{O}$) were measured using a vapor equilibration method (Wassenaar et al., 2008) by cavity ring down spectroscopy (CRDS). Major element concentrations were determined by inductively coupled plasma – optical emission spectroscopy (ICP-OES) on samples acidified to pH < 2 using trace-metal grade nitric acid. Thermodynamic equilibrium modelling of pore-water geochemistry was performed using the PHREEQCi (Version 3.1.5) code with the MINTEQA2 V4 database (Parkhurst and Appelo, 2013).

4.1.3. Solid-phase analyses

Gravimetric water contents were determined in triplicate for 24 samples by weighing before and after oven drying at 105°C for at least 24 hours. Cation exchange capacity was determined for 19 samples following a modified methylene blue method described by Holden et al. (2012). Briefly, 20g equivalent

dry weight of each sample was dispersed in 500 mL of deionized water (DI) and then titrated using a 0.02 M methylene blue solution. The titration endpoint corresponded to volume of methylene blue solution required to produce a blue halo around sample suspensions pipetted onto filter paper (Holden et al., 2012). Final CEC values were calculated using the formula reported by Holden et al. (2012). The CEC determinations were performed in triplicate on two core samples to assess the reproducibility of this method.

Exchangeable ions concentrations were measured for 24 core samples using a modified LiCl method described by Holden et al. (2012). Briefly, fresh sub-sample was combined with DI water to form a saturated paste, 10 g of which was then combined with 25 mL of 0.4 M LiCl solution prepared in DI water. This mixture was then shaken and centrifuged, and the supernatant was decanted and passed through a 0.2 μm PES filter membrane. This process was repeated two additional times and the filtered supernatant samples were pooled prior to quantification of Na, K, Ca and Mg by ICP-OES. Exchangeable ion concentrations were determined by subtracting mass of dissolved ions associated with soil pore water (§ 3.2.1) from the total mass present in solution following the extraction procedure.

X-ray diffraction (XRD) was performed with a Co $K\alpha_1$ source (1.78901 Angstroms), and a Fe beta filter at 45 mA and 40 kV. Air-dried samples were lightly ground in an agate mortar and pestle and mounted on glass slides (Moore and Reynolds, 1997). The XRD instrument (Empyrean, PANalytical) was operated using a 3-80° 2 θ step size and 50-minute counting. Phase identification was performed with Match! (v. 2.3.3), using the Crystallography Open Database (Gražulis et al., 2009).

4.2. Laboratory columns

Column experiments were conducted to examine ion exchange reactions within individual reclamation cover materials under dynamic flow conditions. Two simulated waters and three reclamation materials were considered in these controlled laboratory experiments.

4.2.1. Setup

Column experiments were conducted on the laboratory benchtop with the three principal materials used during construction of the Sandhill Fen: (i) clay-rich Pleistocene till; (ii) dewatered peat; and (iii) Pleistocene fluvial (Pf) sand. Each material was packed into two separate acrylic columns (L: 10 cm; ID: 7.6 cm) producing a total of six columns (Figure 4.2). The final columns contained an 8-cm interval of reclamation material between two 1-cm layers of acid-washed 20–40 mesh Ottawa sand. Each packed column was fitted with one inlet and one outlet port. The inlet port was connected with polytetrafluoroethylene (PTFE) tubing to a high-precision, low-flow multi-channel peristaltic pump (Model 2058, Watson-Marlow, Inc.). The outlet port was connected in series to a sealed overflow

sampling cell and then to an overflow waste jug. The columns were wrapped in Al foil to limit growth of phototrophs and to minimize photochemical reactions. Prior to starting the experiment, the columns were flushed for 48 hours with CO_{2(g)}, which is highly soluble in water and, therefore, helps to minimize trapped bubbles during saturation.

4.2.2. Input Solutions

Two input solutions were prepared to simulate groundwater chemistry observed in monitoring wells located below the reclamation cover within Sandhill Fen (Table 4.2). The chemistry for input solutions 1 and 2 were based upon 2013 groundwater chemistry data provided by Dr. C. Mendoza for SH-GW-23-D and EIP-08-10-D, respectively. These solutions were prepared by dissolving reagent-grade salts (i.e., Na₂SO₄, NaCl, NaHCO₃, CaCl₂·2H₂O, MgCl₂·6H₂O, KCl) in DI water. These solutions were then transferred into 2 L amber-glass bottles and pumped into the columns in an upward direction using a multi-channel peristaltic pump (Watson Marlow 2058). The composition (Table 4.1) of the stock solution remained constant throughout the experiment and was refilled weekly from a stored stock solution of both water chemistries. All glassware was cleaned in 10 % (v/v) hydrochloric acid bath and thoroughly rinsed in DI water before use.

4.2.3. Sample collection and analysis

Column influent and effluent samples were collected weekly to monitor ion exchange reactions as a function of time. The input samples were collected directly from the stock solution, while effluent samples were collected from the sampling cell. Samples were collected into PP syringes either transferred directly into glass culture tubes or passed through 0.45 μm PES syringe filters. Measurements of pH were made on unfiltered samples using a ROSS pH electrode (Orion 9678BNWP, Thermo Scientific, USA) that was calibrated to NIST-traceable pH 4, 7 and 10 buffers. Electrical conductivity measurements were performed using an EC cell (Orion 013010MD, Thermo Scientific, USA) that was calibrated to NIST-traceable conductivity standards. Calibrations were checked before each measurement and recalibration was performed as required. Alkalinity was determined on filtered samples by titration with 1.6 N H₂SO₄ to the bromocresol green methyl red endpoint (i.e., 4.5). Filtered samples were collected into HDPE bottles and stored at 4°C until analysis. Inorganic anions were quantified by IC on non-acidified samples, whereas major elements were quantified by ICP-OES on samples first acidified to pH < 2 using trace metal grade HNO₃.

4.3. Geochemical modeling

Geochemical modeling was performed to assess data quality and to assist with data interpretation. Modeling was performed using the PHREEQCi software package (version 3.1.5.9113; Parkhurst and Appelo, 2013) with the integrated WATEQ4F thermodynamic database (Ball and Nordstrom, 1991). Data

quality for the chemical analyses was assessed using speciated charge balance errors (CBE) calculated using PHREEQCi. These modeled CBE values – ion balance expressed as a percentage – provide a better indication of data quality than those calculated solely from total major ion concentrations. The saturation state of water samples with respect to relevant mineral phases (e.g., calcite, dolomite, gypsum) was also determined. These values provide insight into the thermodynamic potential for the precipitation or dissolution of a given phase.

Speciated CBE values calculated with PHREEQCi for field samples were consistently smaller than $\pm 5\%$, which is generally indicative of accurate analyses. In contrast, initial speciated CBE values for column samples were indicative of analytical issues, which were later attributed to Ca and Na values determined by ICP-MS. Consequently, samples were re-analyzed by ICP-OES to determine Ca and Na concentrations and substantial differences were noted. The modeled CBE values for including ICP-OES data from the re-analyzed samples were greatly improved, with 82 % of samples ($n = 204$) exhibiting values smaller than $\pm 5\%$. In total, 96 % of samples exhibited speciated CBE values smaller than $\pm 7\%$, while values for two samples were greater than 10 %. Overall, these results are indicative of high-quality data; however, the challenging chemistry of these samples (i.e., high dissolved salt concentrations) clearly presented analytical challenges.

5. RESULTS AND DISCUSSION

5.1. Field sampling

5.1.1. Solid-phase characteristics

Moisture content of the cores ranged from 0.17 to 0.85 % (w/w), but were consistently lower within the sub-soil relative to the peat. The sub-soil moisture content averaged $23 \pm 4.0\%$ (w/w), whereas the peat moisture content averaged $69 \pm 19\%$ (w/w). Measured CEC values for the sub-soil samples ranged from 6.4 to 14 meq 100 g⁻¹ with an average value for all samples ($n = 16$) of 10 ± 2.0 meq 100 g⁻¹ (Table 5.1). Samples from locations US-SHF-06 (18-24) and US-SHF-06 were analyzed in triplicate and results were highly reproducible at 12 ± 0.1 meq 100 g⁻¹ and 9.6 ± 0.4 meq 100 g⁻¹, respectively. These values are slightly higher than methylene blue CEC values previously reported for Pleistocene till in the AOSR (Holden et al., 2012). Methylene blue titrations were attempted for the peat samples; however, visual determination of the titration endpoint was challenging and calculated CEC values were not reproducible. Mineralogical analysis of the sub-soil samples revealed that the clay content was dominated by kaolinite, illite and chlorite (Figure 5.1). The measured CEC values are generally consistent with the clay mineralogy and content of the sub-soil samples (Carrol, 1959).

Exchangeable ions concentrations among all sub-soil samples followed the general order $Mg > Ca > Na > K$ (Figure 5.2). However, distinct differences were observed between sampling locations positioned along transect B – B'. Exchangeable ions at locations US-SHF-04 and US-SHF-05 followed the general order $Ca > Na > Mg > K$, whereas the order was $Mg > Na > Ca > K$ among the remaining sites. These results are inconsistent with Pleistocene till from the AOSR, which exhibit exchangeable ion concentrations that follow the general order $Ca > Mg > K > Na$ (Holden et al., 2012). An important difference between the current study and these previous results is that the sub-soil within Sandhill Fen has, potentially, encountered OSPW from the underlying tailings deposit. Although the difference in exchangeable Ca and Mg concentration between sites remained unclear, the relative abundance of Na within these samples is greater than Pleistocene till from the AOSR.

Average exchangeable Mg (0.62 ± 0.21 meq 100 g^{-1}) was greater than Ca (0.47 ± 0.805 meq 100 g^{-1}) among all samples (Figure 5.2). Although spatial trends in Mg were not apparent, exchangeable Ca was substantially higher (1.5 ± 0.86 meq 100 g^{-1}) than the overall average at locations US-SHF-04 and US-SHF-05. Exchangeable Na ranged from 0.09 to 1.7 meq 100 g^{-1} (average 0.39 ± 0.45 meq 100 g^{-1}), but averaged 0.96 ± 0.52 meq 100 g^{-1} at locations US-SHF-04 and US-SHF-05. In contrast to both Ca and Na, exchangeable K concentrations (average 0.04 ± 0.03 meq 100 g^{-1}) were relatively low and exhibited limited spatial variability. In addition to higher exchangeable Ca and Na concentrations at locations US-SHF-04 and US-SHF-05, the fraction of exchangeable ions normalized to measured CEC was up to 10 times higher.

5.1.2. Pore-water chemistry

Pore-water pH ranged 5.55 to 8.31 (average 7.03 ± 0.72) with values less than 7.0 limited to the peat layer (Figure 5.3). The lowest pH values were observed in uppermost sample from locations US-SHF-04 and US-SHF-05. Alkalinity exhibited a wide range from 43 to 610 mg L^{-1} (as CaCO_3) among all samples. These values generally increased with depth at locations US-SHF-04, US-SHF-05, US-SHF-08, and US-SHF-09. An opposite trend was observed at US-SHF-07, which was located within a zone of sub-soil with no overlying peat layer (i.e., till extending from surface to 1.0 m). Alkalinity averaged 270 ± 150 mg L^{-1} (as CaCO_3) among all sites and depth dependent variation was generally greater than variations among individual sites. However, the lowest measured alkalinity values, which were less than 60 mg L^{-1} as CaCO_3 , occurred at depths where pore-water pH was < 6.0 . For samples with pH was greater than 6.4, HCO_3^- is the dominant contributor to alkalinity. Electrical conductivity averaged 2200 ± 800 $\mu\text{S cm}^{-1}$ and generally decreased from location US-SHF-04 to US-SHF-08. However, elevated EC values of up to 4000 $\mu\text{S cm}^{-1}$ were observed in the uppermost sample at locations US-SHF-04, US-SHF-05 and US-SHF-07, which was attributed to evaporation.

In general, pore-water Cl concentrations followed a similar spatial trend to EC values. Concentrations ranged from 28 to 880 mg L⁻¹ (average 220 ± 230 mg L⁻¹) with the highest concentrations observed in the uppermost samples from locations US-SHF-04 and US-SHF-05 (Figure 5.4). Average Cl concentrations for given locations generally decreased along the transect from location US-SHF-04 (680 ± 110 mg L⁻¹) to US-SHF-08 (64 ± 5.6 mg L⁻¹). Despite similar spatial trends, Cl concentrations and EC values were poorly correlated, suggesting different ions contribute to measured EC at different sampling locations or depths. Dissolved sulfate concentrations generally exhibited an opposite spatial trend to that of Cl. Sulfate concentrations ranged from 262 to 2206 mg L⁻¹ (average 830 ± 410 mg L⁻¹) among all sites, with the highest location-averaged concentration found at US-SHF-07 (1140 ± 530 mg L⁻¹). Similar to EC, concentrations of both Cl and SO₄ exhibited increases near surface at locations US-SHF-04, US-SHF-05 and US-SHF-07.

Pore-water Ca concentrations (Figure 5.5) averaged 250 ± 110 mg L⁻¹ among all samples; however, location-averaged concentrations were much lower at US-SHF-04 (140 ± 78 mg L⁻¹) compared to US-SHF-06 (360 ± 46 mg L⁻¹) and US-SHF-07 (360 ± 130 mg L⁻¹). Corresponding Mg concentrations followed similar spatial trends and averaged (65 ± 34 mg L⁻¹) overall. In contrast, average pore-water Na concentrations were more than five times higher at US-SHF-04 (560 ± 30 mg L⁻¹) than at US-SHF-07 (100 ± 50 mg L⁻¹) or US-SHF-08 (88 ± 11 mg L⁻¹). These Na concentrations follow a similar spatial trend to that of Cl, where the highest location-averaged concentrations were also observed at US-SHF-04. These trends are generally opposite to observed trends in Ca, Mg and SO₄, suggesting soil pore water within Sandhill Fen is derived from more than one source.

Statistical analysis of pore-water chemistry data including Pearson correlation and principal component analysis (PCA) revealed positive relationships between: Na and Cl; Mg, Ca and SO₄; K and HCO₃ (Figure 5.6). The PCA results revealed a strong negative correlation on the PC3 axis between K and HCO₃. While on the PC1 axis there is a well-defined opposing relationship between Ca, Mg, SO₄ and on the other side lies Na and Cl. These trends are apparent in a spatial association within the geochemical data along transect B – B' through Sandhill Fen. The composition of these waters was compared to that of shallow groundwater within Pleistocene tills of the Canadian Prairies (Hendry et al., 2004, Hendry et al., 1986) and to that of OSPW (Gibson et al., 2013). This comparison was undertaken to compare soil pore-water chemistry from Sandhill Fen to likely end-member waters. The Piper diagram generated from these data (Figure 5.7) revealed a mixing trend between Na-Cl type water characteristic of OSPW to a Ca-Mg-SO₄ type water characteristic of Pleistocene till pore waters. This trend suggests that soil pore-water obtained from location US-SHF-04 is dominated by OSPW, whereas pore-water from locations US-SHF-

07, US-SHF-08 and US-SHF-09 was more characteristic of shallow groundwater in regional Pleistocene tills.

To further constrain the two sources of water, and mixing between these sources along transect B – B', stable isotopes of water (i.e., $\delta^{18}\text{O}$, $\delta^2\text{H}$) were also measured. Values of $\delta^{18}\text{O}$ ranged from -11.23 ‰ to -18.16 ‰ while $\delta^2\text{H}$ values ranged from -107.0 ‰ to -146.6 ‰ (Figure 5.8). Comparison of these isotopic signatures to data recently published by Baer et al. (2016) on natural waters and OSPW in the AOSR revealed similar trends to the pore-water samples. More specifically, samples from locations US-SHF-07 and US-SHF-08 exhibited $\delta^2\text{H}$ and $\delta^{18}\text{O}$ values that fall on weighted local meteoric water line (LMWL) for the Mildred Lake Mine (Baer et al. 2016) and were, therefore, consistent with local precipitation. In contrast, samples for US-SHF-04 and US-SHF-05 exhibited $\delta^2\text{H}$ and $\delta^{18}\text{O}$ values more indicative of evaporation, which is consistent with OSPW from the Mildred Lake Settling Basin and tailings pore waters from West-In-Pit (Baer et al., 2016). A mixing line between samples obtained along transect B – B' was also apparent, providing further evidence for spatial differences in the presence of OSPW within soil pore waters.

Spatial trends in pore-water composition are generally consistent with previous hydrogeological modeling (BGC, 2016). These models predicted a discharge zone at the south margin of the Sandhill Fen wetland area, which is well aligned with locations where pore-water chemistry and isotopic signatures are most consistent with OSPW. Comparison of depth profiles for major ions (i.e., Na, Ca, Mg, Cl, SO_4) concentrations in meq L^{-1} reinforced the transition in soil pore-water chemistry from OSPW to background shallow groundwater along the B – B' transect (Figure X). These data also suggest that capacity for Na attenuation via ion exchange was likely limited at location US-SHF-04 and declining at locations US-SHF-05 and US-SHF-06.

These spatial trends are also reinforced by calculated sodium adsorption ratio (SAR) values, which are used as an indicator of the potential for clay particles to flocculate or disperse within soils. The SAR ratio for each pore-water sample was calculated using the following equation:

$$SAR = \frac{[Na]}{\sqrt{\frac{[Ca] + [Mg]}{2}}}$$

where concentrations of Na, Ca, and Mg are in meq L^{-1} . The SAR values ranged from 0.8 to 14 meq L^{-1} and exhibited an average value of $3.9 \pm 3.9 \text{ meq L}^{-1}$ (Figure 5.9). Values $> 9 \text{ meq L}^{-1}$, which suggests clay dispersion are likely to have negative impacts on soil permeability, were observed only at location US-SHF-04. In contrast, SAR values were < 3 in sub-soil samples at US-SHF-06 and for all samples at US-

SHF-07, US-SHF-08, and US-SHF-09. These low SAR values generally correspond to locations where pore-water composition was consistent with background shallow groundwater.

5.2. Laboratory columns

5.2.1. Column Solids

Cation exchange capacity for the fresh Pleistocene till (sub-soil) averaged 7.8 ± 0.33 meq 100g^{-1} . The CEC of peat and Pf sand used in these experiments were not quantified in this study. However, previous studies have reported CEC values of 100 to 500 meq 100g^{-1} for peat (Grim, 1953) and 0.6 to 2.0 meq 100g^{-1} for quartz-feldspar sand (Ganguly, 1951; Nash and Marshall, 1956). Additional method development or different methods would need to be used to quantify the CEC of these materials.

5.2.2. Flow characteristics

Porosity was not measured directly, but was estimated from column volumes, and material mass and density, to be 0.45, 0.80, and 0.35 in the till, peat, and sand columns, respectively. The input solutions were passed through the columns at a rate of approximately 28 mL per day during the experiment. Over the entire 28-week experiment, between 4.8 and 5.2 L of input solution were passed through each column. These volumes corresponded to approximately 31, 17, and 38 pore volumes for the till, peat, and sand columns, respectively. Transport within the till and peat columns was likely influenced by the dual porosity characteristics (Rezanezhad et al., 2012); however, this aspect of the experiments will be evaluated through future reactive transport modeling.

5.2.3. Effluent geochemistry

The pH of input solutions 1 and 2 steadily increased from approximately 8.5 to 9.4 during the experiment. Effluent pH for both till columns (SFX-01, SFX-02) and both peat columns (SFX-03, SFX-04) was near-neutral (i.e., 6.9 to 7.1) over the first 14 to 21 days of the experiment (Figure 5.10). Like the input solutions, effluent pH in these columns increased with time and stabilized between 7.7 and 8.1 after approximately 75 days. Effluent pH for both sand columns (SFX-05, SFX-06) increased during the first 75 days and remained between 8.9 and 9.1 for the remainder of the experiment. Geochemical modeling indicated initial pH values were controlled by $\text{CO}_{2(\text{g})}$ dissolution associated with initial column setup.

Alkalinity was initially elevated within all columns, but decreased over the first 25 days when values were generally consistent with the input solutions. Alkalinity within both till and sand column effluents subsequently mirrored that of the input solution, which averaged 800 mg L^{-1} (as CaCO_3). In contrast, alkalinity within the peat columns increased again after 25 days, peaking at approximately 1400 mg L^{-1} (as CaCO_3) after 40 days, and declining again to near input values. This alkalinity increase was attributed

to microbial oxidation of organic carbon within the peat columns. Observed increases in effluent Fe and Mn concentrations, combined with SO₄ removal, are consistent with this interpretation (Figure 11).

Electrical conductivity in column effluent was consistent with the input solutions after approximately 30 days. However, during the initial 30 days of the experiment, EC values were elevated in column effluent relative to the input solutions. The largest observed difference was for the peat columns (SFX-03, SFX-04), where initial effluent EC values approached two times the input value. Geochemical modeling indicated that these trends were associated with initial dissolution of gypsum or other minerals within the columns. Effluent Cl tracked the input solution values throughout the experiment, confirming that Cl transport is conservative within these materials.

Substantial differences in effluent Na relative to input concentrations were observed within the till and peat columns (Figure 12). During the first 7 d of the experiment, effluent Na concentrations within these columns were approximately one half of the input concentrations (i.e., $C/C_0 = 0.5$). The magnitude of this initial decrease is generally consistent with Na attenuation in batch experiments conducted on Pleistocene tills (Holden et al., 2011). Nevertheless, effluent Na concentrations in all columns were consistently greater than 500 mg L⁻¹ during the experiment. Sodium attenuation also declined over time and, after approximately 75 d, effluent Na concentrations were consistently greater than 800 mg L⁻¹. Over 80 % of the cumulative Na mass removal occurred during the initial 75 d and, overall, only 13 to 16% of Na introduced into the till (SFX-01, SFX-02) and peat (SFX-03, SFX-04) columns was attenuated. Results were generally consistent among columns receiving input solutions 1 and 2, suggesting that the presence of SO₄ had limited impact on Na attenuation. Overall, these results suggest that the Na attenuation capacities of the till and peat were largely exhausted within 12 and 7 pore volumes, respectively. In contrast, Na attenuation within the Pf sand columns (SFX-05, SFX-06) was limited throughout the experiment.

Effluent Ca concentrations were initially elevated relative to the input solutions, but decreased rapidly over the first 25 to 75 days of the experiment (Figure 12). Initial effluent Ca concentrations exceeded 1000 mg L⁻¹ for the peat columns (SFX-03, SFX-04) and exceeded 350 mg L⁻¹ for the till columns (SFX-01, SFX-02). Calcium release from the sand columns produced initial effluent concentrations of approximately 350 mg L⁻¹ (SFX-05) and 140 mg L⁻¹ (SFX-06). Calcium concentrations decreased rapidly and reached an apparent steady state at approximately 10 and 40 times the input concentrations for till and peat columns, respectively. Geochemical modeling indicated that effluent from the till and sand columns was consistently undersaturated with respect to gypsum, whereas initial effluent collected from the peat columns during the first three weeks was supersaturated with respect to gypsum. Similar trends in early effluent concentrations of both Ca and SO₄ from the peat columns suggest that

gypsum dissolution likely contributed Ca to solution. A relative increase in effluent EC from the peat columns during this time is also consistent with mineral dissolution. Speciation modeling indicated effluent from all columns was consistently supersaturated with respect to calcite and dolomite, which suggests that carbonate-mineral dissolution was unlikely an important source of dissolved Ca after the first 1 to 2 pore volumes.

Magnesium concentrations in column effluents followed similar trends to Ca; however, the magnitude was substantially lower in the till and peat columns (Figure 12). Early effluent Mg concentrations ranged from 100 to 200 mg L⁻¹ for the till columns and from approximately 150 to 300 mg L⁻¹ for the peat columns. These concentrations decreased to near input solution concentrations after 75 to 100 d for the peat and till columns. In contrast to Ca, this observation suggests that long-term Mg release was limited for these materials. Although effluent Mg concentrations from the sand columns were slightly greater than input concentrations at the first sampling time (7 d), this difference was minimal for the remainder of the experiment.

Potassium transport through the Pf sand columns (SFX-05, SFX-06) was largely conservative (Figure 12). Effluent K concentrations for the peat columns were slightly greater than the input solutions over the first 14 to 21 d, and then slightly less than the input solutions for the remainder of the experiment. Considerable K attenuation was observed over the duration of the experiment for both till columns (i.e., SFX-01, SFX-02). Nevertheless, input and effluent K concentrations were consistently lower than that of Na, Ca, and Mg.

5.2.4. Mass Balance Calculations

Mass balance calculations were performed to examine the influence of ion exchange reactions on Na, Ca, Mg and K concentrations within each column. The change in mass storage, dM_j , for a given solute, j , was calculated by subtracting the effluent solute mass, $M_{j,out}$, from the input solute mass, $M_{j,in}$:

$$dM_j = M_{j,in} - M_{j,out} \quad (\text{Eq. 5.1})$$

where $M_{j,out}$ and $M_{j,in}$ were calculated as the product of water volume (L), dV_i , over a given sampling interval, i , by the mean effluent concentration (mmol L⁻¹) of the solute, $\bar{m}_{j,i}$, over that time interval, and by the valence (meq mmol⁻¹) of the solute ion, z_j :

$$M_{j,i} = dV_i \cdot \bar{m}_{j,i} \cdot z_j \quad (\text{Eq. 5.2})$$

The cumulative mass, $M_{j,sum}$, was determined by summation of masses determined at each sampling interval:

$$M_{j,sum} = \sum_{i=1}^n M_{j,i} \quad (\text{Eq. 5.3})$$

Comparison of cumulative input and effluent masses revealed that a relatively small proportion of total Na was stored within the till and peat columns (Figure 13). In contrast, both Ca and Mg were released (i.e., negative mass storage) from the columns during the experiment. Column effluent was consistently understatured with respect to Na-bearing mineral phases, and ion exchange reactions involving Ca and Mg were, therefore, assumed the principal Na attenuation mechanism. Consequently, deviation from a 1:1 milliequivalent mass ratio between Na (plus K) and Ca plus Mg would be indicative of other reactions.

These calculations revealed an apparent excess of Ca plus Mg milliequivalents discharged from the peat columns (SFX-03, SFX-04), when assuming ion exchange was the only Na attenuation mechanism. Additionally, these calculations indicated that excess Na was discharged from the till columns (SFX-01, SFX-02) relative to Ca and Mg. However, geochemical equilibrium (thermodynamic) modeling predicted extensive aqueous complexation of Ca, Mg and Na. For example, only 30 to 40% of total Ca and Mg, and 70 to 80% of total Na, were predicted to occur as free ions (i.e., Ca^{2+} , Mg^{2+} , Na^+) in the till column. This result is important because free ions – not complexed ions – are available for ion exchange reactions.

The mass balance calculations were, therefore, also performed using free ion (i.e., Ca^{2+} , Mg^{2+} , Na^+) activities to further examine relationships between Na attenuation and the release of Ca and Mg from the columns:

$$M_{j,i} = dV_i \cdot \bar{a}_{j,i} \cdot z_j \quad (\text{Eq. 5.4})$$

where $\bar{a}_{j,i}$ was the mean activity of a solute ion, j , predicted by thermodynamic equilibrium modeling.

Calculations using activities also revealed excess Ca and Mg released from the till columns compared to Na attenuation (Figure 14). This result suggests that precipitation of a Ca-bearing mineral phase likely occurred within these columns. Modeled saturation indices suggested that precipitation of secondary calcite [CaCO_3] or another Ca-bearing carbonate phase could have influenced Ca discharge from the till columns. Despite initial Ca release, Na attenuation within the peat columns approximately equaled Ca and Mg release during the experiment. This observation suggests ion exchange reactions were the dominant controls major ion concentrations within the peat columns. Results for the sand columns were more variable due to small cumulative storage or release of exchangeable ions.

6. CONCLUSIONS

The field sampling campaign indicated that Na attenuation is likely limited and short-lived. Results of solid-phase and pore-water analyses revealed that elevated Ca concentrations observed in Sandhill Fen surface waters was unlikely derived from ion exchange with Na during migration of OSPW through the reclamation soil cover. Instead, the chemical and isotopic signatures of soil pore water suggest that the

elevated Ca concentrations may be associated with background shallow groundwater typical of Pleistocene tills found in the Canadian Prairies. Analysis of soil pore-water samples obtained along a south to north transect of the Sandhill Fen revealed a mixing trend between OSPW-influenced groundwater to the south and background shallow groundwater within the wetland area. This distribution of OSPW-type water was generally consistent with previously modeled groundwater discharge zones (BGC, 2015). The apparent absence of a vertical Na breakthrough curve within soil pore water vertical trends in pore water composition (i.e., increasing dissolved Na concentrations with depth) at individual sampling locations suggests that ion exchange reactions have limited impact on Na migration.

The column experiments demonstrated that substantial Na exchange may be achieved by till and peat during initial pore volumes. However, Na attenuation declined rapidly and breakthrough eventually occurred with continual input of simulated OSPW. Although effluent concentrations decreased by up to one half during the first pore volume, Na concentrations were consistently elevated throughout the experiment. Sodium attenuation was controlled by ion exchange reactions, whereas dissolved Ca and Mg concentrations were likely influenced by mineral precipitation-dissolution reactions.

Results of the field study and column experiments indicated that ion exchange reactions will not effectively limit Na transport over time. Initial Na attenuation within till and peat was controlled by ion exchange reactions involving Ca and Mg, yet pore-water and effluent Na concentrations remained elevated. These results suggest that decision-making related to soil cover system design should take into consideration the limited influence of till and peat on long-term Na migration.

7. REFERENCES

- Allen, E.W. (2008). Process water treatment in Canada's oil sands industry: I. Target pollutants and treatment objectives. *Journal of Environmental Engineering and Science*, 7, 123–138.
- Baer, T., Barbour, S.L., Gibson, J.J. (2016). The stable isotopes of site wide waters at an oil sands mine in northern Alberta, Canada. *Journal of Hydrology*, 541, 1155–1164.
- BGC Engineering Inc. (2015). Sandhill Fen: Numerical Groundwater Modeling, Project No. 0534135. Submitted to Syncrude Canada Ltd., June 12, 2015.
- Carroll, D. (1959). Ion Exchange in Clays and Other Minerals. *Geological Society of America Bulletin*, 70, 749–779.
- Ganguly, A.K. (1951). Base-exchange capacity of silica and silicate minerals: *Journal of Physical and Colloid Chemistry*, 55, 1417–1428.

- Gibson, J.J., Fennell, J., Birks, S.J., Yi, Y., Moncur, M.C., Hansen, B., Jasechko, S. (2013). Evidence of discharging saline formation water to the Athabasca River in the oil sands mining region, northern Alberta. *Canadian Journal of Earth Sciences*, 50, 1244–1257.
- Grim, R.E. (1953). *Clay mineralogy*: New York, McGraw Hill Book Co., Inc., 384.
- Gražulis, S., Chateigner, D., Downs, R.T., Yokochi, A.F.T., Quirós, M., Lutterotti, L., Manakova, E., Butkus, J., Moeck, P., Le Bail, A., 2009. Crystallography open database - an open-access collection of crystal structures. *Journal of Applied Crystallography*, 42, 726–729.
- Hendry, M.J., Cherry, J.A., Wallick, E.I. (1986). Origin and Distribution of Sulfate in a Fractured Till in Southern Alberta, Canada. *Water Resources Research*, 22, 45–61.
- Hendry, M.J., Wassenaar, L.I. (2004). Transport and geochemical controls on the distribution of solutes and stable isotopes in a thick clay-rich till aquitard, Canada. *Isotopes in Environmental and Health Studies*, 40, 3–19.
- Holden, A.A., Donahue, R.B., Ulrich, A.C. (2011). Geochemical interactions between process-affected water from oil sands tailings ponds and North Alberta surficial sediments. *Journal of Contaminant Hydrology*, 119, 55–68.
- Holden, A.A., Mayer, K.U., Ulrich, A.C. (2012). Evaluating methods for quantifying cation exchange in mildly calcareous sediments in Northern Alberta. *Applied Geochemistry*, 27, 2511–2523.
- Kasperski, K.L., Mikula, R.J. (2011). Waste Streams of Mined Oil Sands: Characteristics and Remediation. *Elements*, 7, 387–392.
- Matthews, J.G., Shaw, W.H., MacKinnon, M.D., Cuddy, R.G. (2002). Development of Composite Tailings Technology at Syncrude. *International Journal of Surface Mining, Reclamation and Environment*, 16, 24–39.
- Moncur, M.C., Blowes, D.W., Ptacek, C.J. (2013). Pore-water extraction from the unsaturated and saturated zones. *Canadian Journal of Earth Sciences*, 50, 1051–1058.
- Moore, D.M., & Reynolds, R.C. (1997). X-Ray diffraction and the identification and analysis of clay minerals.
- Nash, V.E., Marshall, C.E. (1956). The surface reactions of silicate minerals. II. Reactions of feldspar surfaces with salt solutions: Univ. Missouri Coll. Agriculture Research Bull. 614, 36.
- Parkhurst, D.L., Appelo, C.A.J., 2013. Description of Input and Examples for PHREEQC Version 3—A Computer Program for Speciation, Batch-Reaction, One-Dimensional Transport, and Inverse

- Geochemical Calculations. In: *Techniques and Methods 6-A43*, U.S. Geological Survey, Denver, USA, 497 pp.
- Reid, M.L., Warren, L.A. (2016). S reactivity of an oil sands composite tailings deposit undergoing reclamation wetland construction. *Journal of Environmental Management*, 166, 321–329.
- Rezanezhad, R., Price, J.S., Craig, J.R. (2012) The effects of dual porosity on transport and retardation in peat: A laboratory experiment. *Canadian Journal of Soil Science*, 92, 723–732.
- Wassenaar, L.I., Hendry, M.J., Chostner, V.L., Lis, G.P. (2008). High resolution pore water $\delta^2\text{H}$ and $\delta^{18}\text{O}$ measurements by $\text{H}_2\text{O}_{(\text{liquid})}$ - $\text{H}_2\text{O}_{(\text{vapor})}$ equilibration laser spectroscopy. *Environmental Science and Technology*, 42, 9262–9267.

DRAFT

Table 4.1. Locations of soil cores obtained during the field sampling campaign.

Transect	Location ID	Latitude	Longitude	Elevation (masl)
A – A'	US-SHF-01	57.03943	-111.58878	332
	US-SHF-02	57.03954	-111.58887	318
	US-SHF-03	57.03922	-111.58889	323
	US-SHF-10	57.04026	-111.58862	312
B – B'	US-SHF-04	57.03899	-111.59110	319
	US-SHF-05	57.03957	-111.59130	315
	US-SHF-06	57.03995	-111.59143	314
	US-SHF-07	57.04015	-111.59139	313
	US-SHF-08	57.04068	-111.59155	314
	US-SHF-09	57.04100	-111.59143	315

DRAFT

Table 4.2. Target input solution chemistry for column experiments.

Parameter	Units	Solution 1	Solution 2
pH		8.5	8.5
sodium (Na ⁺)	mg L ⁻¹	1000	1000
magnesium (Mg ²⁺)	mg L ⁻¹	16	7
potassium (K ⁺)	mg L ⁻¹	18	18
calcium (Ca ²⁺)	mg L ⁻¹	24	12
bicarbonate (HCO ₃ ⁻)	mg L ⁻¹	1100	1100
chloride (Cl ⁻)	mg L ⁻¹	650	900
sulfate (SO ₄ ²⁻)	mg L ⁻¹	900	100

DRAFT

Table 5.1. Cation exchange capacity determined by the methylene blue method for soil core samples collected along transect B – B’.

Location	Mean Depth (m)	CEC (meq 100 g⁻¹)	<i>n</i>
US-SHF-04	0.53	9.6	3
US-SHF-04	0.69	9.4	1
US-SHF-04	0.84	9.3	1
US-SHF-05	0.53	8.5	3
US-SHF-05	0.84	8.0	1
US-SHF-06	0.53	11.3	3
US-SHF-06	0.84	9.6	1
US-SHF-07	0.23	10.4	3
US-SHF-07	0.53	10.2	1
US-SHF-07	0.84	9.1	1
US-SHF-08	0.53	10.3	3
US-SHF-08	0.84	6.4	1
US-SHF-09	0.69	10.0	3
US-SHF-09	0.84	9.0	1



Figure 3.1. Satellite image of Sandhill Fen showing sampling transects A – A' and B – B'. (Image from August 26, 2015, ©2017 DigitalGlobe)

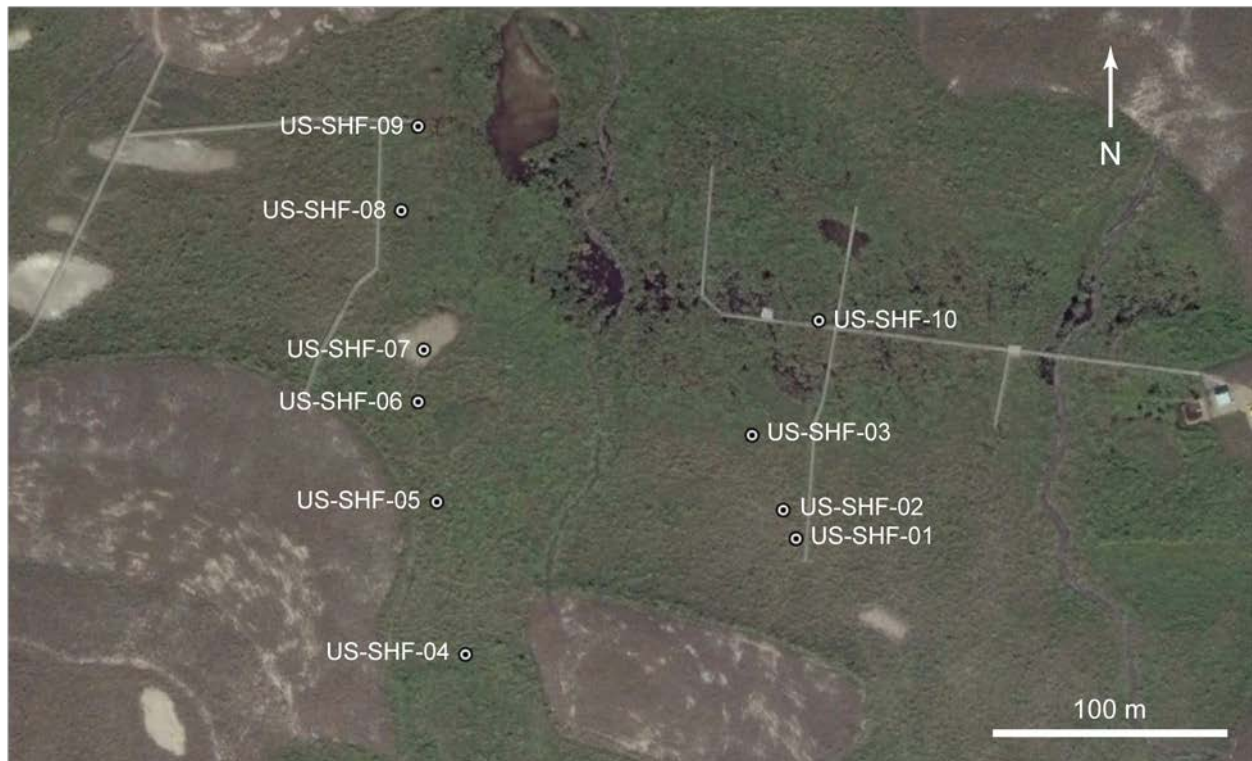


Figure 4.1. Satellite image of Sandhill Fen showing soil core sample locations (Image from August 26, 2015, ©2017 DigitalGlobe).



Figure 4.2. Photograph of experimental setup used for the column experiments.

DRAFT

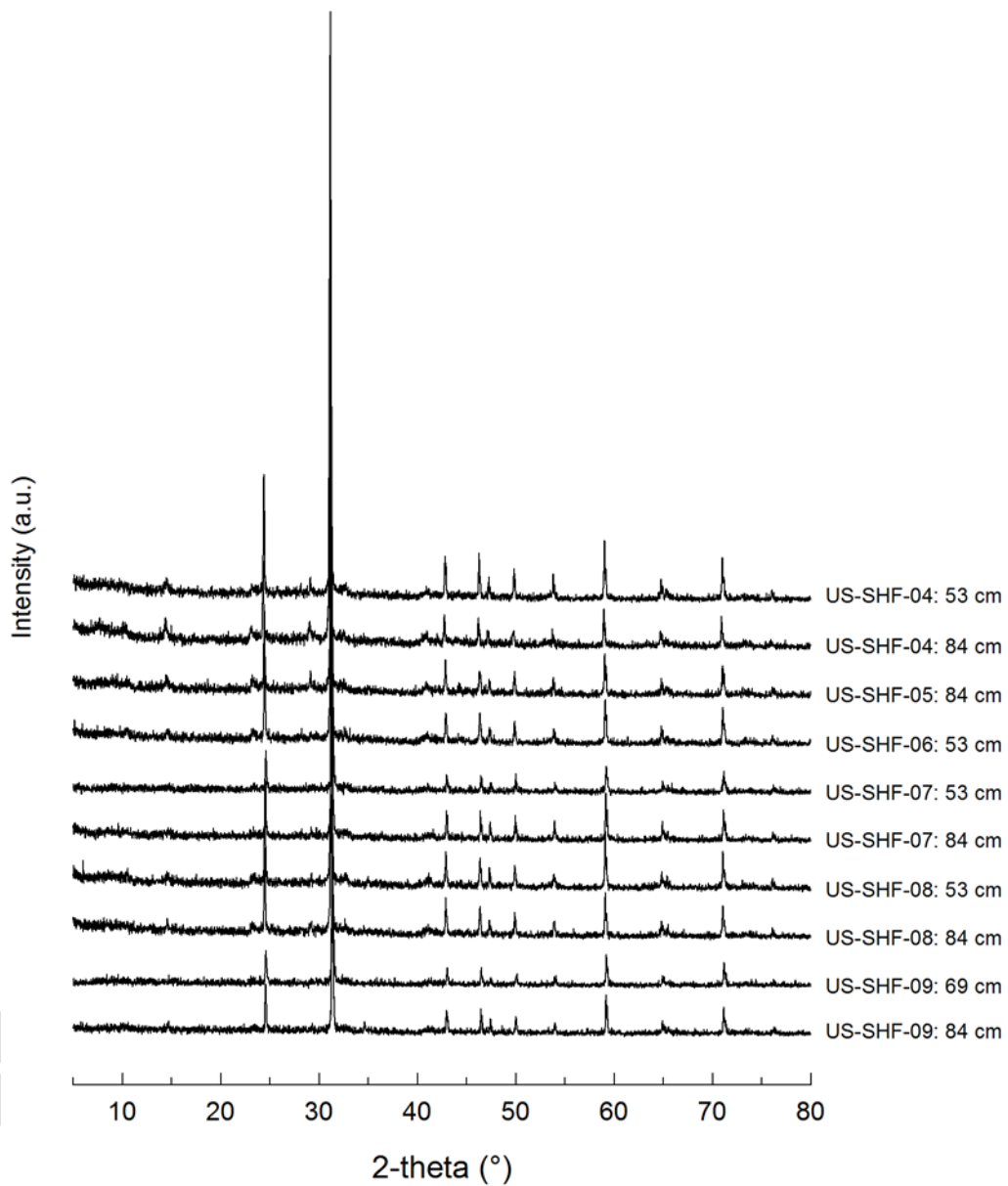


Figure 5.1. X-ray diffraction patterns obtained for soil core samples collected along transect B – B’.

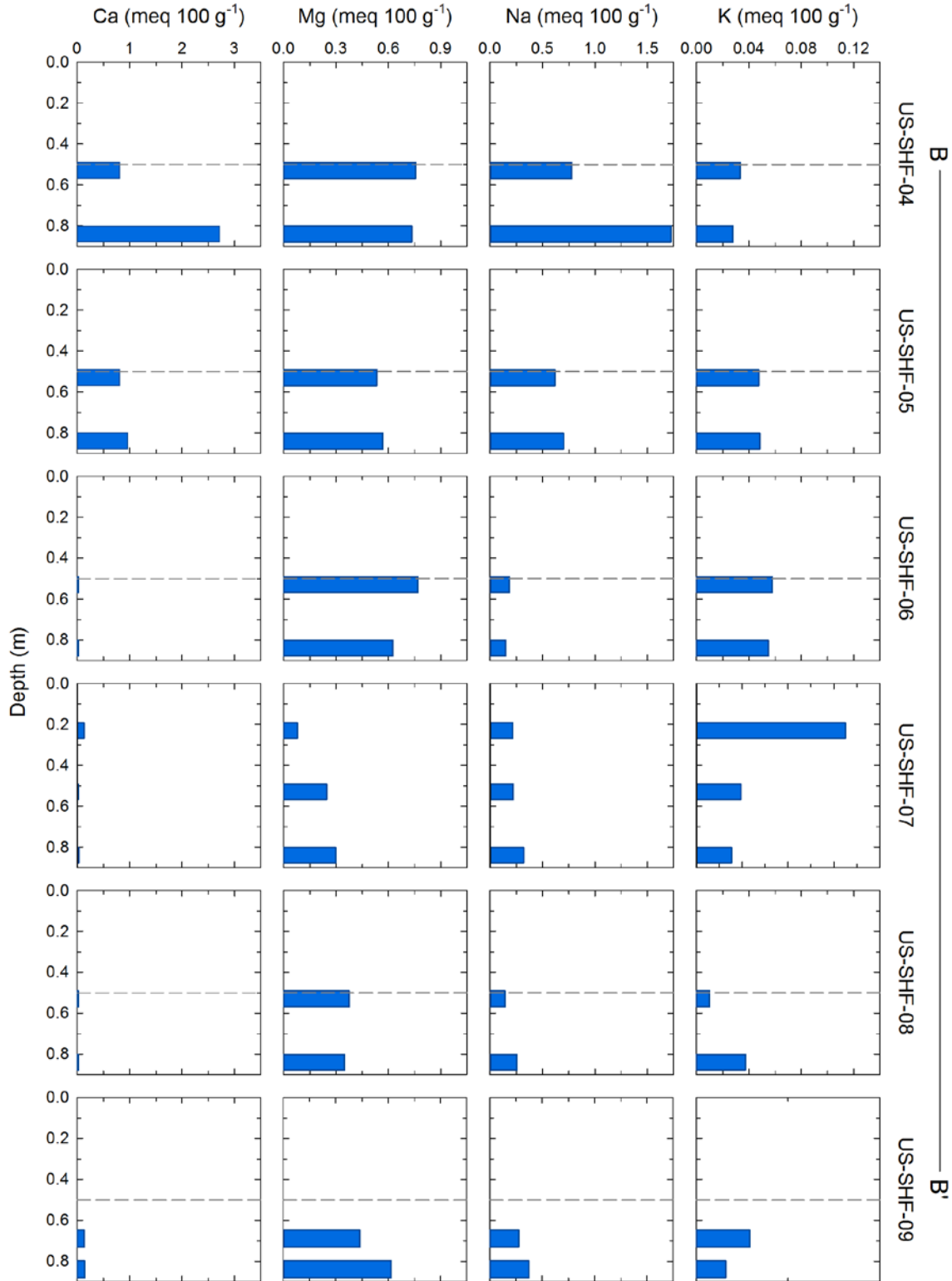


Figure 5.2. Exchangeable ion concentrations determined by LiCl extraction and normalized per unit mass of dry soil sample.

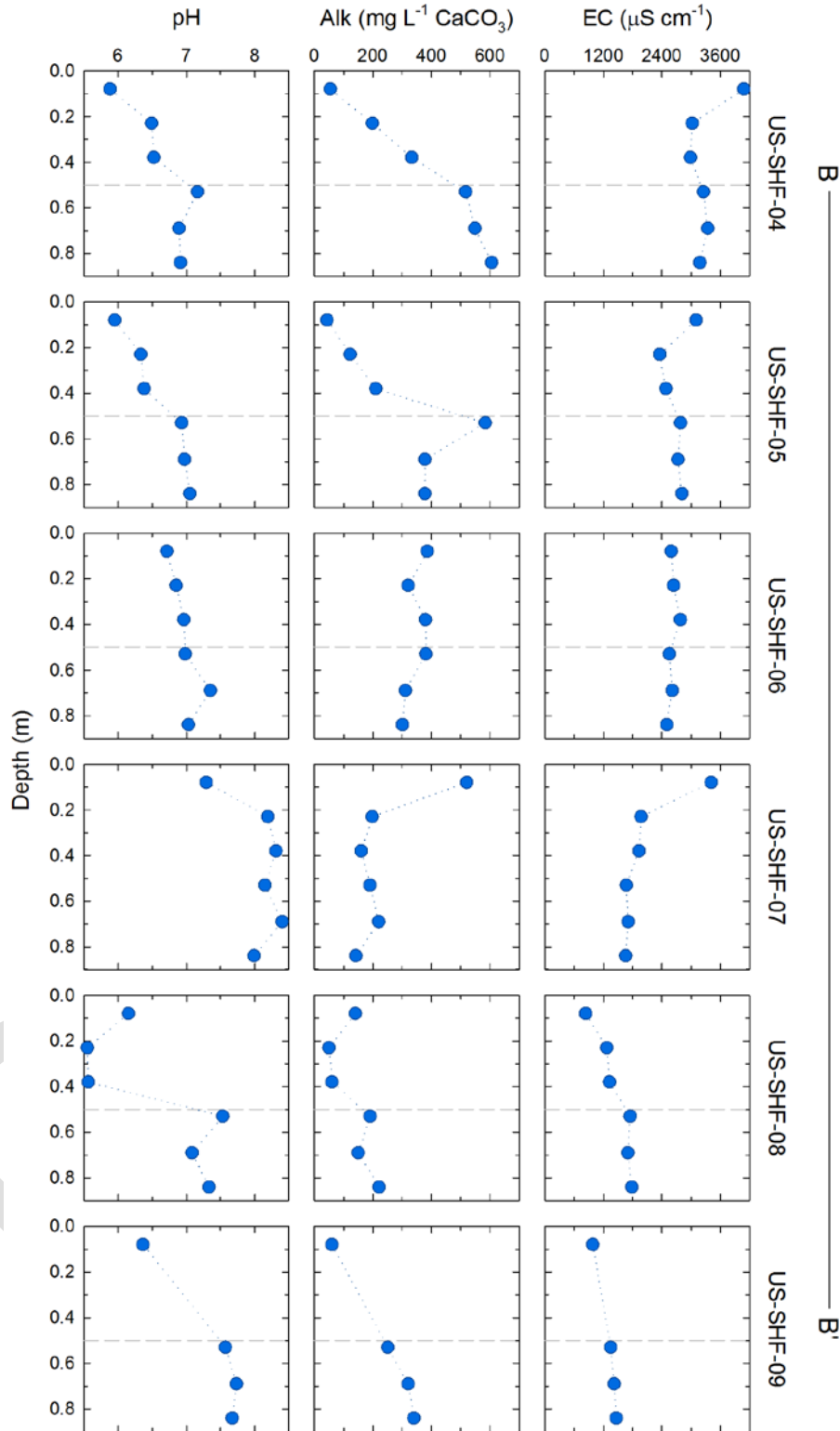


Figure 5.3. Pore-water pH, alkalinity (Alk) and electrical conductivity (EC) for soil core samples collected along transect B – B'.

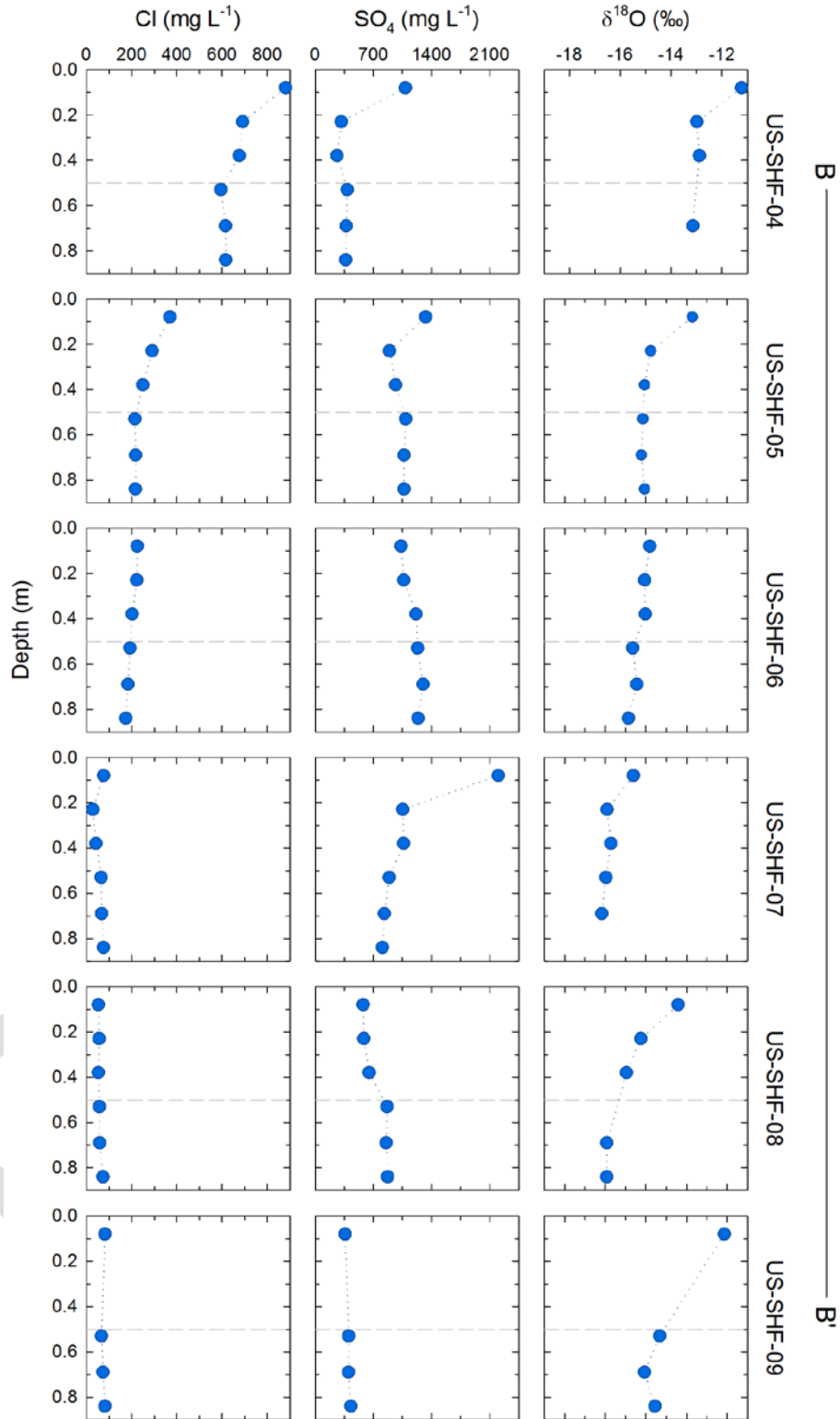


Figure 5.4. Depth profiles of pore-water chloride (Cl), sulfate (SO₄) and oxygen-18 (δ¹⁸O) concentrations for soil core samples collected along transect B – B’.

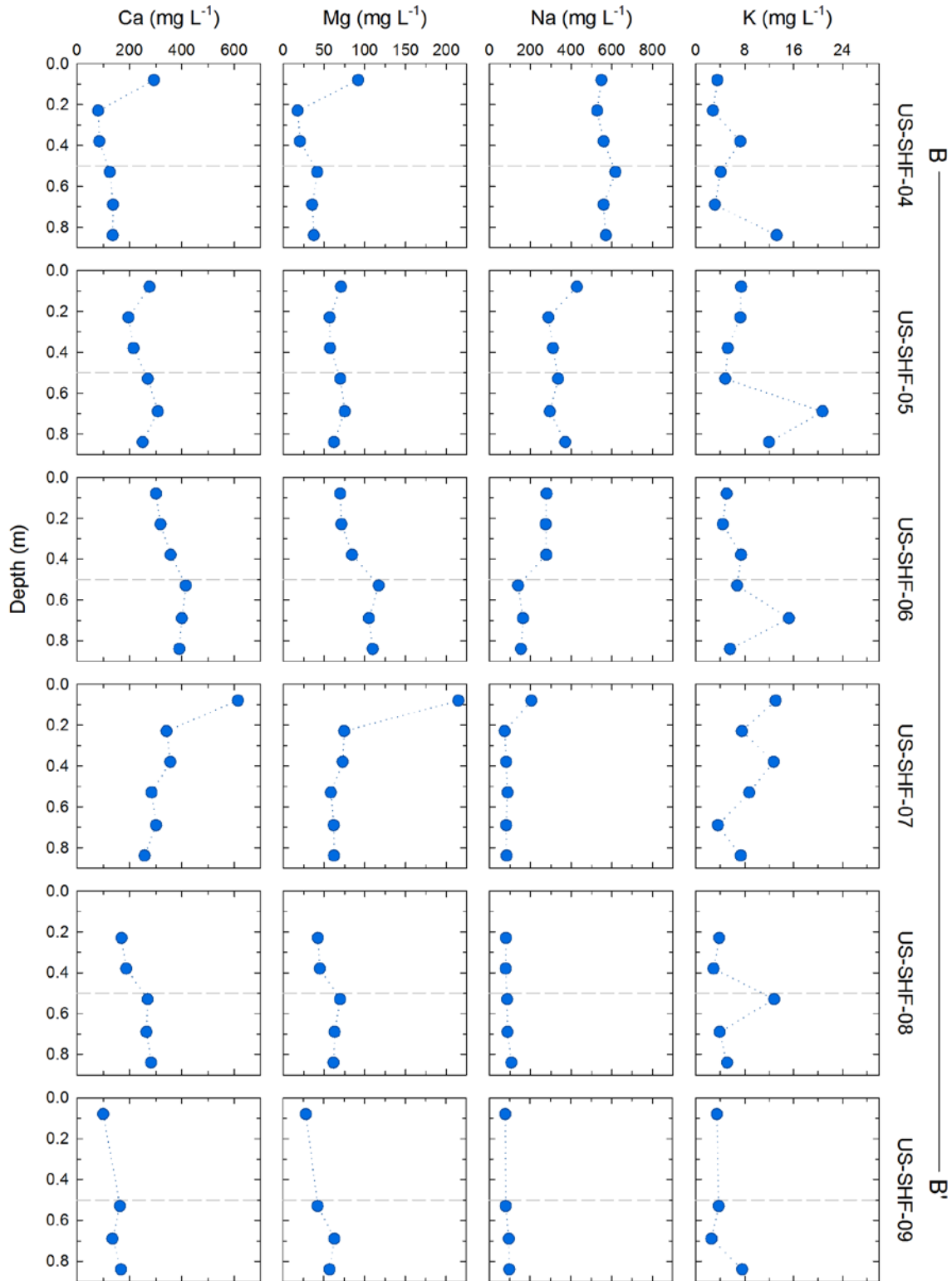


Figure 5.5. Depth profiles of pore-water calcium (Ca), magnesium (Mg), sodium (Na) and potassium (K) concentrations for soil core samples collected along transect B – B'.

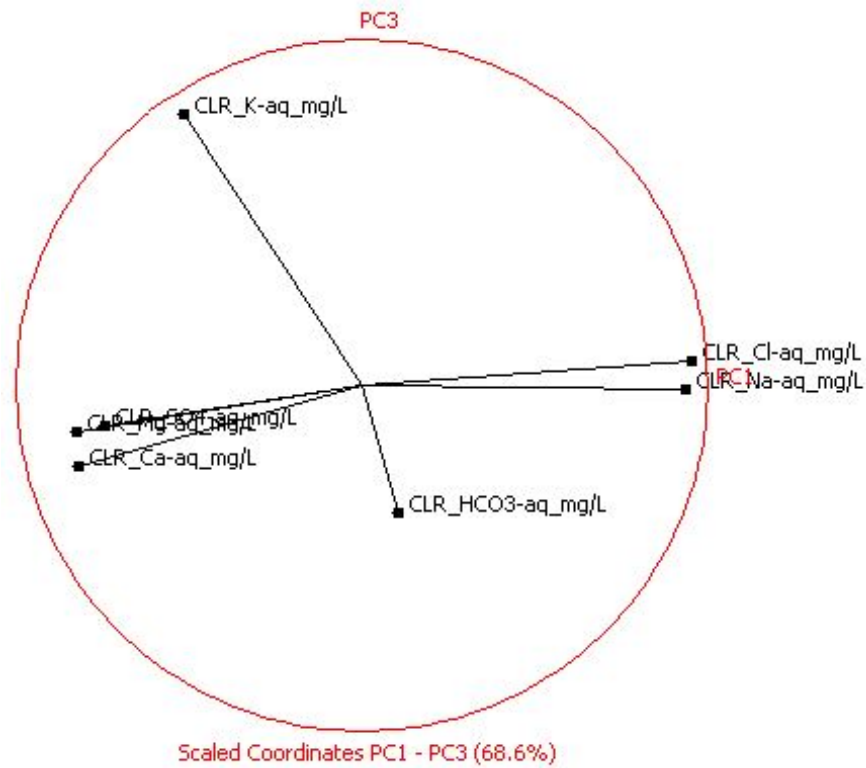


Figure 5.6. Principal component analysis (PCA) diagram showing statistical relationships between the major cations and anions.

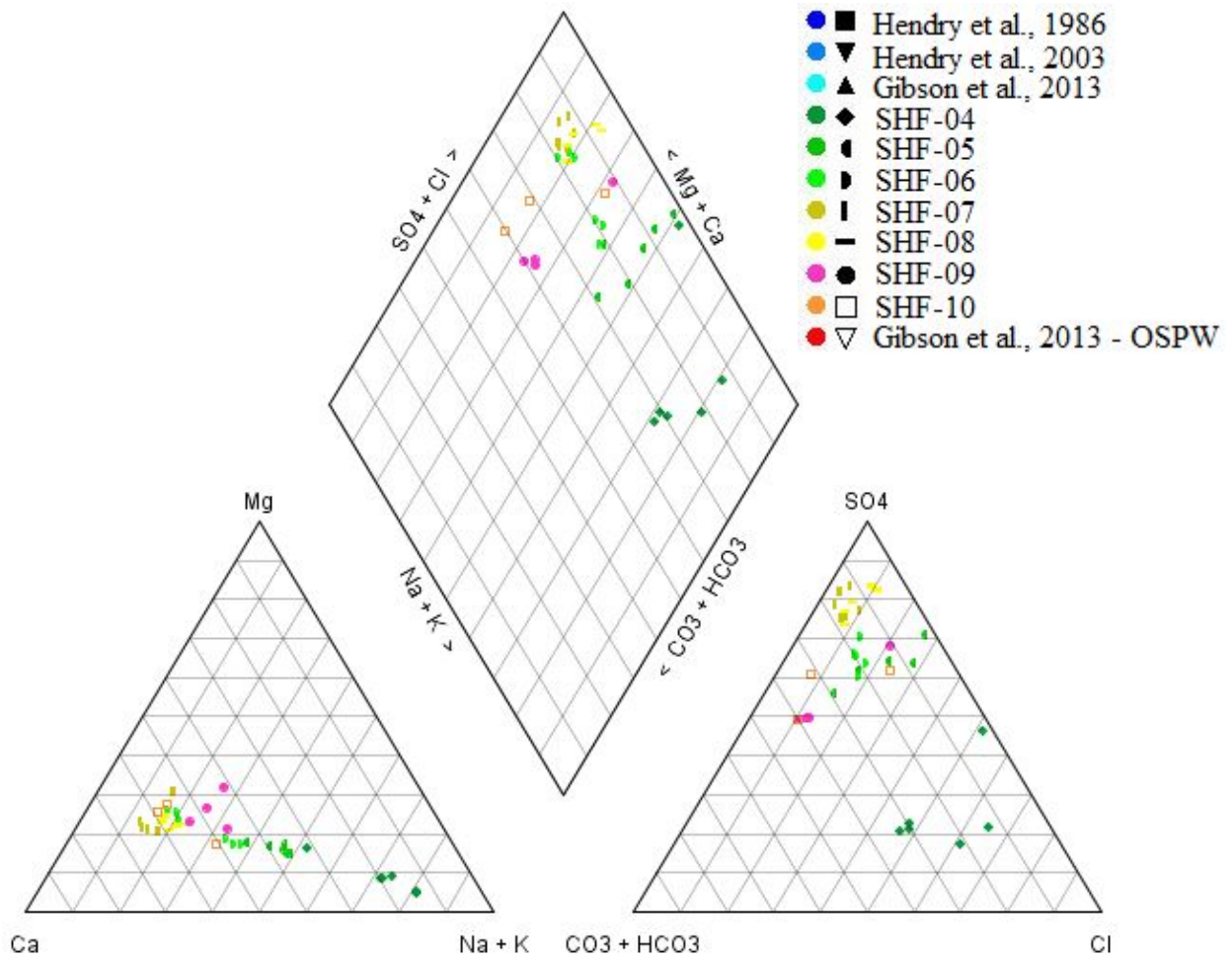


Figure 5.7. Piper diagram of pore-water chemistry from soil core samples collected along transect B – B’.

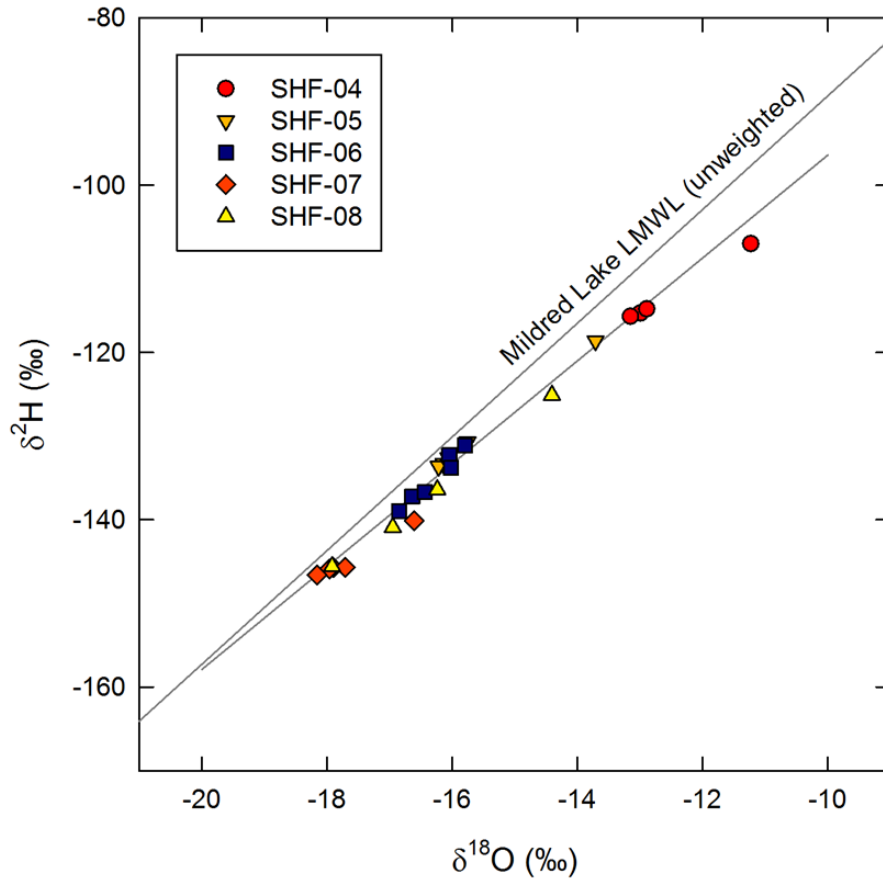


Figure 5.8. Plot of $\delta^2\text{H}$ versus $\delta^{18}\text{O}$ for pore-water from soil core samples collected along transect B – B'. Local meteoric water line (LMWL) from Baer et al (2016) and linear regression line through all data.

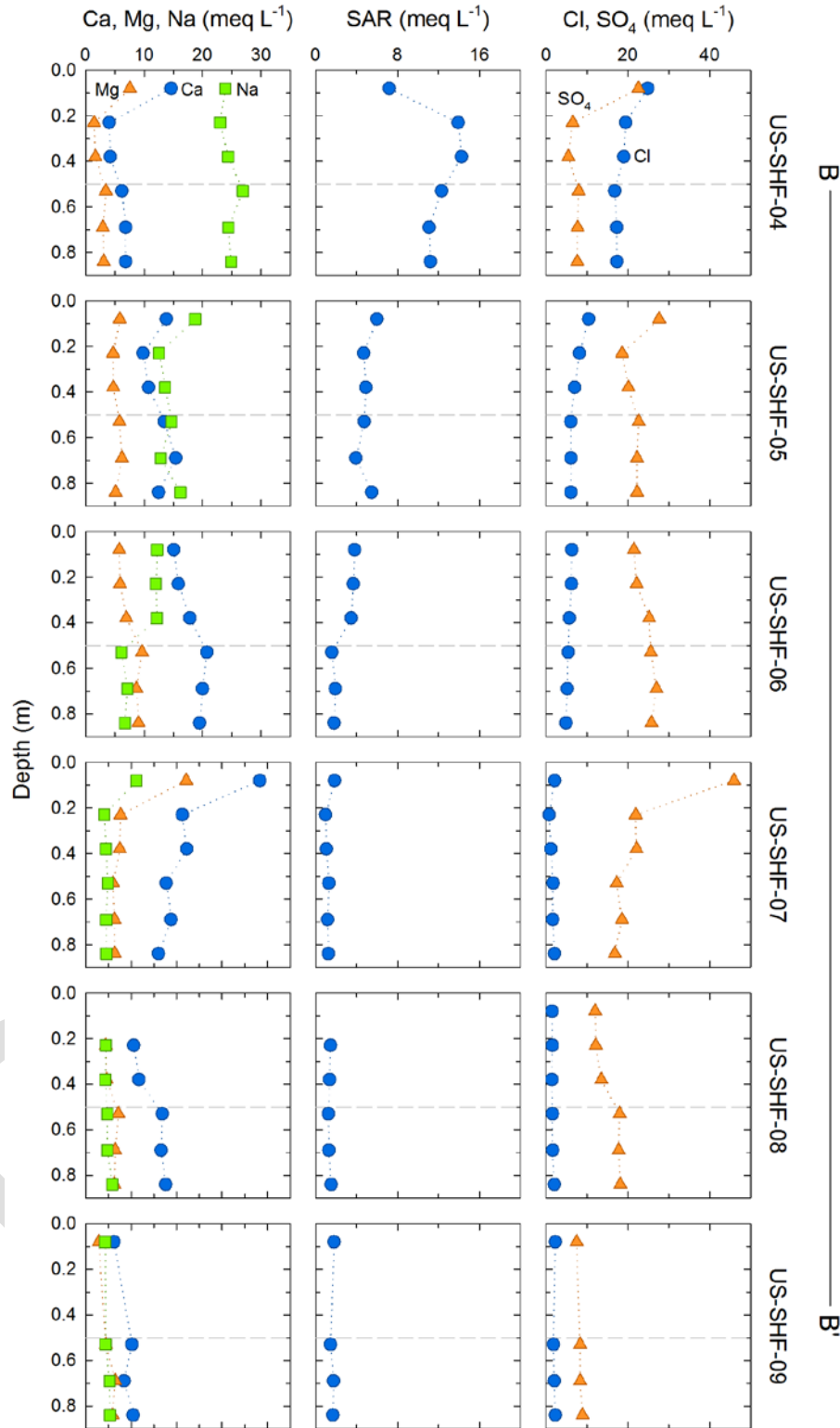


Figure 5.9. Depth profiles of pore-water calcium (Ca), magnesium (Mg), sodium adsorption ratio (SAR), chloride (Cl) and sulfate (SO₄) in milliequivalents for soil core samples collected along transect B – B'.

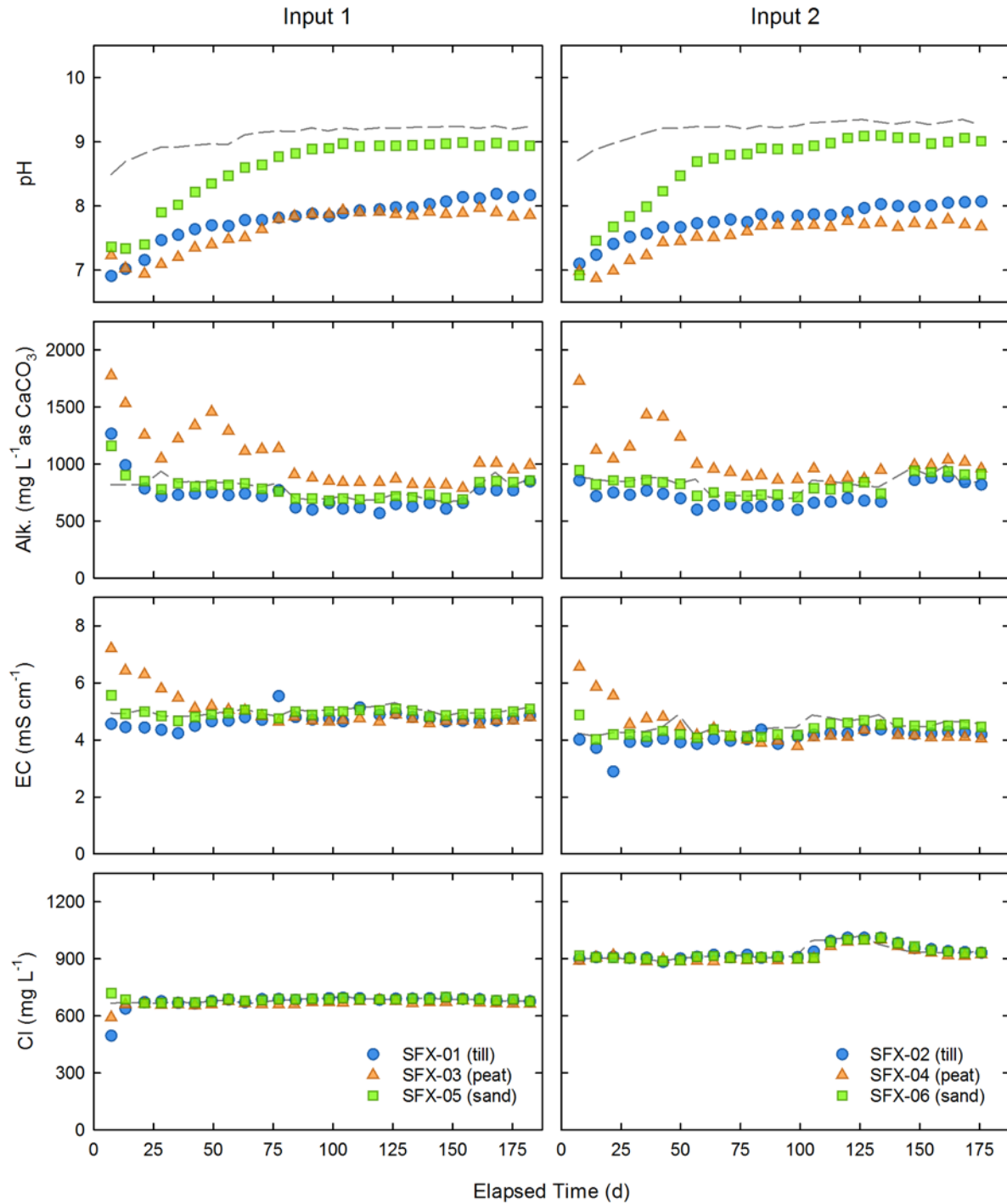


Figure 5.10. Values of pH, alkalinity (Alk.), electrical conductivity (EC), and chloride (Cl) in column effluent (symbols) and input solutions (dashed lines) over time.

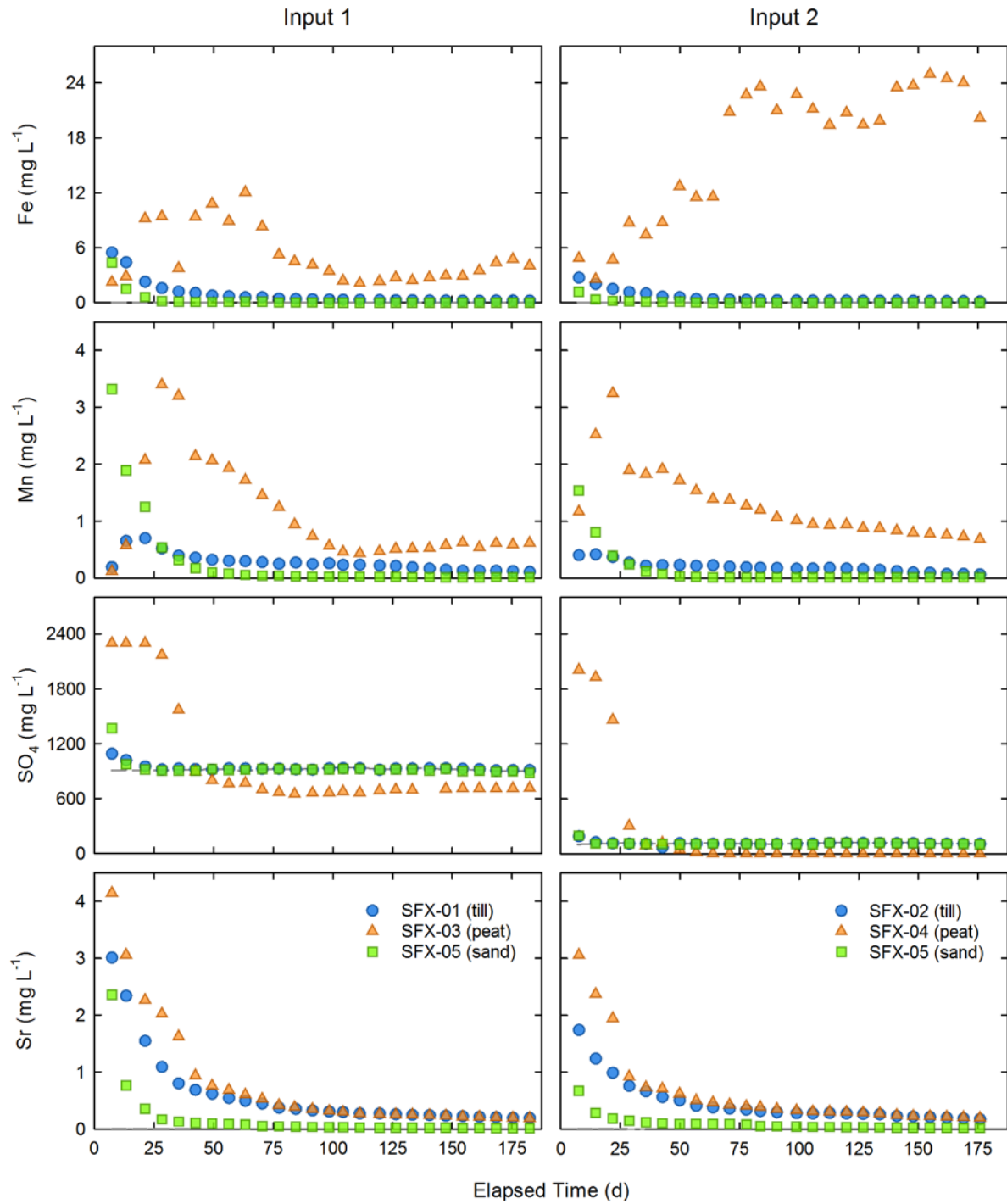


Figure 5.11. Dissolved concentrations of total iron (Fe), total manganese (Mn), sulfate (SO₄) and strontium (Sr) in column effluent (symbols) for input solutions (dashed lines) over time.

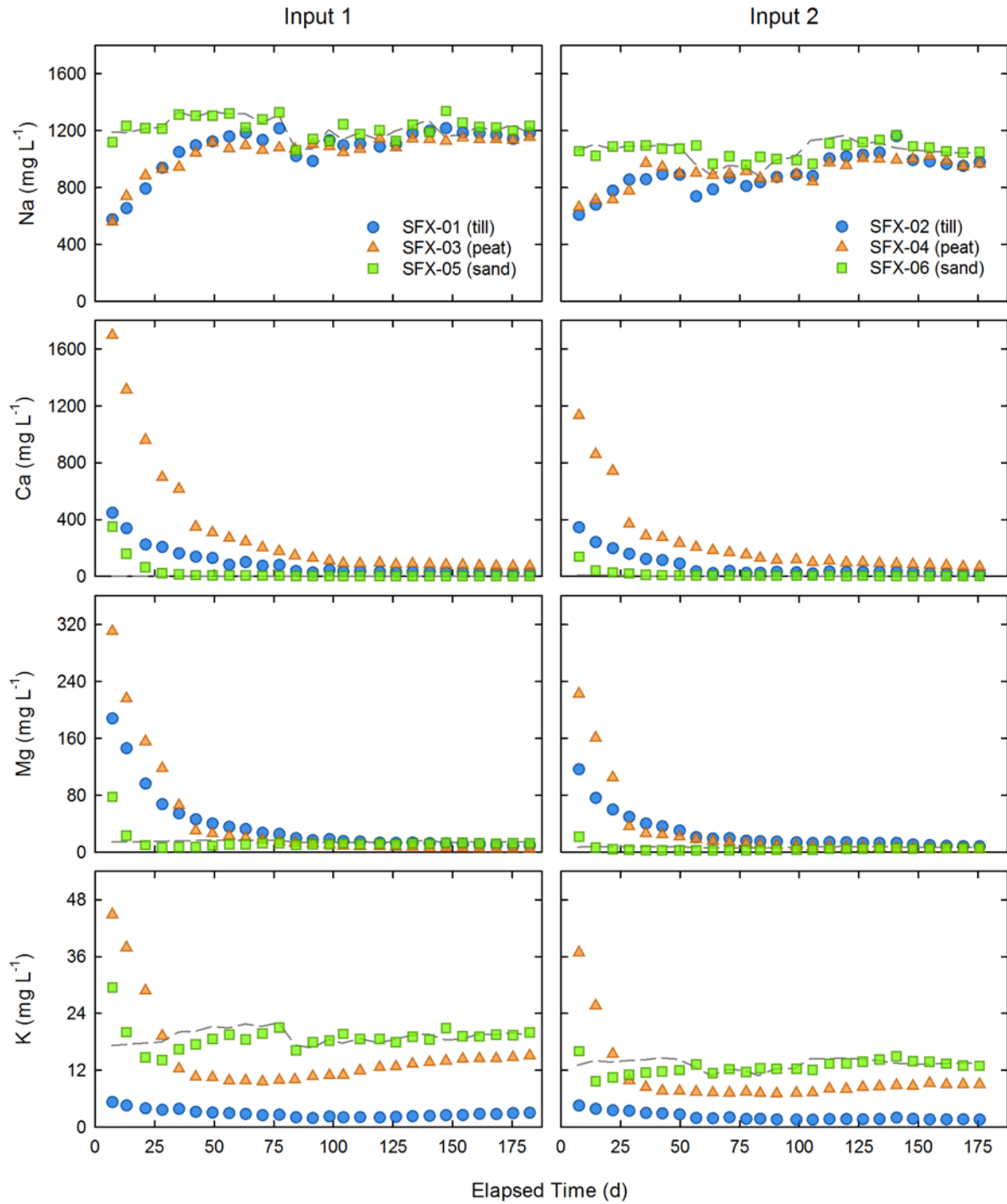


Figure 5.12. Dissolved concentrations of sodium (Na), calcium (Ca), magnesium (Mg), and potassium (K) in column effluent (symbols) for input solutions (dashed lines) over time.

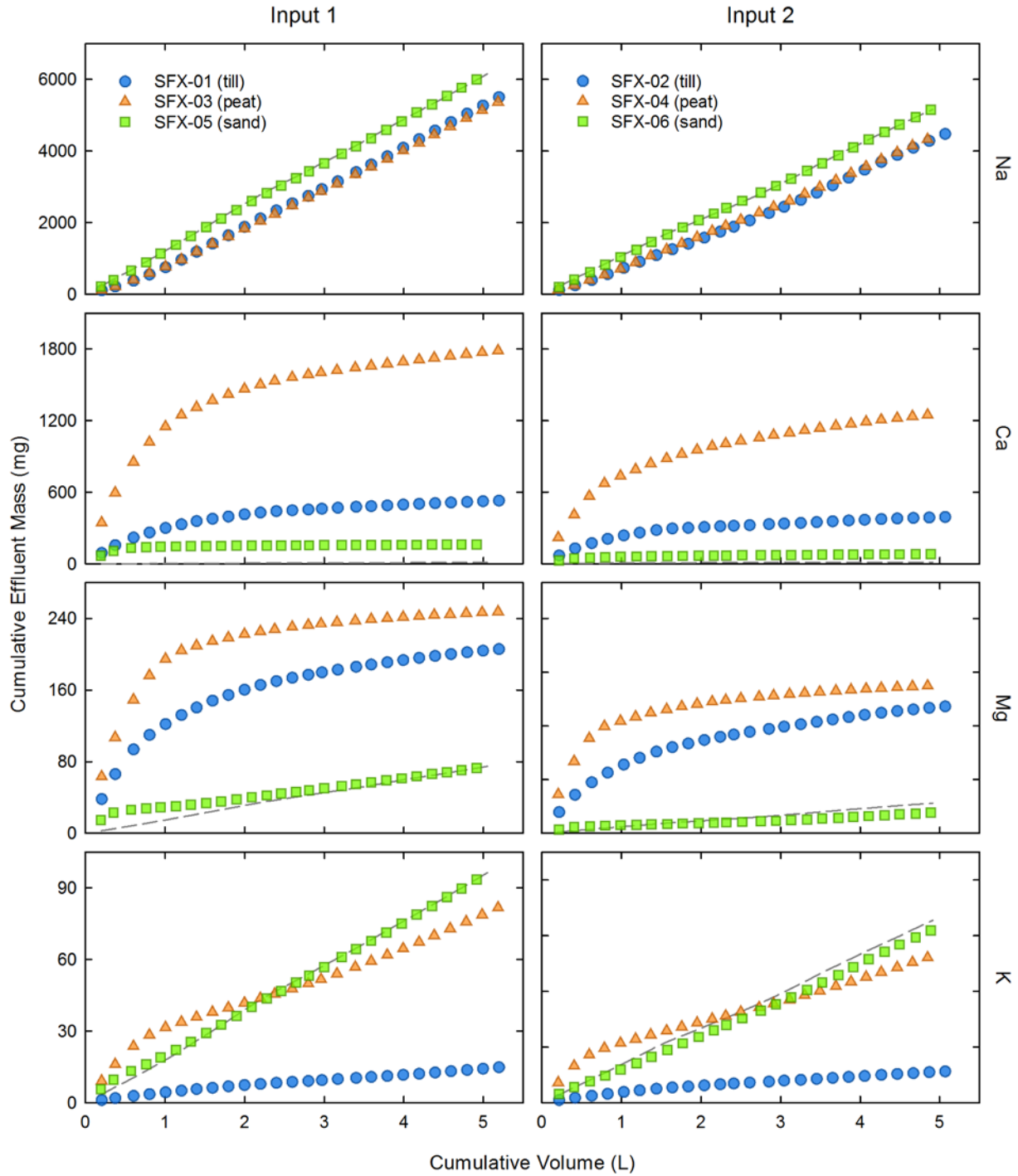


Figure 5.13. Cumulative masses of sodium (Na), calcium (Ca), magnesium (Mg) and potassium (K) calculated for column effluent (symbols) for input solutions (dashed lines) over time.

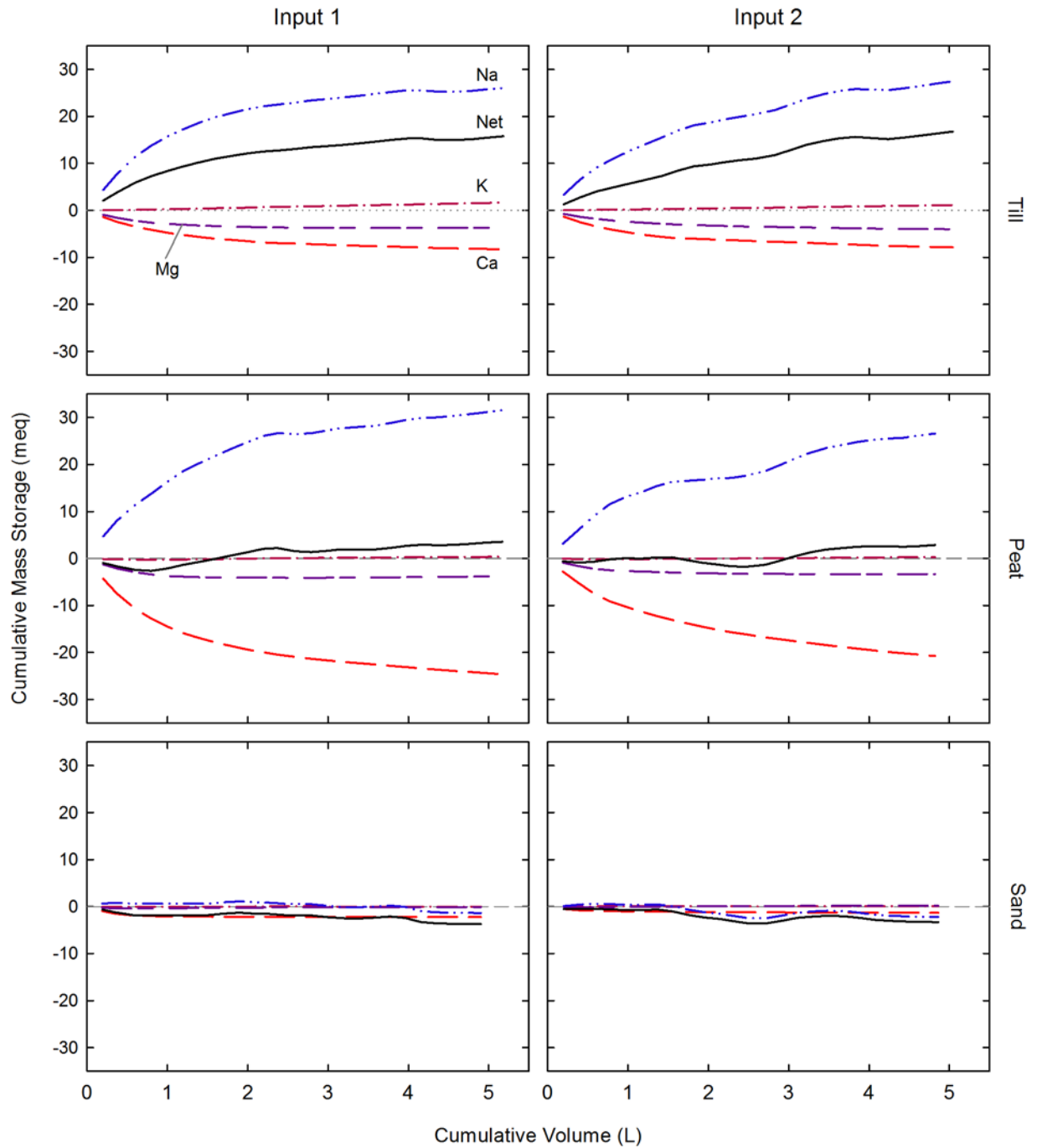


Figure 5.14. Cumulative mass storage versus cumulative volume calculated in milliequivalents for sodium (Na), calcium (Ca), magnesium (Mg) and potassium (K) from modeled free ion activities in column effluent.

BIBLIOGRAPHY



Sandhill Fen, July 2018

Appendix D

Development of Composite Tailings Technology at Syncrude Canada

Development of Composite Tailings Technology at Syncrude Canada

J.G. Matthews, W. H. Shaw, M. D. MacKinnon, & R. G. Cuddy
Syncrude Canada Ltd., Alberta, CANADA

(SWEMP 2000 Sixth International Symposium on Environmental Issues and Waste Management and Mineral Production. Calgary, Alberta. May 30-June 2, 2000. Eds. R. Singhal and A.K. Mehrotra. Pp455)

ABSTRACT: During extraction of bitumen from the Athabasca Oil Sands, an aqueous fines suspension, called mature fine tails (MFT), is produced. The geotechnical characteristics of MFT demand long term storage in geotechnically secure containment areas. The composite tailings (CT) process involves mixing a coarse tailings stream with a MFT stream and adding a coagulant to form slurry that rapidly releases water when deposited and binds the MFT in a coarse tailings/MFT deposit. Thus, more of the fines can be stored in a geotechnical soil matrix, which reduces the inventory of fluid-fine tails and enables a wider range of reclamation alternatives. CT process optimization, coupled with public and regulatory consultation at key milestones, has led to a corporate commitment to implement this technology. This paper reviews key aspects of the evolution of the CT process at Syncrude, including segregation, depositional and geotechnical characteristics of CT mixes that are formed with various chemical aids. Some of the treatments discussed include those based on the use of acid, lime, gypsum, alum, and organic polymers as the coagulant aids.

1 INTRODUCTION

Processing of Athabasca Oil Sands using a water-based extraction process at the current commercial oil sands operations, Syncrude Canada Ltd. and Suncor Energy Inc., generates an increasing volume of clay-rich fine tailings (Fig. 1). In response to the challenge of fine tailings management, Syncrude plans to begin making composite tailings (CT) on a commercial scale in 2000. Initial placement of CT will be in the mined-out area of the present base mine east of Hwy 63 on Lease 17.

This paper will describe the composite tailings process, the benefits of CT, and outline some of the research and development work carried out at Syncrude Canada Ltd. to develop this tailings management technique.

1.1 The Composite Tailings (CT) Process

The CT process involves addition of a chemical coagulant to a slurry, comprising of sufficient solids content and clay minerals fraction, that there is a shift in the coarse-fines segregation boundary. As a result of the treatment, the slurry mix becomes non-segregating during transport, discharge, and deposition (Fig. 2). The product is a material containing the coarse- and fine-grained tailings solids from which a particle-free water is rapidly released upon deposition. The solids are retained

within a homogenous and uniform deposit. While these deposits are initially soft and require containment, an increase in strength to allow a relatively rapid reclamation is anticipated.

The water released from the CT deposit is essentially suspended solids-free. It will comprise a significant portion of the Plant recycle water used in Syncrude's bitumen extraction process and other plant operations (MacKinnon et al 2000).



Figure 1: Aerial photo of Syncrude and Suncor oil sands plants.

Composite Tailings Process Schematic

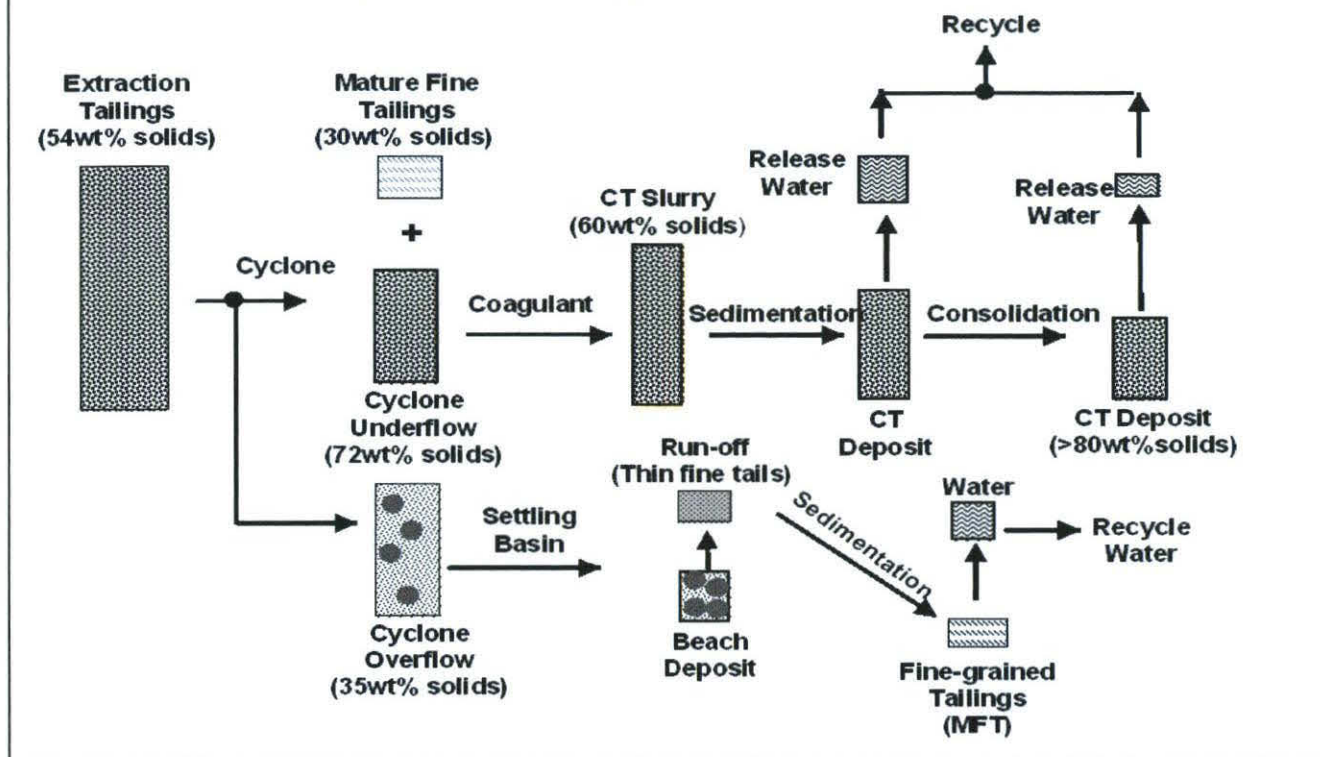


Figure 2: Outline of the CT Process.

1.2 Benefits of Composite Tailings

Syncrude, through the implementation of CT, will accrue a number of benefits:

- Existing volumes of fine tailings (MFT) on Leases 17/22 will be maintained or reduced,
- Disturbed areas will be reclaimed faster,
- The percentage of dry landscape at lease closure will be increased — a positive response to public and regulatory concerns expressed regarding the long term management of fluid fine tailings, and
- Tailings management and storage costs will be reduced. Increased reclamation and mine planning flexibility may also provide opportunities for further production cost savings.

2 BACKGROUND

Current tailings management practices at Syncrude involve discharging the tailings slurry onto beaches or into cells. The coarse fraction ($>44\mu\text{m}$) of the mixture settles rapidly to form a loose water-saturated sand deposit (beaches, dykes). Approximately 50 to 70 percent of the fines ($<44\mu\text{m}$) in the extraction tailings slurry segregate from this deposit and wash into a settling basin along with the process-affected waters released during dis-

charge and deposition. This thin slurry of fines (6–10wt% solids) eventually develops into MFT ($>30\text{wt}\%$ solids).

Without changes to the current tailings management strategy, it is estimated that Syncrude's Leases 17/22 MFT inventory could increase from the current 360 million cubic metres to one billion cubic metres by 2030. This provides incentive to create tailings that do not require fluid containment.

2.1 Previous Research Efforts in Tailings

Over the past three decades, the chemical amendment of whole tailings to initiate coagulation of the fines has been assessed. This research has included dry tailings filtration (Liu et al 1977; Coward 1996), centrifugation (Cymerman 1991), and other mechanical enhancements. In the 1980s, work focused on applying the benefits of coagulation to tailings deposition (FTFC 1995; Shaw et al 1996).

Research in the early 1980s indicated that Syncrude coarse extraction tailings could be made non-segregating with the addition of lime (FTFC 1995). Though not developed to commercial implementation, this work set the stage for further development of chemical amendment processes in support of creating non-segregating tailings (CT).

In 1990, lime was added to a Syncrude extraction tailings stream to create a non-segregating beach deposit, but it was very soft and had low beach angles (Cuddy et al 1991). Subsequent laboratory work at the University of Alberta confirmed that SCL extraction tailings could be made non-segregating through the addition of lime (Caughill 1992). Laboratory testing of the deposits created in this work indicated acceptable long-term geotechnical characteristics that would allow a “dry” landscape for reclamation, but they would require containment during placement and dewatering.

These findings coincided with an in-house mine plan review in 1993 and an opportunity was identified to place non-segregating tailings into below-grade mined-out pits. The decision to pursue this opportunity prompted a more comprehensive laboratory program. Combined with these positive technical results and identified opportunities, a number of significant achievements since 1993 supported continued evaluation and development of the CT process including:

- Successful field pilot trial of CT at SCL in 1995 (Shaw et al 1996),
- Suncor initiated commercial operation of CT process in 1996, and,
- Successful full-scale prototype demonstration of CT at Syncrude in 1997/98.

3 CT TECHNICAL ASPECTS

Through extensive research and development initiatives CT has evolved through a number of process changes (FTFC 1995). Factors identified as influencing segregation of CT mixes include:

- fines content (fraction of total solids),
- total solids content (density),
- particle size gradation,
- mineralogy of fines fraction, and
- water chemistry).

These factors can be manipulated individually or in combination to shift the segregation boundaries. The segregation character can be further manipulated with chemical amendments.

3.1 Segregation Mechanics

Two segregation boundary curves are given in Figure 3. One curve is for Syncrude tailings without chemical amendment and the other is for gypsum treated tailings (1000g CaSO₄·2H₂O per m³ of CT slurry). The curves represent segregation curves under laboratory testing conditions and a shift in these boundaries would be expected under full-scale discharge and deposition conditions. All %fines - %solids combinations plotting above the segregation line (Fig.3) are non-segregating, those falling below the line will be segregating.

Three basic means of slurry manipulation have been evaluated in the course of the CT development:

1. Increased solids content, primarily by hydrocyclone densification,
2. Increased fines content, primarily through enrichment with settled fine tailings, and,
3. Chemical adjustment by addition of coagulants.

The effect of each of these factors is depicted in Figure 3. Initial slurry with 23% fines and 63% solids (*point A*) plots below the segregation curve for untreated Syncrude tailings and is a segregating mix. This slurry is made non-segregating using three basic approaches above:

In the first case, the slurry is densified (as with hydrocyclones or a thickener) to 68% solids without a change in the %fines in the tailings slurry (*point B*). This shifts the slurry composition above the segregation curve for untreated Syncrude tailings and the slurry becomes non-segregating.

Alternately, the mix can be made non-segregating by enriching the slurry with fines (relative to coarse solids and without a change in slurry solids content). In this case the fines content is increased to 28% (*point C*) and again the new slurry “state” is on the non-segregating side of segregation boundary curve.

Finally, the mix can be made non-segregating by addition of a coagulant (*point A*). In this case, the slurry composition does not shift in %solids-%fines space but instead the appropriate segregation curve for reference dramatically shifted. This example depicts a gypsum-treatment curve. With gypsum, point A is well above the segregation boundary curve and the slurry is non-segregating.

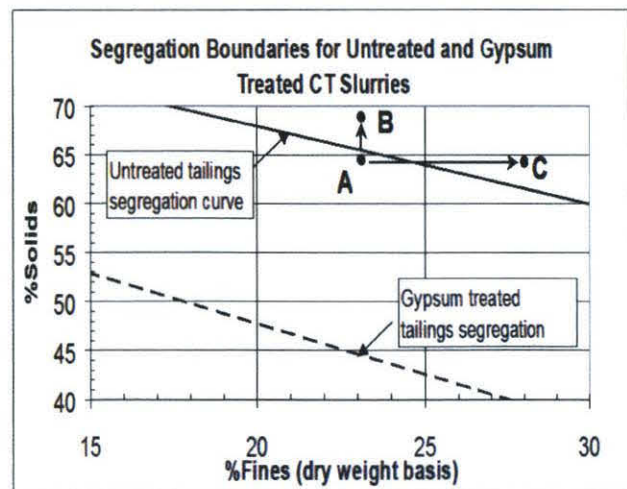


Figure 3: Segregation curves for “raw” and gypsum treated CT slurry.

3.2 Role of coagulants

Addition of a coagulant to the CT mixture (coarse tailings-MFT mixture) is an essential component of the CT process. The coagulant produces changes in the properties of the clays in the CT mixture. Coagulation of clays can be initiated by pH adjustment, salinity or specific cation adjustment, or through cation exchange (MacKinnon et al 2000).

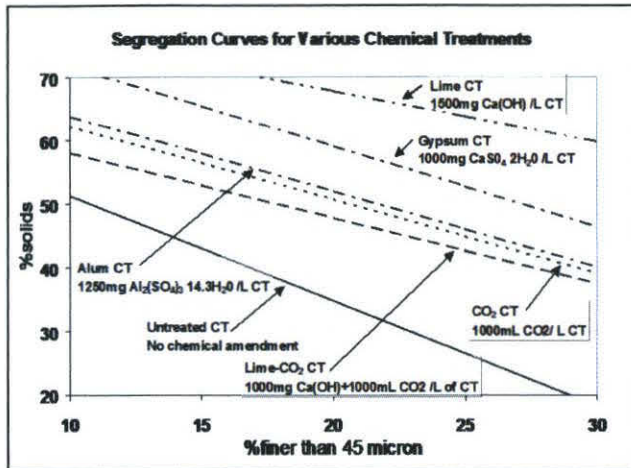


Figure 4: Segregation curves for various coagulant treatments

Without addition of a coagulant, coarse tailings slurry exhibits a gap-graded particle size distribution; it is the gap-graded nature of the PSD that leads to segregation of the fines from the slurry during discharge and deposition (FTFC 1995). Addition of a coagulant causes the colloidal particles to aggregate. This has the effect of changing the particle size distribution of the solids in the slurry to provide a more uniformly graded mixture that can suppress or eliminate segregation. With the addition of a coagulant, the coarse tailings slurry can be made non-segregating during transport, discharge, and deposition (Scott et al 1993).

During the development of the CT process, various coagulant aids were assessed including acid (H_2SO_4), lime (CaO , $Ca(OH)_2$), acid-lime ($H_2SO_4 - CaO$), gypsum ($CaSO_4 \cdot 2H_2O$), sodium aluminate ($Na_2Al_2O_3$), alum ($48\% Al_2(SO_4)_3 \cdot 14.3H_2O$), lime- CO_2 , CO_2 , and organic polymers (polyacrylamides).

Segregation curves for untreated, lime-, gypsum-, alum-, lime- CO_2 , and CO_2 -treated tailings slurry are given (Fig. 4). Each curve represents the segregation boundary for a given coagulant treatment and coagulant dosage in %fines-%solids space.

3.2.1 Coagulant Impact on Water Chemistry

In MacKinnon et al (2000), the impact of coagulant on the quality of CT waters is discussed. Laboratory and field studies were undertaken to evaluate these impacts.

CT made using inorganic coagulants exhibited the greatest effect on water quality, generally with a resulting increase in overall or specific ionic loading and a shift in the relative ionic composition of the CT release waters. While CT produced using organic flocculants showed no net increase in overall ionic loading of produced waters, the performance of the resulting CT was not deemed acceptable based on its geotechnical properties.

3.2.2 Coagulant Screening Process

Following Syncrude's 1990 Field Trial using lime treatment of extraction tailings streams (Cuddy et al 1991), acid and lime were considered as candidate coagulants. As part of this comparison, the release water quality from lime, acid, and acid-lime and gypsum produced CT mixes was assessed (MacKinnon et al 2000). Though all coagulant treatments were found to produce acceptable non-segregating slurries at appropriate dosages (Fig. 4), significant differences were noted in the CT pore- and release-waters quality. As well, the segregation characteristics, deposit dewatering and consolidation rates, and economics were factors in coagulant selection.

Based on on-going research efforts (FTFC 1995), gypsum was proven to be a robust, effective, easy to handle, and readily available alternative to lime and acid-lime treatment. As a result, Syncrude decided to use gypsum as the coagulant for a 1995 field demonstration and the 1997/98 prototype programs. In these programs, slurries that were non-segregating during transport, discharge and deposition and which displayed suitable geotechnical characteristics were produced under operational conditions. Through this evaluation process, gypsum was selected as the coagulant for the commercial application of CT at Syncrude.

Though gypsum has been demonstrated as an affordable and effective coagulant for the CT process, work continues in screening alternative coagulants. Key factors assessed in screening alternatives include supply cost, dosage, effects on pore and release water, segregation susceptibility, depositional performance and geotechnical performance.



Figure 5: Syncrude's 1997/98 CT Prototype trial.

3.2.3 Gypsum Dosages at Field Scale

In the development of the gypsum-based CT process, differences were noted in dosages required to prevent segregation of the CT solids when lab-scale performance was compared with field-scale performance. Gypsum dosages required for full-scale operation have been found to be as much as twice the dosage recommended based on laboratory findings. Laboratory testing on gypsum treated CT was carried out at the University of Alberta to identify minimum and recommended gypsum dosages for use in the 1995 Field Demonstration program. Through this study, a dosage of 900 grams gypsum per cubic metre of CT was selected for the program. When this dosage was tried during the initial stages of the 1995 Field Demonstration, it was found to be inadequate to prevent segregation of most of the CT slurry produced. In response to this, gypsum dosages were incrementally increased and a minimum field dosage of 1200 grams gypsum per cubic metre of CT slurry was identified. To ensure effective production of non-segregating slurry, the field dosage was boosted further to 1400 grams gypsum per cubic metre of CT slurry. Some of this difference reflects the moisture content and debris in the available (agricultural grade from Domtar).

3.3 Densification of the Coarse Tailings Stream

In Scott et al (1993), it was shown that Syncrude coarse tailings streams can be made non-segregating without a densification step. These predictions are made based on results from laboratory standpipe testing programs. In practice, most Syncrude coarse tailings slurry cannot be made non-segregating without some degree of densification as part of the CT process (Shaw et al 1996).

The process step of coarse tailings densification provides a number of process benefits including

reduced treatment costs and an opportunity to consume MFT inventory.

3.3.1 Reduced treatment costs.

Densification increases the solids content of slurry. For a fixed fines content, increasing the solids content reduces the likelihood for the slurry to segregate. Therefore, if the densification process is implemented and dosage rates are left unchanged, the slurry is less susceptible to segregation for a given fines content.

3.3.2 Opportunity to consume MFT inventory.

Densification of the coarse tailings stream, followed by the addition of MFT, creates an opportunity to consume existing MFT inventory. When CT, with a sand-to-fines ratio (SFR) of 4:1 (< 44µm basis) is produced it has almost twice as much of the <5.5µm fines fraction as an "unenriched" extraction coarse tailings stream with a SFR of 5:1 (Fig. 6). Since the finest mineral particles are the primary MFT-formers (FTFC 1995), this difference has a significant impact of MFT production. More MFT can be consumed through the densification of the coarse tailings stream, followed by addition of MFT, than can be achieved by capturing all available fines in the extraction coarse tailings slurry alone.

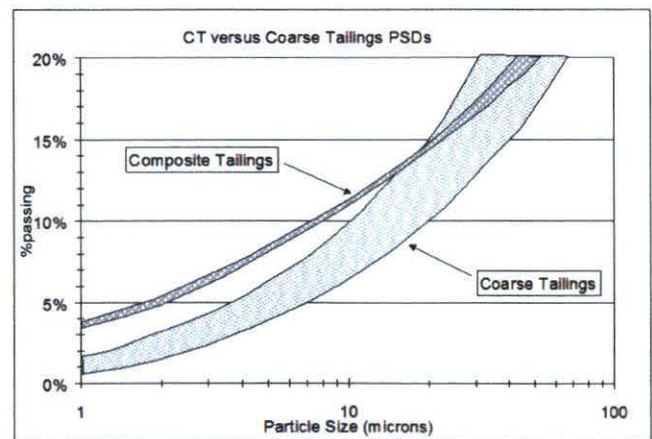


Figure 6: Fines consumption with CT

3.4 Addition of Mature Fine Tailings

One of Syncrude's biggest challenges is management of fluid fine tailings inventory. In 1997, Syncrude carried a base mine MFT inventory of approximately 360 million cubic metres. PSDs for typical Syncrude tailings streams are given in Figure 7. CT provides an opportunity to manage the fines content of the CT slurry produced, providing a means of engineering the solids storage efficiency and geotechnical performance of the deposit(s)

created. A primary incentive of CT is to create non-segregating slurries with higher fines contents and a resulting consumption of MFT-forming fines. In contrast, controlling the fines-enrichment factor must be considered to optimize tailings storage. The aim of designing the CT slurry is to ensure that these interests are balanced to provide optimum tailings storage efficiency and acceptable geotechnical performance, while maintaining mine planning flexibility.

Factors which were considered in support of fines enrichment included dosage efficiency, MFT content and long-term and depth dependence of the geotechnical integrity of the deposit. Factors that may limit the fine content of the CT product included slower dewatering and consolidation rates, reduced hydraulic conductivity and reduction in short term/shallow deposit integrity.

The field scale demonstration and prototype programs were important in increasing understanding of the CT geotechnical performance.

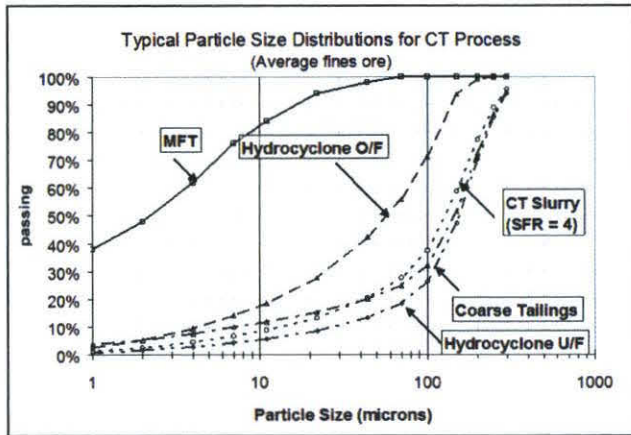


Figure 7: Typical PSDs for CT Process

Laboratory work done in advance of the field programs was extensive, but it was unable to account for all of the processes at play at full-scale implementation. Almost all of the geotechnical models required re-calibration after the field trials to account for significant differences in process rates and effects between the laboratory and field scale. The current consolidation and permeability models for Syncrude CT are discussed below. These models were initially developed from carefully controlled laboratory testing programs and then re-calibrated based on observed field behaviour from the 1995 and 1997/98 field programs (Pollock et al 2000).

3.4.1 Fines Content and CT Compressibility

Compressibility curves for various sand-to-fines ratios (SFRs, $>44\mu\text{m}/<44\mu\text{m}$) are given (Fig. 8). These curves represent the state of knowledge re-

garding anticipated stress-strain performance of the CT deposits based on all work done to date (including laboratory and field data, with precedence given to performance from the 1995 and 1997 field trial programs). Although these curves depict the current state of knowledge, careful monitoring will be necessary with commercial start-up to verify the model parameters and account for a number of significant influences including; larger deposition areas, winter CT deposition, extraction tailings stream variability, and deeper deposit thickness. It may be seen that current models predict increased CT deposit compressibility with increased fines contents (Fig. 8).

Storage efficiency of CT can be represented in terms of tonnes of dry solids stored per cubic metre of CT deposit across a range of effective stress conditions (Fig. 9). Model analyses indicate that greater storage efficiency is associated with higher fines contents at depths in excess of approximately two metres (i.e. effective stresses in excess of approximately 20 kPa).

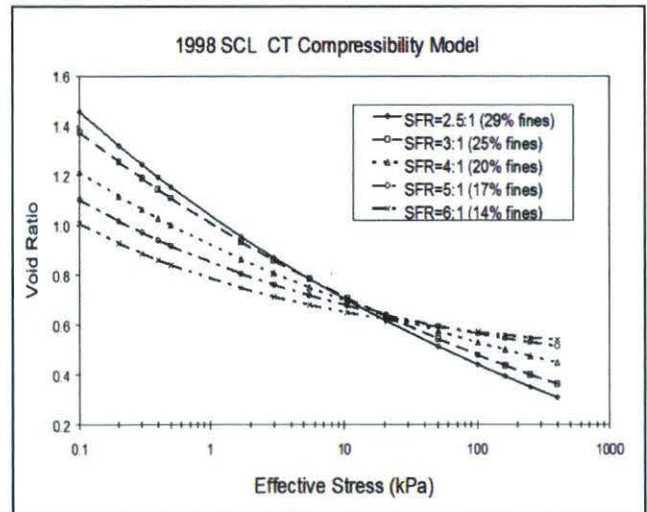


Figure 8: CT Compressibility

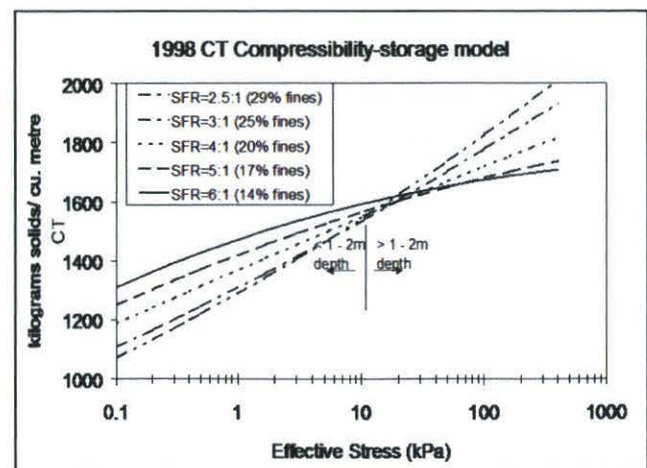


Figure 9: CT Solids Storage Efficiency

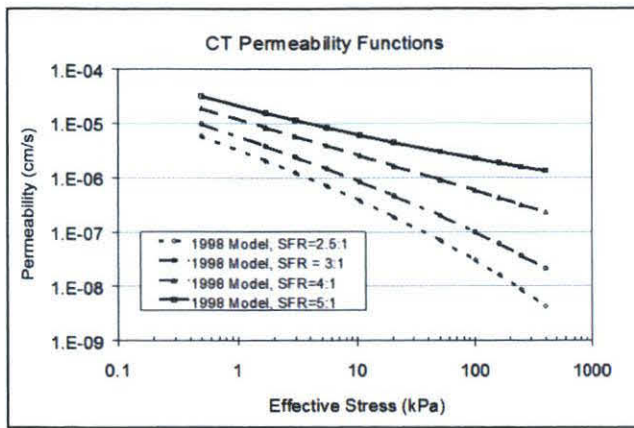


Figure 10: CT Permeability

3.4.2 SFR Influence on CT Permeability

The permeability of CT at a given void ratio decreases with increased fines contents (Fig. 10). In the plot of the permeability-fines void ratio, there is a single curve describing the permeability of CT across the range of SFRs evaluated (<44 μ m basis). After deposition and completion of initial sedimentation and consolidation, the permeability of the CT appears to be almost wholly influenced by the fines (<44 μ m) content of the deposit (Pollock 2000).

3.4.3 SFR for Commercial Implementation

A target SFR of 4:1 (<44 μ m basis) has been chosen for commercial implementation in 2000. This choice was influenced by precedent established through research and development efforts and by a desire to optimize the rate of consolidation. Most Syncrude field experience included a ratio of 4:1, providing confidence that this SFR will provide adequate geotechnical performance and satisfy planning needs.

3.5 CT Implementation and MFT Inventory

While the CT process consumes existing MFT, thin fine tails (TFT) continue to be generated from the hydrocyclone overflow stream and from other tailings streams (Fig. 2). The new TFT will densify and continue to produce MFT in the active settling basins. With the implementation of CT in 2000, it is anticipated that net MFT production will be eliminated at Syncrude's base mine operation. The immediate benefit to Syncrude will be reduced fluid containment requirements. This plan assumes production of CT slurry at 58wt% solids with a SFR of 4:1 produced with 95 percent efficiency in creating non-segregating slurries. Sensitivities factored into this prediction include the assumed hydrocyclone solids and fines capture efficiency and CT plant operating efficiency. Should deposit per-

formance warrant it, there is potential to increase MFT consumption through increased fine solids enrichment.

4 FUTURE CHALLENGES FOR R & D

Certain technical issues require continued evaluation and development, including:

- Assessment of water quality impacts on extraction processability, plant operations, and reclamation,
- Continued assessment of alternative coagulants,
- Monitoring and evaluation of environmental and reclamation aspects, including substrate design, vegetation selection, and landscape alternatives, and
- Monitoring and prediction of depositional and geotechnical performance including ongoing optimization of sand-to-fines ratio (i.e. fines consumption versus geotechnical integrity and performance).

4.1 Water Impacts

Water chemistry changes will be associated with implementation of the CT process. Issues to continue monitoring and addressing include effects of changes on ore processability and plant operations and reclamation design. Due regard must be given to these issues to ensure that potential detrimental effects of water chemistry changes are mitigated (MacKinnon et al 2000).

4.2 Reclamation Design

Reclaimed composite tailings deposits will comprise a significant part of Syncrude's final landscape. It is anticipated that approximately two thirds of the CT deposits will be capped with tailings sand and will be reclaimed using established reclamation practices. The remaining one third of the deposits will not be capped with sand but will be amended with peat or capped with reclamation materials and vegetated. Most of this uncapped landscape will be found in lowlands areas and will be developed to support wetland communities. CT reclamation research is currently focussed on:

- Evaluating the effects of CT water on plant growth, survival, and propagation,
- Selection of salt tolerant species for vegetation,
- Determination of most effective capping strategies (including materials, depth, timing) to mitigate effects of CT release water on root zones, and,
- Evaluation of methods to develop and improve soils on CT surfaces.

4.3 Geotechnical Performance

Development of effective consolidation models for a range of CT mixtures allows assessment of various deposition and volume-balancing scenarios in support of optimized mining and extraction tailings objectives. With a focus on maximizing the depletion of mature fine tailings (MFT) reserves, there is a potential to create non-segregating slurries with lower sand-to-fines ratios. Balancing this potential is the recognition that as the fines content goes up, the rate of water release and consolidation goes down, potentially adding more pressure on site tailings and water storage capacity needs. Continued refinement of consolidation models for CT, based on field performance at increasing scales, will offer increased confidence regarding the prediction of future performance and consequential identification of planning sensitivities.

5 SUMMARY

Syncrude Canada Ltd. is committed to continuous improvements in the areas of productivity and environmental performance. The company is also committed to restoring the land to an acceptable and sustainable use.

One challenge facing Syncrude is fine tailings management. To meet the challenges associated with fine tailings management and to support its commitment for continuous improvements, Syncrude maintains a strong research and development focus on tailings management alternatives.

Over recent years, composite tailings (CT) technology has been developed to become an important part of the tailings management solution. Much of the CT development process has taken place through the concerted and collaborative efforts of the oil sands industry, consultants, academics and regulatory agencies. The technology began initially as a simple process of adding lime to a coarse tailings stream and has developed through a number of key modifications to become a robust and commercially viable tailings management technology.

Commercial implementation of the CT process provides Syncrude an opportunity to improve tailings management efficiency and reduce the volumes of fluid fines to be managed in the long term.

More research and development work is planned to continue improving the CT process. In particular, challenges remain in assessing reclamation alternatives, assessing potential negative effects of CT release water on bitumen recovery and plant operations efficiency, seeking continuous process improvements (including alternative coagulants), and optimization of storage plans through manipulation of the CT mixtures.

6 CONCLUSIONS & RECOMENDATIONS

A process has been developed which will enable Syncrude to achieve improved fine tailings management performance. The process was developed through programs of progressive and increasing scale and scope, from bench scale testing to the creation of a prototype scale deposit. This effort has been an example of successful partnering of university and industry research initiatives and close cooperation and support from development and operational groups. The composite tailings (CT) process, which emerged from these ongoing research and development improvements, has been tested and found to be robust and effective in producing a non-segregating tailings slurry through a wide range of operating conditions with favourable economics.

Though much has been learned about the CT process, there are a number of areas requiring further investigation. Specific aspects to monitor with full-scale production will include field deposit performance (consolidation and water release rates) and release water chemistry changes. As well, consideration will be given to potential differences between CT produced from Clark Hot Water Extraction (CHWE) tailings and CT made at Aurora using Low Energy Extraction (LEE) tailings.

AKNOWLEDGEMENTS

The authors wish to graciously acknowledge the efforts of everyone that has contributed to the successful development of the composite tailings process. Many dedicated people worked to make this project a success including: the geotechnical engineering group at the University of Alberta, research partners at CANMET (Devon), industry partners at Suncor Energy Inc., consultant expertise from Golder Associates and AGRA Earth and Environmental, and the many Syncrude employees and contract support staff. Collectively, many hours of effort have gone into the development of the CT process. Congratulations to all involved for a job well done.

REFERENCES

- Caughill, D.L. 1992. *Geotechnics of Non-segregating Oil Sand Tailings*. University of Alberta, M.Sc. Thesis. June 1992.
- Coward, J. 1996. *Feasibility and Economics of Whole Tailings Filtration*. Edmonton, Syncrude Research Department, Progress Report, 25 (1) pp. 80 – 124, 1996.
- Cuddy, G., R. Lahaie, & W. Mimura 1991. *1990 Sand-fine tails field program*. Edmonton,

- Syncrude Research Dept. Research Report, 91-5, 3v., 1991.
- Cymerman, G. 1991. *Fine Tails Compaction Tests at Bird Laboratory*. Edmonton, Syncrude Research Department, Progress Report, 20 (1) pp. 83 – 113, 1991.
- FTFC (Fine Tailings Fundamentals Consortium) 1995. In: *Advances in Oil Sands Tailings Research*, Alberta Department of Energy, Oil Sands and Research Division. 1995.
- Liu, J. K. 1977. *Dry Tailings Disposal — Filtration Demonstration Run*. Edmonton, Syncrude Canada Ltd. Research Department, Progress Report, 6 (7) pp. 84-91, 1977.
- MacKinnon, M.D., J.G. Matthews, W.H. Shaw, & R.G. Cuddy 2000. Water quality issues associated with implementation of composite tailings (CT) technology for managing oil sands tailings. In: *Proceedings of SWEMP 2000*, Calgary, Alberta, May 30 – June 2, 2000.
- Pollock, G.W., E.C. McRoberts, G. Livingstone, G.T. McKenna, & J.G. Matthews 2000. Consolidation behaviour and modeling of oil sands composite tailings in the Syncrude CT prototype. In: *Tailings and Mine Waste '00*. Rotterdam: 2000 Balkema. Fort Collins, January 2000. pp121-130..
- Scott, J. D., Y. (Bill) Liu, & D.L. Caughill 1993. Fine Tails Disposal Utilizing Nonsegregating mixes. In: *Proceedings of Oil Sands — Our Petroleum Future Conference*, Edmonton, Alberta, Canada. Apr. 4 – 7, F18, 1993.
- Shaw, W., G. Cuddy, G. McKenna, & M. MacKinnon 1996. *Non-segregating Tailings: 1995 NST Field Demonstration*. Edmonton, 96-2: Syncrude Canada Ltd. 4 vols.